



HAL
open science

Coordination chemistry and catalysis with mixed ligands associating iminophosphorane to thiolate or phenolate

Thi-Phuong-Anh Cao

► **To cite this version:**

Thi-Phuong-Anh Cao. Coordination chemistry and catalysis with mixed ligands associating iminophosphorane to thiolate or phenolate. Coordination chemistry. Ecole Polytechnique X, 2012. English. NNT: . pastel-00765632

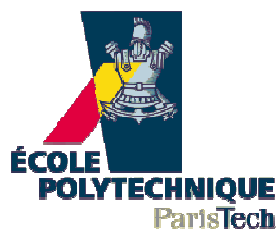
HAL Id: pastel-00765632

<https://pastel.hal.science/pastel-00765632>

Submitted on 18 Dec 2012

HAL is a multi-disciplinary open access archive for the deposit and dissemination of scientific research documents, whether they are published or not. The documents may come from teaching and research institutions in France or abroad, or from public or private research centers.

L'archive ouverte pluridisciplinaire **HAL**, est destinée au dépôt et à la diffusion de documents scientifiques de niveau recherche, publiés ou non, émanant des établissements d'enseignement et de recherche français ou étrangers, des laboratoires publics ou privés.



THESE

Présentée pour obtenir le titre de

Docteur de l'École Polytechnique,

Spécialité Chimie

Par **Thi Phuong Anh CAO**

COORDINATION CHEMISTRY AND CATALYSIS WITH MIXED LIGANDS ASSOCIATING IMINOPHOSPHORANE TO THIOLATE OR PHENOLATE

Thèse soutenue le lundi 24 septembre 2012 à 14h00

à Ecole Polytechnique 91128 Palaiseau Cedex FRANCE

Composition du jury

Fanny BONNET	CNRS, Ecole Nationale de Chimie de Lille	Examinatrice
Vincent GANDON	CNRS, Université Paris-sud 11	Examinateur
Guy LAVIGNE	CNRS, LCC Toulouse	Rapporteur
Dominique MATT	CNRS, Institut de Chimie de Strasbourg	Rapporteur
François NIEF	CNRS, Ecole Polytechnique	Directeur de Laboratoire
Audrey AUFRANT	CNRS, Ecole Polytechnique	Directrice de thèse
Pascal LE FLOCH		Directeur de thèse

Acknowledgements

What is reported in this thesis results from the efforts and contributions of many people.

It is first and foremost the one of professor Pascal Le Floch, with whom I've started the PhD. Though the time was short, I've learned a lot from him.

I would like to thank Doctor Audrey Auffrant, who had accepted to take the direction of my thesis after Pascal had passed away. It was not easy, for her and for me. But we've successfully passed through it.

During my thesis, which covers quite a large range of domains in chemistry, I had the opportunity to work with many great people. They are:

- 1) Dr. Elina Payet, who worked in the development of ligands associating PN and heteroatom (other than sulfur) of the structure NPCH_2X (chapter 1).
- 2) Thibault Cheisson and Dr. Christian Klemps who worked on the oligomerisation of ethylene (chapter 2).
- 3) Dr. Stéphanie Labouille, who worked on the DFT calculations for our first study on the phosphasalen ligand (chapter 3).
- 4) Dr. Gregory Nocton and Dr. Louis Ricard, who worked on the EPR spectroscopies and the related DFT study on the Ni(III)-phosphasalen complex (chapter 4).
- 5) Dr. Antoin Buchard, who gave me precious guide and advice on the first study of rac-lactide polymerisation (chapter 5).
- 6) Clare M. Bakewell, who helped me with the activity study of the complexes in rac-lactide polymerisation (chapter 5, part IV).

Many thanks are dedicated to Dr. Xavier F. Legoff and Dr. Louis Ricard for all the X-ray diffraction experiments and magnetic study, for their carefulness, enthusiasm and patience. I would like to thank Pr. Yves Jean, who guided me for all the DFT studies, and who in particular has contributed to the DFT studies on the Nickel-Phosphasalen complexes.

Special thanks are given to Dr. Charlotte K. Williams, whose precious discussions have helped me all along the development of complexes for the polymerisation of lactide.

I would like to thank Dr. François Nief for his help in administration procedures, and his scientific advice for the development of iminophosphorane compounds. I would like to give a special thank to Anne-Florence Eyssautier, without whose help and smile my PhD life would be much less enjoyable.

And finally, I want like to thank all the members of the Laboratoire de Heteroelements et Coordination who had been there during my PhD and who had made that time memorable, as well as the members of Dr. Williams' group for their warm welcome during my stay at the Imperial College of London .

Publications and notable communications

- [1] Clare M. Bakewell, Thi-Phuong-Anh Cao, Nicholas Long, Xavier F. Le Goff, Audrey Auffrant and Charlotte K. Williams, “*Yttrium Phosphasalen Initiators for rac-Lactide Polymerization: Excellent Rates and High iso-Selectivities*”, **Journal of the American Chemical Society**, **2012** (DOI: 10.1021/ja310003v).
- [2] Thi-Phuong-Anh Cao, Antoine Buchard, Xavier F. Le Goff, Audrey Auffrant and Charlotte K. Williams, “*PhosphaSalen Yttrium Complexes: Highly Active and Stereoselective Initiators for Lactide Polymerization*”, **Inorganic Chemistry**, **2012**, 51(4), 2157-2169.
- [3] Thi-Phuong-Anh Cao, Stéphanie Labouille, Audrey Auffrant, Yves Jean, Xavier F. Le Goff and Pascal Le Floch, “*Pd(II) and Ni(II) Complexes Featuring a “Phosphasalen” Ligand: Synthesis and DFT Study*”, **Dalton Transactions**, **2011**, 40, 10029-10037.
- [4] Thi-Phuong-Anh Cao, Elina Payet, Audrey Auffrant, Xavier F. Le Goff and Pascal Le Floch “*Facile Synthesis of Bifunctional Ligands Using LiCH₂PPh₂=NPh Obtained From [PhNH-PPh₃]⁺[Br⁻]*”, **Organometallics**, **2010**, 29, 3991-3996.
- [5] Clare M. Bakewell, Thi-Phuong-Anh Cao, Nicholas Long, Xavier F. Le Goff, Audrey Auffrant and Charlotte K. Williams, “*Yttrium Phosphasalen Initiators for rac-Lactide Polymerization*”, submitted to **Organometallics**.
- [6] Thi-Phuong-Anh Cao, Xavier F. Le Goff, Gregory Nocton, Audrey Auffrant, “*Tuning of Oxidation Locus on Metal Complex: the Geometric and Electronic Structure of One-Electron Oxidated Nickel Phosphasalen Complex*”, working paper.
- [7] Thi-Phuong-Anh Cao, Thibault Cheisson, Xavier F. Le Goff, Pascal Le Floch and Audrey Auffrant, “*Nickel Complexes as Highly Active Catalysts for the Dimerisation of Ethylene*”, working paper.
- [8] Thi-Phuong-Anh Cao, Stéphanie Labouille, Antoine Buchard, Xavier F. Le Goff, Duncan Carmichael, Jean Yves, Audrey Auffrant, Pascal Le Floch and Charlotte K. Williams, “*Phosphasalen complexes: what phosphorus changes*”, Oral Communication (20 min), Congress “*European Workshop in Phosphorus Chemistry*”, 22-23 March **2012**, Rennes.
- [9] Thi-Phuong-Anh Cao, Stéphanie Labouille, Audrey Auffrant, Yves Jean, Xavier F. Le Goff and Pascal Le Floch, “*Synthesis and Coordination of a Phosphasalen ligand*”, Oral Communication (20 min), Congress: “*Journées de chimie de coordination de la Societe Chimique de France*”, 3-4 February **2011**, Angers.

Guide to the reading

Compound numbering

Synthesised compounds are numbered as **1,2,3**, etc. Reference compounds existing in the literature are named using a letter and a number. The letter refers to the metal if the compounds are metal complexes (e.g. **Al1**, **Ni2**, **Y3**, etc.), and is **X** if not (e.g. **X1**).

List of abbreviations

COD: 1,5-cyclooctadiene

DABCO: 1,4-diazabicyclo[2,2,2]octane

DFT: Density Functional Theory

DME: Dimethoxyethane

EPR: Electron Paramagnetic Resonance

Et: Ethyl

Fc: Ferrocene

GPC: Gel Permeation Chromatography

HOMO: Highest Occupied Molecular Orbital

iPA: isoPropanol

iPr: isoPropyl

KHMDS: Potassium bis(trimethylsilyl)amide

LA: Lactide

LUMO: Lowest Occupied Molecular Orbital

M: mol/L

MALDI-ToF: Matrix Assisted Laser Desorption Ionisation-Time of Flight

MAO: Methylaluminoxane

Me: Methyl

NBO: Natural Bond Orbital

nBu: n-Butyl

NMR: Nuclear Magnetic Resonance

ORTEP: Oak Ridge Thermal-Ellipsoid Plot Program

PCM: Polarisable Continuum Model

PDI: Polydispersity Index

Ph: Phenyl

PLA: Polylactic Acid

rac-: racemic mixture

ROP: Ring Opening Polymerisation

SOMO: Singly Occupied Molecular Orbital

tBu: *tert*-Butyl

THF: Tetrahydrofuran

TMS: Trimethylsilyl

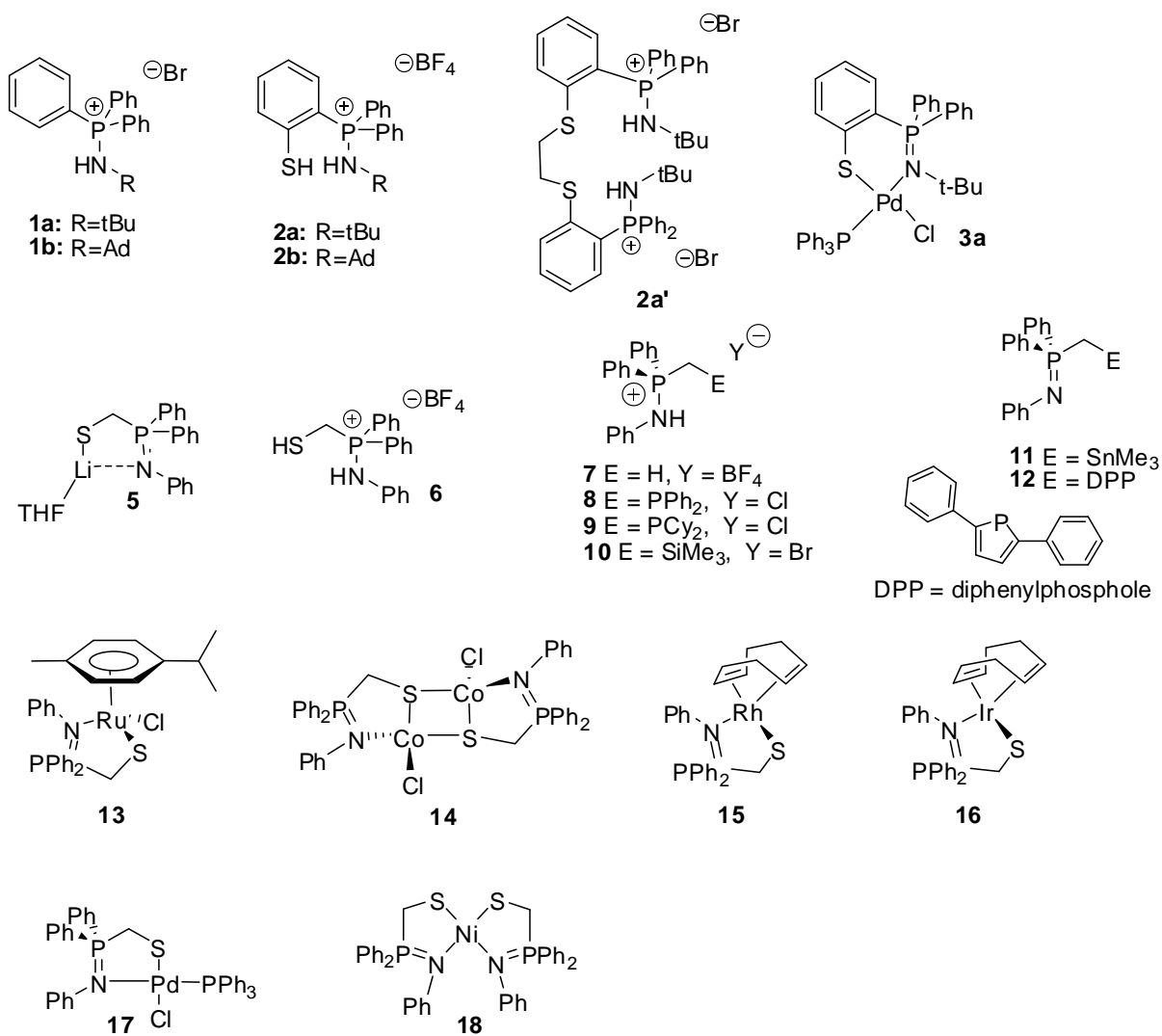
TOF: Turn Over Frequency

TON: Turn Over Number

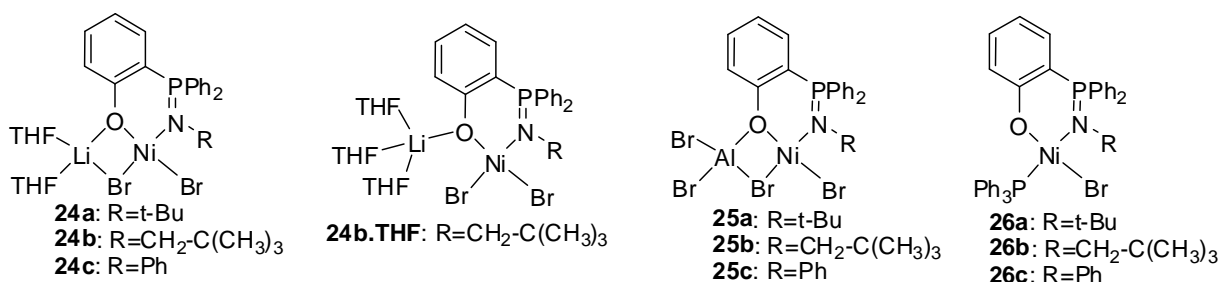
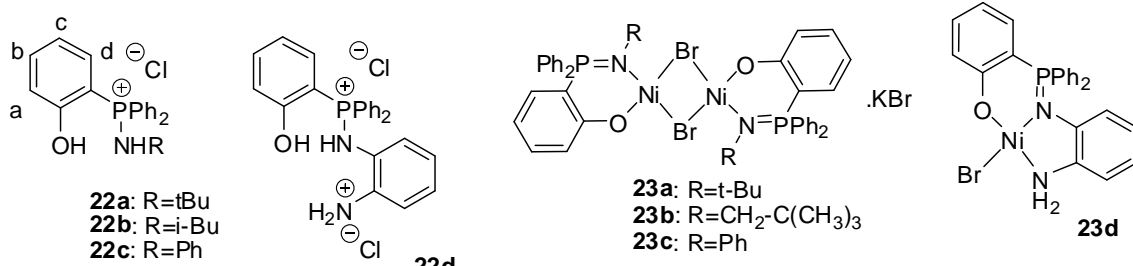
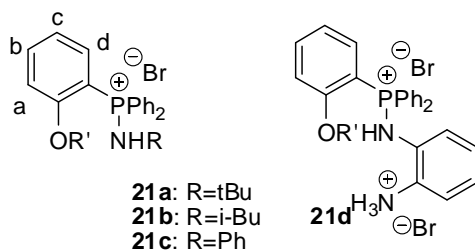
TS: Transition State

List of Synthesised Compounds

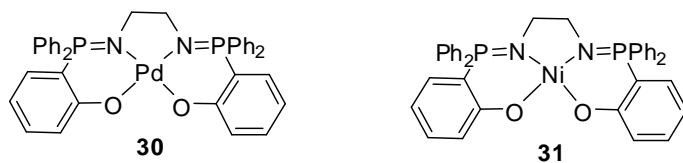
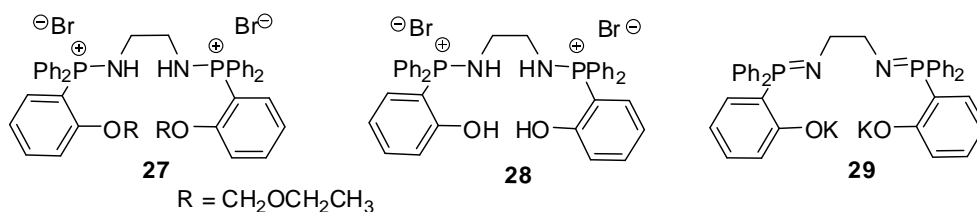
Chapter 1



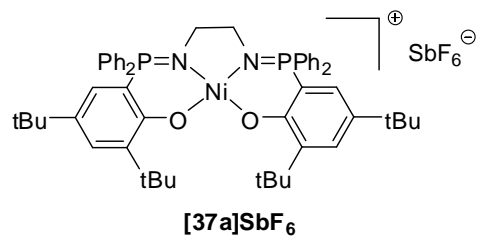
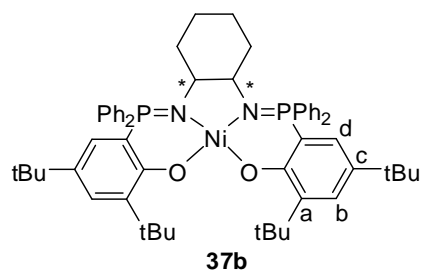
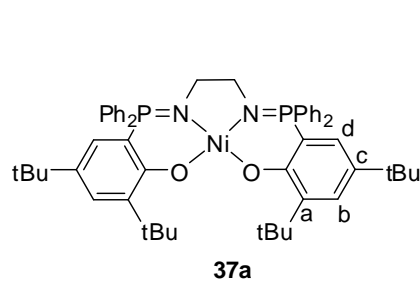
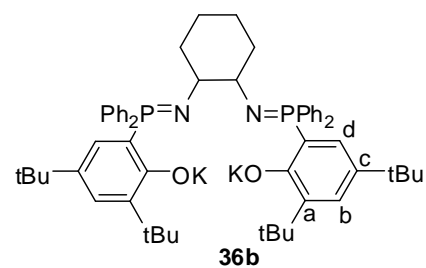
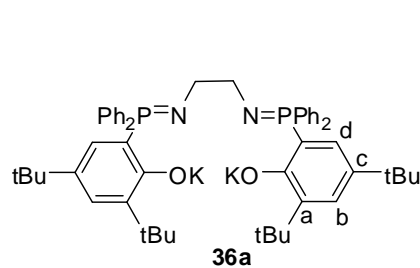
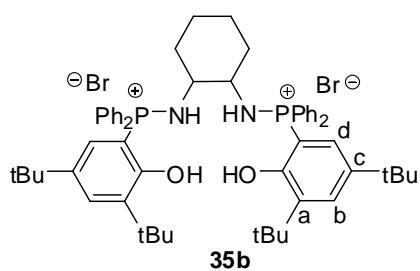
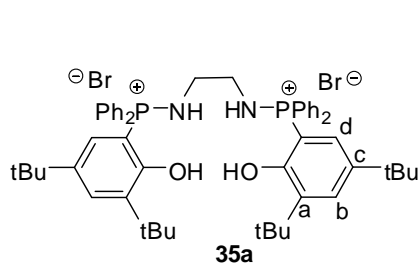
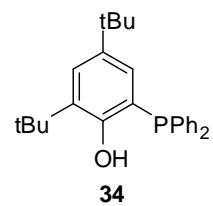
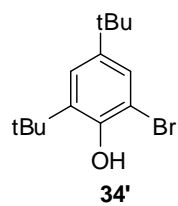
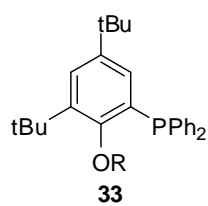
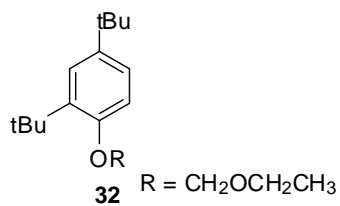
Chapter 2.



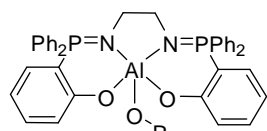
Chapter 3



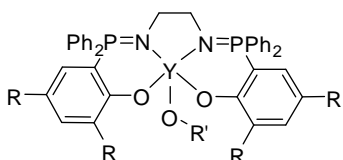
Chapter 4



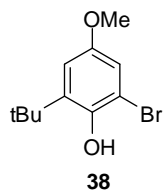
Chapter 5



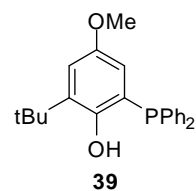
41: R = Et
42: R = tBu



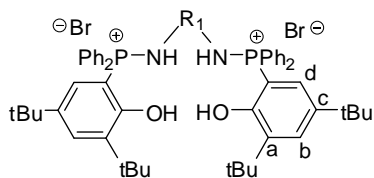
43: R=H, R'=Et
44: R=H, R'=t-Bu
45: R=t-Bu, R'=t-Bu



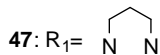
38



39

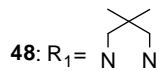


35b: R₁ = (*rac*)-

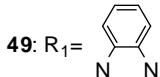


47: R₁ =

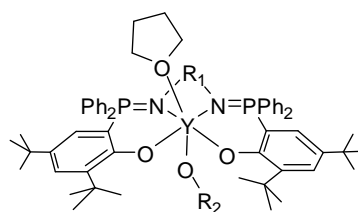
46: R₁ = (*R,R*)-



48: R₁ =



49: R₁ =



51: R₁ = (*rac*)- R₂ = *t*-Bu

54a: R₁ = N N R₂ = *t*-Bu

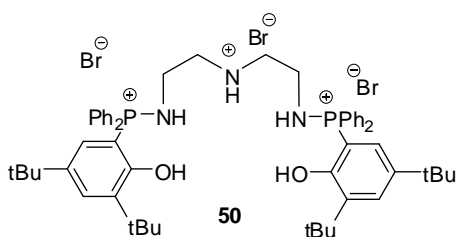
52: R₁ = (*R,R*)- R₂ = *t*-Bu

54b: R₁ = N N R₂ = Et

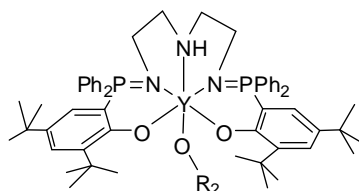
53a: R₁ = N N R₂ = *t*-Bu

55: R₁ = N N R₂ = *t*-Bu

53b: R₁ = N N R₂ = Et

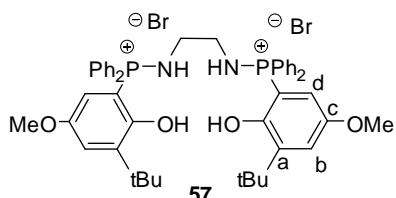


50

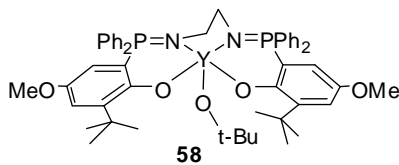


56a: R₂ = *t*-Bu

56b: R₂ = Et



57



58

Table of Contents

Introduction. The Iminophosphoranes	-1-
I. Introduction to Iminophosphorane	-1-
1. Synthesis	-2-
Staudinger Reaction	-2-
Kirsanov Reaction.....	-2-
Aza-Mitsunobu Reaction	-3-
2. Structural Data and Electronic Properties: DFT Calculations	-4-
3. Reactivities.....	-7-
Basicity	-7-
Aza-Wittig Reaction	-8-
Hydrolysis	-10-
Alkylation	-10-
Insertion	-11-
4. Applications in Coordination Chemistry: Overview.....	-11-
II. Objectives	-14-
REFERENCES.....	-15-

Chapter 1. Sulfur Containing Iminophosphoranes	-18-
I. Sulfur-Containing Ligands in Coordination Chemistry	-18-
II. Bidentate PN-S Ligands by an Ortho-Lithiation Reaction	-21-
1. Bidentate PN-S Ligand Synthesis by Ortho-Lithiation Reaction.....	-21-
2. Reactivities and Coordination Test of Thiolate-Iminophosphorane Ligand.	-23-
2.1 Basicity of the P=N Function.....	-23-
2.2 Coordination Test.....	-25-
III. Synthesis of PN-S Ligand by a Substitution Reaction	-26-
1. Ligand Synthesis	-26-
2. Synthesis of Mixed Ligand Containing Iminophosphorane and other Heteroatoms-Based Groups by Substitution Reactions.....	-28-
3. Coordination Chemistry of Thiolate-Iminophosphorane Ligand 5	-30-
3.1 Coordination of PN-S Ligand with Group VIII-Metal Centre: Ru(II).....	-30-

3.2 Coordination of PN-S Ligand with Group IX-Metal Centres: Co(II), Rh(I), Ir(I) ..	-30-
3.3 Coordination of PN-S Ligand with Group X-Metal Centres: Pd(II) and Ni(II)	-32-
IV. Conclusion	-36-
REFERENCES	-38-

Chapter 2. Iminophosphorane-Phenoxide Bidentate Ligands & Applications in Oligomerisation of Ethylene.....-41-

I. Introduction	-41-
1. Oligomerisation of Ethylene	-41-
2. Nickel Catalysts for Dimerisation of Ethylene.	-42-
2.1 Mechanism of the Oligomerisation and Polymerisation of Ethylene using Ni Complexes	-43-
2.2 Catalysts	-44-
Indenyl Nickel Complexes	-44-
Nickel Complexes of Tridentate Ligands	-45-
Nickel Complexes of Bidentate Ligands (N,N), (N,P), (P,P)	-45-
Nickel Complexes of (N,O) or (P,O) Chelating Ligands	-48-
Nickel Complexes of Iminophosphoranes	-49-
II. Synthesis and Activities of Ni-PO Complexes	-50-
1. Ligand Synthesis	-50-
2. Complexes Synthesis	-52-
3. Catalytic Activities	-57-
III. Conclusion	-59-
REFERENCES	-61-

Chapter 3. Phosphasalen Ligand: Synthesis, Coordination and Properties....-64-

I. Introduction to Salen Ligands	-64-
1. Synthesis, Coordination and Application of Salens	-64-
2. Configuration of Salen Complexes and Importance of <i>cis</i> -Complexes	-69-
2.1 Configurations and Conformations for Salen Complexes	-69-
2.2 <i>Cis</i> -Complex and Catalytic Activity.	-70-
II. Phosphasalen Ligand: Synthesis, Coordination and Properties	-74-
1. Phosphasalen Synthesis	-74-
2. Coordination with Group 10 Metals and Studies of the Ligand Properties	-76-

2.1 Complexes Synthesis and Characterisations	-76-
2.2 Electrochemical Studies on Nickel and Palladium Complexes.	-79-
2.2.1. Electrochemistry of Nickel and Palladium Salen Complexes.....	-79-
2.2.2 Electrochemistry of Iminophosphoranes.....	-80-
2.2.3 Electrochemical Study of the Ni- and Pd-Phosphasalen Complexes	-81-
2.2.4 Magnetic Properties of Nickel phosphasalen Complex and Theoretical Studies-83-	
Orbital Analysis for Singlet and Triplet States	-85-
III. Conclusion	-89-
REFERENCES.....	-91-

Chapter 4. Oxidised Ni(II) Phosphasalen Complexes -96-

I. Introduction	-96-
1. Phenoxy Radical Complexes	-96-
2. Mixed-Valence Compounds and Oxidized Nickel Salen Complexes.....	-98-
3. Nickel (III) Complexes	-102-
II. Results	-105-
1. Methods for Substituted Phosphasalen Ligand Synthesis.....	-105-
2. Neutral Complex Synthesis and Characterisation.....	-107-
2.1 Neutral Complexes Synthesis	-107-
2.2. Electrochemistry of Nickel Complexes.	-110-
3. Oxidised Complexes Synthesis and Characterisation	-112-
4. EPR and Magnetic Studies of the Complex [37a][SbF ₆]	-115-
5. DFT Studies of the Complex [37a][SbF ₆]	-116-
III. Conclusion	-120-
REFERENCES.....	-121-

Chapter 5. Phosphasalen Complexes in Ring-Opening Polymerisation of Lactide..

.....	-124-
I. Introduction: PLA and ROP of Lactide	-124-
1. PLA: Utility and Synthesis	-124-
2. Controlled Polymerisation: Meaningful Indicators.....	-125-
2.1 PDI and Molar Mass Distribution.....	-125-
2.2 Stereochemistry of Polymer and Tacticities	-126-
2.2.1 Introduction to Tacticity.....	-126-

2.2.2 Statistic of Polymerisation and Bernoulli Trials	-129-
3. Mechanism of Ring-Opening Polymerisation of Lactide	-131-
4. Initiators for ROP of Lactide	-133-
4.1. Aluminium Complexes	-134-
4.2. Yttrium Complexes	-135-
II. Aluminium-Phosphasalen Complexes	-137-
1. Synthesis	-137-
2. Catalytic Activites in ROP of Lactide.....	-140-
III. Yttrium Phosphasalen Complexes: First Study	-141-
1. Synthesis	-141-
2. Catalytic Activities and Kinetics Studies.....	-146-
2.1 Overall.....	-146-
2.2 Catalytic Activities and Kinetics Studies: Dimeric Complexes.....	-147-
2.2.1 Complex 43	-147-
2.2.2 Complex 44	-150-
2.3 Catalytic Activities and Kinetics Studies: Monomeric Complex.....	-153-
2.3.1 General.....	-153-
2.3.2 NMR Studies of the Addition of <i>iso</i> -Propanol on Complex 45	-156-
2.4 Stereoselectivity of the Polymerisations	-159-
3. Discussion	-160-
3.1 Generalities	-160-
3.2 Comparisons with Other Yttrium Complexes.....	-162-
4. DFT calculations.....	-164-
4.1. Initiation step	-165-
2. Propagation step.....	-168-
IV. Monomeric yttrium complexes: factors influencing the activity	-169-
1. New yttrium phosphasalen complexes.....	-169-
1.1 New complexes with modified steric properties.....	-169-
1.2 New complexes with modified electronic properties.....	-175-
2. Activities	-177-
3. Conclusion	-180-
REFERENCES.....	-182-
 Conclusion	 -186-

Experimental Section	-189-
I. Chapter 1.....	-189-
II. Chapter 2.....	-197-
III. Chapter 3.....	-202-
IV. Chapter 4.....	-206-
V. Chapter 5.....	-213-
REFERENCES	-229-

Appendix 1. Crystallographic Data	-230-
Chapter 1.....	-231-
Chapter 2.....	-272-
Chapter 3.....	-292-
Chapter 4.....	-311-
Chapter 5.....	-340-

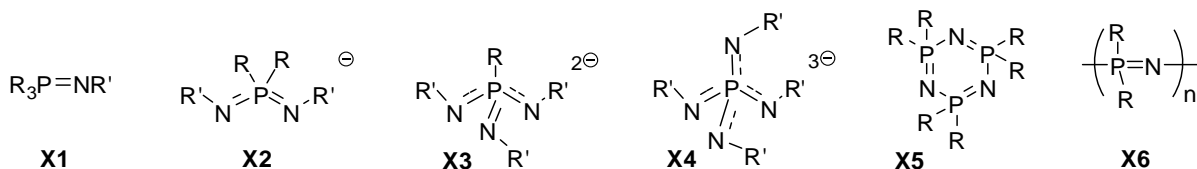
Appendix 2. Optimised Structures by DFT	-436-
Chapter 1.....	-437-
Chapter 3.....	-442-
Chapter 4.....	-448-
Chapter 5.....	-458-

Introduction

The Iminophosphoranes

I . Introduction to Iminophosphorane

The class of iminophosphoranes, compounds with formal P-N double bonds, is a well established, yet still not thoroughly explored class of compounds in coordination chemistry and synthesis. The first iminophosphoranes were synthesized by Staudinger and Meyer in 1919,¹ they exist under various nomenclatures: iminophosphorane, phosphazene, phosphinimine. Successive replacement of R group at the phosphorus atom in simple neutral iminophosphoranes **X1** (Scheme 1) leads to monoanionic diiminophosphinate **X2**, dianionic triiminophosphonate **X3** and trianionic tetraiminophosphate **X4**.² These compounds could also exist in polymeric or cyclic forms (**X5** and **X6** respectively). Cyclic and polymeric forms of neutral iminophosphorane are commonly called cyclophosphazene and polyphosphazene. They are interesting agents in biochemistry, especially in drug design and drug delivery,³ as their metabolisms yield only ammonium and phosphate, ions already largely involved in the cellular functioning.



Scheme 1. Different forms of iminophosphorane compounds

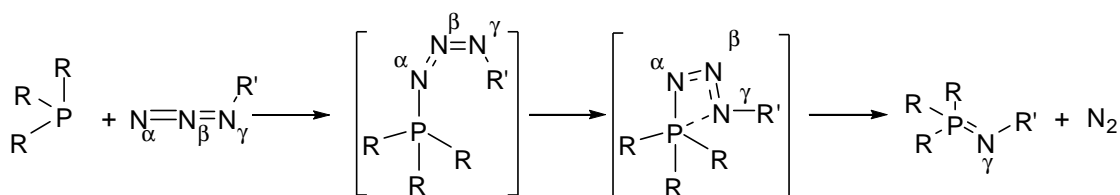
The work presented here focuses on simple neutral iminophosphoranes of the form **X1**.

1. Synthesis

Whereas a great number of synthetic approaches exist for the preparation of iminophosphoranes, only the three most used methods are presented here, which are the Staudinger reaction (first reported in 1919), the Kirsanov reactions (discovered in 1950), which was modified by Horner and Oediger in 1959, and more recently, the aza-Mitsunobu reaction.

Staudinger Reaction

The Staudinger reaction, discovered in 1919,¹ is the oldest synthetic approach to iminophosphoranes, yet it is still by far the most commonly used method.⁴ The reaction involves an nucleophilic addition of an azide $R'N_3$ to a P^{III} centre (e.g. a phosphine R_3P), followed by nitrogen elimination (Scheme 2). The Staudinger mechanism has been studied by DFT calculations by the group of Wang.⁵ Experimentally, since 1968, by the use of ^{15}N , Bock and coworkers have identified that the nitrogen in the iminophosphorane function is indeed the N^γ atom. The phosphazide intermediate was also isolated in some case by using factors inhibiting the formation of the four-membered ring, such as steric effects (bulky substituents on phosphorus or nitrogen atoms),⁶ or electronic effect (increasing electron density on the phosphorus atom and decreasing the one on the N^γ atom).⁷ A review about stabilized phosphazide intermediates was published by Bourissou and coworkers in 2009.⁸

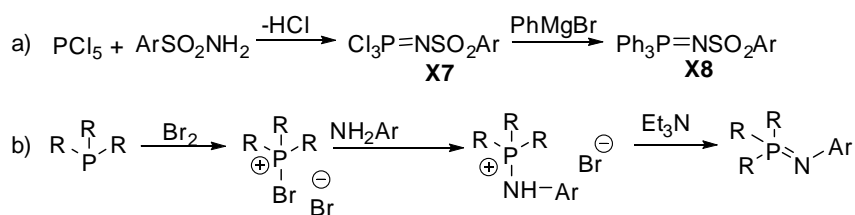


Scheme 2. Staudinger reaction

The advantages of the Staudinger method may in part be ascribed to the fact that during this reaction, nitrogen (N_2) is released as the only side product, thus rendering unnecessary further purification of the iminophosphorane product. Furthermore, the reaction could be applied to a wide range of P^{III} centres containing different types of substituents. However, the major inconvenience of this method is the risk of explosion associated with most azide derivatives. This is a major drawback to the variation of the nitrogen substituent R' , as well as for large-scale synthesis.

Kirsanov Reaction

The Kirsanov method for the synthesis of iminophosphoranes originated from a reaction discovered by Kirsanov in 1950 (Scheme 3a).⁹ Reaction of PCl_5 with phenylsulfonamide resulted in the formation of compound **X7** by nucleophilic substitution on two chlorides. This compound **X7** in turn was transformed into P,P,P-triphenyl iminophosphorane **X8** by nucleophilic substitution of the three remaining chlorides with phenyl magnesium bromide.



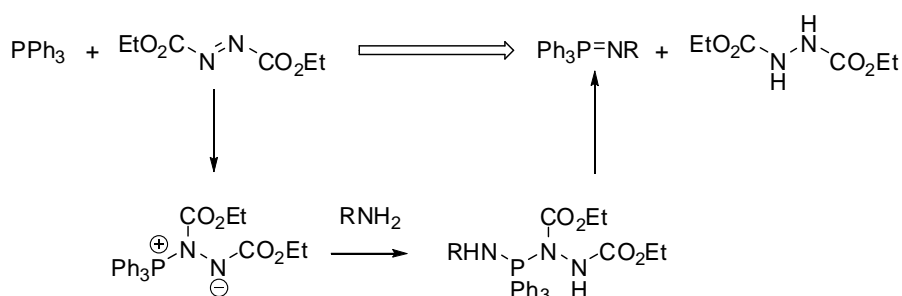
Scheme 3. Kirsanov reaction (a) and Horner/Oedinger variation (b).

In 1959, Horner and Oedinger developed the modern version of the Kirsanov reaction by using in situ generated PR_3Br_2 compounds, obtained from the bromination of a tertiary phosphine, instead of PCl_5 (Scheme 3b).¹⁰ The bromination product underwent a nucleophilic substitution with aromatic amine in the presence of two equiv. of triethylamine, to give the corresponding iminophosphoranes in high yields.

Several years later, Zimmer and Singh applied this method to alkylamines and found that the reaction got stuck at the formation of the aminophosphonium bromide salt $[\text{R}_3\text{PNHR}']^+[\text{Br}]^-$.¹¹ Likely, triethylamine is not strong enough to deprotonate these salts. A second step, employing stronger bases such as MeLi, KHMDS is required to generate the corresponding iminophosphoranes. This necessity of a second step is not a drawback, but quite the opposite: aminophosphonium salts, as opposed to their iminophosphorane analogues, are air- and water stable, and thus easy to manipulate and in most cases easy to isolate from the reaction mixture. They can be prepared in big quantities.

Another advantage of this method over the Staudinger reaction is the variability brought to the nitrogen residue R' , as virtually any primary amine may be employed in this reaction. This opens the route towards a great variety of derivatives, including chiral iminophosphoranes, which is important notably for catalysis. Furthermore, the scope of applications of this reaction does not involve solely amines (aromatic and aliphatic), but also hydrazines (H_2NNXY),¹² hydrazones ($\text{H}_2\text{NN}=\text{CXY}$),¹³ hydrazide (RC(O)-NHNH_2),¹⁴ etc.

Aza-Mitsunobu Reaction



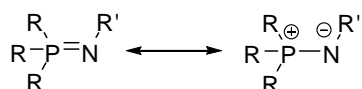
Scheme 4. Aza-Mitsunobu reaction

The aza-Mitsunobu method for the synthesis of iminophosphorane was developed in the 1970s. It is based on the reaction of triphenylphosphine with diethylazodicarboxylate (DEAD) and a primary amine $\text{R}'\text{NH}_2$ (Scheme 4). Even though this one-pot reaction proceeds with excellent

yields, its scope is limited to amines with electron withdrawing groups, with a proton sufficiently acidic to allow its abstraction by the azodicarboxylate.

2. Structural Data and Electronic Properties: DFT Calculations

Two electronic configurations are conceivable for an iminophosphorane: a compound with double bond P-N or a zwitterion.



Scheme 5. Two descriptions of an iminophosphorane

Based on literature data, the bond length of an iminophosphorane in the solid state is comprised between 1.54 Å and 1.64 Å. Taking into account the fact that the sum of the covalent radii of nitrogen and phosphorus is 1.84 Å for a single bond and 1.62 Å for a double bond,¹⁵ these two limiting values indicate that structurally, the P-N bond in iminophosphoranes is closer to a double bond.

According to the Valence Shell Electron Pair Repulsion (VSEPR), the angle P-N-R in iminophosphorane would be around 109° if the P-N bond is single bond (in zwitterionic structure), and around 120° if it is a double bond. Experimentally, this angle is measured between 119° and 143°. Thus, this observation also points towards a double bond P-N in iminophosphorane.

However, the hypothesis of the double bond P-N is inconsistent with calculated energy required for the free rotation around the P-N bond, which is very low (2.1 kcal/mol). Theoretical studies have been carried out in order to understand the electronic nature of this P-N bond.¹⁶ Another study was done by NBO (natural bonding orbital) calculations¹⁷ on model compound PH₃NH, using density functional theory (DFT) with b3lyp functional and 6-31G* basis set for all atoms. Calculations for model compound of imines were also carried out for the sake of comparisons.

	qP +1.07	qC -0.10
	$\begin{array}{c} H \\ \diagdown \\ H-P=N \\ \diagup \\ H \end{array}$	$\begin{array}{c} H \\ \diagdown \\ H-C=N \\ \diagup \\ H \end{array}$
	qN -1.32	qN -0.63
Wiberg index	1.34	2.03
π orbital occupancy	1.76	1.99

q_X: NBO charge at atom X

Scheme 6. NBO analysis for model compounds of iminophosphorane and imine

In fact, NBO analysis tends to neglect the delocalisation of the systems and tries to localise the electrons in 1-centre and 2-centre regions of the molecules. Thus, NBO analysis gives a vision

very close to the Lewis model. The results obtained for the model compounds were in favour of a single bond P-N in iminophosphorane. Whereas the Wiberg index of the imine model is 2.03, indicative of a double bond, the one for the iminophosphorane model is close to 1 (1.34 vs 2.03 in imine). Furthermore, the charges at N and P atoms fit perfectly to the dipolar description of the P-N bond. Thus according to these results, for iminophosphoranes, the zwitterionic form seems to be more suitable than a double bond model.

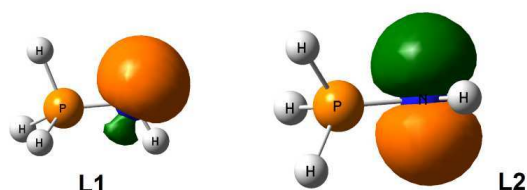


Figure 1. Two lone pairs on Nitrogen atom

According to the zwitterionic form, two lone pairs of electron should be present on nitrogen. Indeed, the NBO analysis supports the existence of these two free electron pairs, which are of highest energies among the occupied orbitals in the molecule (Figure 1). The first one is a hybrid sp^x (47%*s*, 53%*p*, occupancy 1.88) and the second one a pure *p* orbital (occupancy 1.75). These values of occupancies less than 2 imply a certain degree of delocalisation of electrons on to other atoms. Indeed, as would be seen later, the electron delocalisation from these two orbitals to the unoccupied $\sigma^*(P-H)$ and Rydberg *d*-orbitals of the phosphorus atom is significant. It is responsible for the negative hyper-conjugation which reinforces the P-N bond, hence the shortening of the P-N bond (Figure 2 and 3) .

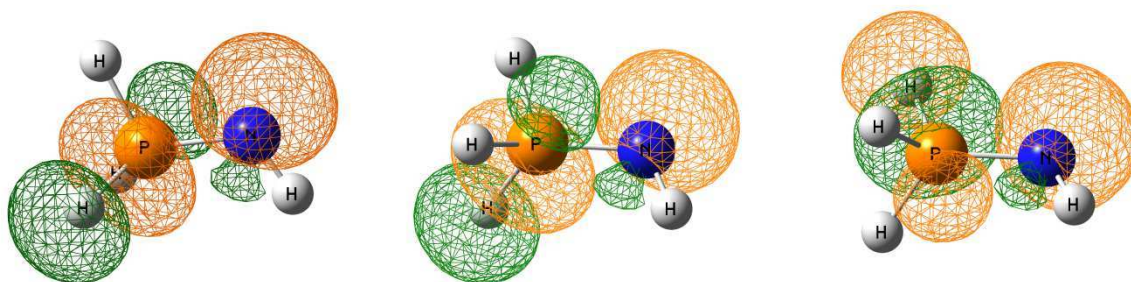


Figure 2. Stabilising interactions between the first lone pair L1 of nitrogen and three $\sigma^(P-H)$. Stabilisation energy ~17.3 kcal/mol*

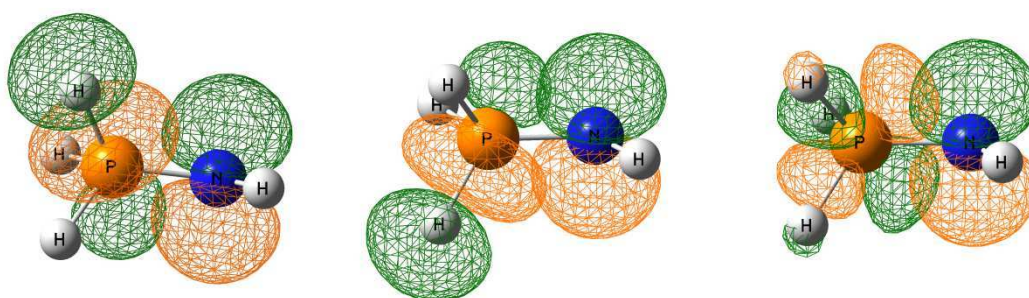


Figure 3. Stabilising interactions between the second lone pair **L2** of nitrogen and two $\sigma^*(\text{P-H})$ (~ 16.5 kcal/mol each), and d -orbital of the phosphorus atom (~ 9.0 kcal).

Both lone pairs L1 and L2 participate in π -interactions with $\sigma^*(\text{P-H})$ orbitals or Rydberg orbitals on P of appropriate symmetry. As these orbitals are of higher energy, these interactions are stabilising for L1 and L2. In total, such hyper-conjugations bring stabilisation energy of approximately 18 kcal/mol to L1 and 45 kcal/mol to L2.

The real molecular orbitals are obviously different from these natural orbitals described above. But the difference is not huge: the corresponding Kohn-Sham orbitals from DFT calculations on the model compound of iminophosphorane are presented in Figure 4. They sensibly have the same forms as L1 and L2. Just as L1 and L2, they are the two highest occupied orbitals of the molecule and their relative energies do not change.

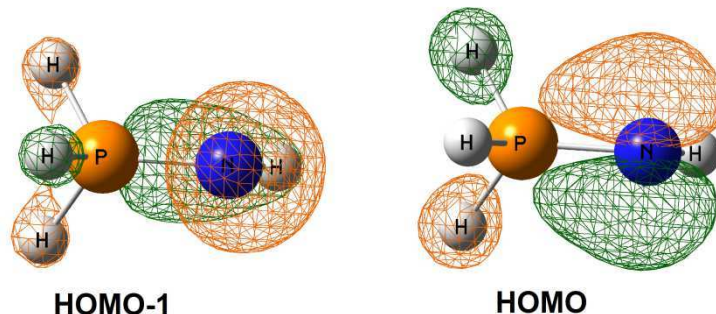


Figure 4. HOMO and HOMO-1 in the real DFT description.

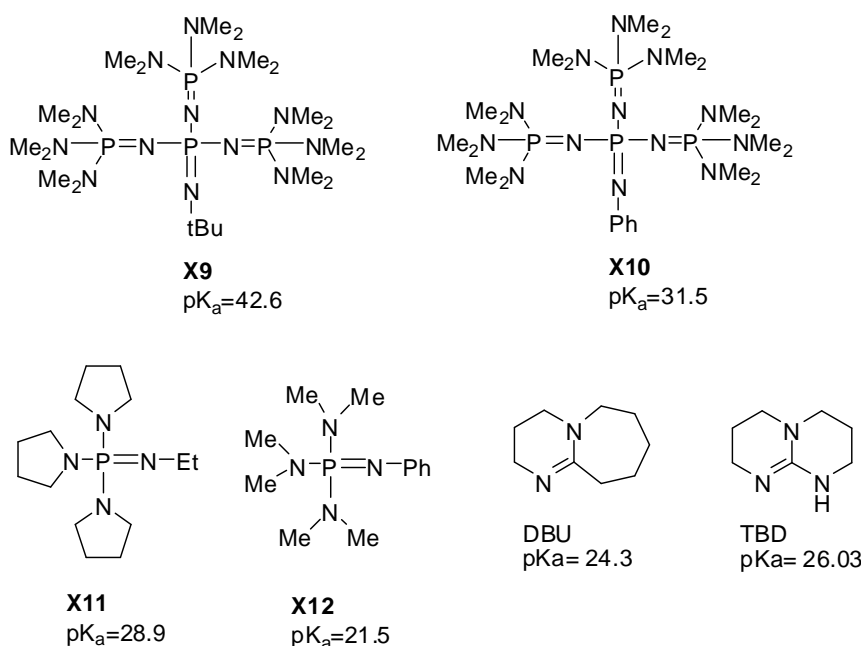
Thus from the calculational analysis, it is clear that the P-N bond in iminophosphorane is in reality a single bond, reinforced with negative hyper-conjugations from the lone pairs of the nitrogen onto other orbitals on the phosphorus atoms. The zwitterionic form correctly represents the nature of the bond, as well as the charge at P and N atoms, but could not describe these hyper-conjugations which are responsible for the strong bond P-N (hence the shortening of P-N bond, for example). The official representation $\text{P}=\text{N}$ double bond, even though less correct, is adopted for the sake of simplicity and the coherence with the literature.

3. Reactivities

The reactivities of iminophosphoranes revolve around the positive charge on the phosphorus atom and the negative charge on the nitrogen atom. They could be seen as to resemble a lot to those of phosphorus ylides and amides.

Basicity

Thanks to the important negative charge at nitrogen, iminophosphoranes behave as strong bases. The first representative of iminophosphorane bases was prepared in the 1970s by Lischewski and co-workers.¹⁸ In 1987, Schwesinger and co-workers synthesised the iminophosphorane **X9**, which is the strongest neutral base that has been developed to date. Since then, the design of superbases from iminophosphoranes has been thoroughly studied, especially by the Koppel group, both theoretically and experimentally.¹⁹ The basicity of the iminophosphoranes increases with the donating ability of substituents. On going from simple iminophosphoranes, to amino-, and then phosphazo-substituted iminophosphoranes, significant enhancements in basicity have been observed. By careful selection of substituents, various iminophosphorane-containing superbases have been prepared, which are among the strongest ever to exist. Fine tuning of basicity on these systems is also possible. Indeed, bases of pK_a ranging from 10 to 42 (in acetonitrile) have been obtained.^{19b, 20} Examples of these systems are presented in Scheme 7, along with several other bases for comparison.

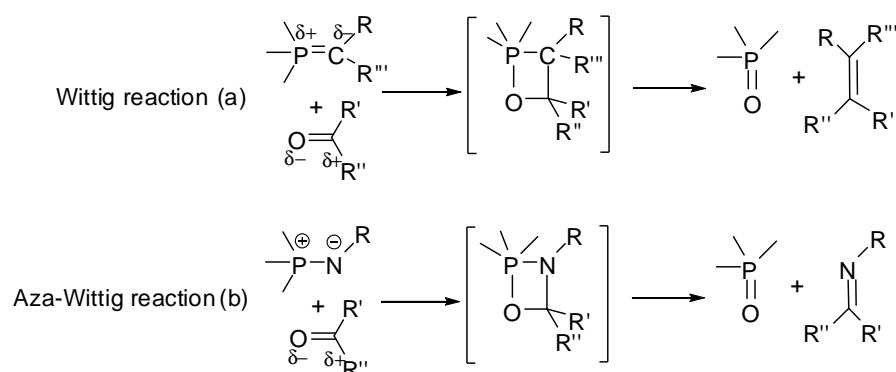


Scheme 7. Examples of iminophosphorane bases and some common non-iminophosphorane bases.

These bases present various advantages for utilities in organic chemistry. Firstly, thanks to their common bulkiness, their nucleophilicity is greatly reduced. Thus, they could give excellent

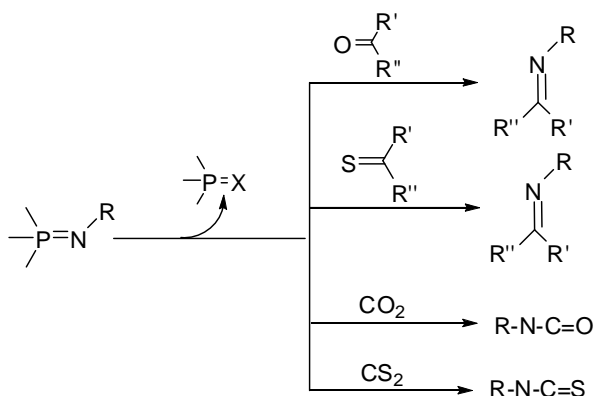
selectivity in reactions requiring activation by basicity, but not nucleophilicity (e.g. enolate and peptide alkylations, catalytic aldol reactions, desilylations, and even aromatic and alkynyl deprotonations). Secondly, as they act without metallic cations and due to their bulkiness, the anions obtained from the deprotonation by these bases are often “naked”, and thus highly reactive. Thirdly, as they are generally soluble in organic solvents and exist in solid form at room temperature, their handling is generally easy.

Aza-Wittig Reaction



Scheme 8. Wittig and Aza-Wittig reaction

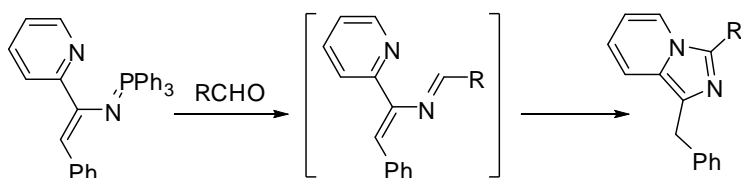
The Aza-Wittig reaction is the most common applications of iminophosphoranes, as has been evidenced by many reviews from different groups.²¹ First discovered by Staudinger in 1921 (two years after he synthesised the first iminophosphorane), the reaction is an analogue of Wittig reaction, applied for phosphorus ylides.²² When an iminophosphorane reacts with a carbonyl or thiocarbonyl, an imine is formed along with the elimination of one phosphinoyl molecule. The mechanism of the reaction is supposed to be similar to the one of the Wittig reaction. Several theoretical studies have been carried out, confirming this hypothesis.²³ In some cases, intermediates were also isolated.²⁴



Scheme 9. Aza-Wittig reaction

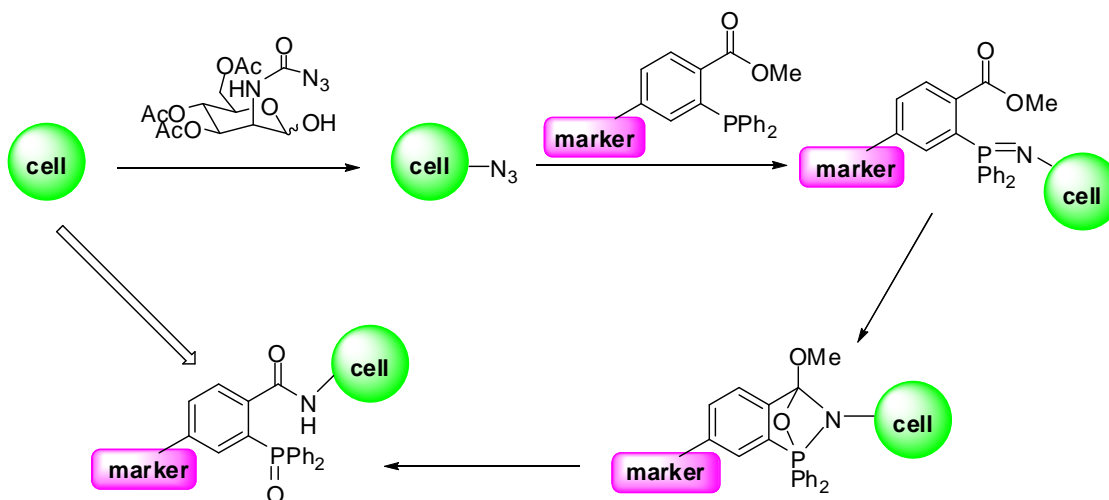
The reaction is not limited only to carbonyl or thiocarbonyl, but could be applied to isocyanates ($R'N=C=O$), or thiocyanates ($R'N=C=S$), giving hetero-disubstituted carbodiimides ($R-N=C=N-R'$). On the other hand, using CO_2 and CS_2 allows the synthesis of isocyanates and thiocyanates.

The Aza-Wittig reaction is often used for the synthesis of heterocycles in organic chemistry. This application has been the subject of various reviews in the literature.²⁵ An example of one of those syntheses is presented in Scheme 10.



Scheme 10. Example of Aza-Wittig reaction in heterocycles synthesis.²⁶

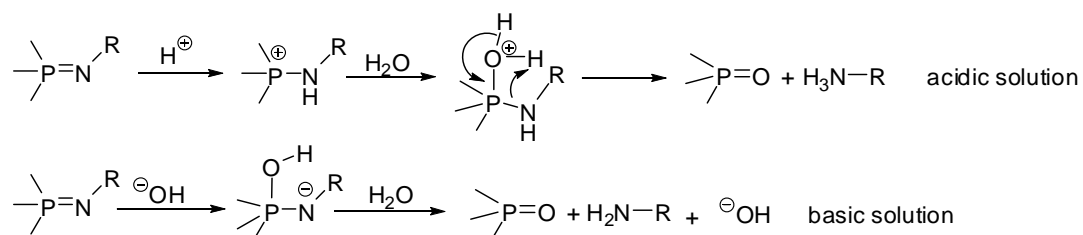
This reaction could be coupled to a Staudinger reaction, and the total process is called a Staudinger ligation.²⁷ The advantage of such process lies in the highly selectivity of the reactions and the absence of water in the final mixture, which is helpful in some cases. The reaction is mostly used in biochemistry for the grafting of phosphorus-containing marker to the glycoside on the cellular surface. The phosphine, bearing the marker, and the azide, grafted on to the cell's surface, react quickly and selectively in aqueous environment to give iminophosphorane. This latter is however not stable in water, but is trapped quickly by an intramolecular Aza-Wittig reaction with an ester in close proximity to give a stable amide. The marker is thus linked to the cell's surface by this amide bond.



Scheme 11. Staudinger ligation in cell surface engineering.

Hydrolysis

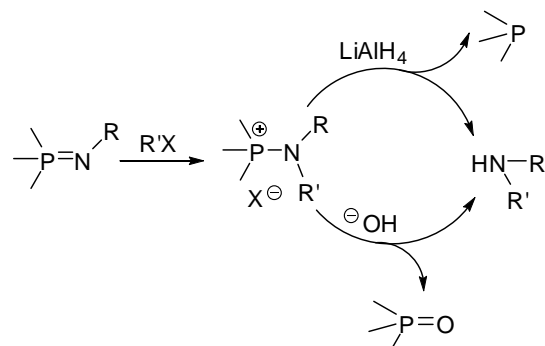
Because of the zwitterionic structure, iminophosphoranes are generally decomposed by water. This involves either the attack of proton on the negatively charged nitrogen, or the nucleophilic attack of hydroxide on the positively charged phosphorus, depending on the pH. This decomposition explains the instability of iminophosphoranes in water and the facile hydrolysis of alkyliminophosphoranes (with better basicity) in air.



Scheme 12. Hydrolysis of iminophosphorane.

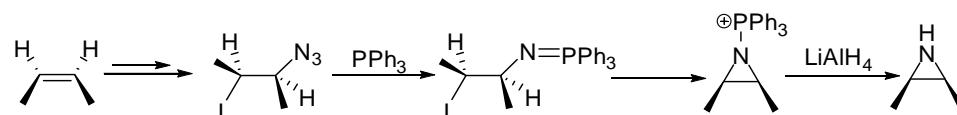
Alkylation

The negatively charged nitrogen could be alkylated by nucleophilic substitution with alkylhalide. The resulting phosphonium salt could be converted into secondary amine by hydrolyse (with hydroxide, for example) or by reduction with LiAlH_4 .



Scheme 13. Alkylation of iminophosphorane

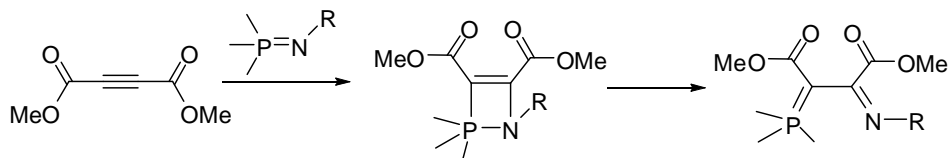
This reaction has been exploited by Hassner and co-workers since 1970 for the synthesis of arizidines.²⁸



Scheme 14. Synthesis of arizidines by alkylation of iminophosphorane.

Insertion

Iminophosphoranes could insert into triple bonds, a mechanism which closely resembles to the Aza-Wittig reaction. A four-membered intermediate is obtained directly from the insertion. The ring-opening of this intermediate gives compounds containing imine and phosphorus ylide functions in the α position.



Scheme 15. Insertion of iminophosphorane into alkynes.

4. Applications in Coordination Chemistry: Overview

The NBO analysis on model compound of iminophosphorane clearly shows the presence of two lone pairs on the nitrogen atom, which are the HOMO and HOMO-1 orbitals, and the absence of a real π -system. The ability of iminophosphorane to coordinate to metal centres lies in these two lone pairs. In fact, iminophosphoranes act as strong σ and π donors (thanks to the HOMO-1 and HOMO respectively), and does not have π -accepting ability. These ligands thus preferably coordinate to “hard” metal centres, as “soft” centres are more stabilised by π -interaction from metal to ligand.

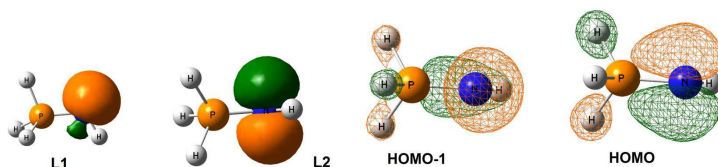
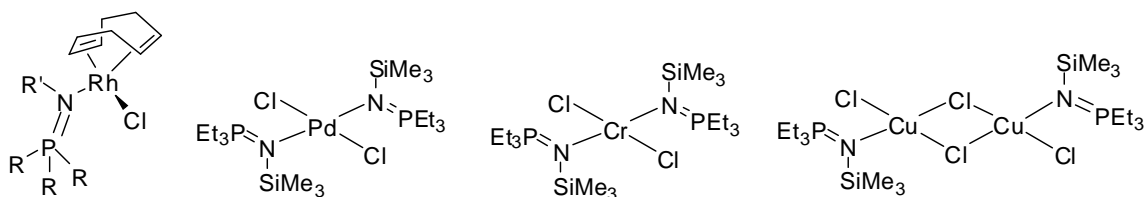


Figure 5. Two lone pairs at the nitrogen atom (NBO analysis) and their respective form (Kohn-Sham orbitals) in real system.

A simple search in the CCDC database shows that in complexes the angle P-N-M has a median value of 115° , and centred around 120° , and the values for P-N-R angle have a median of 122° and centred around 120° . In almost all complexes, the nitrogen atom is in the same plane as R, P, and M. These data clearly indicate that coordination is done by the HOMO-1, and involves the σ -donation from the ligand to the metal.

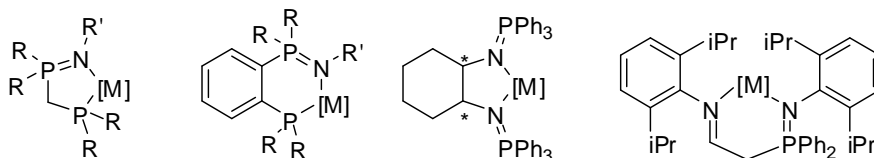
Complexes of simple iminophosphoranes are known, with metals such as magnesium,²⁹ copper, zinc, chromium(II), palladium or rhodium, etc.³⁰ It is however worth reminding that because of the lack of π -accepting ability, the coordination of iminophosphoranes with “soft” metal centres are not very strong. The coordinated iminophosphoranes are easily exchanged with other ligands. For example, the rhodium complexes $[\text{RhL}_2\text{Cl}(\text{R}'\text{N}=\text{PR}_3)]$ ($\text{L}_2 = \text{COD}$) exist in

equilibrium with the parent compounds $[\text{RhL}_2\text{Cl}]_2$ and $\text{R}'\text{N}=\text{PR}_3$, this equilibrium being dependent on substituents on N and P, temperature, and the ratio $\text{Rh}/\text{R}'\text{N}=\text{PR}_3$.



Scheme 16. Examples for complexes of simple iminophosphorane ligands.

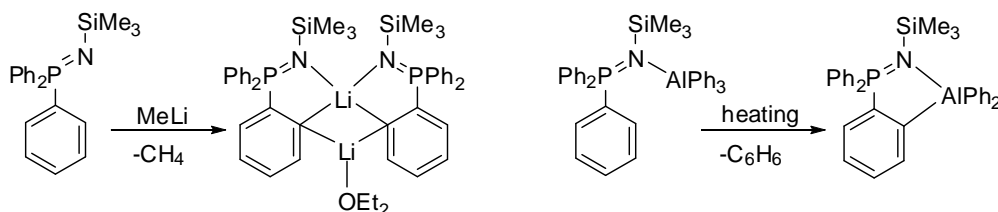
In order to circumvent this limitation, iminophosphoranes are often combined with other donors to obtain multidentate ligands, very often hetero-multidentate ligands. These ligands offer a much larger scope of coordination and could give more stable complexes. Scheme 17 shows examples of such systems: phosphino-iminophosphoranes reported by Cavell and co-workers,³¹ chiral bis-iminophosphoranes elaborated by Reetz and co-workers,³² imine-iminophosphorane ligand by Stephan and coworkers³³.



Scheme 17. Examples of multidentate ligands containing iminophosphorane group(s).

Among the most interesting ligands based on iminophosphorane function are those containing carbanions. In fact, the particular dipolar structure of iminophosphorane allows the stabilisation of carbanions in close proximity by different effects.

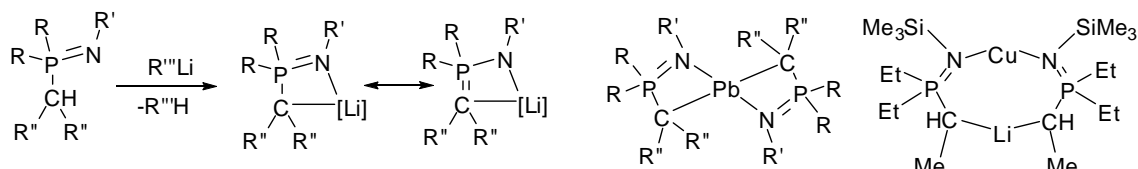
Firstly, the iminophosphorane function could direct the ortho-deprotonation reaction and stabilise the product. Many complexes of this family have been elaborated, either from the reaction of metal precursors with an iminophosphorane-carbanion ligand (such as the lithium compounds in Scheme 18),³⁴ or from the intramolecular ortho-deprotonation of an already-existed metal-iminophosphorane complex (second reaction, Scheme 18).³⁵



Scheme 18. Ortho-deprotonation reactions

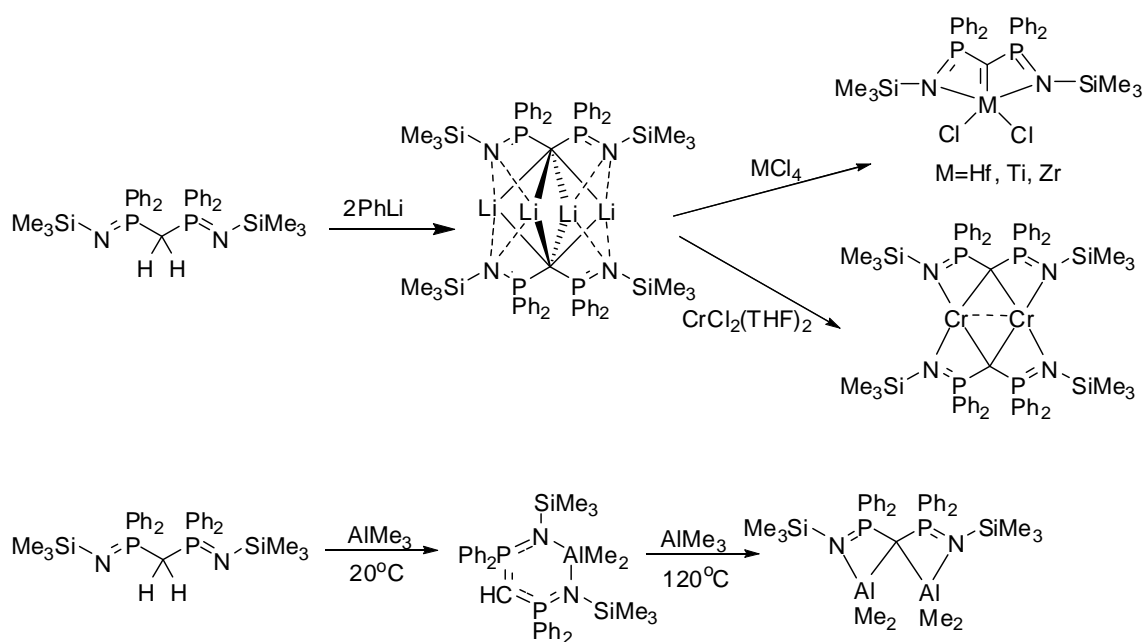
Secondly, the important positive charge at the phosphorus atom opens the possibility of functionalising α C-H bond by deprotonation reaction. Indeed, monoanions and geminal

dianions of P-alkyl iminophosphorane have been the subjects pursued by many groups. By reacting with organolithiums, P-alkyl iminophosphanes are deprotonated at the α positions, yielding lithium complexes in which the lithium centres are chelated in a bidentate fashion by C and N centres.³⁶ The negative charge on the ligand is delocalised on both C and N atoms, due to resonance structures (Scheme 19).



Scheme 19. Monocarbanion from iminophosphorane and several complexes.

These lithium complexes exist in oligomeric form, the extent of which depends on steric bulk of the ligand(s) and the nature of coordinating solvent (Et_2O , THF, etc.) By reacting with metal precursors, they give iminophosphorane complexes of the corresponding metals. Several complexes of the iminophosphorane- monocarbanion ligands with metals other than lithium are presented on Scheme 19.



Scheme 20. Examples for the synthesis of complexes of bis(iminophosphorane)methandiide ligand.

Of particular interests are geminal dianions generated from the bis(iminophosphorane)methane and derivatives (e.g. $\text{H}_2\text{C}(\text{Ph}_2\text{P}=\text{NSiMe}_3)_2$). In fact, both methylene protons of these compounds are sufficiently acidic to be displaced directly by organolithium. In 1999, the Stephan³⁷ and Cavell³⁸ groups independently reported the first dilithio-methandiide complex by deprotonation of $\text{H}_2\text{C}(\text{Ph}_2\text{P}=\text{NSiMe}_3)_2$ with two equiv. of PhLi or with excess of MeLi (Scheme 20).

Complexes of the corresponding ligands can be generated either by direct reaction of such dianions with metal precursors, or by reaction of the corresponding monoanion with alkyl or amide metal precursors (to yield intramolecular deprotonation) (Scheme 20). The interest of such ligands lie in the various possible coordination modes, the formation of clusters, and in particular the formation of carbene complexes. Various reviews have been dedicated to the chemistry of these species.^{36c, 39a, 2, 39b, c}

II. Objectives

The objective of the work is to develop new iminophosphorane-based systems and to evaluate their applications in coordination chemistry and catalysis. They involve thus three important tasks 1) Organic synthesis of targeted ligands; 2) Coordination chemistry of such ligands and studies on properties/activities of the corresponding complexes; 3) Studies of the complexes in catalysis.

We are interested in developing new ligands combining iminophosphorane with an anionic coordinating group, which has been chosen to be thiolate or phenoxide. The synthesis of such ligands is targeted to be simple, easy to scale-up and based on inexpensive, commercially available starting materials.

Once synthesised, the ligands would be studied in coordination chemistry with different metal centres. Studies of such complexes sometimes leads to modifying existing ligands and re-synthesising the desired complexes. Theoretical studies are carried out in some cases in order to better understand the electronic properties of the ligand in coordination.

The activities of selected complexes in catalysis are then tested. Just like at the coordination step, study on catalytic activities sometimes leads to the developing of new appropriate ligands for “tuning” of the activity. Also, DFT calculations are used in some cases to clarify some aspects of the catalysis when possible.

REFERENCES

1. Staudinger, H.; Meyer, J., *Helv. Chim. Acta* **1919**, 2 (1), 635-646.
2. Steiner, A.; Zacchini, S.; Richards, P. I., *Coord. Chem. Rev.* **2002**, 227 (2), 193-216.
3. (a) Potin, P.; Dejaeger, R., *Eur. Polym. J.* **1991**, 27 (4-5), 341-348; (b) Laurencin, C. T.; Koh, H. J.; Neenan, T. X.; Allcock, H. R.; Langer, R., *J. Biomed. Mat. Res.* **1987**, 21 (10), 1231-1246; (c) Allcock, H. R.; Morozowich, N. L., *Polym. Chem.* **2012**, 3 (3), 578-590; (d) Morozowich, N. L.; Nichol, J. L.; Mondschein, R. J.; Allcock, H. R., *Polym. Chem.* **2012**, 3 (3), 778-786.
4. (a) Gololobov, Y. G.; Kasukhin, L. F., *Tetrahedron* **1992**, 48 (8), 1353-1406; (b) Gololobov, Y. G.; Zhmurova, I. N.; Kasukhin, L. F., *Tetrahedron* **1981**, 37 (3), 437-472.
5. Tian, W. Q.; Wang, Y. A., *J. Org. Chem.* **2004**, 69 (13), 4299-4308.
6. Alajarín, M.; Molina, P.; López-Lázaro, A.; Foces-Foces, C., *Angew. Chem. -Int. Ed.* **1997**, 36 (1-2), 67-70.
7. Widauer, C.; Grützmacher, H.; Shevchenko, I.; Gramlich, V., *Eur. J. Inorg. Chem.* **1999**, 1999 (10), 1659-1664.
8. Bebbington, M. W. P.; Bourissou, D., *Coord. Chem. Rev.* **2009**, 253 (9-10), 1248-1261.
9. Kirsanov, A. V., *Isv. Akad. Nauk. SSSR* **1950**, 426.
10. Horner, L.; Oediger, H., *Justus Liebigs Annalen der Chemie* **1959**, 627 (1), 142-162.
11. Zimmer, H.; Singh, G., *J. Org. Chem.* **1963**, 28 (2), 483-486.
12. Zimmer, H.; Singh, G., *J. Org. Chem.* **1964**, 29 (6), 1579-1581.
13. Singh, G.; Zimmer, H., *J. Org. Chem.* **1965**, 30 (2), 417-420.
14. Walker, C. C.; Shechter, H., *J. Am. Chem. Soc.* **1968**, 90 (20), 5626-5627.
15. Pauling, L., *Nature of the chemical bond*. 3rd ed.; Cornell University Press: New York, 1960.
16. (a) Boubekur, L. Les iminophosphoranes: synthèse, propriétés en coordination et applications en catalyse. Les iminophosphoranes: synthèse, propriétés en coordination et applications en catalyse, Ecole Polytechnique, 2006; (b) Buchard, A. Chimie de coordination des iminophosphoranes et nouveaux systèmes catalytiques. Ecole Polytechnique, 2009.
17. (a) Foster, J. P.; Weinhold, F., *J. Am. Chem. Soc.* **1980**, 102 (24), 7211-7218; (b) Reed, A. E.; Curtiss, L. A.; Weinhold, F., *Chem. Rev.* **1988**, 88 (6), 899-926.
18. Issleib, K.; Lischewski, M., *Synth. React. Inorg. Met.-Org. Chem.* **1973**, 3 (3), 255-266.

19. (a) Koppel, I. A.; Schwesinger, R.; Breuer, T.; Burk, P.; Herodes, K.; Koppel, I.; Leito, I.; Mishima, M., *J. Phys. Chem. A* **2001**, *105* (41), 9575-9586; (b) Kaljurand, I.; Kütt, A.; Sooväli, L.; Rodima, T.; Mäemets, V.; Leito, I.; Koppel, I. A., *J. Org. Chem.* **2005**, *70* (3), 1019-1028; (c) Kaljurand, I.; Rodima, T.; Pihl, A.; Mäemets, V.; Leito, I.; Koppel, I. A.; Mishima, M., *J. Org. Chem.* **2003**, *68* (26), 9988-9993; (d) Rodima, T.; Kaljurand, I.; Pihl, A.; Mäemets, V.; Leito, I.; Koppel, I. A., *J. Org. Chem.* **2002**, *67* (6), 1873-1881; (e) Rõõm, E.-I.; Kaljurand, I.; Leito, I.; Rodima, T.; Koppel, I. A.; Vlasov, V. M., *J. Org. Chem.* **2003**, *68* (20), 7795-7799; (f) Kolomeitsev, A. A.; Koppel, I. A.; Rodima, T.; Barten, J.; Lork, E.; Röschenthaler, G.-V.; Kaljurand, I.; Kütt, A.; Koppel, I.; Mäemets, V.; Leito, I., *J. Am. Chem. Soc.* **2005**, *127* (50), 17656-17666; (g) Kaljurand, I.; Koppel, I. A.; Kütt, A.; Rõõm, E.-I.; Rodima, T.; Koppel, I.; Mishima, M.; Leito, I., *J. Phys. Chem. A* **2007**, *111* (7), 1245-1250.
20. Schwesinger, R.; Hasenfratz, C.; Schlemper, H.; Walz, L.; Peters, E.-M.; Peters, K.; von Schnering, H. G., *Angew. Chem. -Int. Ed.* **1993**, *32* (9), 1361-1363.
21. (a) Eguchi, S.; Matsushita, Y.; Yamashita, K., *Org. Prep. Proced. Int.* **1992**, *24* (2), 209-&; (b) Molina, P.; Vilaplana, M. J., *Synthesis-Stuttgart* **1994**, 1197-1218; (c) Palacios, F.; Alonso, C.; Aparicio, D.; Rubiales, G.; de los Santos, J. M., *Tetrahedron* **2007**, *63* (3), 523-575.
22. Staudinger, H.; Hauser, E., *Helv. Chim. Acta* **1921**, *4* (1), 861-886.
23. Koketsu, J.; Ninomiya, Y.; Suzuki, Y.; Koga, N., *Inorg. Chem.* **1997**, *36* (4), 694-702.
24. Sasaki, T.; Eguchi, S.; Okano, T., *J. Am. Chem. Soc.* **1983**, *105* (18), 5912-5913.
25. (a) Fresneda, P. M.; Molina, P., *Synlett* **2004**, *2004* (EFirst), 1,17; (b) Takeuchi, H.; Yanagida, S.; Ozaki, T.; Hagiwara, S.; Eguchi, S., *J. Org. Chem.* **1989**, *54* (2), 431-434; (c) Takeuchi, H.; Hagiwara, S.; Eguchi, S., *Tetrahedron* **1989**, *45* (20), 6375-6386.
26. Palacios, F.; Alonso, C.; Rubiales, G., *Tetrahedron* **1995**, *51* (12), 3683-3690.
27. (a) Kohn, M.; Breinbauer, R., *Angew. Chem. Int. Ed* **2004**, *43* (24), 3106-3116; (b) Saxon, E.; Armstrong, J. I.; Bertozzi, C. R., *Org. Lett.* **2000**, *2* (14), 2141-2143; (c) Saxon, E.; Bertozzi, C. R., *Science* **2000**, *287* (5460), 2007-2010.
28. Hassner, A.; Galle, J. E., *J. Am. Chem. Soc.* **1970**, *92* (12), 3733-3739.
29. Müller, A.; Krieger, M.; Neumüller, B.; Dehnicke, K.; Magull, J., *Z. Anorg. Allg. Chem.* **1997**, *623* (7), 1081-1087.
30. (a) Imhoff, P.; Elsevier, C. J.; Stam, C. H., *Inorg. Chim. Acta* **1990**, *175* (2), 209-216; (b) Miekisch, T.; Mai, H. J.; zu Köcker, R. M.; Dehnicke, K.; Magull, J.; Goesmann, H., *Z. Anorg. Allg. Chem.* **1996**, *622* (3), 583-588.
31. (a) Katti, K. V.; Cavell, R. G., *Inorg. Chem.* **1989**, *28* (3), 413-416; (b) Reed, R. W.; Santarsiero, B.; Cavell, R. G., *Inorg. Chem.* **1996**, *35* (15), 4292-4300.
32. T. Reetz, M.; Bohres, E., *Chem. Commun.* **1998**, (8), 935-936.
33. Masuda, J. D.; Wei, P.; Stephan, D. W., *Dalton Trans.* **2003**, (18), 3500-3505.
34. Steiner, A.; Stalke, D., *Angew. Chem. -Int. Ed.* **1995**, *34* (16), 1752-1755.

35. Schmidbaur, H.; Wolfsberger, W., *Chem. Ber.* **1967**, *100* (3), 1016-1022.
36. (a) Müller, A.; Neumüller, B.; Dehnicke, K., *Chem. Ber.* **1996**, *129* (2), 253-257; (b) Müller, A.; Neumüller, B.; Dehnicke, K., *Angew. Chem. -Int. Ed.* **1997**, *36* (21), 2350-2352; (c) Cristau, H.-J., *Chem. Rev.* **1994**, *94* (5), 1299-1313.
37. Ong, C. M.; Stephan, D. W., *J. Am. Chem. Soc.* **1999**, *121* (12), 2939-2940.
38. Kasani, A.; Kamalesh Babu, R. P.; McDonald, R.; Cavell, R. G., *Angew. Chem. Int. Ed.* **1999**, *38* (10), 1483-1484.
39. (a) Harder, S., *Coord. Chem. Rev.* **2011**, *255* (11-12), 1252-1267; (b) Heuclin, H.; Fustier, M.; Auffrant, A.; Mezailles, N., *Lett. Org. Chem.* **2010**, *7* (8), 596-611; (c) Cantat, T.; Mezailles, N.; Auffrant, A.; Le Floch, P., *Dalton Trans.* **2008**, (15), 1957-1972.

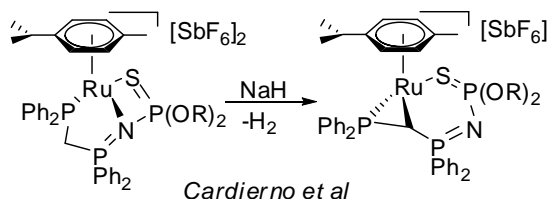
Chapter 1

Sulfur Containing Iminophosphoranes

I. Sulfur-Containing Ligands in Coordination Chemistry

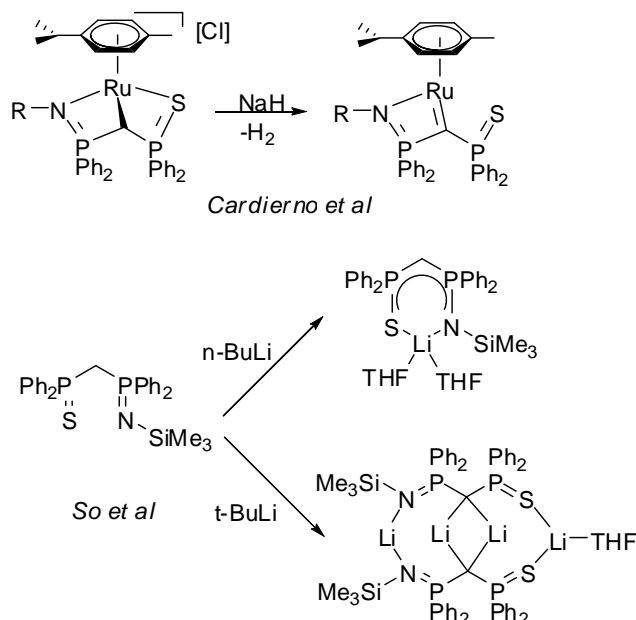
Sulfur containing ligands are of great importance in coordination and catalysis. This might be directly related to the occurrence of sulfur in many enzymatic systems. Of notable examples are iron-sulfur clusters in nitrogenases¹ and aconitase² (enzyme catalysing the transformation citrate-isocitrate). The importance of sulfur is also shown by the roles of cysteinyl residues in enzymes such as zinc-fingers³, alcohol dehydrogenases,⁴ which facilitate the interconversion of alcohols and aldehyde/ketones, thus serving to breakdown alcohols that are otherwise toxic, and recover helpful aldehyde, ketones and alcohols in human and animals. The occurrence of sulfur-containing groups as ligands is also evidenced in blue copper proteins⁵ (cupredoxins, for example, are characterized by a single copper atom coordinated by two histidine residues and a cysteine residue in a trigonal planar structure, and a variable axial ligand, function as electron transfer shuttles between proteins), or in hydrogenases⁶ (enzymes enabling cells to use molecular hydrogen), etc. Many efforts have been made in order to develop biomimetic models with the aim of elucidating the mechanisms of enzymes and constructing catalytic systems.⁷

Despite the abundance of sulfur containing ligands, systems having both a sulfur-containing group and iminophosphorane (P=N) are still rare. Most of them employ sulfur in thiophosphinate function (P=S, also called thiophosphorane), sometimes as a substituent at the nitrogen atom of P=N group. Examples include the hetero-trifunctional ligand $\text{Ph}_2\text{PCH}_2\text{P}=\text{N}(\text{=X})(\text{OR})_2\text{Ph}_2$ developed by Cardierno and coworkers (Scheme 1).⁸ These ligands were synthesized by a direct Staudinger reaction of diphenylphosphinomethane (dppm) with the corresponding thiophosphorylated azide. These compounds acted as versatile ligands in coordination to ruthenium centre, generating unusual systems containing Ru-C bond after selective transformation.



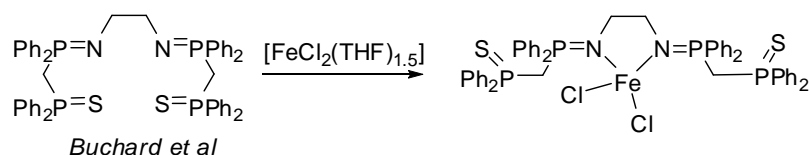
Scheme 1. Example of $\text{P}=\text{S}$ function as a substituent at the iminophosphorane group.

The same group, following their interest in the iminophosphorane-ruthenium chemistry, developed mixed iminophosphoranyl thiophosphoranyl methane ligands for the preparation of new ruthenium carbene species (Scheme 2).⁹ These carbene species, however, do not include a $\text{P}=\text{S}$ -metal coordination bond. Later, the same molecular structure (iminophosphoranyl thiophosphoranyl methane) was adopted by So and coworkers to successfully obtain methanide dianionic lithium complexes,¹⁰ this time the metal centre is coordinated by the $\text{P}=\text{S}$ group (Scheme 2).



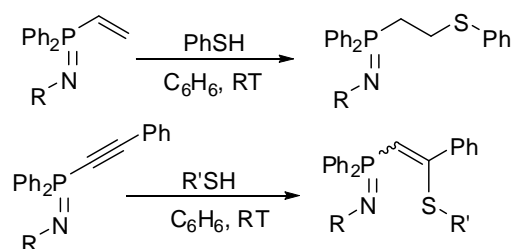
Scheme 2. Iminophosphoranyl thiophosphoranyl methane ligands

In addition to all these reports, our laboratory has developed iron complex of iminophosphorane-thiophosphorane ligand as active catalyst in transfer-hydrogenation of ketones (Scheme 3).¹¹ The coordination ability of $\text{P}=\text{S}$ group is limited, as has been shown by the fact that in these iron species, no $\text{P}=\text{S}$ -metal coordination bond existed in solution or in solid state.

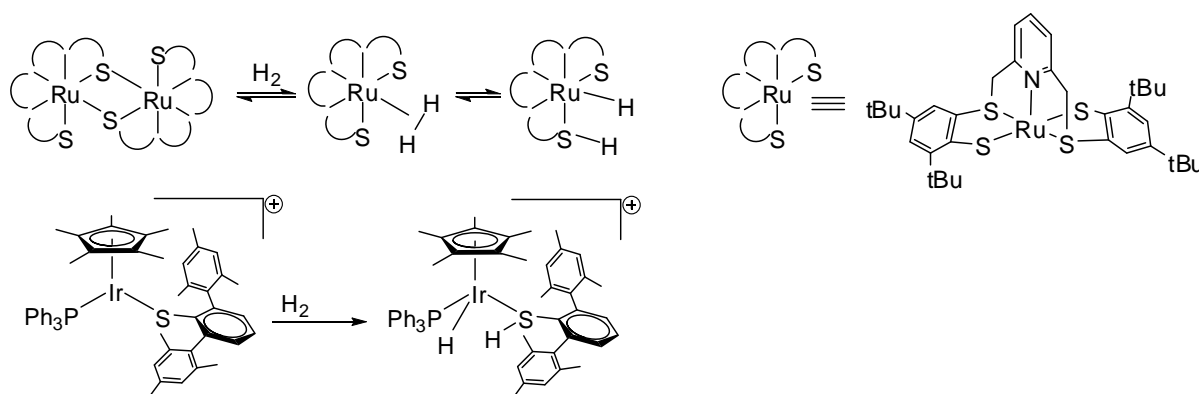


Scheme 3. Tetradentate ($P=S$, $P=N$) ligand developed in the laboratory.

Examples of iminophosphoranes incorporating the thioether or the thiolate function are much rarer in the literature. Thioether-iminophosphoranes were prepared first by Alajarin and coworkers using Michael-type addition reaction of thiol to diphenylvinyl iminophosphorane (Scheme 4).¹² This method could also be applied to alkynyl iminophosphorane.¹³



Scheme 4. Synthesis of thioether-iminophosphoranes by Michael addition.



Scheme 5. Examples of molecular hydrogen activation by thiolate complexes, from Sellmann group¹⁴ (top) and from Ohki group¹⁵ (bottom).

On the other hand, no ligand associating thiolate and iminophosphorane has been reported. These ligands could be of interest as the electronic properties of thiolates, thioethers and thiophosphinates ($P=S$) are very different. Even after coordination, the sulfur of the thiolate function with its diffused orbitals can participate in other chemical transformation such as S -metallation or S -alkylation. Furthermore, the presence of thiolate function give to many complexes the ability to activate molecular hydrogen,^{16a-h, 15, 16i} an activity relevant to hydrogenases.

Indeed, the Sellmann group has reported various studies of heterolytic activation of dihydrogen using ruthenium or rhodium complex of mixed tetradentate thioether-thiolate ligand “S4” (1,2-bis((2-mercaptophenyl)thio)ethane) and derivatives (Scheme 5).^{7g, 16b, 14} In approaching the M-S

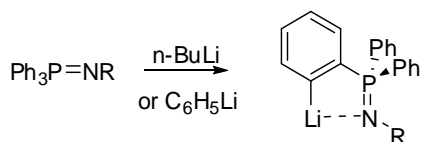
bond, the molecular hydrogen is cleaved into a proton that goes to the thiolate and a hydride that is coordinated to the metal centre. Thus the thiolate acts as a base to trap the formed proton and facilitate the cleavage reaction. In the same manner, the thiolate ligand (2,6-dimesitylphenyl thiolate) reported by Ohki and coworkers, in the rhodium or iridium complexes, is protonated upon exposition to hydrogen to become a thiol which is subsequently decoordinates from the metal centre (Scheme 5).¹⁵ The group has then successfully exploited this activation for the catalytic hydrogenation of C=N and C=O bond with molecular hydrogen.^{16f}

Taking into account all these information, and our interest in developing new iminophosphorane ligands incorporating different heteroatoms, we work on the synthesis of thiolate-iminophosphorane ligands through different but simple routes.

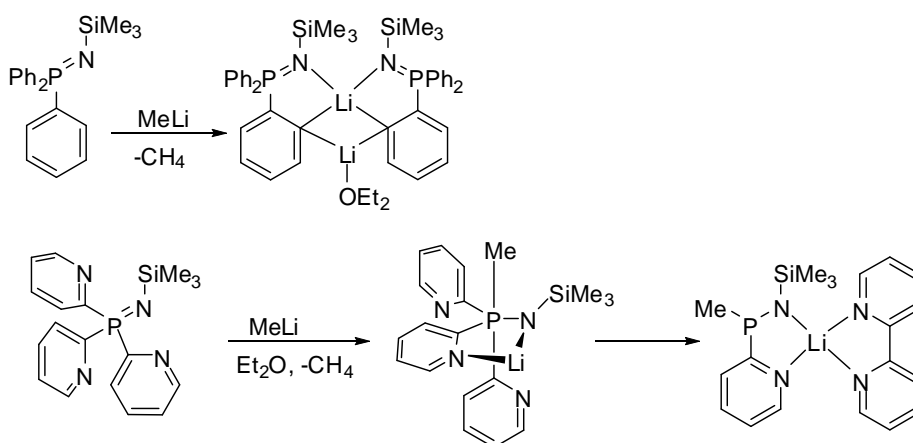
II. Bidentate PN-S Ligands by Ortho-Lithiation Reaction

1. Bidentate PN-S Ligand Synthesis by Ortho-Lithiation Reaction

Selective ortho-lithiation of iminophosphorane derivatives is a valuable synthetic way to the introduction of other donors group giving access to iminophosphorane containing bidentate ligands. The possibility of P=N to favor the α -deprotonation of a phenyl group at P atom has been reported for the first time in 1976 by C. G. Stuckwisch.¹⁷ They found that the reaction of $\text{Ph}_3\text{P}=\text{NPh}$ with phenyllithium or n-butyllithium gives primarily a metallation product (Scheme 6).



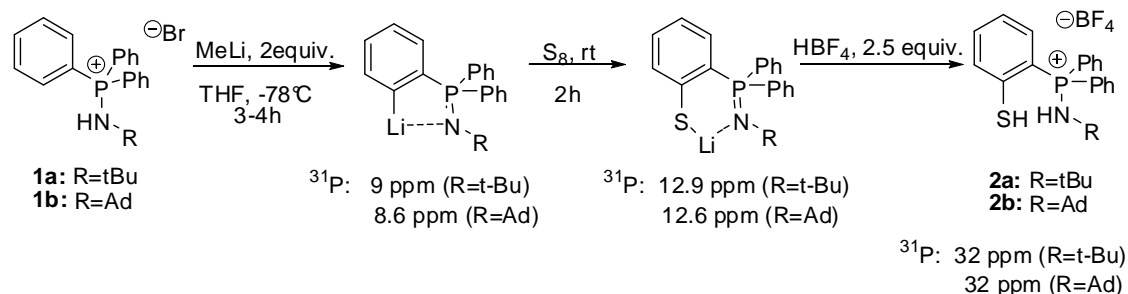
Scheme 6. Ortholithiation reaction



Scheme 7. Substituents-controlled reactions of iminophosphoranes with MeLi.

Later, Steiner and Stalke reported the clean formation of the anionic salt $[(\text{Ph}_2(\text{C}_6\text{H}_4\text{-Li})\text{P}=\text{NTMS})_2(\text{Et}_2\text{O})]$ over the reaction of $[\text{Ph}_3\text{P}=\text{NTMS}]$ with methyllithium¹⁸. This reaction is however very sensitive to substituents on the phosphorus atom, as has been shown by a totally different behavior for the reaction between $[\text{Py}_3\text{P}=\text{NTMS}]$ with methyllithium. Instead of the product from the ortho-lithiation or the exchange reaction, a monomeric amide was immediately formed at -78°C along with the reduction of P^{V} to P^{III} (Scheme 7).

The coordination ability of the ortho-lithiation products of different triphenylphosphinimines has been investigated with different metals by the groups of D. W. Stephan¹⁹ and of Stalke.²⁰ Furthermore, the trapping of this ortho-lithiation product with chlorophosphine was demonstrated in our laboratory to be an efficient route to mixed phosphine-iminophosphorane ligands.²¹ Adopting the strategy of the ortho-lithiation reaction, we developed a route to novel thiolate-iminophosphorane ligands.



Scheme 8. Synthesis of thiol-aminophosphonium ligands from ortholithiation reaction.

The aminophosphonium salts **1a-b** were directly reacted with 2 equiv. of MeLi to yield the ortholithiated product (R=tBu, Ad). In the case of R=tBu, the addition of MeLi (2eq) led to the formation of various products as evidenced by $^{31}\text{P}\{^1\text{H}\}$ -NMR spectra. After one night, only one product remained exhibiting a singlet at 9 ppm. For R=Ad, the deprotonation reaction was completed after several hours, a unique product was formed showing a chemical shift of 8.6 ppm in $^{31}\text{P}\{^1\text{H}\}$ -NMR spectrum. All these values of chemical shifts are indicative for the formation of ortho-lithiation products where the iminophosphorane function is in weak coordination with lithium cation. Both these two solutions presented a red wine color, which faded rapidly upon addition of solid S_8 . In $^{31}\text{P}\{^1\text{H}\}$ -NMR spectra, both the obtained solutions exhibited a unique singlet with lower field shift at 12.9 ppm for R=tBu and 12.6 ppm for R=Ad, indicating the completion of the reactions with sulfur.

The resulting solution could be used directly for complexation test. Nevertheless, the ligands were isolated and fully characterised as aminophosphonium salts **2a,b** after protonation with two equivalents of HBF_4 . The X-ray structure of the product **2a** is shown in Figure 1.

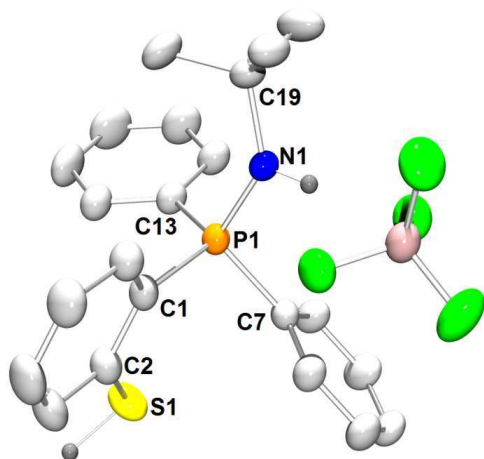


Figure 1. ORTEP view of complex **2a**. Hydrogen atoms have been omitted for clarity. Thermal ellipsoids drawn at the 50% probability level. Selected distances (Å) and angles (°): S1-C2 1.781 (2), P1-N1 1.623 (1), P1-C1 1.807 (2), P1-C7 1.797 (2), P1-C13 1.791 (2), N1-C19 1.505 (2), P1-N1-C19 134.1 (1).

2. Reactivities and Coordination Test of the Thiolate-Iminophosphorane Ligand.

2.1 Basicity of the P=N Function

One particular behavior of compound **2a** is that its mono-deprotonation yielded a zwitterion combining a thiolate and an aminophosphonium function. Indeed, addition of one equiv. of MeLi into a slurry of the thiol-aminophosphonium salt in THF gave a pale orange-red solution which presents a unique singlet at +36.2 ppm in $^{31}\text{P}\{^1\text{H}\}$ -NMR spectrum, characteristic of the aminophosphonium function. Furthermore, X-ray diffraction experiments on single crystals obtained from slow diffusion of petroleum ether on THF solution of the product shows no presence of counter ion. Importantly, the P-N bond (1.631(1) Å) of the product is slightly longer than the one in the corresponding fully protonated compound (1.623(1) Å), and is significantly longer than P=N bonds found on other iminophosphorane compounds based on the data retrieved from the Cambridge database (1.605). Thus, it is not a P=N bond of an iminophosphorane. On the other hand, the S1-C2 bond (1.741(2) Å) is significantly shortened compared to the one in the fully protonated salt (1.781(2) Å), which could be explained by the stabilisation of the thiolate anionic charge by the phenyl ring.

This result is in perfect agreement with DFT calculations carried out on the possible product(s) from the protonation of the ligand with one equiv. of acid. Optimisation on three possible structures: (1) the proton attached to S, (2) the proton attached to N, (3) the proton located between S and N, all led to a unique stable geometry in which the proton is attached to N.

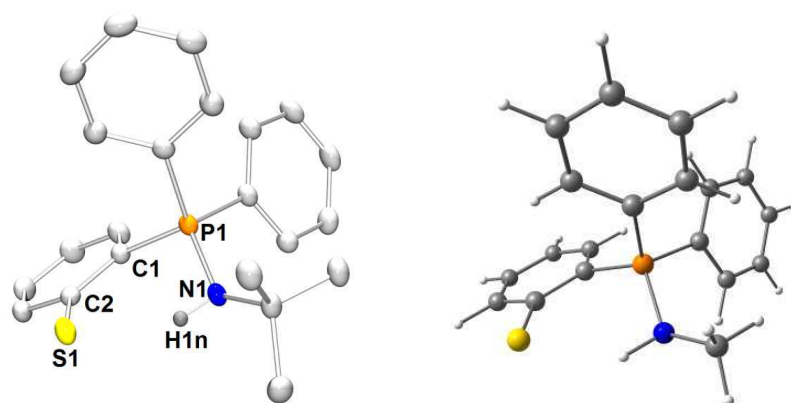
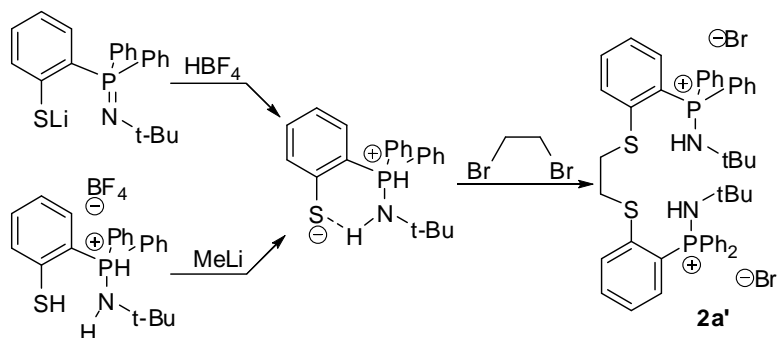


Figure 2. (a) X-ray structure of the monoprotonated compound. Hydrogen atoms have been omitted for clarity (except the one attached to N atom). Thermal ellipsoids drawn at the 50% probability level. Selected distances (\AA) and angles ($^\circ$): P1-N1 1.631 (1), P1-C1 1.797 (1), C2-S1 1.741 (2), C1-C2 1.428 (2). (b) optimised model compound. Tert-butyl group has been replaced with Me in order to simplify the calculations. Selected distances (\AA) and angles ($^\circ$): P1-N1 1.674, P1-C1 1.786, C2-S1 1.733, C1-C2 1.430.

This behavior could be explained by the greater basicity of the iminophosphorane compared to the thiolate function. Many of the powerful bases are indeed designed based on iminophosphorane function, as indicated in the introduction.

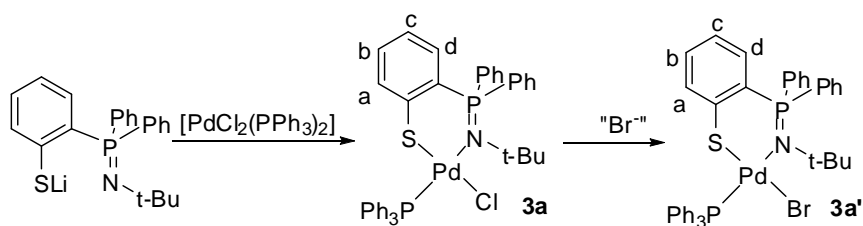
This property of thiolate-iminophosphorane function has been exploited to selectively functionalise the thiolate. The compound reacted with $\frac{1}{2}$ equiv. of dibromoethane to give the bis(thioether) bis(aminophosphonium) salt as a result of nucleophilic substitution (Scheme 9). This product, upon deprotonation, could give tetradentate ligand incorporating thioether and iminophosphorane groups. Thus, the reaction could be a versatile method of synthesising tetradentate ligands of this type. However, this strategy and chemistry of the possible so-formed species was not exploited further as we concentrated on other ligands which seemed to be more interesting in coordination and catalysis.



Scheme 9. Functionalisation of S in thiolate-aminophosphonium compound.

2.2 Coordination Test

Preliminary coordination study of the thiolate-iminophosphorane ligand resulted from **2a** has been done with a palladium precursor. The thiol-aminophosphonium salt was first deprotonated with 2 equiv. of MeLi. Addition of $[\text{PdCl}_2(\text{PPh}_3)_2]$ into the obtained solution induced a rapid color change from deep red wine to bright orange-red. Completeness of the reaction after one day was monitored in $^{31}\text{P}\{^1\text{H}\}$ -NMR spectrum. The signal of the free ligand at +12.9 ppm disappeared, and two doublets at +31.8 ppm ($J_{\text{P,P}}=3.5$ Hz) and + 15.4 ppm ($J_{\text{P,P}}=3.5$ Hz) were observed, corresponding to the coordinated iminophosphorane group and PPh_3 group, respectively. This indicated the clean formation of the palladium complex **3a** (Scheme 10).



Scheme 10. Coordination of **2a'** with palladium(II) and exchange reaction.

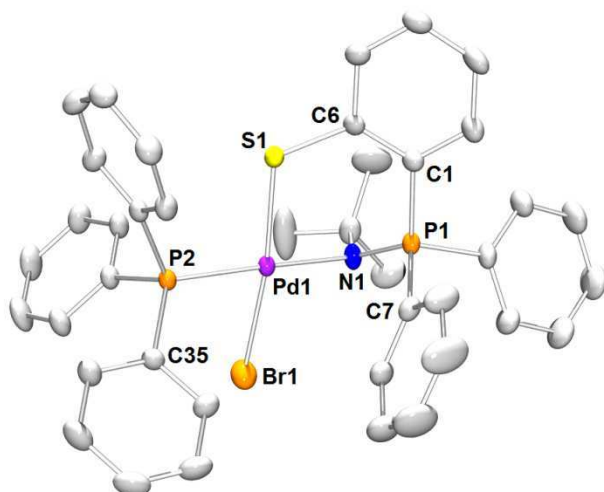


Figure 3. ORTEP view of complex **3a'**. Hydrogen atoms and solvent molecules have been omitted for clarity. Thermal ellipsoids drawn at the 50% probability level. Selected distances (Å) and angles ($^\circ$): Pd1–N1 2.116(2), S1–Pd1 2.283(1), Pd1–P2 2.2676(8), Pd1–Br1 2.4781(6), N1–P1 1.608(3), P1–C1 1.809(3), P1–C7 1.803(3), C6–S1 1.757(3), P2–C35 1.825(3), N1–Pd1–S1 92.53(8), P2–Pd1–S1 90.51(3), N1–Pd1–Br1 91.97(8), P2–Pd1–Br1 84.65(3), C6–S1–Pd1 115.4(1).

Interestingly, when coordination test was done directly on in situ prepared thiolate-iminophosphorane ligand by the ortho-lithiation reaction, two set of doublets were found in the final reactional medium: the two as described above, and two other doublets at +31.3 ppm ($J_{\text{P,P}}=3.5$ Hz) and + 15.5 ppm ($J_{\text{P,P}}=3.5$ Hz). These two latters increased in intensity when excess LiBr was added, along with the total disappearance of the first set of doublets corresponding to

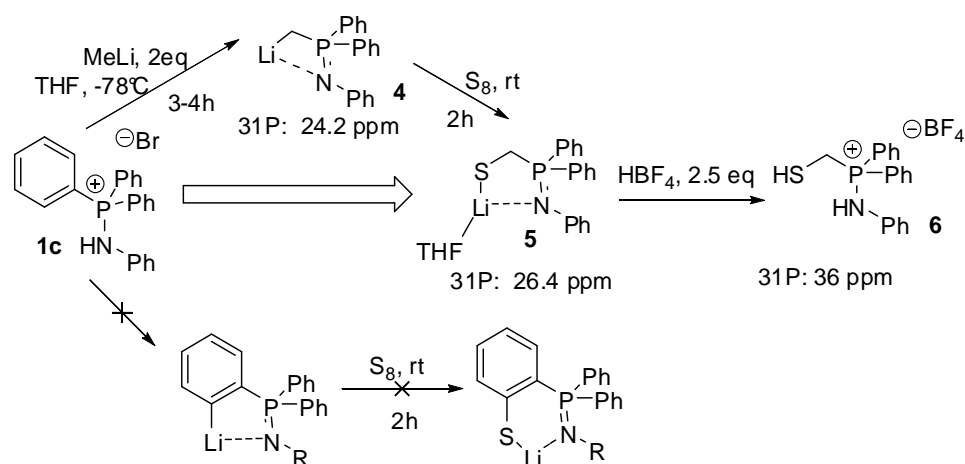
compound **3a**. Thus, these doublets are supposed to belong to the product with Br- ligand at the place of Cl-. Indeed, from this solution, an orange-red solid precipitated out after 3 days of staying at room temperature. $^1\text{H-NMR}$ and $^{13}\text{C-NMR}$ of this compound presents no difference from those of **3a**, only slight chemical shift difference in $^{31}\text{P}\{^1\text{H}\}$ -NMR spectrum was detected. X-ray diffraction experiment on single crystals of this compound by slow diffusion of petroleum ether over a dichloromethane solution showed the presence of a coordinated bromine, thus confirming the exchange reaction Cl-Br on the Pd centre.

The coordination chemistry of the ligands corresponding to the proligands **2a,b** were not pursued further as we chose to concentrate on other ligand systems. However, this preliminary coordination test shows the ability of these ligands to coordinate easily and quite strongly to metal centres. This ability could be exploited to synthesize specific complexes when needed.

III. Synthesis of PN-S Ligand by Substitution Reaction

1. Ligand Synthesis

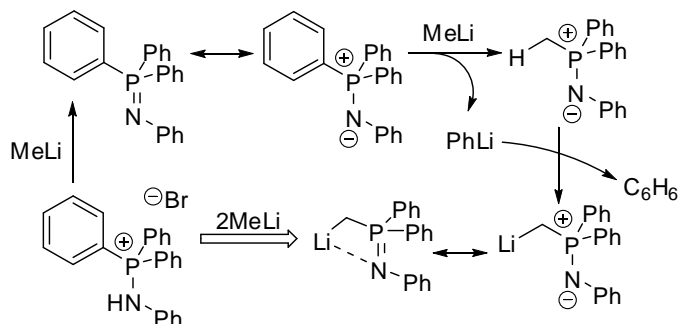
Working on ortho-lithiation of iminophosphorane, we have found that this reaction depends highly on the nature of the substituents at nitrogen and the experimental conditions. Especially, when applying the same strategy of thiolate-iminophosphorane ligand synthesis on N-phenyl triphenyl-aminophosphonium bromide **1c**, we observed the unexpected clean formation of the thiolate **5** (Scheme 11). The compound is soluble in pyridine and has been found to contain one THF per ligand molecule. The protonation of this lithium complex with 2 equiv. of HBF_4 yielded the thiol-aminophosphonium salt **6** which was also fully characterised.



Scheme 11. Thiolate-iminophosphorane formation from nucleophilic substitution.

The formation of this ligand must have arisen from the nucleophilic substitution of MeLi on the iminophosphorane group which leads to anion **4**, prior to the addition of S_8 step. Following this

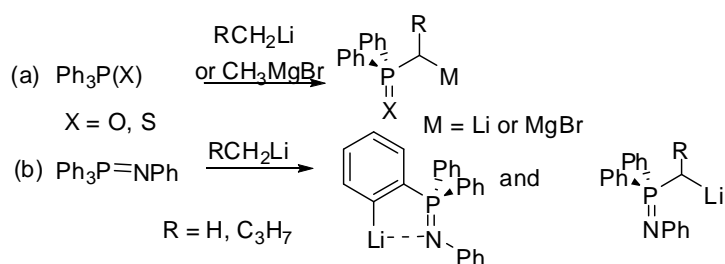
observation, conditions for the clean formation of the anion **4** were found. Indeed, adding two equivalents of MeLi (1.6 M in diethyl ether) to a suspension of N-phenyl triphenylaminophosphonium bromide in THF induced a marked color change, the white suspension disappeared giving an orange-red solution.



Scheme 12. Mechanism of the nucleophilic substitution on iminophosphorane

$^{31}\text{P}\{^1\text{H}\}$ NMR spectrum of the crude mixture showed a singlet at $\delta(\text{THF}) = 24.2$ ppm, which is in the range of the chemical shift observed for ortholithiated derivatives obtained from $\text{Ph}_3\text{P}=\text{NR}$ ($\text{R} = \text{CH}(\text{CH}_3)\text{CH}(\text{CH}_3)_2$, CH_2^tBu , $i\text{-Pr}$)²¹ in diethyl ether, but is too high compared to the ortho-lithiation products of N-tBu and N-Ad compounds **1a-b** in THF (Scheme 8). ^1H NMR spectrum of the crude mixture in $\text{d}_8\text{-THF}$ showed a broad singlet at $\delta(\text{THF}) = -0.11$ ppm integrating for 2 protons, and the presence of only two phenyl rings on the phosphorus atom.

These observations were strongly in favor of the formation of a methanide substituent on the phosphorus atom which results from the displacement of one phenyl substituent by methyl lithium, followed by the deprotonation of the so-formed species by the released phenyl lithium. Indeed, NMR characterisation of the compound in THF presented data very similar to those described by Davidson and Lopez-Ortiz group, who synthesized this anion from $\text{CH}_3\text{PPh}_2=\text{NPh}$ and characterized it in solution and in the solid state.²²



Scheme 13. Metallation of $\text{PPh}_3(\text{X})$ derivatives

This reaction resembles the reactivity of thiophosphines and phosphine oxides towards alkyllithium or Grignard reagents reported by D. Seyferth *et al.* in the early 60ies.²³ Indeed, as described in Scheme 13, they have showed that such reaction lead to the formation of diphenylphosphinylalkyl organometallic reagent $(\text{MCH}_2)\text{P}(\text{X})\text{Ph}_2$ ($\text{M} = \text{MgBr}$, Li ; $\text{X} = \text{O}$, S). However, no report has been found for a clean exchange reaction in the case of

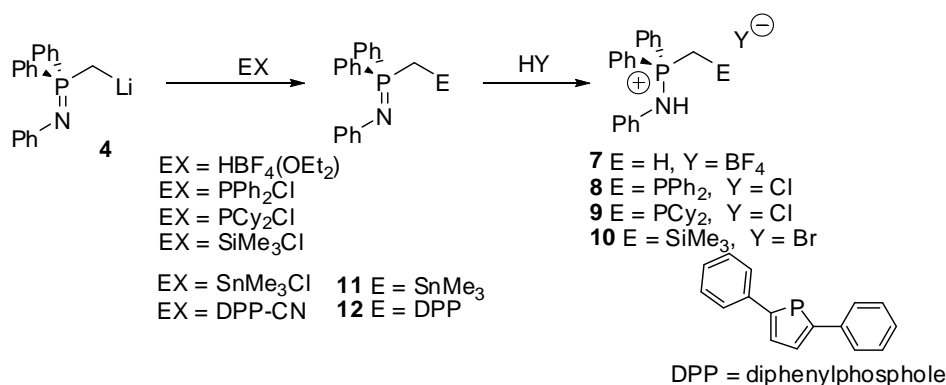
iminophosphoranes. In fact, for $\text{PPh}_3=\text{NPh}$, C. G. Stuckwisch¹⁷ mentioned that a competitive reaction takes place when performing the ortho-lithiation, metalated diphenylalkylphosphine N-phenylimide was indeed observed as by-product.

The formation of **4** from $\text{PPh}_3=\text{NPh}$ was found to depend highly on the reaction conditions. When using *n*-BuLi instead of MeLi in THF two different products were obtained, one coming from ortho-lithiation and the other from a phenyl displacement followed by α -metallation. Moreover, the lithiation carried out with MeLi (1.6 M in diethyl ether) in toluene leads also to a mixture of two product: **4** and the ortho-lithiated derivative corresponding to a singlet at $\delta(\text{toluene}) = 16.9$ ppm in $^{31}\text{P}\{\text{H}\}$ NMR spectrum. The latter can also be obtained as the sole product by using *n*-BuLi in toluene.

The reaction is also very sensitive to the nature of the nitrogen substituent. Indeed, with alkyl substituent at the nitrogen, whatever the nature of the base or solvent used, only ortho-lithiation was observed as we described earlier (Scheme 6)²¹.

2. Synthesis of Mixed Ligand Containing Iminophosphorane and other Heteroatoms-Based Groups by Substitution Reactions.

After having determined the experimental conditions enabling a clean preparation of **4**, this anion was trapped with various electrophiles (Scheme 14). These reactions were carried out not only to test the reactivity of **4**, but also to test the possibility to prepare ligands containing iminophosphoranes and heteroatoms. Contrary to bidentate iminophosphorane-phosphine ligands which are quite well-known, the combination of iminophosphorane with other donating groups containing heteroatoms still remains scarce, not least because of the synthesis difficulty.



Scheme 14. Electrophilic trapping of **4**

Protonation of **4** with HBF_4 results immediately in a colorless solution. In $^{31}\text{P}\{\text{H}\}$ NMR spectrum, the phosphorus signal is strongly deshielded ($\delta(\text{THF}) = +36.6$ ppm). The aminophosphonium salt **7** was isolated in 70% yield as a white solid. The presence of the

methyl group is attested by a doublet at $\delta(\text{THF}) = 2.44$ ppm (${}^2J_{\text{P,H}} = 69.5$ Hz) in the ${}^1\text{H}$ NMR spectrum.

Reaction of **4** with one equivalent of PPh_2Cl induced the formation of the (P, P=N) adduct as evidenced by the presence of two doublet at $\delta(\text{THF}) = 0.80$ ppm and -26.6 ppm (${}^2J_{\text{P,P}} = 51.5$ Hz) in the ${}^{31}\text{P}\{\text{H}\}$ NMR of the crude mixture, corresponding respectively to P^{III} and P^{V} . After protonation the aminophosphonium salt **8** can be isolated. NMR spectra of **8** correspond exactly to the ones reported for this compound earlier.²¹

In fact, compound **8** has already been prepared in the lab using Kirsavov reaction on bis(diphenylphosphine)methane (dppm, $\text{CH}_2(\text{PPh}_2)_2$). However, this previous method could not be used to prepare mixed phosphine-iminophosphorane ligands, in which the two phosphorus atoms do not bear the same substituents. With the new synthesis strategy using **4**, the preparation of such compounds is possible. For example the reaction of **4** with PCy_2PCl , followed by acidic work-up gave compound **9** in good yield. In ${}^{31}\text{P}\{\text{H}\}$ NMR spectroscopy two doublet at $\delta(\text{CD}_2\text{Cl}_2) = -22.2$ ppm and 34.80 (${}^2J_{\text{P,P}} = 87.5$ Hz) were observed corresponding respectively to the P^{III} and P^{V} atoms. The bridging methylene appears as doublet at $\delta(\text{CD}_2\text{Cl}_2) = 3.22$ ppm (${}^2J_{\text{P,H}} = 16.5$ Hz) and a doublet of doublet at $\delta(\text{CD}_2\text{Cl}_2) = 18.7$ ppm (${}^2J_{\text{P,C}} = 39.0$ Hz and 68.0 Hz) in the ${}^1\text{H}$ and ${}^{13}\text{C}$ NMR spectra respectively.

In the same manner, reaction of **4** with trimethylsilylchloride also proceeded cleanly, giving after acidic work up the aminophosphonium salt **10** in high yield. The methylene group gave rise to a doublet at $\delta(\text{CDCl}_3) = 2.71$ ppm (${}^2J_{\text{P,H}} = 18.0$ Hz) in ${}^1\text{H}$ -NMR spectrum and a doublet at $\delta(\text{CDCl}_3) = 14.5$ ppm (${}^2J_{\text{P,C}} = 58.5$ Hz) in ${}^{13}\text{C}$ NMR spectrum.

Reaction of anion **4** with trimethyltin chloride gave **11** as a white solid in 75% yield. In ${}^{31}\text{P}\{\text{H}\}$ NMR spectroscopy **11** exhibited a singlet at $\delta(\text{C}_6\text{D}_6) = 7.40$ ppm and satellites due to tin isotope (${}^2J_{\text{P,Sn}} = 60.0$ Hz). In ${}^1\text{H}$ NMR the methylene protons appears as a doublet with tin satellites centered at $\delta(\text{C}_6\text{D}_6) = 2.71$ ppm (${}^2J_{\text{Sn,H}} = 52.0$ Hz, ${}^2J_{\text{P,H}} = 11.0$ Hz).

Finally, reaction of **4** with 1-cyano-2,5-diphenylphosphole gave access to **12** in 85 % yield. The formation of **12** was ascertained by NMR spectroscopy. ${}^{31}\text{P}\{\text{H}\}$ NMR spectrum of the compound showed a doublet at $\delta(\text{C}_6\text{D}_6) = -23.7$ ppm for the phosphole P-atom and another doublet at 0.8 ppm for the P(V) atom. This mixed bidentate ligand is very promising since it features coordination sites with very different electronic properties iminophosphorane as a strong σ and π donor and the phosphole ring as a phosphine with greater accepting ability.

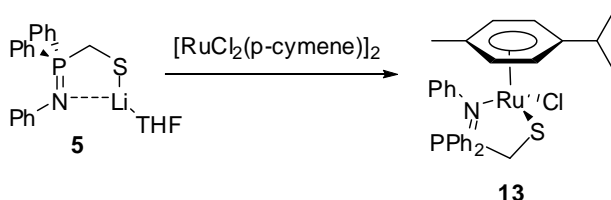
As we focused in the development and reactivities of sulfur-containing iminophosphorane ligands, the coordination chemistry and reactivities of these compounds have not been studied. However, taking into account the differences in electronic and steric properties of these groups, they could make interesting ligands for other studies.

3. Coordination Chemistry of the Thiolate-Iminophosphorane **5**

As first coordination experiments, the thiolate-iminophosphorane anion **5** was coordinated to metals of group 8, 9, 10 (Ru, Co, Rh, Ir, Pd and Ni). Some of these metals are chosen also for their potential applications related to thiolate ligands: many thiolate complexes of Ru(II), Rh(I) and Ir(I) give high activity for hydrogen activation.

3.1 Coordination of PN-S Ligand with a Group VIII-Metal Centre: Ru(II)

The iminophosphorane-thiolate anion **5** was easily coordinated to Ru(II) centre. Addition of THF to a mixture of **5** and dichloro(p-cymene)ruthenium(II) dimer in the solid state led rapidly to a red solution. The disappearance of the precipitated anion was a good sign of coordination which was confirmed by $^{31}\text{P}\{\text{H}\}$ NMR of the crude mixture showing the formation of a unique product exhibiting a singlet at $\delta(\text{THF}) = 36.9$ ppm. After 3h at room temperature, the solvent was evaporated, the lithium salt was filtered-off after precipitation in dichloromethane and **13** was isolated as a red solid in 76% yield.



Scheme 15. Coordination of the thiolate-iminophosphorane ligand with Ru(II)

In the ^1H NMR spectrum the methylene protons appear as two doublets at 2.67 and 4.12 ppm, this accounts for the chirality of the Ru centre which bears four different substituents. In the same manner the protons of the coordinated p-cymene ring are differentiated giving three doublets at 4.64, 4.76, and 4.90 ppm integrating respectively for 1, 2, and 1 protons. In the aromatic area, the differentiation of the protons of the phenyl rings on the phosphorus atom can also be seen. In the ^{13}C spectrum most of the carbons of both the p-cymene and phenyl rings (on P) are differentiated. All these data suggest the structure depicted in Scheme 15 for complex **13**.

3.2 Coordination of PN-S Ligand with Group IX-Metal Centres: Co(II), Rh(I), Ir(I)

Reaction of the ligand with one equivalent of CoCl_2 in THF gives first a green solution, from which a green solid precipitated out after 3 hours. If stirring is stopped just after the introduction of the ligand and the solution was allowed to stay for one day, green crystals are formed. X-ray diffraction experiment carried out on these crystals showed a dimeric $[(\text{o-C}_6\text{H}_4(\text{S})\text{P}(\text{Ph}_2)=\text{N}(\text{Ph}))\text{CoCl}]$ complex (Figure 4), the sulfur atoms serving as bridges forming a planar four-membered ring Co_2S_2 .

The complex is symmetric with an inversion point at the centre of this ring. The metals adopt distorted tetrahedral geometry, the values of P=N and other bonds on the ligand are in the usual range as in other complexes. The distance Co-Co (2.87 Å) is larger than the sum of covalent radii of the two Co atoms (1.26 Å each) and significantly longer than the average value of Co-Co distances (2.50 Å) in all compounds containing any type of Co-Co bond (from the CCDC database). The complex **14** is thus a simple dimeric complex and does not contain any special metal-metal bond. (Indeed, DFT calculations performed on this complex do not show any special metal-metal interaction).

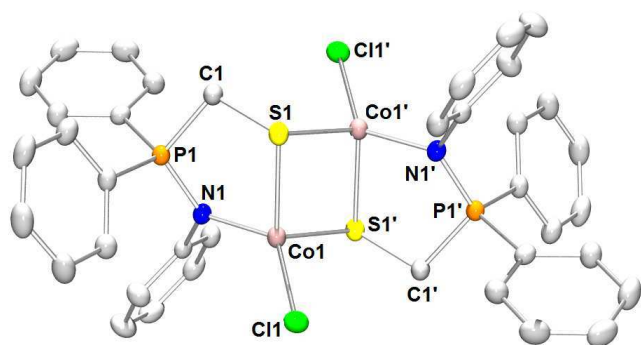
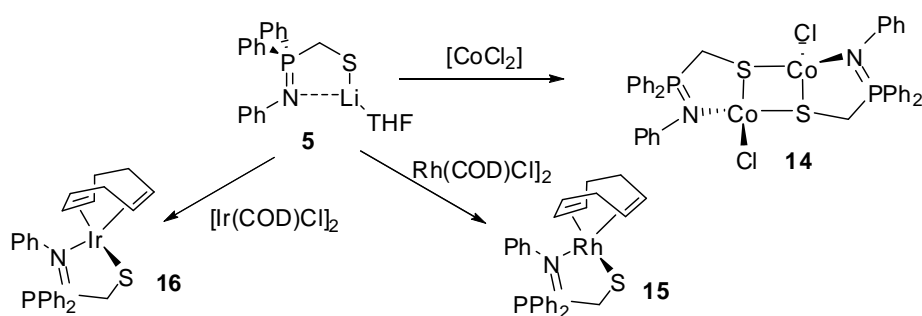


Figure 4. ORTEP view of complex **14**. Hydrogen atoms have been omitted for clarity. Thermal ellipsoids drawn at the 50% probability level. The molecule has an inversion point at the centre of the 4-membered ring Co₂S₂. Selected distances (Å) and angles (°): Co1-N1 1.977 (2), Co1-Cl1 2.2501 (7), Co1-S1 2.3643 (8), Co1-S1' 2.3465 (7), Co1-Co1' 2.8689 (7), N1-P1 1.613 (2), N1-Co1-S1' 105.4 (6), Cl1-Co1-S1 109.14 (3), S1-Co1-S1' 104.97 (2), Co1-S1-Co1' 75.04 (2), S1-Co1-S1'-Co1' 0.



Scheme 16. Coordination of the thiolate-iminophosphorane ligand with Co(II), Rh(I), Ir(I)

Addition of **5** to a solution of [Rh(COD)Cl]₂ or [Ir(COD)Cl]₂ in toluene at room temperature immediately resulted in the change of color from yellow to light orange. ³¹P{H} NMR of the crude mixture showed a unique product exhibiting a singlet at δ(THF) = 63.0 ppm for the reaction with iridium precursor. In the case of reaction with rhodium precursor, a unique doublet was observed at δ(THF) = 47.7 ppm with a coupling constant of 5.0 Hz, clearly showing the formation of the rhodium complex of iminophosphorane ligand. After removal of lithium salts and evaporation of solvent, rhodium and iridium complexes (**15** and **16**) could be obtained as

orange solids. Single crystals of **15** suitable for X-ray diffraction were obtained by slow diffusion of petroleum ether over a solution in CH_2Cl_2 (Figure 5). The complex adopts a square-planar geometry, the rhodium centre being coordinated by the thiolate and iminophosphorane from the ligand, and two double bonds from the cyclooctadiene. No special effect has been found on the structure of the complex.

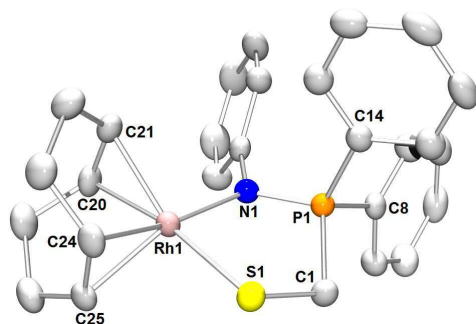
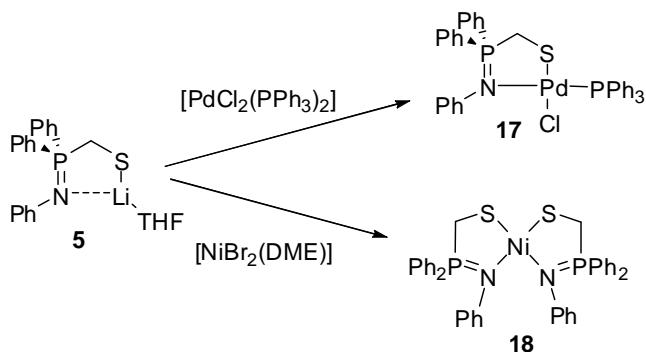


Figure 5. ORTEP view of complex **15**. Hydrogen atoms have been omitted for clarity. Thermal ellipsoids drawn at the 50% probability level. Selected distances (\AA) and angles ($^\circ$): Rh1-N1 2.118 (2), Rh1-S1 2.3291 (8), Rh1-C21 2.118 (3), Rh1-C20 2.157 (3), Rh1-C24 2.133 (3), Rh1-C25 2.138 (3), S1-C1 1.821 (3), P1-N1 1.613 (2), P1-C1 1.788 (3), P1-C14 1.808 (3), P1-C8 1.812 (3), N1-Rh1-S1 88.32 (7), N1-Rh1-C21 93.9 (1), N1-Rh1-C20 94.7 (1), S1-Rh1-C24 89.5 (1), S1-Rh1-C25 91.1 (1), N1-P1-C1 107.2 (1), P1-C1-S1 106.8 (2), C1-S1-Rh1 103.4 (1).

3.3 Coordination of PN-S Ligand with Group X-Metal Centres: Pd(II) and Ni(II)



Scheme 17. Coordination of the thiolate-iminophosphorane ligand with Pd(II), Ni(II)

Due to the low solubility of **5** in THF, complexation reactions were carried out by addition of THF onto a mixture of isolated **5** and the appropriate metal precursor. With [*trans*- $\text{PdCl}_2(\text{PPh}_3)_2$], after 4h hours at room temperature, the yellow slurry had turned to an orange solution. Compared with the analog thiolate-iminophosphorane **2a'**, the coordination of **5** is thus much faster, probably due to the more important donating ability of the thiolate attached to an alkyl group, and the greater flexibility of the ligand.

The $^{31}\text{P}\{\text{H}\}$ NMR spectrum of the crude mixture showed the presence of one equivalent of free triphenylphosphine ($\delta(\text{THF}) = -5.1$ ppm) and an AB signal pattern evidencing the coordination of the ligand to the palladium centre. The complex $[(\text{PhNPPh}_2\text{CH}_2\text{S})\text{Pd}(\text{PPh}_3)\text{Cl}]$ **17** exhibited two doublets ($^3J_{\text{P,P}} = 6.5$ Hz) at $\delta(\text{THF}) = 34.2$ ppm and $\delta(\text{THF}) = 45.0$ ppm corresponding respectively to the coordinated triphenylphosphine and iminophosphorane function. This complex was isolated in 87% yield and was characterized by multinuclear NMR, elemental analysis and X-Ray diffraction analysis.

Single crystals were obtained by slow diffusion of petroleum ether into a concentrated CH_2Cl_2 solution of **17**. An Ortep plot of **17** is depicted in Figure 6 together with the most relevant structural data. The complex adopts a slightly distorted square-planar geometry, the iminophosphorane and the phosphine being located *trans* to each other. This *trans*-configuration is probably due to the initial configuration of the palladium precursor.

The deviation from planarity was measured at $16.70(9)$. The P-N bond distance is normal at $1.597(3)$ Å, the P3-C1 bond is shortened compared to the P-C bond in $[(\text{PhNCH}_2\text{PPh}_2)\text{PdCl}_2]$ featuring bidentate phosphine-iminophosphorane ligand ($1.801(3)$ Å vs $1.842(2)$ Å). On the contrary both the N-Pd ($2.100(2)$ Å) and the Pd-Cl ($2.3869(7)$ Å) are elongated compared to the same reference (N-Pd = $2.076(2)$ Å and Pd-Cl = $2.3668(5)$ Å, $2.3035(6)$ Å). Compared with complex **3a'** $[(o\text{-C}_6\text{H}_4(\text{S})\text{P}(\text{Ph}_2)=\text{N}(\text{t-Bu}))\text{Pd}(\text{PPh}_3)\text{Cl}]$ of another thiolate-iminophosphorane ligand resulted from the ortho-lithiation reaction, the Pd-S, Pd-N and Pd-PPh₃ bonds are almost of the same values

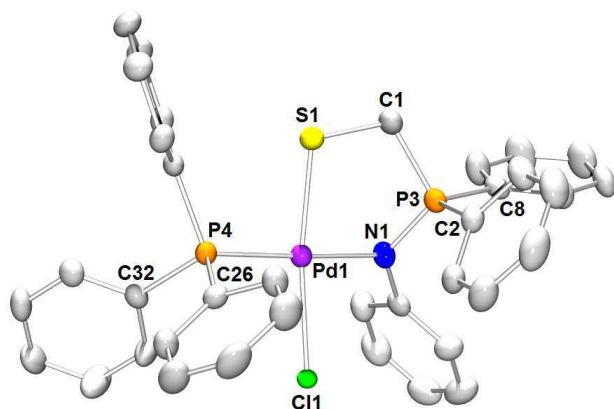
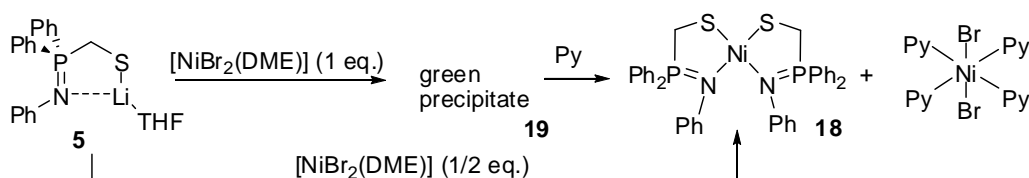


Figure 6. ORTEP view of complex **17**. Hydrogen atoms have been omitted for clarity. Thermal ellipsoids drawn at the 50% probability level. Selected distances (Å) and angles ($^\circ$): Pd1–N1 $2.100(2)$, S1–Pd1 $2.289(1)$, Pd1–P4 $2.2528(8)$, Pd1–Cl1 $2.3869(7)$, N1–P3 $1.597(3)$, P3–C1 $1.801(3)$, P3–C2 $1.799(3)$, P3–C8 $1.808(3)$, C1–S1 $1.824(3)$, P4–C32 $1.829(3)$, P4–C26 $1.818(3)$, N1–Pd1–S1 $88.52(7)$, P4–Pd1–S $89.87(3)$, N1–Pd1–Cl1 $92.45(7)$, P4–Pd1–Cl1 $89.73(3)$, P3–C1–S1 $109.5(2)$, N1–P3–C1 $104.9(2)$, C1–S1–Pd1 $103.6(1)$, S1–Pd1–N1–Cl1 $16.70(9)$.

Along with the Pd complex described above, nickel complex of the thiolate-iminophosphorane ligand **5** was synthesised with the aim of studying the coordination chemistry of the ligand, because tetracoordinated Ni^{II} complexes, in difference from Pd complexes, could adopt

tetrahedral or square-planar geometry, and exist in singlet or triplet state, depending on the rigidity of ligand and its field-strength.

Reaction of the iminophosphorane-thiolate ligand with one equivalent of $[\text{NiBr}_2(\text{DME})]$ gives a deep green solution, from which a green precipitate appears after 1h. Elemental analysis of this product shows that it corresponds to the formula $[(\text{CH}_2(\text{S})\text{P}(\text{Ph}_2)=\text{N}(\text{Ph}))\text{NiBr}]$. SQUID measurement showed that only half of the nickel centres are in triplet state. Attempts to obtain single crystals suitable for X-ray diffraction measurement have been carried out. However, due to the very limited solubility of the complex in common solvents, no crystals have been obtained. The complex is soluble in pyridine, but in this solvent, crystallisation yields two types of crystals: $[\text{NiBr}_2(\text{Py})_4]$ (pale green) and deep green crystals corresponding to a complex in which the nickel centre is coordinated by two iminophosphorane groups in *cis*-position, forming a distorted square planar geometry (**18**, deep green crystals).



Scheme 18. Reaction of **5** with $[\text{NiBr}_2(\text{DME})]$.

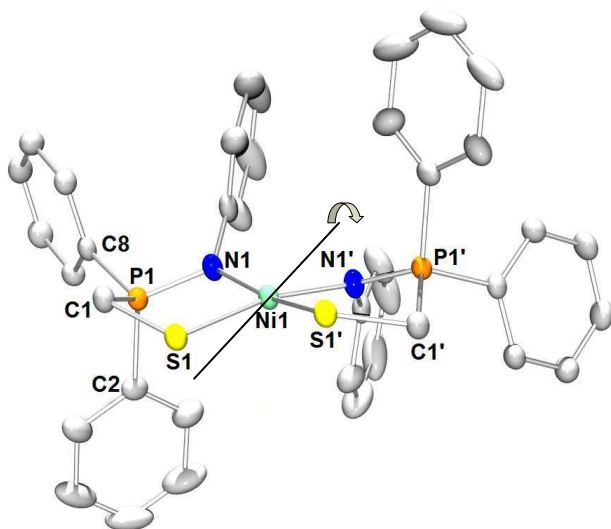


Figure 7. ORTEP view of complex **18**. Hydrogen atoms have been omitted for clarity. Thermal ellipsoids drawn at the 50% probability level. The molecule has a C_2 axis passing through Ni1. Selected distances (\AA) and angles ($^\circ$): Ni1-Ni1.961 (1), Ni1-S1 2.1996 (5), S1-C1 1.834 (2), P1-Ni1 1.612 (1), P1-C1 1.787 (2), P1-C8 1.800 (2), Ni1-Ni1-S1 91.38 (4), Ni1-Ni1-Ni1' 94.61 (8), S1-Ni1-S1' 84.62 (2), Ni1-Ni1-S1' 168.2 (4), C1-S1-Ni1 104.35 (5), P1-Ni1-Ni1 115.35 (8).

Intrigued by this result, we tested the coordination to Ni(II) using 2 equiv. of the thiolate ligand **5**. Reaction of two equivalents of ligand **5** with $[\text{NiBr}_2(\text{DME})]$ in THF yielded immediately a bright green solution, from which a green slurry was formed after 4h. After removal of lithium

salts by dissolving the solid in CH_2Cl_2 and evaporation of solvent, $[(\text{CH}_2(\text{S})\text{P}(\text{Ph}_2)=\text{N}(\text{Ph}))_2\text{Ni}]$ was isolated as green solid at high yield. X-ray diffraction experiment carried out on monocrystals of the complex obtained from slow diffusion of petroleum ether over CH_2Cl_2 solution showed the same complex **18**.

The complex, even though having a geometry close to square-planar in solid state, is paramagnetic in solution. Magnetic measurement with Evans method on a solution of this complex in CH_2Cl_2 showed a magnetic moment of $2.3 \mu_{\text{B}}$, suggesting that the majority of the complex molecules in solution are high-spin. DFT calculations has been carried out to rationalise this behavior. Nickel was represented by the relativistic effective core potential of Hay and Wadt²⁴ and the associated triple zeta quality basis set²⁵, augmented by a f polarization function as proposed by Frenking²⁶ (lanl2tz(f)). S was described with 6-31+G* basis set. All other atoms were described with the 6-31G* Pople basis set²⁷. Optimisations were done in nonsymmetric condition. It was then found that the triplet state which is in tetrahedral geometry is much more stable than the singlet state, which adopts a distorted-square planar geometry very close to the structure resolved with X-ray diffraction experiment. The difference in free energy is 9.0 kcal/mol. This result explains paramagnetic behavior of the complex in solution.

In solid state, however, π -stacking interactions between phenyl rings of neighboring molecules were detected from the X-ray crystal structure (the distances between these phenyl rings, i.e centroid perpendicular distances, being approximately 3.35-3.39 Å). These interactions, along with weak hydrogen bonds between H(phenyl) and Sulfur atoms ($d(\text{H}-\text{S})$ being approximately 2.90-2.94 Å), are stabilising for the square-planar geometry in the singlet state.

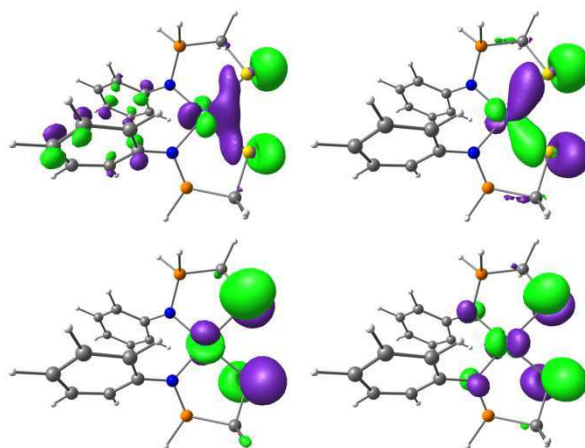
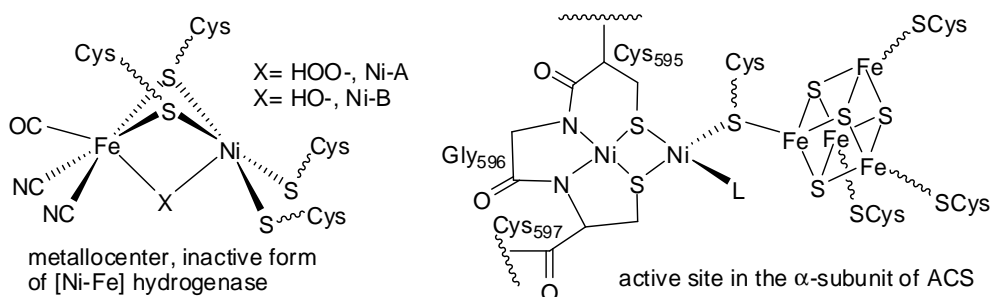


Figure 8. Orbitals in singlet cis-complex for in σ - and π -donating interaction.

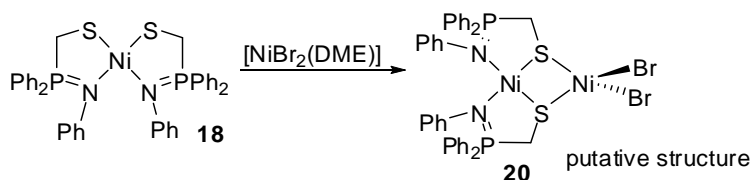
One interesting finding for the *cis*-complex in square-planar geometry is that, the HOMO, HOMO-1 and two other occupied molecular orbitals resulted essentially from orbitals p of S in antibonding/ bonding interaction with d-block orbitals of Ni are in good steric and electronic conditions to enter in σ - and π -interaction with other d-orbitals of a second metal. Thus, this species can behave as a bidentate ligand.

Indeed, multinuclear complexes having discrete $[\text{NiS}_2]$ units, and in particular $[\text{Ni}_2\text{S}_2]$ units serving as S-donor ligand are common in coordination chemistry, because of the tendency of mercapto groups to form bridge between metals. Most of them are synthesised as structural mimics of biological species such as the α -subunit of the acetyl CoA synthase²⁸, or $[\text{Ni-Fe}]$ hydrogenase^{6b, 29}, whose active site are presented in Scheme 19.



Scheme 19. active site of acetyl CoA synthase^{28a, b}, or $[\text{Ni-Fe}]$ hydrogenase^{6b}.

Reaction of complex **18** with $[\text{NiBr}_2(\text{DME})]$ in CH_2Cl_2 gave a green suspension after 2 hours. After solvent removal, a deep green solid was obtained which also corresponds to the formula $[(\text{CH}_2(\text{S})\text{P}(\text{Ph}_2)=\text{N}(\text{Ph}))\text{NiBr}]$ as **19** as attested by elemental analysis. SQUID measurement of this species also showed that one half of the nickel centre is in triplet state. This suggest the formation of dinuclear complex **20**, as shown in scheme 17. The first nickel centre is in square-planar geometry ($S \approx 0$) and the second in tetrahedral geometry ($S \approx 3$). From experimental results, this complex might also be the same species as **19** (Scheme 18). However, no definite evidence was obtained as this product is hardly soluble in common solvents, just like the case with **19**.



Scheme 20. Reaction of **18** with $[\text{NiBr}_2(\text{DME})]$.

Complex **18** was reacted with other metal precursor, especially $[\text{Fe}(\text{CO})_4\text{Br}_2]$. However, as the products are all insoluble in common solvents, their characterisations would not be carried out. Nevertheless, the well controlled formation of **18** and its stability, as well as the electronic properties conferred by iminophosphorane function which differ largely from amines or imines make this species an interesting ligand in synthesizing multinuclear complexes.

IV. Conclusion

Taking into account the importance of sulfur-containing ligands in nature and in coordination chemistry, we were interested in developing new systems combining iminophosphorane and

different sulfur-containing functions. In particular, different bidentate thiolate-iminophosphorane ligands has been synthesised using the ortho-lithiation reaction or nucleophilic substitution. This second synthetic route is in fact based on the first report on a clean nucleophilic substitution on iminophosphorane. Other mixed bidentate ligands combining iminophosphorane and different heteroatoms-containing groups (phosphine, phosphole, silane, borane, etc) have been developed thanks to this reaction. Though coordination chemistry has not been further studied for these ligand precursors, this demonstrated a versatile route to a series of possible bidentate ligands combining iminophosphorane and other donating groups that are very different in steric and electronic properties.

Among the bidentate thiolate iminophosphorane ligands, coordination study has been done extensively on the more flexible ligand **5**. This latter has been coordinated with different transition metal precursors of groups 8, 9, 10. In particular, discrete [NiN₂S₂] complex resulted from the reaction of **5** with 2 equiv. of [NiBr₂(DME)] could act as bidentate ligand through electron pairs on sulfur atoms, leading to bimetallic complexes. Although definite evidence of the coordination ability of this species was not established due to the insolubility of the complexes, along with other ligands synthesised, it enlarges greatly the library of iminophosphorane with sulfur-containing group, in particular, and hetero-atom containing group in general, for further studies in coordination chemistry and catalysis.

REFERENCES

1. (a) Burgess, B. K.; Lowe, D. J., *Chem. Rev.* **1996**, *96* (7), 2983-3011; (b) Howard, J. B.; Rees, D. C., *Chem. Rev.* **1996**, *96* (7), 2965-2982; (c) Kim, J. S.; Rees, D. C., *Science* **1992**, *257* (5077), 1677-1682; (d) Barney, B. M.; Lee, H. I.; Dos Santos, P. C.; Hoffmann, B. M.; Dean, D. R.; Seefeldt, L. C., *Dalton Trans.* **2006**, (19), 2277-2284.
2. Beinert, H.; Kennedy, M. C.; Stout, C. D., *Chem. Rev.* **1996**, *96* (7), 2335-2373.
3. (a) Szczepek, M.; Brondani, V.; Buchel, J.; Serrano, L.; Segal, D. J.; Cathomen, T., *Nat. Biotechnol.* **2007**, *25* (7), 786-793; (b) Jamieson, A. C.; Miller, J. C.; Pabo, C. O., *Nat. Rev. Drug Discov.* **2003**, *2* (5), 361-368; (c) Bibikova, M.; Beumer, K.; Trautman, J. K.; Carroll, D., *Science* **2003**, *300* (5620), 764-764.
4. (a) Blair, A. H.; Vallee, B. L., *Biochemistry* **1966**, *5* (6), 2026-&; (b) Jornvall, H., *Eur. J. Biochem.* **1970**, *16* (1), 25-&; (c) Fisher, H. F.; Conn, E. E.; Vennesland, B.; Westheimer, F. H., *J. Biol. Chem.* **1953**, *202* (2), 687-697; (d) Hayes, J. E.; Velick, S. F., *J. Biol. Chem.* **1954**, *207* (1), 225-244; (e) Racker, E., *J. Biol. Chem.* **1950**, *184* (1), 313-319.
5. (a) Solomon, E. I.; Szilagyi, R. K.; George, S. D.; Basumallick, L., *Chem. Rev.* **2004**, *104* (2), 419-458; (b) Sykes, A. G., *Adv. Inorg. Chem.* **1991**, *36*, 377-408; (c) Solomon, E. I.; Hare, J. W.; Dooley, D. M.; Dawson, J. H.; Stephens, P. J.; Gray, H. B., *J. Am. Chem. Soc.* **1980**, *102* (1), 168-178.
6. (a) Fontecilla-Camps, J. C.; Volbeda, A.; Cavazza, C.; Nicolet, Y., *Chem. Rev.* **2007**, *107* (10), 4273-4303; (b) Tard, C.; Pickett, C. J., *Chem. Rev.* **2009**, *109* (6), 2245-2274; (c) Vignais, P. M.; Billoud, B., *Chem. Rev.* **2007**, *107* (10), 4206-4272.
7. (a) Liu, X. M.; Ibrahim, S. K.; Tard, C.; Pickett, C. J., *Coord. Chem. Rev.* **2005**, *249* (15-16), 1641-1652; (b) Canaguier, S.; Artero, V.; Fontecave, M., *Dalton Trans.* **2008**, (3), 315-325; (c) Jiang, J. F.; Maruani, M.; Solaimanzadeh, J.; Lo, W. F.; Koch, S. A.; Millar, M., *Inorg. Chem.* **2009**, *48* (14), 6359-6361; (d) Ott, S.; Kritikos, M.; Akermark, B.; Sun, L. C.; Lomoth, R., *Angew. Chem. Int. Ed* **2004**, *43* (8), 1006-1009; (e) Holland, P. L.; Tolman, W. B., *J. Am. Chem. Soc.* **2000**, *122* (26), 6331-6332; (f) Randall, D. W.; George, S. D.; Holland, P. L.; Hedman, B.; Hodgson, K. O.; Tolman, W. B.; Solomon, E. I., *J. Am. Chem. Soc.* **2000**, *122* (47), 11632-11648; (g) Sellmann, D.; Fursattel, A., *Angew. Chem. Int. Ed* **1999**, *38* (13-14), 2023-2026; (h) Barriere, F., *Coord. Chem. Rev.* **2003**, *236* (1-2), 71-89; (i) Durrant, M. C., *Inorg. Chem. Commun.* **2001**, *4* (1), 60-62.
8. (a) Cadierno, V.; Diez, J.; Garcia-Alvarez, J.; Gimeno, J., *Organometallics* **2004**, *23* (14), 3425-3436; (b) Cadierno, V.; Diez, J.; Garcia-Alvarez, J.; Gimeno, J., *J. Organomet. Chem.* **2005**, *690* (8), 2087-2096.
9. Cadierno, V.; Diez, J.; Garcia-Alvarez, J.; Gimeno, J., *Organometallics* **2008**, *27* (8), 1809-1822.

10. Chen, J. H.; Guo, J. Y.; Li, Y. X.; So, C. W., *Organometallics* **2009**, 28 (15), 4617-4620.
11. Buchard, A.; Heuclin, H.; Auffrant, A.; Le Goff, X. F.; Le Floch, P., *Dalton Trans.* **2009**, (9), 1659-1667.
12. Alajarin, M.; Lopez-Leonardo, C.; Llamas-Lorente, P.; Bautista, D.; Jones, P. G., *Dalton Trans.* **2003**, (3), 426-434.
13. Alajarín, M.; López-Leonardo, C.; Llamas-Lorente, P.; Raja, R., *Tetrahedron Lett.* **2007**, 48 (39), 6987-6991.
14. Sellmann, D.; Prakash, R.; Heinemann, F. W.; Moll, M.; Klimowicz, M., *Angew. Chem. Int. Ed* **2004**, 43 (14), 1877-1880.
15. Ohki, Y.; Sakamoto, M.; Tatsumi, K., *J. Am. Chem. Soc.* **2008**, 130 (35), 11610-+.
16. (a) Sellmann, D.; Hille, A.; Heinemann, F. W.; Moll, M.; Reiher, M.; Hess, B. A.; Bauer, W., *Chem. Eur. J.* **2004**, 10 (17), 4214-4224; (b) Sellmann, D.; Rackelmann, G. H.; Heinemann, F. W., *Chem. Eur. J.* **1997**, 3 (12), 2071-2080; (c) Sellmann, D.; Prakash, R.; Heinemann, F. W., *Dalton Trans.* **2004**, (23), 3991-3996; (d) Dahlenburg, L.; Gotz, R., *Eur. J. Inorg. Chem.* **2004**, (4), 888-905; (e) Sellmann, D.; Gottschalk-Gaudig, T.; Heinemann, F. W., *Inorg. Chem.* **1998**, 37 (16), 3982-3988; (f) Sakamoto, M.; Ohki, Y.; Kehr, G.; Erker, G.; Tatsumi, K., *J. Organomet. Chem.* **2009**, 694 (17), 2820-2824; (g) Ienco, A.; Calhorda, M. J.; Reinhold, J.; Reineri, F.; Bianchini, C.; Peruzzini, M.; Vizza, F.; Mealli, C., *J. Am. Chem. Soc.* **2004**, 126 (38), 11954-11965; (h) Misumi, Y.; Seino, H.; Mizobe, Y., *J. Am. Chem. Soc.* **2009**, 131 (41), 14636-+; (i) Sweeney, Z. K.; Polse, J. L.; Bergman, R. G.; Andersen, R. A., *Organometallics* **1999**, 18 (26), 5502-5510.
17. Stuckwisch, C. G., *J. Org. Chem.* **1976**, 41 (7), 1173-1176.
18. Steiner, A.; Stalke, D., *Angew. Chem. Int. Ed.* **1995**, 34 (16), 1752-1755.
19. (a) Wei, P.; Chan, K. T. K.; Stephan, D. W., *Dalton Trans.* **2003**, (19), 3804-3810; (b) Chan, K. T. K.; Spencer, L. P.; Masuda, J. D.; McCahill, J. S. J.; Wei, P.; Stephan, D. W., *Organometallics* **2003**, 23 (3), 381-390.
20. (a) Wingerter, S.; Pfeiffer, M.; Stey, T.; Bolboacă, M.; Kiefer, W.; Chandrasekhar, V.; Stalke, D., *Organometallics* **2001**, 20 (13), 2730-2735; (b) Wingerter, S.; Gornitzka, H.; Bertrand, G.; Stalke, D., *Eur. J. Inorg. Chem.* **1999**, 1999 (1), 173-178.
21. Boubekour, L.; Ricard, L.; Mezailles, N.; Demange, M.; Auffrant, A.; Le Floch, P., *Organometallics* **2006**, 25 (12), 3091-3094.
22. Gomez, G. R.; Fernandez, I.; Ortiz, F. L.; Price, R. D.; Davidson, M. G.; Mahon, M. F.; Howard, J. A. K., *Organometallics* **2007**, 26 (3), 514-518.
23. (a) Seyferth, D.; Welch, D. E., *J. Organomet. Chem.* **1964**, 2 (1), 1-7; (b) Seyferth, D.; Heeren, J. K.; Welch, D. E., *J. Am. Chem. Soc.* **1963**, 85 (5), 642-647; (c) Seyferth, D.; Welch, D. E.; Heeren, J. K., *J. Am. Chem. Soc.* **1964**, 86 (6), 1100-1105.
24. Hay, P. J.; Wadt, W. R., *J. Chem. Phys.* **1985**, 82 (1), 270-283.

25. Roy, L. E.; Hay, P. J.; Martin, R. L., *J. Chem. Theory Comput.* **2008**, *4* (7), 1029-1031.
26. Ehlers, A. W.; Bohme, M.; Dapprich, S.; Gobbi, A.; Hollwarth, A.; Jonas, V.; Kohler, K. F.; Stegmann, R.; Veldkamp, A.; Frenking, G., *Chem. Phys. Lett.* **1993**, *208* (1-2), 111-114.
27. Petersson, G. A.; Bennett, A.; Tensfeldt, T. G.; Allaham, M. A.; Shirley, W. A.; Mantzaris, J., *J. Chem. Phys.* **1988**, *89* (4), 2193-2218.
28. (a) Darnault, C.; Volbeda, A.; Kim, E. J.; Legrand, P.; Vernede, X.; Lindahl, P. A.; Fontecilla-Camps, J. C., *Nat Struct Mol Biol* **2003**, *10* (4), 271-279; (b) Doukov, T. I.; Iverson, T. M.; Seravalli, J.; Ragsdale, S. W.; Drennan, C. L., *Science* **2002**, *298* (5593), 567-572; (c) Matsumoto, T.; Ito, M.; Kotera, M.; Tatsumi, K., *Dalton Trans.* **2010**, *39* (12), 2995-2997.
29. Oudart, Y.; Artero, V.; Pécaut, J.; Fontecave, M., *Inorg. Chem.* **2006**, *45* (11), 4334-4336.

Chapter 2

Iminophosphorane-Phenoxide Bidentate Ligands & Applications in Oligomerisation of Ethylene

I. Introduction

1. Oligomerisation of Ethylene

Linear alpha olefins (LAOs) are important chemicals in industry, with important applications in various domains. The main uses of alpha molecules are represented in the table 1.¹ The low carbon numbered compounds (C4-C8) are mainly used as co-monomer in polyethylene production because the addition of alpha olefines co-monomers creates branches and renders the polymer more flexible. It's also thanks to the presence of these branches that many polyalphaolefines, from the polymerisation of alpha olefine (C12 and more) do not easily crystallise or solidify and remain oily even at low temperature and thus could serve as lubricants in a wide temperature range. LAOs (mainly C4-C8) are also used for the production of linear aldehydes by hydroformylation (addition of CO and H₂) for latter production of short-chain fatty acids or alcohols (used as plasticizers). C10-C14 linear alpha olefines are used to make surfactants for aqueous detergent formulations, the higher C16-C16 LAOS are used as the hydrophobes in oil soluble surfactants, etc.

Table 1. Main use of LAOs, from Forestiere et al¹

Polyethylene comonomer C4-C8	Oxo alcohols C6-C16	Poly alpha olefins C10-C14	others
40%	19%	14%	27%

The main route to LAOs is the oligomerisation of ethylene. A remarkable catalytic system for the selective production of linear alpha olefins is the Shell Higher Olefin Process (SHOP), developed by Keim and coworkers², using $[\text{Ni}(\text{P},\text{O})(\text{PR}_3)\text{R}']$ system. Alpha olefins C6-C18 could be obtained from the process following a geometric Schulz-Flory distribution.

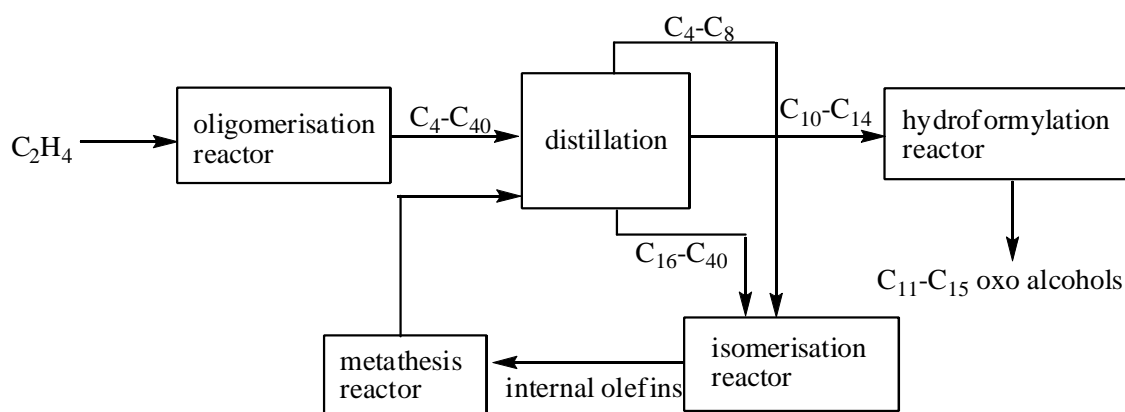


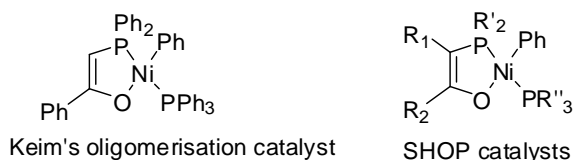
Figure 1. SHOP process^{3a, 2b, 3b}

The two important industrial processes allowing the selective production of hexene and butene are the Philips trimerisation process, based on the work of Morgan and co-workers⁴ and employed by Chevron-Philips,^{5, 1} and the Alphabutol process, developed by Chauvin and coworkers at IFP.⁶ The latter utilises titanium alkoxide complexes along with alkyl aluminum as co-catalyst, accounts for nearly 25% of 1-butene serving as co-monomer in PE units. The selectivity of 1-butene could be up to 93% in optimised condition. The modified process, called AlphaSelect, using a different catalyst, produces C4-C10 alpha olefins with high selectivity and the ability of adjusting the olefins distribution.

2. Nickel Catalysts for Dimerisation of Ethylene.

The use of nickel complexes in homogenous catalysis and in particular, in olefin oligomerisation dated back to the 50s from a discovery of Karl Ziegler and co-workers, latter called the “nickel effect”. They found that the presence of nickel salt in catalytic system for the polymerisation of ethylene by titanium complexes and alkyl aluminum compounds changed the product nature: instead of polymers, they obtained 1-butene.

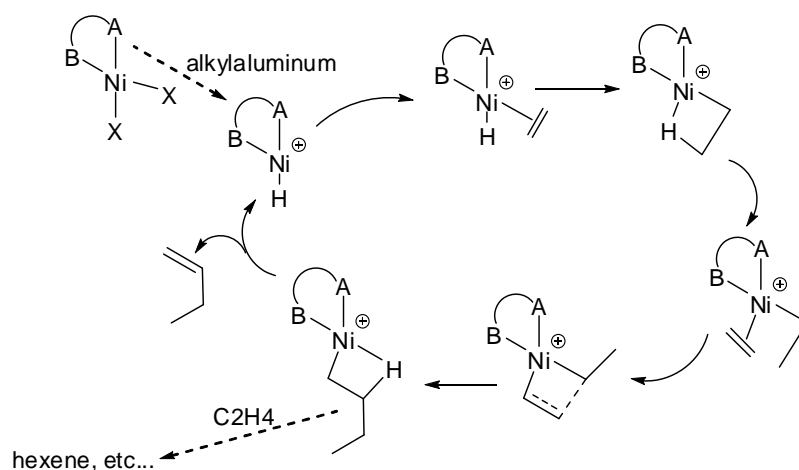
The SHOP process described above used nickel complexes (Scheme 1). Following its success, many other nickel complexes have been made in order to obtain highly active and selective catalysts for the oligomerisation of ethylene, and in particularly the di- or tri-merisation of this compound, as the commercial demands for alpha olefins C4-C10 is high and has increased these years. Variations for the ligand close to the ones in SHOP process would not be detailed here and could be found in publications by Keim and coworkers.^{2a, 7} Notable systems using nickel complexes for the oligomerisation/polymerisation of ethylene will be briefly discussed.



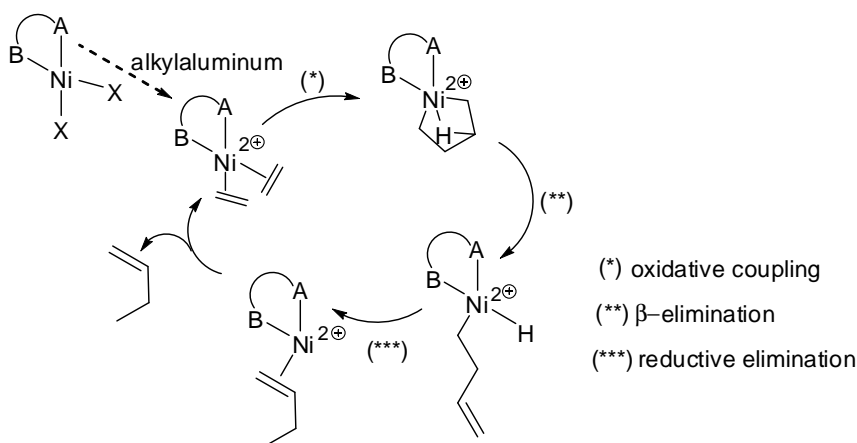
Scheme 1. Nickel complexes for the oligomerisation of ethylene: SHOP complexes and Keim's complexes.

2.1 Mechanism of the Oligomerisation and Polymerisation of Ethylene using Ni Complexes

The oligomerisation/polymerisation of ethylene using nickel complexes is often assumed to go through a Cossee mechanism (Scheme 2),⁸ although a metallacyclic mechanism^{9, 1} (Scheme 3) as in the case of the titanium catalysts involved in the Alphabutol process and the chromium catalysts in the Phillips trimerisation process is also conceivable. In our laboratory, full DFT calculations on the two possible mechanisms have shown that the Cossee mechanism is the more suitable one.¹⁰



Scheme 2. Simplified representative Cossee mechanism of the dimerisation of ethylene with nickel complex



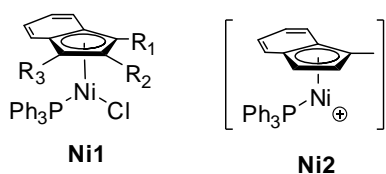
Scheme 3. Simplified representative metallacyclic mechanism of the dimerisation of ethylene with nickel complex

2.2 Catalysts

Nickel complexes tested in oligomerisation and polymerisation of ethylene often include a bi/tri-dentate ligand, as multidentate ligands could offer better control of the intermediate configurations and thus better control over the catalytic reaction of ethylene. Except several examples of indenyl nickel complexes where the multidentate ligands is aromatic ring, other ligands for nickel complexes could be divided into several groups based on the atoms coordinated to Ni: (P,P), (N,N), (N, P), (O,N), (O, P)

Indenyl Nickel Complexes

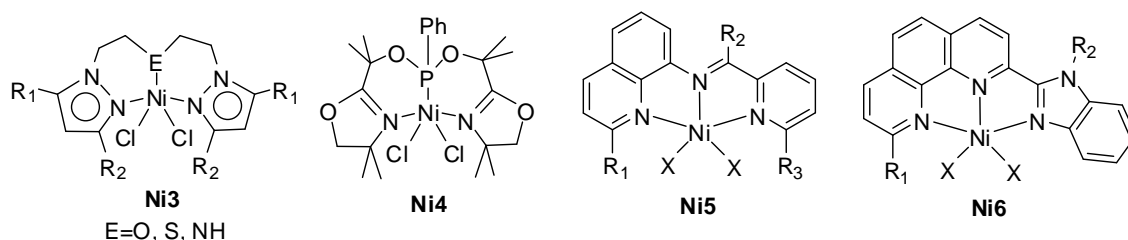
The phosphine nickel indenyl complexes have been used successfully. The neutral complex **Ni1** synthesized by Collins et al acts along with MAO as catalysts for the polymerisation of ethylene,¹¹ giving PE with PDI from 1.7-2.0. On the other hand, the cationic complex **Ni2** arising from the abstraction of the chloride, described by the same group,¹² gives only 1-butene, as shown by GC/MS analyses with an ethylene consumption rate of *ca.* 390 000 mol(C₂H₄)/mol(Ni)/h. The species was not isolated but has been trapped with several agents which allowed the isolation of more stable complexes.



Scheme 4. Nickel indenyl complexes

Nickel Complexes of Tridentate Ligands

The coordination of tridentate N,X,N ligands to NiCl₂ gave penta-coordinated Ni complexes which are efficient for the oligomerisation of ethylene. The best example is given by Carpentier et al. Their nickel complexes with tridentate pyrazolyl ligands¹³ (general structure **Ni3**, Scheme 5) can achieve performance up to TOF=80 000 mol(C₂H₄)/mol(Ni)/h. The selectivity of these systems could be up to 93% in 1-butene, all in maintaining a very high TOF (60 000 mol(C₂H₄)/mol(Ni)/h). A very similar system of penta-coordinated Ni with bidentate ligand developed by Braunstein¹⁴ (**Ni4**, Scheme 5) gave a TOF of 31 400 during 35 min, with 70% selection in C₄, using a very low loading of co-catalyst Al/Ni=6/1. The content in alpha-olefin in the product was not high, however.

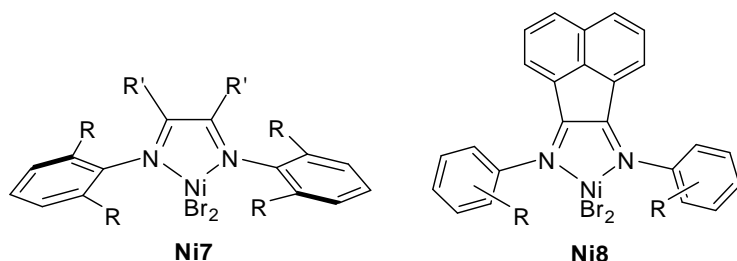


Scheme 5. Nickel complexes with tridentate ligands

A more rigid system as the one reported by Sun¹⁵ based on N-((pyridin-2-yl)methylene)quinolin-8-amine (general structure **Ni5**, Scheme 5) could give generally high TOFs, and in the same time achieve high selectivity in butane and 1-butene. When R₁=*i*-Pr, R₃=Me, X=Cl, the TOF of the oligomerisation was up to 120 000 mol(C₂H₄)/mol(Ni)/h during 20 min, with 92.9% of C₄ and 91.2% 1-C₄. These systems use however a very important amount of Et₂AlCl as co-catalyst (Al/Ni=500/1). A similar systems, based on the more rigid and less-donor ligands (2-(benzimidazol-2-yl)-1,10-phenanthrolines), reported by Lu¹⁶ and coworkers are also highly active (general structure **Ni6**, Scheme 5). One of the most active complex, with R₁=R₂=H, X=Cl, gave a TOF of up to 314 000 mol(C₂H₄)/mol(Ni)/h during 20 min with 89.9% C₄ (66% in 1-C₄). However, just like complexes **Ni5**, these systems use very high charge of co-catalyst (Et₂AlCl/Ni=1000/1).

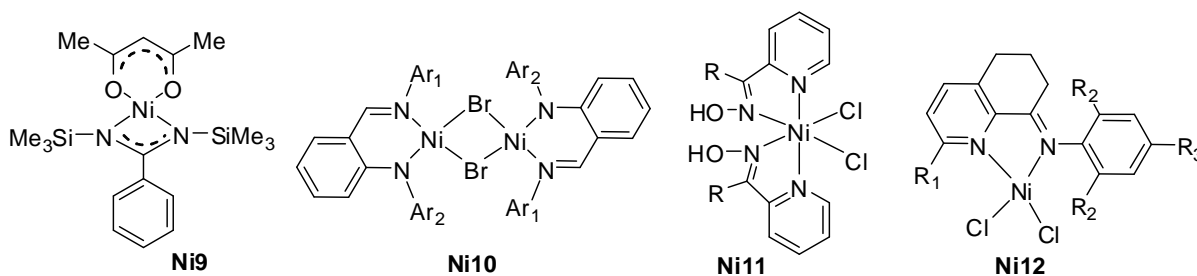
Nickel Complexes of Bidentate Ligands (N,N), (N,P), (P,P)

Bidentate (N,N) and (N,P) ligands based one amine, imine, amide and phosphine functions are very often used and fine tuning of the steric and electronic properties of these ligands could provide strong catalysts. Among the notable systems are α -diimine nickel(II) complexes, studied by Brookhart and coworkers.¹⁷ They could catalyse either the polymerization (Complexes **Ni8**, Scheme 6) or the oligomerisation of ethylene (Complexes **Ni7**, Scheme 6), depending on the steric bulk of the α -diimine ligands. The oligomerisations are however not selective and follow Schulz-Flory distributions just like in the case of SHOP catalysts.



Scheme 6. α -diimine nickel(II) complex.,

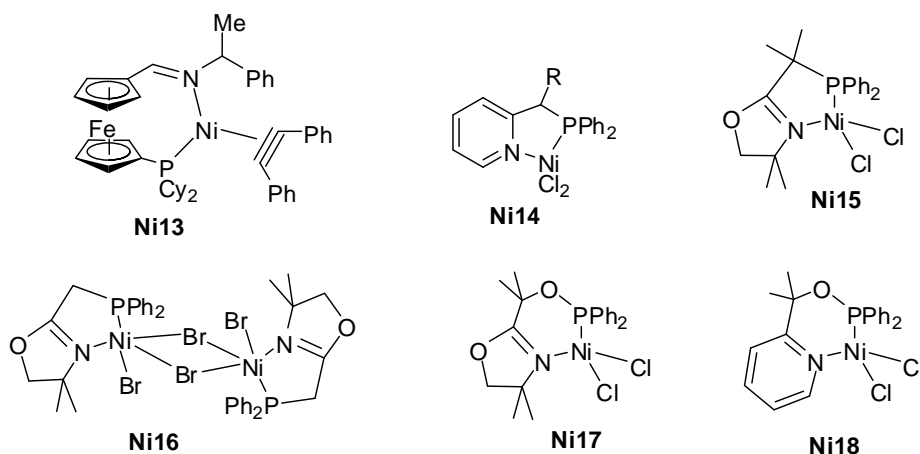
The nickel complexes based on other bidentate (N,N) ligands, but combining imine-amide functions reported by Wu¹⁸ (**Ni10**, Scheme 7) and Eisen¹⁹ (**Ni9**, Scheme 7) are also unselective in the oligomerisation of ethylene. Better selectivities have been observed with systems using imine-pyridine bidentate ligands. For example, Mukerjee²⁰ and coworkers reported nickel complexes of general structures **Ni11** (Scheme 7) which gave very high values of TOFs (around 130 000-170 000 mol(C₂H₄)/mol(Ni)/h) over a period of 30 min, along with a selectivity of 92% in butane. A reasonable amount of Et₂AlCl as co-catalysts (Al/Ni=100/1) is needed for the oligomerisation. Same order of activity has been observed for other complexes with imine-pyridine ligand reported by Sun and coworkers (general structure **Ni12**, Scheme 7).²¹ The group also claimed that changes of co-catalyst from Et₂AlCl to ethylenealuminum sesquichloride (ESAC) was beneficial. High TOFs (up to 310 000 mol(C₂H₄)/mol(Ni)/h over a period of 30 min, when R₁=Cl, R₂= i-Pr, R₃=H) and high selectivities (89.6% in C₄ (of which >99% 1-C₄)) were obtained. The experiments were done under 10 bar of ethylene. Note that in these examples, the charge in ESAC was very high (Al/Ni=400/1).



Scheme 7. Nickel complexes of bidentate imine-amide and imine-pyridine ligands

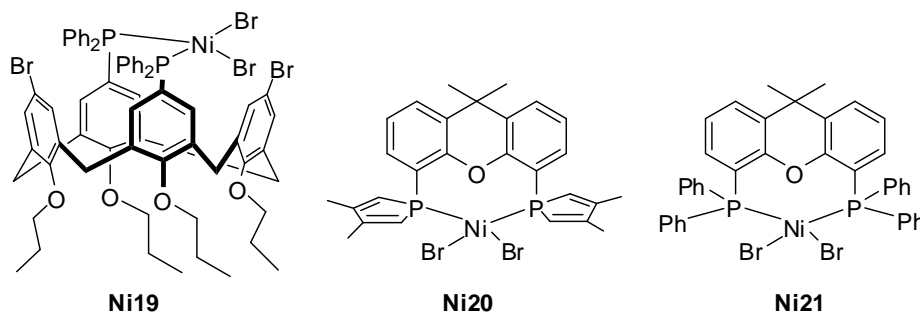
Hor²² developed complexes of (P,N) ferrocenediyl imine-phosphine bidentate ligands (**Ni13**, Scheme 8) which are very active (TOF up to 91 600 mol(C₂H₄)/mol(Ni)/h during 3h with a reasonable amount of cocatalyst Et₂AlCl/Ni=146), but not very selective for the oligomerisation of ethylene (69.9% C₄, 45.9% alpha olefins). Other complexes with (P,N) bidentate ligands, such as phosphinopyridine²³ (**Ni14**), phosphino oxazoline²⁴ (monomer **Ni15**, or dimer **Ni16**), phosphinito oxazoline²⁵ (**Ni17**), phosphinito (**Ni18**) and phosphonito-pyridine^{23b} developed by Braunstein and coworkers also present the same behavior: high activity and limited selectivity in C₄. For example, with a very low loading of co-catalyst EtAlCl₂/Ni=6/1, the phosphino

pyridine complexes **Ni14**^{23a} with R=Me could give TOF up to 55 200 over 35 min run, under p(C₂H₄)=10 bar. The selectivities are however not excellent: for the same cited reference the products contained 66% C₄ and 30% C₆, selection 11% in α -C₄. Details about (P,N) chelating ligands and dimerisation of ethylene have been the objects of a review by the same group.²⁶



Scheme 8. Examples of nickel complexes of (N,P) bidentate ligands

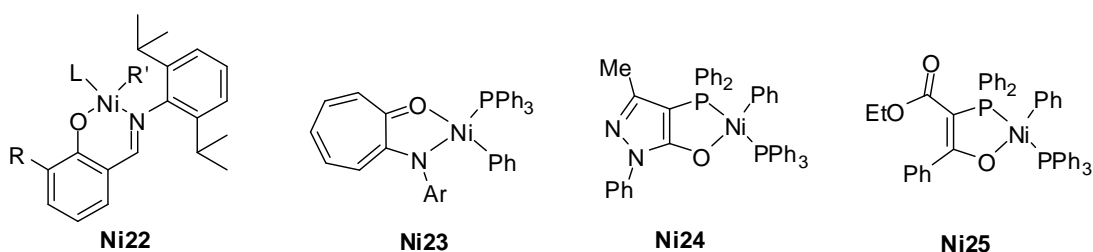
Matt's group suggested that the use of a ligand with large bite angle would facilitate the elimination step terminating the catalytic cycle, thus increase the catalytic activity. They successfully synthesised diphosphinated calix[4]arenes systems which upon coordination to Ni^{II} centres give strongly active complexes for the dimerisation of ethylene (for example, **Ni19**, Scheme 9).²⁷ Complex **Ni19** could give a TOF of up to 830 000 mol(C₂H₄)/mol(Ni)/h for a run during 15 min at 20 bar (C₂H₄). The selectivity in 1-butene was limited due to the isomerisation reactions. In the laboratory, other complexes based on diphospholes with large bite angle were synthesized (**Ni20**, **Ni21**, Scheme 9).²⁸ They act as highly selective catalysts for the dimerisation: oligomerisation catalysed by **Ni20** gave 97% selection in C₄ (90% in 1-C₄) for a high TOF of 43 000 mol(C₂H₄)/mol(Ni)/h. Complex **Ni21**, however, is less active: under the same conditions, the TOF was of 14 000 mol(C₂H₄)/mol(Ni)/h, with 96% selection in C₄ (88% in 1-C₄).



Scheme 9. Complexes of bidentate (P,P) ligands with large bite angle.

Nickel Complexes of (N,O) or (P,O) Chelating Ligands.

As the complexes in the SHOP process are based on (P,O) bidentate ligands, many systems employing (N,O) and (P,O) bidentate ligands have been elaborated. However, most of them direct the polymerisation of ethylene and very few are active for the oligomerisation. For example, nickel salicylaldimine complexes **Ni22** (Scheme 10) developed by Grubbs and coworkers²⁹ or the anilintropone complexes **Ni23** (Scheme 10) reported by Brookhart and coworkers³⁰ are highly active in polymerisation. **Ni22** with R=9-anthracene, R'=Ph, L=PPh₃, catalysed exclusively the polymerization of ethylene with high efficiency (TOF=1.2x10⁶ g(PE)/mol(Ni)/h, M_w= 347 000, PDI=3.0, without co-catalyst). **Ni23** with Ar = C₆H₃(iPr)₂ is also highly active in the polymerization of ethylene, with a TOF of 1.34x10⁶ g(PE)/mol(Ni)/h, giving polymers with M_n=104 000 and a rather low polydispersity PDI=1.95.



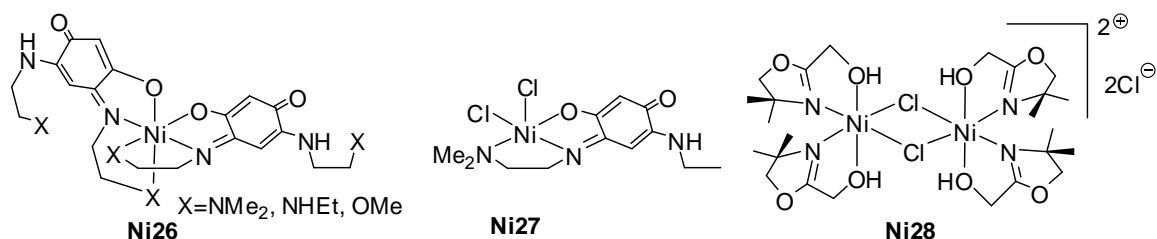
Scheme 10. Complexes of (N,O) and (P,O) bidentate ligands.

When electron poor (P,O) ligands⁷ were employed, as those reported by Matt and coworkers, short chain olefins were formed instead of polyethylene. For example, oligomerisation catalysed by **Ni25** (Scheme 10) could attain TOF=68 000 for 1h run, with a selection on C₄-C₁₆ equals to 12.3% (in weight), the Schulz-Flory parameter $\alpha = \text{mol}(C_{n+2})/\text{mol}(C_n)$ being 0.93.^{7b} Alpha olefins were yielded primarily (wt%=95.8).

Under a constant pressure of ethylene (p=5 bar), in 30 min, **Ni24** catalysed the formation of C₄-C₁₆ in 80.2% weight (of which 96.2% weight of alpha olefins), the TOF was of 14 400 mol(C₂H₄)/mol(Ni)/h. The in situ generated complex obtained from **Ni24**, where the coordinated phenyl was replaced by a coordinated ethylene molecule, catalysed the formation of polyethylene.^{7a}

The Ni complexes (general structures **Ni26**, **Ni27**, Scheme 11) supported by benzoquinonemonoimine (N,O) chelates developed by Braunstein and coworkers show much better selectivity in oligomerisation of ethylene, with selectivity in C₄ up to 90% with TOF of 24 000 mol(C₂H₄)/mol(Ni)/h.³¹ The amount of α -olefins is however very limited (9.4%). The same group also developed (4,5-dihydro-4,4-dimethyloxazol-2-yl)methanol as (N,O) chelating ligands for Ni complexes (for example, **Ni28**, Scheme 11).³² These complexes are generally very active and selective in oligomerisation of olefins. Complex **Ni28** offered a TOF of 20 700 mol(C₂H₄)/mol(Ni)/h, with 92% in C₄ (with 62% in 1-C₄), using a very low co-catalyst charge

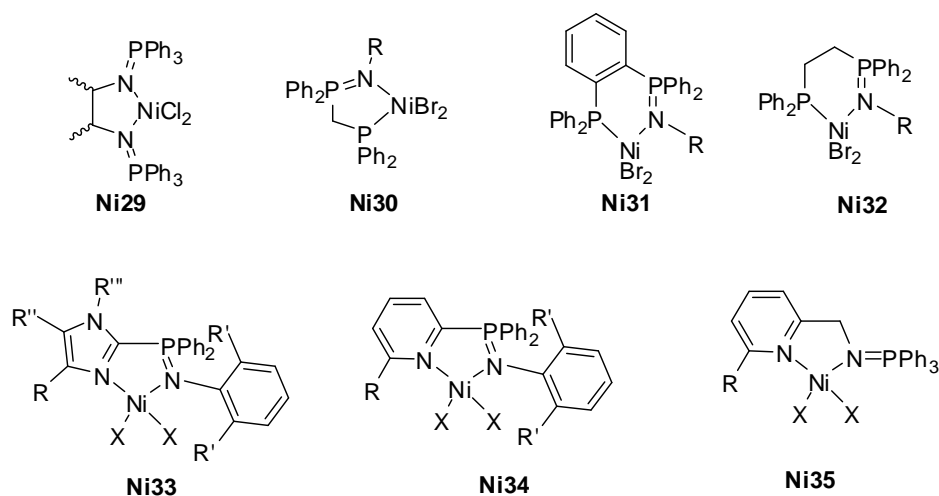
(AlEtCl₂/Ni=2/1). Activities could be increased with increasing the amount of Al, but this led to a dramatic decrease in C₄-selectivity.



Scheme 11. Nickel complexes of (N,O) ligands, developed by Braunstein and coworkers.

Nickel Complexes of Iminophosphoranones

The use of iminophosphoranones for nickel-catalysed oligomerisation has been reported by several groups. All of them are bidentate (N,N) or (N,P) ligands. In 2001, Reau and coworkers reported the synthesis and activities of bis(iminophosphorane) nickel complexes (general structure **Ni29**, Scheme 12).³³ For an 1h run under very low pressure of C₂H₄ (p(C₂H₄)=1.1 bar), the most active catalyst (with phenylene bridge) offered a TOF of 11 000 mol(C₂H₄)/mol(Ni)/h with 61% selectivity in C₄ (2% of 1-C₄).

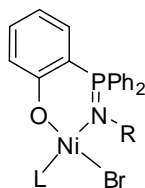


Scheme 12. Nickel-iminophosphorane complexes for the oligomerisation of ethylene.

In 2003, Stephan et coworkers reported on nickel complexes of bidentate ligands combining iminophosphorane and pyridine- or imidazole (**Ni33-35**, Scheme 12).³⁴ They showed at best an activity of 48 g oligomer/g cat/h/atm, i.e. TOF<1000 mol(C₂H₄)/mol(Ni)/h, with very low content in alpha olefins (1-C₄/2-C₄=1%/99%). If, however, the iminophosphoranones are associated with a softer donor group (phosphine for example), just as the complexes developed in our laboratory in 2007 (**Ni30-32**, Scheme 12), the resulted complexes offer much better performance in dimerisation of olefins, in terms of both activity and selectivity.³⁵ As an

example, oligomerisation of ethylene catalysed by **Ni31**, with R=iPr, gave TOF up to 166 000 mol(C₂H₄)/mol(Ni)/h for a run of 1h under 30 bar of ethylene. The selectivity was 97% in C₄ (73.6% in 1-C₄).

As the examples of iminophosphorane nickel complexes active in oligomerisation of ethylene remains relatively scarce in comparison with amine or imine functions, and as a continuation of our work in developing bidentate ligands associating one iminophosphorane and one anionic donor group, we were interested in nickel complexes of these types of ligands.



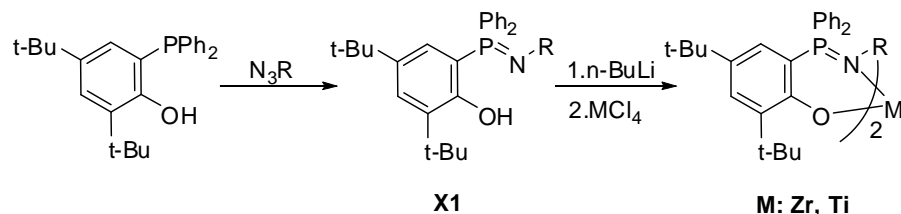
Scheme 13. Targeted nickel complexes

Bidentate ligands containing iminophosphorane and phenoxide were chosen to be studied (Scheme 13). In fact, as has been observed above, nickel complexes of (N,O) or (P,O) chelating ligands are not highly active in oligomerisation of ethylene. On the other hand, it seems that the combination of iminophosphorane with a soft, electron-rich donating group is beneficial for the performance of the complexes. It would be thus difficult to predict the performance of such systems in oligomerisation of ethylene.

II. Synthesis and Activities of Ni-PO Complexes

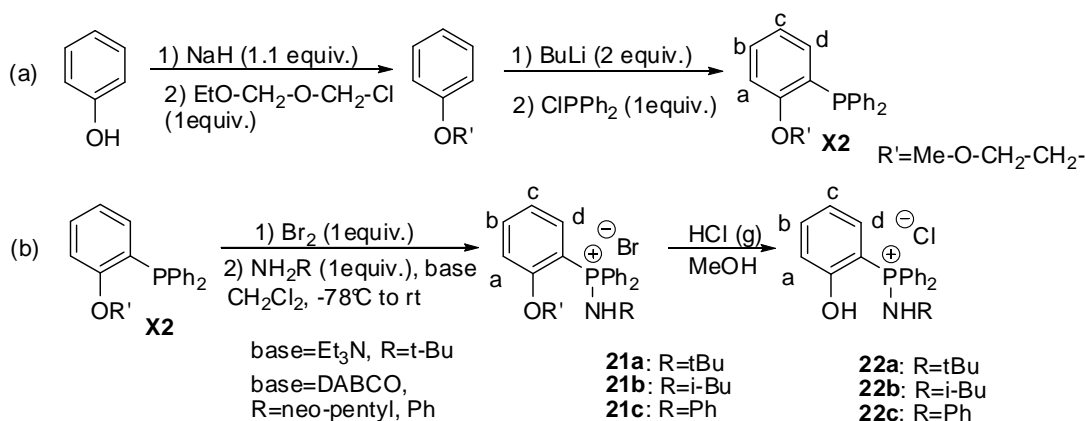
1. Ligand Synthesis

In fact, an example of one ligand phenoxide-iminophosphorane already existed in the literature. In 2005, the group of Zhang synthesized the iminophosphorane **X1** by the Staudinger method (Scheme 14).³⁶ The resulting ligand was coordinated to zirconium and titanium centres. These two complexes showed little activities in polymerization of ethylene: under various activation conditions with MAO (Al/M=2000/1) or *i*-Bu₃Al/Ph₃CB(C₆F₅)₄ (Al/M = 100/1) as co-catalysts, only traces of polymer was obtained.



Scheme 14. Synthesis of alkolate-iminophosphorane ligands by Zhang and coworkers

As the use of azides may restrain the possible substitution pattern at the nitrogen atom, another approach was developed using the Kirsanov reaction on the protected phosphinophenol **X2** (Scheme 15). This latter in turn was prepared from phenol according to a procedure described by Bianchi and coworkers (Scheme 15 (a)).³⁷ After the formation of the aminophosphonium salt, a simple deprotection of the phenol group gave the phenol aminophosphonium salt as colorless crystals or white solid in reasonable yields (60-71% of total yield for the synthesis of **2a-c** from **X2**).



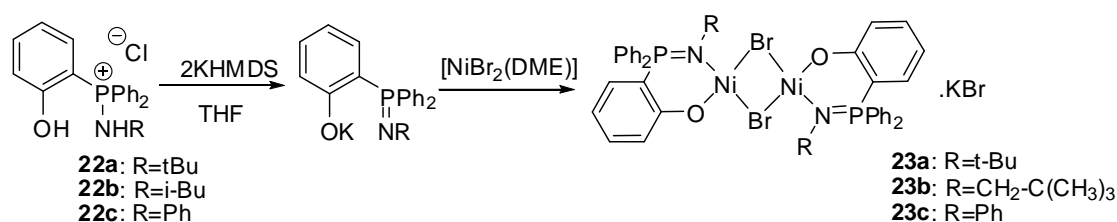
Scheme 15. Synthesis of alcohol-aminophosphonium ligand.

All compounds **22a-c** were fully characterized by NMR multinuclear. In ³¹P{¹H}NMR spectra, each of the three compounds **22a-c** exhibits a unique singlet in the zone (**22a**: 35.2 ppm, **22b**: 36.4 ppm, **22c**: 39.9 ppm), corresponding to the chemical shift of the aminophosphonium groups.

After a double deprotonation with 2 equiv. of KHMDS, colorless solutions were obtained for all three ligands with significant high field chemical shift in ³¹P{¹H} NMR spectra (**22a**: 12 ppm, **22b**: 14.6 ppm, **22c**: 8.4 ppm). These values are much higher than the simple iminophosphorane function in THF (typically from -10 ppm to -20 ppm for the iminophosphorane without a phenoxide function), and differ by the way of deprotonation (when using MeLi, values of chemical shifts are slightly higher). Thus, they are supposed to be the one of the phenoxide iminophosphorane with coordinated potassium (or lithium) cation. However, definitive evidence of this coordination by X-ray diffraction experiments was not obtained due to the difficulty to grow mono-crystal.

As it is unnecessary to isolate the anionic iminophosphorane-phenoxide ligands, coordination tests were carried out on in situ generated ligands from reaction of **22a-c** with KHMDS.

2. Complexes Synthesis

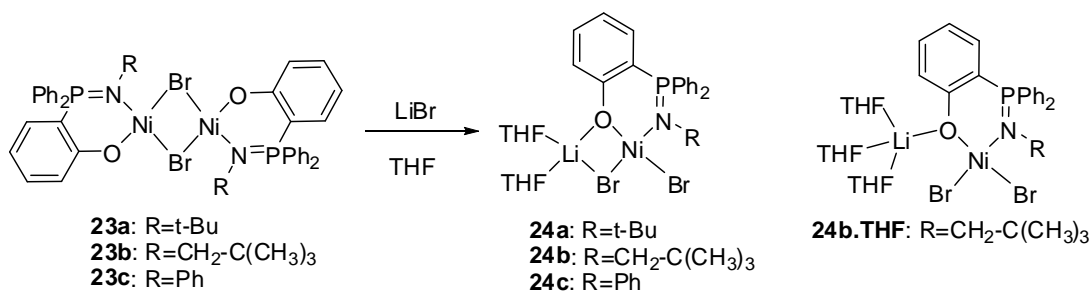


Scheme 16. Coordination of iminophosphorane-phenoxide ligands with $[\text{NiBr}_2(\text{DME})]$

Addition of $[\text{NiBr}_2(\text{DME})]$ into the solutions issued from the deprotonation of **22a-c** with 2 equiv. of KHMDS in THF immediately yielded pale purple-to-red solutions along with the formation of a white insoluble potassium bromide salt. The complete disappearance of the signal in $^{31}\text{P}\{^1\text{H}\}$ NMR spectrum indicates the completeness of the coordination reaction and the formation of paramagnetic nickel(II) compounds. After removal of insoluble potassium salts by centrifugation, evaporation of THF and washing of the resulting solid with petroleum ether, nickel complexes **23a-c** were isolated in good yield as pale purple solids for **23a-b**, and a green solid for **23c**.

Elemental analyses correspond to the presence of one molecule of KBr for two Ni centres. This stoichiometry for KBr and the difficulty of complete removal of this molecule suggest that KBr is coordinated to the nickel complex(es), maybe through the interaction with the oxygen of the phenoxides. Structures of complexes **23a-c** as presented in Scheme 16 are just putative simplistic representations. Attempts have been carried out in order to obtain crystals of **23a-c** for X-ray diffraction experiments, using various solvent systems at different temperatures, but no crystal was obtained.

As the coordination of this oxygen with hard cation such as Li is stronger than the one with potassium, lithium could replace the potassium in the above-mentioned complexes. Indeed, the addition of one equivalent of lithium bromide into the solution of **23a-c** in THF results immediately in a change of color from pale purple-blue to deep blue-purple (**24a-b**) or deep green (**24c**). In decreasing the solvent volumes, lithium-nickel complexes precipitated out as purple crystals (**24a-b**) or green crystals (**24c**).



Scheme 17. Formation of bimetallic nickel-lithium complexes.

Single crystals of **24a-c** suitable for X-ray diffraction experiments were obtained by slow diffusion of petroleum ether into a THF solution of the complexes at -40°C . These crystals are extremely sensitive towards the raise of temperature, probably because of the incorporation of many THF molecules in the crystals structures.

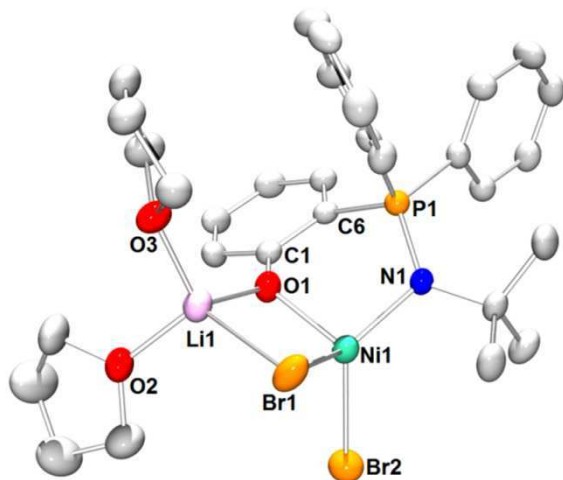


Figure 2. Ortep view of complex **24a**. Hydrogen atoms and non-coordinated THF molecules have been omitted for clarity. Thermal ellipsoids are drawn at the 50% probability level. Selected distances (\AA) and angles ($^{\circ}$): Ni1-N1 1.977(2), Ni1-O1 1.954(2), Ni1-Br1 2.4526(5), Ni1-Br2 2.3799(5), Li1-Br1 2.535(5), Li1-O1 1.893(5), Li1-O2 1.915(6), Li1-O3 1.915(6), N1-P1 1.602(2), O1-C1 1.332(3), O1-Ni1-N1 98.30 (8), N1-Ni1-Br2 116.17(7), Br2-Ni1-Br1 104.99(2), Br1-Ni1-O1 91.47(6), Li1-O1-Ni1 102.2 (2), Li1-Br1-Ni1 73.8 (1), Br1-Li1-O1 90.4 (2), O1-Li1-O3 117.3 (3), O3-Li1-O2 104.4(3), O2-Li1-Br1 16.5(2),

24a is a bimetallic complex (Figure 2). The driving force of the formation of this bimetallic structure is probably the strong interaction between $\text{O}_{\text{phenoxide}}$ and Li atoms. Both the nickel and lithium are in tetrahedral geometry. The two metallic centres Li and Ni are bridged by Br and O-phenoxide atoms, forming a nearly-planar four-membered ring, as shown by the value of the distortion angle O1-Li1-Br1-N1 close to 10° , the two angles at Ni and Li being very close to 90° . Both Li and Ni adopt slightly distorted tetrahedral geometry. The Ni1-Br1 bond (2.4526(5) \AA) is slightly longer than Ni1-Br2 (2.3799(5) \AA) due to the bridging position of the Br1 atom.

The crystals comprise one non-coordinated THF molecule and is very sensitive to air and temperature. Despite this fragility, the structure described above of the dinuclear complex is maintained in dried solid state, as elemental analysis done on vacuum-dried crystals evidences the presence of LiBr and two molecules of THF.

Elemental analysis results showed the same composition for the two other compounds **24b-c** in the solid state after drying, i.e. the formation of bimetallic complexes with the presence of one LiBr and two molecules of THF. However, X-ray diffraction on single crystals of **24b** obtained from slow diffusion of petroleum ether over a solution in THF shows a different structure (Figure 3). The complex is still binuclear, but this time the Li cation is linked only to the

phenoxide oxygen and surrounded by three THF molecules. Upon drying the solid in vacuum, a four-membered ring similar to the one in **24a** is probably formed along with the release of one coordinated THF, which explains the composition found in elemental analysis.

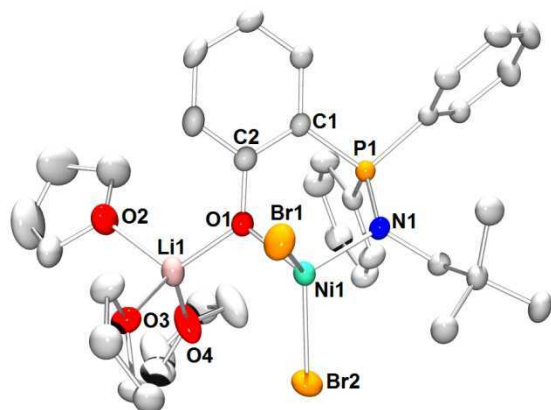


Figure 3. Ortep view of complex **24b-THF**. Hydrogen atoms and non-coordinated THF molecules have been omitted for clarity. Thermal ellipsoids are drawn at the 50% probability level. Exchange between Br and Cl anions is observed for the coordinated bromides, probably because of traces of chloride anions from the deprotonation step. Selected distances (Å) and angles (°): Ni1-N1 1.981(3), Ni1-O1 1.975(2), Ni1-Br1 2.4020(8), Ni1-Br2 2.381(2), Li1-O1 1.930(7), Li1-O2 2.006(7), Li1-O3 1.945(7), Li1-O4 1.917(7), N1-P1 1.607(3), O1-C2 1.338(4), O1-Ni1-N1 98.9 (1), N1-Ni1-Br2 107.5(1), Br2-Ni1-Br1 124.39(4).

The solid state structure of **24c** resembles to the one of **24a**. Green crystals of the complexes were obtained by slow diffusion of petroleum ether over a THF solution at -40°C . Though these crystals did not diffract well, X-ray diffraction experiment allowed to establish the connectivity as shown in Figure 4. The two metallic centres Li and Ni are bridged by Br and O-phenoxide atoms, forming a nearly-planar four-membered ring, the lithium being coordinated with two molecules of THF (Figure 4). Elemental analysis on the isolated complex is consistent with the composition in complex **24c**.

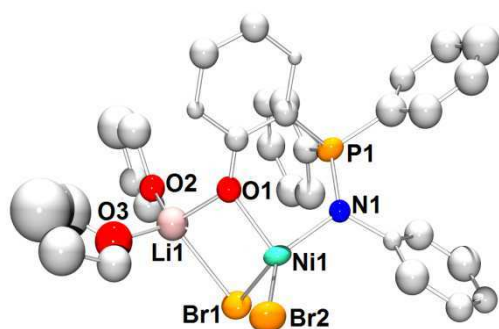
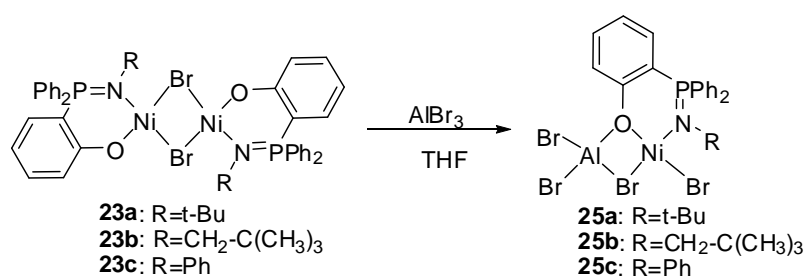
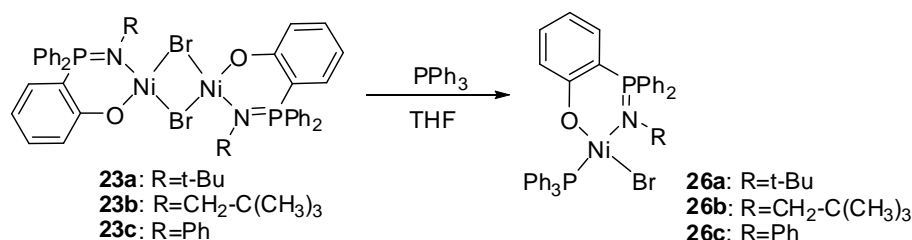


Figure 4. Ortep view of complex **24c**. Hydrogen atoms and non-coordinated THF molecules have been omitted for clarity. Thermal ellipsoids drawn at the 50% probability level. The poor resolution of the structure does not allow any discussion about distances and angles.



Scheme 18. Formation of bimetallic nickel-aluminum complexes

The formation of binuclear complexes of Ni and Li in **24a-c** demonstrates the strong vocation of the phenoxide oxygen to coordinate to hard Lewis centres. We thus attempted the synthesis of binuclear Al-Ni complexes from **23a-c** (Scheme 18). Indeed, the additions of AlBr₃ into the solutions of **23a-c** in THF yielded blue precipitates after overnight stirring at room temperature. Though X-ray structures for these complexes were not obtained, elemental analysis evidenced the incorporation of AlBr₃ into the nickel complexes and suggested the formation of Al-Ni complexes like the case with Li.



Scheme 19. Formation of nickel-iminophosphorane complex with PPh₃

In an attempt to break the suspected multimetallic structures in **23a-c**, PPh₃ was added (Scheme 19). The addition of PPh₃ into a solution of **23a-c** in THF resulted in a change of color to deep green in all cases, with the formation of green solid with reduced solubility in THF compared to **23a-c**. These complexes are paramagnetic, suggesting that the nickel centres are still in tetrahedral geometry. These products have been characterised with elemental analysis.

Definite structure of one of these complexes, **26a**, was obtained by X-ray diffraction (Figure 5). Suitable crystals for this experiment have been grown by slow diffusion of petroleum ether over a solution of **26a** in THF at -40°C. The complex adopts tetrahedral geometry, with Ni1-Br1, Ni1-N1, N1-P1 bond lengths having very close values to those observed in **24a,b**. The Ni1-O1 bond length is however significantly shorter (1.921(3) Å in **26a** compared to 1.954(2) Å in **24a** and 1.975(2) Å in **24b**), as a consequence of the fact that the oxygen atom is only coordinated to one metal centre in **26a**, whereas it is coordinated to two metal centres in **24a,b**.

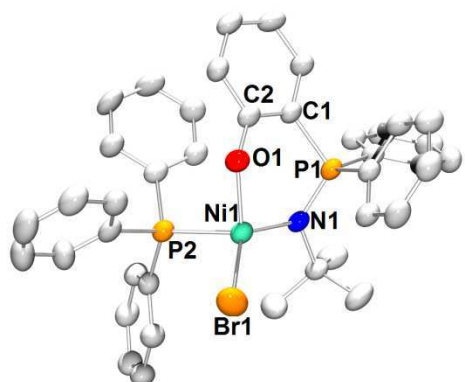
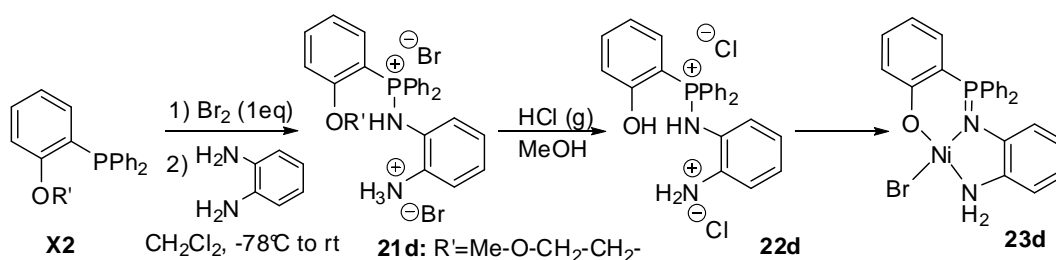


Figure 5. Ortep view of complex **26a**. Hydrogen atoms and non-coordinated THF molecules have been omitted for clarity. Thermal ellipsoids drawn at the 50% probability level. Selected distances (Å) and angles (°): Ni1-N1 1.971(3), Ni1-O1 1.921(3), Ni1-Br1 2.3712(7), Ni1-P2 2.321(1), N1-P1 1.616(4), O1-C2 1.314(5), O1-Ni1-N1 99.4 (1), N1-Ni1-Br1 127.8(1), Br1-Ni1-O1 109.7(1), P2-Ni1-Br1 102.25(4).

From the results of the described complexes, it has been observed that the nickel completes its coordination sphere with one extra ligand coming from different sources: KBr, LiBr, AlBr₃ or PPh₃. To circumvent this problem, we have thus developed a tridentate N2O proligand similar to **22a-c**, using *o*-phenylenediamine instead of monoamines. The Kirsanov reaction did not need any additional amine as base, thanks to the presence of another amino group in the diamine. This facilitates greatly the purification step, as the product **21d** was isolated after a simple evaporation of dichloromethane and washing with THF. Deprotection of **21d** was much easier than for **21a-c** and gave the proligands **22d** in high yield (80% starting from **X2**). In ³¹P{¹H}NMR spectrum, **22d** is characterised by a singlet at 39 ppm, a value very close to the ones obtained for **22a-c**.



Scheme 20. Synthesis and coordination to Ni(II) of tridentate iminophosphorane-phenoxide ligand.

Addition of 3 equiv. of KHMDS into a slurry of **22d** in THF yielded a cloudy solution, with the disappearance of the signal of the proligand at 39 ppm and apparition of one unique singlet at 15 ppm, indicating the formation of the anionic phenolate- iminophosphorane ligand. After removal of insoluble potassium salt, addition of [NiBr₂(DME)] into the obtained solution gave a

deep red solution. Insoluble potassium salt was removed by centrifugation, THF was evaporated and petroleum ether was introduced to wash traces of HMDS. The nickel complex **23d** was isolated as a deep red solid in high yield (73%). This compound however decomposes slowly in solution to give metallic Ni: a mirror could be seen after several weeks on the wall-side of the vial containing **23d** in THF or dichloromethane. This decomposition is likely due to the reductive ability of the amino group on a very-electron donating ligand.

3. Catalytic Activities

The synthesized nickel complexes were tested in oligomerisation of ethylene, with Et₂AlCl as co-catalyst (it was found that Et₂AlCl is much more efficient than MAO as co-catalyst, giving higher TOF at much lower Al/Ni ratio). In general, the activities and selectivities of these iminophosphorane-phenoxide complexes are in general significantly higher than complexes of (N,O) and (P,O) ligands existed in the literature. Details of the activities are given in Table 2, as well as the activities of related nickel iminophosphorane complexes reported in the literature for the sake of comparison.

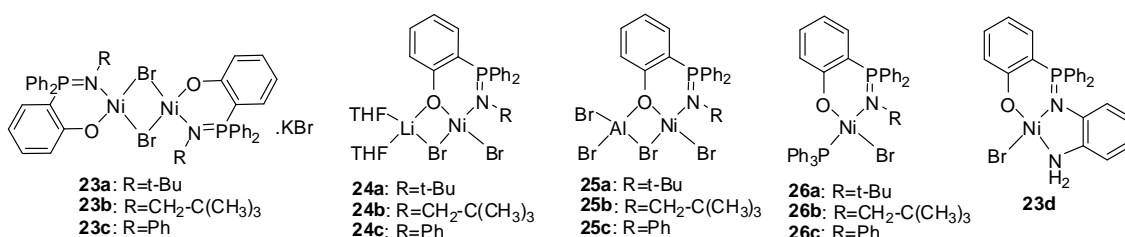


Table 2. Activities of nickel-iminophosphorane complexes in oligomerisation of ethylene.^a

entry	complex	Co-catalyst	Al/Ni	Time	TOF (x10 ⁻³ mol(C ₂ H ₄)/ mol(Ni)/h)	% C4 (% 1-C4)	% 1-C6
	[NiBr ₂ (DME)]	MAO	300	0.5h	15.0	94.0 (85)	1.7 ^b
1	23b	MAO	300	1h	20.1	98.1 (79.1)	1.9
2	23b	AlEt ₂ Cl	22.5	1h	36.9	98.4 (73.4)	1.6
3	23a	AlEt ₂ Cl	22.5	1h	39.6	98.2 (74.3)	1.8
4	23c	AlEt ₂ Cl	22.5	1h	68.1	98.2 (59.8)	1.8
5	23c	AlEt ₂ Cl	22.5	0.5h	67.5	97.9 (44.0)	2.1
6	23c	AlEt ₂ Cl	45	1h	72.1	97.0 (48.1)	3.0
7	24a	AlEt ₂ Cl	22.5	1h	23.7	97.6 (73.1)	2.4
8	24b	AlEt ₂ Cl	22.5	1h	30.3	98.4 (78.1)	1.6
9	24c	AlEt ₂ Cl	22.5	1h	14.0	98.1 (82.7)	1.9
10	25a	AlEt ₂ Cl	22.5	1h	18.5	98.7 (85.9)	1.3
11	25b	AlEt ₂ Cl	22.5	1h	28.9	98.5 (82.4)	1.5
12	25c	AlEt ₂ Cl	22.5	1h	7.3	98.7 (93.5)	1.3
13	26a	AlEt ₂ Cl	22.5	1h			
14	26b	AlEt ₂ Cl	22.5	1h	14.5	99.4 (48.9)	0.6
15	26c	AlEt ₂ Cl	22.5	1h	15.8	99.0 (55.0)	1.0
16	23d	AlEt ₂ Cl	22.5	1h	41.2	97.1 (55.6)	3.0

^{a)} experimental conditions: T=25°C, P(C₂H₄)=30 bar, 8x10⁻³ mmol (Ni), toluene 20 mL. TOF and selectivities are determined by gas-phase chromatography, using n-heptane as internal reference. ^{b)} other isomers of hexene are formed

The synthesized nickel complexes show high activities (TOF up to 67 000 mol(C₂H₄)/mol(Ni)/h) and high selectivities in the dimerisation (>97% of C₄ in all cases). No trace of polymer was found.

As stated above, two tendencies were expected concerning the performance of these complexes. Firstly, nickel complexes of (N,O) or (P,O) chelating ligands are not highly active in oligomerisation of ethylene, at least not as active as those featuring (N,N), (N,P), (P,P) ligands. As has been seen in the previous section, they either direct the polymerisation or the oligomerisation of ethylene with a wide product distribution. One of the most active and selective systems in the oligomerisation of ethylene (**Ni26-Ni28**), developed by Braunstein and coworkers, offer *ca.* 90-92% selection in C₄ (with at best 62% selection in 1-C₄), and TOFs between 20 000-24 000 mol(C₂H₄)/mol(Ni)/h). Secondly, it seems that the combination of iminophosphorane with a soft, electron-rich donating group is beneficial for the performance of the complexes. Indeed, for the nickel complexes developed in this study, their activities are higher than the nickel complexes of pyridine or oxazoline-iminophosphorane ligands reported by Stephan and coworkers,³⁴ but not as high as those of phosphine-iminophosphorane ligands previously synthesized in the laboratory.³⁵

Inside the series of the synthesized complexes, it clearly appears that with the same iminophosphorane-phenoxide ligand, the more difficultly the auxiliary ligand is removed from the coordination sphere, the lower the activities of the complexes in dimerisation. This is easy to understand, as according to both Cosse and metallacyclic mechanisms, it requires at least two coordination sites in order for the dimerisation/oligomerisation to occur. Thus complexes **26a-b** which have a strongly coordinated PPh₃ as auxiliary ligand are the less active. The bimetallic lithium-nickel complexes are better for the dimerisation, probably because the lithium bromide easily goes away, leaving two possible coordination sites (from two bromides). The most active ones are complexes **23a-b**, as they are supposed to be more exposed in solution (the possible multinuclear structures being easily broken).

The electronic properties probably play an important role. Complex **23c** with phenyl substituent at nitrogen is much more active than complex **23a,b**, which has the same structure but bear alkyl substituents at the nitrogen atom.

The selectivities in alpha olefins vary greatly among the complexes. The formation of 2-C₄ probably results from the capacity of the complexes to catalyse the isomerisation of C₄. In fact, it has been observed that the longer the systems are kept at low temperature after stopping the C₂H₄ alimentation and before the quenching of the catalysts with MeOH, the lower the selectivities in 1-C₄ are, and the more 2-C₄ are obtained. Extreme care was thus taken in order to reduce this isomerisation due to the handling conditions, and to represent correctly the state

of the product mixture just after stopping the ethylene alimentation. It is interesting to notice that bimetallic nickel-lithium and nickel-aluminum offer very good selectivities in 1-C4 (more than 70% in all cases and up to 93.5% for **25c**), whereas the complexes with PPh₃ and the complex **23d** of a tridentate ligand are much less selective in terms of 1-C4.

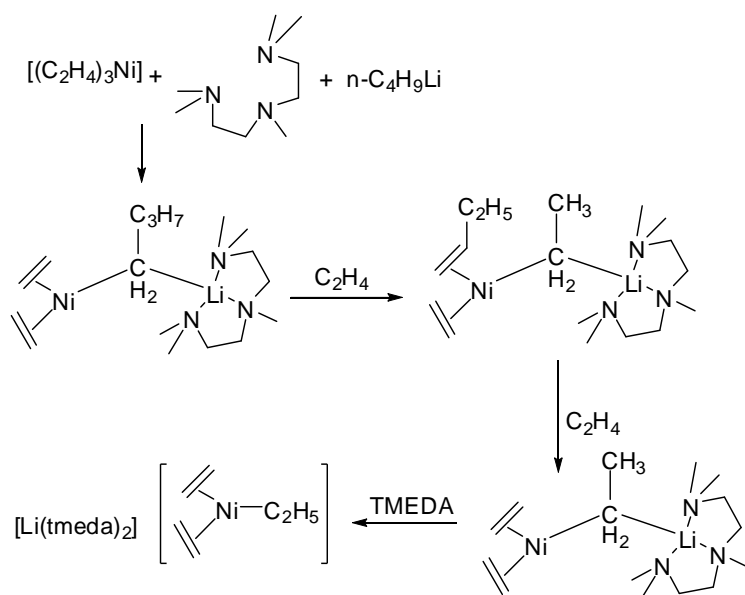
In conclusion, from these results, it could be concluded that during the oligomerisation, the complexes incorporating lithium, aluminum or PPh₃ do not simply act as if these “added” components were removed and left aside, leaving solely the iminophosphorane-phenoxide nickel complexes acting on their own. The formation of bimetallic nickel-lithium and nickel-aluminum complexes **24a-c** and **25a-c** are beneficial for the selectivities of the dimerisation of ethylene, though they are less active than the simple nickel complexes **23a-c**.

III. Conclusion

A new method for the synthesis of bidentate iminophosphorane-phenoxide ligands have been developed using Kirsanov reaction. This method allows a large variation of substituents on the ligand (in particular at the nitrogen atom), uses inexpensive starting materials and could be applied for large scale synthesis.

The newly synthesized iminophosphorane-phenoxide ligands were coordinated to nickel(II). In particular, the presence of anionic phenoxide group on the ligands allows then coordination of a second metal centre, such as lithium or aluminum. Thus monometallic and bimetallic complexes of nickel-iminophosphorane have been obtained, containing tetrahedral nickel centres. Some of their structures have been evidenced by X-ray diffraction experiments. These nickel complexes were studied in the oligomerisation of ethylene. The activities and selectivities of these iminophosphorane-phenoxide complexes are in general significantly higher than complexes of (N,O) and (P,O) ligands existed in the literature. Their performances in terms of TOF and selectivities (in C4 and in 1-C4) vary greatly in function of the auxiliary ligand or substituents at the nitrogen atoms. The comparisons of performance between the synthesized complexes could be used for the fine design of new nickel complexes efficient for the dimerisation of ethylene.

Furthermore, the formation of bimetallic nickel-lithium and nickel-aluminum complexes is interesting and opens the possibility to develop self-activated bimetallic nickel-aluminum complexes for the oligomerisation of ethylene, based on iminophosphorane ligands. In fact, it has been suggested by many groups (e.g the Wilke and Eisch groups) that one of the key intermediates in the Ziegler nickel effect in polymerization/oligomerisation of olefins are multimetallic complexes of the type Ni(μ -C)Al or Ni(μ -C)Li, or the bridging hydride of Ni and Al (Scheme 21, next page).³⁸ Thus the formation of such self-activated complexes might contribute to the clarification of the mechanism of the Ziegler polymerization/oligomerisation of olefins.



Scheme 21. Model demonstrating the “nickel effect”, from Wilke and coworkers.^{38b}

REFERENCES

1. Forestiere, A.; Olivier-Bourbigou, H.; Saussine, L., *Oil Gas Sci. Technol. Rev.* **2009**, *64* (6), 649-667.
2. (a) Keim, W., *Angew. Chem. Int. Ed.* **1990**, *29* (3), 235-244; (b) Skupinska, J., *Chem. Rev.* **1991**, *91* (4), 613-648.
3. (a) Reuben, B.; Wittcoff, H., *J. Chem. Educ.* **1988**, *65* (7), 605; (b) Lutz, E. F., *J. Chem. Educ.* **1986**, *63* (3), 202.
4. Dixon, J. T.; Green, M. J.; Hess, F. M.; Morgan, D. H., *J. Organomet. Chem.* **2004**, *689* (23), 3641-3668.
5. McGuinness, D. S., *Chem. Rev.* **2010**, *111* (3), 2321-2341.
6. (a) Chauvin, Y., *Angew. Chem. Int. Edit.* **2006**, *45* (23), 3740-3747; (b) Commereuc, D.; Chauvin, Y.; Gaillard, J.; Leonard, J.; Andrews, J., *Hydrocarb. Process.* **1984**, *63* (11), 118-120.
7. (a) Kuhn, P.; Semeril, D.; Jeunesse, C.; Matt, D.; Neuburger, M.; Mota, A., *Chem. Eur. J.* **2006**, *12* (20), 5210-5219; (b) Kuhn, P.; Semeril, D.; Jeunesse, C.; Matt, D.; Lutz, P.; Welter, R., *Eur. J. Inorg. Chem.* **2005**, (8), 1477-1481.
8. (a) Heyndrickx, W.; Occhipinti, G.; Minenkov, Y.; Jensen, V. R., *Chem. Eur. J.* **2011**, *17* (51), 14628-14642; (b) Fan, L.; Krzywicki, A.; Somogyvari, A.; Ziegler, T., *Inorg. Chem.* **1996**, *35* (13), 4003-4006; (c) Deng, L. Q.; Margl, P.; Ziegler, T., *J. Am. Chem. Soc.* **1997**, *119* (5), 1094-1100.
9. (a) Emrich, R.; Heinemann, O.; Jolly, P. W.; Kruger, C.; Verhovnik, G. P. J., *Organometallics* **1997**, *16* (8), 1511-1513; (b) Overett, M. J.; Blann, K.; Bollmann, A.; Dixon, J. T.; Haasbroek, D.; Killian, E.; Maumela, H.; McGuinness, D. S.; Morgan, D. H., *J. Am. Chem. Soc.* **2005**, *127* (30), 10723-10730.
10. Buchard, A. Chimie de coordination des iminophosphoranes et nouveaux systemes catalytiques. Ecole Polytechnique, Palaiseau, 2009.
11. Dubois, M. A.; Wang, R. P.; Zargarian, D.; Tian, J.; Vollmerhaus, R.; Li, Z. M.; Collins, S., *Organometallics* **2001**, *20* (4), 663-666.
12. Vollmerhaus, R.; BelangerGaripey, F.; Zargarian, D., *Organometallics* **1997**, *16* (22), 4762-4764.
13. Ajellal, N.; Kuhn, M. C. A.; Boff, A. D. G.; Horner, M.; Thomas, C. M.; Carpentier, J. F.; Casagrande, O. L., *Organometallics* **2006**, *25* (5), 1213-1216.
14. Speiser, F.; Braunstein, P.; Saussine, L., *Dalton Trans.* **2004**, (10), 1539-1545.

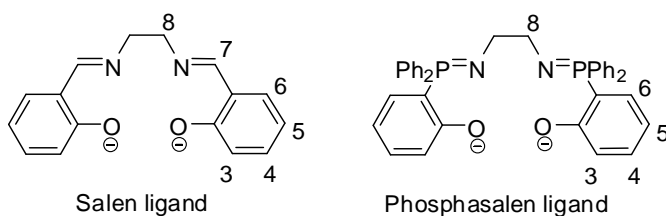
15. Sun, W. H.; Wang, K. F.; Wedeking, K.; Zhang, D. H.; Zhang, S.; Cai, J. J.; Li, Y., *Organometallics* **2007**, *26* (19), 4781-4790.
16. Zhang, M.; Zhang, S.; Hao, P.; Jie, S.; Sui, W. H.; Li, P. Z.; Lu, X. M., *Eur. J. Inorg. Chem.* **2007**, (24), 3816-3826.
17. Svejda, S. A.; Brookhart, M., *Organometallics* **1999**, *18* (1), 65-74.
18. Gao, H. Y.; Guo, W. J.; Bao, F.; Gui, G. Q.; Zhang, J. K.; Zhu, F. M.; Wu, Q., *Organometallics* **2004**, *23* (26), 6273-6280.
19. Nelkenbaum, E.; Kapon, M.; Eisen, M. S., *Organometallics* **2005**, *24* (11), 2645-2659.
20. Mukherjee, S.; Patel, B. A.; Bhaduri, S., *Organometallics* **2009**, *28* (10), 3074-3078.
21. Yu, J. G.; Hu, X. Q.; Zeng, Y. N.; Zhang, L. P.; Ni, C. H.; Hao, X. A.; Sun, W. H., *New J. Chem.* **2011**, *35* (1), 178-183.
22. Weng, Z. Q.; Teo, S.; Hor, T. S. A., *Organometallics* **2006**, *25* (20), 4878-4882.
23. (a) Speiser, F.; Braunstein, P.; Saussine, L., *Organometallics* **2004**, *23* (11), 2625-2632;
(b) Kermagoret, A.; Braunstein, P., *Organometallics* **2008**, *27* (1), 88-99.
24. Speiser, F.; Braunstein, P.; Saussine, L.; Welter, R., *Organometallics* **2004**, *23* (11), 2613-2624.
25. Speiser, F.; Braunstein, P.; Saussine, L.; Welter, R., *Inorg. Chem.* **2004**, *43* (5), 1649-1658.
26. Speiser, F.; Braunstein, P.; Saussine, W., *Acc. Chem. Res.* **2005**, *38* (10), 784-793.
27. Lejeune, M.; Semeril, D.; Jeunesse, C.; Matt, D.; Peruch, F.; Lutz, P. L.; Ricard, L., *Chem. Eur. J.* **2004**, *10* (21), 5354-5360.
28. Mora, G.; van Zutphen, S.; Klemps, C.; Ricard, L.; Jean, Y.; Le Floch, P.; Bernache-Assollant, D., *Inorg. Chem.* **2007**, *46* (24), 10365-10371.
29. Younkin, T. R.; Connor, E. F.; Henderson, J. I.; Friedrich, S. K.; Grubbs, R. H.; Bansleben, D. A., *Science* **2000**, *287* (5452), 460-462.
30. Hicks, F. A.; Brookhart, M., *Organometallics* **2001**, *20* (15), 3217-3219.
31. Yang, Q. Z.; Kermagoret, A.; Agostinho, M.; Siri, O.; Braunstein, P., *Organometallics* **2006**, *25* (23), 5518-5527.
32. Kermagoret, A.; Braunstein, P., *Dalton Trans.* **2008**, (12), 1564-1573.
33. Sauthier, M.; Leca, F.; de Souza, R. F.; Bernardo-Gusmao, K.; Queiroz, L. F. T.; Toupet, L.; Reau, R., *New J. Chem.* **2002**, *26* (5), 630-635.

34. Spencer, L. P.; Altwer, R.; Wei, P. R.; Gelmini, L.; Gauld, J.; Stephan, D. W., *Organometallics* **2003**, 22 (19), 3841-3854.
35. Buchard, A.; Auffrant, A.; Klemps, C.; Vu-Do, L.; Boubekour, L.; Le Goff, X. F.; Le Floch, P., *Chem. Commun.* **2007**, (15), 1502-1504.
36. Qi, C. H.; Zhang, S. B.; Sun, J. H., *J. Organomet. Chem.* **2005**, 690 (17), 3946-3950.
37. Bianchi, A.; Bernardi, A., *J. Org. Chem.* **2006**, 71 (12), 4565-4577.
38. (a) Weng, Z.; Teo, S.; Koh, L. L.; Hor, T. S. A., *Chem. Commun.* **2006**, (12), 1319-1321; (b) Wilke, G., *Angew. Chem. Int. Ed.* **1988**, 27 (1), 185-206; (c) Eisch, J. J.; Ma, X.; Singh, M.; Wilke, G., *J. Organomet. Chem.* **1997**, 527 (1-2), 301-304.

Chapter 3

Phosphasalen Ligand: Synthesis, Coordination and Properties

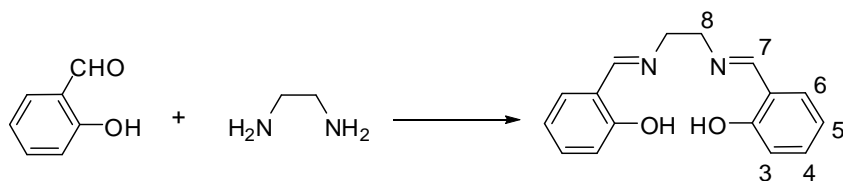
Following our interest in new systems of ligands associating iminophosphorane(s) with anionic donating group, and as a continuation to the work on bidentate iminophosphorane-phenoxide ligands, we developed tetradentate ligands combining two iminophosphorane functions and two phenoxides. These latter, termed “phosphasalen”, are the phosphorus analogues of the well known Salen ligands in chemistry.



I. Introduction to Salen Ligands

1. Synthesis, Coordination and Application of Salens

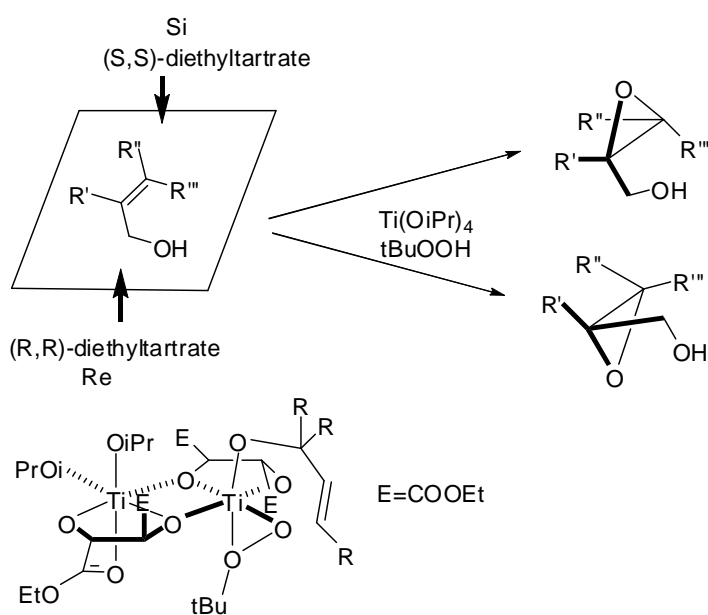
The chemistry of Salen ligands and their complexes, as well as their applications in catalysis is a well elaborated yet still fertilised domain.¹ Strictly speaking the term Salen is reserved to the diimine diphenol product (N,N'-bis(salicylaldehyde)ethylenediamine) from the condensation of two equivalents of salicylaldehyde with one equivalent of ethylenediamine. Variations of substituents on the diamine linker, the phenoxide rings or on the carbon of the imine functions extend largely the Salen ligands class. Recently, the term Salen is even used to describe general tetradentate N₂O₂ ligands resulting from the condensation of a diamine and two aldehydes.



Scheme 1. Synthesis of unsubstituted Salen ligand and its conventional numbering.

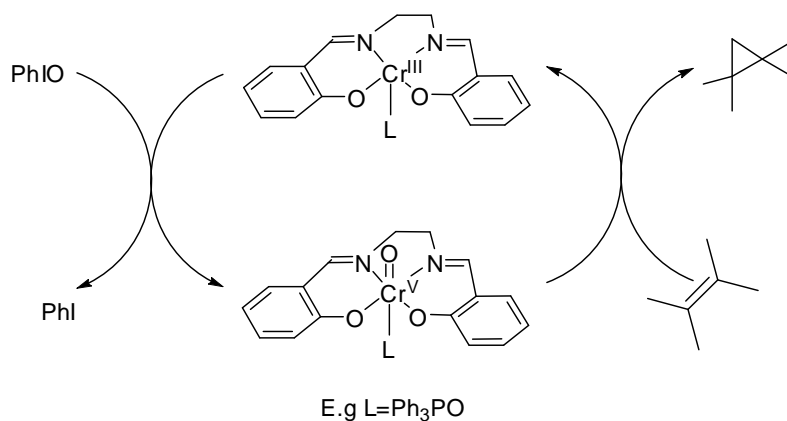
The double deprotonation of Salens gives tetradentate ligands which could bind strongly to metal centers through the phenoxide and imine groups. The ease of synthesis, the large scope of possible variations on ligand structure, and the ease of complex structure control when dealing with tetradentate ligands makes Salens ligands of choice in many studies. Their complexes have been successfully employed in various chemical transformations. The most significant ones being asymmetric epoxidation, epoxide ring-opening and co-polymerisation of carbon dioxide and epoxides.

The major breakthrough in asymmetric epoxidation was reported by Sharpless and Katsuki with titanium systems.² This method allows the enantioselective epoxidation of prochiral allylic alcohols. The asymmetric induction is achieved by adding an enantiomerically enriched tartrate derivative (Scheme 2). The catalyst is supposed to be a titanium dimer, and the reaction is thought to happen through a key intermediate in which the hydroperoxide, the allylic alcohol group, and the asymmetric tartrate ligand are bound to the titanium centres via oxygen atoms.³ This discovery and the development of the reaction has led to what is now called the Sharpless AE (AE: asymmetric epoxidation). In 2001, Sharpless was given the Nobel prize in Chemistry "for his work on chirally catalysed oxidation reactions" together with William S. Knowles and Ryoji Noyori "for their work on chirally catalysed hydrogenation reactions".



Scheme 2. Sharpless asymmetric epoxidation and putative key intermediate.

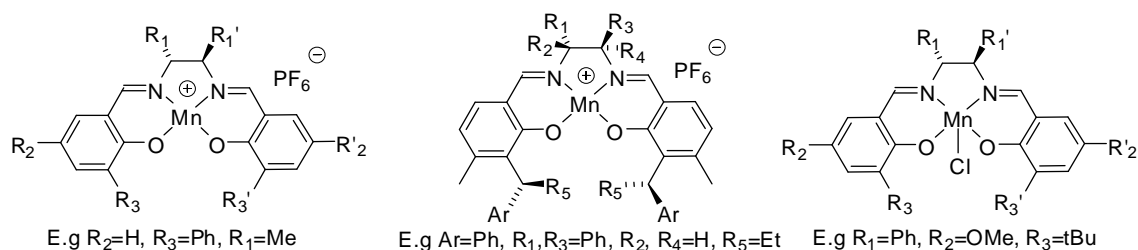
This method is however restricted to functionalised alkenes. On the other hands, in the 80ies, Koichi and co-workers first found that both Cr(Salen) and Mn(Salen) complexes were effective catalysts in epoxidation of unfunctionalised alkenes using PhIO as terminal oxidants.⁴ Their studies on the mechanism of the reaction showed the roles of oxo-chromium or oxo-manganese salen complexes as active species in the oxygen transfer.



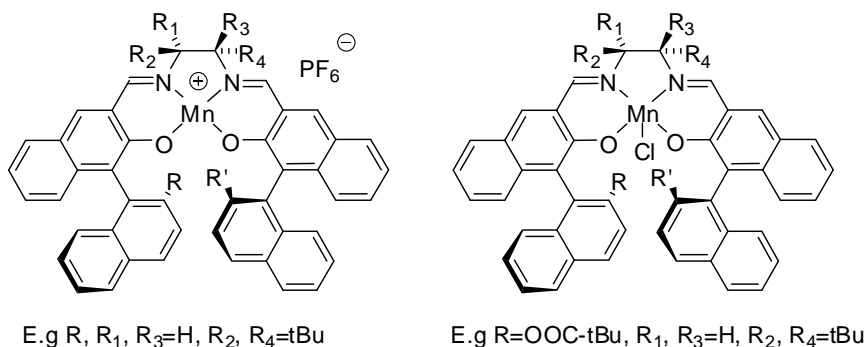
Scheme 3. Mechanism of the epoxidation of alkenes with PhIO, catalysed by Cr(Salen) complexes.

The potential of developing asymmetric catalysts on the Kochi catalyst was noticed by Jacobsen and Katsuki, both had worked under Sharpless. Compared to systems of two or three dentate ligands as used in AEs developed by Sharpless et coworkers, Salen complexes do not normally dissociate in solution, thus the control on the composition and geometries of metal complexes in solution becomes easier. As a consequence, the enantiomeric control should also be better.

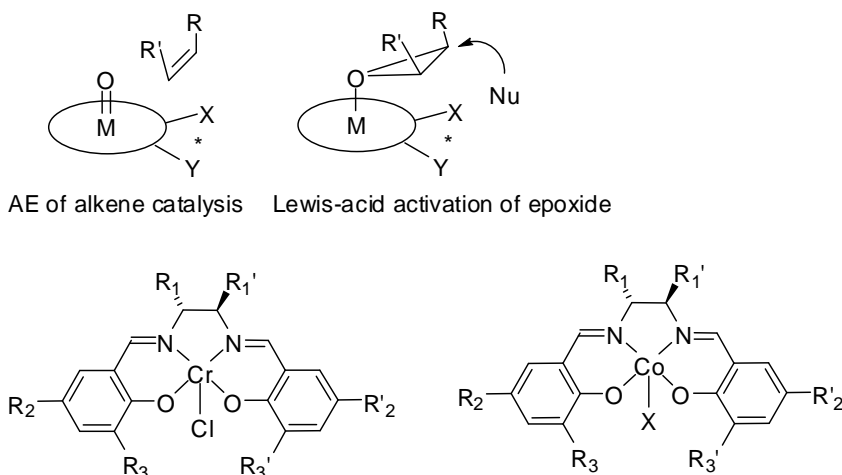
In 1990, Jacobsen and Katsuki independently reported the AEs of unfunctionalised alkenes with ArIOs as oxidants using manganese salen complexes. Since then the area of metal salen mediated asymmetric reaction in general, and AE in particular has expanded rapidly.^{4a, 5} The possible introduction of asymmetric centers at many different places on the salen ligands, and its relative rigid frame offers fine tunings of the salen ligands to better catalytic performances. Scheme 4 and Scheme 5 present examples of Jacobsen's first and second generation catalysts as a small demonstration for these mentioned possibilities.



Scheme 4. Jacobsen's catalysts

Scheme 5. Katsuki's second generation catalysts.^{4a}

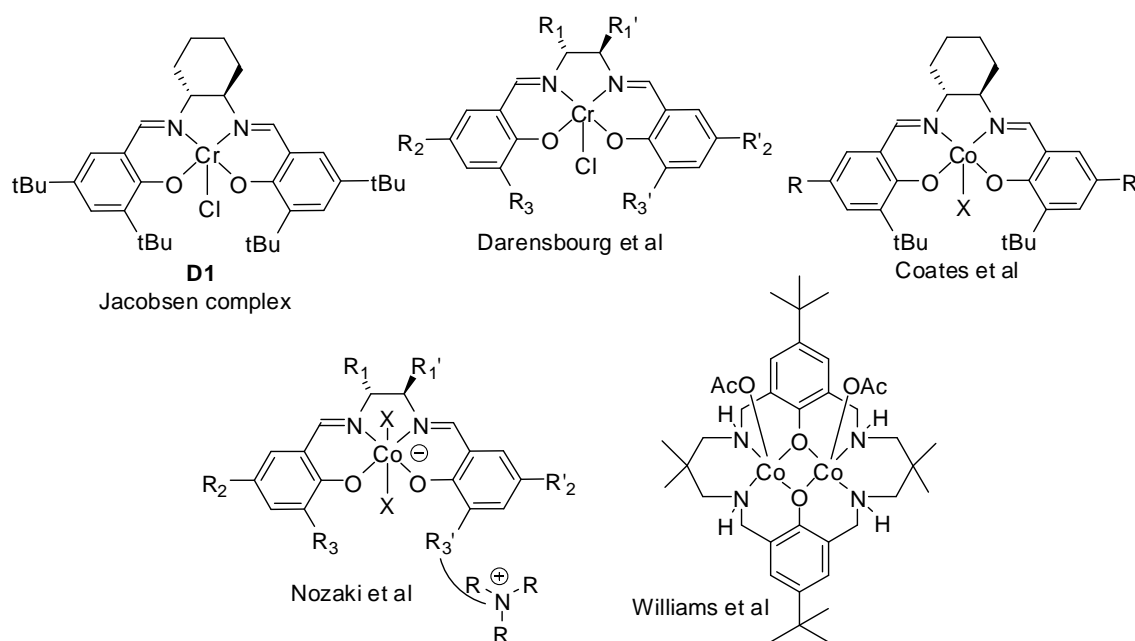
From the studies of asymmetric epoxidation, an apparent relationship between the transition state of epoxidation and the ground state of coordinated epoxides was established. This relation led to one question whether the same catalysts which are able to discriminate effectively the two faces of olefins would be able to create an asymmetric environment and thus favor one particular attack on the epoxide (Scheme 6). Following this direction, Jacobsen and coworkers have developed powerful catalysts for the epoxide ring-opening reaction based on chromium and cobalt salen complexes⁶ (though the mechanism for ring-opening of epoxides has been shown to be much more complicated and involve in the same time the activation of the epoxide and the nucleophile by two catalyst molecules).

Scheme 6. (top) Side-on approach in AE and possible mode of activation in Asymmetric ring-opening of epoxies by chiral metal catalyst, adopted from Jacobsen *et al*^{6c}, (bottom) Jacobsen's catalysts in asymmetric epoxide resolution

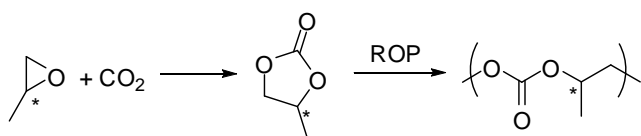
Another important application in catalysis of Salen complexes is the copolymerisation of epoxides and CO₂. The heterogeneously catalysed reaction of CO₂ and propylene oxide to give polycarbonate was first discovered by Inoue's group in 1969.⁷ Following this discovery, many heterogeneous and homogeneous catalytic systems have been developed.

The success of Jacobsen's catalysts in the ring-opening of epoxides suggested that these same compounds could be active in the stereo-regular copolymerization of epoxides and CO₂. Indeed, in 2000, Jacobsen and coworkers reported in a patent that the (R,R)-chromium complex **D1** (Scheme 7) catalysed the selective reaction of CO₂ (1 bar) with the (S)-enantiomer of *rac*-1,2-epoxyhexane to afford polycarbonate.⁸ In the same period, Paddock and Nguyen studied the use of various chromium salen complexes for the coupling of epoxides and CO₂ to give cyclic carbonate.⁹

Since then, the use of salen ligands in designing catalysts for this transformation has expanded. Indeed, cobalt and chromium salen complexes were demonstrated to be among the most effective catalysts up to date for this process.¹⁰ Scheme 7 presents some of these systems.^{10c, d} With carefully modification of the substituents on the salen ligand, the catalysts could afford stereo-regular enriched polycarbonate. This subject is actively studied by many groups (mainly Coates', Nozaki's and Lu's).^{10d}



Scheme 7. Selective catalysts for the copolymerization of CO₂ and epoxides, based on Salens and derivatives.



Scheme 8. Polycarbonate production from cyclic carbonate.

One other interesting method, but less direct, for the production of stereo-regular polycarbonate from CO₂ and epoxides also originated from the studies in asymmetric epoxide ring opening. As mentioned before, the use of salen complex to catalyse the formation of cyclic carbonate from

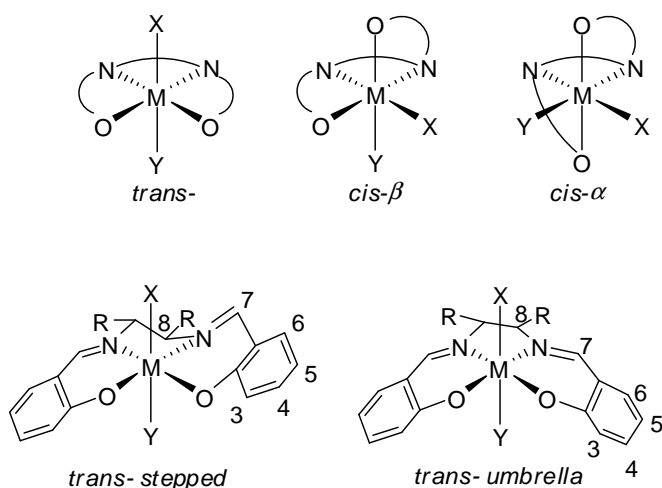
CO₂ and epoxide was first reported by Paddock and Nguyen.⁹ The products are however racemic mixtures. Lu and coworkers used chiral Co(Salen) catalysts for the coupling of epoxides and CO₂ to obtain enantiomerically enriched cyclic carbonates,¹¹ which could then give enantiomerically enriched polycarbonate by ring-opening polymerization.

Applications of Salen ligands in catalysis could be found in many other reactions. For metal-based catalysts for selective asymmetric sulfoxidation, salens and derivatives are ligands of choice and give most of the effective catalysts.¹² Environmentally friendly metals such as titanium¹³ or iron¹⁴ are the preferred metals for this transformation. Other examples include Nguyen's ruthenium salen complexes for cyclopropanation reaction of alkenes,¹⁵ Salen complexes of titanium and vanadium for the asymmetric cyanosilylation of carbonyl compounds,¹⁶ BINOL-Salen ligands for the asymmetric addition of alkynes to aldehydes with zinc complexes,¹⁷ chromium and cobalt salen complexes for asymmetric hetero Diels-Alder reaction,¹⁸ cobalt and zirconium-salen complexes for the Bayer-Villiger reaction.¹⁹

2. Configuration of Salen Complexes and Importance of *cis*-Complexes

2.1 Configurations and Conformations for Salen Complexes

Catalytic activities of Salen complexes strongly depend on the geometry and electronic properties conferred by the ligands. The rigidity of salen ligands due to the presence of the imine functions in conjugation with the phenoxide ring is at the same time an advantage and a drawback. The advantage is that the geometry of the complex is well controlled. The drawback is the limited flexibility, which may be detrimental for many catalytic transformations. However, this rigidity of the imine functions is often overcome by the flexibility endowed by the two C_{sp}³ in the diamine backbone.



Scheme 9. Configurations and conformations of salen complexes.

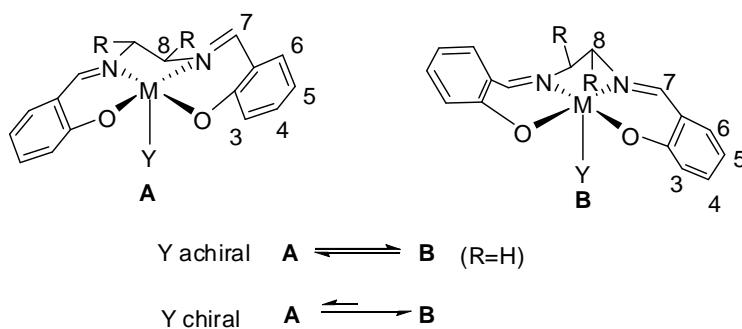
Upon coordination to a metal, the [O,N,N,O] frame can adopt many configurations: *trans*-configuration, in which the [O,N,N,O] occupy all the four equatorial positions and the two

ancillary ligands occupy two apical positions, *cis-β* in which the two ancillary ligands occupy one apical and one equatorial position, and *cis-α* where they take two equatorial positions.

The most usually seen configuration for salen complexes is *trans*-.^{1b, 12} A *trans*-metallo-salen complex in its turn could exist in different conformations, due to the flexibility of the diamine backbone. Two typical ones are stepped and umbrella conformations.

The choice of stepped or umbrella conformation is often determined by the substituents on the diamine backbone, which govern the conformation of the five-membered ring formed by the metal center and the diamine (half-chair or envelope), which would in turn govern the conformation of the complex. The chelate ring in *trans*-stepped salen complexes generally exists in half-chair conformer, and that of the *trans*-umbrella complexes exists in envelope conformer. For example, salen complexes with substituents at 8,8' positions often exist in stepped configuration, with the chelate ring in half-chair conformation, so that the two substituents could be in equatorial positions (Scheme 9).

Just as the substituents on the diamine backbone, the steric elements from the ancillary ligands could also be determinant for the conformation of the salen ligands. For example, *trans*-step metallo-salen exist in two possible step conformations which are in equilibrium. The introduction of one chiral element in Y shifts the equilibrium to one side (Scheme 10).



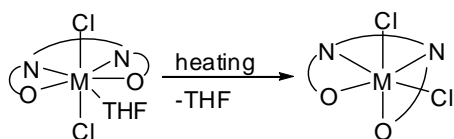
Scheme 10. Influence of ancillary ligands to the conformation of Salen.

2.2 *Cis-Complex and Catalytic Activity.*

When the ancillary ligand is multidentate, metallo-salen adopt *cis*-configuration. For example, Co(II) salen complexes often adopt *trans*- configuration with stepped or umbrella conformations.²⁰ When treated with acetylacetonate or oxalate, both bidentate ligands, they change to *cis-β* configuration.²¹

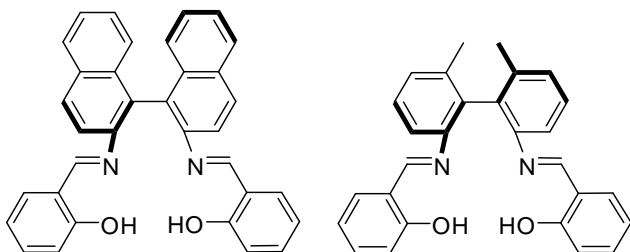
Salen complexes of some metals preferentially adopt *cis*- configuration with or without multidentate ancillary ligand. Zirconium and hafnium salen complexes adopt seven-coordinated pentagonal bipyramidal geometry, in which one solvent molecule (THF) takes an equatorial

position along with the salen ligands in *trans*-configuration. When heated in toluene, they lose the solvent molecule and adopt octahedral geometry with *cis-β* configuration (Scheme 11).²²



Scheme 11. Transition *trans-cis* configurations of zirconium and hafnium salen complexes

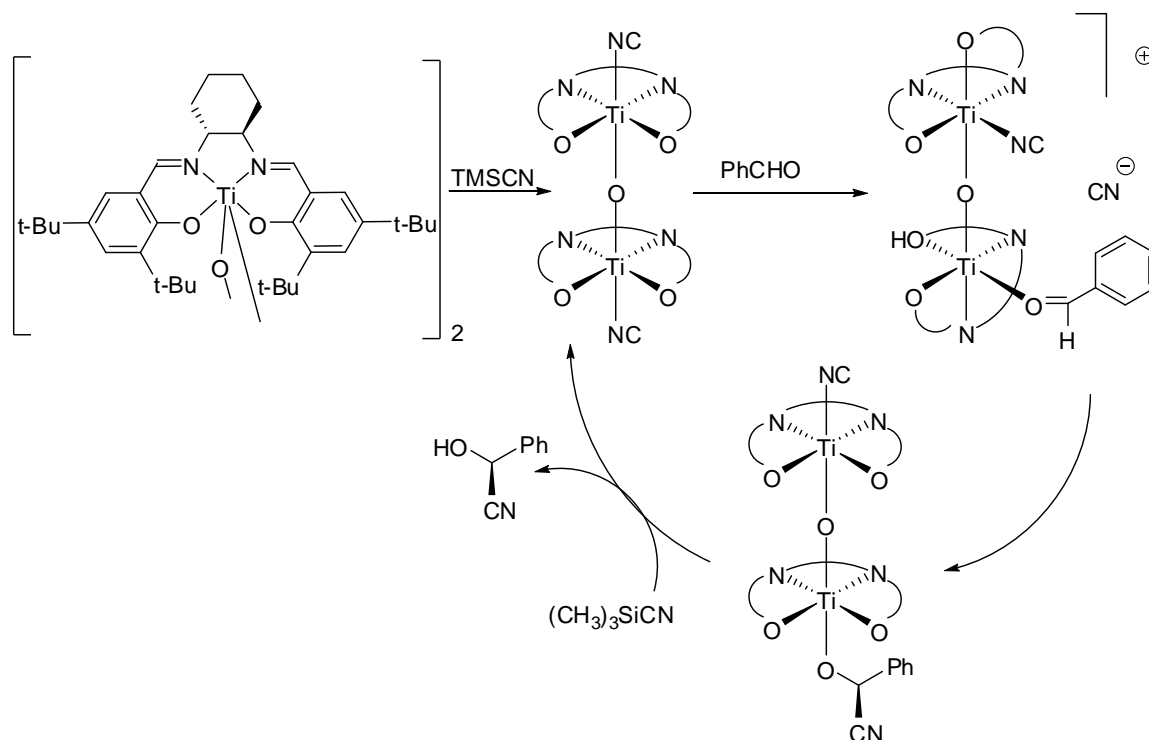
Substituents can also direct the configuration of the ligand: chiral metallosalen complexes of titanium having substituents at C7 and C8 (C7' and C8') adopt *cis-β* configuration to avoid steric repulsions between these substituents,²³ whereas the complex with only substituents at C7 and C7' exists in *trans*-configuration (Scheme 9). Some bulky chiral salen ligands also adopt *cis-β* configuration, such as those derived from 2,2'-diamino-1,1'-binaphthyl or 2,2'-diamino-6,6'-dimethyl-1,1'-biphenyl (Scheme 12).²⁴



Scheme 12. Salens derived from 2,2'-diamino-1,1'-binaphthyl (left) or 2,2'-diamino-6,6'-dimethyl-1,1'-biphenyl (right).

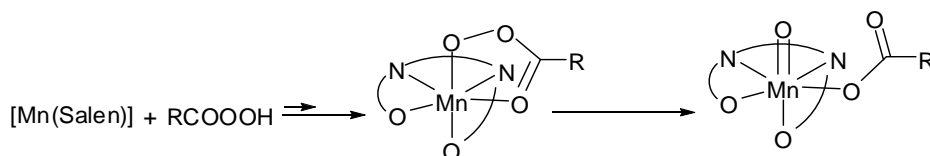
Though *cis*-metallosalen complexes are not as abundant as those for *trans*-configurations, it has been shown that *cis*-configurations offer unique catalytic activities compared to *trans*-configurations.¹² For example, in these complexes interactions between two ancillary ligands could be favored, this aspect being important in catalytic transformations involving two or more agents. In some cases it has been shown that a *trans*-complex isomerises to the *cis*-complex to participate in the catalytic cycle.

The most well-known example is the case of titanium complexes in asymmetric addition of TMSCN to aldehydes (Scheme 13). The active species is considered to be a *cis-β-μ-oxo* titanium complex. Upon treatment with TMSCN, a *trans-μ-oxo* dimer was formed. With the arrival of the aldehyde in equatorial position, an apical CN is displaced by one arm of the ligand, this moiety being in *cis-β* configuration. On the other moiety of the complex, the CN anion changes position from apical to equatorial. In the so formed intermediate, CN ligand and the aldehyde are placed close to each other and could react in an intramolecular fashion.



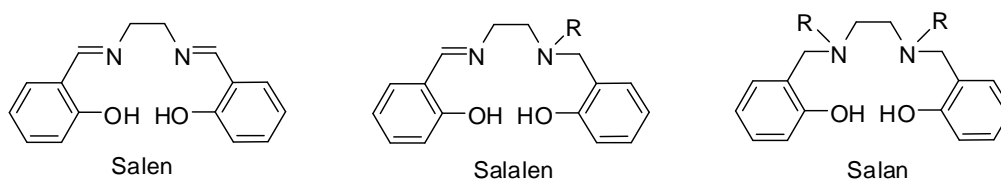
Scheme 13. Mechanism of Ti-catalysed asymmetric addition of TMSCN to aldehydes.

Another example includes Mn-salen complexes in epoxidation reaction using a mixture of molecular oxygen and aldehyde. These complexes are often considered to adopt trans-configuration.²⁵ But later studies suggested the participation of *cis-β* peroxy complexes in the catalytic cycle (Scheme 14).²⁶



Scheme 14. Formation of oxo-complex from $[Mn(Salen)]$ complex and organic peroxy acid.

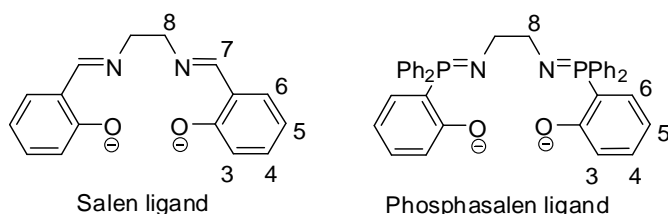
The need for new ligands presenting different electronic environment and especially a more important degree of flexibility has led to a rapid development of Salan ligands, featuring two amine functions instead of imines, and their derivatives as well as the hybrid Salalens (containing an imine and an amine group) recently (Scheme 15).



Scheme 15. Salen, Salalen and Salan ligands

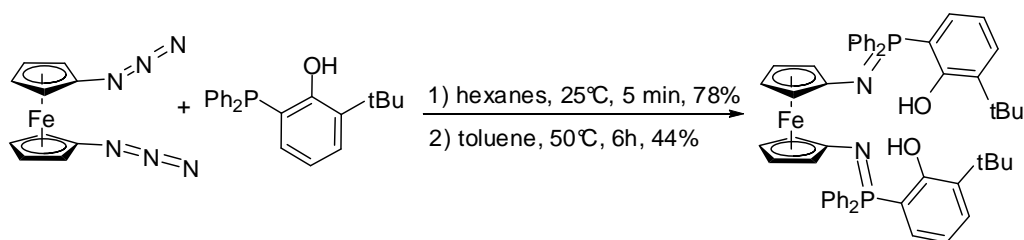
As expected, the change from a double bond C=N in the imine group of Salen to a single one in the amine group of Salan renders the [O,N,N,O] skeleton more flexible, thus in some cases favors the formation of *cis*-complexes.²⁷ For example Goldberg or Zigler^{27b} has reported the formation of *cis-β* complexes of titanium or zirconium^{27c} or molybdenum with salalen ligands. Complexes of Salan ligands have shown unique catalytic activities.^{27b, 28} The titanium salan complexes^{28c, 28a} are efficient catalysts in asymmetric epoxidation. In sulfoxidation with H₂O₂, salan complexes of iron or titanium offer high activity.^{14a, 29} Other applications of salan or salalen ligands are still to be actively investigated,³⁰ such as in copolymerisation of epoxide and CO₂^{30b} or in aerobic oxidation.^{30a}

Following this trend, we noticed that replacing imines by iminophosphoranes in salen ligands could be interesting. As we have seen, the P=N bond in iminophosphorane is not a real double bond and thus could be free to rotations.³¹ Furthermore, electronic properties of P=N is very different from imine, amine, or amide. We thus developed a new class of ligand which we called Phosphasalen, whose general structure is presented in Scheme 16.



Scheme 16. Salen ligand and Phosphasalen ligand.

Independently, and unknown to our group, in the same time, the group of Diaconescu developed a new ferrocene diphosphazene ligand based on Staudinger reaction of diazidoferrocene and a phosphinophenol³² (Scheme 17).

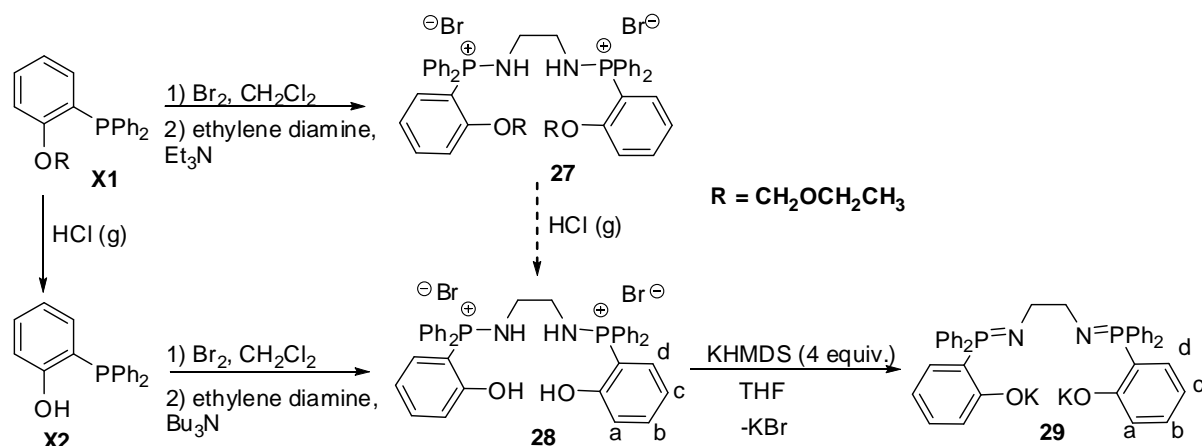


Scheme 17. Synthesis of ferrocene diphosphazene by Diaconescu et al.

The ligand also contains two iminophosphoranes and two phenoxide functions, but the molecule has a ferrocenediyl linker instead of ethylene. Its electronic and steric properties are thus completely different from phosphasalen ligands. Furthermore, the synthesis of phosphasalen ligands was achieved using Kirsanov reaction, thus giving access to a broad, completely different range of compounds.

II. Phosphasalen Ligand: Synthesis, Coordination and Properties

1. Phosphasalen Synthesis



Scheme 18. Synthesis of Phosphasalen ligand.

Following the synthesis of bidentate (PN,O) ligand reported in chapter 2, the synthesis of unsubstituted phosphasalen ligand **29** featuring an ethylene diamine link was first attempted from the protected o-diphenylphosphinophenol **X1** (Scheme 18), which was prepared starting from phenol following a literature procedure reported by Bianchi and coworkers.³³ After oxidation of the phosphine function with bromine, the corresponding phosphonium bromide salt was reacted with ethylenediamine (0.5 equiv.) in presence of triethylamine (1 equiv.) to give the bis-aminophosphonium salt **27** in 70% yield after aqueous work-up. The deprotection of the protected group by HCl-saturated MeOH solution gave the proligand **28** in high yield (81%).

However, contrary to the deprotection leading to bidentate (PN,O) proligand, this reaction was very sensitive to the experimental conditions, and the factors allowing the formation of **28** proved to be difficult to control. We thus modified the synthesis strategy and performed first the deprotection of the phenol functionality and then the Kirsanov reaction. O-diphenylphosphinophenol **X2** was obtained from **X1** by deprotection in HCl-saturated MeOH.³³ Its bromination followed by nucleophilic substitution with ethylenediamine (0.5 equiv.) in presence of tributylamine (1 equiv.) gave the expected bis-aminophosphonium salt **28** in 63% yield (Scheme 18). The compound has limited solubility in dichloromethane and could be isolated by precipitation in THF. For this reason, tributylamine was used in place of triethylamine because of the solubility of its ammonium hydrobromide salt in THF which enabled its easy removal.

28 was characterised by multinuclear NMR spectroscopies in CDCl_3 , despite its poor solubility in this solvent. In $^{31}\text{P}\{^1\text{H}\}$ spectroscopy the equivalent phosphorus atoms of **28** appear as a

singlet at $\delta(\text{CDCl}_3) = 39.3$ ppm which is in the range of the signals for bidentate phenol-aminophosphonium salts reported in chapter 2. In ^1H NMR spectrum, the bridging ethylene protons appear as a doublet ($^3J_{\text{P,H}} = 10.5$ Hz) with a chemical shift ($\delta(\text{CDCl}_3) = 3.43$ ppm) similar to the one observed for bis(phosphine-aminophosphonium) salts featuring such ethylenediamine linker.³⁴

Monocrystals suitable for X-ray diffraction of **28** were obtained by slow evaporation of a solution in chloroform. The structure of **28** is depicted in Figure 1. No hydrogen bonds between O, N and the protons of the phenol or aminophosphonium group has been detected. The two bromide anions stay quite far away from the diaminophosphonium cation and exert only weak hydrogen bonds with the protons of OH and NH groups, and the proton in chloroform (the distance between O, N, Cl_3C and the nearest Br being 3.120, 3.402, 3.592 Å respectively). π -stacking exists for one phenyl ring on each phosphorus atom, the perpendicular distance between two stacked rings being ~ 3.37 Å.

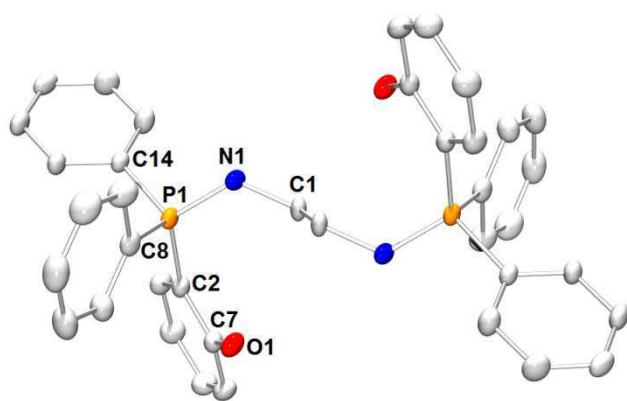


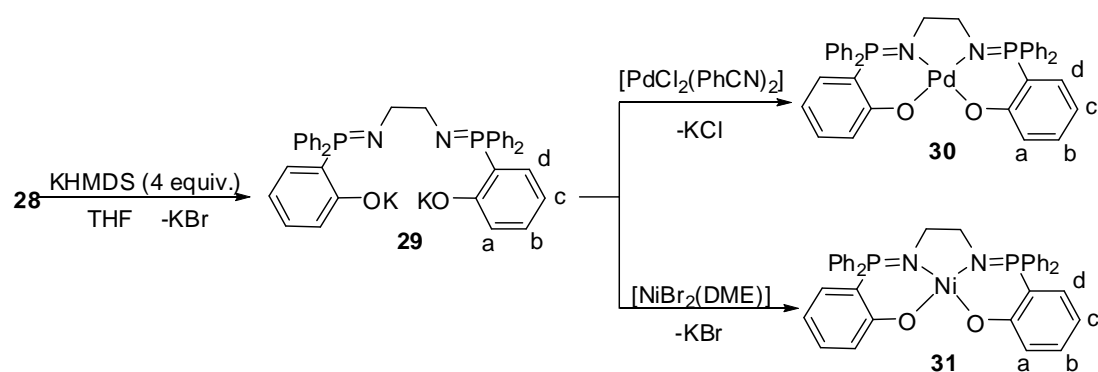
Figure 1. ORTEP view of **28**. Hydrogen atoms, solvent molecules and bromide anions have been omitted for clarity. Thermal ellipsoids drawn at the 50% probability level. Selected distances (Å): P1-N1 1.623 (2), P1-C2 1.790 (2), P1-C8 1.792 (2), O1-C7 1.355 (3).

The phosphasalen ligand **29** was generated from **28** by deprotonation using potassium hexamethyldisilazane (KHMDs, 4 equiv.) in THF at room temperature (Scheme 18). The formation of **29** was monitored by in situ $^{31}\text{P}\{^1\text{H}\}$ NMR, the completeness of the reaction was indicated by the presence of one singlet at $\delta(\text{THF}) = 18.6$ ppm indicating completion of the reaction. After removal of insoluble potassium salts and evaporation of solvent, the obtained residue was washed with petroleum ether to deliver **29** as a white powder in 99% yield. The structure of **29** was unambiguously established by NMR spectroscopy, and elemental analysis.

2. Coordination with Group 10 Metals and Studies of the Ligand Properties

2.1 Complexes Synthesis and Characterisations

In order to study the coordination properties of the phosphasalen ligand, it was first coordinated to group 10 metals: Pd(II) and Ni(II) (Scheme 19). As it was unnecessary to isolate the free ligand **29**, all coordination experiments were conducted from the bis-aminophosphonium salt **28**.



Scheme 19. Coordination of **29** to Pd(II) and Ni(II) metal centers.

For the synthesis of the palladium complex **30**, deprotonation of **28** was carried out in THF, the potassium bromide salts were removed and $[\text{PdCl}_2(\text{PhCN})_2]$ was added to the *in situ* generated ligand **29**. The solution turned immediately yellow and after one night stirring at room temperature a brown solid precipitated from the reaction mixture. This solid was dissolved in dichloromethane to eliminate the insoluble potassium salt(s). After evaporation of dichloromethane and washing of the residue with petroleum ether, palladium complex **30** was obtained in 73% yield as a yellow solid. It was characterised by multinuclear NMR spectroscopies and elemental analysis. In $^{31}\text{P}\{^1\text{H}\}$ NMR, the phosphorus nuclei appear as a singlet at $\delta(\text{CD}_2\text{Cl}_2) = 33.7$ ppm, thus significantly deshielded compared to the anionic ligand **29**. This indicated the coordination of the iminophosphorane group to the metal center. In contrast, in the ^1H NMR spectrum little change was seen from the ligand **29** except the resonance of the ethylene protons which are shifted upfield ($\delta(\text{CD}_2\text{Cl}_2) = 2.54$ ppm vs $\delta(\text{CDCl}_3) = 3.42$ ppm in **29**).

Note that reactions performed with other palladium precursors failed; with $[\text{Pd}(\text{PPh}_3)_2\text{Cl}_2]$ no coordination was observed whereas with $[\text{Pd}(\text{COD})\text{Cl}_2]$ the reaction was very slow. Importantly whereas the free ligand is sensitive to moisture, the obtained complex proved to be stable on the bench for weeks as already shown for other iminophosphorane complexes.

Definitive evidence concerning the structure of **30** was provided by X-ray crystal analysis of the complex. Suitable crystals were obtained from slow diffusion of petroleum ether over a saturated dichloromethane solution of **30** at room temperature. Ortep view of complex **30** is presented in Figure 2. The complex crystallised with four molecules of dichloromethane. As expected for a diamagnetic d^8 complex **30** adopts a square planar geometry around the metal with almost no deviation from planarity (O2-N2-N1-O1 dihedral angle $0.05(13)^\circ$). The four coordination sites are occupied by the iminophosphorane and phenoxide groups. The $O_{\text{phenoxide}}-C_{\text{phenyl}}$ bond length is significantly shorter in the complex than in the free proligand **28** ($1.314(4)$ Å vs $1.355(3)$ Å in **28**) as a consequence of the charge delocalisation from $O_{\text{phenoxide}}$ into the phenoxide ring. The $P-C_{\text{phenoxide}}$ bond does not change much ($1.777(4)$ Å vs. $1.790(2)$ Å in **28**).

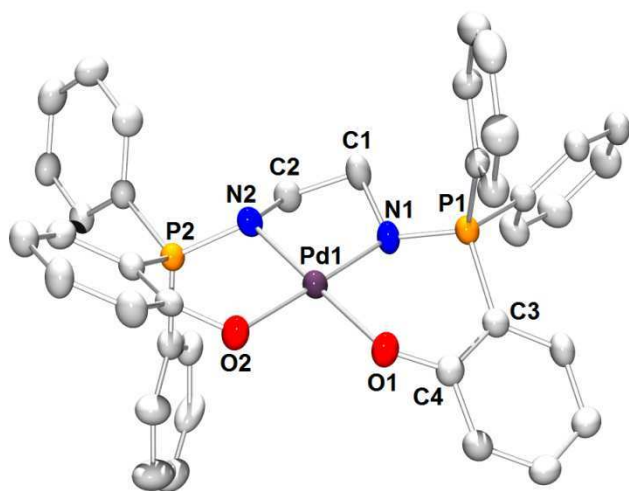


Figure 2. ORTEP view of complex **30**. Hydrogen atoms and solvent molecules have been omitted for clarity. Thermal ellipsoids drawn at the 50% probability level. Selected distances (Å) and angles ($^\circ$): Pd1–N1 2.014(3), Pd1–N2 2.017(3), N1–P1 1.620(3), N2–P2 1.623(3), Pd1–O1 2.029(2), Pd1–O2 2.039(2), O1–C4 1.314(4), P1–C3 1.777(4), N1–Pd1–O1 96.6(1), N1–Pd1–N2 82.6(1), N2–Pd1–O2 96.1(1), O1–Pd1–O2 84.7(2), N1–P1–C3 107.4(2), N2–P2–C21 106.6(2), N1–C1–C2–N2 55.76(29), N1–C4–C3–P1 25.64(38), O2–N2–N1–O1 0.05(13).

In comparison with the salen complex, the bond lengths of the Pd–N and Pd–O were measured at 2.014(3), 2.017(3) and 2.029(2), 2.039(2) Å respectively, which are all longer than the Pd–N and Pd–O distances (1.952(2), 1.957(2) and 1.9981(16), 2.0087(16) Å respectively) measured in the corresponding salen complex.³⁵ Due to the tetrahedral configuration of the phosphorus atoms, the molecule is also much less planar than related [Pd(salen)].³⁵ For example the dihedral angle N1–C4–C3–P1 was measured at $25.64(38)^\circ$ vs -3.02° in the imine derivative. In the same manner the flexible ethylene diamine chain is also much more largely deviated from the median plan in **30** than in [Pd(salen)] (N1–C1–C2–N2: $55.76(29)^\circ$ vs 34.5°), probably because the geometry around the coordinated nitrogen atom in iminophosphorane is not exactly as planar as the one around the coordinated nitrogen in imine function (C2–Pd1–P2–N1 $\sim 25^\circ$ in **30**, C1–Pd1–C=N $\sim 1.0^\circ$ in [Pd(salen)]). Concerning the crystal packing no peculiarity was observed for **30**

whereas the molecules of the salen complex axially packed because of π -stacking interactions between the phenyl rings (the centroid perpendicular distance being $\sim 3.3\text{ \AA}$).

A similar procedure was adopted to prepare the phosphasalen nickel complex **31** (Scheme 19). $[\text{NiBr}_2(\text{DME})_2]$ was added to an *in situ* generated potassium bromide salt free THF solution of **29**, leading to a rapid colour change of the solution from pale yellow to deep purple. After 30 min a purple solid precipitated out of the reaction mixture, the colour of which faded. This solid was isolated by centrifugation and a work-up similar to that described for **30** was carried out. This allowed the isolation of **31** as a purple solid in 82% yield. As for **30**, no decomposition of **31** in air was detected. This complex was characterised by multinuclear NMR spectroscopies and elemental analysis. Interestingly, the $^{31}\text{P}\{^1\text{H}\}$ NMR spectrum carried out in CD_2Cl_2 at room temperature exhibited a broad signal around 33 ppm whereas at -80°C the signal sharpened to give a nice singlet at $\delta(\text{CD}_2\text{Cl}_2) = 32.8$ ppm, confirming the coordination of the iminophosphorane moieties. ^1H and $^{13}\text{C}\{^1\text{H}\}$ NMR were recorded at room temperature on a concentrated CD_2Cl_2 solution. Spectra were very similar to those of complex **30**, except that the resolution of peaks was lower.

Definitive evidence concerning the structure of **31** was brought by X-ray diffraction analysis (Figure 3) realised on single crystals obtained from slow diffusion of petroleum ether over a saturated dichloromethane solution of **31** at room temperature.

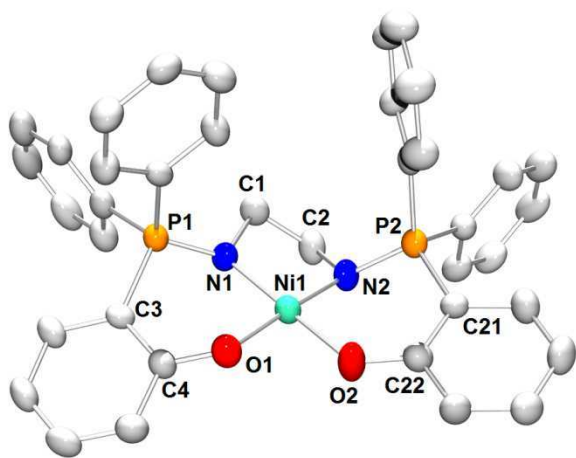


Figure 3. ORTEP view of complex **31**. Hydrogen atoms and solvent molecule have been omitted for clarity. Thermal ellipsoids drawn at the 50% probability level. Selected distances (\AA) and angles ($^\circ$): Ni1–N1 1.905(4), Ni1–N2 1.888(4), P1–N1 1.613(4), P2–N2 1.617(4), Ni1–O1 1.881(3), Ni1–O2 1.863(4), O1–C4 1.301 (6), O2–C22 (1.319 (6), C3–P1 1.774 (5), C21–P2 1.771 (5), O1–Ni1–N1 95.4(2), N2–Ni1–N1 85.4(2), O2–Ni1–N2 95.4(2), O2–Ni1–O1 83.9(2), N1–P1–C3 108.2(2), N2–P2–C21 108.1(2), N2–C2–C1–N1 $-45.00(56)$, N1–C4–C3–P1 22.57(68), N2–N1–O1–O2 3.64(35).

The complex crystallised with one molecule of dichloromethane. In the solid state, complex **31** adopts a nearly square planar geometry with a small deviation from planarity (N2–N1–O1–O2 dihedral angle at $3.64(35)^\circ$). Just like the case with the palladium complex, the $\text{O}_{\text{phenoxide}}-\text{C}_{\text{phenyl}}$

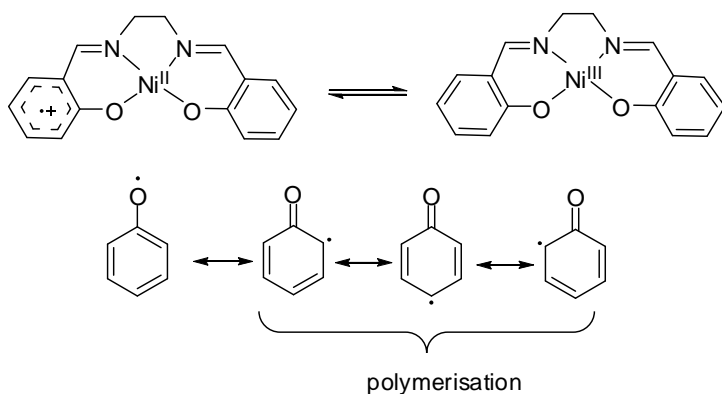
bond length is significantly shorter in **31** than in the free proligand **28** (1.301 (6) and 1.319 (6) vs 1.355 (3)) as a consequence of the charge delocalisation from O_{phenoxide} into the phenoxide ring.

The Ni-O bonds are measured at 1.863(4) and 1.881(3) Å while the Ni-N distances are at 1.888(4) and 1.905(4) Å. These bond lengths are on average longer than those recorded for the [Ni(salen)] complex³⁶ (1.853 and 1.851 Å for the Ni-O bonds and 1.851 and 1.849 Å for the Ni-N bonds). As observed for palladium complex **30**, the overall geometry of the phosphasalen complex is much less planar than the salen counterpart. The dihedral angle N1-C4-C3-P2 was measured at 22.57(68)° vs 3.30° on average in the imine derivative. Moreover, while molecules of [Ni(salen)] complexes axially packed either thanks to π -stacking interactions between the phenyl rings when the carbon of the imine function is unsubstituted^{36a} or through weak hydrogen bond when this carbon bears a phenyl group,³⁷ no particular packing was seen for **31**.

2.2 Electrochemical Studies on Nickel and Palladium Complexes.

2.2.1. Electrochemistry of Nickel and Palladium Salen Complexes

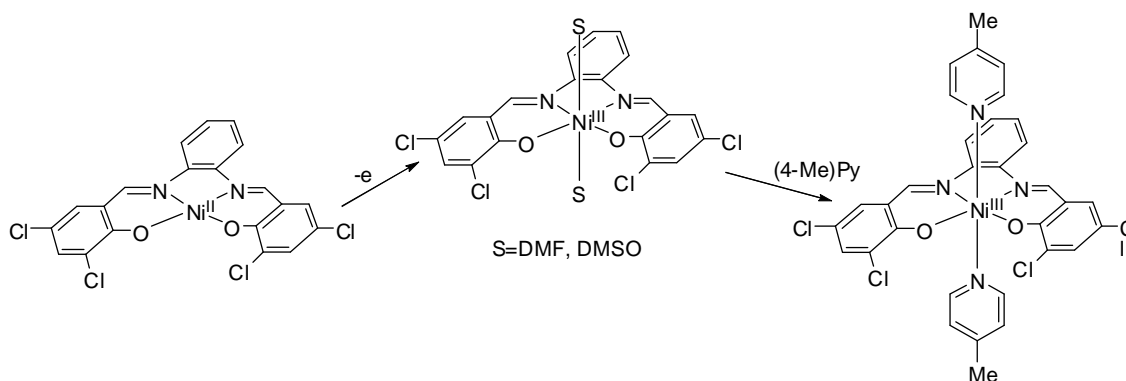
The oxidative chemistry of nickel(II)-Salen complexes and their derivatives has been the subjects of various studies. Two alternatives are imaginable for the oxidation of these complexes: either a ligand-based process (yielding phenoxyl radicals) or metal-based process (yielding high valent Ni(III)). In acetonitrile and other weak donor solvents (with donicity number (DN) inferior to that of acetonitrile (DN=14.1)), they are reversibly reduced to Ni(I) complexes but is oxidatively polymerized at the electrode to generate electroactive film, a process which has been proposed by Goldsby et al. to be ligand-based and probably takes place through a mixture of o- and p-linking of the phenyl ring (Scheme 20).³⁸



Scheme 20. Oxidation of [Ni(Salen)] complexes in weak donor solvents. The canonical forms of phenoxyl radical lead to polymerization of the complexes through o- and p-linking of the phenyl rings.

In strong coordinating solvent (DN \gg 14, e.g dimethylformamide, dimethylsulfoxide), these Ni(II) salen complexes are oxidized to hexa-coordinated Ni(III) complexes, as shown by the group of Freire and Castro by electrochemical techniques and EPR spectroscopy of the oxidized

products (Scheme 21).³⁹ The two coordinated solvents are displaced with the addition of two equiv. of 4-methylpyridine. The explanation for these observations lies in the electronic structure of the square-planar Ni(II) Salen complexes. For these complexes where the π energy levels of the ligand and those of the central Ni(II) ion are very similar, oxidation can be ligand-localized or metal-localized, the final oxidation site depends on the ability of surrounding environment (solvents and other donors) to stabilize the oxidation state of the metal. Axial coordination can shift d-orbitals with z-component above the filled ligand orbitals, thus making metal oxidation the preferred process.



Scheme 21. Oxidation of $[Ni(3,5-Cl_2Saloph)]$, from Freire and coworker

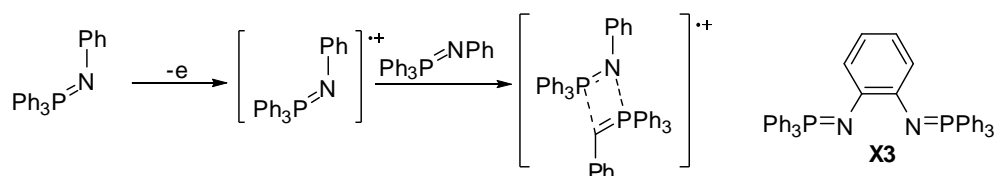
Freire, Castro and coworkers later studied the effects of substituents at the imine bridge on the oxidation of Ni(II) Salen complexes and found that the introduction of substituents not only affects the electronic structure but also imposes steric constraints on the axial coordination.³⁷ Increasing electron donor ability of the ligand would decrease the half-cell potential $E^{1/2}$, but steric constraints may play a more important role. The presence of steric repulsion between the substituents and the ligands at axial positions would destabilise the oxidized Nickel complex and $E^{1/2}$ of the oxidative process increases as a consequence.

If studies on the comparisons between electronic properties of salen ligands common in the literature, fewer have been done on the comparisons between salens and their analogs, which is partly likely related to the few salen analogs existing in the literature. Elias et al. compared the ligand Salen and tetrahydroSalen (or Salan) through their coordination properties and electrochemistry of their complexes with Ni(II), Co(II) and Cu(II).⁴⁰ They found that in contrast to the corresponding Schiff-base complexes NiL, the Ni[H4]L undergo a fast reversible oxidation and irreversible reduction in acetonitrile. Although not stated, the difference of the oxidation process probably lies in the more electron-donor property of the tetrahydroSalen.

2.2.2 Electrochemistry of Iminophosphoranes

The oxidation of free iminophosphorane has been studied in the laboratory.⁴¹ $Ph_3P=NPh$, for example, presents an irreversible oxidation wave at 0.8 V (vs. SCE) in dichloromethane, using tetrabutylammonium tetrafluoroborate salt as electrolyte. Studies on EPR spectroscopy and DFT

calculations allowed to assert that the oxidation takes place at the nitrogen atom. As a consequence, the spin density is delocalised between the nitrogen atom and the associated phenyl group. The radical cation is not stable and tend to associate with a non-oxidised iminophosphorane through the P=N group (Scheme 22). Bis(iminophosphorane) having two nitrogen atoms being able to communicate with each other through a systems of π -electrons present a first oxidation wave at lower potential (0.3-0.5V vs. SCE), and this oxidation process is often reversible.^{42, 41b} As the case with **X3**, the spin density of the oxidised species is delocalized on the two nitrogen atoms and the bridge between them.



Scheme 22. Oxidation of iminophosphoranes

Cyclic voltammetry measurements on the anionic free ligand was carried out in THF. The oxidation wave is very broad, ranging from 0.2 to 0.8 V (vs SCE). The study was thus not conclusive.

2.2.3 Electrochemical Study of the Ni- and Pd-Phosphasalen Complexes

The cyclic voltammetry measurements for Ni and Pd phosphasalen complexes were not carried out in DMF or acetonitrile which are the solvents often used for the measurements on Ni-Salen complexes. The reason lie in the limited solubilities of the complexes in these solvents. Thus all measurements were done in a mixture of dichloromethane and DMF or acetonitrile at room temperature. A gold disk was used as working electrode and a Pt gauze as counter electrode. For the sake of comparison with literature data, the potential of ferrocene in the same solvent system is also indicated.

Table 1. Electrochemical data for nickel-phosphasalen complex **31**^a in MeCN/CH₂Cl₂ (60/40 volume)

Complex	E ^a ₁ , V	E ^c ₁ , V	E ^{1/2} ₁	i _{pa} /i _{pc}
31 ^b	0.76	0.64	0.70	1.21 ^c
Fc	0.50	0.40	0.45	1.01

^a Tetrabutylammonium tetrafluoroborate salt as electrolyte (c = 0.12 mol L⁻¹); scan rate= 100 mV s⁻¹; the potential values are relative to SCE; ^b c = 4.5 mmol L⁻¹; ^c ratio was observed to change with scan rate with a value of 1.40 at 50 mV s⁻¹;

In MeCN/CH₂Cl₂, Nickel Phosphasalen complex presents a quasi-reversible oxidation process, whereas Nickel Salen complex presents an irreversible process in MeCN and other solvents of lower coordination donocity, as mentioned before. It is worth noting that the E^{1/2} of Nickel Phosphasalen complex in this solvent system is 0.25V higher than E^{1/2}(Fc⁺/Fc), a value lower than the difference between E^{1/2}([Ni-Salen]⁺/[Ni-Salen]) and E^{1/2}(Fc⁺/Fc) in DMF, a better

donor solvent. Thus it clearly shows that either the phosphasalen ligand stabilises better the oxidised Nickel metal center, or this ligand is easier to be oxidated. The anodic-cathodic peak potential separation is larger than expected theoretically for one-electron process (59 mV). However, under similar conditions, peak separation for the couple ferrocenium/ferrocene is about 100mV. This same phenomenon has been reported for Ni-Salen complexes.³⁹

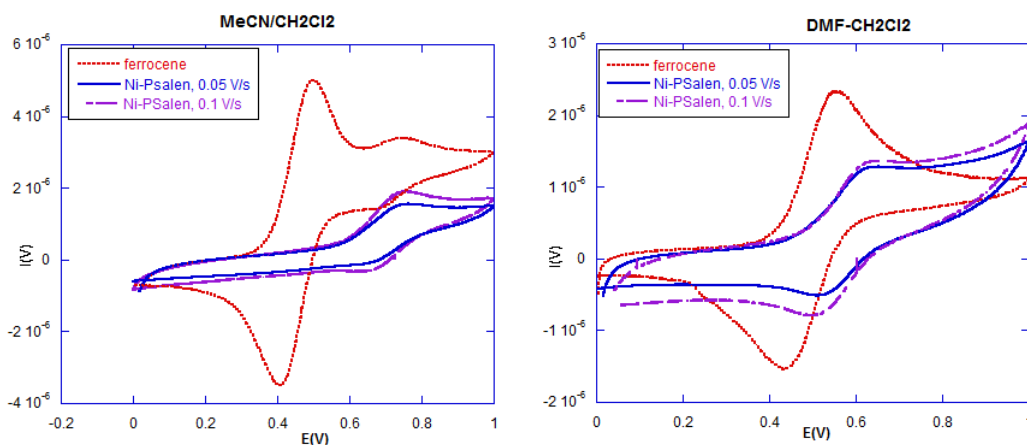


Figure 4. Cyclic voltammetric spectra of Ni-Phosphasalen complex in different systems of solvents.

For the sake of comparison and in order to better stabilise the oxidised species, DMF/CH₂Cl₂ was employed as system of solvent. In this solvent systems, similar to the case with Nickel (salen) complexes, the oxidized species are likely hexa-coordinated Ni(III) complexes, the coordination sphere of the nickel being completed by two solvent molecules.

Table 2. Electrochemical data for phosphasalen complexes **30** and **31**^a in DMF/CH₂Cl₂ (60/40 volume)

Complex	E ^a _{P1} , V	E ^c _{P1} , V	E ¹ _{1/2}	i _{pa} /i _{pc}	E ^a _{P2} , V	E ^c _{P2} , V	E ¹ _{1/2}	i _{pa} /i _{pc}
31 ^b	0.65	0.51	0.58	1.00 ^c				
30 ^d	0.76				1.10	1.03	1.06	1.12
Fc	0.55	0.43	0.49	1.01				

^a Tetrabutylammonium tetrafluoroborate salt as electrolyte ($c = 0.12 \text{ mol L}^{-1}$); scan rate = 100 mV s^{-1} ; the potential values are relative to SCE; ^b $c = 3.8 \text{ mmol L}^{-1}$; ^c ratio was observed to change with scan rate with a value of 1.46 at 50 mV s^{-1} ; ^d $c = 2.0 \text{ mmol L}^{-1}$; ^e ratio was observed to change with scan rate with a value of 1.27 at 50 mV s^{-1} .

Indeed the change for a solvent with better donocity reduced the oxidation potential and stabilised even more the oxidised species. For nickel complex **31**, no reduction was observed within the potential window (0 V, -2.0 V) considered, and a reversible one electron oxidation took place at 0.58 V ($\Delta E_p = 152 \text{ mV}$). Interestingly for the salen complex oxidation takes place at $E_{1/2} = 0.81 \text{ V}$ in DMF, in conditions where oxidation of ferrocene occurs at 0.48 V.³⁷ Thus,

the oxidation potential of phosphasalen nickel complex **31** is only 0.1 V higher than that of ferrocene, whereas that of the [Ni(salen)] derivative is 0.33 V higher compared to the same reference. This clearly illustrates the better donating ability of the phosphasalen ligand which renders the nickel centre more electron rich and allows an easier oxidation.

For the palladium complex **30**, electrochemical studies were more difficult due to the more limited solubility of this complex in presence of DMF, thus lower concentrations were employed. Similarly to the case of the nickel-phosphasalen complex, no reduction was observed within the potential range explored. Interestingly, two oxidation waves were seen. The first one is irreversible at 0.76 V and the second one at 1.06 V which is pseudo-reversible ($I_{pc}/I_{pa} \sim 1.12$). Thus, the first oxidation of the palladium complex **30** occurred at a higher potential compared to the nickel counterpart **31** which implies a less electron rich metal centre. Nevertheless a second oxidation can only be seen in the case of the palladium derivative which may be related to the increase of the thermodynamic stability of the highest oxidation states of elements within the row Ni-Pd-Pt.⁴³

Indeed, for the [Pd(salen)] complex two irreversible oxidation waves were observed⁴⁴ at 0.96 and 1.07 V in acetonitrile namely 0.44 and 0.55 V higher than the oxidation potential of ferrocene in the same conditions (0.518 V). The first oxidation is thus easier for the phosphasalen derivative (only 0.27 V higher than the ferrocene oxidation potential) in agreement with the presence of a better electron-donating ligand. However, the second oxidation of the phosphasalen complex occurs at comparable potential as the salen derivative (namely 0.55 and 0.58 V higher than $E_{1/2}^1(\text{Fc}^+/\text{Fc})$), but as already established this oxidation in [Pd(salen)] complex corresponds to the electron transfer from a molecular orbital localised predominantly on the ligand and not on the metal centre.^{44a}

2.2.4 Magnetic Properties of Nickel phosphasalen Complex and Theoretical Studies

Whereas the palladium phosphasalen complex always give finely resolved NMR spectra, which is quite usual for a diamagnetic compound, it is difficult to obtain nicely resolved spectra for the nickel phosphasalen complex at room temperature. This suggests either a rapid exchange between different conformations of a diamagnetic complex, or the existence of a partially populated triplet state of the complex at room temperature. Indeed, if at room temperature the phosphasalen nickel complex **31** would exist under two different spin states (a singlet and a triplet one), the latter would perturb the NMR measurements. Magnetic moment of phosphasalen complex **31** has been measured using Evans method⁴⁵ showing a value of $1.40 \mu_B$ at room temperature. At first view, this value is very low compared to literature values of 3.0-4.0 μ_B expected for fully tetrahedral Ni(II) complexes.⁴⁶ However, values around 1.3 μ_B were reported by Braunstein and coworkers for Ni(II) complexes adopting a distorted tetrahedral

geometry in solution.⁴⁷ This was attributed to the dependence of magnetic moment on the ligand field, and the occurrence of structural equilibria in solution.⁴⁸

As such observation was neither made for salen Ni(II) complexes we undertook a theoretical study to compare the electronic properties of the [Ni(salen)] and [Ni(phosphasalén)]. Density Functional Theory (DFT) calculations were performed on these two complexes with the Gaussian 03 set of programs⁴⁹ in combination with the B3PW91 functional⁵⁰. Nickel was represented by the relativistic effective core potential of Hay and Wadt⁵¹ and the associated triple zeta quality basis set,⁵² augmented by a f polarization function as proposed by Frenking⁵³ (lanl2tz(f)). All other atoms were described with the 6-31G* Pople basis set.⁵⁴

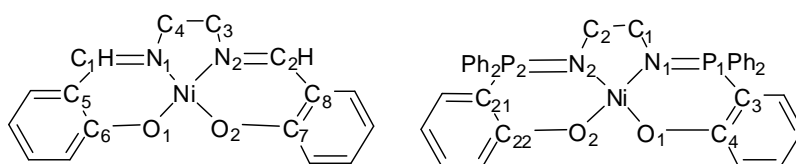


Table 3. Comparison of selected geometric parameters coming from X-ray diffraction analysis and DFT calculations

	[Ni(salen)]			[Ni(phosphasalén)]		
	X-ray	Optimised singlet structure	Optimised triplet structure	X-ray	Optimised singlet structure	Optimised triplet structure
N2-Ni1	1.851(3)	1.857	1.986	1.888(4)	1.897	1.966
N1-Ni1	1.849(3)	1.856	1.989	1.905(4)	1.894	2.011
Ni-O2	1.853(3)	1.847	1.900	1.863(4)	1.865	1.914
Ni-O1	1.851(5)	1.848	1.899	1,881(3)	1.883	1.953
O2-Ni-N2	94.1(4)	94.31	91.6	95.4(2)	94.7	97,5
O1-Ni-N1	94.2(4)	93.99	91.5	95.4(2)	95.1	96,3
O1-Ni-O2	85.5(4)	85.4	105.2	83.9(2)	84.4	101.1
N1-Ni-N2	86.3(5)	86.4	82.9	85.4(2)	85.8	85.8
N1-Ni-N2-O2	178,5	177.5	153.4	176.40(35)	179.4	127.2
N2-Ni-N1-O1	178.6	177.8	151.4	178.68(39)	178.8	155.1
O2-Ni-O1-N1	178.7	177.5	158.5	176.38(42)	179.4	130.6
O1-Ni-O2-N2	178.5	177.8	156.1	178.64(39)	178.8	162.0

Optimizations of both complexes **31** and [Ni(salen)] were performed in the singlet and triplet states. Table 3 gathers some selected geometric parameters for each optimised structure together with the available experimental data from X-ray diffraction analysis.¹³ On the whole there is an excellent agreement between the experimental structure and the theoretical parameters optimised for the singlet state. A nearly square planar geometry was found for both complexes with dihedral angles around the metal centre lying between 176 and 179°. Mean deviations of 0.01 Å were found for the bond lengths and 1° for the bond angles.

In optimized triplet states, both complexes adopt distorted tetrahedral geometry. This change in geometry is illustrated by the dihedral angles given in Table 3 which vary from nearly 180° (the value for an ideal square planar arrangement) in the singlet state to values between 162 and 127° (instead of 120° for an ideal tetrahedral structure) in the triplet state. The phosphasalen ligand seems to be more flexible than the salen one, as demonstrated by the larger geometrical evolution of the phosphasalen complex than the salen one (mean value of 143.7° for the dihedral angles instead of 154.9° for the latter). It's also observed that the metal-ligand bond distances are significantly longer in the triplet than in the singlet state, by 0.094 and 0.076 Å in the salen and the phosphasalen complexes, respectively (mean values).

Orbital Analysis for Singlet and Triplet States

Nickel(Salen) Complex

To decrypt these observation and have an insight into the low spin-high spin process, orbital analysis has been carried out. In fact, formation of the triplet state in the square planar singlet state involves first removing one electron and then placing it in another orbital. For the Ni-Salen complex, a correlation has been clearly established between different spin states and geometries of the two major orbitals: that from which the electron was removed and that which accepts the removed electron (Figure 5, Figure 6).

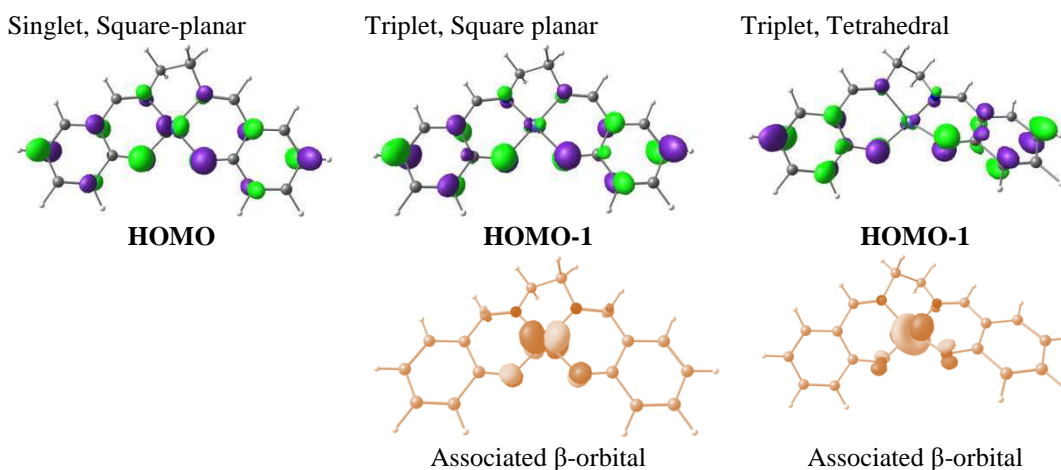


Figure 5. Evolution of MO orbital from which one electron is transferred

The electron is removed from the HOMO, which involves a d orbital in π -antibonding interaction with p- π orbitals from O and N. This orbital loses its component in d and becomes essentially ligand-based (the lost d component now resides essentially in the beta-orbital associated, which is unoccupied). The electron is placed in the $d_{x^2-y^2}$ orbital in strong σ -antibonding interaction with the ligands.

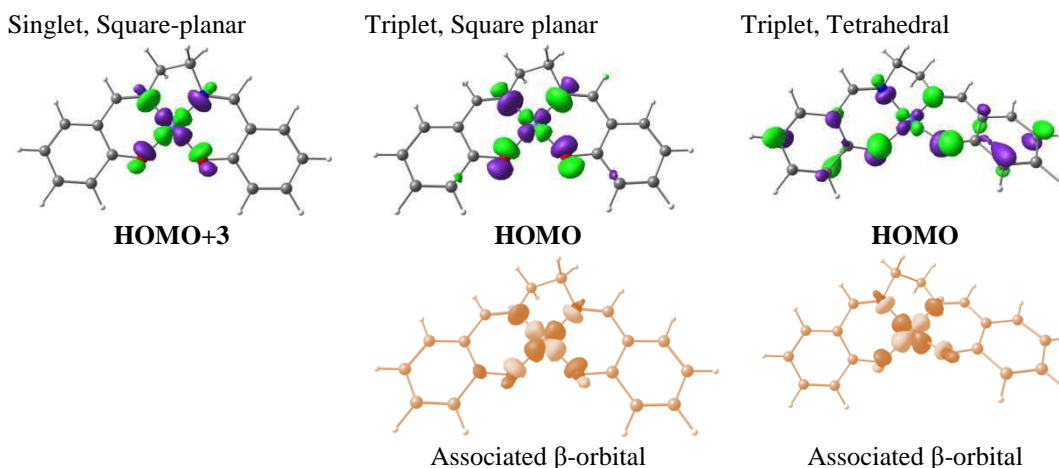


Figure 6. Evolution of MO orbital to which one electron is transferred

According to the metal-ligand π antibonding character of the HOMO orbital of the nickel Salen complex (Figure 5), taking one electron from this should shorten the metal-ligand bond distances. However the electron left from the HOMO now occupies an orbital which was vacant in the singlet state, the fifth d orbital of these d^8 complexes ($d_{x^2-y^2}$). Since it is strongly σ -antibonding between the metal and the ligands (Figure 4), its occupation entails a lengthening of the metal-ligand bonds. So two factors work in opposite direction but the latter dominates (the σ antibonding interactions are stronger than the π ones). A lengthening of the metal-ligand distances thus occurs on going to the triplet spin state, a trend which is preserved upon distortion towards a pseudo-tetrahedral arrangement.

Nickel(Phosphasalen) Complex

The same reasoning of the elongated M-O and M-N bonds applies for the nickel-phosphasalen complex. Indeed, in the case of Ni-Psalen complex, the electron is also removed from the HOMO and placed in $d_{x^2-y^2}$ -orbital in strong σ -antibonding interaction with p-orbitals from N and O, which was vacant in the singlet state.

The correlation of orbitals in the singlet, non-relaxed triplet ($S=3$ PC) and in the relaxed triplet ($S=3$ Td) states are undoubtful for this $d_{x^2-y^2}$ -orbital for both the occupied alpha orbital and the associated unoccupied beta-orbital (Figure 7). But it was not obvious for the occupied alpha-orbital which the HOMO has become, as the large molecule has many wave functions with close eigen values, i.e orbitals with close energy, and the singly occupied orbital seems to have

made various combinations with other orbitals which render its identification difficult. However, the associated beta-orbital could be easily identified (Figure 8). This orbital is metal-centered and allows us to conclude that the singly occupied orbital from HOMO has lost most of its component in d-orbital, and that electron is taken from this d-component to placed in the $d_{x^2-y^2}$ orbital.

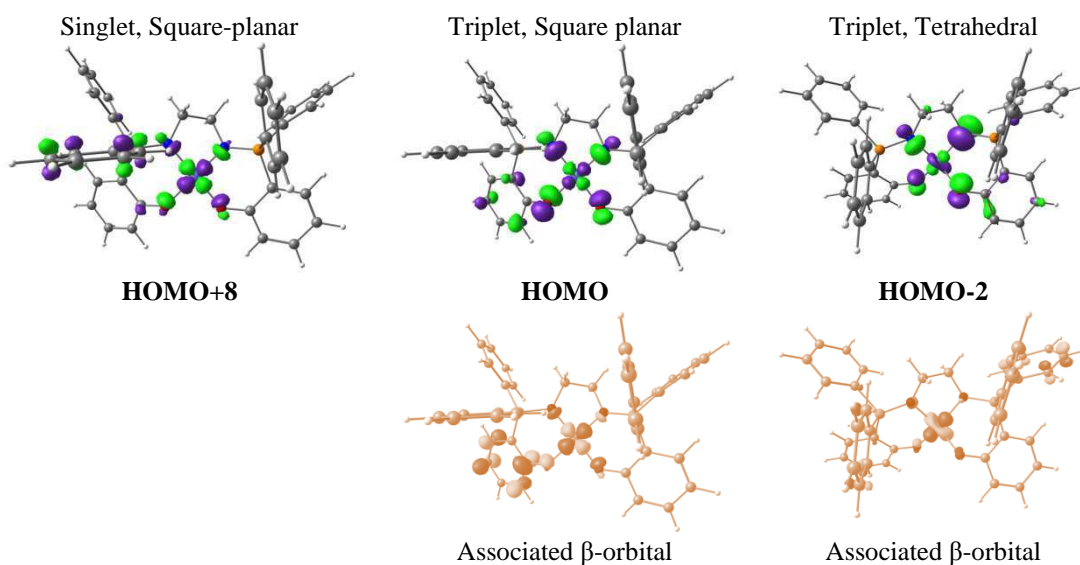


Figure 7. Evolution of MO orbital to which one electron is transferred

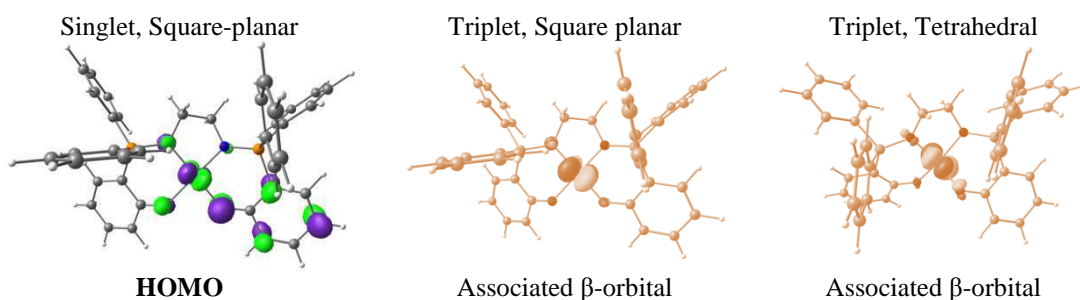


Figure 8. Evolution of MO orbital from which one electron is transferred

Just as the previous case with Ni-Salen complex, the charge at Ni and negative charges at O and N should increase. That is indeed the case: the charge at Ni changes from +0.456 in singlet state to +0.621 in triplet state (square planar), at N from -0.662 and -0.650 to -0.700 and -0.715, at O from -0.580 and -0.571 to -0.605 and -0.599. The spin density is mainly on Ni (+1.59), the rest of spin densities are mainly on N and O atoms. When the geometry is relaxed, the alpha orbital

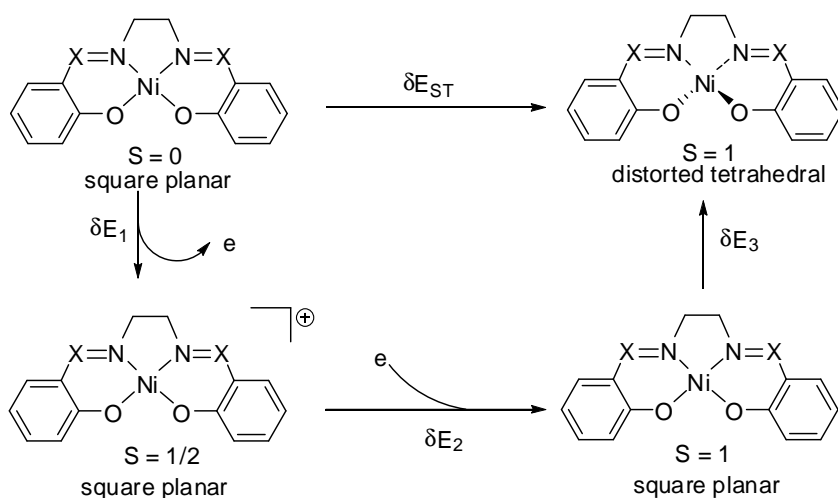
from $d_{x^2-y^2}$ is more ligand-centered and the associated beta orbital is more metal-centered, so the charge at Ni increases to +0.682, the spin density at Ni is +1.65.

Magnetic Moment of Ni-Phosphasalén Complex

As could be seen from the orbital analysis before, the HOMO in both complexes involves a d orbital on the metal centre in π -antibonding interaction with the oxygen and nitrogen ligands. However the HOMO of the phosphasalén complex is significantly higher in energy than that of the salen complex (-4.56 instead of -5.12 eV). As a consequence the vertical ionisation energy calculated for the phosphasalén complex (5.73 eV) is lower than that for the salen complex (6.49 eV), a result in agreement with the easier oxidation found experimentally for the former.

From an energetic point of view the singlet state was found 9.0 kcal mol⁻¹ more stable than the triplet state for the salen complex in agreement with the experimental evidence for a low spin complex in solution.⁵⁵ A strikingly different situation was found for the phosphasalén complex with a triplet state slightly more stable than the singlet state ($\Delta E = -1.4$ kcal mol⁻¹). A triplet ground state in solution as well as a small singlet-triplet energy difference (which suggests that both spin configurations could coexist in solution), are in agreement with the experimental measure of the magnetic moment of complex **31**.

In order to rationalise the singlet-triplet energy difference (δE_{ST}), we made use of the thermodynamical cycle as described in Scheme 23. Starting from the optimised square planar singlet state, one electron is removed from the HOMO keeping the geometry of the complex unchanged (δE_1). This removed electron is then placed in the antibonding d orbital leading to a triplet state in the square planar geometry (δE_2). Finally, the geometry is relaxed to reach the optimised geometry for the triplet state (δE_3).



Scheme 23. Thermodynamical cycle to determine the singlet-triplet energy difference (δE_{ST})

The values of δE_1 , δE_2 , δE_3 and δE_{ST} are reported in Table 4 for both salen and phosphasalen complexes. It clearly appears that the electronic factor responsible for the difference of δE_{ST} between salen and phosphasalen complex (by $10.4 \text{ kcal mol}^{-1}$) is the major lowering (by $17.5 \text{ kcal mol}^{-1}$) of the ionisation energy in going from the salen to the phosphasalen complex. Thus it could be said that the low-lying triplet state of the nickel phosphasalen complex is due to the better donating ability of phosphasalen ligand.

Table 4. Energy decomposition (kcal mol^{-1}), according to Scheme 4, of the singlet-triplet energy difference for salen and phosphasalen complexes.

	δE_1	δE_2	δE_3	δE_{ST}
[Ni(salen)]	149.6	-129.6	-11.0	+9.0
[Ni(phosphasalen)]	132.1	-122.0	-11.5	-1.4
$\Delta E([\text{Ni}(\text{salen})] - [\text{Ni}(\text{phosphasalen})])$	-17.5	+7.0	-0.5	-10.4

III. Conclusion

Taken into account the importance of salen ligands in coordination chemistry and catalysis, as well as the need to develop salen-like ligands with different electronic properties and improved flexibility, phosphasalen ligands have been developed in the laboratory. This new class of ligand combines two iminophosphorane and two phenoxide groups. The proligand (bis(aminophosphonium) salt) was synthesized by a Kirsanov reaction between ethylene diamine and phosphinophenol in good yield. Although only the unsubstituted proligand has been synthesized, it is well conceivable that this simple method could be apply to the synthesis of other ligands with variations on the phenoxide rings, as well as on the diamine linker. These possibilities would be developed further.

The phosphasalen ligand was easily and cleanly coordinated with nickel(II) and palladium(II) metal centers, giving stable complexes. Chemical study by cyclic voltammetry showed that all these two complexes present oxidation waves at lower potential than the salen analogs, clearly demonstrating the better donating ability of the phosphasalen ligand compared to salen.

In particular, the nickel phosphasalen complex presents a non-negligible magnetic moment in solution, whereas in the solid state it is diamagnetic and adopts square-planar geometry. This behavior is very different from the nickel salen complex and suggest the existence of a low-lying triplet state. DFT calculations carried out on nickel salen and phosphasalen complexes in singlet and triplet states not only elucidate the orbitals involved in the singlet-triplet transition for both complexes, but also explain the origin of this “strange” behavior of the phosphasalen complex. It has been found that the triplet state of phosphasalen complex is slightly lower in

energy than the singlet state, whereas for the salen complex, the triplet state is much higher in energy than the singlet state. The small difference in energy in singlet-triplet state for phosphasalen complex explains the magnetic moment measured in solution for this compound. And this small difference in energy is a direct consequence of the better donating ability of phosphasalen ligand.

REFERENCES

1. (a) Canali, L.; Sherrington, D. C., *Chem. Soc. Rev.* **1999**, 28 (2), 85-93; (b) Cozzi, P. G., *Chem. Soc. Rev.* **2004**, 33 (7), 410-421; (c) Baleizao, C.; Garcia, H., *Chem. Rev.* **2006**, 106 (9), 3987-4043.
2. Katsuki, T.; Sharpless, K. B., *J. Am. Chem. Soc.* **1980**, 102 (18), 5974-5976.
3. Sharpless, K. B.; Woodard, S. S.; Finn, M. G., *Pure Appl. Chem.* **1983**, 55 (11), 1823-1836.
4. (a) McGarrigle, E. M.; Gilheany, D. G., *Chem. Rev.* **2005**, 105 (5), 1563-1602; (b) Siddall, T. L.; Miyaura, N.; Huffman, J. C.; Kochi, J. K., *J. Chem. Soc.-Chem. Commun.* **1983**, (21), 1185-1186; (c) Srinivasan, K.; Michaud, P.; Kochi, J. K., *J. Am. Chem. Soc.* **1986**, 108 (9), 2309-2320; (d) Samsel, E. G.; Srinivasan, K.; Kochi, J. K., *J. Am. Chem. Soc.* **1985**, 107 (25), 7606-7617.
5. Katsuki, T., *Adv. Synth. Catal.* **2002**, 344 (2), 131-147.
6. (a) Yoon, T. P.; Jacobsen, E. N., *Science* **2003**, 299 (5613), 1691-1693; (b) Annis, D. A.; Jacobsen, E. N., *J. Am. Chem. Soc.* **1999**, 121 (17), 4147-4154; (c) Jacobsen, E. N., *Acc. Chem. Res.* **2000**, 33 (6), 421-431; (d) Ready, J. M.; Jacobsen, E. N., *J. Am. Chem. Soc.* **2001**, 123 (11), 2687-2688.
7. Inoue, S.; Koinuma, H.; Tsuruta, T., *J. Polym. Sci. B: Polym. Lett.* **1969**, 7 (4), 287-292.
8. Jacobsen, E. N.; Tokunaga, M.; Larrow, J. F. WO2000009463. 2000.
9. Paddock, R. L.; Nguyen, S. T., *J. Am. Chem. Soc.* **2001**, 123 (46), 11498-11499.
10. (a) Darensbourg, D. J.; Mackiewicz, R. M.; Rodgers, J. L.; Fang, C. C.; Billodeaux, D. R.; Reibenspies, J. H., *Inorg. Chem.* **2004**, 43 (19), 6024-6034; (b) Darensbourg, D. J.; Frantz, E. B., *Inorg. Chem.* **2007**, 46 (15), 5967-5978; (c) Darensbourg, D. J., *Chem. Rev.* **2007**, 107 (6), 2388-2410; (d) Lu, X.-B.; Darensbourg, D. J., *Chem. Soc. Rev.* **2012**, 41 (4), 1462-1484.
11. Lu, X.-B.; Liang, B.; Zhang, Y.-J.; Tian, Y.-Z.; Wang, Y.-M.; Bai, C.-X.; Wang, H.; Zhang, R., *J. Am. Chem. Soc.* **2004**, 126 (12), 3732-3733.
12. Katsuki, T., *Chem. Soc. Rev.* **2004**, 33 (7), 437-444.
13. (a) Saito, B.; Katsuki, T., *Tetrahedron Lett.* **2001**, 42 (47), 8333-8336; (b) Saito, B.; Katsuki, T., *Tetrahedron Lett.* **2001**, 42 (23), 3873-3876; (c) Matsumoto, K.; Sawada, Y.; Saito, B.; Sakai, K.; Katsuki, T., *Angew. Chem. Int. Ed.* **2005**, 44 (31), 4935-4939.

14. (a) Egami, H.; Katsuki, T., *J. Am. Chem. Soc.* **2007**, *129*, 8940-+; (b) Sivasubramanian, V. K.; Ganesan, M.; Rajagopal, S.; Ramaraj, R., *J. Org. Chem.* **2002**, *67* (5), 1506-1514; (c) Chattopadhyay, T.; Das, D., *J. Coord. Chem.* **2009**, *62* (5), 845-853; (d) Wang, C. H.; Lu, J. W.; Wei, H. H.; Takeda, M., *Inorg. Chim. Acta* **2007**, *360* (9), 2944-2952; (e) Mukherjee, C.; Stammler, A.; Boege, H.; Glaser, T., *Chem. Eur. J.* **2010**, *16* (33), 10137-10149; (f) Mekmouche, Y.; Menage, S.; Toia-Duboc, C.; Fontecave, M.; Galey, J. B.; Lebrun, C.; Pecaut, J., *Angew. Chem. Int. Ed.* **2001**, *40* (5), 949-952; (g) Legros, J.; Bolm, C., *Angew. Chem. Int. Ed.* **2004**, *43* (32), 4225-4228.
15. (a) Lebel, H.; Marcoux, J. F.; Molinaro, C.; Charette, A. B., *Chem. Rev.* **2003**, *103* (4), 977-1050; (b) Maas, G., *Chem. Soc. Rev.* **2004**, *33* (3), 183-190.
16. (a) Kim, S. S.; Lee, S. H.; Kwak, J. M., *Tetrahedron Asym.* **2006**, *17* (8), 1165-1169; (b) Baleizao, C.; Gigante, B.; Garcia, H.; Corma, A., *Tetrahedron Lett.* **2003**, *44* (36), 6813-6816; (c) Baleizao, C.; Gigante, B.; Garcia, H.; Corma, A., *Tetrahedron* **2004**, *60* (46), 10461-10468; (d) Baleizao, C.; Gigante, B.; Garcia, H.; Corma, A., *J. Catal.* **2004**, *221* (1), 77-84; (e) Lv, C. W.; Cheng, Q. G.; Xu, D. Q.; Wang, S. F.; Xia, C. G.; Sun, W., *Eur. J. Org. Chem.* **2011**, (19), 3407-3411; (f) Belokon, Y.; Moscalenko, M.; Ikonnikov, N.; Yashkina, L.; Antonov, D.; Vorontsov, E.; Rozenberg, V., *Tetrahedron Asym.* **1997**, *8* (19), 3245-3250; (g) Belokon, Y.; Ikonnikov, N.; Moscalenko, M.; North, M.; Orlova, S.; Tararov, V.; Yashkina, L., *Tetrahedron Asym.* **1996**, *7* (3), 851-855; (h) Belokon, Y. N.; Caveda-Cepas, S.; Green, B.; Ikonnikov, N. S.; Krustalev, V. N.; Larichev, V. S.; Moscalenko, M. A.; North, M.; Orizu, C.; Tararov, V. I.; Tasinazzo, M.; Timofeeva, G. I.; Yashkina, L. V., *J. Am. Chem. Soc.* **1999**, *121* (16), 3968-3973.
17. (a) Li, Z. B.; Pu, L., *Org. Lett.* **2004**, *6* (6), 1065-1068; (b) Trost, B. M.; Weiss, A. H., *Adv. Synth. Catal.* **2009**, *351* (7-8), 963-983.
18. (a) Li, L. S.; Wu, Y. K.; Hu, Y. J.; Xia, L. J.; Wu, Y. L., *Tetrahedron Asym.* **1998**, *9* (13), 2271-2277; (b) Aikawa, K.; Irie, R.; Katsuki, T., *Tetrahedron* **2001**, *57* (5), 845-851; (c) Chaladaj, W.; Kwiatkowski, P.; Jurczak, J., *Synlett* **2006**, (19), 3263-3266; (d) Schaus, S. E.; Branalt, J.; Jacobsen, E. N., *J. Org. Chem.* **1998**, *63* (2), 403-405; (e) Zulauf, A.; Mellah, M.; Guillot, R.; Schulz, E., *Eur. J. Org. Chem.* **2008**, (12), 2118-2129; (f) Eno, S.; Egami, H.; Uchida, T.; Katsuki, T., *Chem. Lett.* **2008**, *37* (6), 632-633.
19. (a) Uchida, T.; Katsuki, T., *Tetrahedron Lett.* **2001**, *42* (39), 6911-6914; (b) Bianchini, G.; Cavarzan, A.; Scarso, A.; Strukul, G., *Green Chemistry* **2009**, *11* (10), 1517-1520; (c) Watanabe, A.; Uchida, T.; Ito, K.; Katsuki, T., *Tetrahedron Lett.* **2002**, *43* (25), 4481-4485; (d) Watanabe, A.; Uchida, T.; Irie, R.; Katsuki, T., *P. Natl. Acad. Sci. USA* **2004**, *101* (16), 5737-5742.
20. Calligar.M; Randacci.L; Nardin, G., *Coord. Chem. Rev.* **1972**, *7* (4), 385-&.
21. Calligar.M; Manzini, G.; Randacci.L; Nardin, G., *J. Chem. Soc.- Dalton Trans.* **1972**, (4), 543-&.
22. Corazza, F.; Solari, E.; Floriani, C.; Chiesivilla, A.; Guastini, C., *J. Chem. Soc.- Dalton Trans.* **1990**, (4), 1335-1344.
23. P. Corden, J.; Errington, W.; Moore, P.; G. H. Wallbridge, M., *Chem. Commun.* **1999**, (4).

24. (a) Knight, P. D.; Scott, P., *Coord. Chem. Rev.* **2003**, *242* (1-2), 125-143; (b) Che, C. M.; Huang, J. S., *Coord. Chem. Rev.* **2003**, *242* (1-2), 97-113.
25. Yamada, T.; Imagawa, K.; Nagata, T.; Mukaiyama, T., *Chem. Lett.* **1992**, (11), 2231-2234.
26. (a) Khavrutskii, I. V.; Musaev, D. G.; Morokuma, K., *J. Am. Chem. Soc.* **2003**, *125* (45), 13879-13889; (b) Suzuki, M.; Ishikawa, T.; Harada, A.; Ohba, S.; Sakamoto, M.; Nishida, Y., *Polyhedron* **1997**, *16* (15), 2553-2561.
27. (a) Atwood, D. A., *Coord. Chem. Rev.* **1997**, *165*, 267-296; (b) Ziegler, J. E.; Du, G. D.; Fanwick, P. E.; Abu-Omar, M. M., *Inorg. Chem.* **2009**, *48* (23), 11290-11296; (c) Yeori, A.; Gendler, S.; Groysman, S.; Goldberg, I.; Kol, M., *Inorg. Chem. Commun.* **2004**, *7* (2), 280-282.
28. (a) Matsumoto, K.; Oguma, T.; Katsuki, T., *Angew. Chem. Int. Ed.* **2009**, *48* (40), 7432-7435; (b) Saito, B.; Katsuki, T., *Angew. Chem. Int. Ed.* **2005**, *44* (29), 4600-4602; (c) Sawada, Y.; Matsumoto, K.; Kondo, S.; Watanabe, H.; Ozawa, T.; Suzuki, K.; Saito, B.; Katsuki, T., *Angew. Chem. Int. Ed.* **2006**, *45* (21), 3478-3480; (d) Cohen, A.; Yeori, A.; Kopilov, J.; Goldberg, I.; Kol, M., *Chem. Commun.* **2008**, (18), 2149-2151; (e) Matsumoto, K.; Saito, B.; Katsuki, T., *Chem. Commun.* **2007**, (35), 3619-3627; (f) Liu, X. L.; Cui, D. M., *Dalton Trans.* **2009**, (47), 10621-10621; (g) Saito, B.; Egami, H.; Katsuki, T., *J. Am. Chem. Soc.* **2007**, *129* (7), 1978-1986; (h) Yeori, A.; Goldberg, I.; Shuster, M.; Kol, M., *J. Am. Chem. Soc.* **2006**, *128* (40), 13062-13063.
29. Adao, P.; Avecilla, F.; Bonchio, M.; Carraro, M.; Pessoa, J. C.; Correia, I., *Eur. J. Inorg. Chem.* **2010**, (35), 5568-5578.
30. (a) Kunisu, T.; Oguma, T.; Katsuki, T., *J. Am. Chem. Soc.* **2011**, *133* (33), 12937-12939; (b) Darensbourg, D. J.; Poland, R. R.; Strickland, A. L., *J. Polym. Sci., Part A: Polym. Chem.* **2012**, *50* (1), 127-133; (c) Bryliakov, K. P.; Talsi, E. P., *Eur. J. Org. Chem.* **2011**, (24), 4693-4698.
31. Kocher, N.; Leusser, D.; Murso, A.; Stalke, D., *Chem. Eur. J.* **2004**, *10* (15), 3622-3631.
32. Broderick, E. M.; Thuy-Boun, P. S.; Guo, N.; Vogel, C. S.; Sutter, J.; Miller, J. T.; Meyer, K.; Diaconescu, P. L., *Inorg. Chem.* **2011**, *50* (7), 2870-2877.
33. Bianchi, A.; Bernardi, A., *J. Org. Chem.* **2006**, *71* (12), 4565-4577.
34. Buchard, A.; Komly, B.; Auffrant, A.; Le Goff, X. F.; Floch, P. L., *Organometallics* **2008**, *27* (17), 4380-4385.
35. Kumari, N.; Prajapati, R.; Mishra, L., *Polyhedron* **2008**, *27* (1), 241-248.
36. (a) Kondo, M.; Nabari, K.; Horiba, T.; Irie, Y.; Kabir, M. K.; Sarker, R. P.; Shimizu, E.; Shimizu, Y.; Fuwa, Y., *Inorg. Chem. Commun.* **2003**, *6* (2), 154-156; (b) Siegler, M. A.; Lutz, M., *Crystal Growth & Design* **2009**, *9* (2), 1194-1200.
37. Santos, I. C.; Vilas-Boas, M.; Piedade, M. F. M.; Freire, C.; Duarte, M. T.; de Castro, B., *Polyhedron* **2000**, *19* (6), 655-664.

38. (a) Vilas-Boas, M.; Freire, C.; de Castro, B.; Christensen, P. A.; Hillman, A. R., *Chem. Eur. J.* **2001**, *7* (1), 139-150; (b) VilasBoas, M.; Freire, C.; deCastro, B.; Christensen, P. A.; Hillman, A. R., *Inorg. Chem.* **1997**, *36* (22), 4919-4929.
39. De Castro, B.; Freire, C., *Inorg. Chem.* **1990**, *29* (25), 5113-5119.
40. Bottcher, A.; Elias, H.; Jager, E. G.; Langfelderova, H.; Mazur, M.; Muller, L.; Paulus, H.; Pelikan, P.; Rudolph, M.; Valko, M., *Inorg. Chem.* **1993**, *32* (19), 4131-4138.
41. (a) Matni, A.; Boubekeur, L.; Mezailles, N.; Le Floch, P.; Geoffroy, M., *Chem. Phys. Lett.* **2005**, *411* (1-3), 23-27; (b) Matni, A.; Boubekeur, L.; Grosshans, P.; Mezailles, N.; Bernardinelli, G.; Le Floch, P.; Geoffroy, M., *Magn. Reson. Chem.* **2007**, *45* (12), 1011-1017.
42. Escobar, M.; Jin, Z.; Lucht, B. L., *Org. Lett.* **2002**, *4* (13), 2213-2216.
43. Cotton, A. F.; Wilkinson, G., *Advanced Inorganic Chemistry*. Willey: New York, 1988.
44. (a) Vasil'eva, S.; Balashev, K.; Timonov, A., *Russ. J. Electrochem.* **2000**, *36* (1), 75-79; (b) Fonseca, J.; Tedim, J.; Biernacki, K.; Magalhães, A. L.; Gurman, S. J.; Freire, C.; Hillman, A. R., *Electrochim. Acta* **2010**, *55* (26), 7726-7736.
45. (a) Evans, D. F., *J. Chem. Soc.* **1959**, (JUN), 2003-2005; (b) Deutsch, J. L.; Poling, S. M., *J. Chem. Educ.* **1969**, *46* (3), 167-&; (c) Loliger, J.; Scheffol.R, *J. Chem. Educ.* **1972**, *49* (9), 646-&.
46. Frommel, T.; Peters, W.; Wunderlich, H.; Kuchen, W., *Angew. Chem.-Int. Edit. Engl.* **1993**, *32* (6), 907-909.
47. Speiser, F.; Braunstein, P.; Saussine, L., *Organometallics* **2004**, *23* (11), 2625-2632.
48. (a) Hayter, R. G.; Humiec, F. S., *Inorg. Chem.* **1965**, *4* (12), 1701-&; (b) Dori, Z.; Gray, H. B., *J. Am. Chem. Soc.* **1966**, *88* (7), 1394-&.
49. M. J. Frisch; G. W. Trucks; H. B. Schlegel; G. E. Scuseria; M. A. Robb; J. R. Cheeseman; J. A. Montgomery, Jr., T. V.; K. N. Kudin; J. C. Burant; J. M. Millam; S. S. Iyengar; J. Tomasi; V. Barone; B. Mennucci; M. Cossi; G. Scalmani; N. Rega; G. A. Petersson, H. N., M. Hada, M. Ehara, K. Toyota, R. Fukuda, J. Hasegawa, M. Ishida, T. Nakajima, Y. Honda, O. Kitao, H. Nakai, M. Klene, X. Li, J. E. Knox, H. P. Hratchian, J. B. Cross, V. Bakken, C. Adamo, J. Jaramillo, R. Gomperts, R. E. Stratmann, O. Yazyev, A. J. Austin, R. Cammi, C. Pomelli, J. W. Ochterski, P. Y. Ayala, K. Morokuma, G. A. Voth, P. Salvador, J. J. Dannenberg, V. G. Zakrzewski, S. Dapprich, A. D. Daniels, M. C. Strain, O. Farkas, D. K. Malick, A. D. Rabuck, K. Raghavachari, J. B. Foresman, J. V. Ortiz, Q. Cui, A. G. Baboul, S. Clifford, J. Cioslowski, B. B. Stefanov, G. Liu, A. Liashenko, P. Piskorz, I. Komaromi, R. L. Martin, D. J. Fox, T. Keith, M. A. Al-Laham, C. Y. Peng, A. Nanayakkara, M. Challacombe, P. M. W. Gill, B. Johnson, W. Chen, M. W. Wong, C. Gonzalez, and J. A. Pople *Gaussian 03, revision C.02*, Gaussian Inc., Wallingford CT: 2004.
50. (a) Becke, A. D., *J. Chem. Phys.* **1993**, *98* (7), 5648-5652; (b) Perdew, J. P.; Wang, Y., *Phys. Rev. B* **1992**, *45* (23), 13244-13249.
51. Hay, P. J.; Wadt, W. R., *J. Chem. Phys.* **1985**, *82* (1), 270-283.

52. Roy, L. E.; Hay, P. J.; Martin, R. L., *J. Chem. Theory Comput.* **2008**, *4* (7), 1029-1031.
53. Ehlers, A. W.; Bohme, M.; Dapprich, S.; Gobbi, A.; Hollwarth, A.; Jonas, V.; Kohler, K. F.; Stegmann, R.; Veldkamp, A.; Frenking, G., *Chem. Phys. Lett.* **1993**, *208* (1-2), 111-114.
54. Petersson, G. A.; Bennett, A.; Tensfeldt, T. G.; Allaham, M. A.; Shirley, W. A.; Mantzaris, J., *J. Chem. Phys.* **1988**, *89* (4), 2193-2218.
55. Hobday, M. D.; Smith, T. D., *Coord. Chem. Rev.* **1973**, *9* (3-4), 311-337.

Chapter 4

Oxidised Ni(II) Phosphasalen Complexes

From our study on Nickel phosphasalen complex, it has been shown that the phosphasalen ligand is a better donor than the salen one and that the complex is oxidized at lower potential than the salen analog. Furthermore, by cyclic voltammetry study, it was observed that the oxidised species is quite stable, even in solvent with low-coordinating ability such as acetonitrile. Following this direction, and taken into account the interest in Ni(III) and in studying oxidized phenoxide complexes of nickel which has been manifested through Ni-Salen, we carried out the preparation and study of oxidised nickel-phosphasalen complex.

I. Introduction

1. Phenoxy Radical Complexes

The chemistry of oxidized metal-phenoxide complexes has attracted much attention in the last decade. This might be attributed to the direct relation to the phenoxy radical in galactose oxidase,¹ a mononuclear copper enzyme catalyzing the oxidation of primary alcohols to aldehydes along with the reduction of O₂ to H₂O₂. The enzyme functions as a two electron redox unit during the catalytic cycle, and the overall catalytic reaction in fact involves two separable half-reaction: oxidation of a primary alcohol and reduction of oxygen to hydrogen peroxide. The active site of the enzyme is composed of a copper center coordinated by four aminoacid side chains (from Tyr272, Tyr495, His496, His581), along with a solvent molecule, forming a five-coordinated metal complex (Figure 1).

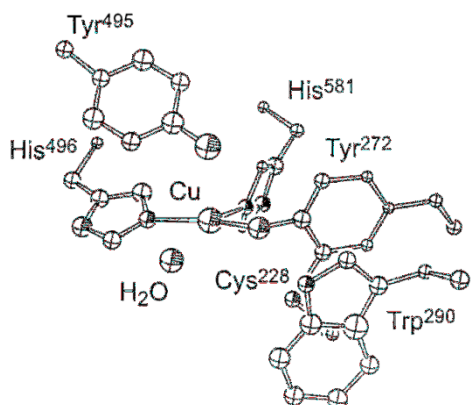
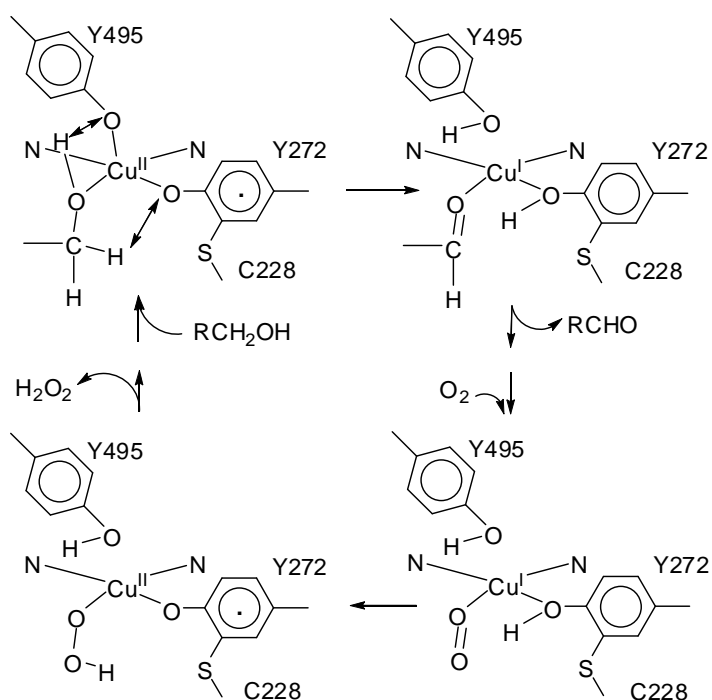


Figure 1. X-ray structure of the active site of galactose oxidase.

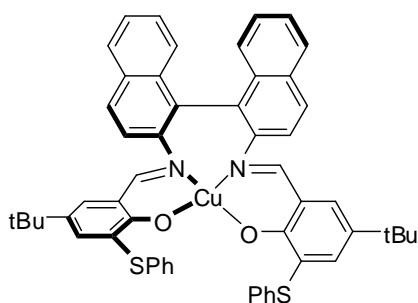
The role of Tyr495 is supposed to act as a general base during the proton transfer. The electron transfer is ensured by the copper ion and Tyr272, which is a modified one and is covalently cross-linked to a cysteine (Cys228) through the sulfur atom. This cross-link has been shown to be redox-active and identified as the protein free radical site in galactose oxidase (Scheme 1). What is important in the mechanism of activity of galactose oxidase is the cooperative and alternative action of the metal center and tyrosine in redox reactions: the copper taking oxidation states of I or II and the tyrosine ligand exists sometimes as a neutral one, sometimes as a radical cation.



Scheme 1. Active site and catalytic mechanism of galactose oxidase (from Whittaker *et al*)^{1a}

The recognition of free radical role in the activity of galactose oxidase has shed insight into the understanding of many other metalloenzyme systems which also contain a redox active metal

center coordinated or adjacent to pro-radical ligand.² In catalysis, the cooperative effect between the metal center and the ligand in these systems have inspired the design of many synthetic system of catalyst³. The group of Stack, for example, developed copper salen complexes (one of which is presented in Scheme 2, named [Cu(II)BST]) which are able to catalyse the oxidation of primary alcohols by O₂ (1 atm), with turnover numbers up to 1300.^{3a} During the catalytic cycles, the complex is oxidized to [Cu(II)BST]⁺, in which the ligand is oxidized to a radical cation.



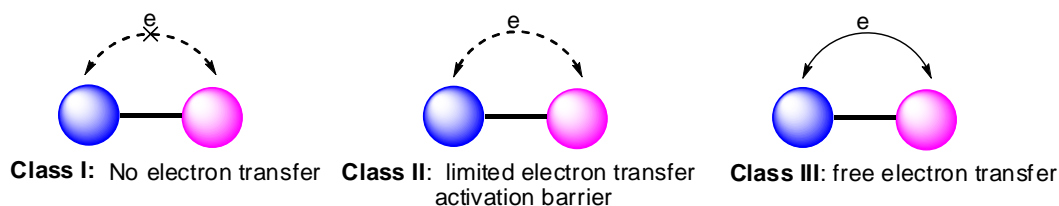
Scheme 2. Copper salen complex [Cu(II)BST]

For the importance of understanding the role of phenoxy radical in biochemistry and the potential applications of these species in catalysis, phenoxide metal complexes have attracted much attention in the last decade. Salen is likely the most important phenoxide-containing ligand in chemistry, and salen complexes have found numerous applications in catalysis (epoxidation, epoxide resolution, copolymerization of epoxides and CO₂, sulfoxidation, etc). Thus, it's easy to understand that a large part of studies on design and electronic structure of oxidized metal-phenoxide species have evolved around the salen complexes. The use of salen ligands constitutes other advantages: they could be easily synthesized from readily available starting material, and the introduction of various types of substituents on different positions on the ligand is possible, allowing the fine tuning of electronic properties of salen complexes and their oxidized species.

2. Mixed-Valence Compounds and Oxidized Nickel Salen Complexes

The oxidized species of a salen complex could not be attributed as phenoxy radical, or high valent metal complex at first sight. What happens inside the oxidized complex is more complicated.

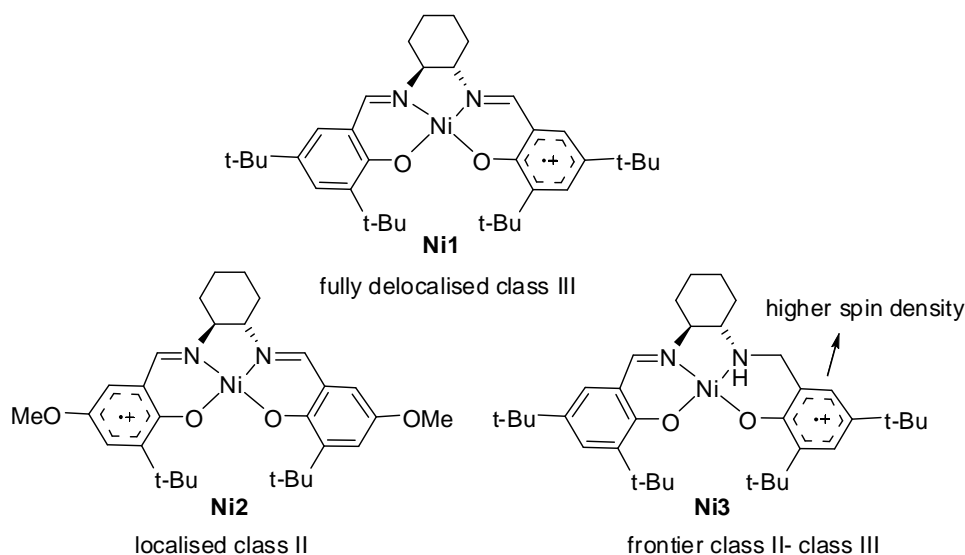
Taking the case of one oxidized metal complexes with a proradical ligand: they could exist in two limiting descriptions: a high valent metal complex [M⁽ⁿ⁺¹⁾⁺-L⁻], or a metal-ligand radical [Mⁿ⁺-L[•]]. These complexes are special case of mixed-valence compounds. The unpaired electron, or the “hole”, could “jump” between the two redox centers which are the metal and the ligand. According to the facility this process, mixed-valence compounds containing two redox centers are divided in three classes (Scheme 3).



Scheme 3. Three classes of mixed-valence compounds.

In class I, no electron transfer occurs between the two centers because they are far apart or because their interaction is symmetry or spin forbidden. In class II, electronic interaction between the two centers exists and thus the electron transfer between these two centers. In class III, the two centers have such strong electronic interaction that there's not activation barrier for electron transfer, leading to free spin delocalisation and an average charge on the two centers (Scheme 3).⁴

Oxidised salen complexes of manganese, iron, cobalt, copper and group 10 metals (Ni, Pd, Pt) have been isolated and studied exclusively. Oxidized nickel salen complexes have been found to be of class III mixed valence complexes, the radical being delocalized over the ligand through the metal bridge, the spin density on the metal center is often low (<20%).⁵ Three directions to tune the electronic configuration of the complexes have been envisaged: 1) localize the spin density on one of the two phenoxide moiety, 2) increase the activation barrier of electron transfer, 3) change the locus of electron density from ligand to metal (Scheme 4). Needless to say, the first and second options often come together.



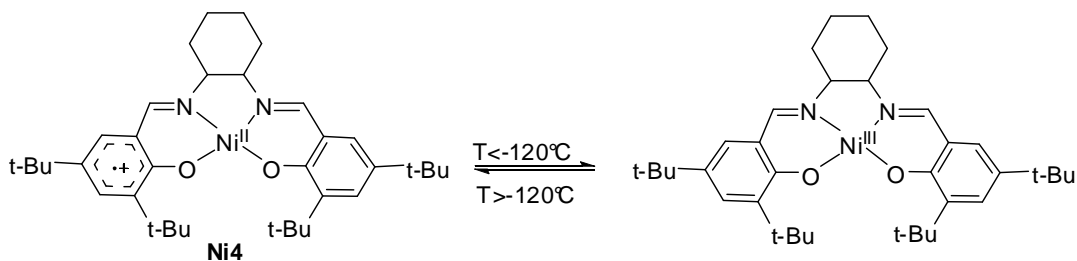
Scheme 4. Nickel salen complexes

The first option has been done for example by using nonsymmetrical salen ligand. Oxidised nickel salen complex **Ni1**, realized by Shimazaki and coworkers^{5b} has equal spin densities on each phenoxide moiety, with 12% contribution from Ni center. By changing the imine functional group by an amine which is more electron donor, the same group obtained the radical

complex **Ni3** with a more localized spin density on the phenoxide ring linked to the amine function, as has been demonstrated by X-ray diffraction experiment and DFT calculations.⁶ The calculations also suggested that the electron transfer between the two phenoxide, presumably mediated through Ni center (orbital d_{yz}), is significantly reduced. The complex is at the frontier class II-class III mixed-valence compounds.

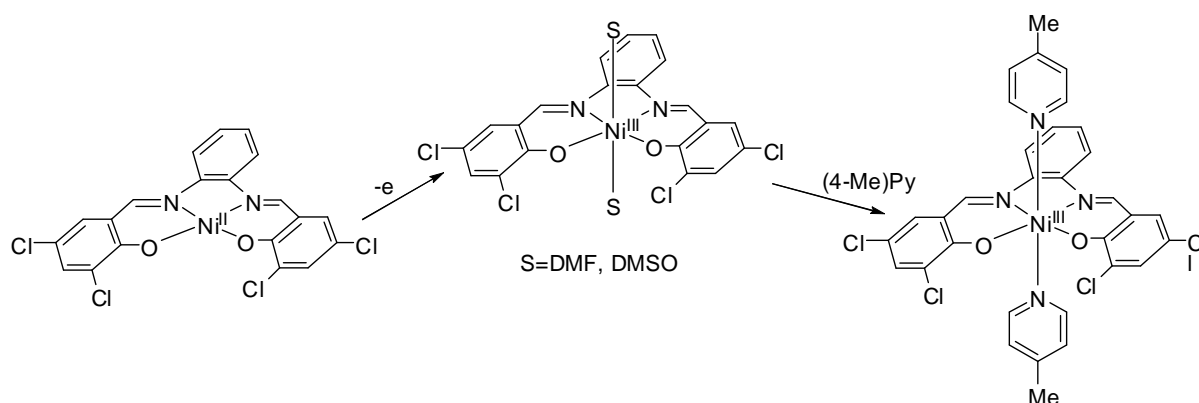
If the activation barrier for the electron transfer is increased, then the spin density can be localized even for complexes of symmetrical ligand. In 2010 Thomas and coworkers reported the complex **Ni2** [Ni(L-OMe)](SbF₆), featuring OMe at the *para*- position of the phenoxide rings, which shows the unsymmetrical structure containing one quinoid and one phenoxide ring (Scheme 4). This has been explained by the interaction of the fluorides on one phenyl ring which render the molecules non-symmetrical. Later, Kurahashi and co workers examined the intervalence charge transfer band (IVTC) of the same complex in solution and found that the complex is a class II mixed valence compound. They explained this by the change of redox potential induced by OMe groups, which modifies the activation barrier for electron transfer.⁴

The third option, changing the locus of oxidation from ligand to metal, has been realized up to now only with the intervention of external factors: the temperature, the nature of solvent or the presence of exogenous ligands. The effect of the temperature has been investigated by Shimazaki and coworkers, who discovered the tautomerism between the two forms of complex **Ni4** (ligand radical or high valent Ni(III)) by increasing or lowering the temperature.⁷ The Ni(III) complex exists under -120°C. (Scheme 5)



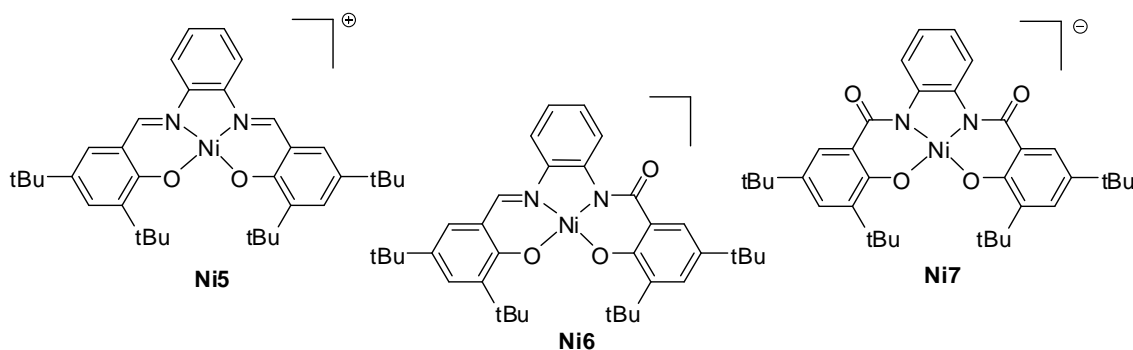
Scheme 5. Tautomerism of oxidized Nickel-salen complex.

The effect of the addition of axial ligands on the stability of oxidised nickel salen complex has been long known in chemistry. Earlier to the studies of nickel-phenoxyl radical complexes and electronic structures of oxidized nickel salens, in 1990, Freire and coworkers studied the oxidation of [Ni(3,5-Cl₂Saloph)] in DMF and (CH₃)₂SO by electrochemistry and formulated the oxidized species as [Ni(3,5-Cl₂Saloph).S₂]⁺ (S=solvent molecule) (Scheme 6).⁸ The products have a large g_{iso} values at room temperature which suggest that the oxidation is metal-based. The EPR spectra of frozen solutions displayed highly anisotropic, large g tensor, typical of Ni(III). Upon addition of 4-methylpyridine, the base replaces the two solvent molecules at the axial position, leading to the apparition of a hyperfin coupling in EPR spectrum of the oxidized species, due to the interaction of the unpaired electron and two equivalent nitrogen atoms.



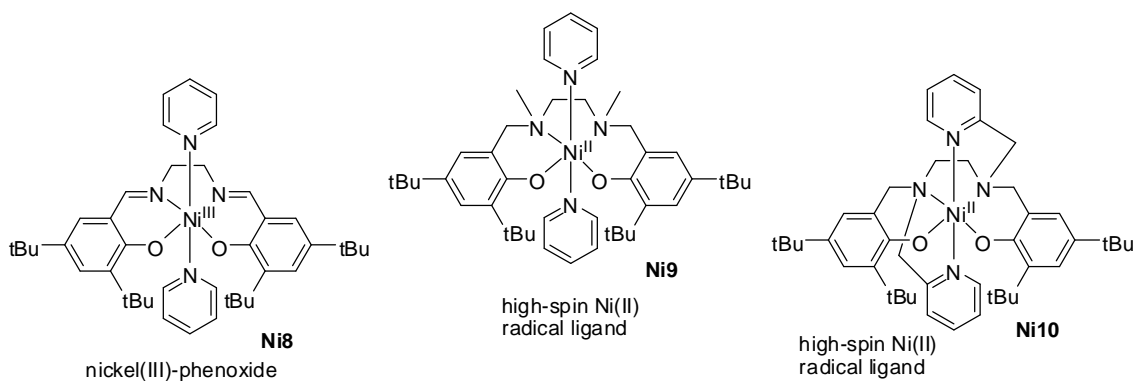
Scheme 6. Oxidation of $[Ni(3,5-Cl_2Saloph)]$, from Freire and coworker.⁸

The role of the axial ligand(s) was more deeply investigated by F. Thomas and coworkers.⁹ They observed that addition of pyridine into electrochemically generated complexes **Ni5-7** (Scheme 7) in CH_2Cl_2 led to the existence of six-coordinated Ni(III) adducts that has been evidenced by EPR spectra.^{9b} This is in contrast to the situation when no pyridine is added: EPR spectra of the oxidized complexes **Ni5-7** in CH_2Cl_2 pointed towards the phenoxyl radical complexes.



Scheme 7. Oxidated nickel salen complexes, from Thomas *et al.*^{9b}

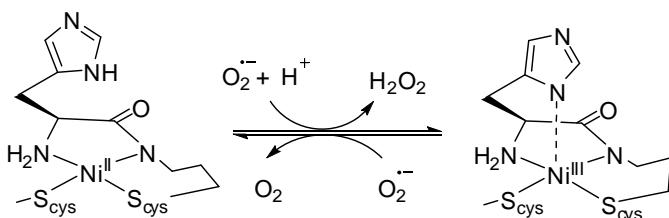
In fact, in square planar nickel salen complexes, the energy level of the d orbitals from the metal and the π -orbitals from the ligands are very close. By changing the relative energies between these orbitals, a metal-based or ligand-based process could be favored, leading to high valent Ni(III) or ligand radical. In those above-cited examples, on going from a square planar to an octahedral geometry, the presence of axial ligands increases the energies of d_{xz} , d_{yz} and d_{z^2} orbitals, probably makes them higher than the energy of π -orbitals from the ligand. This resulted in the formation of a Ni(III) complex. This “tuning” is however very delicate, and adding axial ligand does not systematically leads to a metal-based oxidation process. For examples, in Scheme 8, all the three oxidized nickel complexes adopt octahedral geometries. But whereas **Ni8** is a high valent Ni(III) complex, **Ni9-10** featuring salen ligands are radical complexes of high spin Ni(II).^{9c} For all these three complexes, two-electron oxidations afford bis (phenoxyl) radical species, regardless of the hybridization of the coordinating nitrogen.



Scheme 8. Oxidised nickel complexes of salen-type ligands, from Thomas and coworkers

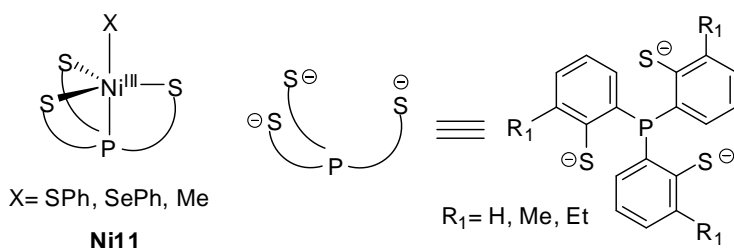
3. Nickel (III) Complexes

In the discussion about oxidized nickel-salen complexes, it has been demonstrated that the formation of Ni(III) complex could only be obtained in the presence of axial ligands leading to an octahedral geometry. Indeed, most of Ni(III) complexes reported in the literature are hexa-coordinated. However, it's the coordinatively unsaturated complexes that could have attractive applications in catalysis, as there's still place to coordinate the substrate(s). Catalytic applications of Ni(III) in nature are known. The Ni-containing superoxide dismutase (NiSOD) is able to catalyse the disproportionation of O_2^- to O_2 and H_2O_2 .¹⁰ The active site of the enzyme features an Ni(II) and a square planar N2S2 ligand set in its first coordination sphere. The oxidation form has N2S2 ligand set in equatorial plane, and an imidazole in axial position, giving a Ni(III) complex in square pyramidal geometry. (Scheme 9)



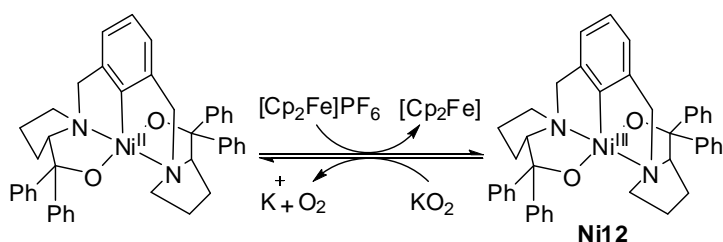
Scheme 9. Active site of Ni-containing superoxide dismutase.

Penta-coordinated Ni(III) complexes are less common than hexa-coordinated Ni(III), but not too rare. For example, Lee C. M. and coworkers synthesised alkyl, thiolate and selenonate penta-coordinated Ni(III) complexes supported by tris(thiolate) phosphine ligand.¹¹ (Scheme 10) The average g value of the alkyl complex at 77K is 2.13, significantly higher than 2.00, indicating that the unpaired electron is primarily located at Ni. SQUID measurement of the same complex in the solid state gave a magnetic moment of $1.85 \mu_B$, which has been judged as "consistent with the Ni^{III} having a low-spin d^7 electron configuration in a distorted trigonal bipyramidal ligand field".



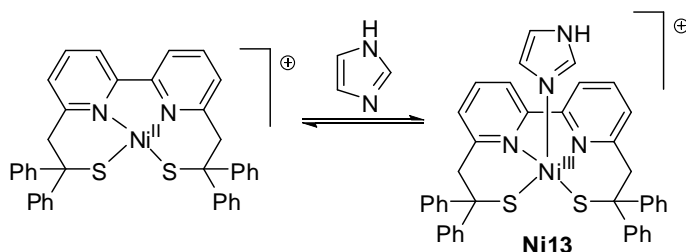
Scheme 10. Penta-dentate nickel(III) complexes, from Lee and coworkers.¹¹

More recently, in 2012, W. Z. Lee and coworkers reported the formation of Ni(III) complex with a penta-dentate N3O2 ligand, which resembles the oxidized form of the active site of Nickel-containing superoxide dismutase (Scheme 11). The complex could react with KO₂ to give O₂ and the corresponding Ni(II) complex, which could then be re-converted into Ni(III) complex by oxidation with [Cp₂Fe]PF₆. Spin density plot of the complex calculated from DFT showed an important contribution from the ligand.



Scheme 11. Synthesis of Ni(III) pentadentate complex, from Lee W.Z. and coworkers.¹²

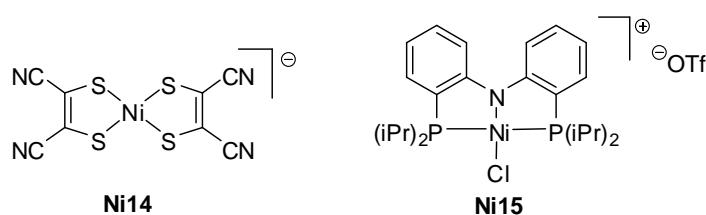
If obtaining of penta-coordinated Ni(III) complexes is already difficult, Ni(III) complexes of lower coordination number are even more difficult to achieve. For example, square-planar pyramidal nickel complex of bisamine dithiolate ligand and apical imidazole ligand has high valent Ni(III)¹³ (Scheme 12). When the imidazole ligand is absent, the metal character of the redox-active molecular orbital drops drastically, and the square-planar complex could be considered as a Ni(II) radical complex.¹⁴



Scheme 12. Reversible apical coordination of imidazole on nickel complex, by Neese and coworkers.

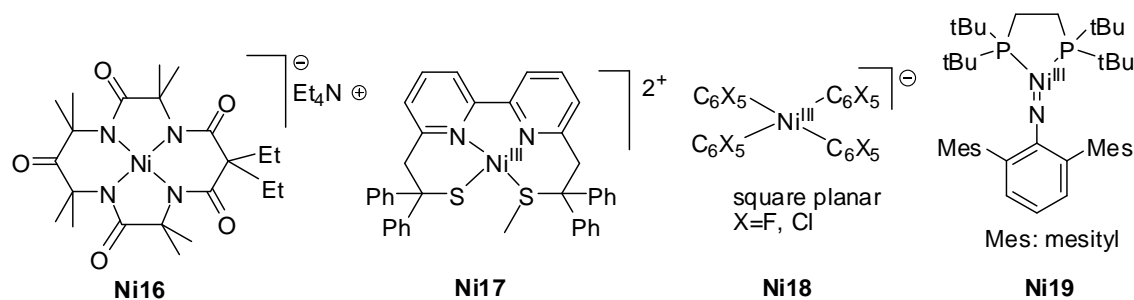
Some lower-coordinated complexes previously denoted as Ni(III) turned out to be Ni(II). For example, the complex **Ni14** [NiL₂]⁺, where L is the doubly deprotonated form of 1,2-

benzodithiol, has been the center of debate for several decades concerning the nature of Ni (Scheme 13). It was first supposed to be a Ni(III) complex in which the SOMO has a large contribution from the ligand.¹⁵ It turned out, as been shown by Neese and Wieghart, that it is a Ni(II) complex, in which the SOMO is primarily ligand-based. This orbital is energetically close to the 3d_{xz} of Ni, and is symmetrically allowed to mix with it, resulting in the 3d-Ni character part in the SOMO.¹⁶ Another example of the ambiguity of formal Ni(III) and true Ni(III) compounds involves formally pincer Ni(III) complexes. They are used as catalysts for the Kharasch reaction and are often denoted as “Ni(III) complexes” but little has been studied about the true oxidation state of Ni.¹⁷ In one of the study, it has been shown that the formally Ni(III) complex **Ni15** [Ni(PNP)Cl]OTf (Scheme 13) contains in fact Ni(II) centre bound to a radical cation.¹⁸



Scheme 13. Ni(II) complexes often denoted as Ni(III)

In 1991, Collins and coworkers reported the first isolation of a square-planar Ni(III) complex, which is based on N4 ligand system (**Ni16**, Scheme 14). In 2011 Neese and coworkers reported thiolate Ni(III) complex **Ni17** of a mixed thiolate-thioether ligand.¹⁴ A three coordinated Ni(III) imide complex **Ni18** has been reported by the group of Hillhouse,¹⁹ as part of their research in low-coordinated species that features multiple bond between nickel and light-elements like C, N, P. Tetra-coordinated homoleptic Ni(III) complexes **Ni19** were reported by Alonso and coworkers, using C6X5 ligands (Scheme 14).²⁰



Scheme 14. Examples of tetra- and tri-coordinated Ni(III) complexes

In summary, due the interest in phenoxy radical and mix-valence complexes, oxidized species of nickel salen complexes have been the subjects pursued by many groups. We were thus interested in studying the oxidation of Ni(II) phosphasalen complexes to see the electronic differences conferred by the phosphasalen ligands compared to salens. Taking into account the rarity of Ni(III) complexes, and the inexistence of a tetracoordinated Ni(III) complex of a Salen-

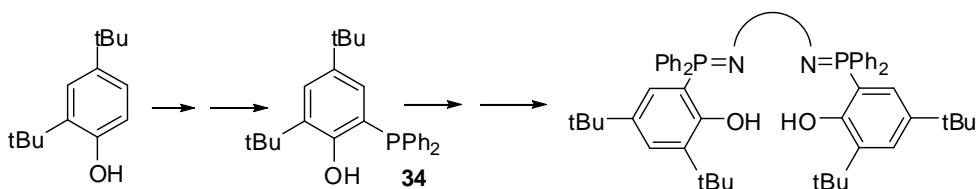
like ligand, and more generally, of a phenoxide-containing ligand, it would be interesting to see if the phosphasalen ligands could afford the high oxidation state Ni(III).

II. Results.

1. Methods for Substituted Phosphasalen Ligand Synthesis

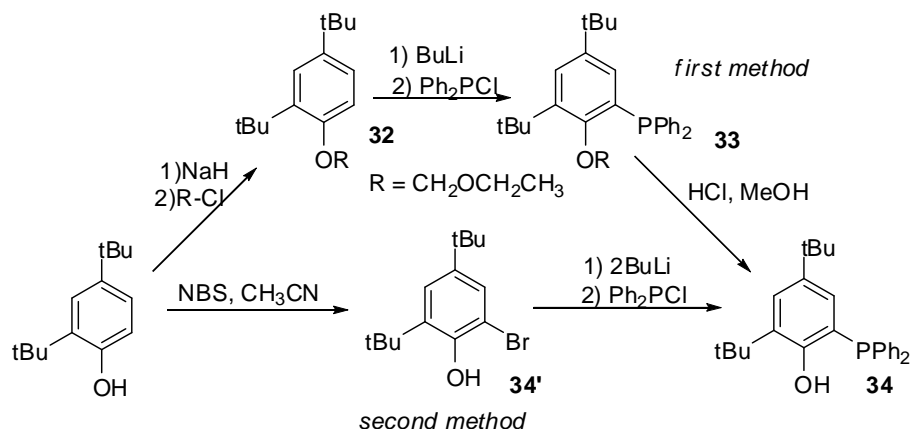
It is worth noting that all oxidised nickel salen complexes that are stable enough to be characterised do have substituents on *ortho*- and *para*- positions of the phenoxide rings. And they were not random choices. In fact, since 1989, Goldsby and co-workers have reported the oxidative polymerisation of Ni(II) salen complexes in moderately/weak donor solvents, giving polymer-modified electrodes.²¹ The group also observed that polymer formation was inhibited by substituents at *para*- positions of the phenoxide rings, and proposed that the polymerisation took place by ligand-radical coupling mechanism with the formation of C-C linkages between phenyl rings, a process related to the oxidative polymerisation of phenol and substituted phenols.

Thus, before the study of any eventual oxidised phosphasalen nickel complex, it's important to develop substituted phosphasalen ligand. We chose to develop phosphasalen ligands with *tert*-butyl substituents on *ortho*- and *para*- positions of the phenoxide rings, starting from a cheap and readily available 2,4-di-*tert*-butylphenol. This starting compound is first converted to phosphinophenol **34** which would then be transformed into phosphasalen ligands by a sequence of Kirsanov reactions-deprotonation as has been seen for the synthesis of the non-substituted phosphasalen ligand. (Scheme 15)



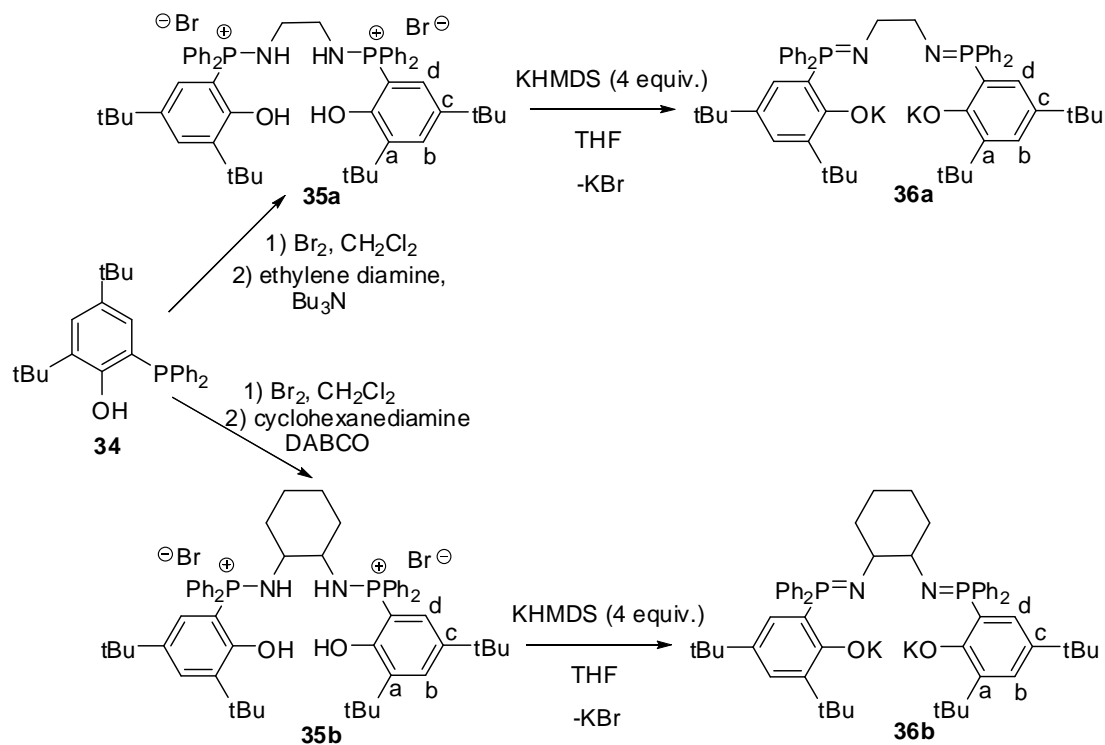
Scheme 15. Synthesis of substituted phosphasalen ligands.

The phosphinophenol **34** was first synthesised following the same procedure as reported for the unsubstituted phosphasalen ligands in chapter 3 (Scheme 16, first method). The phenol function was first protected, then was submitted to an ortholithiation reaction and treatment with diphenylphosphine chloride to introduce PPh_2 functional group at *ortho*-position of the protected phenol. Finally, the protection group of the phenol function was removed by an acidic treatment. This method gave compound **34** with high total yield, but employed an expensive and toxic compound (chloride methyl ethyl ether) to introduce the protecting group. Furthermore, the purification of the intermediate **33** by recrystallation in methanol often took long time. We thus searched for an alternative method.



Scheme 16. First and second synthesis of phosphinophenol

We later noticed that the phosphinophenol **34** could be obtained much faster and more easily by adopting the synthesis reported for dilithium bis(aryloxy)phosphines complexes by Fryzyk and coworkers²² (Scheme 16, second method). The bromination of 2,4-di-*tert*-butylphenol with *N*-bromosuccinimide gave 2-bromo-4,6-di-*tert*-butylphenol **34'** in quantitative yield. Reaction of this product with *n*-BuLi, followed by nucleophilic substitution with chlorodiphenylphosphine and aqueous treatment gave the desired product **34** in high yield as a white crystalline solid. This method is not only faster and simpler than the synthesis of **34** by protection/deprotection, but also employs reagents that are much less expensive and less toxic than the reagents needed in the first method.



Scheme 17. Synthesis of phosphasalen ligands

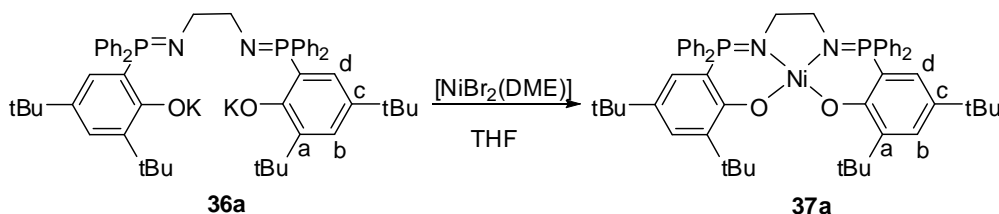
Kirsanov reaction of **34** with ethylenediamine and trans-1,2-cyclohexanediamine in the presence of the appropriate bases gave proligands **35a,b** in high yield (Scheme 17). Though these compounds have very limited solubility in common solvents, their characterisation by NMR multi-nuclear was still successfully carried out. In $^{31}\text{P}\{^1\text{H}\}$ spectroscopy the equivalent phosphorus atoms of **35a** appear as a singlet at $\delta(\text{CDCl}_3) = 40.3$ ppm, and those of **35b** at $\delta(\text{CDCl}_3) = 38.5$ ppm, which are very close to the value reported for the unsubstituted phosphasalen proligand ($\delta(\text{CDCl}_3) = 39.3$ ppm). In ^1H NMR spectrum, the bridging ethylene protons of **35a** appear as a broad signal at $\delta(\text{CDCl}_3) = 3.74$ ppm, those of **35b** at $\delta(\text{CDCl}_3) = 3.82$ ppm, all slightly higher than the values reported for the unsubstituted phosphasalen proligand ($\delta(\text{CDCl}_3) = 3.43$ ppm).

Upon reaction with 4 equiv. of KHMDS in THF, both these compounds are easily deprotonated to give the corresponding anionic phosphasalen ligands. Physically, a cloudy solution (containing KBr and the soluble anionic phosphasalen product) was formed instead of a white suspension (containing insoluble proligand and soluble KHMDS). The completion of reaction was monitored by the apparition of a unique singlet corresponding to the anionic phosphasalen ligands ($\delta(\text{THF}) = 20.6$ ppm for **36a**, 15.8 ppm for **36b**). After removal of KBr by filtration, evaporation of THF and recrystallisation in petroleum ether to remove HMDS, phosphasalen ligand **36a** was obtained as a white solid in quantitative yield. In ^1H NMR spectrum, the bridging ethylene protons of **36a** now as a virtual triplet at $\delta(\text{THF-d}_8) = 3.20$ ppm, due to couplings with two phosphorus atoms ($J_{\text{P,H}} = 5.0$ Hz). Although the formation of **36b** is also very clean, it could not be separated from HMDS. Thus, **36b** was not isolated and but was still characterised by NMR-multinuclear experiments for comparisons.

2. Neutral Complex Synthesis and Characterisation

2.1 Neutral Complexes Synthesis

The synthesis of nickel complex of ligand **36a** was carried out directly by reaction of $[\text{NiBr}_2(\text{DME})]$ with a colorless solution of isolated **36a** in THF, giving immediately a deep purple solution (Scheme 18).



Scheme 18. Synthesis of **37a**.

In $^{31}\text{P}\{^1\text{H}\}$ spectroscopy only one singlet was seen at $\delta(\text{THF}) = 36$ ppm, indicating the completeness of the coordination reaction. THF was evaporated and the residue was taken in dichloromethane to completely precipitate insoluble potassium salt(s). After removal of

insoluble potassium salt by centrifugation and evaporation of dichloromethane, complex **37a** was obtained as a blue purple solid. In ^1H spectroscopy, the ethylene bridge protons appear as a broad signal at $\delta(\text{CD}_2\text{Cl}_2) = 2.05$ ppm, much higher field than in the ligand or proligand.

Definitive evidence concerning the structure of **37a** was provided by X-ray crystal analysis of the complex. Suitable crystals were obtained from slow diffusion of petroleum ether over a saturated dichloromethane solution of **37a** at room temperature. Ortep view of complex **37a** is presented in Figure 2. The complex crystallized with two molecules of dichloromethane. (The same structure of Nickel-complex was obtained by X-ray diffraction on crystals obtained from slow evaporation of a toluene solution at room temperature, and in this case the complex crystallize with two molecules of toluene).

As expected for a diamagnetic d^8 complex **37a** adopts a square planar geometry around the metal and has a C2 axis going through the metal center. The four coordination sites are occupied by the iminophosphorane and phenoxide groups with slight deviation from planarity (O1-N1-N1'-O1' dihedral angle 8.51°). The $\text{O}_{\text{phenoxide}}-\text{C}_{\text{phenyl}}$, Ni-O and Ni-N bond lengths are of almost the same values as those in the nickel complex of unsubstituted phosphasalen ligand. In the same manner, values of bond angles around the nickel center are very close to the ones reported for the unsubstituted complex.

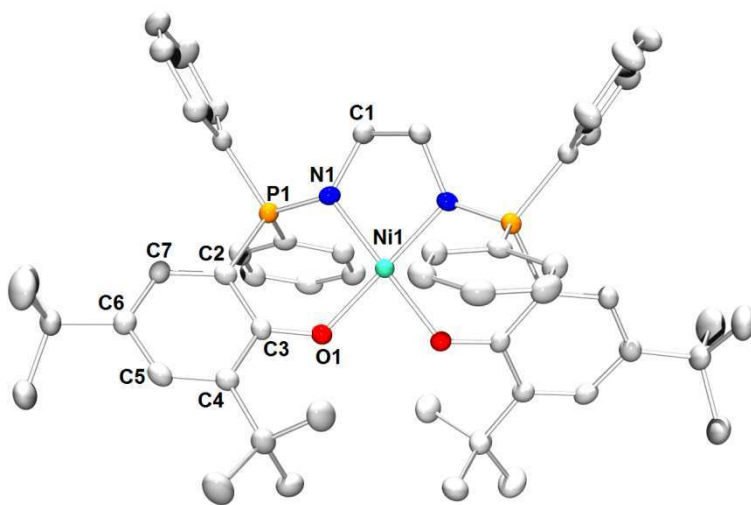
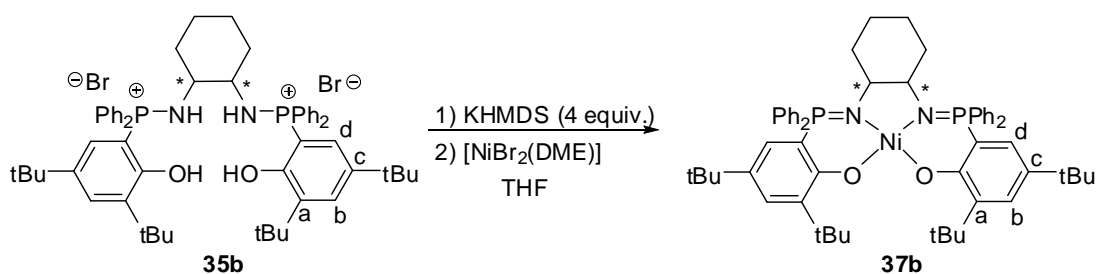


Figure 2. ORTEP view of complex **37a**. Solvent molecules and hydrogen atoms have been omitted for clarity. Thermal ellipsoids drawn at the 50% probability level. The complex has a C2 symmetric axis passing through Ni. Selected distances (\AA) and angles ($^\circ$): Ni-O1 1.881 (2), Ni-N1 1.887 (2), P1-N1 1.613 (2), O1-C3 1.317 (3), C2-C3 1.424 (4), C3-C4 1.426 (4), C4-C5 1.391(4), C5-C6 1.408 (4), C6-C7 1.375(4), C7-C2 1.398 (4), N1-Ni1-O1 95.7 (1), N1-Ni1-N1' 84.7 (1), O1-Ni1-O'1 84.7 (1).

The synthesis of **37b** is slightly different from the one for **37a**. As the anionic phosphasalen ligand **36b** was not isolated as a solid, the coordination was done by the reaction of $[\text{NiBr}_2(\text{DME})]$ with an in situ-generated solution of **36b** in THF, as described above in Scheme

19. The addition of $[\text{NiBr}_2(\text{DME})]$ induced immediately the change from a colourless to a deep blue-purple solution. $^{31}\text{P}\{^1\text{H}\}$ spectrum showed the formation of a unique product at δ (THF) = 30 ppm, which is in lower field compared to the anionic free ligand (δ (THF) = 15.8 ppm). THF was evaporated and the residue was taken in dichloromethane to facilitate the precipitation of insoluble potassium salt(s). After removal of insoluble potassium salt by centrifugation, evaporation of dichloromethane and washing with petroleum ether to remove HMDS, complex **6b** was obtained as a blue solid. In ^1H spectroscopy, the ethylene bridge protons appear as a virtual triplet at $\delta(\text{CD}_2\text{Cl}_2) = 3.02$ ppm, due to couplings with vicinal protons and phosphorus atoms ($^3J_{\text{H,H}} = ^3J_{\text{P,H}} = 9.0$ Hz).



Scheme 19. Synthesis of nickel complex **37b**.

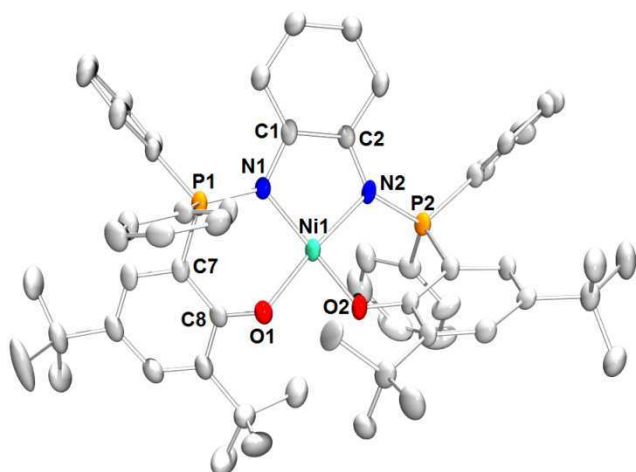


Figure 3. ORTEP view of complex **37b**. Solvent molecules and hydrogen atoms have been omitted for clarity. Thermal ellipsoids drawn at the 50% probability level. Selected distances (\AA) and angles ($^\circ$): Ni-O1 1.877 (3), Ni-O2 1.882(3), Ni-N1 1.912 (4), Ni-N2 1.921(4), P1-N1 1.627 (4), P2-N2 1.618(4), O1-C8 1.303 (6), O2-C_{phenyl} 1.306(6), N1-C1 1.478(6), N2-C2 1.477(6), N1-Ni1-O1 98.1 (2), O2-Ni1-N2 95.2(2), N1-Ni1-N2 85.7 (2), O1-Ni1-O2 83.3 (1), O1-N1-N2-O2 14.57.

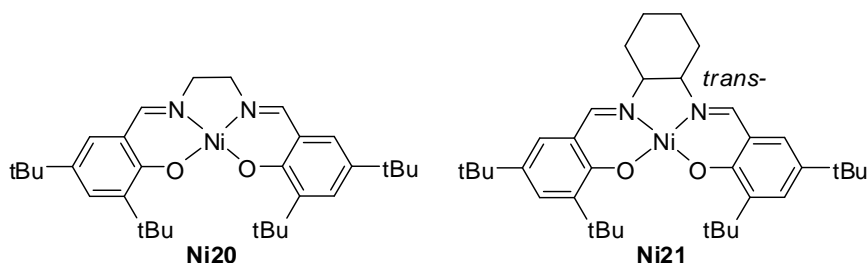
X-ray diffraction experiment was carried out on single crystals of **37b** obtained from slow diffusion of petroleum ether over a saturated dichloromethane solution and gave definite evidence of the structure of **37b** (Figure 3). The complex crystallised with two molecules of dichloromethane.

Whereas the ligand **36b** exists in racemic mixture of (R,R) and (S,S) configuration of the cyclohexane diamine bridge, **37b** crystallised as mixtures of enantiopure crystals (or conglomerates) (this phenomenon, known as chiral resolution by crystallization, concerns about 5-10% of all racemates). Thus the crystal on which X-ray diffraction was carried out is of (R,R) configuration for C1 and C2. Similarly to **37a**, **37b** adopts a slightly distorted square-planar geometry (O1-N1-N2-O2 dihedral angle 14.57°). The $O_{\text{phenoxide}}-C_{\text{phenyl}}$ bonds are slightly shorter than the ones in **37a** (1.303(6) and 1.306(6) vs 1.317(3)), whereas Ni-N bonds are longer (1.912(4) and 1.921(4) vs 1.887(2)). But those differences remain insignificant.

2.2. Electrochemistry of Nickel Complexes.

At the difference of nickel phosphasalens complex with unsubstituted ligand which only has irreversible oxidation wave in dichloromethane, in the same solvent **37a,b** present first oxidation waves which are reversible. This is expected because the change from unsubstituted ligand to ligands with substituents on *ortho*- and *para*- positions of the phenoxide rings would limited side-reactions that could happen to the oxidised nickel complexes, e.g oxidative polymerisation, as has been described before for the Salen complexes.

For reference, whereas simple nickel of unsubstituted salen ligand has irreversible oxidation process in dichloromethane, In this solvent and at room temperature, the complex [Ni(t-Bu-Salen)] (Scheme 20) exhibits a first reversible oxidation wave at $E_{1/2}^1 = +0.58\text{V}$ (vs $E_{1/2}(\text{Fc}^+/\text{Fc})$), and a second quasi-reversible one at $E_{1/2}^2 = +1.04\text{V}$ (vs $E_{1/2}(\text{Fc}^+/\text{Fc})$).^{9c, 23} In the same solvent and at the same temperature, complex [Ni(t-Bu-Salcn)] (Scheme 20) exhibits two quasi-reversible oxidation waves at $E_{1/2}^1 \sim 0.47\text{V}$ and $E_{1/2}^2 \sim 0.79\text{V}$ (vs $E_{1/2}(\text{Fc}^+/\text{Fc})$).⁷ When the temperature was decreased to 230K, these two oxidation waves shift to $E_{1/2}^1 \sim 0.37\text{V}$ and $E_{1/2}^2 \sim 0.85\text{V}$ (vs $E_{1/2}(\text{Fc}^+/\text{Fc})$).^{5b} These oxidations have been established to be ligand-based to give mono- and bis-phenoxyradical species.^{9c} The difference between the two half-wave potentials $E_{1/2}^1$ and $E_{1/2}^2$ is an indication of the communication through bond and space between the two phenoxide moieties: the bigger the difference, the stronger the communication.



Scheme 20. Nickel salen complexes analogs of **37a,b**.

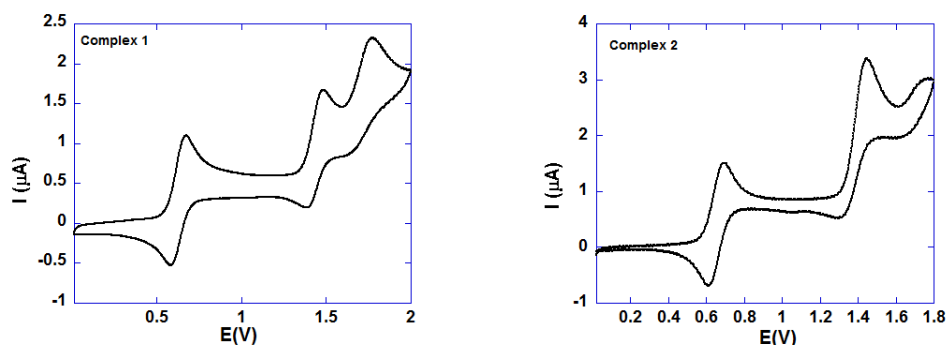


Figure 4. Cyclic voltammetry graphs of **37a** (left) and **37b** (right) in CH_2Cl_2 . The potential values are relative to SCE Tetrabutylammonium tetrafluoroborate salt as electrolyte ($c = 0.12 \text{ mol L}^{-1}$); scan rate = 50 mV s^{-1} ; $c = 3.0 \text{ mmol L}^{-1}$;

To our surprise, for the two phosphasalen complexes, up to three reversible oxidation waves were observed (Figure 4). The first oxidation waves of these two complexes happen at +0.16V and +0.18V higher than $E_{1/2}(\text{Fc}^+/\text{Fc})$, thus much easier than the salen analogs (Table 1 and Table 2) This clearly demonstrate the better donating ability of phosphasalen ligands comparing to salens which render more stable the oxidized species.

Table 1. Electrochemical data for nickel-phosphasalen complexes in CH_2Cl_2 ^a

Complex	E_a^1	E_p^1	E_a^2	E_p^2	E_a^3	E_p^3	$E_{1/2}^1, \text{V}$	$E_{1/2}^2, \text{V}$	$E_{1/2}^3, \text{V}$
37a	0.68	0.59	1.48	1.39	1.77	1.60	0.63	1.43	1.69
37b	0.69	0.61	1.42	1.33	1.75	1.58	0.65	1.37	1.67
Fc									

^a Measurements were done at room temperature. Potential values are relative to SCE. Tetrabutylammonium tetrafluoroborate salt as electrolyte ($c = 0.12 \text{ mol L}^{-1}$); scan rate = 50 mV s^{-1} ; $c = 3.0 \text{ mmol L}^{-1}$;

Table 2. Comparison of Electrochemical data for nickel complexes in CH_2Cl_2 ^a

Complex	$E_{1/2}^1, \text{V}$	$E_{1/2}^2, \text{V}$	$E_{1/2}^3, \text{V}$
37a ^a	0.16	0.96	1.22
37b ^a	0.18	0.90	1.20
[Ni(t-Bu Salen)] ^a	0.58	1.04	
[Ni(t-Bu Salcn)] ^a	0.47	0.79	
[Ni(t-Bu Salcn)] ^b	0.37	0.85	

^a Potential values are relative to $E_{1/2}(\text{Fc}^+/\text{Fc})$. Tetrabutylammonium tetrafluoroborate salt as electrolyte ($c = 0.12 \text{ mol L}^{-1}$); scan rate = 50 mV s^{-1} ; $c = 3.0 \text{ mmol L}^{-1}$; ^a measurements at room temperature; ^b measurements at 230K.

The second and third oxidation waves of complex **37a** are very close to each other, the difference between them being 0.26V. However, the difference between the first and second

oxidation waves is very large (0.8 V, Table 2). This value is much more important than the difference of second and first half wave potential for the analog salen complex **Ni20** (0.46 V).

In the same manner, the difference between the second and the third oxidation waves of complex **37b** is small (0.30 V) whereas the one between the first and the second half wave potentials is very large (0.72 V). Once again, this value of 0.72 V is much more important than the one reported for the analog nickel-salen complex **Ni21** featuring trans-cyclohexane diamine backbone.

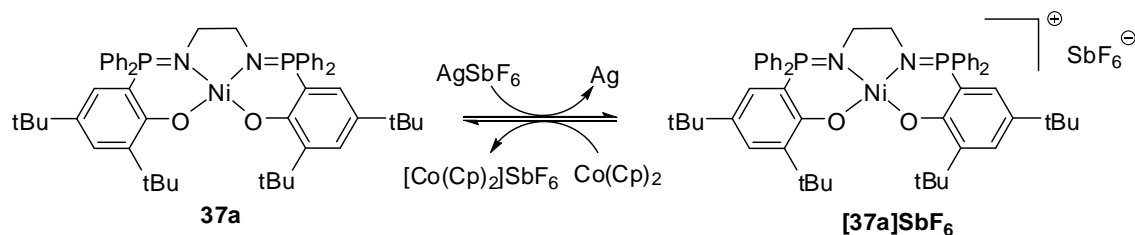
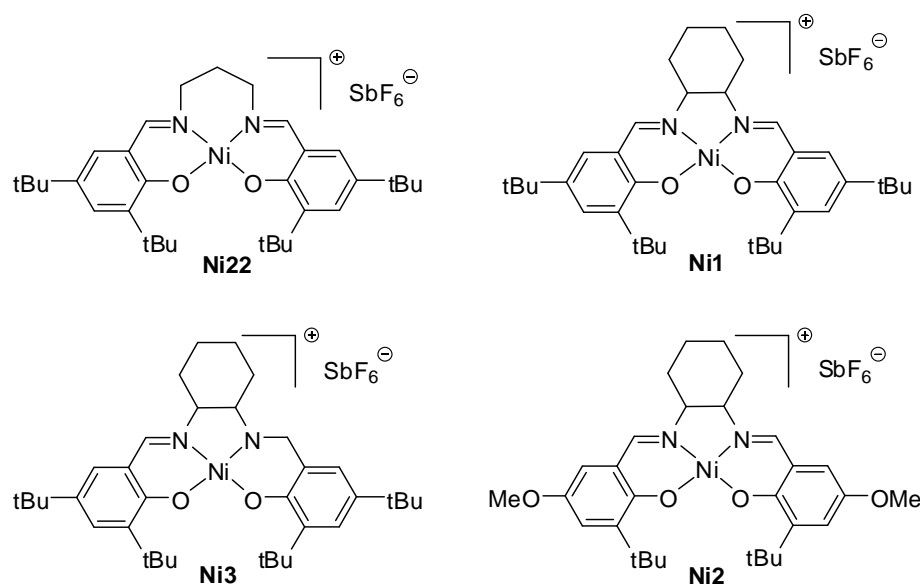
It is worth noting that studies have shown that oxidized species from the two cited nickel-salen complexes are of class III mixed-valence compounds, where there's almost no barrier to electronic communication between the two phenoxide moieties (which is done through the nickel center). Thus, for these complexes, the difference in half wave potentials of first and second oxidations to yield mono- and bisphenoxyl radicals are among the largest one, because the second oxidation is influenced by the first one. Weaker electrochemical communication or less flexibility resulting in weaker structural rearrangement to accommodate such communication would reduce the difference between first and second half-wave potentials.^{9c} Thus for salen complexes, the difference of half wave potentials of processes giving mono- and bisphenoxyl radicals should be around, or less than those values reported for the cited salen complexes (0.46 V for **Ni20** and 0.32 V for **Ni21**).

Therefore the values of difference between first and second half-wave potentials for the two phosphasalens complexes **37a,b** (0.80 V and 0.72 V) suggest that these do not correspond to the formation of mono- and bisphenoxyl radicals. Along with the existence of three oxidation waves for those complexes, they suggest that the first oxidation happens in the metal, and the second and third ones are ligand-based giving phenoxyl or iminophosphoranyl radicals.

3. Oxidised Complexes Synthesis and Characterisation

The electrochemical studies suggests that it's possible to form stable one-electron oxidised species of nickel-phosphasalens complexes by silver salts in CH_2Cl_2 (formal potential of Ag^+/Ag in CH_2Cl_2 is of 0.65V vs $\text{Fc}^+/\text{Fc}^{2+}$). Indeed, addition of a stoichiometric amount of AgPF_6 , AgBF_4 , AgOTf or AgSbF_6 into a solution of complex **37a,b** in CH_2Cl_2 induced immediately a change of colour from blue to deep red, with metal silver precipitated out from the solution, which sometimes gave a mirror layer on the wall-side of the test tube. In $^{31}\text{P}\{^1\text{H}\}$ spectrum recorded after 2 hours of stirring, no signal was detected indicating the disappearance of the starting complex and the formation of a paramagnetic species.

Though for all reactions between **37a** or **37b** with any of those listed silver salts seemed to proceed well and gave the same physical aspects, only in the case of reaction of **37a** with AgSbF_6 did the product crystallise. The further studies are thus centred on this species.

Scheme 21. Oxidation of phosphasalen complex **37a**.Scheme 22. Reported oxidized nickel-salen complexes as evidenced by X-ray diffraction.^{5a, 5c, d, 6}

After removal of Ag by centrifugation, dichloromethane was evaporated almost completely and the residue was dissolved in toluene, giving a deep red-brown solution. Green crystals were obtained after one week of storage at -40°C in almost quantitative yield (89%). The complex is stable for months in solid state or in solution in dichloromethane or toluene. It could be quantitatively reduced to the Ni(II) phosphasalen complex **37a** by one equiv. of $\text{Co}(\text{Cp})_2$ (Scheme 21).

X-ray diffraction was carried out on crystals of the oxidised complex $[\mathbf{37a}][\text{SbF}_6]^+$ giving definite evidence for its structure (Figure 5). The obtainment of X-ray structure of $[\mathbf{37a}][\text{SbF}_6]^+$ is precious because X-ray structures of oxidised nickel-salen complexes and derivatives remain scarce in literature (Scheme 22).^{5a, 5c, d, 6}

The complex $[\mathbf{37a}][\text{SbF}_6]^+$ crystallised with 4 molecules of toluene. The nickel is in a slightly distorted square planar geometry formed by the four donating atoms of the phosphasalen ligand, as seen by the dihedral angle $\text{O1-N1-N2-O2} = 11.06^{\circ}$ (instead of 8.51° in the neutral complex). The anion SbF_6^- was found to be located quite far from the cation. No special stacking effect or hydrogen bonding was detected.

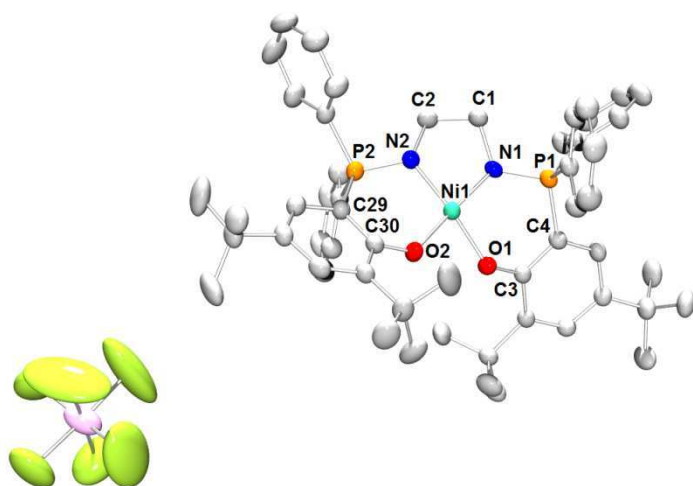
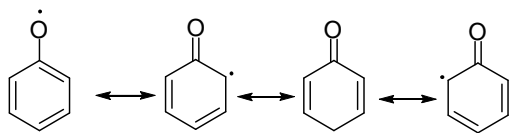


Figure 5. ORTEP view of complex $[37a][SbF_6]$. Solvent molecules and hydrogen atoms have been omitted for clarity. Thermal ellipsoids drawn at the 50% probability level. Selected distances (Å) and angles (°): Ni-O1 1.828 (2), Ni-O2 1.844(2), Ni-N1 1.875 (3), Ni-N2 1.842(3), P1-N1 1.639 (3), P2-N2 1.650 (3), O1-C4 1.327 (4), O2-C30 1.326(5), N1-C1 1.486(5), N2-C2 1.486(5), N1-Ni1-O1 94.9 (1), O2-Ni1-N2 95.3 (1), N1-Ni1-N2 86.8 (1), O1-Ni1-O2 84.2 (1), O1-N1-N2-O2 11.06.

Selected bond lengths around the metal centre of $[37a][SbF_6]$ and **37a** are presented in Table 3. Compared to the neutral complex, the two $O_{\text{phenoxide}}-C_{\text{phenoxide}}$ bonds in $[37a][SbF_6]$ are slightly longer (1.327(4) and 1.326(5) vs. 1.317(3)). This is in contrast with the case of phenoxyl radical salen complexes, where the $O_{\text{phenoxide}}-C_{\text{phenoxide}}$ bonds are shorter than those in the corresponding neutral salen complexes, as a result of semi-quinone character of the phenoxyl radical (Scheme 23). All M-N and M-O bonds are contracted in the oxidised phosphasalens complex. Interestingly, contraction is more important along one axis O1-M-N2 than the other (O2-M-N1).



Scheme 23. Canonical forms of phenoxyl radical.

Table 3. Selected bondlengths in **37a** and $[37a][SbF_6]$

Complex	Ni-N1	Ni-N2	Ni-O1	Ni-O2	O1- $C_{\text{phenoxide}}$	O2- $C_{\text{phenoxide}}$
37a (exp)	1.887 (2)	1.887 (2)	1.881(2)	1.881(2)	1.317(3)	1.317(3)
37a (calc)	1.892	1.892	1.904	1.904	1.309	1.309
$[37a][SbF_6]$ (exp)	1.875 (3)	1.842(3)	1.828 (2)	1.844(2)	1.327 (4)	1.326(5)
$[37a]^+$ (calc)	1.897	1.819	1.819	1.888	1.323	1.327
$[37a][SbF_6]$ (calc)	1.875	1.806	1.827	1.887	1.323	1.320

In most reported X-ray structures of oxidised nickel Salen complexes, which has been shown to be phenoxyl radical species, contraction of O-C_{phenoxide} bonds have been observed, along with the contraction of M-N, M-O bonds.^{5a, 5c, d} The only case where O-C_{phenoxide} bonds are slightly elongated upon comparison with the neutral complex happened to complex with unsymmetrical ligand⁶ (**Ni2**, Scheme 22), and in this case, the M-N and M-O are also elongated. The structural data thus suggest the formation of a nickel(III) complex. Further studies have been carried out in order to assess the nature of complex **[37a][SbF₆]**.

3. EPR and Magnetic Studies of Complex **[37a][SbF₆]**

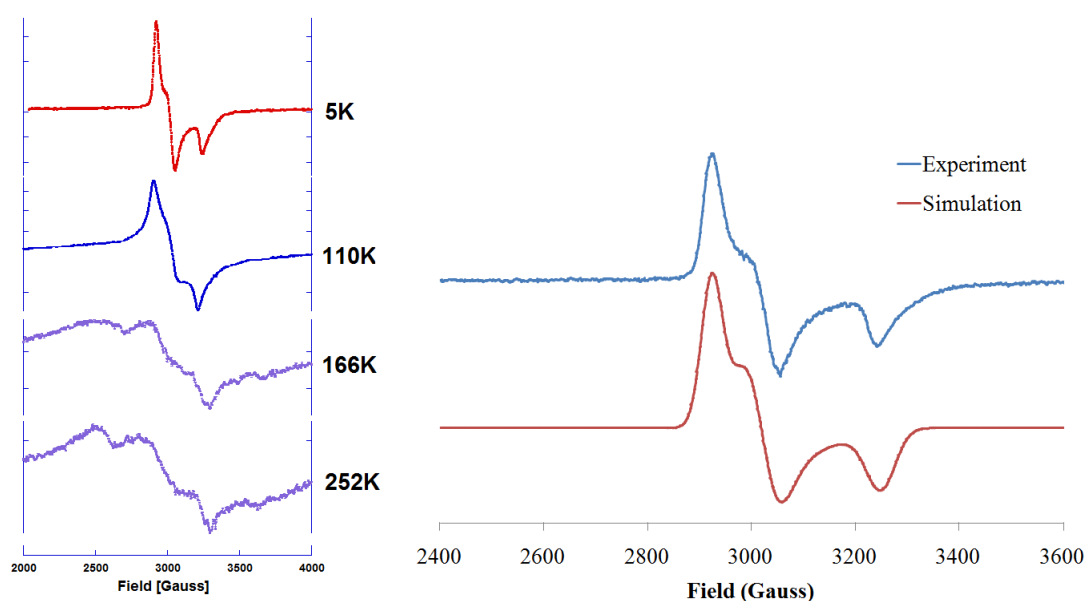


Figure 6. (left) EPR spectra of **[37a][SbF₆]** at different temperature; (right) recorded EPR spectrum of **[37a][SbF₆]** at 5K and the simulated spectrum. Conditions: **[37a][SbF₆]** = 4 mM in toluene:benzene, frequency 9.3690 GHz, power = 0.1 mW at 5K, 60 mW at other temperatures.

EPR spectrum recorded for the complex **[37a][SbF₆]** at 5K exhibited parameters with a large g-tensor anisotropy. Simulations gave three values of g as follow: $g_1=2.290$, $g_2=2.215$, $g_3=2.061$. These data indicate a rhombic symmetry typically known for low spin Ni(III).^{9, 6, 5d, 25, 23, 19}

No transition from Ni(III)-radical was observed in increasing the temperature, instead the intensities of the signals in EPR spectra decreased dramatically (no signal was detected at room temperature). This is markedly different from the behaviour of reported oxidised Ni(Salen) complexes and derivatives. For these compounds, high valent Ni(III) exist at low temperature (less than 160K, sometimes even much lower) and phenoxyl radical complex exists at higher temperatures.^{5d, 7, 23} At these temperatures and above, EPR spectra recorded for these complexes present a fine signal with $g \sim 2.0$, characteristic of an organic radical.

Thus these data clearly evidence the formation of a Ni(III)phosphasalen complex at low temperature and suggest that this oxidised complex is still a Ni(III) species at up to 252K.

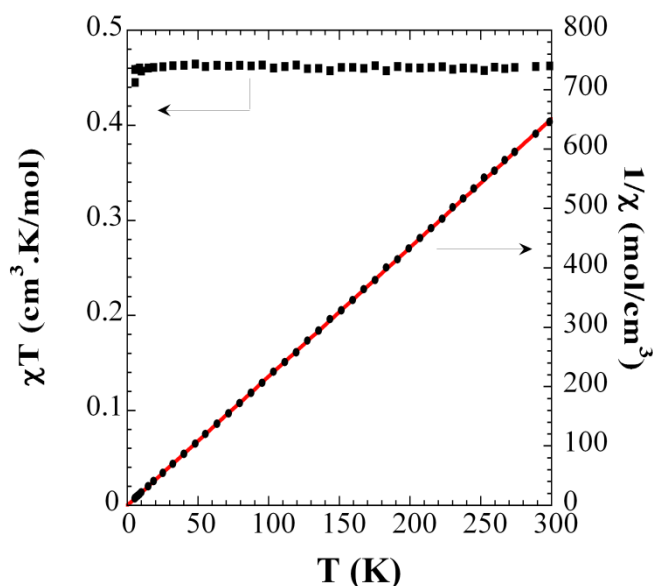


Figure 7. Plots of χT and $1/\chi$ vs. T for $[6a][SbF_6]$.

The solid state SQUID measurements (SQUID = Superconducting Quantum Interference Device) in temperatures were performed at 1000G on dried crystals of $[37a][SbF_6]$. They showed that the magnetic susceptibility χ follows a Curie law ($\chi=C/T$) for a mononuclear complex. The plot of $1/\chi$ vs. T is linear, and the product χT is constant from $\sim 4K$ up to 300K. The constant C was then determined to be $0.46 \text{ cm}^3 \cdot K/\text{mol}$. From this value, g was deduced to be 2.22 ($C = (Ng^2\mu_B^2S(S+1))/k_B$). Note that this value of g is in perfect consistence with the g_{average} calculated from EPR pectra (2.19).

The constant C , and thus g does not vary from $\sim 4K$ up to 300K, strongly suggesting that in this range of temperatures, the complex $[37a][SbF_6]$ remains a Ni(III) species. This hypothesis is consistent with what have been observed from EPR spectroscopy measurements.

Data from EPR and SQUID measurements thus strongly suggest that the complex $[37a][SbF_6]$ is a high valent Ni(III) species and that this species is stable even at high temperature. DFT calculations have been carried out for better understanding of the nature of the complex.

4. DFT Studies of $[37a][SbF_6]$

Density Functional Theory (DFT) calculations were performed on the two complexes **6a** and $[37a][SbF_6]$ with the Gaussian 03 set of programs²⁶ in combination with the B3PW91 functional.²⁷ Nickel was represented by the relativistic effective core potential of Hay and Wadt²⁸ and the associated triple zeta quality basis set²⁹, augmented by a f polarization function as proposed by Frenking³⁰ (lanl2tz(f)). Tert-butyl group on the phenoxide rings were described

with 3-21G Pople basis set to simplify the calculations. Phosphorus atoms were represented by 6-31G* basis set reinforced with an f polarization function. All other atoms were described with the 6-31G* Pople basis set.³¹

DFT calculations correctly represent the geometry of neutral nickel-phosphasalens complexes, the difference between calculated bond lengths and experimental ones are less than 0.02Å. Details of the bonds around metal center could be seen in Table 3.

For the oxidized species, two structures were optimized: the cation with or without a counterion SbF₆. All bond distances on the ligand predicted for [6a]⁺ are very close to the ones predicted for [37a][SbF₆] and they all match experimental values. At the difference from oxidized nickel salen complex Ni2 (Scheme 22) featuring methoxyl group at the *p*-position on the phenoxide rings, whose optimized DFT structure and X-ray structure both shown a non-negligible interaction of SbF₆ and the cationic nickel complex, no such interaction was detected in the optimized DFT structure of [37a][SbF₆], which is coherent with what has been seen in X-ray structure of [37a][SbF₆].

Just like in the structure obtained from X-ray diffraction, in the optimized structures of [37a]⁺ and [37a][SbF₆] the two C_{phenoxide}-O bonds are not shortened but even slightly elongated and show no difference one to the other. The non-symmetric contraction of Ni-N and Ni-O bonds along one particular N-Ni-O axis (more precisely, N2-Ni-O1 axis in X-ray structure) is also correctly represented. Effectively, the calculations attributed an important spin density on the three atoms on this N2-Ni-O1 axis (Figure 8). Those densities are much higher than the ones on other atoms. Spin densities on the phenyl ring attached to O1 are also more important than the ones on the other side. The majority of spin density is on the Ni centre, which suggests that the oxidised complex contains high valent Ni(III) instead of a radical ligand.

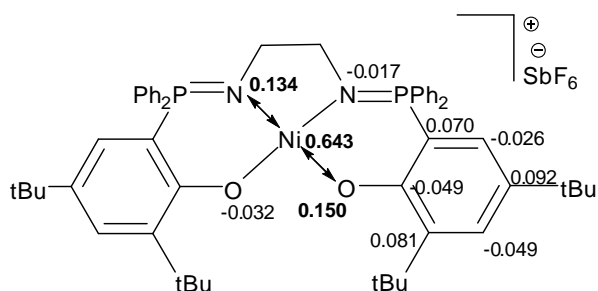
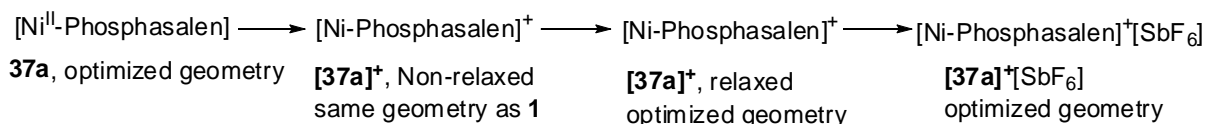


Figure 8. Spin densities on [37a][SbF₆], only the ones >0.02 are printed.

In order to elucidate the electronic structure of the oxidised nickel-phosphasalens species and to understand the oxidation process, natural bond orbital (NBO) analysis was performed on all species involved in the following process:



In neutral complex **37a**, the d-block orbitals of Ni are all in important bonding or anti-bonding interaction with p-orbitals from nitrogen or oxygen. The resulting MOs are among the highest occupied MOs of the molecule and do not differ much in energy. This indicates close energy levels between d-block orbitals of Ni and p_z orbitals of N and O and π -orbitals of aromatic rings. The two highest occupied molecular orbitals are almost of the same energy and result from the anti-bonding combination of d_{xz}/d_{yz} orbital of Ni with p_π orbitals of the phenoxides on the ligand (Figure 9).

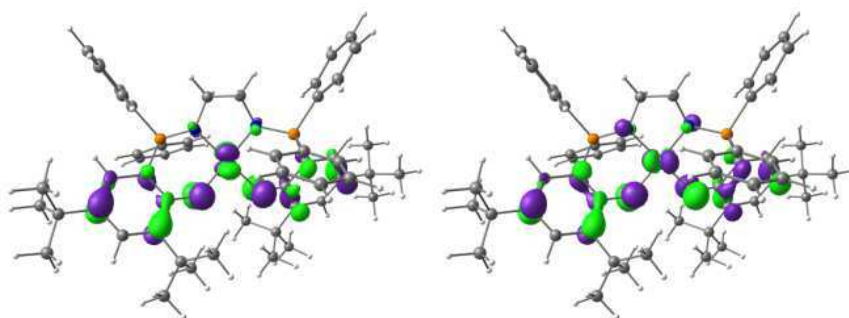


Figure 9. HOMO-1 and HOMO of neutral complex **37a**.

The oxidation was first done by removing one electron from one of these highest occupied orbitals. In the non-relaxed geometry, the resulted cation has two possible ground states with the same energy. According to the Jahn-Teller theorem, the compound will follow a geometric distortion in order to remove this degeneracy (Figure 10). Thus the two degenerate orbitals split in two energy levels: the singly occupied orbital at higher energy level than the doubly occupied one. This latter has been determined in the optimised $[\mathbf{37a}]^+$ and is essentially the d_{xz} of nickel (Figure 10).

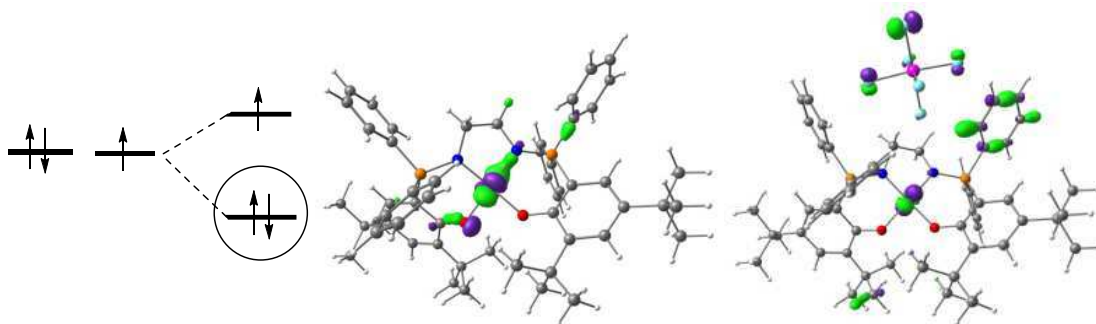


Figure 10. Jahn-Teller effect and the resulted doubly occupied orbital in $[\mathbf{37a}]^+$ and $[\mathbf{37a}][\text{SbF}_6]$

The fact that there's almost no participation from the ligand in this molecular orbital is not surprising. In fact, it has been found that in $[37a]^+$ and $[37a][SbF_6]$ d-block orbitals of Nickel become relatively much more stabilised than other ligand-based ones and they pass from the highest block into the high-medium ones (d_{xz} , d_{xy} , d_{z^2}). On the other hand, the p_π -orbitals of nitrogens and oxygens are still among the highest occupied orbitals. Thus, it is clear that the once existing bonding/antibonding interaction between these orbitals and ligand orbitals no longer exist. The relative stabilization of that d-block orbitals of Nickel is another indication of the high-valent Ni(III) complex.

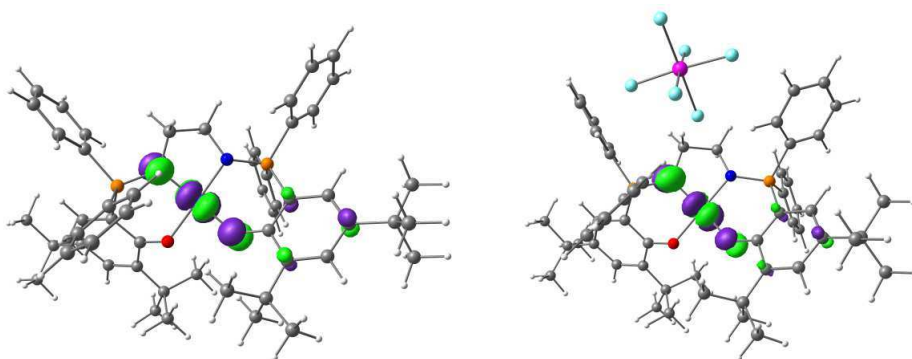


Figure 11. The “hole” in $[37a]^+$ and $[37a][SbF_6]$

The determination of the singly occupied orbital (SOMO) is difficult. In these big systems where energy levels of orbitals (alpha or beta) are very close to others, the SOMO seems to “blend” in combinations with other orbitals. Fortunately, the “hole” corresponding to the orbital from which the electron was removed has been determined (Figure 11). It consists of the d_{yz} of nickel in antibonding interactions with p_π -orbitals of N2 and O1. It is indeed the highest unoccupied molecular orbital (alpha and beta comprised) and is the one in which the electron would be added if the oxidized complex undergoes a reduction to give the neutral one.

The form of this orbital coincides perfectly with the spin density distribution in $[37a]^+$ and $[37a][SbF_6]$. Furthermore, as this orbital consists of d_{yz} of nickel in antibonding interactions with p_π -orbitals of N2 and O1, removal of electron from it would shorten the bonds along the N2-Ni-O1 axis, a result which has been attested by X-ray diffraction and geometry optimization calculations.

In conclusion, from the DFT analysis, it could be seen that

- 1) the biggest spin density is on the Ni, with more than 60%;
- 2) the orbital from which the electron is removed is essentially d_{yz} of nickel in antibonding interactions with p_π -orbitals of N2 and O1, resulting in non-symmetrical shortening of bonds along one axis O1-M-N2;
- 3) in $[37a]^+$ and $[37a][SbF_6]$ d-block orbitals of Nickel become relatively much more stabilised than other ligand-based ones

All these three observations strongly indicate that the oxidized form of Nickel phosphasalen complex **37a** is a high-valent Ni(III) complex.

III. Conclusion

The previous studies on nickel complex of the non-substituted phosphasalen ligand demonstrated the superior donating ability of this ligand compared to salen. This ability suggests that phosphasalens could be used for the obtainment of stabilised oxidised complexes. Taken into account the rarity of isolated Ni(III) complex with low-coordination number, as well as the study on oxidized metal-phenoxide complexes, we decided to study the oxidations of nickel phosphasalen complexes.

Two nickel complexes have been synthesised from modified phosphasalen ligands with *tert*-butyl substituents on the *o*- and *p*- positions of the phenoxide rings. They have been fully characterised and could be cleanly oxidised by one equivalent of silver salt in dichloromethane. X-ray structure was obtained one these two products (complex [**37a**][SbF₆]). At the difference of all reported oxidised nickel-phenoxide complexes up to now, which have been shown to be Ni(II) complexes of phenoxyl radical, the oxidised species [**37a**][SbF₆] is a Ni(III) complex. This has been shown by EPR spectroscopy and DFT calculations. This complex is the first example of four-coordinated high valent Ni(III) phenoxide species, and one of rare example of Ni(III) complexes with coordination number less than 5.

The easy formation and stability of these Ni(III) complexes would allow further studies of the reactivity of Ni(III) complexes and their roles in catalysis. Furthermore, these phosphasalen ligands, which could stabilise high valent Ni(III) state by their donating abilities, are expected to render possible the isolation of other high valent complexes, in particular the oxo complexes of Mn(III), the active intermediate supposed to be present in manganese-catalysed epoxidation of olefins, which has never been evidenced.

REFERENCES

1. (a) Whittaker, J. W., *Chem. Rev.* **2003**, *103* (6), 2347-2364; (b) Baron, A. J.; Stevens, C.; Wilmot, C.; Seneviratne, K. D.; Blakeley, V.; Dooley, D. M.; Phillips, S. E. V.; Knowles, P. F.; McPherson, M. J., *J. Biol. Chem.* **1994**, *269* (40), 25095-25105.
2. Stubbe, J.; van der Donk, W. A., *Chem. Rev.* **1998**, *98* (2), 705-762.
3. (a) Wang, Y. D.; DuBois, J. L.; Hedman, B.; Hodgson, K. O.; Stack, T. D. P., *Science* **1998**, *279* (5350), 537-540; (b) Königsmann, M.; Donati, N.; Stein, D.; Schönberg, H.; Harmer, J.; Sreekanth, A.; Grützmacher, H., *Angew. Chem. Int. Ed.* **2007**, *46* (19), 3567-3570; (c) Chirik, P. J.; Wieghardt, K., *Science* **2010**, *327* (5967), 794-795; (d) Chaudhuri, P.; Hess, M.; Muller, J.; Hildenbrand, K.; Bill, E.; Weyhermuller, T.; Wieghardt, K., *J. Am. Chem. Soc.* **1999**, *121* (41), 9599-9610.
4. Kurahashi, T.; Fujii, H., *J. Am. Chem. Soc.* **2011**, *133* (21), 8307-8316.
5. (a) Orio, M.; Jarjays, O.; Kanso, H.; Philouze, C.; Neese, F.; Thomas, F., *Angew. Chem. Int. Ed.* **2010**, *49* (29), 4989-4992; (b) Shimazaki, Y.; Stack, T. D. P.; Storr, T., *Inorg. Chem.* **2009**, *48* (17), 8383-8392; (c) Storr, T.; Wasinger, E.; Pratt, R.; Stack, T., *Angew. Chem. Int. Ed.* **2007**, *46* (27), 5198-5201; (d) Shimazaki, Y.; Arai, N.; Dunn, T. J.; Yajima, T.; Tani, F.; Ramogida, C. F.; Storr, T., *Dalton Trans.* **2011**, *40* (11), 2469-2479.
6. Storr, T.; Verma, P.; Shimazaki, Y.; Wasinger, E. C.; Stack, T. D. P., *Chem. Eur. J.* **2010**, *16* (30), 8980-8983.
7. Shimazaki, Y.; Tani, F.; Fukui, K.; Naruta, Y.; Yamauchi, O., *J. Am. Chem. Soc.* **2003**, *125* (35), 10512-10513.
8. De Castro, B.; Freire, C., *Inorg. Chem.* **1990**, *29* (25), 5113-5119.
9. (a) Rotthaus, O.; Jarjays, O.; Del Valle, C. P.; Philouze, C.; Thomas, F., *Chem. Commun.* **2007**, (43), 4462-4464; (b) Rotthaus, O.; Jarjays, O.; Thomas, F.; Philouze, C.; Perez Del Valle, C.; Saint-Aman, E.; Pierre, J.-L., *Chem. Eur. J.* **2006**, *12* (8), 2293-2302; (c) Rotthaus, O.; Thomas, F.; Jarjays, O.; Philouze, C.; Saint-Aman, E.; Pierre, J.-L., *Chem. Eur. J.* **2006**, *12* (26), 6953-6962; (d) Rotthaus, O.; Jarjays, O.; Philouze, C.; Del Valle, C. P.; Thomas, F., *Dalton Trans.* **2009**, (10), 1792-1800.
10. Barondeau, D. P.; Kassmann, C. J.; Bruns, C. K.; Tainer, J. A.; Getzoff, E. D., *Biochemistry* **2004**, *43* (25), 8038-8047.
11. (a) Lee, C. M.; Chen, C. H.; Ke, S. C.; Lee, G. H.; Liaw, W. F., *J. Am. Chem. Soc.* **2004**, *126* (27), 8406-8412; (b) Lee, C.-M.; Chen, C.-H.; Liao, F.-X.; Hu, C.-H.; Lee, G.-H., *J. Am. Chem. Soc.* **2010**, *132* (27), 9256-9258.
12. Lee, W.-Z.; Chiang, C.-W.; Lin, T.-H.; Kuo, T.-S., *Chem. Eur. J.* **2012**, *18* (1), 50-53.
13. Gennari, M.; Orio, M.; Pecaut, J.; Neese, F.; Collomb, M. N.; Duboc, C., *Inorg. Chem.* **2010**, *49* (14), 6399-6401.

14. Gennari, M.; Orio, M.; Pecaut, J.; Bothe, E.; Neese, F.; Collomb, M. N.; Duboc, C., *Inorg. Chem.* **2011**, *50* (8), 3707-3716.
15. (a) Schmitt, R. D.; Maki, A. H., *J. Am. Chem. Soc.* **1968**, *90* (9), 2288-2292; (b) Maki, A. H.; Edelstein, N.; Davison, A.; Holm, R. H., *J. Am. Chem. Soc.* **1964**, *86* (21), 4580-4587.
16. Pierpont, C. G., *Coord. Chem. Rev.* **2001**, *219*, 415-433.
17. (a) Spasyuk, D. M.; Zargarian, D.; van der Est, A., *Organometallics* **2009**, *28* (22), 6531-6540; (b) Salah, A. B.; Zargarian, D., *Dalton Trans.* **2011**, *40* (35), 8977-8985.
18. Adhikari, D.; Mossin, S.; Basuli, F.; Huffman, J. C.; Szilagy, R. K.; Meyer, K.; Mindiola, D. J., *J. Am. Chem. Soc.* **2008**, *130* (11), 3676-3682.
19. Iluc, V. M.; Miller, A. J. M.; Anderson, J. S.; Monreal, M. J.; Mehn, M. P.; Hillhouse, G. L., *J. Am. Chem. Soc.* **2011**, *133* (33), 13055-13063.
20. Alonso, P. J.; Arauzo, A. B.; Garcia-Monforte, M. A.; Martin, A.; Menjon, B.; Rillo, C.; Tomas, M., *Chem. Eur. J.* **2009**, *15* (41), 11020-11030.
21. (a) Goldsby, K. A.; Blaho, J. K.; Hoferkamp, L. A., *Polyhedron* **1989**, *8* (1), 113-115; (b) Hoferkamp, L. A.; Goldsby, K. A., *Chem. Mater.* **1989**, *1* (3), 348-352.
22. Carmichael, C. D.; Fryzuk, M. D., *Dalton Trans.* **2008**, (6), 800-806.
23. Shimazaki, Y.; Yajima, T.; Tani, F.; Karasawa, S.; Fukui, K.; Naruta, Y.; Yamauchi, O., *J. Am. Chem. Soc.* **2007**, *129* (9), 2559-2568.
24. Connelly, N. G.; Geiger, W. E., *Chem. Rev.* **1996**, *96* (2), 877-910.
25. Shimazaki, Y.; Huth, S.; Karasawa, S.; Hirota, S.; Naruta, Y.; Yamauchi, O., *Inorg. Chem.* **2004**, *43* (24), 7816-7822.
26. M. J. Frisch; G. W. Trucks; H. B. Schlegel; G. E. Scuseria; M. A. Robb; J. R. Cheeseman; J. A. Montgomery, Jr., T. V.; K. N. Kudin; J. C. Burant; J. M. Millam; S. S. Iyengar; J. Tomasi; V. Barone; B. Mennucci; M. Cossi; G. Scalmani; N. Rega; G. A. Petersson, H. N., M. Hada, M. Ehara, K. Toyota, R. Fukuda, J. Hasegawa, M. Ishida, T. Nakajima, Y. Honda, O. Kitao, H. Nakai, M. Klene, X. Li, J. E. Knox, H. P. Hratchian, J. B. Cross, V. Bakken, C. Adamo, J. Jaramillo, R. Gomperts, R. E. Stratmann, O. Yazyev, A. J. Austin, R. Cammi, C. Pomelli, J. W. Ochterski, P. Y. Ayala, K. Morokuma, G. A. Voth, P. Salvador, J. J. Dannenberg, V. G. Zakrzewski, S. Dapprich, A. D. Daniels, M. C. Strain, O. Farkas, D. K. Malick, A. D. Rabuck, K. Raghavachari, J. B. Foresman, J. V. Ortiz, Q. Cui, A. G. Baboul, S. Clifford, J. Cioslowski, B. B. Stefanov, G. Liu, A. Liashenko, P. Piskorz, I. Komaromi, R. L. Martin, D. J. Fox, T. Keith, M. A. Al-Laham, C. Y. Peng, A. Nanayakkara, M. Challacombe, P. M. W. Gill, B. Johnson, W. Chen, M. W. Wong, C. Gonzalez, and J. A. Pople *Gaussian 03, revision C.02*, Gaussian Inc., Wallingford CT: 2004.
27. (a) Becke, A. D., *J. Chem. Phys.* **1993**, *98* (7), 5648-5652; (b) Perdew, J. P.; Wang, Y., *Phys. Rev. B* **1992**, *45* (23), 13244-13249.
28. Hay, P. J.; Wadt, W. R., *J. Chem. Phys.* **1985**, *82* (1), 270-283.

29. Roy, L. E.; Hay, P. J.; Martin, R. L., *J. Chem. Theory Comput.* **2008**, *4* (7), 1029-1031.
30. Ehlers, A. W.; Bohme, M.; Dapprich, S.; Gobbi, A.; Hollwarth, A.; Jonas, V.; Kohler, K. F.; Stegmann, R.; Veldkamp, A.; Frenking, G., *Chem. Phys. Lett.* **1993**, *208* (1-2), 111-114.
31. Petersson, G. A.; Bennett, A.; Tensfeldt, T. G.; Allaham, M. A.; Shirley, W. A.; Mantzaris, J., *J. Chem. Phys.* **1988**, *89* (4), 2193-2218.

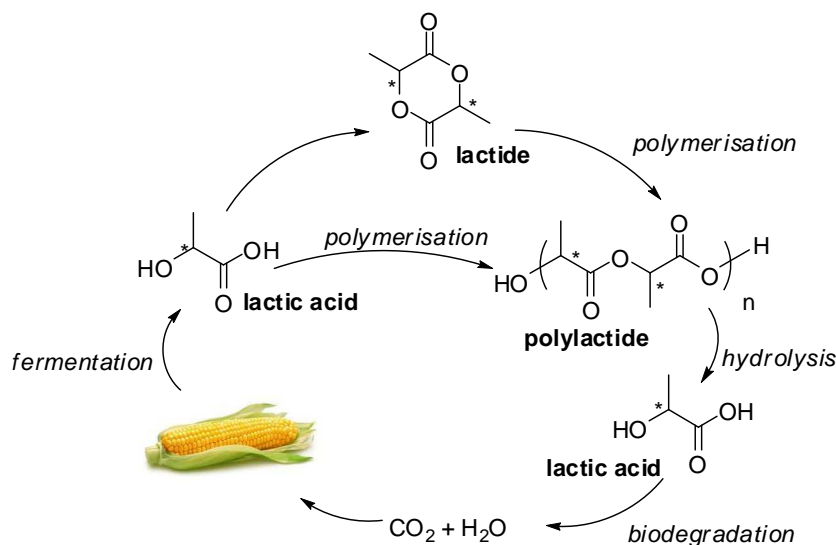
Chapter 5

Phosphasalen Complexes in Ring-Opening Polymerisation of Lactide

I. Introduction: PLA and ROP of Lactide

1. PLA: Utility and Synthesis

Most of polymers for daily utility such as polypropylene, polystyrene, PVC, nylon, synthetic rubber, etc., are derived from petrochemical feedstock. The possible exhaustion of oil and gas feedstock in a near future, and the ecological problems linked to the disposal of those plastics have drawn towards the development of polymer from renewable sources and ideally, biodegradable. Poly(lactic acid) or polylactide (PLA) is a polymer derived from bioresources that fulfils both these criteria and thus its synthesis and development has been an active domain of research in industry and academics. It is up to date the most commercially viable biodegradable material. It is recently manufactured in large scale in US and in smaller scale in EU and Japon.¹ PLA has good mechanical and physical properties and its advantage is even enhanced by its biocompatibility and its ability to be adsorbed and degraded in vivo. PLA is an FDA approved substance for use in therapy.



Scheme 1. Life-cycle of polylactide.

PLA, like other polyester, could be produced by two main ways: condensation-polymerisation of lactic acid which bears both an acid and an alcohol function, or ring-opening polymerisation of lactide (Scheme 1). Lactic acid is obtained from fermentation of sugars, produced from high starch content plants. Direct condensation-polymerisation of lactic acid is often limited by the necessity of adding coupling agents and adjuvants in order to remove water to drive the equilibrium towards the formation of polyester. This method produces polylactide with poorly controlled chain length and often with low molar mass. Thus synthesis of polylactide is often directed to the second method which is ring-opening polymerisation of lactide. This product is formed by the thermal degradation of oligolactic acids, which in turn are produced by the condensation polymerisation of lactic acid.

Compared to condensation polymerisation, ring-opening polymerisation has a crucial advantage which is the possibility of having controlled polymerisation in terms of chain lengths/molar mass, and in terms of stereochemistry. Many researches have been actively carried out to attain polymerisation system which is both viable commercially and effective in producing PLA with special stereochemistry.

Before going any further, it is important to understand the meaning of control polymerisation and stereochemistry of such process. The next section is a brief introduction to all those notions, sometimes in direct relation with polylactide.

2. Controlled Polymerisation: Meaningful Indicators

2.1 PDI and Molar Mass Distribution

Polymer molecular weight is important because it greatly influences many physical properties of the polymer. These includes glass transition temperature (the temperature at which the

polymer changes from a hard and brittle state to a rubber-like one) or melt temperature (the temperature at which semi-crystallised domains of the polymer melt), viscoelasticity, strength, etc. The polymer molecular weight is thus reported for any polymerisation and its control is important.

Polymer masses are often given by physical methods, such as gel-exclusion chromatography, light-scattering, osmometry or viscosity measurements. Unlike small molecules, most synthetic polymers do not have unique molar mass but a range of masses of different polymer molecules. This weight distribution depends on the way the polymer is produced. Thus most physical methods deliver mass distributions. They are the molar mass M_i of a molecule of type i , the total mass $m_i = n_i M_i$ of all molecules i , their mass fraction $w_i = m_i / \sum_i m_i$, or mass concentration $c_i = m_i / V$. Some physical methods deliver higher statistical weights. Common case is z-statistical weight $z_i = m_i M_i = n_i M_i^2$.

For practical purposes, the three most important molar masses are \bar{M}_n (the number average molecular weight), \bar{M}_w (the weight average molecular weight) and \bar{M}_z (the z-average molecular weight). Their definitions are described as follow:

$$\bar{M}_n = \sum_i x_i M_i = \frac{\sum_i n_i M_i}{\sum_i n_i}$$

$$\bar{M}_w = \sum_i w_i M_i = \frac{\sum_i m_i M_i}{\sum_i m_i} = \frac{\sum_i n_i M_i^2}{\sum_i n_i M_i}$$

$$\bar{M}_z = \sum_i Z_i M_i = \frac{\sum_i m_i M_i^2}{\sum_i m_i M_i} = \frac{\sum_i n_i M_i^3}{\sum_i n_i M_i^2}$$

Polymolecular index $Q_{w,n} = \bar{M}_w / \bar{M}_n$, or commonly called polydispersity index (PDI) is often used to determine the quality of control of the polymerisation. The broader the distribution of molar mass is, the higher PDI, thus the lower the degree of control of the polymerisation is.

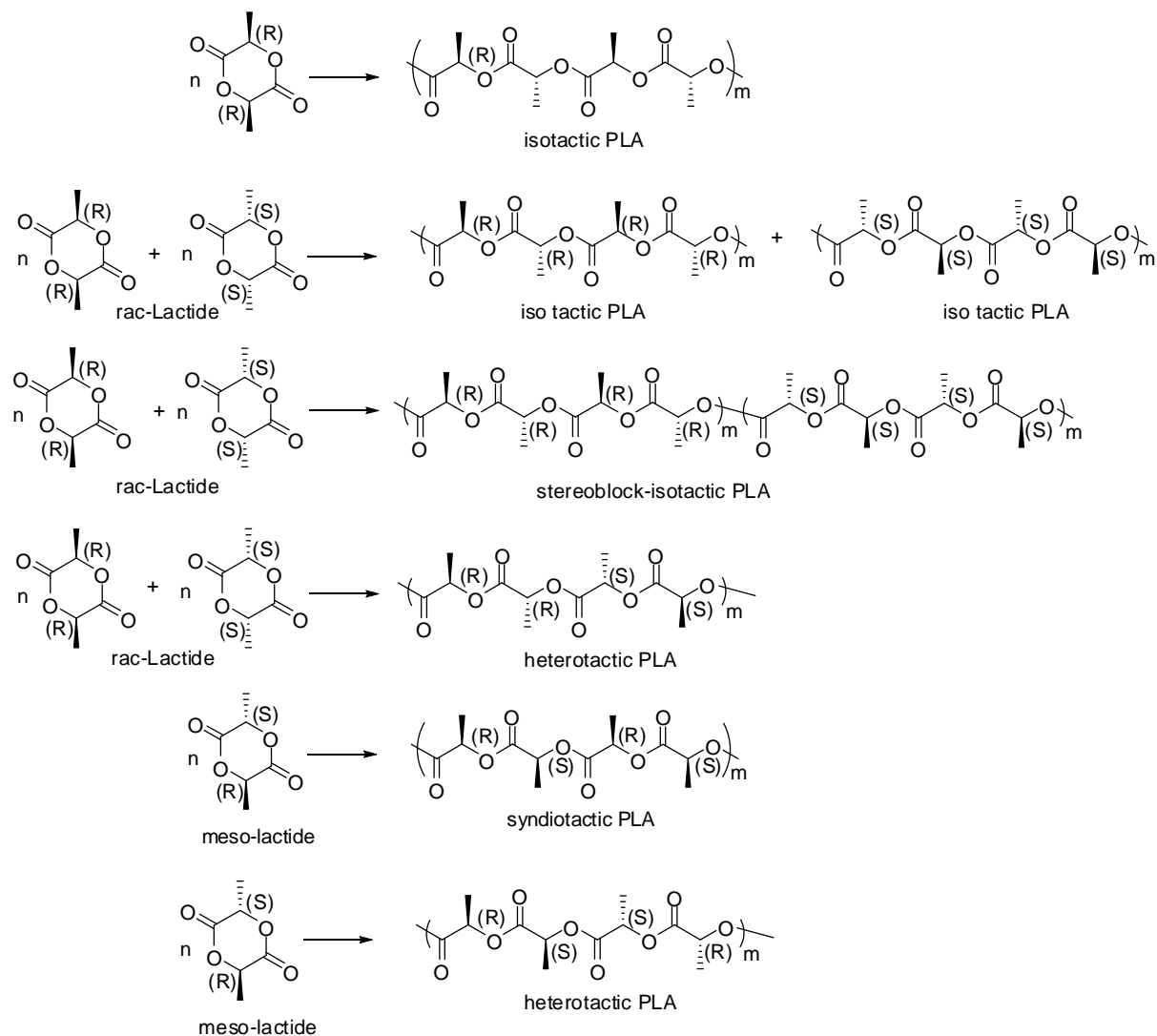
2.2 Stereochemistry of Polymer and Tacticities

2.2.1 Introduction to Tacticity

Stereocontrol is an important issue in polymers containing asymmetric centres. Just like in simple small molecules where diastereoisomers do not have the same melting temperature or solubility, physical properties polymers depend on the enchainment those asymmetric centres. For example, isotactic PLA having only S-lactic acid monomer is crystalline thermoplastic with $T_g \sim 60^\circ\text{C}$ and $T_m \sim 170^\circ\text{C}$, whereas atactic PLA having R-lactic acid monomers and S-lactic acid monomers in non-ordered enchainment is amorphous. The type of stereo-enchainment of monomers in the polymer molecule is called tacticity.

In general, the tacticity of polymer is determined by the probabilities of certain **stereo-sequences**, or stereorepeating units. A repeating unit or constitutional repeating unit is the

smallest constitutional unit whose repetition in a single sequential arrangement described a regular polymer molecule.² For PLA, the constitutional repeating unit is one half the lactide molecule, i.e. $-C(=O)-CH(CH_3)-O-$. An **isotactic sequence** consists of a single constitutional repeating unit, in this case: a single enantiomer R or S. A **syndiotactic sequence** consists of two enantiomeric configurational repeating unit RS or SR. A **heterotactic repeating sequence** has four monomeric units RRSS or SSRR. The repetition of each of these stereosequences gives respectively **isotactic**, **syndiotactic** and **heterotactic** polymer. Different types of tacticity that could be derived from the polymerisation of lactides are shown in Scheme 2.



Scheme 2. Tacticities of PLA

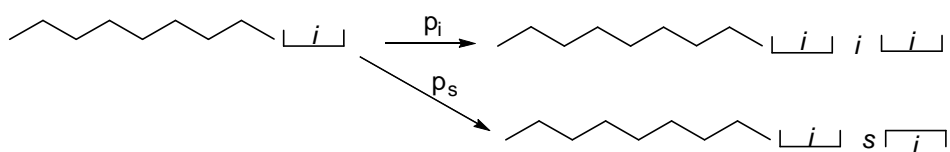
Atactic polymer contains all types of configurational units (i.e. R and S) with equal amounts in random distribution. Stereoblock polymers have different blocks, each of which contains the same type of stereosequences.

2.2.2 Statistic of Polymerisation and Bernoulli Trials

In fact, in stereoselective polymerisation, there's always some influence of the present units which is expressed as a conditional probability of the connecting step, thus the statistics should follow a Markov trial. In Markov first order trials, only the last unit influences the addition of the new unit. For the polymerisation to yield PLA, four conditional probabilities must be considered, corresponding to the probability of adding R-LA or S-LA constitutional unit to a polymer with (r) or (s) propagating centre: $p_{(r)/R}$, $p_{(r)/S}$, $p_{(s)/R}$, $p_{(s)/S}$. These probabilities obey this relation:

$$p_{(r)/R} + p_{(r)/S} = p_{(s)/R} + p_{(s)/S} = 1$$

As defined above, p_i and p_s is respectively the probability of isotactic or heterotactic enchainment, and in simplified cases, the probability of adding R-LA or S-LA constitutional unit to a polymer with (r) or (s) propagating centre only depends on the relative configuration between the arriving and the present units, we have thus $p_{(r)/R} = p_{(s)/S} = p_i$ and $p_{(r)/S} = p_{(s)/R} = p_s$. As only two probabilities exist $p_i + p_s = 1$, the statistics is reduced to a zeroth-order Markovnikov chain or a Bernoulli statistics. That's why the polymerisation of lactide is said to follow Bernoulli statistics.

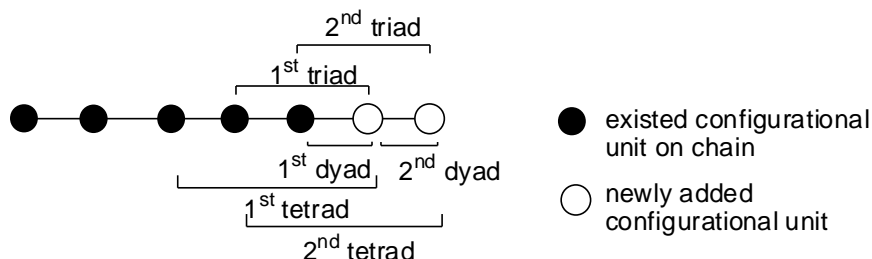


Scheme 4. Chain-growing polymerisation of dimers of lactide (after Coudane et al)^{3a}

For the polymerization of lactide (which is in fact a dimer of constitutional unit), let x_a the proportion of sequences of type a in the polymer. For tetrads levels, we have:

$$x_{iii} + x_{iis} + x_{isi} + x_{iss} + x_{sss} + x_{sis} + x_{ssi} + x_{sii} = 1$$

For polymerisation from *rac*-LA, $x_{sss} = x_{iss} = x_{ssi} = 0$ (because sequences with RSR or SRS are impossible to form), thus we have $x_{iii} + x_{iis} + x_{isi} + x_{sis} + x_{sii} = 1$



Scheme 5. Diads, triads, tetrads formed from the addition of a dimer lactide.

When a new dimer lactide unit is added, two configurational unit are added to the polymer chain, thus two dyads, two triads, and two tetrads are formed (Scheme 5).

By applying some simple probability reasoning, one could find again the values for the probabilities of different dyads, triads, tetrads, pentads or hexads in function of p_i and p_s , as given by Coudane and coworkers^{3a} (Table 1).

Table 1. Probability of n -ads ($n=2-6$) in *rac*-lactide polymerisation with a Bernoullian statistics.

Dyads	<i>i</i>	<i>s</i>				
Ratio	$(1+p_i)/2$	$(1-p_i)/2$				
Triads	<i>ii</i>	<i>is</i>	<i>si</i>			
Ratio	p_i	$(1-p_i)/2$	$(1-p_i)/2$			
Tetrads	<i>iii</i>	<i>iis</i>	<i>isi</i>	<i>sii</i>	<i>sis</i>	
Ratio	$p_i(p_i+1)/2$	$p_i(1-p_i)/2$	$(1-p_i)/2$	$p_i(1-p_i)/2$	$(1-p_i)^2/2$	
Pentads	<i>iiii</i>	<i>iisi</i>	<i>iiis</i>	<i>siii</i>	<i>isii</i>	<i>isis</i>
Ratio	p_i^2	$p_i(1-p_i)/2$	$p_i(1-p_i)/2$	$p_i(1-p_i)/2$	$p_i(1-p_i)/2$	$(1-p_i)^2/2$
Hexads	<i>iiii</i>	<i>isiii</i>	<i>iiis</i>	<i>iisis</i>	<i>isisi</i>	<i>sisis</i>
		<i>iiisi</i>	<i>iisii</i>	<i>siiis</i>		
			<i>siiii</i>	<i>sisii</i>		
Ratio	$p_i^2(p_i+1)/2$	$p_i(1-p_i)/2$	$p_i^2(1-p_i)/2$	$p_i(1-p_i)^2/2$	$(1-p_i)^2/2$	$(1-p_i)^3/2$

Using these formulas, the heteroselectivity p_s for a polymer derived from *rac*-lactide could be calculated from the peak integrals in the homodecoupled ^1H or $^{13}\text{C}\{^1\text{H}\}$ NMR spectra.

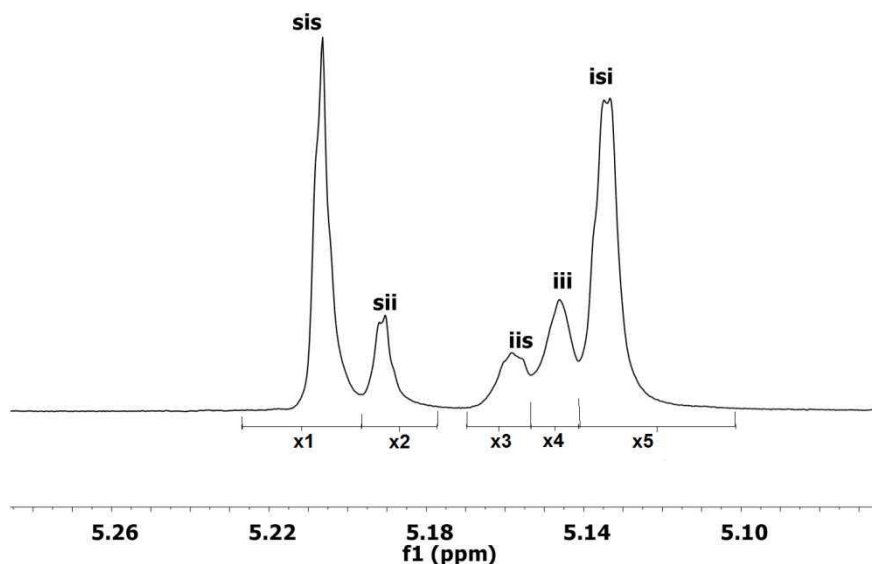


Figure 2. Example of tetrad level of resonances observed in homodecoupled ^1H NMR spectrum.

The integrals of *sis*, *sii*, *iis*, *iii*, *isi* signals being x_1 , x_2 , x_3 , x_4 , x_5 , respectively

From the *sis* signal: $x_{sis} = x_1 / \sum_{i=1}^5 x_i$ and $p_{i1} = 1 - \sqrt{2x_{sis}}$, $p_{s1} = \sqrt{2x_{sis}}$

From the *sii* signal: $x_{sii} = x_2 / \sum_{i=1}^5 x_i$ and

$$p_{i2} = \frac{(1 \pm \sqrt{1 - 8x_{sii}})}{2}, \quad p_{s2} = \frac{(1 \mp \sqrt{1 - 8x_{sii}})}{2}$$

(the value of p_{s2} is the one that is closer to p_{s1})

From the *iss* signal: $x_{iss} = x_3 / \sum_{i=1}^5 x_i$ and

$$p_{i3} = \frac{(1 \pm \sqrt{1 - 8x_{iss}})}{2}, \quad p_{s3} = \frac{(1 \mp \sqrt{1 - 8x_{iss}})}{2}$$

(the value of p_{s3} is the one that is closer to p_{s2})

From the *iii* signal: $x_{iss} = x_4 / \sum_{i=1}^5 x_i$ and

$$p_{i4} = \frac{(-1 + \sqrt{1 + 8x_{iii}})}{2}, \quad p_{s4} = \frac{(3 - \sqrt{1 + 8x_{iii}})}{2}$$

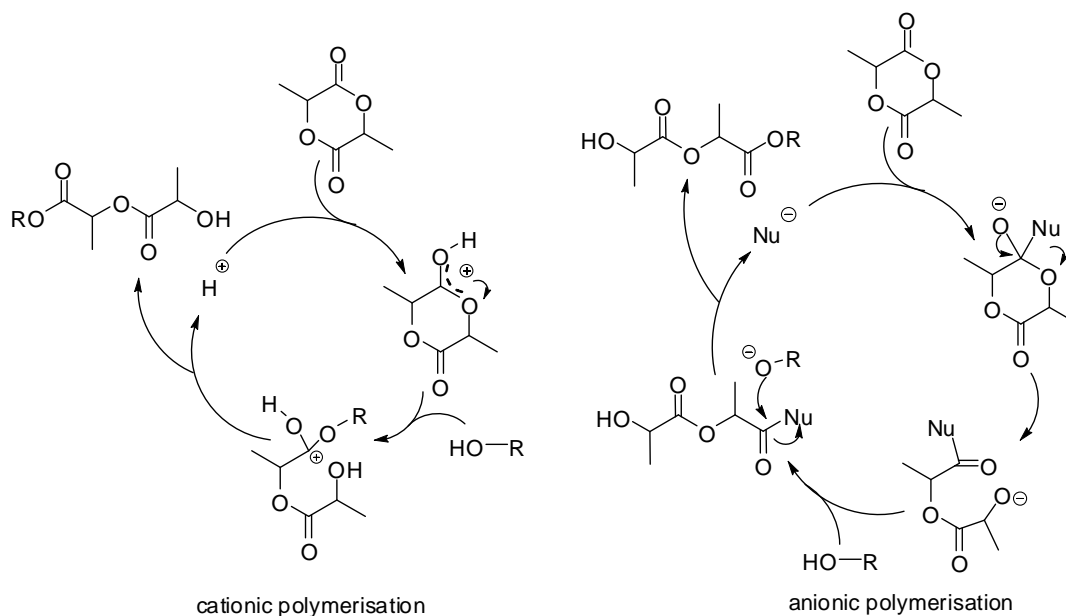
From the *isi* signal: $x_{isi} = x_5 / \sum_{i=1}^5 x_i$ and $p_{i5} = 1 - 2x_5$, $p_{s5} = 2x_5$

The tacticity of the polymer $p_i = \frac{1}{5} \sum_{j=1}^5 p_{ij}$ and $p_s = \frac{1}{5} \sum_{j=1}^5 p_{sj}$

3. Mechanism of Ring-Opening Polymerisation of Lactide

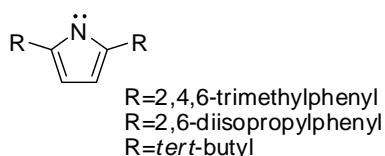
Depending on initiators, ring-opening polymerisation (ROP) of lactide could have different mechanisms. The three most often considered ones are coordination-insertion,⁴ anionic,^{4,5} and cationic^{4,6} polymerisation (Scheme 6, Scheme 8).

The last two mechanisms are often proposed for the organo/cationic initiator and are called monomer-activated mechanism, because the monomer must be activated first by a nucleophile such as a carbene, or an electrophile (very often acid Bronsted) in order for the polymerisation to occur (Scheme 6).



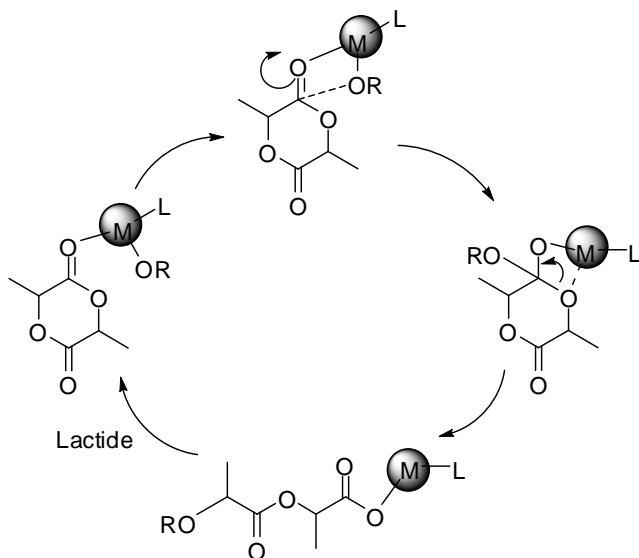
Scheme 6. Cationic and anionic lactide ring-opening polymerization.

In theory, by selecting the cation/nucleophile with appropriate steric properties, stereo-selective ROP can take place. However, to our knowledge, no such selectivity has been reported for ROP systems supposedly following cationic mechanisms. Examples of stereoselective ROP with anionic mechanism are rare. In 2004, Tolman and co-workers reported that ROP using free *N*-heterocyclic carbene and analogs give isotactic enriched PLA ($P_s=0.75$) (Scheme 7).⁷



Scheme 7. Tolman's *N*-heterocyclic carbenes for ROP of lactide

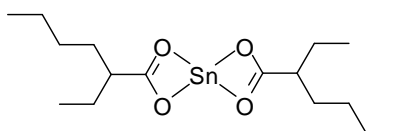
The coordination-insertion mechanism, represented in Scheme 8, involves the catalytic action of metal center and is supposed to be the most common mechanism in ROP of lactide involving organometallic compounds, a result supported by many experimental and theoretical studies. The great advantage of such polymerisation is the possible fine tuning of the steric and electronic properties of the metal centre which in turn would influence the control of the polymerisation process. Indeed, living polymerisation with very good control of M_n and excellent stereoselectivity (for example, heteroselectivity p_r up to 0.98) has been reported using various organometallic complexes. The next section gives more details about the performance of such systems.



Scheme 8. Coordination-insertion ROP of lactide.

4. Initiators for ROP of Lactide

The most widely used complex for industrial preparation of PLA is tin (II) bis(2-ethylhexanoate), commonly referred as tin(II) octanoate $\text{Sn}(\text{Oct})_2$, whose structure is given in Scheme 9.⁸ It is commercially available, easy to handle, and highly active, giving high activity in melt conditions and allows the preparation of PLA with very high molecular weight (up to 10^5 - 10^6 Da). However, the polymers obtained show no stereoselectivity.



Scheme 9. tin(II) octanoate $\text{Sn}(\text{Oct})_2$

Significantly efforts have been placed to the design and synthesis of efficient catalysts for the preparation of polylactide. And despite the existence of some functional catalytic systems, fundamental understanding about the process is still lacking. Thus research has often been draw towards well characterised, discrete systems as these would facilitate the understanding of the factors influencing the efficiency of the catalyst/initiators.

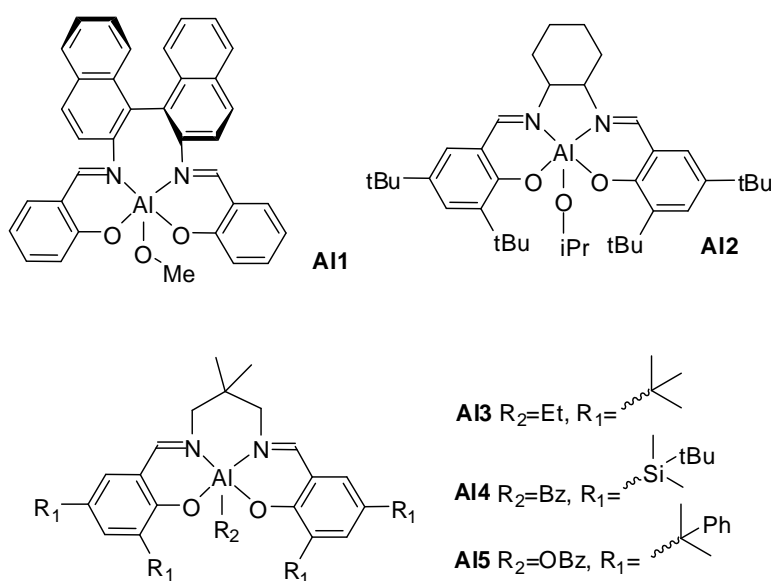
By far the most common organometallic initiators for ROP of LA are amide or alkoxide metal complexes. Almost all earth-alkaline metals, transition metals and rare-earth metals complexes have been tested. The scope of which has been the subjects of several reviews, like the one of Tolman group⁹ in 2001, of Bourissou group¹⁰ in 2004, of Williams group^{1b, 1d} in 2008, or of Feijen group¹¹ in 2011. Of particular interest are metals of group 2 (Ca, Mg) and 12 (Zn) (oxidation state +2), 13 (Al, In) and rare-earth metals (Sc, Y, Nd, etc) (oxidation state +3), or

group 4 (Ti) (oxidation state +4), which are not only commercially viable and non-toxic, but also offer rather high activity and sometimes selectivity.

As salen ligands and derivatives were used in combination with different metals for the ROP of lactide, we were curious to evaluate the performance of phosphasalen complexes in this process. Given the dianionic properties of phosphasalen ligands and common requirement of having an alkoxide/amide group on the complex, we decided to investigate the activities of phosphasalen complexes of yttrium and aluminium. Both these metals are cheap, having non-reported toxicities and their complexes generally offer the best rates or control of polymerations.

4.1. Aluminium Complexes

Although the rate for ROP of aluminium complexes are often lower than other metals, they have been extensively studied as they generally offer very good polymerisation control due to the lack of side reactions (e.g transesterification). More importantly, easily synthesised salen complexes of aluminium are among the most stereoselective initiators for ROP of lactide. In fact, the most important breakthrough in stereoselective polymerisation process was made by Spassky and co-workers. They found that aluminium complex of salen ligand derived from *R*-(+)-1,1'-binaphthyl-2,2'-diamine (Scheme 10, **A11**) initiated the ROP of *rac*-lactide to predominantly isotactic PLA in reasonable time, the polymerisation rate of (*R,R*)-LA being 19 times higher than the one of (*S,S*)-LA.¹²



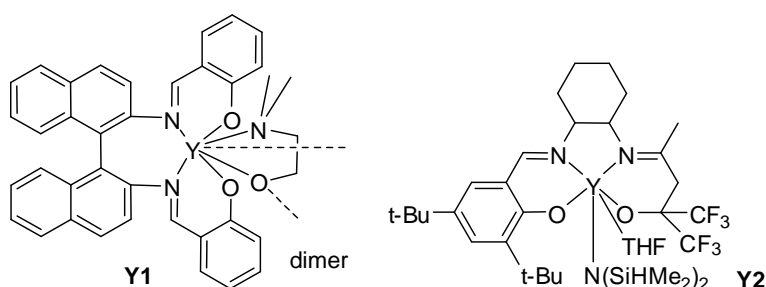
Scheme 10. Aluminium complexes for stereoselective ROP of lactide

This finding started a rapid development in the studies of aluminium complexes of Salen and derivatives, and much has been obtained in terms of stereoselectivity. In a result reported by Feijen and co-workers in 2002, aluminium complex of *rac*-Jacobsen ligand (**A12**, Scheme 10) could initiate and catalyse the formation of stereoblock PLA p_i with $\alpha=0.93$ at 83% conversion of *rac*-lactide.¹³ More interestingly, this excellent stereocontrol is maintained even in bulk

conditions. In 2003, Chen and co-workers reported on the complex **A13**/benzylalcohol (Scheme 10, **A13**) as the catalyst/initiator systems for ROP of rac-lactide which offers a high isoselectivity ($p_i = 0.90$).¹⁴ In 2007, Nomura and co-workers used the aluminium complex of a similar ligand with more bulky substituent $t\text{BuMe}_2\text{Si}$ at the *o*- and *p*- positions of the phenoxide rings (Scheme 10, **A14**), and obtained an excellent isoselectivity of $p_i = 0.98$ with rac-lactide.¹⁵ The complex with Salen ligands featuring bulky cumyl groups (Scheme 10, **A15**) reported by Chen and co-workers in 2012 could initiate the ROP of rac-lactide to give highly isotactic PLA ($p_i = 0.97$) in high conversion (94%) with very narrow PDI (1.07).¹⁶

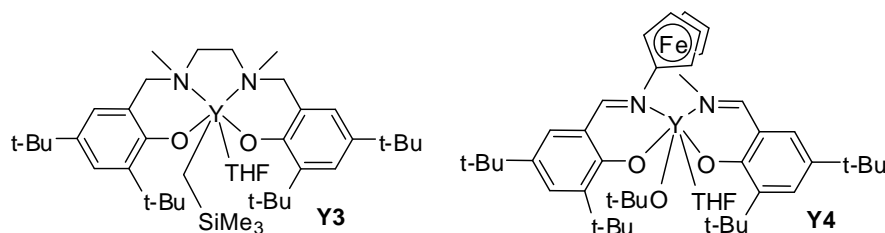
4.2. Yttrium Complexes

Yttrium complexes are particularly promising as they offer very fast rates for ROP of lactide and, through careful selection of the ancillary ligand, can enable stereocontrol. Most of the successful systems employ tetradentate ligands which ensure the stability and prevent redistribution reactions often seen for rare-earth complexes. From this point of view, the use of salen ligands are interesting. Yttrium salen complexes were first investigated nearly a decade ago by Ovitt and Coates, together with the aluminium complex of the same ligand (Scheme 12), for the ROP of meso-lactide. It showed moderate rates but lack polymerization or tacticity control (LA/I=100/1, 14h, 97%).¹⁷ Carpentier and colleagues have also studied alkoxide/phenolate ligands, related to salens, which were slow initiators and produced atactic PLA (LA/I/iPA = 100/1/1, 1d, 91%).¹⁸

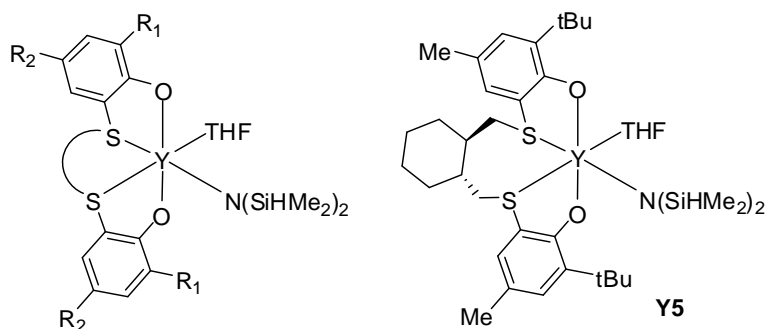


Scheme 11. Yttrium complexes of Salen ligands and derivatives

The activities of yttrium complexes with derivatives of salen ligands have been reported (Scheme 12). The salan complex featured in a report by Cui and co-workers in 2007 afforded PLA with moderate heterotacticity in much higher rate compared to the salen analogues (LA/I=300/1, 1h, 100%, $p_s = 0.65$).¹⁹ Recently, Diaconescu and co-workers have reported a salen derivative with a ferrocenediyl unit in the imine backbone which showed even faster rates, but lacks stereocontrol (LA/I=500/1, 40min, 92%, atactic).²⁰



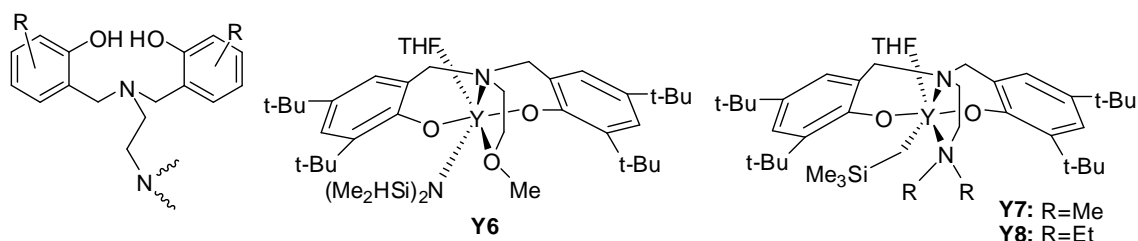
Scheme 12. Yttrium complexes of Salen ligands and derivatives



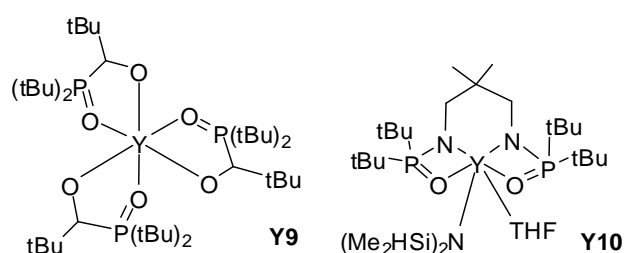
Scheme 13. Yttrium complexes of dithia-alkanediy bridged diphenolate ligands

Okuda has pioneered the use of dithia-alkanediy bridged diphenolate ligands with group 3 metals for the ROP of lactide (Scheme 13). Yttrium complexes of such ligands showed very fast rates and can be used at low initiator concentration (complex **Y5**: LA/I=300/1, 0.75h, 89%, or LA/I=3000/1, 6h, 92%). Some of them showed excellent heteroselectivity via a dynamic monomer recognition process controlled by the inter-conversion of initiator enantiomers ($p_s=0.88$ for the same complex **Y5**).²¹ The complexes also yield highly syndiotactic PLA from *meso*-LA.²²

The most successful ligand systems up to date for the design of catalyst/initiator of the ROP of lactide up to date is tetradentate phenolate-amine ligands (Scheme 14). These compounds were synthesised in single-step Mannich condensation of primary amine, formaldehyde and substituted phenol. Their zirconium/hafnium complexes had given excellent results for olefin polymerisation,²³ as reported by Goldschmidt and coworkers, before Carpentier and co-workers realised the potential of such ligands in ROP of lactide. They reported rare-earth metal complexes of the modified ligands in 2003.²⁴ The yttrium complex (**Y6**, Scheme 14) appeared to be very active in ROP of lactide (LA/I=500/1, 1h, 100%) and afford PLA with high degree of heterotacticity ($p_s=0.80$).²⁵ Eversince, this type of ligands have been studied intensively by the groups of Carpentier, Mountford, and others.²⁶ The complexes studied generally give highly stereocontrolled ROP and offer high rates all in the same time. For yttrium complexes, highly efficient systems with heterotacticity up to 0.99 and high rates have been achieved, for example in the systems reported by Cui and co-workers (LA/I=700/1, 3h, 86%, $p_s=0.99$) (**Y7-8**, Scheme 14).¹⁹



Scheme 14. Tetradentate bis(phenoxy) amine ligands and some notable yttrium complexes.



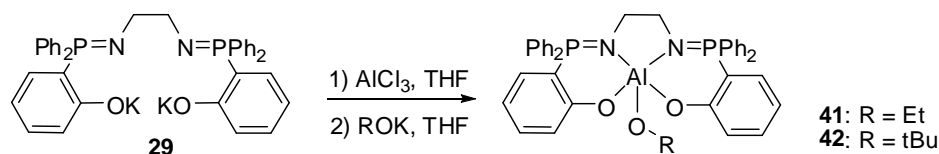
Scheme 15. Notable systems with ligands incorporating phosphinic functions.

Ligands incorporating phosphorus-containing function, such as phosphinic, thiophosphinic has given good results in ROP of lactide. Arnold and co-workers have recently reported an interesting initiating system comprising a racemic mixture of alkoxide-phosphine oxide yttrium complexes, which, in stark contrast of other yttrium systems which give heterotactic PLA, yielded isotactic PLA from *rac*-LA (LA/I=200/1, 10min, 98%, $P_i=0.81$).²⁷ (Y9, Scheme 15). The Williams group prepared yttrium complexes of bis(phosphinic/thiophosphinic)diamido ligands which show very high rates of polymerization and, in some cases, good heteroselectivity ($P_s = 0.85$) (Y10, Scheme 15).²⁸

II. Aluminium-Phosphasalen Complexes.

1. Synthesis

The aluminium phosphasalen complexes were synthesized easily by reaction of the anionic ligand **29** with AlCl_3 in THF, followed by nucleophilic substitution with KOR (R=Et, tBu) (Scheme 16).



Scheme 16. Synthesis of aluminium phosphasalen complexes

The addition of AlCl_3 into a solution of the phosphasalen ligand in THF at room temperature quickly gives a white suspension after 10 minutes of stirring at room temperature. In $^{31}\text{P}\{^1\text{H}\}$ NMR spectrum, the signal of free ligand at +18.6 ppm has disappeared. Although the precipitation of the product prevents its characterization, the total disappearance of the ligand suggested that the product is the phosphasalen aluminum chloride complex **40**.

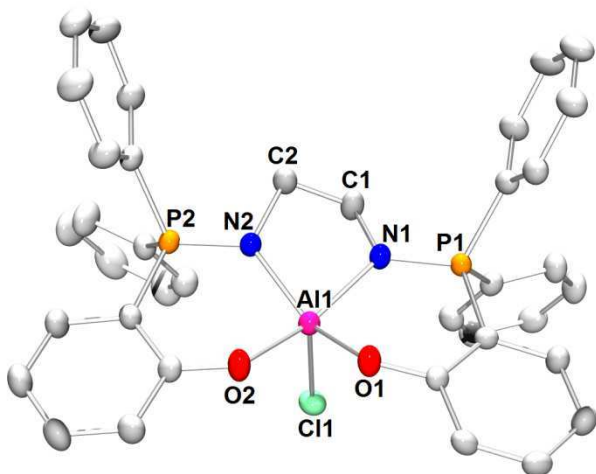


Figure 3. ORTEP view of complex **40**. Solvent molecules and hydrogen atoms have been omitted for clarity. Thermal ellipsoids drawn at the 50% probability level. Selected distances (\AA) and angles ($^\circ$): Al1-Cl1 2.228(1), Al1-O1 1.804(2), Al1-O2 1.817(2), Al1-N1 1.982(2), Al1-N2 1.940(2), N1-P1 1.600(2), N2-P2 1.609(2), O1-Al1-O2 85.86(8), O1-Al1-N1 91.1(1), O2-Al1-N2 91.94(8), N1-Al1-N1 81.64(8), Cl1-Al1-O1 104.02(6), Cl1-Cl1-N2 107.70(7), Cl1-Al1-O2 98.80(7), Cl1-Al1-N1 98.60(7), O1-Cl1-N2-Al1 -1.68, O2-Cl1-N1-Al1 0.72.

Indeed, if stirring was turned off after 2 minutes, crystals of the product was obtained from the solution. X-ray diffraction experiment carried out on these crystals showed clearly the structure of phosphasalen aluminum chloride complex (Figure 3).

The complex crystallized with one molecule of THF, which lies far from the aluminum center and thus no THF coordination was observed. The metal center adopted a distorted square-based pyramidal geometry with the phosphasalen ligand being in *trans*-configuration.

Addition of one equiv. of ROK (R=Et or tBu) into the in situ generated suspension of complex **40** in THF induced slowly the dissolution of the precipitate and yielded a cloudy solution after overnight stirring. $^{31}\text{P}\{^1\text{H}\}$ -NMR spectrum of the solution showed a unique singlet at +35.2 ppm for R=Et, or at +34.8 for R=tBu, indicating the clean formation of a phosphasalen complex. After removal of insoluble potassium salt, aluminum phosphasalen alkoxide complexes **41** and **42** were obtained as ivory solid. Crystals suitable for X-ray diffraction of these compounds were obtained from a saturated solution of **41** (or **42**) in toluene at -40°C .

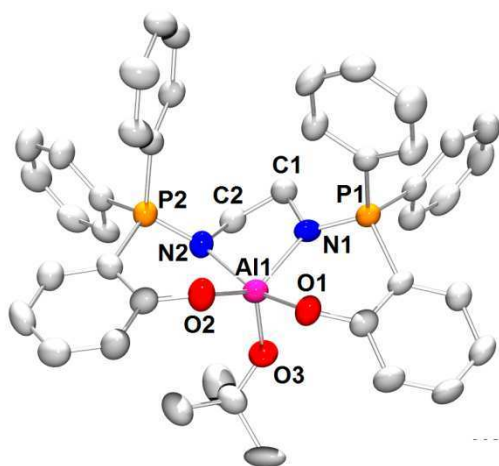


Figure 4. ORTEP view of complex **41**. Hydrogen atoms have been omitted for clarity. Thermal ellipsoids drawn at the 50% probability level. Selected distances (Å) and angles (°): Al1-O3 1.733(4), Al1-O1 1.861(4), Al1-O2 1.827(4), Al1-N1 1.973(4), Al1-N2 2.019(4), N1-P1 1.602(4), N2-P2 1.591(4), O1-Al1-O2 83.9(2), O1-Al1-N1 90.3(2), O2-Al1-N2 89.7(2), N1-Al1-N2 81.3(2), O3-Al1-O1 99.5(2), O3-C11-N2 100.2(2), O3-Al1-O2 117.6(2), O3-Al1-N1 106.4(2), O1-O3-N2-Al1 -2.01, O2-O3-N1-Al1 0.67.

Both complexes adopted distorted square-based pyramidal geometry, with the metal center placed slightly out of the medial plane formed by O2N2 atoms of the phosphasalen ligand. The Al-O_{alkoxide} bonds are slightly shorter than Al-O_{phenoxide} bonds (1.733(4) vs. 1.861(4) and 1.827(4) in **41**, and 1.756(4) vs. 1.853(3) and 1.792(4) in **42**), which results from the better electron donating ability of alkoxides.

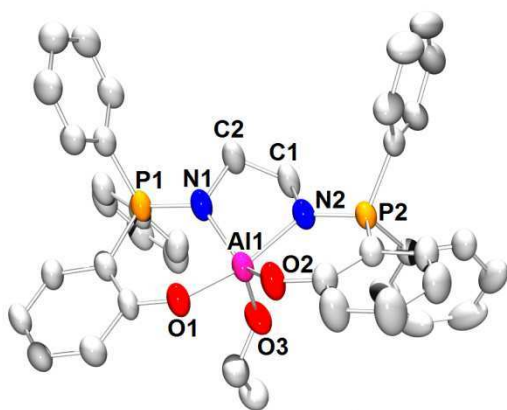


Figure 5. ORTEP view of complex **42**. Hydrogen atoms have been omitted for clarity. Thermal ellipsoids are drawn at the 50% probability level. Selected distances (Å) and angles (°): Al1-O3 1.756(4), Al1-O1 1.853(3), Al1-O2 1.792(4), Al1-N1 1.948(4), Al1-N2 1.991(4), N1-P1 1.597(4), N2-P2 1.586(4), O1-Al1-O2 85.7(2), O1-Al1-N1 90.8(2), O2-Al1-N2 91.3(2), N1-Al1-N2 81.1(2), O3-Al1-O1 99.7(2), O3-Al1-N2 94.9(2), O3-Al1-O2 115.2(2), O3-Al1-N1 108.8(2), O1-O3-N2-Al1 2.33, O2-O3-N1-Al1 -2.30.

2. Catalytic Activities in ROP of Lactide

Both complexes **41** and **42** have been tested as initiators for the ROP of lactide. The choice of solvent is important, as both complexes decompose in dichloromethane and polymerization in THF were extremely slow. The best results have been obtained in toluene at high temperature.

Table 2. Activities of aluminum complexes

Initiator (I)	[LA] ₀ : [I]	T (°C)	Time / d	Conversion/%	P _i
41	100:1	80	1	73	atactic
42	100:1	80	1	70	atactic
rac-Al2 ^{13a}	62:1	70	12	85	0.93
(R,R)-Al2 ^{13a}	62:1	70	24	87.8	-
Al3 ¹⁴	122:1:1 ^{a)}	70	0.42	83.6	0.89
Al4 ¹⁵	100/1/1 ^{b)}	70	0.79	62	0.97
Al5 ¹⁶	100/1	70	0.5	94	0.97

^a presence of isopropanol LA/I/iPA=122/1/1, ^b presence of BzOH LA/I/BzOH=100/1/1,

Both complexes **41** and **42** are active in ROP of lactide. With the loading LA/I=100/1, in toluene at 80°C, initiator **41** gave 73% of conversion after 24h, and initiator **42** gave 70% of conversion after the same duration. These results are comparable with other aluminum initiators. Table 2 presents the performance of **41**, **42** and different initiators in the literature.

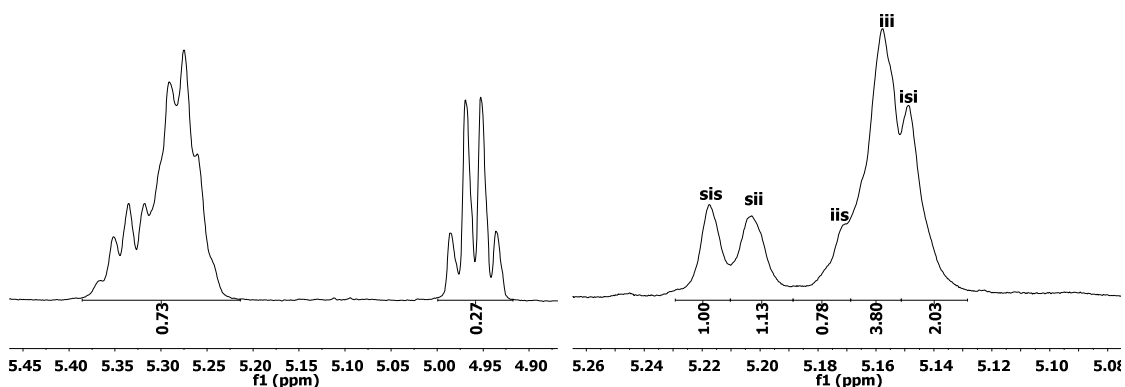
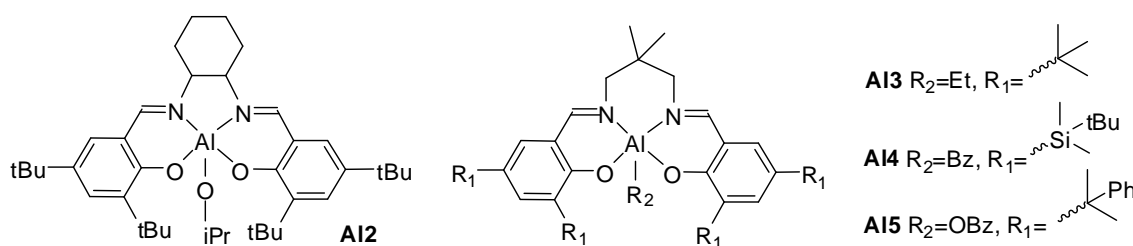


Figure 6. ¹H} and ¹H{¹H} NMR spectrum of PLA in CDCl₃. [LA]₀ = 1M, [41] = 0.01M, toluene, 80 °C, 73 % conversion of rac-LA, atactic

The polymers obtained from **41** and **42** are predominantly atactic, regardless of the conversion. For an example, the methane regions in ¹H} and ¹H{¹H} NMR spectrum of PLA obtained from polymerization with **41** were presented in Figure 6. The poor control in stereochemistry might

probably due to a larger and more flexible phosphasalen ligand, which leaves an important space around the metal center and thus limits the stereocontrol by chain-end configuration.

As the performance in terms of catalytic activity of aluminum complexes are far behind the yttrium phosphasalen complexes (details of which would be presented in the next section), most of the work was focused in the study of yttrium complexes. Though these preliminary tests for ROP of lactide with aluminum complexes do not give good results in terms of stereoselectivity, further modifications brought to the phosphasalen ligands could improve the stereocontrol of ROP of lactide with these initiators. For example, all the examples of aluminum complexes presenting high stereoselectivity are based on very bulky systems (**A2-5**, Scheme 17), which reduce the space around the metal centre and improve the stereocontrol, and thus future work on aluminum phosphasalen complexes for ROP of lactide could be directed in this direction.



Scheme 17. Highly stereoselective aluminum complexes

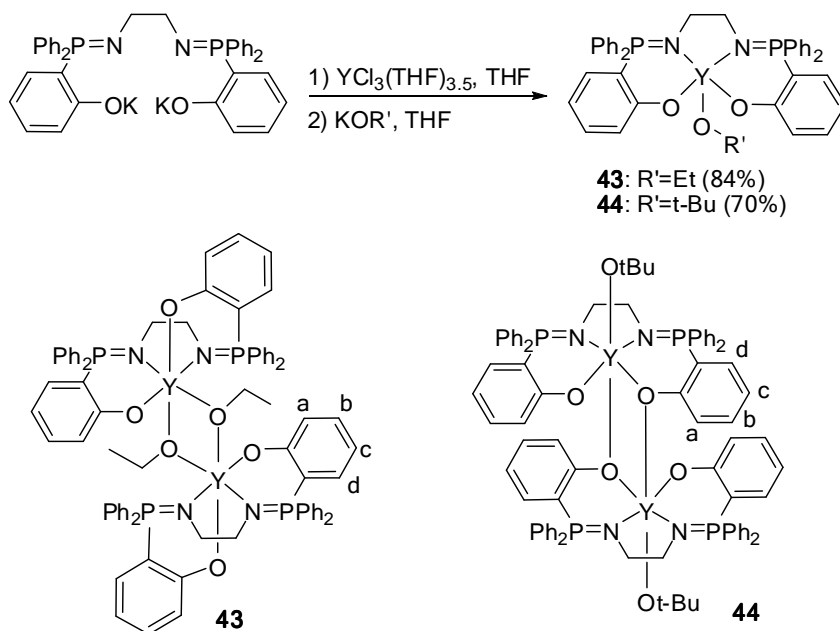
III. Yttrium Phosphasalen Complexes: First Study

1. Synthesis

The synthesis of the anionic phosphasalen ligand **29** has already been reported in chapter 3. Reaction of ligand **29** with $[YCl_3(THF)_{3,5}]$ in tetrahydrofuran resulted in the immediate precipitation of a white product. The $^{31}P\{^1H\}$ NMR spectrum showed the complete consumption of ligand, as evidenced by the disappearance of the signal at 18.6 ppm. The total insolubility of the product prevented any further analysis; the product is believed to be a cluster/polymer of the ligand-yttrium-chloride. A similar effect has been observed by Diaconescu and co-workers using related yttrium chloride Schiff base complexes.^{29, 20} Furthermore, the apparition of an insoluble phosphasalen chloride complex has already happened in the case of aluminum, as has been shown in the previous section.

Despite the insolubility of the product, the addition of an equivalent of potassium *tert*-butoxide/ethoxide into the reaction mixture induced a slow dissolution. The $^{31}P\{^1H\}$ NMR spectrum of the solution presented a single signal, at significantly lower field compared to the dianionic ligand, indicating the coordination of the phosphasalen ligand to the yttrium center. After removal of the potassium salt, the ethoxide and *tert*-butoxide phosphasalen-yttrium

complexes (complexes **43** and **44**, respectively) were isolated as white solids, which were characterized by multinuclear NMR spectroscopy, elemental analyses and using single crystal X-ray diffraction experiments.



Scheme 18. Synthesis of yttrium complexes with unsubstituted phosphasalen ligand.

Both complexes **43** and **44** adopt a dimeric structure in the solid state, with the yttrium centers exhibiting a distorted octahedral geometry formed by the tetradentate phosphasalen ligand, the alkoxide group and a phenoxide/alkoxide bridge. Both dimers are symmetric: there is no difference between the two yttrium centers in either complex, thus all the selected bond lengths and angles are represented for only one yttrium center.

In complex **43**, the ethoxide groups bridge between the two metal centers, forming a $[Y_2O_2]$ four membered ring. The phosphasalen ligand is in *cis*- β configuration: one phenoxide (O2) and one bridging ethoxide group (O3#2) occupy the axial positions. The yttrium center and the other four coordinated atoms (O1, N1, N2, O3) are almost in the same plan (dihedral angle (O1, N1, N2, O3)=1.52(22) Å, (Y, N1, O1, O3)=0.11(25)) Å. The yttrium-phenoxide (Y-O2) bond in axial position is slightly longer than the one in the equatorial position (Y-O1) (2.213(3) Å vs 2.182(3) Å), whereas the Y-ethoxide (Y-O3#2) bond in the axial position is slightly shorter than the one in the equatorial position (Y-O3) (2.243(3) Å vs 2.273(3) Å). The two yttrium-alkoxide bonds are all longer than the yttrium-phenoxide bonds (2.243(3) Å and 2.273(3) Å vs 2.182(3) Å and 2.213(3) Å), probably because they are in bridging positions.

There is almost no difference concerning the bond lengths of Y-N1 and Y-N2, or N1-P1 and N2-P2, respectively, but the distance Y-P1 is significantly longer than Y-P2 (3.561(1) Å vs 3.414(1) Å), and the Y-N1-P1 angle is larger than Y-N2-P2 (123.81(17) vs 114.05(17)). These differences clearly shows that the two phosphorus atoms are in slightly different environments,

which is also in accordance with the fact that they are linked to two phenoxide groups in different environment (axial or equatorial positions).

As a consequent, $^{31}\text{P}\{^1\text{H}\}$ -NMR spectrum of the complex **43** in THF, recorded in a Av500, exhibits two signals very close to each other, of equal intensity. These two signals were not separated and merged into a broad signal in an NMR-spectrum recorded by an Av300 instrument.

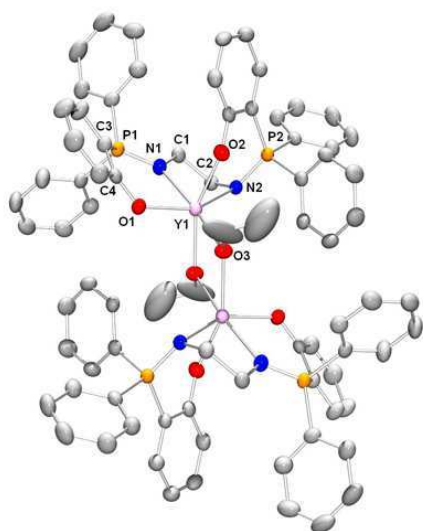


Figure 7. ORTEP view of complex **43** with thermal ellipsoids drawn at the 50% probability level. Hydrogens are omitted for clarity. Selected bond lengths (Å) and angles (deg): Y1-Y1#2 = 3.6492(7), Y1-O1 2.182(3), Y1-O2 2.213(3), Y1-O3 2.273(3), Y1-O3#2 2.243(3), Y1-N1 2.415(3), Y1-N2 2.438(3), P1-N1 1.598(3), P2-N2 1.595(3), O1-Y1-N1 78.8(1), O2-Y1-N1 90.5(1), N1-Y1-N2 70.4(1), N2-Y1-O2 81.4(1), O1-Y1-O2 97.1(1), O2-Y1-O3 90.6(1), O2-Y1-O3#2 156.1(1), N1-Y1-N2-O2 86.40(11), O1-Y1-N2-N1 4.05(25).

Complex **44** is also a dimer in the solid state, however, changing the alkoxide co-ligand from ethoxide to *tert*-butoxide changes the structure of the complex (Figure 8). The two yttrium centers remain in distorted octahedral geometries, but the *tert*-butoxide ligands now occupy the axial positions, presumably due to steric hindrance preventing them adopting bridging coordination modes. The complex adopts a *trans*-coordination geometry with a single μ -phenoxide coordination mode, per ligand. The Y-N and P-N bond lengths are comparable with those in complex **43**, but the Y-O(μ -phenoxide) bond is longer (2.338(2) Å vs 2.203(3) Å in **43**) and the Y-O(alkoxide) bond is significantly shorter (2.079(3) Å vs 2.243(3) Å in **43**).

Although the two phenoxide oxygen atoms adopt different coordination modes, the two phosphorus atoms are in almost identical environments, as shown by close similarity in the P-Y distances (3.490(1) Å vs 3.507(1) Å) and the P-N-Y bond angles ($121.55(18)^\circ$ vs $122.48(18)^\circ$). Indeed, in the $^{31}\text{P}\{^1\text{H}\}$ -NMR spectrum of complex **44**, in THF, only a single doublet is observed, due to the coupling with the yttrium center. The value of the coupling constant ($^2J_{\text{YP}} =$

3.4 Hz) is comparable with other reported values for ${}^2J_{\text{YP}}$ in similar complexes.^{28a-c, 28e} This provides some indication that the solid state structure may be maintained in solution

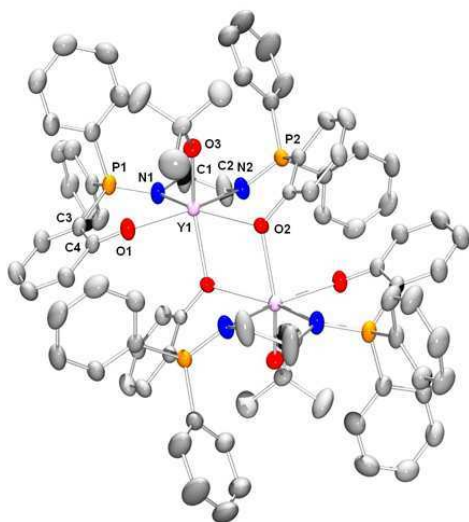


Figure 8. ORTEP view of the solid state structure of complex **44**, with thermal ellipsoids drawn at the 50% probability level. Hydrogen atoms are omitted for clarity. Selected bond lengths (Å) and angles (deg): Y1-O1 2.203(3), Y1-O2 2.338(2), Y1-O3 2.079(3), Y1-O2#2 2.312(2), Y1-N1 2.398(3), Y2-N2 2.372(3), P1-N1 1.596(3), P2-N2 1.586(3), O1-Y1-N1 78.6(1), O2-Y1-N1 143.7(1), N1-Y1-N2 70.4(1), N2-Y1-O2 74.9(1), O1-Y1-O2 133.0(1), O2-Y1-O3 89.2(1), O2#2-Y1-O3 148.8(1), Y1-O2-N2-N1 9.39(24), Y1-O1-N1-N2 6.29(26); O1-N1-Y1-O3 88.49(11), O1-N1-Y1-O2#2 82.27(10).

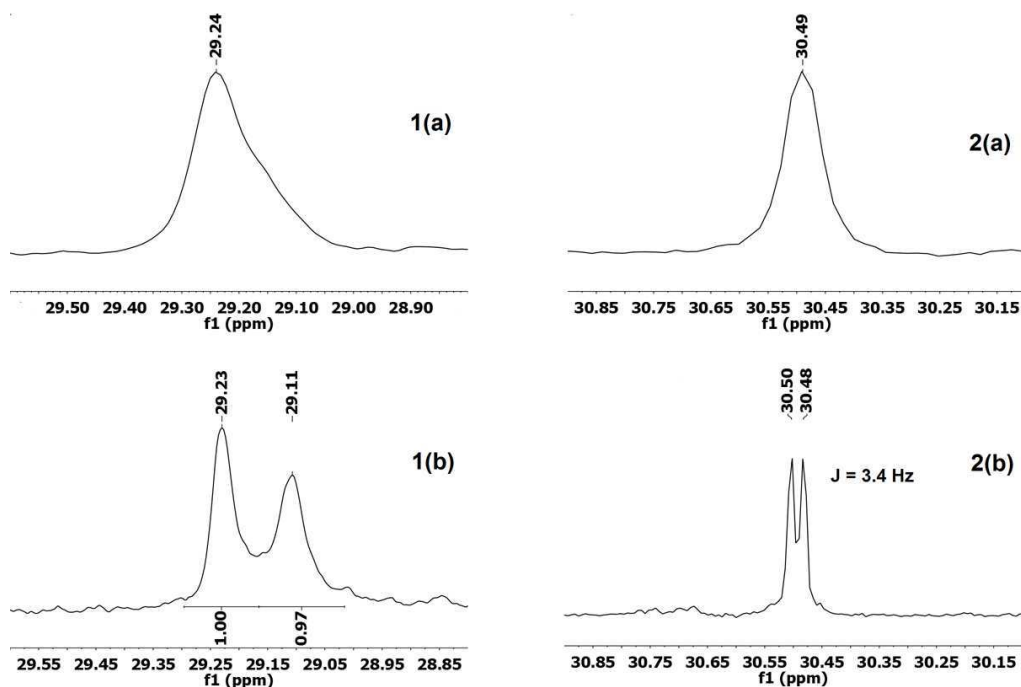
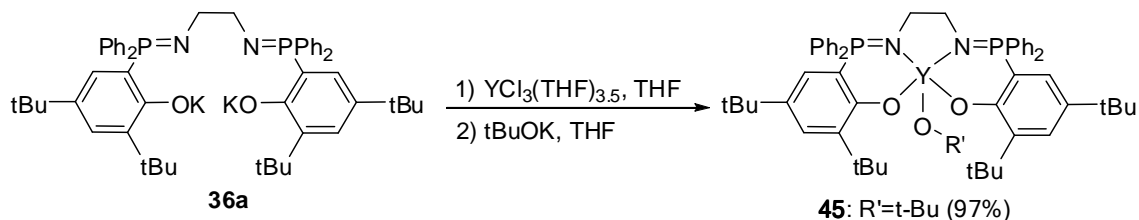


Figure 9. ${}^{31}\text{P}\{^1\text{H}\}$ -NMR spectra of complexes **43** and **44**, recorded in THF on a (a) 300 MHz (b) 500 MHz instrument.

Complex **45** was prepared from the phosphasalen ligand **36a** with sterically hindered *tert*-butyl substituents on the phenoxide ring and with a *tert*-butyl alkoxide co-ligand (Scheme 19). This ligand was deliberately targeted so as to prevent dimerization and enable isolation of a mononuclear yttrium alkoxide complex. Its synthesis was reported in chapter 4.



Scheme 19. Synthesis of the yttrium complex **45**.

Addition of $[\text{YCl}_3(\text{THF})_{3.5}]$ into a solution of ligand **36a** in tetrahydrofuran resulted in a cloudy solution. $^{31}\text{P}\{^1\text{H}\}$ NMR spectrum showed the complete disappearance of the free ligand signal at +20.6 ppm, and the apparition of a unique singlet at lower field (+31.0 ppm). This suggested the clean formation of a phosphasalen yttrium complex. One equiv. of potassium *tert*-butoxide was added into the solution and stirring was continued for 7h. After removal of insoluble potassium salt, THF was evaporated, giving the product as a viscous oil, which turned into an ivory solid after several days of storing at room temperature.

The $^{31}\text{P}\{^1\text{H}\}$ NMR spectrum, in THF, showed a single doublet, at 31.6 ppm, with a coupling constant of 3.0 Hz, suggesting that complex **45** adopts a *trans*-configuration, in a manner analogous to complex **44**. On examination of the NMR spectra of complexes **44** and **45** some clear differences were observed. In particular, the $^{13}\text{C}\{^1\text{H}\}$ NMR spectra showed that the quaternary phenolate carbon atoms are equivalent in the spectrum of compound **45**, whereas they are different in the case of compound **44** (and compound **43**), giving rise to two doublets, likely due to the bridging and non-bridging coordination modes of the phenolate. This supported the notion that complex **45** has a mononuclear structure.

Definitive evidence concerning the structure of complex **45** was obtained by X-ray diffraction analysis of monocrystals grown from a saturated solution of **5** in cyclohexane (Figure 10). The complex adopts square based pyramidal geometry, with the four coordinating atoms of the phosphasalen ligands forming the basal plane, as shown by the dihedral angle O1-N1-N2-O2 (4.13(0.11)). The yttrium center is slightly out of the medial plane of these four atoms (0.7472 (0.0011) Å). The angle at O3 atom is close to 180°, which probably results from the steric hindrance of the phosphasalen ligand in the basal plane. All the yttrium-nitrogen and yttrium-oxygen bonds in complex **45** are slightly shorter compared to the corresponding values in complex **43** and **44**, probably as a result of the penta-coordination mode.

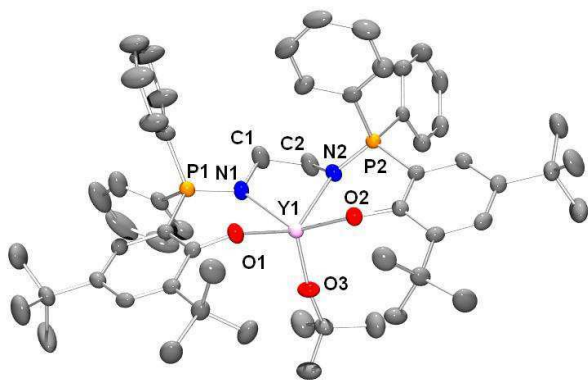


Figure 10. ORTEP view of the solid state structure of complex **45**, with thermal ellipsoids drawn at the 50% probability level. Hydrogen atoms are omitted for clarity. Selected bond lengths (Å) and angles (deg): Y1-O1 2.1671(318), Y1-O2 2.1704(18), Y1-O3 2.025(2), Y1-N1 2.375(2), Y2-N2 2.324(2), P1-N1 1.595(2), P2-N2 1.584(2), O1-Y1-N1 80.51(7), O2-Y1-N1 139.87(8), N1-Y1-N2 71.78(8), N2-Y1-O2 79.68(7), O1-Y1-O2 102.03(7), O2-Y1-O3 109.16(8), O1-Y1-O3 115.03(8), C55-O3-Y1 171.40 (19), O1-N1-N2-O2 4.13(0.11), O1-N1-N2-Y1 25.13(0.10)

2. Catalytic Activities and Kinetics Studies

2.1 Overall

All three complexes were highly active initiators for the ring opening polymerization (ROP) of lactide. The selection of the polymerization solvent was critical, with initiator decomposition occurring in methylene chloride and the partial solubility of lactide in toluene (at ambient temperature) leading to heterogeneous polymerization, albeit extremely rapidly. The optimum solvent for use at ambient temperature (25 °C) was THF; all experiments were conducted using an initial concentration of lactide of 1 M, so as to enable accurate comparison between the different initiators and additives.

Table 3. Data for the ROP of lactide using yttrium initiators **43-45** $[LA]_0 = 1$ M.

Initiator	$[LA]_0:[I]$	Time / s	Conversion ^{a)} / %	$M_n(\text{calc})^b)$ / kg mol ⁻¹	$M_n(\text{exp})^c)$ / kg mol ⁻¹	PDI ^{c)}	$P_s^d)$	$k_{obs}^e)$
43	200:1	3360 (56 min)	90	25.9	27.1	1.36	0.78	0.0031 ^{d)}
44	200:1	40	91	26.2	57.6	1.42	0.78	0.2522 ^{d)}
44	200:1	5	98	28.8	64.6 ^{l)}	1.20 ^{l)}	0.86 ^{m)}	
45	1000:1	45	97	140	223	1.34	0.86	0.0799 ^{g)}

45^{h)}	1000:1:1	70	80	115	105	1.08	0.90	-
45ⁱ⁾	1000:1	120 ^{l)}	99	144	332	1.31	0.87	-
45^{j)}	2000:1	10 min ^{l)}	99	288	330	1.35	0.87	-
45^{k)}	5000:1	30 min ^{l)}	98	720	700	1.23	0.88	-

^a Conversions were determined from the ¹H NMR spectra (CDCl₃) of the crude products, by integration of the methine resonance assigned to LA ($\delta=4.92$ ppm) and to PLA ($\delta=5.00-5.30$ ppm).

^b $M_n(\text{calc}) = 144 \times [\text{LA}]_0 / [\text{I}] \times \% \text{ conversion LA}$.

^c $M_n(\text{exp})$ was determined using GPC, in THF, using multi-angle laser light scattering (GPC-MALLS) according to the method described earlier.^{28a, b} The polydispersity index was also determined from GPC, $\text{PDI} = M_w / M_n$.

^d P_s is the probability of racemic linkages between monomer units and is determined by comparison of the integrals of tetrads in the homonuclear decoupled ¹H NMR spectrum with those calculated using Bernoullian statistics, according to the method described by Coudane *et al.*^{3a}

^e Determined from the gradients of the $\ln\{[\text{LA}]_0 / [\text{LA}]_t\}$ (for first-order reaction) or $1/[\text{LA}]_t$ (for second-order reaction) versus time plots

^f expressed in $\text{M}^{-1}\text{s}^{-1}$. The reaction is second-order in lactide.

^g expressed in s^{-1} . The reaction is first order in lactide, $[\text{I}] = 1 \text{ mM}$.

^h isopropanol was added, $[\text{LA}]/[\text{I}]/[\text{iPA}] = 1000/1/1$

ⁱ A reaction using unpurified lactide.

^j Slurry of 2 mmol lactide in 1 mL THF at 25 °C.

^k Slurry of 5 mmol lactide in 1 mL THF at 25 °C.

^l Reaction time unoptimized.

^m This experiment showed a rapid increase of PDI and decrease of P_s , over time.

The catalytic activities of the dimeric complexes differ markedly from the ones of the monomeric complex. Studies of their catalytic behaviors are presented separately below.

2.2 Catalytic Activities and Kinetics Studies: Dimeric Complexes

2.2.1 Complex 43

The polymerizations using **43** were analyzed by taking aliquots throughout the polymerizations. They were well controlled, as shown by the linear evolution in the molecular weight with conversion and the narrow PDI for the PLA (Figure 11). In general, there was a good agreement between $M_n(\text{calc})$ and $M_n(\text{exp})$, suggesting that both alkoxide groups in the dimer initiate the polymerisation.

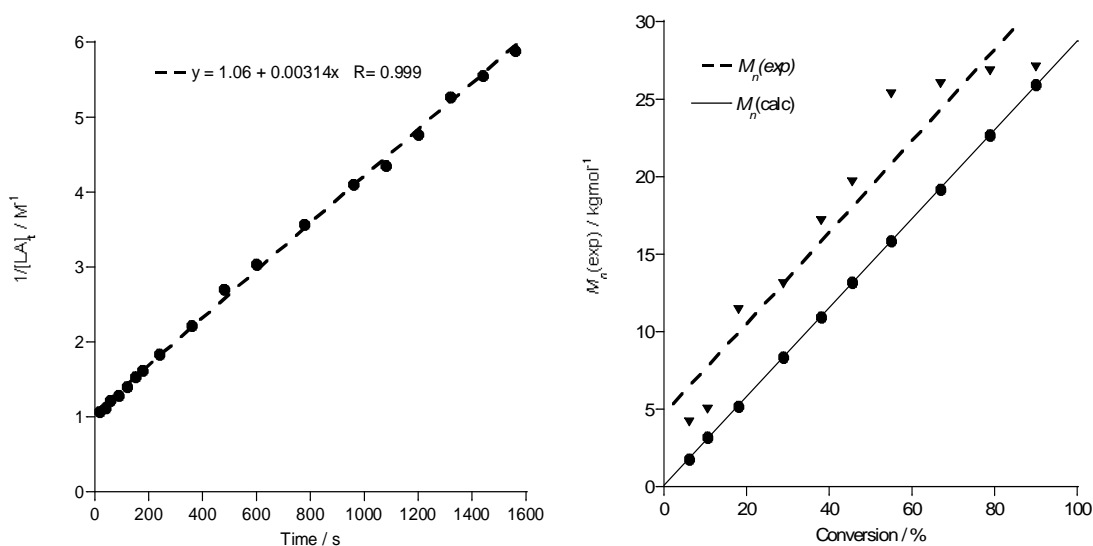


Figure 11. (Left) Plot illustrating $1/[LA]_t$ (M^{-1}) versus time (s) for LA ROP using **43**. (Right) Plot showing the evolution of experimental M_n ($kgmol^{-1}$) vs. conversion (%) for LA ROP using initiator **43**. Polymerization conditions: $[LA]_0 = 1 M$, $[43] = 5 mM$, THF, 25 °C.

For a polymerization initiated and catalysed by an initiator, the rate law can be expressed according to the equation below:

$$\frac{-d[LA]_t}{dt} = k_p [LA]_t^m [I]_t^n \quad (\text{Equation 1})$$

Where $[LA]$: concentration of the lactide ($mol.L^{-1}$), $[I]$: concentration of the initiator ($mol.L^{-1}$), m : order of the reaction on Lactide, n : order of the reaction in initiator, k_p : rate constant of the reaction ($s^{-1} \cdot mol^{-(n+m-1)} \cdot L^{(n+m-1)}$).

Lactide polymerization often follows a first-order in substrate. Curiously the polymerisations with **43** as initiator showed a second order dependence on the concentration of lactide. The plots of $\ln\{[LA]_0/[LA]_t\}$ versus time did not show a linear fit to the data, indicating the reaction was not first order in lactide concentration. In contrast, a plot of $1/[LA]_t$ versus time showed a good linear fit (Figure 11), the y-axis intercept ($t = 0$ s) corresponds well with the starting concentration of lactide (1 M). This indicates a second order dependence on lactide concentration, an unusual finding in this type of polymerisation catalysis. There are only a few other examples of such second order dependence, including a dinuclear Salen-magnesium complex³⁰ and trinuclear zinc- β -diketiminato complex.³¹ Delbridge also observed a second order dependence using lanthanide amide initiators of the type $[L_2LnN(SiMe_3)_2]$, they attributed this to initiation from both the amide and the ancillary ligand, L.³²

The end group of the polymers were analysed by mass spectroscopy using MALDI (Matrix-Assisted Laser Desorption/Ionisation) technique, a soft ionisation one that is often used for the analysis of macromolecules that are often fragile and tend to fragment with other conventional

ionization techniques (Figure 12). A solution containing the matrix (which is a specific crystallisable molecule) and the analyte is spotted on the sample plate. Solvent was evaporated and laser beam is fired at the recrystallised matrix/analyte. The clusters ejected from the surface consists of analyte molecules surrounded by matrix and salt ions. The matrix molecules evaporate away from the clusters to leave the free analyte in the gas-phase. The photo-excited matrix molecules are stabilised through proton/cation transfer to the analyte. It is in this way that the characteristic $[M+X]^+$ ($X = H, Na, K$ etc.) analyte ions are formed, which would then be detected using a mass spectrometer (normally time-of-flight mass spectrometer, hence the notation MALDI-ToF).

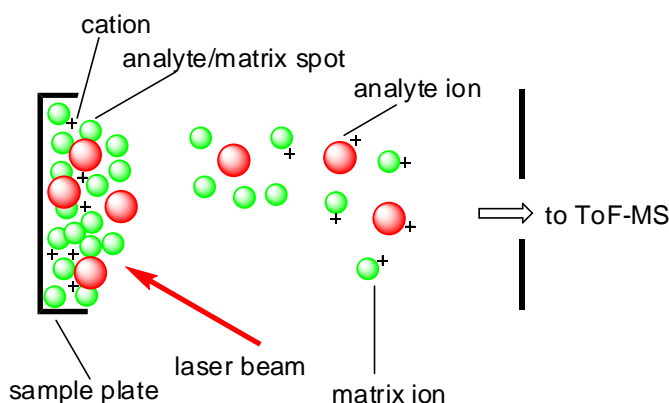


Figure 12. MALDI technique.

The MALDI-ToF spectrum on a sample of polymers obtained from the polymerization with complex **43**, using a dithranol matrix with potassium trifluoroacetate as the cationising agent, showed that all polymers have OEt endgroups (Figure 13). This suggests that the polymerization follows a traditional coordination-insertion mechanism (Scheme 8).

The detailed mechanism of the ROP initiated with **43** is however still non-elucidated, especially the second-order in lactide. This probably have some relation with the dimeric structure of the initiator. A mechanism could be proposed to explain the observations on M_n , kinetic data and end-group analysis. But much data would be needed to put more life into such mechanism. Due to the relatively low activity of complex **3** compared to **44** and **45**, no further investigation was pursued.

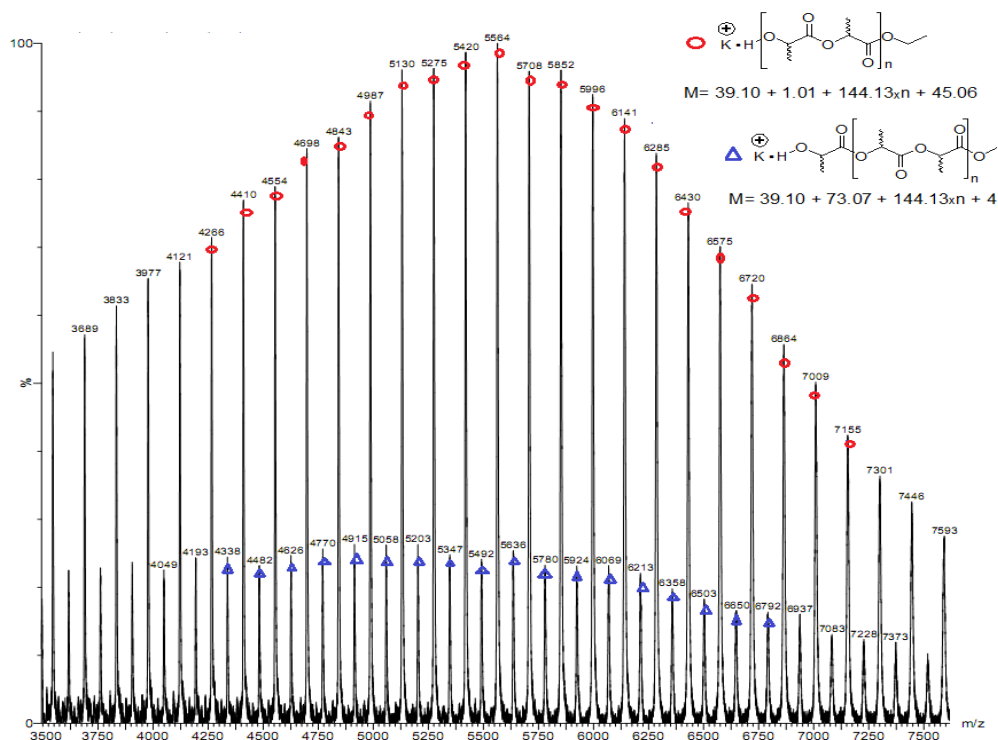


Figure 13. Selected area of the MALDI-ToF mass spectrum of PLA, synthesised by ROP using **43** in THF. Polymerisation conditions: $[LA]_0 = 1\text{ M}$, $[43]_0 = 5\text{ mM}$, reaction stopped at $t=50\text{ s}$ to obtained PLA with $M_n \sim 6\text{ kg mol}^{-1}$ (calculated first from kinetic plots). The MALDI-ToF conditions were using a dithranol matrix, in dichloromethane at a loading of 1:5, with potassium trifluoroacetate as the cationising agent.

2.2.2 Complex 44

The relative high rate of reactions with complex **44** allows studying kinetics of the reactions with different catalytic loading. Thus a full analysis of the kinetics for polymerizations was undertaken for polymerization with this initiator: first k_{obs} was determined from each polymerization run with a known concentration of initiator $[I]_0$, then plot of k_{obs} vs. $[I]_0$ was analysed in order to determined the order in initiator and k_p . (equation 1 and 2).

$$\frac{-d[LA]_t}{dt} = k_p [LA]_t^m [I]_t^n \quad (\text{Equation 1})$$

$$k_{\text{obs}} = k_p [I]_t^n \quad (\text{Equation 2})$$

This species showed a complex kinetic behavior, with a second order dependence in lactide concentration (Figure 14), just like the case with complex **43**, and a third order dependence on yttrium concentration (Figure 15). Such data are indicative of substantial aggregation occurring under the conditions of the catalysis and underscore the importance of the phosphasalen ancillary ligand structure.

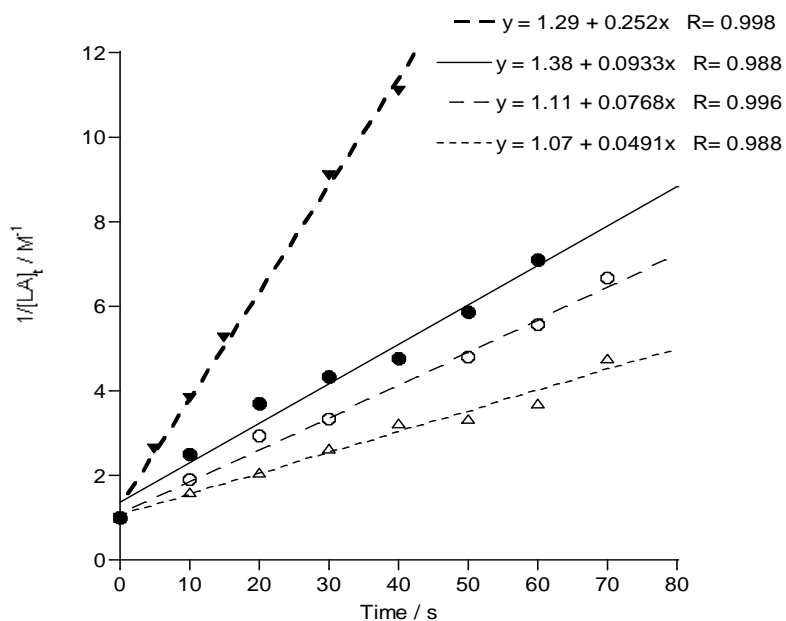


Figure 14. Plot showing $1/[LA]_t$ (M^{-1}) versus time (s) for LA ROP using **44** over the concentration range 2.5-5 mM. Polymerization conditions: $[LA]_0 = 1$ M, THF, 25 °C, $[4] = 5$ mM (filled triangles, $k_{obs} = 0.252$ $M^{-1}s^{-1}$); $[44] = 3.3$ mM (filled circles, $k_{obs} = 0.0933$ $M^{-1}s^{-1}$); $[44] = 2.9$ mM (open circles, $k_{obs} = 0.0768$ $M^{-1}s^{-1}$); $[44] = 2.5$ mM (open triangles, $k_{obs} = 0.0491$ $M^{-1}s^{-1}$).

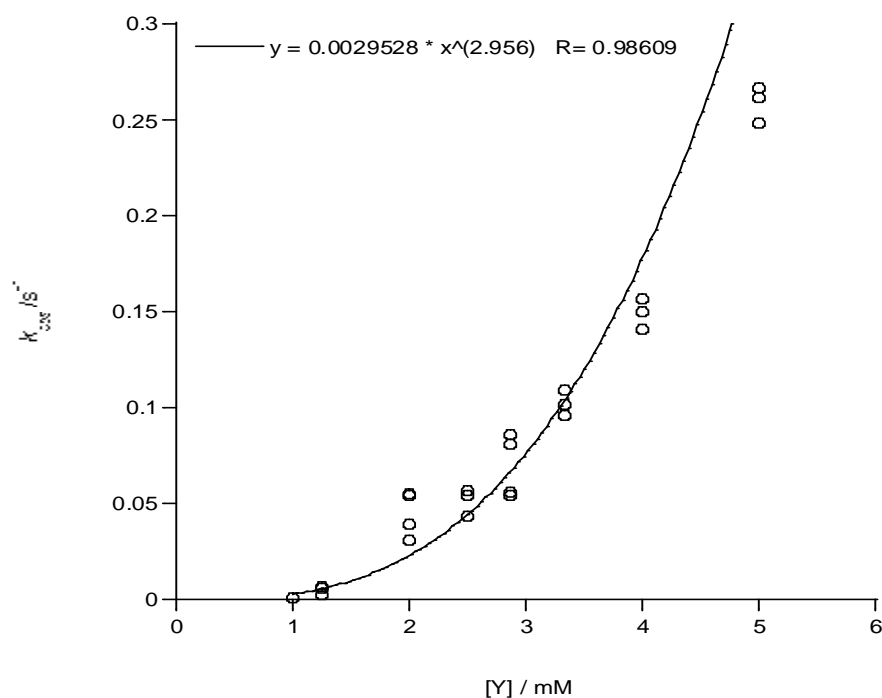


Figure 15. Plot of k_{obs} versus $[Y]$, polymerization conditions; $[LA]_0 = 1$ M, THF, 25 °C, $[44] = 1$ -5 mM.

MALDI-ToF spectrum done on polymers sample obtained from polymerisation with **44** showed that these molecules all have tBuO- endgroup, which is indicative of a coordination-insertion mechanism (Figure 16). At the difference from polymerization with **43**, where $M_n(\text{exp})$ fit with $M_n(\text{calc})$, suggesting that both the ethoxides in the dimer initiate the ROP, for complex **44**, the $M_n(\text{exp})$ values were approximately double the $M_n(\text{calc.})$ (Figure 17). This indicates that only half the alkoxide groups initiate, consistent with only a single site in the dinuclear complex being active.

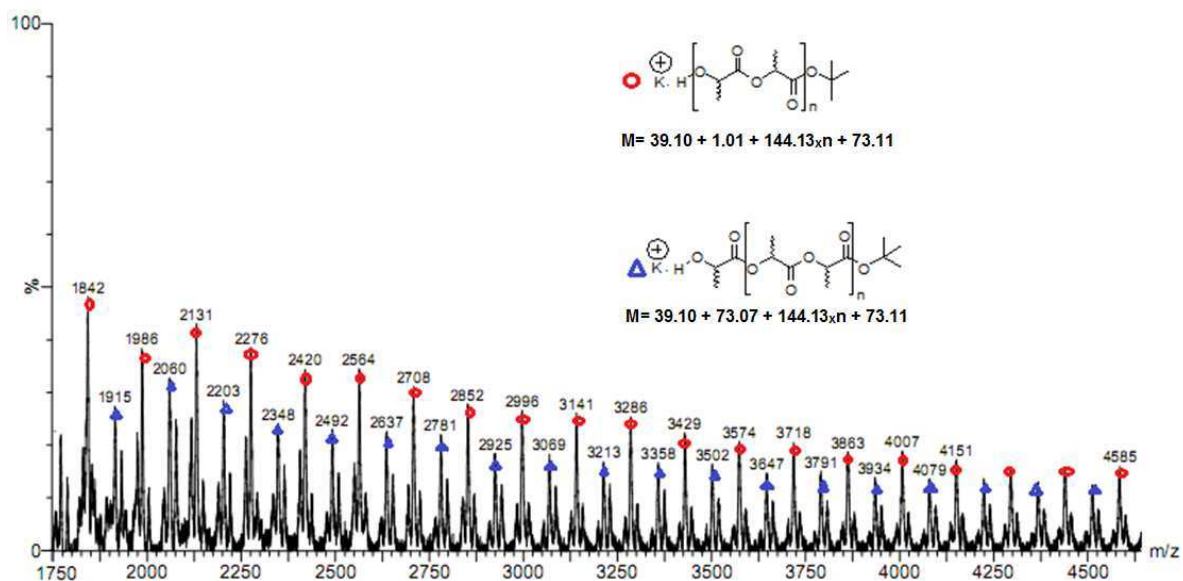


Figure 16. Selected area of the MALDI-ToF mass spectrum of PLA, synthesised by ROP using **44** in THF. Polymerisation conditions: $[LA]_0 = 1 \text{ M}$, $[44]_0 = 2 \text{ mM}$, reaction stopped at $t = 2 \text{ s}$ to obtained PLA with $M_n < 10 \text{ kg mol}^{-1}$ (calculated first from kinetic plots). The MALDI-ToF conditions were using a dithranol matrix, in dichloromethane at a loading of 1:5, with potassium trifluoroacetate as the cationising agent.

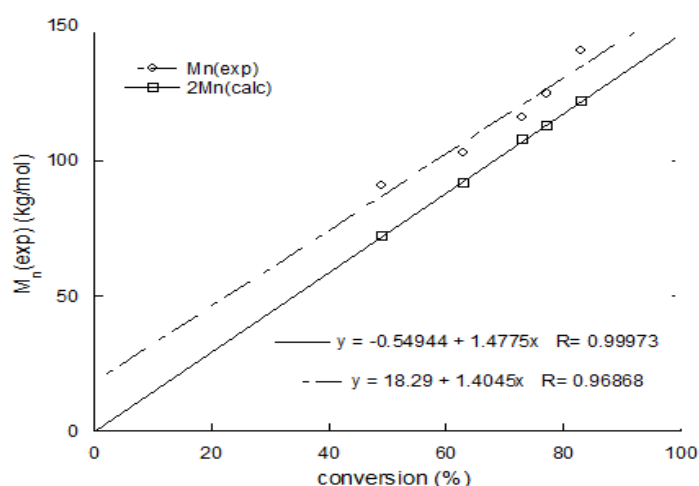


Figure 17. Plot showing evolution of M_n (kg mol^{-1}) vs. conversion (%) for LA ROP using initiator **44**. Polymerisation conditions: $[LA]_0 = 1 \text{ M}$, $[44] = 2 \text{ mM}$, THF, $25 \text{ }^\circ\text{C}$.

In situ $^{31}\text{P}\{^1\text{H}\}$ NMR spectroscopy was used to monitor a mixture of complex **4** and 25 equivalents of LA. The spectrum was quite different to complex **44** alone; it showed four non-equivalent phosphorus nuclei (Figure 18), data which could support aggregation under the conditions of the catalysis. Currently, we are unable to unambiguously assign the solution structure of complex **44**, under the polymerization conditions.

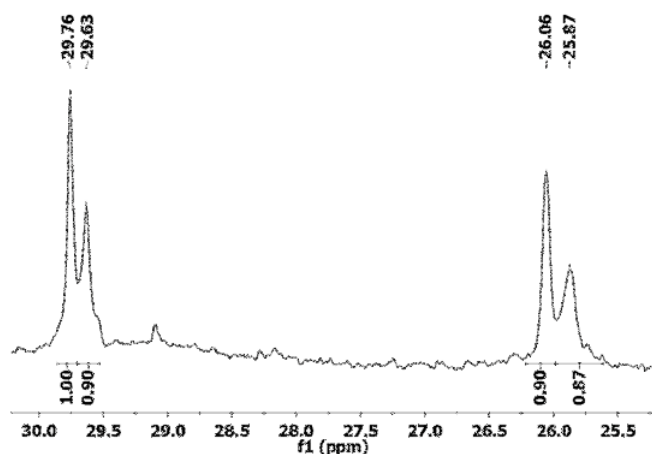


Figure 18. $^{31}\text{P}\{^1\text{H}\}$ NMR spectrum of a mixture of **44** and 25 equiv. of *rac*-lactide in THF recorded with an Av500 instrument.

2.3 Catalytic Activities and Kinetics Studies: Monomeric Complex

2.3.1 General

Complex **45** is extremely active, it is even able to polymerize unpurified lactide; near quantitative conversion is reached within 2 minutes at low initiator loadings ($[\mathbf{45}] = 1 \text{ mM}$). Kinetic study for the polymerizations analysed by taking aliquots showed that the reaction follows a first-order rate in lactide (Figure 19). This rate law is thus the same as common ROP of lactide reactions and contrasts with the cases of complex **43** and **44**. The pseudo first order rate constant, k_{obs} , was 0.08 s^{-1} , at $[\mathbf{45}]$ of 1 mM. The rate of polymerization is thus amongst the highest values reported for this reaction, easily comparing with related yttrium systems and outstripping many other metal centres.

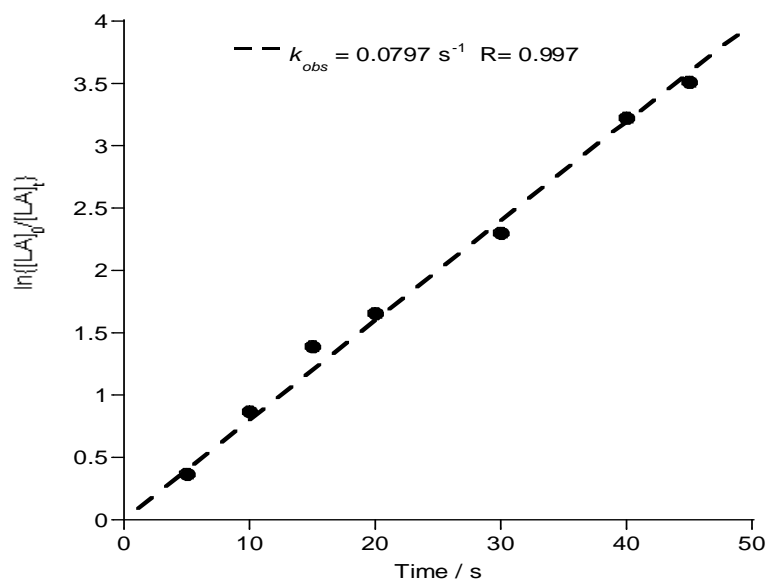


Figure 19. $\ln\{[LA]_0/[LA]_t\}$ versus time for LA ROP using initiator **45**. Polymerization conditions: $[LA]_0 = 1\text{ M}$, $[3] = 1\text{ mM}$, THF, 25 °C.

In comparison with yttrium complexes of salens and derivatives, it is clear that initiator **6** shows remarkably enhanced rates, even under significantly lower loadings, although caution should be applied in comparing values as the experiments were not run under identical conditions (Table 4). For example, complex **Y1**¹⁷ took 14 h to reach complete conversion at 100:1 loading of lactide:initiator, complex **Y3**¹⁹ took an hour to reach complete conversion at a loading of 300:1 and, the ferrocenyl salen complex **Y4**²⁰ took 40 min to reach high conversions at a loading of 500:1. In contrast, complex **45** was able to completely polymerize as many as 5000 equivalents of lactide in 30 mins and 1000 equivalents in less than a minute. It is also notable that initiator **45** can be used at rather low loadings, down to $[LA]:[45] = 5000$, which is useful for production of high molecular weight PLA (up to 700 kg/mol). Finally, it is apparent that the other yttrium salen complexes do not allow significant stereocontrol in *rac*-lactide ROP, in contrast complex **45** enables a high degree of heteroselectivity in *rac*-LA ROP.

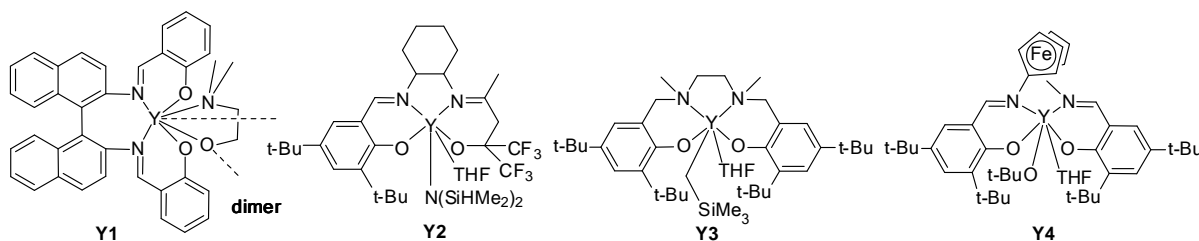


Table 4. Data for the ROP of lactide using yttrium initiators.

Initiator (I)	[LA] ₀ : [I]	Time / s	Conversion/%	$M_n(\text{calc})^{\text{b}}$ / kg mol ⁻¹	$M_n(\text{exp})$ / kg mol ⁻¹	PDI	P _s
45	1000:1	45	97	140	223	1.34	0.86
45^{a)}	2000:1	10 min	99	288	330	1.35	0.87
45^{b)}	5000:1	30 min	98	720	700	1.23	0.88
Y1¹⁷	100:1	14 hours	>98	-	-	-	-
Y2¹⁸	100:1	3 days	80	12	10	1.18	0.72
Y3¹⁹	300:1	60 min	>98	43	37	1.64	0.65
Y4²⁰	500:1	40 min	90	72	93	1.13	-

^a Slurry of 2 mmol lactide in 1 mL THF at 25 °C. ^b Slurry of 5 mmol lactide in 1 mL THF at 25 °C.

The LA ROP using initiator **45** is quite well controlled, with the number averaged molecular weight (M_n) of the PLA increasing linearly with the percentage conversion and the polydispersity indices remaining narrow throughout the polymerization (<1.4).

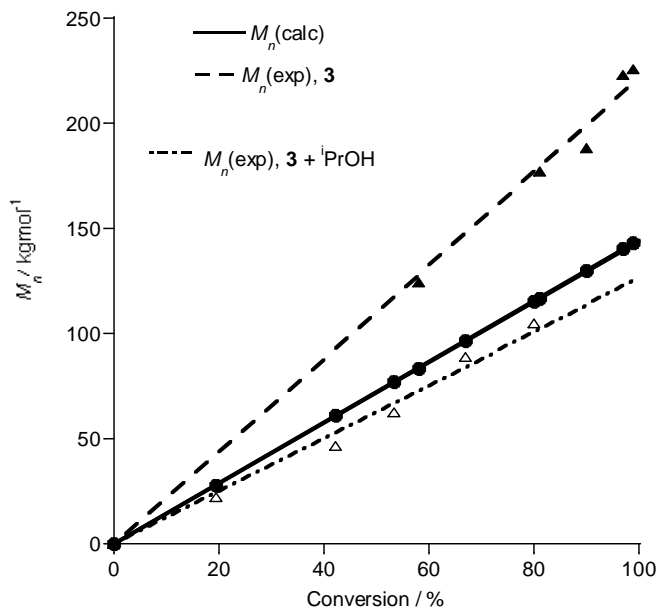


Figure 20. Evolution of M_n (kg/mol) versus conversion (%) for LA ROP using **45** (filled triangles), and with an extra equivalent of *iPrOH* (hollow triangles). Also plotted is the $M_n(\text{calc})$ (filled circles). Polymerization conditions: $[\text{LA}]_0 = 1 \text{ M}$, $[\mathbf{45}] = [\textit{iPrOH}] = 1 \text{ mM}$, THF, 25 °C.

The experimentally determined values for the number averaged molecular weight exceed those calculated (on the basis of initiator concentration and conversion). This could either be due to incomplete initiation from the *tert*-butyl alkoxide groups or to partial deactivation of the initiator.

In order to test the above hypothesis, and to bring the experimental M_n close to its calculated values, an experiment was carried out where an equivalent of *iso*-propyl alcohol was added. An yttrium *iso*-propyl alkoxide complex is expected to be a better initiator due to its reduced steric hindrance and is also a good model for the secondary alkoxide propagating species. The addition of an equivalent of *iso*-propyl alcohol led to an improved control, as evidenced by the excellent agreement between the experimentally determined and calculated values for M_n and the PDI being below 1.10, in almost all samples. These results indicate that *iso*-propyl alcohol is a viable chain transfer agent and a more effective initiator.

NMR experiments at variable temperature (VT-NMR) were carried out to investigate the formation of an yttrium isopropoxide complex upon addition of isopropanol (1 equivalent), and its exchange with the alcohol in solution. Details are presented in the following section. The study showed the formation of an LYOiPr complex and its rapid exchange with free *t*BuOH was demonstrated. As isopropoxide is a better initiating group than *tert*-butoxide, the equilibrium between LYOiPr and LYOtBu is driven towards the formation of the isopropoxide complex during the reaction. Moreover, HO*t*Bu is a poor chain transfer agent. Taking into account all data, the polymerizations are expected to be dominated by the yttrium isopropoxide initiator, hence the good fit between $M_n(\text{exp})$ and $M_n(\text{calc})$ in this case.

2.3.2 NMR Studies of the Addition of *iso*-Propanol on Complex 45.

Upon the addition of 1 equivalent of iPA into a solution of complex **45** in THF-*d*₈, minor changes were observed in the ³¹P-NMR and ¹H-NMR spectra. The protons of the *tert*-butoxide group experienced the largest shift from a broad singlet at 0.68 ppm (in the complex) to a fine one at 0.98 ppm, the methyl protons of isopropoxide appear as a doublet at 0.90 ppm. (Figure 21). When 3 or 5 equivalents of *iso*propanol were added, the changes in the signals for the phosphasalen ligand in both ³¹P-NMR and ¹H-NMR are minor compared to those observed upon the addition of only one equivalent of *iso*propanol. This suggests that the ligand is still coordinated to the yttrium center, and that the complex(es) remain(s) essentially unchanged.

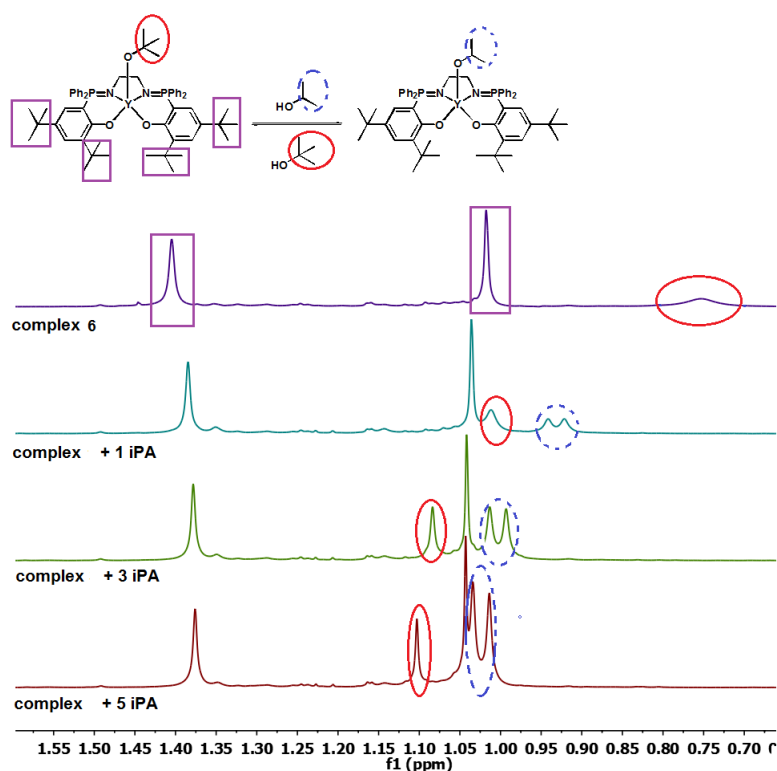


Figure 21. Addition of 1 to 5 equivalents of iPA on **45** (spectra between 0.6 and 1.6 ppm)

From the addition of 3 and 5 equivalents of isopropanol, it was observed that the proton signals of the isopropyl group in both the complex and free isopropanol are almost identical. This may point towards a rapid exchange in the solution between coordinated isopropoxide and isopropanol. In the same manner, rapid exchanges between coordinated *t*BuO and free HO*t*Pr (and the reverse) are conceivable. Therefore variable temperature NMR experiments were performed.

Comparisons between NMR spectra at variable temperatures obtained from a mixture (**6** + iPA) and those from (**45** + 3 iPA) show important differences (Figure 22). In presence of 3 equivalents of isopropanol, at all temperature, the Y-*Ot*Bu complex disappeared (no doublet at 6.33 ppm corresponding to C_dH), and only signals corresponding to the L- Y-*Oi*Pr are observable (doublet at 6.45 ppm for C_dH).

Spectra recorded for **45** in the presence of one equivalent of isopropanol is typical for an exchange process. Signals corresponding to C_dH of the L- Y-*Ot*Bu complex can clearly be seen at 178K (see Figure 22, spectrum of **45** alone and **45**+ iPA at 178K). Upon heating, signals corresponding to L- Y-*Ot*Bu complex (doublet at 6.32 ppm at 178K) and the one corresponding to the L- Y-*Oi*Pr complex (doublet at 6.55 ppm at 198K) merge ($T = 238K$). Afterwards, a clear doublet corresponding to both complexes in rapid exchange appears at 6.47 ppm.

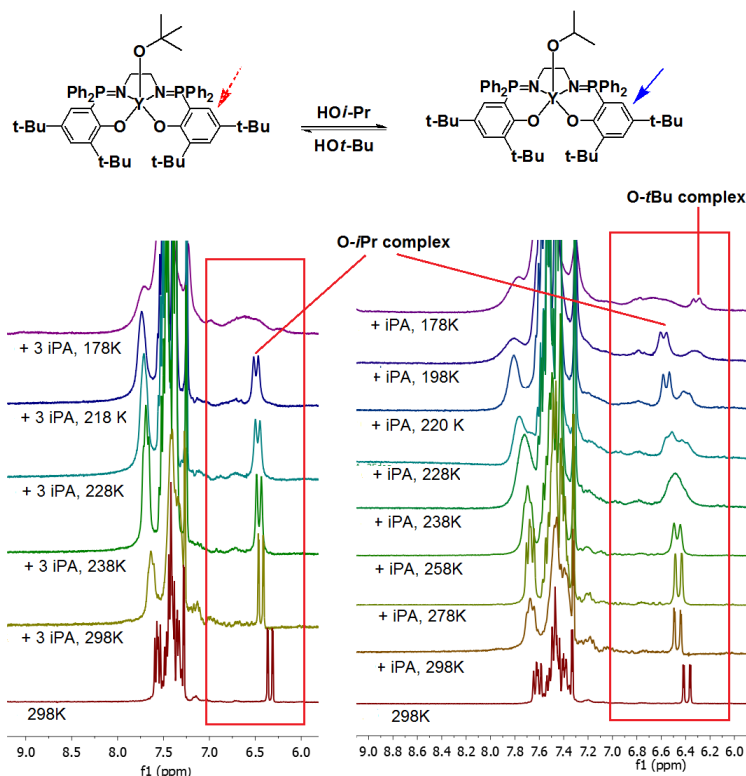
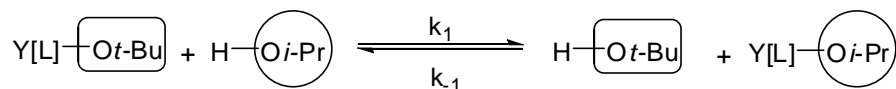


Figure 22. Addition of 1 and 3 equivalents of iPA on **45** at variable temperatures (spectrum between 9.0 and 6.0 ppm).

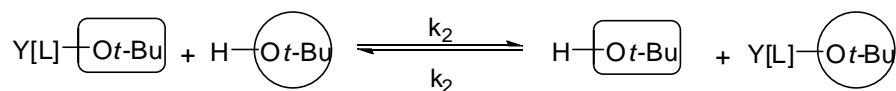
Considering the following reaction which takes place when 1 equiv. of isopropanol is added into a solution of L- Y-O*t*Bu complex



The activation parameters were determined: $\Delta G^\ddagger = 11.4 \text{ kcal.mol}^{-1}$

$$k_{-1} = 1770 \text{ s}^{-1} \text{ mol}^{-1} \text{ L}, k_1 = 7110 \text{ s}^{-1} \text{ mol}^{-1} \text{ L}$$

Variable Temperature-NMR also allowed to study the exchange between coordinated *Ot*Bu and free *HOt*Bu in the solution.



In fact, at $T \leq 238\text{K}$, in presence of 1 equivalent of *HOi*Pr, signals corresponding to coordinated *t*BuO (singlet at 0.69 ppm at 298K) and free *HOt*Bu (singlet at 1.13 ppm) are differentiated (Figure 23). The rate constant was determined $k_2 = 7110 \text{ s}^{-1} \text{ mol}^{-1} \text{ L}$, as well as the activation barrier for such exchange $G^\ddagger = 12.0 \text{ kcal.mol}^{-1}$ at 238K.

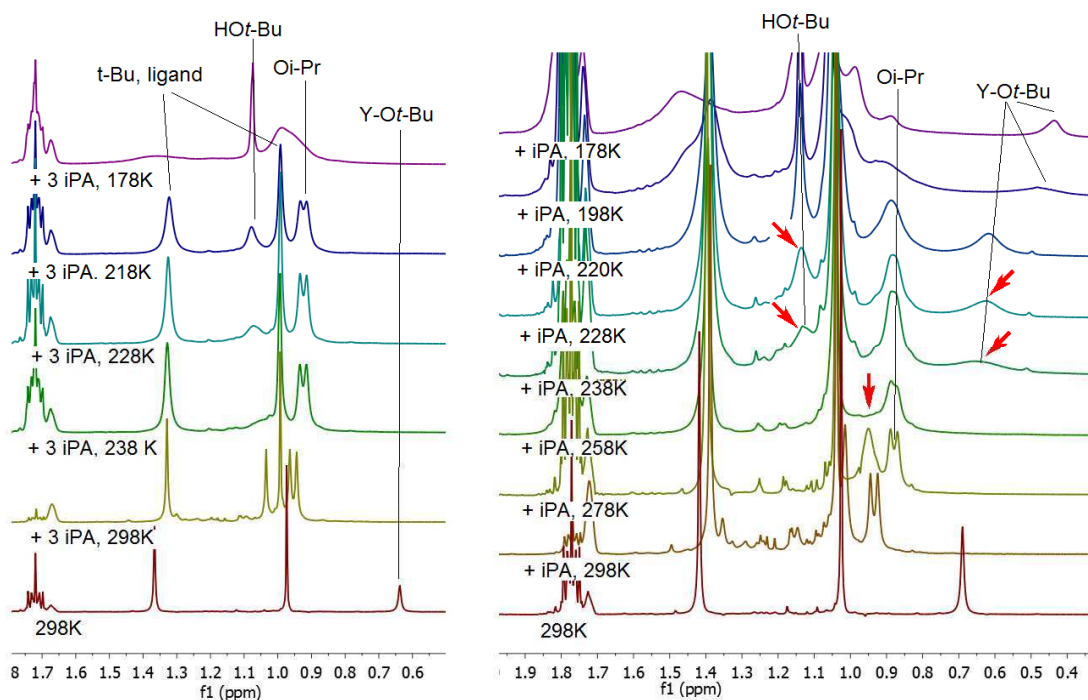


Figure 23. Addition of 1 and 3 equivalents of iPA on **45** at variable temperatures (spectrum between 2.0 and 0.4 ppm).

2.4 Stereoselectivity of the Polymerisations

The polylactide produced from *rac*-lactide using the three initiators shows a heterotactic bias (P_s). The determination of P_s was carried out using the probabilities calculated by Coudane *et al.*,^{3a} every tetrad signal was analysed and the average value for P_s reported (Figure 24 and Figure 25). PLA produced using initiators **43** and **44** had P_s values in the range 0.78-0.81, regardless of the *rac*-LA conversion or initiator concentration.

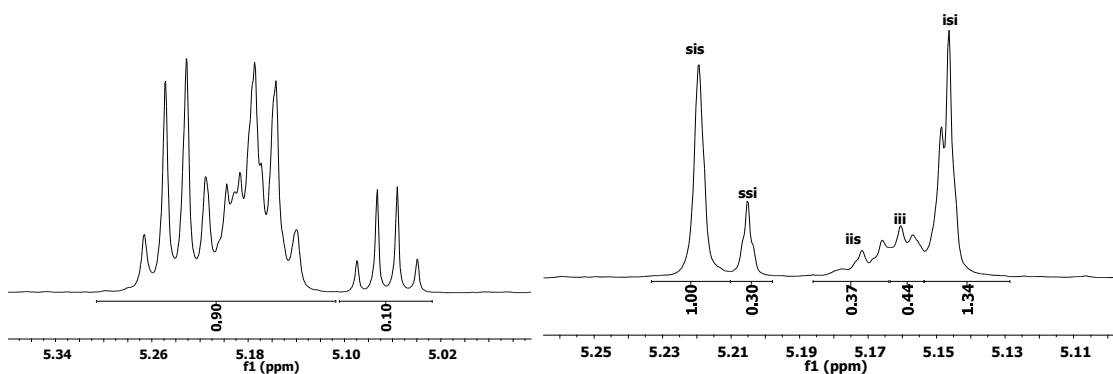


Figure 24. $\{^1\text{H}\}$ and $^1\text{H}\{^1\text{H}\}$ NMR spectra of PLA produced using initiator **43**. $[\text{LA}]_0 = 1 \text{ M}$, $[\text{I}] = 5 \text{ mM}$, 90 % conversion of LA, THF, 25 °C, $P_s = 0.78$.

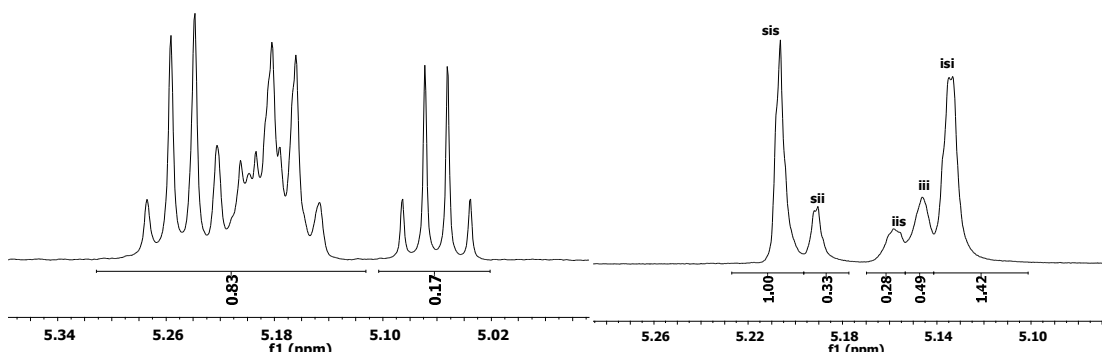


Figure 25. ^1H and $^1\text{H}\{^1\text{H}\}$ NMR spectra of PLA produced using initiator **44**. $[\text{LA}]_0 = 1 \text{ M}$, $[\text{2}] = 2 \text{ mM}$, 83% conversion of LA, THF, 25°C , $P_s = 0.79$.¹

Complex **45** shows considerably enhanced heteroselectivity, with P_s 0.86-0.90. Once again, the probability of heterotactic enchainment was independent of the conversion of *rac*-LA, the addition of *iso*-propyl alcohol or the concentration of the initiator. It is quite interesting to observe that highly heterotactic PLA was produced from either purified or crude LA. As an illustration of the high degrees of heteroselectivity conferred by this initiator, the methyne region of the ^1H NMR spectrum of PLA (Figure 26) is illustrated; it is dominated by two quartets, assigned to heterotactic PLA.

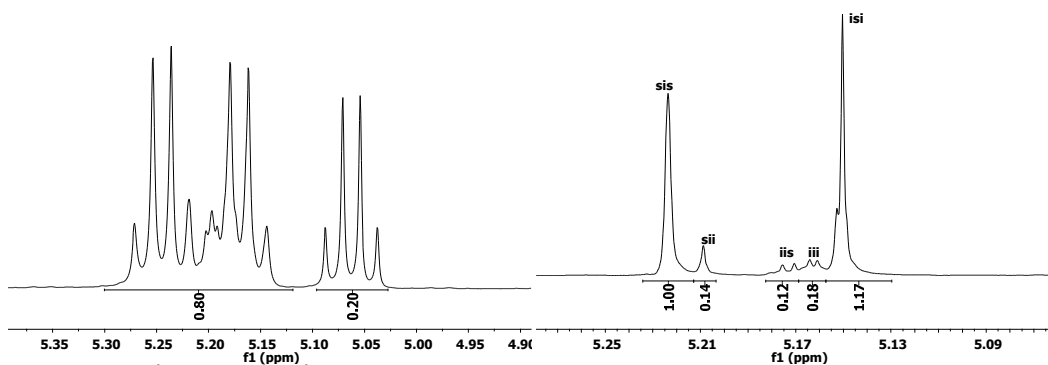


Figure 26. ^1H and $^1\text{H}\{^1\text{H}\}$ NMR spectra of PLA produced using initiator **45**. Polymerisation conditions: $[\text{LA}]_0 = 1 \text{ M}$, $[\text{3}] = [\text{PrOH}] = 1 \text{ mM}$, 80% conversion of LA, THF, 25°C , $P_s = 0.90$.

3. Discussion

3.1 Generalities

Complexes **43** and **44** are proposed to initiate and propagate ROP via a coordination insertion mechanism. The MALDI-TOF spectra of the PLA produced using these initiators show chain end-capped with ethyl ester and *tert*-butyl ester groups respectively (as well as the expected

hydroxyl group at the opposite chain end), consistent with this mechanism. Both complexes exhibit dimeric structures in the solid state, with complex **43** having bridging ethoxide groups whilst complex **44** bridges through a phenoxide group from each phosphasalen ligand. It is likely that the solid state structures are maintained in THF solutions, as the $^{31}\text{P}\{^1\text{H}\}$ -NMR spectra differ despite having the yttrium centre coordinated by the same phosphasalen ligand. Thus, complex **43** displays two signals, assigned to two phosphorus atoms in different chemical environments, in accordance with the solid state structure, whilst complex **44** displays a single doublet, indicating all the phosphorus atoms are in equivalent environments, again in accordance with the solids state structures.

The polymerization data also indicate differences between the two initiators with **43** being significantly slower than **44**. Indeed at 5 mM initiator concentration, complete conversion was observed after approximately 1 h using complex **43** and after only 40 s using complex **44**. Both initiators show a second order dependence of the rate of polymerization on the concentration of lactide, implicating two molecules of lactide in the rate determining step. Even more curiously, the molecular weights agree well with calculated values on the basis of two active sites per molecule of **43** but only for a single active site for complex **44**.

It is proposed that the dimeric structures are maintained under the conditions of the polymerization, with initiation and propagation occurring from both bridging alkoxide groups in the case of **43** and from a single tert-butoxide group in the case of **44**. The order in LA concentration and the molecular weight observations for complex **43** imply that two chains are propagated per dimer molecule. However, in the case of complex **44** it is not clear why a second order dependence in lactide concentration is observed but only a single chain propagates per dimer molecule. But again, this phenomenon has already been observed for some other second-order reactions in LA, where the experimental M_n s imply that only half of the possible initiating groups are active, although they are all in the same environment in the starting complex.^{31, 30} In our case, NMR experiments and full kinetic study showing a third order in initiator suggested an aggregation of the complexes in the conditions of polymerizations. This underlines the importance of having bulky substituents on the phosphasalen ligand to prevent such phenomenon.

Complex **45** was targeted to have a mononuclear structure in solution, via the use of a sterically hindered phopphasalen ancillary ligand and a hindered initiating group, tert-butyl alkoxide. Based on NMR data and solid state structure, it is proposed that this species retains a mononuclear structure in solution. Polymerizations using this initiator show extremely rapid rates, indeed the pseudo first order rate constant (at $[\mathbf{45}] = 1 \text{ mM}$) is very high ($k_{obs} = 0.008 \text{ s}^{-1}$) and the rate depends to the first order in the concentration of LA.

A mixture of complex **45** and 25 eq. of LA was analyzed by $^{31}\text{P}\{^1\text{H}\}$ -NMR spectroscopy which showed that the P=N groups remain coordinated to the yttrium centres, indicating that the ligand is not dissociated during the polymerization. Furthermore, complex **45** shows excellent heteroselectivity for *rac*-LA ROP. This interesting finding further confirms earlier experiments

using bis(phosphinic amido) yttrium complexes developed by the Williams' group, where high degrees of heteroselectivity were only observed from a mononuclear complex.^{28b}

The stereocontrol is proposed to arise via a chain end control mechanism, that is where the stereochemistry of the last inserted lactide unit controls the stereochemistry of the coordination/insertion into the next lactide unit. This enhancement in stereocontrol for yttrium initiators in THF has been reported by many group are is presumably due, in part, to its ability to coordinate to the yttrium centre and control the active site stereochemistry.^{26g, 25, 33a, b, 10, 19, 33c,}

^{1d} An NMR scale experiment involving addition of increasing quantities of THF to a solution of **45** in toluene did not lead to a significant shift in the THF resonances, either due to rapid exchange or a lack of coordination. It is, however, clear that the THF solvent is important for the high stereocontrol as an experiment conducted in toluene ([LA]= 1 M, [**45**] = 1 mM in THF, 80 °C, 91% conversion) yielded a PLA with much lower heteroselectivity ($P_s = 0.73$ vs. 0.89 in pure THF).

3.2 Comparisons with Other Yttrium Complexes

The groups of Coates^{17a} and Carpentier's¹⁸ have both studied yttrium complexes of (substituted) tetradentate salen ligands. The yttrium complexes, either as monomers (**Y2**) or dimers (**Y1**, bridging through the alkoxide group), were not particularly active in lactide ROP and no stereocontrol was reported (Table 4). These phosphasalen yttrium complexes showed markedly different behaviour giving very high activities for lactide polymerisation and heteroselectivity to rac-LA ROP. In fact, the electronic properties of the iminophosphorane functional group, in the phosphasalen ligand, differ notably from the imine moiety in the salen analogue. Figure 27 recalls the divergent electronic properties of the ligands, as a result from NBO (Natural Bond Orbital) analyses on the structures of model compounds optimized using the Density Functional Theory, with the B3PW91 as the functional and the 6-31G* basis set.

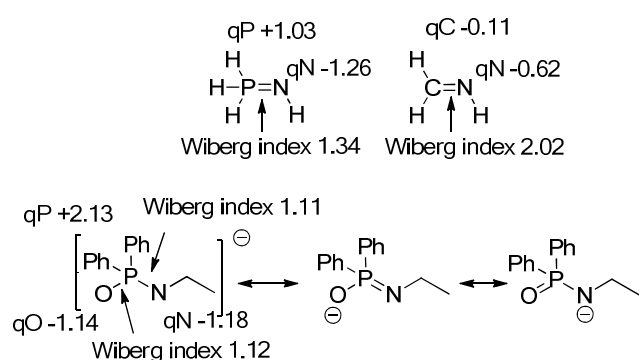
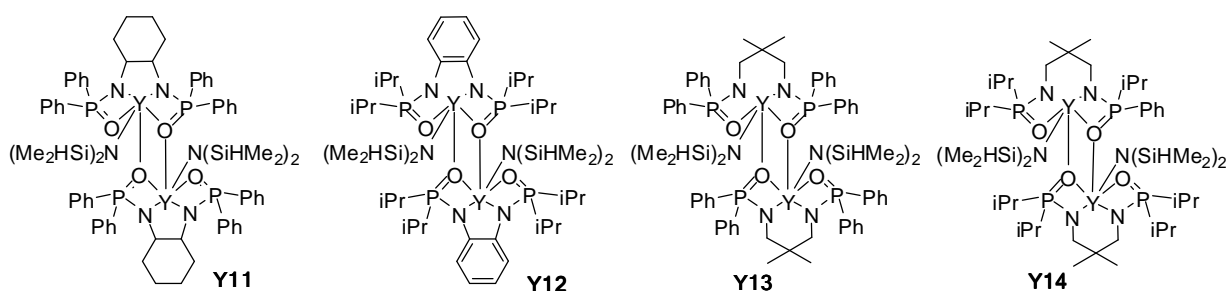


Figure 27. Comparisons of the Wiberg indices and NBO charge for various model compounds, calculated using Gaussian09, using B3PW91 functional and 6-31G* basis set.

With this in mind, it is interesting to re-examine a series of bis(phosphinic)diamido yttrium complexes, developed by the Williams' group and show excellent activities in lactide polymerization.^{28a, b, 28d} All the complexes have tetradentate bis(phosphinic amido) ancillary

ligands, coordinated to the yttrium centres via the N and O atoms. They were highly active; furthermore a monomeric complex gave highly enriched heterotactic PLA ($P_s=0.85$) (whereas the dimeric complexes give moderately heterotactic PLA). An NBO analysis performed on a model of diphenylphosphinic amido derivative shows some similarities with iminophosphorane derivatives (Figure 27). Indeed the NBO charges at P, N, and O were calculated at +2.13, -1.18, and -1.14, respectively. Moreover, both the P-N, and P-O bond indices are close to 1. This is in agreement with the existence of two resonance forms for this functionality, one of which corresponds to an iminophosphorane ($N=P-O^-$). The X-ray crystal structures of these complexes show that the P-N bond lengths and the geometries at the P and N centers fit with the ligands having some degree of iminophosphorane functionality (Scheme 20, Table 5).



Scheme 20. Dimeric bis(phosphinic amido) yttrium complexes, by Williams and coworkers

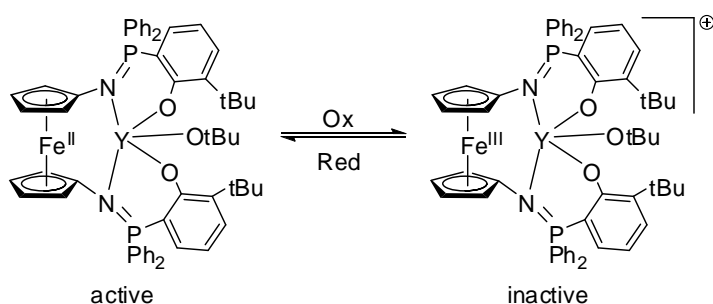
Table 5. Structural data for dimeric bis(phosphinic amido) and phosphasalen yttrium complexes (Y-N and Y-O distances relative to ancillary ligand)

Complex	P-N (Å)	Y-N (Å)	Y-O (Å)
Y11 ^{28b}	1.576(2), 1.568(2)	2.336(2), 2.395(2)	2.3336(17), 2.4444(16)
Y12 ^{28b}	1.5907(18), 1.5989(18)	2.3560(17), 2.3348(17)	2.3409(15), 2.4720(13)
Y13 ^{28b}	1.5922(13), 1.5821(12)	2.3681(12), 2.3542(12),	2.3548(10), 2.4621(10)
Y14 ³⁴	1.596(6), 1.582(6)	2.216(6), 2.345(6)	2.315(5), 2.524(5)
43	1.598(3), 1.595(3)	2.415(3), 2.438(3)	2.182(3), 2.213(3),
44	1.596(3), 1.586(3)	2.398(3), 2.372(3)	2.203(3), 2.338(2),
45	1.595(2), 1.584(2)	2.375(2), 2.324(2)	2.1671(318), 2.1704(18)

Experimentally, it appears that this iminophosphorane ligand motif accelerates ROP at the yttrium centres, leading to much enhanced activities and even enabling stereochemical control. The iminophosphorane functionality is significantly more electron donating than the imine analogue in the salen ligand. In lactide ROP, there is a balance between requiring a Lewis acidic

yttrium centre to facilitate lactide coordination whilst also requiring a labile yttrium alkoxide bond to accelerate insertion of the lactide unit. Thus, it seems that a better donor ligand is desirable, this may be due to weakening or labilizing of the yttrium-alkoxide bond and acceleration of the insertion step.

Diaconescu and coworkers recently reported a switchable activity in lactide ROP using an yttrium alkoxide complex, with a tetradentate ligand featuring in the backbone an iminophosphorane linked to a ferrocene.³⁵ Whereas the complex bearing the neutral ligand (featuring a ferrocene), with an electron rich nitrogen donor group is active for the ROP of lactide, the oxidized complex (featuring a ferrocenium) is completely inactive (Scheme 21). Thus, the polymerization activity is switched ‘off’ when the electron density at the nitrogen decreases. It was hypothesized that although the insertion of the monomer to the oxidized complex is possible, the propagation from such a species is unfavourable, since the alkoxide would be connected to a more electron deficient metal.



Scheme 21. Redox control polymerization, by Diaconescu and coworkers.

This observation strongly supports the benefit of a good donor ligand for the ROP of lactide. The flexibility of the ligand could also play an important role, as the coordination geometry at yttrium is expected to change during the coordination-insertion steps in ROP, and a more flexible ligand could be beneficial.

4. DFT calculations

Following the experimental study on the catalytic activity of complex **45** on ROP of lactide, theoretical studies have been carried out in order to investigate the mechanism of the reaction and to find out, if possible, factors that are important for the ROP of lactide using such systems.

Density Functional Theory (DFT) calculations were performed on these two complexes with the Gaussian 03 set of programs³⁶ in combination with the B3PW91 functional³⁷. The choice of basis sets and functions was made based on the computational costs and validated by comparisons between the optimised and experimental structures of complex **45** (details of which would not be presented here). The optimised structures were characterised by vibration frequencies calculations. Yttrium was represented by the nonrelativistic Stuttgart effective core

potential ECP28MHF and the associated basis set. In fact, on this system, it had been tested that the use of relativistic Stuttgart effective core potential ECP28MDF and the associated basis set ECP28MDF-VTZ gave almost the same values of activation energies for several steps of the mechanism, so nonrelativistic effective core potential was chosen in order to reduce the calculation cost. Phosphorus atoms were described by the SDDALL basis set³⁸ with Stuttgart potentials, reinforced with polarisation functions $P(\zeta(d) = 0.340)$.³⁹ All other atoms were described with the 6-31G* Pople basis set.⁴⁰ Tert-butyl groups were not represented with lower basis sets because steric interactions have been shown to be important in these systems, and calculations using 3-21G basis set for tert-butyl groups gave significantly different activation energies than those using 6-31G* basis sets.

4.1. Initiation step

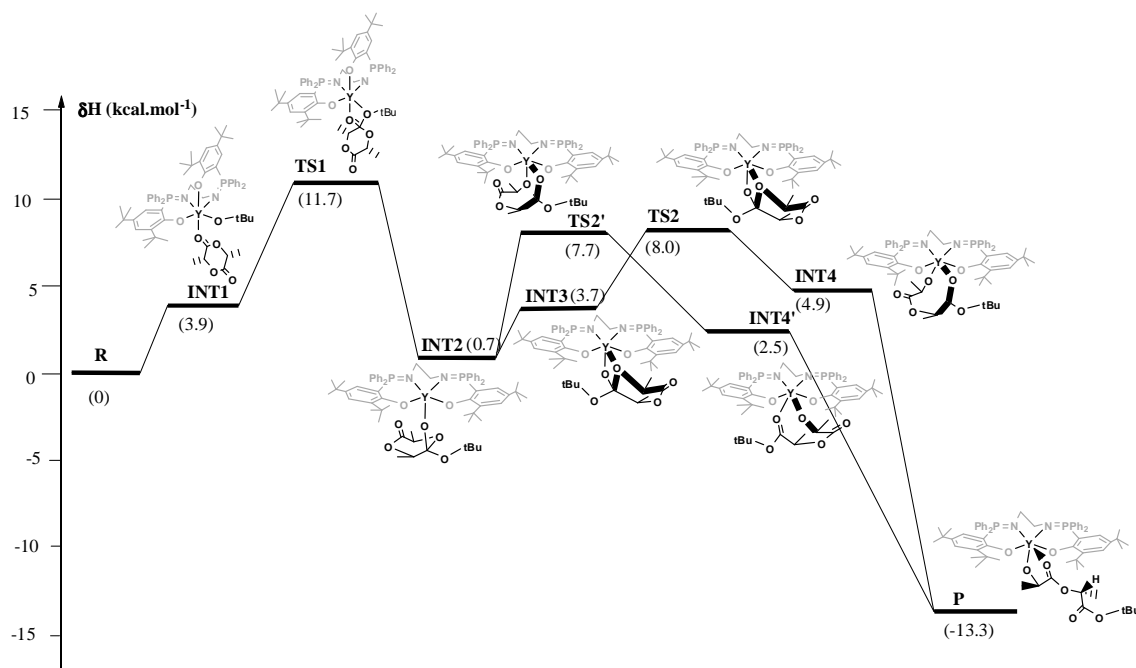
Experimental data on the ROP of lactide initiated by complex **45** were strongly in favor of a coordination-insertion mechanism (Scheme 8). Thus the calculations were directed into this mechanism and were divided into several steps: coordination of the lactide unit to the yttrium center, interaction of this lactide with *tert*-butoxide group in close proximity, leading to the nucleophilic addition of the alkoxide to the coordinated carbonyl function of the lactide, followed by the ring opening of the lactide unit which occur at this carbon.

DFT calculations have been done to determine the structure of **45** in THF, and more precisely, to see whether THF could coordinate to the yttrium center. In fact, one optimized structure of **6**.THF was found. The complex adopts a distorted octahedral geometry, the phosphasalen ligand takes the four positions of the equatorial plane, THF and the *tert*-butoxide group occupy the axial positions. It has been found that ΔH of the reaction $\mathbf{45} + \text{THF} \rightleftharpoons \mathbf{45} \cdot \text{THF} (*)$ is equal to -0.9 kcal/mol, taken into account that THF is solvent, the coordination of THF is likely in solution. Therefore, the mechanism has been calculated starting from **45**.THF. It is however worth noting that because the value of ΔH for (*) is very small, even when supposing that the active species be **45**, almost the same values of ΔH for the steps in the mechanism would be obtained.

Coordination of two molecules of THF to yttrium center in **45** is not possible, as has been shown by DFT calculations: optimization of the supposed molecule **45**.2THF led to the structure of **45**.THF and one separated THF molecule. This is indicative that for complex **45**, hepta-coordination is not possible or strongly disfavored. This would still be seen in the following steps.

Arbitrarily, the first inserted lactide unit was chosen to be (R,R)-lactide. The lactide coordinates to the yttrium center and takes an equatorial position, “pushing” one phenoxide arm to the axial position, and the phosphasalen changes from *trans*-configuration to *cis*-configuration. From this intermediate **INT1**, intramolecular nucleophilic reaction takes place between the *tert*-butoxide group and the activated carbonyl function of the coordinated lactide. The transition state **TS1** is characterised by a four-member ring formed between the yttrium, the two atoms O_{carbonyl} and O_{alkoxide} , and the C_{carbonyl} atom which had become tetrahedral. The $C_{\text{carbonyl}}-O_{\text{carbonyl}}$ bond is

lengthened (1.25 Å vs 1.21 Å in **INT1**), as well as the Y-O_{alkoxide} bond (2.34 Å vs 2.09 Å in **INT1**), whereas the Y-O_{carbonyl} bond is shortened (2.32 Å vs 2.53 Å in **INT1**). The C_{carbonyl}-O_{alkoxide} distance is of 1.91 Å.



Scheme 22. Initiation step for ROP of lactide catalysed by **45**.

The nucleophilic attack results in the formation of intermediate **INT2**. In this intermediate, the Y-O_{alkoxide} bond is completely broken and the complex recover its distorted square-based pyramidal geometry as in **45**, the phosphasalen ligand changes configuration from *cis*- to *trans*-.

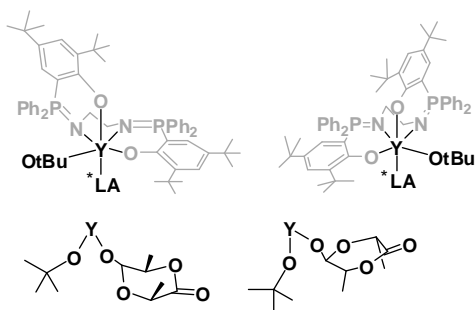
Two possible pathways are possible for the ring-opening step. In the first pathway, **INT2** directly undergoes the ring-opening reaction, as the O_{lactide ring} approaches the yttrium centre. This results in the intermediate **INT4'**, in which both the O_{carbonyl} and the O_{lactide ring} atoms still coordinate to the metal centre, but the C_{carbonyl}-O_{lactide ring} bond has been completely broken. The corresponding transition state is characterised by a four membered-ring composed of Y, O_{lactide ring}, C_{carbonyl}, and O_{carbonyl} atoms.

In the second pathway, rotation of the lactide unit around the Y-O_{carbonyl} bond leads to the formation of the intermediate **INT3**, in which a four-membered ring is formed between Y, C_{carbonyl}, O_{carbonyl}, and O_{lactide ring} atoms. This intermediate is higher in energy than **INT2**, and the Y-O_{lactideRing} bond is quite weak, as evidenced by the long bondlength (2.73 Å). In the corresponding transition state **TS2** this four-membered ring is still maintained, but with significant changes in bond lengths: elongation of the C_{carbonyl}-O_{lactide ring} bond and shortening of the C_{carbonyl}-O_{carbonyl}. The resulted intermediate **INT4** resembles **INT4'** described above, but with different relative orientation of Y-O_{lactideRing} and Y-O_{carbonyl} bonds (Scheme 22).

Both intermediates **INT4** and **INT4'** evolve towards the final product **P**, characterised by a five-membered ring formed from the coordination of the other O_{carbonyl} atom of the former lactide unit to the yttrium center, the phosphasalen ligand being in trans-configuration. This product is the most stable one. Another possible product, **P'**, deprived of this coordination, adopts distorted square-based pyramidal geometry and is higher in energy than **P** of about 3 kcal/mol. In total, the formation of these final products are exothermic, which recompense the possible loss of entropy.

Several observations have been drawn out concerning the mechanism:

1) In order for the insertion to occur, the intermediates resulting from the coordination of lactide to **45** must have the phosphasalen ligand in *cis*-configuration, so that the alkoxide and the lactide are in *cis*-position, close to each other.



Scheme 23. Illustration for the relative configurations

In total, eight configurations could be envisaged, arising from the possibilities of 1) the *tert*-butoxide group to be either on axial or equatorial positions; 2) the (R,R)-lactide to place either with the methyl groups in the same or opposite direction of the alkoxide group; 3) because the lactide is chiral, with the same position of LA and *Ot*Bu groups, two *cis*-conformations of the phosphasalen ligand lead to two different conformations of the product, of different energies (Scheme 23).

In all cases, the enthalpies of these coordination reactions are higher than the total enthalpies of the starting compounds by 3.8-5.4 kcal/mol. These positive and close values suggest that one has to look into the activation barrier of the insertion in order to know which configuration gives better chance for the following steps to occur.

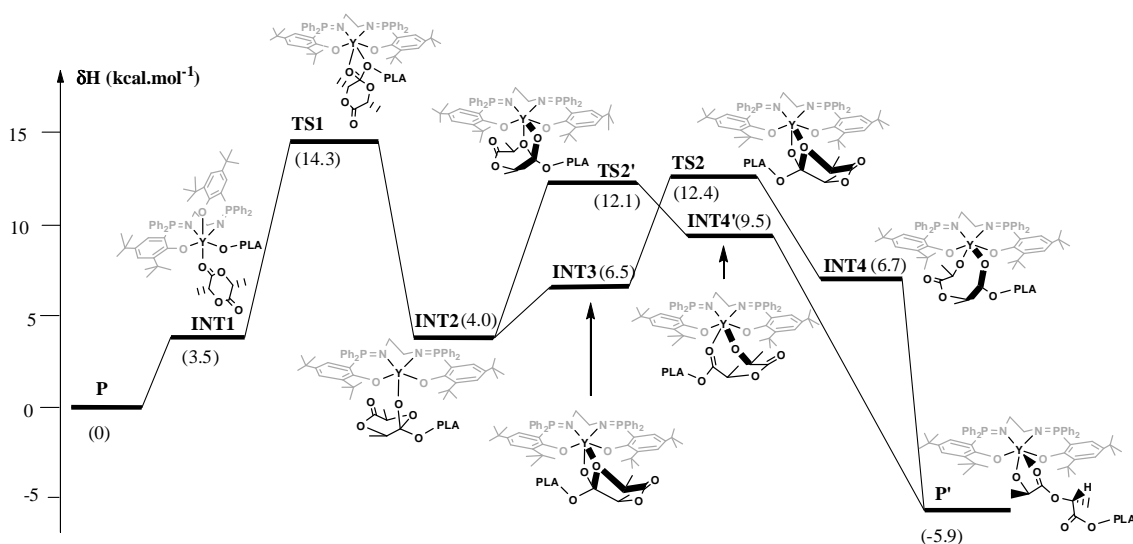
Transition states for the insertion step resulting from such configurations have been determined. **TS1** is the transition state with the lowest activation barrier. All the transition states corresponding to other conformations of **INT1** are higher in energy of 2-5kcal/mol. Steric interactions between the phosphasalen ligand (mainly from the *tert*-butyl and phenyl groups), the *tert*-butoxide group, and the methyl groups on the lactide are important. This explains the necessity of representing the whole molecule in DFT calculations, as well as the difficulty of modeling them.

2) The energy barrier for the ring-opening step is lower than the one for the insertion step. The latter is thus the rate-determining step for the initiation. Not that for the ring-opening step, both transition states **TS2** and **TS2'** have approximately the same energy. Thus it seems that steric influences in this step are not very important.

3) The configuration of the PLA chain is very important and it has been observed that slightly different configurations of this chain may lead to energy difference of several kcal/mol. The configuration with the lowest energy was found to be the one with stabilizing hydrogen bonds between the O_{carbonyl} atoms and the appropriate hydrogen(s) in close proximity, and minimized steric repulsion between methyl and *tert*-butyl groups.

2. Propagation step

The starting species for the first propagation step was supposed to be the most stable product resulted from the initiation step (**P**). The second lactide unit was chosen to be of the same configuration as the first one, i.e. (*R,R*)-lactide, so that comparisons could be made easily between the initiation and propagation step.



Scheme 24. First propagation step for the ROP of lactide initiated by **45**.

The profile of the propagation step in the ROP of lactide by **45** resembles a lot to the one of the initiation step. All transition states and intermediates have similar conformations as the corresponding species in the initiation step, with the exception of **TS1**. The phosphasalen ligand in this transition state adopts a *trans*- configuration, while the first transition state for the initiation step has the ligand in *cis*- configuration. All the energies for the intermediates and transition states in the propagation step are slightly higher than the ones in the initiation step.

In summary, from the calculations for the initiation and the first propagation step of the ROP of *rac*-lactide initiated by **45**, it could be seen that

1) the activation energies are small, thus explaining the excellent rate of this polymerization

- 2) the polymerization is exothermic. The negative value of enthalpy is the driving force of the polymerisation.
- 3) the rate-determining step seems to be the insertion step. In this step, steric interactions are very important and probably determinant for the stereoselectivities of the ROP of lactide.
- 4) the ring-opening step is not much influenced by steric interactions
- 5) the most stable configuration of the propagating chain is characterised by a five-membered ring formed from the coordination of the other O_{carbonyl} atom of the former lactide unit to the yttrium center.

When the second lactide unit was chosen to be (S,S)-lactide in order to modeling the heteroselectivity of the ROP initiated with **45**, it has been found that: 1) the structures and energies of the intermediates are very close to the ones obtained from the above calculations, supposing that the second lactide unit is (R,R)-lactide; 2) the energies of the transition states are slightly higher than the ones obtained from the above calculations, of less than 1 kcal/mol, in gas-phase and in solution (model PCM). These very close values did not allow to draw any conclusion about the heteroselectivity of the ROP of *rac*-lactide initiated by **45**.

As it seems that steric factors are important for the performance of **45** in the ROP of *rac*-lactide, we decided to prepare other yttrium complexes with different steric properties and determine their activities of the ROP of lactide.

IV. Monomeric yttrium complexes: factors influencing the activity

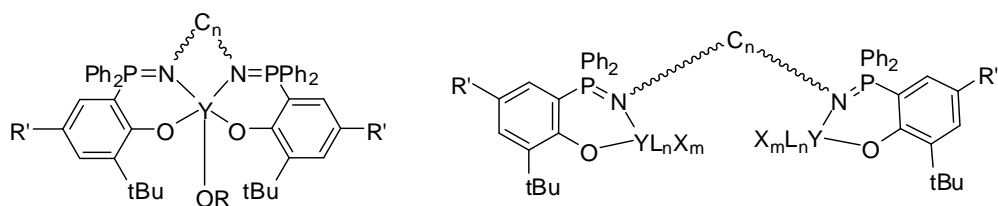
1. New yttrium phosphasalen complexes

1.1 New complexes with modified steric properties

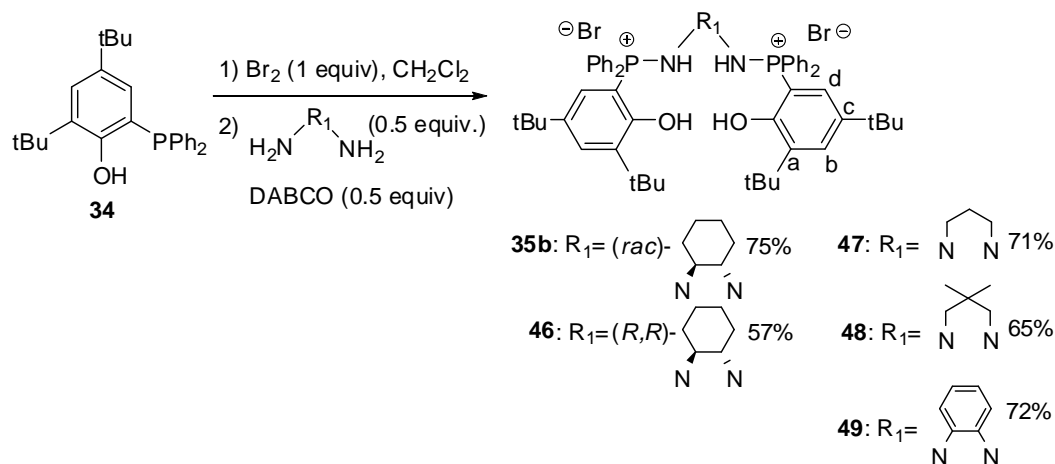
Encouraged by the excellent performance of the monomeric yttrium complex **45**, we decided to synthesise more complexes based on similar systems in order to investigate, experimentally, the factors underlying the rate and stereoselectivity of ROP of lactide by yttrium-phosphasalen systems. Monomeric complexes were targeted as ROP of lactide initiated by dimeric phosphasalen complexes were shown to be complex and less efficient.

In order to achieve well defined monomeric complexes, the presence of bulky substituents on the *ortho*-position of the phenoxide rings is essential. For this purpose, *tert*-butyl groups are maintained at this position. Furthermore, for the formation of well defined monomeric complexes, the diamine bridge must not be too large, otherwise one phosphasalen ligand could coordinate two yttrium centers by the two sides of the ligand, each containing one phenoxide

and one iminophosphorane group (Scheme 25). The diamine bridge are thus chosen to be the ones with 2 or 3 carbons.

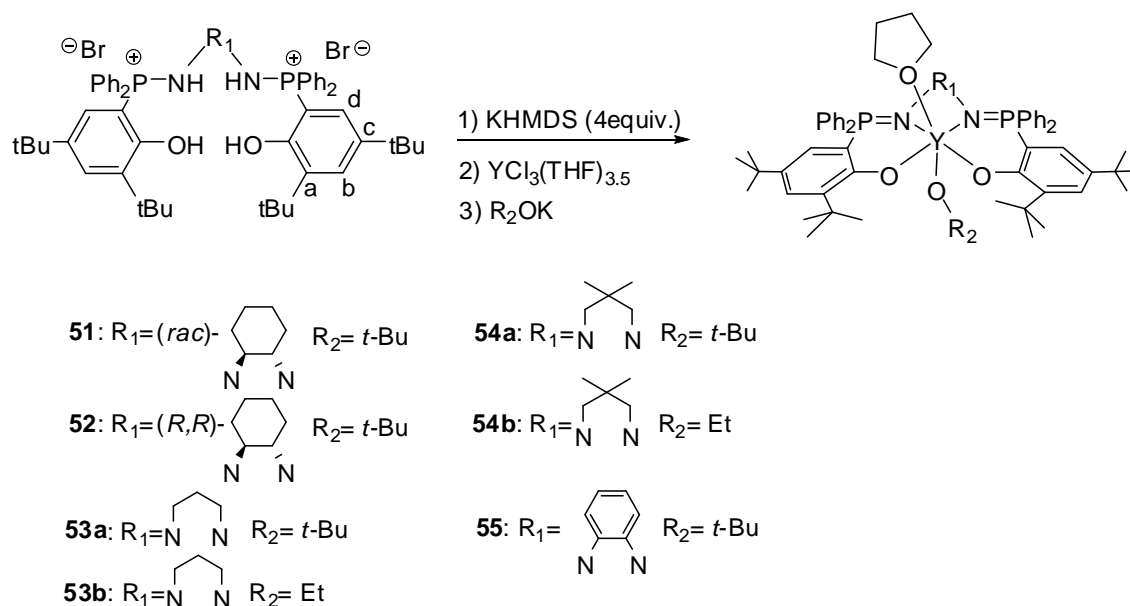


Scheme 25. (left) Monomeric yttrium phosphasalen complexes, small diamine bridge. (right) One phosphasalen ligand coordinated to two yttrium centers, large diamine bridge.



Scheme 26. New Phosphasalen proligands having C2 and C3 diamine bridges

The synthesis of **35b** has been described in chapter 4. The proligands **46-49** were synthesized from 2,4-di-tert-butyl-6-phosphinophenol by the Kisanov reaction with dibromine and the appropriate diamines in dichloromethane, using DABCO as base. After evaporation of dichloromethane, the mixture was taken in THF in order to remove insoluble DABCO salts. THF was evaporated and the solid was washed with Et₂O and the product was isolated as a white solid. This method gave the phosphasalen proligands **46-49** in high yield. They were all fully characterized by NMR multinuclear experiments and elemental analysis.



Scheme 27. Synthesis of yttrium phosphasalen complexes

Addition of 4 equiv. of KHMDS into a slurry of the phosphasalen proligands in THF gave cloudy colorless solutions, indicating the formation of anionic phosphasalen ligands. Completeness of the reaction was verified by $^{31}\text{P}\{^1\text{H}\}$ NMR spectra which showed singlets in much higher field compared to the signals of aminophosphonium salt in the proligands (+18 ppm instead of +38.5 ppm to for **35b** and **46**, +23.8 ppm instead of +40.4 ppm for **47**, +22.3 ppm instead of +41.7 ppm for **48**, +13.2 ppm instead of +38.9 ppm for **49**).

After removal of insoluble potassium salts by centrifugation, addition of $[\text{YCl}_3(\text{THF})_{3.5}]$ into this solution gave a unique product which showed one singlet at lower field in $^{31}\text{P}\{^1\text{H}\}$ NMR spectra, compared to the phosphasalen ligands. This indicated the formation of yttrium phosphasalen complexes. Finally, addition of potassium ethoxide or tert-butoxide into the mixture caused the nucleophilic substitution which yielded the desired phosphasalen alkoxide complexes, with in general an upfield shift in $^{31}\text{P}\{^1\text{H}\}$ NMR spectra. Evaporation of THF and recrystallisation in cyclohexane gave the products as colorless crystals or white solids.

All the complexes have been fully characterized by NMR experiments and elemental analysis. In some cases, crystals suitable for X-ray diffraction has been obtained, allowing to determine the structures of the complexes without ambiguity.

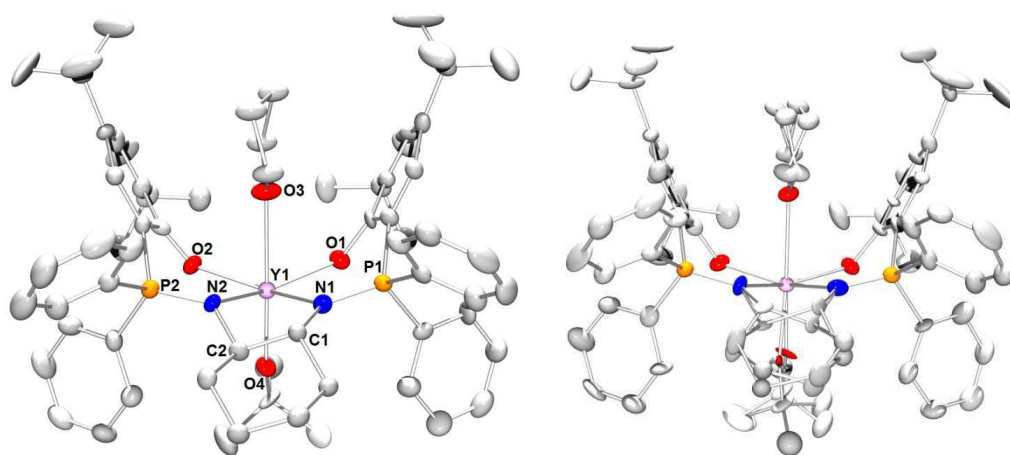


Figure 28. (left) ORTEP view of the solid state structure of complex **52**, with thermal ellipsoids drawn at the 50% probability level. Hydrogen atoms are omitted for clarity. Selected bond lengths (Å) and angles (deg): Y1-O1 2.23(6), Y1-O2 2.25(6), Y1-O3 2.53(6), Y-O4 2.04(2), Y1-N1 2.38(7), Y2-N2 2.40(7), P1-N1 1.59(7), P2-N2 1.59(7), O1-Y1-N1 82(2), N1-Y1-N2 70(1), N2-Y1-O2 83(2), O1-Y1-O2 120(1), O2-Y1-O3 84(3), O2-Y1-O4 95(2), O3-Y1-O4 179(3), O2-Y1-N1 151(2), O1-Y1-N2 148(2). (right) ORTEP view of the solid state structure of complex **51**, showing the existence of two isomers (R,R) and (S,S) with equal percentage. Thermal ellipsoids are drawn at the 50% probability level, hydrogen atoms are omitted for clarity.

Structure of complex **51**, prepared from the phosphasalen ligand with *rac*-1,2-diaminocyclohexane backbone has been resolved. As expected, the two isomers having (R,R) and (S,S)-1,2-diaminocyclohexane backbone cocrystallised in 50/50 proportion (Figure 28), each of them could be seen as a mirror image of each other. Complex **52** featuring the enantiometrically pure (R,R)-1,2-diaminocyclohexane backbone present the same structural data as the one resolved for complex **51**. It has yttrium center in octahedral geometry: the two nitrogen and two oxygen atoms of the phosphasalen ligand occupy the equatorial plane, the tert-butoxide group and one molecule of THF occupy the axial positions. This is very different from complex **45** which also features a C2-backbone diamine and has a penta-coordinated yttrium center.

The bond lengths Y-O_{phosphasalen} and Y-N in **52** are almost comparable to those in **45** (2.23 (6) Å and 2.25(6) Å vs 2.1671(318) Å and 2.1704(318) Å for Y-O bonds, 2.38(7) Å and 2.40(7) Å vs 2.375(2) Å and 2.324(2) Å for Y-N bonds), and the P-N, N-C1/2 and C1-C2 bond lengths in **52** are sensibly the same as those in **45**. Thus, the reason why an extra THF molecule could be accommodated in **52**, rather in **45** does not lay on the hypothesis that bond lengths in the phosphasalen ligand of **52** are longer than those in **45**. It is thought that for **52**, steric interaction between the phenyl groups on P atoms with carbons and hydrogen atoms on the cyclohexylene backbone prevents the contraction of phosphasalen ligand as with **45**, and thus resulted in an “exposed” space around the yttrium center where THF molecule is coordinated.

Probably for the same reason, complex **55** featuring *ortho*-phenylene diamine also present a coordinated THF (Figure 29). It adopts a distorted octahedral geometry, the phosphasalen ligand

occupying the 4 equatorial positions, the two axial positions being occupied by the tert-butoxide group and THF molecule. In general, Y-O_{phosphasalén} and Y-N bond length values in **55** are very close to the ones in **52** and **45**.

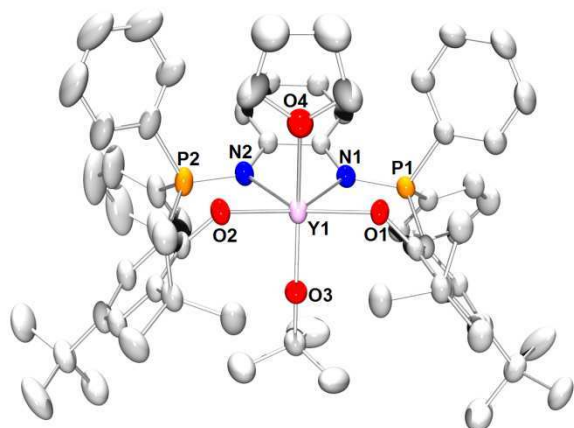


Figure 29. ORTEP view of the solid state structure of complex **55**, with thermal ellipsoids drawn at the 50% probability level. Hydrogen atoms are omitted for clarity. Selected bond lengths (Å) and angles (deg): Y1-O1 2.243(3), Y1-O2 2.220(3), Y1-O3 2.040(3), Y1-O4 2.467(3), Y1-N1 2.389(4), Y1-N2 2.406(3), P1-N1 1.606(4), P2-N2 1.604(4), O1-Y1-N1 80.8(1), N1-Y1-N2 68.3(1), N2-Y1-O2 80.9(1), O1-Y1-O2 126.1(1), O2-Y1-O3 95.5(1), O2-Y1-O4 75.4(1), O3-Y1-O4 160.6(1), O2-Y1-N1 147.6(1), O1-Y1-N2 146.9(1)

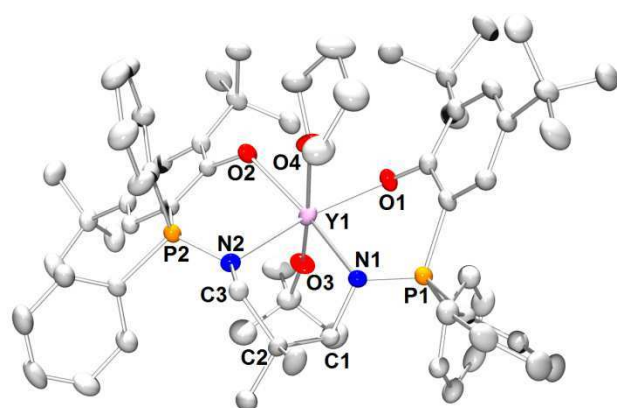
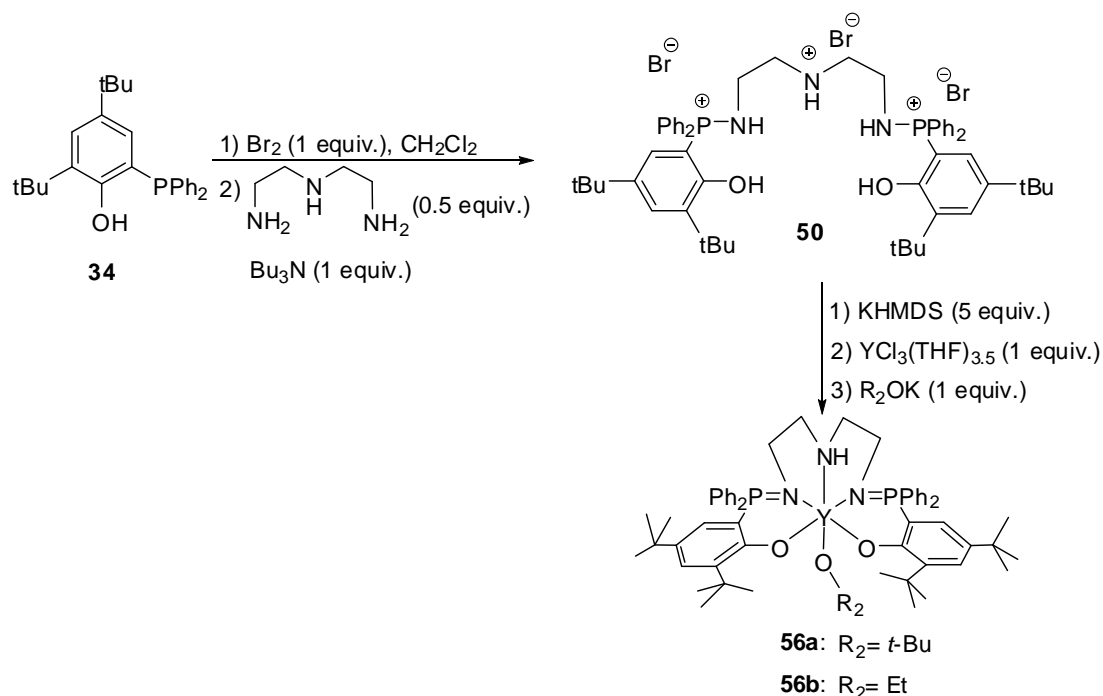


Figure 30. ORTEP view of the solid state structure of complex **54a**, with thermal ellipsoids drawn at the 50% probability level. Hydrogen atoms are omitted for clarity. Selected bond lengths (Å) and angles (deg): Y1-O1 2.232(3), Y1-O2 2.191(3), Y1-O3 2.072(3), Y1-O4 2.462(3), Y1-N1 2.432(4), Y1-N2 2.402(4), P1-N1 1.597(4), P2-N2 1.599(4), O1-Y1-N1 84.0(1), N1-Y1-N2 80.8(1), N2-Y1-O2 83.2(1), O1-Y1-O2 109.3(1), O2-Y1-O3 95.6(1), O2-Y1-O4 78.3(1), O3-Y1-O4 173.5(1), O2-Y1-N1 155.8(1), O1-Y1-N2 163.7(1)

A phosphasalén ligand with C3 diamine backbone, which is longer than the ethylene diamine backbone, logically give a larger “exposed” space around the yttrium center compared to complex **45**. Thus, complex **54a** featuring a 2,2-dimethyl-1,3-diaminopropane backbone also has a coordinated THF molecule (Figure 30). No particularity has been found for the structural data of this complex.

Though X-ray structures has not obtained for other phosphasalen complexes of this series, based on these observations, it is supposed that these compounds would also carry a coordinated THF, which has been attested by elemental analysis and NMR analysis.

A modified phosphasalen ligand presenting a supplementary coordination site on the diamine backbone has also been prepared (Scheme 28). Kisanov reaction on 2,4-di-tert-butyl-6-phosphinophenol with dibromine and diethylene triamine in dichloromethane, using Bu_3N (only in 1 equiv. quantity) as base yielded a cloudy solution. After evaporation of dichloromethane, the mixture was taken in THF and the product precipitated, giving a white solid, which was isolated by centrifugation and washed several times with THF in order to remove tributylammonium salt. After drying under vacuum, the phosphasalen proligand **50** was isolated in high yield (78%) and was fully characterized by NMR multinuclear experiments and elemental analysis.



Scheme 28. Synthesis of yttrium complex of a modified penta-dentate phosphasalen ligand.

Addition of 5 equiv. of KHMDS into a slurry of the phosphasalen proligands **50** in THF gave cloudy colorless solutions after 4h, indicating the formation of anionic phosphasalen ligand. In $^{31}\text{P}\{^1\text{H}\}$ NMR spectrum, a unique singlet was observed at 24.2 ppm, thus in much higher field compared to the signal of aminophosphonium salt in the proligand (41.8 ppm). Insoluble potassium salts were removed by centrifugation. Addition of $[\text{YCl}_3(\text{THF})_{3.5}]$ into the resulting solution gave a unique product which showed one singlet at lower field in $^{31}\text{P}\{^1\text{H}\}$ NMR spectra (35.0 ppm). This indicated the clean formation of yttrium phosphasalen complexes. Finally, addition of potassium ethoxide or tert-butoxide into the mixture led to the nucleophilic substitution which yielded the desired phosphasalen alkoxide complexes **56a,b**, which presented

a unique singlet in $^{31}\text{P}\{^1\text{H}\}$ NMR spectra (+33.6 ppm for **56a**, 34.2 ppm for **56b**). Evaporation of THF and recrystallisation in cyclohexane gave the products as white solids. All the complexes have been fully characterized by NMR experiments and elemental analysis.

No crystals of suitable size for X-ray diffraction has been obtained for complexes **56a,b**. The few crystals obtained from the crystallization tests were those of partly hydrolysed compounds. One resolved structure is presented in Figure 31. Though this structure is not the one of the desired or isolated product, based on this structure, several observations could be made: 1) the amine group on the backbone is coordinated strongly to the yttrium center; 2) even though the phosphasalen ligand takes up to five coordination positions, there's still space around the yttrium center to coordinate two more groups (this is important, because the ROP of lactide could thus proceed).

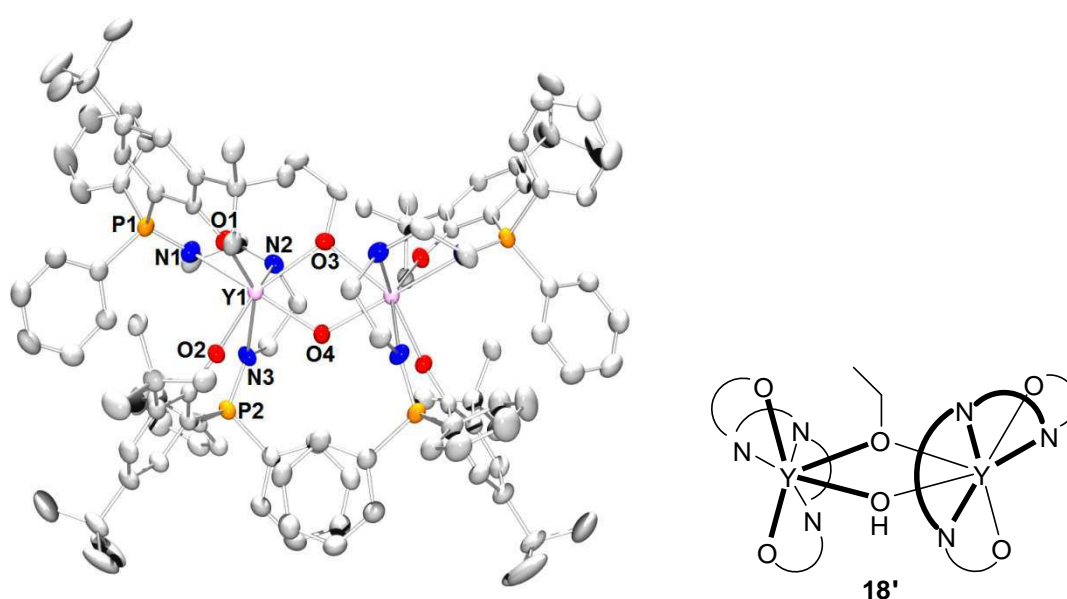
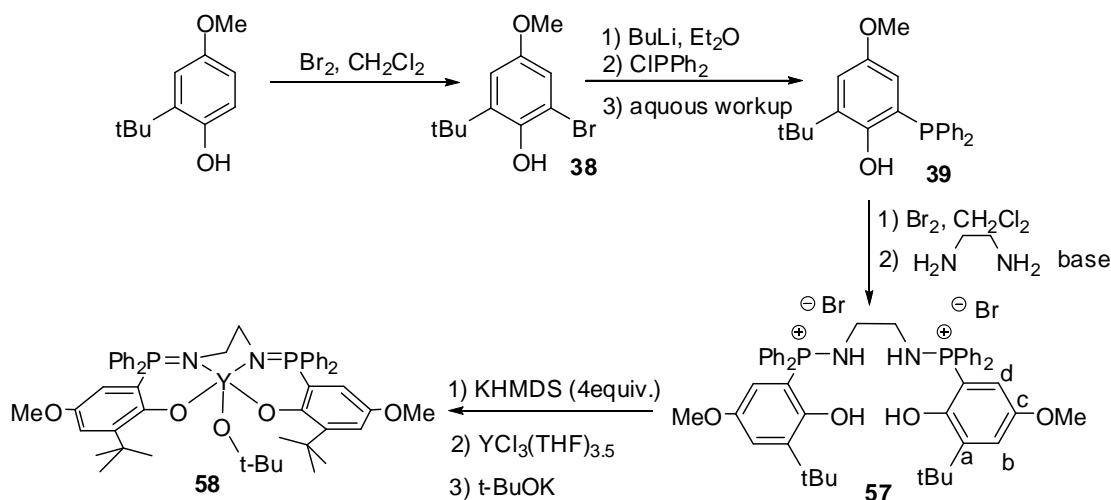


Figure 31. ORTEP view of the solid state structure of complex one yttrium complex with penta-dentate phosphasalen ligand **56'**, with thermal ellipsoids drawn at the 50% probability level. Hydrogen atoms are omitted for clarity. Selected bond lengths (Å) and angles (deg): Y1-O1 2.271(2), Y1-O2 2.230(2), Y1-O3 2.411(2), Y1-O4 2.248(2), Y1-N1 2.433(3), Y1-N2 2.511(3), Y1-N3 2.517(3), P1-N1 1.583(3), P2-N3 1.596(3), O1-Y1-N1 75.7(1), N1-Y1-N2 68.1(1), N2-Y1-N3 65.9(1), N3-Y1-O2 74.5(1), O3-Y1-O4 64.8(1).

1.2 New complexes with modified electronic properties

For all the phosphasalen yttrium alkoxide complexes described above, only modifications on the diamine backbone have been made with the main objective of modifying the steric properties of the yttrium complexes. In fact, based on the structures of yttrium phosphasalen complexes obtained by X-ray diffraction experiments, it could be seen that substituents on the phenoxide rings, except the ones at the *ortho*-position of the phenoxide, would not exert much influence on the steric properties of the complexes. However, these substituents may have great influence in terms of electronic properties on the phenoxide, thus on the yttrium complexes. We thus

targeted the modifications on the phenoxide rings with the objective of modifying the electronic properties. From the earlier observations on the activities of complex **45**, it has been speculated that the better donating ability of the phosphasalen ligand, compared to salen, might contribute largely to the better performance of this complex. We were then interested in the synthesis of the phosphasalen proligand **57** having OMe groups at the *para*-position of the phenoxide rings (Scheme 29).



Scheme 29. Synthesis of the phosphasalen proligand having OMe groups on phenoxide rings, and the corresponding yttrium complex

The bromination of 4-methoxy-2-*tert*-butylphenol with Br₂ in dichloromethane at 0°C gave 2-bromo-4-methoxy-6-*tert*-butylphenol **38** which was isolated by chromatography (71%). Reaction of this product with *n*-BuLi, followed by nucleophilic substitution with chlorodiphenylphosphine and aqueous treatment gave the desired product **39** in 84% yield as a yellow viscous oil.

Kirsanov reaction of **39** with bromine and ethylenediamine in the presence of tributylamine as base gave proligand **57** in 69% yield (Scheme 29). This compound, isolated as a white solid, has been fully characterized by multinuclear NMR spectroscopy and elemental analysis. In ³¹P{¹H} spectroscopy the equivalent phosphorus atoms of **57** appear as a singlet at δ(CDCl₃) = 40.1 ppm, which is very close to the value reported for the phosphasalen proligand having ethylene diamine bridge and *tert*-butyl groups at *ortho*- and *para*- positions of the phenoxide rings (compound **35a**, δ(CDCl₃) = 40.3 ppm). In ¹H NMR spectrum, the bridging ethylene protons of **57** appear as a doublet of doublet, due to couplings with two phosphorus atoms (³J_{P,H} = 6.5 Hz, ⁴J_{P,H} = 2.0 Hz), at 3.66 ppm. These values are also very close to the chemical shift of the ethylene protons in the same reference (δ(CDCl₃) = 3.74 ppm).

Addition of 4 equiv. of KHMDS into a slurry of the phosphasalen proligand **57** in THF gave a cloudy colorless solution after 4h, which is indicative of the formation of soluble anionic phosphasalen ligand. Completion of the deprotonation was monitored by ³¹P{¹H} NMR spectrum, which showed a unique singlet at 20.3 ppm, thus in much higher field compared to

the signal of aminophosphonium salt in the proligand (40.1 ppm). Insoluble potassium salts were removed by centrifugation. Addition of $[\text{YCl}_3(\text{THF})_{3.5}]$ into the resulting solution gave a unique product which showed one singlet at lower field in $^{31}\text{P}\{^1\text{H}\}$ NMR spectra (31.5 ppm), indicating the clean formation of the yttrium phosphasalen complex. Finally, addition of potassium tert-butoxide into the mixture entrained the nucleophilic substitution which yielded the desired phosphasalen alkoxide complex **58**.

Evaporation of THF and recrystallisation in cyclohexane gave the products as white solids. The complex has been fully characterized by NMR experiments and elemental analysis. The complex presented a unique singlet in $^{31}\text{P}\{^1\text{H}\}$ NMR spectra at 31.6 ppm, which is quite close to the chemical shift of the in situ generated phosphasalen yttrium chloride complex, but its ^1H NMR and $^{13}\text{C}\{^1\text{H}\}$ NMR spectra evidenced the incorporation of *tert*-butoxide group and its structure as described in Scheme 29.

Though single crystals were easily obtained, they did not diffract well and thus X-ray structure for this compound was not obtained. However, based on NMR data and elemental analysis, it is strongly believed that the structure in solid state and in solution of **58** resembles the one of complex **45**. This compound has the same chemical structure as **58**, but with *tert*-butyl groups at the *para*-positions of the phenoxide rings, instead of methoxy groups.

2. Activities

The experiences determining the activities of different synthesized complexes in the ROP of *rac*-lactide were done in collaboration with the Williams group at Imperial College, London. Preliminary results are given in Table 6. The solvent of choice for use at ambient temperature (25 °C) was THF; all experiments were conducted using an initial concentration of lactide of 1 M, so as to enable accurate comparison between the different initiators and additives.

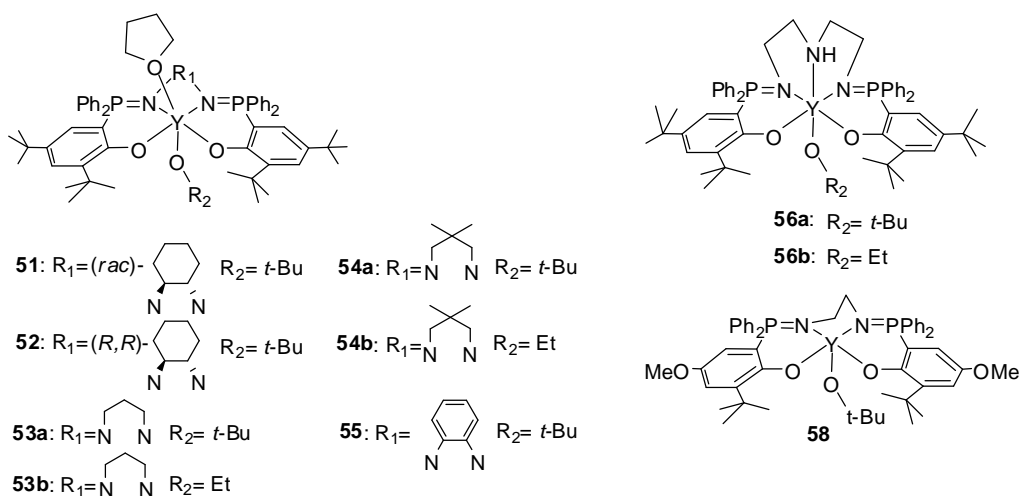


Table 6. Activities of different yttrium phosphasalene complexes in ROP of rac-lactide.

Initiator (I)	[LA] ₀ : [I]	Time / s	Conversion ^a /%	$M_n(\text{calc})^{\text{b}}$ / kg mol ⁻¹	$M_n(\text{exp})^{\text{c}}$ / kg mol ⁻¹	$k_{\text{obs}}(\text{s}^{-1})^{\text{d}}$	P_n
45	1000:1	45	97	140	223 (1.34)		0.86
51	500:1	240	89	64.08	84.0 (1.05)	0.0085	0.75
52	500:1	240	95	68.4	120.5 (1.07)	0.0123	0.76
53a	500:1	480	84	60.5	66.8 (1.07)	0.0038	0.68
53b	500:1	600	82	-	-	0.0027	-
54a	500:1	1200	91	65.5	76.5 (1.02)	0.0020	0.71
54b	500:1	1560	89	64.1	70.9 (1.01)	0.0015	0.65
55	500:1	360	90	64.8	196.2 (1.05)	0.0067	0.83
56a	500:1	2160	87	-	-	0.0011	0.74 (P_n)
56b	500:1	2520	84	60.5	61.6 (1.04)	0.0007	0.66 (P_n)
58	1000:1	90	83				0.85

^a Conversions were determined from the ¹H NMR spectra (CDCl₃) of the crude products, by integration of the methine resonance assigned to LA ($\delta=4.92$ ppm) and to PLA ($\delta=5.00-5.30$ ppm).

^b $M_n(\text{calc}) = 144 \times [\text{LA}]_0 / [\text{I}] \times \% \text{ conversion LA}$.

^c $M_n(\text{exp})$ was determined using GPC, in THF, using multi-angle laser light scattering (GPC-MALLS) according to the method described earlier.^{28a, b} The polydispersity index was also determined from GPC, $\text{PDI} = M_w / M_n$.

^d Determined from the gradients of the $\ln\{[\text{LA}]_0 / [\text{LA}]_t\}$ versus time plots, expressed in s⁻¹. The reactions are first order in lactide, $[\text{I}] = 1$ mM

As expected from monomeric complexes, all ROP reactions initiated by these yttrium phosphasalene complexes are first-order in lactide. Activities in ROP of lactide vary drastically with the change of the steric properties, induced by modifying the diamine bridge.

Several clear observations can be made:

1) All complexes **51-56a,b** are far less active than complex **45**. Even complexes with C2 linkers like **51**, **52**, **55** have activities that are incomparable with the activity of complex **45**, which could polymerise the lactide in very low catalytic loading (1000/1) in less than one minutes. The reason of such drastic change in catalytic activities lie in fact in the structure of complex. It has been seen, from the complexes characterizations above, that **51**, **52**, **54a**, **55** adopt monomeric

structures, but with the coordination of one molecule of THF, and that it is strongly believe that other complexes (**53a,b**, **54b**) have the same structure, i.e. containing one coordinated THF molecule. As to complex **45**, its solid structure shows no coordination of THF. So probably, because of the coordination of THF, the space for the coordination of lactide is reduced, and the ROP of lactide is rendered more difficult.

Poly lactides obtained from ROP of lactide initiated with complexes **51-56a,b** are less hetero-enriched than those obtained from the action of complex **45**. Once again, the presence of one more ligand (THF in case of **51-55**, NH in case of **56a,b**) seems to render the systems more “rigid” and lowers the stereoselectivity of the ROP.

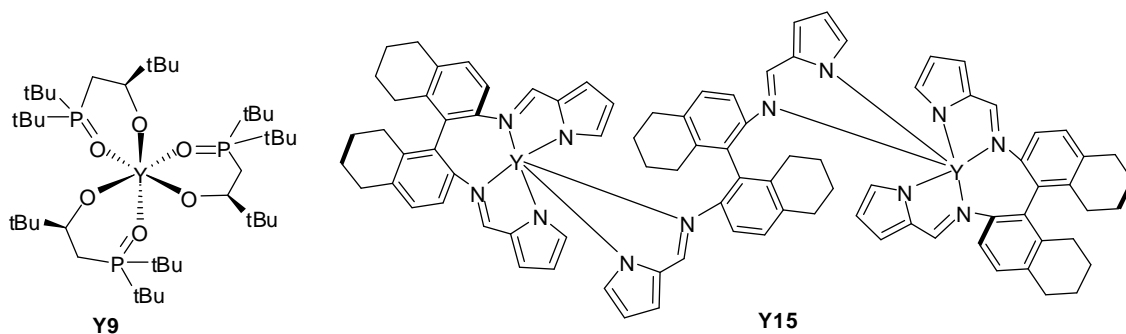
The ideal yttrium complex for the ROP of lactide should thus be the one where the yttrium center is only penta-coordinated. Complex **58**, with the ethylenediamine linker like complex **45**, is expected to adopt the same structure as **45** and to offer a better activity in ROP of lactide compared to complexes **51-56a,b**. Indeed, complex **58** is highly active in ROP of lactide. The polymerization of *rac*-lactide initiated by **58**, using only a very low catalyst loading (LA/I=1000/1), is fast (83% after 90s) and offers highly heterotactic polymers ($P_s=0.85$). The activity and heteroselectivity of complex **58** are thus comparable with the ones of complex **45**.

2) In general, complexes with C2 linkers are much more active than complexes with C3 linkers. For example, for a ratio LA/I=500/1, ROP of *rac*-lactide initiated by the complexes **51**, **52**, **55** require between 240-360s to achieve high conversion (more than 90%), whereas those initiated by **53a,b**, **54a,b** attained conversions about 80% in longer time (480-1600s). This could also be seen by comparing k_{obs} for ROP of lactide initiated by these complexes.

3) When comparing the performances of complexes with C3 linker, with or without substituents on the diamine linker, it is observed that the introduction of these substituents is not beneficial. Hence, the ROP of lactide initiated by **53a,b** require only 480-600 s to attain approximately the same conversions as those initiated by complexes **54a,b** after more than 900s. The k_{obs} for ROP initiated by **53a,b** are two or three times higher than k_{obs} for ROP initiated by **54a,b**. The reason of these differences in performance is probably because the presence of additional bulkiness renders difficult the coordination of lactide to the yttrium center.

4) Interestingly, complexes **56a,b** with additional coordination site of the diamine linker initiated the polymerization of *rac*-lactide to give isotactic polymers. The isotacticity is reasonable at room temperature ($P_i=0.74$ for **56a** and 0.66 for **56b**) and could be greatly improved by lowering the temperature ($P_i=0.81$ for **56a** at -15°C , and 0.76 for **56b** at -18°C). These complexes are among the very rare examples of yttrium complexes catalyse the formation of isotactic PLA from *rac*-lactide. Other examples are the systems of Arnold and coworkers (**Y9**, Scheme 30),⁴¹ and of Zi and coworkers (**Y15**, Scheme 30).⁴² ROP of *rac*-lactide initiated by **Y9** (LA/I=200/1) in dichloromethane, at -18°C , achieved 98% of conversion after 10 min and gave polymers with $P_i=0.81$. At 40°C and in THF, complex **Y15** initiated the ROP of *rac*-lactide (LA/I=1000/1), giving 45% of conversion after 3h and polymers with $P_i=0.67$.

Compared to these systems, complexes **56a,b** offer better activity and iso-selectivity. More studies about the performances of these two complexes are being carried out.



Scheme 30. Examples of yttrium complexes having isoselectivity in ROP of *rac*-lactide

3. Conclusion

New yttrium phosphasalen complexes **51-55a,b**, **58** have been synthesized their activities in ROP of lactide have been studied in order to evaluate the influences of steric and electronic factors in their performance. They are targeted to be monomeric and indeed, X-ray structures obtained for several of them are in accord with this hypothesis. Compared to complex **45**, complexes **51-55** present different C2 and C3 diamine linkers. From this minor change in chemical structure, whereas complex **45** is penta-coordinated and adopts distorted square-based pyramidal geometry, these complexes have hexa-coordinated yttrium centers with the coordination of one THF molecule, completing the coordination sphere constituted by the phosphasalen ligand occupying the four positions of the equatorial plane and the alkoxide group. Because of this difference, these complexes (**51-55**) are much less active than complex **45** in ROP of lactide, likely because the space available for the coordination of lactide is expected to be reduced which renders the ROP difficult. Their heteroselectivities also decrease.

Complex **58** is formed from a ligand with ethylenediamine linker as in **45**, but presenting methoxy groups, which are strong electron donating, instead of *tert*-butyl group at the *para*-positions of the phenoxide rings. This complex is strongly believe to adopt the same distorted square-planar geometry as complex **45**, with a penta-coordinated yttrium center. It presents comparable activity in ROP of lactide as complex **45**.

Complex **56a,b** feature a phosphasalen ligand with an additional amine group which could act as additional coordination site upon complexation. These two complexes are among the rare examples of yttrium complexes presenting isoselectivity in ROP of *rac*-lactide.

These results thus evidence the strong and subtle influence of steric factors in the performance of these yttrium complexes in ROP of *rac*-lactide. In particular, the shift from excellent heteroselectivities achieved with **45** and **58**, to very good isoselectivities with **56a,b** suggests a great potential in tuning the activities and stereoselectivities in yttrium-phosphasalen complexes by careful design of the phosphasalen ligands.

REFERENCES

1. (a) Ragauskas, A. J.; Williams, C. K.; Davison, B. H.; Britovsek, G.; Cairney, J.; Eckert, C. A.; Frederick, W. J.; Hallett, J. P.; Leak, D. J.; Liotta, C. L.; Mielenz, J. R.; Murphy, R.; Templer, R.; Tschaplinski, T., *Science* **2006**, *311* (5760), 484-489; (b) Williams, C. K.; Hillmyer, M. A., *Polym. Rev.* **2008**, *48* (1), 1-10; (c) Dove, A. P., *Chem. Commun.* **2008**, (48), 6446-6470; (d) Platel, R. H.; Hodgson, L. M.; Williams, C. K., *Polym. Rev.* **2008**, *48* (1), 11-63; (e) Inkinen, S.; Hakkarainen, M.; Albertsson, A. C.; Sodergard, A., *Biomacromolecules* **2011**, *12* (3), 523-532.
2. H.-G., E., *Macromolecules*. 2005 ed.; Wiley-VCH: Vol. 1.
3. (a) Coudane, J.; UstarizPeyret, C.; Schwach, G.; Vert, M., *J. Polym. Sci., Part A: Polym. Chem.* **1997**, *35* (9), 1651-1658; (b) Chamberlain, B. M.; Cheng, M.; Moore, D. R.; Ovitt, T. M.; Lobkovsky, E. B.; Coates, G. W., *J. Am. Chem. Soc.* **2001**, *123* (14), 3229-3238; (c) Kricheldorf, H. R.; Boettcher, C.; Tönnes, K.-U., *Polymer* **1992**, *33* (13), 2817-2824.
4. (a) Khanna, A.; Sudha, Y.; Pillai, S.; Rath, S., *J. Mol. Model.* **2008**, *14* (5), 367-374; (b) Stridsberg, K.; Ryner, M.; Albertsson, A.-C., Controlled Ring-Opening Polymerization: Polymers with designed Macromolecular Architecture. In *Degradable Aliphatic Polyesters*, Springer Berlin / Heidelberg: 2002; Vol. 157, pp 41-65.
5. Connor, E. F.; Nyce, G. W.; Myers, M.; Mock, A.; Hedrick, J. L., *J. Am. Chem. Soc.* **2002**, *124* (6), 914-915.
6. (a) Kim, M. S.; Seo, K. S.; Khang, G.; Lee, H. B., *Macromol. Rapid Commun.* **2005**, *26* (8), 643-648; (b) Bourissou, D.; Martin-Vaca, B.; Dumitrescu, A.; Graullier, M.; Lacombe, F., *Macromolecules* **2005**, *38* (24), 9993-9998.
7. Jensen, T. R.; Breyfogle, L. E.; Hillmyer, M. A.; Tolman, W. B., *Chem. Commun.* **2004**, (21), 2504-2505.
8. (a) Jacobsen, S.; Degee, P. H.; Fritz, H. G.; Dubois, P. H.; Jerome, R., *Polym. Eng. Sci.* **1999**, *39* (7), 1311-1319; (b) Degee, P.; Dubois, P.; Jerome, R.; Jacobsen, S.; Fritz, H. G., *Macromolecular Symposia* **1999**, *144*, 289-302.
9. O'Keefe, B. J.; Hillmyer, M. A.; Tolman, W. B., *J. Chem. Soc.- Dalton Trans.* **2001**, (15), 2215-2224.
10. Dechy-Cabaret, O.; Martin-Vaca, B.; Bourissou, D., *Chem. Rev.* **2004**, *104* (12), 6147-6176.
11. Dijkstra, P. J.; Du, H. Z.; Feijen, J., *Polymer Chemistry* **2011**, *2* (3), 520-527.
12. Spassky, N.; Wisniewski, M.; Pluta, C.; LeBorgne, A., *Macromol. Chem. Phys.* **1996**, *197* (9), 2627-2637.
13. (a) Zhong, Z. Y.; Dijkstra, P. J.; Feijen, J., *Angew. Chem. Int. Ed* **2002**, *41* (23), 4510-4513; (b) Zhong, Z. Y.; Dijkstra, P. J.; Feijen, J., *J. Am. Chem. Soc.* **2003**, *125* (37), 11291-11298.

14. Tang, Z. H.; Chen, X. S.; Pang, X.; Yang, Y. K.; Zhang, X. F.; Jing, X. B., *Biomacromolecules* **2004**, *5* (3), 965-970.
15. Nomura, N.; Ishii, R.; Yamamoto, Y.; Kondo, T., *Chem. Eur. J.* **2007**, *13* (16), 4433-4451.
16. Chen, H. L.; Dutta, S.; Huang, P. Y.; Lin, C. C., *Organometallics* **2012**, *31* (5), 2016-2025.
17. (a) Ovitt, T. M.; Coates, G. W., *J. Am. Chem. Soc.* **2002**, *124* (7), 1316-1326; (b) Ovitt, T. M.; Coates, G. W., *J. Am. Chem. Soc.* **1999**, *121* (16), 4072-4073.
18. Alaaeddine, A.; Thomas, C. M.; Roisnel, T.; Carpentier, J. F., *Organometallics* **2009**, *28* (5), 1469-1475.
19. Liu, X.; Shang, X.; Tang, T.; Hu, N.; Pei, F.; Cui, D.; Chen, X.; Jing, X., *Organometallics* **2007**, *26* (10), 2747-2757.
20. Broderick, E. M.; Diaconescu, P. L., *Inorg. Chem.* **2009**, *48* (11), 4701-4706.
21. (a) Ma, H.; Spaniol, T. P.; Okuda, J., *Inorg. Chem.* **2008**, *47* (8), 3328-3339; (b) Ma, H. Y.; Spaniol, T. P.; Okuda, J., *Angew. Chem. Int. Ed.* **2006**, *45* (46), 7818-7821; (c) Ma, H.; Okuda, J., *Macromolecules* **2005**, *38*, 2665-2673.
22. Buffet, J. C.; Kapelski, A.; Okuda, J., *Macromolecules* **2010**, *43* (24), 10201-10203.
23. (a) Tshuva, E. Y.; Groysman, S.; Goldberg, I.; Kol, M.; Goldschmidt, Z., *Organometallics* **2002**, *21* (4), 662-670; (b) Tshuva, E. Y.; Goldberg, I.; Kol, M.; Goldschmidt, Z., *Organometallics* **2001**, *20* (14), 3017-3028.
24. Cai, C.-X.; Toupet, L.; Lehmann, C. W.; Carpentier, J.-F., *J. Organomet. Chem.* **2003**, *683* (1), 131-136.
25. Cai, C. X.; Amgoune, A.; Lehmann, C. W.; Carpentier, J. F., *Chem. Commun.* **2004**, (3), 330-331.
26. (a) Bouyahyi, M.; Ajellal, N.; Kirillov, E.; Thomas, C. M.; Carpentier, J. F., *Chem. Eur. J.* **2011**, *17* (6), 1872-1883; (b) Nie, K.; Gu, X. Y.; Yao, Y. M.; Zhang, Y.; Shen, Q., *Dalton Trans.* **2010**, *39* (29), 6832-6840; (c) Clark, L.; Cushion, M. G.; Dyer, H. E.; Schwarz, A. D.; Duchateau, R.; Mountford, P., *Chem. Commun.* **2010**, *46* (2), 273-275; (d) Zhang, Z. J.; Xu, X. P.; Li, W. Y.; Yao, Y. M.; Zhang, Y.; Shen, Q.; Luo, Y. J., *Inorg. Chem.* **2009**, *48* (13), 5715-5724; (e) Dyer, H. E.; Huijser, S.; Schwarz, A. D.; Wang, C.; Duchateau, R.; Mountford, P., *Dalton Trans.* **2008**, (1), 32-35; (f) Amgoune, A.; Thomas, C. M.; Roisnel, T.; Carpentier, J. F., *Chem.-Eur. J.* **2006**, *12*, 169-179; (g) Bonnet, F.; Cowley, A. R.; Mountford, P., *Inorg. Chem.* **2005**, *44* (24), 9046-9055; (h) Cai, C. X.; Amgoune, A.; Lehmann, C. W.; Carpentier, J. F., *Chem. Commun.* **2004**, 330-331; (i) Shang, X. M.; Liu, X. L.; Cui, D. M., *J. Polym. Sci., Part A: Polym. Chem.* **2007**, *45* (23), 5662-5672; (j) Miao, W.; Li, S. H.; Zhang, H. X.; Cui, D.; Wang, Y. R.; Huang, B. T., *J. Organomet. Chem.* **2007**, *692* (22), 4828-4834; (k) Liu, X. L.; Shang, X. M.; Tang, T.; Hu, N. H.; Pei, F. K.; Cui, D. M.; Chen, X. S.; Jing, X. B., *Organometallics* **2007**, *26* (10), 2747-2757; (l) Amgoune, A.; Thomas, C. M.; Carpentier, J. F., *Pure Appl. Chem.* **2007**, *79* (11), 2013-2030; (m) Amgoune, A.; Thomas, C. M.; Carpentier, J. F., *Macromol. Rapid*

Commun. **2007**, 28 (6), 693-697; (n) Zhao, W.; Cui, D. M.; Liu, X. L.; Chen, X. S., *Macromolecules* **2010**, 43 (16), 6678-6684.

27. (a) Arnold, P. L.; Buffet, J. C.; Blaudeck, R.; Sujecki, S.; Wilson, C., *Chem. Eur. J.* **2009**, 15 (33), 8241-8250; (b) Arnold, P. L.; Buffet, J. C.; Blaudeck, R. P.; Sujecki, S.; Blake, A. J.; Wilson, C., *Angew. Chem. Int. Ed.* **2008**, 47 (32), 6033-6036.

28. (a) Platel, R. H.; White, A. J. P.; Williams, C. K., *Inorg. Chem.* **2008**, 47 (15), 6840-6849; (b) Platel, R. H.; White, A. J. P.; Williams, C. K., *Chem. Commun.* **2009**, (27), 4115-4117; (c) Hodgson, L. M.; Platel, R. H.; White, A. J. P.; Williams, C. K., *Macromolecules* **2008**, 41 (22), 8603-8607; (d) Platel, R. H.; Hodgson, L. M.; White, A. J. P.; Williams, C. K., *Organometallics* **2007**, 26 (20), 4955-4963; (e) Hodgson, L. M.; White, A. J. P.; Williams, C. K., *J. Polym. Sci., Part A: Polym. Chem.* **2006**, 44 (22), 6646-6651.

29. Broderick, E. M.; Thuy-Boun, P. S.; Guo, N.; Vogel, C. S.; Sutter, J.; Miller, J. T.; Meyer, K.; Diaconescu, P. L., *Inorg. Chem.* **2011**, 50 (7), 2870-2877.

30. Wu, J. C.; Huang, B. H.; Hsueh, M. L.; Lai, S. L.; Lin, C. C., *Polymer* **2005**, 46 (23), 9784-9792.

31. Chen, H.-Y.; Huang, B.-H.; Lin, C.-C., *Macromolecules* **2005**, 38 (13), 5400-5405.

32. Binda, P. I.; Delbridge, E. E., *Dalton Trans.* **2007**, (41), 4685-4692.

33. (a) Chisholm, M. H.; Gallucci, J.; Phomphrai, K., *Chem. Commun.* **2003**, (1), 48-49; (b) Chmura, A. J.; Davidson, M. G.; Frankis, C. J.; Jones, M. D.; Lunn, M. D., *Chem. Commun.* **2008**, (11), 1293-1295; (c) Ma, H. Y.; Spaniol, T. P.; Okuda, J., *Angew. Chem. Int. Ed.* **2006**, 45 (46), 7818-7821.

34. Platel, R.; Hodgson, L.; White, A.; Williams, C., *Organometallics* **2007**, 26, 4955-4963.

35. Broderick, E. M.; Guo, N.; Vogel, C. S.; Xu, C.; Sutter, J. r.; Miller, J. T.; Meyer, K.; Mehrkhodavandi, P.; Diaconescu, P. L., *J. Am. Chem. Soc.* **2011**, 133 (24), 9278-9281.

36. M. J. Frisch; G. W. Trucks; H. B. Schlegel; G. E. Scuseria; M. A. Robb; J. R. Cheeseman; J. A. Montgomery, Jr., T. V.; K. N. Kudin; J. C. Burant; J. M. Millam; S. S. Iyengar; J. Tomasi; V. Barone; B. Mennucci; M. Cossi; G. Scalmani; N. Rega; G. A. Petersson, H. N., M. Hada, M. Ehara, K. Toyota, R. Fukuda, J. Hasegawa, M. Ishida, T. Nakajima, Y. Honda, O. Kitao, H. Nakai, M. Klene, X. Li, J. E. Knox, H. P. Hratchian, J. B. Cross, V. Bakken, C. Adamo, J. Jaramillo, R. Gomperts, R. E. Stratmann, O. Yazyev, A. J. Austin, R. Cammi, C. Pomelli, J. W. Ochterski, P. Y. Ayala, K. Morokuma, G. A. Voth, P. Salvador, J. J. Dannenberg, V. G. Zakrzewski, S. Dapprich, A. D. Daniels, M. C. Strain, O. Farkas, D. K. Malick, A. D. Rabuck, K. Raghavachari, J. B. Foresman, J. V. Ortiz, Q. Cui, A. G. Baboul, S. Clifford, J. Cioslowski, B. B. Stefanov, G. Liu, A. Liashenko, P. Piskorz, I. Komaromi, R. L. Martin, D. J. Fox, T. Keith, M. A. Al-Laham, C. Y. Peng, A. Nanayakkara, M. Challacombe, P. M. W. Gill, B. Johnson, W. Chen, M. W. Wong, C. Gonzalez, and J. A. Pople *Gaussian 03, revision C.02*, Gaussian Inc., Wallingford CT: 2004.

37. (a) Becke, A. D., *J. Chem. Phys.* **1993**, 98 (7), 5648-5652; (b) Perdew, J. P.; Wang, Y., *Phys. Rev. B* **1992**, 45 (23), 13244-13249.

38. (a) Haussermann, U.; Dolg, M.; Stoll, H.; Preuss, H.; Schwerdtfeger, P.; Pitzer, R. M., *Mol. Phys.* **1993**, 78 (5), 1211-1224; (b) Dolg, M.; Wedig, U.; Stoll, H.; Preuss, H., *J. Chem. Phys.* **1987**, 86 (2), 866-872.
39. Ehlers, A. W.; Bohme, M.; Dapprich, S.; Gobbi, A.; Hollwarth, A.; Jonas, V.; Kohler, K. F.; Stegmann, R.; Veldkamp, A.; Frenking, G., *Chem. Phys. Lett.* **1993**, 208 (1-2), 111-114.
40. Petersson, G. A.; Bennett, A.; Tensfeldt, T. G.; Allaham, M. A.; Shirley, W. A.; Mantzaris, J., *J. Chem. Phys.* **1988**, 89 (4), 2193-2218.
41. Arnold, P. L.; Buffet, J.-C.; Blaudeck, R. P.; Sujecki, S.; Blake, A. J.; Wilson, C., *Angew. Chem. Int. Ed.* **2008**, 47 (32), 6033-6036.
42. Zi, G.; Xiang, L.; Liu, X.; Wang, Q.; Song, H., *Inorg. Chem. Commun.* **2010**, 13 (3), 445-448.

Conclusion

The presented work describes the development of new multidentate ligands combining iminophosphorane and anionic donors such as thiolate or phenolate. These ligands can be easily synthesised from inexpensive, readily available starting materials and in large scale.

Chapter 1 is centered on the development of bidentate ligands [S, P=N], taking into account the importance of sulfur-containing ligands in nature and in coordination chemistry. The synthesis of such ligands relied on ortho-lithiation reaction. Working on such syntheses, we discovered the conditions for a clean nucleophilic substitution on iminophosphorane. This reaction opened a way to various mixed bidentate ligands combining iminophosphorane and different heteroatoms-containing groups (phosphine, phosphole, silane, borane, etc) with a special ligand skeleton [N=P-CH₂-X]. The thiolate-containing ligand having such skeleton showed a great coordination ability and was coordinated to different transition metal precursors of groups 8, 9, 10. In particular, the discrete [NiN₂S₂] complex resulted from the reaction of the ligand with 2 equiv. of [NiBr₂(DME)] could act as bidentate ligand through electron pairs on sulfur atoms, leading to bimetallic complexes.

Chapter 2 describes the development of nickel complexes of new bidentate [O, P=N] ligands, containing phenoxide and iminophosphorane groups for the oligomerisation of ethylene. The presence of the anionic phenoxide group on the ligands allowed the coordination of a second metal centre, such as lithium or aluminum, leading to bimetallic complexes. Mono-nuclear complexes were obtained by using additional auxiliary ligands. The activities and selectivities of the synthesized nickel iminophosphorane-phenoxide complexes are in general significantly higher than complexes of (N,O) and (P,O) ligands existing in the literature. Their performances in terms of TOF and selectivities (in C₄ and in 1-C₄) vary greatly in function of the auxiliary ligand or substituents at the nitrogen atoms. The comparisons of performances between the synthesized complexes could be used for the fine design of new nickel complexes efficient for the dimerisation of ethylene. Furthermore, the formation of bimetallic nickel-lithium and nickel-aluminum complexes is interesting and opens the possibility to develop of self-activated bimetallic nickel-aluminum complexes for the oligomerisation of ethylene, based on iminophosphorane ligands.

Chapters 3, 4, 5 focused on the development of tetradentate phosphasalen ligands, associating two iminophosphoranes and two phenoxides. They are the phosphorus analogues of a well-known and important class of ligands in coordination and catalysis: the salens. Chapter 3 described the conception and the synthesis of phosphasalen ligands in general, and the unsubstituted phosphasalen in particular. Experimental and theoretical studies have been carried

out on nickel and palladium complexes, in order to better understand their differences from the salen analogs. It has been found that as expected, the phosphasalen ligand is better donating and slightly more flexible than the analogue salen.

These properties prompted us to test the utility of phosphasalens in the stabilization of oxidized metal complexes. Due to the interest in phenoxyl radical and mix-valence complexes, oxidized species of nickel salen complexes have been the subjects pursued by many groups. We were thus interested in studying the oxidation of Ni(II) phosphasalen complexes to see the electronic differences conferred by the phosphasalen ligands compared to salens. This is the subject of chapter 4. Two new nickel phosphasalen complexes were synthesised and were cleanly oxidised by one equivalent of silver salt in dichloromethane. X-ray structure was obtained for one of these two products (complex **[6a][SbF₆]**). At the difference of all reported oxidised nickel-phenoxide complexes up to now, which have been shown to be Ni(II) complexes of phenoxyl radical, the oxidised species **[6a][SbF₆]** is a Ni(III) complex. This has been shown by EPR spectroscopy and DFT calculations. This complex is one of rare example of Ni(III) complexes with coordination number less than 5, and is the first example of four-coordinated high valent Ni(III) phenoxide species.

The obtainment of this Ni(III) complex could be seen as the first, encouraging example for the use of phosphasalen ligands in stabilising high-valent metal centres. One can imagine, for example, the development of phosphasalen oxo complexes of metals such as chromium or manganese in order to shed more light into the mechanism of catalysed asymmetric epoxidation, as this process is often carried out using chromium or manganese salen complexes and is suspected to involve an oxo intermediate. Up to date, no oxo salen complex of manganese has been isolated, likely because of their instability. Due to their better donating ability, phosphasalen ligands could help stabilise such oxidised complexes.

Chapter 5 presents the use of aluminium and yttrium phosphasalen complexes in the ring opening polymerisation of lactide. In particular, interesting results have been obtained for the yttrium complexes, both in terms of coordination chemistry and catalysis.

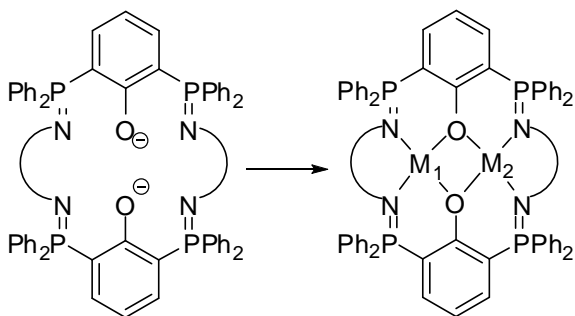
In the coordination point of view, it has been observed that due to the flexibilities of the phosphasalen ligands, their complexes adopt completely different geometries, depending on the diamine linker, the substituents on the phosphasalen ligands, the auxiliary alkoxide ligand. Dimeric and monomeric complexes were obtained, and showed completely different activities in ROP of rac-lactide. Whereas ROP initiated by the dimeric complexes follow a second-order in lactide, the ones initiated by monomeric complexes are first order in lactide. Inside the monomeric complexes, activities change drastically with different structures. The most active and heteroselective complexes are the monomeric ones with ethylene diamine linker. Interestingly, yttrium complexes of a penta-dentate phosphasalen ligand even offer good isoselectivities, which is really rare for yttrium chemistry. The comparisons of activities between different complexes help clarify the design of the ideal initiator for the ROP of lactide.

In particular, whereas the yttrium salen complexes only have limited performance in ring-opening polymerisation of lactide, yttrium complexes of phosphasalen ligands are among the

Conclusion

best initiators in terms of both activity and stereo-selectivity. These results demonstrate the various perspectives of phosphasalen ligands in catalysis.

The method for the synthesis of phosphasalen ligands, and the very encouraging results obtained with their complexes in coordination and catalysis could also inspired new phosphasalen-like ligands, such as the hexa-dentate ones (whose general structure is presented below) for the development of bimetallic species.



Experimental Section

I. Chapter 1.

General Considerations

All experiments, unless otherwise stated, were performed under an atmosphere of dry nitrogen or argon using standard schlenk and glove box techniques. Solvents were freshly distilled under dry nitrogen from Na/benzophenone (THF, diethylether, petroleum ether), from P₂O₅ (dichloromethane). **1a,c**,¹ [NiBr₂(DME)],² [Ir(COD)Cl]₂, [Rh(COD)Cl]₂,³ [RuCl₂(*p*-cymene)]⁴ were prepared according to the literature. All other reagents and chemicals were obtained commercially and used without further purification.

Nuclear magnetic resonance spectra were recorded on Bruker Avance 300 spectrometer operating at 300 MHz for ¹H, 75.5 MHz for ¹³C and 121.5 MHz for ³¹P. Solvent peaks were used as internal references for ¹H and ¹³C chemical shifts (ppm). ³¹P{¹H} are relative to a 85% H₃PO₄ external reference. Coupling constant are expressed in hertz. The following abbreviations are used: br, broad; s, singlet; d, doublet; dd, doublet of doublets; t, triplet; m, multiple; v, virtual. The labeling schemes of the ligands and ligand precursors are given in schemes 7 and 9. Elemental analyses (for several compounds) were performed by the Elemental analysis service of the London Metropolitan University (United Kingdom).

Synthesis of aminophosphonium compounds by Kirsanov reaction

1b: Br₂ (0.98 mL, 19.07 mmol) was added dropwise to a solution of PPh₃ (5g, 19.07 mmol) in CH₂Cl₂ (200 mL) at -78°C under nitrogen. The cold bath was removed and stirring was continued for 45 minutes at room temperature. The obtained suspension was then cooled again to -78°C and Et₃N (2.65 mL, 19.07 mmol) was added, followed by the addition of adamantylamine RNH₂ (2.88 g, 19.07 mmol). Stirring was continued for several hours at room temperature to give a transparent solution. After washing twice with H₂O, the organic layer was dried over MgSO₄, the solvent was reduced in volume and THF was added. The white precipitated product was separated by filtration, dried in vacuum. (6.0 g, 64%)

1b: ³¹P{¹H} NMR (CDCl₃): δ 32.0 (s, *P*^V); ¹H NMR (CDCl₃): δ 7.94 (ddd, ⁴J_{H,H}=1.0 Hz, ³J_{H,H}=7.5 Hz, ³J_{P,H}=13.0 Hz, 6H, *o*-CH(PPh₃)), 7.69 (vtd, ⁴J_{H,H}= 1.0 Hz, ³J_{H,H}=7.5 Hz, 3H, *p*-

$CH(PPh_2)$), 7.59 (vtd, $^3J_{H,H}=^3J'_{H,H}=7.5$ Hz, $^4J_{P,H}=3.5$ Hz, 6H, $m-CH(PPh_2)$), 7.18 (d, $^2J_{P,H}=6.0$ Hz, 1H, NH), 1.89 (s, 9H, NH- CH_2-CH- and $-CH(CH_2)_3$), 1.44 (m, 6H, $-CH-CH_2-CH-$); $^{13}C\{^1H\}$ NMR ($CDCl_3$): δ 134.8 (d, $^4J_{P,C}=2.8$ Hz, $p-CH(PPh_3)$), 134.0 (d, $^2J_{P,C}=11.5$ Hz, $o-CH(PPh_3)$), 129.6 (d, $^3J_{P,C}=13.0$ Hz, $o-CH(PPh_3)$), 123.4 (d, $^1J_{P,C}=102.1$ Hz, $C^{IV}(PPh_3)$), 57.7 (d, $^2J_{P,C}=4.7$ Hz, NH- $C(CH_2)_3$), 44.7 (d, $^3J_{P,C}=4.4$ Hz, NH- $C(CH_2)_3$), 36.6 (s, $-CH-CH_2-CH-$), 30.0 (s, $-CH(CH_2)_3$);

Synthesis of 2a,b

MeLi (1.6M in Et_2O , 1.25 mL, 2 mmol) was added dropwise to a suspension of the starting aminophosphonium salt (1 mmol) in THF (10 mL) at $-78^\circ C$. The cold bath was removed and stirring is continued at room temperature for 3h to give an orange-red (or red wine) solution. S_8 (32 mg, 1/8 mmol) was then added in the dry box to give a yellow-to-orange solution. Stirring was continued for 30 minutes. $HBF_4 \cdot Et_2O$ (322 mg, 2mmol) was added to protonate the thiolate-iminophosphorane. THF was removed in vacuum and CH_2Cl_2 (25mL) was added. The reaction mixture was washed twice with an aqueous solution of HBF_4 0.1M (15 mL), once with a saturated solution of $NaBF_4$ (15 mL) in water and dried over $MgSO_4$. CH_2Cl_2 was evaporated and the recrystallisation was taken in THF, giving the desired product as a white solid.

2a: (370 mg, 81%). $^{31}P\{^1H\}$ NMR ($CDCl_3$): δ 36.1 (s, P^V); 1H NMR ($CDCl_3$): δ 7.85 (ddd, $^4J_{H,H}=2.0$ Hz, $^3J_{H,H}=7.5$ Hz, $^3J_{P,H}=13.2$ Hz, 4H, $o-CH(PPh_2)$), 7.85 (m, 1H, C_dH), 7.75 (vtd, $^4J_{H,H}=2.0$ Hz, $^3J_{H,H}=7.5$ Hz, 2H, $p-CH(PPh_2)$), 7.65 (vtd, $^3J_{H,H}=^3J'_{H,H}=7.5$ Hz, $^4J_{P,H}=3.5$ Hz, 4H, $m-CH(PPh_2)$), 7.60 (m, 2H, C_bH and $C_{a/c}H$), 7.47 (vtdd, $^3J_{H,H}=^3J'_{H,H}=7.5$ Hz, $^4J_{H,H}=1.0$ Hz, $^4J_{P,H}=3.0$ Hz, 1H, $C_{a/c}H$), 4.82 (d, $^2J_{P,H}=8.0$ Hz, 1H, NH), 4.02 (s, 1H, SH), 1.29 (s, 9H, $C^{IV}(CH_3)_3$); $^{13}C\{^1H\}$ NMR ($CDCl_3$): δ 138.8 (d, $^2J_{P,C}=8.4$ Hz, SC^{IV}), 136.6 (d, $^2J_{P,C}=11.50$ Hz, C_dH), 135.5 (d, $^3J_{P,C}=10.0$ Hz, $C_{a/c}H$), 135.5 (s, C_bH), 135.3 (d, $^4J_{P,C}=3.0$ Hz, $p-CH(PPh_2)$), 133.9 (d, $^2J_{P,C}=11.3$ Hz, $o-CH(PPh_2)$), 130.4 (d, $^3J_{P,C}=13.5$ Hz, $m-CH(PPh_2)$), 127.4 (d, $^3J_{P,C}=12.7$ Hz, $C_{a/c}H$), 122.2 (d, $^1J_{P,C}=103.8$ Hz, $C^{IV}(PPh_2)$), 121.8 (d, $^1J_{P,C}=105.1$ Hz, $C^{IV}-PPh_2$), 57.2 (d, $^2J_{P,C}=4.5$ Hz, $C^{IV}(CH_3)_3$), 32.0 (d, $^3J_{P,C}=4.0$ Hz, $C^{IV}(CH_3)_3$)

2b: (345 mg, 65%). $^{31}P\{^1H\}$ NMR ($CDCl_3$): δ 34 (s, P^V); 1H NMR ($CDCl_3$): δ 7.88 (ddd, $^4J_{H,H}=2.0$ Hz, $^3J_{H,H}=7.0$ Hz, $^3J_{P,H}=13.5$ Hz, 4H, $o-CH(PPh_2)$), 7.78 (m, 1H, C_dH), 7.74 (vtd, $^4J_{H,H}=2.0$ Hz, $^3J_{H,H}=7.0$ Hz, 2H, $p-CH(PPh_2)$), 7.65 (vtd, $^3J_{H,H}=^3J'_{H,H}=7.0$ Hz, $^4J_{P,H}=3.5$ Hz, 4H, $m-CH(PPh_2)$), 7.59 (m, 2H, C_bH and C_aH), 7.48 (vtdd, $^3J_{H,H}=^3J'_{H,H}=7.5$ Hz, $^4J_{H,H}=1.0$ Hz, $^4J_{P,H}=3.0$ Hz, 1H, C_cH), 4.78 (d, $^2J_{P,H}=7.5$ Hz, 1H, NH), 1.97 (m, 3H, $CH(CH_2)_3$), 1.86 (s, 6H, NH- CH_2-CH-), 1.50 (m, 6H, $-CH-CH_2-CH-$); $^{13}C\{^1H\}$ NMR ($CDCl_3$): δ 140.3 (d, $^2J_{P,C}=6.0$ Hz, SC^{IV}), 136.4 (d, $^2J_{P,C}=12.50$ Hz, C_dH), 135.5 (d, $^3J_{P,C}=9.5$ Hz, $C_{a/c}H$), 135.2 (d, $^4J_{P,C}=2.5$ Hz, C_bH), 135.0 (d, $^4J_{P,C}=2.7$ Hz, $p-CH(PPh_2)$), 134.2 (d, $^2J_{P,C}=11.3$ Hz, $o-CH(PPh_2)$), 130.0 (d, $^3J_{P,C}=13.3$ Hz, $m-CH(PPh_2)$), 126.8 (d, $^3J_{P,C}=13.1$ Hz, $C_{a/c}H$), 123.2 (d, $^1J_{P,C}=102.9$ Hz, $C^{IV}(PPh_2)$), 122.1 (d, $^1J_{P,C}=105.5$ Hz, $C^{IV}-PPh_2$), 58.4 (d, $^2J_{P,C}=5.1$ Hz, NH- $C(CH_2)_3$), 44.7 (d, $^3J_{P,C}=4.0$ Hz, NH- $C(CH_2)_3$), 35.9 (s, $-CH-CH_2-CH-$), 30.3 (s, $-CH(CH_2)_3$)

Synthesis of 2a' from 2a

MeLi (1.6M in Et₂O, 250 μ L, 0.4 mmol) was added dropwise to a suspension of the starting thiol aminophosphonium salt **2a** (181 mg, 0.4 mmol) in THF (4 mL) at -20°C. The cold bath was removed and stirring is continued at room temperature for 15 min to give a bright orange solution. ³¹P{¹H} NMR exhibited a singlet at +36 ppm. Addition of dibromoethane (17 μ L, 0.2 mmol) into the solution yielded a white slurry after overnight stirring at room temperature. The precipitate was isolated, washed with THF and dried in vacuum. (104 mg, 55%)

2a': ³¹P{¹H} NMR (CDCl₃): δ 32 (s, P^V); ¹H NMR (CDCl₃): δ 7.99 (dd, ³J_{H,H}=7.5 Hz, ³J_{H,H}=14.0 Hz, 2H, C_dH), 7.92 (vtd, ³J_{H,H}=³J_{H,H}=7.5 Hz, ⁴J_{P,H}=4.0 Hz, 4H, *m*-CH(PPh₂)), 7.85 (dd, ³J_{H,H}=7.5 Hz, ³J_{P,H}=13.0 Hz, 4H, *o*-CH(PPh₂)), 7.61 (m, 16H, CH(PPh₂) + C_{a/c,b}H), 7.48 (vtd, ³J_{H,H}=³J_{H,H}=7.5 Hz, ⁴J_{P,H}=3.0 Hz, 2H, C_{a/c}H), 2.32 (s, 2H, CH₂-CH₂), 1.42 (s, 2H, CH₂-CH₂), 1.41 (s, 18H, C(CH₃)₃); ¹³C{¹H} NMR (CDCl₃): δ 142.2 (d, ²J_{P,C}=6.0 Hz, SC^{IV}), 136.3 (d, ²J_{P,C}=12.0 Hz, C_dH), 135.8 (d, ⁴J_{P,C}=1.0 Hz, C_bH), 134.6 (d, ⁴J_{P,C}=2.5 Hz, *p*-CH(PPh₂)), 133.7 (d, ^{2/3}J_{P,C}=11.3 Hz, *o*- or *m*-CH(PPh₂)), 133.3 (d, ³J_{P,C}=9.5 Hz, C_{a/c}H), 129.9 (d, ^{2/3}J_{P,C}=9.5 Hz, *o*- or *m*-CH(PPh₂)), 127.7 (d, ³J_{P,C}=12.5 Hz, C_{a/c}H), 124.0 (d, ¹J_{P,C}=101.5 Hz, C^{IV}-PPh₂), 123.5 (d, ¹J_{P,C}=104.0 Hz, C^{IV}(PPh₂)), 57.0 (d, ²J_{P,C}=4.5 Hz, C^{IV}(CH₃)₃), 34.3 (s, CH₂-CH₂), 30.8 (d, ³J_{P,C}=4.0 Hz, C^{IV}(CH₃)₃)

Synthesis of 3a

Addition of 2 equiv. of MeLi (1.6M, 250 μ L, 0.4 mmol) into a slurry of the thiol-aminophosphonium salt **2a** (90.6 mg, 0.2 mmol) in THF gave rapidly a cloudy colorless solution. After 30 min, [PdCl₂(PPh₃)₂] (140.4 mg, 0.2 mmol) was added, inducing a rapid change of color from deep red wine to bright orange-red. Completeness of the reaction after one day was monitored in ³¹P{¹H}-NMR spectrum by the disappearance of the signal of free ligand at +12.9 ppm, and the apparition of two doublets at +31.8 ppm (J_{P,P}=3.5 Hz) and +15.4 ppm (J_{P,P}=3.5 Hz). THF was evaporated and dichloromethane was introduced to precipitate insoluble lithium salt, which were then removed by centrifugation. The product was isolated by evaporation of dichloromethane as a red solid. (120 mg, 78%)

3a: ³¹P{¹H} NMR (CDCl₃): δ 31.3 (d, ³J_{P,P}=3.5 Hz, P^V), 15.5 (d, ³J_{P,P}=3.5 Hz, PPh₃); ¹H NMR (CDCl₃): δ 8.18 (m, 2H, *o*-CH(PPh₂)), 7.68 (m, 4H, C_dH + *o*-CH(PPh₂) + *p*-CH(PPh₂)), 7.29 (m, 13H, *o*-CH(PPh₃) + *p*-CH(PPh₃) + *m*-CH(PPh₂)), 7.17 (m, 7H, *m*-CH(PPh₃) + C_bH), 7.07 (m, 2H, C_aH + *p*-CH(PPh₂)), 6.87 (m, 1H, C_cH); ¹³C{¹H} NMR (CDCl₃): δ 152.0 (dd, ²J_{P,C}=7.0 Hz, ³J_{P,C}=4.0 Hz, SC^{IV}), 134.9 (d, ²J_{P,C}=10.5 Hz, *o*-CH(PPh₂)), 134.4 (d, ²J_{P,C}=10.5 Hz, *o*-CH(PPh₂) and C_dH), 134.3 (d, ²J_{P,C}=10.5 Hz, *o*-CH(PPh₃)), 133.9 (d, ³J_{P,C}=11.0 Hz, C_aH), 131.6 (d, ⁴J_{P,C}=3.0 Hz, *p*-CH(PPh₂)), 131.3 (s, C_cH), 130.1 (d, ⁴J_{P,C}=2.5 Hz, *p*-CH(PPh₂)), 129.6 (d, ¹J_{P,C}=52.0 Hz, C^{IV}(PPh₃)), 129.4 (d, ⁴J_{P,C}=2.5 Hz, *p*-CH(PPh₃)), 128.7 (d, ¹J_{P,C}=56.0 Hz, C^{IV}(PPh₂)), 127.7 (d, ³J_{P,C}=12.0 Hz, *m*-CH(PPh₂)), 121.0 (d, ¹J_{P,C}=93.5 Hz, C^{IV}-PPh₂), 119.8 (d, ³J_{P,C}=11.0 Hz, C_cH), 57.3 (dd, ²J_{P,C}=4.5 Hz, ³J_{P,C}=2.0 Hz, C^{IV}(CH₃)₃), 25.0 (s, C^{IV}(CH₃)₃)

Synthesis of **5**

MeLi (1.6 M in Et₂O, 4 mL, 6.4 mmol) was added dropwise to a suspension of **1c** (1.390 g, 3.2 mmol) in THF (32 mL) at -78°C. The cold bath was removed and stirring is continued at room temperature for four hours to give an orange-red solution. S₈ (102 mg, 0.4 mmol) was then added in the dry box to give a yellow-to-orange solution. A precipitate appeared after one hour. After three hours, the precipitate was isolated, washed with THF and dried in vacuum. This white solid, which is **5** could be used for further complexation tests. (710 mg, 55%)

5: ³¹P {¹H} NMR (Pyr-d₅) δ 21.3 (s); ¹H NMR (Pyr-d₅) δ 8.22 (dd, ³J_{H,H} = 7.5 Hz, ³J_{P,H} = 9.5 Hz, 4H, *o*-CH(PPh₂)), 7.64 (t, ³J_{H,H} = 7.5 Hz, 2H, *p*-CH (PPh₂)), 7.54 (td, ³J_{H,H} = 7.5 Hz, ⁴J_{P,H} = 1.0 Hz, 4H, *m*-CH(PPh₂)), 7.40 (t, ³J_{H,H} = 7.0 Hz, 2H, *o*-CH(NPh)), 7.28 (t, ³J_{H,H} = 7.0 Hz, 2H, *m*-CH(NPh)), 6.89 (t, ³J_{H,H} = 7.0 Hz, 1H, *p*-CH(NPh)), 4.18 (d, ²J_{P,H} = 7.0 Hz, 2H, PCH₂), 3.84 (m, 4H, OCH₂(THF)), 1.80 (m, 4H, CH₂(THF)); ¹³C NMR (Pyr-d₅): δ 155.8 (d, ²J_{P,C} = 5.5 Hz, C^{IV}(NPh)), 135.4 (d, ²J_{P,C} = 8.0 Hz, *o*-CH(PPh₂)), 134.1 (d, ⁴J_{P,C} = 2.5 Hz, *p*-CH(PPh₂)), 133.6 (d, ¹J_{P,C} = 78.5 Hz, C^{IV}(PPh₂)), 131.6 (d, ³J_{P,C} = 1.0 Hz, *m*-CH(NPh)), 131.1 (d, ³J_{P,C} = 10.5 Hz *m*-CH(PPh₂)), 125.4 (d, ³J_{P,C} = 17.6 Hz, *o*-CH(NPh)), 119.8 (s, *p*-CH(NPh)), 70.2 (s, OCH₂(THF)), 31.5 (d, ¹J_{P,C} = 88.0 Hz, PCH₂), 28.2 (s, CH₂(THF)).

Synthesis of **6**

HBF₄(Et₂O)₂ (0.46 mmol, 63 μl) was added to a solution of **5** (92 mg, 0.23 mmol) in THF giving a colorless solution. The solvent was removed and the residue was taken in CH₂Cl₂ (5 mL). After removal of insoluble lithium salts by filtration under N₂, the solvent was evaporated to afford aminophosphonium salt **6** (67 mg, 70%).

6: ³¹P {¹H} NMR (CDCl₃) δ 35.9 (s); ¹H NMR (CDCl₃) δ 7.86 (dd, ³J_{H,H} = 7.5 Hz, ³J_{P,H} = 9.5 Hz, 4H, *o*-CH(PPh₂)), 7.69 (t, ³J_{H,H} = 7.5 Hz, 2H, *p*-CH (PPh₂)), 7.56 (td, ³J_{H,H} = 7.5 Hz, ⁴J_{P,H} = 3.5 Hz, 4H, *m*-CH(PPh₂)), 7.34 (d, ²J_{P,H} = 9.5 Hz, 1H, NH), 7.00 (t, ³J_{H,H} = 7.5 Hz, 2H, *m*-CH(NPh)), 6.87 (t, ³J_{H,H} = 7.5 Hz, 1H, *p*-CH(NPh)), 6.80 (d, ³J_{H,H} = 7.5 Hz, 2H, *o*-CH(NPh)), 3.85 (d, ²J_{P,H} = 7.5 Hz, 2H, PCH₂), 2.00 (td, ³J_{H,H} = 9.0 Hz, ³J_{P,H} = 2.0 Hz, 1H, SH); ¹³C NMR (CDCl₃) δ 18.7 (d, ¹J_{P,C} = 69.0 Hz, PCH₂), 116.8 (d, ¹J_{P,C} = 99.5 Hz, C^{IV}(PPh₂)), 119.0 (d, ³J_{P,C} = 17.6 Hz, *o*-CH(NPh)), 123.1 (s, *p*-CH(NPh)), 128.6 (s, *m*-CH(NPh)), 129.2 (d, ³J_{P,C} = 13.5 Hz, *m*-CH(PPh₂)), 132.5 (d, ²J_{P,C} = 10.5 Hz, *o*-CH(PPh₂)), 134.7 (d, ⁴J_{P,C} = 3.0 Hz, *p*-CH(PPh₂)), 136.3 (d, ²J_{P,C} = 3.0 Hz, C^{IV}(NPh)). Anal. Calcd for C₁₉H₁₉BF₄NPS: C, 55.50; H, 4.66; N, 3.41. Found: C, 55.21; H, 4.94; N, 3.09.

Synthesis of **9**

MeLi (1.6 M in Et₂O, 725 μL, 1.16 mmol) was added dropwise to a suspension of **1c** (0.58 mmol, 250 mg) in THF (6 mL) at -78°C. The cold bath was removed and stirring is continued at room temperature for four hours to give an orange-red solution. Dicyclohexylphosphine chloride (0.58 mmol, 128 μl) was added giving a clear yellow solution. After 30 minutes of stirring at room temperature, solvent was evaporated, the residue was taken in dichloromethane (7 mL). The reaction mixture was washed with aqueous HCl 2M solution (2x7 mL), the organic

phase was then dried on Na₂SO₄ and filtered under N₂. The solvent was evaporated and the product was precipitated in petroleum ether was a white solid (228 mg, 75%).

9: ³¹P {¹H} NMR (CD₂Cl₂): δ -22.2 (d, ²J_{P,P} = 87.5 Hz, PCy₂), 34.8 (d, ²J_{P,P} = 87.5 Hz, PPh₂); ¹H NMR (CD₂Cl₂): δ 8.01 (dd, ³J_{H,H} = 8.0 Hz, ³J_{P,H} = 13.0 Hz, 4H, *o*-CH(Ph₂P)), 7.57 (m, 6H, *m*- and *p*-CH(Ph₂P)), 6.99 (d, ³J_{H,H} = 7.5 Hz, 2H, *m*-CH(NPh)), 6.90 (d, ³J_{H,H} = 7.5 Hz, 2H, *o*-CH(NPh)), 6.82 (t, ³J_{H,H} = 7.5 Hz, 1H, *p*-CH(NPh)), 3.22 (d, ²J_{P,H} = 16.5 Hz, 2H, PCH₂), 0.80-1.52 (22H, m, Cy); ¹³C NMR (CD₂Cl₂): δ 138.5 (d, ²J_{P,C} = 3.0 Hz, C^{IV}(NPh)), 133.8 (d, ⁴J_{P,C} = 3.0 Hz, *p*-CH(PPh₂)), 133.0 (dd, ³J_{P,C} = 10.1 and ³J_{P,C} = 4.5 Hz, *o*-CH(PPh₂)), 128.2 (s, *m*-CH(NPh)), 128.7 (d, ²J_{P,C} = 13.0 Hz, *m*-CH(PPh₂)), 122.0 (s, *p*-CH(NPh)), 119.7 (d, ¹J_{P,C} = 97.5 Hz, C^{IV}(PPh₂)), 119.3 (d, ³J_{P,C} = 7.5 Hz, *o*-CH(NPh)), 33.1 (dd, ³J_{P,C} = 8.0 Hz and ¹J_{P,C} = 15.0 Hz, CH(Cy)), 28.2 (t, ³J_{P,C} = 13.0 Hz, CH₂(Cy)), 26.2 (d, ¹J_{P,C} = 12.0 Hz, CH₂(Cy)), 25.2 (s, CH₂(Cy)), 18.7 (dd, ¹J_{P,C} = 39.0 Hz and ¹J_{P,C} = 68.0 Hz, PCH₂). Anal. Calcd for C₃₁H₄₀ClNP₂: C, 71.05; H, 7.69; N, 2.67. Found: C, 71.28; H, 7.47; N, 2.36.

Synthesis of 10

10 (0.139 g, 60 %) was obtained with a procedure similar to that used for **9** using trimethylsilylchloride (0.58 mmol, 75 μl) as the electrophile.

10: ³¹P {¹H} NMR (CDCl₃): δ 37.2 (s); ¹H NMR (CDCl₃): δ 7.91 (dd, ³J_{H,H} = 7.5 Hz, ²J_{P,H} = 13.0 Hz, 4H, *o*-CH(PPh₂)), 7.78 (dd, ³J_{H,H} = 7.5 Hz, ⁴J_{P,H} = 6.0 Hz, 2H, *p*-CH (PPh₂)), 7.57 (td, ³J_{H,H} = 7.5 Hz, ³J_{P,H} = 3.5 Hz, 4H, *m*-CH (PPh₂)), 7.03 (m, ³J_{H,H} = 7.5 Hz, 4H, *o*- and *m*-CH(NPh)), 6.86 (t, ³J_{H,H} = 7.0 Hz, 1H, *p*-CH(NPh)), 2.71 (d, ²J_{P,H} = 18.0 Hz, 2H, PCH₂), 0.0 (s, 9H, CH₃); ¹³C NMR (CDCl₃): δ 139.0 (d, ²J_{P,C} = 2.5 Hz, C^{IV}(NPh)), 134.4 (d, ⁴J_{P,C} = 3.0 Hz, *p*-CH(PPh₂)), 132.6 (d, ³J_{P,C} = 11.0 Hz, *m*-CH(PPh₂)), 129.7 (d, ²J_{P,C} = 13.0 Hz, *o*-CH(PPh₂)), 129.0 (s, *m*-CH(NPh)), 122.9 (s, *p*-CH(NPh)), 122.5 (d, ¹J_{P,C} = 96.5 Hz, C^{IV}(PPh₂)), 120.0 (d, ³J_{P,C} = 6.0 Hz, *o*-CH(NPh)), 14.5 (d, ¹J_{P,C} = 58.5 Hz, PCH₂), 0.0 (s, CH₃). Anal. Calcd for C₂₂H₂₇BrNPSi: C, 59.46; H, 6.12; N, 3.50. Found: C, 58.81; H, 5.93; N, 3.40.

Synthesis of 11

MeLi (1.6 M in Et₂O, 725 μL, 1.16 mmol) was added dropwise to a suspension of **1c** (0.58 mmol, 250 mg) in THF (6 mL) at -78°C. The cold bath was removed and stirring is continued at room temperature for four hours to give an orange-red solution. A solution of trimethyltinchloride (0.58 mmol, 0.116 g) in THF (2 mL) was added, giving a pale yellow solution. After 20 minutes of stirring at room temperature, solvent was removed and toluene was added to filter off the lithium salts. After evaporation of toluene, iminophosphorane **11** was obtained as a white solid (341 mg, 75 %).

11: ³¹P {¹H} NMR (C₆D₆): δ -6.88 (s+sat, ²J_{P,Sn} = 60.0 Hz); ¹H NMR (C₆D₆): δ 7.66 (m, 4H, *o*-CH(PPh₂)), 7.18 (m, 2H, *p*-CH(NPh)), 6.99 (m, 6H, *p*- and *m*-CH(PPh₂)), 6.76 (m, 3H, *p*- and *m*-CH(NPh)), 1.55 (d+sat, ²J_{P,H} = 11.0 Hz, ²J_{Sn,H} = 52.0 Hz, 2H, CH₂P), 0.10 (s +sat, ²J_{Sn,H} = 50.0 Hz, 9H, Sn(CH₃)₃). ¹³C NMR (C₆D₆): δ 152.8 (²J_{P,C} = 3.0 Hz, C^{IV}(NPh)), 134.9 (d, ¹J_{P,C} = 87.0 Hz, C^{IV}(PPh₂)), 133.8 (d, ³J_{P,C} = 3.0 Hz, *p*-CH(PPh₂)), 131.6 (d, ²J_{P,C} = 9.0 Hz, *o*-CH(PPh₂)),

129.7 (d, $^3J_{P,C} = 12.0$ Hz, *m*-CH(PPh₂)), 128.6 (d, $^3J_{P,C} = 11.0$ Hz, *o*-CH(NPh)), 123.2 (d, $^3J_{P,C} = 20.0$ Hz, *m*-CH(NPh)), 117.1 (s, *p*-CH(NPh)), 12.0 (d+sat, $^1J_{P,C} = 75.0$ Hz, $^1J_{Sn,C} = 296.0$ Hz, CH₂P), -7.4 (d+sat, $^3J_{P,C} = 1.5$ Hz, $^1J_{Sn,C} = 362.0$ Hz, Sn(CH₃)₃).

Synthesis of 12

12 (260 mg, 85 %) was obtained with a procedure similar to that employed for **11** using a solution of 1-cyano-2,5-diphenylphosphole (0.58 mmol, 0.15 g) in THF.

12: ^{31}P { 1H } NMR (C₆D₆): δ -23.7 (d, $^2J_{P,P} = 48.5$ Hz, P^{III}), 0.8 (d, $^2J_{P,P} = 48.5$ Hz, PPh₂); 1H NMR (C₆D₆): δ 7.61 (m, 2H, *o*-CH(NPh)), 7.52 (dd, $^3J_{H,H} = 7.0$ Hz, $^4J_{P,H} = 1.0$ Hz, 4H, *o*-CH(Ph_{phosphole})), 7.45 (dd, $^3J_{P,H} = 11.5$ Hz, $^3J_{H,H} = 7.0$ Hz, 4H, *o*-CH(PPh₂)), 7.07 (d, $^3J_{P,H} = 8.0$ Hz, 2H, CH _{β} phosphole), 6.91 (m, 6H, *m* and *p*-CH(Ph_{phosphole})), 7.02 (m, 6H, *m*- and *p*-CH(NPh)), 6.82 (td, $J_{H,H} = 7.5$ Hz, $J_{P,H} = 3.0$ Hz, 6H, *m*- and *p*-CH(PPh₂)), 2.75 (dd, $^2J_{P,H} = 10.0$ Hz, $^2J_{P,H} = 4.0$ Hz, 2H, PCH₂P); ^{13}C NMR (C₆D₆): δ 152.4 (d, $^1J_{P,C} = 68.0$ Hz, C _{α} phosphole), 136.5 (d, $^2J_{P,C} = 17.0$ Hz, C^{IV}(NPh)), 135.6 (dd, $^1J_{P,C} = 97.0$ Hz, $^3J_{P,C} = 8.0$ Hz, C^{IV}(PPh₂)), 132.5 (d, $^2J_{P,C} = 9.0$ Hz, C _{β} phosphole), 132.3 (d, $^2J_{P,C} = 9.0$ Hz, *o*-CH(PPh₂)), 131.8 (d, $J_{P,C} = 3.0$ Hz, CH(Ph)), 131.5 (s, CH(Ph)), 131.3 (s, CH(Ph)), 128.8 (d, $J_{P,C} = 9.0$ Hz, CH(Ph)), 127.8 (d, $^3J_{P,C} = 8.0$ Hz, *o*-CH(NPh)), 126.7 (d, $^3J_{P,C} = 5.0$ Hz, *o*-CH(Ph_{phosphole})), 123.9 (s, CH(Ph)), 123.6 (s, C^{IV}(Ph_{phosphole})), 117.6 (s, CH(Ph)), 24.8 (dd, $^1J_{P,C} = 44.0$ Hz, $^1J_{P,C} = 37.5$ Hz, PCH₂).

Synthesis of 13

THF (1 mL) was added to a mixture of dichloro(*p*-cymene)ruthenium(II) dimer (23.2 mg, 0.38 mmol) and **5** (30 mg, 0.075 mmol) at room temperature giving immediately a red solution. After 2h of stirring, THF was removed and the residue was dissolved in dichloromethane (3 mL). After removal of the insoluble lithium salts by filtration and evaporation of dichloromethane, the obtained solid was washed with hexanes (3 mL) to give **13** as a red solid (25 mg, 76%).

13: ^{31}P { 1H } NMR (*d*⁸-THF): δ 36.9 (s); 1H NMR (CDCl₃): δ 7.82 (td, $^3J_{H,H} = 7.0$ Hz, $^3J_{P,H} = 10.1$ Hz, 2H, *m*-CH (PPh₂)), 7.57 (d, $^3J_{H,H} = 7.0$ Hz, 1H, *p*-CH (PPh₂)), 7.52 (dd, $^3J_{H,H} = 7.0$ Hz, $^3J_{P,H} = 11.5$ Hz, 4H, *o*-CH(PPh₂)), 7.38 (d, $^3J_{H,H} = 7.5$ Hz, 2H, *m*-CH(NPh)), 7.25 (t, $^3J_{H,H} = 7.0$ Hz, 1H, *p*-CH(PPh₂)), 7.18 (m, 2H, *m*-CH(PPh₂)), 6.85 (t, $^3J_{H,H} = 7.5$ Hz, 2H, *o*-CH(PPh₂)), 6.64 (vtd, $^3J_{H,H} = 7.5$ Hz, $^4J_{H,H} = 0.5$ Hz, 1H, *p*-CH(NPh)), 4.90 (d, $^3J_{H,H} = 5.5$ Hz, 1H, CH(*p*-cymene)), 4.76 (d, $^3J_{H,H} = 5.5$ Hz, 2H, CH(*p*-cymene)), 4.64 (d, $^3J_{H,H} = 5.5$ Hz, 1H, CH(*p*-cymene)), 4.12 (vt, $^3J_{H,H} = ^2J_{P,H} = 13.0$ Hz, 1H, PCH₂), 2.80 (sept., $^3J_{H,H} = 7.0$ Hz, 1H, CH(CH₃)₂), 2.67 (d, $^3J_{H,H} = 13.0$ Hz, 1H, PCH₂), 1.99 (3H, s, CH₃), 1.15 (d, $^3J_{H,H} = 7.0$ Hz, 6H, C(CH₃)₂); ^{13}C NMR (CDCl₃): δ 151.2 (s, C^{IV}(NPh)), 130.1 (d, $J_{P,C} = 9.0$ Hz, CH(PPh₂)), 129.8 (d, $J_{P,C} = 9.0$ Hz, CH(PPh₂)), 128.4 (s, CH(PPh₂)), 127.9 (s, CH(PPh₂)), 126.1 (d, $^1J_{P,C} = 89.0$ Hz, C^{IV}(PPh₂)), 125.3 (d, $J_{P,C} = 7.0$ Hz, CH(NPh)), 124.6 (d, $J_{P,C} = 11.5$ Hz, CH(PPh₂)), 124.4 (d, $J_{P,C} = 9.0$ Hz, CH(PPh₂)), 124.0 (d, $J_{P,C} = 1.0$ Hz, CH(NPh)), 118.3 (d, $J_{P,C} = 2.0$ Hz, *p*-CH(NPh)), 99.0 (s, C^{IV}-(*p*-cymene)), 90.9 (s, C^{IV}-(*p*-cymene)), 80.8 (s, CH(*p*-cymene)), 79.3 (s, CH(*p*-cymene)), 79.2 (s, CH(*p*-cymene)), 73.2 (s, CH(*p*-cymene)), 28.8 (d, $^1J_{P,C} = 84.0$ Hz, PCH₂), 27.1 (s,

CH(CH₃)₂), 18.5 (s, CH(CH₃)₂), 18.3 (s, CH(CH₃)₂), 14.0 (s, CH₃). Anal. Calcd for C₂₉H₃₁ClNPRuS: C, 58.72; H, 5.27; N, 2.36. Found: C, 58.61; H, 5.20; N, 2.21.

Synthesis of 14

THF (1 mL) was added to a mixture of CoCl₂ (9.8 mg, 0.075 mmol) and **5** (30 mg, 0.075 mmol) at room temperature giving immediately a blue solution, then a blue suspension after 10 minutes. After 2h of stirring, THF was removed and the residue was dissolved in dichloromethane (3 mL). After removal of the insoluble lithium salts by filtration and evaporation of dichloromethane, the obtained solid was washed with hexanes (3 mL) to give **14** as a blue/green solid (24 mg, 76%). Single crystals suitable for X-ray diffraction was obtained by slow diffusion of petroleum ether over a solution in dichloromethane.

Synthesis of 15

Toluene (1 mL) was added to a mixture of chloro(1,5-cyclooctadiene)rhodium(I) dimer (19 mg, 0.038 mmol) and **5** (30 mg, 0.075 mmol) at room temperature giving immediately a yellow solution. After 2h of stirring, THF was removed and the residue was dissolved in dichloromethane (3 mL). After removal of insoluble lithium salts by filtration and evaporation of dichloromethane, the obtained solid was washed with hexanes (3 mL) to give **15** as a yellow solid (20 mg, 68%).

15: ³¹P {¹H} NMR (CD₂Cl₂): δ 47.7 (d, ²J_{Rh,P} = 5.0 Hz, P=N); ¹H NMR (CD₂Cl₂): δ 7.81 (ddd, ³J_{H,H} = 7.5 Hz, ³J_{P,H} = 10.0 Hz, ⁴J_{H,H} = 1.0 Hz, 4H, *o*-CH(PPh₂)), 7.56 (vtd, ³J_{H,H} = 7.5 Hz, ⁴J_{H,H} = 1.0 Hz, 2H, *p*-CH(PPh₂)), 7.47 (vtd, ³J_{H,H} = ³J_{H,H} = 7.5 Hz, ⁴J_{P,H} = 2.5 Hz, 4H, *m*-CH(PPh₂)), 6.93 (vt, ³J_{H,H} = ³J_{H,H} = 7.0 Hz, 2H, *m*-CH(NPh)), 6.83 (d, ³J_{H,H} = 7.0 Hz, 2H, *o*-CH(NPh)), 6.75 (d, ³J_{H,H} = 7.0 Hz, 1H, *p*-CH(NPh)), 3.87 (m, 4H, CH(COD)), 3.23 (d, ²J_{P,H} = 5.5 Hz, 2H, PCH₂), 2.37 (m, 4H, CH₂(COD)), 1.80 (m, 4H, CH₂(COD)); ¹³C NMR (CD₂Cl₂): δ 147.9 (s, C^{IV}(NPh)), 133.7 (d, ²J_{P,C} = 9.0 Hz, *o*-CH(PPh₂)), 132.6 (d, ⁴J_{P,C} = 2.0 Hz, *p*-CH(PPh₂)), 129.3 (s, CH(COD)), 129.0 (d, ³J_{P,C} = 7.5 Hz, *o*-CH(NPh)), 128.6 (d, ³J_{P,C} = 11.5 Hz, *m*-CH(PPh₂)), 128.5 (s, CH(COD)), 128.3 (d, ⁴J_{P,C} = 1.5 Hz, *m*-CH(NPh)), 127.7 (d, ¹J_{P,C} = 83.0 Hz, C^{IV}(PPh₂)), 125.6 (s, CH(COD)), 123.0 (d, ⁵J_{P,C} = 2.0 Hz, *p*-CH(NPh)), 31.1 (s, b, CH₂(COD)), 25.9 (d, ¹J_{P,C} = 90.0 Hz, PCH₂),

Synthesis of 16

THF (1 mL) was added to a mixture of chloro(1,5-cyclooctadiene)Iridium(I) dimer (25.5 mg, 0.038 mmol) and **5** (150 mg, 0.38 mmol) at room temperature giving immediately an orange-red solution. After 2h of stirring, THF was removed and the residue was dissolved in dichloromethane (3 mL). After removal of insoluble lithium salts by filtration and evaporation of dichloromethane, the obtained solid was washed with hexanes (3 mL) to give **16** as a red solid (25 mg, 71%).

16: ³¹P {¹H} NMR (CD₂Cl₂): δ 63.0 (s); ¹H NMR (CD₂Cl₂): δ 7.77 (ddd, ³J_{H,H} = 7.5 Hz, ³J_{P,H} = 11.0 Hz, ⁴J_{H,H} = 1.5 Hz, 4H, *o*-CH(PPh₂)), 7.56 (vtd, ³J_{H,H} = 7.5 Hz, ⁴J_{H,H} = 1.5 Hz, 2H, *p*-

CH(PPh₂)), 7.45 (vtd, ³J_{H,H} = ³J'_{H,H} = 7.5 Hz, ⁴J_{P,H} = 3.0 Hz, 4H, *m-CH*(PPh₂)), 6.94 (vt, ³J_{H,H} = ³J'_{H,H} = 7.5 Hz, 2H, *m-CH*(NPh)), 6.79 (dd, ³J_{H,H} = 7.5 Hz, ⁴J_{H,H} = 1.5 Hz, 2H, *o-CH*(NPh)), 6.77 (td, ³J_{H,H} = 7.5 Hz, ⁴J_{H,H} = 1.5 Hz, 1H, *p-CH*(NPh)), 3.41 (m, 2H, *CH*(COD)), 3.35 (d, ²J_{P,H} = 5.5 Hz, 2H, PCH₂), 3.05 (m, 2H, *CH*(COD)), 2.15 (m, 4H, CH₂(COD)), 1.57 (m, 2H, CH₂(COD)), 1.45 (m, 2H, CH₂(COD)); ¹³C NMR (CD₂Cl₂): δ 146.2 (s, C^{IV}(NPh)), 134.0 (d, ²J_{P,C} = 9.0 Hz, *o-CH*(PPh₂)), 132.9 (d, ⁴J_{P,C} = 2.0 Hz, *p-CH*(PPh₂)), 129.4 (d, ³J_{P,C} = 7.0 Hz, *o-CH*(NPh)), 128.6 (d, ³J_{P,C} = 11.5 Hz, *m-CH*(PPh₂)), 128.1 (d, ⁴J_{P,C} = 1.0 Hz, *m-CH*(NPh)), 126.6 (d, ¹J_{P,C} = 86.0 Hz, C^{IV}(PPh₂)), 123.8 (d, ⁵J_{P,C} = 2.0 Hz, *p-CH*(NPh)), 65.0 (s, *CH*(COD)), 56.5 (s, *CH*(COD)), 31.9 1 (s, CH₂(COD)), 31.3 (s, CH₂(COD)), 25.3 (d, ¹J_{P,C} = 89.0 Hz, PCH₂),

Synthesis of 17

THF (1 mL) was added to a mixture of trans-[PdCl₂(PPh₃)₂] (53 mg, 0.075 mmol) and **5** (30 mg, 0.075 mmol). After 4h stirring the yellow slurry has turned to an orange solution. THF was removed by evaporation and the residue was taken in dichloromethane (4 mL). Insoluble lithium salts were removed by filtration. After evaporation of dichloromethane, the obtained solid residue was washed with hexanes (3 mL) to give **17** as an orange solid (31.7 mg, 87%).

17: ³¹P {¹H} NMR (CD₂Cl₂): δ 33.5 (d, ³J_{P,P} = 6.5 Hz, P^{III}), 46.2 (d, ³J_{P,P} = 6.5 Hz, P^V); ¹H NMR (CD₂Cl₂): δ 7.83 (ddd, ³J_{H,H} = 7.5 Hz, ³J_{P,H} = 11.5 Hz, ⁴J_{H,H} = 1.5 Hz, 4H, *o-CH*(PPh₂)), 7.65 (ddd, ³J_{H,H} = 7.5 Hz, ³J_{P,H} = 11.5 Hz, ⁴J_{H,H} = 1.5 Hz, 6H, *o-CH*(PPh₃)), 7.64 (tt, ³J_{H,H} = 7.5 Hz, ⁴J_{H,H} = 1.5 Hz, 2H, *p-CH*(PPh₂)), 7.63 (vtd, ³J_{H,H} = ³J'_{H,H} = 7.5 Hz, ⁴J_{P,H} = 3.0 Hz, 4H, *m-CH*(PPh₂)), 7.46 (tt, ³J_{H,H} = 7.5 Hz, ⁴J_{H,H} = 1.5 Hz, 2H, *p-CH*(PPh₃)), 7.37 (vtd, ³J_{H,H} = ³J'_{H,H} = 7.5 Hz, ⁴J_{P,H} = 2.5 Hz, 6H, *m-CH*(PPh₃)), 7.37 (vt, ³J_{H,H} = ³J'_{H,H} = 6.0 Hz, 2H, *m-CH*(NPh)), 6.94 (dd, ³J_{H,H} = 6.0 Hz, ⁴J_{H,H} = 2.5 Hz, 2H, *o-CH*(NPh)), 6.67 (td, ³J_{H,H} = 6.0 Hz, ⁴J_{H,H} = 2.5 Hz, 1H, *p-CH*(NPh)), 3.14 (d, ²J_{P,H} = 6.0 Hz, 2H, PCH₂); ¹³C NMR (CD₂Cl₂): δ 149.6 (dd, ²J_{P,C} = 3.0 Hz, ³J_{P,C} = 1.5 Hz, C^{IV}(NPh)), 136.5 (d, ²J_{P,C} = 11.0 Hz, *o-CH*(PPh₃)), 134.9 (d, ²J_{P,C} = 9.0 Hz, *o-CH*(PPh₂)), 134.4 (d, ⁴J_{P,C} = 2.5 Hz, *p-CH*(PPh₂)), 132.2 (d, ²J_{P,C} = 2.5 Hz, *p-CH*(PPh₃)), 131.9 (d, ¹J_{P,C} = 53.5 Hz, C^{IV}(PPh₃)), 130.3 (d, ³J_{P,C} = 11.5 Hz, *m-CH*(PPh₂)), 130.1 (dd, ³J_{P,C} = 10.5 Hz, ⁴J_{P,C} = 1.0 Hz, *o-CH*(NPh)), 129.4 (d, ³J_{P,C} = 11.0 Hz, *m-CH*(PPh₃)), 129.0 (s, *m-CH*(NPh)), 128.5 (d, ¹J_{P,C} = 86.0 Hz, C^{IV}(PPh₂)), 123.3 (s, *p-CH*(NPh)), 29.5 (dd, ¹J_{P,C} = 85.0 Hz, ³J_{P,C} = 4.5 Hz, PCH₂); Anal. Calcd for C₃₇H₃₂ClNPdP₂S: C, 61.17; H, 4.44; N, 1.93. Found: C, 61.03; H, 4.364; N, 2.02.

Synthesis of 18

THF (1 mL) was added to a mixture of [NiBr₂(DME)] (11.6 mg, 0.038 mmol) and **5** (30 mg, 0.075 mmol) at room temperature giving immediately deep green solution, then a green suspension after 10 minutes. After 2h of stirring, THF was removed and the residue was dissolved in dichloromethane (3 mL). After removal of insoluble lithium salts by filtration and evaporation of dichloromethane, the obtained solid was washed with hexanes (3 mL) to give **18** as a green solid (22 mg, 82%). Single crystals suitable for X-ray diffraction was obtained from slow diffusion of petroleum ether over a solution in dichloromethane.

Experimental Section

II. Chapter 2

General considerations

All experiments, unless otherwise stated, were performed under an atmosphere of dry nitrogen or argon using standard schlenk and glove box techniques. Solvents were taken directly from a M-Braun MB-SPS 800 Solvent Purification Machine. *O*-diphenylphosphinophenol,⁵ [NiBr₂(DME)]² were prepared according to the literature. Methylaluminoxane (10% wt in toluene) and diethylaluminum chloride was purchased from Acros. Ethylene (N25 grade) was purchased from Air Liquide. All other reagents and chemicals were obtained commercially and used without further purification.

Nuclear magnetic resonance spectra were recorded on Bruker Avance 300 spectrometer operating at 300 MHz for ¹H, 75.5 MHz for ¹³C and 121.5 MHz for ³¹P. Solvent peaks were used as internal references for ¹H and ¹³C chemical shifts (ppm). ³¹P{¹H} are relative to a 85% H₃PO₄ external reference. Coupling constant are expressed in hertz. The following abbreviations are used: br, broad; s, singlet; d, doublet; dd, doublet of doublets; t, triplet; m, multiple; v, virtual. The labeling of the ligands and ligand precursors are given in scheme 15. Elemental analyses were performed by the Elemental analysis service of the London Metropolitan University (United Kingdom).

General procedure for ethylene oligomerisation

All catalytic reactions were carried out in glass container in a magnetically stirred stainless steel autoclave (40 mL), equipped with a pressure gauge and needle valves for injections. The interior of the autoclave was protected from corrosion by a Teflon protective coating. A typical reaction was performed by introducing in the reactor under nitrogen atmosphere a suspension of the complex (8 μmol) in toluene (20 mL). After injection of the cocatalyst solution (in toluene), the reactor was immediately brought to the desired working pressure, and continuously fed with ethylene using a reserve bottle. The reaction was stopped by closing the ethylene supply and cooling down the system to -70°C. After release of residual pressure, the reaction was quenched by adding methanol (5 mL). *n*-heptane used as internal standard was also introduced and the

mixture was analyzed by quantitative GC (PERICROM 2100 gas chromatograph equipped with a HP PONA column (50 m × 0.2 mm × 0.5 μm)), first calibrated with authentic samples.

Kirsanov reaction

21a-c: 1equiv. of Br₂ (200 μL, 3.883 mmol) was added dropwise to a solution of the protected phosphinophenol **X2** (1304 mg, 3.883 mmol) in CH₂Cl₂ (38 mL) at -78°C under nitrogen. The cold bath was removed and stirring was continued for 45 minutes at room temperature. The obtained suspension was then cooled again to -78°C and DABCO (218 mg, 1.942 mmol) was added, followed by the addition of 1 equiv. of RNH₂. Stirring was continued overnight at room temperature to give a white suspension. Dichloromethane was evaporated and the residue was taken in THF (50 mL). After removal of DABCO salts by centrifugation, the solvent was evaporated in vacuum, giving white solid. The products were verified in ³¹P{¹H} NMR spectrum and are used directly without further purification for the deprotection step.

21d: 1equiv. of Br₂ (200 μL, 3.883 mmol) was added dropwise to a solution of the protected phosphinophenol **X2** (1304 mg, 3.883 mmol) in CH₂Cl₂ (10mL/mmol) at -78°C under nitrogen. The cold bath was removed and stirring was continued for 45 minutes at room temperature. The obtained suspension was then cooled again to -78°C and o-phenylenediamine (420 mg, 3.883 mmol) was added. Stirring was continued overnight at room temperature to give a pale yellow slurry. Dichloromethane was evaporated and the residue was washed with THF (2x10 mL), giving a white solid. verified in ³¹P{¹H} NMR spectrum and are used directly without further purification for the deprotection step.

Deprotection reaction

The aminophosphonium salt resulted from the Kirsanov reaction was put into distilled dichloromethane (15mL) and the solution was saturated with HCl gaseous. After 15 minutes of stirring, a cloudy pale yellow solution was formed.

22a: Dichloromethane and HCl was evaporated, the residue was taken in MeOH (10 mL) giving a pale pink solution. Water (3 mL) was added dropwise, leading to the formation of colorless crystallised solid. The white solid was separated by centrifugation, washed with THF (3x5 mL) and dried in vacuum.

22b-d: Dichloromethane and HCl were evaporated, the residue was taken in THF (20 mL) giving a yellow slurry. The white solid was separated by centrifugation, washed again with THF (5 mL) and dried in vacuum.

22a: (0.87 g, 2.2 mmol, 57%). ³¹P{¹H} NMR (CDCl₃): δ 35.2 (s, P^V); ¹H NMR (CDCl₃): δ 7.96 (ddd, ³J_{H,H}=7.5 Hz, ⁴J_{H,H}=1.8 Hz, ⁴J_{P,H}=5.5 Hz, 1H, C_aH), 7.75 (dd, ³J_{H,H}=7.5 Hz, ³J_{P,H}=13.0 Hz, 4H, *o*-CH(PPh₂)), 7.70 (vt, ³J_{H,H}=7.5 Hz, 2H, *p*-CH(PPh₂)), 7.58 (vtd, ³J_{H,H}=³J'_{H,H}=7.5 Hz, ⁴J_{P,H}=2.4 Hz, 4H, *m*-CH(PPh₂)), 7.41 (vtd, ³J_{H,H}=³J'_{H,H}=7.5 Hz, ⁴J_{H,H}=3.0 Hz, 1H, C_bH), 6.80 (m, 2H, C_cH+C_dH), 4.94 (s, 1H, NH), 1.15 (s, 9H, C^{IV}(CH₃)₃); ¹³C{¹H} NMR (CDCl₃): δ 161.6 (d, ²J_{P,C}=1.8 Hz, OC^{IV}), 136.7 (d, ⁴J_{P,C}=1.7 Hz, C_bH), 134.8 (d, ⁴J_{P,C}=3.0 Hz, *p*-CH(PPh₂)), 134.0

(d, $^2J_{P,C}=11.4$ Hz, *o*-CH(PPh₂)), 132.1 (d, $^2J_{P,C}=10.5$ Hz, *C_dH*), 129.8 (d, $^3J_{P,C}=13.3$ Hz, *m*-CH(PPh₂)), 128.8 (d, $^3J_{P,C}=12.4$ Hz, *C_acH*), 122.7 (d, $^1J_{P,C}=101.8$ Hz, *C^{IV}*(PPh₂)), 120.2 (d, $^3J_{P,C}=13.9$ Hz, *C_acH*), 107.1 (d, $^1J_{P,C}=107.3$ Hz, *C^{IV}*-PPh₂), 55.8 (d, $^2J_{P,C}=4.8$ Hz, *C^{IV}*(CH₃)₃), 32.1 (d, $^3J_{P,C}=4.4$ Hz, *C^{IV}*(CH₃)₃)

22b: (1.24 g, 2.8 mmol, 72%). $^{31}P\{^1H\}$ NMR (CDCl₃): δ 36.4 (s, *P^V*); 1H NMR (CDCl₃): δ 8.15 (s, b, *OH*), 8.02 (dd, $^3J_{H,H}=7.5$ Hz, $^4J_{P,H}=6.5$ Hz, 1H, *C_aH*), 7.80 (ddd, $^4J_{H,H}=1.0$ Hz, $^3J_{H,H}=7.5$ Hz, $^3J_{P,H}=13.5$ Hz, 4H, *o*-CH(PPh₂)), 7.75 (vtt, $^4J_{H,H}=1.0$ Hz, $^3J_{H,H}=7.5$ Hz, 2H, *p*-CH(PPh₂)), 7.62 (vtd, $^3J_{H,H}=^3J'_{H,H}=7.5$ Hz, $^4J_{P,H}=3.0$ Hz, 4H, *m*-CH(PPh₂)), 7.46 (vtd, $^3J_{H,H}=^3J'_{H,H}=7.5$ Hz, $^4J_{H,H}=2.0$ Hz, 1H, *C_bH*), 6.88 (m, 2H, *C_cH+C_dH*), 4.96 (d, $^2J_{P,H}=2.0$ Hz, 1H, *NH*), 1.46 (s, 2H, *CH₂-C^{IV}*(CH₃)₃), 1.19 (s, 9H, *C^{IV}*(CH₃)₃); $^{13}C\{^1H\}$ NMR (CDCl₃): δ 161.4 (d, $^2J_{P,C}=1.8$ Hz, *OC^{IV}*), 136.7 (d, $^4J_{P,C}=2.0$ Hz, *C_bH*), 134.8 (d, $^4J_{P,C}=2.8$ Hz, *p*-CH(PPh₂)), 133.9 (d, $^2J_{P,C}=11.7$ Hz, *o*-CH(PPh₂)), 132.4 (d, $^{2,3}J_{P,C}=11.0$ Hz, *C_dcH*), 129.8 (d, $^3J_{P,C}=12.0$ Hz, *m*-CH(PPh₂)), 122.7 (d, $^1J_{P,C}=102.0$ Hz, *C^{IV}*(PPh₂)), 120.3 (d, $^{2,3}J_{P,C}=13.5$ Hz, *C_cdH*), 119.4 (d, $^2J_{P,C}=7.4$ Hz, *C_dH*), 107.2 (d, $^1J_{P,C}=106.3$ Hz, *C^{IV}*-PPh₂), 55.8 (d, $^2J_{P,C}=5.0$ Hz, *CH₂-C^{IV}*(CH₃)₃), 53.5 (s, *C^{IV}*(CH₃)₃), 32.1 (d, $^3J_{P,C}=4.3$ Hz, *C^{IV}*(CH₃)₃)

22c: (1.35 g, 3.01 mmol, 78%). $^{31}P\{^1H\}$ NMR (CDCl₃): δ 39.9 (s, *P^V*); 1H NMR (CDCl₃): δ 7.97 (ddd, $^3J_{H,H}=6.5$ Hz, $^4J_{H,H}=1.0$ Hz, $^4J_{P,H}=8.5$ Hz, 1H, *C_aH*), 7.68 (vtt, $^4J_{H,H}=1.0$ Hz, $^3J_{H,H}=7.5$ Hz, 2H, *p*-CH(PPh₂)), 7.66 (ddd, $^4J_{H,H}=1.0$ Hz, $^3J_{H,H}=7.5$ Hz, $^3J_{P,H}=14.0$ Hz, 4H, *o*-CH(PPh₂)), 7.54 (vtd, $^3J_{H,H}=^3J'_{H,H}=7.5$ Hz, $^4J_{P,H}=3.0$ Hz, 4H, *m*-CH(PPh₂)), 7.54 (m, 1H, *C_bH*), 7.10 (vt, $^3J_{H,H}=^3J'_{H,H}=7.5$ Hz, 2H, *m*-CH(NPh)), 7.02 (vtd, $^3J_{H,H}=^3J'_{H,H}=6.5$ Hz, $^4J_{H,H}=1.0$ Hz, 1H, *C_cH*), 7.00 (t, $^3J_{H,H}=7.5$ Hz, 1H, *p*-CH(PPh₂)), 6.93 (ddd, $^3J_{H,H}=6.5$ Hz, $^4J_{H,H}=1.0$ Hz, $^3J_{P,H}=3.5$ Hz, 1H, *C_dH*), 6.85 (d, $^3J_{H,H}=7.5$ Hz, 2H, *o*-CH(PPh₂)); $^{13}C\{^1H\}$ NMR (CDCl₃): δ 161.8 (d, $^2J_{P,C}=2.5$ Hz, *OC^{IV}*), 137.8 (d, $^2J_{P,C}=3.0$ Hz, *C^{IV}*(NPh)), 137.6 (d, $^4J_{P,C}=2.0$ Hz, *C_bH*), 135.2 (d, $^4J_{P,C}=3.0$ Hz, *p*-CH(PPh₂)), 133.8 (d, $^2J_{P,C}=11.5$ Hz, *o*-CH(PPh₂)), 133.1 (d, $^3J_{P,C}=10.5$ Hz, *C_cH*), 130.0 (d, $^3J_{P,C}=13.6$ Hz, *m*-CH(PPh₂)), 129.6 (s, *m*-CH(NPh)), 124.5 (s, *p*-CH(NPh)), 121.6 (d, $^3J_{P,C}=6.0$ Hz, *o*-CH(NPh)), 120.6 (d, $^3J_{P,C}=13.8$ Hz, *C_aH*), 120.3 (d, $^1J_{P,C}=104.0$ Hz, *C^{IV}*(PPh₂)), 119.5 (d, $^2J_{P,C}=7.5$ Hz, *C_dH*), 105.9 (d, $^1J_{P,C}=105.2$ Hz, *C^{IV}*-PPh₂)

22d: (1.95 g, 3.56 mmol, 92%). $^{31}P\{^1H\}$ NMR (MeOD-*d*₄): δ 39.0 (s); 1H NMR (MeOD-*d*₄): δ 7.93 (ddd, $^4J_{H,H}=1.0$ Hz, $^3J_{H,H}=7.5$ Hz, $^3J_{P,H}=14.0$ Hz, 4H, *o*-CH(PPh₂)), 7.85 (tdt, $^4J_{H,H}=1.0$ Hz, $^3J_{H,H}=8.0$ Hz, $^5J_{P,H}=2.0$ Hz, 2H, *p*-CH(PPh₂)), 7.79 (dddd, $^3J_{H,H}=8.5$ Hz, $^3J_{H,H}=7.5$ Hz, $^4J_{H,H}=1.0$ Hz, $^5J_{P,H}=1.5$ Hz, 1H, *C_bH*), 7.71 (vtd, $^3J_{H,H}=^3J'_{H,H}=7.5$ Hz, $^4J_{P,H}=4.0$ Hz, 4H, *m*-CH(PPh₂)), 7.53 (ddd, $^4J_{H,H}=1.0$ Hz, $^3J_{H,H}=8.0$ Hz, $^3J_{P,H}=15.0$ Hz, 1H, *C_dH*), 7.46 (dvt, $^4J_{H,H}=1.0$ Hz, $^3J_{H,H}=8.0$ Hz, $^4J_{P,H}=1.0$ Hz, 1H, *C_eH*), 7.26 (vtd, $^3J_{H,H}=^3J'_{H,H}=8.0$ Hz, $^4J_{H,H}=1.0$ Hz, 1H, *C_fH*), 7.20 (vtdd, $^4J_{H,H}=1.0$ Hz, $^3J_{H,H}=^3J'_{H,H}=8.0$ Hz, $^4J_{P,H}=3.0$ Hz, 1H, *C_cH*), 7.15 (ddd, $^4J_{H,H}=1.0$ Hz, $^3J_{H,H}=8.0$ Hz, $^4J_{P,H}=6.0$ Hz, 1H, *C_aH*), 7.15 (vtd, $^3J_{H,H}=^3J'_{H,H}=8.0$ Hz, $^4J_{H,H}=1.0$ Hz, 1H, *C_gH*), 6.93 (dd, $^3J_{H,H}=8.0$ Hz, $^4J_{H,H}=1.0$ Hz, 1H, *C_hH*); $^{13}C\{^1H\}$ NMR (MeOD-*d*₄): δ 162.8 (d, $^2J_{P,C}=3.5$ Hz, *C^{IV}*-O), 140.0 (d, $^4J_{P,C}=2.0$ Hz, *C_bH*), 136.8 (d, $^4J_{P,C}=3.0$ Hz, *p*-CH(PPh₂)), 136.3 (d, $^2J_{P,C}=9.5$ Hz, *C_dH*), 135.4 (d, $^2J_{P,C}=11.5$ Hz, *o*-CH(PPh₂)), 133.3 (d, $^2J_{P,C}=1.0$ Hz, *C^{IV}*-N-P), 132.7 (d, $^3J_{P,C}=14.0$ Hz, *m*-CH(PPh₂)), 130.9 (s, *C_fH*), 128.4 (s, *C_gH*), 127.7 (d, $^3J_{P,C}=8.0$ Hz,

C^{IV} -N-C), 127.1(d, $^3J_{P,C} = 4.0$ Hz, C_eH), 126.4 (s, C_hH), 122.7 (d, $^3J_{P,C} = 13.5$ Hz, C_eH), 121.6 (d, $^1J_{P,C} = 106.0$ Hz, $C^{IV}(PPh_2)$), 118.8 (d, $^3J_{P,C} = 7.5$ Hz, C_aH), 107.8 (d, $^1J_{P,C} = 104.5$ Hz, $C^{IV}-PPh_2$).

Synthesis of complexes **23a-d**

KHMDS (200 mg, 1 mmol and 300 mg, 1.5 mmol in the case of **23d**) was added into a slurry of the phenolaminophosphonium salt (0.5 mmol) in THF (10 mL). After 30 min of stirring at RT, insoluble potassium salts (KCl) was removed by centrifugation. $[NiBr_2(DME)]$ (154 mg, 0.5 mmol) was added resulting immediately in a change of color. Stirring was continued for 2h. Insoluble potassium salt was removed by centrifugation. THF was evaporated to give the product as a pale solid which is washed with petroleum ether to remove traces of HMDS. **23a** (220 mg, 0.21 mmol, 82%), pale purple solid. Anal. Calcd for **23a** ($C_{44}H_{46}Br_3KN_2Ni_2O_2P_2$): C, 48.35; H, 4.24; N, 2.56. Found: C, 48.82; H, 5.38; N, 2.73. **23b**. (195 mg, 0.18 mmol, 74%). pale blue solid. Anal. Calcd for **23b** ($C_{46}H_{50}Br_3KN_2Ni_2O_2P_2$): C, 49.28; H, 4.50; N, 2.50. Found: C, 49.09; H, 4.82; N, 4.08. **23c**. (230 mg, 0.21 mmol, 84%). pale green solid. Anal. Calcd for **23c** ($C_{48}H_{38}Br_3KN_2Ni_2O_2P_2$): C, 50.89; H, 3.38; N, 2.47. Found: C, 49.22; H, 4.82; N, 2.97. **23d** (200 mg, 0.39 mmol, 78%) deep red solid. Anal. Calcd for **23d** ($C_{24}H_{20}BrN_2NiOP$): C, 55.22; H, 3.86; N, 5.37. Found: C, 55.15; H, 3.75; N, 5.28.

Synthesis of complexes **24a-c**

KHMDS (200 mg, 1 mmol) was added into a slurry of the phenolaminophosphonium salt (0.5 mmol) in THF (10 mL). After 30 min of stirring at RT, insoluble potassium salts (KCl) was removed by centrifugation. $[NiBr_2(DME)]$ (154 mg, 0.5 mmol) was added resulting immediately in a change of color. Stirring was continued for 2h. Insoluble potassium salt was removed by centrifugation. LiBr (44 mg, 0.5 mmol) was added. The solution changed immediately to a deep blue/purple one. THF was reduced in volume (0.2 mL). The crystallised solid was washed with petroleum ether to remove traces of HMDS. **24a**. (329 mg, 0.46 mmol, 92 %). blue purple solid. Anal. Calcd for **24a** ($C_{30}H_{37}Br_2LiNNiO_3P$): C, 50.32; H, 5.21; N, 1.96. Found: C, 49.91; H, 5.61; N, 1.80. **24b**. (300 mg, 0.42 mmol, 84%). blue solid. Anal. Calcd for **24b** ($C_{31}H_{39}Br_2LiNNiO_3P$): C, 51.00; H, 5.38; N, 1.92. Found: C, 50.76; H, 5.63; N, 1.83. **24c**. (300 mg, 0.41 mmol, 82%). green solid. Anal. Calcd for **24c** ($C_{32}H_{33}Br_2LiNNiO_3P$): C, 52.22; H, 4.52; N, 1.90. Found: C, 51.87; H, 4.68; N, 1.79.

Synthesis of complexes **25a-c**

KHMDS (200 mg, 1 mmol) was added into a slurry of the phenolaminophosphonium salt (0.5 mmol) in THF (10 mL). After 30 min of stirring at RT, insoluble potassium salts (KCl) was removed by centrifugation. $[NiBr_2(DME)]$ (154 mg, 0.5 mmol) was added resulting immediately in a change of color. Stirring was continued for 2h. Insoluble potassium salt was removed by centrifugation. $AlBr_3$ (134 mg, 0.5 mmol) was added. The solution changed immediately to a deep blue/purple one. After one night stirring, blue solid precipitated out. THF was reduced in volume (2 mL) to favor the precipitation. The solid was separated by centrifugation, washed with petroleum ether to remove traces of HMDS, dried in vacuum. **25a**.

(240 mg, 0.32 mmol, 64%). brown solid. Anal. Calcd for **25a** ($C_{22}H_{23}AlBr_4NNiOP$): C, 35.06; H, 3.08; N, 1.86. Found: C, 35.15; H, 3.12; N, 1.76. **25b**. (230 mg, 0.31 mmol, 62%). brown solid. Anal. Calcd for **25b** ($C_{23}H_{25}AlBr_4NNiOP$): C, 35.98; H, 3.28; N, 1.82. Found: C, 36.08; H, 3.40; N, 1.92. **5c**. (240 mg, 0.31 mmol, 62%). brown solid. Anal. Calcd for **25c** ($C_{24}H_{19}AlBr_4NNiOP$): C, 37.26; H, 2.48; N, 1.81. Found: C, 37.33; H, 2.55; N, 1.75.

Synthesis of complexes **26a-c**

KHMDS (200 mg, 1 mmol) was added into a slurry of the phenolaminophosphonium salt (0.5 mmol) in THF (10 mL). After 30 min of stirring at RT, insoluble potassium salts (KCl) was removed by centrifugation. $[NiBr_2(DME)]$ (154 mg, 0.5 mmol) was added resulting immediately in a change of color. Stirring was continued for 2h. Insoluble potassium salt was removed by centrifugation. PPh_3 (122 mg, 0.5 mmol) was added. The solution changed immediately to a deep green one. After stirring overnight, THF was reduced in volume (1 mL) and a green solid precipitated out. The solid was separated by centrifugation and washed with petroleum ether to remove traces of HMDS, dried in vacuum. **26a**. (260 mg, 0.35 mmol, 70%). green solid. Anal. Calcd for **26a** ($C_{40}H_{38}BrNNiOP_2$): C, 64.12; H, 5.11; N, 1.87. Found: C, 63.98; H, 5.22; N, 1.76. **26b**. (280 mg, 0.37 mmol, 73 %). Green solid. Anal. Calcd for **26b** ($C_{41}H_{40}BrNNiOP_2$): C, 64.51; H, 5.28; N, 1.84. Found: C, 65.08; H, 4.40; N, 1.92. **26c**. (315 mg, 0.41 mmol, 83%). green solid. Anal. Calcd for **26c** ($C_{42}H_{34}BrNNiOP_2$): C, 65.58; H, 4.45; N, 1.82. Found: C, 65.44; H, 4.52; N, 1.90.

Experimental Section

III. Chapter 3

General considerations

All experiments, unless otherwise stated, were performed under an atmosphere of dry nitrogen or argon using standard schlenk and glove box techniques. Solvents were freshly distilled under dry nitrogen from Na/benzophenone (THF, diethylether, petroleum ether), from P₂O₅ (dichloromethane). (Protected) *o*-phosphinophenol compounds **X1** and **X2**,⁵ [NiBr₂(DME)]² and [PdCl₂(PhCN)₂]⁶ were prepared according to the literature. All other reagents and chemicals were obtained commercially and used without further purification.

Nuclear magnetic resonance spectra were recorded on Bruker Avance 300 spectrometer operating at 300 MHz for ¹H, 75.5 MHz for ¹³C and 121.5 MHz for ³¹P. Solvent peaks were used as internal references for ¹H and ¹³C chemical shifts (ppm). ³¹P{1H} are relative to a 85% H₃PO₄ external reference. Coupling constant are expressed in hertz. The following abbreviations are used: br, broad; s, singlet; d, doublet; dd, doublet of doublets; t, triplet; m, multiple; v, virtual. The labeling schemes of the phosphasalen derivatives are given in schemes 1 and 2. IR spectra were recorded on a Perkin Elmer spectrometer and are reported in terms of frequency of absorption (cm⁻¹) using for the intensity the following abbreviations: w (weak), m (medium), s (strong). Electronic ionization mass spectra (EI-MS) were recorded with a JEOL GCmate instrument. Elemental analyses were performed by the Elemental analysis service of the London Metropolitan University (United Kingdom).

Electrochemical study

The electrochemical experiments were performed using a Vestastat potentiostat/galvanostat with a three-electrode cell using a Au disk as the working electrode, a Pt gauze as the counter electrode, and a Saturated Calomel Electrode as the reference electrode. Measurements were made in a CH₂Cl₂/DMF solvent mixture (60/40) with a concentration, of 3.8 mmol L⁻¹ and 2.0 mmol L⁻¹ for the nickel and palladium complexes respectively. Tetrabutylammonium tetrafluoroborate salt served as electrolyte (concentration 0.12 mol L⁻¹). Potentials were recorded at 50 mV s⁻¹.

Synthesis of 27

150 μL of Br_2 (2.92 mmol) is added to the solution of the protected phosphine (981.1 mg, 2.92 mmol) in dichloromethane (15 mL) at -78°C under N_2 . The cold bath was then removed. After one hour of stirring at room temperature, the resulting lemonade solution is cooled down to -78°C . Triethylamine (407 μL , 2.92 mmol) and then ethylenediamine (97.6 μL , 1.96 mmol) is added to this solution. Stirring is continued for 2 days at room temperature to yield a yellow solution and a white precipitate (probably the oxidation byproducts). The mixture is extracted three times with water (3x15 mL); the organic layer is dried over MgSO_4 and dichloromethane is evaporated in vacuum. The residue is dissolved in THF (5 mL) and the product precipitates from this solution as a white solid. (900 mg, 70%). It is easily oxidized in solution, especially in MeOH solution to give the phosphorane oxide.

27: ^{31}P { ^1H } NMR (CDCl_3): δ 38.9 (s, P^{V}); ^1H NMR (CDCl_3): δ 7.62 (m, 24H, $\text{CH}(\text{PPh}_2) + \text{C}_b\text{H} + \text{C}_d\text{H}$), 7.17 (m, 4H, $\text{C}_a\text{H} + \text{C}_c\text{H}$), 5.02 (s, 4H, $\text{O-CH}_2\text{-O}$), 3.30 (b, 4H, $\text{NH-CH}_2\text{-CH}_2\text{-NH}$), 3.01 (q, $^3\text{J}_{\text{H,H}}=7.0$ Hz, 4H, $\text{O-CH}_2\text{-CH}_3$), 0.86 (t, $^3\text{J}_{\text{H,H}}=7.0$ Hz, 6H, $\text{O-CH}_2\text{-CH}_3$); ^{13}C NMR (CDCl_3): δ 159.1 (d, $^2\text{J}_{\text{P,C}}=3.0$ Hz, OC^{IV}), 136.7 (d, $^4\text{J}_{\text{P,C}}=1.0$ Hz, C_bH), 134.9 (d, $^2\text{J}_{\text{P,C}}=8.5$ Hz, C_dH), 133.8 (d, $^4\text{J}_{\text{P,C}}=3.0$ Hz, $p\text{-CH}(\text{PPh}_2)$), 132.7 (d, $^2\text{J}_{\text{P,C}}=11.5$ Hz, $o\text{-CH}(\text{PPh}_2)$), 129.2 (d, $^3\text{J}_{\text{P,C}}=13.5$ Hz, $m\text{-CH}(\text{PPh}_2)$), 122.2 (d, $^3\text{J}_{\text{P,C}}=14.0$ Hz, C_{ac}H), 120.8 (d, $^1\text{J}_{\text{P,C}}=106.5$ Hz, $\text{C}^{\text{IV}}(\text{PPh}_2)$), 114.3 (d, $^3\text{J}_{\text{P,C}}=7.0$ Hz, C_{ca}H), 109.2 (d, $^2\text{J}_{\text{P,C}}=104.5$ Hz, $\text{C}^{\text{IV}}\text{-PPh}_2$), 92.7 (s, $\text{O-CH}_2\text{-O}$), 64.2 (s, $\text{CH}_3\text{-CH}_2\text{-O}$), 42.9 (d, $^2\text{J}_{\text{P,C}}=7.5$ Hz, $\text{N-CH}_2\text{-CH}_2\text{-N}$), 14.3 (s, $\text{CH}_3\text{-CH}_2\text{-O}$)

Synthesis of 28

From **27**: The protected diamminophosphonium salt (2 g, 2.92 mmol) was added into a solution of CH_2Cl_2 (20 mL) saturated with $\text{HCl}(\text{g})$. The solution $\text{HCl}/\text{CH}_2\text{Cl}_2$ was prepared under N_2 whereas the addition was not under N_2 . The resulting clear yellow solution became slightly cloudy and after ten minutes, the quantity of solid became significant. The schlenk was exposed to air during one minute and then reclosed. After another ten minutes, the solution had turned into heavy white slurry. HCl and CH_2Cl_2 was evaporated, then CH_2Cl_2 (20 mL) was reintroduced and the solid was separated by centrifugation, washed with CH_2Cl_2 (2.1 g, 2.35 mmol, 81%).

From **X2**: Br_2 (213 μL , 4.14 mmol) is added to a solution of *o*-diphenylphosphinophenol **X2** (1.153 g, 4.14 mmol) in dichloromethane (30 mL) at -78°C . The cold bath was then removed. After one hour stirring at room temperature, the resulting pale yellow solution is cooled down to -78°C . Tributylamine (987 μL , 4.14 mmol) and then ethylenediamine (138.5 μL , 2.07 mmol) is added to this solution. Stirring is continued for 2 days at room temperature to yield a yellow solution and a white precipitate. Dichloromethane was evaporated in vacuum. THF (30 mL) was introduced resulting in the formation of a heavy white slurry. The white solid was separated by filtration under N_2 , washed with THF (4x10mL), dried in vacuum (1.060 g, 63%).

^{31}P { ^1H } NMR (CDCl_3): δ 39.3 (s, P^{V}); ^1H NMR (CDCl_3): δ 7.67-7.59 (12H, m, $p\text{-CH}(\text{PPh}_2)$, $o\text{-CH}(\text{PPh}_2)$), 7.52-7.46 (12H, m, $m\text{-CH}(\text{PPh}_2)$, CH_a , CH_b), 6.86-6.75 (4H, m, CH_c , NH), 6.57

(2H, dd, $^3J_{\text{H,H}} = 8.0$ Hz, $^3J_{\text{P,H}} = 14.5$ Hz, CH_d), 3.43 (4H, d, $^3J_{\text{P,H}} = 10.5$ Hz, CH_2); ^{13}C NMR (CDCl_3): δ 159.7 (d, $^2J_{\text{P,C}} = 0.5$ Hz, OC^{IV}), 136.1 (d, $^4J_{\text{P,C}} = 1.0$ Hz, C_bH), 133.3 (d, $^2J_{\text{P,C}} = 11.5$ Hz, C_dH), 133.1 (d, $^4J_{\text{P,C}} = 3.0$ Hz, $p\text{-CH}(\text{PPh}_2)$), 131.9 (d, $^2J_{\text{P,C}} = 11.5$ Hz, $o\text{-CH}(\text{PPh}_2)$), 128.5 (d, $^3J_{\text{P,C}} = 13.5$ Hz, $m\text{-CH}(\text{PPh}_2)$), 121.4 (d, $^1J_{\text{P,C}} = 106.5$ Hz, $\text{C}^{\text{IV}}(\text{PPh}_2)$), 119.6 (d, $^3J_{\text{P,C}} = 13.5$ Hz, C_cH), 117.7 (d, $^3J_{\text{P,C}} = 7.0$ Hz, C_aH), 106.8 (d, $^2J_{\text{P,C}} = 104.0$ Hz, $\text{PPh}_2\text{C}^{\text{IV}}$), 43.3 (d, $^2J_{\text{P,C}} = 1.5$ Hz, CH_2). HR-EI-MS: 307.1132 ($[\text{M}-2\text{Br}]^{2+}$; $\text{C}_{38}\text{H}_{36}\text{N}_2\text{O}_2\text{P}_2^{2+}$; calcd 307.1126).

Synthesis of 29

KHMDS (7.0 g, 35.1 mmol) was added to a suspension of the aminophosphonium salt (8.8 mmol) in THF (320 mL) at ambient temperature. After 16 h, a cloudy solution was formed. The white potassium bromide by-product was removed by centrifugation. The solvent was removed in vacuum and the residue was dissolved in petroleum ether (60 mL). After 5 minutes of sonification, a white slurry was formed. The white solid was separated by centrifugation, washed with petroleum ether (20 mL) and dried in vacuum.

29: (6.0 g, 8.7 mmol, 99%). $^{31}\text{P}\{^1\text{H}\}$ NMR ($\text{THF}-d_8$): δ 18.6 (s, P^{V}); ^1H NMR ($\text{THF}-d_8$): δ 7.73-7.67 (m, 8H, $o\text{-CH}(\text{PPh}_2)$), 7.62-7.57 (m, $^5J_{\text{P,H}} = 1.5$ Hz, 4H, $p\text{-CH}(\text{PPh}_2)$), 7.55-7.49 (d, $^4J_{\text{P,H}} = 2.0$ Hz, 8H, $m\text{-CH}(\text{PPh}_2)$), 7.09 (m, 2H, $^3J_{\text{H,H}} = 8.5$ Hz, $^3J_{\text{H,H}} = 7.0$ Hz, $^4J_{\text{H,H}} = 1.5$ Hz, 2H, C_bH), 6.6-6.61 (m, 2H, $^3J_{\text{H,H}} = 8.5$ Hz, 2H, C_aH), 6.47 (ddd, $^4J_{\text{H,H}} = 1.5$ Hz, $^3J_{\text{H,H}} = 7.0$ Hz, $^3J_{\text{P,H}} = 16.0$ Hz, 2H, C_dH), 6.05 (ddd, $^3J_{\text{H,H}} = ^3J'_{\text{H,H}} = 7.0$ Hz, $^4J_{\text{P,H}} = 3.0$ Hz, 2H, C_cH), 3.42 (dd, $^3J_{\text{P,H}} = 6.0$ Hz, $^3J'_{\text{P,H}} = 6.5$ Hz, 4H, $\text{N-CH}_2\text{-CH}_2\text{-N}$); $^{13}\text{C}\{^1\text{H}\}$ NMR ($\text{THF}-d_8$): δ 174.3 (d, $^2J_{\text{P,C}} = 3.6$ Hz, O-C^{IV}), 132.9 (d, $^2J_{\text{P,C}} = 12.9$ Hz, C_dH), 132.8 (d, $^1J_{\text{P,C}} = 77.2$ Hz, $\text{C}^{\text{IV}}(\text{PPh}_2)$), 132.1 (d, $^4J_{\text{P,C}} = 1.3$ Hz, C_bH), 131.7 ($^2J_{\text{P,C}} = 8.2$ Hz, $o\text{-CH}(\text{PPh}_2)$), 129.0 (d, $^4J_{\text{P,C}} = 2.1$ Hz, $p\text{-CH}(\text{PPh}_2)$), 127.0 (d, $^3J_{\text{P,C}} = 10.3$ Hz, $m\text{-CH}(\text{PPh}_2)$), 121.8 (d, $^3J_{\text{P,C}} = 9.0$ Hz, C_aH), 112.5 (d, $^1J_{\text{P,C}} = 128.7$ Hz, $\text{C}^{\text{IV}}\text{-PPh}_2$), 107.0 (d, $^3J_{\text{P,C}} = 15.2$ Hz, C_cH), 50.4 (dd, $^2J_{\text{P,C}} = 26.9$ Hz, $^3J_{\text{P,C}} = 8.0$ Hz, $\text{N-CH}_2\text{-CH}_2\text{-N}$). Anal. Calcd for $\text{C}_{38}\text{H}_{32}\text{K}_2\text{N}_2\text{O}_2\text{P}_2$: C, 66.26; H, 4.68; N, 4.07. Found: C, 66.19; H, 4.73; N, 3.99.

Synthesis of 30

THF (5 mL) was added to a mixture of KHMDS (94.3 mg, 0.47 mmol) and **28** (91.4 mg, 0.12 mmol). After 2h, potassium salt was removed by centrifugation and $[\text{PdCl}_2(\text{PhCN})_2]$ (45.3 mg, 0.12 mmol) was added to the obtained colorless solution, which became immediately yellow. After 16h, the precipitated brown solid was separated by centrifugation, dissolved in dichloromethane to remove the insoluble potassium salt. Then the solvent was evaporated and the obtained residue was washed with petroleum ether (5 mL) to give **30** as a yellow solid (63 mg, 73%)

30: $^{31}\text{P}\{^1\text{H}\}$ NMR (CD_2Cl_2): δ 33.7 (s, P^{V}); ^1H NMR (CD_2Cl_2): δ 7.55-7.46 (12H, m, $o\text{-CH}(\text{PPh}_2)$, $p\text{-CH}(\text{PPh}_2)$), 7.44-7.38 (8H, m, $m\text{-CH}(\text{PPh}_2)$), 7.07 (2H, vtdd, $^3J_{\text{H,H}} = 7.0$ Hz, $^3J_{\text{H,H}} = 8.5$ Hz, $^4J_{\text{H,H}} = 1.5$ Hz, $^5J_{\text{P,H}} = 0.5$ Hz, C_bH), 6.78 (2H, ddd, $^3J_{\text{H,H}} = 8.5$ Hz, $^4J_{\text{H,H}} = 1.0$ Hz, $^4J_{\text{P,H}} = 6.5$ Hz, C_aH), 6.32 (2H, ddd, $^3J_{\text{H,H}} = 8.0$ Hz, $^4J_{\text{H,H}} = 1.5$ Hz, $^3J_{\text{P,H}} = 16.0$ Hz, C_dH), 6.18 (2H, dddd, $^3J_{\text{H,H}} = 8.0$ Hz, $^3J_{\text{H,H}} = 7.0$ Hz, $^4J_{\text{H,H}} = 1.0$ Hz, $^4J_{\text{P,H}} = 3.0$ Hz, C_cH), 2.54 (4H, vt, $J_{\text{P,H}} = 4.5$ Hz, CH_2); $^{13}\text{C}\{^1\text{H}\}$ NMR (CD_2Cl_2): δ 172.5 (s, OC^{IV}), 134.9 (br, s, C_bH); 134.2 (d, $^2J_{\text{P,C}} = 10.0$ Hz, $o\text{-$

CH(PPh₂)), 133.3 (br. s, ⁴J_{P,C} = 1.0 Hz, *p*-CH(PPh₂)), 133.1 (²J_{P,C} = 13.0 Hz, C_dH), 129.7 (d, ³J_{P,C} = 12.0 Hz, *m*-CH(PPh₂)), 127.2 (d, ¹J_{P,C} = 89.0 Hz, C^{IV}(PPh₂)), 122.8 (d, ³J_{P,C} = 8.0 Hz, C_aH), 114.0 (d, ³J_{P,C} = 15.0 Hz, C_eH), 110.4 (d, ¹J_{P,C} = 122.0 Hz, C^{IV}-PPh₂), 53.8 (dd, ²J_{P,C} = 17.5 Hz, ³J_{P,C} = 5.0 Hz, CH₂); IR (cm⁻¹): 1586 (m), 1534 (w), 1459 (m, ν_{CC} aromatic), 1442 (s), 1327 (m), 1257 (m), 1124 (w), 1110(s), 1084(w), 1069(w), 1020 (w), 1000 (w), 867 (m, b), 800 (m), 769 (w), 747 (s), 722 (w), 710 (w), 693 (s). Anal. Calcd for C₃₈H₃₂N₂O₂P₂Pd: C, 63.65; H, 4.50; N, 3.91. Found: C, 63.74; H, 4.30; N, 3.94.

Synthesis of 31

THF (5 mL) was added to a mixture of KHMDS (94.3 mg, 0.47 mmol) and **28** (91.4 mg, 0.12 mmol). After 2h, potassium salt was removed by centrifugation and [NiBr₂(DME)] (36.4 mg, 0.12 mmol) was added to the obtained colorless solution which became immediately deep purple. After 30 min, a purple solid precipitated out from the mixture and the color of the solution faded. The solid was separated by centrifugation, and then dissolved in dichloromethane to remove the insoluble potassium salt. After evaporation of the solvent residue was washed with petroleum ether (5mL) giving **31** as a purple solid (65 mg, 82%).

31: ³¹P{¹H} NMR (CD₂Cl₂): δ 32.8 (s, P^V); ¹H NMR (CD₂Cl₂): δ 7.76-7.66 (12H, m, *o*-CH(PPh₂), *p*-CH(PPh₂)), 7.62-7.56 (8H, m, *m*-CH(PPh₂)), 7.10 (2H, vtd, ³J_{H,H} = 7.5 Hz, ⁴J_{H,H} = 1.5 Hz, C_bH), 6.69 (2H, dd, ³J_{H,H} = 7.5 Hz, ³J_{P,H} = 6.5 Hz, C_aH), 6.49 (2H, ddd, ³J_{H,H} = 7.5 Hz, ⁴J_{H,H} = 1.5 Hz, ³J_{P,H} = 15.0 Hz, C_dH), 6.26 (2H, vtd, ³J_{H,H} = 7.5 Hz, ⁴J_{P,H} = 3.0 Hz, C_eH), 2.16-2.13 (4H, m, CH₂); ¹³C{¹H} NMR (CD₂Cl₂): δ 170.1 (s, OC^{IV}), 133.3 (d, ⁴J_{P,C} = 1.0 Hz, C_bH), 133.1 (d, ²J_{P,C} = 10.0 Hz, *o*-CH(PPh₂)), 132.3 (d, ⁴J_{P,C} = 2.0 Hz, *p*-CH(PPh₂)), 131.2 (²J_{P,C} = 12.0 Hz, C_dH), 128.9 (d, ³J_{P,C} = 12.0 Hz, *m*-CH(PPh₂)), 127.4 (d, ¹J_{P,C} = 90.5 Hz, C^{IV}(PPh₂)), 122.7 (d, ³J_{P,C} = 8.0 Hz, C_aH), 113.1 (d, ³J_{P,C} = 14.5 Hz, C_eH), 108.0 (d, ¹J_{P,C} = 119.6 Hz, C^{IV}-PPh₂), 50.0 (dd, ²J_{P,C} = 16.0 Hz, ³J_{P,C} = 2.0 Hz, CH₂); IR (cm⁻¹): 1586 (m), 1534 (w), 1459 (m), 1440 (s), (1300 m), 1275 (m), 1137 (w), 1116(s), 1098(m), 1081(m), 1027 (m), 1000 (w), 889 (w), 867 (w), 861(w), 811 (m), 778 (w), 752 (s), 727 (w), 710 (w), 697 (s). Anal. Calcd for C₃₈H₃₂N₂NiO₂P₂: C, 68.19; H, 4.82; N, 4.19. Found: C, 68.00; H, 4.74; N, 4.05.

Experimental Section

IV. Chapter 4

General considerations

All experiments, unless otherwise stated, were performed under an atmosphere of dry nitrogen or argon using standard schlenk and glove box techniques. Solvents were directly taken from a MBraun MB-SPS 800 Solvent Purification Machine. $[\text{NiBr}_2(\text{DME})]_2$ was prepared according to the literature. All other reagents and chemicals were obtained commercially and used without further purification.

Nuclear magnetic resonance spectra were recorded on Bruker Avance 300 spectrometer operating at 300 MHz for ^1H , 75.5 MHz for ^{13}C and 121.5 MHz for ^{31}P . Solvent peaks were used as internal references for ^1H and ^{13}C chemical shifts (ppm). $^{31}\text{P}\{^1\text{H}\}$ are relative to a 85% H_3PO_4 external reference. Coupling constant are expressed in hertz. The following abbreviations are used: br, broad; s, singlet; d, doublet; dd, doublet of doublets; t, triplet; m, multiple; v, virtual. The labeling schemes of the phosphasalen derivatives are given in schemes 1 and 2. Elemental analyses were performed by the Elemental analysis service of the London Metropolitan University (United Kingdom).

Electrochemical study

The electrochemical experiments were performed using a Vestastat potentiostat/galvanostat with a three-electrode cell using a Au disk as working electrode, a Pt gauze as the counter electrode, and a Saturated Calomel Electrode as reference electrode. Measurements were made in CH_2Cl_2 with a concentration, of 3.0 mmol L^{-1} for the nickel complexes. Tetrabutylammonium tetrafluoroborate salt served as electrolyte (concentration 0.12 mol L^{-1}). Potentials were recorded at 50 mV s^{-1} .

Synthesis of 32

At 0°C , 2,4-ditert-butyl phenol (23.127 g, 112.1 mmol) was added to a slurry of NaH (60% in mineral oil, 5.605 g, 140.1 mmol) in DMF (60 mL), resulted in a yellow slurry. Stirring was continued for 90 minutes at 0°C , then chloromethyl ethyl ether (13 mL, 140.1 mmol) was added dropwise and the cold bath was removed. After 90 minutes of stirring at room temperature, 90 mL of distilled water was added. The mixture was extracted with petroleum ether (4x100 mL).

The organic layer was dried over Na₂SO₄. Petroleum ether was evaporated at low temperature (the product was rather volatile), resulting in a yellow oil. The crude oil contains traces of solvent and will be used for the next step without further purification (30g, 112 mmol, 100%).

32: ¹H NMR (CDCl₃): δ 7.34 (d, ⁴J_{H,H} = 2.5 Hz, 1H, tBu-C^{IV}-CH-C^{IV}-tBu), 7.17 (dd, ³J_{H,H} = 8.5 Hz, ⁴J_{H,H} = 2.5 Hz, 1H, tBu-C^{IV}-CH-CH), 7.08 (d, ³J_{H,H} = 8.5 Hz, 1H, tBu-C^{IV}-CH-CH), 5.27 (s, 2H, O-CH₂-O), 3.75 (q, ³J_{H,H} = 7.0 Hz, 2H, O-CH₂-CH₃), 1.41 (s, 9H, C^{IV}(CH₃)₃), 1.32 (s, 9H, C^{IV}(CH₃)₃), 1.26 (t, ³J_{H,H} = 7.0 Hz, 3H, O-CH₂-CH₃)

Synthesis of 33

At -78°C, a solution containing n-BuLi (1.6M/hexanes, 76 mL, 121 mmol) and TMEDA (tetramethylethylenediamine, 18 mL, 121 mol) in petroleum ether (20 mL) was added into a solution of **32** (30g, 112 mmol) in petroleum ether (100 mL). The cold bath was removed and stirring was continued at room temperature. After 2h, ClPPh₂ (20.3 mL, 115 mmol) was added into the resulted yellow suspension at -78°C. After removal of the cold bath, a red-purple solution was obtained, which transformed into an orange slurry after 16h. The solvents were evaporated and the residue was taken in Et₂O (170 mL) and extracted with H₂O (100 mL). The aqueous phase is extracted three times with Et₂O (3x100 mL) and the total organic layer was dried over Na₂SO₄. After evaporation of Et₂O, the viscous residue was recrystallised in dried MeOH, giving the product as colorless crystals (42g, 93mmol, 83%)

33: ³¹P{¹H} NMR (CDCl₃): δ -12.6 (s, P^V); ¹H NMR (CDCl₃): δ 7.29 (d, ⁴J_{H,H} = 2.5 Hz, 1H, C_bH), 7.24-7.21 (m, 6H, CH(PPh₂)), 7.17-7.12 (m, 4H, CH(PPh₂)), 6.57 (dd, ⁴J_{H,H} = 2.5 Hz, ³J_{P,H} = 4.6 Hz, 1H, C_dH), 5.15 (d, ³J_{H,H} = 1.7 Hz, 2H, O-CH₂-O), 3.67 (q, ³J_{H,H} = 7.0 Hz, 2H, O-CH₂-CH₃), 1.33 (s, 9H, C(CH₃)₃), 1.03 (t, ³J_{H,H} = 7.0 Hz, O-CH₂-CH₃), 0.98 (s, 9H, C(CH₃)₃); ¹³C{¹H} NMR (CDCl₃): δ 156.7 (d, ²J_{P,C} = 19.7 Hz, OC^{IV}), 146.0 (s, C_c^{IV}), 142.4 (d, ⁴J_{P,C} = 3.0 Hz, C_a^{IV}), 137.8 (d, ¹J_{P,C} = 11.5 Hz, C^{IV}(PPh₂)), 133.9 (d, ^{2/3}J_{P,C} = 19.9 Hz, *o*-or *m*-CH(PPh₂)), 130.6 (d, ¹J_{P,C} = 11.5 Hz, C^{IV}-PPh₂), 130.5 (d, ²J_{P,C} = 2.6 Hz, C_dH), 130.2 (s, *p*-CH(PPh₂)), 130.0 (d, ^{2/3}J_{P,C} = 7.0 Hz, *o*-or *m*-CH(PPh₂)), 125.9 (d, ⁴J_{P,C} = 1.5 Hz, C_bH), 98.8 (d, ⁴J_{P,C} = 17.5 Hz, O-CH₂-O), 65.7 (s, O-CH₂-CH₃), 35.7 (s, C(CH₃)₃), 34.8 (s, C(CH₃)₃), 31.6 (s, C(CH₃)₃), 31.5 (s, C(CH₃)₃), 31.3 (s, C(CH₃)₃), 15.5 (s, O-CH₂-CH₃)

Synthesis of 34'

At 0°C, NBS (N-bromosuccinimide, 18.2g, 102,3 mmol) was added into a solution of 2,4-di-tert-butylphenol (20.1 g, 97.4 mmol) in acetonitrile (300 mL). Stirring was continued at room temperature overnight, giving an orange solution. 10 mL of saturated aqueous solution of sodium bisulfide was added and induced the precipitation of a white solid. After filtration of this precipitate, the mixture was extracted four times with petroleum ether (4x70 mL). The total organic layer was dried over Na₂SO₄. The solvent was evaporated, giving the product as a slightly yellow solid (24.9g, 90%).

34': ^1H NMR (CDCl_3): δ 7.33 (d, $^4J_{\text{H,H}} = 2.5$ Hz, 1H, $\text{tBu-C}^{\text{IV}}\text{-CH-C}^{\text{IV}}\text{-tBu}$), 7.25 (d, $^4J_{\text{H,H}} = 2.5$ Hz, 1H, $\text{tBu-C}^{\text{IV}}\text{-CH-CBr}$), 5.65 (s, 1H, OH), 1.41 (s, 9H, $\text{C}^{\text{IV}}(\text{CH}_3)_3$), 1.29 (s, 9H, $\text{C}^{\text{IV}}(\text{CH}_3)_3$).

Synthesis of 34

From **33**: The protected phosphine (2g, 4.46 mmol) was added into a solution of dry MeOH (20 mL) saturated with HCl (g) at room temperature and under N_2 . After 45 minutes, HCl and MeOH was evaporated. 15 mL of dry MeOH was added to dissolve the residue, resulting in a colorless solution with several small drops of oil. 1mL of petroleum ether was added to extract the oil. 5 mL of H_2O was added. Scrubbing the flask with a glass pipette led to formation of colorless crystals. More water (7 mL) was added and methanol was evaporated under vacuum for 5 minutes, resulting in more crystal formation and a clear solution. The white solid was separated and dried in vacuum. (1.64 g, 94%)

From **34'**: n-BuLi (1.6M in hexanes, 107.8 mL, 173 mmol) was added into a solution of **3'** (23g, 80.6 mmol) in Et_2O (170 mL) at -78°C , giving immediately a white suspension. The cold bath was removed and stirring was continued at room temperature for 30 min, giving a pale yellow solution. ClPPh_2 (14.5 mL, 80.6 mmol) was added into this solution at -78°C . After overnight stirring, a white suspension was formed. The mixture was extracted quickly twice with aqueous solutions of NaH_2PO_4 (0.1M, 2x100 mL). the organic layer was filtered to removed inorganic salts. MeOH (30 mL) was added and the solution was evaporated under vacuum until the volume of the remaining solvent was about 30 mL. A white solid precipitated out from the green solution. This solid was separated by filtration, washed with MeOH (2x5mL) and dried in vacuum. (28 g, 90%)

34: $^{31}\text{P}\{^1\text{H}\}$ NMR (CDCl_3): δ -30.8 (s, P); ^1H NMR (CDCl_3): δ 7.26-7.25 (m, 11H, $\text{CH}(\text{PPh}_2) + \text{C}_b\text{H}$), 6.81 (dd, $^4J_{\text{H,H}} = 1.5$ Hz, $^3J_{\text{P,H}} = 5.5$ Hz, 1H, C_dH), 6.60 (d, $^4J_{\text{P,H}} = 10.0$ Hz, 1H, OH), 1.34 (s, 9H, $\text{C}_a\text{-C}(\text{CH}_3)_3$), 1.08 (s, 9H, $\text{C}_c\text{-C}(\text{CH}_3)_3$); $^{13}\text{C}\{^1\text{H}\}$ NMR (CDCl_3): δ 156.3 (d, $^2J_{\text{P,C}} = 19.2$ Hz, OC^{IV}), 142.5 (d, $^3J_{\text{P,C}} = 3.0$ Hz, C_c^{IV}), 135.6 (d, $^1J_{\text{P,C}} = 3.0$ Hz, $\text{C}^{\text{IV}}(\text{PPh}_2)$), 135.5 (d, $^3J_{\text{P,C}} = 1.0$ Hz, C_a^{IV}), 133.6 (d, $^{2/3}J_{\text{P,C}} = 18.5$ Hz, *o*- or *m*- $\text{CH}(\text{PPh}_2)$), 129.5 (d, $^2J_{\text{P,C}} = 3.5$ Hz, C_dH), 129.1 (s, *p*- $\text{CH}(\text{PPh}_2)$), 128.8 (d, $^{2/3}J_{\text{P,C}} = 7.5$ Hz, *o*- or *m*- $\text{CH}(\text{PPh}_2)$), 126.6 (s, C_bH), 120.1 (s, $\text{C}^{\text{IV}}\text{-PPh}_2$), 35.4 (d, $^4J_{\text{P,C}} = 2.0$ Hz, $\text{C}_c\text{-C}(\text{CH}_3)_3$), 34.7 (s, $\text{C}_a\text{-C}(\text{CH}_3)_3$), 31.7 (s, $\text{C}_c\text{-C}(\text{CH}_3)_3$), 29.2 (s, $\text{C}_a\text{-C}(\text{CH}_3)_3$),

Synthesis of 35a

At -78°C , bromine (200 μL , 3.88 mmol) was added dropwise to a solution of the phenolphosphine (1.516 g, 3.88 mmol) in CH_2Cl_2 (30 mL). The cold bath was removed and stirring was continued for 45 minutes at room temperature. Then the solution was cooled down to -78°C . Bu_3N (926 μL , 3.88 mmol) was added, followed by ethylene diamine (129.8 μL , 1.94 mmol). The cold bath was removed. After 16h, a cloudy yellow solution was formed. CH_2Cl_2 was evaporated, 15 mL of THF was added. With sonification, a heavy white slurry was formed. The white solid was separated by filtration, washed with THF (5x7 mL), dried in vacuum (1.47 g, 71%)

35a.THF: $^{31}\text{P}\{^1\text{H}\}$ NMR (CDCl_3): δ 40.3 (s, P^{V}); ^1H NMR (CDCl_3): δ 8.15(b, 2H, $\text{CH}(\text{PPh}_2)$), 7.75-7.56 (m, 18H, $\text{CH}(\text{PPh}_2)$), 6.93 (b, 2H, C_bH), 6.44 (dd, $^4\text{J}_{\text{H,H}}=2.1$ Hz, $^3\text{J}_{\text{P,H}}=15.2$ Hz, 2H, C_dH), 3.78 (m, 4H, $\text{O}-\text{CH}_2$ (THF)), 3.74 (b, 4H, $\text{N}-\text{CH}_2-\text{CH}_2-\text{N}$), 1.85 (m, 4H, $\text{O}-\text{CH}_2-\text{CH}_2$ (THF)), 1.59 (b, 2H, OH), 1.52 (s, 18H, $\text{C}_a-\text{C}(\text{CH}_3)_3$), 1.08 (s, 18H, $\text{C}_c-\text{C}(\text{CH}_3)_3$).

The insolubility of the product in all regular deuterated solvents prevents $^{13}\text{C}\{^1\text{H}\}$ NMR characterization.

Synthesis of 35b

At -78°C , bromine (500 μL , 9.71 mmol) was added dropwise to a solution of the phenolphosphine (3.781 g, 9.71 mmol) in CH_2Cl_2 (120 mL). The cold bath was removed and stirring was continued for 3 hours at RT. Then the solution was cooled down to -78°C . DABCO (1,4-diazabicyclo[2.2.2]octane, 545 mg, 4.86 mmol) was added, followed by *rac*-1,2-diaminocyclohexane (582.9 μL , 4.86 mmol). The cold bath was removed. After 16h, a cloudy yellow solution was formed. CH_2Cl_2 was evaporated, 200 mL of THF was added. The insoluble DABCO salt was removed by centrifugation. THF was evaporated and the white solid was washed with Et_2O (2x5 mL), dried in vacuum (3.8 g, 75%)

35b: $^{31}\text{P}\{^1\text{H}\}$ NMR (CDCl_3): δ 38.5 (s, P^{V}); ^1H NMR (CDCl_3): δ 8.59 (s, 2H, NH), 7.77 (dd, $^3\text{J}_{\text{H,H}}=7.5$ Hz, $^3\text{J}_{\text{P,H}}=12.8$ Hz, 4H, *o*- $\text{CH}(\text{PPh}_2)$), 7.69 (dd, $^3\text{J}_{\text{H,H}}=7.5$ Hz, $^3\text{J}_{\text{P,H}}=14.2$ Hz, 4H, *o*- $\text{CH}(\text{PPh}_2)$), 7.70 (s, 1H, OH), 7.69 (s, 1H, OH), 7.50 (vtd, $^3\text{J}_{\text{H,H}}=^3\text{J}'_{\text{H,H}}=7.5$ Hz, $^4\text{J}_{\text{P,H}}=3.0$ Hz, 2H, *m*- $\text{CH}(\text{PPh}_2)$), 7.63 (vt, $^3\text{J}_{\text{H,H}}=^3\text{J}'_{\text{H,H}}=7.5$ Hz, 2H, *m*- $\text{CH}(\text{PPh}_2)$), 7.40 (vt, $^3\text{J}_{\text{H,H}}=^3\text{J}'_{\text{H,H}}=7.5$ Hz, 4H, *m*- $\text{CH}(\text{PPh}_2)$), 7.13 (vtd, $^3\text{J}_{\text{H,H}}=^3\text{J}'_{\text{H,H}}=7.5$ Hz, $^4\text{J}_{\text{P,H}}=3.3$ Hz, 4H, *p*- $\text{CH}(\text{PPh}_2)$), 6.56 (dd, $^4\text{J}_{\text{H,H}}=2.2$ Hz, $^5\text{J}_{\text{P,H}}=8.0$ Hz, 1H, C_bH), 6.53 (dd, $^4\text{J}_{\text{H,H}}=2.2$ Hz, $^5\text{J}_{\text{P,H}}=8.0$ Hz, 1H, C_bH), 6.37 (dd, $^4\text{J}_{\text{H,H}}=2.2$ Hz, $^3\text{J}_{\text{P,H}}=15.6$ Hz, 2H, C_bH), 3.82 (m, 2H, $\text{N}-\text{CH}-\text{CH}-\text{N}$), 2.05 (m, 2H, $\text{CH}_2(\text{cyclohexane})$), 1.59 (m, 2H, $\text{CH}_2(\text{cyclohexane})$), 1.53 (s, 18H, $\text{C}_a-\text{C}(\text{CH}_3)_3$), 1.30 (m, 2H, $\text{CH}_2(\text{cyclohexane})$), 1.03 (s, 18H, $\text{C}_c-\text{C}(\text{CH}_3)_3$), 0.93 (m, 2H, $\text{CH}_2(\text{cyclohexane})$); $^{13}\text{C}\{^1\text{H}\}$ NMR (CDCl_3): δ 155.9 (d, $^3\text{J}_{\text{P,C}}=0.9$ Hz, $\text{C}^{\text{IV}}-\text{O}$), 145.7 (d, $^3\text{J}_{\text{P,C}}=8.2$ Hz, $\text{C}_{c,a}^{\text{IV}}$); 144.5 (d, $^3\text{J}_{\text{P,C}}=7.0$ Hz, $\text{C}_{a,c}^{\text{IV}}$), 135.0-133.0 (m, $\text{CH}(\text{PPh}_2)$), 131.8 (d, $^4\text{J}_{\text{P,C}}=0.9$ Hz, *p*- $\text{CH}(\text{PPh}_2)$), 131.5 (d, $^4\text{J}_{\text{P,C}}=0.9$ Hz, *p*- $\text{CH}(\text{PPh}_2)$), 129.7-128.9 (m, $\text{CH}(\text{PPh}_2)$ + C_bH), 128.6 (d, $^2\text{J}_{\text{P,C}}=12.2$ Hz, C_dH), 123.0 (d, $^1\text{J}_{\text{P,C}}=109.7$ Hz, $\text{C}^{\text{IV}}(\text{PPh}_2)$), 121.7 (d, $^1\text{J}_{\text{P,C}}=97.5$ Hz, $\text{C}^{\text{IV}}-\text{PPh}_2$), 116.0 (d, $^1\text{J}_{\text{P,C}}=106.2$ Hz, $\text{C}^{\text{IV}}(\text{PPh}_2)$), 59.0 (m, $\text{N}-\text{CH}-\text{CH}-\text{N}$), 35.6 (s, $\text{C}_a^{\text{IV}}-\text{C}(\text{CH}_3)_3$), 34.7 (s, $\text{C}_c^{\text{IV}}-\text{C}(\text{CH}_3)_3$), 30.2 (s, $\text{CH}_2(\text{cyclohexane})$), 30.0 (s, $\text{CH}_2(\text{cyclohexane})$), 29.8 (s, $\text{C}_{c,a}^{\text{IV}}-\text{C}(\text{CH}_3)_3$), 29.7 (s, $\text{C}_{a,c}^{\text{IV}}-\text{C}(\text{CH}_3)_3$), 29.5 (s, $\text{C}_{a,c}^{\text{IV}}-\text{C}(\text{CH}_3)_3$), 29.4 (s, $\text{CH}_2(\text{cyclohexane})$), 28.8 (s, $\text{CH}_2(\text{cyclohexane})$). Anal. Calcd for $\text{C}_{58}\text{H}_{74}\text{Br}_2\text{N}_2\text{O}_2\text{P}_2$: C, 66.16; H, 7.08; N, 2.66. Found: C, 66.29; H, 7.15; N, 2.67.

Synthesis of 36a

KHMDS (7.0 g, 35.1 mmol) was added to a suspension of the aminophosphonium salt (8.8 mmol) in THF (320 mL) at ambient temperature. After 16 h, a cloudy solution was formed. The white potassium bromide by-product was removed by centrifugation. The solvent was removed *in vacuo* and the residue was dissolved in petroleum ether (60 mL). After 5 minutes of

sonification, a white slurry was formed. The white solid was separated by centrifugation, washed with petroleum ether (20 mL) and dried *in vacuo* (7.2 g, 78%)

36a.2THF. $^{31}\text{P}\{^1\text{H}\}$ NMR (THF- d_8): δ 20.6 (s, P^{V}); ^1H NMR (Toluene- d_8): δ 7.52-7.50 (m, 10H, $\text{CH}(\text{PPh}_2) + \text{C}_b\text{H}$), 7.05-7.01 (m, 12H, $\text{CH}(\text{PPh}_2)$), 6.30 (dd, $^4J_{\text{H,H}}=2.4$ Hz, $^3J_{\text{P,H}}=17.1$ Hz, 2H, C_dH), 3.41-3.38 (m, 8H, $\text{O-CH}_2(\text{THF})$), 3.20 (vt, $J_{\text{P,H}}=J'_{\text{P,H}}=5.0$ Hz, 4H, $\text{N-CH}_2\text{-CH}_2\text{-N}$), 1.70 (s, 18H, $\text{C}_a\text{-C}(\text{CH}_3)_3$), 1.36 (m, 8H, $\text{O-CH}_2\text{-CH}_2(\text{THF})$), 1.08 (s, 18H, $\text{C}_c\text{-C}(\text{CH}_3)_3$); $^{13}\text{C}\{^1\text{H}\}$ NMR (THF- d_8): δ 173.4 (d, $^2J_{\text{P,C}}=4.0$ Hz, $\text{C}^{\text{IV}}\text{-O}$), 140.1 (d, $^3J_{\text{P,C}}=9.5$ Hz, C_c^{IV}), 134.2 (d, $^1J_{\text{P,C}}=81.4$ Hz, $\text{C}^{\text{IV}}(\text{PPh}_2)$), 133.7 (d, $^{2/3}J_{\text{P,C}}=7.5$ Hz, *o*- or *m*- $\text{CH}(\text{PPh}_2)$), 130.5 (d, $^4J_{\text{P,C}}=1.9$ Hz, *p*- $\text{CH}(\text{PPh}_2)$), 128.8 (d, $^2J_{\text{P,C}}=15.6$ Hz, C_dH), 128.6 (d, $^3J_{\text{P,C}}=17$ Hz, C_a^{IV}), 128.4 (d, $^{2/3}J_{\text{P,C}}=10.3$ Hz, *o*- or *m*- $\text{CH}(\text{PPh}_2)$), 127.4 (d, $^4J_{\text{P,C}}=0.8$ Hz, C_bH), 112.8 (d, $^1J_{\text{P,C}}=134.2$ Hz, $\text{C}^{\text{IV}}\text{-PPh}_2$), 52.1 (dd, $J_{\text{P,C}}=9.3$ Hz, $J'_{\text{P,C}}=29.7$ Hz, $\text{N-CH}_2\text{-CH}_2\text{-N}$), 36.0 (d, $^4J_{\text{P,C}}=2.1$ Hz, $\text{C}_a^{\text{IV}}\text{-C}(\text{CH}_3)_3$), 34.0 (d, $^4J_{\text{P,C}}=0.6$ Hz, $\text{C}_c^{\text{IV}}\text{-C}(\text{CH}_3)_3$), 31.9 (s, $\text{C}(\text{CH}_3)_3$), 29.9 (s, $\text{C}(\text{CH}_3)_3$). Anal. Calcd for $\text{C}_{62}\text{H}_{80}\text{K}_2\text{N}_2\text{O}_4\text{P}_2$: C, 70.42; H, 7.63; N, 2.65. Found: C, 70.57; H, 7.80; N, 2.49.

Synthesis of 36b

36b was synthesised following the same procedure as **36a**.

36b.HMDS. $^{31}\text{P}\{^1\text{H}\}$ NMR (benzen- d_6): δ 15.8 (s, P^{V}); ^1H NMR (benzen- d_6): δ 7.72 (m, 4H, $\text{CH}(\text{PPh}_2)$), 7.65 (m, 4H, $\text{CH}(\text{PPh}_2)$), 7.65 (d, $^4J_{\text{H,H}}=2.6$ Hz, 2H, C_bH), 7.14 (m, 6H, $\text{CH}(\text{PPh}_2)$), 7.02 (m, 6H, $\text{CH}(\text{PPh}_2)$), 6.29 (dd, $^4J_{\text{H,H}}=2.6$ Hz, $^3J_{\text{P,H}}=16.8$ Hz, 2H, C_dH), 3.09 (m, 2H, N-CH-CH-N), 2.26 (m, 2H, $\text{CH}_2(\text{cyclohexane})$), 1.82 (s, 18H, $\text{C}_a^{\text{IV}}\text{-C}^{\text{IV}}(\text{CH}_3)_3$), 1.49 (m, 2H, $\text{CH}_2(\text{cyclohexane})$), 1.22 (m, 2H, $\text{CH}_2(\text{cyclohexane})$), 1.17 (s, 18H, $\text{C}_c^{\text{IV}}\text{-C}^{\text{IV}}(\text{CH}_3)_3$), 0.87 (m, 2H, $\text{CH}_2(\text{cyclohexane})$), 0.02 (18H, $\text{CH}_3\text{-HMDS}$); $^{13}\text{C}\{^1\text{H}\}$ NMR (benzen- d_6): δ 173.3 (d, $^3J_{\text{P,C}}=3.4$ Hz, $\text{C}^{\text{IV}}\text{-O}$), 140.3 (d, $^1J_{\text{P,C}}=73.2$ Hz, $\text{C}^{\text{IV}}(\text{PPh}_2)$), 140.3 (d, $^3J_{\text{P,C}}=9.2$ Hz, $\text{C}_{c,a}^{\text{IV}}$), 133.8 (d, $^{2/3}J_{\text{P,C}}=13.8$ Hz, *m*- or *o*- $\text{CH}(\text{PPh}_2)$), 133.5 (d, $^{2/3}J_{\text{P,C}}=12.5$ Hz, *m*- or *o*- $\text{CH}(\text{PPh}_2)$), 133.2 (d, $^{2/3}J_{\text{P,C}}=8.4$ Hz, *m*- or *o*- $\text{CH}(\text{PPh}_2)$), 133.0 (d, $^{2/3}J_{\text{P,C}}=9.8$ Hz, *m*- or *o*- $\text{CH}(\text{PPh}_2)$), 130.2 (d, $^2J_{\text{P,C}}=17.2$ Hz, C_dH), 130.3 (d, $^4J_{\text{P,C}}=1.0$ Hz, *p*- $\text{CH}(\text{PPh}_2)$), 129.8 (d, $^3J_{\text{P,C}}=15.7$ Hz, $\text{C}_{c,a}^{\text{IV}}$), 128.4 (d, $^{2/3}J_{\text{P,C}}=10.6$ Hz, *m*- or *o*- $\text{CH}(\text{PPh}_2)$), 128.0 (d, $^4J_{\text{P,C}}=1.0$ Hz, *p*- $\text{CH}(\text{PPh}_2)$), 127.8 (s, C_bH), 127.7 (d, $^{2/3}J_{\text{P,C}}=11.0$ Hz, *m*- or *o*- $\text{CH}(\text{PPh}_2)$), 112.1 (d, $^1J_{\text{P,C}}=133.9$ Hz, $\text{C}^{\text{IV}}\text{-PPh}_2$), 65.7 (dd, $J_{\text{P,C}}=9.2$ Hz, $J'_{\text{P,C}}=26.1$ Hz, N-CH-CH-N), 40.7 (s, b, $\text{CH}_2(\text{cyclohexane})$), 36.2 (d, $^4J_{\text{P,C}}=1.7$ Hz, $\text{C}_a^{\text{IV}}\text{-C}^{\text{IV}}(\text{CH}_3)_3$), 34.1 (s, $\text{C}_c^{\text{IV}}\text{-C}^{\text{IV}}(\text{CH}_3)_3$), 32.3-31.7 (m, $\text{C}_c^{\text{IV}}\text{-C}^{\text{IV}}(\text{CH}_3)_3 + \text{CH}_2(\text{cyclohexane})$), 30.2 (s, $\text{C}_a^{\text{IV}}\text{-C}^{\text{IV}}(\text{CH}_3)_3$), 30.1 (s, $\text{C}_c^{\text{IV}}\text{-C}^{\text{IV}}(\text{CH}_3)_3$), 2.0 (s, $\text{CH}_3\text{-HMDS}$).

Synthesis of 37a

To a solution of the phosphasalen dianion **36a** (372 mg, 0.35 mmol) in THF (10 mL) was added $[\text{NiBr}_2(\text{DME})]$ (108 mg, 0.35 mmol) resulting immediately in a purple solution. After overnight stirring, precipitated KBr salt was removed by filtration under nitrogen. The product was obtained after evaporation of THF as a purple solid (285 mg, 0.32 mmol, 92%).

37a: $^{31}\text{P}\{^1\text{H}\}$ NMR (CD_2Cl_2): δ 36.8 (s, P^{V}); ^1H NMR (CD_2Cl_2): δ 7.94 (m, 8H, $\text{CH}(\text{PPh}_2)$), 7.60 (m, 12H, $\text{CH}(\text{PPh}_2)$), 7.21 (s, 2H, C_bH), 6.12 (d, b, $^3J_{\text{P,H}}=14.2$ Hz, 2H, C_dH), 2.05 (b, 4H, $\text{N-CH}_2\text{-CH}_2\text{-N}$), 1.36 (s, 18H, $\text{C}_a\text{-C}(\text{CH}_3)_3$), 1.02 (s, 18H, $\text{C}_c\text{-C}(\text{CH}_3)_3$); $^{13}\text{C}\{^1\text{H}\}$ NMR

(CD₂Cl₂): δ 168.2 (s, C^{IV}-O), 142.2 (d, ³J_{P,C} = 7.8 Hz, C_c^{IV}), 134.7 (d, ³J_{P,C} = 15.2 Hz, C_a^{IV}), 133.9 (d, ^{2/3}J_{P,C} = 9.2 Hz, *o*- or *m*-CH(PPh₂)), 132.4 (s, *p*-CH(PPh₂)), 129.0 (d, ^{2/3}J_{P,C} = 11.4 Hz, *o*- or *m*-CH(PPh₂)), 128.2 (s, C_bH), 127.8 (d, ¹J_{P,C} = 87.8 Hz, C^{IV}(PPh₂)), 124.6 (d, ²J_{P,C} = 13.2 Hz, C_dH), 112.2 (d, ¹J_{P,C} = 120.8 Hz, C^{IV}-PPh₂), 50.5 (dd, J_{P,C} = 3.8 Hz, J_{P,C} = 18.8 Hz, N-CH₂-CH₂-N), 35.8 (s, C_a-C(CH₃)₃), 34.0 (s, C_c-C(CH₃)₃), 31.4 (s, C_c-C(CH₃)₃), 29.7 (s, C_a-C(CH₃)₃). Anal. Calcd for C₅₄H₆₄N₂NiO₂P₂: C, 72.57; H, 7.22; N, 3.13. Found: C, 72.42; H, 7.13; N, 3.05.

Synthesis of **37b**

KHMDS (299 mg, 1.5 mmol) was added into a suspension of **35b** (398 mg, 0.374 mmol) in THF (10 mL), inducing the rapid dissolution of the solid and the formation of a colorless solution. After 2h, the insoluble potassium salt was removed by centrifugation. [NiBr₂(DME)] (115 mg, 0.37 mmol) was added into the solution, leading immediately to a color change to deep purple/blue. After 3h, the insoluble potassium salt was removed by centrifugation, THF was evaporated. The blue/purple solid was washed with petroleum ether (8 mL), dried under vacuum. (300mg, 85%)

37b: ³¹P{¹H} NMR (CD₂Cl₂): δ 30.0 (s, P^V); ¹H NMR (CD₂Cl₂): δ 8.67 (ddd, ⁴J_{H,H}=1.5 Hz, ³J_{H,H}=7.5 Hz, ³J_{P,H}=12.5 Hz, 4H, *o*-CH(PPh₂)), 7.65 (vtd, ⁴J_{H,H}=1.5 Hz, ³J_{H,H}=³J_{H,H} = 7.5 Hz, 2H, *p*-CH(PPh₂)), 7.57 (vtd, ⁴J_{P,H}=2.5 Hz, ³J_{H,H}=³J_{H,H} = 7.5 Hz, 4H, *m*-CH(PPh₂)), 7.56 (vtd, ⁴J_{H,H}=1.5 Hz, ³J_{H,H}=³J_{H,H} = 7.5 Hz, 2H, *p*-CH(PPh₂)), 7.48 (ddd, ⁴J_{H,H}=1.5 Hz, ³J_{H,H}=7.5 Hz, ³J_{P,H}=12.5 Hz, 4H, *o*-CH(PPh₂)), 7.41 (vtd, ⁴J_{P,H}=2.5 Hz, ³J_{H,H}=³J_{H,H} = 7.5 Hz, 4H, *m*-CH(PPh₂)), 7.17 (d, ⁴J_{H,H}=2.5 Hz, 2H, C_bH), 6.34 (dd, ⁴J_{H,H}=2.5 Hz, ³J_{P,H} = 15.5 Hz, 2H, C_dH), 3.02 (vtd, ³J_{H,H}=³J_{P,H} = 9.0 Hz, ⁴J_{P,H} = 3.0 Hz, 2H, N-CH-CH-N), 1.13 (s, b, 18H, C_{c,a}^{IV}-C^{IV}(CH₃)₃), 1.10 (s, 18H, C_{c,a}^{IV}-C^{IV}(CH₃)₃), 1.01 (m, 2H, CH₂(cyclohexane)), 0.86 (m, 2H, CH₂(cyclohexane)), 0.63 (m, 2H, CH₂(cyclohexane)), 0.47 (m, 2H, CH₂(cyclohexane)); ¹³C{¹H} NMR (CD₂Cl₂): δ 168.4 (d, ³J_{P,C}=2.5 Hz, C^{IV}-O), 141.9 (d, ³J_{P,C}=8.2 Hz, C_a^{IV}), 134.7 (d, ^{2/3}J_{P,C}=9.7 Hz, *m*- or *o*-CH(PPh₂)), 133.8 (d, ¹J_{P,C}=82.1 Hz, C^{IV}(PPh₂)), 133.7 (d, ³J_{P,C}=15.2 Hz, C_a^{IV}), 133.7 (d, ^{2/3}J_{P,C}=9.8 Hz, *m*- or *o*-CH(PPh₂)), 132.7 (d, ⁴J_{P,C}=2.9 Hz, *p*-CH(PPh₂)), 131.8 (d, ⁴J_{P,C}=2.9 Hz, *p*-CH(PPh₂)), 130.4 (d, ¹J_{P,C}=88.5 Hz, C^{IV}(PPh₂)), 129.0 (d, ^{2/3}J_{P,C}=11.8 Hz, *m*- or *o*-CH(PPh₂)), 128.5 (d, ^{2/3}J_{P,C}=11.5 Hz, *m*- or *o*-CH(PPh₂)), 128.1 (d, ⁴J_{P,C}=1.8 Hz, C_bH), 126.2 (d, ²J_{P,C}=13.2 Hz, C_dH), 112.1 (d, ¹J_{P,C}=124.2 Hz, C^{IV}-PPh₂), 67.3 (dd, J_{P,C}=5.8 Hz, J_{P,C}=15.8 Hz, N-CH-CH-N), 35.6 (d, ⁴J_{P,C}=1.7 Hz, C_{a,c}^{IV}-C^{IV}(CH₃)₃), 35.4 (s, CH₂(cyclohexanediamine)), 34.1 (d, ⁴J_{P,C}=1.0 Hz, C_c^{IV}-C^{IV}(CH₃)₃), 31.6 (s, C^{IV}(CH₃)₃), 29.8 (s, C^{IV}(CH₃)₃), 25.5 (s, CH₂(cyclohexanediamine)). Anal. Calcd for C₅₈H₇₀N₂NiO₂P₂: C, 73.50; H, 7.44; N, 2.96. Found: C, 73.66; H, 7.35; N, 3.01.

Synthesis of **[37a][SbF₆]**

Addition of AgSbF₆ (34.4 mg, 0.1 mmol) into a solution of complex **37a** (89.4 mg, 0.1 mmol) in CH₂Cl₂ (5 mL) induced a rapid colour change from blue to deep red and precipitation of silver. After removal of Ag by centrifugation, dichloromethane was evaporated and the residue was dissolved in toluene (1.5 mL), giving a deep red-brown solution. Green crystals were obtained

Experimental Section

after one week of storage at -40°C , which was then isolated by centrifugation and dried under vacuum. (104 mg, 95 %). Anal. Calcd for **[37a][SbF₆]** C₅₄H₆₄F₆N₂NiO₂P₂Sb: C, 57.42; H, 5.71; N, 2.48. Found: C, 57.50; H, 5.80; N, 2.37.

Experimental Section

V. Chapter 5.

General considerations

All reactions were conducted under an atmosphere of dry nitrogen, or argon, using standard Schlenk and glovebox techniques. Solvents and reagents were obtained from commercial sources. Tetrahydrofuran, toluene, pentane, hexane and petroleum ether were distilled from sodium/benzophenone, under dry nitrogen. Dichloromethane was distilled from CaH₂, under dry nitrogen. *Rac*-lactide was recrystallised from anhydrous toluene and sublimed three times prior to use. [YCl₃(THF)_{3.5}]⁷ was prepared following literature procedure.

Nuclear magnetic resonance (NMR) spectra were recorded on a Bruker Av300 spectrometer operating at 300 MHz for ¹H, 75.5 MHz for ¹³C{¹H}, and 121.5 MHz for ³¹P{¹H}. Solvent peaks were used as internal references for ¹H and ¹³C chemical shifts (ppm). ³¹P peaks were referenced to external 85% H₃PO₄. When needed, higher resolution ³¹P{¹H} NMR and ¹H{¹H} NMR (homo-decoupled spectroscopy) experiments were performed on a Bruker Av500 spectrometer, equipped with a z-gradient bbo/5 mm tuneable probe and a BSMS GAB 10 A gradient amplifier providing a maximum gradient output of 5.35 G/cmA. ¹H NMR spectra for all lactide polymerizations were performed on a Bruker Av400 instrument. Coupling constant are expressed in hertz. The following abbreviations are used: br, broad; s, singlet; d, doublet; dd, doublet of doublets; t, triplet; m, multiple; v, virtual.

Elemental analyses were determined by Mr. Stephen Boyer at London Metropolitan University, Science Centre. Mass spectra were performed on a Micromass MALDI micro MX, using potassium salts for ionisation. PLA number averaged molecular weight, M_n , and polydispersity index (M_w/M_n ; PDI) were determined using gel permeation chromatography, equipped with multi-angle laser light scattering (GPC-MALLS). Two Polymer laboratories Mixed D columns were used in series, with THF as the eluent, at a flow rate of 1 mL min⁻¹, on a Polymer laboratories PL GPC-50 instrument at 35 °C. The light scattering detector was a triple-angle detector (Dawn 8, Wyatt Technology), and the data were analyzed using Astra V version 5.3.4.18. The refractive angle increment for polylactide (dn/dc) in THF was 0.042 mL g⁻¹.⁸

General procedure for lactide polymerization

To a rapidly stirred solution of *rac*-lactide (288 mg, 2 mmol) in THF, in a vial in the glovebox, was added the appropriate quantity of a solution of the initiator, in tetrahydrofuran; the overall concentration of *rac*-lactide was therefore kept at 1 M. Aliquots of the reaction mixture were taken at regular intervals, precipitated in hexane and quenched in air. The solvent was allowed to evaporate slowly, in air, yielding a crude product which was analyzed by ^1H NMR spectroscopy (to determine % conversion) and by GPC (to determine the M_n and PDI). The probability of syndiotactic linkages between monomer units (P_s) is determined from the homonuclear decoupled ^1H NMR spectrum: δ 5.14 and 5.22 ppm in CDCl_3 for heterotactic PLA.⁹

Synthesis of 38

At 0°C, bromine (2 mL, 38.83 mmol) was added into a solution of 2-tert-butyl-4-methoxyphenol (7.00 g, 38.83 mmol) in dichloromethane (200 mL), leading to immediate liberation of HBr(g) and the formation of a pale yellow solution. Stirring was continued at room temperature for 48h. Dichloromethane and HBr was evaporated, the residue was taken in Et_2O (200 mL), washed with an aqueous solution of Na_2CO_3 (1M, 200 mL) and dried over Na_2SO_4 . The solvent was evaporated again. The product was purified by chromatography (eluent Et_2O /petroleum ether = 2.5/97.5).

38 (7.15g, 71%): ^1H NMR (CDCl_3): δ 6.88 (d, $^4J_{\text{H,H}} = 3.0$ Hz, 1H, $\text{C}_{\text{phenyl}}\text{H}$), 6.84 (d, $^4J_{\text{H,H}} = 3.0$ Hz, 1H, $\text{C}_{\text{phenyl}}\text{H}$), 5.42 (s, 1H, OH), 3.74 (s, 3H, O- CH_3), 1.38 (s, 9H, $\text{C}^{\text{IV}}(\text{CH}_3)_3$).

Synthesis of 39

n-BuLi (1.6M in hexanes, 34.5 mL, 55.2 mmol) was added into a solution of **S1** (7.15 g, 27.6 mmol) in Et_2O (70 mL) at -78°C. After the addition, the cold bath was removed, an yellowish solution was obtained and stirring was continued at room temperature for 2h. ClPPh₂ (4.95 mL, 27.6 mmol) was added giving immediately a white suspension. After overnight stirring at room temperature, the solid was isolated by filtration under inert atmosphere and was then put into 80 mL of Et_2O . An aqueous solution (40 mL) of HBF_4 (1 M) was added, giving a biphasic system with the total disappearance of the solid. The organic phase was washed with H_2O (40 mL), dried over MgSO_4 . The solvent was isolated, giving the product as a yellow viscous oil (8.4 g, 84%).

39: $^{31}\text{P}\{^1\text{H}\}$ NMR (CDCl_3): δ -28.3 (s, P^{III}); ^1H NMR (CDCl_3): δ 7.36 (m, 10H, $\text{CH}(\text{PPh}_2)$), 6.94 (d, $^4J_{\text{H,H}} = 3.0$ Hz, 1H, C_bH), 6.49 (d, $^2J_{\text{P,H}} = 10.0$ Hz, 1H, OH), 6.35 (dd, $^3J_{\text{P,H}} = 5.0$ Hz, $^4J_{\text{H,H}} = 3.0$ Hz, 1H, C_dH), 3.58 (s, 3H, O- CH_3), 1.41 (s, 9H, $\text{C}^{\text{IV}}(\text{CH}_3)_3$); $^{13}\text{C}\{^1\text{H}\}$ NMR (CDCl_3): δ 152.9 (d, $^2J_{\text{P,C}} = 3.0$ Hz, $\text{C}^{\text{IV}}\text{-OH}$), 152.6 (d, $^3J_{\text{P,C}} = 19.0$ Hz, $\text{C}^{\text{IV}}\text{-OMe}$), 137.9 (d, $J_{\text{P,C}} = 1.5$ Hz, C^{IV}), 135.0 (d, $J_{\text{P,C}} = 1.5$ Hz, C^{IV}), 133.5 (d, $^{2/3}J_{\text{P,C}} = 19.0$ Hz, *m*-or *o*- $\text{CH}(\text{PPh}_2)$), 129.1 (s, *p*- $\text{CH}(\text{PPh}_2)$), 128.8 (d, $^{2/3}J_{\text{P,C}} = 7.5$ Hz, *m*-or *o*- $\text{CH}(\text{PPh}_2)$), 121.3 (d, $J_{\text{P,C}} = 1.0$ Hz, C^{IV}), 116.7 (s, C_bH), 115.2 (d, $^2J_{\text{P,C}} = 3.0$ Hz, C_dH), 55.5 (s, O- CH_3), 35.2 (s, $\text{C}_{\text{c,a}}^{\text{IV}}\text{-C}^{\text{IV}}(\text{CH}_3)_3$), 29.6 (s, $\text{C}_{\text{c,a}}^{\text{IV}}\text{-C}^{\text{IV}}(\text{CH}_3)_3$).

Synthesis of 41

At -40°C , AlCl_3 (93.3 mg, 0.7 mmol) was added into a solution of the unsubstituted phosphasalen ligand **29** (490 mg, 0.7 mmol) in THF (20 mL), giving a cloudy solution which quickly turned into a white slurry. Stirring was continued at room temperature. After 2h, KOEt (58.9 mg, 0.7 mmol) was added, inducing the slow dissolution of the solid. After 20h, a cloudy solution was obtained. The insoluble salts were removed by centrifugation. THF was evaporated in vacuum, giving an ivory solid, which was then recrystallised in toluene (2 mL). The product was isolated as white solid. (350 mg, 73%)

41. $^{31}\text{P}\{^1\text{H}\}$ NMR (THF- d_8): δ 35.1 (s, P^{V}); ^1H NMR (THF- d_8): δ 8.04 (vddt, $^4J_{\text{H,H}}=^4J'_{\text{H,H}}=1.5$ Hz, $^3J_{\text{H,H}}=6.7$ Hz, $^3J_{\text{P,H}}=11.9$ Hz, 4 H, *o*-CH(PPh₂)), 7.55-7.35 (m, br, 16 H, CH(PPh₂)), 7.12 (dddd, $^3J_{\text{H,H}}=8.7$ Hz, $^3J_{\text{H,H}}=7.0$ Hz, $^4J_{\text{H,H}}=1.7$ Hz, $^5J_{\text{P,H}}=1.2$ Hz, 2H, C_bH), 6.79 (ddd, $^3J_{\text{H,H}}=8.0$ Hz, $^4J_{\text{H,H}}=1.7$ Hz, $^3J_{\text{P,H}}=15.0$ Hz, 2H, C_dH), 6.73 (ddd, $^3J_{\text{H,H}}=8.7$ Hz, $^4J_{\text{H,H}}=1.0$ Hz, $^4J_{\text{P,H}}=5.7$ Hz, 2H, C_aH), 6.36 (dddd, $^3J_{\text{H,H}}=8.0$ Hz, $^3J_{\text{H,H}}=7.0$ Hz, $^4J_{\text{H,H}}=1.0$ Hz, $^4J_{\text{P,H}}=3.2$ Hz, 2H, C_cH), 3.57 (q, $^3J_{\text{H,H}}=7.0$ Hz, 2H, O-CH₂-CH₃), 2.93 (m, 2H, N-CH₂-CH₂-N), 2.48 (m, 2H, N-CH₂-CH₂-N), 0.87 (t, $^3J_{\text{H,H}}=7.0$ Hz, 3H, O-CH₂-CH₃); $^{13}\text{C}\{^1\text{H}\}$ NMR (THF- d_8): δ 170.2 (d, $^3J_{\text{P,C}}=3.0$ Hz, C^{IV}-O), 134.3(d, $^3J_{\text{P,C}}=10.4$ Hz, *o*-CH(PPh₂)), 134.2(s, C_bH), 133.9 (d, $^3J_{\text{P,C}}=8.9$ Hz, *o*-CH(PPh₂)), 132.7 (d, $^5J_{\text{P,C}}=1.8$ Hz, *p*-CH(PPh₂)), 132.5 (d, $^5J_{\text{P,C}}=2.2$ Hz, *p*-CH(PPh₂)), 132.0 (d, $^3J_{\text{P,C}}=11.5$ Hz, C_dH), 130.3 (d, $^1J_{\text{P,C}}=90.2$ Hz, C^{IV}(PPh₂)), 129.5 (d, $^1J_{\text{P,C}}=89.2$ Hz, C^{IV}(PPh₂)); 129.3 (d, $^4J_{\text{P,C}}=11.8$ Hz, *m*-CH(PPh₂)), 129.1 (d, $^4J_{\text{P,C}}=14.0$ Hz, *m*-CH(PPh₂)), 124.0 (d, $^4J_{\text{P,C}}=9.4$ Hz, C_aH), 114.7 (d, $^4J_{\text{P,C}}=14.4$ Hz, C_cH), 108.1 (d, $^1J_{\text{P,C}}=116.1$ Hz, C^{IV}-PPh₂), 58.3 (s, O-CH₂-CH₃), 51.3 (d, $J_{\text{P,C}}=13.8$ Hz, N-CH₂-CH₂-N), 21.8 (s, O-CH₂-CH₃). Anal. Calcd for C₄₀H₃₇AlN₂O₃P₂: C, 70.38; H, 5.46; N, 4.10. Found: C, 70.50; H, 5.39; N, 4.00.

Synthesis of 42.

42 was synthesised using the same method as **41**, except that tBuOK (78.6 mg, 0.7 mmol) was used instead of KOEt. The product was purified by crystallisation in toluene (2 mL) and isolated as white solid. (420 mg, 84%).

42. $^{31}\text{P}\{^1\text{H}\}$ NMR (THF- d_8): δ 35.1 (s, P^{V}); ^1H NMR (THF- d_8): δ 8.07 (vddt, $^4J_{\text{H,H}}=^4J'_{\text{H,H}}=1.5$ Hz, $^3J_{\text{H,H}}=6.7$ Hz, $^3J_{\text{P,H}}=12.0$ Hz, 4 H, *o*-CH(PPh₂)), 7.62-7.41 (m, 16 H, CH(PPh₂)), 7.19 (dddd, $^3J_{\text{H,H}}=8.7$ Hz, $^3J_{\text{H,H}}=7.0$ Hz, $^4J_{\text{H,H}}=1.7$ Hz, $^5J_{\text{P,H}}=1.1$ Hz, 2H, C_bH), 6.86 (ddd, $^3J_{\text{H,H}}=8.0$ Hz, $^4J_{\text{H,H}}=1.7$ Hz, $^3J_{\text{P,H}}=15.2$ Hz, 2H, C_dH), 6.77 (ddd, $^3J_{\text{H,H}}=8.7$ Hz, $^4J_{\text{H,H}}=1.0$ Hz, $^4J_{\text{P,H}}=5.6$ Hz, 2H, C_aH), 6.41 (dddd, $^3J_{\text{H,H}}=8.0$ Hz, $^3J_{\text{H,H}}=7.0$ Hz, $^4J_{\text{H,H}}=1.0$ Hz, $^4J_{\text{P,H}}=3.0$ Hz, 2H, C_cH), 3.03 (m, 2H, N-CH₂-CH₂-N), 2.56 (m, 2H, N-CH₂-CH₂-N), 1.03 (s, 9H, O-C^{IV}(CH₃)₃); $^{13}\text{C}\{^1\text{H}\}$ NMR (THF- d_8): δ 170.1 (d, $^3J_{\text{P,C}}=3.1$ Hz, C^{IV}-O), 134.4(d, $^3J_{\text{P,C}}=10.0$ Hz, *o*-CH(PPh₂)), 134.1(d, $^5J_{\text{P,C}}=1.6$ Hz, C_bH), 133.8 (d, $^3J_{\text{P,C}}=9.6$ Hz, *o*-CH(PPh₂)), 132.6 (d, $^5J_{\text{P,C}}=3.7$ Hz, *p*-CH(PPh₂)), 132.5 (d, $^5J_{\text{P,C}}=2.8$ Hz, *p*-CH(PPh₂)), 132.2 (d, $^3J_{\text{P,C}}=12.4$ Hz, C_dH), 130.4 (d, $^1J_{\text{P,C}}=90.0$ Hz, C^{IV}(PPh₂)), 129.9 (d, $^1J_{\text{P,C}}=92.5$ Hz, C^{IV}(PPh₂)), 129.2 (d, $^4J_{\text{P,C}}=11.4$ Hz, *m*-CH(PPh₂)), 129.1 (d, $^4J_{\text{P,C}}=10.9$ Hz, *m*-CH(PPh₂)), 124.2 (d, $^4J_{\text{P,C}}=9.4$ Hz, C_aH), 114.6 (d, $^4J_{\text{P,C}}=14.4$ Hz, C_cH), 107.0 (d, $^1J_{\text{P,C}}=115.5$ Hz, C^{IV}-PPh₂), 46.0 (d, $J_{\text{P,C}}=14.7$ Hz, $J_{\text{P,C}}=1.7$ Hz, N-CH₂-CH₂-N), 34.1 (s, O-

$C^{IV}(CH_3)_3$). Anal. Calcd for $C_{42}H_{41}AlN_2O_3P_2$: C, 70.98; H, 5.81; N, 3.94. Found: C, 70.84; H, 5.72; N, 3.83.

Synthesis of 43

$[YCl_3(THF)_{3.5}]$ (313 mg, 0.7 mmol) was added to a solution of the unsubstituted phosphasalen ligand **29** (491 mg, 0.7 mmol), in THF (30 mL) at $-40\text{ }^\circ\text{C}$. A white slurry was formed after 2 min, stirring was continued at room temperature for 1 h. Potassium ethoxide (59 mg, 0.7 mmol) was added, giving a cloudy solution after 7 h. The solid was removed by centrifugation and the filtrate was evaporated to give an ivory solid. Crystallization from toluene yielded the product as colorless crystals (430 mg, 0.59 mmol, 84%)

43: $^{31}P\{^1H\}$ NMR (THF- d_8): δ 29.3 (s, P^V); 1H NMR (THF- d_8): δ 7.77-7.24 (m, b, 20H, $CH(PPh_2)$), 7.09 (dddd, $^3J_{H,H}=8.7$ Hz, $^3J_{H,H}=7.0$ Hz, $^4J_{H,H}=1.7$ Hz, $^5J_{P,H}=1.2$ Hz, 2H, C_bH), 6.79 (ddd, $^3J_{H,H}=7.7$ Hz, $^4J_{H,H}=1.7$ Hz, $^3J_{P,H}=13.9$ Hz, 2H, C_dH), 6.52 (ddd, $^3J_{H,H}=8.7$ Hz, $^4J_{H,H}=0.7$ Hz, $^4J_{P,H}=8.3$ Hz, 2H, C_aH), 6.31 (dddd, $^3J_{H,H}=7.7$ Hz, $^3J_{H,H}=7.0$ Hz, $^4J_{H,H}=0.7$ Hz, $^4J_{P,H}=3.5$ Hz, 2H, C_cH), 3.42 (br, 2H, O- CH_2-CH_3), 3.08 (br, 2H, N- CH_2-CH_2-N), 2.84 (b, 2H, N- CH_2-CH_2-N), 1.01 (br, 1H, O- CH_2-CH_3); 0.62 (b, 2H, O- CH_2-CH_3); $^{13}C\{^1H\}$ NMR (THF- d_8): δ 172.1 (d, $^3J_{P,C}=2.3$ Hz, $C^{IV}-O$), 172.0 (d, $^3J_{P,C}=2.7$ Hz, $C^{IV}-O$), 134.0 (s, $p-CH(PPh_2)$), 134.0 (d, $^{2/3}J_{P,C}=9.5$ Hz, o - or $m-CH(PPh_2)$), 133.1 (d, $^4J_{P,C}=10.9$ Hz, C_bH), 132.0 (m, b, C_dH); 131.8 (m, b, $C(Ar)$), 129.1 (m, b, $C(Ar)$), 122.7 (d, $^3J_{P,C}=7.5$ Hz, C_aH), 114.9 (d, $^1J_{P,C}=113.8$ Hz, $C^{IV}-PPh_2$), 113.0 (d, $^3J_{P,C}=14.9$ Hz, C_cH), 51.3 (dd, $J_{P,C}=6.3$ Hz, $J'_{P,C}=13.1$ Hz, N- CH_2-CH_2-N), 68.0 (s, O- CH_2-CH_3), 25.1 (s, O- CH_2-CH_3). Anal. Calcd for $C_{80}H_{74}N_4O_6P_4Y_2$: C, 64.52; H, 5.01; N, 3.76. Found: C, 64.44; H, 5.07; N, 3.72.

Synthesis of 44

$[YCl_3(THF)_{3.5}]$ (313 mg, 0.7 mmol) was added to a solution of the unsubstituted phosphasalen ligand **29** (491 mg, 0.7 mmol) in THF (50 mL) at $-40\text{ }^\circ\text{C}$. A white slurry was formed after 2 min, stirring was continued at room temperature for 1 h. Potassium *tert*-butoxide (78.6 mg, 0.7 mmol) was added into the mixture, giving a cloudy solution after 7 h. The solid was removed by centrifugation. The solution was concentrated (to 10 mL). The product precipitated from the solution as a white solid (380 mg, 0.49 mmol, 70 %). Crystals suitable for X-ray diffraction experiments were obtained from a solution of complex **44** in THF/toluene (1/3 volume)

44: $^{31}P\{^1H\}$ NMR (THF- d_8): δ 30.4 (s, P^V); 1H NMR (THF- d_8): δ 7.73-7.30 (m, b, 20H, $CH(PPh_2)$), 7.08 (dddd, $^3J_{H,H}=8.7$ Hz, $^3J_{H,H}=7.0$ Hz, $^4J_{H,H}=1.7$ Hz, $^5J_{P,H}=1.0$ Hz, 2H, C_bH), 6.53 (ddd, $^3J_{H,H}=8.0$ Hz, $^4J_{H,H}=1.7$ Hz, $^3J_{P,H}=14.6$ Hz, 2H, C_dH), 6.50 (ddd, $^3J_{H,H}=8.7$ Hz, $^4J_{H,H}=1.0$ Hz, $^4J_{P,H}=5.5$ Hz, 2H, C_aH), 6.18 (dddd, $^3J_{H,H}=8.0$ Hz, $^3J_{H,H}=7.0$ Hz, $^4J_{H,H}=1.0$ Hz, $^4J_{P,H}=3.5$ Hz, 2H, C_cH), 3.42 (b, 2H, O- CH_2-CH_3), 3.22 (b, 2H, N- CH_2-CH_2-N), 2.99 (b, 2H, N- CH_2-CH_2-N), 0.88 (b, 9H, O- $C^{IV}(CH_3)_3$); $^{13}C\{^1H\}$ NMR (THF- d_8): δ 172.7 (d, $^3J_{P,C}=2.3$ Hz, $C^{IV}-O$), 172.6 (d, $^3J_{P,C}=2.5$ Hz, $C^{IV}-O$), 134.0 (d, $^{2/3}J_{P,C}=9.2$ Hz, o - or $m-CH(PPh_2)$), 134.0 (d, $^{2/3}J_{P,C}=8.6$ Hz, o - or $m-CH(PPh_2)$), 133.1 (d, $^4J_{P,C}=12.6$ Hz, C_dH), 131.8 (d, $^4J_{P,C}=2.3$ Hz, $p-CH(PPh_2)$), 131.6 (d, $^1J_{P,C}=74.6$ Hz, $C^{IV}(PPh_2)$), 131.5 (d, $^4J_{P,C}=2.8$ Hz, C_bH), 131.5 (d, $^1J_{P,C}=75.0$ Hz, $C^{IV}(PPh_2)$),

128.9 (d, $^{23}\text{J}_{\text{P,C}}=11.5$ Hz, *o*- or *m*-CH(PPh₂)), 128.7 (d, $^{23}\text{J}_{\text{P,C}}=10.7$ Hz, *o*- or *m*-CH(PPh₂)), 122.0 (d, $^3\text{J}_{\text{P,C}}=8.0$ Hz, C_aH), 114.2 (d, $^1\text{J}_{\text{P,C}}=121.3$ Hz, C^{IV}-P(Ph₂)), 112.4 (d, $^3\text{J}_{\text{P,C}}=15.0$ Hz, C_cH), 68.0 (s, O-C^{IV}(CH₃)₃), 51.9 (dd, $\text{J}_{\text{P,C}}=5.2$ Hz, $\text{J}'_{\text{P,C}}=15.5$ Hz, N-CH₂-CH₂-N), 32.7 (s, b, O-C^{IV}(CH₃)₃). Anal. Calcd for C₈₄H₈₂N₄O₆P₄Y₂: C, 65.29; H, 5.35; N, 3.63. Found: C, 65.27; H, 5.25; N, 3.76.

Synthesis of 45

[YCl₃(THF)_{3.5}] (313 mg, 0.7 mmol) was added to a solution of the phosphasalen ligand **36a** (745 mg, 0.7 mmol) in THF (25 mL) at -40°C. After 2 h of stirring at room temperature, potassium *tert*-butoxide (78.6 mg, 0.7 mmol) was added into the mixture, giving a cloudy solution. Stirring was continued for 7 h and the solid was removed by centrifugation. The solvents were removed from the filtrate yielding a pale yellow oil, which transformed into a white solid after one week of storing at room temperature (680 mg, 0.68 mmol, 97 %).

45: $^{31}\text{P}\{^1\text{H}\}$ NMR (THF-*d*₈): δ 30.8 (s, P^V); ^1H NMR (THF-*d*₈): δ 7.57 (d, $^3\text{J}_{\text{H,H}}=7.0$ Hz, $^3\text{J}_{\text{P,H}}=11.2$ Hz, 4H, *o*-CH(PPh₂)), 7.61 (vt, $^3\text{J}_{\text{H,H}}=7.0$ Hz, $^5\text{J}_{\text{P,H}}=1.0$ Hz, 2H, *p*-CH(PPh₂)), 7.43 (vt, $^3\text{J}_{\text{H,H}}=^3\text{J}'_{\text{H,H}}=7.0$ Hz, 4H, *m*-CH(PPh₂)), 7.42 (dd, $^3\text{J}_{\text{H,H}}=7.0$ Hz, $^3\text{J}_{\text{P,H}}=10.7$ Hz, 4H, *o*-CH(PPh₂)), 7.42 (vt, $^3\text{J}_{\text{H,H}}=7.0$ Hz, 2H, *p*-CH(PPh₂)), 7.34 (vtd, $^3\text{J}_{\text{H,H}}=^3\text{J}'_{\text{H,H}}=7.0$ Hz, $^4\text{J}_{\text{P,H}}=2.5$ Hz, 4H, *m*-CH(PPh₂)), 7.28 (d, $^3\text{J}_{\text{H,H}}=2.5$ Hz, 2H, C_bH), 6.34 (dd, $^3\text{J}_{\text{H,H}}=2.5$ Hz, $^3\text{J}_{\text{P,H}}=15.9$ Hz, 2H, C_dH), 3.31 (m, 2H, N-CH₂-CH₂-N), 3.18 (m, 2H, N-CH₂-CH₂-N), 1.37 (s, 18H, C_a-C(CH₃)₃), 0.98 (s, 18H, C_c-C(CH₃)₃), 0.68 (s, b, 9H, O-C(CH₃)₃); $^{13}\text{C}\{^1\text{H}\}$ NMR (THF-*d*₈): δ 169.7 (d, $^3\text{J}_{\text{P,C}}=2.7$ Hz, C^{IV}-O), 139.0 (d, $^3\text{J}_{\text{P,C}}=8.2$ Hz, C_c^{IV}); 134.0 (d, $^3\text{J}_{\text{P,C}}=15.4$ Hz, C_a^{IV}), 134.1 (d, $^{23}\text{J}_{\text{P,C}}=8.7$ Hz, *o*-CH(PPh₂)), 133.5 (d, $^{23}\text{J}_{\text{P,C}}=8.9$ Hz, *o*-CH(PPh₂)), 132.7 (d, $^1\text{J}_{\text{P,C}}=86.6$ Hz, C^{IV}(PPh₂)), 131.7 (d, $^1\text{J}_{\text{P,C}}=89.0$ Hz, C^{IV}(PPh₂)), 131.9 (d, $^4\text{J}_{\text{P,C}}=1.7$ Hz, *p*-CH(PPh₂)), 131.5 (d, $^4\text{J}_{\text{P,C}}=1.8$ Hz, *p*-CH(PPh₂)), 128.9 (d, $^{23}\text{J}_{\text{P,C}}=9.6$ Hz, *m*-CH(PPh₂)), 128.8 (d, $^{23}\text{J}_{\text{P,C}}=10.0$ Hz, *m*-CH(PPh₂)), 128.3 (s, C_bH), 127.8 (d, $^2\text{J}_{\text{P,C}}=13.9$ Hz, C_dH), 112.5 (d, $^1\text{J}_{\text{P,C}}=122.2$ Hz, C^{IV}-PPh₂), 47.3 (dd, $\text{J}_{\text{P,C}}=7.5$ Hz, $\text{J}'_{\text{P,C}}=19.0$ Hz, N-CH₂-CH₂-N), 35.8 (s, C_a^{IV}-C(CH₃)₃+O-C(CH₃)₃), 34.3 (s, C_c^{IV}-C(CH₃)₃), 31.7 (s, C_c^{IV}-C(CH₃)₃+O-C(CH₃)₃), 30.4 (s, C_a^{IV}-C(CH₃)₃). Anal. Calcd for C₅₈H₇₃N₂O₃P₂Y: C, 69.87; H, 7.38; N, 2.81. Found: C, 69.55; H, 7.26; N, 2.76.

Synthesis of 46

At -78°C, bromine (200 μL , 3.88 mmol) was added dropwise to a solution of the phenolphosphine (1.516 g, 3.88 mmol) in CH₂Cl₂ (45 mL). The cold bath was removed and stirring was continued for 1 hour at room temperature. Then the solution was cooled down to -78°C. DABCO (1,4-diazabicyclo[2.2.2]octane, 218 mg, 1.94 mmol) was added, followed by (R,R)-1,2-diaminocyclohexane (222 mg, 1.94 mmol). The cold bath was removed. After 16h, a white slurry was formed. CH₂Cl₂ was evaporated, 50 mL of THF was added. The insoluble DABCO salt was removed by centrifugation. THF was evaporated and the white solid was washed with Et₂O (7 mL), dried in vacuum (1.04g, 57%).

46: $^{31}\text{P}\{^1\text{H}\}$ NMR (CDCl_3): δ 38.5 (s, P^V); ^1H NMR (CDCl_3): δ 8.59 (s, 2H, NH), 7.77 (dd, $^3J_{\text{H,H}}=7.5$ Hz, $^3J_{\text{P,H}}=12.8$ Hz, 4H, *o*-CH(PPh₂)), 7.69 (dd, $^3J_{\text{H,H}}=7.5$ Hz, $^3J_{\text{P,H}}=14.2$ Hz, 4H, *o*-CH(PPh₂)), 7.70 (s, 1H, OH), 7.69 (s, 1H, OH), 7.50 (vtd, $^3J_{\text{H,H}}=^3J_{\text{H,H}}=7.5$ Hz, $^4J_{\text{P,H}}=3.0$ Hz, 2H, *m*-CH(PPh₂)), 7.63 (vt, $^3J_{\text{H,H}}=^3J_{\text{H,H}}=7.5$ Hz, 2H, *p*-CH(PPh₂)), 7.40 (vt, $^3J_{\text{H,H}}=^3J_{\text{H,H}}=7.5$ Hz, 4H, *p*-CH(PPh₂)), 7.13 (vtd, $^3J_{\text{H,H}}=^3J_{\text{H,H}}=7.5$ Hz, $^4J_{\text{P,H}}=3.3$ Hz, 4H, *m*-CH(PPh₂)), 6.56 (dd, $^4J_{\text{H,H}}=2.2$ Hz, $^5J_{\text{P,H}}=8.0$ Hz, 1H, C_bH), 6.53 (dd, $^4J_{\text{H,H}}=2.2$ Hz, $^5J_{\text{P,H}}=8.0$ Hz, 1H, C_bH), 6.37 (dd, $^4J_{\text{H,H}}=2.2$ Hz, $^3J_{\text{P,H}}=15.6$ Hz, 2H, C_bH), 3.82 (m, 2H, N-CH-CH-N), 2.05 (m, 2H, CH₂(cyclohexane)), 1.59 (m, 2H, CH₂(cyclohexane)), 1.53 (s, 18H, C_a-C(CH₃)₃), 1.30 (m, 2H, CH₂(cyclohexane)), 1.03 (s, 18H, C_c-C(CH₃)₃), 0.93 (m, 2H, CH₂(cyclohexane)); $^{13}\text{C}\{^1\text{H}\}$ NMR (CDCl_3): δ 155.9 (d, $^3J_{\text{P,C}}=0.9$ Hz, C^{IV}-O), 145.7 (d, $^3J_{\text{P,C}}=8.2$ Hz, C_{c,a}^{IV}); 144.5 (d, $^3J_{\text{P,C}}=7.0$ Hz, C_{a,c}^{IV}), 135.0-133.0 (m, CH(PPh₂)), 131.8 (d, $^4J_{\text{P,C}}=0.9$ Hz, *p*-CH(PPh₂)), 131.5 (d, $^4J_{\text{P,C}}=0.9$ Hz, *p*-CH(PPh₂)), 129.7-128.9 (m, CH(PPh₂) + C_bH), 128.6 (d, $^2J_{\text{P,C}}=12.2$ Hz, C_dH), 123.0 (d, $^1J_{\text{P,C}}=109.7$ Hz, C^{IV}(PPh₂)), 121.7 (d, $^1J_{\text{P,C}}=97.5$ Hz, C^{IV}-PPh₂), 116.0 (d, $^1J_{\text{P,C}}=106.2$ Hz, C^{IV}(PPh₂)), 59.0 (m, N-CH-CH-N), 35.6 (s, C_a^{IV}-C(CH₃)₃), 34.7 (s, C_c^{IV}-C(CH₃)₃), 30.2 (s, CH₂(cyclohexane)), 30.0 (s, CH₂(cyclohexane)), 29.8 (s, C_{c,a}^{IV}-C(CH₃)₃), 29.7 (s, C_{a,c}^{IV}-C(CH₃)₃), 29.5 (s, C_{a,c}^{IV}-C(CH₃)₃), 29.4 (s, CH₂(cyclohexane)), 28.8 (s, CH₂(cyclohexane)). Anal. Calcd for C₅₈H₇₄Br₂N₂O₂P₂: C, 66.16; H, 7.08; N, 2.66. Found: C, 66.25; H, 6.96; N, 2.56.

Synthesis of 47

47 was synthesized using the same protocol as the synthesis of **46**, but using 1,3-diaminopropane (162 μL , 1.942 mmol) instead of (R,R)-1,2-diaminocyclohexane. It was isolated as a white solid (1.5g, 71%)

47: $^{31}\text{P}\{^1\text{H}\}$ NMR (CDCl_3): δ 40.4 (s, P^V); ^1H NMR (CDCl_3): δ 7.74-7.56 (m, 22H, CH(PPh₂) + C_bH), 6.54 (dd, $^4J_{\text{H,H}}=2.0$ Hz, $^3J_{\text{P,H}}=15.5$ Hz, 2H, C_dH), 3.37 (vq, $^3J_{\text{H,H}}=^3J_{\text{P,H}}=7.0$ Hz, 4H, N-CH₂-CH₂-CH₂-N), 2.32 (qt, $^3J_{\text{H,H}}=7.0$ Hz, 2H, N-CH₂-CH₂-CH₂-N), 1.49 (s, b, 18H, C_{c,a}^{IV}-C^{IV}(CH₃)₃), 1.11 (s, 18H, C_{c,a}^{IV}-C^{IV}(CH₃)₃); $^{13}\text{C}\{^1\text{H}\}$ NMR (CDCl_3): δ 156.0 (d, $^3J_{\text{P,C}}=1.0$ Hz, C^{IV}-O), 145.4 (d, $^3J_{\text{P,C}}=13.5$ Hz, C_{c,a}^{IV}), 143.6 (d, $^3J_{\text{P,C}}=7.0$ Hz, C_{a,c}^{IV}), 134.1 (m, CH(PPh₂)), 133.7 (d, $^{2/3}J_{\text{P,C}}=10.0$ Hz, *o*-or *m*-CH(PPh₂)), 133.4 (d, $^{2/3}J_{\text{P,C}}=10.0$ Hz, *o*-or *m*-CH(PPh₂)), 131.9 (d, $^4J_{\text{P,C}}=0.9$ Hz, *p*-CH(PPh₂)), 131.6 (d, $^4J_{\text{P,C}}=0.9$ Hz, *p*-CH(PPh₂)), 129.7-128.9 (m, CH(PPh₂) + C_bH), 128.3 (d, $^2J_{\text{P,C}}=12.2$ Hz, C_dH), 122.8 (d, $^1J_{\text{P,C}}=103.7$ Hz, C^{IV}(PPh₂)), 114.9 (d, $^1J_{\text{P,C}}=109.1$ Hz, C^{IV}-PPh₂), 41.9 (m, N-CH₂), 35.3 (s, C_{a,c}^{IV}-C(CH₃)₃), 34.5 (s, C_{c/a}^{IV}-C(CH₃)₃), 31.0 (s, N-CH₂-CH₂-CH₂-N), 30.6 (s, C_{c,a}^{IV}-C(CH₃)₃), 29.7 (s, C_{a,c}^{IV}-C(CH₃)₃). Anal. Calcd for C₅₅H₇₀Br₂N₂O₂P₂: C, 65.22; H, 6.97; N, 2.77. Found: C, 65.19; H, 7.03; N, 2.70.

Synthesis of 48

48 was synthesized using the same protocol as the synthesis of **46**, but using 1,3-diamino-2,2-dimethylpropane (198 mg, 1.942 mmol) instead of (R,R)-1,2-diaminocyclohexane. It was isolated as a white solid (1.32g, 65%)

48: $^{31}\text{P}\{^1\text{H}\}$ NMR (CDCl_3): δ 41.7 (s, P^V); ^1H NMR (CDCl_3): δ 7.72 (dd, $^3J_{\text{H,H}}=7.5$ Hz, $^3J_{\text{P,H}}=13.0$ Hz, 8H, *o*-CH(PPh_2)), 7.65 (vt, $^3J_{\text{H,H}}=^3J'_{\text{H,H}}=7.5$ Hz, 4H, *p*-CH(PPh_2)), 7.56 (s, br, 2H, $C_b\text{H}$), 7.55 (vtd, $^4J_{\text{P,H}}=3.0$ Hz, $^3J_{\text{H,H}}=^3J'_{\text{H,H}}=7.5$ Hz, 8H, *m*-CH(PPh_2)), 6.73 (d, b, $^3J_{\text{P,H}}=14.0$ Hz, 2H, $C_d\text{H}$), 3.17 (s, 2H, NH), 3.14 (d, $^3J_{\text{P,H}}=9.0$ Hz, 4H, N- CH_2), 1.29 (s, b, 18H, $C_{c,a}^{\text{IV}}-\text{C}^{\text{IV}}(\text{CH}_3)_3$), 1.10 (s, 18H, $C_{c,a}^{\text{IV}}-\text{C}^{\text{IV}}(\text{CH}_3)_3$), 0.74 (s, br, 6H, N- $\text{CH}_2-\text{C}^{\text{IV}}(\text{CH}_3)_2$); $^{13}\text{C}\{^1\text{H}\}$ NMR (CDCl_3): δ 141.9 (d, $^3J_{\text{P,C}}=2.5$ Hz, $C_{c,a}^{\text{IV}}$), 133.9 (s, b, *p*-CH(PPh_2)), 133.7 (d, $^{2/3}J_{\text{P,C}}=10.5$ Hz, *m*- or *o*-CH(PPh_2)), 131.6 (s, b, $C_b\text{H}$), 129.5 (d, $^{2/3}J_{\text{P,C}}=13.0$ Hz, *m*- or *o*-CH(PPh_2)), 128.7 (d, $^2J_{\text{P,C}}=12.0$ Hz, $C_d\text{H}$), 50.6 (m,b, N- CH_2), 37.06 (t, $^3J_{\text{P,C}}=8.0$ Hz, N- $\text{CH}_2-\text{C}^{\text{IV}}-\text{CH}_2-\text{N}$), 35.2 (s, $C_{c,a}^{\text{IV}}-\text{C}^{\text{IV}}(\text{CH}_3)_3$), 34.6 (s, $C_{c,a}^{\text{IV}}-\text{C}^{\text{IV}}(\text{CH}_3)_3$), 31.3 (s, $C_{c,a}^{\text{IV}}-\text{C}^{\text{IV}}(\text{CH}_3)_3$), 30.6 (s, N- $\text{CH}_2-\text{C}^{\text{IV}}(\text{CH}_3)_2$), ($\text{C}^{\text{IV}}-\text{OH}$, $\text{C}^{\text{IV}}-\text{PPh}_2$, $\text{C}^{\text{IV}}(\text{PPh}_2)$ and one of $C_{c,a}^{\text{IV}}$) were not observed at all, even in increasing the number of acquisition). Anal. Calcd for $\text{C}_{57}\text{H}_{74}\text{Br}_2\text{N}_2\text{O}_2\text{P}_2$: C, 65.77; H, 7.17; N, 2.69. Found: C, 65.88; H, 7.08; N, 2.81.

Synthesis of 49

49 was synthesized using the same protocol as the synthesis of **46**, but using ortho-phenylenediamine (210 mg, 1.942 mmol) instead of (R,R)-1,2-diaminocyclohexane. It was isolated as a white solid (1.47 g, 72%)

49: $^{31}\text{P}\{^1\text{H}\}$ NMR (CDCl_3): δ 38.9 (s, P^V); ^1H NMR (CDCl_3): δ 8.88 (d, $^2J_{\text{P,H}}=8.5$ Hz, 2H, NH), 7.76 (d, 2H, $^4J_{\text{H,H}}=2.0$ Hz, $C_b\text{H}$), 7.74 (vt, $^3J_{\text{P,H}}=^3J_{\text{H,H}}=8.0$ Hz, 4H, *o*-CH(PPh_2)), 7.73 (vt, $^3J_{\text{P,H}}=^3J_{\text{H,H}}=8.0$ Hz, 4H, *o*-CH(PPh_2)), 7.71 (vt, $^3J_{\text{H,H}}=^3J'_{\text{H,H}}=8.0$ Hz, 4H, *p*-CH(PPh_2)), 7.56 (vtd, $^3J_{\text{H,H}}=^3J'_{\text{H,H}}=8.0$ Hz, $^4J_{\text{P,H}}=4.0$ Hz, 8H, *m*-CH(PPh_2)), 7.48 (b, 2H, OH), 6.90 (dd, $^3J_{\text{P,H}}=16.0$ Hz, $^4J_{\text{H,H}}=2.0$ Hz, $C_d\text{H}$), 6.65 (dd, $^3J_{\text{H,H}}=6.0$ Hz, $^4J_{\text{H,H}}=3.5$ Hz, 2H, $C_f\text{H}$), 6.53 (ddd, $^3J_{\text{H,H}}=6.0$ Hz, $^4J_{\text{H,H}}=3.5$ Hz, $^4J_{\text{P,H}}=1.0$ Hz, 2H, $C_e\text{H}$), 1.33 (s, 18H, $C_{c,a}^{\text{IV}}-\text{C}^{\text{IV}}(\text{CH}_3)_3$), 1.15 (s, 18H, $C_{c,a}^{\text{IV}}-\text{C}^{\text{IV}}(\text{CH}_3)_3$); $^{13}\text{C}\{^1\text{H}\}$ NMR (CDCl_3): δ 155.8 (d, $^3J_{\text{P,C}}=2.0$ Hz, $\text{C}^{\text{IV}}-\text{O}$), 145.8 (d, $^3J_{\text{P,C}}=13$ Hz, $C_{c,a}^{\text{IV}}$), 141.6 (d, $^3J_{\text{P,C}}=7.5$ Hz, $C_{c,a}^{\text{IV}}$), 134.8 (d, $^4J_{\text{P,C}}=3.0$ Hz, *p*-CH(PPh_2)), 133.7 (d, $^{2/3}J_{\text{P,C}}=11.0$ Hz, *m*- or *o*-CH(PPh_2)), 132.9 (d, $^4J_{\text{P,C}}=2.0$ Hz, $C_b\text{H}$), 132.5 (d, $^2J_{\text{P,C}}=6.5$ Hz, $\text{C}^{\text{IV}}-\text{N}$), 129.9 (d, $^{2/3}J_{\text{P,C}}=13.5$ Hz, *m*- or *o*-CH(PPh_2)), 129.1 (d, $^2J_{\text{P,C}}=11.5$ Hz, $C_d\text{H}$), 125.3 (d, $^4J_{\text{P,C}}=1.0$ Hz, $C_f\text{H}$), 125.0 (d, $^3J_{\text{P,C}}=3.0$ Hz, $C_e\text{H}$), 121.5 (d, $^1J_{\text{P,C}}=104.5$ Hz, $\text{C}^{\text{IV}}(\text{PPh}_2)$), 111.0 (d, $^1J_{\text{P,C}}=110.5$ Hz, $\text{C}^{\text{IV}}-\text{PPh}_2$), 35.1 (s, $C_{c,a}^{\text{IV}}-\text{C}^{\text{IV}}(\text{CH}_3)_3$), 34.8 (s, $C_{c,a}^{\text{IV}}-\text{C}^{\text{IV}}(\text{CH}_3)_3$), 31.2 (s, $C_{c,a}^{\text{IV}}-\text{C}^{\text{IV}}(\text{CH}_3)_3$), 30.7 (s, $C_{c,a}^{\text{IV}}-\text{C}^{\text{IV}}(\text{CH}_3)_3$). Anal. Calcd for $\text{C}_{58}\text{H}_{68}\text{Br}_2\text{N}_2\text{O}_2\text{P}_2$: C, 66.54; H, 6.55; N, 2.68. Found: C, 66.68; H, 6.55; N, 2.58.

Synthesis of 50

12 was synthesized using the same protocol as the synthesis of **46**, but using diethylenetriamine (210 μL , 1.942 mmol) instead of (R,R)-1,2-diaminocyclohexane, and tributylamine (463 μL , 1.942 mmol) instead of DABCO as base. It was isolated as a white solid (1.8 g, 78%)

50: $^{31}\text{P}\{^1\text{H}\}$ NMR (CDCl_3): δ 41.8 (s, P^V); ^1H NMR (CDCl_3): δ 7.74 (m, 2H, CH(PPh_2)), 7.65 (m, 20H, CH(PPh_2) + $C_b\text{H}$), 6.72 (m, b, 2H, OH or NH), 6.56 (dd, $^3J_{\text{H,H}}=2.0$ Hz, $^3J_{\text{P,H}}=16.0$ Hz, 2H, $C_d\text{H}$), 3.70 (s, b, 4H, $\text{CH}_2-\text{NH}_2-\text{CH}_2$), 3.52 (s, b, 4H, $P^V-\text{NH}-\text{CH}_2$), 2.02 (s, b, 4H, OH or NH), 1.47 (s, 18H, $C_{c,a}^{\text{IV}}-\text{C}^{\text{IV}}(\text{CH}_3)_3$), 1.10 (s, 18H, $C_{c,a}^{\text{IV}}-\text{C}^{\text{IV}}(\text{CH}_3)_3$); $^{13}\text{C}\{^1\text{H}\}$ NMR (CDCl_3):

δ 155.7 (d, $^2J_{P,C}$ = 1.0 Hz, C^{IV} -OH), 145.5 (d, $^3J_{P,C}$ = 14.0 Hz, $C_{c/a}^{IV}$), 141.9 (d, $^3J_{P,C}$ = 7.0 Hz, $C_{c/a}^{IV}$), 134.7 (d, $^4J_{P,C}$ = 3.0 Hz, p -CH(PPh₂)), 133.5 (d, $^{2/3}J_{P,C}$ = 11.5 Hz, m -or o -CH(PPh₂)), 132.3 (d, $^4J_{P,C}$ = 1.5 Hz, C_bH), 130.0 (d, $^{2/3}J_{P,C}$ = 13.0 Hz, m -or o -CH(PPh₂)), 128.6 (d, $^2J_{P,C}$ = 12.5 Hz, C_dH), 121.7 (d, $^1J_{P,C}$ = 105.0 Hz, C^{IV} (PPh₂)), 114.5 (d, $^1J_{P,C}$ = 98.0 Hz, C^{IV} -PPh₂), 113.1 (d, $^1J_{P,C}$ = 107.2 Hz, C^{IV} -PPh₂), 49.0 (d, $^2J_{P,C}$ = 9.0 Hz, P^V -N-CH₂), 40.0 (s, P^V -N-CH₂-CH₂), 35.1 (d, $^4J_{P,C}$ = 2.0 Hz, $C_{c,a}^{IV}$ - C^{IV} (CH₃)₃), 34.7 (d, $^4J_{P,C}$ = 1.0 Hz, $C_{c,a}^{IV}$ - C^{IV} (CH₃)₃), 31.2 (s, $C_{c,a}^{IV}$ - C^{IV} (CH₃)₃), 30.6 (s, N-CH₂- C^{IV} (CH₃)₂). Anal. Calcd for C₅₆H₇₄Br₃N₃O₂P₂: C, 59.90; H, 6.64; N, 3.74. Found: C, 59.78; H, 7.66.536; N, 3.74.

Synthesis of 51

KHMDS (240 mg, 1.2 mmol) was added into a slurry of **35b** (316 mg, 0.3 mmol) in THF (20 mL). After 4h, a cloudy solution was yielded. The completion of the deprotonation was verified by $^{31}P\{^1H\}$ NMR spectrum which showed only one singlet at +18 ppm. Insoluble potassium salt was removed by centrifugation. [YCl₃(THF)_{3.5}] (134.3 mg, 0.3 mmol) was added. After 4 h of stirring at room temperature, $^{31}P\{^1H\}$ NMR spectrum showed the clean formation of a complex with two singlets of equal intensity at 27.5 ppm and 22.6 ppm. Potassium *tert*-butoxide (33.7 mg, 0.3 mmol) was added into the mixture, giving a cloudy solution. Stirring was continued for 7 h and the solid was removed by centrifugation. The solvents was evaporated in vacuum and the residue was recrystallised in cyclohexane (5 mL), giving the product as colorless crystals (265 mg, 79%).

51: $^{31}P\{^1H\}$ NMR (THF- d_8): δ 27.6 (s, P^V), 20.8 (s, P^V); 1H NMR (THF- d_8): δ 7.89 (ddd, $^3J_{P,H}$ = 10.6 Hz, $^3J_{H,H}$ = 7.5 Hz, $^4J_{H,H}$ = 1.0 Hz, 2H, o -CH(PPh₂)), 7.75 (ddd, $^3J_{P,H}$ = 12.3 Hz, $^3J_{H,H}$ = 7.5 Hz, $^4J_{H,H}$ = 1.0 Hz, 2H, o -CH(PPh₂)), 7.62 (ddd, $^3J_{P,H}$ = 11.2 Hz, $^3J_{H,H}$ = 7.5 Hz, $^4J_{H,H}$ = 1.0 Hz, 2H, o -CH(PPh₂)), 7.56 (ddd, $^3J_{P,H}$ = 11.0 Hz, $^3J_{H,H}$ = 7.5 Hz, $^4J_{H,H}$ = 1.0 Hz, 2H, o -CH(PPh₂)), 7.51-7.42 (m, 5H, p -CH(PPh₂) + m -CH(PPh₂)), 7.38 (vtd, $^4J_{P,H}$ = 2.2 Hz, $^3J_{H,H}$ = $^3J'_{H,H}$ = 7.5 Hz, 2H, m -CH(PPh₂)), 7.32 (vtd, $^4J_{P,H}$ = 2.2 Hz, $^3J_{H,H}$ = $^3J'_{H,H}$ = 7.5 Hz, 2H, m -CH(PPh₂)), 7.27 (d, $^4J_{H,H}$ = 2.0 Hz, 1H, C_bH), 7.21 (d, $^4J_{H,H}$ = 2.0 Hz, 1H, C_bH), 7.17 (vtd, $^4J_{H,H}$ = 1.0 Hz, $^3J_{H,H}$ = $^3J'_{H,H}$ = 7.5 Hz, 1H, p -CH(PPh₂)), 6.84 (dd, $^4J_{H,H}$ = 2.0 Hz, $^3J_{P,H}$ = 16.0 Hz, 1H, C_dH), 6.82 (vtd, $^4J_{P,H}$ = 2.2 Hz, $^3J_{H,H}$ = $^3J'_{H,H}$ = 7.5 Hz, 2H, m -CH(PPh₂)), 6.47 (dd, $^4J_{H,H}$ = 2.0 Hz, $^3J_{P,H}$ = 16.0 Hz, 1H, C_dH), 4.62 (vqd, $^3J_{H,H}$ = $^3J'_{H,H}$ = $^3J_{P,H}$ = 9.0 Hz, $^4J_{P,H}$ = 3.0 Hz, 1H, N-CH-CH-N), 2.97 (vqd, $^3J_{H,H}$ = $^3J'_{H,H}$ = $^3J_{P,H}$ = 9.0 Hz, $^4J_{P,H}$ = 3.0 Hz, 1H, N-CH-CH-N), 1.57 (m, 2H, CH₂(cyclohexane)), 1.31 (s, 9H, $C_{c,a}^{IV}$ - C^{IV} (CH₃)₃), 1.12 (m, 2H, CH₂(cyclohexane)), 1.12 (s, b, 9H, O- C^{IV} (CH₃)₃), 1.10 (s, 9H, $C_{c,a}^{IV}$ - C^{IV} (CH₃)₃), 1.09 (s, 9H, $C_{c,a}^{IV}$ - C^{IV} (CH₃)₃), 0.96 (s, 9H, $C_{c,a}^{IV}$ - C^{IV} (CH₃)₃), 0.82 (m, 2H, CH₂(cyclohexane)), 0.66 (m, 1H, CH₂(cyclohexane)), 0.48 (m, 1H, CH₂(cyclohexane)); $^{13}C\{^1H\}$ NMR (THF- d_8): δ 168.7 (vt, $^3J_{P,C}$ = $^2J_{Y,C}$ = 2.7 Hz, C^{IV} -O), 168.5 (vt, $^3J_{P,C}$ = $^2J_{Y,C}$ = 2.7 Hz, C^{IV} -O), 139.5 (d, $^3J_{P,C}$ = 8.2 Hz, $C_{c,a}^{IV}$), 138.8 (d, $^3J_{P,C}$ = 7.8 Hz, $C_{c,a}^{IV}$), 136.7 (d, $^1J_{P,C}$ = 82.9 Hz, C^{IV} (PPh₂)), 136.5 (d, $^1J_{P,C}$ = 86.2 Hz, C^{IV} (PPh₂)), 134.9 (d, $^{2/3}J_{P,C}$ = 9.3 Hz, m -or o -CH(PPh₂)), 134.3 (d, $^1J_{P,C}$ = 108.5 Hz, C^{IV} (PPh₂)), 134.1 (d, $^3J_{P,C}$ = 8.2 Hz, $C_{c,a}^{IV}$), 134.0 (d, $^2J_{P,C}$ = 9.2 Hz, C_dH), 133.9 (d, $^{2/3}J_{P,C}$ = 9.0 Hz, m -or o -CH(PPh₂)), 133.8 (d, $^{2/3}J_{P,C}$ = 10.0 Hz, m -or o -CH(PPh₂)), 133.0 (d, $^1J_{P,C}$ = 82.1 Hz, C^{IV} (PPh₂)), 132.0 (d, $^4J_{P,C}$ = 2.6 Hz, p -CH(PPh₂)), 131.8 (d, $^4J_{P,C}$ = 2.1 Hz, p -CH(PPh₂)), 131.6 (d, $^4J_{P,C}$ = 2.4 Hz, p -CH(PPh₂)), 130.9 (d, $^4J_{P,C}$ = 2.4 Hz, p -CH(PPh₂)),

128.9 (d, $^{23}\text{J}_{\text{P,C}} = 11.6$ Hz, *m*-or *o*-CH(PPh₂)), 128.7 (d, $^{23}\text{J}_{\text{P,C}} = 11.6$ Hz, *m*-or *o*-CH(PPh₂)), 128.5 (d, $^{23}\text{J}_{\text{P,C}} = 12.1$ Hz, *m*-or *o*-CH(PPh₂)), 128.4 (d, $^2\text{J}_{\text{P,C}} = 12.0$ Hz, C_dH), 128.1 (d, $^4\text{J}_{\text{P,C}} = 1.5$ Hz, C_bH), 128.0 (d, $^4\text{J}_{\text{P,C}} = 1.5$ Hz, C_bH), 70.0 (s, O-C^{IV}(CH₃)₃), 64.0 (d, $^2\text{J}_{\text{P,C}} = 7.9$ Hz, N-CH-CH-N), 63.8 (d, $^2\text{J}_{\text{P,C}} = 8.3$ Hz, N-CH-CH-N), 37.7 (s, CH₂(cyclohexane ring)), 37.6 (s, CH₂(cyclohexane ring)), 36.3 (s, CH₂(cyclohexane ring)), 35.9 (s, C^{IV}(CH₃)₃), 35.8 (s, C^{IV}(CH₃)₃), 35.6 (s, C^{IV}(CH₃)₃), 35.5 (s, C^{IV}(CH₃)₃), 35.1 (s, C^{IV}(CH₃)₃), 31.8 (s, C^{IV}(CH₃)₃), 30.3 (s, C^{IV}(CH₃)₃), 29.6 (s, C^{IV}(CH₃)₃), 27.1 (s, CH₂(cyclohexane ring)). Anal. Calcd for C₆₂H₇₉N₂O₃P₂Y: C, 70.84; H, 7.58; N, 2.67. Found: C, 70.66; H, 7.65; N, 2.59.

Synthesis of 52

KHMDS (240 mg, 1.2 mmol) was added into a slurry of **46** (316 mg, 0.3 mmol) in THF (20 mL). After 4h, a cloudy solution was yielded. The completion of the deprotonation was verified by $^{31}\text{P}\{^1\text{H}\}$ NMR spectrum which showed only one singlet at +18 ppm. Insoluble potassium salt was removed by centrifugation. [YCl₃(THF)_{3.5}] (134.3 mg, 0.3 mmol) was added. After 4 h of stirring at room temperature, $^{31}\text{P}\{^1\text{H}\}$ NMR spectrum showed the clean formation of a complex with two singlets of equal intensity at 27.5 ppm and 22.6 ppm. Potassium *tert*-butoxide (33.7 mg, 0.3 mmol) was added into the mixture, giving a cloudy solution. Stirring was continued for 7 h and the solid was removed by centrifugation. The solvents was evaporated in vacuum and the residue was recrystallised in cyclohexane (5 mL), giving the product as colorless crystals (293 g, 87%).

52: $^{31}\text{P}\{^1\text{H}\}$ NMR (THF-*d*₈): δ 27.6 (s, P^V), 20.8 (s, P^V); ^1H NMR (THF-*d*₈): δ 7.89 (ddd, $^3\text{J}_{\text{P,H}} = 10.6$ Hz, $^3\text{J}_{\text{H,H}} = 7.5$ Hz, $^4\text{J}_{\text{H,H}} = 1.0$ Hz, 2H, *o*-CH(PPh₂)), 7.75 (ddd, $^3\text{J}_{\text{P,H}} = 12.3$ Hz, $^3\text{J}_{\text{H,H}} = 7.5$ Hz, $^4\text{J}_{\text{H,H}} = 1.0$ Hz, 2H, *o*-CH(PPh₂)), 7.62 (ddd, $^3\text{J}_{\text{P,H}} = 11.2$ Hz, $^3\text{J}_{\text{H,H}} = 7.5$ Hz, $^4\text{J}_{\text{H,H}} = 1.0$ Hz, 2H, *o*-CH(PPh₂)), 7.56 (ddd, $^3\text{J}_{\text{P,H}} = 11.0$ Hz, $^3\text{J}_{\text{H,H}} = 7.5$ Hz, $^4\text{J}_{\text{H,H}} = 1.0$ Hz, 2H, *o*-CH(PPh₂)), 7.51-7.42 (m, 5H, *p*-CH(PPh₂) + *m*-CH(PPh₂)), 7.38 (vtd, $^4\text{J}_{\text{P,H}} = 2.2$ Hz, $^3\text{J}_{\text{H,H}} = ^3\text{J}'_{\text{H,H}} = 7.5$ Hz, 2H, *m*-CH(PPh₂)), 7.32 (vtd, $^4\text{J}_{\text{P,H}} = 2.2$ Hz, $^3\text{J}_{\text{H,H}} = ^3\text{J}'_{\text{H,H}} = 7.5$ Hz, 2H, *m*-CH(PPh₂)), 7.27 (d, $^4\text{J}_{\text{H,H}} = 2.0$ Hz, 1H, C_bH), 7.21 (d, $^4\text{J}_{\text{H,H}} = 2.0$ Hz, 1H, C_bH), 7.17 (vtd, $^4\text{J}_{\text{H,H}} = 1.0$ Hz, $^3\text{J}_{\text{H,H}} = ^3\text{J}'_{\text{H,H}} = 7.5$ Hz, 1H, *p*-CH(PPh₂)), 6.84 (dd, $^4\text{J}_{\text{H,H}} = 2.0$ Hz, $^3\text{J}_{\text{P,H}} = 16.0$ Hz, 1H, C_dH), 6.82 (vtd, $^4\text{J}_{\text{P,H}} = 2.2$ Hz, $^3\text{J}_{\text{H,H}} = ^3\text{J}'_{\text{H,H}} = 7.5$ Hz, 2H, *m*-CH(PPh₂)), 6.47 (dd, $^4\text{J}_{\text{H,H}} = 2.0$ Hz, $^3\text{J}_{\text{P,H}} = 16.0$ Hz, 1H, C_dH), 4.62 (vqd, $^3\text{J}_{\text{H,H}} = ^3\text{J}'_{\text{H,H}} = ^3\text{J}_{\text{P,H}} = 9.0$ Hz, $^4\text{J}_{\text{P,H}} = 3.0$ Hz, 1H, N-CH-CH-N), 2.97 (vqd, $^3\text{J}_{\text{H,H}} = ^3\text{J}'_{\text{H,H}} = ^3\text{J}_{\text{P,H}} = 9.0$ Hz, $^4\text{J}_{\text{P,H}} = 3.0$ Hz, 1H, N-CH-CH-N), 1.57 (m, 2H, CH₂(cyclohexane)), 1.31 (s, 9H, C_{c,a}^{IV} - C^{IV}(CH₃)₃), 1.12 (m, 2H, CH₂(cyclohexane)), 1.12 (s, b, 9H, O - C^{IV}(CH₃)₃), 1.10 (s, 9H, C_{c,a}^{IV} - C^{IV}(CH₃)₃), 1.09 (s, 9H, C_{c,a}^{IV} - C^{IV}(CH₃)₃), 0.96 (s, 9H, C_{c,a}^{IV} - C^{IV}(CH₃)₃), 0.82 (m, 2H, CH₂(cyclohexane)), 0.66 (m, 1H, CH₂(cyclohexane)), 0.48 (m, 1H, CH₂(cyclohexane)); $^{13}\text{C}\{^1\text{H}\}$ NMR (THF-*d*₈): δ 168.7 (vt, $^3\text{J}_{\text{P,C}} = ^2\text{J}_{\text{Y,C}} = 2.7$ Hz, C^{IV}-O), 168.5 (vt, $^3\text{J}_{\text{P,C}} = ^2\text{J}_{\text{Y,C}} = 2.7$ Hz, C^{IV}-O), 139.5 (d, $^3\text{J}_{\text{P,C}} = 8.2$ Hz, C_{c,a}^{IV}), 138.8 (d, $^3\text{J}_{\text{P,C}} = 7.8$ Hz, C_{c,a}^{IV}), 136.7 (d, $^1\text{J}_{\text{P,C}} = 82.9$ Hz, C^{IV}(PPh₂)), 136.5 (d, $^1\text{J}_{\text{P,C}} = 86.2$ Hz, C^{IV}(PPh₂)), 134.9 (d, $^{23}\text{J}_{\text{P,C}} = 9.3$ Hz, *m*-or *o*-CH(PPh₂)), 134.3 (d, $^1\text{J}_{\text{P,C}} = 108.5$ Hz, C^{IV}(PPh₂)), 134.1 (d, $^3\text{J}_{\text{P,C}} = 8.2$ Hz, C_{c,a}^{IV}), 134.0 (d, $^2\text{J}_{\text{P,C}} = 9.2$ Hz, C_dH), 133.9 (d, $^{23}\text{J}_{\text{P,C}} = 9.0$ Hz, *m*-or *o*-CH(PPh₂)), 133.8 (d, $^{23}\text{J}_{\text{P,C}} = 10.0$ Hz, *m*-or *o*-CH(PPh₂)), 133.0 (d, $^1\text{J}_{\text{P,C}} = 82.1$ Hz, C^{IV}(PPh₂)), 132.0 (d, $^4\text{J}_{\text{P,C}} = 2.6$ Hz, *p*-CH(PPh₂)), 131.8 (d, $^4\text{J}_{\text{P,C}} = 2.1$ Hz, *p*-CH(PPh₂)), 131.6 (d, $^4\text{J}_{\text{P,C}} = 2.4$ Hz, *p*-CH(PPh₂)), 130.9 (d, $^4\text{J}_{\text{P,C}} = 2.4$ Hz, *p*-CH(PPh₂)),

128.9 (d, ${}^2J_{P,C} = 11.6$ Hz, *m*-or *o*-CH(PPh₂)), 128.7 (d, ${}^2J_{P,C} = 11.6$ Hz, *m*-or *o*-CH(PPh₂)), 128.5 (d, ${}^2J_{P,C} = 12.1$ Hz, *m*-or *o*-CH(PPh₂)), 128.4 (d, ${}^2J_{P,C} = 12.0$ Hz, C_dH), 128.1 (d, ${}^4J_{P,C} = 1.5$ Hz, C_bH), 128.0 (d, ${}^4J_{P,C} = 1.5$ Hz, C_bH), 70.0 (s, O-C^{IV}(CH₃)₃), 64.0 (d, ${}^2J_{P,C} = 7.9$ Hz, N-CH-CH-N), 63.8 (d, ${}^2J_{P,C} = 8.3$ Hz, N-CH-CH-N), 37.7 (s, CH₂(cyclohexane ring)), 37.6 (s, CH₂(cyclohexane ring)), 36.3 (s, CH₂(cyclohexane ring)), 35.9 (s, C^{IV}(CH₃)₃), 35.8 (s, C^{IV}(CH₃)₃), 35.6 (s, C^{IV}(CH₃)₃), 35.5 (s, C^{IV}(CH₃)₃), 35.1 (s, C^{IV}(CH₃)₃), 31.8 (s, C^{IV}(CH₃)₃), 30.3 (s, C^{IV}(CH₃)₃), 29.6 (s, C^{IV}(CH₃)₃), 27.1 (s, CH₂(cyclohexane ring)). Anal. Calcd for C₆₂H₇₉N₂O₃P₂Y: C, 70.84; H, 7.58; N, 2.67. Found: C, 70.47; H, 7.97; N, 2.53.

Synthesis of 53a

KHMDS (240 mg, 1.2 mmol) was added into a slurry of **47** (304 mg, 0.3 mmol) in THF (20 mL). After 4h, a cloudy solution was yielded. The completion of the deprotonation was verified by ${}^{31}\text{P}\{^1\text{H}\}$ NMR spectrum which showed only one singlet at +23.8 ppm. Insoluble potassium salt was removed by centrifugation. [YCl₃(THF)_{3.5}] (134.3 mg, 0.3 mmol) was added. After 4h of stirring at room temperature, ${}^{31}\text{P}\{^1\text{H}\}$ NMR spectrum showed the clean formation of a complex with one singlet at 36.9 ppm. Potassium *tert*-butoxide (33.7 mg, 0.3 mmol) was added into the mixture, giving a cloudy solution. Stirring was continued for 7 h and the solid was removed by centrifugation. The solvents was evaporated in vacuum and the residue was recrystallised in cyclohexane (5 mL), giving the product as colorless crystals (240 mg, 74%).

53a: ${}^{31}\text{P}\{^1\text{H}\}$ NMR (THF-*d*₈): δ 33.8 (s); ${}^1\text{H}$ NMR (THF-*d*₈): δ 7.63 (dd, ${}^3J_{H,H} = 7.0$ Hz, ${}^3J_{P,H} = 10.5$ Hz, 4H, *o*-CH(PPh₂)), 7.50 (dd, ${}^3J_{H,H} = 7.0$ Hz, ${}^3J_{P,H} = 10.5$ Hz, 4H, *o*-CH(PPh₂)), 7.48 (vt, ${}^3J_{H,H} = {}^3J'_{H,H} = 7.0$ Hz, 2H, *p*-CH(PPh₂)), 7.41 (vtd, ${}^3J_{H,H} = {}^3J'_{H,H} = 7.0$ Hz, ${}^4J_{P,H} = 2.0$ Hz, 4H, *m*-CH(PPh₂)), 7.40 (vt, ${}^3J_{H,H} = {}^3J'_{H,H} = 7.0$ Hz, 2H, *p*-CH(PPh₂)), 7.32 (vtd, ${}^3J_{H,H} = {}^3J'_{H,H} = 7.0$ Hz, ${}^4J_{P,H} = 2.0$ Hz, 4H, *m*-CH(PPh₂)), 7.29 (d, ${}^4J_{H,H} = 2.5$ Hz, 2H, C_bH), 6.37 (dd, ${}^4J_{H,H} = 2.5$ Hz, ${}^3J_{P,H} = 15.5$ Hz, 2H, C_dH), 3.51 (m, 2H, N-CH₂-CH₂-CH₂-N), 3.16 (m, 2H, N-CH₂-CH₂-CH₂-N), 1.90 (m, 1H, N-CH₂-CH₂-CH₂-N), 1.63 (m, 1H, N-CH₂-CH₂-CH₂-N), 1.42 (s, 18H, C(CH₃)₃), 1.09 (s, 18H, C(CH₃)₃), 0.86 (s, 9H, O-C(CH₃)₃); ${}^{13}\text{C}\{^1\text{H}\}$ NMR (THF-*d*₈): 169.3 (d, ${}^3J_{P,C} = 1.5$ Hz, C^{IV}-O), 139.0 (d, ${}^3J_{P,C} = 8.0$ Hz, C_{c,a}^{IV}), 134.3 (d, ${}^2J_{P,C} = 9.0$ Hz, *m*-or *o*-CH(PPh₂)), 134.1 (d, ${}^2J_{P,C} = 9.0$ Hz, *m*-or *o*-CH(PPh₂)), 133.9 (d, ${}^3J_{P,C} = 10.5$ Hz, C_{c,a}^{IV}), 132.6 (d, ${}^1J_{P,C} = 87.8$ Hz, C^{IV}-PPh₂), 131.9 (d, ${}^4J_{P,C} = 1.0$ Hz, *p*-CH(PPh₂)), 131.8 (d, ${}^4J_{P,C} = 1.0$ Hz, *p*-CH(PPh₂)), 128.9 (d, ${}^2J_{P,C} = 11.5$ Hz, *m*-or *o*-CH(PPh₂)), 128.4 (s, C_bH), 128.1 (d, ${}^2J_{P,C} = 14.0$ Hz, C_dH), 113.3 (d, ${}^1J_{P,C} = 121.0$ Hz, C^{IV}(PPh₂)), 69.8 (s, O-C^{IV}(CH₃)₃), 47.1 (d, ${}^2J_{P,C} = 7.0$ Hz, N-CH₂-CH₂-CH₂-N), 36.4 (t, ${}^3J_{P,C} = 9.0$ Hz, N-CH₂-CH₂-CH₂-N), 34.6 (s, O-C^{IV}(CH₃)₃), 31.9 (s, C_{c,a}^{IV}-C^{IV}(CH₃)₃), 31.7 (s, C_{c,a}^{IV}-C^{IV}(CH₃)₃), 31.4 (s, C_{c,a}^{IV}-C^{IV}(CH₃)₃), 30.4 (s, C_{c,a}^{IV}-C^{IV}(CH₃)₃). Anal. Calcd for C₆₃H₈₃N₂O₄P₂Y: C, 69.86; H, 7.72; N, 2.59. Found: C, 69.72; H, 7.66; N, 2.67.

Synthesis of 53b

KHMDS (240 mg, 1.2 mmol) was added into a slurry of **47** (304 mg, 0.3 mmol) in THF (20 mL). After 4h, a cloudy solution was yielded. The completion of the deprotonation was verified by ${}^{31}\text{P}\{^1\text{H}\}$ NMR spectrum which showed only one singlet at +23.8 ppm. Insoluble potassium salt was removed by centrifugation. [YCl₃(THF)_{3.5}] (134.3 mg, 0.3 mmol) was added. After 4h

of stirring at room temperature, $^{31}\text{P}\{^1\text{H}\}$ NMR spectrum showed the clean formation of a complex with one singlet at 36.9 ppm. Potassium ethoxide (25.2 mg, 0.3 mmol) was added into the mixture, giving a cloudy solution. Stirring was continued for 7 h and the solid was removed by centrifugation. The solvents was evaporated in vacuum and the residue was recrystallised in cyclohexane (5 mL), giving the product as white solid (240 mg, 74%).

53b: $^{31}\text{P}\{^1\text{H}\}$ NMR (THF- d_8): δ 34.3 (s); ^1H NMR (THF- d_8): δ 7.66 (dd, $^3J_{\text{H,H}}=7.0$ Hz, $^3J_{\text{P,H}}=12.5$ Hz, 4H, *o*-CH(PPh₂)), 7.48 (vt, $^3J_{\text{H,H}}=^3J'_{\text{H,H}}=7.0$ Hz, 4H, *p*-CH(PPh₂)), 7.34 (vtd, $^3J_{\text{H,H}}=^3J'_{\text{H,H}}=7.0$ Hz, $^4J_{\text{P,H}}=2.0$ Hz, 4H, *m*-CH(PPh₂)), 7.33 (d, $^4J_{\text{H,H}}=2.5$ Hz, 2H, C_bH), 7.16 (vtd, $^3J_{\text{H,H}}=^3J'_{\text{H,H}}=7.0$ Hz, $^4J_{\text{P,H}}=2.0$ Hz, 4H, *m*-CH(PPh₂)), 6.73 (dd, $^4J_{\text{H,H}}=2.5$ Hz, $^3J_{\text{P,H}}=15.5$ Hz, 2H, C_dH), 3.27 (m, 2H, O-CH₂-CH₃), 3.07 (m, 2H, N-CH₂-CH₂-CH₂-N), 3.05 (m, 2H, N-CH₂-CH₂-CH₂-N), 1.58 (m, 2H, N-CH₂-CH₂-CH₂-N), 1.22 (s, 18H, C(CH₃)₃), 1.16 (s, 18H, C(CH₃)₃), 1.12 (t, 3H, O-CH₂-CH₃); $^{13}\text{C}\{^1\text{H}\}$ NMR (THF- d_8): 168.7 (d, $^3J_{\text{P,C}}=2.5$ Hz, C^{IV}-O), 139.1 (d, $^3J_{\text{P,C}}=8.0$ Hz, C_{c,a}^{IV}), 134.1 (d, $^{2/3}J_{\text{P,C}}=9.0$ Hz, *m*-or *o*-CH(PPh₂)), 133.9 (d, $^3J_{\text{P,C}}=14.5$ Hz, C_{c,a}^{IV}), 132.5 (d, $^1J_{\text{P,C}}=91.5$ Hz, C^{IV}-PPh₂), 131.7 (d, $^4J_{\text{P,C}}=1.0$ Hz, *p*-CH(PPh₂)), 128.8 (d, $^{2/3}J_{\text{P,C}}=11.5$ Hz, *m*-or *o*-CH(PPh₂)), 128.2 (s, C_bH), 127.8 (d, $^2J_{\text{P,C}}=13.5$ Hz, C_dH), 114.3 (d, $^1J_{\text{P,C}}=119.5$ Hz, C^{IV}(PPh₂)), 60.9 (s, O-CH₂-CH₃), 48.5 (d, $^2J_{\text{P,C}}=6.0$ Hz, N-CH₂-CH₂-CH₂-N), 35.7 (t, $^3J_{\text{P,C}}=5.0$ Hz, N-CH₂-CH₂-CH₂-N), 34.3 (s, C_{c,a}^{IV}-C^{IV}(CH₃)₃), 32.0 (s, O-CH₂-CH₃), 31.8 (s, C_{c,a}^{IV}-C^{IV}(CH₃)₃), 30.1 (s, C_{c,a}^{IV}-C^{IV}(CH₃)₃), 26.5 (s, C_{c,a}^{IV}-C^{IV}(CH₃)₃). Anal. Calcd for C₆₁H₇₉N₂O₄P₂Y: C, 69.44; H, 7.55; N, 2.65. Found: C, 69.29; H, 7.52; N, 2.65.

Synthesis of 54a

KHMDS (240 mg, 1.2 mmol) was added into a slurry of **48** (312 mg, 0.3 mmol) in THF (20 mL). After 4h, a cloudy solution was yielded. The completion of the deprotonation was verified by $^{31}\text{P}\{^1\text{H}\}$ NMR spectrum which showed only one singlet at +22.3 ppm. Insoluble potassium salt was removed by centrifugation. [YCl₃(THF)_{3.5}] (134.3 mg, 0.3 mmol) was added. After 4h of stirring at room temperature, $^{31}\text{P}\{^1\text{H}\}$ NMR spectrum showed the clean formation of a complex with one singlet at 36.5 ppm. Potassium *tert*-butoxide (33.7 mg, 0.3 mmol) was added into the mixture, giving a cloudy solution. Stirring was continued for 7 h and the solid was removed by centrifugation. The solvents was evaporated in vacuum and the residue was recrystallised in cyclohexane (5 mL), giving the product as colorless crystals (295 mg, 88%).

54a: $^{31}\text{P}\{^1\text{H}\}$ NMR (THF- d_8): δ 33.4 (s); ^1H NMR (THF- d_8): δ 7.70 (ddd, $^4J_{\text{H,H}}=1.5$ Hz, $^3J_{\text{H,H}}=8.0$ Hz, $^3J_{\text{P,H}}=10.5$ Hz, 4H, *o*-CH(PPh₂)), 7.49 (ddd, $^4J_{\text{H,H}}=1.5$ Hz, $^3J_{\text{H,H}}=8.0$ Hz, $^3J_{\text{P,H}}=10.5$ Hz, 4H, *o*-CH(PPh₂)), 7.42(vtd, $^4J_{\text{P,H}}=2.5$ Hz, $^3J_{\text{H,H}}=^3J'_{\text{H,H}}=8.0$ Hz, 4H, *m*-CH(PPh₂)), 7.34 (vtd, $^4J_{\text{P,H}}=2.5$ Hz, $^3J_{\text{H,H}}=^3J'_{\text{H,H}}=8.0$ Hz, 4H, *m*-CH(PPh₂)), 7.29 (d, $^4J_{\text{H,H}}=2.0$ Hz, 2H, C_bH), 7.15 (vtd, $^4J_{\text{H,H}}=1.5$ Hz, $^3J_{\text{H,H}}=^3J'_{\text{H,H}}=8.0$ Hz, 2H, *p*-CH(PPh₂)), 7.07 (vtd, $^4J_{\text{H,H}}=1.5$ Hz, $^3J_{\text{H,H}}=^3J'_{\text{H,H}}=8.0$ Hz, 2H, *p*-CH(PPh₂)), 6.43 (dd, $^4J_{\text{H,H}}=2.0$ Hz, $^3J_{\text{P,H}}=15.5$ Hz, 2H, C_dH), 3.39 (d, $^3J_{\text{P,H}}=12.5$ Hz, 1H, N-CH₂), 3.34 (d, $^3J_{\text{P,H}}=12.5$ Hz, 1H, N-CH₂), 2.85 (d, $^3J_{\text{P,H}}=12.0$ Hz, 1H, N-CH₂), 2.79 (d, $^3J_{\text{P,H}}=12.5$ Hz, 1H, N-CH₂), 1.36 (s, 18H, C_{c,a}^{IV}-C^{IV}(CH₃)₃), 1.02 (s, 18H, C_{c,a}^{IV}-C^{IV}(CH₃)₃), 0.80 (s, 9H, O-C^{IV}(CH₃)₃), 0.62 (s, 3H, N-CH₂-C^{IV}(CH₃)₂), 0.50 (s, 3H, N-CH₂-C^{IV}(CH₃)₂); $^{13}\text{C}\{^1\text{H}\}$ NMR (THF- d_8): 168.8 (d, $^3J_{\text{P,C}}=2.5$ Hz, C^{IV}-O), 168.7 (d, $^3J_{\text{P,C}}=2.5$ Hz,

$C^{IV}-O$), 137.9 (d, $^3J_{P,C}=7.7$ Hz, $C_{c,a}^{IV}$), 133.8 (d, $^{2/3}J_{P,C}=8.5$ Hz, *m*-or *o*-CH(PPh₂)), 133.6 (d, $^{2/3}J_{P,C}=8.5$ Hz, *m*-or *o*-CH(PPh₂)), 132.8 (d, $^1J_{P,C}=97.0$ Hz, $C^{IV}(PPh_2)$), 131.7 (d, $^1J_{P,C}=87.4$ Hz, $C^{IV}(PPh_2)$), 130.9 (s, *p*-CH(PPh₂)), 130.8 (s, *p*-CH(PPh₂)), 127.9 (d, $^{2/3}J_{P,C}=11.0$ Hz, *m*-or *o*-CH(PPh₂)), 128.8 (d, $^{2/3}J_{P,C}=11.0$ Hz, *m*-or *o*-CH(PPh₂)), 127.5 (s, C_bH), 127.5 (d, $^2J_{P,C}=12.5$ Hz, C_dH), 112.4 (d, $^1J_{P,C}=121.0$ Hz, $C^{IV}-PPh_2$), 69.2 (s, O- $C^{IV}(CH_3)_3$), 58.1 (d, $^2J_{P,C}=7.5$ Hz, N-CH₂), 38.1 (t, $^3J_{P,C}=12.5$ Hz, N-CH₂- $C^{IV}-CH_2-N$), 35.1 (s, $C_{c,a}^{IV}-C^{IV}(CH_3)_3$), 33.7 (s, O- $C^{IV}(CH_3)_3$), 33.5 (s, $C_{c,a}^{IV}-C^{IV}(CH_3)_3$), 31.0 (s, $C_{c,a}^{IV}-C^{IV}(CH_3)_3$), 29.6 (s, $C_{c,a}^{IV}-C^{IV}(CH_3)_3$), 26.1 (s, $C^{IV}(CH_3)_2$), 25.2 (s, N-CH₂- $C^{IV}(CH_3)_2$). Anal. Calcd for C₆₅H₈₆N₂O₄P₂Y: C, 70.32; H, 7.81; N, 2.52. Found: C, 70.40; H, 7.74; N, 2.61.

Synthesis of 54b

KHMDS (240 mg, 1.2 mmol) was added into a slurry of **48** (312 mg, 0.3 mmol) in THF (20 mL). After 4h, a cloudy solution was yielded. The completion of the deprotonation was verified by $^{31}P\{^1H\}$ NMR spectrum which showed only one singlet at +22.3 ppm. Insoluble potassium salt was removed by centrifugation. [YCl₃(THF)_{3.5}] (134.3 mg, 0.3 mmol) was added. After 4h of stirring at room temperature, $^{31}P\{^1H\}$ NMR spectrum showed the clean formation of a complex with one singlet at 36.5 ppm. Potassium ethoxide (25.2 mg, 0.3 mmol) was added into the mixture, giving a cloudy solution. Stirring was continued for 7 h and the solid was removed by centrifugation. The solvents was evaporated in vacuum and the residue was recrystallised in cyclohexane (5 mL), giving the product as white solid (265 mg, 81%).

54b: $^{31}P\{^1H\}$ NMR (THF-*d*₈): δ 33.4 (s); 1H NMR (THF-*d*₈): δ 7.75 (ddd, $^4J_{H,H}=1.5$ Hz, $^3J_{H,H}=7.0$ Hz, $^3J_{P,H}=11.5$ Hz, 4H, *o*-CH(PPh₂)), 7.58 (ddd, $^4J_{H,H}=1.5$ Hz, $^3J_{H,H}=7.0$ Hz, $^3J_{P,H}=11.5$ Hz, 4H, *o*-CH(PPh₂)), 7.45 (m, 8H, *m*-CH(PPh₂) + *p*-CH(PPh₂)), 7.35 (d, $^4J_{H,H}=2.0$ Hz, 2H, C_bH), 7.33 (vtd, $^4J_{P,H}=2.5$ Hz, $^3J_{H,H}=^3J_{H,H}=7.0$ Hz, 4H, *m*-CH(PPh₂)), 6.77 (dd, $^4J_{H,H}=2.0$ Hz, $^3J_{P,H}=15.0$ Hz, 2H, C_dH), 4.03 (t, $^3J_{H,H}=6.0$ Hz, 1H, O-CH₂-CH₃), 4.01 (t, $^3J_{H,H}=6.0$ Hz, 1H, O-CH₂-CH₃), 3.69 (d, $^3J_{P,H}=15.0$ Hz, 1H, N-CH₂), 3.64 (d, $^3J_{P,H}=15.0$ Hz, 1H, N-CH₂), 2.68 (d, $^3J_{P,H}=12.5$ Hz, 1H, N-CH₂), 2.61 (d, $^3J_{P,H}=12.5$ Hz, 1H, N-CH₂), 1.29 (s, 18H, $C_{c,a}^{IV}-C^{IV}(CH_3)_3$), 1.19 (s, 18H, $C_{c,a}^{IV}-C^{IV}(CH_3)_3$), 0.90 (m, 3H, O-CH₂-CH₃), 0.46 (s, 3H, N-CH₂- $C^{IV}(CH_3)_2$), 0.44 (s, 3H, N-CH₂- $C^{IV}(CH_3)_2$); $^{13}C\{^1H\}$ NMR (THF-*d*₈): 169.1 (d, $^3J_{P,C}=2.5$ Hz, $C^{IV}-O$), 169.0 (d, $^3J_{P,C}=2.5$ Hz, $C^{IV}-O$), 139.0 (d, $^3J_{P,C}=7.5$ Hz, $C_{c,a}^{IV}$), 134.8 (d, $^{2/3}J_{P,C}=9.0$ Hz, *m*-or *o*-CH(PPh₂)), 134.3 (d, $^{2/3}J_{P,C}=9.0$ Hz, *m*-or *o*-CH(PPh₂)), 134.0 (d, $^3J_{P,C}=14.5$ Hz, $C_{c,a}^{IV}$), 133.1 (d, $^1J_{P,C}=88.5$ Hz, $C^{IV}(PPh_2)$), 131.7 (d, $^1J_{P,C}=90.5$ Hz, $C^{IV}(PPh_2)$), 131.7 (s, *p*-CH(PPh₂)+ C_bH), 127.9 (d, $^2J_{P,C}=13.0$ Hz, C_dH), 114.4 (d, $^1J_{P,C}=120.0$ Hz, $C^{IV}-PPh_2$), 61.6 (s, O-CH₂-CH₃), 58.2 (d, $^2J_{P,C}=7.5$ Hz, N-CH₂), 37.5 (t, $^3J_{P,C}=12.5$ Hz, N-CH₂- $C^{IV}-CH_2-N$), 34.9 (s, $C_{c,a}^{IV}-C^{IV}(CH_3)_3$), 33.5 (s, $C_{c,a}^{IV}-C^{IV}(CH_3)_3$), 31.3 (s, O-CH₂-CH₃), 30.9 (s, $C_{c,a}^{IV}-C^{IV}(CH_3)_3$), 29.3 (s, $C_{c,a}^{IV}-C^{IV}(CH_3)_3$), 26.2 (s, $C^{IV}(CH_3)_2$), 22.3 (s, N-CH₂- $C^{IV}(CH_3)_2$). Anal. Calcd for C₆₃H₈₂N₂O₄P₂Y: C, 69.92; H, 7.64; N, 2.59. Found: C, 69.96; H, 7.66; N, 2.65.

Synthesis of 55

KHMDS (240 mg, 1.2 mmol) was added into a slurry of **49** (314 mg, 0.3 mmol) in THF (20 mL). After 4h, a cloudy solution was yielded. The completion of the deprotonation was verified

by $^{31}\text{P}\{^1\text{H}\}$ NMR spectrum which showed only one singlet at +13.2 ppm. Insoluble potassium salt was removed by centrifugation. $[\text{YCl}_3(\text{THF})_{3.5}]$ (134.3 mg, 0.3 mmol) was added. After 4h of stirring at room temperature, $^{31}\text{P}\{^1\text{H}\}$ NMR spectrum showed the clean formation of a complex with one singlet at 27.3 ppm. Potassium *tert*-butoxide (33.7 mg, 0.3 mmol) was added into the mixture, giving a cloudy solution. Stirring was continued for 7 h and the solid was removed by centrifugation. The solvents was evaporated in vacuum and the residue was recrystallised in cyclohexane (5 mL), giving the product as colorless crystals (290 mg, 87%).

55: $^{31}\text{P}\{^1\text{H}\}$ NMR (THF- d_8): δ 24.9 (s); ^1H NMR (THF- d_8): δ 7.71 (ddd, $^4J_{\text{H,H}}=1.5$ Hz, $^3J_{\text{H,H}}=8.0$ Hz, $^3J_{\text{P,H}}=12.0$ Hz, 4H, *o*-CH(PPh₂)), 7.58 (ddd, $^4J_{\text{H,H}}=1.5$ Hz, $^3J_{\text{H,H}}=8.0$ Hz, $^3J_{\text{P,H}}=12.0$ Hz, 4H, *o*-CH(PPh₂)), 7.58 (vtvt, $^4J_{\text{H,H}}=^5J_{\text{P,H}}=1.5$ Hz, $^3J_{\text{H,H}}=^3J'_{\text{H,H}}=8.0$ Hz, 2H, *p*-CH(PPh₂)), 7.51 (vtd, $^4J_{\text{P,H}}=3.0$ Hz, $^3J_{\text{H,H}}=^3J'_{\text{H,H}}=8.0$ Hz, 4H, *m*-CH(PPh₂)), 7.45 (vtvt, $^4J_{\text{H,H}}=^5J_{\text{P,H}}=1.5$ Hz, $^3J_{\text{H,H}}=^3J'_{\text{H,H}}=8.0$ Hz, 2H, *p*-CH(PPh₂)), 7.31 (d, $^4J_{\text{H,H}}=3.0$ Hz, 2H, C_bH), 7.30 (vtd, $^4J_{\text{P,H}}=3.0$ Hz, $^3J_{\text{H,H}}=^3J'_{\text{H,H}}=8.0$ Hz, 4H, *m*-CH(PPh₂)), 6.37 (dd, $^4J_{\text{H,H}}=3.0$ Hz, $^3J_{\text{P,H}}=15.5$ Hz, 2H, C_dH), 6.27 (ddd, $^3J_{\text{H,H}}=6.0$ Hz, $^4J_{\text{H,H}}=3.5$ Hz, $^4J_{\text{P,H}}=3.0$ Hz, 2H, C_eH), 6.01 (dd, $^3J_{\text{H,H}}=6.0$ Hz, $^4J_{\text{H,H}}=3.5$ Hz, 2H, C_fH), 1.27 (s, 18H, C_{c,a}^{IV}-C^{IV}(CH₃)₃), 1.04 (s, 18H, C_{c,a}^{IV}-C^{IV}(CH₃)₃), 0.56 (b, 9H, O-C^{IV}(CH₃)₃); $^{13}\text{C}\{^1\text{H}\}$ NMR (THF- d_8): 169.7 (s, C^{IV}-O), 144.8 (dd, $^2J_{\text{P,C}}=19.0$ Hz, $^3J_{\text{P,C}}=4.0$ Hz, C^{IV}-N), 139.0 (d, $^3J_{\text{P,C}}=7.5$ Hz, C_{c,a}^{IV}), 134.4 (d, $^3J_{\text{P,C}}=16.0$ Hz, C_{c,a}^{IV}), 134.0 (d, $^{2,3}J_{\text{P,C}}=10.0$ Hz, *m*-or *o*-CH(PPh₂)), 132.3 (s, *p*-CH(PPh₂)), 132.0 (s, *p*-CH(PPh₂)), 132.0 (d, $^1J_{\text{P,C}}=88.5$ Hz, C^{IV}(PPh₂)), 131.1 (d, $^1J_{\text{P,C}}=87.0$ Hz, C^{IV}(PPh₂)), 129.3 (d, $^{2,3}J_{\text{P,C}}=11.5$ Hz, *m*-or *o*-CH(PPh₂)), 128.8 (s, C_bH), 128.7 (d, $^{2,3}J_{\text{P,C}}=11.5$ Hz, *m*-or *o*-CH(PPh₂)), 128.4 (d, $^2J_{\text{P,C}}=14.0$ Hz, C_dH), 122.2 (d, $^3J_{\text{P,C}}=10.0$ Hz, C_eH), 118.3 (s, C_fH), 114.8 (d, $^1J_{\text{P,C}}=124.0$ Hz, C^{IV}-PPh₂), 35.7 (s, C_{c,a}^{IV}-C^{IV}(CH₃)₃), 34.3 (s, C_{c,a}^{IV}-C^{IV}(CH₃)₃), 33.9 (b, O-C^{IV}(CH₃)₃), 31.8 (s, (b, O-C^{IV}(CH₃)₃), 31.7 (s, C_{c,a}^{IV}-C^{IV}(CH₃)₃), 30.3 (s, C_{c,a}^{IV}-C^{IV}(CH₃)₃). Anal. Calcd for C₆₆H₈₀N₂O₄P₂Y: C, 71.02; H, 7.22; N, 2.51. Found: C, 70.85; H, 7.43; N, 2.55.

Synthesis of 56a

KHMDS (300 mg, 1.5 mmol) was added into a slurry of **50** (350 mg, 0.3 mmol) in THF (20 mL). After 4h, a cloudy solution was yielded. The completion of the deprotonation was verified by $^{31}\text{P}\{^1\text{H}\}$ NMR spectrum which showed only one singlet at +24.2 ppm. Insoluble potassium salt was removed by centrifugation. $[\text{YCl}_3(\text{THF})_{3.5}]$ (134.3 mg, 0.3 mmol) was added. After 4h of stirring at room temperature, $^{31}\text{P}\{^1\text{H}\}$ NMR spectrum showed the clean formation of a complex with one singlet at 35.0 ppm. Potassium *tert*-butoxide (33.7 mg, 0.3 mmol) was added into the mixture, giving a cloudy solution. Stirring was continued for 7 h and the solid was removed by centrifugation. The solvents was evaporated in vacuum and the residue was recrystallised in cyclohexane (5 mL), giving the product as colorless crystals (260 mg, 83%).

56a: $^{31}\text{P}\{^1\text{H}\}$ NMR (THF- d_8): δ 33.6 (s); ^1H NMR (THF- d_8): δ 7.60 (ddd, $^4J_{\text{H,H}}=1.5$ Hz, $^3J_{\text{H,H}}=7.0$ Hz, $^3J_{\text{P,H}}=11.5$ Hz, 4H, *o*-CH(PPh₂)), 7.57 (ddd, $^4J_{\text{H,H}}=1.5$ Hz, $^3J_{\text{H,H}}=7.0$ Hz, $^3J_{\text{P,H}}=11.5$ Hz, 4H, *o*-CH(PPh₂)), 7.50 (tvq, $^4J_{\text{H,H}}=1.5$ Hz, $^3J_{\text{H,H}}=7.0$ Hz, $^5J_{\text{P,H}}=1.5$ Hz, 2H, *p*-CH(PPh₂)), 7.42 (vtd, $^4J_{\text{P,H}}=2.5$ Hz, $^3J_{\text{H,H}}=^3J'_{\text{H,H}}=7.0$ Hz, 4H, *m*-CH(PPh₂)), 7.40 (tvq, $^4J_{\text{H,H}}=1.5$ Hz, $^3J_{\text{H,H}}=7.0$ Hz, $^5J_{\text{P,H}}=1.5$ Hz, 2H, *p*-CH(PPh₂)), 7.24 (vtd, $^4J_{\text{P,H}}=2.5$ Hz, $^3J_{\text{H,H}}=^3J'_{\text{H,H}}=7.0$ Hz, 4H, *m*-

$CH(PPh_2)$), 7.21 (d, $^4J_{H,H}=2.0$ Hz, 2H, C_bH), 6.59 (dd, $^4J_{H,H}=2.0$ Hz, $^3J_{P,H}=15.5$ Hz, 2H, C_dH), 3.24 (m, 4H, $P=N-CH_2$), 2.93 (m, 2H, $P=N-CH_2-CH_2$), 2.58 (m, 2H, $P=N-CH_2-CH_2$), 1.15 (s, 18H, $C_{c,a}^{IV}-C^{IV}(CH_3)_3$), 1.10 0.80 (s, 9H, $O-C^{IV}(CH_3)_3$), 1.09 (s, 18H, $C_{c,a}^{IV}-C^{IV}(CH_3)_3$); $^{13}C\{^1H\}$ NMR (THF- d_8): 169.1 (d, $^3J_{P,C}=3.0$ Hz, $C^{IV}-O$), 169.0 (d, $^3J_{P,C}=3.0$ Hz, $C^{IV}-O$), 139.9 (d, $^3J_{P,C}=8.0$ Hz, $C_{c,a}^{IV}$), 133.8 (d, $^{2/3}J_{P,C}=9.5$ Hz, m -or o - $CH(PPh_2)$), 133.7 (d, $^{2/3}J_{P,C}=9.5$ Hz, m -or o - $CH(PPh_2)$), 133.6 (d, $^3J_{P,C}=8.0$ Hz, $C_{c,a}^{IV}$), 133.3 (d, $^1J_{P,C}=87.5$ Hz, $C^{IV}(PPh_2)$), 132.1 (d, $^1J_{P,C}=90.0$ Hz, $C^{IV}(PPh_2)$), 131.8 (d, $^4J_{P,C}=2.5$ Hz, p - $CH(PPh_2)$), 131.6 ($^4J_{P,C}=2.5$ Hz, p - $CH(PPh_2)$), 128.9 (d, $^{2/3}J_{P,C}=11.0$ Hz, m -or o - $CH(PPh_2)$), 128.8 (d, $^{2/3}J_{P,C}=11.0$ Hz, m -or o - $CH(PPh_2)$), 128.2 (d, $^4J_{P,C}=2.5$ Hz, C_bH), 127.5 (d, $^2J_{P,C}=12.5$ Hz, C_dH), 111.8 (d, $^1J_{P,C}=118.0$ Hz, $C^{IV}-PPh_2$), 69.7 (s, $O-C^{IV}(CH_3)_3$), 54.0 (d, $^2J_{P,C}=16.0$ Hz, $P^{IV}-N-CH_2$), 48.6 (d, $^3J_{P,C}=5.0$ Hz, $P^{IV}-N-CH_2-CH_2$), 35.8 (s, $C_{c,a}^{IV}-C^{IV}(CH_3)_3$), 35.2 (s, $O-C^{IV}(CH_3)_3$), 34.3 (s, $C_{c,a}^{IV}-C^{IV}(CH_3)_3$), 31.8 (s, $C_{c,a}^{IV}-C^{IV}(CH_3)_3$), 30.2 (s, $C_{c,a}^{IV}-C^{IV}(CH_3)_3$). Anal. Calcd for $C_{60}H_{78}N_3O_3P_2Y$: C, 69.28; H, 7.56; N, 4.04. Found: C, 69.16; H, 7.64; N, 3.95.

Synthesis of 56b

KHMDS (300 mg, 1.5 mmol) was added into a slurry of **50** (350 mg, 0.3 mmol) in THF (20 mL). After 4h, a cloudy solution was yielded. The completion of the deprotonation was verified by $^{31}P\{^1H\}$ NMR spectrum which showed only one singlet at +24.2 ppm. Insoluble potassium salt was removed by centrifugation. $[YCl_3(THF)_{3.5}]$ (134.3 mg, 0.3 mmol) was added. After 4h of stirring at room temperature, $^{31}P\{^1H\}$ NMR spectrum showed the clean formation of a complex with one singlet at 35.0 ppm. Potassium ethoxide (25.2 mg, 0.3 mmol) was added into the mixture, giving a cloudy solution. Stirring was continued for 7 h and the solid was removed by centrifugation. The solvents was evaporated in vacuum and the residue was recrystallised in cyclohexane (5 mL), giving the product as colorless crystals (265 mg, 87%).

56b: $^{31}P\{^1H\}$ NMR (THF- d_8): δ 34.2 (s); 1H NMR (THF- d_8): δ 7.61 (ddd, $^4J_{H,H}=1.5$ Hz, $^3J_{H,H}=8.0$ Hz, $^3J_{P,H}=9.0$ Hz, 4H, o - $CH(PPh_2)$), 7.55 (ddd, $^4J_{H,H}=1.5$ Hz, $^3J_{H,H}=8.0$ Hz, $^3J_{P,H}=9.0$ Hz, 4H, o - $CH(PPh_2)$), 7.49 (tt, $^4J_{H,H}=1.5$ Hz, $^3J_{H,H}=8.0$ Hz, 2H, p - $CH(PPh_2)$), 7.39 (vtd, $^4J_{P,H}=2.5$ Hz, $^3J_{H,H}=^3J'_{H,H}=8.0$ Hz, 4H, m - $CH(PPh_2)$), 7.37 (tt, $^4J_{H,H}=1.5$ Hz, $^3J_{H,H}=8.0$ Hz, 2H, p - $CH(PPh_2)$), 7.22 (vtd, $^4J_{P,H}=2.5$ Hz, $^3J_{H,H}=^3J'_{H,H}=8.0$ Hz, 4H, m - $CH(PPh_2)$), 7.21 (d, $^4J_{H,H}=2.0$ Hz, 2H, C_bH), 6.65 (dd, $^4J_{H,H}=2.0$ Hz, $^3J_{P,H}=15.5$ Hz, 2H, C_dH), 3.96 (m, 1H, $O-CH_2-CH_3$), 3.32 (m, 1H, $O-CH_2-CH_3$), 3.27 (m, 4H, $P=N-CH_2$), 2.83 (m, 2H, $P=N-CH_2-CH_2$), 2.58 (m, 2H, $P=N-CH_2-CH_2$), 1.12 (s, 36H, $C_{c,a}^{IV}-C^{IV}(CH_3)_3$), 0.90 (m, 3H, $O-CH_2-CH_3$); $^{13}C\{^1H\}$ NMR (THF- d_8): 168.9 (d, $^3J_{P,C}=3.0$ Hz, $C^{IV}-O$), 168.8 (d, $^3J_{P,C}=3.0$ Hz, $C^{IV}-O$), 139.9 (d, $^3J_{P,C}=7.5$ Hz, $C_{c,a}^{IV}$), 133.7 (d, $^{2/3}J_{P,C}=8.0$ Hz, m -or o - $CH(PPh_2)$), 133.6 (d, $^{2/3}J_{P,C}=8.0$ Hz, m -or o - $CH(PPh_2)$), 133.5 (d, $^3J_{P,C}=8.0$ Hz, $C_{c,a}^{IV}$), 133.3 (d, $^1J_{P,C}=83.0$ Hz, $C^{IV}(PPh_2)$), 131.8 ($^4J_{P,C}=2.5$ Hz, p - $CH(PPh_2)$), 131.6 (d, $^1J_{P,C}=88.0$ Hz, $C^{IV}(PPh_2)$), 131.6 (d, $^4J_{P,C}=2.5$ Hz, p - $CH(PPh_2)$), 128.9 (d, $^{2/3}J_{P,C}=11.0$ Hz, m -or o - $CH(PPh_2)$), 128.8 (d, $^{2/3}J_{P,C}=11.0$ Hz, m -or o - $CH(PPh_2)$), 128.3 (d, $^4J_{P,C}=2.0$ Hz, C_bH), 127.2 (d, $^2J_{P,C}=12.5$ Hz, C_dH), 113.0 (d, $^1J_{P,C}=119.0$ Hz, $C^{IV}-PPh_2$), 62.5 (s, $O-CH_2-CH_3$), 53.7 (d, $^2J_{P,C}=16.0$ Hz, $P^{IV}-N-CH_2$), 48.8 (d, $^3J_{P,C}=5.0$ Hz, $P^{IV}-N-CH_2-CH_2$), 35.7 (s, $C_{c,a}^{IV}-C^{IV}(CH_3)_3$), 34.3 (s, $C_{c,a}^{IV}-C^{IV}(CH_3)_3$), 31.9 (s, $C_{c,a}^{IV}-C^{IV}(CH_3)_3$), 29.9

(s, $C_{c,a}^{IV}-C^{IV}(CH_3)_3$), 23.3 (s, O-CH₂-CH₃). Anal. Calcd for C₅₈H₇₄N₃O₃P₂Y: C, 68.83; H, 7.37; N, 4.74. Found: C, 68.14; H, 7.54; N, 4.27.

Synthesis of 57

At -78°C, bromine (300 μL, 5.825 mmol) was added dropwise to a solution of the phenolphosphine **39** (2.018 g, 5.825 mmol) in CH₂Cl₂ (100 mL). The cold bath was removed and stirring was continued for 2 hours at room temperature. Then the solution was cooled down to -78°C. Tributylamine (1.39 mL, 5.825 mmol) was added, followed by ethylenediamine (195 μL, 2.913 mmol). The cold bath was removed. After 16h, a cloudy solution was formed. CH₂Cl₂ was evaporated and the residue was washed with THF (5x10 mL) to remove tributylammonium salt. The product was isolated as a white solid and dried under vacuum (1.9 g, 69%).

57: ³¹P{¹H} NMR (CDCl₃): δ 40.1 (s, P^V); ¹H NMR (CDCl₃): δ 7.66 (t, ³J_{H,H}=8.0 Hz, 4H, *p*-CH(PPh₂)), 7.63 (dd, ³J_{P,H}=12.5 Hz, ³J_{H,H}=8.0 Hz, 8H, *o*-CH(PPh₂)), 7.53 (vtd, ⁴J_{P,H}=3.5 Hz, ³J_{H,H}=³J'_{H,H}=8.0 Hz, 8H, *m*-CH(PPh₂)), 7.17 (d, ⁴J_{H,H}=2.5 Hz, 2H, C_bH), 5.95 (dd, ³J_{P,H}=16.5 Hz, ⁴J_{H,H}=2.5 Hz, 2H, C_dH), 3.66 (dd, ³J_{P,H}=6.5 Hz, ⁴J_{P,H}=2.0 Hz, 4H, N-CH₂-CH₂-N), 3.50 (s, 6H, -OCH₃), 1.50 (s, 18H, C^{IV}(CH₃)₃); ¹³C{¹H} NMR (CDCl₃): δ 154.4 (C^{IV}-O or C_{c,a}^{IV}), 151.8 (weak, C^{IV}-O or C_{c,a}^{IV}), 145.7 (C^{IV}-O or C_{c,a}^{IV}), 134.3 (s, *p*-CH(PPh₂)), 133.6 (d, ²J_{P,C}=9.0 Hz, *o*-CH(PPh₂)), 129.7 (d, ³J_{P,C}=13.5 Hz, *m*-CH(PPh₂)), 122.1 (d, ¹J_{P,C}=105 Hz, C^{IV}(PPh₂)), 121.2 (s, C_bH), 116.0 (d, ¹J_{P,C}=120 Hz, C^{IV}-PPh₂), 115.0 (d, ²J_{P,C}=13.5 Hz, C_dH), 55.6 (s, O-CH₃), 44.2 (dd, ²J_{P,C}=7.5 Hz, ³J_{P,C}=1.0 Hz, N-CH₂-CH₂-N), 35.4 (s, C_a^{IV}-C^{IV}(CH₃)₃), 30.3 (s, b, C_a^{IV}-C^{IV}(CH₃)₃). Anal. Calcd for C₄₈H₅₆Br₂N₂O₄P₂: C, 60.90; H, 5.96; N, 2.96. Found: C, 60.71; H, 6.02; N, 3.02.

Synthesis of 58

KHMDS (240 mg, 1.2 mmol) was added into a slurry of **57** (295 mg, 0.3 mmol) in THF (20 mL). After 4h, a cloudy solution was yielded. The completion of the deprotonation was verified by ³¹P{¹H} NMR spectrum which showed only one singlet at +20.3 ppm. Insoluble potassium salt was removed by centrifugation. [YCl₃(THF)_{3,5}] (134.3 mg, 0.3 mmol) was added. After 4h of stirring at room temperature, ³¹P{¹H} NMR spectrum showed the clean formation of a complex with one singlet at 31.5 ppm. Potassium *tert*-butoxide (33.7 mg, 0.3 mmol) was added into the mixture, giving a cloudy solution. Stirring was continued for 7 h and the solid was removed by centrifugation. The solvents was evaporated in vacuum and the residue was recrystallised in cyclohexane (5 mL), giving the product as colorless crystals (250 mg, 88%).

58: ³¹P{¹H} NMR (THF-*d*₈): δ 31.6 (s); ¹H NMR (THF-*d*₈): δ 7.63 (dd, ³J_{P,H}=11.5 Hz, ³J_{H,H}=7.0 Hz, 4H, *o*-CH(PPh₂)), 7.54 (m, 2H, *p*-CH(PPh₂)), 7.48 (m, 5H, *p*-CH(PPh₂) + *m*-CH(PPh₂)), 7.40 (dd, ³J_{P,H}=11.5 Hz, ³J_{H,H}=7.0 Hz, 4H, *o*-CH(PPh₂)), 7.39 (vt, ³J_{H,H}=³J'_{H,H}=7.0 Hz, 1H, *m*-CH(PPh₂)), 6.92 (d, ⁴J_{H,H}=3.0 Hz, 2H, C_bH), 5.94 (dd, ³J_{P,H}=15.5 Hz, ⁴J_{H,H}=3.0 Hz, 2H, C_dH), 3.35 (s, 6H, -OCH₃), 3.31 (m,b, 2H, N-CH₂-CH₂-N), 3.18 (m,b, 2H, N-CH₂-CH₂-N), 1.39 (s, 18H, C_a^{IV}-C^{IV}(CH₃)₃), 0.84 (s, b, 9H, O-C^{IV}(CH₃)₃); ¹³C{¹H} NMR (THF-*d*₈): 166.8 (s, C^{IV}-O), 148.2 (d, ³J_{P,C}=20.0 Hz, C_c^{IV}), 141.1 (d, ³J_{P,C}=9.5 Hz, C_a^{IV}), 134.1 (d, ²J_{P,C}=9.0 Hz, *o*-

CH(PPh₂)), 133.6 (d, ²J_{P,C} = 9.0 Hz, *o*-CH(PPh₂)), 132.3 (d, ¹J_{P,C} = 88.0 Hz, C^{IV}(PPh₂)), 132.0 (d, ⁴J_{P,C} = 1.5 Hz, *p*-CH(PPh₂)), 131.7 (d, ¹J_{P,C} = 90.0 Hz, C^{IV}(PPh₂)), 131.7 (d, ⁴J_{P,C} = 1.5 Hz, *p*-CH(PPh₂)), 129.0 (d, ³J_{P,C} = 10.5 Hz, *m*-CH(PPh₂)), 128.9 (d, ³J_{P,C} = 10.5 Hz, *m*-CH(PPh₂)), 120.3 (d, ⁴J_{P,C} = 1.0 Hz, C_bH), 114.2 (d, ²J_{P,C} = 14.5 Hz, C_dH), 111.6 (d, ¹J_{P,C} = 123.0 Hz, C^{IV}-PPh₂), 55.5 (s, O-CH₃), 52.1 (dd, ^{2/3}J_{P,C} = 6.5 Hz, ^{3/3}J_{P,C} = 18.0 Hz, N-CH₂-CH₂-N), 35.7 (s, C_a^{IV}-C^{IV}(CH₃)₃), 33.3 (s, O-C^{IV}(CH₃)₃), 30.2 (s, C_a^{IV}-C^{IV}(CH₃)₃), 26.0 (s, O-C^{IV}(CH₃)₃). Anal. Calcd for C₅₂H₆₁N₂O₅P₂Y: C, 66.10; H, 6.51; N, 2.96. Found: C, 65.89; H, 6.42; N, 2.85.

REFERENCES

1. (a) Zimmer, H.; Singh, G., *J. Org. Chem.* **1963**, *28* (2), 483-486; (b) Borowitz, I. J.; Kirby, K. C.; Rusek, P. E.; Casper, E. W. R., *J. Org. Chem.* **1971**, *36* (1), 88-97.
2. King, R. B., *Organometallic syntheses academic*. 1965; Vol. 1, p 71.
3. Giordano, G.; Crabtree, R. H., *Inorg. Synth.* **1990**, *28*, 88-90.
4. Bennett, M. A.; Huang, T. N.; Matheson, T. W.; Smith, A. K.; Ittel, S.; Nickerson, W., *Inorg. Synth.* **1982**, *21*, 74-78.
5. Bianchi, A.; Bernardi, A., *J. Org. Chem.* **2006**, *71* (12), 4565-4577.
6. Anderson, G. K.; Lin, M.; Sen, A.; Gretz, E., *Inorg. Synth.* **1990**, *28*, 60-63.
7. Sobota, P.; Utoko, J.; Szafert, S., *Inorg. Chem.* **1994**, *33* (23), 5203-5206.
8. Dorgan, J. R.; Janzen, J.; Knauss, D. M.; Hait, S. B.; Limoges, B. R.; Hutchinson, M. H., *J. Polym. Sci., Part B: Polym. Phys.* **2005**, *43* (21), 3100-3111.
9. Coudane, J.; UstarizPeyret, C.; Schwach, G.; Vert, M., *J. Polym. Sci., Part A: Polym. Chem.* **1997**, *35* (9), 1651-1658.

Crystallographic Data

Chapter 1

Compound 2a

Table 1. Crystal data for pa058

Compound	pa058
Molecular formula	C ₂₂ H ₂₅ NPS, BF ₄
Molecular weight	453.27
Crystal habit	Colorless Block
Crystal dimensions(mm)	0.30x0.12x0.08
Crystal system	orthorhombic
Space group	Pbca
a(Å)	15.666(1)
b(Å)	16.486(1)
c(Å)	17.614(1)
α(°)	90.00
β(°)	90.00
γ(°)	90.00
V(Å ³)	4549.2(5)
Z	8
d(g·cm ⁻³)	1.324
F(000)	1888
μ(cm ⁻¹)	0.254
Absorption corrections	multi-scan ; 0.9278 min, 0.9800 max
Diffractionmeter	KappaCCD
X-ray source	MoKα
λ(Å)	0.71069
Monochromator	graphite
T (K)	150.0(1)
Scan mode	phi and omega scans
Maximum θ	27.45
HKL ranges	-20 16 ; -17 20 ; -15 22
Reflections measured	21003
Unique data	5177
Rint	0.0258
Reflections used	3908
Criterion	I > 2σ(I)
Refinement type	Fsqd
Hydrogen atoms	mixed
Parameters refined	280
Reflections / parameter	13
wR2	0.1107
R1	0.0382
Weights a, b	0.0541 ; 1.0556
GoF	1.066
difference peak / hole (e Å ⁻³)	0.348(0.045) / -0.514(0.045)

Appendix 1. Crystallographic data

Table 2. Atomic Coordinates (A x 10⁴) and equivalent isotropic displacement parameters (A² x 10³) for pa058

atom	x	y	z	U(eq)
S(1)	4444(1)	1284(1)	4211(1)	45(1)
P(1)	5259(1)	2165(1)	5734(1)	26(1)
F(1)	4080(1)	3504(1)	7281(1)	43(1)
F(2)	4001(1)	4263(1)	6219(1)	44(1)
F(3)	2926(1)	4301(1)	7080(1)	55(1)
F(4)	4203(1)	4873(1)	7360(1)	56(1)
N(1)	5511(1)	2754(1)	6438(1)	29(1)
C(1)	5059(1)	2702(1)	4858(1)	30(1)
C(2)	4697(1)	2337(1)	4213(1)	34(1)
C(3)	4524(1)	2814(1)	3576(1)	42(1)
C(4)	4726(1)	3632(1)	3574(1)	47(1)
C(5)	5073(1)	3997(1)	4207(1)	43(1)
C(6)	5228(1)	3536(1)	4848(1)	35(1)
C(7)	4259(1)	1706(1)	5991(1)	28(1)
C(8)	4210(1)	924(1)	6289(1)	38(1)
C(9)	3423(1)	607(1)	6484(1)	45(1)
C(10)	2687(1)	1053(1)	6380(1)	42(1)
C(11)	2734(1)	1821(1)	6078(1)	41(1)
C(12)	3519(1)	2155(1)	5883(1)	34(1)
C(13)	6095(1)	1439(1)	5595(1)	32(1)
C(14)	6525(1)	1387(1)	4902(1)	38(1)
C(15)	7229(1)	878(1)	4839(1)	51(1)
C(16)	7490(2)	423(1)	5451(2)	58(1)
C(17)	7059(1)	458(1)	6135(1)	52(1)
C(18)	6362(1)	969(1)	6214(1)	38(1)
C(19)	6329(1)	3141(1)	6700(1)	35(1)
C(20)	7037(1)	3083(1)	6112(1)	46(1)
C(21)	6600(2)	2725(1)	7434(1)	55(1)
C(22)	6135(1)	4035(1)	6858(1)	42(1)
B(1)	3797(1)	4248(1)	6983(1)	33(1)

U(eq) is defined as 1/3 the trace of the U_{ij} tensor.

Appendix 1. Crystallographic data

Table 3. Bond lengths (A) and angles (deg) for pa058

S(1)-C(2)	1.781(2)	S(1)-H(1S)	1.34(2)
P(1)-N(1)	1.623(1)	P(1)-C(13)	1.791(2)
P(1)-C(7)	1.797(2)	P(1)-C(1)	1.807(2)
F(1)-B(1)	1.406(2)	F(2)-B(1)	1.384(2)
F(3)-B(1)	1.378(2)	F(4)-B(1)	1.382(2)
N(1)-C(19)	1.505(2)	N(1)-H(1N)	0.900(1)
C(1)-C(6)	1.400(2)	C(1)-C(2)	1.405(2)
C(2)-C(3)	1.396(2)	C(3)-C(4)	1.385(3)
C(3)-H(3)	0.9500	C(4)-C(5)	1.378(3)
C(4)-H(4)	0.9500	C(5)-C(6)	1.383(2)
C(5)-H(5)	0.9500	C(6)-H(6)	0.9500
C(7)-C(12)	1.389(2)	C(7)-C(8)	1.395(2)
C(8)-C(9)	1.383(3)	C(8)-H(8)	0.9500
C(9)-C(10)	1.380(3)	C(9)-H(9)	0.9500
C(10)-C(11)	1.374(3)	C(10)-H(10)	0.9500
C(11)-C(12)	1.391(3)	C(11)-H(11)	0.9500
C(12)-H(12)	0.9500	C(13)-C(14)	1.396(2)
C(13)-C(18)	1.401(2)	C(14)-C(15)	1.390(3)
C(14)-H(14)	0.9500	C(15)-C(16)	1.376(3)
C(15)-H(15)	0.9500	C(16)-C(17)	1.383(3)
C(16)-H(16)	0.9500	C(17)-C(18)	1.387(3)
C(17)-H(17)	0.9500	C(18)-H(18)	0.9500
C(19)-C(20)	1.520(3)	C(19)-C(21)	1.524(3)
C(19)-C(22)	1.531(2)	C(20)-H(20A)	0.9800
C(20)-H(20B)	0.9800	C(20)-H(20C)	0.9800
C(21)-H(21A)	0.9800	C(21)-H(21B)	0.9800
C(21)-H(21C)	0.9800	C(22)-H(22A)	0.9800
C(22)-H(22B)	0.9800	C(22)-H(22C)	0.9800
C(2)-S(1)-H(1S)	97(1)	N(1)-P(1)-C(13)	109.06(8)
N(1)-P(1)-C(7)	105.72(7)	C(13)-P(1)-C(7)	113.01(7)
N(1)-P(1)-C(1)	113.66(7)	C(13)-P(1)-C(1)	109.75(8)
C(7)-P(1)-C(1)	105.64(8)	C(19)-N(1)-P(1)	134.1(1)
C(19)-N(1)-H(1N)	113(1)	P(1)-N(1)-H(1N)	113(1)
C(6)-C(1)-C(2)	119.2(2)	C(6)-C(1)-P(1)	117.3(1)
C(2)-C(1)-P(1)	123.4(1)	C(3)-C(2)-C(1)	119.1(2)
C(3)-C(2)-S(1)	120.3(1)	C(1)-C(2)-S(1)	120.6(1)
C(4)-C(3)-C(2)	120.4(2)	C(4)-C(3)-H(3)	119.8
C(2)-C(3)-H(3)	119.8	C(5)-C(4)-C(3)	120.8(2)
C(5)-C(4)-H(4)	119.6	C(3)-C(4)-H(4)	119.6
C(4)-C(5)-C(6)	119.4(2)	C(4)-C(5)-H(5)	120.3
C(6)-C(5)-H(5)	120.3	C(5)-C(6)-C(1)	121.0(2)
C(5)-C(6)-H(6)	119.5	C(1)-C(6)-H(6)	119.5
C(12)-C(7)-C(8)	119.9(2)	C(12)-C(7)-P(1)	118.0(1)
C(8)-C(7)-P(1)	122.1(1)	C(9)-C(8)-C(7)	119.5(2)
C(9)-C(8)-H(8)	120.3	C(7)-C(8)-H(8)	120.3
C(10)-C(9)-C(8)	120.7(2)	C(10)-C(9)-H(9)	119.7
C(8)-C(9)-H(9)	119.7	C(11)-C(10)-C(9)	119.9(2)
C(11)-C(10)-H(10)	120.1	C(9)-C(10)-H(10)	120.1
C(10)-C(11)-C(12)	120.5(2)	C(10)-C(11)-H(11)	119.7
C(12)-C(11)-H(11)	119.7	C(7)-C(12)-C(11)	119.6(2)
C(7)-C(12)-H(12)	120.2	C(11)-C(12)-H(12)	120.2
C(14)-C(13)-C(18)	120.2(2)	C(14)-C(13)-P(1)	120.9(1)
C(18)-C(13)-P(1)	118.7(1)	C(15)-C(14)-C(13)	119.3(2)
C(15)-C(14)-H(14)	120.3	C(13)-C(14)-H(14)	120.3
C(16)-C(15)-C(14)	120.2(2)	C(16)-C(15)-H(15)	119.9
C(14)-C(15)-H(15)	119.9	C(15)-C(16)-C(17)	121.0(2)
C(15)-C(16)-H(16)	119.5	C(17)-C(16)-H(16)	119.5
C(16)-C(17)-C(18)	119.8(2)	C(16)-C(17)-H(17)	120.1
C(18)-C(17)-H(17)	120.1	C(17)-C(18)-C(13)	119.5(2)
C(17)-C(18)-H(18)	120.2	C(13)-C(18)-H(18)	120.2
N(1)-C(19)-C(20)	112.7(2)	N(1)-C(19)-C(21)	107.9(1)
C(20)-C(19)-C(21)	110.2(2)	N(1)-C(19)-C(22)	107.2(1)
C(20)-C(19)-C(22)	109.2(2)	C(21)-C(19)-C(22)	109.5(2)
C(19)-C(20)-H(20A)	109.5	C(19)-C(20)-H(20B)	109.5

Appendix 1. Crystallographic data

H(20A)-C(20)-H(20B)	109.5	C(19)-C(20)-H(20C)	109.5
H(20A)-C(20)-H(20C)	109.5	H(20B)-C(20)-H(20C)	109.5
C(19)-C(21)-H(21A)	109.5	C(19)-C(21)-H(21B)	109.5
H(21A)-C(21)-H(21B)	109.5	C(19)-C(21)-H(21C)	109.5
H(21A)-C(21)-H(21C)	109.5	H(21B)-C(21)-H(21C)	109.5
C(19)-C(22)-H(22A)	109.5	C(19)-C(22)-H(22B)	109.5
H(22A)-C(22)-H(22B)	109.5	C(19)-C(22)-H(22C)	109.5
H(22A)-C(22)-H(22C)	109.5	H(22B)-C(22)-H(22C)	109.5
F(3)-B(1)-F(4)	110.4(2)	F(3)-B(1)-F(2)	110.4(2)
F(4)-B(1)-F(2)	110.4(2)	F(3)-B(1)-F(1)	108.7(2)
F(4)-B(1)-F(1)	109.0(2)	F(2)-B(1)-F(1)	107.8(2)

Appendix 1. Crystallographic data

Table 4. Anisotropic displacement parameters ($\text{\AA}^2 \times 10^3$) for pa058

atom	U11	U22	U33	U23	U13	U12
S(1)	63(1)	32(1)	39(1)	-2(1)	-11(1)	-5(1)
P(1)	28(1)	23(1)	27(1)	2(1)	2(1)	-2(1)
F(1)	47(1)	40(1)	42(1)	9(1)	2(1)	12(1)
F(2)	48(1)	51(1)	33(1)	7(1)	2(1)	-9(1)
F(3)	33(1)	57(1)	76(1)	21(1)	11(1)	10(1)
F(4)	66(1)	46(1)	58(1)	-18(1)	8(1)	-8(1)
N(1)	24(1)	32(1)	31(1)	-3(1)	1(1)	-3(1)
C(1)	33(1)	27(1)	29(1)	3(1)	3(1)	0(1)
C(2)	41(1)	30(1)	31(1)	0(1)	2(1)	0(1)
C(3)	57(1)	39(1)	31(1)	1(1)	-2(1)	4(1)
C(4)	65(1)	41(1)	35(1)	12(1)	3(1)	4(1)
C(5)	55(1)	29(1)	46(1)	9(1)	5(1)	-2(1)
C(6)	40(1)	28(1)	36(1)	2(1)	4(1)	-3(1)
C(7)	31(1)	27(1)	27(1)	-1(1)	1(1)	-4(1)
C(8)	34(1)	32(1)	47(1)	9(1)	-2(1)	-3(1)
C(9)	43(1)	38(1)	55(1)	15(1)	0(1)	-13(1)
C(10)	32(1)	45(1)	49(1)	3(1)	5(1)	-10(1)
C(11)	31(1)	42(1)	49(1)	1(1)	4(1)	2(1)
C(12)	35(1)	28(1)	40(1)	3(1)	4(1)	0(1)
C(13)	30(1)	26(1)	39(1)	-1(1)	3(1)	0(1)
C(14)	38(1)	33(1)	44(1)	-2(1)	7(1)	-3(1)
C(15)	45(1)	46(1)	61(1)	-10(1)	20(1)	1(1)
C(16)	46(1)	45(1)	84(2)	-3(1)	8(1)	15(1)
C(17)	45(1)	40(1)	69(2)	10(1)	0(1)	10(1)
C(18)	34(1)	32(1)	47(1)	5(1)	2(1)	0(1)
C(19)	28(1)	37(1)	39(1)	0(1)	-5(1)	-7(1)
C(20)	29(1)	45(1)	64(1)	-6(1)	7(1)	-6(1)
C(21)	52(1)	59(1)	55(1)	12(1)	-22(1)	-18(1)
C(22)	34(1)	42(1)	51(1)	-12(1)	-3(1)	-8(1)
B(1)	32(1)	31(1)	36(1)	4(1)	4(1)	2(1)

The anisotropic displacement factor exponent takes the form
 $2 \pi^2 [h^2 a^{*2} U(11) + \dots + 2 h k a^* b^* U(12)]$

Table 5. Hydrogen Coordinates ($\text{\AA} \times 10^4$) and equivalent isotropic displacement parameters ($\text{\AA}^2 \times 10^3$) for pa058

atom	x	y	z	U(eq)
H(1S)	4330(20)	1220(10)	3460(10)	67
H(1N)	5052(8)	2920(10)	6700(10)	43
H(3)	4267	2576	3142	51
H(4)	4623	3944	3131	56
H(5)	5204	4559	4202	52
H(6)	5454	3790	5289	42
H(8)	4714	611	6358	46
H(9)	3389	76	6692	54
H(10)	2149	829	6516	50
H(11)	2226	2125	6003	49
H(12)	3547	2687	5677	41
H(14)	6338	1697	4478	46
H(15)	7530	845	4372	61
H(16)	7975	81	5403	70
H(17)	7239	131	6549	62
H(18)	6067	1001	6684	45
H(20A)	7200	2514	6045	69
H(20B)	7532	3395	6286	69
H(20C)	6833	3303	5628	69
H(21A)	6136	2760	7806	83
H(21B)	7109	2994	7637	83
H(21C)	6730	2154	7331	83
H(22A)	5965	4303	6384	64
H(22B)	6646	4300	7062	64
H(22C)	5669	4075	7228	64

Monodeprotonation from 2a

Table 1. Crystal data for pa069

Compound	pa069
Molecular formula	$\text{C}_{22}\text{H}_{24}\text{NPS}$
Molecular weight	365.45
Crystal habit	Pale Yellow Plate
Crystal dimensions(mm)	0.20x0.16x0.04
Crystal system	monoclinic
Space group	$P2_1/c$
a(\AA)	10.459(1)
b(\AA)	10.181(1)
c(\AA)	18.909(1)
α ($^\circ$)	90.00
β ($^\circ$)	109.043(3)
γ ($^\circ$)	90.00
V(\AA^3)	1903.3(3)
Z	4
d(g·cm $^{-3}$)	1.275
F(000)	776
μ (cm $^{-1}$)	0.258
Absorption corrections	multi-scan ; 0.9501 min, 0.9897 max
Diffractometer	KappaCCD
X-ray source	MoK α
λ (\AA)	0.71069
Monochromator	graphite
T (K)	150.0(1)
Scan mode	phi and omega scans
Maximum θ	30.02
HKL ranges	-13 14 ; -14 12 ; -26 26
Reflections measured	15481
Unique data	5554
Rint	0.0306
Reflections used	3919
Criterion	$I > 2\sigma(I)$
Refinement type	Fsqd
Hydrogen atoms	mixed
Parameters refined	229
Reflections / parameter	17
wR2	0.0964
R1	0.0379
Weights a, b	0.0402 ; 0.2099
GoF	1.028
difference peak / hole (e \AA^{-3})	0.340(0.055) / -0.350(0.055)

Appendix 1. Crystallographic data

Table 2. Atomic Coordinates (A x 10⁴) and equivalent isotropic displacement parameters (A² x 10³) for pa069

atom	x	y	z	U(eq)
S(1)	2019(1)	-4073(1)	-2994(1)	23(1)
P(1)	1923(1)	-5253(1)	-1341(1)	18(1)
N(1)	454(1)	-5271(1)	-1999(1)	19(1)
C(1)	3131(1)	-5776(1)	-1775(1)	19(1)
C(2)	3151(1)	-5240(2)	-2470(1)	19(1)
C(3)	4183(1)	-5720(2)	-2730(1)	23(1)
C(4)	5095(2)	-6661(2)	-2358(1)	27(1)
C(5)	5049(2)	-7182(2)	-1688(1)	29(1)
C(6)	4074(2)	-6733(2)	-1401(1)	25(1)
C(7)	1898(1)	-6432(2)	-636(1)	20(1)
C(8)	2729(2)	-6289(2)	111(1)	24(1)
C(9)	2718(2)	-7250(2)	629(1)	27(1)
C(10)	1906(2)	-8346(2)	418(1)	28(1)
C(11)	1098(2)	-8504(2)	-324(1)	27(1)
C(12)	1104(1)	-7555(2)	-847(1)	23(1)
C(13)	-912(1)	-4768(2)	-2027(1)	21(1)
C(14)	-1347(2)	-5351(2)	-1397(1)	26(1)
C(15)	-1865(2)	-5258(2)	-2781(1)	30(1)
C(16)	-933(2)	-3266(2)	-2005(1)	27(1)
C(17)	2499(1)	-3720(2)	-858(1)	20(1)
C(18)	1899(2)	-3203(2)	-357(1)	25(1)
C(19)	2319(2)	-2008(2)	-9(1)	29(1)
C(20)	3345(2)	-1319(2)	-159(1)	30(1)
C(21)	3956(2)	-1828(2)	-646(1)	29(1)
C(22)	3539(1)	-3023(2)	-995(1)	24(1)

U(eq) is defined as 1/3 the trace of the Uij tensor.

Appendix 1. Crystallographic data

Table 3. Bond lengths (A) and angles (deg) for pa069

S(1)-C(2)	1.741(2)	P(1)-N(1)	1.631(1)
P(1)-C(1)	1.797(1)	P(1)-C(7)	1.799(1)
P(1)-C(17)	1.809(2)	N(1)-C(13)	1.502(2)
C(1)-C(6)	1.402(2)	C(1)-C(2)	1.428(2)
C(2)-C(3)	1.412(2)	C(3)-C(4)	1.372(2)
C(4)-C(5)	1.389(2)	C(5)-C(6)	1.381(2)
C(7)-C(12)	1.393(2)	C(7)-C(8)	1.405(2)
C(8)-C(9)	1.387(2)	C(9)-C(10)	1.380(2)
C(10)-C(11)	1.390(2)	C(11)-C(12)	1.385(2)
C(13)-C(14)	1.526(2)	C(13)-C(16)	1.530(2)
C(13)-C(15)	1.532(2)	C(17)-C(22)	1.393(2)
C(17)-C(18)	1.399(2)	C(18)-C(19)	1.384(2)
C(19)-C(20)	1.386(2)	C(20)-C(21)	1.382(2)
C(21)-C(22)	1.385(2)		
N(1)-P(1)-C(1)	106.02(6)	N(1)-P(1)-C(7)	108.63(6)
C(1)-P(1)-C(7)	108.84(7)	N(1)-P(1)-C(17)	118.04(6)
C(1)-P(1)-C(17)	108.56(6)	C(7)-P(1)-C(17)	106.51(6)
C(13)-N(1)-P(1)	132.2(1)	C(6)-C(1)-C(2)	120.7(1)
C(6)-C(1)-P(1)	117.3(1)	C(2)-C(1)-P(1)	122.0(1)
C(3)-C(2)-C(1)	115.5(1)	C(3)-C(2)-S(1)	119.5(1)
C(1)-C(2)-S(1)	125.0(1)	C(4)-C(3)-C(2)	123.0(1)
C(3)-C(4)-C(5)	120.6(1)	C(6)-C(5)-C(4)	118.8(1)
C(5)-C(6)-C(1)	121.3(1)	C(12)-C(7)-C(8)	119.2(1)
C(12)-C(7)-P(1)	119.1(1)	C(8)-C(7)-P(1)	121.5(1)
C(9)-C(8)-C(7)	119.5(1)	C(10)-C(9)-C(8)	120.8(1)
C(9)-C(10)-C(11)	120.0(1)	C(12)-C(11)-C(10)	119.8(2)
C(11)-C(12)-C(7)	120.6(1)	N(1)-C(13)-C(14)	111.2(1)
N(1)-C(13)-C(16)	111.2(1)	C(14)-C(13)-C(16)	110.9(1)
N(1)-C(13)-C(15)	104.1(1)	C(14)-C(13)-C(15)	109.2(1)
C(16)-C(13)-C(15)	109.9(1)	C(22)-C(17)-C(18)	119.0(1)
C(22)-C(17)-P(1)	119.8(1)	C(18)-C(17)-P(1)	121.2(1)
C(19)-C(18)-C(17)	120.6(1)	C(18)-C(19)-C(20)	119.7(1)
C(21)-C(20)-C(19)	120.2(2)	C(20)-C(21)-C(22)	120.4(2)
C(21)-C(22)-C(17)	120.2(1)		

Appendix 1. Crystallographic data

Table 4. Anisotropic displacement parameters ($\text{\AA}^2 \times 10^3$) for pa069

atom	U11	U22	U33	U23	U13	U12
S(1)	25(1)	25(1)	23(1)	5(1)	11(1)	3(1)
P(1)	20(1)	18(1)	17(1)	0(1)	8(1)	1(1)
N(1)	20(1)	23(1)	17(1)	1(1)	9(1)	1(1)
C(1)	19(1)	20(1)	19(1)	-2(1)	7(1)	-1(1)
C(2)	20(1)	20(1)	19(1)	-3(1)	6(1)	-3(1)
C(3)	22(1)	29(1)	21(1)	-3(1)	10(1)	-3(1)
C(4)	22(1)	34(1)	29(1)	-5(1)	12(1)	2(1)
C(5)	25(1)	31(1)	29(1)	1(1)	8(1)	9(1)
C(6)	27(1)	29(1)	21(1)	2(1)	9(1)	4(1)
C(7)	22(1)	20(1)	19(1)	1(1)	9(1)	3(1)
C(8)	28(1)	24(1)	21(1)	0(1)	9(1)	1(1)
C(9)	33(1)	30(1)	19(1)	4(1)	10(1)	8(1)
C(10)	34(1)	26(1)	28(1)	9(1)	17(1)	8(1)
C(11)	28(1)	22(1)	33(1)	4(1)	13(1)	1(1)
C(12)	26(1)	21(1)	23(1)	0(1)	10(1)	2(1)
C(13)	19(1)	23(1)	23(1)	2(1)	9(1)	3(1)
C(14)	26(1)	26(1)	30(1)	4(1)	15(1)	4(1)
C(15)	23(1)	37(1)	27(1)	0(1)	6(1)	-1(1)
C(16)	30(1)	25(1)	29(1)	5(1)	13(1)	6(1)
C(17)	21(1)	20(1)	17(1)	0(1)	4(1)	1(1)
C(18)	27(1)	26(1)	24(1)	-2(1)	11(1)	0(1)
C(19)	31(1)	30(1)	26(1)	-7(1)	8(1)	4(1)
C(20)	30(1)	24(1)	30(1)	-8(1)	1(1)	0(1)
C(21)	28(1)	26(1)	32(1)	-3(1)	8(1)	-6(1)
C(22)	25(1)	24(1)	22(1)	-1(1)	8(1)	-1(1)

The anisotropic displacement factor exponent takes the form
 $2 \pi^2 [h^2 a^{*2} U(11) + \dots + 2 h k a^* b^* U(12)]$

Appendix 1. Crystallographic data

Table 5. Hydrogen Coordinates ($\text{\AA} \times 10^4$) and equivalent isotropic displacement parameters ($\text{\AA}^2 \times 10^3$) for pa069

atom	x	y	z	U(eq)
H(1N)	643	-4995	-2398	23
H(3)	4249	-5375	-3184	28
H(4)	5763	-6958	-2561	33
H(5)	5678	-7835	-1432	35
H(6)	4040	-7079	-941	30
H(8)	3294	-5540	261	29
H(9)	3277	-7154	1135	32
H(10)	1898	-8992	779	33
H(11)	543	-9261	-471	32
H(12)	561	-7671	-1355	28
H(14A)	-1350	-6311	-1430.9999	39
H(14B)	-2258	-5040	-1444	39
H(14C)	-713	-5075	-913.0001	39
H(15A)	-1562.0001	-4921	-3185	44
H(15B)	-2785	-4947	-2851.0002	44
H(15C)	-1857	-6221	-2788	44
H(16A)	-384.0000	-2961	-1507	41
H(16B)	-1866	-2961	-2115	41
H(16C)	-562	-2913.9998	-2380	41
H(18)	1196	-3675	-254	30
H(19)	1907	-1662	330	35
H(20)	3629	-494.0000	74	36
H(21)	4665	-1356	-741.9999	34
H(22)	3964	-3368	-1329	29

Complex 3a'

Table 1. Crystal data for pa074

Compound	pa074
Molecular formula	2(C ₄₀ H ₃₈ BrNP ₂ PdS),CH ₂ Cl ₂
Molecular weight	855.49
Crystal habit	orange plate
Crystal dimensions(mm)	0.22x0.20x0.12
Crystal system	triclinic
Space group	P -1
a(Å)	9.798(1)
b(Å)	9.884(1)
c(Å)	20.216(1)
α(°)	87.730(1)
β(°)	83.800(1)
γ(°)	72.090(1)
V(Å ³)	1852.0(3)
Z	2
d(g·cm ⁻³)	1.534
F(000)	866
μ(cm ⁻¹)	1.825
Absorption corrections	multi-scan ; 0.6896 min, 0.8107 max
Diffractionmeter	KappaCCD
X-ray source	MoKα
λ(Å)	0.71073
Monochromator	graphite
T (K)	150.0(1)
Scan mode	phi and omega scans
Maximum θ	30.02
HKL ranges	-13 13 ; -12 13 ; -28 27
Reflections measured	23799
Unique data	10763
Rint	0.0199
Reflections used	9318
Criterion	I > 2σ(I)
Refinement type	Fsqd
Hydrogen atoms	mixed
Parameters refined	445
Reflections / parameter	20
wR2	0.1442
R1	0.0456
Weights a, b	0.0790 ; 4.4523
GoF	1.033
difference peak / hole (e Å ⁻³)	1.076(0.131) / -2.924(0.131)

Table 2. Atomic Coordinates (A x 10⁴) and equivalent isotropic displacement parameters (A² x 10³) for pa074

atom	x	y	z	U(eq)
Pd(1)	1518(1)	1604(1)	2415(1)	17(1)
Br(1)	3427(1)	-346(1)	2886(1)	38(1)
S(1)	32(1)	3508(1)	1904(1)	25(1)
P(1)	-1134(1)	2435(1)	3430(1)	19(1)
P(2)	2722(1)	784(1)	1418(1)	17(1)
N(1)	543(3)	2333(3)	3374(1)	21(1)
C(1)	-2269(4)	3805(3)	2936(2)	23(1)
C(2)	1302(6)	2795(5)	4454(2)	45(1)
C(3)	-4597(4)	5551(4)	2788(2)	33(1)
C(4)	-3978(4)	6095(4)	2235(2)	30(1)
C(5)	-2552(4)	5466(3)	2013(2)	25(1)
C(6)	-1669(3)	4277(3)	2340(2)	21(1)
C(7)	-1270(4)	761(4)	3168(2)	22(1)
C(8)	-2535(5)	673(5)	2948(2)	40(1)
C(9)	-2657(6)	-635(6)	2801(3)	57(1)
C(10)	-1531(6)	-1854(5)	2866(3)	55(1)
C(11)	-255(5)	-1785(4)	3082(2)	42(1)
C(12)	-130(4)	-483(4)	3240(2)	28(1)
C(13)	-1971(4)	2628(4)	4285(2)	25(1)
C(14)	-1720(4)	1404(4)	4677(2)	33(1)
C(15)	-2210(5)	1491(5)	5348(2)	45(1)
C(16)	-2969(6)	2786(6)	5633(2)	49(1)
C(17)	-3240(5)	4011(5)	5251(2)	41(1)
C(18)	-2746(4)	3946(4)	4578(2)	32(1)
C(19)	1142(4)	3296(4)	3735(2)	27(1)
C(20)	2625(6)	3217(7)	3399(3)	64(2)
C(21)	-3746(4)	4420(4)	3134(2)	29(1)
C(22)	201(6)	4841(5)	3725(3)	53(1)
C(23)	4490(3)	1056(3)	1372(2)	21(1)
C(24)	5790(4)	50(4)	1158(2)	28(1)
C(25)	7072(4)	386(5)	1136(2)	38(1)
C(26)	7068(4)	1729(5)	1321(2)	37(1)
C(27)	5769(4)	2737(4)	1538(2)	31(1)
C(28)	4493(4)	2398(4)	1569(2)	24(1)
C(29)	1950(3)	1694(3)	676(1)	19(1)
C(30)	714(4)	1446(4)	491(2)	25(1)
C(31)	29(4)	2179(4)	-40(2)	30(1)
C(32)	558(4)	3188(4)	-389(2)	31(1)
C(33)	1783(4)	3428(4)	-213(2)	31(1)
C(34)	2484(4)	2686(4)	318(2)	25(1)
C(35)	2950(3)	-1063(3)	1221(2)	21(1)
C(36)	3683(4)	-1637(4)	613(2)	27(1)
C(37)	3813(4)	-3037(4)	455(2)	33(1)
C(38)	3185(5)	-3840(4)	893(2)	36(1)
C(39)	2424(5)	-3268(4)	1479(2)	35(1)
C(40)	2295(4)	-1870(4)	1652(2)	27(1)
Cl(1)	3749(4)	2179(5)	5717(2)	90(1)
Cl(2)	5288(4)	60(6)	4719(2)	84(1)
C(41)	4630(20)	430(20)	5560(7)	72(4)

U(eq) is defined as 1/3 the trace of the Uij tensor.

Appendix 1. Crystallographic data

Table 3. Bond lengths (Å) and angles (deg) for pa074

Pd(1)-N(1)	2.116(2)	Pd(1)-P(2)	2.2676(8)
Pd(1)-S(1)	2.283(1)	Pd(1)-Br(1)	2.4781(6)
S(1)-C(6)	1.757(3)	P(1)-N(1)	1.608(3)
P(1)-C(7)	1.803(3)	P(1)-C(1)	1.809(3)
P(1)-C(13)	1.823(3)	P(2)-C(23)	1.825(3)
P(2)-C(35)	1.825(3)	P(2)-C(29)	1.829(3)
N(1)-C(19)	1.507(4)	C(1)-C(21)	1.406(5)
C(1)-C(6)	1.409(4)	C(2)-C(19)	1.526(6)
C(3)-C(4)	1.384(6)	C(3)-C(21)	1.387(5)
C(4)-C(5)	1.376(5)	C(5)-C(6)	1.416(4)
C(7)-C(8)	1.390(5)	C(7)-C(12)	1.399(5)
C(8)-C(9)	1.381(6)	C(9)-C(10)	1.374(8)
C(10)-C(11)	1.390(7)	C(11)-C(12)	1.382(5)
C(13)-C(14)	1.390(5)	C(13)-C(18)	1.408(5)
C(14)-C(15)	1.386(5)	C(15)-C(16)	1.380(7)
C(16)-C(17)	1.381(7)	C(17)-C(18)	1.391(5)
C(19)-C(20)	1.517(6)	C(19)-C(22)	1.523(6)
C(23)-C(24)	1.391(4)	C(23)-C(28)	1.401(4)
C(24)-C(25)	1.390(5)	C(25)-C(26)	1.392(6)
C(26)-C(27)	1.393(6)	C(27)-C(28)	1.385(5)
C(29)-C(34)	1.392(4)	C(29)-C(30)	1.399(4)
C(30)-C(31)	1.385(5)	C(31)-C(32)	1.395(5)
C(32)-C(33)	1.377(6)	C(33)-C(34)	1.396(5)
C(35)-C(40)	1.396(5)	C(35)-C(36)	1.402(4)
C(36)-C(37)	1.397(5)	C(37)-C(38)	1.385(6)
C(38)-C(39)	1.372(6)	C(39)-C(40)	1.404(5)
Cl(1)-C(41)	1.70(2)	Cl(2)-C(41)#2	0.74(1)
Cl(2)-Cl(2)#2	1.23(1)	Cl(2)-C(41)	1.76(2)
N(1)-Pd(1)-P(2)	175.78(8)	N(1)-Pd(1)-S(1)	92.53(8)
P(2)-Pd(1)-S(1)	90.51(3)	N(1)-Pd(1)-Br(1)	91.97(8)
P(2)-Pd(1)-Br(1)	84.65(3)	S(1)-Pd(1)-Br(1)	171.51(3)
C(6)-S(1)-Pd(1)	115.4(1)	N(1)-P(1)-C(7)	108.3(2)
N(1)-P(1)-C(1)	116.5(2)	C(7)-P(1)-C(1)	106.7(2)
N(1)-P(1)-C(13)	112.7(1)	C(7)-P(1)-C(13)	104.2(2)
C(1)-P(1)-C(13)	107.6(2)	C(23)-P(2)-C(35)	109.2(2)
C(23)-P(2)-C(29)	104.0(1)	C(35)-P(2)-C(29)	101.0(1)
C(23)-P(2)-Pd(1)	107.9(1)	C(35)-P(2)-Pd(1)	117.1(1)
C(29)-P(2)-Pd(1)	116.7(1)	C(19)-N(1)-P(1)	124.3(2)
C(19)-N(1)-Pd(1)	118.7(2)	P(1)-N(1)-Pd(1)	109.3(1)
C(21)-C(1)-C(6)	118.8(3)	C(21)-C(1)-P(1)	121.4(3)
C(6)-C(1)-P(1)	119.7(2)	C(4)-C(3)-C(21)	119.3(3)
C(5)-C(4)-C(3)	119.9(3)	C(4)-C(5)-C(6)	122.1(3)
C(1)-C(6)-C(5)	117.7(3)	C(1)-C(6)-S(1)	128.3(2)
C(5)-C(6)-S(1)	113.8(2)	C(8)-C(7)-C(12)	119.4(3)
C(8)-C(7)-P(1)	120.9(3)	C(12)-C(7)-P(1)	119.5(2)
C(9)-C(8)-C(7)	120.0(4)	C(10)-C(9)-C(8)	120.5(4)
C(9)-C(10)-C(11)	120.3(4)	C(12)-C(11)-C(10)	119.6(4)
C(11)-C(12)-C(7)	120.2(4)	C(14)-C(13)-C(18)	119.0(3)
C(14)-C(13)-P(1)	117.1(3)	C(18)-C(13)-P(1)	123.6(3)
C(15)-C(14)-C(13)	120.2(4)	C(16)-C(15)-C(14)	120.6(4)
C(15)-C(16)-C(17)	120.0(4)	C(16)-C(17)-C(18)	120.2(4)
C(17)-C(18)-C(13)	119.9(4)	N(1)-C(19)-C(20)	108.9(3)
N(1)-C(19)-C(22)	112.3(3)	C(20)-C(19)-C(22)	108.1(4)
N(1)-C(19)-C(2)	109.9(3)	C(20)-C(19)-C(2)	108.2(4)
C(22)-C(19)-C(2)	109.4(4)	C(3)-C(21)-C(1)	121.8(3)
C(24)-C(23)-C(28)	119.2(3)	C(24)-C(23)-P(2)	125.1(2)
C(28)-C(23)-P(2)	115.6(2)	C(25)-C(24)-C(23)	120.0(3)
C(24)-C(25)-C(26)	120.6(4)	C(25)-C(26)-C(27)	119.6(3)
C(28)-C(27)-C(26)	119.9(3)	C(27)-C(28)-C(23)	120.7(3)
C(34)-C(29)-C(30)	118.9(3)	C(34)-C(29)-P(2)	122.8(2)
C(30)-C(29)-P(2)	118.2(2)	C(31)-C(30)-C(29)	120.6(3)
C(30)-C(31)-C(32)	120.2(3)	C(33)-C(32)-C(31)	119.6(3)
C(32)-C(33)-C(34)	120.5(3)	C(29)-C(34)-C(33)	120.3(3)
C(40)-C(35)-C(36)	119.8(3)	C(40)-C(35)-P(2)	119.9(2)

Appendix 1. Crystallographic data

C(36)-C(35)-P(2)	120.1(2)	C(37)-C(36)-C(35)	119.8(3)
C(38)-C(37)-C(36)	119.9(3)	C(39)-C(38)-C(37)	120.6(3)
C(38)-C(39)-C(40)	120.5(4)	C(35)-C(40)-C(39)	119.3(3)
C(41)#2-C1(2)-Cl(2)#2	125(2)	C(41)#2-C1(2)-C(41)	145(1)
Cl(2)#2-C1(2)-C(41)	20.0(5)	Cl(1)-C(41)-Cl(2)	114.2(8)

Estimated standard deviations are given in the parenthesis.

Symmetry operators ::

1: x, y, z 2: -x, -y, -z

Appendix 1. Crystallographic data

Table 4. Anisotropic displacement parameters ($\text{Å}^2 \times 10^3$) for pa074

atom	U11	U22	U33	U23	U13	U12
Pd(1)	16(1)	18(1)	15(1)	-1(1)	0(1)	-5(1)
Br(1)	31(1)	45(1)	33(1)	4(1)	-4(1)	-3(1)
S(1)	27(1)	22(1)	20(1)	4(1)	5(1)	-1(1)
P(1)	18(1)	23(1)	15(1)	0(1)	1(1)	-5(1)
P(2)	16(1)	17(1)	17(1)	-2(1)	1(1)	-5(1)
N(1)	20(1)	27(1)	17(1)	-6(1)	2(1)	-9(1)
C(1)	23(2)	23(1)	19(1)	0(1)	-2(1)	-2(1)
C(2)	62(3)	48(2)	36(2)	2(2)	-22(2)	-26(2)
C(3)	26(2)	34(2)	27(2)	-7(1)	-3(1)	6(1)
C(4)	32(2)	23(2)	30(2)	-2(1)	-9(1)	1(1)
C(5)	31(2)	20(1)	23(2)	1(1)	-4(1)	-4(1)
C(6)	24(2)	17(1)	19(1)	-2(1)	-1(1)	-3(1)
C(7)	25(2)	26(2)	19(1)	3(1)	-4(1)	-12(1)
C(8)	37(2)	39(2)	50(2)	14(2)	-21(2)	-18(2)
C(9)	60(3)	57(3)	76(4)	17(3)	-40(3)	-40(3)
C(10)	72(4)	39(2)	69(3)	5(2)	-23(3)	-34(2)
C(11)	48(2)	28(2)	53(3)	5(2)	-6(2)	-18(2)
C(12)	26(2)	26(2)	32(2)	2(1)	-1(1)	-11(1)
C(13)	20(1)	35(2)	18(1)	1(1)	1(1)	-5(1)
C(14)	38(2)	36(2)	20(2)	5(1)	1(1)	-8(2)
C(15)	56(3)	52(3)	21(2)	9(2)	4(2)	-13(2)
C(16)	53(3)	66(3)	19(2)	0(2)	7(2)	-10(2)
C(17)	38(2)	48(2)	27(2)	-11(2)	4(2)	-2(2)
C(18)	30(2)	36(2)	23(2)	-3(1)	1(1)	-1(1)
C(19)	31(2)	31(2)	24(2)	-7(1)	0(1)	-15(1)
C(20)	50(3)	107(5)	56(3)	-46(3)	20(2)	-56(3)
C(21)	25(2)	35(2)	21(2)	-1(1)	0(1)	-1(1)
C(22)	68(3)	26(2)	71(3)	-3(2)	-23(3)	-20(2)
C(23)	17(1)	24(1)	21(1)	-3(1)	0(1)	-7(1)
C(24)	22(2)	30(2)	31(2)	-9(1)	2(1)	-5(1)
C(25)	19(2)	49(2)	45(2)	-15(2)	4(1)	-7(2)
C(26)	25(2)	55(2)	38(2)	-12(2)	4(1)	-22(2)
C(27)	31(2)	38(2)	29(2)	-5(1)	0(1)	-20(2)
C(28)	21(2)	26(2)	26(2)	-5(1)	2(1)	-9(1)
C(29)	19(1)	19(1)	17(1)	-3(1)	0(1)	-4(1)
C(30)	20(2)	29(2)	25(2)	1(1)	-1(1)	-7(1)
C(31)	23(2)	37(2)	29(2)	-1(1)	-7(1)	-5(1)
C(32)	34(2)	30(2)	24(2)	4(1)	-7(1)	-1(1)
C(33)	43(2)	29(2)	23(2)	6(1)	-5(1)	-12(2)
C(34)	31(2)	25(2)	22(1)	0(1)	-2(1)	-11(1)
C(35)	22(1)	17(1)	23(1)	-1(1)	-3(1)	-5(1)
C(36)	27(2)	25(2)	28(2)	-6(1)	1(1)	-7(1)
C(37)	32(2)	27(2)	38(2)	-14(2)	4(2)	-4(1)
C(38)	43(2)	20(2)	46(2)	-3(1)	-18(2)	-7(2)
C(39)	46(2)	23(2)	39(2)	7(1)	-13(2)	-16(2)
C(40)	32(2)	25(2)	26(2)	2(1)	-5(1)	-13(1)
Cl(1)	78(2)	91(3)	80(2)	15(2)	-22(2)	6(2)
Cl(2)	67(2)	123(4)	73(2)	-17(2)	-16(2)	-38(2)
C(41)	90(10)	90(10)	53(8)	12(7)	-22(7)	-60(10)

The anisotropic displacement factor exponent takes the form
 $2 \pi^2 [h^2 a^{*2} U(11) + \dots + 2 h k a^* b^* U(12)]$

Appendix 1. Crystallographic data

Table 5. Hydrogen Coordinates ($\text{Å} \times 10^4$) and equivalent isotropic displacement parameters ($\text{Å}^2 \times 10^3$) for pa074

atom	x	y	z	U(eq)
H(2A)	345	2922	4692	68
H(2B)	1796	3353	4671	68
H(2C)	1866	1788	4462	68
H(3)	-5594	5948	2930	39
H(4)	-4538	6901	2008	36
H(5)	-2147	5841	1627	30
H(8)	-3314	1513	2897	47
H(9)	-3527	-692	2655	69
H(10)	-1624.0001	-2748	2761	66
H(11)	527	-2628	3122	50
H(12)	732	-433	3398	33
H(14)	-1210	506	4484	39
H(15)	-2023	652	5613	54
H(16)	-3305	2834	6093	58
H(17)	-3765	4901	5448	49
H(18)	-2931	4791	4317	38
H(20A)	3210	2219	3345	96
H(20B)	3094	3703	3673	96
H(20C)	2531	3679	2961	96
H(21)	-4173	4052	3516	35
H(22A)	-13	5123	3268	79
H(22B)	713	5447	3890	79
H(22C)	-701	4946	4009	79
H(24)	5802	-866	1027	34
H(25)	7957	-308	995	46
H(26)	7946	1956	1298	45
H(27)	5759	3656	1665	37
H(28)	3612	3082	1726	29
H(30)	341	768	730	30
H(31)	-802	1993	-166	36
H(32)	77	3705	-747	38
H(33)	2153	4105	-454	37
H(34)	3328	2858	435	30
H(36)	4091	-1076	308	32
H(37)	4330	-3439	48	39
H(38)	3282	-4795	787	43
H(39)	1980	-3824	1770	41
H(40)	1769	-1478	2059	32
H(41A)	3959	-129	5698	86
H(41B)	5445	108	5836	86

Complex 14

Table 1. Crystal data for pa321

Compound	pa321
Molecular formula	C ₃₈ H ₃₄ Cl ₂ Co ₂ N ₂ P ₂ S ₂
Molecular weight	833.49
Crystal habit	Green Block
Crystal dimensions(mm)	0.20x0.10x0.08
Crystal system	monoclinic
Space group	P2 ₁ /c
a(Å)	9.002(1)
b(Å)	17.784(1)
c(Å)	12.158(1)
α(°)	90.00
β(°)	113.901(2)
γ(°)	90.00
V(Å ³)	1779.5(3)
Z	2
d(g·cm ⁻³)	1.556
F(000)	852
μ(cm ⁻¹)	1.321
Absorption corrections	multi-scan ; 0.7780 min, 0.9017 max
Diffractometer	KappaCCD
X-ray source	MoKα
λ(Å)	0.71069
Monochromator	graphite
T (K)	150.0(1)
Scan mode	phi and omega scans
Maximum θ	30.03
HKL ranges	-12 12 ; -25 22 ; -17 17
Reflections measured	15358
Unique data	5174
Rint	0.0338
Reflections used	4305
Criterion	I > 2σI
Refinement type	Fsqd
Hydrogen atoms	constr
Parameters refined	217
Reflections / parameter	19
wR2	0.1050
R1	0.0452
Weights a, b	0.0362 ; 3.8823
GoF	1.066
difference peak / hole (e Å ⁻³)	1.082(0.094) / -0.639(0.094)

Table 2. Atomic Coordinates (A x 10⁴) and equivalent isotropic displacement parameters (Å² x 10³) for pa321

atom	x	y	z	U(eq)
Co(1)	4924(1)	-4499(1)	4054(1)	20(1)
Cl(1)	6161(1)	-4733(1)	2811(1)	26(1)
S(1)	3153(1)	-5505(1)	3944(1)	21(1)
P(1)	1442(1)	-4012(1)	3464(1)	18(1)
N(1)	3303(2)	-3728(1)	3981(2)	19(1)
C(1)	1448(3)	-4967(2)	3984(2)	23(1)
C(2)	219(3)	-3472(2)	4032(2)	21(1)
C(3)	593(3)	-3508(2)	5267(2)	26(1)
C(4)	-368(4)	-3133(2)	5737(3)	31(1)
C(5)	-1691(4)	-2713(2)	4981(3)	33(1)
C(6)	-2036(4)	-2656(2)	3774(3)	32(1)
C(7)	-1092(3)	-3037(2)	3286(2)	25(1)
C(8)	465(3)	-4044(2)	1846(2)	21(1)
C(9)	-1134(3)	-4298(2)	1261(3)	27(1)
C(10)	-1830(4)	-4347(2)	7(3)	32(1)
C(11)	-959(4)	-4130(2)	-646(3)	32(1)
C(12)	628(4)	-3879(2)	-71(2)	30(1)
C(13)	1344(3)	-3842(2)	1175(2)	23(1)
C(14)	3700(3)	-2952(2)	4274(2)	19(1)
C(15)	3459(4)	-2407(2)	3393(3)	27(1)
C(16)	3884(4)	-1662(2)	3711(3)	33(1)
C(17)	4538(4)	-1451(2)	4910(3)	31(1)
C(18)	4779(3)	-1987(2)	5789(3)	29(1)
C(19)	4370(3)	-2733(2)	5479(2)	25(1)

U(eq) is defined as 1/3 the trace of the Uij tensor.

Appendix 1. Crystallographic data

Table 3. Bond lengths (Å) and angles (deg) for pa321

Co(1)-N(1)	1.977(2)	Co(1)-Cl(1)	2.2501(7)
Co(1)-S(1)#3	2.3465(7)	Co(1)-S(1)	2.3643(8)
Co(1)-Co(1)#3	2.8689(7)	S(1)-C(1)	1.827(3)
S(1)-Co(1)#3	2.3465(7)	P(1)-N(1)	1.613(2)
P(1)-C(2)	1.797(3)	P(1)-C(8)	1.801(3)
P(1)-C(1)	1.812(3)	N(1)-C(14)	1.435(3)
C(1)-H(1A)	0.9900	C(1)-H(1B)	0.9900
C(2)-C(7)	1.395(4)	C(2)-C(3)	1.401(4)
C(3)-C(4)	1.386(4)	C(3)-H(3)	0.9500
C(4)-C(5)	1.390(5)	C(4)-H(4)	0.9500
C(5)-C(6)	1.376(4)	C(5)-H(5)	0.9500
C(6)-C(7)	1.393(4)	C(6)-H(6)	0.9500
C(7)-H(7)	0.9500	C(8)-C(13)	1.394(4)
C(8)-C(9)	1.397(4)	C(9)-C(10)	1.396(4)
C(9)-H(9)	0.9500	C(10)-C(11)	1.378(5)
C(10)-H(10)	0.9500	C(11)-C(12)	1.386(4)
C(11)-H(11)	0.9500	C(12)-C(13)	1.387(4)
C(12)-H(12)	0.9500	C(13)-H(13)	0.9500
C(14)-C(19)	1.394(4)	C(14)-C(15)	1.395(4)
C(15)-C(16)	1.389(4)	C(15)-H(15)	0.9500
C(16)-C(17)	1.384(4)	C(16)-H(16)	0.9500
C(17)-C(18)	1.382(5)	C(17)-H(17)	0.9500
C(18)-C(19)	1.388(4)	C(18)-H(18)	0.9500
C(19)-H(19)	0.9500		
N(1)-Co(1)-Cl(1)	130.91(7)	N(1)-Co(1)-S(1)#3	105.40(6)
Cl(1)-Co(1)-S(1)#3	109.84(3)	N(1)-Co(1)-S(1)	93.08(7)
Cl(1)-Co(1)-S(1)	109.14(3)	S(1)#3-Co(1)-S(1)	104.97(2)
N(1)-Co(1)-Co(1)#3	105.16(7)	Cl(1)-Co(1)-Co(1)#3	123.22(3)
S(1)#3-Co(1)-Co(1)#3	52.77(2)	S(1)-Co(1)-Co(1)#3	52.20(2)
C(1)-S(1)-Co(1)#3	104.2(1)	C(1)-S(1)-Co(1)	99.0(1)
Co(1)#3-S(1)-Co(1)	75.04(2)	N(1)-P(1)-C(2)	112.6(1)
N(1)-P(1)-C(8)	114.0(1)	C(2)-P(1)-C(8)	109.4(1)
N(1)-P(1)-C(1)	107.5(1)	C(2)-P(1)-C(1)	106.4(1)
C(8)-P(1)-C(1)	106.4(1)	C(14)-N(1)-P(1)	120.8(2)
C(14)-N(1)-Co(1)	123.4(2)	P(1)-N(1)-Co(1)	115.6(1)
P(1)-C(1)-S(1)	111.5(1)	P(1)-C(1)-H(1A)	109.3
S(1)-C(1)-H(1A)	109.3	P(1)-C(1)-H(1B)	109.3
S(1)-C(1)-H(1B)	109.3	H(1A)-C(1)-H(1B)	108.0
C(7)-C(2)-C(3)	119.7(2)	C(7)-C(2)-P(1)	122.3(2)
C(3)-C(2)-P(1)	118.0(2)	C(4)-C(3)-C(2)	120.0(3)
C(4)-C(3)-H(3)	120.0	C(2)-C(3)-H(3)	120.0
C(3)-C(4)-C(5)	119.8(3)	C(3)-C(4)-H(4)	120.1
C(5)-C(4)-H(4)	120.1	C(6)-C(5)-C(4)	120.5(3)
C(6)-C(5)-H(5)	119.8	C(4)-C(5)-H(5)	119.8
C(5)-C(6)-C(7)	120.4(3)	C(5)-C(6)-H(6)	119.8
C(7)-C(6)-H(6)	119.8	C(6)-C(7)-C(2)	119.6(3)
C(6)-C(7)-H(7)	120.2	C(2)-C(7)-H(7)	120.2
C(13)-C(8)-C(9)	119.8(2)	C(13)-C(8)-P(1)	119.3(2)
C(9)-C(8)-P(1)	120.9(2)	C(10)-C(9)-C(8)	119.4(3)
C(10)-C(9)-H(9)	120.3	C(8)-C(9)-H(9)	120.3
C(11)-C(10)-C(9)	120.2(3)	C(11)-C(10)-H(10)	119.9
C(9)-C(10)-H(10)	119.9	C(10)-C(11)-C(12)	120.7(3)
C(10)-C(11)-H(11)	119.6	C(12)-C(11)-H(11)	119.6
C(11)-C(12)-C(13)	119.6(3)	C(11)-C(12)-H(12)	120.2
C(13)-C(12)-H(12)	120.2	C(12)-C(13)-C(8)	120.3(3)
C(12)-C(13)-H(13)	119.9	C(8)-C(13)-H(13)	119.9
C(19)-C(14)-C(15)	118.7(3)	C(19)-C(14)-N(1)	119.2(2)
C(15)-C(14)-N(1)	122.1(2)	C(16)-C(15)-C(14)	120.6(3)
C(16)-C(15)-H(15)	119.7	C(14)-C(15)-H(15)	119.7
C(17)-C(16)-C(15)	120.3(3)	C(17)-C(16)-H(16)	119.9
C(15)-C(16)-H(16)	119.9	C(18)-C(17)-C(16)	119.6(3)
C(18)-C(17)-H(17)	120.2	C(16)-C(17)-H(17)	120.2
C(17)-C(18)-C(19)	120.5(3)	C(17)-C(18)-H(18)	119.7
C(19)-C(18)-H(18)	119.7	C(18)-C(19)-C(14)	120.4(3)

Appendix 1. Crystallographic data

C(18)-C(19)-H(19) 119.8 C(14)-C(19)-H(19) 119.8

 Estimated standard deviations are given in the parenthesis.
 Symmetry operators ::
 1: x, y, z 2: -x, y+1/2, -z+1/2 3: -x, -y, -z
 4: x, -y-1/2, z-1/2

Appendix 1. Crystallographic data

Table 4. Anisotropic displacement parameters ($\text{\AA}^2 \times 10^3$) for pa321

atom	U11	U22	U33	U23	U13	U12
Co(1)	19(1)	20(1)	20(1)	1(1)	7(1)	1(1)
Cl(1)	32(1)	28(1)	25(1)	2(1)	19(1)	2(1)
S(1)	21(1)	19(1)	21(1)	-1(1)	5(1)	0(1)
P(1)	17(1)	19(1)	17(1)	0(1)	6(1)	0(1)
N(1)	17(1)	19(1)	20(1)	-1(1)	6(1)	0(1)
C(1)	19(1)	22(1)	28(1)	4(1)	7(1)	0(1)
C(2)	18(1)	21(1)	24(1)	-2(1)	9(1)	-2(1)
C(3)	28(1)	25(1)	26(1)	1(1)	13(1)	1(1)
C(4)	39(2)	31(2)	29(1)	-6(1)	21(1)	-6(1)
C(5)	31(1)	30(2)	44(2)	-13(1)	22(1)	-4(1)
C(6)	25(1)	30(2)	37(2)	-8(1)	8(1)	5(1)
C(7)	25(1)	24(1)	24(1)	-3(1)	8(1)	2(1)
C(8)	20(1)	20(1)	18(1)	-2(1)	5(1)	2(1)
C(9)	22(1)	28(1)	27(1)	-5(1)	7(1)	2(1)
C(10)	23(1)	34(2)	30(1)	-9(1)	1(1)	5(1)
C(11)	36(2)	33(2)	20(1)	-4(1)	4(1)	9(1)
C(12)	36(2)	34(2)	21(1)	0(1)	11(1)	8(1)
C(13)	25(1)	23(1)	21(1)	-2(1)	9(1)	1(1)
C(14)	16(1)	18(1)	22(1)	-1(1)	7(1)	1(1)
C(15)	35(1)	22(1)	24(1)	-2(1)	11(1)	-2(1)
C(16)	42(2)	21(1)	37(2)	2(1)	18(1)	-4(1)
C(17)	27(1)	23(1)	45(2)	-10(1)	17(1)	-6(1)
C(18)	21(1)	32(2)	30(1)	-12(1)	7(1)	-1(1)
C(19)	22(1)	27(1)	23(1)	-2(1)	6(1)	0(1)

The anisotropic displacement factor exponent takes the form
 $2 \pi^2 [h^2 a^{*2} U(11) + \dots + 2 h k a^* b^* U(12)]$

Appendix 1. Crystallographic data

Table 5. Hydrogen Coordinates ($\text{\AA} \times 10^4$) and equivalent isotropic displacement parameters ($\text{\AA}^2 \times 10^3$) for pa321

atom	x	y	z	U(eq)
H(1A)	416	-5217.0005	3470	28
H(1B)	1517	-4957	4818	28
H(3)	1506	-3790	5783	31
H(4)	-124	-3162	6572	37
H(5)	-2363	-2464	5301	39
H(6)	-2922	-2354	3270	39
H(7)	-1339	-3001	2450	30
H(9)	-1741	-4437	1711	32
H(10)	-2908	-4530	-397	38
H(11)	-1452	-4153	-1500	38
H(12)	1222	-3732.9998	-528	36
H(13)	2438	-3678	1573	28
H(15)	2999	-2546	2568	33
H(16)	3726	-1297	3104	39
H(17)	4820	-939.9999	5126	37
H(18)	5228	-1843	6612	35
H(19)	4548	-3097	6091	30

Complex 15

Table 1. Crystal data for pa163

Compound	pa163
Molecular formula	C ₂₇ H ₂₉ NPRhS
Molecular weight	533.45
Crystal habit	Yellow Block
Crystal dimensions(mm)	0.16x0.12x0.08
Crystal system	monoclinic
Space group	P2 ₁ /c
a(Å)	15.329(1)
b(Å)	10.354(1)
c(Å)	15.839(1)
α(°)	90.00
β(°)	112.885(1)
γ(°)	90.00
V(Å ³)	2316.0(3)
Z	4
d(g·cm ⁻³)	1.530
F(000)	1096
μ(cm ⁻¹)	0.912
Absorption corrections	multi-scan ; 0.8678 min, 0.9306 max
Diffractionmeter	KappaCCD
X-ray source	MoKα
λ(Å)	0.71069
Monochromator	graphite
T (K)	150.0(1)
Scan mode	phi and omega scans
Maximum θ	27.48
HKL ranges	-19 14 ; -13 12 ; -20 20
Reflections measured	14478
Unique data	5290
Rint	0.0453
Reflections used	3973
Criterion	I > 2σ(I)
Refinement type	Fsqd
Hydrogen atoms	constr
Parameters refined	280
Reflections / parameter	14
wR2	0.1087
R1	0.0407
Weights a, b	0.0583 ; 0.0000
GoF	1.040
difference peak / hole (e Å ⁻³)	1.213(0.101) / -0.831(0.101)

Table 2. Atomic Coordinates (A x 10⁴) and equivalent isotropic displacement parameters (Å² x 10³) for pa163

atom	x	y	z	U(eq)
Rh(1)	3075(1)	-350(1)	6884(1)	24(1)
S(1)	2803(1)	-1963(1)	5786(1)	31(1)
P(1)	2055(1)	412(1)	4803(1)	24(1)
N(1)	2235(2)	905(2)	5823(2)	24(1)
C(1)	1862(2)	-1292(3)	4779(2)	29(1)
C(2)	1978(2)	2214(3)	5911(2)	26(1)
C(3)	1252(2)	2469(3)	6198(2)	36(1)
C(4)	937(3)	3716(4)	6230(2)	47(1)
C(5)	1367(3)	4741(3)	5986(3)	46(1)
C(6)	2102(3)	4519(3)	5717(2)	41(1)
C(7)	2410(2)	3259(3)	5682(2)	32(1)
C(8)	1025(2)	1217(3)	3981(2)	27(1)
C(9)	129(2)	829(4)	3903(2)	35(1)
C(10)	-665(2)	1506(4)	3364(2)	42(1)
C(11)	-567(2)	2602(4)	2902(2)	41(1)
C(12)	306(3)	3001(4)	2972(2)	42(1)
C(13)	1113(2)	2303(3)	3512(2)	34(1)
C(14)	3010(2)	688(3)	4425(2)	27(1)
C(15)	2893(2)	348(3)	3532(2)	33(1)
C(16)	3623(3)	525(3)	3237(2)	37(1)
C(17)	4470(2)	1051(4)	3826(2)	40(1)
C(18)	4593(2)	1389(3)	4707(2)	37(1)
C(19)	3870(2)	1199(3)	5014(2)	32(1)
C(20)	3141(2)	939(3)	7977(2)	32(1)
C(21)	3888(2)	1169(3)	7716(2)	31(1)
C(22)	4906(2)	702(4)	8227(2)	41(1)
C(23)	4966(2)	-705(4)	8495(2)	39(1)
C(24)	4168(2)	-1502(3)	7838(2)	32(1)
C(25)	3313(2)	-1761(3)	7935(2)	29(1)
C(26)	3034(2)	-1212(4)	8678(2)	41(1)
C(27)	3237(3)	225(4)	8842(2)	42(1)

U(eq) is defined as 1/3 the trace of the Uij tensor.

Table 3. Bond lengths (Å) and angles (deg) for pal63

Rh(1)-N(1)	2.118(2)	Rh(1)-C(21)	2.118(3)
Rh(1)-C(24)	2.133(3)	Rh(1)-C(25)	2.138(3)
Rh(1)-C(20)	2.157(3)	Rh(1)-S(1)	2.3291(8)
S(1)-C(1)	1.821(3)	P(1)-N(1)	1.613(2)
P(1)-C(1)	1.788(3)	P(1)-C(14)	1.808(3)
P(1)-C(8)	1.812(3)	N(1)-C(2)	1.432(4)
C(1)-H(1A)	0.9900	C(1)-H(1B)	0.9900
C(2)-C(3)	1.382(4)	C(2)-C(7)	1.389(4)
C(3)-C(4)	1.386(5)	C(3)-H(3)	0.9500
C(4)-C(5)	1.381(5)	C(4)-H(4)	0.9500
C(5)-C(6)	1.370(6)	C(5)-H(5)	0.9500
C(6)-C(7)	1.396(5)	C(6)-H(6)	0.9500
C(7)-H(7)	0.9500	C(8)-C(13)	1.383(4)
C(8)-C(9)	1.390(4)	C(9)-C(10)	1.376(5)
C(9)-H(9)	0.9500	C(10)-C(11)	1.390(5)
C(10)-H(10)	0.9500	C(11)-C(12)	1.363(5)
C(11)-H(11)	0.9500	C(12)-C(13)	1.401(5)
C(12)-H(12)	0.9500	C(13)-H(13)	0.9500
C(14)-C(19)	1.390(4)	C(14)-C(15)	1.400(4)
C(15)-C(16)	1.382(5)	C(15)-H(15)	0.9500
C(16)-C(17)	1.383(5)	C(16)-H(16)	0.9500
C(17)-C(18)	1.379(5)	C(17)-H(17)	0.9500
C(18)-C(19)	1.386(4)	C(18)-H(18)	0.9500
C(19)-H(19)	0.9500	C(20)-C(21)	1.381(4)
C(20)-C(27)	1.513(5)	C(20)-H(20)	0.9500
C(21)-C(22)	1.530(4)	C(21)-H(21)	0.9500
C(22)-C(23)	1.510(5)	C(22)-H(22A)	0.9900
C(22)-H(22B)	0.9900	C(23)-C(24)	1.507(5)
C(23)-H(23A)	0.9900	C(23)-H(23B)	0.9900
C(24)-C(25)	1.403(4)	C(24)-H(24)	0.9500
C(25)-C(26)	1.510(5)	C(25)-H(25)	0.9500
C(26)-C(27)	1.521(5)	C(26)-H(26A)	0.9900
C(26)-H(26B)	0.9900	C(27)-H(27A)	0.9900
C(27)-H(27B)	0.9900		
N(1)-Rh(1)-C(21)	93.9(1)	N(1)-Rh(1)-C(24)	166.8(1)
C(21)-Rh(1)-C(24)	82.2(1)	N(1)-Rh(1)-C(25)	154.7(1)
C(21)-Rh(1)-C(25)	98.1(1)	C(24)-Rh(1)-C(25)	38.4(1)
N(1)-Rh(1)-C(20)	94.7(1)	C(21)-Rh(1)-C(20)	37.7(1)
C(24)-Rh(1)-C(20)	89.9(1)	C(25)-Rh(1)-C(20)	81.8(1)
N(1)-Rh(1)-S(1)	88.32(7)	C(21)-Rh(1)-S(1)	152.6(1)
C(24)-Rh(1)-S(1)	89.5(1)	C(25)-Rh(1)-S(1)	91.1(1)
C(20)-Rh(1)-S(1)	169.1(1)	C(1)-S(1)-Rh(1)	103.4(1)
N(1)-P(1)-C(1)	107.2(1)	N(1)-P(1)-C(14)	115.9(1)
C(1)-P(1)-C(14)	107.3(2)	N(1)-P(1)-C(8)	109.6(1)
C(1)-P(1)-C(8)	110.4(1)	C(14)-P(1)-C(8)	106.3(1)
C(2)-N(1)-P(1)	116.8(2)	C(2)-N(1)-Rh(1)	127.5(2)
P(1)-N(1)-Rh(1)	114.5(1)	P(1)-C(1)-S(1)	106.8(2)
P(1)-C(1)-H(1A)	110.4	S(1)-C(1)-H(1A)	110.4
P(1)-C(1)-H(1B)	110.4	S(1)-C(1)-H(1B)	110.4
H(1A)-C(1)-H(1B)	108.6	C(3)-C(2)-C(7)	117.6(3)
C(3)-C(2)-N(1)	120.0(3)	C(7)-C(2)-N(1)	122.3(3)
C(2)-C(3)-C(4)	121.8(3)	C(2)-C(3)-H(3)	119.1
C(4)-C(3)-H(3)	119.1	C(5)-C(4)-C(3)	119.6(4)
C(5)-C(4)-H(4)	120.2	C(3)-C(4)-H(4)	120.2
C(6)-C(5)-C(4)	119.9(3)	C(6)-C(5)-H(5)	120.1
C(4)-C(5)-H(5)	120.1	C(5)-C(6)-C(7)	120.1(3)
C(5)-C(6)-H(6)	120.0	C(7)-C(6)-H(6)	120.0
C(2)-C(7)-C(6)	121.0(3)	C(2)-C(7)-H(7)	119.5
C(6)-C(7)-H(7)	119.5	C(13)-C(8)-C(9)	119.2(3)
C(13)-C(8)-P(1)	121.3(2)	C(9)-C(8)-P(1)	119.0(2)
C(10)-C(9)-C(8)	120.8(3)	C(10)-C(9)-H(9)	119.6
C(8)-C(9)-H(9)	119.6	C(9)-C(10)-C(11)	119.5(3)
C(9)-C(10)-H(10)	120.2	C(11)-C(10)-H(10)	120.2
C(12)-C(11)-C(10)	120.5(3)	C(12)-C(11)-H(11)	119.7

C(10)-C(11)-H(11)	119.7	C(11)-C(12)-C(13)	120.0(3)
C(11)-C(12)-H(12)	120.0	C(13)-C(12)-H(12)	120.0
C(8)-C(13)-C(12)	120.0(3)	C(8)-C(13)-H(13)	120.0
C(12)-C(13)-H(13)	120.0	C(19)-C(14)-C(15)	119.3(3)
C(19)-C(14)-P(1)	121.1(2)	C(15)-C(14)-P(1)	119.5(2)
C(16)-C(15)-C(14)	120.4(3)	C(16)-C(15)-H(15)	119.8
C(14)-C(15)-H(15)	119.8	C(15)-C(16)-C(17)	119.7(3)
C(15)-C(16)-H(16)	120.2	C(17)-C(16)-H(16)	120.2
C(18)-C(17)-C(16)	120.4(3)	C(18)-C(17)-H(17)	119.8
C(16)-C(17)-H(17)	119.8	C(17)-C(18)-C(19)	120.3(3)
C(17)-C(18)-H(18)	119.8	C(19)-C(18)-H(18)	119.8
C(18)-C(19)-C(14)	119.8(3)	C(18)-C(19)-H(19)	120.1
C(14)-C(19)-H(19)	120.1	C(21)-C(20)-C(27)	123.8(3)
C(21)-C(20)-Rh(1)	69.6(2)	C(27)-C(20)-Rh(1)	112.5(2)
C(21)-C(20)-H(20)	118.1	C(27)-C(20)-H(20)	118.1
Rh(1)-C(20)-H(20)	87.9	C(20)-C(21)-C(22)	125.5(3)
C(20)-C(21)-Rh(1)	72.7(2)	C(22)-C(21)-Rh(1)	109.1(2)
C(20)-C(21)-H(21)	117.3	C(22)-C(21)-H(21)	117.3
Rh(1)-C(21)-H(21)	88.2	C(23)-C(22)-C(21)	113.1(3)
C(23)-C(22)-H(22A)	109.0	C(21)-C(22)-H(22A)	109.0
C(23)-C(22)-H(22B)	109.0	C(21)-C(22)-H(22B)	109.0
H(22A)-C(22)-H(22B)	107.8	C(24)-C(23)-C(22)	112.9(3)
C(24)-C(23)-H(23A)	109.0	C(22)-C(23)-H(23A)	109.0
C(24)-C(23)-H(23B)	109.0	C(22)-C(23)-H(23B)	109.0
H(23A)-C(23)-H(23B)	107.8	C(25)-C(24)-C(23)	124.8(3)
C(25)-C(24)-Rh(1)	71.0(2)	C(23)-C(24)-Rh(1)	112.7(2)
C(25)-C(24)-H(24)	117.6	C(23)-C(24)-H(24)	117.6
Rh(1)-C(24)-H(24)	86.2	C(24)-C(25)-C(26)	125.0(3)
C(24)-C(25)-Rh(1)	70.6(2)	C(26)-C(25)-Rh(1)	109.6(2)
C(24)-C(25)-H(25)	117.5	C(26)-C(25)-H(25)	117.5
Rh(1)-C(25)-H(25)	89.8	C(25)-C(26)-C(27)	113.6(3)
C(25)-C(26)-H(26A)	108.9	C(27)-C(26)-H(26A)	108.9
C(25)-C(26)-H(26B)	108.9	C(27)-C(26)-H(26B)	108.9
H(26A)-C(26)-H(26B)	107.7	C(20)-C(27)-C(26)	112.4(3)
C(20)-C(27)-H(27A)	109.1	C(26)-C(27)-H(27A)	109.1
C(20)-C(27)-H(27B)	109.1	C(26)-C(27)-H(27B)	109.1
H(27A)-C(27)-H(27B)	107.8		

Appendix 1. Crystallographic data

Table 4. Anisotropic displacement parameters ($\text{Å}^2 \times 10^3$) for pal63

atom	U11	U22	U33	U23	U13	U12
Rh(1)	27(1)	20(1)	24(1)	2(1)	10(1)	1(1)
S(1)	40(1)	21(1)	31(1)	-1(1)	11(1)	3(1)
P(1)	25(1)	21(1)	24(1)	0(1)	9(1)	-1(1)
N(1)	28(1)	18(1)	27(1)	0(1)	11(1)	1(1)
C(1)	32(2)	23(2)	30(2)	0(1)	9(1)	0(1)
C(2)	27(2)	25(2)	21(1)	0(1)	5(1)	-1(1)
C(3)	40(2)	29(2)	45(2)	-2(2)	22(2)	0(2)
C(4)	52(2)	46(2)	47(2)	-2(2)	25(2)	15(2)
C(5)	72(3)	23(2)	44(2)	-3(2)	25(2)	13(2)
C(6)	69(3)	20(2)	36(2)	3(2)	20(2)	-1(2)
C(7)	42(2)	25(2)	32(2)	0(2)	15(1)	-2(2)
C(8)	31(2)	29(2)	22(1)	-1(1)	11(1)	1(1)
C(9)	33(2)	37(2)	33(2)	4(2)	12(1)	-2(2)
C(10)	27(2)	59(3)	38(2)	3(2)	11(2)	2(2)
C(11)	34(2)	54(2)	31(2)	-1(2)	7(1)	17(2)
C(12)	51(2)	40(2)	35(2)	6(2)	17(2)	5(2)
C(13)	31(2)	33(2)	37(2)	5(2)	14(1)	2(2)
C(14)	30(2)	24(2)	29(2)	1(1)	13(1)	2(1)
C(15)	36(2)	28(2)	35(2)	2(1)	15(2)	4(2)
C(16)	50(2)	33(2)	36(2)	8(2)	26(2)	10(2)
C(17)	38(2)	34(2)	57(2)	17(2)	29(2)	11(2)
C(18)	30(2)	30(2)	51(2)	7(2)	15(2)	1(2)
C(19)	33(2)	29(2)	34(2)	2(2)	12(1)	4(2)
C(20)	40(2)	31(2)	23(1)	-5(1)	10(1)	4(2)
C(21)	36(2)	26(2)	27(2)	-3(1)	7(1)	-2(2)
C(22)	35(2)	37(2)	44(2)	-2(2)	7(2)	-4(2)
C(23)	34(2)	41(2)	37(2)	4(2)	7(2)	6(2)
C(24)	36(2)	29(2)	29(2)	7(1)	10(1)	10(2)
C(25)	32(2)	26(2)	27(2)	7(1)	10(1)	2(1)
C(26)	43(2)	49(2)	33(2)	10(2)	17(2)	3(2)
C(27)	50(2)	47(2)	32(2)	1(2)	20(2)	8(2)

The anisotropic displacement factor exponent takes the form
 $2\pi^2 [h^2 a^{*2} U(11) + \dots + 2hka^* b^* U(12)]$

Appendix 1. Crystallographic data

Table 5. Hydrogen Coordinates ($\text{Å} \times 10^4$) and equivalent isotropic displacement parameters ($\text{Å}^2 \times 10^3$) for pal63

atom	x	y	z	U(eq)
H(1A)	1882	-1672	4213	35
H(1B)	1235	-1480	4797	35
H(3)	960	1771	6379	43
H(4)	428	3865	6418	56
H(5)	1154	5598	6005	55
H(6)	2402	5223	5553	50
H(7)	2924	3115	5500	39
H(9)	64	87	4227	42
H(10)	-1275	1226	3308	50
H(11)	-1113	3076	2533	49
H(12)	367	3752	2655	50
H(13)	1720	2575	3556	40
H(15)	2308	-6.0000	3125	40
H(16)	3543	286	2632	45
H(17)	4970	1180	3623	48
H(18)	5176	1755	5105	44
H(19)	3963	1417	5626	39
H(20)	2532	1247	7592	39
H(21)	3759	1658	7173	38
H(22A)	5265	837	7834	49
H(22B)	5208	1230	8787	49
H(23A)	5576	-1062	8523	47
H(23B)	4958	-774	9116	47
H(24)	4250	-1856	7320	38
H(25)	2877	-2323	7501	35
H(26A)	3380	-1683	9256	49
H(26B)	2349	-1361	8509	49
H(27A)	2791	602	9090	50
H(27B)	3887	342	9306	50

Complex 17

Table 1. Crystal data for pa136

Compound	pa136
Molecular formula	C ₃₇ H ₃₂ CINP ₂ PdS
Molecular weight	726.49
Crystal habit	Orange Block
Crystal dimensions(mm)	0.14x0.12x0.10
Crystal system	monoclinic
Space group	P2 ₁ /c
a(Å)	9.612(1)
b(Å)	16.430(1)
c(Å)	21.208(1)
α(°)	90.00
β(°)	102.9220(10)
γ(°)	90.00
V(Å ³)	3264.5(4)
Z	4
d(g·cm ⁻³)	1.478
F(000)	1480
μ(cm ⁻¹)	0.840
Absorption corrections	multi-scan ; 0.8915 min, 0.9207 max
Diffractionmeter	KappaCCD
X-ray source	MoKα
λ(Å)	0.71069
Monochromator	graphite
T (K)	150.0(1)
Scan mode	phi and omega scans
Maximum θ	27.47
HKL ranges	-9 12 ; -21 19 ; -27 27
Reflections measured	23979
Unique data	7391
Rint	0.0449
Reflections used	4991
Criterion	I > 2σI
Refinement type	Fsqd
Hydrogen atoms	constr
Parameters refined	388
Reflections / parameter	12
wR2	0.0970
R1	0.0405
Weights a, b	0.0465 ; 0.0000
GoF	0.956
difference peak / hole (e Å ⁻³)	0.938(0.090) / -0.626(0.090)

Table 2. Atomic Coordinates (A x 10⁴) and equivalent isotropic displacement parameters (A² x 10³) for pa136

atom	x	y	z	U(eq)
Pd(1)	8406(1)	1829(1)	4144(1)	23(1)
Cl(1)	8917(1)	2153(1)	3122(1)	21(1)
S(1)	7289(1)	1681(1)	4983(1)	33(1)
P(3)	6208(1)	453(1)	3970(1)	26(1)
P(4)	9152(1)	3078(1)	4509(1)	22(1)
N(1)	7755(3)	643(1)	3847(1)	26(1)
C(1)	6323(4)	723(2)	4803(2)	34(1)
C(2)	4779(3)	1044(2)	3490(2)	28(1)
C(3)	3373(4)	926(2)	3543(2)	37(1)
C(4)	2280(4)	1371(2)	3170(2)	47(1)
C(5)	2590(4)	1958(2)	2754(2)	47(1)
C(6)	3973(4)	2088(2)	2706(2)	40(1)
C(7)	5079(4)	1630(2)	3061(2)	30(1)
C(8)	5736(4)	-611(2)	3867(2)	28(1)
C(9)	6653(4)	-1165(2)	4249(2)	41(1)
C(10)	6319(5)	-1983(2)	4219(2)	54(1)
C(11)	5087(4)	-2261(2)	3817(2)	49(1)
C(12)	4185(4)	-1724(2)	3415(2)	37(1)
C(13)	4513(4)	-902(2)	3449(2)	32(1)
C(14)	8429(3)	139(2)	3457(2)	27(1)
C(15)	7788(4)	-81(2)	2832(2)	34(1)
C(16)	8472(5)	-606(2)	2483(2)	47(1)
C(17)	9814(5)	-910(2)	2757(2)	47(1)
C(18)	10460(4)	-689(2)	3388(2)	47(1)
C(19)	9783(4)	-175(2)	3735(2)	38(1)
C(20)	8831(3)	3349(2)	5299(2)	24(1)
C(21)	7981(3)	4005(2)	5380(2)	28(1)
C(22)	7725(4)	4178(2)	5987(2)	34(1)
C(23)	8308(4)	3688(2)	6513(2)	36(1)
C(24)	9141(4)	3036(2)	6433(2)	33(1)
C(25)	9413(3)	2860(2)	5835(2)	28(1)
C(26)	8209(3)	3850(2)	3962(2)	26(1)
C(27)	6752(4)	3750(2)	3727(2)	32(1)
C(28)	5968(4)	4339(2)	3335(2)	43(1)
C(29)	6652(4)	5029(2)	3168(2)	43(1)
C(30)	8097(4)	5120(2)	3385(2)	41(1)
C(31)	8874(4)	4536(2)	3785(2)	32(1)
C(32)	11054(3)	3292(2)	4602(2)	26(1)
C(33)	11759(4)	3836(2)	5073(2)	29(1)
C(34)	13194(4)	3995(2)	5144(2)	34(1)
C(35)	13959(4)	3624(2)	4751(2)	43(1)
C(36)	13257(4)	3095(3)	4278(2)	63(1)
C(37)	11821(4)	2928(2)	4208(2)	47(1)

U(eq) is defined as 1/3 the trace of the Uij tensor.

Table 3. Bond lengths (Å) and angles (deg) for pal36

Pd(1)-N(1)	2.100(2)	Pd(1)-P(4)	2.2528(8)
Pd(1)-S(1)	2.289(1)	Pd(1)-Cl(1)	2.3869(7)
S(1)-C(1)	1.824(3)	P(3)-N(1)	1.597(3)
P(3)-C(2)	1.799(3)	P(3)-C(1)	1.801(3)
P(3)-C(8)	1.808(3)	P(4)-C(26)	1.818(3)
P(4)-C(20)	1.825(3)	P(4)-C(32)	1.829(3)
N(1)-C(14)	1.424(4)	C(1)-H(1A)	0.9900
C(1)-H(1B)	0.9900	C(2)-C(3)	1.394(5)
C(2)-C(7)	1.398(4)	C(3)-C(4)	1.376(5)
C(3)-H(3)	0.9500	C(4)-C(5)	1.383(6)
C(4)-H(4)	0.9500	C(5)-C(6)	1.372(5)
C(5)-H(5)	0.9500	C(6)-C(7)	1.380(5)
C(6)-H(6)	0.9500	C(7)-H(7)	0.9500
C(8)-C(13)	1.388(4)	C(8)-C(9)	1.393(5)
C(9)-C(10)	1.379(5)	C(9)-H(9)	0.9500
C(10)-C(11)	1.374(5)	C(10)-H(10)	0.9500
C(11)-C(12)	1.387(5)	C(11)-H(11)	0.9500
C(12)-C(13)	1.386(4)	C(12)-H(12)	0.9500
C(13)-H(13)	0.9500	C(14)-C(15)	1.380(4)
C(14)-C(19)	1.401(5)	C(15)-C(16)	1.394(5)
C(15)-H(15)	0.9500	C(16)-C(17)	1.384(5)
C(16)-H(16)	0.9500	C(17)-C(18)	1.392(5)
C(17)-H(17)	0.9500	C(18)-C(19)	1.375(5)
C(18)-H(18)	0.9500	C(19)-H(19)	0.9500
C(20)-C(21)	1.386(4)	C(20)-C(25)	1.402(4)
C(21)-C(22)	1.393(4)	C(21)-H(21)	0.9500
C(22)-C(23)	1.386(5)	C(22)-H(22)	0.9500
C(23)-C(24)	1.371(5)	C(23)-H(23)	0.9500
C(24)-C(25)	1.382(4)	C(24)-H(24)	0.9500
C(25)-H(25)	0.9500	C(26)-C(27)	1.387(4)
C(26)-C(31)	1.387(4)	C(27)-C(28)	1.384(5)
C(27)-H(27)	0.9500	C(28)-C(29)	1.395(5)
C(28)-H(28)	0.9500	C(29)-C(30)	1.370(5)
C(29)-H(29)	0.9500	C(30)-C(31)	1.384(5)
C(30)-H(30)	0.9500	C(31)-H(31)	0.9500
C(32)-C(37)	1.369(5)	C(32)-C(33)	1.398(4)
C(33)-C(34)	1.379(4)	C(33)-H(33)	0.9500
C(34)-C(35)	1.371(5)	C(34)-H(34)	0.9500
C(35)-C(36)	1.384(5)	C(35)-H(35)	0.9500
C(36)-C(37)	1.383(5)	C(36)-H(36)	0.9500
C(37)-H(37)	0.9500		
N(1)-Pd(1)-P(4)	177.26(7)	N(1)-Pd(1)-S(1)	88.52(7)
P(4)-Pd(1)-S(1)	89.87(3)	N(1)-Pd(1)-Cl(1)	92.45(7)
P(4)-Pd(1)-Cl(1)	89.73(3)	S(1)-Pd(1)-Cl(1)	163.28(3)
C(1)-S(1)-Pd(1)	103.6(1)	N(1)-P(3)-C(2)	115.0(2)
N(1)-P(3)-C(1)	104.9(2)	C(2)-P(3)-C(1)	107.1(2)
N(1)-P(3)-C(8)	112.8(1)	C(2)-P(3)-C(8)	108.3(2)
C(1)-P(3)-C(8)	108.4(2)	C(26)-P(4)-C(20)	104.6(1)
C(26)-P(4)-C(32)	106.1(1)	C(20)-P(4)-C(32)	103.0(1)
C(26)-P(4)-Pd(1)	110.0(1)	C(20)-P(4)-Pd(1)	115.6(1)
C(32)-P(4)-Pd(1)	116.5(1)	C(14)-N(1)-P(3)	122.8(2)
C(14)-N(1)-Pd(1)	124.8(2)	P(3)-N(1)-Pd(1)	111.0(1)
P(3)-C(1)-S(1)	109.5(2)	P(3)-C(1)-H(1A)	109.8
S(1)-C(1)-H(1A)	109.8	P(3)-C(1)-H(1B)	109.8
S(1)-C(1)-H(1B)	109.8	H(1A)-C(1)-H(1B)	108.2
C(3)-C(2)-C(7)	119.5(3)	C(3)-C(2)-P(3)	120.7(3)
C(7)-C(2)-P(3)	119.8(3)	C(4)-C(3)-C(2)	120.6(4)
C(4)-C(3)-H(3)	119.7	C(2)-C(3)-H(3)	119.7
C(3)-C(4)-C(5)	119.4(4)	C(3)-C(4)-H(4)	120.3
C(5)-C(4)-H(4)	120.3	C(6)-C(5)-C(4)	120.4(4)
C(6)-C(5)-H(5)	119.8	C(4)-C(5)-H(5)	119.8
C(5)-C(6)-C(7)	121.0(4)	C(5)-C(6)-H(6)	119.5
C(7)-C(6)-H(6)	119.5	C(6)-C(7)-C(2)	119.0(3)
C(6)-C(7)-H(7)	120.5	C(2)-C(7)-H(7)	120.5

C(13)-C(8)-C(9)	118.8(3)	C(13)-C(8)-P(3)	124.3(2)
C(9)-C(8)-P(3)	116.9(3)	C(10)-C(9)-C(8)	119.9(3)
C(10)-C(9)-H(9)	120.0	C(8)-C(9)-H(9)	120.0
C(11)-C(10)-C(9)	120.8(4)	C(11)-C(10)-H(10)	119.6
C(9)-C(10)-H(10)	119.6	C(10)-C(11)-C(12)	120.2(3)
C(10)-C(11)-H(11)	119.9	C(12)-C(11)-H(11)	119.9
C(13)-C(12)-C(11)	118.9(3)	C(13)-C(12)-H(12)	120.5
C(11)-C(12)-H(12)	120.5	C(12)-C(13)-C(8)	121.3(3)
C(12)-C(13)-H(13)	119.4	C(8)-C(13)-H(13)	119.4
C(15)-C(14)-C(19)	118.7(3)	C(15)-C(14)-N(1)	123.2(3)
C(19)-C(14)-N(1)	118.1(3)	C(14)-C(15)-C(16)	120.7(3)
C(14)-C(15)-H(15)	119.7	C(16)-C(15)-H(15)	119.7
C(17)-C(16)-C(15)	120.5(4)	C(17)-C(16)-H(16)	119.8
C(15)-C(16)-H(16)	119.8	C(16)-C(17)-C(18)	118.9(4)
C(16)-C(17)-H(17)	120.6	C(18)-C(17)-H(17)	120.6
C(19)-C(18)-C(17)	120.8(4)	C(19)-C(18)-H(18)	119.6
C(17)-C(18)-H(18)	119.6	C(18)-C(19)-C(14)	120.5(4)
C(18)-C(19)-H(19)	119.7	C(14)-C(19)-H(19)	119.7
C(21)-C(20)-C(25)	119.0(3)	C(21)-C(20)-P(4)	121.9(2)
C(25)-C(20)-P(4)	119.0(2)	C(20)-C(21)-C(22)	120.2(3)
C(20)-C(21)-H(21)	119.9	C(22)-C(21)-H(21)	119.9
C(23)-C(22)-C(21)	120.1(3)	C(23)-C(22)-H(22)	119.9
C(21)-C(22)-H(22)	119.9	C(24)-C(23)-C(22)	119.8(3)
C(24)-C(23)-H(23)	120.1	C(22)-C(23)-H(23)	120.1
C(23)-C(24)-C(25)	120.9(3)	C(23)-C(24)-H(24)	119.6
C(25)-C(24)-H(24)	119.6	C(24)-C(25)-C(20)	120.0(3)
C(20)-C(25)-H(25)	120.0	C(20)-C(25)-H(25)	120.0
C(27)-C(26)-C(31)	119.2(3)	C(27)-C(26)-P(4)	117.7(2)
C(28)-C(27)-C(26)	123.0(3)	C(28)-C(27)-C(26)	120.2(3)
C(26)-C(27)-H(27)	119.9	C(26)-C(27)-H(27)	119.9
C(27)-C(28)-C(29)	119.8(4)	C(27)-C(28)-H(28)	120.1
C(29)-C(28)-H(28)	120.1	C(30)-C(29)-C(28)	120.2(3)
C(30)-C(29)-H(29)	119.9	C(28)-C(29)-H(29)	119.9
C(29)-C(30)-C(31)	119.8(3)	C(29)-C(30)-H(30)	120.1
C(31)-C(30)-H(30)	120.1	C(30)-C(31)-C(26)	120.7(3)
C(30)-C(31)-H(31)	119.6	C(26)-C(31)-H(31)	119.6
C(37)-C(32)-C(33)	118.4(3)	C(37)-C(32)-P(4)	120.8(3)
C(33)-C(32)-P(4)	120.9(2)	C(34)-C(33)-C(32)	120.8(3)
C(34)-C(33)-H(33)	119.6	C(32)-C(33)-H(33)	119.6
C(35)-C(34)-C(33)	120.6(3)	C(35)-C(34)-H(34)	119.7
C(33)-C(34)-H(34)	119.7	C(34)-C(35)-C(36)	118.6(3)
C(34)-C(35)-H(35)	120.7	C(36)-C(35)-H(35)	120.7
C(37)-C(36)-C(35)	121.0(4)	C(37)-C(36)-H(36)	119.5
C(35)-C(36)-H(36)	119.5	C(32)-C(37)-C(36)	120.6(3)
C(32)-C(37)-H(37)	119.7	C(36)-C(37)-H(37)	119.7

Appendix 1. Crystallographic data

Table 4. Anisotropic displacement parameters ($\text{\AA}^2 \times 10^3$) for pal36

atom	U11	U22	U33	U23	U13	U12
Pd(1)	25(1)	23(1)	22(1)	-1(1)	6(1)	-3(1)
C1(1)	23(1)	23(1)	18(1)	-3(1)	9(1)	-5(1)
S(1)	40(1)	37(1)	25(1)	-5(1)	13(1)	-13(1)
P(3)	27(1)	24(1)	27(1)	1(1)	8(1)	-3(1)
P(4)	23(1)	23(1)	21(1)	0(1)	4(1)	-2(1)
N(1)	26(2)	21(1)	33(2)	-4(1)	8(1)	-1(1)
C(1)	37(2)	38(2)	29(2)	0(2)	10(2)	-13(2)
C(2)	27(2)	25(2)	31(2)	-7(1)	5(2)	0(1)
C(3)	30(2)	32(2)	52(2)	-8(2)	15(2)	1(2)
C(4)	28(2)	44(2)	66(3)	-12(2)	8(2)	3(2)
C(5)	41(3)	40(2)	52(3)	-9(2)	-7(2)	12(2)
C(6)	47(3)	31(2)	37(2)	2(2)	-1(2)	1(2)
C(7)	31(2)	28(2)	30(2)	-2(2)	3(2)	-5(2)
C(8)	28(2)	24(2)	34(2)	2(1)	13(2)	-2(1)
C(9)	33(2)	37(2)	50(2)	7(2)	-1(2)	-3(2)
C(10)	48(3)	30(2)	77(3)	17(2)	2(2)	2(2)
C(11)	52(3)	25(2)	69(3)	4(2)	10(2)	-5(2)
C(12)	27(2)	30(2)	53(2)	-4(2)	10(2)	-7(2)
C(13)	29(2)	28(2)	37(2)	1(2)	6(2)	0(2)
C(14)	29(2)	22(2)	34(2)	2(1)	12(2)	-4(1)
C(15)	41(2)	31(2)	32(2)	0(2)	12(2)	5(2)
C(16)	69(3)	38(2)	35(2)	1(2)	15(2)	3(2)
C(17)	60(3)	28(2)	61(3)	-1(2)	34(2)	5(2)
C(18)	36(2)	37(2)	71(3)	-3(2)	19(2)	6(2)
C(19)	29(2)	37(2)	48(2)	-6(2)	7(2)	0(2)
C(20)	26(2)	24(2)	24(2)	-3(1)	8(2)	-7(1)
C(21)	31(2)	25(2)	26(2)	-1(1)	4(2)	0(1)
C(22)	38(2)	32(2)	35(2)	-6(2)	14(2)	1(2)
C(23)	47(2)	40(2)	24(2)	-8(2)	12(2)	-8(2)
C(24)	42(2)	34(2)	20(2)	4(2)	2(2)	-6(2)
C(25)	28(2)	27(2)	28(2)	-1(1)	2(2)	-1(1)
C(26)	30(2)	26(2)	21(2)	-1(1)	7(2)	0(1)
C(27)	30(2)	32(2)	32(2)	3(2)	2(2)	-3(2)
C(28)	41(2)	43(2)	40(2)	5(2)	-2(2)	3(2)
C(29)	56(3)	39(2)	27(2)	6(2)	-4(2)	8(2)
C(30)	57(3)	32(2)	31(2)	7(2)	3(2)	-6(2)
C(31)	30(2)	32(2)	31(2)	2(2)	2(2)	-5(2)
C(32)	25(2)	25(2)	28(2)	2(1)	7(2)	-3(1)
C(33)	30(2)	23(2)	33(2)	0(1)	7(2)	0(1)
C(34)	30(2)	26(2)	40(2)	-1(2)	-1(2)	-6(2)
C(35)	25(2)	62(3)	42(2)	-2(2)	7(2)	-13(2)
C(36)	34(3)	111(4)	47(3)	-32(3)	18(2)	-15(2)
C(37)	27(2)	79(3)	38(2)	-28(2)	11(2)	-15(2)

The anisotropic displacement factor exponent takes the form
 $2\pi^2 [h^2 a^{*2} U(11) + \dots + 2hka^* b^* U(12)]$

Appendix 1. Crystallographic data

Table 5. Hydrogen Coordinates ($\text{\AA} \times 10^4$) and equivalent isotropic displacement parameters ($\text{\AA}^2 \times 10^3$) for pal36

atom	x	y	z	U(eq)
H(1A)	6825	288	5089	41
H(1B)	5351	780	4883	41
H(3)	3168	536	3840	45
H(4)	1320	1276	3198	56
H(5)	1842	2273	2500	57
H(6)	4172	2499	2424	48
H(7)	6029	1712	3015	36
H(9)	7506	-980	4530	50
H(10)	6950	-2358	4479	65
H(11)	4851	-2823	3814	59
H(12)	3356	-1917	3121	44
H(13)	3890	-530	3182	38
H(15)	6871	128	2637	41
H(16)	8014	-757	2054	56
H(17)	10287	-1263.0001	2518	56
H(18)	11379	-895.9999	3582	56
H(19)	10237	-31	4165	46
H(21)	7572	4339	5019	33
H(22)	7149	4631	6041	41
H(23)	8132	3805	6926	44
H(24)	9537	2701	6793	40
H(25)	9995	2407	5786	34
H(27)	6291	3276	3836	38
H(28)	4968	4274	3180	51
H(29)	6114	5437	2903	52
H(30)	8564	5583	3261	49
H(31)	9873	4605	3940	38
H(33)	11243	4099	5349	35
H(34)	13657	4365	5468	40
H(35)	14950	3729	4802	52
H(36)	13770	2843	3996	75
H(37)	11362	2557	3884	57

Complex 18

Table 1. Crystal data for pa118

Compound	pa118
Molecular formula	C ₃₈ H ₃₄ N ₂ NiP ₂ S ₂
Molecular weight	703.44
Crystal habit	blue plate
Crystal dimensions(mm)	0.20x0.12x0.02
Crystal system	monoclinic
Space group	C2/c
a(Å)	12.469(1)
b(Å)	25.716(1)
c(Å)	11.930(1)
α(°)	90.00
β(°)	121.135(1)
γ(°)	90.00
V(Å ³)	3274.3(4)
Z	4
d(g·cm ⁻³)	1.427
F(000)	1464
μ(cm ⁻¹)	0.849
Absorption corrections	multi-scan ; 0.8485 min, 0.9832 max
Diffraction	KappaCCD
X-ray source	MoKα
λ(Å)	0.71069
Monochromator	graphite
T (K)	150.0(1)
Scan mode	phi and omega scans
Maximum θ	27.46
HKL ranges	-12 16 ; -33 30 ; -15 15
Reflections measured	14046
Unique data	3756
Rint	0.0294
Reflections used	3025
Criterion	I > 2σI
Refinement type	Fsqd
Hydrogen atoms	constr
Parameters refined	204
Reflections / parameter	14
wR2	0.0689
R1	0.0283
Weights a, b	0.0263 ; 1.7209
GoF	1.039
difference peak / hole (e Å ⁻³)	0.333(0.050) / -0.330(0.050)

Table 2. Atomic Coordinates (A x 10⁴) and equivalent isotropic displacement parameters (A² x 10³) for pa118

atom	x	y	z	U(eq)
Ni(1)	0	2014(1)	2500	20(1)
S(1)	1284(1)	2646(1)	2723(1)	23(1)
P(1)	2570(1)	1691(1)	3077(1)	20(1)
N(1)	1340(1)	1497(1)	3075(1)	23(1)
C(1)	2845(1)	2350(1)	3633(2)	24(1)
C(2)	2381(2)	1685(1)	1472(2)	26(1)
C(3)	1425(2)	1395(1)	491(2)	40(1)
C(4)	1308(2)	1367(1)	-731(2)	60(1)
C(5)	2142(3)	1623(1)	-967(2)	57(1)
C(6)	3098(2)	1904(1)	5(2)	49(1)
C(7)	3228(2)	1939(1)	1230(2)	35(1)
C(8)	3905(1)	1286(1)	4092(2)	21(1)
C(9)	4484(2)	1318(1)	5453(2)	26(1)
C(10)	5453(2)	984(1)	6244(2)	29(1)
C(11)	5855(2)	616(1)	5696(2)	31(1)
C(12)	5299(2)	584(1)	4347(2)	30(1)
C(13)	4324(2)	917(1)	3543(2)	26(1)
C(14)	1423(1)	1055(1)	3836(2)	25(1)
C(15)	1464(2)	555(1)	3435(2)	43(1)
C(16)	1559(2)	129(1)	4198(3)	61(1)
C(17)	1595(2)	197(1)	5358(3)	60(1)
C(18)	1553(2)	688(1)	5763(2)	53(1)
C(19)	1478(2)	1118(1)	5022(2)	36(1)

U(eq) is defined as 1/3 the trace of the Uij tensor.

Table 3. Bond lengths (Å) and angles (deg) for pall8

Ni(1)-N(1)#2	1.961(1)	Ni(1)-N(1)	1.961(1)
Ni(1)-S(1)	2.1996(5)	Ni(1)-S(1)#2	2.1996(5)
S(1)-C(1)	1.834(2)	P(1)-N(1)	1.612(1)
P(1)-C(1)	1.787(2)	P(1)-C(8)	1.800(2)
P(1)-C(2)	1.805(2)	N(1)-C(14)	1.424(2)
C(1)-H(1A)	0.9900	C(1)-H(1B)	0.9900
C(2)-C(3)	1.379(3)	C(2)-C(7)	1.393(2)
C(3)-C(4)	1.389(3)	C(3)-H(3)	0.9500
C(4)-C(5)	1.378(3)	C(4)-H(4)	0.9500
C(5)-C(6)	1.363(3)	C(5)-H(5)	0.9500
C(6)-C(7)	1.388(3)	C(6)-H(6)	0.9500
C(7)-H(7)	0.9500	C(8)-C(9)	1.397(2)
C(8)-C(13)	1.398(2)	C(9)-C(10)	1.381(2)
C(9)-H(9)	0.9500	C(10)-C(11)	1.383(2)
C(10)-H(10)	0.9500	C(11)-C(12)	1.387(2)
C(11)-H(11)	0.9500	C(12)-C(13)	1.388(2)
C(12)-H(12)	0.9500	C(13)-H(13)	0.9500
C(14)-C(15)	1.383(3)	C(14)-C(19)	1.391(2)
C(15)-C(16)	1.389(3)	C(15)-H(15)	0.9500
C(16)-C(17)	1.374(4)	C(16)-H(16)	0.9500
C(17)-C(18)	1.364(4)	C(17)-H(17)	0.9500
C(18)-C(19)	1.388(3)	C(18)-H(18)	0.9500
C(19)-H(19)	0.9500		
N(1)#2-Ni(1)-N(1)	94.61(8)	N(1)#2-Ni(1)-S(1)	168.20(4)
N(1)-Ni(1)-S(1)	91.38(4)	N(1)#2-Ni(1)-S(1)#2	91.38(4)
N(1)-Ni(1)-S(1)#2	168.20(4)	S(1)-Ni(1)-S(1)#2	84.62(2)
C(1)-S(1)-Ni(1)	104.35(5)	N(1)-P(1)-C(1)	107.16(7)
N(1)-P(1)-C(8)	111.73(7)	C(1)-P(1)-C(8)	111.47(8)
N(1)-P(1)-C(2)	113.17(8)	C(1)-P(1)-C(2)	107.27(8)
C(8)-P(1)-C(2)	106.02(7)	C(14)-N(1)-P(1)	119.4(1)
C(14)-N(1)-Ni(1)	122.2(1)	P(1)-N(1)-Ni(1)	115.35(8)
P(1)-C(1)-S(1)	103.46(8)	P(1)-C(1)-H(1A)	111.1
S(1)-C(1)-H(1A)	111.1	P(1)-C(1)-H(1B)	111.1
S(1)-C(1)-H(1B)	111.1	H(1A)-C(1)-H(1B)	109.0
C(3)-C(2)-C(7)	119.5(2)	C(3)-C(2)-P(1)	119.2(1)
C(7)-C(2)-P(1)	121.2(1)	C(2)-C(3)-C(4)	119.7(2)
C(2)-C(3)-H(3)	120.2	C(4)-C(3)-H(3)	120.2
C(5)-C(4)-C(3)	120.6(2)	C(5)-C(4)-H(4)	119.7
C(3)-C(4)-H(4)	119.7	C(6)-C(5)-C(4)	120.0(2)
C(6)-C(5)-H(5)	120.0	C(4)-C(5)-H(5)	120.0
C(5)-C(6)-C(7)	120.3(2)	C(5)-C(6)-H(6)	119.9
C(7)-C(6)-H(6)	119.9	C(6)-C(7)-C(2)	120.0(2)
C(6)-C(7)-H(7)	120.0	C(2)-C(7)-H(7)	120.0
C(9)-C(8)-C(13)	119.4(2)	C(9)-C(8)-P(1)	119.3(1)
C(13)-C(8)-P(1)	121.1(1)	C(10)-C(9)-C(8)	120.1(2)
C(10)-C(9)-H(9)	120.0	C(8)-C(9)-H(9)	120.0
C(9)-C(10)-C(11)	120.4(2)	C(9)-C(10)-H(10)	119.8
C(11)-C(10)-H(10)	119.8	C(10)-C(11)-C(12)	120.2(2)
C(10)-C(11)-H(11)	119.9	C(12)-C(11)-H(11)	119.9
C(11)-C(12)-C(13)	119.9(2)	C(11)-C(12)-H(12)	120.0
C(13)-C(12)-H(12)	120.0	C(12)-C(13)-C(8)	120.0(2)
C(12)-C(13)-H(13)	120.0	C(8)-C(13)-H(13)	120.0
C(15)-C(14)-C(19)	118.0(2)	C(15)-C(14)-N(1)	121.7(2)
C(19)-C(14)-N(1)	120.3(2)	C(14)-C(15)-C(16)	120.9(2)
C(14)-C(15)-H(15)	119.6	C(16)-C(15)-H(15)	119.6
C(17)-C(16)-C(15)	120.5(2)	C(17)-C(16)-H(16)	119.8
C(15)-C(16)-H(16)	119.8	C(18)-C(17)-C(16)	119.2(2)
C(18)-C(17)-H(17)	120.4	C(16)-C(17)-H(17)	120.4
C(17)-C(18)-C(19)	121.0(2)	C(17)-C(18)-H(18)	119.5
C(19)-C(18)-H(18)	119.5	C(18)-C(19)-C(14)	120.5(2)
C(18)-C(19)-H(19)	119.8	C(14)-C(19)-H(19)	119.8

Estimated standard deviations are given in the parenthesis.

Symmetry operators ::
 1: x, y, z
 2: -x, y, -z+1/2
 3: x+1/2, y+1/2, z
 4: -x+1/2, y+1/2, -z+1/2
 5: -x, -y, -z
 6: x, -y, z-1/2
 7: -x+1/2, -y+1/2, -z
 8: x+1/2, -y+1/2, z-1/2

Appendix 1. Crystallographic data

Table 4. Anisotropic displacement parameters ($\text{\AA}^2 \times 10^3$) for pall18

atom	U11	U22	U33	U23	U13	U12
Ni(1)	18(1)	20(1)	23(1)	0	12(1)	0
S(1)	22(1)	22(1)	26(1)	1(1)	14(1)	0(1)
P(1)	19(1)	24(1)	21(1)	-1(1)	12(1)	0(1)
N(1)	20(1)	22(1)	31(1)	4(1)	15(1)	1(1)
C(1)	21(1)	25(1)	27(1)	-1(1)	14(1)	-2(1)
C(2)	27(1)	28(1)	24(1)	3(1)	15(1)	9(1)
C(3)	41(1)	45(1)	28(1)	-3(1)	14(1)	3(1)
C(4)	79(2)	59(2)	27(1)	-7(1)	17(1)	10(1)
C(5)	93(2)	55(2)	33(1)	12(1)	40(1)	33(1)
C(6)	67(2)	53(2)	52(1)	24(1)	49(1)	32(1)
C(7)	36(1)	42(1)	37(1)	10(1)	25(1)	11(1)
C(8)	18(1)	23(1)	26(1)	1(1)	13(1)	-1(1)
C(9)	23(1)	29(1)	27(1)	-2(1)	14(1)	1(1)
C(10)	26(1)	36(1)	25(1)	2(1)	13(1)	2(1)
C(11)	25(1)	31(1)	34(1)	7(1)	14(1)	5(1)
C(12)	30(1)	28(1)	37(1)	-1(1)	21(1)	4(1)
C(13)	27(1)	28(1)	26(1)	-2(1)	16(1)	0(1)
C(14)	16(1)	25(1)	34(1)	4(1)	13(1)	1(1)
C(15)	51(1)	28(1)	70(2)	3(1)	46(1)	4(1)
C(16)	59(2)	27(1)	120(2)	20(1)	63(2)	12(1)
C(17)	37(1)	57(2)	87(2)	46(2)	35(1)	16(1)
C(18)	41(1)	73(2)	36(1)	25(1)	14(1)	1(1)
C(19)	32(1)	42(1)	28(1)	4(1)	11(1)	-4(1)

The anisotropic displacement factor exponent takes the form
 $2 \pi^2 [h^2 a^{*2} U(11) + \dots + 2 h k a^* b^* U(12)]$

Appendix 1. Crystallographic data

Table 5. Hydrogen Coordinates ($\text{\AA} \times 10^4$) and equivalent isotropic displacement parameters ($\text{\AA}^2 \times 10^3$) for pall18

atom	x	y	z	U(eq)
H(1A)	3430	2523	3425	29
H(1B)	3192	2369	4589	29
H(3)	850	1216	649	48
H(4)	647	1169	-1409	72
H(5)	2050	1605	-1808	68
H(6)	3678	2077	-157	59
H(7)	3894	2136	1904	42
H(9)	4212	1570	5835	31
H(10)	5845	1008	7169	35
H(11)	6515	385	6246	37
H(12)	5583	334	3974	36
H(13)	3941	895	2619	31
H(15)	1427	501	2628	52
H(16)	1599	-212	3914	73
H(17)	1648	-95	5873	71
H(18)	1575	737	6564	64
H(19)	1465	1456	5328	43

Chapter 2

Complex 24a

Table 1. Crystal data for pa209

Compound	pa209
Molecular formula	C ₃₀ H ₃₉ Br ₂ LiNNiO ₃ P ₄ C ₄ H ₈ O
Molecular weight	790.17
Crystal habit	Blue Block
Crystal dimensions(mm)	0.28x0.20x0.18
Crystal system	monoclinic
Space group	P2 ₁ /c
a(Å)	9.169(1)
b(Å)	23.772(1)
c(Å)	18.710(1)
α(°)	90.00
β(°)	118.751(3)
γ(°)	90.00
V(Å ³)	3575.4(5)
Z	4
d(g·cm ⁻³)	1.468
F(000)	1624
μ(cm ⁻¹)	2.859
Absorption corrections	multi-scan ; 0.5016 min, 0.6272 max
Diffractometer	KappaCCD
X-ray source	MoKα
λ(Å)	0.71069
Monochromator	graphite
T (K)	150.0(1)
Scan mode	phi and omega scans
Maximum θ	27.48
HKL ranges	-9 11 ; -30 30 ; -24 22
Reflections measured	19718
Unique data	8125
Rint	0.0338
Reflections used	5770
Criterion	I > 2σ(I)
Refinement type	Fsqd
Hydrogen atoms	constr
Parameters refined	400
Reflections / parameter	14
wR2	0.1014
R1	0.0389
Weights a, b	0.0467 ; 0.3463
GoF	1.041
difference peak / hole (e Å ⁻³)	0.989(0.075) / -0.554(0.075)

Table 2. Atomic Coordinates (A x 10⁴) and equivalent isotropic displacement parameters (A² x 10³) for pa209

atom	x	y	z	U(eq)
Br (1)	-7289 (1)	-2595 (1)	2740 (1)	42 (1)
Br (2)	-3219 (1)	-2283 (1)	2708 (1)	43 (1)
Ni (1)	-5837 (1)	-1875 (1)	2382 (1)	31 (1)
P (1)	-7228 (1)	-723 (1)	1708 (1)	25 (1)
O (1)	-7473 (2)	-1930 (1)	1228 (1)	33 (1)
O (2)	-8232 (3)	-3237 (1)	703 (1)	46 (1)
O (3)	-11016 (3)	-2546 (1)	692 (1)	42 (1)
N (1)	-5864 (3)	-1049 (1)	2498 (1)	26 (1)
C (1)	-7465 (3)	-1586 (1)	667 (2)	28 (1)
C (2)	-7654 (4)	-1797 (1)	-70 (2)	33 (1)
C (3)	-7656 (4)	-1442 (1)	-654 (2)	37 (1)
C (4)	-7476 (4)	-867 (1)	-521 (2)	35 (1)
C (5)	-7313 (3)	-649 (1)	195 (2)	30 (1)
C (6)	-7298 (3)	-998 (1)	801 (2)	25 (1)
C (7)	-6894 (3)	27 (1)	1685 (2)	27 (1)
C (8)	-8048 (4)	426 (1)	1634 (2)	34 (1)
C (9)	-7703 (4)	998 (1)	1643 (2)	41 (1)
C (10)	-6228 (4)	1176 (1)	1701 (2)	38 (1)
C (11)	-5068 (4)	781 (1)	1745 (2)	35 (1)
C (12)	-5396 (4)	213 (1)	1734 (2)	30 (1)
C (13)	-9328 (3)	-809 (1)	1562 (2)	27 (1)
C (14)	-9548 (4)	-1048 (1)	2186 (2)	33 (1)
C (15)	-11121 (4)	-1117 (1)	2093 (2)	41 (1)
C (16)	-12497 (4)	-949 (1)	1380 (2)	40 (1)
C (17)	-12301 (4)	-719 (1)	761 (2)	42 (1)
C (18)	-10717 (4)	-653 (1)	845 (2)	36 (1)
C (19)	-4859 (4)	-824 (1)	3357 (2)	30 (1)
C (20)	-3143 (4)	-657 (1)	3496 (2)	43 (1)
C (21)	-5671 (4)	-329 (1)	3555 (2)	46 (1)
C (22)	-4656 (4)	-1305 (1)	3942 (2)	40 (1)
C (23)	-9304 (5)	-3419 (2)	-119 (2)	61 (1)
C (24)	-8171 (6)	-3637 (2)	-419 (3)	86 (2)
C (25)	-6776 (6)	-3889 (2)	334 (3)	72 (1)
C (26)	-6649 (5)	-3514 (2)	1010 (2)	60 (1)
C (27)	-11904 (4)	-2182 (2)	1 (2)	52 (1)
C (28)	-13654 (4)	-2128 (2)	-131 (2)	50 (1)
C (29)	-13653 (4)	-2466 (2)	557 (2)	50 (1)
C (30)	-11846 (4)	-2507 (1)	1178 (2)	44 (1)
Li (1)	-8641 (7)	-2594 (2)	1198 (3)	38 (1)
O (4)	-50 (6)	-4011 (2)	1990 (3)	149 (2)
C (31)	-1730 (7)	-4048 (2)	1245 (3)	117 (2)
C (32)	-1898 (6)	-4503 (2)	770 (2)	69 (1)
C (33)	-543 (8)	-4778 (3)	1097 (4)	128 (2)
C (34)	510 (7)	-4624 (2)	1996 (4)	127 (2)

U(eq) is defined as 1/3 the trace of the U_{ij} tensor.

Table 3. Bond lengths (Å) and angles (deg) for pa209

Br(1)-Ni(1)	2.4526(5)	Br(1)-Li(1)	2.535(5)
Br(2)-Ni(1)	2.3799(5)	Ni(1)-O(1)	1.954(2)
Ni(1)-N(1)	1.977(2)	Ni(1)-Li(1)	2.994(5)
P(1)-N(1)	1.602(2)	P(1)-C(6)	1.792(3)
P(1)-C(7)	1.813(3)	P(1)-C(13)	1.822(3)
O(1)-C(1)	1.332(3)	O(1)-Li(1)	1.893(5)
O(2)-C(23)	1.437(4)	O(2)-C(26)	1.439(4)
O(2)-Li(1)	1.915(6)	O(3)-C(27)	1.439(4)
O(3)-C(30)	1.441(4)	O(3)-Li(1)	1.915(6)
N(1)-C(19)	1.515(3)	C(1)-C(2)	1.398(4)
C(1)-C(6)	1.415(4)	C(2)-C(3)	1.381(4)
C(2)-H(2)	0.9500	C(3)-C(4)	1.384(4)
C(3)-H(3)	0.9500	C(4)-C(5)	1.376(4)
C(4)-H(4)	0.9500	C(5)-C(6)	1.400(4)
C(5)-H(5)	0.9500	C(7)-C(8)	1.389(4)
C(7)-C(12)	1.403(4)	C(8)-C(9)	1.396(4)
C(8)-H(8)	0.9500	C(9)-C(10)	1.371(4)
C(9)-H(9)	0.9500	C(10)-C(11)	1.392(4)
C(10)-H(10)	0.9500	C(11)-C(12)	1.382(4)
C(11)-H(11)	0.9500	C(12)-H(12)	0.9500
C(13)-C(18)	1.384(4)	C(13)-C(14)	1.398(4)
C(14)-C(15)	1.377(4)	C(14)-H(14)	0.9500
C(15)-C(16)	1.382(5)	C(15)-H(15)	0.9500
C(16)-C(17)	1.369(5)	C(16)-H(16)	0.9500
C(17)-C(18)	1.394(4)	C(17)-H(17)	0.9500
C(18)-H(18)	0.9500	C(19)-C(20)	1.519(4)
C(19)-C(21)	1.531(4)	C(19)-C(22)	1.533(4)
C(20)-H(20A)	0.9800	C(20)-H(20B)	0.9800
C(20)-H(20C)	0.9800	C(21)-H(21A)	0.9800
C(21)-H(21B)	0.9800	C(21)-H(21C)	0.9800
C(22)-H(22A)	0.9800	C(22)-H(22B)	0.9800
C(22)-H(22C)	0.9800	C(23)-C(24)	1.491(5)
C(23)-H(23A)	0.9900	C(23)-H(23B)	0.9900
C(24)-C(25)	1.499(6)	C(24)-H(24A)	0.9900
C(24)-H(24B)	0.9900	C(25)-C(26)	1.504(5)
C(25)-H(25A)	0.9900	C(25)-H(25B)	0.9900
C(26)-H(26A)	0.9900	C(26)-H(26B)	0.9900
C(27)-C(28)	1.507(5)	C(27)-H(27A)	0.9900
C(27)-H(27B)	0.9900	C(28)-C(29)	1.516(5)
C(28)-H(28A)	0.9900	C(28)-H(28B)	0.9900
C(29)-C(30)	1.500(5)	C(29)-H(29A)	0.9900
C(29)-H(29B)	0.9900	C(30)-H(30A)	0.9900
C(30)-H(30B)	0.9900	O(4)-C(31)	1.503(6)
O(4)-C(34)	1.544(7)	C(31)-C(32)	1.362(6)
C(31)-H(31A)	0.9900	C(31)-H(31B)	0.9900
C(32)-C(33)	1.271(7)	C(32)-H(32A)	0.9900
C(32)-H(32B)	0.9900	C(33)-C(34)	1.528(8)
C(33)-H(33A)	0.9900	C(33)-H(33B)	0.9900
C(34)-H(34A)	0.9900	C(34)-H(34B)	0.9900
Ni(1)-Br(1)-Li(1)	73.8(1)	O(1)-Ni(1)-N(1)	98.30(8)
O(1)-Ni(1)-Br(2)	113.52(6)	N(1)-Ni(1)-Br(2)	116.17(7)
O(1)-Ni(1)-Br(1)	91.47(6)	N(1)-Ni(1)-Br(1)	128.82(7)
Br(2)-Ni(1)-Br(1)	104.99(2)	O(1)-Ni(1)-Li(1)	38.2(1)
N(1)-Ni(1)-Li(1)	126.6(1)	Br(2)-Ni(1)-Li(1)	111.0(1)
Br(1)-Ni(1)-Li(1)	54.4(1)	N(1)-P(1)-C(6)	110.7(1)
N(1)-P(1)-C(7)	115.6(1)	C(6)-P(1)-C(7)	105.4(1)
N(1)-P(1)-C(13)	112.6(1)	C(6)-P(1)-C(13)	105.3(1)
C(7)-P(1)-C(13)	106.6(1)	C(1)-O(1)-Li(1)	134.9(2)
C(1)-O(1)-Ni(1)	122.5(2)	Li(1)-O(1)-Ni(1)	102.2(2)
C(23)-O(2)-C(26)	109.2(3)	C(23)-O(2)-Li(1)	124.4(3)
C(26)-O(2)-Li(1)	124.6(3)	C(27)-O(3)-C(30)	106.6(2)
C(27)-O(3)-Li(1)	119.8(3)	C(30)-O(3)-Li(1)	120.8(2)
C(19)-N(1)-P(1)	127.9(2)	C(19)-N(1)-Ni(1)	115.7(2)
P(1)-N(1)-Ni(1)	115.1(1)	O(1)-C(1)-C(2)	120.8(2)

O(1)-C(1)-C(6)	120.6(2)	C(2)-C(1)-C(6)	118.6(3)
C(3)-C(2)-C(1)	121.0(3)	C(3)-C(2)-H(2)	119.5
C(1)-C(2)-H(2)	119.5	C(2)-C(3)-C(4)	120.4(3)
C(2)-C(3)-H(3)	119.8	C(4)-C(3)-H(3)	119.8
C(5)-C(4)-C(3)	119.6(3)	C(5)-C(4)-H(4)	120.2
C(3)-C(4)-H(4)	120.2	C(4)-C(5)-C(6)	121.3(3)
C(4)-C(5)-H(5)	119.3	C(6)-C(5)-H(5)	119.3
C(5)-C(6)-C(1)	119.0(2)	C(5)-C(6)-P(1)	122.2(2)
C(1)-C(6)-P(1)	118.7(2)	C(8)-C(7)-C(12)	118.6(2)
C(8)-C(7)-P(1)	122.7(2)	C(12)-C(7)-P(1)	118.7(2)
C(7)-C(8)-C(9)	120.3(3)	C(7)-C(8)-H(8)	119.9
C(9)-C(8)-H(8)	119.9	C(10)-C(9)-C(8)	120.7(3)
C(10)-C(9)-H(9)	119.6	C(8)-C(9)-H(9)	119.6
C(9)-C(10)-C(11)	119.6(3)	C(9)-C(10)-H(10)	120.2
C(11)-C(10)-H(10)	120.2	C(12)-C(11)-C(10)	120.3(3)
C(12)-C(11)-H(11)	119.9	C(10)-C(11)-H(11)	119.9
C(11)-C(12)-C(7)	120.5(3)	C(11)-C(12)-H(12)	119.7
C(7)-C(12)-H(12)	119.7	C(18)-C(13)-C(14)	119.0(3)
C(18)-C(13)-P(1)	121.9(2)	C(14)-C(13)-P(1)	119.1(2)
C(15)-C(14)-C(13)	120.4(3)	C(15)-C(14)-H(14)	119.8
C(13)-C(14)-H(14)	119.8	C(14)-C(15)-C(16)	120.2(3)
C(14)-C(15)-H(15)	119.9	C(16)-C(15)-H(15)	119.9
C(17)-C(16)-C(15)	120.1(3)	C(17)-C(16)-H(16)	120.0
C(15)-C(16)-H(16)	120.0	C(16)-C(17)-H(17)	119.9
C(13)-C(18)-C(17)	120.1(3)	C(13)-C(18)-H(18)	119.9
C(17)-C(18)-H(18)	119.9	N(1)-C(19)-C(20)	109.0(2)
N(1)-C(19)-C(21)	114.2(2)	C(20)-C(19)-C(21)	110.0(3)
N(1)-C(19)-C(22)	107.3(2)	C(20)-C(19)-C(22)	108.2(2)
C(21)-C(19)-C(22)	107.9(2)	C(19)-C(20)-H(20A)	109.5
C(19)-C(20)-H(20B)	109.5	H(20A)-C(20)-H(20B)	109.5
C(19)-C(20)-H(20C)	109.5	H(20A)-C(20)-H(20C)	109.5
H(20B)-C(20)-H(20C)	109.5	C(19)-C(21)-H(21A)	109.5
C(19)-C(21)-H(21B)	109.5	H(21A)-C(21)-H(21B)	109.5
C(19)-C(21)-H(21C)	109.5	H(21A)-C(21)-H(21C)	109.5
H(21B)-C(21)-H(21C)	109.5	C(19)-C(22)-H(22A)	109.5
C(19)-C(22)-H(22B)	109.5	H(22A)-C(22)-H(22B)	109.5
C(19)-C(22)-H(22C)	109.5	H(22A)-C(22)-H(22C)	109.5
H(22B)-C(22)-H(22C)	109.5	O(2)-C(23)-C(24)	105.4(3)
O(2)-C(23)-H(23A)	110.7	C(24)-C(23)-H(23A)	110.7
O(2)-C(23)-H(23B)	110.7	C(24)-C(23)-H(23B)	110.7
H(23A)-C(23)-H(23B)	108.8	C(23)-C(24)-C(25)	102.6(3)
C(23)-C(24)-H(24A)	111.2	C(25)-C(24)-H(24A)	111.2
C(23)-C(24)-H(24B)	111.2	C(25)-C(24)-H(24B)	111.2
H(24A)-C(24)-H(24B)	109.2	C(24)-C(25)-C(26)	103.9(3)
C(24)-C(25)-H(25A)	111.0	C(1)-C(25)-H(25A)	111.0
C(24)-C(25)-H(25B)	111.0	C(26)-C(25)-H(25B)	111.0
H(25A)-C(25)-H(25B)	109.0	O(2)-C(26)-C(25)	106.3(3)
O(2)-C(26)-H(26A)	110.5	C(25)-C(26)-H(26A)	110.5
O(2)-C(26)-H(26B)	110.5	C(25)-C(26)-H(26B)	110.5
H(26A)-C(26)-H(26B)	108.7	O(3)-C(27)-C(28)	107.2(3)
O(3)-C(27)-H(27A)	110.3	C(28)-C(27)-H(27A)	110.3
O(3)-C(27)-H(27B)	110.3	C(28)-C(27)-H(27B)	110.3
H(27A)-C(27)-H(27B)	108.5	C(27)-C(28)-C(29)	104.5(3)
C(27)-C(28)-H(28A)	110.9	C(29)-C(28)-H(28A)	110.9
C(27)-C(28)-H(28B)	110.9	C(29)-C(28)-H(28B)	110.9
H(28A)-C(28)-H(28B)	108.9	C(30)-C(29)-C(28)	104.0(3)
C(30)-C(29)-H(29A)	111.0	C(28)-C(29)-H(29A)	111.0
C(30)-C(29)-H(29B)	111.0	C(28)-C(29)-H(29B)	111.0
H(29A)-C(29)-H(29B)	109.0	O(3)-C(30)-C(29)	103.8(3)
O(3)-C(30)-H(30A)	111.0	C(29)-C(30)-H(30A)	111.0
O(3)-C(30)-H(30B)	111.0	C(29)-C(30)-H(30B)	111.0
H(30A)-C(30)-H(30B)	109.0	O(1)-Li(1)-O(3)	117.3(3)
O(1)-Li(1)-O(2)	116.1(3)	O(3)-Li(1)-O(2)	104.4(3)
O(1)-Li(1)-Br(1)	90.4(2)	O(3)-Li(1)-Br(1)	112.3(2)
O(2)-Li(1)-Br(1)	116.5(2)	O(1)-Li(1)-Ni(1)	39.6(1)
O(2)-Li(1)-Ni(1)	134.4(2)	O(2)-Li(1)-Ni(1)	121.0(2)
Br(1)-Li(1)-Ni(1)	51.9(1)	C(31)-O(4)-C(34)	98.1(4)

Appendix 1. Crystallographic data

C(32)-C(31)-O(4)	113.3(5)	C(32)-C(31)-H(31A)	108.9
O(4)-C(31)-H(31A)	108.9	C(32)-C(31)-H(31B)	108.9
O(4)-C(31)-H(31B)	108.9	H(31A)-C(31)-H(31B)	107.7
C(33)-C(32)-C(31)	108.5(4)	C(33)-C(32)-H(32A)	110.0
C(31)-C(32)-H(32A)	110.0	C(33)-C(32)-H(32B)	110.0
C(31)-C(32)-H(32B)	110.0	H(32A)-C(32)-H(32B)	108.4
C(32)-C(33)-C(34)	111.1(5)	C(32)-C(33)-H(33A)	109.4
C(34)-C(33)-H(33A)	109.4	C(32)-C(33)-H(33B)	109.4
C(34)-C(33)-H(33B)	109.4	H(33A)-C(33)-H(33B)	108.0
C(33)-C(34)-O(4)	100.8(4)	C(33)-C(34)-H(34A)	111.6
O(4)-C(34)-H(34A)	111.6	C(33)-C(34)-H(34B)	111.6
O(4)-C(34)-H(34B)	111.6	H(34A)-C(34)-H(34B)	109.4

Appendix 1. Crystallographic data

Table 4. Anisotropic displacement parameters ($\text{\AA}^2 \times 10^3$) for pa209

atom	U11	U22	U33	U23	U13	U12
Br(1)	35(1)	52(1)	30(1)	11(1)	9(1)	-8(1)
Br(2)	40(1)	44(1)	49(1)	5(1)	26(1)	3(1)
Ni(1)	33(1)	27(1)	26(1)	4(1)	9(1)	0(1)
P(1)	23(1)	25(1)	25(1)	1(1)	12(1)	1(1)
O(1)	40(1)	28(1)	24(1)	3(1)	10(1)	-3(1)
O(2)	38(1)	45(1)	43(1)	-12(1)	10(1)	0(1)
O(3)	34(1)	53(1)	34(1)	2(1)	11(1)	6(1)
N(1)	26(1)	26(1)	22(1)	-1(1)	9(1)	0(1)
C(1)	23(1)	30(2)	28(2)	2(1)	9(1)	2(1)
C(2)	35(2)	30(2)	28(2)	-3(1)	11(1)	6(1)
C(3)	39(2)	46(2)	25(2)	-1(1)	15(1)	12(2)
C(4)	37(2)	44(2)	28(2)	9(1)	18(1)	7(1)
C(5)	27(2)	32(2)	28(2)	4(1)	11(1)	4(1)
C(6)	21(1)	28(1)	24(2)	3(1)	9(1)	4(1)
C(7)	30(2)	27(1)	24(2)	-1(1)	14(1)	0(1)
C(8)	31(2)	33(2)	39(2)	2(1)	18(1)	2(1)
C(9)	42(2)	28(2)	53(2)	3(2)	22(2)	5(1)
C(10)	46(2)	29(2)	35(2)	0(1)	17(2)	-5(1)
C(11)	37(2)	35(2)	31(2)	1(1)	16(1)	-7(1)
C(12)	31(2)	30(1)	30(2)	1(1)	15(1)	1(1)
C(13)	28(2)	23(1)	31(2)	0(1)	16(1)	2(1)
C(14)	33(2)	37(2)	29(2)	-2(1)	16(1)	-3(1)
C(15)	44(2)	47(2)	44(2)	-2(2)	30(2)	-8(2)
C(16)	31(2)	34(2)	63(2)	-7(2)	30(2)	-1(1)
C(17)	25(2)	36(2)	57(2)	6(2)	15(2)	1(1)
C(18)	32(2)	33(2)	41(2)	10(2)	16(2)	3(1)
C(19)	31(2)	33(2)	21(2)	0(1)	8(1)	-2(1)
C(20)	33(2)	52(2)	34(2)	1(2)	9(2)	-8(2)
C(21)	51(2)	47(2)	31(2)	-11(2)	12(2)	3(2)
C(22)	49(2)	43(2)	25(2)	-2(1)	16(2)	-6(2)
C(23)	51(2)	69(2)	44(2)	-22(2)	8(2)	0(2)
C(24)	93(4)	106(4)	58(3)	-8(3)	35(3)	33(3)
C(25)	79(3)	79(3)	65(3)	1(2)	39(3)	26(2)
C(26)	41(2)	69(2)	57(2)	-1(2)	15(2)	9(2)
C(27)	49(2)	65(2)	38(2)	7(2)	16(2)	12(2)
C(28)	41(2)	51(2)	40(2)	-8(2)	5(2)	2(2)
C(29)	35(2)	59(2)	50(2)	-5(2)	15(2)	2(2)
C(30)	42(2)	45(2)	44(2)	1(2)	20(2)	4(2)
Li(1)	37(3)	38(3)	34(3)	-2(2)	12(2)	-3(2)
O(4)	117(4)	157(4)	148(4)	-6(3)	44(3)	12(3)
C(31)	105(4)	78(3)	81(4)	-12(3)	-25(3)	23(3)
C(32)	80(3)	64(3)	38(2)	-5(2)	8(2)	-16(2)
C(33)	81(4)	145(6)	135(6)	-81(5)	34(4)	-21(4)
C(34)	65(3)	111(5)	161(6)	49(4)	20(4)	52(3)

The anisotropic displacement factor exponent takes the form
 $2 \pi^2 [h^2 a^{*2} U(11) + \dots + 2 h k a^* b^* U(12)]$

Table 5. Hydrogen Coordinates ($\text{\AA} \times 10^4$) and equivalent isotropic displacement parameters ($\text{\AA}^2 \times 10^3$) for pa209

atom	x	y	z	U(eq)
H(2)	-7783	-2190	-170.0000	39
H(3)	-7781.9995	-1593	-1151	44
H(4)	-7465	-624	-922.0001	42
H(5)	-7208	-254	280	36
H(8)	-9077	308	1592	41
H(9)	-8500	1267	1609	50
H(10)	-6000	1567	1712	46
H(11)	-4047	903	1782	42
H(12)	-4601	-54	1759	36
H(14)	-8606	-1162	2678	39
H(15)	-11260.9990	-1282	2518	49
H(16)	-13580	-993	1320	48
H(17)	-13250	-604	272	50
H(18)	-10589	-500	409	43
H(20A)	-2643	-974	3356	64
H(20B)	-2439	-557	4071	64
H(20C)	-3239.0002	-333	3153	64
H(21A)	-5695.0005	0	3233	69
H(21B)	-5029	-239	4137	69
H(21C)	-6810	-429	3422	69
H(22A)	-5756.0005	-1437	3836	60
H(22B)	-4032	-1172	4506	60
H(22C)	-4052	-1615.9999	3859	60
H(23A)	-9976	-3101	-460	73
H(23B)	-10065	-3719	-130	73
H(24A)	-7768	-3328.9998	-635	103
H(24B)	-8731	-3924	-849	103
H(25A)	-5727	-3886	305	87
H(25B)	-7037	-4280	413	87
H(26A)	-6408	-3740.0002	1499	72
H(26B)	-5748	-3235	1158	72
H(27A)	-11913	-2343	-488	63
H(27B)	-11364	-1808	109	63
H(28A)	-14466	-2284	-666.9999	60
H(28B)	-13936	-1729.0001	-103	60
H(29A)	-14290	-2270	785	60
H(29B)	-14138	-2843.9998	366	60
H(30A)	-11478	-2169	1530	53
H(30B)	-11629	-2845	1523	53
H(31A)	-2594	-4064	1418	141
H(31B)	-1922	-3702	917	141
H(32A)	-2822	-4743	721	83
H(32B)	-2152	-4379	217	83
H(33A)	93	-4698	806	154
H(33B)	-791	-5186	1049	154
H(34A)	1715	-4647	2174	152
H(34B)	250	-4866	2350	152

Complex 24b'

Table 1. Crystal data for pa278

Compound	pa278
Molecular formula	$\text{C}_{35}\text{H}_{49}\text{Br}_{1.70}\text{Cl}_{0.31}\text{LiNiO}_4\text{P}$
Molecular weight	790.63
Crystal habit	Blue Block
Crystal dimensions(mm)	0.28x0.14x0.10
Crystal system	monoclinic
Space group	$P2_1/c$
a(\AA)	9.793(1)
b(\AA)	17.973(1)
c(\AA)	22.786(1)
α ($^\circ$)	90.00
β ($^\circ$)	114.646(3)
γ ($^\circ$)	90.00
V(\AA^3)	3645.2(5)
Z	4
d(g·cm $^{-3}$)	1.441
F(000)	1634
μ (cm $^{-1}$)	2.493
Absorption corrections	multi-scan ; 0.5419 min, 0.7886 max
Diffractometer	KappaCCD
X-ray source	MoK α
λ (\AA)	0.71069
Monochromator	graphite
T (K)	150.0(1)
Scan mode	phi and omega scans
Maximum θ	27.46
HKL ranges	-12 8 ; -17 23 ; -19 29
Reflections measured	18906
Unique data	8073
Rint	0.0453
Reflections used	6116
Criterion	$I > 2\sigma(I)$
Refinement type	Fsqd
Hydrogen atoms	constr
Parameters refined	417
Reflections / parameter	14
wR2	0.1001
R1	0.0500
Weights a, b	0.0262 ; 7.8434
GoF	1.091
difference peak / hole (e \AA^{-3})	0.584(0.083) / -0.427(0.083)

Appendix 1. Crystallographic data

Table 2. Atomic Coordinates ($\text{\AA} \times 10^4$) and equivalent isotropic displacement parameters ($\text{\AA}^2 \times 10^3$) for pa278

atom	x	y	z	U(eq)
Br(1A)	-1094(1)	-2664(1)	-2592(1)	43(1)
Cl(1B)	-660(30)	-2560(10)	-2490(10)	43(1)
Br(2A)	3187(2)	-1972(1)	-2420(1)	41(1)
Cl(2B)	3350(20)	-2123(8)	-2433(8)	41(1)
Ni(1)	993(1)	-2724(1)	-2885(1)	26(1)
P(1)	413(1)	-3491(1)	-4150(1)	21(1)
O(1)	1591(3)	-3781(1)	-2727(1)	28(1)
O(2)	3563(3)	-5082(2)	-1660(1)	47(1)
O(3)	3147(3)	-3621(1)	-1157(1)	36(1)
O(4)	5224(3)	-3795(2)	-1905(1)	51(1)
N(1)	324(3)	-2703(1)	-3834(1)	23(1)
C(1)	-152(4)	-4224(2)	-3765(2)	23(1)
C(2)	525(4)	-4264(2)	-3080(2)	27(1)
C(3)	52(4)	-4835(2)	-2787(2)	33(1)
C(4)	-1022(4)	-5345(2)	-3148(2)	34(1)
C(5)	-1667(4)	-5306(2)	-3818(2)	31(1)
C(6)	-1224(4)	-4753(2)	-4122(2)	27(1)
C(7)	-830(4)	-3519(2)	-5006(2)	24(1)
C(8)	-2383(4)	-3447(2)	-5193(2)	29(1)
C(9)	-3352(4)	-3432(2)	-5841(2)	35(1)
C(10)	-2797(5)	-3468(2)	-6308(2)	39(1)
C(11)	-1277(5)	-3541(2)	-6131(2)	38(1)
C(12)	-283(4)	-3572(2)	-5477(2)	29(1)
C(13)	2258(4)	-3717(2)	-4107(2)	27(1)
C(14)	2657(4)	-4449(2)	-4182(2)	34(1)
C(15)	4063(5)	-4593(2)	-4168(2)	43(1)
C(16)	5075(4)	-4026(2)	-4085(2)	39(1)
C(17)	4698(4)	-3309(2)	-4007(2)	38(1)
C(18)	3303(4)	-3152(2)	-4016(2)	34(1)
C(19)	471(4)	-2015(2)	-4168(2)	26(1)
C(20)	-677(4)	-1402(2)	-4238(2)	28(1)
C(21)	-2270(4)	-1702(2)	-4567(2)	38(1)
C(22)	-417(4)	-1059(2)	-3589(2)	34(1)
C(23)	-435(5)	-799(2)	-4663(2)	39(1)
C(24)	3581(6)	-2086(2)	-5678(2)	59(1)
C(25)	4435(7)	-6292(3)	-1660(3)	80(2)
C(26)	5390(8)	-5956(4)	-1052(3)	88(2)
C(27)	4601(5)	-5254(2)	-1015(2)	49(1)
C(28)	1779(5)	-3731(2)	-1080(2)	44(1)
C(29)	1574(5)	-3068(2)	-722(2)	44(1)
C(30)	2572(5)	-2478(2)	-829(2)	43(1)
C(31)	3831(5)	-2938(2)	-846(2)	41(1)
C(32)	6692(5)	-3721(3)	-1415(2)	55(1)
C(33)	7664(6)	-4190(4)	-1623(3)	79(2)
C(34)	6783(6)	-4323(3)	-2330(2)	57(1)
C(35)	5420(6)	-3833(4)	-2492(2)	70(2)
Li(1)	3286(7)	-4010(3)	-1928(3)	33(1)

U(eq) is defined as 1/3 the trace of the Uij tensor.

Appendix 1. Crystallographic data

Table 3. Bond lengths (\AA) and angles (deg) for pa278

Br(1A)-Ni(1)	2.4020(8)	Cl(1B)-Ni(1)	2.17(2)
Br(2A)-Ni(1)	2.381(2)	Cl(2B)-Ni(1)	2.36(2)
Ni(1)-O(1)	1.975(2)	Ni(1)-N(1)	1.981(3)
P(1)-N(1)	1.607(3)	P(1)-C(1)	1.794(3)
P(1)-C(13)	1.815(4)	P(1)-C(7)	1.820(3)
O(1)-C(2)	1.338(4)	O(1)-Li(1)	1.930(7)
O(2)-C(27)	1.429(5)	O(2)-C(24)	1.451(5)
O(2)-Li(1)	2.006(7)	O(3)-C(28)	1.436(5)
O(3)-C(31)	1.437(4)	O(3)-Li(1)	1.945(7)
O(4)-C(32)	1.411(5)	O(4)-C(35)	1.431(5)
O(4)-Li(1)	1.917(7)	N(1)-C(19)	1.490(4)
C(1)-C(6)	1.398(5)	C(1)-C(2)	1.419(5)
C(2)-C(3)	1.405(5)	C(3)-C(4)	1.379(5)
C(3)-H(3)	0.9500	C(4)-C(5)	1.390(5)
C(4)-H(4)	0.9500	C(5)-C(6)	1.382(5)
C(5)-H(5)	0.9500	C(6)-H(6)	0.9500
C(7)-C(12)	1.389(5)	C(7)-C(8)	1.403(5)
C(8)-C(9)	1.382(5)	C(8)-H(8)	0.9500
C(9)-C(10)	1.385(6)	C(9)-H(9)	0.9500
C(10)-C(11)	1.376(6)	C(10)-H(10)	0.9500
C(11)-C(12)	1.401(5)	C(11)-H(11)	0.9500
C(12)-H(12)	0.9500	C(13)-C(18)	1.394(5)
C(13)-C(14)	1.402(5)	C(14)-C(15)	1.388(5)
C(14)-H(14)	0.9500	C(15)-C(16)	1.379(6)
C(15)-H(15)	0.9500	C(16)-C(17)	1.372(6)
C(16)-H(16)	0.9500	C(17)-C(18)	1.388(5)
C(17)-H(17)	0.9500	C(18)-H(18)	0.9500
C(19)-C(20)	1.534(5)	C(19)-H(19A)	0.9900
C(19)-H(19B)	0.9900	C(20)-C(21)	1.520(5)
C(20)-C(22)	1.524(5)	C(20)-C(23)	1.536(5)
C(21)-H(21A)	0.9800	C(21)-H(21B)	0.9800
C(21)-H(21C)	0.9800	C(22)-H(22A)	0.9800
C(22)-H(22B)	0.9800	C(22)-H(22C)	0.9800
C(23)-H(23A)	0.9800	C(23)-H(23B)	0.9800
C(23)-H(23C)	0.9800	C(24)-C(25)	1.478(7)
C(24)-H(24A)	0.9900	C(24)-H(24B)	0.9900
C(25)-C(26)	1.441(8)	C(25)-H(25A)	0.9900
C(25)-H(25B)	0.9900	C(26)-C(27)	1.500(7)
C(26)-H(26A)	0.9900	C(26)-H(26B)	0.9900
C(27)-H(27A)	0.9900	C(27)-H(27B)	0.9900
C(28)-C(29)	1.504(6)	C(28)-H(28A)	0.9900
C(28)-H(28B)	0.9900	C(29)-C(30)	1.528(6)
C(29)-H(29A)	0.9900	C(29)-H(29B)	0.9900
C(30)-C(31)	1.498(6)	C(30)-H(30A)	0.9900
C(30)-H(30B)	0.9900	C(31)-H(31A)	0.9900
C(31)-H(31B)	0.9900	C(32)-C(33)	1.489(7)
C(32)-H(32A)	0.9900	C(32)-H(32B)	0.9900
C(33)-C(34)	1.497(7)	C(33)-H(33A)	0.9900
C(33)-H(33B)	0.9900	C(34)-C(35)	1.510(7)
C(34)-H(34A)	0.9900	C(34)-H(34B)	0.9900
C(35)-H(35A)	0.9900	C(35)-H(35B)	0.9900

O(1)-Ni(1)-N(1)	98.9(1)	O(1)-Ni(1)-Cl(1B)	105.9(7)
N(1)-Ni(1)-Cl(1B)	119.0(7)	O(1)-Ni(1)-Cl(2B)	101.5(3)
N(1)-Ni(1)-Cl(2B)	106.6(4)	Cl(1B)-Ni(1)-Cl(2B)	121.0(8)
O(1)-Ni(1)-Br(2A)	108.69(8)	N(1)-Ni(1)-Br(2A)	107.5(1)
Cl(1B)-Ni(1)-Br(2A)	115.2(7)	Cl(2B)-Ni(1)-Br(2A)	7.7(3)
O(1)-Ni(1)-Br(1A)	102.43(7)	N(1)-Ni(1)-Br(1A)	111.73(8)
Cl(1B)-Ni(1)-Br(1A)	9.3(7)	Cl(2B)-Ni(1)-Br(1A)	130.3(3)
Br(2A)-Ni(1)-Br(1A)	124.39(4)	N(1)-P(1)-C(1)	110.1(2)
N(1)-P(1)-C(13)	114.4(2)	C(1)-P(1)-C(13)	108.2(2)
N(1)-P(1)-C(7)	111.6(2)	C(1)-P(1)-C(7)	107.4(2)
C(13)-P(1)-C(7)	104.9(2)	C(2)-O(1)-Li(1)	125.3(3)
C(2)-O(1)-Ni(1)	114.6(2)	Li(1)-O(1)-Ni(1)	116.7(2)
C(27)-O(2)-C(24)	109.1(3)	C(27)-O(2)-Li(1)	117.9(3)

Appendix 1. Crystallographic data

C(24)-O(2)-Li(1)	122.9(3)	C(28)-O(3)-C(31)	108.9(3)
C(28)-O(3)-Li(1)	118.8(3)	C(31)-O(3)-Li(1)	123.9(3)
C(32)-O(4)-C(35)	104.8(4)	C(32)-O(4)-Li(1)	135.3(3)
C(35)-O(4)-Li(1)	118.9(3)	C(19)-N(1)-P(1)	117.9(2)
C(19)-N(1)-Ni(1)	121.0(2)	P(1)-N(1)-Ni(1)	114.6(2)
C(6)-C(1)-C(2)	119.9(3)	C(6)-C(1)-P(1)	121.6(3)
C(2)-C(1)-P(1)	118.4(2)	O(1)-C(2)-C(3)	121.2(3)
O(1)-C(2)-C(1)	121.2(3)	C(3)-C(2)-C(1)	117.6(3)
C(4)-C(3)-C(2)	121.6(3)	C(4)-C(3)-H(3)	119.2
C(2)-C(3)-H(3)	119.2	C(3)-C(4)-C(5)	120.3(3)
C(3)-C(4)-H(4)	119.8	C(5)-C(4)-H(4)	119.8
C(6)-C(5)-C(4)	119.6(3)	C(6)-C(5)-H(5)	120.2
C(4)-C(5)-H(5)	120.2	C(5)-C(6)-C(1)	120.9(3)
C(5)-C(6)-H(6)	119.6	C(1)-C(6)-H(6)	119.6
C(12)-C(7)-C(8)	119.3(3)	C(12)-C(7)-P(1)	122.0(3)
C(8)-C(7)-P(1)	118.7(3)	C(9)-C(8)-C(7)	120.1(4)
C(9)-C(8)-H(8)	120.0	C(7)-C(8)-H(8)	120.0
C(8)-C(9)-C(10)	120.3(4)	C(8)-C(9)-H(9)	119.8
C(10)-C(9)-H(9)	119.8	C(11)-C(10)-C(9)	120.2(3)
C(11)-C(10)-H(10)	119.9	C(9)-C(10)-H(10)	119.9
C(10)-C(11)-C(12)	120.1(4)	C(10)-C(11)-H(11)	119.9
C(12)-C(11)-H(11)	119.9	C(7)-C(12)-C(11)	119.9(3)
C(7)-C(12)-H(12)	120.0	C(11)-C(12)-H(12)	120.0
C(18)-C(13)-C(14)	118.5(3)	C(18)-C(13)-P(1)	119.8(3)
C(14)-C(13)-P(1)	121.7(3)	C(15)-C(14)-C(13)	119.8(3)
C(15)-C(14)-H(14)	120.1	C(13)-C(14)-H(14)	120.1
C(16)-C(15)-C(14)	121.0(4)	C(16)-C(15)-H(15)	119.5
C(14)-C(15)-H(15)	119.5	C(17)-C(16)-C(15)	119.7(4)
C(17)-C(16)-H(16)	120.2	C(15)-C(16)-H(16)	120.2
C(16)-C(17)-C(18)	120.3(4)	C(16)-C(17)-H(17)	119.8
C(18)-C(17)-H(17)	119.8	C(17)-C(18)-C(13)	120.7(3)
C(17)-C(18)-H(18)	119.6	C(13)-C(18)-H(18)	119.6
N(1)-C(19)-C(20)	115.2(3)	N(1)-C(19)-H(19A)	108.5
C(20)-C(19)-H(19A)	108.5	N(1)-C(19)-H(19B)	108.5
C(20)-C(19)-H(19B)	108.5	H(19A)-C(19)-H(19B)	107.5
C(21)-C(20)-C(22)	110.1(3)	C(21)-C(20)-C(19)	110.7(3)
C(22)-C(20)-C(19)	111.8(3)	C(21)-C(20)-C(23)	109.7(3)
C(22)-C(20)-C(23)	108.6(3)	C(19)-C(20)-C(23)	105.9(3)
C(20)-C(21)-H(21A)	109.5	C(20)-C(21)-H(21B)	109.5
H(21A)-C(21)-H(21B)	109.5	C(20)-C(21)-H(21C)	109.5
H(21A)-C(21)-H(21C)	109.5	H(21B)-C(21)-H(21C)	109.5
C(20)-C(22)-H(22A)	109.5	C(20)-C(22)-H(22B)	109.5
H(22A)-C(22)-H(22B)	109.5	C(20)-C(22)-H(22C)	109.5
H(22A)-C(22)-H(22C)	109.5	H(22B)-C(22)-H(22C)	109.5
C(20)-C(23)-H(23A)	109.5	C(20)-C(23)-H(23B)	109.5
H(23A)-C(23)-H(23B)	109.5	C(20)-C(23)-H(23C)	109.5
H(23A)-C(23)-H(23C)	109.5	H(23B)-C(23)-H(23C)	109.5
O(2)-C(24)-C(25)	105.8(4)	O(2)-C(24)-H(24A)	110.6
C(25)-C(24)-H(24A)	110.6	O(2)-C(24)-H(24B)	110.6
C(25)-C(24)-H(24B)	110.6	H(24A)-C(24)-H(24B)	108.7
C(26)-C(25)-C(24)	106.3(5)	C(26)-C(25)-H(25A)	110.5
C(24)-C(25)-H(25A)	110.5	C(26)-C(25)-H(25B)	110.5
C(24)-C(25)-H(25B)	110.5	H(25A)-C(25)-H(25B)	108.7
C(25)-C(26)-C(27)	105.3(4)	C(25)-C(26)-H(26A)	110.7
C(27)-C(26)-H(26A)	110.7	C(25)-C(26)-H(26B)	110.7
C(27)-C(26)-H(26B)	110.7	H(26A)-C(26)-H(26B)	108.8
O(2)-C(27)-C(26)	106.6(4)	O(2)-C(27)-H(27A)	110.4
C(26)-C(27)-H(27A)	110.4	O(2)-C(27)-H(27B)	110.4
C(26)-C(27)-H(27B)	110.4	H(27A)-C(27)-H(27B)	108.6
O(3)-C(28)-C(29)	107.5(3)	O(3)-C(28)-H(28A)	110.2
C(29)-C(28)-H(28A)	110.2	O(3)-C(28)-H(28B)	110.2
C(29)-C(28)-H(28B)	110.2	H(28A)-C(28)-H(28B)	108.5
C(28)-C(29)-C(30)	102.9(3)	C(28)-C(29)-H(29A)	111.2
C(30)-C(29)-H(29A)	111.2	C(28)-C(29)-H(29B)	111.2
C(30)-C(29)-H(29B)	111.2	H(29A)-C(29)-H(29B)	109.1
C(31)-C(30)-C(29)	102.2(3)	C(31)-C(30)-H(30A)	111.3
C(29)-C(30)-H(30A)	111.3	C(31)-C(30)-H(30B)	111.3
C(29)-C(30)-H(30B)	111.3	H(30A)-C(30)-H(30B)	109.2

Appendix 1. Crystallographic data

O(3)-C(31)-C(30)	105.3(3)	O(3)-C(31)-H(31A)	110.7
C(30)-C(31)-H(31A)	110.7	O(3)-C(31)-H(31B)	110.7
C(30)-C(31)-H(31B)	110.7	H(31A)-C(31)-H(31B)	108.8
O(4)-C(32)-C(33)	105.7(4)	O(4)-C(32)-H(32A)	110.6
C(33)-C(32)-H(32A)	110.6	O(4)-C(32)-H(32B)	110.6
C(33)-C(32)-H(32B)	110.6	H(32A)-C(32)-H(32B)	108.7
C(32)-C(33)-C(34)	106.0(4)	C(32)-C(33)-H(33A)	110.5
C(34)-C(33)-H(33A)	110.5	C(32)-C(33)-H(33B)	110.5
C(34)-C(33)-H(33B)	110.5	H(33A)-C(33)-H(33B)	108.7
C(33)-C(34)-C(35)	103.0(4)	C(33)-C(34)-H(34A)	111.2
C(35)-C(34)-H(34A)	111.2	C(33)-C(34)-H(34B)	111.2
C(35)-C(34)-H(34B)	111.2	H(34A)-C(34)-H(34B)	109.1
O(4)-C(35)-C(34)	104.4(4)	O(4)-C(35)-H(35A)	110.9
C(34)-C(35)-H(35A)	110.9	O(4)-C(35)-H(35B)	110.9
C(34)-C(35)-H(35B)	110.9	H(35A)-C(35)-H(35B)	108.9
O(4)-Li(1)-O(1)	115.8(3)	O(4)-Li(1)-O(3)	110.1(3)
O(1)-Li(1)-O(3)	114.8(3)	O(4)-Li(1)-O(2)	100.3(3)
O(1)-Li(1)-O(2)	116.5(3)	O(3)-Li(1)-O(2)	97.1(3)

Appendix 1. Crystallographic data

Table 4. Anisotropic displacement parameters ($\text{Å}^2 \times 10^3$) for pa278

atom	U11	U22	U33	U23	U13	U12
Br(1A)	41(1)	46(1)	51(1)	5(1)	30(1)	3(1)
Cl(1B)	41(1)	46(1)	51(1)	5(1)	30(1)	3(1)
Br(2A)	28(1)	46(1)	42(1)	-7(1)	7(1)	-4(1)
Cl(2B)	28(1)	46(1)	42(1)	-7(1)	7(1)	-4(1)
Ni(1)	29(1)	26(1)	23(1)	-1(1)	11(1)	1(1)
P(1)	22(1)	21(1)	22(1)	0(1)	10(1)	0(1)
O(1)	28(1)	25(1)	29(1)	3(1)	9(1)	1(1)
O(2)	55(2)	34(2)	41(2)	1(1)	10(1)	9(1)
O(3)	36(2)	32(1)	45(2)	-6(1)	23(1)	-3(1)
O(4)	31(2)	86(2)	35(2)	11(2)	13(1)	12(2)
N(1)	25(1)	20(1)	24(1)	1(1)	12(1)	1(1)
C(1)	25(2)	19(2)	26(2)	1(1)	13(1)	2(1)
C(2)	27(2)	23(2)	31(2)	1(1)	13(2)	2(1)
C(3)	41(2)	31(2)	31(2)	7(2)	19(2)	4(2)
C(4)	41(2)	25(2)	45(2)	8(2)	26(2)	1(2)
C(5)	31(2)	22(2)	42(2)	-2(2)	17(2)	-3(1)
C(6)	31(2)	23(2)	29(2)	-1(1)	13(2)	2(1)
C(7)	26(2)	18(2)	24(2)	-1(1)	8(1)	-1(1)
C(8)	24(2)	26(2)	36(2)	-2(2)	10(2)	4(1)
C(9)	28(2)	26(2)	37(2)	-6(2)	2(2)	2(1)
C(10)	45(2)	34(2)	26(2)	-2(2)	3(2)	7(2)
C(11)	47(2)	41(2)	25(2)	1(2)	14(2)	2(2)
C(12)	32(2)	27(2)	27(2)	0(1)	10(2)	-1(1)
C(13)	25(2)	28(2)	25(2)	1(1)	8(1)	2(1)
C(14)	28(2)	29(2)	47(2)	-10(2)	16(2)	-1(2)
C(15)	38(2)	34(2)	60(3)	-8(2)	23(2)	7(2)
C(16)	28(2)	47(2)	47(2)	-1(2)	21(2)	5(2)
C(17)	31(2)	38(2)	52(2)	1(2)	23(2)	-4(2)
C(18)	28(2)	27(2)	49(2)	0(2)	18(2)	0(1)
C(19)	31(2)	23(2)	26(2)	-2(1)	15(2)	-3(1)
C(20)	33(2)	22(2)	26(2)	2(1)	10(2)	3(1)
C(21)	36(2)	30(2)	43(2)	-2(2)	12(2)	7(2)
C(22)	43(2)	27(2)	35(2)	-3(2)	18(2)	4(2)
C(23)	54(3)	27(2)	37(2)	6(2)	20(2)	4(2)
C(24)	73(3)	40(3)	60(3)	-10(2)	24(3)	10(2)
C(25)	75(4)	50(3)	100(5)	-7(3)	22(4)	27(3)
C(26)	83(4)	93(5)	81(4)	29(4)	29(4)	48(4)
C(27)	47(3)	46(3)	48(3)	14(2)	12(2)	1(2)
C(28)	44(2)	40(2)	60(3)	-5(2)	34(2)	-6(2)
C(29)	46(2)	47(2)	47(2)	-4(2)	27(2)	4(2)
C(30)	46(2)	38(2)	42(2)	-6(2)	14(2)	2(2)
C(31)	38(2)	39(2)	42(2)	-14(2)	13(2)	-9(2)
C(32)	40(2)	62(3)	59(3)	-12(2)	15(2)	-12(2)
C(33)	41(3)	128(5)	62(4)	13(4)	15(3)	27(3)
C(34)	55(3)	68(3)	62(3)	-6(3)	37(3)	-2(2)
C(35)	43(3)	128(5)	41(3)	8(3)	20(2)	11(3)
Li(1)	35(3)	35(3)	30(3)	3(3)	15(3)	7(3)

The anisotropic displacement factor exponent takes the form
 $2 \pi^2 [h^2 a^{*2} U(11) + \dots + 2 h k a^* b^* U(12)]$

Appendix 1. Crystallographic data

Table 5. Hydrogen Coordinates ($\text{Å} \times 10^4$) and equivalent isotropic displacement parameters ($\text{Å}^2 \times 10^3$) for pa278

atom	x	y	z	U(eq)
H(3)	482	-4871	-2329	40
H(4)	-1323	-5725	-2937	41
H(5)	-2407	-5658	-4065	37
H(6)	-1654	-4731	-4580	32
H(8)	-2768	-3407.9998	-4875	35
H(9)	-4404	-3397.0002	-5966	42
H(10)	-3466	-3441.9998	-6752	47
H(11)	-901	-3569	-6452.9995	45
H(12)	765	-3630	-5356	35
H(14)	1966	-4844	-4244	41
H(15)	4332	-5090	-4215	52
H(16)	6029	-4132	-4081	47
H(17)	5396	-2918	-3948	46
H(18)	3055	-2654	-3959	41
H(19A)	376	-2153	-4604	31
H(19B)	1492	-1810	-3926.9998	31
H(21A)	-2425	-2082	-4292	56
H(21B)	-2426	-1922	-4983	56
H(21C)	-2986	-1295	-4637	56
H(22A)	-1111	-641	-3656	51
H(22B)	621	-879	-3376	51
H(22C)	-592	-1435	-3316	51
H(23A)	-1128	-384.0000	-4716	59
H(23B)	-626	-1008	-5087	59
H(23C)	602	-618	-4457	59
H(24A)	4077	-5511.9995	-2364	70
H(24B)	2545	-5838.9995	-2366	70
H(25A)	3743	-6654.0005	-1600	96
H(25B)	5047	-6555	-1848	96
H(26A)	6391	-5843	-1038	105
H(26B)	5516	-6292	-688.9999	105
H(27A)	4063	-5327	-736	59
H(27B)	5333	-4844	-834.0001	59
H(28A)	1841	-4192	-833	52
H(28B)	917	-3775	-1507	52
H(29A)	1911	-3177.9998	-257	53
H(29B)	512	-2906	-903	53
H(30A)	2031	-2210	-1241	52
H(30B)	2942	-2115	-470.0000	52
H(31A)	4315	-2681	-1094	49
H(31B)	4599	-3034	-404.0000	49
H(32A)	6734	-3896	-996	67
H(32B)	7020	-3195	-1368.9999	67
H(33A)	7901	-4667	-1384	95
H(33B)	8616	-3929	-1542	95
H(34A)	6493	-4853	-2419	69
H(34B)	7363	-4174	-2578.0002	69
H(35A)	5596	-3332	-2628	84
H(35B)	4527	-4055	-2843	84

Complex 26a

Table 1. Crystal data for pa874bis

Compound	pa874bis
Molecular formula	C ₄₀ H ₃₈ BrNNiOP ₂ , C ₄ H ₈ O
Molecular weight	821.38
Crystal habit	Dark Green Block
Crystal dimensions(mm)	0.22x0.18x0.16
Crystal system	Triclinic
Space group	P -1
a(Å)	9.656(1)
b(Å)	12.252(1)
c(Å)	17.162(1)
α(°)	92.016(1)
β(°)	96.257(1)
γ(°)	99.969(1)
V(Å ³)	1984.8(3)
Z	2
d(g·cm ⁻³)	1.374
F(000)	852
μ(cm ⁻¹)	1.613
Absorption corrections	multi-scan ; 0.7179 min, 0.7824 max
Diffractionmeter	KappaCCD
X-ray source	MoKα
λ(Å)	0.71069
Monochromator	graphite
T (K)	150.0(1)
Scan mode	phi and omega scans
Maximum θ	25.01
HKL ranges	-9 11 ; -14 14 ; -17 20
Reflections measured	18156
Unique data	6780
Rint	0.0531
Reflections used	5658
Criterion	I > 2σI
Refinement type	Fsqd
Hydrogen atoms	constr
Parameters refined	418
Reflections / parameter	13
wR2	0.1372
R1	0.0565
Weights a, b	0.0568 ; 4.3728
GoF	1.072
difference peak / hole (e Å ⁻³)	0.831(0.084) / -0.450(0.084)

Table 2. Atomic Coordinates (A x 10⁴) and equivalent isotropic displacement parameters (A² x 10³) for pa874bis

atom	x	y	z	U(eq)
Br(1)	-321(1)	7523(1)	3561(1)	59(1)
Ni(1)	1392(1)	8146(1)	2709(1)	36(1)
P(1)	3885(1)	10026(1)	2925(1)	33(1)
P(2)	737(1)	6873(1)	1643(1)	35(1)
O(1)	883(3)	9389(2)	2166(2)	38(1)
N(1)	3433(4)	8702(3)	2991(2)	35(1)
C(1)	3155(4)	10423(3)	1992(2)	34(1)
C(2)	1710(4)	10038(3)	1749(2)	34(1)
C(3)	1131(5)	10399(4)	1026(3)	39(1)
C(4)	1954(5)	11094(4)	585(3)	43(1)
C(5)	3369(5)	11486(4)	840(3)	43(1)
C(6)	3960(5)	11166(4)	1543(3)	39(1)
C(7)	5788(4)	10486(4)	3004(3)	36(1)
C(8)	6550(5)	11015(4)	3683(3)	42(1)
C(9)	8011(5)	11224(4)	3767(3)	51(1)
C(10)	8733(5)	10916(4)	3172(3)	54(1)
C(11)	7989(5)	10395(4)	2482(3)	47(1)
C(12)	6525(5)	10187(4)	2402(3)	41(1)
C(13)	3227(4)	10879(4)	3639(2)	35(1)
C(14)	3537(5)	12029(4)	3606(3)	42(1)
C(15)	2985(5)	12707(4)	4108(3)	47(1)
C(16)	2129(5)	12243(4)	4644(3)	45(1)
C(17)	1810(5)	11107(4)	4676(3)	45(1)
C(18)	2343(5)	10423(4)	4170(2)	39(1)
C(19)	4239(5)	7987(4)	3512(3)	39(1)
C(20)	4300(6)	8339(5)	4372(3)	60(1)
C(21)	5756(6)	7981(5)	3324(3)	60(1)
C(22)	3443(6)	6815(4)	3366(4)	66(2)
C(23)	1534(5)	7391(4)	782(2)	38(1)
C(24)	812(5)	7224(4)	29(3)	45(1)
C(25)	1465(5)	7666(5)	-594(3)	54(1)
C(26)	2803(5)	8286(5)	-479(3)	53(1)
C(27)	3529(5)	8461(4)	267(3)	47(1)
C(28)	2889(5)	8005(4)	895(3)	40(1)
C(29)	-1163(4)	6597(4)	1335(2)	38(1)
C(30)	-1896(5)	5580(4)	1016(3)	50(1)
C(31)	-3323(6)	5421(5)	802(3)	60(1)
C(32)	-4057(5)	6287(5)	883(3)	58(1)
C(33)	-3338(5)	7307(5)	1190(3)	52(1)
C(34)	-1904(5)	7472(4)	1415(3)	43(1)
C(35)	1184(4)	5498(4)	1743(3)	38(1)
C(36)	1971(5)	5036(4)	1233(3)	44(1)
C(37)	2299(5)	3998(4)	1355(3)	50(1)
C(38)	1846(6)	3411(4)	1979(3)	52(1)
C(39)	1066(6)	3864(4)	2488(3)	51(1)
C(40)	742(5)	4902(4)	2384(3)	46(1)

U(eq) is defined as 1/3 the trace of the Uij tensor.

Table 3. Bond lengths (Å) and angles (deg) for pa874bis

Br(1)-Ni(1)	2.3712(7)	Ni(1)-O(1)	1.921(3)
Ni(1)-N(1)	1.971(3)	Ni(1)-P(2)	2.321(1)
P(1)-N(1)	1.616(4)	P(1)-C(1)	1.796(4)
P(1)-C(7)	1.815(4)	P(1)-C(13)	1.819(4)
P(2)-C(35)	1.819(4)	P(2)-C(29)	1.822(4)
P(2)-C(23)	1.824(4)	O(1)-C(2)	1.314(5)
N(1)-C(19)	1.522(5)	C(1)-C(6)	1.400(6)
C(1)-C(2)	1.406(6)	C(2)-C(3)	1.422(6)
C(3)-C(4)	1.368(7)	C(3)-H(3)	0.9500
C(4)-C(5)	1.384(7)	C(4)-H(4)	0.9500
C(5)-C(6)	1.377(6)	C(5)-H(5)	0.9500
C(6)-H(6)	0.9500	C(7)-C(8)	1.383(6)
C(7)-C(12)	1.390(6)	C(8)-C(9)	1.379(7)
C(8)-H(8)	0.9500	C(9)-C(10)	1.375(7)
C(9)-H(9)	0.9500	C(10)-C(11)	1.390(7)
C(10)-H(10)	0.9500	C(11)-C(12)	1.383(6)
C(11)-H(11)	0.9500	C(12)-H(12)	0.9500
C(13)-C(18)	1.382(6)	C(13)-C(14)	1.393(6)
C(14)-C(15)	1.385(6)	C(14)-H(14)	0.9500
C(15)-C(16)	1.375(7)	C(15)-H(15)	0.9500
C(16)-C(17)	1.377(7)	C(16)-H(16)	0.9500
C(17)-C(18)	1.384(6)	C(17)-H(17)	0.9500
C(18)-H(18)	0.9500	C(19)-C(22)	1.505(7)
C(19)-C(20)	1.516(7)	C(19)-C(21)	1.534(7)
C(20)-H(20A)	0.9800	C(20)-H(20B)	0.9800
C(20)-H(20C)	0.9800	C(21)-H(21A)	0.9800
C(21)-H(21B)	0.9800	C(21)-H(21C)	0.9800
C(22)-H(22A)	0.9800	C(22)-H(22B)	0.9800
C(22)-H(22C)	0.9800	C(23)-C(28)	1.382(6)
C(23)-C(24)	1.390(6)	C(24)-C(25)	1.380(7)
C(24)-H(24)	0.9500	C(25)-C(26)	1.371(7)
C(25)-H(25)	0.9500	C(26)-C(27)	1.382(7)
C(26)-H(26)	0.9500	C(27)-C(28)	1.387(6)
C(27)-H(27)	0.9500	C(28)-H(28)	0.9500
C(29)-C(30)	1.384(7)	C(29)-C(34)	1.399(6)
C(30)-C(31)	1.365(7)	C(30)-H(30)	0.9500
C(31)-C(32)	1.386(8)	C(31)-H(31)	0.9500
C(32)-C(33)	1.377(8)	C(32)-H(32)	0.9500
C(33)-C(34)	1.374(7)	C(33)-H(33)	0.9500
C(34)-H(34)	0.9500	C(35)-C(36)	1.387(6)
C(35)-C(40)	1.407(6)	C(36)-C(37)	1.380(6)
C(36)-H(36)	0.9500	C(37)-C(38)	1.379(7)
C(37)-H(37)	0.9500	C(38)-C(39)	1.376(7)
C(38)-H(38)	0.9500	C(39)-C(40)	1.374(7)
C(39)-H(39)	0.9500	C(40)-H(40)	0.9500
O(1)-Ni(1)-N(1)	99.4(1)	O(1)-Ni(1)-P(2)	95.6(1)
N(1)-Ni(1)-P(2)	117.2(1)	O(1)-Ni(1)-Br(1)	109.7(1)
N(1)-Ni(1)-Br(1)	127.8(1)	P(2)-Ni(1)-Br(1)	102.25(4)
N(1)-P(1)-C(1)	109.8(2)	N(1)-P(1)-C(7)	113.2(2)
C(1)-P(1)-C(7)	107.2(2)	N(1)-P(1)-C(13)	115.1(2)
C(1)-P(1)-C(13)	104.3(2)	C(7)-P(1)-C(13)	106.7(2)
C(35)-P(2)-C(29)	103.9(2)	C(35)-P(2)-C(23)	104.8(2)
C(29)-P(2)-C(23)	105.0(2)	C(35)-P(2)-Ni(1)	117.8(1)
C(29)-P(2)-Ni(1)	113.2(2)	C(23)-P(2)-Ni(1)	111.0(2)
C(2)-O(1)-Ni(1)	125.1(3)	C(19)-N(1)-P(1)	125.3(3)
C(19)-N(1)-Ni(1)	116.5(3)	P(1)-N(1)-Ni(1)	113.7(2)
C(6)-C(1)-C(2)	120.3(4)	C(6)-C(1)-P(1)	121.5(3)
C(2)-C(1)-P(1)	118.0(3)	O(1)-C(2)-C(1)	123.0(4)
O(1)-C(2)-C(1)	119.5(4)	C(1)-C(2)-C(3)	117.4(4)
C(4)-C(3)-C(2)	121.1(4)	C(4)-C(3)-H(3)	119.5
C(2)-C(3)-H(3)	119.5	C(3)-C(4)-C(5)	120.8(4)
C(3)-C(4)-H(4)	119.6	C(5)-C(4)-H(4)	119.6
C(6)-C(5)-C(4)	119.7(4)	C(6)-C(5)-H(5)	120.1
C(4)-C(5)-H(5)	120.1	C(5)-C(6)-C(1)	120.6(4)

C(5)-C(6)-H(6)	119.7	C(1)-C(6)-H(6)	119.7
C(8)-C(7)-C(12)	118.6(4)	C(8)-C(7)-P(1)	121.9(3)
C(12)-C(7)-P(1)	119.0(3)	C(9)-C(8)-C(7)	120.8(4)
C(9)-C(8)-H(8)	119.6	C(7)-C(8)-H(8)	119.6
C(10)-C(9)-C(8)	120.3(5)	C(10)-C(9)-H(9)	119.8
C(8)-C(9)-H(9)	119.8	C(9)-C(10)-C(11)	119.8(4)
C(9)-C(10)-H(10)	120.1	C(11)-C(10)-H(10)	120.1
C(12)-C(11)-C(10)	119.5(4)	C(12)-C(11)-H(11)	120.3
C(10)-C(11)-H(11)	120.3	C(11)-C(12)-C(7)	120.9(4)
C(11)-C(12)-H(12)	119.5	C(7)-C(12)-H(12)	119.5
C(18)-C(13)-C(14)	119.2(4)	C(18)-C(13)-P(1)	122.1(3)
C(14)-C(13)-P(1)	118.5(3)	C(15)-C(14)-C(13)	120.4(4)
C(15)-C(14)-H(14)	119.8	C(13)-C(14)-H(14)	119.8
C(16)-C(15)-C(14)	119.9(5)	C(16)-C(15)-H(15)	120.1
C(14)-C(15)-H(15)	120.1	C(15)-C(16)-C(17)	120.1(4)
C(15)-C(16)-H(16)	120.0	C(17)-C(16)-H(16)	120.0
C(16)-C(17)-C(18)	120.4(4)	C(16)-C(17)-H(17)	119.8
C(18)-C(17)-H(17)	119.8	C(13)-C(18)-C(17)	120.1(4)
C(13)-C(18)-H(18)	120.0	C(17)-C(18)-H(18)	120.0
C(22)-C(19)-C(20)	109.5(4)	C(22)-C(19)-N(1)	106.3(3)
C(20)-C(19)-N(1)	111.3(4)	C(22)-C(19)-C(21)	107.0(4)
C(20)-C(19)-C(21)	108.4(4)	N(1)-C(19)-C(21)	114.2(4)
C(19)-C(20)-H(20A)	109.5	C(19)-C(20)-H(20B)	109.5
H(20A)-C(20)-H(20B)	109.5	C(19)-C(20)-H(20C)	109.5
H(20B)-C(20)-H(20C)	109.5	H(20B)-C(20)-H(20C)	109.5
C(19)-C(21)-H(21A)	109.5	C(19)-C(21)-H(21B)	109.5
H(21A)-C(21)-H(21B)	109.5	C(19)-C(21)-H(21C)	109.5
H(21B)-C(21)-H(21C)	109.5	H(21B)-C(21)-H(21C)	109.5
C(19)-C(22)-H(22A)	109.5	C(19)-C(22)-H(22B)	109.5
H(22A)-C(22)-H(22B)	109.5	C(19)-C(22)-H(22C)	109.5
H(22B)-C(22)-H(22C)	109.5	H(22B)-C(22)-H(22C)	109.5
C(28)-C(23)-C(24)	119.5(4)	C(28)-C(23)-P(2)	118.0(3)
C(24)-C(23)-P(2)	122.4(4)	C(25)-C(24)-C(23)	119.5(5)
C(25)-C(24)-H(24)	120.3	C(23)-C(24)-H(24)	120.3
C(26)-C(25)-C(24)	120.9(4)	C(26)-C(25)-H(25)	119.5
C(24)-C(25)-H(25)	119.5	C(25)-C(26)-C(27)	120.1(4)
C(25)-C(26)-H(26)	119.9	C(27)-C(26)-H(26)	119.9
C(26)-C(27)-C(28)	119.3(5)	C(26)-C(27)-H(27)	120.3
C(28)-C(27)-H(27)	120.3	C(23)-C(28)-C(27)	120.6(4)
C(23)-C(28)-H(28)	119.7	C(27)-C(28)-H(28)	119.7
C(30)-C(29)-C(34)	118.8(4)	C(30)-C(29)-P(2)	123.5(4)
C(34)-C(29)-P(2)	117.7(3)	C(31)-C(30)-C(29)	120.8(5)
C(31)-C(30)-H(30)	119.6	C(29)-C(30)-H(30)	119.6
C(30)-C(31)-C(32)	120.3(5)	C(30)-C(31)-H(31)	119.8
C(32)-C(31)-H(31)	119.8	C(33)-C(32)-C(31)	119.4(5)
C(31)-C(32)-H(32)	120.3	C(31)-C(32)-H(32)	120.3
C(34)-C(33)-C(32)	120.7(5)	C(34)-C(33)-H(33)	119.7
C(32)-C(33)-H(33)	119.7	C(33)-C(34)-C(29)	119.9(5)
C(29)-C(34)-H(34)	120.0	C(29)-C(34)-H(34)	120.0
C(36)-C(35)-C(40)	119.2(4)	C(36)-C(35)-P(2)	123.0(3)
C(40)-C(35)-P(2)	117.8(3)	C(37)-C(36)-C(35)	119.9(5)
C(37)-C(36)-H(36)	120.0	C(35)-C(36)-H(36)	120.0
C(38)-C(37)-C(36)	120.6(5)	C(38)-C(37)-H(37)	119.7
C(36)-C(37)-H(37)	119.7	C(39)-C(38)-C(37)	119.9(5)
C(39)-C(38)-H(38)	120.1	C(37)-C(38)-H(38)	120.1
C(40)-C(39)-C(38)	120.5(5)	C(40)-C(39)-H(39)	119.7
C(38)-C(39)-H(39)	119.7	C(39)-C(40)-C(35)	119.9(5)
C(39)-C(40)-H(40)	120.1	C(35)-C(40)-H(40)	120.1

Appendix 1. Crystallographic data

Table 4. Anisotropic displacement parameters ($\text{Å}^2 \times 10^3$) for pa874bis

atom	U11	U22	U33	U23	U13	U12
Br(1)	63(1)	63(1)	53(1)	5(1)	29(1)	4(1)
Ni(1)	37(1)	41(1)	30(1)	6(1)	5(1)	9(1)
P(1)	33(1)	41(1)	27(1)	5(1)	3(1)	11(1)
P(2)	34(1)	40(1)	32(1)	5(1)	4(1)	11(1)
O(1)	36(2)	41(2)	40(2)	10(1)	4(1)	11(1)
N(1)	34(2)	43(2)	28(2)	8(2)	0(1)	10(2)
C(1)	38(2)	39(2)	26(2)	4(2)	2(2)	12(2)
C(2)	39(2)	40(2)	27(2)	3(2)	5(2)	16(2)
C(3)	37(2)	44(2)	37(2)	3(2)	-3(2)	12(2)
C(4)	51(3)	51(3)	32(2)	9(2)	2(2)	23(2)
C(5)	53(3)	50(3)	34(2)	17(2)	14(2)	23(2)
C(6)	37(2)	45(3)	36(2)	8(2)	6(2)	11(2)
C(7)	31(2)	41(2)	38(2)	10(2)	4(2)	10(2)
C(8)	45(3)	43(3)	39(2)	10(2)	7(2)	10(2)
C(9)	41(3)	55(3)	54(3)	6(2)	-6(2)	6(2)
C(10)	35(3)	66(3)	64(3)	18(3)	5(2)	15(2)
C(11)	44(3)	55(3)	50(3)	13(2)	16(2)	20(2)
C(12)	41(2)	48(3)	38(2)	9(2)	7(2)	18(2)
C(13)	35(2)	42(2)	30(2)	4(2)	2(2)	14(2)
C(14)	43(3)	51(3)	35(2)	11(2)	7(2)	13(2)
C(15)	53(3)	49(3)	43(3)	7(2)	8(2)	22(2)
C(16)	43(3)	57(3)	39(2)	-2(2)	3(2)	22(2)
C(17)	39(2)	63(3)	35(2)	2(2)	8(2)	13(2)
C(18)	41(2)	47(3)	32(2)	6(2)	2(2)	12(2)
C(19)	37(2)	44(2)	37(2)	11(2)	0(2)	14(2)
C(20)	68(3)	78(4)	37(3)	10(3)	-2(2)	30(3)
C(21)	59(3)	70(4)	59(3)	21(3)	14(3)	31(3)
C(22)	65(4)	51(3)	76(4)	19(3)	-20(3)	11(3)
C(23)	41(2)	44(2)	35(2)	6(2)	7(2)	20(2)
C(24)	42(3)	59(3)	35(2)	8(2)	5(2)	12(2)
C(25)	53(3)	83(4)	28(2)	14(2)	3(2)	19(3)
C(26)	50(3)	75(4)	43(3)	24(3)	17(2)	22(3)
C(27)	43(3)	54(3)	47(3)	7(2)	14(2)	15(2)
C(28)	40(2)	49(3)	35(2)	3(2)	8(2)	18(2)
C(29)	36(2)	54(3)	26(2)	7(2)	5(2)	11(2)
C(30)	41(3)	54(3)	52(3)	-4(2)	0(2)	3(2)
C(31)	49(3)	67(4)	59(3)	-8(3)	-2(2)	1(3)
C(32)	34(3)	89(4)	49(3)	-2(3)	1(2)	7(3)
C(33)	44(3)	75(4)	43(3)	8(3)	7(2)	26(3)
C(34)	41(3)	53(3)	37(2)	4(2)	5(2)	9(2)
C(35)	37(2)	41(2)	38(2)	4(2)	0(2)	9(2)
C(36)	50(3)	44(3)	40(2)	5(2)	4(2)	16(2)
C(37)	55(3)	51(3)	46(3)	0(2)	1(2)	21(2)
C(38)	60(3)	44(3)	54(3)	8(2)	-5(2)	17(2)
C(39)	64(3)	43(3)	44(3)	10(2)	1(2)	9(2)
C(40)	51(3)	46(3)	43(3)	6(2)	5(2)	11(2)

The anisotropic displacement factor exponent takes the form
 $2 \pi^2 [h^2 a^{*2} U_{11} + \dots + 2 h k a^* b^* U_{12}]$

Appendix 1. Crystallographic data

Table 5. Hydrogen Coordinates ($\text{Å} \times 10^4$) and equivalent isotropic displacement parameters ($\text{Å}^2 \times 10^3$) for pa874bis

atom	x	y	z	U(eq)
H(3)	158	10152	845	47
H(4)	1550	11311	98	51
H(5)	3929	11973	532	52
H(6)	4924	11452	1726	47
H(8)	6062	11237	4096	50
H(9)	8520	11583	4239	61
H(10)	9739	11059	3233	65
H(11)	8482	10183	2067	57
H(12)	6014	9835	1929	49
H(14)	4132	12350	3237	50
H(15)	3197	13490	4081	56
H(16)	1759	12707	4992	54
H(17)	1219	10790	5047	54
H(18)	2102	9640	4188	47
H(20A)	4762	9118	4461	89
H(20B)	4839	7874	4692	89
H(20C)	3336	8254	4520	89
H(21A)	5747	7832	2759	90
H(21B)	6143	7402	3610	90
H(21C)	6345	8705	3483	90
H(22A)	2466	6784	3482	99
H(22B)	3903	6324	3705	99
H(22C)	3441	6575	2815	99
H(24)	-123.0000	6809	-56.0000	54
H(25)	980	7539	-1111	65
H(26)	3231	8596	-913.0001	64
H(27)	4458	8888	348	56
H(28)	3387	8117	1408	48
H(30)	-1400	4985	946	60
H(31)	-3815	4713	595	73
H(32)	-5049	6178	729	70
H(33)	-3837.0002	7903	1246	63
H(34)	-1417	8180	1625	52
H(36)	2285	5432	801	52
H(37)	2842	3685	1005	60
H(38)	2071	2694	2056	63
H(39)	750	3456	2915	61
H(40)	220	5215	2744	55

Chapter 3

Compound 28

Table 1. Crystal data for pa370

Compound	pa370
Molecular formula	C ₃₈ H ₃₆ N ₂ O ₂ P ₂ ,2(CHCl ₃) ₂ (Br)
Molecular weight	1015.20
Crystal habit	Colorless Block
Crystal dimensions(mm)	0.60x0.58x0.54
Crystal system	monoclinic
Space group	P2 ₁ /c
a(Å)	13.347(1)
b(Å)	11.074(1)
c(Å)	15.874(1)
α(°)	90.00
β(°)	111.514(1)
γ(°)	90.00
V(Å ³)	2182.8(3)
Z	2
d(g·cm ⁻³)	1.545
F(000)	1024
μ(cm ⁻¹)	2.334
Absorption corrections	multi-scan ; 0.3348 min, 0.3654 max
Diffractometer	KappaCCD
X-ray source	MoKα
λ(Å)	0.71069
Monochromator	graphite
T (K)	150.0(1)
Scan mode	phi and omega scans
Maximum θ	30.01
HKL ranges	-18 18 ; -14 15 ; -20 22
Reflections measured	14803
Unique data	6278
Rint	0.0242
Reflections used	5351
Criterion	I > 2σ(I)
Refinement type	Fsqd
Hydrogen atoms	mixed
Parameters refined	251
Reflections / parameter	21
wR2	0.0860
R1	0.0388
Weights a, b	0.0261 ; 3.1298
GoF	1.078
difference peak / hole (e Å ⁻³)	1.157(0.074) / -0.748(0.074)

Table 2. Atomic Coordinates (A x 10⁴) and equivalent isotropic displacement parameters (Å² x 10³) for pa370

atom	x	y	z	U(eq)
P(1)	1655(1)	6312(1)	4350(1)	20(1)
O(1)	-477(1)	7410(2)	3992(1)	27(1)
C(1A)	143(2)	4759(2)	4609(2)	21(1)
N(1A)	1260(2)	5114(2)	4730(2)	31(1)
C(1B)	490(10)	5320(10)	5301(8)	21(1)
N(1B)	1260(2)	5114(2)	4730(2)	31(1)
C(2)	670(2)	6710(2)	3270(2)	22(1)
C(3)	867(2)	6480(2)	2477(2)	26(1)
C(4)	82(2)	6708(2)	1635(2)	32(1)
C(5)	-910(2)	7165(2)	1580(2)	32(1)
C(6)	-1115(2)	7405(2)	2360(2)	29(1)
C(7)	-329(2)	7185(2)	3206(2)	23(1)
C(8)	1971(2)	7587(2)	5097(2)	24(1)
C(9)	1647(2)	8761(2)	4806(2)	30(1)
C(10)	2003(2)	9713(3)	5409(2)	37(1)
C(11)	2684(2)	9498(3)	6299(2)	39(1)
C(13)	3001(2)	8342(3)	6591(2)	40(1)
C(14)	2648(2)	7379(3)	5995(2)	34(1)
C(15)	2879(2)	5897(2)	4207(1)	21(1)
C(16)	3684(2)	6756(2)	4322(2)	24(1)
C(17)	4594(2)	6441(2)	4142(2)	28(1)
C(18)	4699(2)	5292(2)	3844(2)	28(1)
C(19)	3905(2)	4434(2)	3734(2)	31(1)
C(20)	2992(2)	4734(2)	3918(2)	28(1)
Cl(1)	2323(1)	-633(1)	2815(1)	44(1)
Cl(2)	4611(1)	-613(1)	3190(1)	56(1)
Cl(3)	3704(1)	961(1)	4194(1)	62(1)
C(21)	3489(2)	270(3)	3142(2)	43(1)
Br(1)	2838(1)	2041(1)	1115(1)	28(1)

U(eq) is defined as 1/3 the trace of the U_{ij} tensor.

Table 3. Bond lengths (Å) and angles (deg) for pa370

P(1)-N(1A)	1.623(2)	P(1)-C(15)	1.790(2)
P(1)-C(2)	1.790(2)	P(1)-C(8)	1.792(2)
O(1)-C(7)	1.355(3)	O(1)-H(10)	0.8400
C(1A)-N(1A)	1.485(3)	C(1A)-C(1A)#3	1.524(5)
C(1A)-H(1A1)	0.9900	C(1A)-H(1A2)	0.9900
N(1A)-H(1NA)	0.75(2)	N(1A)-H(1NB)	0.75(2)
C(1B)-C(1B)#3	1.48(2)	C(1B)-H(1B1)	0.9900
C(1B)-H(1B2)	0.9900	C(2)-C(3)	1.401(3)
C(2)-C(7)	1.402(3)	C(3)-C(4)	1.387(3)
C(3)-H(3)	0.9500	C(4)-C(5)	1.391(3)
C(4)-H(4)	0.9500	C(5)-C(6)	1.388(3)
C(5)-H(5)	0.9500	C(6)-C(7)	1.389(3)
C(6)-H(6)	0.9500	C(8)-C(9)	1.395(3)
C(8)-C(14)	1.399(3)	C(9)-C(10)	1.385(4)
C(9)-H(9)	0.9500	C(10)-C(11)	1.391(4)
C(10)-H(10)	0.9500	C(11)-C(13)	1.375(4)
C(11)-H(11)	0.9500	C(13)-C(14)	1.388(4)
C(13)-H(13)	0.9500	C(14)-H(14)	0.9500
C(15)-C(20)	1.393(3)	C(15)-C(16)	1.396(3)
C(16)-C(17)	1.391(3)	C(16)-H(16)	0.9500
C(17)-C(18)	1.383(4)	C(17)-H(17)	0.9500
C(18)-C(19)	1.386(4)	C(18)-H(18)	0.9500
C(19)-C(20)	1.393(3)	C(19)-H(19)	0.9500
C(20)-H(20)	0.9500	C1(1)-C(21)	1.760(3)
C1(2)-C(21)	1.767(3)	C1(3)-C(21)	1.762(3)
C(21)-H(21)	1.0000		
N(1A)-P(1)-C(15)	105.8(1)	N(1A)-P(1)-C(2)	109.4(1)
C(15)-P(1)-C(2)	109.0(1)	N(1A)-P(1)-C(8)	115.3(1)
C(15)-P(1)-C(8)	106.4(1)	C(2)-P(1)-C(8)	110.6(1)
C(7)-O(1)-H(10)	109.6	N(1A)-C(1A)-C(1A)#3	110.0(3)
N(1A)-C(1A)-H(1A1)	109.7	C(1A)#3-C(1A)-H(1A1)	109.7
N(1A)-C(1A)-H(1A2)	109.7	C(1A)#3-C(1A)-H(1A2)	109.7
H(1A1)-C(1A)-H(1A2)	108.2	C(1A)-N(1A)-P(1)	128.0(2)
C(1A)-N(1A)-H(1NA)	114(1)	P(1)-N(1A)-H(1NA)	118(1)
C(1A)-N(1A)-H(1NB)	114(1)	P(1)-N(1A)-H(1NB)	118(1)
H(1NA)-N(1A)-H(1NB)	0(3)	C(1B)#3-C(1B)-H(1B1)	111.9
C(1B)#3-C(1B)-H(1B2)	111.9	H(1B1)-C(1B)-H(1B2)	109.6
C(3)-C(2)-C(7)	119.4(2)	C(3)-C(2)-P(1)	120.1(2)
C(7)-C(2)-P(1)	120.5(2)	C(4)-C(3)-C(2)	120.6(2)
C(4)-C(3)-H(3)	119.7	C(2)-C(3)-H(3)	119.7
C(3)-C(4)-C(5)	119.4(2)	C(3)-C(4)-H(4)	120.3
C(5)-C(4)-H(4)	120.3	C(6)-C(5)-C(4)	120.6(2)
C(6)-C(5)-H(5)	119.7	C(4)-C(5)-H(5)	119.7
C(5)-C(6)-C(7)	120.2(2)	C(5)-C(6)-H(6)	119.9
C(7)-C(6)-H(6)	119.9	O(1)-C(7)-C(6)	123.0(2)
O(1)-C(7)-C(2)	117.2(2)	C(6)-C(7)-C(2)	119.8(2)
C(9)-C(8)-C(14)	119.8(2)	C(9)-C(8)-P(1)	123.1(2)
C(14)-C(8)-P(1)	116.9(2)	C(10)-C(9)-C(8)	119.6(2)
C(10)-C(9)-H(9)	120.2	C(8)-C(9)-H(9)	120.2
C(9)-C(10)-C(11)	120.2(3)	C(9)-C(10)-H(10)	119.9
C(11)-C(10)-H(10)	119.9	C(13)-C(11)-C(10)	120.5(3)
C(13)-C(11)-H(11)	119.8	C(10)-C(11)-H(11)	119.8
C(11)-C(13)-C(14)	120.0(2)	C(11)-C(13)-H(13)	120.0
C(14)-C(13)-H(13)	120.0	C(13)-C(14)-C(8)	119.9(3)
C(13)-C(14)-H(14)	120.0	C(8)-C(14)-H(14)	120.0
C(20)-C(15)-C(16)	120.2(2)	C(20)-C(15)-P(1)	119.5(2)
C(16)-C(15)-P(1)	120.2(2)	C(17)-C(16)-C(15)	119.4(2)
C(17)-C(16)-H(16)	120.3	C(15)-C(16)-H(16)	120.3
C(18)-C(17)-C(16)	120.5(2)	C(18)-C(17)-H(17)	119.8
C(16)-C(17)-H(17)	119.8	C(17)-C(18)-C(19)	120.3(2)
C(17)-C(18)-H(18)	119.8	C(19)-C(18)-H(18)	119.8
C(18)-C(19)-C(20)	119.8(2)	C(18)-C(19)-H(19)	120.1
C(20)-C(19)-H(19)	120.1	C(19)-C(20)-C(15)	119.8(2)
C(19)-C(20)-H(20)	120.1	C(15)-C(20)-H(20)	120.1

C1(1)-C(21)-C1(3)	110.2(2)	C1(1)-C(21)-C1(2)	110.0(2)
C1(3)-C(21)-C1(2)	111.0(2)	C1(1)-C(21)-H(21)	108.5
C1(3)-C(21)-H(21)	108.5	C1(2)-C(21)-H(21)	108.5

 Estimated standard deviations are given in the parenthesis.

Symmetry operators ::

1: x, y, z 2: -x, y+1/2, -z+1/2 3: -x, -y, -z
 4: x, -y-1/2, z-1/2

Appendix 1. Crystallographic data

Table 4. Anisotropic displacement parameters ($\text{Å}^2 \times 10^3$) for pa370

atom	U11	U22	U33	U23	U13	U12
P(1)	15(1)	26(1)	22(1)	4(1)	10(1)	0(1)
O(1)	19(1)	37(1)	28(1)	2(1)	11(1)	3(1)
C(1A)	19(1)	22(1)	24(1)	-1(1)	10(1)	-6(1)
N(1A)	18(1)	36(1)	42(1)	19(1)	15(1)	6(1)
C(1B)	19(1)	22(1)	24(1)	-1(1)	10(1)	-6(1)
N(1B)	18(1)	36(1)	42(1)	19(1)	15(1)	6(1)
C(2)	18(1)	24(1)	23(1)	4(1)	8(1)	-1(1)
C(3)	23(1)	33(1)	25(1)	2(1)	11(1)	3(1)
C(4)	33(1)	39(1)	23(1)	3(1)	10(1)	3(1)
C(5)	29(1)	39(1)	25(1)	5(1)	5(1)	4(1)
C(6)	21(1)	34(1)	31(1)	6(1)	7(1)	5(1)
C(7)	20(1)	24(1)	24(1)	3(1)	9(1)	-1(1)
C(8)	21(1)	32(1)	22(1)	1(1)	12(1)	-2(1)
C(9)	32(1)	31(1)	26(1)	1(1)	11(1)	-4(1)
C(10)	43(1)	34(1)	36(1)	-3(1)	17(1)	-8(1)
C(11)	41(1)	48(2)	31(1)	-12(1)	17(1)	-14(1)
C(13)	37(1)	58(2)	23(1)	-4(1)	9(1)	-1(1)
C(14)	32(1)	46(2)	23(1)	1(1)	10(1)	6(1)
C(15)	15(1)	27(1)	20(1)	3(1)	7(1)	-1(1)
C(16)	19(1)	28(1)	26(1)	4(1)	10(1)	-2(1)
C(17)	18(1)	39(1)	30(1)	6(1)	12(1)	-2(1)
C(18)	19(1)	44(1)	23(1)	6(1)	10(1)	6(1)
C(19)	30(1)	34(1)	31(1)	-3(1)	14(1)	5(1)
C(20)	23(1)	32(1)	29(1)	-3(1)	12(1)	-3(1)
Cl(1)	44(1)	46(1)	41(1)	-1(1)	15(1)	-4(1)
Cl(2)	48(1)	66(1)	61(1)	13(1)	27(1)	-2(1)
Cl(3)	67(1)	62(1)	42(1)	-10(1)	3(1)	-3(1)
C(21)	49(2)	39(2)	35(1)	7(1)	9(1)	-5(1)
Br(1)	21(1)	31(1)	34(1)	1(1)	13(1)	1(1)

The anisotropic displacement factor exponent takes the form
 $2 \pi^2 [h^2 a^{*2} U(11) + \dots + 2 h k a^* b^* U(12)]$

Appendix 1. Crystallographic data

Table 5. Hydrogen Coordinates ($\text{Å} \times 10^4$) and equivalent isotropic displacement parameters ($\text{Å}^2 \times 10^3$) for pa370

atom	x	y	z	U(eq)
H(10)	-1101	7679	3878	41
H(1A1)	80	3868	4585	25
H(1A2)	-365	5088	4030	25
H(1NA)	1680(10)	4720(20)	5060(10)	46
H(1B1)	787	4943	5908	25
H(1B2)	347	6186	5362	25
H(1NB)	1680(10)	4720(20)	5060(10)	46
H(3)	1544	6164	2517	32
H(4)	221	6553	1099	38
H(5)	-1452	7315	1004	39
H(6)	-1795	7719	2315	35
H(9)	1184	8907	4198	36
H(10)	1782	10513	5213	44
H(11)	2931	10154	6707	47
H(13)	3462	8202	7201	48
H(14)	2865	6579	6197	40
H(16)	3611	7548	4523	28
H(17)	5147	7020	4224	34
H(18)	5319	5089	3714	34
H(19)	3982	3644	3533	37
H(20)	2448	4147	3847	33
H(21)	3382	916	2676	51

Complex 30

Table 1. Crystal data for pa236

Compound	pa236
Molecular formula	C ₃₈ H ₃₂ N ₂ O ₂ P ₂ Pd ₄ (CH ₂ Cl ₂)
Molecular weight	1056.70
Crystal habit	Orange Block
Crystal dimensions(mm)	0.28x0.18x0.16
Crystal system	orthorhombic
Space group	Pna2 ₁
a(Å)	23.441(1)
b(Å)	10.218(1)
c(Å)	19.401(1)
α(°)	90.00
β(°)	90.00
γ(°)	90.00
V(Å ³)	4646.9(6)
Z	4
d(g·cm ⁻³)	1.510
F(000)	2136
μ(cm ⁻¹)	0.965
Absorption corrections	multi-scan ; 0.7738 min, 0.8608 max
Diffractionmeter	KappaCCD
X-ray source	MoKα
λ(Å)	0.71069
Monochromator	graphite
T (K)	150.0(1)
Scan mode	phi and omega scans
Maximum θ	30.02
HKL ranges	-33 31 ; -10 14 ; -27 20
Reflections measured	44198
Unique data	12183
Rint	0.0323
Reflections used	10068
Criterion	I > 2σ(I)
Refinement type	Fsqd
Hydrogen atoms	constr
Parameters refined	516
Reflections / parameter	19
wR2	0.1165
R1	0.0433
Flack's parameter	0.38(2)
Weights a, b	0.0609 ; 1.5094
GoF	1.091
difference peak / hole (e Å ⁻³)	0.835(0.065) / -0.501(0.065)

Table 2. Atomic Coordinates (A x 10⁴) and equivalent isotropic displacement parameters (A² x 10³) for pa236

atom	x	y	z	U(eq)
Pd(1)	-6221(1)	-1849(1)	-3994(1)	26(1)
P(1)	-7426(1)	-3000(1)	-4108(1)	27(1)
P(2)	-5012(1)	-2965(1)	-3893(1)	26(1)
O(1)	-6776(1)	-390(2)	-4225(1)	33(1)
O(2)	-5667(1)	-367(2)	-3780(1)	34(1)
N(1)	-6756(1)	-3343(3)	-4199(2)	31(1)
N(2)	-5679(1)	-3319(3)	-3765(2)	28(1)
C(1)	-6539(1)	-4557(3)	-3873(3)	38(1)
C(2)	-5904(1)	-4579(3)	-4033(3)	35(1)
C(3)	-7579(1)	-1649(4)	-4654(2)	29(1)
C(4)	-7223(1)	-521(4)	-4629(2)	30(1)
C(5)	-7381(2)	544(4)	-5056(2)	34(1)
C(6)	-7849(2)	473(4)	-5487(2)	36(1)
C(7)	-8179(2)	-652(4)	-5526(2)	36(1)
C(8)	-8050(2)	-1705(4)	-5107(2)	33(1)
C(9)	-7842(1)	-4375(4)	-4392(2)	30(1)
C(10)	-7675(2)	-5006(4)	-5012(2)	38(1)
C(11)	-7992(2)	-6025(5)	-5267(3)	47(1)
C(12)	-8482(2)	-6438(4)	-4924(2)	44(1)
C(13)	-8651(2)	-5825(4)	-4323(2)	39(1)
C(14)	-8337(1)	-4799(3)	-4054(2)	33(1)
C(15)	-7648(1)	-2638(4)	-3230(2)	29(1)
C(16)	-7642(2)	-3631(4)	-2732(2)	36(1)
C(17)	-7800(2)	-3347(5)	-2065(2)	46(1)
C(18)	-7953(2)	-2097(6)	-1878(2)	51(1)
C(19)	-7957(2)	-1100(5)	-2375(2)	45(1)
C(20)	-7805(2)	-1378(4)	-3045(2)	37(1)
C(21)	-4858(1)	-1586(4)	-3368(2)	29(1)
C(22)	-5217(1)	-479(3)	-3381(2)	28(1)
C(23)	-5070(2)	580(4)	-2944(2)	35(1)
C(24)	-4605(2)	528(4)	-2514(2)	36(1)
C(25)	-4257(2)	-591(4)	-2491(2)	36(1)
C(26)	-4384(2)	-1638(4)	-2914(2)	32(1)
C(27)	-4581(1)	-4330(3)	-3616(2)	28(1)
C(28)	-4107(1)	-4757(3)	-3982(2)	31(1)
C(29)	-3797(1)	-5810(4)	-3742(2)	37(1)
C(30)	-3949(2)	-6435(4)	-3136(2)	42(1)
C(31)	-4414(2)	-5985(4)	-2759(2)	39(1)
C(32)	-4729(2)	-4945(4)	-3005(2)	36(1)
C(33)	-4817(1)	-2599(4)	-4766(2)	33(1)
C(34)	-4828(2)	-3577(5)	-5279(2)	37(1)
C(35)	-4695(2)	-3250(5)	-5954(2)	46(1)
C(36)	-4554(2)	-1986(5)	-6134(2)	48(1)
C(37)	-4552(2)	-1021(6)	-5636(3)	58(1)
C(38)	-4687(2)	-1317(4)	-4963(2)	41(1)
Cl(1)	-6342(1)	-1024(2)	-1954(1)	86(1)
Cl(2)	-5851(1)	-3470(2)	-1532(1)	142(1)
C(39)	-5811(3)	-2199(6)	-2076(3)	77(2)
Cl(3)	-6397(1)	2823(2)	-2594(1)	89(1)
Cl(4)	-7408(1)	2421(1)	-3425(1)	63(1)
C(40)	-6821(2)	1665(5)	-3008(3)	60(1)
Cl(5)	-8236(1)	3021(2)	-1514(1)	109(1)
Cl(6)	-8775(1)	671(2)	-1003(1)	70(1)
C(41)	-8676(2)	2360(7)	-862(3)	70(2)
Cl(7)	-9159(1)	-3328(3)	-726(1)	144(1)
Cl(8)	-9925(1)	-2515(1)	370(1)	66(1)
C(42)	-9247(3)	-3125(6)	129(3)	71(2)

U(eq) is defined as 1/3 the trace of the Uij tensor.

Table 3. Bond lengths (Å) and angles (deg) for pa236

Pd(1)-N(1)	2.014(3)	Pd(1)-N(2)	2.017(3)
Pd(1)-O(1)	2.029(2)	Pd(1)-O(2)	2.039(2)
P(1)-N(1)	1.620(3)	P(1)-C(3)	1.777(4)
P(1)-C(9)	1.795(4)	P(1)-C(15)	1.819(4)
P(2)-N(2)	1.623(3)	P(2)-C(21)	1.777(4)
P(2)-C(33)	1.793(4)	P(2)-C(27)	1.804(3)
O(1)-C(4)	1.314(4)	O(2)-C(22)	1.313(4)
N(1)-C(1)	1.482(5)	N(2)-C(2)	1.484(4)
C(1)-C(2)	1.521(4)	C(1)-H(1A)	0.9900
C(1)-H(1B)	0.9900	C(2)-H(2A)	0.9900
C(2)-H(2B)	0.9900	C(3)-C(8)	1.412(5)
C(3)-C(4)	1.425(5)	C(4)-C(5)	1.417(5)
C(5)-C(6)	1.381(5)	C(5)-H(5)	0.9500
C(6)-C(7)	1.388(6)	C(6)-H(6)	0.9500
C(7)-C(8)	1.383(6)	C(7)-H(7)	0.9500
C(8)-H(8)	0.9500	C(9)-C(14)	1.402(5)
C(9)-C(10)	1.420(6)	C(10)-C(11)	1.371(6)
C(10)-H(10)	0.9500	C(11)-C(12)	1.393(6)
C(11)-H(11)	0.9500	C(12)-C(13)	1.382(6)
C(12)-H(12)	0.9500	C(13)-C(14)	1.383(5)
C(13)-H(13)	0.9500	C(14)-H(14)	0.9500
C(15)-C(20)	1.387(6)	C(15)-C(16)	1.402(6)
C(16)-C(17)	1.377(6)	C(16)-H(16)	0.9500
C(17)-C(18)	1.375(7)	C(17)-H(17)	0.9500
C(18)-C(19)	1.403(7)	C(18)-H(18)	0.9500
C(19)-C(20)	1.377(6)	C(19)-H(19)	0.9500
C(20)-H(20)	0.9500	C(21)-C(22)	1.411(5)
C(21)-C(26)	1.417(5)	C(22)-C(23)	1.417(5)
C(23)-C(24)	1.373(5)	C(23)-H(23)	0.9500
C(24)-C(25)	1.406(5)	C(24)-H(24)	0.9500
C(25)-C(26)	1.381(6)	C(25)-H(25)	0.9500
C(26)-H(26)	0.9500	C(27)-C(32)	1.386(5)
C(27)-C(28)	1.390(5)	C(28)-C(29)	1.380(5)
C(28)-H(28)	0.9500	C(29)-C(30)	1.384(6)
C(29)-H(29)	0.9500	C(30)-C(31)	1.392(6)
C(30)-H(30)	0.9500	C(31)-C(32)	1.378(5)
C(31)-H(31)	0.9500	C(32)-H(32)	0.9500
C(33)-C(38)	1.399(6)	C(33)-C(34)	1.410(6)
C(34)-C(35)	1.387(6)	C(34)-H(34)	0.9500
C(35)-C(36)	1.378(7)	C(35)-H(35)	0.9500
C(36)-C(37)	1.380(7)	C(36)-H(36)	0.9500
C(37)-C(38)	1.378(6)	C(37)-H(37)	0.9500
C(38)-H(38)	0.9500	Cl(1)-C(39)	1.745(6)
Cl(2)-C(39)	1.677(6)	C(39)-H(39A)	0.9900
C(39)-H(39B)	0.9900	Cl(3)-C(40)	1.741(5)
Cl(4)-C(40)	1.774(5)	C(40)-H(40A)	0.9900
C(40)-H(40B)	0.9900	Cl(5)-C(41)	1.765(6)
Cl(6)-C(41)	1.763(7)	C(41)-H(41A)	0.9900
C(41)-H(41B)	0.9900	Cl(7)-C(42)	1.684(7)
Cl(8)-C(42)	1.770(6)	C(42)-H(42A)	0.9900
C(42)-H(42B)	0.9900		
N(1)-Pd(1)-N(2)	82.6(1)	N(1)-Pd(1)-O(1)	96.6(1)
N(2)-Pd(1)-O(1)	179.1(1)	N(1)-Pd(1)-O(2)	178.7(1)
N(2)-Pd(1)-O(2)	96.1(1)	O(1)-Pd(1)-O(2)	84.7(1)
N(1)-P(1)-C(3)	107.4(2)	N(1)-P(1)-C(9)	108.9(2)
C(3)-P(1)-C(9)	108.4(2)	N(1)-P(1)-C(15)	115.0(2)
C(3)-P(1)-C(15)	110.0(2)	C(9)-P(1)-C(15)	106.9(2)
N(2)-P(2)-C(21)	106.6(2)	N(2)-P(2)-C(33)	115.9(2)
C(21)-P(2)-C(33)	108.9(2)	N(2)-P(2)-C(27)	108.8(2)
C(21)-P(2)-C(27)	109.1(2)	C(33)-P(2)-C(27)	107.4(2)
C(4)-O(1)-Pd(1)	124.6(2)	C(22)-O(2)-Pd(1)	124.6(2)
C(1)-N(1)-P(1)	117.9(2)	C(1)-N(1)-Pd(1)	109.7(2)
P(1)-N(1)-Pd(1)	114.7(2)	C(2)-N(2)-P(2)	118.8(2)
C(2)-N(2)-Pd(1)	110.2(2)	P(2)-N(2)-Pd(1)	114.0(2)

N(1)-C(1)-C(2)	105.1(3)	N(1)-C(1)-H(1A)	110.7
C(2)-C(1)-H(1A)	110.7	N(1)-C(1)-H(1B)	110.7
C(2)-C(1)-H(1B)	110.7	H(1A)-C(1)-H(1B)	108.8
N(2)-C(2)-C(1)	105.3(3)	N(2)-C(2)-H(2A)	110.7
C(1)-C(2)-H(2A)	110.7	N(2)-C(2)-H(2B)	110.7
C(1)-C(2)-H(2B)	110.7	H(2A)-C(2)-H(2B)	108.8
C(8)-C(3)-C(4)	120.9(3)	C(8)-C(3)-P(1)	119.8(3)
C(4)-C(3)-P(1)	119.3(3)	O(1)-C(4)-C(5)	118.7(3)
O(1)-C(4)-C(3)	124.8(3)	C(5)-C(4)-C(3)	116.5(3)
C(6)-C(5)-C(4)	121.5(4)	C(6)-C(5)-H(5)	119.3
C(4)-C(5)-H(5)	119.3	C(5)-C(6)-C(7)	121.3(4)
C(5)-C(6)-H(6)	119.3	C(7)-C(6)-H(6)	119.3
C(8)-C(7)-C(6)	119.3(4)	C(8)-C(7)-H(7)	120.3
C(6)-C(7)-H(7)	120.3	C(7)-C(8)-C(3)	120.4(4)
C(7)-C(8)-H(8)	119.8	C(3)-C(8)-H(8)	119.8
C(14)-C(9)-C(10)	118.9(3)	C(14)-C(9)-P(1)	123.2(3)
C(10)-C(9)-P(1)	117.8(3)	C(11)-C(10)-C(9)	120.2(4)
C(11)-C(10)-H(10)	119.9	C(9)-C(10)-H(10)	119.9
C(10)-C(11)-C(12)	120.3(4)	C(10)-C(11)-H(11)	119.9
C(12)-C(11)-H(11)	119.9	C(13)-C(12)-C(11)	120.1(4)
C(13)-C(12)-H(12)	119.9	C(11)-C(12)-H(12)	119.9
C(12)-C(13)-C(14)	120.7(4)	C(12)-C(13)-H(13)	119.6
C(14)-C(13)-H(13)	119.6	C(13)-C(14)-C(9)	119.9(4)
C(13)-C(14)-H(14)	120.1	C(9)-C(14)-H(14)	120.1
C(20)-C(15)-C(16)	119.7(4)	C(20)-C(15)-P(1)	120.5(3)
C(16)-C(15)-P(1)	119.8(3)	C(17)-C(16)-C(15)	119.6(4)
C(17)-C(16)-H(16)	120.2	C(15)-C(16)-H(16)	120.2
C(18)-C(17)-C(16)	120.9(4)	C(18)-C(17)-H(17)	119.6
C(16)-C(17)-H(17)	119.6	C(17)-C(18)-C(19)	119.7(4)
C(17)-C(18)-H(18)	120.2	C(19)-C(18)-H(18)	120.2
C(20)-C(19)-C(18)	119.8(5)	C(20)-C(19)-H(19)	120.1
C(18)-C(19)-H(19)	120.1	C(19)-C(20)-C(15)	120.3(4)
C(19)-C(20)-H(20)	119.8	C(15)-C(20)-H(20)	119.8
C(22)-C(21)-C(26)	120.6(3)	C(22)-C(21)-P(2)	120.3(3)
C(26)-C(21)-P(2)	119.1(3)	O(2)-C(22)-C(21)	124.1(3)
O(2)-C(22)-C(23)	118.8(3)	C(21)-C(22)-C(23)	117.2(3)
C(24)-C(23)-C(22)	121.8(3)	C(24)-C(23)-H(23)	119.1
C(22)-C(23)-H(23)	119.1	C(23)-C(24)-C(25)	120.7(4)
C(23)-C(24)-H(24)	119.6	C(25)-C(24)-H(24)	119.6
C(26)-C(25)-C(24)	119.1(3)	C(26)-C(25)-H(25)	120.5
C(24)-C(25)-H(25)	120.5	C(25)-C(26)-C(21)	120.6(4)
C(25)-C(26)-H(26)	119.7	C(21)-C(26)-H(26)	119.7
C(32)-C(27)-C(28)	119.6(3)	C(32)-C(27)-P(2)	117.8(3)
C(28)-C(27)-P(2)	122.6(3)	C(29)-C(28)-C(27)	119.6(4)
C(29)-C(28)-H(28)	120.2	C(27)-C(28)-H(28)	120.2
C(28)-C(29)-C(30)	120.7(4)	C(28)-C(29)-H(29)	119.6
C(30)-C(29)-H(29)	119.6	C(29)-C(30)-C(31)	119.7(4)
C(29)-C(30)-H(30)	120.1	C(31)-C(30)-H(30)	120.1
C(32)-C(31)-C(30)	119.5(4)	C(32)-C(31)-H(31)	120.3
C(30)-C(31)-H(31)	120.3	C(31)-C(32)-C(27)	120.8(3)
C(31)-C(32)-H(32)	119.6	C(27)-C(32)-H(32)	119.6
C(38)-C(33)-C(34)	118.3(4)	C(38)-C(33)-P(2)	120.6(3)
C(34)-C(33)-P(2)	120.9(3)	C(35)-C(34)-C(33)	119.5(4)
C(35)-C(34)-H(34)	120.3	C(33)-C(34)-H(34)	120.3
C(36)-C(35)-C(34)	121.2(4)	C(36)-C(35)-H(35)	119.4
C(34)-C(35)-H(35)	119.4	C(35)-C(36)-C(37)	119.6(4)
C(35)-C(36)-H(36)	120.2	C(37)-C(36)-H(36)	120.2
C(38)-C(37)-C(36)	120.3(5)	C(38)-C(37)-H(37)	119.8
C(36)-C(37)-H(37)	119.8	C(37)-C(38)-C(33)	121.0(4)
C(37)-C(38)-H(38)	119.5	C(33)-C(38)-H(38)	119.5
Cl(2)-C(39)-Cl(1)	114.1(3)	Cl(2)-C(39)-H(39A)	108.7
Cl(1)-C(39)-H(39A)	108.7	Cl(2)-C(39)-H(39B)	108.7
Cl(1)-C(39)-H(39B)	108.7	H(39A)-C(39)-H(39B)	107.6
Cl(3)-C(40)-Cl(4)	110.9(3)	Cl(3)-C(40)-H(40A)	109.5
Cl(4)-C(40)-H(40A)	109.5	Cl(3)-C(40)-H(40B)	109.5
Cl(4)-C(40)-H(40B)	109.5	H(40A)-C(40)-H(40B)	108.0
Cl(6)-C(41)-Cl(5)	109.9(3)	Cl(6)-C(41)-H(41A)	109.7
Cl(5)-C(41)-H(41A)	109.7	Cl(6)-C(41)-H(41B)	109.7

Appendix 1. Crystallographic data

Cl(5)-C(41)-H(41B)	109.7	H(41A)-C(41)-H(41B)	108.2
Cl(7)-C(42)-Cl(8)	114.4(4)	Cl(7)-C(42)-H(42A)	108.7
Cl(8)-C(42)-H(42A)	108.7	Cl(7)-C(42)-H(42B)	108.7
Cl(8)-C(42)-H(42B)	108.7	H(42A)-C(42)-H(42B)	107.6

Appendix 1. Crystallographic data

Table 4. Anisotropic displacement parameters ($\text{Å}^2 \times 10^3$) for pa236

atom	U11	U22	U33	U23	U13	U12
Pd(1)	23(1)	25(1)	30(1)	1(1)	1(1)	1(1)
P(1)	22(1)	28(1)	31(1)	1(1)	2(1)	0(1)
P(2)	22(1)	28(1)	29(1)	1(1)	1(1)	2(1)
O(1)	27(1)	28(1)	44(2)	-1(1)	-4(1)	5(1)
O(2)	30(1)	28(1)	44(2)	0(1)	-8(1)	-1(1)
N(1)	20(1)	28(2)	44(2)	-1(1)	-2(1)	-2(1)
N(2)	23(1)	24(1)	36(2)	0(1)	4(1)	2(1)
C(1)	24(1)	28(2)	62(3)	2(2)	0(2)	0(1)
C(2)	30(1)	25(2)	49(2)	1(2)	0(2)	2(1)
C(3)	26(2)	30(2)	30(2)	1(2)	4(1)	2(1)
C(4)	29(2)	32(2)	30(2)	-1(2)	1(1)	3(1)
C(5)	32(2)	32(2)	38(2)	5(2)	1(1)	-1(1)
C(6)	37(2)	41(2)	30(2)	7(2)	3(2)	5(2)
C(7)	33(2)	44(2)	30(2)	5(2)	0(2)	3(2)
C(8)	23(2)	35(2)	40(2)	-3(2)	1(1)	-2(1)
C(9)	26(2)	31(2)	33(2)	4(2)	0(1)	-2(1)
C(10)	35(2)	37(2)	43(2)	-5(2)	7(2)	-5(2)
C(11)	49(2)	43(2)	50(3)	-4(2)	9(2)	-3(2)
C(12)	43(2)	39(2)	51(3)	-3(2)	-5(2)	-10(2)
C(13)	28(2)	41(2)	49(2)	5(2)	-4(2)	-4(2)
C(14)	24(1)	37(2)	37(2)	1(2)	2(2)	-1(1)
C(15)	23(2)	35(2)	28(2)	2(2)	-3(1)	0(1)
C(16)	34(2)	42(2)	32(2)	4(2)	-4(2)	-2(2)
C(17)	41(2)	60(3)	38(2)	10(2)	-4(2)	-11(2)
C(18)	37(2)	86(4)	31(2)	-9(2)	2(2)	-9(2)
C(19)	45(2)	55(3)	37(2)	-7(2)	3(2)	2(2)
C(20)	34(2)	42(2)	35(2)	-3(2)	2(2)	1(2)
C(21)	25(2)	34(2)	27(2)	2(2)	2(1)	-3(1)
C(22)	27(2)	28(2)	28(2)	3(2)	3(1)	-4(1)
C(23)	34(2)	27(2)	45(2)	-5(2)	1(2)	0(1)
C(24)	30(2)	38(2)	41(2)	-11(2)	-3(2)	0(1)
C(25)	31(2)	39(2)	39(2)	-2(2)	-2(2)	-2(2)
C(26)	31(2)	37(2)	27(2)	2(2)	2(1)	2(1)
C(27)	24(1)	27(2)	32(2)	-1(2)	-1(1)	1(1)
C(28)	24(1)	34(2)	33(2)	-4(2)	1(2)	1(1)
C(29)	27(2)	43(2)	41(2)	-2(2)	-2(1)	5(1)
C(30)	37(2)	39(2)	49(3)	-2(2)	-7(2)	7(2)
C(31)	44(2)	39(2)	35(2)	4(2)	1(2)	10(2)
C(32)	34(2)	36(2)	36(2)	-5(2)	5(2)	7(2)
C(33)	25(2)	38(2)	37(2)	1(2)	2(2)	4(1)
C(34)	32(2)	45(2)	35(2)	-6(2)	-4(2)	4(2)
C(35)	41(2)	69(3)	28(2)	-11(2)	-6(2)	18(2)
C(36)	50(2)	63(3)	31(2)	6(2)	3(2)	14(2)
C(37)	67(3)	60(3)	48(3)	18(3)	8(2)	6(3)
C(38)	47(2)	41(2)	35(2)	4(2)	7(2)	4(2)
Cl(1)	82(1)	104(1)	73(1)	11(1)	12(1)	38(1)
Cl(2)	196(3)	102(2)	128(2)	63(1)	99(2)	68(2)
C(39)	95(4)	70(4)	65(4)	10(3)	24(3)	23(3)
Cl(3)	98(1)	64(1)	104(1)	-19(1)	-61(1)	21(1)
Cl(4)	49(1)	54(1)	87(1)	6(1)	-19(1)	-9(1)
C(40)	68(3)	47(3)	66(4)	-2(2)	-23(3)	0(2)
Cl(5)	123(2)	129(2)	73(1)	-4(1)	-14(1)	-41(1)
Cl(6)	59(1)	103(1)	48(1)	-11(1)	1(1)	16(1)
C(41)	77(4)	94(5)	40(3)	-5(3)	-3(2)	18(3)
Cl(7)	113(2)	240(3)	79(1)	27(2)	38(1)	32(2)
Cl(8)	54(1)	62(1)	82(1)	-5(1)	10(1)	-6(1)
C(42)	64(3)	76(4)	73(4)	21(3)	4(3)	14(3)

The anisotropic displacement factor exponent takes the form
 $2\pi^2 [h^2 a^{*2} U_{11} + \dots + 2hka^* b^* U_{12}]$

Table 5. Hydrogen Coordinates ($\text{\AA} \times 10^4$) and equivalent isotropic displacement parameters ($\text{\AA}^2 \times 10^3$) for pa236

atom	x	y	z	U(eq)
H(1A)	-6730	-5335.9995	-4069	46
H(1B)	-6605	-4540	-3369	46
H(2A)	-5716	-5327	-3801	42
H(2B)	-5838.9995	-4651	-4535	42
H(5)	-7161	1324	-5044.9995	41
H(6)	-7946	1209	-5762	43
H(7)	-8491	-697.9999	-5838.9995	43
H(8)	-8280	-2471	-5123	39
H(10)	-7343.9995	-4723	-5251	46
H(11)	-7877	-6451	-5680	57
H(12)	-8701	-7141	-5104	53
H(13)	-8985	-6111.9995	-4092.0002	47
H(14)	-8457	-4382	-3641	39
H(16)	-7530	-4494	-2852.9998	44
H(17)	-7803	-4023.9998	-1729.0001	56
H(18)	-8056	-1910	-1415	61
H(19)	-8063	-235.0000	-2250	54
H(20)	-7808	-703	-3382	44
H(23)	-5299	1347	-2949	42
H(24)	-4518	1257	-2229	43
H(25)	-3939	-626	-2189	44
H(26)	-4152	-2400	-2901	38
H(28)	-3996.9998	-4327	-4396	37
H(29)	-3476.0002	-6111	-3995.0002	44
H(30)	-3736	-7167	-2978	50
H(31)	-4515	-6393	-2336	47
H(32)	-5050	-4646	-2752	43
H(34)	-4927	-4451	-5163	45
H(35)	-4702	-3910	-6299	55
H(36)	-4459	-1781	-6597	58
H(37)	-4456	-147	-5759	70
H(38)	-4692	-640	-4628	50
H(39A)	-5837	-2532	-2555	92
H(39B)	-5434	-1776	-2022	92
H(40A)	-6964	1024	-2666.0002	72
H(40B)	-6590	1186	-3352	72
H(41A)	-8496	2500	-406.0000	84
H(41B)	-9050	2810	-864	84
H(42A)	-8951	-2515	299	85
H(42B)	-9186	-3978	359	85

Complex 3I

Table 1. Crystal data for pa185

Compound	pa185
Molecular formula	$\text{C}_{38}\text{H}_{32}\text{N}_2\text{NiO}_2\text{P}_2\text{CH}_2\text{Cl}_2$
Molecular weight	754.23
Crystal habit	Purple Needle
Crystal dimensions(mm)	0.32x0.10x0.04
Crystal system	monoclinic
Space group	Pc
a(\AA)	14.095(1)
b(\AA)	9.040(1)
c(\AA)	16.233(1)
α ($^\circ$)	90.00
β ($^\circ$)	122.384(4)
γ ($^\circ$)	90.00
V(\AA^3)	1746.7(3)
Z	2
d(g $\cdot\text{cm}^{-3}$)	1.434
F(000)	780
μ (cm^{-1})	0.838
Absorption corrections	multi-scan ; 0.7753 min, 0.9672 max
Diffractometer	KappaCCD
X-ray source	MoK α
λ (\AA)	0.71069
Monochromator	graphite
T (K)	150.0(1)
Scan mode	phi and omega scans
Maximum θ	26.00
HKL ranges	-13 17 ; -10 11 ; -19 20
Reflections measured	9847
Unique data	5021
Rint	0.0244
Reflections used	4499
Criterion	I > 2 σ (I)
Refinement type	Fsqd
Hydrogen atoms	constr
Parameters refined	433
Reflections / parameter	10
wR2	0.1219
R1	0.0449
Flack's parameter	0.022(16)
Weights a, b	0.0739 ; 0.7114
GoF	1.044
difference peak / hole (e \AA^{-3})	0.909(0.069) / -0.722(0.069)

Appendix 1. Crystallographic data

Table 2. Atomic Coordinates (A x 10⁴) and equivalent isotropic displacement parameters (A² x 10³) for pa185

atom	x	y	z	U(eq)
Ni(1)	913(1)	-9383(1)	-2668(1)	32(1)
P(2)	-1253(1)	-10212(1)	-2808(1)	31(1)
P(3)	2546(1)	-11573(1)	-2605(1)	32(1)
O(1)	-137(3)	-7837(4)	-3246(3)	40(1)
O(2)	1695(4)	-8318(4)	-3102(4)	57(1)
N(1)	83(3)	-10482(4)	-2259(3)	33(1)
N(2)	2024(4)	-10855(5)	-2019(3)	36(1)
C(1)	576(4)	-11954(5)	-1867(4)	38(1)
C(2)	1824(4)	-11742(6)	-1365(4)	41(1)
C(3)	-1491(4)	-8282(5)	-2830(3)	29(1)
C(4)	-872(4)	-7338(5)	-3065(4)	33(1)
C(5)	-1112(5)	-5799(5)	-3131(4)	43(1)
C(6)	-1890(5)	-5272(6)	-2941(4)	42(1)
C(7)	-2465(5)	-6201(6)	-2679(4)	42(1)
C(8)	-2286(4)	-7705(5)	-2627(4)	36(1)
C(9)	-1810(4)	-11099(5)	-2156(4)	35(1)
C(10)	-1172(5)	-11027(6)	-1137(4)	45(1)
C(11)	-1551(6)	-11702(6)	-605(5)	54(2)
C(12)	-2569(6)	-12427(7)	-1075(6)	62(2)
C(13)	-3219(5)	-12487(6)	-2089(5)	52(2)
C(14)	-2843(4)	-11819(5)	-2621(4)	38(1)
C(15)	-2065(4)	-10853(5)	-4053(4)	31(1)
C(16)	-3147(4)	-10288(6)	-4707(4)	43(1)
C(17)	-3762(5)	-10764(7)	-5661(4)	48(1)
C(18)	-3326(4)	-11789(6)	-5990(4)	43(1)
C(19)	-2264(5)	-12351(6)	-5368(4)	47(1)
C(20)	-1631(5)	-11876(6)	-4405(4)	40(1)
C(21)	3011(4)	-10114(5)	-3031(4)	32(1)
C(22)	2528(5)	-8692(5)	-3209(4)	39(1)
C(23)	2962(5)	-7592(5)	-3534(4)	43(1)
C(24)	3827(5)	-7877(6)	-3681(4)	43(1)
C(25)	4290(5)	-9283(6)	-3514(4)	46(1)
C(26)	3894(5)	-10369(6)	-3191(4)	43(1)
C(27)	3722(4)	-12758(5)	-1808(4)	34(1)
C(28)	4385(4)	-12397(5)	-824(4)	40(1)
C(29)	5300(4)	-13269(6)	-167(4)	49(1)
C(30)	5556(5)	-14517(6)	-535(5)	51(2)
C(31)	4914(5)	-14857(6)	-1497(5)	49(1)
C(32)	4011(5)	-13983(6)	-2149(4)	41(1)
C(33)	1596(4)	-12746(5)	-3642(4)	33(1)
C(34)	1132(5)	-12268(6)	-4581(4)	45(1)
C(35)	399(5)	-13157(7)	-5347(4)	51(1)
C(36)	115(5)	-14539(6)	-5194(4)	49(2)
C(37)	576(4)	-15040(6)	-4246(4)	43(1)
C(38)	1309(4)	-14151(6)	-3473(4)	39(1)
Cl(1)	2951(3)	-5630(3)	-217(3)	138(1)
Cl(2)	4293(2)	-7980(3)	-276(3)	121(1)
C(39)	3020(10)	-7270(10)	-730(10)	126(4)

U(eq) is defined as 1/3 the trace of the Uij tensor.

Appendix 1. Crystallographic data

Table 3. Bond lengths (A) and angles (deg) for pa185

Ni(1)-O(2)	1.863(4)	Ni(1)-O(1)	1.881(3)
Ni(1)-N(2)	1.888(4)	Ni(1)-N(1)	1.905(4)
P(2)-N(1)	1.613(4)	P(2)-C(3)	1.774(5)
P(2)-C(15)	1.804(5)	P(2)-C(9)	1.807(5)
P(3)-N(2)	1.617(4)	P(3)-C(21)	1.771(5)
P(3)-C(27)	1.809(5)	P(3)-C(33)	1.827(5)
O(1)-C(4)	1.301(6)	O(2)-C(22)	1.319(6)
N(1)-C(1)	1.478(6)	N(2)-C(2)	1.474(6)
C(1)-C(2)	1.502(7)	C(3)-C(4)	1.410(7)
C(3)-C(8)	1.425(7)	C(4)-C(5)	1.421(7)
C(5)-C(6)	1.373(8)	C(6)-C(7)	1.382(8)
C(7)-C(8)	1.378(7)	C(9)-C(14)	1.391(7)
C(9)-C(10)	1.398(8)	C(10)-C(11)	1.378(8)
C(11)-C(12)	1.38(1)	C(12)-C(13)	1.39(1)
C(13)-C(14)	1.373(8)	C(15)-C(20)	1.389(7)
C(15)-C(16)	1.407(7)	C(16)-C(17)	1.377(8)
C(17)-C(18)	1.368(8)	C(18)-C(19)	1.378(8)
C(19)-C(20)	1.390(8)	C(21)-C(22)	1.410(7)
C(21)-C(26)	1.419(7)	C(22)-C(23)	1.409(7)
C(23)-C(24)	1.387(8)	C(24)-C(25)	1.387(8)
C(25)-C(26)	1.366(8)	C(27)-C(28)	1.390(7)
C(27)-C(32)	1.392(7)	C(28)-C(29)	1.397(7)
C(29)-C(30)	1.41(1)	C(30)-C(31)	1.36(1)
C(31)-C(32)	1.386(8)	C(33)-C(34)	1.367(7)
C(33)-C(38)	1.404(7)	C(34)-C(35)	1.372(8)
C(35)-C(36)	1.375(8)	C(36)-C(37)	1.387(8)
C(37)-C(38)	1.378(7)	Cl(1)-C(39)	1.72(1)
Cl(2)-C(39)	1.66(1)		
O(2)-Ni(1)-O(1)	83.9(2)	O(2)-Ni(1)-N(2)	95.4(2)
O(1)-Ni(1)-N(2)	176.3(2)	O(2)-Ni(1)-N(1)	178.5(2)
O(1)-Ni(1)-N(1)	95.4(2)	N(2)-Ni(1)-N(1)	85.4(2)
N(1)-P(2)-C(3)	108.2(2)	N(1)-P(2)-C(15)	115.0(2)
C(3)-P(2)-C(15)	107.1(2)	N(1)-P(2)-C(9)	110.8(2)
C(3)-P(2)-C(9)	108.2(2)	C(15)-P(2)-C(9)	107.4(2)
N(2)-P(3)-C(21)	108.1(2)	N(2)-P(3)-C(27)	110.4(2)
C(21)-P(3)-C(27)	109.3(2)	N(2)-P(3)-C(33)	115.8(2)
C(21)-P(3)-C(33)	108.3(2)	C(27)-P(3)-C(33)	104.7(2)
C(4)-O(1)-Ni(1)	130.9(3)	C(22)-O(2)-Ni(1)	131.7(3)
C(1)-N(1)-P(2)	121.0(3)	C(1)-N(1)-Ni(1)	112.6(3)
P(2)-N(1)-Ni(1)	118.8(2)	C(2)-N(2)-P(3)	121.9(3)
C(2)-N(2)-Ni(1)	111.3(3)	P(3)-N(2)-Ni(1)	117.2(2)
N(1)-C(1)-C(2)	105.3(4)	N(2)-C(2)-C(1)	107.4(4)
C(4)-C(3)-C(8)	121.2(4)	C(4)-C(3)-P(2)	117.6(3)
C(8)-C(3)-P(2)	121.2(4)	O(1)-C(4)-C(3)	122.3(4)
O(1)-C(4)-C(5)	120.5(4)	C(3)-C(4)-C(5)	117.1(4)
C(6)-C(5)-C(4)	120.5(5)	C(5)-C(6)-C(7)	121.9(5)
C(8)-C(7)-C(6)	120.1(5)	C(7)-C(8)-C(3)	119.2(5)
C(14)-C(9)-C(10)	119.1(5)	C(14)-C(9)-P(2)	123.1(4)
C(10)-C(9)-P(2)	117.7(4)	C(11)-C(10)-C(9)	120.1(6)
C(12)-C(11)-C(10)	120.1(6)	C(11)-C(12)-C(13)	120.3(6)
C(14)-C(13)-C(12)	119.7(6)	C(13)-C(14)-C(9)	120.6(6)
C(20)-C(15)-C(16)	118.0(5)	C(20)-C(15)-P(2)	121.3(4)
C(16)-C(15)-P(2)	120.6(4)	C(17)-C(16)-C(15)	120.7(5)
C(18)-C(17)-C(16)	120.4(5)	C(17)-C(18)-C(19)	120.2(5)
C(18)-C(19)-C(20)	120.1(5)	C(15)-C(20)-C(19)	120.6(5)
C(22)-C(21)-C(26)	119.1(5)	C(22)-C(21)-P(3)	121.3(4)
C(26)-C(21)-P(3)	119.6(4)	O(2)-C(22)-C(23)	117.6(4)
O(2)-C(22)-C(21)	125.0(5)	C(23)-C(22)-C(21)	117.4(5)
C(24)-C(23)-C(22)	122.1(5)	C(25)-C(24)-C(23)	120.1(5)
C(26)-C(25)-C(24)	119.2(5)	C(25)-C(26)-C(21)	122.1(5)
C(28)-C(27)-C(32)	118.9(5)	C(28)-C(27)-P(3)	118.5(4)
C(32)-C(27)-P(3)	122.6(4)	C(27)-C(28)-C(29)	121.5(5)
C(28)-C(29)-C(30)	118.0(5)	C(31)-C(30)-C(29)	120.3(5)
C(30)-C(31)-C(32)	121.5(6)	C(31)-C(32)-C(27)	119.7(5)

Appendix 1. Crystallographic data

C(34)-C(33)-C(38)	119.2(5)	C(34)-C(33)-P(3)	121.4(4)
C(38)-C(33)-P(3)	119.4(4)	C(33)-C(34)-C(35)	120.2(5)
C(34)-C(35)-C(36)	121.3(5)	C(35)-C(36)-C(37)	119.2(5)
C(38)-C(37)-C(36)	119.8(5)	C(37)-C(38)-C(33)	120.2(5)
C1(2)-C(39)-C1(1)	116.4(6)		

Appendix 1. Crystallographic data

Table 4. Anisotropic displacement parameters ($\text{Å}^2 \times 10^3$) for pal85

atom	U11	U22	U33	U23	U13	U12
Ni(1)	34(1)	29(1)	35(1)	3(1)	20(1)	3(1)
P(2)	32(1)	29(1)	33(1)	1(1)	19(1)	2(1)
P(3)	31(1)	31(1)	34(1)	4(1)	17(1)	4(1)
O(1)	45(2)	34(2)	47(2)	9(2)	28(2)	5(2)
O(2)	63(3)	37(2)	100(4)	20(2)	64(3)	12(2)
N(1)	30(2)	28(2)	39(2)	7(2)	18(2)	4(2)
N(2)	41(2)	39(2)	37(2)	4(2)	28(2)	2(2)
C(1)	44(3)	28(2)	43(3)	9(2)	24(3)	6(2)
C(2)	40(3)	48(3)	36(3)	12(2)	21(2)	12(2)
C(3)	37(3)	26(2)	24(2)	-3(2)	15(2)	-1(2)
C(4)	38(3)	29(2)	34(3)	2(2)	21(2)	3(2)
C(5)	47(3)	32(3)	51(3)	-2(2)	26(3)	-3(2)
C(6)	53(3)	27(2)	41(3)	3(2)	22(3)	7(2)
C(7)	43(3)	41(3)	42(3)	-1(3)	23(2)	12(2)
C(8)	39(3)	35(3)	32(3)	2(2)	17(2)	11(2)
C(9)	37(3)	27(2)	46(3)	7(2)	26(3)	7(2)
C(10)	51(3)	43(3)	46(3)	6(3)	31(3)	9(2)
C(11)	80(5)	45(3)	57(4)	13(3)	50(4)	18(3)
C(12)	84(5)	41(3)	101(6)	16(3)	75(5)	13(3)
C(13)	54(4)	41(3)	78(5)	9(3)	48(4)	8(3)
C(14)	37(3)	35(3)	49(3)	1(2)	27(3)	4(2)
C(15)	39(3)	26(2)	36(3)	-3(2)	25(2)	-4(2)
C(16)	35(3)	47(3)	45(3)	-2(3)	19(3)	5(2)
C(17)	36(3)	58(4)	43(3)	-10(3)	17(3)	-6(2)
C(18)	42(3)	44(3)	42(3)	-6(2)	23(3)	-13(2)
C(19)	57(4)	43(3)	47(3)	-10(3)	32(3)	-4(3)
C(20)	42(3)	39(3)	42(3)	2(2)	24(3)	7(2)
C(21)	34(3)	27(2)	34(3)	-2(2)	18(2)	-3(2)
C(22)	44(3)	33(3)	45(3)	-2(2)	27(3)	-2(2)
C(23)	51(3)	30(3)	55(4)	4(2)	35(3)	-1(2)
C(24)	52(3)	41(3)	44(3)	0(2)	30(3)	-5(2)
C(25)	46(3)	57(3)	47(3)	7(3)	32(3)	1(3)
C(26)	43(3)	42(3)	48(3)	6(3)	28(3)	8(2)
C(27)	32(3)	33(3)	37(3)	-3(2)	18(2)	-1(2)
C(28)	35(3)	33(3)	45(3)	8(2)	16(2)	1(2)
C(29)	32(3)	52(3)	46(3)	7(3)	10(3)	-3(2)
C(30)	30(3)	41(3)	61(4)	18(3)	10(3)	5(2)
C(31)	39(3)	38(3)	63(4)	6(3)	22(3)	5(2)
C(32)	37(3)	37(3)	42(3)	3(2)	16(2)	7(2)
C(33)	30(3)	34(3)	36(3)	3(2)	19(2)	5(2)
C(34)	45(3)	39(3)	38(3)	6(2)	14(3)	3(2)
C(35)	50(4)	53(3)	35(3)	2(3)	12(3)	-4(3)
C(36)	46(4)	44(3)	41(3)	-7(3)	13(3)	0(2)
C(37)	37(3)	33(3)	46(3)	-1(3)	14(3)	-3(2)
C(38)	33(3)	42(3)	36(3)	0(2)	14(2)	-4(2)
C1(1)	177(3)	63(1)	250(4)	-23(2)	165(3)	-15(1)
C1(2)	94(2)	92(2)	176(3)	40(2)	72(2)	16(1)
C(39)	125(8)	86(6)	109(8)	-33(6)	23(7)	0(6)

The anisotropic displacement factor exponent takes the form
 $2 \pi^2 [h^2 a^{*2} U_{11} + \dots + 2 h k a^* b^* U_{12}]$

Table 5. Hydrogen Coordinates ($\text{\AA} \times 10^4$) and equivalent isotropic displacement parameters ($\text{\AA}^2 \times 10^3$) for pa185

atom	x	y	z	U(eq)
H(1A)	304	-12687	-2400	46
H(1B)	378	-12299	-1399	46
H(2A)	2121	-11221	-736	49
H(2B)	2205	-12711.9990	-1233	49
H(5)	-731	-5130	-3308	52
H(6)	-2037.9999	-4240	-2991	51
H(7)	-2984.0002	-5801	-2536	50
H(8)	-2687	-8350	-2457	44
H(10)	-476	-10512	-812.0001	54
H(11)	-1109	-11668	87	65
H(12)	-2829	-12887	-706	75
H(13)	-3921	-12988	-2411	62
H(14)	-3291.0002	-11849	-3314	46
H(16)	-3456	-9570	-4489	52
H(17)	-4493	-10378	-6093.9995	57
H(18)	-3757	-12115	-6648	51
H(19)	-1964	-13063	-5599	57
H(20)	-894	-12255	-3983	48
H(23)	2652	-6625	-3656	51
H(24)	4104	-7109	-3897	52
H(25)	4875	-9487	-3623	56
H(26)	4220	-11327	-3069	51
H(28)	4211	-11537	-594	48
H(29)	5737	-13030	508	58
H(30)	6181	-15121	-106	62
H(31)	5088	-15714	-1729.9999	59
H(32)	3592	-14218	-2824	49
H(34)	1318	-11318.0010	-4703	54
H(35)	82	-12810	-5995	61
H(36)	-392	-15144	-5730.9995	59
H(37)	388	-15993	-4130	52
H(38)	1621	-14490	-2823	47
H(39A)	2554	-8009	-653.9999	151
H(39B)	2675	-7104	-1436	151

Chapter 4

Complex 37a

Table 1. Crystal data for pa646

Compound	pa646
Molecular formula	$\text{C}_{54}\text{H}_{64}\text{N}_2\text{NiO}_2\text{P}_2 \cdot 2(\text{C}_7\text{H}_8)$
Molecular weight	1077.99
Crystal habit	Dark Blue Block
Crystal dimensions(mm)	0.22x0.12x0.06
Crystal system	monoclinic
Space group	C2/c
a(\AA)	31.194(1)
b(\AA)	10.777(1)
c(\AA)	19.804(1)
α ($^\circ$)	90.00
β ($^\circ$)	112.805(1)
γ ($^\circ$)	90.00
V(\AA^3)	6137.2(7)
Z	4
d(g·cm $^{-3}$)	1.167
F(000)	2304
μ (cm $^{-1}$)	0.412
Absorption corrections	multi-scan ; 0.9148 min, 0.9757 max
Diffractometer	KappaCCD
X-ray source	MoK α
λ (\AA)	0.71069
Monochromator	graphite
T (K)	150.0(1)
Scan mode	phi and omega scans
Maximum θ	27.48
HKL ranges	-38 40 ; -13 13 ; -25 25
Reflections measured	24477
Unique data	6920
Rint	0.0511
Reflections used	5745
Criterion	I > 2 σ (I)
Refinement type	Fsqd
Hydrogen atoms	constr
Parameters refined	346
Reflections / parameter	16
wR2	0.1019
R1	0.0486
Weights a, b	0.0267 ; 15.563
GoF	1.060
difference peak / hole (e \AA^{-3})	0.605(0.061) / -0.332(0.061)

Appendix 1. Crystallographic data

Table 2. Atomic Coordinates (A x 10⁴) and equivalent isotropic displacement parameters (A² x 10³) for pa646

atom	x	y	z	U(eq)
Ni(1)	0	6409(1)	2500	17(1)
P(1)	507(1)	7358(1)	4017(1)	18(1)
O(1)	340(1)	5126(1)	3117(1)	21(1)
N(1)	307(1)	7699(2)	3154(1)	19(1)
C(1)	73(1)	8909(2)	2911(1)	24(1)
C(2)	804(1)	8692(2)	4545(1)	21(1)
C(3)	1224(1)	9070(2)	4510(1)	28(1)
C(4)	1437(1)	10154(2)	4861(1)	33(1)
C(5)	1233(1)	10873(2)	5231(2)	38(1)
C(6)	815(1)	10513(2)	5260(2)	40(1)
C(7)	601(1)	9423(2)	4920(1)	30(1)
C(8)	64(1)	6925(2)	4353(1)	21(1)
C(9)	174(1)	6715(2)	5100(1)	25(1)
C(10)	-171(1)	6372(2)	5341(1)	29(1)
C(11)	-625(1)	6230(2)	4839(1)	28(1)
C(12)	-735(1)	6410(2)	4100(1)	28(1)
C(13)	-390(1)	6764(2)	3857(1)	23(1)
C(14)	906(1)	6119(2)	4157(1)	19(1)
C(15)	764(1)	5156(2)	3627(1)	19(1)
C(16)	1094(1)	4194(2)	3690(1)	22(1)
C(17)	1509(1)	4200(2)	4299(1)	23(1)
C(18)	1637(1)	5102(2)	4853(1)	23(1)
C(19)	1331(1)	4761(2)	4761(1)	22(1)
C(20)	981(1)	3176(2)	3104(1)	28(1)
C(21)	1404(1)	2343(3)	3217(2)	41(1)
C(22)	828(1)	3751(2)	2333(1)	37(1)
C(23)	589(1)	2347(2)	3146(2)	35(1)
C(24)	2098(1)	5054(2)	5525(1)	29(1)
C(25)	2358(1)	3836(3)	5578(2)	60(1)
C(26)	2412(1)	6117(3)	5482(2)	50(1)
C(27)	2004(1)	5206(4)	6224(2)	56(1)
C(28)	2998(1)	1751(4)	2077(2)	62(1)
C(29)	3388(1)	1975(4)	1947(2)	60(1)
C(30)	3665(1)	2972(5)	2246(2)	73(1)
C(31)	3561(2)	3762(4)	2689(2)	82(1)
C(32)	3173(2)	3573(5)	2834(2)	87(2)
C(33)	2888(1)	2581(5)	2532(2)	77(1)
C(34)	2705(2)	663(6)	1730(3)	129(2)

U(eq) is defined as 1/3 the trace of the Uij tensor.

Appendix 1. Crystallographic data

Table 3. Bond lengths (A) and angles (deg) for pa646

Ni(1)-O(1)	1.878(1)	Ni(1)-O(1)#2	1.878(1)
Ni(1)-N(1)#2	1.888(2)	Ni(1)-N(1)	1.888(2)
P(1)-N(1)	1.619(2)	P(1)-C(14)	1.772(2)
P(1)-C(2)	1.808(2)	P(1)-C(8)	1.811(2)
O(1)-C(15)	1.315(2)	N(1)-C(1)	1.479(3)
C(1)-C(1)#2	1.511(4)	C(1)-H(1A)	0.9900
C(1)-H(1B)	0.9900	C(2)-C(7)	1.393(3)
C(2)-C(3)	1.399(3)	C(3)-C(4)	1.389(3)
C(3)-H(3)	0.9500	C(4)-C(5)	1.381(4)
C(4)-H(4)	0.9500	C(5)-C(6)	1.381(4)
C(5)-H(5)	0.9500	C(6)-C(7)	1.390(3)
C(6)-H(6)	0.9500	C(7)-H(7)	0.9500
C(8)-C(13)	1.387(3)	C(8)-C(9)	1.402(3)
C(9)-C(10)	1.386(3)	C(9)-H(9)	0.9500
C(10)-C(11)	1.389(3)	C(10)-H(10)	0.9500
C(11)-C(12)	1.380(3)	C(11)-H(11)	0.9500
C(12)-C(13)	1.394(3)	C(12)-H(12)	0.9500
C(13)-H(13)	0.9500	C(14)-C(19)	1.400(3)
C(14)-C(15)	1.420(3)	C(15)-C(16)	1.431(3)
C(16)-C(17)	1.387(3)	C(16)-C(20)	1.537(3)
C(17)-C(18)	1.402(3)	C(17)-H(17)	0.9500
C(18)-C(19)	1.382(3)	C(18)-C(24)	1.536(3)
C(19)-H(19)	0.9500	C(20)-C(21)	1.538(3)
C(20)-C(22)	1.541(3)	C(20)-C(23)	1.542(3)
C(21)-H(21A)	0.9800	C(21)-H(21B)	0.9800
C(21)-H(21C)	0.9800	C(22)-H(22A)	0.9800
C(22)-H(22B)	0.9800	C(22)-H(22C)	0.9800
C(23)-H(23A)	0.9800	C(23)-H(23B)	0.9800
C(23)-H(23C)	0.9800	C(24)-C(25)	1.524(4)
C(24)-C(26)	1.529(4)	C(24)-C(27)	1.533(4)
C(25)-H(25A)	0.9800	C(25)-H(25B)	0.9800
C(25)-H(25C)	0.9800	C(26)-H(26A)	0.9800
C(26)-H(26B)	0.9800	C(26)-H(26C)	0.9800
C(27)-H(27A)	0.9800	C(27)-H(27B)	0.9800
C(27)-H(27C)	0.9800	C(28)-C(29)	1.360(5)
C(28)-C(33)	1.403(6)	C(28)-C(34)	1.481(6)
C(29)-C(30)	1.363(6)	C(29)-H(29)	0.9500
C(30)-C(31)	1.349(6)	C(30)-H(30)	0.9500
C(31)-C(32)	1.362(7)	C(31)-H(31)	0.9500
C(32)-C(33)	1.370(7)	C(32)-H(32)	0.9500
C(33)-H(33)	0.9500	C(34)-H(34A)	0.9800
C(34)-H(34B)	0.9800	C(34)-H(34C)	0.9800
O(1)-Ni(1)-O(1)#2	85.2(1)	O(1)-Ni(1)-N(1)#2	175.47(7)
O(1)#2-Ni(1)-N(1)#2	95.03(7)	O(1)-Ni(1)-N(1)	95.03(7)
O(1)#2-Ni(1)-N(1)	175.47(7)	N(1)#2-Ni(1)-N(1)	85.1(1)
N(1)-P(1)-C(14)	107.3(1)	N(1)-P(1)-C(2)	109.4(1)
C(14)-P(1)-C(2)	109.7(1)	N(1)-P(1)-C(8)	114.2(1)
C(14)-P(1)-C(8)	109.8(1)	C(2)-P(1)-C(8)	106.6(1)
C(15)-O(1)-Ni(1)	128.9(1)	C(1)-N(1)-P(1)	118.9(1)
C(1)-N(1)-Ni(1)	111.8(1)	P(1)-N(1)-Ni(1)	116.2(1)
N(1)-C(1)-C(1)#2	104.7(1)	N(1)-C(1)-H(1A)	110.8
C(1)#2-C(1)-H(1A)	110.8	N(1)-C(1)-H(1B)	110.8
C(1)#2-C(1)-H(1B)	110.8	H(1A)-C(1)-H(1B)	108.9
C(7)-C(2)-C(3)	119.4(2)	C(7)-C(2)-P(1)	121.4(2)
C(3)-C(2)-P(1)	118.9(2)	C(4)-C(3)-C(2)	119.7(2)
C(4)-C(3)-H(3)	120.1	C(2)-C(3)-H(3)	120.1
C(5)-C(4)-C(3)	120.5(2)	C(5)-C(4)-H(4)	119.8
C(3)-C(4)-H(4)	119.8	C(4)-C(5)-C(6)	120.1(2)
C(4)-C(5)-H(5)	120.0	C(6)-C(5)-H(5)	120.0
C(5)-C(6)-C(7)	120.1(2)	C(5)-C(6)-H(6)	119.9
C(7)-C(6)-H(6)	119.9	C(6)-C(7)-C(2)	120.2(2)
C(6)-C(7)-H(7)	119.9	C(2)-C(7)-H(7)	119.9
C(13)-C(8)-C(9)	119.5(2)	C(13)-C(8)-P(1)	119.1(2)
C(9)-C(8)-P(1)	121.4(2)	C(10)-C(9)-C(8)	120.1(2)

Appendix 1. Crystallographic data

C(10)-C(9)-H(9)	119.9	C(8)-C(9)-H(9)	119.9
C(9)-C(10)-C(11)	119.7(2)	C(9)-C(10)-H(10)	120.1
C(11)-C(10)-H(10)	120.1	C(12)-C(11)-C(10)	120.6(2)
C(12)-C(11)-H(11)	119.7	C(10)-C(11)-H(11)	119.7
C(11)-C(12)-C(13)	119.8(2)	C(11)-C(12)-H(12)	120.1
C(13)-C(12)-H(12)	120.1	C(8)-C(13)-C(12)	120.2(2)
C(8)-C(13)-H(13)	119.9	C(12)-C(13)-H(13)	119.9
C(19)-C(14)-C(15)	121.9(2)	C(19)-C(14)-P(1)	122.3(2)
C(15)-C(14)-P(1)	115.8(2)	O(1)-C(15)-C(14)	121.2(2)
O(1)-C(15)-C(16)	121.6(2)	C(14)-C(15)-C(16)	117.2(2)
C(17)-C(16)-C(15)	118.1(2)	C(17)-C(16)-C(20)	121.6(2)
C(15)-C(16)-C(20)	120.4(2)	C(16)-C(17)-C(18)	124.8(2)
C(16)-C(17)-H(17)	117.6	C(18)-C(17)-H(17)	117.6
C(19)-C(18)-C(17)	116.8(2)	C(19)-C(18)-C(24)	120.5(2)
C(17)-C(18)-C(24)	122.8(2)	C(18)-C(19)-C(14)	121.0(2)
C(18)-C(19)-H(19)	119.5	C(14)-C(19)-H(19)	119.5
C(16)-C(20)-C(21)	112.0(2)	C(16)-C(20)-C(22)	110.7(2)
C(21)-C(20)-C(22)	107.4(2)	C(16)-C(20)-C(23)	109.0(2)
C(21)-C(20)-C(23)	107.9(2)	C(22)-C(20)-C(23)	109.8(2)
C(20)-C(21)-H(21A)	109.5	C(20)-C(21)-H(21B)	109.5
H(21A)-C(21)-H(21B)	109.5	C(20)-C(21)-H(21C)	109.5
H(21A)-C(21)-H(21C)	109.5	H(21B)-C(21)-H(21C)	109.5
C(20)-C(22)-H(22A)	109.5	C(20)-C(22)-H(22B)	109.5
H(22A)-C(22)-H(22B)	109.5	C(20)-C(22)-H(22C)	109.5
H(22A)-C(22)-H(22C)	109.5	H(22B)-C(22)-H(22C)	109.5
C(20)-C(23)-H(23A)	109.5	C(20)-C(23)-H(23B)	109.5
H(23A)-C(23)-H(23B)	109.5	C(20)-C(23)-H(23C)	109.5
H(23A)-C(23)-H(23C)	109.5	H(23B)-C(23)-H(23C)	109.5
C(25)-C(24)-C(26)	108.4(2)	C(25)-C(24)-C(27)	108.2(3)
C(26)-C(24)-C(27)	108.7(2)	C(25)-C(24)-C(18)	112.5(2)
C(26)-C(24)-C(18)	109.3(2)	C(27)-C(24)-C(18)	109.6(2)
C(24)-C(25)-H(25A)	109.5	C(24)-C(25)-H(25B)	109.5
H(25A)-C(25)-H(25B)	109.5	C(24)-C(25)-H(25C)	109.5
H(25A)-C(25)-H(25C)	109.5	H(25B)-C(25)-H(25C)	109.5
C(24)-C(26)-H(26A)	109.5	C(24)-C(26)-H(26B)	109.5
H(26A)-C(26)-H(26B)	109.5	C(24)-C(26)-H(26C)	109.5
H(26A)-C(26)-H(26C)	109.5	H(26B)-C(26)-H(26C)	109.5
C(24)-C(27)-H(27A)	109.5	C(24)-C(27)-H(27B)	109.5
H(27A)-C(27)-H(27B)	109.5	C(24)-C(27)-H(27C)	109.5
H(27A)-C(27)-H(27C)	109.5	H(27B)-C(27)-H(27C)	109.5
C(29)-C(28)-C(33)	117.9(4)	C(29)-C(28)-C(34)	119.3(4)
C(33)-C(28)-C(34)	122.9(4)	C(28)-C(29)-C(30)	121.4(4)
C(28)-C(29)-H(29)	119.3	C(30)-C(29)-H(29)	119.3
C(31)-C(30)-C(29)	120.5(4)	C(31)-C(30)-H(30)	119.8
C(29)-C(30)-H(30)	119.8	C(30)-C(31)-C(32)	120.0(5)
C(30)-C(31)-H(31)	120.0	C(32)-C(31)-H(31)	120.0
C(31)-C(32)-C(33)	120.3(4)	C(31)-C(32)-H(32)	119.9
C(33)-C(32)-H(32)	119.9	C(32)-C(33)-C(28)	119.9(4)
C(32)-C(33)-H(33)	120.0	C(28)-C(33)-H(33)	120.0
C(28)-C(34)-H(34A)	109.5	C(28)-C(34)-H(34B)	109.5
H(34A)-C(34)-H(34B)	109.5	C(28)-C(34)-H(34C)	109.5
H(34A)-C(34)-H(34C)	109.5	H(34B)-C(34)-H(34C)	109.5

Estimated standard deviations are given in the parenthesis.

Symmetry operators ::

1: x, y, z 2: -x, y, -z+1/2 3: x+1/2, y+1/2, z
 4: -x+1/2, y+1/2, -z+1/2 5: -x, -y, -z 6: x, -y, z-1/2
 7: -x+1/2, -y+1/2, -z 8: x+1/2, -y+1/2, z-1/2

Appendix 1. Crystallographic data

Table 4. Anisotropic displacement parameters ($\text{\AA}^2 \times 10^3$) for pa646

atom	U11	U22	U33	U23	U13	U12
Ni(1)	17(1)	15(1)	17(1)	0	5(1)	0
P(1)	19(1)	17(1)	18(1)	-2(1)	6(1)	0(1)
O(1)	20(1)	17(1)	22(1)	2(1)	2(1)	1(1)
N(1)	21(1)	15(1)	18(1)	0(1)	6(1)	0(1)
C(1)	29(1)	16(1)	24(1)	-1(1)	7(1)	1(1)
C(2)	23(1)	19(1)	18(1)	-2(1)	3(1)	-1(1)
C(3)	28(1)	25(1)	29(1)	-1(1)	8(1)	-3(1)
C(4)	28(1)	29(1)	36(1)	-2(1)	5(1)	-9(1)
C(5)	41(1)	27(1)	37(1)	-8(1)	6(1)	-8(1)
C(6)	48(2)	30(1)	43(2)	-15(1)	20(1)	-3(1)
C(7)	32(1)	25(1)	35(1)	-6(1)	14(1)	-2(1)
C(8)	22(1)	17(1)	24(1)	0(1)	10(1)	2(1)
C(9)	27(1)	24(1)	24(1)	2(1)	10(1)	2(1)
C(10)	38(1)	26(1)	27(1)	5(1)	18(1)	4(1)
C(11)	32(1)	21(1)	39(1)	3(1)	22(1)	2(1)
C(12)	23(1)	25(1)	37(1)	-2(1)	13(1)	-1(1)
C(13)	22(1)	22(1)	26(1)	0(1)	10(1)	1(1)
C(14)	18(1)	19(1)	19(1)	1(1)	8(1)	1(1)
C(15)	19(1)	18(1)	19(1)	3(1)	6(1)	-1(1)
C(16)	23(1)	20(1)	22(1)	2(1)	8(1)	1(1)
C(17)	19(1)	24(1)	26(1)	3(1)	8(1)	4(1)
C(18)	18(1)	25(1)	23(1)	1(1)	5(1)	-1(1)
C(19)	22(1)	23(1)	20(1)	-1(1)	6(1)	-3(1)
C(20)	31(1)	22(1)	26(1)	-2(1)	7(1)	6(1)
C(21)	41(2)	36(1)	38(1)	-9(1)	8(1)	14(1)
C(22)	49(2)	36(1)	25(1)	-5(1)	12(1)	8(1)
C(23)	37(1)	24(1)	36(1)	-4(1)	4(1)	-1(1)
C(24)	19(1)	33(1)	27(1)	3(1)	1(1)	1(1)
C(25)	35(2)	48(2)	65(2)	-5(2)	-16(1)	14(1)
C(26)	32(1)	58(2)	48(2)	0(1)	3(1)	-14(1)
C(27)	37(2)	92(3)	29(1)	7(2)	1(1)	7(2)
C(28)	69(2)	71(2)	46(2)	23(2)	20(2)	6(2)
C(29)	67(2)	75(2)	45(2)	21(2)	32(2)	36(2)
C(30)	49(2)	118(4)	47(2)	33(2)	13(2)	14(2)
C(31)	87(3)	78(3)	54(2)	9(2)	-3(2)	10(2)
C(32)	103(4)	99(3)	50(2)	5(2)	19(2)	58(3)
C(33)	59(2)	133(4)	53(2)	37(3)	37(2)	41(3)
C(34)	156(6)	126(5)	88(4)	27(3)	30(4)	-51(4)

The anisotropic displacement factor exponent takes the form
 $2 \pi^2 [h^2 a^{*2} U(11) + \dots + 2 h k a^* b^* U(12)]$

Table 5. Hydrogen Coordinates ($\text{\AA} \times 10^4$) and equivalent isotropic displacement parameters ($\text{\AA}^2 \times 10^3$) for pa646

atom	x	y	z	U(eq)
H(1A)	289	9602	3137	29
H(1B)	-201	8986	3044	29
H(3)	1363	8588	4248	34
H(4)	1725	10403	4845	40
H(5)	1380	11615	5467	45
H(6)	674	11013	5511	48
H(7)	315	9175	4944	36
H(9)	486	6807	5442	30
H(10)	-97	6235	5848	34
H(11)	-863	6007	5005	34
H(12)	-1045	6292	3759	33
H(13)	-465	6894	3349	28
H(17)	1723	3546	4345	28
H(19)	1411	6725	5112	27
H(21A)	1321	1723	2825	61
H(21B)	1499	1923	3692	61
H(21C)	1662	2852	3207	61
H(22A)	541	4225	2224	56
H(22B)	773	3089	1970	56
H(22C)	1073	4305	2316	56
H(23A)	318	2860	3088	53
H(23B)	697	1928	3622	53
H(23C)	502	1726	2754	53
H(25A)	2644	3840	6021	90
H(25B)	2436	3741	5147	90
H(25C)	2160	3143	5600	90
H(26A)	2255	6911	5468	75
H(26B)	2475	6027	5037	75
H(26C)	2705	6093	5912	75
H(27A)	1841	5991	6204	84
H(27B)	2300	5209	6651	84
H(27C)	1811	4515	6266	84
H(29)	3468	1424	1641	71
H(30)	3934	3113	2142	87
H(31)	3758	4449	2900	99
H(32)	3100	4131	3145	104
H(33)	2617	2456	2632	93
H(34A)	2680	585	1223	193
H(34B)	2394	774	1734	193
H(34C)	2847	-89	2002	193

Complex 37b

Table 1. Crystal data for pa748

Compound	pa748
Molecular formula	$\text{C}_{58}\text{H}_{70}\text{N}_2\text{NiO}_2\text{P}_2, 2(\text{CH}_2\text{Cl}_2)$
Molecular weight	1117.66
Crystal habit	Blue Needle
Crystal dimensions(mm)	0.40x0.12x0.12
Crystal system	monoclinic
Space group	$\text{P2}_1/\text{c}$
a(\AA)	15.723(1)
b(\AA)	20.228(1)
c(\AA)	18.106(1)
α ($^\circ$)	90.00
β ($^\circ$)	94.940(1)
γ ($^\circ$)	90.00
V(\AA^3)	5737.1(6)
Z	4
d(g-cm $^{-3}$)	1.294
F(000)	2360
μ (cm $^{-1}$)	0.623
Absorption corrections	multi-scan ; 0.7886 min, 0.9289 max
Diffractometer	KappaCCD
X-ray source	MoK α
λ (\AA)	0.71069
Monochromator	graphite
T (K)	150.0(1)
Scan mode	phi and omega scans
Maximum θ	25.03
HKL ranges	-18 18 ; -23 24 ; -17 21
Reflections measured	25515
Unique data	9844
Rint	0.0780
Reflections used	8140
Criterion	$I > 2\sigma(I)$
Refinement type	Fsqd
Hydrogen atoms	constr
Parameters refined	598
Reflections / parameter	13
wR2	0.2234
R1	0.0901
Weights a, b	0.1091 ; 12.643
GoF	1.149
difference peak / hole (e \AA^{-3})	0.971(0.106) / -1.040(0.106)

Appendix 1. Crystallographic data

Table 2. Atomic Coordinates (A x 10⁴) and equivalent isotropic displacement parameters (A² x 10³) for pa748

atom	x	y	z	U(eq)
Ni(2)	3011(1)	3615(1)	4694(1)	24(1)
P(1)	2114(1)	4304(1)	5845(1)	25(1)
P(2)	3826(1)	3809(1)	3358(1)	25(1)
O(1)	2228(2)	3029(2)	5069(2)	31(1)
O(2)	3585(2)	2830(2)	4479(2)	29(1)
N(1)	2590(2)	4419(2)	5092(2)	24(1)
N(2)	3694(3)	4176(2)	4134(2)	27(1)
C(1)	3247(3)	4934(2)	5026(2)	27(1)
C(2)	3477(3)	4880(2)	4220(3)	27(1)
C(3)	4183(3)	5358(3)	4073(3)	35(1)
C(4)	3965(4)	6063(3)	4269(3)	40(1)
C(5)	3742(4)	6107(3)	5072(3)	39(1)
C(6)	3029(4)	5633(3)	5227(3)	36(1)
C(7)	1281(3)	3711(2)	5684(2)	26(1)
C(8)	1467(3)	3142(2)	5274(2)	26(1)
C(9)	797(3)	2671(3)	5134(3)	34(1)
C(10)	60(3)	2756(3)	5479(3)	36(1)
C(11)	-106(3)	3292(3)	5940(3)	34(1)
C(12)	516(3)	3774(3)	6023(2)	30(1)
C(13)	914(4)	2072(3)	4621(3)	43(1)
C(14)	1592(5)	1611(3)	4979(4)	60(2)
C(15)	1186(4)	2318(3)	3866(3)	55(2)
C(16)	82(4)	1690(4)	4458(5)	68(2)
C(17)	-917(4)	3320(3)	6348(3)	42(1)
C(18)	-748(5)	2949(5)	7088(4)	87(3)
C(19)	-1163(4)	4037(4)	6505(4)	57(2)
C(20)	-1671(4)	3008(3)	5892(4)	52(2)
C(21)	1592(3)	5045(2)	6143(3)	28(1)
C(22)	1832(3)	5365(3)	6820(3)	37(1)
C(23)	1424(4)	5954(3)	6985(3)	41(1)
C(24)	794(4)	6224(3)	6514(3)	41(1)
C(25)	546(4)	5896(3)	5838(3)	39(1)
C(26)	955(3)	5320(3)	5663(3)	34(1)
C(27)	2807(3)	3998(2)	6622(2)	27(1)
C(28)	3640(3)	3821(2)	6521(3)	30(1)
C(29)	4168(4)	3548(2)	7092(3)	37(1)
C(30)	3853(4)	3451(3)	7788(3)	37(1)
C(31)	3026(4)	3610(3)	7886(3)	40(1)
C(32)	2494(4)	3881(3)	7314(3)	36(1)
C(33)	4516(3)	3127(2)	3571(2)	28(1)
C(34)	4311(3)	2747(2)	4192(2)	26(1)
C(35)	4898(3)	2254(2)	4463(2)	27(1)
C(36)	5634(3)	2159(2)	4096(3)	28(1)
C(37)	5815(3)	2510(2)	3457(2)	27(1)
C(38)	5245(3)	2992(2)	3201(2)	28(1)
C(39)	4734(3)	1825(3)	5137(3)	34(1)
C(40)	4574(4)	2273(3)	5808(3)	44(1)
C(41)	3936(4)	1401(3)	4945(3)	38(1)
C(42)	5482(4)	1369(3)	5380(3)	48(2)
C(43)	6655(3)	2373(3)	3099(3)	34(1)
C(44)	7413(3)	2533(3)	3660(3)	43(1)
C(45)	6728(4)	2791(3)	2410(3)	51(2)
C(46)	6701(4)	1644(3)	2882(3)	46(1)
C(47)	2845(3)	3533(2)	2859(3)	31(1)
C(48)	2873(4)	3056(3)	2313(3)	44(1)
C(49)	2136(5)	2860(3)	1891(4)	60(2)
C(50)	1367(5)	3153(4)	2029(4)	63(2)
C(51)	1328(4)	3633(4)	2574(4)	57(2)
C(52)	2067(3)	3812(3)	2994(3)	40(1)
C(53)	4316(3)	4321(2)	2687(2)	27(1)
C(54)	5174(3)	4499(2)	2806(3)	30(1)
C(55)	5543(4)	4894(3)	2295(3)	35(1)

Appendix 1. Crystallographic data

C(56)	5051(4)	5125(3)	1662(3)	42(1)
C(57)	4206(4)	4958(3)	1556(3)	43(1)
C(58)	3825(4)	4551(2)	2056(3)	33(1)

U(eq) is defined as 1/3 the trace of the Uij tensor.

Table 3. Bond lengths (Å) and angles (deg) for pa748

Ni(2)-O(1)	1.877(3)	Ni(2)-O(2)	1.882(3)
Ni(2)-N(2)	1.912(4)	Ni(2)-N(1)	1.921(4)
P(1)-N(1)	1.627(4)	P(1)-C(7)	1.781(5)
P(1)-C(27)	1.813(5)	P(1)-C(21)	1.814(5)
P(2)-N(2)	1.618(4)	P(2)-C(33)	1.777(5)
P(2)-C(47)	1.808(5)	P(2)-C(53)	1.817(5)
O(1)-C(8)	1.303(6)	O(2)-C(34)	1.306(6)
N(1)-C(1)	1.478(6)	N(2)-C(2)	1.477(6)
C(1)-C(6)	1.507(7)	C(1)-C(2)	1.537(6)
C(1)-H(1)	1.0000	C(2)-C(3)	1.513(7)
C(2)-H(2)	1.0000	C(3)-C(4)	1.514(7)
C(3)-H(3A)	0.9900	C(3)-H(3B)	0.9900
C(4)-C(5)	1.527(7)	C(4)-H(4A)	0.9900
C(4)-H(4B)	0.9900	C(5)-C(6)	1.519(7)
C(5)-H(5A)	0.9900	C(5)-H(5B)	0.9900
C(6)-H(6A)	0.9900	C(6)-H(6B)	0.9900
C(7)-C(12)	1.403(7)	C(7)-C(8)	1.415(7)
C(8)-C(9)	1.427(7)	C(9)-C(10)	1.373(7)
C(9)-C(13)	1.546(7)	C(10)-C(11)	1.406(8)
C(10)-H(10)	0.9500	C(11)-C(12)	1.381(7)
C(11)-C(17)	1.530(7)	C(12)-H(12)	0.9500
C(13)-C(14)	1.52(1)	C(13)-C(16)	1.527(8)
C(13)-C(15)	1.549(8)	C(14)-H(14A)	0.9800
C(14)-H(14B)	0.9800	C(14)-H(14C)	0.9800
C(15)-H(15A)	0.9800	C(15)-H(15B)	0.9800
C(15)-H(15C)	0.9800	C(16)-H(16A)	0.9800
C(16)-H(16B)	0.9800	C(16)-H(16C)	0.9800
C(17)-C(20)	1.52(1)	C(17)-C(19)	1.53(1)
C(17)-C(18)	1.538(8)	C(18)-H(18A)	0.9800
C(18)-H(18B)	0.9800	C(18)-H(18C)	0.9800
C(19)-H(19A)	0.9800	C(19)-H(19B)	0.9800
C(19)-H(19C)	0.9800	C(20)-H(20A)	0.9800
C(20)-H(20B)	0.9800	C(20)-H(20C)	0.9800
C(21)-C(26)	1.385(7)	C(21)-C(22)	1.408(7)
C(22)-C(23)	1.398(8)	C(22)-H(22)	0.9500
C(23)-C(24)	1.364(8)	C(23)-H(23)	0.9500
C(24)-C(25)	1.416(8)	C(24)-H(24)	0.9500
C(25)-C(26)	1.381(7)	C(25)-H(25)	0.9500
C(26)-H(26)	0.9500	C(27)-C(28)	1.385(7)
C(27)-C(32)	1.404(7)	C(28)-C(29)	1.384(7)
C(28)-H(28)	0.9500	C(29)-C(30)	1.407(8)
C(29)-H(29)	0.9500	C(30)-C(31)	1.365(8)
C(30)-H(30)	0.9500	C(31)-C(32)	1.387(7)
C(31)-H(31)	0.9500	C(32)-H(32)	0.9500
C(33)-C(38)	1.404(7)	C(33)-C(34)	1.421(6)
C(34)-C(35)	1.417(7)	C(35)-C(36)	1.397(7)
C(35)-C(39)	1.537(6)	C(36)-C(37)	1.408(6)
C(36)-H(36)	0.9500	C(37)-C(38)	1.377(7)
C(37)-C(43)	1.544(7)	C(38)-H(38)	0.9500
C(39)-C(42)	1.529(8)	C(39)-C(41)	1.535(7)
C(39)-C(40)	1.554(7)	C(40)-H(40A)	0.9800
C(40)-H(40B)	0.9800	C(40)-H(40C)	0.9800
C(41)-H(41A)	0.9800	C(41)-H(41B)	0.9800
C(41)-H(41C)	0.9800	C(42)-H(42A)	0.9800
C(42)-H(42B)	0.9800	C(42)-H(42C)	0.9800
C(43)-C(45)	1.520(8)	C(43)-C(46)	1.529(8)
C(43)-C(44)	1.532(7)	C(44)-H(44A)	0.9800
C(44)-H(44B)	0.9800	C(44)-H(44C)	0.9800
C(45)-H(45A)	0.9800	C(45)-H(45B)	0.9800
C(45)-H(45C)	0.9800	C(46)-H(46A)	0.9800
C(46)-H(46B)	0.9800	C(46)-H(46C)	0.9800
C(47)-C(48)	1.384(7)	C(47)-C(52)	1.386(8)
C(48)-C(49)	1.390(8)	C(48)-H(48)	0.9500
C(49)-C(50)	1.39(1)	C(49)-H(49)	0.9500
C(50)-C(51)	1.39(1)	C(50)-H(50)	0.9500
C(51)-C(52)	1.381(8)	C(51)-H(51)	0.9500

C(52)-H(52)	0.9500	C(53)-C(54)	1.394(7)
C(53)-C(58)	1.403(7)	C(54)-C(55)	1.386(7)
C(54)-H(54)	0.9500	C(55)-C(56)	1.405(8)
C(55)-H(55)	0.9500	C(56)-C(57)	1.369(8)
C(56)-H(56)	0.9500	C(57)-C(58)	1.397(7)
C(57)-H(57)	0.9500	C(58)-H(58)	0.9500
O(1)-Ni(2)-O(2)	83.3(1)	O(1)-Ni(2)-N(2)	169.1(2)
O(2)-Ni(2)-N(2)	95.2(2)	O(1)-Ni(2)-N(1)	98.1(2)
O(2)-Ni(2)-N(1)	168.1(2)	N(2)-Ni(2)-N(1)	85.6(2)
N(1)-P(1)-C(7)	110.1(2)	N(1)-P(1)-C(27)	114.2(2)
C(7)-P(1)-C(27)	106.4(2)	N(1)-P(1)-C(21)	112.6(2)
C(7)-P(1)-C(21)	105.0(2)	C(27)-P(1)-C(21)	107.9(2)
N(2)-P(2)-C(33)	106.8(2)	N(2)-P(2)-C(47)	114.1(2)
C(33)-P(2)-C(47)	110.4(2)	N(2)-P(2)-C(53)	114.3(2)
C(33)-P(2)-C(53)	107.6(2)	C(47)-P(2)-C(53)	103.6(2)
C(8)-O(1)-Ni(2)	129.8(3)	C(34)-O(2)-Ni(2)	129.9(3)
C(1)-N(1)-P(1)	122.9(3)	C(1)-N(1)-Ni(2)	107.5(3)
P(1)-N(1)-Ni(2)	113.0(2)	C(2)-N(2)-P(2)	125.6(3)
C(2)-N(2)-Ni(2)	111.8(3)	P(2)-N(2)-Ni(2)	107.9(2)
N(1)-C(1)-C(6)	117.8(4)	N(1)-C(1)-C(2)	104.5(4)
C(6)-C(1)-C(2)	111.9(4)	N(1)-C(1)-H(1)	107.4
C(6)-C(1)-H(1)	107.4	C(2)-C(1)-H(1)	107.4
N(2)-C(2)-C(3)	114.7(4)	N(2)-C(2)-C(1)	104.1(4)
C(3)-C(2)-C(1)	111.0(4)	N(2)-C(2)-H(2)	108.9
C(3)-C(2)-H(2)	108.9	C(1)-C(2)-H(2)	108.9
C(2)-C(3)-C(4)	112.1(4)	C(2)-C(3)-H(3A)	109.2
C(4)-C(3)-H(3A)	109.2	C(2)-C(3)-H(3B)	109.2
C(4)-C(3)-H(3B)	109.2	H(3A)-C(3)-H(3B)	107.9
C(3)-C(4)-C(5)	110.7(4)	C(3)-C(4)-H(4A)	109.5
C(5)-C(4)-H(4A)	109.5	C(3)-C(4)-H(4B)	109.5
C(5)-C(4)-H(4B)	109.5	H(4A)-C(4)-H(4B)	108.1
C(6)-C(5)-C(4)	111.9(4)	C(6)-C(5)-H(5A)	109.2
C(4)-C(5)-H(5A)	109.2	C(6)-C(5)-H(5B)	109.2
C(4)-C(5)-H(5B)	109.2	H(5A)-C(5)-H(5B)	107.9
C(1)-C(6)-C(5)	111.1(4)	C(1)-C(6)-H(6A)	109.4
C(5)-C(6)-H(6A)	109.4	C(1)-C(6)-H(6B)	109.4
C(5)-C(6)-H(6B)	109.4	H(6A)-C(6)-H(6B)	108.0
C(12)-C(7)-C(8)	121.8(5)	C(12)-C(7)-P(1)	120.9(4)
C(8)-C(7)-P(1)	116.9(4)	O(1)-C(8)-C(7)	121.8(4)
O(1)-C(8)-C(9)	121.0(4)	C(7)-C(8)-C(9)	117.0(4)
C(10)-C(9)-C(8)	118.3(5)	C(10)-C(9)-C(13)	121.4(5)
C(8)-C(9)-C(13)	120.3(4)	C(9)-C(10)-C(11)	125.0(5)
C(9)-C(10)-H(10)	117.5	C(11)-C(10)-H(10)	117.5
C(12)-C(11)-C(10)	116.4(5)	C(12)-C(11)-C(17)	122.1(5)
C(10)-C(11)-C(17)	121.4(5)	C(11)-C(12)-C(7)	120.9(5)
C(11)-C(12)-H(12)	119.6	C(7)-C(12)-H(12)	119.6
C(14)-C(13)-C(16)	109.3(5)	C(14)-C(13)-C(9)	109.9(5)
C(16)-C(13)-C(9)	111.6(5)	C(14)-C(13)-C(15)	109.7(5)
C(9)-C(13)-C(15)	106.8(5)	C(9)-C(13)-C(15)	109.6(5)
C(13)-C(14)-H(14A)	109.5	C(13)-C(14)-H(14B)	109.5
H(14A)-C(14)-H(14B)	109.5	C(13)-C(14)-H(14C)	109.5
H(14A)-C(14)-H(14C)	109.5	H(14B)-C(14)-H(14C)	109.5
C(13)-C(15)-H(15A)	109.5	C(13)-C(15)-H(15B)	109.5
H(15A)-C(15)-H(15B)	109.5	C(13)-C(15)-H(15C)	109.5
H(15A)-C(15)-H(15C)	109.5	C(13)-C(16)-H(16A)	109.5
C(13)-C(16)-H(16A)	109.5	C(13)-C(16)-H(16B)	109.5
H(16A)-C(16)-H(16B)	109.5	C(13)-C(16)-H(16C)	109.5
H(16A)-C(16)-H(16C)	109.5	H(16B)-C(16)-H(16C)	109.5
C(20)-C(17)-C(11)	111.4(5)	C(20)-C(17)-C(19)	107.2(5)
C(11)-C(17)-C(19)	111.0(5)	C(20)-C(17)-C(18)	109.7(6)
C(11)-C(17)-C(18)	108.2(5)	C(19)-C(17)-C(18)	109.2(6)
C(17)-C(18)-H(18A)	109.5	C(17)-C(18)-H(18B)	109.5
H(18A)-C(18)-H(18B)	109.5	C(17)-C(18)-H(18C)	109.5
H(18A)-C(18)-H(18C)	109.5	H(18B)-C(18)-H(18C)	109.5
C(17)-C(19)-H(19A)	109.5	C(17)-C(19)-H(19B)	109.5
H(19A)-C(19)-H(19B)	109.5	C(17)-C(19)-H(19C)	109.5

Appendix 1. Crystallographic data

H(19A)-C(19)-H(19C)	109.5	H(19B)-C(19)-H(19C)	109.5
C(17)-C(20)-H(20A)	109.5	C(17)-C(20)-H(20B)	109.5
H(20A)-C(20)-H(20B)	109.5	C(17)-C(20)-H(20C)	109.5
H(20A)-C(20)-H(20C)	109.5	H(20B)-C(20)-H(20C)	109.5
C(26)-C(21)-C(22)	119.1(5)	C(26)-C(21)-P(1)	117.8(4)
C(22)-C(21)-P(1)	123.0(4)	C(23)-C(22)-C(21)	119.0(5)
C(23)-C(22)-H(22)	120.5	C(21)-C(22)-H(22)	120.5
C(24)-C(23)-C(22)	122.0(5)	C(24)-C(23)-H(23)	119.0
C(22)-C(23)-H(23)	119.0	C(23)-C(24)-C(25)	118.9(5)
C(23)-C(24)-H(24)	120.6	C(25)-C(24)-H(24)	120.6
C(26)-C(25)-C(24)	119.7(5)	C(26)-C(25)-H(25)	120.2
C(24)-C(25)-H(25)	120.2	C(25)-C(26)-C(21)	121.4(5)
C(25)-C(26)-H(26)	119.3	C(21)-C(26)-H(26)	119.3
C(28)-C(27)-C(32)	118.9(4)	C(28)-C(27)-P(1)	119.8(3)
C(32)-C(27)-P(1)	121.1(4)	C(29)-C(28)-C(27)	121.2(5)
C(29)-C(28)-H(28)	119.4	C(27)-C(28)-H(28)	119.4
C(28)-C(29)-C(30)	119.4(5)	C(28)-C(29)-H(29)	120.3
C(30)-C(29)-H(29)	120.3	C(31)-C(30)-C(29)	119.7(5)
C(31)-C(30)-H(30)	120.2	C(29)-C(30)-H(30)	120.2
C(30)-C(31)-C(32)	121.1(5)	C(30)-C(31)-H(31)	119.5
C(32)-C(31)-H(31)	119.5	C(31)-C(32)-C(27)	119.8(5)
C(31)-C(32)-H(32)	120.1	C(27)-C(32)-H(32)	120.1
C(38)-C(33)-C(34)	121.5(4)	C(38)-C(33)-P(2)	123.7(4)
C(34)-C(33)-P(2)	114.6(4)	O(2)-C(34)-C(35)	121.2(4)
O(2)-C(34)-C(33)	120.7(4)	C(35)-C(34)-C(33)	118.0(4)
C(36)-C(35)-C(34)	118.3(4)	C(36)-C(35)-C(39)	120.1(4)
C(34)-C(35)-C(39)	121.6(4)	C(35)-C(36)-C(37)	123.8(4)
C(35)-C(36)-H(36)	118.1	C(37)-C(36)-H(36)	118.1
C(38)-C(37)-C(36)	117.5(4)	C(38)-C(37)-C(43)	122.8(4)
C(36)-C(37)-C(43)	119.6(4)	C(37)-C(38)-C(33)	120.7(4)
C(37)-C(38)-H(38)	119.6	C(33)-C(38)-H(38)	119.6
C(42)-C(39)-C(41)	108.7(4)	C(42)-C(39)-C(35)	113.1(4)
C(41)-C(39)-C(35)	109.0(4)	C(42)-C(39)-C(40)	107.3(4)
C(41)-C(39)-C(40)	108.6(5)	C(35)-C(39)-C(40)	110.0(4)
C(39)-C(40)-H(40A)	109.5	C(39)-C(40)-H(40B)	109.5
H(40A)-C(40)-H(40B)	109.5	C(39)-C(40)-H(40C)	109.5
H(40A)-C(40)-H(40C)	109.5	H(40B)-C(40)-H(40C)	109.5
C(39)-C(41)-H(41A)	109.5	C(39)-C(41)-H(41B)	109.5
H(41A)-C(41)-H(41B)	109.5	C(39)-C(41)-H(41C)	109.5
H(41A)-C(41)-H(41C)	109.5	H(41B)-C(41)-H(41C)	109.5
C(39)-C(42)-H(42A)	109.5	C(39)-C(42)-H(42B)	109.5
H(42A)-C(42)-H(42B)	109.5	C(39)-C(42)-H(42C)	109.5
H(42A)-C(42)-H(42C)	109.5	H(42B)-C(42)-H(42C)	109.5
C(45)-C(43)-C(46)	108.4(5)	C(45)-C(43)-C(44)	108.4(5)
C(46)-C(43)-C(44)	108.8(5)	C(45)-C(43)-C(37)	111.9(4)
C(46)-C(43)-C(37)	110.0(4)	C(44)-C(43)-C(37)	109.2(4)
C(43)-C(44)-H(44A)	109.5	C(43)-C(44)-H(44B)	109.5
H(44A)-C(44)-H(44B)	109.5	C(43)-C(44)-H(44C)	109.5
H(44A)-C(44)-H(44C)	109.5	H(44B)-C(44)-H(44C)	109.5
C(43)-C(45)-H(45A)	109.5	C(43)-C(45)-H(45B)	109.5
H(45A)-C(45)-H(45B)	109.5	C(43)-C(45)-H(45C)	109.5
H(45A)-C(45)-H(45C)	109.5	H(45B)-C(45)-H(45C)	109.5
C(43)-C(46)-H(46A)	109.5	C(43)-C(46)-H(46B)	109.5
H(46A)-C(46)-H(46B)	109.5	C(43)-C(46)-H(46C)	109.5
H(46A)-C(46)-H(46C)	109.5	H(46B)-C(46)-H(46C)	109.5
C(48)-C(47)-C(52)	119.5(5)	C(48)-C(47)-P(2)	119.5(4)
C(52)-C(47)-P(2)	120.9(4)	C(47)-C(48)-C(49)	121.0(6)
C(47)-C(48)-H(48)	119.5	C(49)-C(48)-H(48)	119.5
C(50)-C(49)-C(48)	118.5(6)	C(50)-C(49)-H(49)	120.7
C(48)-C(49)-H(49)	120.7	C(51)-C(50)-C(49)	121.2(6)
C(51)-C(50)-H(50)	119.4	C(49)-C(50)-H(50)	119.4
C(52)-C(51)-C(50)	119.2(6)	C(52)-C(51)-H(51)	120.4
C(50)-C(51)-H(51)	120.4	C(51)-C(52)-C(47)	120.6(6)
C(51)-C(52)-H(52)	119.7	C(47)-C(52)-H(52)	119.7
C(54)-C(53)-C(58)	119.8(4)	C(54)-C(53)-P(2)	120.3(4)
C(58)-C(53)-P(2)	119.9(4)	C(55)-C(54)-C(53)	120.0(5)
C(55)-C(54)-H(54)	120.0	C(53)-C(54)-H(54)	120.0
C(54)-C(55)-C(56)	120.2(5)	C(54)-C(55)-H(55)	119.9

Appendix 1. Crystallographic data

C(56)-C(55)-H(55)	119.9	C(57)-C(56)-C(55)	119.4(5)
C(57)-C(56)-H(56)	120.3	C(55)-C(56)-H(56)	120.3
C(56)-C(57)-C(58)	121.3(5)	C(56)-C(57)-H(57)	119.3
C(58)-C(57)-H(57)	119.3	C(57)-C(58)-C(53)	119.1(5)
C(57)-C(58)-H(58)	120.4	C(53)-C(58)-H(58)	120.4

Appendix 1. Crystallographic data

Table 4. Anisotropic displacement parameters ($\text{Å}^2 \times 10^3$) for pa748

atom	U11	U22	U33	U23	U13	U12
N1(2)	32(1)	29(1)	10(1)	0(1)	6(1)	0(1)
P(1)	32(1)	34(1)	11(1)	1(1)	5(1)	1(1)
P(2)	34(1)	31(1)	10(1)	0(1)	5(1)	0(1)
O(1)	35(2)	32(2)	26(2)	2(1)	11(2)	-1(1)
O(2)	37(2)	32(2)	21(2)	1(1)	14(1)	4(1)
N(1)	33(2)	28(2)	14(2)	1(2)	7(2)	0(2)
N(2)	40(2)	30(2)	13(2)	-1(2)	12(2)	4(2)
C(1)	30(2)	40(3)	11(2)	-2(2)	2(2)	0(2)
C(2)	36(3)	34(3)	13(2)	0(2)	6(2)	-3(2)
C(3)	43(3)	44(3)	19(3)	-6(2)	12(2)	-1(2)
C(4)	48(3)	42(3)	32(3)	-4(2)	15(2)	-7(3)
C(5)	56(3)	38(3)	23(3)	-8(2)	10(2)	-6(3)
C(6)	46(3)	43(3)	19(3)	-7(2)	8(2)	-4(2)
C(7)	26(2)	38(3)	15(2)	4(2)	0(2)	1(2)
C(8)	34(3)	32(2)	14(2)	7(2)	4(2)	-1(2)
C(9)	41(3)	40(3)	23(3)	4(2)	11(2)	-3(2)
C(10)	40(3)	40(3)	28(3)	6(2)	7(2)	-8(2)
C(11)	35(3)	46(3)	21(2)	12(2)	5(2)	1(2)
C(12)	36(3)	45(3)	10(2)	5(2)	2(2)	2(2)
C(13)	48(3)	41(3)	41(3)	-10(3)	15(3)	-9(3)
C(14)	76(5)	32(3)	74(5)	-4(3)	17(4)	3(3)
C(15)	68(4)	63(4)	35(3)	-14(3)	16(3)	-6(3)
C(16)	56(4)	69(5)	84(6)	-38(4)	26(4)	-22(4)
C(17)	37(3)	59(4)	33(3)	14(3)	14(2)	4(3)
C(18)	51(4)	160(10)	53(5)	61(5)	25(3)	21(5)
C(19)	43(3)	81(5)	52(4)	-13(3)	23(3)	-8(3)
C(20)	35(3)	63(4)	60(4)	-1(3)	17(3)	1(3)
C(21)	35(3)	32(3)	18(2)	0(2)	11(2)	0(2)
C(22)	40(3)	53(3)	18(3)	-3(2)	7(2)	3(2)
C(23)	51(3)	47(3)	28(3)	-10(2)	13(2)	4(3)
C(24)	48(3)	36(3)	40(3)	0(2)	15(3)	7(2)
C(25)	43(3)	41(3)	32(3)	3(2)	4(2)	9(2)
C(26)	44(3)	41(3)	17(2)	5(2)	8(2)	-3(2)
C(27)	40(3)	30(2)	11(2)	4(2)	1(2)	-3(2)
C(28)	41(3)	37(3)	14(2)	1(2)	4(2)	4(2)
C(29)	48(3)	33(3)	29(3)	0(2)	0(2)	5(2)
C(30)	56(4)	36(3)	17(2)	4(2)	-9(2)	-7(2)
C(31)	50(3)	51(3)	18(3)	11(2)	3(2)	-5(3)
C(32)	40(3)	49(3)	19(3)	2(2)	4(2)	0(2)
C(33)	37(3)	35(3)	12(2)	-1(2)	5(2)	-2(2)
C(34)	36(3)	31(2)	12(2)	-5(2)	4(2)	0(2)
C(35)	40(3)	31(2)	10(2)	-2(2)	6(2)	-2(2)
C(36)	38(3)	30(2)	16(2)	2(2)	0(2)	3(2)
C(37)	40(3)	28(2)	13(2)	-5(2)	5(2)	-3(2)
C(38)	38(3)	37(3)	11(2)	-3(2)	7(2)	-2(2)
C(39)	49(3)	37(3)	16(2)	4(2)	6(2)	5(2)
C(40)	80(4)	46(3)	8(2)	-2(2)	10(2)	4(3)
C(41)	50(3)	37(3)	28(3)	3(2)	12(2)	-5(2)
C(42)	62(4)	54(4)	30(3)	16(3)	13(3)	2(3)
C(43)	38(3)	44(3)	21(3)	0(2)	8(2)	4(2)
C(44)	32(3)	62(4)	35(3)	-5(3)	7(2)	3(3)
C(45)	51(4)	73(4)	33(3)	5(3)	20(3)	11(3)
C(46)	52(3)	48(3)	39(3)	-11(3)	14(3)	5(3)
C(47)	41(3)	36(3)	16(2)	4(2)	-2(2)	-4(2)
C(48)	63(4)	37(3)	29(3)	-6(2)	-11(3)	7(3)
C(49)	83(5)	46(4)	45(4)	-8(3)	-24(4)	-10(3)
C(50)	56(4)	82(5)	46(4)	12(4)	-26(3)	-28(4)
C(51)	45(4)	89(5)	37(4)	14(3)	1(3)	-4(3)
C(52)	37(3)	62(4)	22(3)	7(2)	4(2)	-1(3)
C(53)	37(3)	35(3)	11(2)	1(2)	5(2)	0(2)
C(54)	45(3)	29(2)	17(2)	-4(2)	10(2)	2(2)
C(55)	47(3)	39(3)	22(3)	-5(2)	17(2)	-11(2)
C(56)	69(4)	39(3)	23(3)	1(2)	20(3)	-9(3)

Appendix 1. Crystallographic data

C(57)	73(4)	37(3)	18(3)	5(2)	4(3)	-5(3)
C(58)	51(3)	32(3)	16(2)	0(2)	6(2)	0(2)

The anisotropic displacement factor exponent takes the form
 $2 \pi^2 [h^2 a^{*2} U(11) + \dots + 2hka^* b^* U(12)]$

Appendix 1. Crystallographic data

Table 5. Hydrogen Coordinates ($\text{\AA} \times 10^4$) and equivalent isotropic displacement parameters ($\text{\AA}^2 \times 10^3$) for pa748

atom	x	y	z	U(eq)
H(1)	3763	4801	5353	32
H(2)	2960	4986	3880	33
H(3A)	4287	5337	3542	42
H(3B)	4715	5224	4367	42
H(4A)	3475	6218	3934	48
H(4B)	4458	6353	4199	48
H(5A)	4255	6003	5407	47
H(5B)	3564	6564	5176	47
H(6A)	2931	5654	5759	43
H(6B)	2495	5769	4937	43
H(10)	-370	2427	5400	43
H(12)	424	4154	6315	36
H(14A)	1436	1478	5468	90
H(14B)	2144	1840	5030	90
H(14C)	1635	1218	4667	90
H(15A)	1248	1939	3538	82
H(15B)	1732	2552	3943	82
H(15C)	750	2619	3638	82
H(16A)	173	1326	4116	103
H(16B)	-359	1987	4232	103
H(16C)	-102	1511	4921	103
H(18A)	-623	2484	6989	131
H(18B)	-1253	2977	7367	131
H(18C)	-259	3149	7377	131
H(19A)	-732.9999	4232	6865	86
H(19B)	-1720.9999	4046	6706	86
H(19C)	-1190	4292	6043	86
H(20A)	-1725	3203	5394	78
H(20B)	-2196	3089	6134	78
H(20C)	-1579	2531	5854	78
H(22)	2264	5183	7159	44
H(23)	1590	6172	7439	50
H(24)	526	6626	6637	49
H(25)	100	6072	5508	46
H(26)	796	5108	5202	40
H(28)	3853	3889	6052	36
H(29)	4737	3428	7015	44
H(30)	4214	3274	8187	44
H(31)	2812	3533	8353	48
H(32)	1920	3987	7390	43
H(36)	6036	1839	4290	33
H(38)	5347	3236	2768	34
H(40A)	5073	2556	5927	66
H(40B)	4480	1996	6238	66
H(40C)	4070	2548	5684	66
H(41A)	3446	1689	4812	57
H(41B)	3823	1131	5375	57
H(41C)	4031	1112	4525	57
H(42A)	5571	1056	4982	72
H(42B)	5355	1126	5826	72
H(42C)	6000	1634	5489	72
H(44A)	7395	2247	4095	64
H(44B)	7382	2997	3811	64
H(44C)	7947	2458	3431	64
H(45A)	7276	2701	2209	77
H(45B)	6696	3260	2539	77
H(45C)	6261	2681	2037	77
H(46A)	6696	1368	3327	69
H(46B)	7228	1564	2645	69
H(46C)	6208	1533	2536	69
H(48)	3404	2861	2225	52
H(49)	2158	2532	1518	71

Appendix 1. Crystallographic data

H(50)	858	3024	1745	76
H(51)	800	3835	2657	68
H(52)	2043	4128	3379	48
H(54)	5506	4350	3237	36
H(55)	6130	5008	2372	42
H(56)	5304	5395	1312	51
H(57)	3872	5123	1134	51
H(58)	3240	4430	1969	39

Complex [37a][SbF₆]

Table 1. Crystal data for pa845

Compound	pa845
Molecular formula	C ₅₄ H ₆₄ N ₂ NiO ₂ P ₂ ,4(C ₇ H ₈),F ₆ Sb
Molecular weight	1498.01
Crystal habit	Black Plate
Crystal dimensions(mm)	0.24x0.22x0.06
Crystal system	triclinic
Space group	Pbar1
a(Å)	9.993(1)
b(Å)	19.417(2)
c(Å)	20.297(2)
α(°)	77.163(1)
β(°)	88.532(1)
γ(°)	78.116(1)
V(Å ³)	3756.7(7)
Z	2
d(g·cm ⁻³)	1.324
F(000)	1562
μ(cm ⁻¹)	0.715
Absorption corrections	multi-scan ; 0.8472 min, 0.9584 max
Diffractionmeter	KappaCCD
X-ray source	MoKα
λ(Å)	0.71069
Monochromator	graphite
T (K)	150.0(1)
Scan mode	phi and omega scans
Maximum θ	25.02
HKL ranges	-11 11 ; -22 23 ; -23 24
Reflections measured	26224
Unique data	12512
Rint	0.0338
Reflections used	10755
Criterion	I > 2σ(I)
Refinement type	Fsqd
Hydrogen atoms	constr
Parameters refined	949
Reflections / parameter	11
wR2	0.1398
R1	0.0590
Weights a, b	0.0590 ; 9.1274
GoF	1.077
difference peak / hole (e Å ⁻³)	1.584(0.087) / -1.703(0.087)

Table 2. Atomic Coordinates (A x 10⁴) and equivalent isotropic displacement parameters (Å² x 10³) for pa845

atom	x	y	z	U(eq)
Ni (1)	3901(1)	2429(1)	7345(1)	27(1)
P (1)	3647(1)	3007(1)	8617(1)	29(1)
P (2)	4387(1)	1002(1)	6924(1)	29(1)
O (1)	3028(3)	3377(1)	7121(1)	33(1)
O (2)	4373(3)	2581(1)	6447(1)	35(1)
N (1)	3601(3)	2323(2)	8274(1)	29(1)
N (2)	4498(3)	1442(2)	7522(2)	30(1)
C (1)	4344(4)	1603(2)	8647(2)	35(1)
C (2)	4203(4)	1084(2)	8221(2)	35(1)
C (3)	2431(4)	3747(2)	8154(2)	31(1)
C (4)	2177(4)	3779(2)	7466(2)	28(1)
C (5)	1012(4)	4272(2)	7139(2)	29(1)
C (6)	290(4)	4760(2)	7499(2)	32(1)
C (7)	602(4)	4778(2)	8161(2)	31(1)
C (8)	1671(4)	4246(2)	8492(2)	33(1)
C (9)	593(4)	4310(2)	6405(2)	35(1)
C (10)	707(6)	3558(3)	6261(2)	55(1)
C (11)	-893(4)	4706(3)	6255(2)	47(1)
C (12)	1515(5)	4717(3)	5925(2)	50(1)
C (13)	-179(4)	5345(2)	8526(2)	41(1)
C (14A)	-1312(8)	5874(4)	8082(3)	59(3)
C (15A)	-868(8)	4945(4)	9160(4)	53(2)
C (16A)	800(10)	5741(4)	8759(5)	50(2)
C (14B)	-110(50)	6150(10)	8020(20)	110(20)
C (15B)	-1600(40)	5310(20)	8580(30)	130(20)
C (16B)	620(50)	5430(30)	9120(20)	130(20)
C (17)	5327(4)	3201(2)	8626(2)	33(1)
C (18)	5638(4)	3767(2)	8137(2)	40(1)
C (19)	6949(5)	3889(3)	8095(2)	49(1)
C (20)	7970(5)	3450(3)	8536(3)	49(1)
C (21)	7670(5)	2888(2)	9024(2)	46(1)
C (22)	6355(4)	2760(2)	9074(2)	36(1)
C (23)	3029(4)	2820(2)	9466(2)	32(1)
C (24)	1827(4)	2555(2)	9551(2)	42(1)
C (25)	1221(5)	2449(3)	10176(2)	50(1)
C (26)	1815(5)	2611(3)	10713(2)	50(1)
C (27)	2993(5)	2868(3)	10633(2)	52(1)
C (28)	3616(5)	2982(2)	10007(2)	42(1)
C (29)	5201(4)	1419(2)	6205(2)	31(1)
C (30)	5148(4)	2164(2)	6089(2)	31(1)
C (31)	5932(4)	2483(2)	5549(2)	32(1)
C (32)	6591(4)	2040(2)	5139(2)	35(1)
C (33)	6578(4)	1302(2)	5222(2)	35(1)
C (34)	5895(4)	998(2)	5769(2)	35(1)
C (35)	6027(5)	3280(2)	5432(2)	42(1)
C (36)	4613(6)	3759(2)	5235(3)	58(1)
C (37)	6569(7)	3424(3)	6076(3)	70(2)
C (38)	7006(5)	3485(3)	4864(3)	56(1)
C (39)	7310(4)	890(2)	4708(2)	43(1)
C (40)	6671(6)	1247(4)	4001(3)	70(2)
C (41)	8824(5)	925(3)	4692(2)	50(1)
C (42)	7219(6)	96(3)	4889(3)	71(2)
C (43)	5366(4)	103(2)	7209(2)	33(1)
C (44)	6715(5)	44(2)	7399(3)	50(1)
C (45)	7548(6)	-626(3)	7629(3)	61(1)
C (46)	7024(6)	-1235(3)	7681(3)	64(2)
C (47)	5697(7)	-1186(3)	7500(3)	66(2)
C (48)	4847(5)	-519(2)	7258(2)	48(1)
C (49)	2642(4)	996(2)	6729(2)	35(1)
C (50)	1865(4)	582(2)	7168(2)	42(1)
C (51)	504(5)	629(3)	7011(3)	53(1)
C (52)	-95(5)	1091(3)	6427(3)	54(1)

Appendix 1. Crystallographic data

C(53)	667(5)	1510(3)	5998(3)	52(1)
C(54)	2034(4)	1462(2)	6147(2)	42(1)
Sb(1)	7959(1)	1665(1)	1406(1)	71(1)
F(1)	8159(5)	1751(3)	492(2)	120(2)
F(2)	7710(10)	1521(5)	2324(2)	219(4)
F(3)	8489(8)	2506(4)	1339(4)	190(3)
F(4)	6130(4)	2064(3)	1246(3)	139(2)
F(5)	7508(6)	755(2)	1457(2)	124(2)
F(6)	9770(5)	1277(6)	1528(4)	268(6)
C(55)	-210(10)	2255(6)	3111(4)	143(4)
C(56)	643(6)	2409(4)	3635(3)	67(2)
C(57)	270(8)	3010(4)	3885(3)	84(2)
C(58)	970(10)	3167(4)	4335(4)	110(3)
C(59)	2140(10)	2756(6)	4574(4)	103(3)
C(60)	2677(7)	2144(6)	4362(4)	115(4)
C(61)	1845(8)	1947(4)	3867(3)	90(2)
C(62)	4597(7)	2960(3)	2700(3)	77(2)
C(63)	4976(5)	3601(3)	2893(3)	52(1)
C(64)	4124(5)	4016(3)	3251(2)	52(1)
C(65)	4484(6)	4608(3)	3420(3)	59(1)
C(66)	5688(6)	4795(3)	3239(3)	62(1)
C(67)	6568(6)	4388(3)	2879(3)	70(2)
C(68)	6232(6)	3796(3)	2704(3)	70(2)
C(69)	230(10)	9498(6)	770(6)	141(4)
C(70)	563(7)	8882(4)	1351(3)	82(2)
C(71)	-352(6)	8446(4)	1565(4)	82(2)
C(72)	-78(7)	7896(5)	2102(4)	87(2)
C(73)	1125(7)	7757(4)	2442(4)	82(2)
C(74)	2076(6)	8172(4)	2267(4)	75(2)
C(75)	1788(6)	8749(4)	1716(4)	81(2)
C(76)	5520(20)	-850(10)	-620(10)	74(7)
C(77)	5150(10)	-284(5)	-225(4)	57(3)
C(78)	6158(8)	48(6)	-58(5)	70(10)
C(79)	5840(10)	574(5)	320(5)	84(4)
C(80)	4510(20)	767(5)	531(5)	90(10)
C(81)	3500(10)	435(6)	364(6)	75(4)
C(82)	3816(8)	-91(5)	-14(5)	64(8)
C(83)	4610(10)	5246(5)	10447(6)	87(6)
C(84)	5000(10)	4696(6)	11017(4)	87(5)
C(85)	5820(10)	4045(5)	10953(4)	107(6)
C(86)	6260(10)	3944(5)	10320(5)	84(4)
C(87)	5880(10)	4494(6)	9750(4)	70(5)
C(88)	5050(10)	5145(5)	9813(5)	93(5)
C(89)	4540(10)	5761(7)	9187(6)	150(10)

U(eq) is defined as 1/3 the trace of the Uij tensor.

Appendix 1. Crystallographic data

Table 3. Bond lengths (Å) and angles (deg) for pa845

Ni(1)-O(1)	1.828(2)	Ni(1)-N(2)	1.842(3)
Ni(1)-O(2)	1.844(2)	Ni(1)-N(1)	1.875(3)
P(1)-N(1)	1.639(3)	P(1)-C(3)	1.779(4)
P(1)-C(17)	1.796(4)	P(1)-C(23)	1.799(4)
P(2)-N(2)	1.650(3)	P(2)-C(29)	1.769(4)
P(2)-C(43)	1.794(4)	P(2)-C(49)	1.800(4)
O(1)-C(4)	1.327(4)	O(2)-C(30)	1.326(5)
N(1)-C(1)	1.486(5)	N(2)-C(2)	1.486(5)
C(1)-C(2)	1.494(5)	C(1)-H(1A)	0.9900
C(1)-H(1B)	0.9900	C(2)-H(2A)	0.9900
C(2)-H(2B)	0.9900	C(3)-C(8)	1.397(5)
C(3)-C(4)	1.412(5)	C(4)-C(5)	1.417(5)
C(5)-C(6)	1.397(5)	C(5)-C(9)	1.541(5)
C(6)-C(7)	1.397(5)	C(6)-H(6)	0.9500
C(7)-C(8)	1.391(5)	C(7)-C(13)	1.533(5)
C(8)-H(8)	0.9500	C(9)-C(12)	1.528(6)
C(9)-C(11)	1.529(6)	C(9)-C(10)	1.532(6)
C(10)-H(10A)	0.9800	C(10)-H(10B)	0.9800
C(10)-H(10C)	0.9800	C(11)-H(11A)	0.9800
C(11)-H(11B)	0.9800	C(11)-H(11C)	0.9800
C(12)-H(12A)	0.9800	C(12)-H(12B)	0.9800
C(12)-H(12C)	0.9800	C(13)-C(15B)	1.43(3)
C(13)-C(16A)	1.50(1)	C(13)-C(16B)	1.52(3)
C(13)-C(14A)	1.520(7)	C(13)-C(15A)	1.569(8)
C(13)-C(14B)	1.69(3)	C(14A)-H(14A)	0.9800
C(14A)-H(14B)	0.9800	C(14A)-H(14C)	0.9800
C(15A)-H(15A)	0.9800	C(15A)-H(15B)	0.9800
C(15A)-H(15C)	0.9800	C(16A)-H(16A)	0.9800
C(16A)-H(16B)	0.9800	C(16A)-H(16C)	0.9800
C(14B)-H(14D)	0.9800	C(14B)-H(14E)	0.9800
C(14B)-H(14F)	0.9800	C(15B)-H(15D)	0.9800
C(15B)-H(15E)	0.9800	C(15B)-H(15F)	0.9800
C(16B)-H(16D)	0.9800	C(16B)-H(16E)	0.9800
C(16B)-H(16F)	0.9800	C(17)-C(18)	1.388(6)
C(17)-C(22)	1.399(5)	C(18)-C(19)	1.376(6)
C(18)-H(18)	0.9500	C(19)-C(20)	1.385(7)
C(19)-H(19)	0.9500	C(20)-C(21)	1.378(7)
C(20)-H(20)	0.9500	C(21)-C(22)	1.384(6)
C(21)-H(21)	0.9500	C(22)-H(22)	0.9500
C(23)-C(28)	1.384(6)	C(23)-C(24)	1.393(6)
C(24)-C(25)	1.382(6)	C(24)-H(24)	0.9500
C(25)-C(26)	1.379(7)	C(25)-H(25)	0.9500
C(26)-C(27)	1.363(7)	C(26)-H(26)	0.9500
C(27)-C(28)	1.393(6)	C(27)-H(27)	0.9500
C(28)-H(28)	0.9500	C(29)-C(30)	1.402(5)
C(29)-C(34)	1.410(5)	C(30)-C(31)	1.433(5)
C(31)-C(32)	1.386(5)	C(31)-C(35)	1.534(5)
C(32)-C(33)	1.408(6)	C(32)-H(32)	0.9500
C(33)-C(34)	1.371(6)	C(33)-C(39)	1.534(5)
C(34)-H(34)	0.9500	C(35)-C(37)	1.530(7)
C(35)-C(38)	1.530(6)	C(35)-C(36)	1.531(7)
C(36)-H(36A)	0.9800	C(36)-H(36B)	0.9800
C(36)-H(36C)	0.9800	C(37)-H(37A)	0.9800
C(37)-H(37B)	0.9800	C(37)-H(37C)	0.9800
C(38)-H(38A)	0.9800	C(38)-H(38B)	0.9800
C(38)-H(38C)	0.9800	C(39)-C(42)	1.526(7)
C(39)-C(41)	1.528(6)	C(39)-C(40)	1.540(7)
C(40)-H(40A)	0.9800	C(40)-H(40B)	0.9800
C(40)-H(40C)	0.9800	C(41)-H(41A)	0.9800
C(41)-H(41B)	0.9800	C(41)-H(41C)	0.9800
C(42)-H(42A)	0.9800	C(42)-H(42B)	0.9800
C(42)-H(42C)	0.9800	C(43)-C(44)	1.387(6)
C(43)-C(48)	1.392(6)	C(44)-C(45)	1.381(7)
C(44)-H(44)	0.9500	C(45)-C(46)	1.372(8)
C(45)-H(45)	0.9500	C(46)-C(47)	1.363(8)
C(46)-H(46)	0.9500	C(47)-C(48)	1.387(7)

Appendix 1. Crystallographic data

C(47)-H(47)	0.9500	C(48)-H(48)	0.9500
C(49)-C(54)	1.385(6)	C(49)-C(50)	1.395(6)
C(50)-C(51)	1.385(6)	C(50)-H(50)	0.9500
C(51)-C(52)	1.382(7)	C(51)-H(51)	0.9500
C(52)-C(53)	1.381(7)	C(52)-H(52)	0.9500
C(53)-C(54)	1.386(6)	C(53)-H(53)	0.9500
C(54)-H(54)	0.9500	Sb(1)-F(3)	1.795(5)
Sb(1)-F(6)	1.812(5)	Sb(1)-F(1)	1.835(4)
Sb(1)-F(4)	1.839(4)	Sb(1)-F(2)	1.840(5)
Sb(1)-F(5)	1.892(5)	C(55)-C(56)	1.50(1)
C(55)-H(55A)	0.9800	C(55)-H(55B)	0.9800
C(55)-H(55C)	0.9800	C(56)-C(57)	1.35(1)
C(56)-C(61)	1.37(1)	C(57)-C(58)	1.29(1)
C(57)-H(57)	0.9500	C(58)-C(59)	1.31(1)
C(58)-H(58)	0.9500	C(59)-C(60)	1.36(1)
C(59)-H(59)	0.9500	C(60)-C(61)	1.48(1)
C(60)-H(60)	0.9500	C(61)-H(61)	0.9500
C(62)-C(63)	1.503(7)	C(62)-H(62A)	0.9800
C(62)-H(62B)	0.9800	C(62)-H(62C)	0.9800
C(63)-C(64)	1.359(7)	C(63)-C(68)	1.405(8)
C(64)-C(65)	1.387(7)	C(64)-H(64)	0.9500
C(65)-C(66)	1.346(8)	C(65)-H(65)	0.9500
C(66)-C(67)	1.366(8)	C(66)-H(66)	0.9500
C(67)-C(68)	1.381(8)	C(67)-H(67)	0.9500
C(68)-H(68)	0.9500	C(69)-C(70)	1.47(1)
C(69)-H(69A)	0.9800	C(69)-H(69B)	0.9800
C(69)-H(69C)	0.9800	C(70)-C(71)	1.37(1)
C(70)-C(75)	1.39(1)	C(71)-C(72)	1.34(1)
C(71)-H(71)	0.9500	C(72)-C(73)	1.35(1)
C(72)-H(72)	0.9500	C(73)-C(74)	1.36(1)
C(73)-H(73)	0.9500	C(74)-C(75)	1.38(1)
C(74)-H(74)	0.9500	C(75)-H(75)	0.9500
C(76)-C(77)	1.49(2)	C(76)-H(76A)	0.9800
C(76)-H(76B)	0.9800	C(76)-H(76C)	0.9800
C(77)-C(78)	1.3900	C(77)-C(82)	1.3900
C(78)-C(79)	1.3900	C(78)-H(78)	0.9500
C(79)-C(80)	1.3900	C(79)-H(79)	0.9500
C(80)-C(81)	1.3900	C(80)-H(80)	0.9500
C(81)-C(82)	1.3900	C(81)-H(81)	0.9500
C(82)-H(82)	0.9500	C(83)-C(84)	1.3900
C(83)-C(88)	1.3900	C(83)-H(83)	0.9500
C(84)-C(85)	1.3900	C(84)-H(84)	0.9500
C(85)-C(86)	1.3900	C(85)-H(85)	0.9500
C(86)-C(87)	1.3900	C(86)-H(86)	0.9500
C(87)-C(88)	1.3900	C(87)-H(87)	0.9500
C(88)-C(89)	1.5518	C(89)-H(89A)	0.9800
C(89)-H(89B)	0.9800	C(89)-H(89C)	0.9800
O(1)-Ni(1)-N(2)	170.0(1)	O(1)-Ni(1)-O(2)	84.2(1)
N(2)-Ni(1)-O(2)	95.3(1)	O(1)-Ni(1)-N(1)	94.9(1)
N(2)-Ni(1)-N(1)	86.8(1)	O(2)-Ni(1)-N(1)	173.1(1)
N(1)-P(1)-C(3)	106.0(2)	N(1)-P(1)-C(17)	112.9(2)
C(3)-P(1)-C(17)	112.5(2)	N(1)-P(1)-C(23)	109.0(2)
C(3)-P(1)-C(23)	106.2(2)	C(17)-P(1)-C(23)	109.9(2)
N(2)-P(2)-C(29)	107.2(2)	N(2)-P(2)-C(43)	107.2(2)
C(29)-P(2)-C(43)	107.4(2)	N(2)-P(2)-C(49)	112.2(2)
C(29)-P(2)-C(49)	111.3(2)	C(43)-P(2)-C(49)	111.3(2)
C(4)-O(1)-Ni(1)	131.4(2)	C(30)-O(2)-Ni(1)	132.6(2)
C(1)-N(1)-P(1)	116.4(2)	C(1)-N(1)-Ni(1)	110.1(2)
P(1)-N(1)-Ni(1)	118.4(2)	C(2)-N(2)-P(2)	116.8(2)
C(2)-N(2)-Ni(1)	112.7(2)	P(2)-N(2)-Ni(1)	119.6(2)
N(1)-C(1)-C(2)	106.1(3)	N(1)-C(1)-H(1A)	110.5
C(2)-C(1)-H(1A)	110.5	N(1)-C(1)-H(1B)	110.5
C(2)-C(1)-H(1B)	110.5	H(1A)-C(1)-H(1B)	108.7
N(2)-C(2)-C(1)	105.3(3)	N(2)-C(2)-H(2A)	110.7
C(1)-C(2)-H(2A)	110.7	N(2)-C(2)-H(2B)	110.7
C(1)-C(2)-H(2B)	110.7	H(2A)-C(2)-H(2B)	108.8

Appendix 1. Crystallographic data

C(8)-C(3)-C(4)	121.6(3)	C(8)-C(3)-P(1)	119.3(3)
C(4)-C(3)-P(1)	118.8(3)	O(1)-C(4)-C(3)	121.2(3)
O(1)-C(4)-C(5)	120.3(3)	C(3)-C(4)-C(5)	118.5(3)
C(6)-C(5)-C(4)	117.1(3)	C(6)-C(5)-C(9)	120.4(3)
C(4)-C(5)-C(9)	122.4(3)	C(5)-C(6)-C(7)	124.8(3)
C(5)-C(6)-H(6)	117.6	C(7)-C(6)-H(6)	117.6
C(8)-C(7)-C(6)	116.9(3)	C(8)-C(7)-C(13)	119.9(3)
C(6)-C(7)-C(13)	123.2(3)	C(7)-C(8)-C(3)	120.4(3)
C(7)-C(8)-H(8)	119.8	C(3)-C(8)-H(8)	119.8
C(12)-C(9)-C(11)	108.8(3)	C(12)-C(9)-C(10)	109.2(4)
C(11)-C(9)-C(10)	106.9(4)	C(12)-C(9)-C(5)	109.0(3)
C(11)-C(9)-C(5)	110.9(3)	C(10)-C(9)-C(5)	112.0(3)
C(9)-C(10)-H(10A)	109.5	C(9)-C(10)-H(10B)	109.5
H(10A)-C(10)-H(10B)	109.5	C(9)-C(10)-H(10C)	109.5
H(10A)-C(10)-H(10C)	109.5	H(10B)-C(10)-H(10C)	109.5
C(9)-C(11)-H(11A)	109.5	C(9)-C(11)-H(11B)	109.5
H(11A)-C(11)-H(11B)	109.5	C(9)-C(11)-H(11C)	109.5
H(11A)-C(11)-H(11C)	109.5	H(11B)-C(11)-H(11C)	109.5
C(9)-C(12)-H(12A)	109.5	C(9)-C(12)-H(12B)	109.5
H(12A)-C(12)-H(12B)	109.5	C(9)-C(12)-H(12C)	109.5
H(12A)-C(12)-H(12C)	109.5	H(12B)-C(12)-H(12C)	109.5
C(15B)-C(13)-C(16A)	139(1)	C(15B)-C(13)-C(16B)	121(3)
C(16A)-C(13)-C(16B)	34(3)	C(15B)-C(13)-C(14A)	56(2)
C(16A)-C(13)-C(14A)	110.4(5)	C(16B)-C(13)-C(14A)	131(1)
C(16A)-C(13)-C(7)	111(1)	C(16A)-C(13)-C(7)	109.9(4)
C(16B)-C(13)-C(7)	113(1)	C(14A)-C(13)-C(7)	111.9(4)
C(16A)-C(13)-C(15A)	54(2)	C(16A)-C(13)-C(15A)	108.9(5)
C(16B)-C(13)-C(15A)	76(3)	C(14A)-C(13)-C(15A)	107.4(5)
C(7)-C(13)-C(15A)	108.2(4)	C(15B)-C(13)-C(14B)	106(3)
C(16A)-C(13)-C(14B)	65(2)	C(16B)-C(13)-C(14B)	97(3)
C(14A)-C(13)-C(14B)	52(2)	C(7)-C(13)-C(14B)	106(1)
C(15A)-C(13)-C(14B)	145(1)	C(13)-C(14A)-H(14A)	109.5
C(13)-C(14A)-H(14B)	109.5	C(13)-C(14A)-H(14C)	109.5
C(13)-C(15A)-H(15A)	109.5	C(13)-C(15A)-H(15B)	109.5
C(13)-C(15A)-H(15C)	109.5	C(13)-C(16A)-H(16A)	109.5
C(13)-C(16A)-H(16B)	109.5	C(13)-C(16A)-H(16C)	109.5
C(13)-C(14B)-H(14D)	109.5	C(13)-C(14B)-H(14E)	109.5
H(14D)-C(14B)-H(14E)	109.5	C(13)-C(14B)-H(14F)	109.5
H(14E)-C(14B)-H(14F)	109.5	H(14E)-C(14B)-H(14F)	109.5
C(13)-C(15B)-H(15D)	109.5	C(13)-C(15B)-H(15E)	109.5
H(15D)-C(15B)-H(15E)	109.5	C(13)-C(15B)-H(15F)	109.5
H(15E)-C(15B)-H(15F)	109.5	H(15E)-C(15B)-H(15F)	109.5
C(13)-C(16B)-H(16D)	109.5	C(13)-C(16B)-H(16E)	109.5
H(16D)-C(16B)-H(16E)	109.5	C(13)-C(16B)-H(16F)	109.5
H(16E)-C(16B)-H(16F)	109.5	H(16E)-C(16B)-H(16F)	109.5
C(18)-C(17)-C(22)	119.4(4)	C(18)-C(17)-P(1)	118.8(3)
C(22)-C(17)-P(1)	121.5(3)	C(19)-C(18)-C(17)	120.1(4)
C(19)-C(18)-H(18)	120.0	C(17)-C(18)-H(18)	120.0
C(18)-C(19)-C(20)	120.6(4)	C(18)-C(19)-H(19)	119.7
C(20)-C(19)-H(19)	119.7	C(21)-C(20)-C(19)	119.8(4)
C(21)-C(20)-H(20)	120.1	C(19)-C(20)-H(20)	120.1
C(20)-C(21)-C(22)	120.3(4)	C(20)-C(21)-H(21)	119.8
C(22)-C(21)-H(21)	119.8	C(21)-C(22)-C(17)	119.8(4)
C(21)-C(22)-H(22)	120.1	C(17)-C(22)-H(22)	120.1
C(28)-C(23)-C(24)	119.8(4)	C(28)-C(23)-P(1)	123.5(3)
C(24)-C(23)-P(1)	116.5(3)	C(25)-C(24)-C(23)	120.4(4)
C(25)-C(24)-H(24)	119.8	C(23)-C(24)-H(24)	119.8
C(26)-C(25)-C(24)	119.4(4)	C(26)-C(25)-H(25)	120.3
C(24)-C(25)-H(25)	120.3	C(27)-C(26)-C(25)	120.6(4)
C(27)-C(26)-H(26)	119.7	C(25)-C(26)-H(26)	119.7
C(26)-C(27)-C(28)	121.0(4)	C(26)-C(27)-H(27)	119.5
C(28)-C(27)-H(27)	119.5	C(23)-C(28)-C(27)	118.8(4)
C(23)-C(28)-H(28)	120.6	C(27)-C(28)-H(28)	120.6
C(30)-C(29)-C(34)	121.7(3)	C(30)-C(29)-P(2)	118.7(3)
C(34)-C(29)-P(2)	119.6(3)	O(2)-C(30)-C(29)	122.3(3)
O(2)-C(30)-C(31)	119.3(3)	C(29)-C(30)-C(31)	118.3(3)
C(32)-C(31)-C(30)	116.9(3)	C(32)-C(31)-C(35)	121.9(3)
C(30)-C(31)-C(35)	121.2(3)	C(31)-C(32)-C(33)	125.3(4)

Appendix 1. Crystallographic data

C(31)-C(32)-H(32)	117.4	C(33)-C(32)-H(32)	117.4
C(34)-C(33)-C(32)	116.6(3)	C(34)-C(33)-C(39)	124.2(4)
C(32)-C(33)-C(39)	119.1(4)	C(33)-C(34)-C(29)	120.9(4)
C(33)-C(34)-H(34)	119.5	C(29)-C(34)-H(34)	119.5
C(37)-C(35)-C(38)	107.5(4)	C(37)-C(35)-C(36)	110.3(4)
C(38)-C(35)-C(36)	107.9(4)	C(37)-C(35)-C(31)	109.6(4)
C(38)-C(35)-C(31)	112.0(4)	C(36)-C(35)-C(31)	109.6(4)
C(35)-C(36)-H(36A)	109.5	C(35)-C(36)-H(36B)	109.5
H(36A)-C(36)-H(36B)	109.5	C(35)-C(36)-H(36C)	109.5
H(36A)-C(36)-H(36C)	109.5	H(36B)-C(36)-H(36C)	109.5
C(35)-C(37)-H(37A)	109.5	C(35)-C(37)-H(37B)	109.5
H(37A)-C(37)-H(37B)	109.5	C(35)-C(37)-H(37C)	109.5
H(37A)-C(37)-H(37C)	109.5	H(37B)-C(37)-H(37C)	109.5
C(35)-C(38)-H(38A)	109.5	C(35)-C(38)-H(38B)	109.5
H(38A)-C(38)-H(38B)	109.5	C(35)-C(38)-H(38C)	109.5
H(38A)-C(38)-H(38C)	109.5	H(38B)-C(38)-H(38C)	109.5
C(42)-C(39)-C(41)	107.6(4)	C(42)-C(39)-C(33)	111.8(4)
C(41)-C(39)-C(33)	109.9(3)	C(42)-C(39)-C(40)	109.9(5)
C(41)-C(39)-C(40)	108.5(4)	C(33)-C(39)-C(40)	109.1(4)
C(39)-C(40)-H(40A)	109.5	C(39)-C(40)-H(40B)	109.5
H(40A)-C(40)-H(40B)	109.5	C(39)-C(40)-H(40C)	109.5
H(40A)-C(40)-H(40C)	109.5	H(40B)-C(40)-H(40C)	109.5
C(39)-C(41)-H(41A)	109.5	C(39)-C(41)-H(41B)	109.5
H(41A)-C(41)-H(41B)	109.5	C(39)-C(41)-H(41C)	109.5
H(41A)-C(41)-H(41C)	109.5	H(41B)-C(41)-H(41C)	109.5
C(39)-C(42)-H(42A)	109.5	C(39)-C(42)-H(42B)	109.5
H(42A)-C(42)-H(42B)	109.5	C(39)-C(42)-H(42C)	109.5
H(42A)-C(42)-H(42C)	109.5	H(42B)-C(42)-H(42C)	109.5
C(44)-C(43)-C(48)	119.6(4)	C(44)-C(43)-P(2)	116.2(3)
C(48)-C(43)-P(2)	124.2(3)	C(45)-C(44)-C(43)	120.4(5)
C(45)-C(44)-H(44)	119.8	C(43)-C(44)-H(44)	119.8
C(46)-C(45)-C(44)	119.5(5)	C(46)-C(45)-H(45)	120.3
C(44)-C(45)-H(45)	120.3	C(47)-C(46)-C(45)	120.7(5)
C(47)-C(46)-H(46)	119.6	C(45)-C(46)-H(46)	119.6
C(46)-C(47)-C(48)	120.8(5)	C(46)-C(47)-H(47)	119.6
C(48)-C(47)-H(47)	119.6	C(47)-C(48)-C(43)	118.9(5)
C(47)-C(48)-H(48)	120.6	C(43)-C(48)-H(48)	120.6
C(54)-C(49)-C(50)	119.5(4)	C(54)-C(49)-P(2)	118.1(3)
C(50)-C(49)-P(2)	122.2(3)	C(51)-C(50)-C(49)	119.8(4)
C(51)-C(50)-H(50)	120.1	C(49)-C(50)-H(50)	120.1
C(52)-C(51)-C(50)	120.4(4)	C(52)-C(51)-H(51)	119.8
C(50)-C(51)-H(51)	119.8	C(53)-C(52)-C(51)	119.8(4)
C(53)-C(52)-H(52)	120.1	C(51)-C(52)-H(52)	120.1
C(52)-C(53)-C(54)	120.2(4)	C(52)-C(53)-H(53)	119.9
C(54)-C(53)-H(53)	119.9	C(49)-C(54)-C(53)	120.3(4)
C(49)-C(54)-H(54)	119.9	C(53)-C(54)-H(54)	119.9
F(3)-Sb(1)-F(6)	84.1(5)	F(3)-Sb(1)-F(1)	89.7(3)
F(6)-Sb(1)-F(1)	89.2(3)	F(3)-Sb(1)-F(4)	95.7(3)
F(6)-Sb(1)-F(4)	177.7(3)	F(1)-Sb(1)-F(4)	88.5(3)
F(3)-Sb(1)-F(2)	94.2(3)	F(6)-Sb(1)-F(2)	91.5(4)
F(1)-Sb(1)-F(2)	176.0(3)	F(4)-Sb(1)-F(2)	90.9(4)
F(3)-Sb(1)-F(5)	176.4(3)	F(6)-Sb(1)-F(5)	92.7(4)
F(1)-Sb(1)-F(5)	88.5(2)	F(4)-Sb(1)-F(5)	87.4(2)
F(2)-Sb(1)-F(5)	87.5(3)	C(56)-C(55)-H(55A)	109.5
C(56)-C(55)-H(55B)	109.5	H(55A)-C(55)-H(55B)	109.5
C(56)-C(55)-H(55C)	109.5	H(55A)-C(55)-H(55C)	109.5
H(55B)-C(55)-H(55C)	109.5	C(57)-C(56)-C(61)	117.9(6)
C(57)-C(56)-C(55)	121.7(8)	C(61)-C(56)-C(55)	120.5(8)
C(58)-C(57)-C(56)	124.0(7)	C(58)-C(57)-H(57)	118.0
C(56)-C(57)-H(57)	118.0	C(57)-C(58)-C(59)	122(1)
C(57)-C(58)-H(58)	119.2	C(59)-C(58)-H(58)	119.2
C(58)-C(59)-C(60)	121.6(8)	C(58)-C(59)-H(59)	119.2
C(60)-C(59)-H(59)	119.2	C(59)-C(60)-C(61)	116.7(6)
C(59)-C(60)-H(60)	121.6	C(61)-C(60)-H(60)	121.6
C(56)-C(61)-C(60)	118.1(7)	C(56)-C(61)-H(61)	120.9
C(60)-C(61)-H(61)	120.9	C(63)-C(62)-H(62A)	109.5
C(63)-C(62)-H(62B)	109.5	H(62A)-C(62)-H(62B)	109.5
C(63)-C(62)-H(62C)	109.5	H(62A)-C(62)-H(62C)	109.5

Appendix 1. Crystallographic data

H(62B)-C(62)-H(62C)	109.5	C(64)-C(63)-C(68)	117.3(5)
C(64)-C(63)-C(62)	121.9(5)	C(68)-C(63)-C(62)	120.9(5)
C(63)-C(64)-C(65)	121.2(5)	C(63)-C(64)-H(64)	119.4
C(65)-C(64)-H(64)	119.4	C(66)-C(65)-C(64)	121.5(5)
C(66)-C(65)-H(65)	119.3	C(64)-C(65)-H(65)	119.3
C(65)-C(66)-C(67)	118.8(5)	C(65)-C(66)-H(66)	120.6
C(67)-C(66)-H(66)	120.6	C(66)-C(67)-C(68)	120.8(5)
C(66)-C(67)-H(67)	119.6	C(68)-C(67)-H(67)	119.6
C(67)-C(68)-C(63)	120.5(5)	C(67)-C(68)-H(68)	119.8
C(63)-C(68)-H(68)	119.8	C(70)-C(69)-H(69A)	109.5
C(70)-C(69)-H(69B)	109.5	H(69A)-C(69)-H(69B)	109.5
C(70)-C(69)-H(69C)	109.5	H(69A)-C(69)-H(69C)	109.5
H(69B)-C(69)-H(69C)	109.5	C(71)-C(70)-C(75)	118.5(7)
C(71)-C(70)-C(69)	120.7(8)	C(75)-C(70)-C(69)	120.7(8)
C(72)-C(71)-C(70)	121.3(7)	C(72)-C(71)-H(71)	119.3
C(70)-C(71)-H(71)	119.3	C(71)-C(72)-C(73)	119.9(7)
C(71)-C(72)-H(72)	120.1	C(73)-C(72)-H(72)	120.1
C(72)-C(73)-C(74)	122.3(8)	C(72)-C(73)-H(73)	118.9
C(74)-C(73)-H(73)	118.9	C(73)-C(74)-C(75)	118.0(6)
C(73)-C(74)-H(74)	121.0	C(75)-C(74)-H(74)	121.0
C(74)-C(75)-C(70)	119.9(7)	C(74)-C(75)-H(75)	120.0
C(70)-C(75)-H(75)	120.0	C(78)-C(77)-C(82)	120.0
C(78)-C(77)-C(76)	119(1)	C(82)-C(77)-C(76)	121(1)
C(79)-C(78)-C(77)	120.0	C(79)-C(78)-H(78)	120.0
C(77)-C(78)-H(78)	120.0	C(78)-C(79)-C(80)	120.0
C(78)-C(79)-H(79)	120.0	C(80)-C(79)-H(79)	120.0
C(79)-C(80)-C(81)	120.0	C(79)-C(80)-H(80)	120.0
C(81)-C(80)-H(80)	120.0	C(82)-C(81)-C(80)	120.0
C(82)-C(81)-H(81)	120.0	C(80)-C(81)-H(81)	120.0
C(81)-C(82)-C(77)	120.0	C(81)-C(82)-H(82)	120.0
C(77)-C(82)-H(82)	120.0	C(84)-C(83)-C(88)	120.0
C(84)-C(83)-H(83)	120.0	C(88)-C(83)-H(83)	120.0
C(85)-C(84)-C(83)	120.0	C(85)-C(84)-H(84)	120.0
C(83)-C(84)-H(84)	120.0	C(84)-C(85)-C(86)	120.0
C(84)-C(85)-H(85)	120.0	C(86)-C(85)-H(85)	120.0
C(87)-C(86)-C(85)	120.0	C(87)-C(86)-H(86)	120.0
C(85)-C(86)-H(86)	120.0	C(86)-C(87)-C(88)	120.0
C(86)-C(87)-H(87)	120.0	C(88)-C(87)-H(87)	120.0
C(87)-C(88)-C(83)	120.0	C(87)-C(88)-C(89)	121.7
C(83)-C(88)-C(89)	118.2		

Appendix 1. Crystallographic data

Table 4. Anisotropic displacement parameters ($\text{\AA}^2 \times 10^3$) for pa845

atom	U11	U22	U33	U23	U13	U12
N1(1)	30(1)	26(1)	24(1)	-4(1)	2(1)	-6(1)
P(1)	29(1)	33(1)	24(1)	-6(1)	0(1)	-6(1)
P(2)	32(1)	27(1)	31(1)	-6(1)	2(1)	-9(1)
O(1)	37(2)	31(1)	26(1)	-5(1)	4(1)	0(1)
O(2)	49(2)	28(1)	26(1)	-5(1)	10(1)	-6(1)
N(1)	33(2)	32(2)	21(1)	-3(1)	-3(1)	-5(1)
N(2)	36(2)	28(2)	25(2)	-4(1)	2(1)	-9(1)
C(1)	43(2)	32(2)	26(2)	-1(2)	-1(2)	-6(2)
C(2)	43(2)	30(2)	29(2)	2(2)	1(2)	-10(2)
C(3)	30(2)	34(2)	29(2)	-7(2)	-1(2)	-7(2)
C(4)	30(2)	29(2)	26(2)	-6(1)	1(1)	-8(2)
C(5)	32(2)	30(2)	27(2)	-5(2)	2(2)	-10(2)
C(6)	29(2)	32(2)	32(2)	-5(2)	-1(2)	-4(2)
C(7)	27(2)	35(2)	33(2)	-10(2)	2(2)	-5(2)
C(8)	35(2)	39(2)	29(2)	-12(2)	3(2)	-7(2)
C(9)	37(2)	36(2)	28(2)	-4(2)	-2(2)	-5(2)
C(10)	69(3)	50(3)	48(3)	-21(2)	-21(2)	-5(2)
C(11)	39(2)	63(3)	35(2)	-11(2)	-4(2)	-3(2)
C(12)	50(3)	66(3)	30(2)	-1(2)	6(2)	-12(2)
C(13)	42(2)	42(2)	39(2)	-18(2)	1(2)	1(2)
C(14A)	55(5)	64(5)	51(4)	-27(4)	-7(3)	21(4)
C(15A)	54(4)	63(4)	48(4)	-30(3)	18(3)	-10(3)
C(16A)	48(4)	47(4)	62(5)	-28(4)	2(4)	-9(3)
C(14B)	170(40)	40(10)	100(20)	-30(10)	80(20)	-10(20)
C(15B)	100(30)	130(40)	210(60)	-130(40)	110(40)	-60(30)
C(16B)	150(40)	110(30)	110(30)	-90(30)	-80(30)	80(30)
C(17)	30(2)	38(2)	31(2)	-10(2)	0(2)	-8(2)
C(18)	39(2)	43(2)	37(2)	-6(2)	0(2)	-9(2)
C(19)	51(3)	49(3)	49(3)	-6(2)	7(2)	-19(2)
C(20)	34(2)	53(3)	64(3)	-19(2)	5(2)	-17(2)
C(21)	37(2)	51(3)	52(3)	-14(2)	-5(2)	-8(2)
C(22)	35(2)	40(2)	34(2)	-8(2)	-2(2)	-8(2)
C(23)	34(2)	34(2)	26(2)	-4(2)	2(2)	-4(2)
C(24)	42(2)	53(3)	33(2)	-10(2)	2(2)	-12(2)
C(25)	43(3)	60(3)	43(2)	-2(2)	10(2)	-11(2)
C(26)	49(3)	58(3)	33(2)	-5(2)	10(2)	2(2)
C(27)	52(3)	68(3)	32(2)	-16(2)	1(2)	0(2)
C(28)	43(2)	50(2)	33(2)	-12(2)	1(2)	-9(2)
C(29)	34(2)	31(2)	29(2)	-6(2)	1(2)	-8(2)
C(30)	34(2)	33(2)	26(2)	-5(2)	-2(2)	-7(2)
C(31)	33(2)	36(2)	27(2)	-6(2)	2(2)	-9(2)
C(32)	30(2)	44(2)	29(2)	-5(2)	4(2)	-8(2)
C(33)	31(2)	41(2)	33(2)	-14(2)	1(2)	-4(2)
C(34)	35(2)	32(2)	37(2)	-9(2)	-2(2)	-5(2)
C(35)	51(3)	39(2)	40(2)	-8(2)	13(2)	-17(2)
C(36)	70(3)	34(2)	61(3)	1(2)	24(3)	-5(2)
C(37)	106(5)	67(3)	58(3)	-21(3)	11(3)	-55(3)
C(38)	62(3)	49(3)	59(3)	-5(2)	23(2)	-26(2)
C(39)	38(2)	52(3)	42(2)	-23(2)	6(2)	-3(2)
C(40)	58(3)	109(5)	46(3)	-43(3)	-2(2)	6(3)
C(41)	40(2)	58(3)	53(3)	-22(2)	11(2)	-2(2)
C(42)	68(4)	69(3)	94(4)	-53(3)	35(3)	-23(3)
C(43)	38(2)	28(2)	34(2)	-6(2)	3(2)	-7(2)
C(44)	45(3)	39(2)	62(3)	-10(2)	-7(2)	-3(2)
C(45)	57(3)	54(3)	63(3)	-8(2)	-6(3)	6(2)
C(46)	78(4)	40(3)	55(3)	3(2)	-2(3)	13(3)
C(47)	86(4)	32(2)	80(4)	-11(2)	13(3)	-12(3)
C(48)	55(3)	34(2)	57(3)	-12(2)	2(2)	-12(2)
C(49)	36(2)	34(2)	37(2)	-11(2)	1(2)	-11(2)
C(50)	40(2)	47(2)	40(2)	-7(2)	2(2)	-14(2)
C(51)	42(3)	68(3)	57(3)	-21(2)	9(2)	-26(2)
C(52)	36(2)	74(3)	59(3)	-25(3)	-4(2)	-13(2)
C(53)	44(3)	63(3)	50(3)	-14(2)	-10(2)	-8(2)

Appendix 1. Crystallographic data

C(54)	41(2)	45(2)	40(2)	-7(2)	-4(2)	-10(2)
Sb(1)	50(1)	108(1)	51(1)	6(1)	-1(1)	-31(1)
F(1)	138(4)	174(5)	53(2)	5(2)	11(2)	-78(3)
F(2)	270(8)	400(10)	65(3)	-55(5)	34(4)	-240(10)
F(3)	229(7)	208(7)	205(7)	-83(5)	59(6)	-175(6)
F(4)	62(3)	119(4)	233(6)	-37(4)	13(3)	-14(2)
F(5)	151(4)	86(3)	115(4)	22(3)	15(3)	-24(3)
F(6)	44(3)	430(10)	225(8)	110(8)	-44(4)	4(5)
C(55)	170(10)	200(10)	85(6)	-8(6)	-16(6)	-110(10)
C(56)	61(3)	93(4)	46(3)	-4(3)	4(2)	-32(3)
C(57)	94(5)	82(4)	57(4)	-4(3)	16(3)	9(4)
C(58)	200(10)	70(4)	60(4)	4(3)	-8(5)	-36(6)
C(59)	111(7)	143(8)	69(5)	2(5)	-1(5)	-82(6)
C(60)	54(4)	180(10)	55(4)	44(5)	11(3)	20(5)
C(61)	114(6)	79(4)	55(4)	1(3)	30(4)	13(4)
C(62)	96(5)	54(3)	85(4)	-16(3)	-5(4)	-20(3)
C(63)	55(3)	47(3)	52(3)	-5(2)	-4(2)	-11(2)
C(64)	44(3)	58(3)	52(3)	-7(2)	1(2)	-13(2)
C(65)	58(3)	51(3)	62(3)	-10(2)	-13(2)	1(2)
C(66)	74(4)	49(3)	60(3)	4(2)	-17(3)	-20(3)
C(67)	65(4)	84(4)	64(3)	-1(3)	6(3)	-39(3)
C(68)	59(3)	81(4)	71(4)	-20(3)	18(3)	-16(3)
C(69)	122(8)	140(10)	140(10)	-19(7)	10(7)	-10(7)
C(70)	73(4)	91(5)	75(4)	-27(4)	11(3)	8(4)
C(71)	43(3)	119(6)	104(5)	-68(5)	4(3)	-18(4)
C(72)	60(4)	111(6)	102(5)	-46(5)	10(4)	-20(4)
C(73)	65(4)	104(5)	87(5)	-36(4)	4(3)	-22(4)
C(74)	45(3)	107(5)	83(4)	-46(4)	-2(3)	-13(3)
C(75)	56(4)	109(5)	96(5)	-56(4)	16(3)	-21(4)
C(76)	80(10)	70(10)	70(10)	-10(10)	0(10)	0(10)
C(77)	78(8)	46(6)	36(5)	4(4)	-13(5)	2(6)
C(78)	50(10)	80(20)	60(10)	20(10)	-10(10)	-40(10)
C(79)	100(10)	80(10)	69(8)	5(7)	-21(8)	-40(10)
C(80)	180(30)	50(10)	40(10)	3(8)	-10(10)	-10(10)
C(81)	100(10)	49(7)	62(8)	1(6)	14(7)	4(7)
C(82)	80(20)	50(10)	60(10)	-10(10)	0(10)	0(10)
C(83)	60(10)	150(20)	80(10)	-70(10)	30(10)	-60(10)
C(84)	100(10)	90(10)	100(10)	-50(10)	10(10)	-35(8)
C(85)	120(10)	130(10)	110(10)	-70(10)	30(10)	-60(10)
C(86)	80(10)	130(10)	70(8)	-40(10)	12(7)	-70(10)
C(87)	45(8)	90(10)	100(10)	-60(10)	19(8)	-29(7)
C(88)	100(10)	120(10)	90(10)	-10(10)	10(10)	-90(10)
C(89)	150(20)	220(30)	100(20)	20(20)	-40(20)	-140(20)

The anisotropic displacement factor exponent takes the form
 $2\pi^2 [h^2 a^{*2} U(11) + \dots + 2hka^* b^* U(12)]$

Appendix 1. Crystallographic data

Table 5. Hydrogen Coordinates ($\text{\AA} \times 10^4$) and equivalent isotropic displacement parameters ($\text{\AA}^2 \times 10^3$) for pa845

atom	x	y	z	U(eq)
H(1A)	3939	1467	9095	41
H(1B)	5320	1608	8713	41
H(2A)	4861	621	8373	42
H(2B)	3265	989	8245	42
H(6)	-470.0000	5105	7276	38
H(8)	1886	4222	8951	40
H(10A)	190	3277	6597	82
H(10B)	1670	3312	6286	82
H(10C)	332	3605	5808	82
H(11A)	-1485	4481	6591	70
H(11B)	-1166	4679	5802	70
H(11C)	-980	5213	6276	70
H(12A)	1259	4740	5457	75
H(12B)	2471	4464	6013	75
H(12C)	1409	5207	5999	75
H(14A)	-1964	5611	7952	88
H(14B)	-916	6126	7676	88
H(14C)	-1787	6226	8333	88
H(15A)	-1348	5297	9409	79
H(15B)	-164	4593	9454	79
H(15C)	-1522	4694	9012	79
H(16A)	1220	5999	8365	75
H(16B)	1507	5395	9053	75
H(16C)	297	6087	9009	75
H(14D)	-228	6135	7549	159
H(14E)	775	6274	8085	159
H(14F)	-846	6524	8138	159
H(15D)	-2090	5718	8764	194
H(15E)	-1691	4857	8887	194
H(15F)	-1976.0001	5338	8135	194
H(16D)	104	5823	9310	195
H(16E)	1507	5539	8965	195
H(16F)	769	4979	9467	195
H(18)	4944	4070	7832	48
H(19)	7155	4277	7760	59
H(20)	8874	3536	8502	58
H(21)	8369	2588	9327	56
H(22)	6152	2373	9412	44
H(24)	1421	2446	9179	51
H(25)	403	2267	10233	60
H(26)	1398	2543	11142	59
H(27)	3395	2971	11010	62
H(28)	4429	3169	9954	50
H(32)	7091	2252	4773	41
H(34)	5890	498	5855	42
H(36A)	3963	3630	5588	88
H(36B)	4306	3686	4806	88
H(36C)	4666	4266	5187	88
H(37A)	5933	3326	6443	106
H(37B)	6655	3930	5996	106
H(37C)	7468	3109	6200	106
H(38A)	7038	3996	4805	84
H(38B)	6682	3402	4443	84
H(38C)	7923	3190	4981	84
H(40A)	6688	1763	3898	105
H(40B)	5722	1186	3991	105
H(40C)	7195	1018	3662	105
H(41A)	9273	688	4343	75
H(41B)	9255	680	5133	75
H(41C)	8914	1430	4589	75
H(42A)	7751	-157	4569	106
H(42B)	6261	55	4866	106

Appendix 1. Crystallographic data

H(42C)	7588	-122	5348	106
H(44)	7069	468	7371	59
H(45)	8477	-665	7751	74
H(46)	7591	-1696	7845	76
H(47)	5350	-1613	7541	79
H(48)	3926	-487	7127	57
H(50)	2268	268	7573	50
H(51)	-22	341	7306	63
H(52)	-1028	1119	6320	65
H(53)	253	1833	5599	63
H(54)	2555	1749	5849	50
H(55A)	6.0000	2515	2663	215
H(55B)	-1180	2414	3199	215
H(55C)	-11	1736	3129	215
H(57)	-557	3336	3718	100
H(58)	626	3591	4498	133
H(59)	2634	2891	4904	124
H(60)	3542	1855	4524	139
H(61)	2138	1513	3714	109
H(62A)	3837	2821	2976	116
H(62B)	5387	2556	2776	116
H(62C)	4320	3087	2221	116
H(64)	3268	3898	3387	62
H(65)	3867	4889	3670	70
H(66)	5922	5202	3358	75
H(67)	7421	4514	2748	84
H(68)	6855	3518	2454	84
H(69A)	598	9350	359	211
H(69B)	644	9892	842	211
H(69C)	-761	9662	721	211
H(71)	-1198	8537	1326	98
H(72)	-730	7602	2245	105
H(73)	1314	7356	2816	99
H(74)	2913	8069	2516	90
H(75)	2425	9054	1587	98
H(76A)	5218	-649.0001	-1094	111
H(76B)	5072	-1254.0001	-433	111
H(76C)	6514	-1026	-602	111
H(78)	7069	-84	-202.0000	82
H(79)	6527	800	434	101
H(80)	4285	1126	789	110
H(81)	2584	567	508	90
H(82)	3125	-318.0000	-128	77
H(83)	4051	5691	10490	104
H(84)	4699	4765	11450	105
H(85)	6087	3669	11343	129
H(86)	6826	3499	10276	101
H(87)	6179	4425	9317	84
H(89A)	5281	6017	9032	226
H(89B)	3758	6098	9311	226
H(89C)	4273	5554	8825	226

Chapter 5**Complex 40**

Table 1. Crystal data for pa582

Compound	pa582
Molecular formula	C ₃₈ H ₃₂ AlClN ₂ O ₂ P ₂ .C ₄ H ₈ O
Molecular weight	745.13
Crystal habit	Colorless Block
Crystal dimensions(mm)	0.26x0.24x0.24
Crystal system	monoclinic
Space group	P2 ₁
a(Å)	12.236(1)
b(Å)	12.934(1)
c(Å)	12.697(1)
α(°)	90.00
β(°)	116.183(1)
γ(°)	90.00
V(Å ³)	1803.2(2)
Z	2
d(g·cm ⁻³)	1.372
F(000)	780
μ(cm ⁻¹)	0.263
Absorption corrections	multi-scan ; 0.9348 min, 0.9396 max
Diffractometer	KappaCCD
X-ray source	MoKα
λ(Å)	0.71069
Monochromator	graphite
T (K)	150.0(1)
Scan mode	phi and omega scans
Maximum θ	30.01
HKL ranges	-17 17 ; -18 9 ; -17 17
Reflections measured	16855
Unique data	7237
Rint	0.0280
Reflections used	6957
Criterion	I > 2σ(I)
Refinement type	Fsqd
Hydrogen atoms	constr
Parameters refined	460
Reflections / parameter	15
wR2	0.1012
R1	0.0383
Flack's parameter	0.04(6)
Weights a, b	0.0558 ; 0.8069
GoF	1.052
difference peak / hole (e Å ⁻³)	0.790(0.054) / -0.412(0.054)

Appendix 1. Crystallographic data

Table 2. Atomic Coordinates (A x 10⁴) and equivalent isotropic displacement parameters (A² x 10³) for pa582

atom	x	y	z	U(eq)
C1(1)	-6857(1)	4538(1)	-15734(1)	29(1)
P(1)	-5412(1)	4537(1)	-12193(1)	20(1)
P(2)	-10364(1)	4506(1)	-15813(1)	21(1)
Al	-7587(1)	3731(1)	-14629(1)	20(1)
O(1)	-6525(1)	2689(1)	-13957(2)	26(1)
O(2)	-8526(1)	2772(2)	-15687(2)	29(1)
N(1)	-6789(1)	4581(2)	-13189(2)	23(1)
N(2)	-9007(1)	4491(2)	-14756(1)	22(1)
C(1)	-7493(2)	5513(2)	-13216(2)	32(1)
C(2)	-8824(2)	5201(2)	-13777(2)	30(1)
C(3)	-4704(2)	3404(2)	-12398(2)	21(1)
C(4)	-5353(2)	2653(2)	-13267(2)	20(1)
C(5)	-4671(2)	1810(2)	-13370(2)	24(1)
C(6)	-3439(2)	1715(2)	-12667(2)	28(1)
C(7)	-2815(2)	2450(2)	-11809(2)	30(1)
C(8)	-3446(2)	3289(2)	-11685(2)	26(1)
C(9)	-4524(2)	5652(2)	-12216(2)	23(1)
C(10)	-4839(2)	6155(2)	-13278(2)	27(1)
C(11)	-4155(2)	6985(2)	-13346(2)	32(1)
C(12)	-3129(2)	7296(2)	-12366(3)	33(1)
C(13)	-2794(2)	6798(2)	-11307(2)	35(1)
C(14)	-3492(2)	5976(2)	-11216(2)	30(1)
C(15)	-5273(2)	4521(2)	-10707(2)	24(1)
C(16)	-5383(2)	5438(2)	-10179(2)	31(1)
C(17)	-5314(3)	5422(3)	-9059(2)	39(1)
C(18)	-5133(2)	4509(3)	-8448(2)	40(1)
C(19)	-5024(2)	3589(3)	-8958(2)	35(1)
C(20)	-5099(2)	3598(2)	-10087(2)	27(1)
C(21)	-10530(2)	3491(2)	-16814(2)	24(1)
C(22)	-9594(2)	2769(2)	-16613(2)	24(1)
C(23)	-9852(2)	1969(2)	-17446(2)	30(1)
C(24)	-10970(2)	1896(2)	-18411(2)	35(1)
C(25)	-11887(2)	2605(3)	-18597(2)	36(1)
C(26)	-11665(2)	3403(2)	-17811(2)	32(1)
C(27)	-10712(2)	5715(2)	-16604(2)	27(1)
C(28)	-11912(2)	6079(3)	-17216(3)	41(1)
C(29)	-12132(3)	6985(3)	-17861(3)	50(1)
C(30)	-11183(3)	7536(3)	-17905(3)	48(1)
C(31)	-9996(3)	7169(3)	-17306(3)	45(1)
C(32)	-9758(3)	6266(2)	-16661(2)	34(1)
C(33)	-11528(2)	4333(2)	-15317(2)	24(1)
C(34)	-11964(2)	3346(2)	-15299(2)	33(1)
C(35)	-12825(3)	3184(3)	-14879(3)	42(1)
C(36)	-13233(2)	3999(3)	-14462(3)	41(1)
C(37)	-12783(2)	4977(3)	-14448(3)	40(1)
C(38)	-11943(2)	5164(2)	-14892(2)	32(1)
O(3)	-9351(3)	4562(3)	-10754(2)	70(1)
C(39)	-8490(3)	4579(5)	-9542(4)	71(1)
C(40)	-9214(3)	4620(10)	-8892(4)	137(3)
C(41)	-10423(4)	4805(7)	-9655(4)	102(3)
C(42)	-10531(4)	4754(6)	-10837(3)	94(2)

U(eq) is defined as 1/3 the trace of the U_{ij} tensor.

Appendix 1. Crystallographic data

Table 3. Bond lengths (A) and angles (deg) for pa582

C1(1)-Al	2.228(1)	P(1)-N(1)	1.600(2)
P(1)-C(3)	1.778(2)	P(1)-C(9)	1.813(3)
P(1)-C(15)	1.819(2)	P(2)-N(2)	1.609(2)
P(2)-C(21)	1.776(2)	P(2)-C(27)	1.805(3)
P(2)-C(33)	1.807(2)	Al-O(1)	1.804(2)
Al-O(2)	1.817(2)	Al-N(2)	1.940(2)
Al-N(1)	1.982(2)	O(1)-C(4)	1.311(2)
O(2)-C(22)	1.318(3)	N(1)-C(1)	1.474(3)
N(2)-C(2)	1.481(3)	C(1)-C(2)	1.517(3)
C(1)-H(1A)	0.9900	C(1)-H(1B)	0.9900
C(2)-H(2A)	0.9900	C(2)-H(2B)	0.9900
C(3)-C(8)	1.408(3)	C(3)-C(4)	1.421(3)
C(4)-C(5)	1.414(3)	C(5)-C(6)	1.378(3)
C(5)-H(5)	0.9500	C(6)-C(7)	1.392(4)
C(6)-H(6)	0.9500	C(7)-C(8)	1.381(3)
C(7)-H(7)	0.9500	C(8)-H(8)	0.9500
C(9)-C(10)	1.389(3)	C(9)-C(14)	1.403(3)
C(10)-C(11)	1.388(4)	C(10)-H(10)	0.9500
C(11)-C(12)	1.381(4)	C(11)-H(11)	0.9500
C(12)-C(13)	1.380(4)	C(12)-H(12)	0.9500
C(13)-C(14)	1.401(4)	C(13)-H(13)	0.9500
C(14)-H(14)	0.9500	C(15)-C(20)	1.394(4)
C(15)-C(16)	1.397(4)	C(16)-C(17)	1.388(4)
C(16)-H(16)	0.9500	C(17)-C(18)	1.376(5)
C(17)-H(17)	0.9500	C(18)-C(19)	1.388(5)
C(18)-H(18)	0.9500	C(19)-C(20)	1.396(3)
C(19)-H(19)	0.9500	C(20)-H(20)	0.9500
C(21)-C(22)	1.411(3)	C(21)-C(26)	1.411(3)
C(22)-C(23)	1.412(4)	C(23)-C(24)	1.380(3)
C(23)-H(23)	0.9500	C(24)-C(25)	1.386(4)
C(24)-H(24)	0.9500	C(25)-C(26)	1.378(4)
C(25)-H(25)	0.9500	C(26)-H(26)	0.9500
C(27)-C(32)	1.397(4)	C(27)-C(28)	1.405(3)
C(28)-C(29)	1.385(4)	C(28)-H(28)	0.9500
C(29)-C(30)	1.385(5)	C(29)-H(29)	0.9500
C(30)-C(31)	1.392(5)	C(30)-H(30)	0.9500
C(31)-C(32)	1.381(4)	C(31)-H(31)	0.9500
C(32)-H(32)	0.9500	C(33)-C(34)	1.388(4)
C(33)-C(38)	1.395(3)	C(34)-C(35)	1.391(3)
C(34)-H(34)	0.9500	C(35)-C(36)	1.369(5)
C(35)-H(35)	0.9500	C(36)-C(37)	1.377(5)
C(36)-H(36)	0.9500	C(37)-C(38)	1.393(4)
C(37)-H(37)	0.9500	C(38)-H(38)	0.9500
O(3)-C(39)	1.423(5)	O(3)-C(39)	1.431(5)
C(39)-C(40)	1.453(6)	C(39)-H(39A)	0.9900
C(39)-H(39B)	0.9900	C(40)-C(41)	1.386(5)
C(40)-H(40A)	0.9900	C(40)-H(40B)	0.9900
C(41)-C(42)	1.449(6)	C(41)-H(41A)	0.9900
C(41)-H(41B)	0.9900	C(42)-H(42A)	0.9900
C(42)-H(42B)	0.9900		
N(1)-P(1)-C(3)	109.0(1)	N(1)-P(1)-C(9)	112.9(1)
C(3)-P(1)-C(9)	108.6(1)	N(1)-P(1)-C(15)	113.8(1)
C(3)-P(1)-C(15)	108.3(1)	C(9)-P(1)-C(15)	104.1(1)
N(2)-P(2)-C(21)	109.8(1)	N(2)-P(2)-C(27)	112.2(1)
C(21)-P(2)-C(27)	108.5(1)	N(2)-P(2)-C(33)	112.9(1)
C(21)-P(2)-C(33)	107.4(1)	C(27)-P(2)-C(33)	105.8(1)
O(1)-Al-O(2)	85.86(8)	O(1)-Al-N(2)	148.2(1)
O(2)-Al-N(2)	91.94(8)	O(1)-Al-N(1)	91.1(1)
O(2)-Al-N(1)	162.6(1)	N(2)-Al-N(1)	81.64(8)
O(1)-Al-C1(1)	104.02(6)	O(2)-Al-C1(1)	98.80(7)
N(2)-Al-C1(1)	107.70(7)	N(1)-Al-C1(1)	98.60(7)
C(4)-O(1)-Al	133.6(2)	C(22)-O(2)-Al	135.8(2)
C(1)-N(1)-P(1)	116.7(2)	C(1)-N(1)-Al	112.8(1)
P(1)-N(1)-Al	128.9(1)	C(2)-N(2)-P(2)	114.2(2)

Appendix 1. Crystallographic data

C(2)-N(2)-A1	116.5(1)	P(2)-N(2)-A1	129.2(1)
N(1)-C(1)-C(2)	106.8(2)	N(1)-C(1)-H(1A)	110.4
C(2)-C(1)-H(1A)	110.4	N(1)-C(1)-H(1B)	110.4
C(2)-C(1)-H(1B)	110.4	H(1A)-C(1)-H(1B)	108.6
N(2)-C(2)-C(1)	107.0(2)	N(2)-C(2)-H(2A)	110.3
C(1)-C(2)-H(2A)	110.3	N(2)-C(2)-H(2B)	110.3
C(1)-C(2)-H(2B)	110.3	H(2A)-C(2)-H(2B)	108.6
C(8)-C(3)-C(4)	120.3(2)	C(8)-C(3)-P(1)	117.2(2)
C(4)-C(3)-P(1)	122.4(2)	O(1)-C(4)-C(5)	118.8(2)
O(1)-C(4)-C(3)	124.5(2)	C(5)-C(4)-C(3)	116.7(2)
C(6)-C(5)-C(4)	122.0(2)	C(6)-C(5)-H(5)	119.0
C(4)-C(5)-H(5)	119.0	C(5)-C(6)-C(7)	120.7(2)
C(5)-C(6)-H(6)	119.6	C(7)-C(6)-H(6)	119.6
C(8)-C(7)-C(6)	119.1(2)	C(8)-C(7)-H(7)	120.5
C(6)-C(7)-H(7)	120.5	C(7)-C(8)-C(3)	121.1(2)
C(7)-C(8)-H(8)	119.4	C(3)-C(8)-H(8)	119.4
C(10)-C(9)-C(14)	119.5(2)	C(10)-C(9)-P(1)	118.4(2)
C(14)-C(9)-P(1)	121.9(2)	C(11)-C(10)-C(9)	120.4(2)
C(11)-C(10)-H(10)	119.8	C(9)-C(10)-H(10)	119.8
C(12)-C(11)-C(10)	120.2(2)	C(12)-C(11)-H(11)	119.9
C(10)-C(11)-H(11)	119.9	C(13)-C(12)-C(11)	120.2(2)
C(13)-C(12)-H(12)	119.9	C(11)-C(12)-H(12)	119.9
C(12)-C(13)-C(14)	120.3(2)	C(12)-C(13)-H(13)	119.8
C(14)-C(13)-H(13)	119.8	C(13)-C(14)-C(9)	119.4(2)
C(13)-C(14)-H(14)	120.3	C(9)-C(14)-H(14)	120.3
C(20)-C(15)-C(16)	118.6(2)	C(20)-C(15)-P(1)	121.1(2)
C(16)-C(15)-P(1)	120.2(2)	C(17)-C(16)-C(15)	120.3(3)
C(17)-C(16)-H(16)	119.9	C(15)-C(16)-H(16)	119.9
C(18)-C(17)-C(16)	120.8(3)	C(18)-C(17)-H(17)	119.6
C(16)-C(17)-H(17)	119.6	C(17)-C(18)-C(19)	119.8(2)
C(17)-C(18)-H(18)	120.1	C(19)-C(18)-H(18)	120.1
C(18)-C(19)-C(20)	119.7(3)	C(18)-C(19)-H(19)	120.2
C(20)-C(19)-H(19)	120.2	C(15)-C(20)-C(19)	120.8(3)
C(15)-C(20)-H(20)	119.6	C(19)-C(20)-H(20)	119.6
C(22)-C(21)-C(26)	120.5(2)	C(22)-C(21)-P(2)	122.1(2)
C(26)-C(21)-P(2)	117.3(2)	O(2)-C(22)-C(21)	124.5(2)
O(2)-C(22)-C(23)	118.4(2)	C(21)-C(22)-C(23)	117.0(2)
C(24)-C(23)-C(22)	121.5(3)	C(24)-C(23)-H(23)	119.3
C(22)-C(23)-H(23)	119.3	C(23)-C(24)-C(25)	121.1(3)
C(23)-C(24)-H(24)	119.4	C(25)-C(24)-H(24)	119.4
C(26)-C(25)-C(24)	119.1(2)	C(26)-C(25)-H(25)	120.4
C(24)-C(25)-H(25)	120.4	C(25)-C(26)-C(21)	120.8(2)
C(25)-C(26)-H(26)	119.6	C(21)-C(26)-H(26)	119.6
C(32)-C(27)-C(28)	119.5(3)	C(32)-C(27)-P(2)	118.2(2)
C(28)-C(27)-P(2)	122.1(2)	C(29)-C(28)-C(27)	119.6(3)
C(29)-C(28)-H(28)	120.2	C(27)-C(28)-H(28)	120.2
C(28)-C(29)-C(30)	120.7(3)	C(28)-C(29)-H(29)	119.6
C(30)-C(29)-H(29)	119.6	C(29)-C(30)-C(31)	119.6(3)
C(29)-C(30)-H(30)	120.2	C(31)-C(30)-H(30)	120.2
C(32)-C(31)-C(30)	120.6(3)	C(32)-C(31)-H(31)	119.7
C(30)-C(31)-H(31)	119.7	C(31)-C(32)-C(27)	120.0(3)
C(31)-C(32)-H(32)	120.0	C(27)-C(32)-H(32)	120.0
C(34)-C(33)-C(38)	119.6(2)	C(34)-C(33)-P(2)	119.1(2)
C(38)-C(33)-P(2)	121.2(2)	C(33)-C(34)-C(35)	120.5(3)
C(33)-C(34)-H(34)	119.8	C(35)-C(34)-H(34)	119.8
C(36)-C(35)-C(34)	119.9(3)	C(36)-C(35)-H(35)	120.0
C(34)-C(35)-H(35)	120.0	C(35)-C(36)-C(37)	120.0(2)
C(35)-C(36)-H(36)	120.0	C(37)-C(36)-H(36)	120.0
C(36)-C(37)-C(38)	121.0(3)	C(36)-C(37)-H(37)	119.5
C(38)-C(37)-H(37)	119.5	C(37)-C(38)-C(33)	118.9(3)
C(37)-C(38)-H(38)	120.6	C(33)-C(38)-H(38)	120.6
C(42)-O(3)-C(39)	108.5(3)	O(3)-C(39)-C(40)	105.5(3)
O(3)-C(39)-H(39A)	110.6	C(40)-C(39)-H(39A)	110.6
O(3)-C(39)-H(39B)	110.6	C(40)-C(39)-H(39B)	110.6
H(39A)-C(39)-H(39B)	108.8	C(41)-C(40)-C(39)	109.8(4)
C(41)-C(40)-H(40A)	109.7	C(39)-C(40)-H(40A)	109.7
C(41)-C(40)-H(40B)	109.7	C(39)-C(40)-H(40B)	109.7
H(40A)-C(40)-H(40B)	108.2	C(40)-C(41)-C(42)	107.3(4)

Appendix 1. Crystallographic data

C(40)-C(41)-H(41A)	110.3	C(42)-C(41)-H(41A)	110.3
C(40)-C(41)-H(41B)	110.3	C(42)-C(41)-H(41B)	110.3
H(41A)-C(41)-H(41B)	108.5	O(3)-C(42)-C(41)	107.8(3)
O(3)-C(42)-H(42A)	110.2	C(41)-C(42)-H(42A)	110.2
O(3)-C(42)-H(42B)	110.2	C(41)-C(42)-H(42B)	110.2
H(42A)-C(42)-H(42B)	108.5		

Appendix 1. Crystallographic data

Table 4. Anisotropic displacement parameters ($\text{\AA}^2 \times 10^3$) for pa582

atom	U11	U22	U33	U23	U13	U12
C1(1)	34(1)	31(1)	26(1)	1(1)	17(1)	-2(1)
P(1)	19(1)	19(1)	20(1)	-2(1)	8(1)	0(1)
P(2)	18(1)	22(1)	23(1)	-1(1)	8(1)	0(1)
Al	20(1)	18(1)	22(1)	-2(1)	8(1)	1(1)
O(1)	24(1)	19(1)	28(1)	-2(1)	5(1)	1(1)
O(2)	23(1)	24(1)	32(1)	-7(1)	3(1)	2(1)
N(1)	20(1)	22(1)	24(1)	-3(1)	7(1)	2(1)
N(2)	19(1)	23(1)	32(1)	-4(1)	8(1)	1(1)
C(1)	25(1)	27(1)	36(1)	-9(1)	7(1)	5(1)
C(2)	26(1)	30(1)	29(1)	-8(1)	9(1)	2(1)
C(3)	23(1)	20(1)	21(1)	0(1)	11(1)	2(1)
C(4)	22(1)	19(1)	19(1)	3(1)	9(1)	3(1)
C(5)	31(1)	21(1)	20(1)	-1(1)	11(1)	3(1)
C(6)	34(1)	25(1)	29(1)	1(1)	17(1)	8(1)
C(7)	23(1)	34(1)	32(1)	-1(1)	11(1)	6(1)
C(8)	22(1)	26(1)	28(1)	-4(1)	8(1)	1(1)
C(9)	23(1)	19(1)	28(1)	-1(1)	11(1)	1(1)
C(10)	31(1)	24(1)	27(1)	-3(1)	12(1)	-3(1)
C(11)	39(1)	26(1)	34(1)	0(1)	20(1)	-4(1)
C(12)	36(1)	25(1)	44(1)	-6(1)	23(1)	-10(1)
C(13)	29(1)	30(1)	39(1)	-2(1)	8(1)	-8(1)
C(14)	27(1)	25(1)	31(1)	-1(1)	7(1)	-3(1)
C(15)	22(1)	27(1)	23(1)	-5(1)	10(1)	-4(1)
C(16)	38(1)	28(1)	30(1)	-6(1)	17(1)	-1(1)
C(17)	46(1)	41(2)	36(1)	-14(1)	26(1)	-6(1)
C(18)	45(1)	51(2)	30(1)	-7(2)	23(1)	-10(2)
C(19)	36(1)	41(2)	29(1)	-1(1)	17(1)	-7(1)
C(20)	25(1)	29(1)	26(1)	-2(1)	11(1)	-3(1)
C(21)	22(1)	26(1)	21(1)	-2(1)	8(1)	-1(1)
C(22)	22(1)	21(1)	26(1)	-2(1)	10(1)	-3(1)
C(23)	30(1)	27(1)	31(1)	-7(1)	12(1)	-2(1)
C(24)	37(1)	36(2)	27(1)	-10(1)	9(1)	-5(1)
C(25)	30(1)	42(2)	29(1)	-7(1)	5(1)	-3(1)
C(26)	26(1)	38(2)	26(1)	-3(1)	6(1)	5(1)
C(27)	25(1)	27(1)	26(1)	1(1)	9(1)	0(1)
C(28)	31(1)	43(2)	43(1)	15(1)	12(1)	6(1)
C(29)	43(2)	48(2)	50(2)	21(2)	14(1)	18(1)
C(30)	68(2)	32(2)	38(2)	10(1)	17(1)	2(2)
C(31)	52(2)	38(2)	43(2)	9(1)	19(1)	-7(1)
C(32)	35(1)	32(2)	35(1)	4(1)	15(1)	-1(1)
C(33)	20(1)	27(1)	25(1)	1(1)	10(1)	0(1)
C(34)	35(1)	29(1)	40(1)	-2(1)	22(1)	-4(1)
C(35)	41(1)	39(2)	54(2)	-3(1)	29(1)	-10(1)
C(36)	30(1)	56(2)	42(1)	3(1)	22(1)	-1(1)
C(37)	34(1)	49(2)	44(2)	-7(1)	24(1)	7(1)
C(38)	30(1)	31(1)	37(1)	-2(1)	16(1)	3(1)
O(3)	94(2)	57(2)	69(2)	-13(2)	44(2)	-4(2)
C(39)	52(2)	78(3)	83(3)	38(3)	29(2)	27(2)
C(40)	40(2)	320(10)	46(2)	-2(5)	9(1)	20(4)
C(41)	49(2)	192(8)	58(2)	20(3)	18(2)	16(3)
C(42)	56(2)	162(7)	48(2)	18(3)	7(2)	-46(3)

The anisotropic displacement factor exponent takes the form
 $2 \pi^2 [h^2 a^{*2} U_{11} + \dots + 2 h k a^* b^* U_{12}]$

Appendix 1. Crystallographic data

Table 5. Hydrogen Coordinates ($\text{\AA} \times 10^4$) and equivalent isotropic displacement parameters ($\text{\AA}^2 \times 10^3$) for pa582

atom	x	y	z	U(eq)
H(1A)	-7349	6065	-13681.9990	38
H(1B)	-7249	5775	-12411	38
H(2A)	-9032	4851	-13196	36
H(2B)	-9350	5819	-14076	36
H(5)	-5075	1293	-13943	29
H(6)	-3010	1140	-12767	34
H(7)	-1967.9999	2375	-11317	36
H(8)	-3023	3798	-11108	32
H(10)	-5528	5930	-13961	33
H(11)	-4392	7340	-14069	38
H(12)	-2653	7855	-12421	40
H(13)	-2085	7014	-10635.9990	42
H(14)	-3270	5641	-10484	35
H(16)	-5505	6074	-10589	38
H(17)	-5394	6049	-8709	46
H(18)	-5082	4508	-7680	48
H(19)	-4899	2957	-8540	41
H(20)	-5030	2967	-10437	32
H(23)	-9242	1471	-17340	36
H(24)	-11115	1350	-18957	42
H(25)	-12658	2541	-19258	44
H(26)	-12283	3899	-17941	38
H(28)	-12568.0010	5707	-17189	49
H(29)	-12944	7231	-18276	59
H(30)	-11341	8160	-18342	58
H(31)	-9345	7542	-17341	54
H(32)	-8946	6021	-16256	41
H(34)	-11672	2778	-15575	39
H(35)	-13128.9990	2508	-14881.0010	50
H(36)	-13828	3890	-14183	49
H(37)	-13048	5534	-14130	48
H(38)	-11659	5845	-14905	39
H(39A)	-7957	5195	-9367	85
H(39B)	-7975.9995	3951	-9335	85
H(40A)	-9145	3951	-8482	165
H(40B)	-8905	5171	-8294	165
H(41A)	-10670	5497	-9504	122
H(41B)	-10954	4280	-9548	122
H(42A)	-11095.9990	4192	-11280	113
H(42B)	-10855	5414	-11252	113

Complex 4I

Table 1. Crystal data for pa575

Compound	pa575
Molecular formula	C ₄₂ H ₄₁ AlN ₂ O ₃ P ₂
Molecular weight	710.69
Crystal habit	Colorless Block
Crystal dimensions(mm)	0.22x0.14x0.08
Crystal system	monoclinic
Space group	Pc
a(Å)	14.115(1)
b(Å)	9.151(1)
c(Å)	16.812(1)
α(°)	90.00
β(°)	124.486(4)
γ(°)	90.00
V(Å ³)	1789.9(3)
Z	2
d(g·cm ⁻³)	1.319
F(000)	748
μ(cm ⁻¹)	0.189
Absorption corrections	multi-scan ; 0.9595 min, 0.9850 max
Diffractometer	KappaCCD
X-ray source	MoKα
λ(Å)	0.71069
Monochromator	graphite
T (K)	150.0(1)
Scan mode	phi and omega scans
Maximum θ	25.35
HKL ranges	-13 16 ; -11 10 ; -20 17
Reflections measured	8740
Unique data	4892
Rint	0.0391
Reflections used	4480
Criterion	I > 2σ(I)
Refinement type	Fsqd
Hydrogen atoms	constr
Parameters refined	485
Reflections / parameter	9
wR2	0.1180
R1	0.0516
Flack's parameter	-0.05(12)
Weights a, b	0.0424 ; 2.1544
GoF	1.063
difference peak / hole (e Å ⁻³)	0.856(0.051) / -0.238(0.051)

Table 2. Atomic Coordinates (A x 10⁴) and equivalent isotropic displacement parameters (A² x 10³) for pa575

atom	x	y	z	U(eq)
P(1)	-895(1)	-9855(1)	-6027(1)	37(1)
P(2)	-4666(1)	-8518(1)	-6190(1)	37(1)
Al(1)	-3193(1)	-11001(2)	-6353(1)	40(1)
O(1)	-1920(3)	-12197(4)	-5589(2)	46(1)
O(2)	-3461(3)	-11353(4)	-5427(3)	51(1)
N(1)	-2243(3)	-9623(4)	-6519(3)	40(1)
N(2)	-4232(3)	-9236(4)	-6791(3)	38(1)
C(1)	-2757(4)	-8180(5)	-6929(4)	45(1)
C(2)	-4034(4)	-8360(5)	-7414(3)	42(1)
C(3)	-596(4)	-11753(5)	-6004(3)	36(1)
C(4)	-1177(4)	-12695(5)	-5759(3)	42(1)
C(5)	-941(5)	-14203(5)	-5713(4)	48(1)
C(6)	-168(5)	-14698(5)	-5895(4)	54(1)
C(7)	387(5)	-13764(5)	-6146(4)	49(1)
C(8)	176(4)	-12275(5)	-6206(4)	45(1)
C(9)	-16(4)	-9214(5)	-4795(3)	38(1)
C(10)	1112(4)	-9625(6)	-4175(4)	52(1)
C(11)	1751(5)	-9172(7)	-3226(4)	62(2)
C(12)	1261(5)	-8265(6)	-2890(4)	51(1)
C(13)	143(5)	-7857(6)	-3499(4)	53(1)
C(14)	-508(5)	-8332(5)	-4448(4)	45(1)
C(15)	-417(4)	-8976(5)	-6697(3)	41(1)
C(16)	626(4)	-8256(5)	-6275(4)	47(1)
C(17)	964(5)	-7674(6)	-6838(5)	62(2)
C(18)	226(6)	-7782(7)	-7830(5)	65(2)
C(19)	-801(6)	-8458(6)	-8262(4)	60(2)
C(20)	-1127(5)	-9081(5)	-7702(4)	48(1)
C(21)	-5079(4)	-9972(5)	-5740(3)	39(1)
C(22)	-4375(4)	-11226(5)	-5397(3)	43(1)
C(23)	-4672(5)	-12366(6)	-5015(4)	51(1)
C(24)	-5632(5)	-12261(6)	-5000(4)	52(1)
C(25)	-6329(5)	-11057(7)	-5358(4)	53(1)
C(26)	-6054(4)	-9909(6)	-5725(3)	45(1)
C(27)	-3669(4)	-7368(5)	-5184(3)	40(1)
C(28)	-3300(5)	-6060(5)	-5354(4)	44(1)
C(29)	-2562(4)	-5117(6)	-4603(4)	48(1)
C(30)	-2144(5)	-5498(6)	-3664(4)	50(1)
C(31)	-2489(5)	-6809(6)	-3484(4)	60(2)
C(32)	-3238(4)	-7737(6)	-4234(3)	50(1)
C(33)	-5894(4)	-7352(5)	-6936(3)	41(1)
C(34)	-6617(4)	-7602(6)	-7919(4)	50(1)
C(35)	-7568(5)	-6703(6)	-8487(4)	56(1)
C(36)	-7810(5)	-5569(7)	-8088(4)	62(2)
C(37)	-7109(5)	-5341(7)	-7106(4)	61(2)
C(38)	-6149(5)	-6216(6)	-6530(4)	49(1)
O(3A)	-3936(3)	-12052(4)	-7392(3)	67(1)
C(39A)	-4968(5)	-12779(6)	-7949(4)	52(1)
C(40A)	-5730(10)	-11860(20)	-8826(8)	83(4)
C(41A)	-5540(10)	-13000(10)	-7404(7)	65(3)
C(42A)	-4790(10)	-14270(10)	-8233(8)	75(4)
O(3B)	-3936(3)	-12052(4)	-7392(3)	67(1)
C(39B)	-4968(5)	-12779(6)	-7949(4)	52(1)
C(40B)	-6020(20)	-12050(20)	-8160(10)	77(6)
C(41B)	-4680(20)	-14120(20)	-7390(10)	72(5)
C(42B)	-5320(20)	-13300(20)	-8980(10)	76(6)

U(eq) is defined as 1/3 the trace of the Uij tensor.

Table 3. Bond lengths (Å) and angles (deg) for pa575

P(1)-N(1)	1.602(4)	P(1)-C(3)	1.783(4)
P(1)-C(15)	1.798(5)	P(1)-C(9)	1.807(5)
P(2)-N(2)	1.591(4)	P(2)-C(21)	1.784(5)
P(2)-C(27)	1.803(5)	P(2)-C(33)	1.803(5)
Al(1)-O(3A)	1.733(4)	Al(1)-O(2)	1.827(4)
Al(1)-O(1)	1.861(4)	Al(1)-N(1)	1.973(4)
Al(1)-N(2)	2.019(4)	O(1)-C(4)	1.315(6)
O(2)-C(22)	1.324(6)	N(1)-C(1)	1.476(6)
N(2)-C(2)	1.466(6)	C(1)-C(2)	1.509(7)
C(1)-H(1A)	0.9900	C(1)-H(1B)	0.9900
C(2)-H(2A)	0.9900	C(2)-H(2B)	0.9900
C(3)-C(8)	1.398(6)	C(3)-C(4)	1.401(7)
C(4)-C(5)	1.411(7)	C(5)-C(6)	1.366(7)
C(5)-H(5)	0.9500	C(6)-C(7)	1.378(7)
C(6)-H(6)	0.9500	C(7)-C(8)	1.386(7)
C(7)-H(7)	0.9500	C(8)-H(8)	0.9500
C(9)-C(10)	1.371(6)	C(9)-C(14)	1.391(6)
C(10)-C(11)	1.379(7)	C(10)-H(10)	0.9500
C(11)-C(12)	1.389(8)	C(11)-H(11)	0.9500
C(12)-C(13)	1.360(7)	C(12)-H(12)	0.9500
C(13)-C(14)	1.385(7)	C(13)-H(13)	0.9500
C(14)-H(14)	0.9500	C(15)-C(16)	1.387(7)
C(15)-C(20)	1.396(7)	C(16)-C(17)	1.385(7)
C(16)-H(16)	0.9500	C(17)-C(18)	1.38(1)
C(17)-H(17)	0.9500	C(18)-C(19)	1.349(8)
C(18)-H(18)	0.9500	C(19)-C(20)	1.384(7)
C(19)-H(19)	0.9500	C(20)-H(20)	0.9500
C(21)-C(26)	1.392(7)	C(21)-C(22)	1.410(7)
C(22)-C(23)	1.408(7)	C(23)-C(24)	1.374(7)
C(23)-H(23)	0.9500	C(24)-C(25)	1.369(8)
C(24)-H(24)	0.9500	C(25)-C(26)	1.382(7)
C(25)-H(25)	0.9500	C(26)-H(26)	0.9500
C(27)-C(32)	1.392(7)	C(27)-C(28)	1.397(7)
C(28)-C(29)	1.391(7)	C(28)-H(28)	0.9500
C(29)-C(30)	1.381(7)	C(29)-H(29)	0.9500
C(30)-C(31)	1.391(8)	C(30)-H(30)	0.9500
C(31)-C(32)	1.386(7)	C(31)-H(31)	0.9500
C(32)-H(32)	0.9500	C(33)-C(34)	1.384(7)
C(33)-C(38)	1.398(7)	C(34)-C(35)	1.393(7)
C(34)-H(34)	0.9500	C(35)-C(36)	1.379(8)
C(35)-H(35)	0.9500	C(36)-C(37)	1.378(8)
C(36)-H(36)	0.9500	C(37)-C(38)	1.389(7)
C(37)-H(37)	0.9500	C(38)-H(38)	0.9500
O(3A)-C(39A)	1.377(6)	C(39A)-C(40A)	1.50(1)
C(39A)-C(42A)	1.52(1)	C(39A)-C(41A)	1.54(1)
C(40A)-H(40A)	0.9800	C(40A)-H(40B)	0.9800
C(40A)-H(40C)	0.9800	C(41A)-H(41A)	0.9800
C(41A)-H(41B)	0.9800	C(41A)-H(41C)	0.9800
C(42A)-H(42A)	0.9800	C(42A)-H(42B)	0.9800
C(42A)-H(42C)	0.9800	C(40B)-H(40D)	0.9800
C(40B)-H(40E)	0.9800	C(40B)-H(40F)	0.9800
C(41B)-H(41D)	0.9800	C(41B)-H(41E)	0.9800
C(41B)-H(41F)	0.9800	C(42B)-H(42D)	0.9800
C(42B)-H(42E)	0.9800	C(42B)-H(42F)	0.9800
N(1)-P(1)-C(3)	109.7(2)	N(1)-P(1)-C(15)	111.9(2)
C(3)-P(1)-C(15)	106.4(2)	N(1)-P(1)-C(9)	113.2(2)
C(3)-P(1)-C(9)	106.9(2)	C(15)-P(1)-C(9)	108.4(2)
N(2)-P(2)-C(21)	107.3(2)	N(2)-P(2)-C(27)	117.4(2)
C(21)-P(2)-C(27)	107.9(2)	N(2)-P(2)-C(33)	111.5(2)
C(21)-P(2)-C(33)	108.7(2)	C(27)-P(2)-C(33)	103.8(2)
O(3A)-Al(1)-O(2)	117.6(2)	O(3A)-Al(1)-O(1)	99.5(2)
O(2)-Al(1)-O(1)	83.9(2)	O(3A)-Al(1)-N(1)	106.4(2)
O(2)-Al(1)-N(1)	136.0(2)	O(1)-Al(1)-N(1)	90.3(2)
O(3A)-Al(1)-N(2)	100.2(2)	O(2)-Al(1)-N(2)	89.7(2)

O(1)-Al(1)-N(2)	160.1(2)	N(1)-Al(1)-N(2)	81.3(2)
C(4)-O(1)-Al(1)	129.2(3)	C(22)-O(2)-Al(1)	133.9(3)
C(1)-N(1)-P(1)	119.1(3)	C(1)-N(1)-Al(1)	116.4(3)
P(1)-N(1)-Al(1)	123.1(2)	C(2)-N(2)-P(2)	121.7(3)
C(2)-N(2)-Al(1)	107.8(3)	P(2)-N(2)-Al(1)	124.1(2)
N(1)-C(1)-C(2)	106.0(4)	N(1)-C(1)-H(1A)	110.5
C(2)-C(1)-H(1A)	110.5	N(1)-C(1)-H(1B)	110.5
C(2)-C(1)-H(1B)	110.5	H(1A)-C(1)-H(1B)	108.7
N(2)-C(2)-C(1)	109.1(4)	N(2)-C(2)-H(2A)	109.9
C(1)-C(2)-H(2A)	109.9	N(2)-C(2)-H(2B)	109.9
C(1)-C(2)-H(2B)	109.9	H(2A)-C(2)-H(2B)	108.3
C(8)-C(3)-C(4)	121.9(4)	C(8)-C(3)-P(1)	122.3(4)
C(4)-C(3)-P(1)	115.8(3)	O(1)-C(4)-C(3)	121.4(4)
O(1)-C(4)-C(5)	121.3(5)	C(3)-C(4)-C(5)	117.3(4)
C(6)-C(5)-C(4)	120.4(5)	C(6)-C(5)-H(5)	119.8
C(4)-C(5)-H(5)	119.8	C(5)-C(6)-C(7)	121.8(5)
C(5)-C(6)-H(6)	119.1	C(7)-C(6)-H(6)	119.1
C(6)-C(7)-C(8)	119.8(5)	C(6)-C(7)-H(7)	120.1
C(8)-C(7)-H(7)	120.1	C(7)-C(8)-C(3)	118.8(5)
C(7)-C(8)-H(8)	120.6	C(3)-C(8)-H(8)	120.6
C(10)-C(9)-C(14)	118.8(4)	C(10)-C(9)-P(1)	122.0(4)
C(14)-C(9)-P(1)	119.1(4)	C(9)-C(10)-C(11)	120.9(5)
C(9)-C(10)-H(10)	119.5	C(11)-C(10)-H(10)	119.5
C(10)-C(11)-C(12)	120.0(5)	C(10)-C(11)-H(11)	120.0
C(12)-C(11)-H(11)	120.0	C(13)-C(12)-H(12)	120.3
C(13)-C(12)-H(12)	120.3	C(12)-C(13)-C(14)	120.8(5)
C(12)-C(13)-C(14)	120.8(5)	C(14)-C(13)-H(13)	119.6
C(14)-C(13)-H(13)	119.6	C(13)-C(14)-C(9)	120.1(5)
C(13)-C(14)-H(14)	119.9	C(9)-C(14)-H(14)	119.9
C(16)-C(15)-C(20)	118.6(5)	C(16)-C(15)-P(1)	124.0(4)
C(20)-C(15)-P(1)	117.4(4)	C(17)-C(16)-C(15)	120.7(5)
C(17)-C(16)-H(16)	119.7	C(15)-C(16)-H(16)	119.7
C(18)-C(17)-C(16)	118.8(6)	C(18)-C(17)-H(17)	120.6
C(16)-C(17)-H(17)	120.6	C(19)-C(18)-C(17)	121.9(5)
C(19)-C(18)-H(18)	119.1	C(17)-C(18)-H(18)	119.1
C(18)-C(19)-C(20)	119.5(6)	C(18)-C(19)-H(19)	120.2
C(20)-C(19)-H(19)	120.2	C(19)-C(20)-C(15)	120.5(6)
C(19)-C(20)-H(20)	119.7	C(15)-C(20)-H(20)	119.7
C(26)-C(21)-C(22)	120.1(4)	C(26)-C(21)-P(2)	122.7(4)
C(22)-C(21)-P(2)	117.2(3)	O(2)-C(22)-C(23)	120.0(4)
O(2)-C(22)-C(21)	122.1(4)	C(23)-C(22)-C(21)	117.8(4)
C(24)-C(23)-C(22)	120.6(5)	C(24)-C(23)-H(23)	119.7
C(22)-C(23)-H(23)	119.7	C(25)-C(24)-C(23)	121.3(5)
C(25)-C(24)-H(24)	119.4	C(23)-C(24)-H(24)	119.4
C(24)-C(25)-C(26)	119.7(5)	C(24)-C(25)-H(25)	120.2
C(26)-C(25)-H(25)	120.2	C(25)-C(26)-C(21)	120.5(5)
C(25)-C(26)-H(26)	119.7	C(21)-C(26)-H(26)	119.7
C(32)-C(27)-C(28)	118.1(5)	C(32)-C(27)-P(2)	122.4(4)
C(28)-C(27)-P(2)	119.5(4)	C(29)-C(28)-C(27)	121.4(5)
C(29)-C(28)-H(28)	119.3	C(27)-C(28)-H(28)	119.3
C(30)-C(29)-C(28)	119.8(5)	C(30)-C(29)-H(29)	120.1
C(28)-C(29)-H(29)	120.1	C(29)-C(30)-C(31)	119.4(5)
C(29)-C(30)-H(30)	120.3	C(31)-C(30)-H(30)	120.3
C(32)-C(31)-C(30)	120.8(5)	C(32)-C(31)-H(31)	119.6
C(30)-C(31)-H(31)	119.6	C(31)-C(32)-C(27)	120.6(5)
C(31)-C(32)-H(32)	119.7	C(27)-C(32)-H(32)	119.7
C(34)-C(33)-C(38)	119.1(5)	C(34)-C(33)-P(2)	120.1(4)
C(33)-C(33)-P(2)	120.8(4)	C(33)-C(34)-C(35)	119.6(5)
C(33)-C(34)-H(34)	120.2	C(35)-C(34)-H(34)	120.2
C(36)-C(35)-C(34)	121.3(5)	C(36)-C(35)-H(35)	119.4
C(34)-C(35)-H(35)	119.4	C(37)-C(36)-C(35)	119.3(5)
C(37)-C(36)-H(36)	120.4	C(35)-C(36)-H(36)	120.4
C(36)-C(37)-C(38)	120.2(5)	C(36)-C(37)-H(37)	119.9
C(38)-C(37)-H(37)	119.9	C(37)-C(38)-C(33)	120.5(5)
C(37)-C(38)-H(38)	119.7	C(33)-C(38)-H(38)	119.7
C(39A)-O(3A)-Al(1)	139.1(3)	O(3A)-C(39A)-C(40A)	107.1(6)
O(3A)-C(39A)-C(42A)	110.3(6)	C(40A)-C(39A)-C(42A)	110.6(8)
O(3A)-C(39A)-C(41A)	111.7(5)	C(40A)-C(39A)-C(41A)	109.2(7)

Appendix 1. Crystallographic data

C(42A)-C(39A)-C(41A)	107.9(7)	H(40D)-C(40B)-H(40E)	109.5
H(40D)-C(40B)-H(40F)	109.5	H(40E)-C(40B)-H(40F)	109.5
H(41D)-C(41B)-H(41E)	109.5	H(41D)-C(41B)-H(41F)	109.5
H(41E)-C(41B)-H(41F)	109.5	H(42D)-C(42B)-H(42E)	109.5
H(42D)-C(42B)-H(42F)	109.5	H(42E)-C(42B)-H(42F)	109.5

Appendix 1. Crystallographic data

Table 4. Anisotropic displacement parameters ($\text{\AA}^2 \times 10^3$) for pa575

atom	U11	U22	U33	U23	U13	U12
P(1)	43(1)	27(1)	45(1)	-1(1)	28(1)	0(1)
P(2)	39(1)	33(1)	41(1)	3(1)	24(1)	2(1)
Al(1)	46(1)	28(1)	50(1)	-3(1)	31(1)	-3(1)
O(1)	58(2)	34(2)	63(2)	8(2)	45(2)	7(2)
O(2)	60(2)	38(2)	70(2)	18(2)	47(2)	12(2)
N(1)	44(2)	20(2)	54(2)	3(2)	27(2)	1(2)
N(2)	41(2)	34(2)	42(2)	6(2)	26(2)	5(2)
C(1)	49(3)	31(3)	58(3)	2(2)	33(3)	0(2)
C(2)	49(3)	35(3)	41(2)	3(2)	25(2)	5(2)
C(3)	43(3)	27(2)	38(2)	-2(2)	22(2)	4(2)
C(4)	50(3)	33(3)	44(2)	2(2)	27(2)	5(2)
C(5)	63(4)	27(2)	60(3)	4(2)	38(3)	2(2)
C(6)	65(4)	26(3)	73(4)	-6(2)	41(3)	4(3)
C(7)	55(3)	43(3)	56(3)	-7(3)	36(3)	9(3)
C(8)	45(3)	42(3)	49(3)	-1(2)	28(2)	3(2)
C(9)	44(3)	30(2)	47(3)	-5(2)	29(2)	-3(2)
C(10)	46(3)	52(3)	49(3)	-9(3)	22(3)	10(3)
C(11)	52(3)	63(4)	64(4)	-1(3)	29(3)	9(3)
C(12)	61(4)	40(3)	47(3)	-8(2)	27(3)	-7(3)
C(13)	66(4)	47(3)	55(3)	-10(2)	40(3)	8(3)
C(14)	48(3)	42(3)	48(3)	1(2)	30(2)	7(2)
C(15)	51(3)	29(2)	53(3)	0(2)	35(3)	6(2)
C(16)	46(3)	42(3)	63(3)	1(2)	37(3)	3(2)
C(17)	65(4)	46(3)	96(5)	2(3)	58(4)	0(3)
C(18)	91(5)	52(4)	96(5)	19(3)	79(5)	13(4)
C(19)	94(5)	45(3)	62(3)	6(3)	56(4)	16(3)
C(20)	63(3)	37(3)	58(3)	3(2)	42(3)	5(3)
C(21)	40(3)	38(3)	39(2)	-1(2)	23(2)	-4(2)
C(22)	58(3)	32(3)	48(3)	0(2)	36(3)	-1(2)
C(23)	67(4)	35(3)	66(3)	6(2)	48(3)	4(3)
C(24)	69(4)	43(3)	52(3)	-3(2)	40(3)	-10(3)
C(25)	46(3)	72(4)	50(3)	-5(3)	32(3)	-14(3)
C(26)	47(3)	46(3)	46(3)	0(2)	28(2)	2(2)
C(27)	40(3)	31(2)	50(3)	0(2)	26(2)	1(2)
C(28)	57(3)	39(3)	46(3)	2(2)	35(2)	3(2)
C(29)	52(3)	35(3)	60(3)	-1(2)	34(3)	-3(2)
C(30)	47(3)	39(3)	51(3)	-6(2)	20(2)	-5(2)
C(31)	66(4)	52(3)	43(3)	9(2)	20(3)	-3(3)
C(32)	52(3)	40(3)	49(3)	4(2)	24(3)	-4(3)
C(33)	43(3)	35(3)	46(3)	6(2)	27(2)	1(2)
C(34)	40(3)	38(3)	63(3)	-2(2)	23(3)	-6(2)
C(35)	44(3)	47(3)	57(3)	9(3)	16(3)	-4(3)
C(36)	52(4)	49(3)	75(4)	15(3)	30(3)	9(3)
C(37)	58(4)	62(4)	68(4)	6(3)	38(3)	16(3)
C(38)	47(3)	48(3)	51(3)	4(2)	28(3)	11(3)
O(3A)	60(3)	62(3)	84(3)	-40(2)	44(2)	-20(2)
C(39A)	53(3)	49(3)	53(3)	1(3)	30(3)	-9(3)
C(40A)	76(8)	100(10)	76(7)	18(7)	46(7)	3(7)
C(41A)	60(7)	73(7)	68(6)	-10(6)	40(6)	-20(6)
C(42A)	120(10)	36(5)	84(8)	-20(5)	70(8)	-35(6)
O(3B)	60(3)	62(3)	84(3)	-40(2)	44(2)	-20(2)
C(39B)	53(3)	49(3)	53(3)	1(3)	30(3)	-9(3)
C(40B)	90(10)	50(10)	90(10)	0(10)	60(10)	0(10)
C(41B)	80(10)	80(10)	50(10)	-8(8)	35(8)	-20(10)
C(42B)	90(10)	90(10)	60(10)	-30(10)	50(10)	-20(10)

The anisotropic displacement factor exponent takes the form
 $2 \pi^2 [h^2 a^{*2} U(11) + \dots + 2 h k a^* b^* U(12)]$

Table 5. Hydrogen Coordinates ($\text{\AA} \times 10^4$) and equivalent isotropic displacement parameters ($\text{\AA}^2 \times 10^3$) for pa575

atom	x	y	z	U(eq)
H(1A)	-2591	-7874	-7404	54
H(1B)	-2445	-7434	-6414	54
H(2A)	-4401	-7390	-7530	50
H(2B)	-4378	-8853	-8045	50
H(5)	-1322	-14878	-5554.9995	58
H(6)	-9	-15714.9990	-5847	64
H(7)	913	-14139	-6278	59
H(8)	551	-11619.9990	-6382	53
H(10)	1456	-10230	-4403	62
H(11)	2527	-9480	-2802	75
H(12)	1703	-7932	-2240	61
H(13)	-196	-7240	-3271	63
H(14)	-1293	-8054.9995	-4863	54
H(16)	1114	-8161	-5593	57
H(17)	1690	-7209	-6547	75
H(18)	449	-7368.9995	-8219	78
H(19)	-1297	-8506	-8946	72
H(20)	-1839	-9584	-8003	58
H(23)	-4203	-13214.9990	-4765	61
H(24)	-5817.0005	-13040	-4736	62
H(25)	-6998.9995	-11011	-5353.9995	64
H(26)	-6534	-9069	-5970	55
H(28)	-3558	-5809.9995	-5995	53
H(29)	-2346	-4214	-4736	57
H(30)	-1625	-4870	-3145	60
H(31)	-2208	-7070	-2839	72
H(32)	-3459.9998	-8633	-4098	60
H(34)	-6465	-8382	-8204	60
H(35)	-8060	-6874	-9162	67
H(36)	-8454	-4952	-8486	74
H(37)	-7282	-4582	-6822	74
H(38)	-5662.9995	-6042	-5855	58
H(40A)	-5913	-10946	-8635	124
H(40B)	-6447	-12394	-9274	124
H(40C)	-5342	-11643	-9142	124
H(41A)	-5021	-13549	-6810	97
H(41B)	-6258.9995	-13542	-7813	97
H(41C)	-5704	-12043.9990	-7244	97
H(42A)	-4466	-14159	-8615	112
H(42B)	-5526.0005	-14785	-8617	112
H(42C)	-4255	-14840	-7650	112
H(40D)	-5924.9995	-11789	-7558	115
H(40E)	-6672.0005	-12718	-8532	115
H(40F)	-6154	-11167.0010	-8542	115
H(41D)	-4008	-14567	-7318	108
H(41E)	-5335.9995	-14794	-7735.0005	108
H(41F)	-4521	-13893	-6758.0005	108
H(42D)	-5195.9995	-12501	-9302	115
H(42E)	-6131	-13583	-9372	115
H(42F)	-4846	-14141.0010	-8911	115

Complex 42

Table 1. Crystal data for pa573_a_recolleter

Compound	pa573_a_recolleter
Molecular formula	$\text{C}_{40}\text{H}_{37}\text{AlN}_2\text{O}_3\text{P}_2$, 1.5 (C_7H_8)
Molecular weight	820.84
Crystal habit	Colorless Block
Crystal dimensions(mm)	0.10x0.08x0.02
Crystal system	triclinic
Space group	P-1
a(\AA)	9.510(1)
b(\AA)	12.413(1)
c(\AA)	19.634(1)
α ($^\circ$)	97.531(1)
β ($^\circ$)	101.550(1)
γ ($^\circ$)	105.694(1)
V(\AA^3)	2143.6(3)
Z	2
d($\text{g}\cdot\text{cm}^{-3}$)	1.272
F(000)	866
μ (cm^{-1})	0.168
Absorption corrections	multi-scan ; 0.9834 min, 0.9967 max
Diffractometer	KappaCCD
X-ray source	MoK α
λ (\AA)	0.71069
Monochromator	graphite
T (K)	150.0(1)
Scan mode	phi and omega scans
Maximum θ	25.03
HKL ranges	-11 11 ; -14 14 ; -23 23
Reflections measured	24544
Unique data	7522
Rint	0.0544
Reflections used	5680
Criterion	$I > 2\sigma(I)$
Refinement type	Fsqd
Hydrogen atoms	mixed
Parameters refined	434
Reflections / parameter	13
wR2	0.2374
R1	0.0903
Weights a, b	0.1045 ; 4.0645
GoF	1.111
difference peak / hole ($\text{e}\cdot\text{\AA}^{-3}$)	0.402(0.100) / -0.402(0.100)

Appendix 1. Crystallographic data

Table 2. Atomic Coordinates ($\text{\AA} \times 10^4$) and equivalent isotropic displacement parameters ($\text{\AA}^2 \times 10^3$) for pa573_a_recolleter

atom	x	y	z	U(eq)
P(1)	7992(1)	8818(1)	2673(1)	43(1)
P(2)	3371(1)	4615(1)	1366(1)	40(1)
Al(1)	4560(2)	7228(1)	2217(1)	41(1)
O(1)	4782(4)	8446(2)	2928(2)	49(1)
O(2)	3172(4)	6427(3)	2607(2)	56(1)
O(3)	3839(5)	7742(3)	1474(2)	61(1)
N(1)	6739(4)	7607(3)	2366(2)	45(1)
N(2)	4655(4)	5803(3)	1656(2)	42(1)
C(1)	7288(6)	6728(4)	2006(3)	52(1)
C(2)	6008(6)	6022(4)	1383(3)	51(1)
C(3)	7206(6)	9803(4)	3075(2)	43(1)
C(4)	5726(5)	9466(3)	3153(2)	42(1)
C(5)	5258(6)	10314(4)	3530(3)	52(1)
C(6)	6219(6)	11409(4)	3791(3)	51(1)
C(7)	7657(6)	11738(4)	3685(2)	51(1)
C(8)	8150(6)	10936(4)	3335(2)	48(1)
C(9)	8706(6)	9407(4)	1969(2)	49(1)
C(10)	7650(6)	9220(4)	1328(3)	53(1)
C(11)	8083(8)	9708(4)	778(3)	65(2)
C(12)	9545(8)	10367(4)	862(3)	67(2)
C(13)	10599(7)	10556(4)	1490(3)	64(2)
C(14)	10183(6)	10080(4)	2048(3)	53(1)
C(15)	9566(5)	8718(4)	3324(2)	45(1)
C(16)	10717(6)	8354(4)	3129(3)	53(1)
C(17)	11843(6)	8192(4)	3633(3)	58(1)
C(18)	11816(7)	8393(5)	4345(3)	65(2)
C(19)	10638(7)	8721(5)	4536(3)	62(1)
C(20)	9542(6)	8903(4)	4038(3)	52(1)
C(21)	2057(5)	4504(4)	1906(2)	43(1)
C(22)	2131(6)	5408(4)	2446(3)	49(1)
C(23)	1018(7)	5219(5)	2829(3)	67(2)
C(24)	-110(7)	4191(5)	2674(3)	76(2)
C(25)	-183(7)	3325(5)	2153(3)	65(2)
C(26)	883(6)	3483(4)	1766(3)	51(1)
C(27)	2358(5)	4420(4)	458(2)	45(1)
C(28)	2337(6)	5403(5)	186(3)	55(1)
C(29)	1487(8)	5312(6)	-483(3)	71(2)
C(30)	656(7)	4266(7)	-889(3)	77(2)
C(31)	670(6)	3277(6)	-627(3)	67(2)
C(32)	1517(6)	3366(4)	44(3)	52(1)
C(33)	4135(5)	3425(4)	1392(3)	49(1)
C(34)	4663(6)	3010(4)	841(3)	65(2)
C(35)	5379(7)	2161(5)	909(5)	91(2)
C(36)	5573(8)	1772(6)	1523(6)	101(3)
C(37)	5090(10)	2171(6)	2073(5)	94(2)
C(38)	4357(7)	3005(5)	2015(3)	68(2)
C(39)	3310(7)	8671(4)	1465(3)	65(2)
C(40)	3018(7)	8923(5)	732(3)	66(2)

U(eq) is defined as 1/3 the trace of the Uij tensor.

Appendix 1. Crystallographic data

Table 3. Bond lengths (\AA) and angles (deg) for pa573_a_recolleter

P(1)-N(1)	1.597(4)	P(1)-C(3)	1.775(5)
P(1)-C(15)	1.808(5)	P(1)-C(9)	1.809(5)
P(2)-N(2)	1.586(4)	P(2)-C(21)	1.783(5)
P(2)-C(27)	1.799(5)	P(2)-C(33)	1.816(5)
Al(1)-O(3)	1.756(4)	Al(1)-O(2)	1.792(4)
Al(1)-O(1)	1.853(3)	Al(1)-N(1)	1.948(4)
Al(1)-N(2)	1.991(4)	O(1)-C(4)	1.298(5)
O(2)-C(22)	1.331(5)	O(3)-C(39)	1.378(6)
N(1)-C(1)	1.488(6)	N(2)-C(2)	1.465(6)
C(1)-C(2)	1.515(7)	C(1)-H(1A)	0.9900
C(1)-H(1B)	0.9900	C(2)-H(2A)	0.9900
C(2)-H(2B)	0.9900	C(3)-C(4)	1.402(7)
C(3)-C(8)	1.411(6)	C(4)-C(5)	1.425(6)
C(5)-C(6)	1.380(7)	C(5)-H(5)	0.9500
C(6)-C(7)	1.383(7)	C(6)-H(6)	0.9500
C(7)-C(8)	1.374(7)	C(7)-H(7)	0.9500
C(8)-H(8)	0.9500	C(9)-C(10)	1.393(7)
C(9)-C(14)	1.393(7)	C(10)-C(11)	1.385(7)
C(10)-H(10)	0.9500	C(11)-C(12)	1.374(8)
C(11)-H(11)	0.9500	C(12)-C(13)	1.372(8)
C(12)-H(12)	0.9500	C(13)-C(14)	1.386(7)
C(13)-H(13)	0.9500	C(14)-H(14)	0.9500
C(15)-C(16)	1.393(7)	C(15)-C(20)	1.397(7)
C(16)-C(17)	1.382(8)	C(16)-H(16)	0.9500
C(17)-C(18)	1.393(8)	C(17)-H(17)	0.9500
C(18)-C(19)	1.392(8)	C(18)-H(18)	0.9500
C(19)-C(20)	1.368(7)	C(19)-H(19)	0.9500
C(20)-H(20)	0.9500	C(21)-C(26)	1.396(6)
C(21)-C(22)	1.415(7)	C(22)-C(23)	1.405(7)
C(23)-C(24)	1.378(8)	C(23)-H(23)	0.9500
C(24)-C(25)	1.359(8)	C(24)-H(24)	0.9500
C(25)-C(26)	1.372(7)	C(25)-H(25)	0.9500
C(26)-H(26)	0.9500	C(27)-C(32)	1.381(6)
C(27)-C(28)	1.399(7)	C(28)-C(29)	1.371(7)
C(28)-H(28)	0.9500	C(29)-C(30)	1.37(1)
C(29)-H(29)	0.9500	C(30)-C(31)	1.39(1)
C(30)-H(30)	0.9500	C(31)-C(32)	1.373(7)
C(31)-H(31)	0.9500	C(32)-H(32)	0.9500
C(33)-C(34)	1.378(8)	C(33)-C(38)	1.391(7)
C(34)-C(35)	1.409(8)	C(34)-H(34)	0.9500
C(35)-C(36)	1.35(1)	C(35)-H(35)	0.9500
C(36)-C(37)	1.34(1)	C(36)-H(36)	0.9500
C(37)-C(38)	1.40(1)	C(37)-H(37)	0.9500
C(38)-H(38)	0.9500	C(39)-C(40)	1.500(7)
C(39)-H(39A)	0.9900	C(39)-H(39B)	0.9900
C(40)-H(40A)	0.9800	C(40)-H(40B)	0.9800
C(40)-H(40C)	0.9800		
N(1)-P(1)-C(3)	110.3(2)	N(1)-P(1)-C(15)	111.8(2)
C(3)-P(1)-C(15)	108.5(2)	N(1)-P(1)-C(9)	110.8(2)
C(3)-P(1)-C(9)	107.2(2)	C(15)-P(1)-C(9)	108.1(2)
N(2)-P(2)-C(21)	108.4(2)	N(2)-P(2)-C(27)	114.4(2)
C(21)-P(2)-C(27)	108.3(2)	N(2)-P(2)-C(33)	111.6(2)
C(21)-P(2)-C(33)	109.0(2)	C(27)-P(2)-C(33)	105.0(2)
O(3)-Al(1)-O(2)	115.2(2)	O(3)-Al(1)-O(1)	99.7(2)
O(2)-Al(1)-O(1)	85.7(2)	O(3)-Al(1)-N(1)	108.8(2)
O(2)-Al(1)-N(1)	135.8(2)	O(1)-Al(1)-N(1)	90.8(2)
O(3)-Al(1)-N(2)	94.9(2)	O(2)-Al(1)-N(2)	91.3(2)
O(1)-Al(1)-N(2)	165.0(2)	N(1)-Al(1)-N(2)	81.1(2)
C(4)-O(1)-Al(1)	134.7(3)	C(22)-O(2)-Al(1)	137.4(3)
C(39)-O(3)-Al(1)	127.7(3)	C(1)-N(1)-P(1)	114.2(3)
C(1)-N(1)-Al(1)	115.7(3)	P(1)-N(1)-Al(1)	128.7(2)
C(2)-N(2)-P(2)	119.1(3)	C(2)-N(2)-Al(1)	111.0(3)
P(2)-N(2)-Al(1)	128.7(2)	N(1)-C(1)-C(2)	106.7(4)
N(1)-C(1)-H(1A)	110.4	C(2)-C(1)-H(1A)	110.4

Appendix 1. Crystallographic data

N(1)-C(1)-H(1B)	110.4	C(2)-C(1)-H(1B)	110.4
H(1A)-C(1)-H(1B)	108.6	N(2)-C(2)-C(1)	105.3(4)
N(2)-C(2)-H(2A)	110.7	C(1)-C(2)-H(2A)	110.7
N(2)-C(2)-H(2B)	110.7	C(1)-C(2)-H(2B)	110.7
H(2A)-C(2)-H(2B)	108.8	C(4)-C(3)-C(8)	121.0(4)
C(4)-C(3)-P(1)	121.7(3)	C(8)-C(3)-P(1)	117.2(4)
O(1)-C(4)-C(3)	125.0(4)	O(1)-C(4)-C(5)	118.4(4)
C(3)-C(4)-C(5)	116.5(4)	C(6)-C(5)-C(4)	121.0(5)
C(6)-C(5)-H(5)	119.5	C(4)-C(5)-H(5)	119.5
C(5)-C(6)-C(7)	121.7(4)	C(5)-C(6)-H(6)	119.2
C(7)-C(6)-H(6)	119.2	C(8)-C(7)-C(6)	118.7(4)
C(8)-C(7)-H(7)	120.7	C(6)-C(7)-H(7)	120.7
C(7)-C(8)-C(3)	121.0(5)	C(7)-C(8)-H(8)	119.5
C(3)-C(8)-H(8)	119.5	C(10)-C(9)-C(14)	119.5(4)
C(10)-C(9)-P(1)	115.9(4)	C(14)-C(9)-P(1)	124.4(4)
C(11)-C(10)-C(9)	119.5(5)	C(11)-C(10)-H(10)	120.3
C(9)-C(10)-H(10)	120.3	C(12)-C(11)-C(10)	120.4(6)
C(12)-C(11)-H(11)	119.8	C(10)-C(11)-H(11)	119.8
C(13)-C(12)-C(11)	120.8(5)	C(13)-C(12)-H(12)	119.6
C(11)-C(12)-H(12)	119.6	C(12)-C(13)-C(14)	119.7(5)
C(12)-C(13)-H(13)	120.2	C(14)-C(13)-H(13)	120.2
C(13)-C(14)-C(9)	120.2(5)	C(13)-C(14)-H(14)	119.9
C(9)-C(14)-H(14)	119.9	C(16)-C(15)-C(20)	119.3(5)
C(16)-C(15)-P(1)	121.9(4)	C(20)-C(15)-P(1)	118.5(4)
C(17)-C(16)-C(15)	120.8(5)	C(17)-C(16)-H(16)	119.6
C(15)-C(16)-H(16)	119.6	C(16)-C(17)-C(18)	119.4(5)
C(16)-C(17)-H(17)	120.3	C(18)-C(17)-H(17)	120.3
C(19)-C(18)-C(17)	119.7(5)	C(19)-C(18)-H(18)	120.1
C(17)-C(18)-H(18)	120.1	C(20)-C(19)-C(18)	120.8(5)
C(20)-C(19)-H(19)	119.6	C(18)-C(19)-H(19)	119.6
C(19)-C(20)-C(15)	119.9(5)	C(19)-C(20)-H(20)	120.0
C(15)-C(20)-H(20)	120.0	C(26)-C(21)-C(22)	119.4(4)
C(26)-C(21)-P(2)	117.5(4)	C(22)-C(21)-P(2)	123.0(3)
O(2)-C(22)-C(23)	118.0(4)	O(2)-C(22)-C(21)	124.4(4)
C(23)-C(22)-C(21)	117.6(4)	C(24)-C(23)-C(22)	120.6(5)
C(24)-C(23)-H(23)	119.7	C(22)-C(23)-H(23)	119.7
C(25)-C(24)-C(23)	121.7(6)	C(25)-C(24)-H(24)	119.2
C(23)-C(24)-H(24)	119.2	C(24)-C(25)-C(26)	119.2(5)
C(24)-C(25)-H(25)	120.4	C(26)-C(25)-H(25)	120.4
C(25)-C(26)-C(21)	121.4(5)	C(25)-C(26)-H(26)	119.3
C(21)-C(26)-H(26)	119.3	C(32)-C(27)-C(28)	119.1(5)
C(32)-C(27)-P(2)	123.5(4)	C(28)-C(27)-P(2)	117.2(4)
C(29)-C(28)-C(27)	120.0(5)	C(29)-C(28)-H(28)	120.0
C(27)-C(28)-H(28)	120.0	C(30)-C(29)-C(28)	120.5(6)
C(30)-C(29)-H(29)	119.7	C(28)-C(29)-H(29)	119.7
C(29)-C(30)-C(31)	120.2(5)	C(29)-C(30)-H(30)	119.9
C(31)-C(30)-H(30)	119.9	C(32)-C(31)-C(30)	119.3(5)
C(32)-C(31)-H(31)	120.3	C(30)-C(31)-H(31)	120.3
C(31)-C(32)-C(27)	120.9(5)	C(31)-C(32)-H(32)	119.6
C(27)-C(32)-H(32)	119.6	C(34)-C(33)-C(38)	118.6(5)
C(34)-C(33)-P(2)	121.8(4)	C(38)-C(33)-P(2)	119.2(4)
C(33)-C(34)-C(35)	120.1(7)	C(33)-C(34)-H(34)	120.0
C(35)-C(34)-H(34)	120.0	C(36)-C(35)-C(34)	119.7(8)
C(36)-C(35)-H(35)	120.2	C(34)-C(35)-H(35)	120.2
C(37)-C(36)-C(35)	121.6(7)	C(37)-C(36)-H(36)	119.2
C(35)-C(36)-H(36)	119.2	C(36)-C(37)-C(38)	119.8(7)
C(36)-C(37)-H(37)	120.1	C(38)-C(37)-H(37)	120.1
C(33)-C(38)-C(37)	120.3(7)	C(33)-C(38)-H(38)	119.9
C(37)-C(38)-H(38)	119.9	O(3)-C(39)-C(40)	110.6(5)
O(3)-C(39)-H(39A)	109.5	C(40)-C(39)-H(39A)	109.5
O(3)-C(39)-H(39B)	109.5	C(40)-C(39)-H(39B)	109.5
H(39A)-C(39)-H(39B)	108.1	C(39)-C(40)-H(40A)	109.5
C(39)-C(40)-H(40B)	109.5	H(40A)-C(40)-H(40B)	109.5
C(39)-C(40)-H(40C)	109.5	H(40A)-C(40)-H(40C)	109.5
H(40B)-C(40)-H(40C)	109.5		

Appendix 1. Crystallographic data

Table 4. Anisotropic displacement parameters ($\text{\AA}^2 \times 10^3$) for pa573_a_recolleter

atom	U11	U22	U33	U23	U13	U12
P(1)	51(1)	31(1)	39(1)	0(1)	13(1)	4(1)
P(2)	48(1)	27(1)	40(1)	5(1)	5(1)	7(1)
Al(1)	51(1)	29(1)	39(1)	4(1)	12(1)	7(1)
O(1)	57(2)	34(2)	48(2)	-1(1)	18(2)	5(2)
O(2)	65(2)	37(2)	58(2)	-2(1)	25(2)	2(2)
O(3)	89(3)	39(2)	52(2)	8(2)	8(2)	22(2)
N(1)	53(2)	32(2)	44(2)	-2(2)	16(2)	5(2)
N(2)	52(2)	30(2)	43(2)	4(2)	16(2)	7(2)
C(1)	51(3)	37(2)	60(3)	-6(2)	24(2)	4(2)
C(2)	61(3)	32(2)	53(3)	-2(2)	26(2)	2(2)
C(3)	55(3)	32(2)	40(2)	2(2)	12(2)	9(2)
C(4)	57(3)	26(2)	38(2)	1(2)	9(2)	5(2)
C(5)	58(3)	40(3)	58(3)	5(2)	17(2)	14(2)
C(6)	61(3)	38(3)	52(3)	-3(2)	11(2)	19(2)
C(7)	69(4)	32(2)	46(3)	-2(2)	9(2)	15(2)
C(8)	50(3)	36(2)	48(3)	0(2)	9(2)	5(2)
C(9)	68(3)	32(2)	42(3)	1(2)	21(2)	5(2)
C(10)	59(3)	47(3)	44(3)	3(2)	12(2)	3(2)
C(11)	92(5)	47(3)	49(3)	8(2)	20(3)	8(3)
C(12)	99(5)	44(3)	60(4)	10(2)	41(3)	10(3)
C(13)	82(4)	37(3)	70(4)	7(2)	33(3)	3(3)
C(14)	63(3)	36(2)	54(3)	3(2)	21(3)	3(2)
C(15)	49(3)	34(2)	47(3)	2(2)	12(2)	6(2)
C(16)	64(3)	42(3)	53(3)	5(2)	22(3)	14(2)
C(17)	56(3)	47(3)	72(4)	8(2)	26(3)	13(2)
C(18)	68(4)	58(3)	65(4)	8(3)	5(3)	21(3)
C(19)	74(4)	60(3)	47(3)	0(2)	11(3)	22(3)
C(20)	59(3)	46(3)	46(3)	0(2)	10(2)	16(2)
C(21)	48(3)	36(2)	40(2)	12(2)	8(2)	6(2)
C(22)	50(3)	40(3)	51(3)	10(2)	11(2)	3(2)
C(23)	76(4)	51(3)	68(4)	4(3)	35(3)	0(3)
C(24)	79(4)	62(4)	78(4)	7(3)	40(3)	-3(3)
C(25)	61(4)	51(3)	71(4)	10(3)	16(3)	-3(3)
C(26)	54(3)	41(3)	46(3)	8(2)	6(2)	-1(2)
C(27)	51(3)	42(2)	39(2)	4(2)	7(2)	17(2)
C(28)	74(4)	60(3)	40(3)	11(2)	16(2)	31(3)
C(29)	96(5)	90(4)	45(3)	16(3)	19(3)	58(4)
C(30)	70(4)	135(6)	38(3)	10(3)	11(3)	57(4)
C(31)	54(3)	88(4)	48(3)	-15(3)	6(3)	19(3)
C(32)	54(3)	50(3)	46(3)	0(2)	9(2)	11(2)
C(33)	43(3)	29(2)	64(3)	7(2)	0(2)	2(2)
C(34)	59(3)	41(3)	88(4)	-1(3)	7(3)	18(2)
C(35)	60(4)	48(4)	149(7)	-9(4)	9(4)	17(3)
C(36)	56(4)	54(4)	180(10)	28(5)	-12(5)	19(3)
C(37)	82(5)	67(4)	127(7)	43(4)	-5(5)	24(4)
C(38)	64(4)	54(3)	79(4)	25(3)	0(3)	10(3)
C(39)	70(4)	43(3)	73(4)	9(2)	5(3)	13(3)
C(40)	89(4)	50(3)	60(3)	19(2)	7(3)	25(3)

The anisotropic displacement factor exponent takes the form
 $2 \pi^2 [h^2 a^{*2} U_{11} + \dots + 2hk a^* b^* U_{12}]$

Table 5. Hydrogen Coordinates ($\text{\AA} \times 10^4$) and equivalent isotropic displacement parameters ($\text{\AA}^2 \times 10^3$) for pa573_a_recolleter

atom	x	y	z	U(eq)
H(1A)	7567	6240	2337	62
H(1B)	8184	7097	1841	62
H(2A)	5910	6447	991	61
H(2B)	6181	5297	1205	61
H(5)	4269	10122	3602	63
H(6)	5884	11950	4049	61
H(7)	8290	12503	3852	61
H(8)	9142	11148	3267	57
H(10)	6639	8761	1268	64
H(11)	7365	9587	341	79
H(12)	9830	10696	480	80
H(13)	11609	11009	1542	77
H(14)	10908	10214	2485	64
H(16)	10728	8214	2643	64
H(17)	12625	7947	3495	69
H(18)	12600	8307	4698	78
H(19)	10595	8819	5019	75
H(20)	8765	9155	4178	62
H(23)	1043	5805	3199	80
H(24)	-856.0001	4084	2937	91
H(25)	-961.9999	2619	2059	78
H(26)	820	2885	1395	61
H(28)	2910	6134	465	66
H(29)	1477	5982	-666.9999	85
H(30)	67	4212	-1351.0001	92
H(31)	99	2548	-910	81
H(32)	1524	2694	225	63
H(34)	4543	3297	414	78
H(35)	5723	1861	526	109
H(36)	6065	1204	1566	121
H(37)	5242	1888	2499	112
H(38)	4010	3286	2403	82
H(39A)	4060	9345	1796	78
H(39B)	2365	8514	1626	78
H(40A)	3938	9033	562	99
H(40B)	2715	9618	743	99
H(40C)	2210	8283	413	99

Complex 43

Table 1. Crystal data for pa570

Compound	pa570
Molecular formula	$\text{C}_{80}\text{H}_{74}\text{N}_4\text{O}_6\text{P}_4\text{Y}_2, 2(\text{C}_7\text{H}_8)$
Molecular weight	1673.40
Crystal habit	Colorless Block
Crystal dimensions(mm)	0.20x0.18x0.12
Crystal system	triclinic
Space group	P-1
a(\AA)	12.950(1)
b(\AA)	13.948(1)
c(\AA)	14.744(1)
α ($^\circ$)	102.175(1)
β ($^\circ$)	108.382(1)
γ ($^\circ$)	112.817(1)
V(\AA^3)	2153.9(3)
Z	1
d(g·cm $^{-3}$)	1.290
F(000)	868
μ (cm $^{-1}$)	1.469
Absorption corrections	multi-scan ; 0.7576 min, 0.8434 max
Diffractometer	KappaCCD
X-ray source	MoK α
λ (\AA)	0.71069
Monochromator	graphite
T (K)	150.0(1)
Scan mode	phi and omega scans
Maximum θ	25.03
HKL ranges	-15 15 ; -16 16 ; -17 17
Reflections measured	27959
Unique data	7575
Rint	0.0512
Reflections used	6201
Criterion	I > 2 σ (I)
Refinement type	Fsqd
Hydrogen atoms	constr
Parameters refined	434
Reflections / parameter	14
wR2	0.1368
R1	0.0539
Weights a, b	0.0731 ; 2.9994
GoF	1.076
difference peak / hole (e \AA^{-3})	1.108(0.086) / -0.503(0.086)

Appendix 1. Crystallographic data

Table 2. Atomic Coordinates (A x 10⁴) and equivalent isotropic displacement parameters (A² x 10³) for pa570

atom	x	y	z	U(eq)
Y(1)	772(1)	4466(1)	857(1)	26(1)
P(1)	2105(1)	2661(1)	881(1)	26(1)
P(2)	-349(1)	3974(1)	2616(1)	26(1)
O(1)	2301(3)	4714(2)	435(2)	33(1)
O(2)	1929(3)	5382(2)	2545(2)	32(1)
O(3)	774(3)	6049(2)	688(2)	33(1)
N(1)	991(3)	2846(3)	967(3)	29(1)
N(2)	-700(3)	3385(3)	1430(2)	27(1)
C(1)	96(4)	2032(3)	1206(3)	29(1)
C(2)	-1033(4)	2211(3)	967(3)	30(1)
C(3)	3498(4)	3925(3)	1206(3)	28(1)
C(4)	3384(4)	4770(3)	877(3)	28(1)
C(5)	4502(4)	5687(4)	1036(4)	39(1)
C(6)	5628(4)	5740(4)	1485(4)	45(1)
C(7)	5738(4)	4913(4)	1837(4)	45(1)
C(8)	4672(4)	4014(4)	1696(4)	37(1)
C(9)	1677(4)	1758(3)	-414(3)	29(1)
C(10)	434(4)	1051(3)	-1093(3)	33(1)
C(11)	85(5)	330(4)	-2078(3)	41(1)
C(12)	1002(5)	358(4)	-2382(3)	43(1)
C(13)	2230(5)	1060(4)	-1728(4)	48(1)
C(14)	2590(4)	1763(4)	-737(4)	45(1)
C(15)	2597(4)	1997(3)	1730(3)	29(1)
C(16)	2729(4)	1056(4)	1406(4)	38(1)
C(17)	3171(5)	628(4)	2112(5)	54(1)
C(18)	3512(5)	1156(5)	3150(5)	57(1)
C(19)	3377(4)	2081(4)	3476(4)	47(1)
C(20)	2932(4)	2512(4)	2778(3)	40(1)
C(21)	1198(4)	4407(3)	3553(3)	27(1)
C(22)	2181(4)	5100(3)	3352(3)	29(1)
C(23)	3411(4)	5461(4)	4057(3)	36(1)
C(24)	3648(4)	5160(4)	4903(3)	39(1)
C(25)	2687(4)	4493(4)	5089(3)	39(1)
C(26)	1461(4)	4117(4)	4407(3)	34(1)
C(27)	-1421(4)	3139(3)	3050(3)	28(1)
C(28)	-1498(4)	2122(3)	3091(3)	34(1)
C(29)	-2338(4)	1461(4)	3386(3)	40(1)
C(30)	-3092(5)	1813(4)	3659(4)	45(1)
C(31)	-3030(4)	2824(4)	3622(4)	44(1)
C(32)	-2195(4)	3481(4)	3319(3)	34(1)
C(33)	-458(4)	5242(3)	2751(3)	29(1)
C(34)	131(4)	6102(3)	3715(3)	35(1)
C(35)	34(5)	7075(4)	3829(4)	44(1)
C(36)	-645(5)	7178(4)	2960(4)	43(1)
C(37)	-1233(4)	6341(4)	1995(3)	36(1)
C(38)	-1143(4)	5371(4)	1890(3)	32(1)
C(39)	2080(10)	7157(7)	1397(6)	146(5)
C(40)	1860(10)	7660(10)	2140(10)	163(5)

U(eq) is defined as 1/3 the trace of the Uij tensor.

Appendix 1. Crystallographic data

Table 3. Bond lengths (A) and angles (deg) for pa570

Y(1)-O(1)	2.182(3)	Y(1)-O(2)	2.213(3)
Y(1)-O(3)#2	2.243(3)	Y(1)-O(3)	2.273(3)
Y(1)-N(1)	2.415(3)	Y(1)-N(2)	2.438(3)
Y(1)-Y(1)#2	3.6492(7)	P(1)-N(1)	1.598(3)
P(1)-C(3)	1.796(4)	P(1)-C(15)	1.810(4)
P(1)-C(9)	1.821(4)	P(2)-N(2)	1.595(3)
P(2)-C(33)	1.803(4)	P(2)-C(21)	1.803(4)
P(2)-C(27)	1.821(4)	O(1)-C(4)	1.309(5)
O(2)-C(22)	1.315(5)	O(3)-C(39)	1.58(1)
O(3)-Y(1)#2	2.243(3)	N(1)-C(1)	1.470(5)
N(2)-C(2)	1.458(5)	C(1)-C(2)	1.523(5)
C(1)-H(1A)	0.9900	C(1)-H(1B)	0.9900
C(2)-H(2A)	0.9900	C(2)-H(2B)	0.9900
C(3)-C(8)	1.404(6)	C(3)-C(4)	1.407(5)
C(4)-C(5)	1.418(6)	C(5)-C(6)	1.363(6)
C(5)-H(5)	0.9500	C(6)-C(7)	1.398(6)
C(6)-H(6)	0.9500	C(7)-C(8)	1.374(6)
C(7)-H(7)	0.9500	C(8)-H(8)	0.9500
C(9)-C(10)	1.379(6)	C(9)-C(14)	1.404(6)
C(10)-C(11)	1.393(6)	C(10)-H(10)	0.9500
C(11)-C(12)	1.386(7)	C(11)-H(11)	0.9500
C(12)-C(13)	1.359(7)	C(12)-H(12)	0.9500
C(13)-C(14)	1.388(6)	C(13)-H(13)	0.9500
C(14)-H(14)	0.9500	C(15)-C(16)	1.394(6)
C(15)-C(20)	1.399(6)	C(16)-C(17)	1.386(6)
C(16)-H(16)	0.9500	C(17)-C(18)	1.388(8)
C(17)-H(17)	0.9500	C(18)-C(19)	1.375(7)
C(18)-H(18)	0.9500	C(19)-C(20)	1.382(6)
C(19)-H(19)	0.9500	C(20)-H(20)	0.9500
C(21)-C(26)	1.384(5)	C(21)-C(22)	1.431(5)
C(22)-C(23)	1.408(6)	C(23)-C(24)	1.380(6)
C(23)-H(23)	0.9500	C(24)-C(25)	1.383(6)
C(24)-H(24)	0.9500	C(25)-C(26)	1.390(6)
C(25)-H(25)	0.9500	C(26)-H(26)	0.9500
C(27)-C(32)	1.390(6)	C(27)-C(28)	1.399(6)
C(28)-C(29)	1.382(6)	C(28)-H(28)	0.9500
C(29)-C(30)	1.377(6)	C(29)-H(29)	0.9500
C(30)-C(31)	1.395(7)	C(30)-H(30)	0.9500
C(31)-C(32)	1.385(6)	C(31)-H(31)	0.9500
C(32)-H(32)	0.9500	C(33)-C(34)	1.389(6)
C(33)-C(38)	1.392(5)	C(34)-C(35)	1.392(6)
C(34)-H(34)	0.9500	C(35)-C(36)	1.379(6)
C(35)-H(35)	0.9500	C(36)-C(37)	1.377(6)
C(36)-H(36)	0.9500	C(37)-C(38)	1.384(6)
C(37)-H(37)	0.9500	C(38)-H(38)	0.9500
C(39)-C(40)	1.34(1)	C(39)-H(39A)	0.9900
C(39)-H(39B)	0.9900	C(40)-H(40A)	0.9800
C(40)-H(40B)	0.9800	C(40)-H(40C)	0.9800
O(1)-Y(1)-O(2)	97.1(1)	O(1)-Y(1)-O(3)#2	100.3(1)
O(2)-Y(1)-O(3)#2	156.1(1)	O(1)-Y(1)-O(3)	93.6(1)
O(2)-Y(1)-O(3)	90.6(1)	O(3)#2-Y(1)-O(3)	72.2(1)
O(1)-Y(1)-N(1)	78.8(1)	O(2)-Y(1)-N(1)	90.5(1)
O(3)#2-Y(1)-N(1)	108.8(1)	O(3)-Y(1)-N(1)	172.4(1)
O(1)-Y(1)-N(2)	149.2(1)	O(2)-Y(1)-N(2)	81.4(1)
O(3)#2-Y(1)-N(2)	91.6(1)	O(3)-Y(1)-N(2)	117.2(1)
N(1)-Y(1)-N(2)	70.4(1)	O(1)-Y(1)-Y(1)#2	98.57(7)
O(2)-Y(1)-Y(1)#2	124.66(7)	O(3)#2-Y(1)-Y(1)#2	36.37(7)
O(3)-Y(1)-Y(1)#2	35.82(7)	N(1)-Y(1)-Y(1)#2	144.61(8)
N(2)-Y(1)-Y(1)#2	107.59(7)	N(1)-P(1)-C(3)	115.0(2)
N(1)-P(1)-C(15)	111.9(2)	C(3)-P(1)-C(15)	105.2(2)
N(1)-P(1)-C(9)	112.8(2)	C(3)-P(1)-C(9)	105.4(2)
C(15)-P(1)-C(9)	105.9(2)	N(2)-P(2)-C(33)	106.9(2)
N(2)-P(2)-C(21)	117.2(2)	C(33)-P(2)-C(21)	105.8(2)
N(2)-P(2)-C(27)	113.8(2)	C(33)-P(2)-C(27)	106.3(2)

Appendix 1. Crystallographic data

C(21)-P(2)-C(27)	106.1(2)	C(4)-O(1)-Y(1)	133.9(2)
C(22)-O(2)-Y(1)	135.7(2)	C(39)-O(3)-Y(1)#2	133.1(3)
C(39)-O(3)-Y(1)	113.5(3)	Y(1)#2-O(3)-Y(1)	107.8(1)
C(1)-N(1)-P(1)	118.6(2)	C(1)-N(1)-Y(1)	117.5(2)
P(1)-N(1)-Y(1)	123.8(2)	C(2)-N(2)-P(2)	122.5(3)
C(2)-N(2)-Y(1)	106.9(2)	P(2)-N(2)-Y(1)	114.1(2)
N(1)-C(1)-C(2)	107.8(3)	N(1)-C(1)-H(1A)	110.1
C(2)-C(1)-H(1A)	110.1	N(1)-C(1)-H(1B)	110.1
C(2)-C(1)-H(1B)	110.1	H(1A)-C(1)-H(1B)	108.5
N(2)-C(2)-C(1)	113.1(3)	N(2)-C(2)-H(2A)	109.0
C(1)-C(2)-H(2A)	109.0	N(2)-C(2)-H(2B)	109.0
C(1)-C(2)-H(2B)	109.0	H(2A)-C(2)-H(2B)	107.8
C(8)-C(3)-C(4)	121.0(4)	C(8)-C(3)-P(1)	120.0(3)
C(4)-C(3)-P(1)	118.7(3)	O(1)-C(4)-C(3)	122.0(4)
O(1)-C(4)-C(5)	121.2(4)	C(3)-C(4)-C(5)	116.7(4)
C(6)-C(5)-C(4)	121.3(4)	C(6)-C(5)-H(5)	119.4
C(4)-C(5)-H(5)	119.4	C(5)-C(6)-C(7)	121.7(4)
C(5)-C(6)-H(6)	119.2	C(7)-C(6)-H(6)	119.2
C(8)-C(7)-C(6)	118.4(4)	C(8)-C(7)-H(7)	120.8
C(6)-C(7)-H(7)	120.8	C(7)-C(8)-C(3)	120.8(4)
C(7)-C(8)-H(8)	119.6	C(3)-C(8)-H(8)	119.6
C(10)-C(9)-C(14)	119.1(4)	C(10)-C(9)-P(1)	119.6(3)
C(14)-C(9)-P(1)	121.3(3)	C(9)-C(10)-C(11)	120.6(4)
C(9)-C(10)-H(10)	119.7	C(11)-C(10)-H(10)	119.7
C(12)-C(11)-C(10)	119.2(4)	C(12)-C(11)-H(11)	120.4
C(10)-C(11)-H(11)	120.4	C(13)-C(12)-C(11)	120.9(4)
C(13)-C(12)-H(12)	119.5	C(11)-C(12)-H(12)	119.5
C(12)-C(13)-C(14)	120.3(4)	C(12)-C(13)-H(13)	119.8
C(14)-C(13)-H(13)	119.8	C(13)-C(14)-C(9)	119.8(4)
C(13)-C(14)-H(14)	120.1	C(9)-C(14)-H(14)	120.1
C(16)-C(15)-C(20)	119.2(4)	C(16)-C(15)-P(1)	123.5(3)
C(20)-C(15)-P(1)	117.1(3)	C(17)-C(16)-C(15)	120.2(4)
C(17)-C(16)-H(16)	119.9	C(15)-C(16)-H(16)	119.9
C(16)-C(17)-C(18)	119.8(5)	C(16)-C(17)-H(17)	120.1
C(18)-C(17)-H(17)	120.1	C(19)-C(18)-C(17)	120.4(4)
C(19)-C(18)-H(18)	119.8	C(17)-C(18)-H(18)	119.8
C(18)-C(19)-C(20)	120.3(5)	C(18)-C(19)-H(19)	119.8
C(20)-C(19)-H(19)	119.8	C(19)-C(20)-C(15)	120.1(4)
C(19)-C(20)-H(20)	120.0	C(15)-C(20)-H(20)	120.0
C(26)-C(21)-C(22)	120.8(4)	C(26)-C(21)-P(2)	124.8(3)
C(22)-C(21)-P(2)	114.4(3)	O(2)-C(22)-C(23)	122.4(4)
O(2)-C(22)-C(21)	120.6(4)	C(23)-C(22)-C(21)	116.9(3)
C(24)-C(23)-C(22)	121.1(4)	C(24)-C(23)-H(23)	119.4
C(22)-C(23)-H(23)	119.4	C(23)-C(24)-C(25)	121.3(4)
C(23)-C(24)-H(24)	119.4	C(25)-C(24)-H(24)	119.4
C(24)-C(25)-C(26)	119.2(4)	C(24)-C(25)-H(25)	120.4
C(26)-C(25)-H(25)	120.4	C(21)-C(26)-C(25)	120.6(4)
C(21)-C(26)-H(26)	119.7	C(25)-C(26)-H(26)	119.7
C(32)-C(27)-C(28)	118.9(4)	C(32)-C(27)-P(2)	121.0(3)
C(28)-C(27)-P(2)	120.0(3)	C(29)-C(28)-C(27)	120.6(4)
C(29)-C(28)-H(28)	119.7	C(27)-C(28)-H(28)	119.7
C(30)-C(29)-C(28)	119.9(4)	C(30)-C(29)-H(29)	120.0
C(28)-C(29)-H(29)	120.0	C(29)-C(30)-C(31)	120.3(4)
C(29)-C(30)-H(30)	119.8	C(31)-C(30)-H(30)	119.8
C(32)-C(31)-C(30)	119.7(4)	C(32)-C(31)-H(31)	120.2
C(30)-C(31)-H(31)	120.2	C(31)-C(32)-C(27)	120.6(4)
C(31)-C(32)-H(32)	119.7	C(27)-C(32)-H(32)	119.7
C(34)-C(33)-C(38)	119.0(4)	C(34)-C(33)-P(2)	120.5(3)
C(38)-C(33)-P(2)	120.5(3)	C(33)-C(34)-C(35)	120.9(4)
C(33)-C(34)-H(34)	119.5	C(35)-C(34)-H(34)	119.5
C(36)-C(35)-C(34)	118.6(4)	C(36)-C(35)-H(35)	120.7
C(34)-C(35)-H(35)	120.7	C(37)-C(36)-C(35)	121.6(4)
C(37)-C(36)-H(36)	119.2	C(35)-C(36)-H(36)	119.2
C(36)-C(37)-C(38)	119.4(4)	C(36)-C(37)-H(37)	120.3
C(38)-C(37)-H(37)	120.3	C(37)-C(38)-C(33)	120.5(4)
C(37)-C(38)-H(38)	119.8	C(33)-C(38)-H(38)	119.8
C(40)-C(39)-O(3)	103(1)	C(40)-C(39)-H(39A)	111.2
O(3)-C(39)-H(39A)	111.2	C(40)-C(39)-H(39B)	111.2

Appendix 1. Crystallographic data

O(3)-C(39)-H(39B)	111.2	H(39A)-C(39)-H(39B)	109.1
C(39)-C(40)-H(40A)	109.5	C(39)-C(40)-H(40B)	109.5
H(40A)-C(40)-H(40B)	109.5	C(39)-C(40)-H(40C)	109.5
H(40A)-C(40)-H(40C)	109.5	H(40B)-C(40)-H(40C)	109.5

 Estimated standard deviations are given in the parenthesis.
 Symmetry operators ::
 1: x, y, z 2: -x, -y, -z

Appendix 1. Crystallographic data

Table 4. Anisotropic displacement parameters ($\text{\AA}^2 \times 10^3$) for pa570

atom	U11	U22	U33	U23	U13	U12
Y(1)	31(1)	31(1)	27(1)	16(1)	16(1)	20(1)
P(1)	26(1)	26(1)	29(1)	12(1)	13(1)	15(1)
P(2)	28(1)	31(1)	26(1)	14(1)	14(1)	18(1)
O(1)	37(2)	44(2)	38(2)	26(1)	24(1)	28(1)
O(2)	33(2)	34(2)	31(2)	15(1)	16(1)	15(1)
O(3)	41(2)	28(2)	29(2)	12(1)	10(1)	19(1)
N(1)	32(2)	31(2)	35(2)	16(2)	19(2)	18(2)
N(2)	29(2)	32(2)	29(2)	17(2)	17(2)	19(2)
C(1)	36(2)	26(2)	31(2)	14(2)	18(2)	17(2)
C(2)	25(2)	34(2)	29(2)	10(2)	11(2)	15(2)
C(3)	23(2)	26(2)	31(2)	11(2)	12(2)	10(2)
C(4)	34(2)	32(2)	24(2)	11(2)	17(2)	19(2)
C(5)	42(3)	33(2)	48(3)	21(2)	24(2)	18(2)
C(6)	38(3)	39(2)	58(3)	22(2)	24(2)	13(2)
C(7)	27(2)	47(3)	58(3)	24(2)	13(2)	17(2)
C(8)	28(2)	37(2)	52(3)	23(2)	17(2)	17(2)
C(9)	34(2)	29(2)	33(2)	14(2)	16(2)	21(2)
C(10)	32(2)	28(2)	37(2)	14(2)	14(2)	14(2)
C(11)	49(3)	30(2)	38(2)	13(2)	16(2)	17(2)
C(12)	63(3)	40(2)	34(2)	14(2)	20(2)	33(3)
C(13)	45(3)	59(3)	49(3)	14(2)	26(3)	34(3)
C(14)	37(3)	51(3)	43(3)	6(2)	17(2)	25(2)
C(15)	23(2)	30(2)	35(2)	17(2)	12(2)	12(2)
C(16)	39(3)	37(2)	51(3)	24(2)	27(2)	22(2)
C(17)	59(3)	56(3)	87(4)	50(3)	45(3)	42(3)
C(18)	49(3)	77(4)	81(4)	60(3)	36(3)	42(3)
C(19)	38(3)	58(3)	42(3)	28(2)	13(2)	18(2)
C(20)	40(3)	42(3)	39(2)	18(2)	16(2)	21(2)
C(21)	26(2)	31(2)	25(2)	9(2)	12(2)	15(2)
C(22)	35(2)	31(2)	26(2)	10(2)	16(2)	20(2)
C(23)	31(2)	40(2)	35(2)	10(2)	16(2)	17(2)
C(24)	35(3)	52(3)	27(2)	9(2)	5(2)	28(2)
C(25)	44(3)	49(3)	30(2)	18(2)	15(2)	29(2)
C(26)	33(2)	40(2)	31(2)	15(2)	15(2)	20(2)
C(27)	29(2)	35(2)	22(2)	13(2)	13(2)	16(2)
C(28)	37(2)	36(2)	38(2)	18(2)	20(2)	20(2)
C(29)	42(3)	36(2)	47(3)	21(2)	24(2)	17(2)
C(30)	47(3)	46(3)	44(3)	19(2)	30(2)	18(2)
C(31)	45(3)	51(3)	46(3)	19(2)	31(2)	24(2)
C(32)	37(2)	35(2)	32(2)	10(2)	16(2)	18(2)
C(33)	28(2)	36(2)	30(2)	17(2)	18(2)	18(2)
C(34)	43(3)	40(2)	28(2)	17(2)	15(2)	24(2)
C(35)	60(3)	37(2)	37(2)	13(2)	19(2)	29(2)
C(36)	58(3)	37(2)	47(3)	22(2)	26(2)	31(2)
C(37)	38(3)	47(3)	37(2)	27(2)	19(2)	27(2)
C(38)	32(2)	41(2)	32(2)	16(2)	18(2)	23(2)
C(39)	310(10)	92(6)	65(5)	54(5)	59(7)	140(10)
C(40)	150(10)	170(10)	290(20)	150(10)	140(10)	110(10)

The anisotropic displacement factor exponent takes the form
 $2 \pi^2 [h^2 a^{*2} U_{11} + \dots + 2hk a^* b^* U_{12}]$

Appendix 1. Crystallographic data

Table 5. Hydrogen Coordinates ($\text{\AA} \times 10^4$) and equivalent isotropic displacement parameters ($\text{\AA}^2 \times 10^3$) for pa570

atom	x	y	z	U(eq)
H(1A)	483	2150	1944	35
H(1B)	-161	1254	781	35
H(2A)	-1508	1940	208	36
H(2B)	-1586	1755	1224	36
H(5)	4465	6276	826	46
H(6)	6355	6355	1561	54
H(7)	6531	4971	2165	54
H(8)	4730	3446	1934	45
H(10)	-190	1055	-888	39
H(11)	-771	-174	-2535.0002	49
H(12)	768	-121	-3058	52
H(13)	2847	1070	-1949.9999	57
H(14)	3450	2246	-278	54
H(16)	2515	706	697	45
H(17)	3240	-25	1887	65
H(18)	3840	878	3638	68
H(19)	3590	2424	4185	57
H(20)	2854	3158	3010	48
H(23)	4089	5920	3948	43
H(24)	4487	5417	5367	47
H(25)	2864	4294	5675	46
H(26)	796	3657	4529	40
H(28)	-969	1883	2913	41
H(29)	-2394	765	3398	48
H(30)	-3658	1366	3875	53
H(31)	-3558	3062	3804	52
H(32)	-2151	4170	3295	41
H(34)	607	6024	4306	42
H(35)	425	7656	4492	53
H(36)	-708	7844	3028	51
H(37)	-1697	6427	1405	43
H(38)	-1551	4788	1227	38
H(39A)	2745	6976	1692	175
H(39B)	2313	7632	1005	175
H(40A)	1130	7753	1819	245
H(40B)	2588	8406	2587	245
H(40C)	1696	7206	2549	245

Complex 44

Table 1. Crystal data for pa574

Compound	pa574
Molecular formula	C ₈₄ H ₈₂ N ₄ O ₆ P ₄ Y ₂ ·2(C ₇ H ₈)
Molecular weight	1821.64
Crystal habit	Colorless Block
Crystal dimensions(mm)	0.20x0.10x0.04
Crystal system	triclinic
Space group	Pbar1
a(Å)	10.5300(10)
b(Å)	14.5750(10)
c(Å)	16.4300(10)
α(°)	65.4360(10)
β(°)	87.9590(10)
γ(°)	89.2980(10)
V(Å ³)	2291.9(3)
Z	1
d(g·cm ⁻³)	1.320
F(000)	950
μ(cm ⁻¹)	1.387
Absorption corrections	multi-scan ; 0.7689 min, 0.9466 max
Diffractionmeter	KappaCCD
X-ray source	MoKα
λ(Å)	0.71069
Monochromator	graphite
T (K)	150.0(1)
Scan mode	phi and omega scans
Maximum θ	25.03
HKL ranges	-12 12 ; -17 17 ; -19 19
Reflections measured	27447
Unique data	8058
Rint	0.0582
Reflections used	6609
Criterion	I > 2σ(I)
Refinement type	Fsqd
Hydrogen atoms	mixed
Parameters refined	518
Reflections / parameter	12
wR2	0.1134
R1	0.0562
Weights a, b	0.0275 ; 6.0762
GoF	1.066
difference peak / hole (e Å ⁻³)	1.193(0.079) / -0.506(0.079)

Table 2. Atomic Coordinates (A x 10⁴) and equivalent isotropic displacement parameters (A² x 10³) for pa574

atom	x	y	z	U(eq)
Y(1)	4452(1)	4295(1)	1229(1)	23(1)
P(1)	5415(1)	2381(1)	3249(1)	30(1)
P(2)	5154(1)	6610(1)	1269(1)	28(1)
O(1)	4094(3)	2688(2)	1573(2)	32(1)
O(2)	4244(2)	5760(2)	-88(2)	25(1)
O(3)	2662(3)	4558(2)	1664(2)	32(1)
N(1)	5691(3)	5528(2)	1430(2)	32(1)
N(2)	5714(3)	3499(2)	2524(2)	33(1)
C(1)	6387(6)	4208(4)	2798(4)	68(2)
C(2)	6739(5)	5116(4)	2044(4)	58(2)
C(3)	5253(4)	1500(3)	2761(3)	30(1)
C(4)	4579(4)	1785(3)	1968(3)	28(1)
C(5)	4427(4)	1056(3)	1622(3)	36(1)
C(6)	4915(5)	99(3)	2060(3)	44(1)
C(7)	5567(5)	-185(3)	2845(3)	44(1)
C(8)	5730(4)	517(3)	3189(3)	40(1)
C(9)	4005(4)	2271(3)	3940(3)	33(1)
C(10)	3341(4)	1372(3)	4364(3)	42(1)
C(11)	2335(5)	1288(4)	4954(3)	47(1)
C(12)	1976(5)	2100(4)	5131(3)	49(1)
C(13)	2595(5)	3005(4)	4688(4)	59(2)
C(14)	3606(5)	3099(4)	4094(3)	51(1)
C(15)	6676(4)	1900(3)	4045(3)	32(1)
C(16)	6455(4)	1563(3)	4964(3)	38(1)
C(17)	7455(5)	1215(4)	5544(3)	46(1)
C(18)	8668(5)	1212(4)	5211(3)	50(1)
C(19)	8900(5)	1545(4)	4301(3)	49(1)
C(20)	7910(4)	1889(3)	3719(3)	42(1)
C(21)	3834(4)	6960(3)	542(3)	27(1)
C(22)	3599(4)	6551(3)	-81(2)	25(1)
C(23)	2634(4)	6984(3)	-698(3)	34(1)
C(24)	1906(4)	7765(3)	-681(3)	37(1)
C(25)	2107(4)	8150(3)	-53(3)	41(1)
C(26)	3051(4)	7752(3)	543(3)	35(1)
C(27)	6346(4)	7589(3)	785(3)	30(1)
C(28)	6136(5)	8579(3)	692(3)	38(1)
C(29)	7056(5)	9307(3)	297(3)	47(1)
C(30)	8193(5)	9066(4)	-8(3)	52(1)
C(31)	8413(5)	8108(4)	63(3)	47(1)
C(32)	7488(4)	7368(3)	456(3)	36(1)
C(33)	4624(5)	6656(3)	2312(3)	38(1)
C(34)	3542(5)	6102(4)	2738(3)	48(1)
C(35)	3187(6)	5974(4)	3597(4)	66(2)
C(36)	3924(8)	6389(5)	4034(4)	88(2)
C(37)	5009(8)	6915(5)	3633(4)	93(3)
C(38)	5364(6)	7061(4)	2771(3)	65(2)
C(39)	1346(4)	4434(3)	1661(3)	34(1)
C(40)	899(5)	3624(4)	2561(4)	68(2)
C(41)	669(5)	5433(4)	1479(4)	59(2)
C(42)	1055(6)	4102(5)	919(4)	70(2)
C(43)	969(7)	10867(5)	2495(4)	83(2)
C(44)	498(6)	9970(4)	2391(3)	58(2)
C(45)	-786(6)	9766(5)	2411(3)	62(2)
C(46)	-1211(7)	8957(6)	2307(4)	80(2)
C(47)	-430(10)	8296(6)	2173(4)	86(2)
C(48)	869(8)	8434(5)	2177(4)	82(2)
C(49)	1342(6)	9284(5)	2277(3)	67(2)

U(eq) is defined as 1/3 the trace of the Uij tensor.

Table 3. Bond lengths (Å) and angles (deg) for pa574

Y(1)-O(3)	2.079(3)	Y(1)-O(1)	2.203(3)
Y(1)-O(2)#2	2.312(2)	Y(1)-O(2)	2.338(2)
Y(1)-N(1)	2.372(3)	Y(1)-N(2)	2.398(3)
Y(1)-Y(1)#2	3.8320(7)	P(1)-N(2)	1.596(3)
P(1)-C(3)	1.786(4)	P(1)-C(9)	1.804(4)
P(1)-C(15)	1.818(4)	P(2)-N(1)	1.586(3)
P(2)-C(21)	1.792(4)	P(2)-C(27)	1.809(4)
P(2)-C(33)	1.811(4)	O(1)-C(4)	1.308(5)
O(2)-C(22)	1.336(4)	O(2)-Y(1)#2	2.312(2)
O(3)-C(39)	1.401(5)	N(1)-C(2)	1.468(5)
N(2)-C(1)	1.484(6)	C(1)-C(2)	1.429(7)
C(1)-H(1A)	0.9900	C(1)-H(1B)	0.9900
C(2)-H(2A)	0.9900	C(2)-H(2B)	0.9900
C(3)-C(8)	1.403(6)	C(3)-C(4)	1.408(6)
C(4)-C(5)	1.409(6)	C(5)-C(6)	1.380(6)
C(5)-H(5)	0.9500	C(6)-C(7)	1.386(7)
C(6)-H(6)	0.9500	C(7)-C(8)	1.373(6)
C(7)-H(7)	0.9500	C(8)-H(8)	0.9500
C(9)-C(10)	1.386(6)	C(9)-C(14)	1.389(6)
C(10)-C(11)	1.381(6)	C(10)-H(10)	0.9500
C(11)-C(12)	1.377(7)	C(11)-H(11)	0.9500
C(12)-C(13)	1.373(7)	C(12)-H(12)	0.9500
C(13)-C(14)	1.386(7)	C(13)-H(13)	0.9500
C(14)-H(14)	0.9500	C(15)-C(20)	1.390(6)
C(15)-C(16)	1.392(6)	C(16)-C(17)	1.390(6)
C(16)-H(16)	0.9500	C(17)-C(18)	1.373(7)
C(17)-H(17)	0.9500	C(18)-C(19)	1.379(7)
C(18)-H(18)	0.9500	C(19)-C(20)	1.383(6)
C(19)-H(19)	0.9500	C(20)-H(20)	0.9500
C(21)-C(26)	1.411(5)	C(21)-C(22)	1.412(5)
C(22)-C(23)	1.408(6)	C(23)-C(24)	1.374(6)
C(23)-H(23)	0.9500	C(24)-C(25)	1.388(6)
C(24)-H(24)	0.9500	C(25)-C(26)	1.367(6)
C(25)-H(25)	0.9500	C(26)-H(26)	0.9500
C(27)-C(32)	1.389(6)	C(27)-C(28)	1.403(6)
C(28)-C(29)	1.376(6)	C(28)-H(28)	0.9500
C(29)-C(30)	1.379(7)	C(29)-H(29)	0.9500
C(30)-C(31)	1.370(7)	C(30)-H(30)	0.9500
C(31)-C(32)	1.391(6)	C(31)-H(31)	0.9500
C(32)-H(32)	0.9500	C(33)-C(34)	1.392(6)
C(33)-C(38)	1.396(7)	C(34)-C(35)	1.382(7)
C(34)-H(34)	0.9500	C(35)-C(36)	1.38(1)
C(35)-H(35)	0.9500	C(36)-C(37)	1.37(1)
C(36)-H(36)	0.9500	C(37)-C(38)	1.378(7)
C(37)-H(37)	0.9500	C(38)-H(38)	0.9500
C(39)-C(40)	1.521(6)	C(39)-C(42)	1.528(7)
C(39)-C(41)	1.531(6)	C(40)-H(40A)	0.9800
C(40)-H(40B)	0.9800	C(40)-H(40C)	0.9800
C(41)-H(41A)	0.9800	C(41)-H(41B)	0.9800
C(41)-H(41C)	0.9800	C(42)-H(42A)	0.9800
C(42)-H(42B)	0.9800	C(42)-H(42C)	0.9800
C(43)-C(44)	1.481(8)	C(43)-H(43A)	0.9800
C(43)-H(43B)	0.9800	C(43)-H(43C)	0.9800
C(44)-C(45)	1.384(8)	C(44)-C(49)	1.395(8)
C(45)-C(46)	1.34(1)	C(45)-H(45)	0.9500
C(46)-C(47)	1.34(1)	C(46)-H(46)	0.9500
C(47)-C(48)	1.38(1)	C(47)-H(47)	0.9500
C(48)-C(49)	1.41(1)	C(48)-H(48)	0.9500
C(49)-H(49)	0.9500		
O(3)-Y(1)-O(1)	94.8(1)	O(3)-Y(1)-O(2)#2	148.8(1)
O(1)-Y(1)-O(2)#2	85.2(1)	O(3)-Y(1)-O(2)	89.2(1)
O(1)-Y(1)-O(2)	133.0(1)	O(2)#2-Y(1)-O(2)	69.0(1)
O(3)-Y(1)-N(1)	101.3(1)	O(1)-Y(1)-N(1)	148.1(1)
O(2)#2-Y(1)-N(1)	94.4(1)	O(2)-Y(1)-N(1)	74.9(1)

O(3)-Y(1)-N(2)	107.6(1)	O(1)-Y(1)-N(2)	78.6(1)
O(2)#2-Y(1)-N(2)	102.9(1)	O(2)-Y(1)-N(2)	143.7(1)
N(1)-Y(1)-N(2)	70.4(1)	O(3)-Y(1)-Y(1)#2	120.54(8)
O(1)-Y(1)-Y(1)#2	111.42(7)	O(2)#2-Y(1)-Y(1)#2	34.72(6)
O(2)-Y(1)-Y(1)#2	34.28(6)	N(1)-Y(1)-Y(1)#2	83.6(1)
N(2)-Y(1)-Y(1)#2	128.8(1)	N(2)-P(1)-C(3)	112.9(2)
N(2)-P(1)-C(9)	114.3(2)	C(3)-P(1)-C(9)	107.1(2)
N(2)-P(1)-C(15)	111.6(2)	C(3)-P(1)-C(15)	106.2(2)
C(9)-P(1)-C(15)	104.1(2)	N(1)-P(2)-C(21)	112.2(2)
N(1)-P(2)-C(27)	112.3(2)	C(21)-P(2)-C(27)	107.5(2)
N(1)-P(2)-C(33)	111.3(2)	C(21)-P(2)-C(33)	107.4(2)
C(27)-P(2)-C(33)	105.7(2)	C(4)-O(1)-Y(1)	143.3(2)
C(22)-O(2)-Y(1)#2	127.5(2)	C(22)-O(2)-Y(1)	120.6(2)
Y(1)#2-O(2)-Y(1)	111.0(1)	C(39)-O(3)-Y(1)	147.2(3)
C(2)-N(1)-P(2)	118.6(3)	C(2)-N(1)-Y(1)	114.4(3)
P(2)-N(1)-Y(1)	122.5(2)	C(1)-N(2)-P(1)	119.2(3)
C(1)-N(2)-Y(1)	114.6(3)	P(1)-N(2)-Y(1)	121.6(2)
C(2)-C(1)-N(2)	111.5(4)	C(2)-C(1)-H(1A)	109.3
N(2)-C(1)-H(1A)	109.3	C(2)-C(1)-H(1B)	109.3
N(2)-C(1)-H(1B)	109.3	H(1A)-C(1)-H(1B)	108.0
C(1)-C(2)-N(1)	112.2(4)	C(1)-C(2)-H(2A)	109.2
N(1)-C(2)-H(2A)	109.2	C(1)-C(2)-H(2B)	109.2
N(1)-C(2)-H(2B)	109.2	H(2A)-C(2)-H(2B)	107.9
C(8)-C(3)-C(4)	120.2(4)	C(8)-C(3)-P(1)	120.4(3)
C(4)-C(3)-P(1)	119.3(3)	O(1)-C(4)-C(3)	121.2(3)
O(1)-C(4)-C(5)	121.2(4)	C(3)-C(4)-C(5)	117.7(4)
C(6)-C(5)-C(4)	120.5(4)	C(6)-C(5)-H(5)	119.8
C(4)-C(5)-H(5)	119.8	C(5)-C(6)-C(7)	121.9(4)
C(5)-C(6)-H(6)	119.0	C(7)-C(6)-H(6)	119.0
C(8)-C(7)-C(6)	118.4(4)	C(8)-C(7)-H(7)	120.8
C(6)-C(7)-H(7)	120.8	C(7)-C(8)-C(3)	121.4(4)
C(7)-C(8)-H(8)	119.3	C(3)-C(8)-H(8)	119.3
C(10)-C(9)-C(14)	118.5(4)	C(10)-C(9)-P(1)	122.2(3)
C(14)-C(9)-P(1)	119.2(3)	C(11)-C(10)-C(9)	120.7(4)
C(11)-C(10)-H(10)	119.6	C(9)-C(10)-H(10)	119.6
C(12)-C(11)-C(10)	120.4(5)	C(12)-C(11)-H(11)	119.8
C(10)-C(11)-H(11)	119.8	C(13)-C(12)-C(11)	119.2(5)
C(13)-C(12)-H(12)	120.4	C(11)-C(12)-H(12)	120.4
C(12)-C(13)-C(14)	120.9(5)	C(12)-C(13)-H(13)	119.6
C(14)-C(13)-H(13)	119.6	C(13)-C(14)-C(9)	120.1(5)
C(13)-C(14)-H(14)	119.9	C(9)-C(14)-H(14)	120.0
C(20)-C(15)-C(16)	119.0(4)	C(20)-C(15)-P(1)	118.5(3)
C(16)-C(15)-P(1)	122.4(3)	C(17)-C(16)-C(15)	120.2(4)
C(17)-C(16)-H(16)	119.9	C(15)-C(16)-H(16)	119.9
C(18)-C(17)-C(16)	119.9(4)	C(18)-C(17)-H(17)	120.0
C(16)-C(17)-H(17)	120.0	C(17)-C(18)-C(19)	120.3(5)
C(17)-C(18)-H(18)	119.8	C(19)-C(18)-H(18)	119.8
C(18)-C(19)-C(20)	120.1(5)	C(18)-C(19)-H(19)	120.0
C(20)-C(19)-H(19)	120.0	C(19)-C(20)-C(15)	120.4(4)
C(19)-C(20)-H(20)	119.8	C(15)-C(20)-H(20)	119.8
C(26)-C(21)-C(22)	118.3(4)	C(26)-C(21)-P(2)	117.6(3)
C(22)-C(21)-P(2)	123.9(3)	O(2)-C(22)-C(23)	119.6(3)
O(2)-C(22)-C(21)	122.0(3)	C(23)-C(22)-C(21)	118.4(3)
C(24)-C(23)-C(22)	121.2(4)	C(24)-C(23)-H(23)	119.4
C(22)-C(23)-H(23)	119.4	C(23)-C(24)-C(25)	120.6(4)
C(23)-C(24)-H(24)	119.7	C(25)-C(24)-H(24)	119.7
C(26)-C(25)-C(24)	119.2(4)	C(26)-C(25)-H(25)	120.4
C(24)-C(25)-H(25)	120.4	C(25)-C(26)-C(21)	122.2(4)
C(25)-C(26)-H(26)	118.9	C(21)-C(26)-H(26)	118.9
C(32)-C(27)-C(28)	118.6(4)	C(32)-C(27)-P(2)	119.1(3)
C(28)-C(27)-P(2)	122.3(3)	C(29)-C(28)-C(27)	120.3(4)
C(29)-C(28)-H(28)	119.8	C(27)-C(28)-H(28)	119.8
C(28)-C(29)-C(30)	120.1(4)	C(28)-C(29)-H(29)	119.9
C(30)-C(29)-H(29)	119.9	C(31)-C(30)-C(29)	120.7(5)
C(31)-C(30)-H(30)	119.7	C(29)-C(30)-H(30)	119.7
C(30)-C(31)-C(32)	119.7(5)	C(30)-C(31)-H(31)	120.2
C(32)-C(31)-H(31)	120.2	C(27)-C(32)-C(31)	120.6(4)
C(27)-C(32)-H(32)	119.7	C(31)-C(32)-H(32)	119.7

Appendix 1. Crystallographic data

C(34)-C(33)-C(38)	119.1(4)	C(34)-C(33)-P(2)	117.0(3)
C(38)-C(33)-P(2)	122.9(4)	C(35)-C(34)-C(33)	120.5(5)
C(35)-C(34)-H(34)	119.7	C(33)-C(34)-H(34)	119.7
C(36)-C(35)-C(34)	119.4(6)	C(36)-C(35)-H(35)	120.3
C(34)-C(35)-H(35)	120.3	C(37)-C(36)-C(35)	120.8(5)
C(37)-C(36)-H(36)	119.6	C(35)-C(36)-H(36)	119.6
C(36)-C(37)-C(38)	120.3(6)	C(36)-C(37)-H(37)	119.8
C(38)-C(37)-H(37)	119.8	C(37)-C(38)-C(33)	119.8(6)
C(37)-C(38)-H(38)	120.1	C(33)-C(38)-H(38)	120.1
O(3)-C(39)-C(40)	109.1(4)	O(3)-C(39)-C(42)	108.5(4)
C(40)-C(39)-C(42)	109.4(5)	O(3)-C(39)-C(41)	110.1(4)
C(40)-C(39)-C(41)	110.5(4)	C(42)-C(39)-C(41)	109.1(4)
C(39)-C(40)-H(40A)	109.5	C(39)-C(40)-H(40B)	109.5
H(40A)-C(40)-H(40B)	109.5	C(39)-C(40)-H(40C)	109.5
H(40A)-C(40)-H(40C)	109.5	H(40B)-C(40)-H(40C)	109.5
C(39)-C(41)-H(41A)	109.5	C(39)-C(41)-H(41B)	109.5
H(41A)-C(41)-H(41B)	109.5	H(41B)-C(41)-H(41C)	109.5
C(39)-C(42)-H(42A)	109.5	C(39)-C(42)-H(42B)	109.5
H(42A)-C(42)-H(42B)	109.5	C(39)-C(42)-H(42C)	109.5
H(42A)-C(42)-H(42C)	109.5	H(42B)-C(42)-H(42C)	109.5
C(44)-C(43)-H(43A)	109.5	C(44)-C(43)-H(43B)	109.5
H(43A)-C(43)-H(43B)	109.5	C(44)-C(43)-H(43C)	109.5
H(43A)-C(43)-H(43C)	109.5	H(43B)-C(43)-H(43C)	109.5
C(45)-C(44)-C(49)	117.0(6)	C(45)-C(44)-C(43)	122.1(6)
C(49)-C(44)-C(43)	120.9(6)	C(46)-C(45)-C(44)	122.0(6)
C(46)-C(45)-H(45)	119.0	C(44)-C(45)-H(45)	119.0
C(45)-C(46)-C(47)	122.6(7)	C(45)-C(46)-H(46)	118.7
C(47)-C(46)-H(46)	118.7	C(46)-C(47)-C(48)	118.5(7)
C(46)-C(47)-H(47)	120.7	C(48)-C(47)-H(47)	120.7
C(47)-C(48)-C(49)	120.0(7)	C(47)-C(48)-H(48)	120.0
C(49)-C(48)-H(48)	120.0	C(44)-C(49)-C(48)	119.9(6)
C(44)-C(49)-H(49)	120.1	C(48)-C(49)-H(49)	120.1

 Estimated standard deviations are given in the parenthesis.
 Symmetry operators ::
 1: x, y, z 2: -x, -y, -z

Appendix 1. Crystallographic data

Table 4. Anisotropic displacement parameters ($\text{\AA}^2 \times 10^3$) for pa574

atom	U11	U22	U33	U23	U13	U12
Y(1)	24(1)	21(1)	22(1)	-8(1)	-1(1)	-2(1)
P(1)	35(1)	24(1)	27(1)	-5(1)	-7(1)	-3(1)
P(2)	32(1)	23(1)	31(1)	-13(1)	-1(1)	-3(1)
O(1)	36(2)	23(2)	34(2)	-10(1)	-9(1)	-4(1)
O(2)	28(2)	23(1)	25(1)	-10(1)	-2(1)	4(1)
O(3)	22(2)	35(2)	36(2)	-13(1)	2(1)	-2(1)
N(1)	27(2)	25(2)	44(2)	-13(2)	-13(2)	1(2)
N(2)	39(2)	24(2)	31(2)	-7(2)	-10(2)	-5(2)
C(1)	88(4)	34(3)	67(4)	-1(3)	-45(3)	-22(3)
C(2)	52(3)	32(3)	83(4)	-15(3)	-39(3)	-1(2)
C(3)	33(2)	26(2)	28(2)	-6(2)	1(2)	-5(2)
C(4)	30(2)	24(2)	27(2)	-8(2)	-1(2)	-7(2)
C(5)	45(3)	30(2)	34(2)	-15(2)	-4(2)	-2(2)
C(6)	57(3)	32(2)	48(3)	-23(2)	7(2)	-3(2)
C(7)	49(3)	30(2)	48(3)	-11(2)	-7(2)	7(2)
C(8)	45(3)	31(2)	36(2)	-7(2)	-11(2)	3(2)
C(9)	34(2)	30(2)	29(2)	-6(2)	-6(2)	2(2)
C(10)	40(3)	30(2)	47(3)	-8(2)	-3(2)	2(2)
C(11)	38(3)	41(3)	50(3)	-6(2)	-1(2)	-4(2)
C(12)	40(3)	64(3)	43(3)	-22(3)	-2(2)	3(3)
C(13)	65(4)	58(3)	67(4)	-39(3)	7(3)	-3(3)
C(14)	56(3)	42(3)	59(3)	-27(3)	6(3)	-9(2)
C(15)	37(3)	24(2)	31(2)	-7(2)	-8(2)	-6(2)
C(16)	36(3)	42(3)	31(2)	-10(2)	-7(2)	1(2)
C(17)	46(3)	55(3)	28(2)	-7(2)	-10(2)	-4(2)
C(18)	46(3)	49(3)	41(3)	-5(2)	-16(2)	-4(2)
C(19)	39(3)	54(3)	37(3)	-2(2)	-5(2)	-5(2)
C(20)	41(3)	43(3)	30(2)	-3(2)	-3(2)	-6(2)
C(21)	28(2)	23(2)	31(2)	-10(2)	3(2)	-4(2)
C(22)	25(2)	21(2)	26(2)	-8(2)	6(2)	-2(2)
C(23)	31(2)	32(2)	34(2)	-9(2)	-4(2)	0(2)
C(24)	29(2)	28(2)	46(3)	-7(2)	-4(2)	5(2)
C(25)	29(2)	29(2)	62(3)	-18(2)	0(2)	5(2)
C(26)	37(3)	28(2)	45(3)	-21(2)	4(2)	-3(2)
C(27)	37(2)	28(2)	25(2)	-12(2)	-1(2)	-7(2)
C(28)	50(3)	30(2)	38(2)	-18(2)	1(2)	-5(2)
C(29)	66(4)	28(2)	47(3)	-16(2)	-6(3)	-11(2)
C(30)	58(4)	48(3)	44(3)	-14(2)	1(2)	-27(3)
C(31)	33(3)	63(3)	47(3)	-24(3)	5(2)	-11(2)
C(32)	36(3)	34(2)	41(3)	-17(2)	-3(2)	0(2)
C(33)	58(3)	30(2)	31(2)	-16(2)	3(2)	-6(2)
C(34)	61(3)	40(3)	40(3)	-15(2)	11(2)	-3(2)
C(35)	95(5)	54(3)	50(3)	-24(3)	26(3)	-12(3)
C(36)	155(7)	72(4)	47(3)	-36(3)	38(4)	-33(5)
C(37)	163(8)	84(5)	42(3)	-38(3)	13(4)	-51(5)
C(38)	101(5)	59(3)	39(3)	-26(3)	7(3)	-33(3)
C(39)	21(2)	41(3)	37(2)	-14(2)	3(2)	-6(2)
C(40)	43(3)	68(4)	59(4)	5(3)	9(3)	-10(3)
C(41)	28(3)	54(3)	87(4)	-23(3)	4(3)	5(2)
C(42)	51(4)	93(5)	80(4)	-47(4)	-24(3)	1(3)
C(43)	104(6)	72(4)	61(4)	-15(3)	-2(4)	-7(4)
C(44)	66(4)	69(4)	28(3)	-8(3)	-2(2)	-1(3)
C(45)	56(4)	69(4)	45(3)	-6(3)	-6(3)	2(3)
C(46)	75(5)	86(5)	72(4)	-26(4)	-11(4)	1(4)
C(47)	108(7)	91(5)	58(4)	-30(4)	-7(4)	-13(5)
C(48)	117(7)	73(5)	46(3)	-15(3)	10(4)	26(4)
C(49)	67(4)	83(5)	34(3)	-9(3)	3(3)	9(3)

 The anisotropic displacement factor exponent takes the form
 $2\pi^2 [h^2 a^{*2} U(11) + \dots + 2hka^*b^*U(12)]$

Table 5. Hydrogen Coordinates ($\text{\AA} \times 10^4$) and equivalent isotropic displacement parameters ($\text{\AA}^2 \times 10^3$) for pa574

atom	x	y	z	U(eq)
H(1A)	5829	4374	3216	82
H(1B)	7159	3878	3119	82
H(2A)	7471	4978	1717	69
H(2B)	7009	5624	2257	69
H(5)	3985	1226	1085	43
H(6)	4801	-380	1815	52
H(7)	5893	-849	3139	53
H(8)	6175	334	3727	47
H(10)	3580	806	4247	50
H(11)	1889	666	5238	57
H(12)	1306	2034	5554	59
H(13)	2328	3574	4789	71
H(14)	4026	3730	3792	61
H(16)	5617	1570	5195	46
H(17)	7299	981	6172	55
H(18)	9351	978	5608	60
H(19)	9741	1538	4074	59
H(20)	8074	2119	3093	50
H(23)	2484	6731	-1134	40
H(24)	1260	8044	-1104	45
H(25)	1594	8684	-37	49
H(26)	3185	8017	973	42
H(28)	5355	8749	903	46
H(29)	6907	9978	234	56
H(30)	8830	9570	-269	62
H(31)	9195	7950	-156	57
H(32)	7637	6705	500	44
H(34)	3044	5809	2437	57
H(35)	2441	5603	3883	79
H(36)	3677	6309	4622	106
H(37)	5521	7180	3949	111
H(38)	6109	7436	2492	77
H(40A)	1370	2999	2680	102
H(40B)	-11	3500	2548	102
H(40C)	1051	3849	3034	102
H(41A)	856	5651	1952	89
H(41B)	-250	5340	1471	89
H(41C)	968	5946	899	89
H(42A)	1362	4616	341	105
H(42B)	136	4016	906	105
H(42C)	1482	3461	1035	105
H(43A)	245	11274	2544	125
H(43B)	1509	11272	1973	125
H(43C)	1464	10650	3037	125
H(45)	-1384	10211	2500	75
H(46)	-2102	8849	2328	96
H(47)	-754	7745	2077	103
H(48)	1442	7957	2112	99
H(49)	2233	9388	2266	80

Complex 45

Table 1. Crystal data for pa653

Compound	pa653
Molecular formula	$\text{C}_{58}\text{H}_{73}\text{N}_2\text{O}_3\text{P}_2\text{Y}$
Molecular weight	997.03
Crystal habit	Colorless Block
Crystal dimensions(mm)	0.30x0.12x0.06
Crystal system	monoclinic
Space group	C2/c
a(\AA)	20.514(1)
b(\AA)	27.064(1)
c(\AA)	22.120(1)
α ($^\circ$)	90.00
β ($^\circ$)	117.231(1)
γ ($^\circ$)	90.00
V(\AA^3)	10919.7(8)
Z	8
d(g·cm $^{-3}$)	1.213
F(000)	4224
μ (cm $^{-1}$)	1.170
Absorption corrections	multi-scan ; 0.7204 min, 0.9331 max
Diffractometer	KappaCCD
X-ray source	MoK α
λ (\AA)	0.71069
Monochromator	graphite
T (K)	150.0(1)
Scan mode	phi and omega scans
Maximum θ	26.02
HKL ranges	-25 21 ; -32 33 ; -27 27
Reflections measured	41731
Unique data	10687
Rint	0.0514
Reflections used	8400
Criterion	I > 2 σ (I)
Refinement type	Fsqd
Hydrogen atoms	constr
Parameters refined	610
Reflections / parameter	13
wR2	0.0813
R1	0.0458
Weights a, b	0.0000 ; 33.731
GoF	1.083
difference peak / hole (e \AA^{-3})	0.416(0.063) / -0.305(0.063)

Appendix 1. Crystallographic data

Table 2. Atomic Coordinates (A x 10⁴) and equivalent isotropic displacement parameters (A² x 10³) for pa653

atom	x	y	z	U(eq)
Y(1)	366(1)	2359(1)	670(1)	22(1)
P(1)	1732(1)	1423(1)	1183(1)	22(1)
P(2)	1206(1)	3388(1)	1646(1)	21(1)
O(1)	595(1)	1991(1)	-81(1)	28(1)
O(2)	109(1)	3104(1)	265(1)	26(1)
O(3)	-496(1)	2084(1)	772(1)	37(1)
N(1)	1391(1)	1877(1)	1404(1)	28(1)
N(2)	1049(1)	2815(1)	1650(1)	25(1)
C(1)	1838(2)	2082(1)	2094(1)	37(1)
C(2)	1429(2)	2483(1)	2237(1)	36(1)
C(3)	1148(2)	1207(1)	334(1)	23(1)
C(4)	645(2)	1516(1)	-188(1)	22(1)
C(5)	198(2)	1299(1)	-837(1)	23(1)
C(6)	302(2)	805(1)	-930(1)	25(1)
C(7)	826(2)	501(1)	-430(1)	25(1)
C(8)	1233(2)	709(1)	202(1)	26(1)
C(9)	-378(2)	1610(1)	-1419(1)	30(1)
C(10)	-930(2)	1839(1)	-1208(2)	43(1)
C(11)	7(2)	2020(1)	-1613(2)	43(1)
C(12)	-823(2)	1297(1)	-2059(2)	43(1)
C(13)	922(2)	-41(1)	-582(2)	31(1)
C(14)	404(3)	-368(1)	-450(3)	73(1)
C(15)	774(2)	-102(1)	-1326(2)	55(1)
C(16)	1714(2)	-210(1)	-152(2)	54(1)
C(17)	2628(2)	1553(1)	1249(1)	30(1)
C(18)	2708(2)	1680(1)	685(2)	48(1)
C(19)	3392(2)	1792(2)	739(2)	63(1)
C(20)	3997(2)	1786(2)	1356(2)	62(1)
C(21)	3926(2)	1672(2)	1926(2)	72(1)
C(22)	3251(2)	1552(2)	1877(2)	57(1)
C(23)	1871(2)	898(1)	1740(1)	28(1)
C(24)	1377(2)	841(1)	1999(2)	41(1)
C(25)	1420(3)	436(2)	2396(2)	65(1)
C(26)	1965(3)	87(2)	2543(2)	77(2)
C(27)	2458(3)	141(1)	2294(2)	66(1)
C(28)	2421(2)	545(1)	1894(2)	45(1)
C(29)	410(2)	3737(1)	1091(1)	23(1)
C(30)	-52(2)	3537(1)	441(1)	23(1)
C(31)	-681(2)	3814(1)	-3(1)	25(1)
C(32)	-780(2)	4277(1)	218(1)	27(1)
C(33)	-304(2)	4492(1)	846(1)	26(1)
C(34)	288(2)	4209(1)	1277(1)	24(1)
C(35)	-1217(2)	3609(1)	-703(1)	30(1)
C(36)	-820(2)	3495(1)	-1129(1)	39(1)
C(37)	-1844(2)	3972(1)	-1109(2)	47(1)
C(38)	-1571(2)	3129(1)	-612(2)	38(1)
C(39)	-449(2)	5019(1)	1020(2)	30(1)
C(40)	-1133(2)	5028(1)	1130(2)	56(1)
C(41)	-561(2)	5372(1)	441(2)	47(1)
C(42)	195(2)	5213(1)	1669(2)	45(1)
C(43)	1905(2)	3528(1)	1385(1)	26(1)
C(44)	2014(2)	4008(1)	1229(2)	38(1)
C(45)	2559(2)	4108(1)	1041(2)	49(1)
C(46)	2993(2)	3734(2)	1004(2)	45(1)
C(47)	2872(2)	3255(1)	1137(2)	44(1)
C(48)	2331(2)	3151(1)	1327(1)	33(1)
C(49)	1523(2)	3635(1)	2494(1)	21(1)
C(50)	2220(2)	3824(1)	2882(1)	31(1)
C(51)	2434(2)	3959(1)	3553(2)	40(1)
C(52)	1963(2)	3903(1)	3834(2)	38(1)
C(53)	1270(2)	3714(1)	3452(2)	35(1)
C(54)	1054(2)	3581(1)	2785(1)	31(1)

Appendix 1. Crystallographic data

C(55)	-1097(2)	1963(1)	882(2)	33(1)
C(56)	-1393(2)	2429(1)	1052(2)	50(1)
C(57)	-1678(2)	1727(1)	236(2)	52(1)
C(58)	-846(2)	1601(1)	1473(2)	60(1)

U(eq) is defined as 1/3 the trace of the U_{ij} tensor.

Table 3. Bond lengths (Å) and angles (deg) for pa653

Y(1)-O(3)	2.025(2)	Y(1)-O(1)	2.167(2)
Y(1)-O(2)	2.170(2)	Y(1)-N(2)	2.324(2)
Y(1)-N(1)	2.375(2)	P(1)-N(1)	1.595(2)
P(1)-C(3)	1.803(3)	P(1)-C(17)	1.812(3)
P(1)-C(23)	1.815(3)	P(2)-N(2)	1.584(2)
P(2)-C(29)	1.797(3)	P(2)-C(49)	1.809(3)
P(2)-C(43)	1.814(3)	O(1)-C(4)	1.319(3)
O(2)-C(30)	1.322(3)	O(3)-C(55)	1.399(3)
N(1)-C(1)	1.483(3)	N(2)-C(2)	1.476(3)
C(1)-C(2)	1.492(4)	C(1)-H(1A)	0.9900
C(1)-H(1B)	0.9900	C(2)-H(2A)	0.9900
C(2)-H(2B)	0.9900	C(3)-C(8)	1.405(4)
C(3)-C(4)	1.416(4)	C(4)-C(5)	1.429(4)
C(5)-C(6)	1.385(4)	C(5)-C(9)	1.541(4)
C(6)-C(7)	1.403(4)	C(6)-H(6)	0.9500
C(7)-C(8)	1.378(4)	C(7)-C(13)	1.538(4)
C(8)-H(8)	0.9500	C(9)-C(11)	1.531(4)
C(9)-C(10)	1.539(4)	C(9)-C(12)	1.541(4)
C(10)-H(10A)	0.9800	C(10)-H(10B)	0.9800
C(10)-H(10C)	0.9800	C(11)-H(11A)	0.9800
C(11)-H(11B)	0.9800	C(11)-H(11C)	0.9800
C(12)-H(12A)	0.9800	C(12)-H(12B)	0.9800
C(12)-H(12C)	0.9800	C(13)-C(14)	1.509(5)
C(13)-C(16)	1.529(5)	C(13)-C(15)	1.540(4)
C(14)-H(14A)	0.9800	C(14)-H(14B)	0.9800
C(14)-H(14C)	0.9800	C(15)-H(15A)	0.9800
C(15)-H(15B)	0.9800	C(15)-H(15C)	0.9800
C(16)-H(16A)	0.9800	C(16)-H(16B)	0.9800
C(16)-H(16C)	0.9800	C(17)-C(18)	1.374(4)
C(17)-C(22)	1.392(4)	C(18)-C(19)	1.387(5)
C(18)-H(18)	0.9500	C(19)-C(20)	1.361(5)
C(19)-H(19)	0.9500	C(20)-C(21)	1.369(5)
C(20)-H(20)	0.9500	C(21)-C(22)	1.377(5)
C(21)-H(21)	0.9500	C(22)-H(22)	0.9500
C(23)-C(24)	1.381(4)	C(23)-C(28)	1.395(4)
C(24)-C(25)	1.381(5)	C(24)-H(24)	0.9500
C(25)-C(26)	1.384(7)	C(25)-H(25)	0.9500
C(26)-C(27)	1.363(7)	C(26)-H(26)	0.9500
C(27)-C(28)	1.388(5)	C(27)-H(27)	0.9500
C(28)-H(28)	0.9500	C(29)-C(34)	1.400(4)
C(29)-C(30)	1.418(4)	C(30)-C(31)	1.426(4)
C(31)-C(32)	1.392(4)	C(31)-C(35)	1.536(4)
C(32)-C(33)	1.408(4)	C(32)-H(32)	0.9500
C(33)-C(34)	1.382(4)	C(33)-C(39)	1.541(4)
C(34)-H(34)	0.9500	C(35)-C(36)	1.533(4)
C(35)-C(37)	1.539(4)	C(35)-C(38)	1.545(4)
C(36)-H(36A)	0.9800	C(36)-H(36B)	0.9800
C(36)-H(36C)	0.9800	C(37)-H(37A)	0.9800
C(37)-H(37B)	0.9800	C(37)-H(37C)	0.9800
C(38)-H(38A)	0.9800	C(38)-H(38B)	0.9800
C(38)-H(38C)	0.9800	C(39)-C(41)	1.529(4)
C(39)-C(40)	1.531(4)	C(39)-C(42)	1.532(4)
C(40)-H(40A)	0.9800	C(40)-H(40B)	0.9800
C(40)-H(40C)	0.9800	C(41)-H(41A)	0.9800
C(41)-H(41B)	0.9800	C(41)-H(41C)	0.9800
C(42)-H(42A)	0.9800	C(42)-H(42B)	0.9800
C(42)-H(42C)	0.9800	C(43)-C(48)	1.388(4)
C(43)-C(44)	1.389(4)	C(44)-C(45)	1.386(4)
C(44)-H(44)	0.9500	C(45)-C(46)	1.377(5)
C(45)-H(45)	0.9500	C(46)-C(47)	1.377(5)
C(46)-H(46)	0.9500	C(47)-C(48)	1.383(4)
C(47)-H(47)	0.9500	C(48)-H(48)	0.9500
C(49)-C(50)	1.383(4)	C(49)-C(54)	1.390(4)
C(50)-C(51)	1.390(4)	C(50)-H(50)	0.9500
C(51)-C(52)	1.375(5)	C(51)-H(51)	0.9500
C(52)-C(53)	1.377(4)	C(52)-H(52)	0.9500

C(53)-C(54)	1.380(4)	C(53)-H(53)	0.9500
C(54)-H(54)	0.9500	C(55)-C(56)	1.518(4)
C(55)-C(57)	1.521(5)	C(55)-C(57)	1.522(4)
C(56)-H(56A)	0.9800	C(56)-H(56B)	0.9800
C(56)-H(56C)	0.9800	C(57)-H(57A)	0.9800
C(57)-H(57B)	0.9800	C(57)-H(57C)	0.9800
C(58)-H(58A)	0.9800	C(58)-H(58B)	0.9800
C(58)-H(58C)	0.9800		
O(3)-Y(1)-O(2)	115.03(8)	O(3)-Y(1)-O(2)	109.16(8)
O(1)-Y(1)-O(2)	102.03(7)	O(3)-Y(1)-N(2)	106.04(8)
O(1)-Y(1)-N(2)	135.21(8)	O(2)-Y(1)-N(2)	79.68(7)
O(3)-Y(1)-N(1)	105.5(1)	O(1)-Y(1)-N(1)	80.51(7)
O(2)-Y(1)-N(1)	139.87(8)	N(2)-Y(1)-N(1)	71.78(8)
N(1)-P(1)-C(3)	113.2(1)	N(1)-P(1)-C(17)	113.4(1)
C(3)-P(1)-C(17)	108.2(1)	N(1)-P(1)-C(23)	110.5(1)
C(3)-P(1)-C(23)	106.0(1)	C(17)-P(1)-C(23)	105.0(1)
N(2)-P(2)-C(29)	113.2(1)	N(2)-P(2)-C(49)	109.5(1)
C(29)-P(2)-C(49)	107.3(1)	N(2)-P(2)-C(43)	113.5(1)
C(29)-P(2)-C(43)	106.0(1)	C(49)-P(2)-C(43)	106.9(1)
C(4)-O(1)-Y(1)	130.4(2)	C(30)-O(2)-Y(1)	138.3(2)
C(55)-O(3)-Y(1)	171.4(2)	C(1)-N(1)-P(1)	116.9(2)
C(1)-N(1)-Y(1)	115.7(2)	P(1)-N(1)-Y(1)	126.1(1)
C(2)-N(2)-P(2)	125.0(2)	C(2)-N(2)-Y(1)	110.3(2)
P(2)-N(2)-Y(1)	123.5(1)	N(1)-C(1)-C(2)	110.4(2)
N(1)-C(1)-H(1A)	109.6	C(2)-C(1)-H(1A)	109.6
N(1)-C(1)-H(1B)	109.6	C(2)-C(1)-H(1B)	109.6
H(1A)-C(1)-H(1B)	108.1	N(2)-C(2)-C(1)	112.2(2)
N(2)-C(2)-H(2A)	109.2	C(1)-C(2)-H(2A)	109.2
N(2)-C(2)-H(2B)	109.2	C(1)-C(2)-H(2B)	109.2
H(2A)-C(2)-H(2B)	107.9	C(8)-C(3)-C(4)	120.7(2)
C(8)-C(3)-P(1)	116.2(2)	C(4)-C(3)-P(1)	123.1(2)
O(1)-C(4)-C(3)	121.1(2)	O(1)-C(4)-C(5)	120.9(2)
C(3)-C(4)-C(5)	118.0(2)	C(6)-C(5)-C(4)	118.3(2)
C(6)-C(5)-C(9)	121.0(2)	C(4)-C(5)-C(9)	120.6(2)
C(5)-C(6)-C(7)	124.3(2)	C(5)-C(6)-H(6)	117.9
C(7)-C(6)-H(6)	117.9	C(8)-C(7)-C(6)	116.8(2)
C(8)-C(7)-C(13)	122.3(3)	C(6)-C(7)-C(13)	121.0(2)
C(7)-C(8)-C(3)	121.8(3)	C(7)-C(8)-H(8)	119.1
C(3)-C(8)-H(8)	119.1	C(11)-C(9)-C(10)	109.8(3)
C(11)-C(9)-C(12)	107.8(2)	C(10)-C(9)-C(12)	107.0(3)
C(11)-C(9)-C(5)	109.5(2)	C(10)-C(9)-C(5)	110.7(2)
C(12)-C(9)-C(5)	111.8(2)	C(9)-C(10)-H(10A)	109.5
C(9)-C(10)-H(10B)	109.5	H(10A)-C(10)-H(10B)	109.5
C(9)-C(10)-H(10C)	109.5	H(10A)-C(10)-H(10C)	109.5
H(10B)-C(10)-H(10C)	109.5	C(9)-C(11)-H(11A)	109.5
C(9)-C(11)-H(11B)	109.5	H(11A)-C(11)-H(11B)	109.5
C(9)-C(11)-H(11C)	109.5	H(11A)-C(11)-H(11C)	109.5
H(11B)-C(11)-H(11C)	109.5	C(9)-C(12)-H(12A)	109.5
C(9)-C(12)-H(12B)	109.5	H(12A)-C(12)-H(12B)	109.5
C(9)-C(12)-H(12C)	109.5	H(12A)-C(12)-H(12C)	109.5
H(12B)-C(12)-H(12C)	109.5	C(14)-C(13)-C(16)	110.3(3)
C(14)-C(13)-C(7)	110.1(3)	C(16)-C(13)-C(7)	110.8(2)
C(14)-C(13)-C(15)	109.4(3)	C(16)-C(13)-C(15)	105.5(3)
C(7)-C(13)-C(15)	110.7(2)	C(13)-C(14)-H(14A)	109.5
C(13)-C(14)-H(14B)	109.5	H(14A)-C(14)-H(14B)	109.5
C(13)-C(14)-H(14C)	109.5	H(14A)-C(14)-H(14C)	109.5
H(14B)-C(14)-H(14C)	109.5	C(13)-C(15)-H(15A)	109.5
C(13)-C(15)-H(15B)	109.5	H(15A)-C(15)-H(15B)	109.5
C(13)-C(15)-H(15C)	109.5	H(15A)-C(15)-H(15C)	109.5
H(15B)-C(15)-H(15C)	109.5	C(13)-C(16)-H(16A)	109.5
C(13)-C(16)-H(16B)	109.5	H(16A)-C(16)-H(16B)	109.5
C(13)-C(16)-H(16C)	109.5	H(16A)-C(16)-H(16C)	109.5
H(16B)-C(16)-H(16C)	109.5	C(18)-C(17)-C(22)	118.1(3)
C(18)-C(17)-P(1)	120.9(2)	C(22)-C(17)-P(1)	121.0(2)
C(17)-C(18)-C(19)	120.9(3)	C(17)-C(18)-H(18)	119.6
C(19)-C(18)-H(18)	119.6	C(20)-C(19)-C(18)	120.4(4)

Appendix 1. Crystallographic data

C(20)-C(19)-H(19)	119.8	C(18)-C(19)-H(19)	119.8
C(19)-C(20)-C(21)	119.6(4)	C(19)-C(20)-H(20)	120.2
C(21)-C(20)-H(20)	120.2	C(20)-C(21)-C(22)	120.5(4)
C(20)-C(21)-H(21)	119.7	C(22)-C(21)-H(21)	119.7
C(21)-C(22)-C(17)	120.5(3)	C(21)-C(22)-H(22)	119.7
C(17)-C(22)-H(22)	119.7	C(24)-C(23)-C(28)	119.1(3)
C(24)-C(23)-P(1)	116.8(2)	C(28)-C(23)-P(1)	124.0(3)
C(25)-C(24)-C(23)	120.4(4)	C(25)-C(24)-H(24)	119.8
C(23)-C(24)-H(24)	119.8	C(24)-C(25)-C(26)	120.0(4)
C(24)-C(25)-H(25)	120.0	C(26)-C(25)-H(25)	120.0
C(27)-C(26)-C(25)	120.1(4)	C(27)-C(26)-H(26)	120.0
C(25)-C(26)-H(26)	120.0	C(26)-C(27)-C(28)	120.5(4)
C(26)-C(27)-H(27)	119.8	C(28)-C(27)-H(27)	119.8
C(27)-C(28)-C(23)	119.8(4)	C(27)-C(28)-H(28)	120.1
C(23)-C(28)-H(28)	120.1	C(34)-C(29)-C(30)	121.3(2)
C(34)-C(29)-P(2)	120.5(2)	C(30)-C(29)-P(2)	118.0(2)
O(2)-C(30)-C(29)	119.6(2)	O(2)-C(30)-C(31)	122.2(2)
C(29)-C(30)-C(31)	118.2(2)	C(32)-C(31)-C(30)	117.6(2)
C(32)-C(31)-C(35)	121.8(2)	C(30)-C(31)-C(35)	120.6(2)
C(31)-C(32)-C(33)	124.9(3)	C(31)-C(32)-H(32)	117.6
C(33)-C(32)-H(32)	117.6	C(34)-C(33)-C(32)	116.4(2)
C(34)-C(33)-C(39)	123.4(3)	C(32)-C(33)-C(39)	120.2(2)
C(33)-C(34)-C(29)	121.5(3)	C(33)-C(34)-H(34)	119.2
C(29)-C(34)-H(34)	119.2	C(36)-C(35)-C(31)	110.7(2)
C(36)-C(35)-C(37)	107.9(3)	C(31)-C(35)-C(37)	112.2(2)
C(36)-C(35)-C(38)	109.0(2)	C(31)-C(35)-C(38)	109.6(2)
C(37)-C(35)-C(38)	107.3(3)	C(35)-C(36)-H(36A)	109.5
C(35)-C(36)-H(36B)	109.5	H(36A)-C(36)-H(36B)	109.5
C(35)-C(36)-H(36C)	109.5	H(36A)-C(36)-H(36C)	109.5
H(36B)-C(36)-H(36C)	109.5	C(35)-C(37)-H(37A)	109.5
C(35)-C(37)-H(37B)	109.5	H(37A)-C(37)-H(37B)	109.5
C(35)-C(37)-H(37C)	109.5	H(37A)-C(37)-H(37C)	109.5
H(37B)-C(37)-H(37C)	109.5	C(35)-C(38)-H(38A)	109.5
C(35)-C(38)-H(38B)	109.5	H(38A)-C(38)-H(38B)	109.5
C(35)-C(38)-H(38C)	109.5	H(38A)-C(38)-H(38C)	109.5
H(38B)-C(38)-H(38C)	109.5	C(41)-C(39)-C(40)	109.1(3)
C(41)-C(39)-C(42)	107.8(3)	C(40)-C(39)-C(42)	107.7(3)
C(41)-C(39)-C(33)	110.0(2)	C(40)-C(39)-C(33)	110.5(2)
C(42)-C(39)-C(33)	111.6(2)	C(39)-C(40)-H(40A)	109.5
C(39)-C(40)-H(40B)	109.5	H(40A)-C(40)-H(40B)	109.5
C(39)-C(40)-H(40C)	109.5	H(40A)-C(40)-H(40C)	109.5
H(40B)-C(40)-H(40C)	109.5	C(39)-C(41)-H(41A)	109.5
C(39)-C(41)-H(41B)	109.5	H(41A)-C(41)-H(41B)	109.5
C(39)-C(41)-H(41C)	109.5	H(41A)-C(41)-H(41C)	109.5
H(41B)-C(41)-H(41C)	109.5	C(39)-C(42)-H(42A)	109.5
C(39)-C(42)-H(42B)	109.5	H(42A)-C(42)-H(42B)	109.5
C(39)-C(42)-H(42C)	109.5	H(42A)-C(42)-H(42C)	109.5
H(42B)-C(42)-H(42C)	109.5	C(48)-C(43)-C(44)	119.1(3)
C(48)-C(43)-P(2)	119.9(2)	C(44)-C(43)-P(2)	121.0(2)
C(45)-C(44)-C(43)	120.0(3)	C(45)-C(44)-H(44)	120.0
C(43)-C(44)-H(44)	120.0	C(46)-C(45)-C(44)	120.5(3)
C(46)-C(45)-H(45)	119.7	C(44)-C(45)-H(45)	119.7
C(47)-C(46)-C(45)	119.7(3)	C(47)-C(46)-H(46)	120.2
C(45)-C(46)-H(46)	120.2	C(46)-C(47)-C(48)	120.3(3)
C(46)-C(47)-H(47)	119.8	C(48)-C(47)-H(47)	119.8
C(47)-C(48)-C(43)	120.4(3)	C(47)-C(48)-H(48)	119.8
C(43)-C(48)-H(48)	119.8	C(50)-C(49)-C(54)	119.3(2)
C(50)-C(49)-P(2)	124.0(2)	C(54)-C(49)-P(2)	116.4(2)
C(49)-C(50)-C(51)	119.4(3)	C(49)-C(50)-H(50)	120.3
C(51)-C(50)-H(50)	120.3	C(52)-C(51)-C(50)	120.6(3)
C(52)-C(51)-H(51)	119.7	C(50)-C(51)-H(51)	119.7
C(51)-C(52)-C(53)	120.3(3)	C(51)-C(52)-H(52)	119.9
C(53)-C(52)-H(52)	119.9	C(52)-C(53)-C(54)	119.4(3)
C(52)-C(53)-H(53)	120.3	C(54)-C(53)-H(53)	120.3
C(53)-C(54)-C(49)	121.0(3)	C(53)-C(54)-H(54)	119.5
C(49)-C(54)-H(54)	119.5	O(3)-C(55)-C(56)	109.5(3)
O(3)-C(55)-C(58)	108.8(3)	C(56)-C(55)-C(58)	109.8(3)
O(3)-C(55)-C(57)	107.9(2)	C(56)-C(55)-C(57)	110.5(3)

Appendix 1. Crystallographic data

C(58)-C(55)-C(57)	110.3(3)	C(55)-C(56)-H(56A)	109.5
C(55)-C(56)-H(56B)	109.5	H(56A)-C(56)-H(56B)	109.5
C(55)-C(56)-H(56C)	109.5	H(56A)-C(56)-H(56C)	109.5
H(56B)-C(56)-H(56C)	109.5	C(55)-C(57)-H(57A)	109.5
C(55)-C(57)-H(57B)	109.5	H(57A)-C(57)-H(57B)	109.5
C(55)-C(57)-H(57C)	109.5	H(57A)-C(57)-H(57C)	109.5
H(57B)-C(57)-H(57C)	109.5	C(55)-C(58)-H(58A)	109.5
C(55)-C(58)-H(58B)	109.5	H(58A)-C(58)-H(58B)	109.5
C(55)-C(58)-H(58C)	109.5	H(58A)-C(58)-H(58C)	109.5
H(58B)-C(58)-H(58C)	109.5		

Appendix 1. Crystallographic data

Table 4. Anisotropic displacement parameters ($\text{Å}^2 \times 10^3$) for pa653

atom	U11	U22	U33	U23	U13	U12
Y(1)	21(1)	23(1)	21(1)	-3(1)	8(1)	-2(1)
P(1)	23(1)	23(1)	18(1)	-1(1)	7(1)	0(1)
P(2)	20(1)	22(1)	19(1)	-2(1)	8(1)	-1(1)
O(1)	36(1)	23(1)	21(1)	-1(1)	10(1)	3(1)
O(2)	29(1)	25(1)	21(1)	-1(1)	10(1)	2(1)
O(3)	29(1)	44(1)	39(1)	-6(1)	17(1)	-11(1)
N(1)	30(1)	27(1)	19(1)	-3(1)	6(1)	6(1)
N(2)	30(1)	23(1)	20(1)	-2(1)	9(1)	-1(1)
C(1)	48(2)	30(2)	21(1)	-1(1)	6(1)	6(2)
C(2)	53(2)	28(2)	20(1)	0(1)	12(1)	4(1)
C(3)	21(2)	26(1)	20(1)	-2(1)	9(1)	-2(1)
C(4)	22(2)	27(1)	20(1)	0(1)	11(1)	0(1)
C(5)	20(2)	29(2)	21(1)	-1(1)	11(1)	-2(1)
C(6)	22(2)	33(2)	21(1)	-6(1)	10(1)	-5(1)
C(7)	27(2)	24(1)	27(1)	-4(1)	14(1)	-4(1)
C(8)	24(2)	26(1)	24(1)	1(1)	8(1)	2(1)
C(9)	29(2)	36(2)	21(1)	-1(1)	7(1)	5(1)
C(10)	33(2)	56(2)	34(2)	-1(2)	10(2)	16(2)
C(11)	51(2)	46(2)	24(2)	8(1)	10(2)	1(2)
C(12)	35(2)	51(2)	28(2)	-4(2)	2(2)	8(2)
C(13)	38(2)	25(2)	33(2)	-7(1)	17(1)	-2(1)
C(14)	102(4)	30(2)	131(4)	-25(2)	93(3)	-20(2)
C(15)	77(3)	44(2)	45(2)	-12(2)	29(2)	9(2)
C(16)	58(3)	32(2)	66(2)	-3(2)	24(2)	10(2)
C(17)	26(2)	36(2)	26(2)	-6(1)	10(1)	-7(1)
C(18)	37(2)	75(3)	32(2)	-3(2)	16(2)	-15(2)
C(19)	48(3)	98(3)	51(2)	-2(2)	29(2)	-20(2)
C(20)	35(2)	84(3)	68(3)	-15(2)	24(2)	-19(2)
C(21)	29(2)	131(4)	47(2)	-13(3)	9(2)	-20(2)
C(22)	33(2)	101(3)	32(2)	-5(2)	10(2)	-14(2)
C(23)	36(2)	24(1)	18(1)	-2(1)	6(1)	-3(1)
C(24)	48(2)	44(2)	28(2)	3(1)	15(2)	-11(2)
C(25)	79(3)	72(3)	36(2)	6(2)	19(2)	-39(3)
C(26)	121(5)	41(2)	36(2)	12(2)	9(3)	-24(3)
C(27)	95(4)	33(2)	40(2)	4(2)	4(2)	15(2)
C(28)	60(2)	38(2)	29(2)	2(1)	12(2)	12(2)
C(29)	21(2)	25(1)	23(1)	0(1)	11(1)	-1(1)
C(30)	25(2)	22(1)	23(1)	2(1)	13(1)	-2(1)
C(31)	21(2)	29(2)	24(1)	3(1)	9(1)	-2(1)
C(32)	23(2)	28(2)	31(2)	9(1)	12(1)	4(1)
C(33)	29(2)	23(1)	31(2)	4(1)	18(1)	1(1)
C(34)	26(2)	24(1)	23(1)	-1(1)	13(1)	-3(1)
C(35)	29(2)	30(2)	24(1)	3(1)	5(1)	1(1)
C(36)	49(2)	41(2)	23(2)	4(1)	13(2)	-1(2)
C(37)	41(2)	46(2)	31(2)	2(2)	-4(2)	6(2)
C(38)	28(2)	38(2)	38(2)	0(1)	8(1)	-6(1)
C(39)	35(2)	22(1)	38(2)	4(1)	21(2)	3(1)
C(40)	56(3)	35(2)	97(3)	-10(2)	54(2)	0(2)
C(41)	70(3)	25(2)	44(2)	6(2)	23(2)	2(2)
C(42)	58(2)	27(2)	46(2)	-4(2)	21(2)	3(2)
C(43)	23(2)	36(2)	18(1)	-4(1)	8(1)	-3(1)
C(44)	40(2)	39(2)	39(2)	-2(2)	22(2)	-4(2)
C(45)	53(2)	56(2)	46(2)	-4(2)	30(2)	-21(2)
C(46)	32(2)	77(3)	33(2)	-10(2)	20(2)	-17(2)
C(47)	33(2)	67(2)	36(2)	-7(2)	20(2)	2(2)
C(48)	27(2)	43(2)	28(2)	-1(1)	13(1)	3(1)
C(49)	22(2)	19(1)	19(1)	-2(1)	7(1)	1(1)
C(50)	25(2)	37(2)	29(2)	-4(1)	11(1)	-1(1)
C(51)	34(2)	48(2)	29(2)	-11(2)	6(2)	-3(2)
C(52)	51(2)	36(2)	21(1)	-3(1)	12(2)	13(2)
C(53)	43(2)	36(2)	30(2)	-3(1)	21(2)	6(2)
C(54)	33(2)	31(2)	28(2)	-4(1)	15(1)	-1(1)
C(55)	34(2)	32(2)	38(2)	-7(1)	22(2)	-8(1)

Appendix 1. Crystallographic data

C(56)	64(3)	45(2)	53(2)	-6(2)	37(2)	4(2)
C(57)	36(2)	66(2)	59(2)	-24(2)	26(2)	-18(2)
C(58)	86(3)	45(2)	62(2)	4(2)	45(2)	-4(2)

The anisotropic displacement factor exponent takes the form
 $2 \pi^2 [h^2 a^{*2} U(11) + \dots + 2hka^* b^* U(12)]$

Appendix 1. Crystallographic data

Table 5. Hydrogen Coordinates ($\text{\AA} \times 10^4$) and equivalent isotropic displacement parameters ($\text{\AA}^2 \times 10^3$) for pa653

atom	x	y	z	U(eq)
H(1A)	2303	2215	2128	44
H(1B)	1958	1816	2436	44
H(2A)	1064	2333	2359	43
H(2B)	1776	2678	2632	43
H(6)	0	662	-1362	30
H(8)	1581	511	558	31
H(10A)	-1329	1995	-1603	65
H(10B)	-681	2088	-854	65
H(10C)	-1129	1580	-1031	65
H(11A)	333	1870	-1776	64
H(11B)	294	2226	-1214	64
H(11C)	-361	2224	-1974	64
H(12A)	-1188	1506	-2415	64
H(12B)	-1072	1029	-1948	64
H(12C)	-492.0000	1156	-2222	64
H(14A)	528	-353	33	109
H(14B)	449	-709	-575	109
H(14C)	-100	-253	-723	109
H(15A)	252	-47	-1629	82
H(15B)	908	-437.0000	-1395.0001	82
H(15C)	1066	139	-1429	82
H(16A)	2046	19	-215	81
H(16B)	1777	-542	-294	81
H(16C)	1825	-216	329	81
H(18)	2289	1691	253	57
H(19)	3439	1874	343	75
H(20)	4465	1861	1391	74
H(21)	4345	1676	2358	87
H(22)	3211	1468	2276	69
H(24)	1005	1082	1903	49
H(25)	1075	398	2568	78
H(26)	1993	-191.0000	2816	92
H(27)	2830	-100	2396	80
H(28)	2769	582	1726	55
H(32)	-1200	4461	-77	33
H(34)	618	4337	1709	29
H(36A)	-625	3802	-1217	58
H(36B)	-1164	3346	-1562.0001	58
H(36C)	-415.0000	3265	-880	58
H(37A)	-1639	4281	-1179	71
H(37B)	-2120	4040	-855	71
H(37C)	-2172	3827	-1551	71
H(38A)	-1918	3001	-1059	56
H(38B)	-1832	3199	-345	56
H(38C)	-1189	2882	-374	56
H(40A)	-1061	4806	1507	84
H(40B)	-1558	4917	715	84
H(40C)	-1217	5365	1240	84
H(41A)	-990	5269	24	71
H(41B)	-126	5366	365	71
H(41C)	-637	5708	561	71
H(42A)	92	5552	1756	67
H(42B)	642	5209	1614	67
H(42C)	263	5001	2054	67
H(44)	1715	4269	1252	46
H(45)	2632	4438	936	58
H(46)	3375	3806	886	54
H(47)	3161	2994	1098	52
H(48)	2251	2819	1418	39
H(50)	2548	3861	2691	37
H(51)	2911	4090	3820	48
H(52)	2116	3996	4294	45

Appendix 1. Crystallographic data

H(53)	945	3676	3646	41
H(54)	576	3450	2521	37
H(56A)	-1005	2585	1456	75
H(56B)	-1805	2343	1141	75
H(56C)	-1559	2658	668	75
H(57A)	-1867	1973	-129	78
H(57B)	-2080	1604	317	78
H(57C)	-1460	1452	103	78
H(58A)	-636.0001	1307	1368	91
H(58B)	-1267	1504	1543	91
H(58C)	-475	1759	1886	91

Complex 5I

Table 1. Crystal data for pa652

Compound	pa652
Molecular formula	C ₆₆ H ₈₇ N ₂ O ₄ P ₂ Y
Molecular weight	1123.23
Crystal habit	Colourless Block
Crystal dimensions(mm)	0.28x0.26x0.22
Crystal system	monoclinic
Space group	P2 ₁
a(Å)	10.654(1)
b(Å)	26.055(1)
c(Å)	11.449(1)
α(°)	90.00
β(°)	107.091(1)
γ(°)	90.00
V(Å ³)	3037.8(4)
Z	2
d(g·cm ⁻³)	1.228
F(000)	1196
μ(cm ⁻¹)	1.060
Absorption corrections	multi-scan ; 0.7556 min, 0.8002 max
Diffractionmeter	KappaCCD
X-ray source	MoKα
λ(Å)	0.71069
Monochromator	graphite
T (K)	150.0(1)
Scan mode	phi and omega scans
Maximum θ	27.48
HKL ranges	-12 13 ; -33 33 ; -14 11
Reflections measured	17115
Unique data	12776
Rint	0.0455
Reflections used	11429
Criterion	I > 2σ(I)
Refinement type	Fsqd
Hydrogen atoms	constr
Parameters refined	749
Reflections / parameter	15
wR2	0.1178
R1	0.0500
Flack's parameter	0.492(11)
Weights a, b	0.0478 ; 3.9788
GoF	1.089
difference peak / hole (e Å ⁻³)	0.728(0.066) / -1.082(0.066)

Table 2. Atomic Coordinates (A x 10⁴) and equivalent isotropic displacement parameters (Å² x 10³) for pa652

atom	x	y	z	U(eq)
Y(1)	7748(1)	2129(1)	4826(1)	21(1)
P(1)	9230(2)	1015(1)	4390(2)	22(1)
P(2)	9243(2)	3241(1)	4397(2)	22(1)
O(1)	7421(6)	2866(3)	5675(6)	27(1)
O(2)	7425(6)	1381(3)	5659(6)	27(1)
N(1)	9134(7)	2659(3)	4007(7)	27(2)
N(2)	9112(7)	1607(3)	3999(7)	23(2)
C(1A)	9100(10)	2378(6)	2890(10)	19(2)
C(2A)	9630(10)	1855(6)	3080(10)	23(3)
C(3A)	9390(30)	1560(10)	1970(30)	33(4)
C(4A)	10040(20)	1847(8)	1040(20)	28(3)
C(5A)	9610(20)	2370(10)	880(30)	32(4)
C(6A)	9780(10)	2682(7)	2040(20)	17(3)
C(1B)	9680(20)	2438(6)	3130(20)	19(2)
C(2B)	9130(20)	1856(8)	2820(20)	23(3)
C(3B)	9810(30)	1580(10)	1970(30)	33(4)
C(4B)	9510(20)	1840(10)	780(20)	28(3)
C(5B)	10030(30)	2420(10)	960(30)	32(4)
C(6B)	9390(20)	2680(10)	1830(20)	17(3)
C(7)	9374(8)	3331(3)	5957(8)	23(2)
C(8)	8349(8)	3182(3)	6392(7)	25(2)
C(9)	8189(7)	3367(3)	7489(7)	22(2)
C(10)	9340(10)	3599(3)	8277(7)	28(2)
C(11)	10520(10)	3682(3)	7999(8)	25(2)
C(12)	10511(7)	3572(3)	6819(8)	23(2)
C(13)	6870(10)	3343(4)	7800(10)	39(2)
C(14)	5910(10)	3623(5)	6790(10)	47(3)
C(15)	6510(10)	2791(4)	7980(10)	55(3)
C(16)	7010(10)	3635(5)	9030(10)	54(3)
C(17)	11730(10)	3878(3)	8990(10)	31(2)
C(18)	12930(10)	3831(6)	8580(10)	81(4)
C(19)	11520(20)	4462(6)	9150(20)	131(8)
C(20)	12020(10)	3548(6)	10130(10)	75(4)
C(21)	10640(10)	3574(3)	4125(8)	26(2)
C(22)	10490(10)	4054(4)	3550(10)	38(2)
C(23)	11480(10)	4295(4)	3300(10)	43(2)
C(24)	12790(10)	4048(5)	3660(10)	54(3)
C(25)	12910(10)	3582(4)	4170(10)	39(2)
C(26)	11820(10)	3344(4)	4420(10)	35(2)
C(27)	7790(8)	3640(3)	3622(8)	26(2)
C(28)	6970(10)	3478(4)	2570(10)	40(2)
C(29)	5930(10)	3786(5)	1950(10)	46(3)
C(30)	5680(10)	4240(4)	2440(10)	42(3)
C(31)	6480(10)	4378(4)	3530(10)	43(3)
C(32)	7570(10)	4096(4)	4160(10)	40(2)
C(33)	9445(8)	923(3)	6026(7)	23(2)
C(34)	8271(8)	1084(3)	6345(7)	23(2)
C(35)	8256(8)	875(3)	7531(8)	30(2)
C(36)	9322(8)	655(3)	8297(8)	28(2)
C(37)	10513(8)	583(3)	7998(8)	26(2)
C(38)	10470(10)	689(4)	6780(8)	28(2)
C(39)	6947(8)	907(3)	7823(7)	27(2)
C(40)	6480(10)	1461(4)	7910(10)	50(3)
C(41)	6970(10)	645(5)	9000(10)	47(3)
C(42)	5790(10)	658(5)	6780(10)	53(3)
C(43)	11739(8)	367(4)	8947(8)	33(2)
C(44)	11680(10)	-191(4)	9090(10)	84(4)
C(45)	11800(10)	569(6)	10210(10)	78(4)
C(46)	13020(10)	489(5)	8630(10)	56(3)
C(47)	7834(8)	633(3)	3649(8)	28(2)
C(48)	6981(8)	779(4)	2486(8)	33(2)
C(49)	5890(10)	479(5)	1890(10)	43(3)

Appendix 1. Crystallographic data

C(50)	5640(10)	28(4)	2410(10)	43(3)
C(51)	6470(10)	-136(5)	3560(10)	54(3)
C(52)	7520(10)	178(4)	4140(10)	40(2)
C(53)	10601(8)	680(4)	4083(8)	27(2)
C(54)	10480(10)	200(4)	3540(10)	36(2)
C(55)	11620(10)	-28(4)	3330(10)	50(3)
C(56)	12730(10)	199(4)	3600(10)	40(2)
C(57)	12910(10)	677(5)	4190(10)	47(3)
C(58)	11864(8)	925(4)	4420(8)	32(2)
O(3A)	9821(2)	2122(4)	6590(2)	27(1)
C(59A)	11130(10)	2190(10)	6470(10)	35(2)
C(60A)	12070(10)	2055(7)	7690(10)	33(2)
C(61A)	11270(10)	1960(8)	8520(10)	34(2)
C(62A)	9910(10)	2150(10)	7871(8)	32(1)
O(3B)	9821(2)	2122(4)	6590(2)	27(1)
C(59B)	11125(8)	2070(10)	6440(10)	35(2)
C(60B)	12020(10)	2299(7)	7590(10)	33(2)
C(61B)	11380(10)	2204(6)	8565(7)	34(2)
C(62B)	9960(10)	2110(10)	7885(7)	32(1)
O(4A)	6040(20)	2078(6)	3270(10)	13(3)
C(63A)	4847(7)	2136(7)	2487(7)	35(1)
C(64A)	5000(10)	2210(6)	1216(8)	51(2)
C(65A)	3950(20)	1675(8)	2440(30)	67(4)
C(66A)	4160(20)	2603(6)	2840(10)	49(3)
O(4B)	6010(20)	2158(8)	3530(10)	25(3)
C(63B)	4634(6)	2128(7)	2990(6)	35(1)
C(64B)	4031(7)	2130(10)	4060(6)	51(2)
C(65B)	4310(20)	1635(8)	2260(30)	67(4)
C(66B)	4110(20)	2606(6)	2220(20)	49(3)

U(eq) is defined as 1/3 the trace of the Uij tensor.

Appendix 1. Crystallographic data

Table 3. Bond lengths (Å) and angles (deg) for pa652

Y(1)-O(4B)	2.00(2)	Y(1)-O(4A)	2.14(2)
Y(1)-O(1)	2.227(7)	Y(1)-O(2)	2.240(7)
Y(1)-N(2)	2.380(7)	Y(1)-N(1)	2.404(7)
Y(1)-O(3A)	2.517(2)	Y(1)-C(1A)	3.05(1)
P(1)-N(2)	1.602(7)	P(1)-C(47)	1.78(1)
P(1)-C(53)	1.82(1)	P(1)-C(33)	1.834(8)
P(2)-N(1)	1.576(8)	P(2)-C(7)	1.77(1)
P(2)-C(21)	1.82(1)	P(2)-C(27)	1.859(8)
O(1)-C(8)	1.36(1)	O(2)-C(34)	1.27(1)
N(1)-C(1B)	1.42(2)	N(1)-C(1A)	1.47(2)
N(2)-C(2A)	1.47(2)	N(2)-C(2B)	1.50(2)
C(1A)-C(2A)	1.46(2)	C(1A)-C(6A)	1.59(2)
C(1A)-H(1A)	1.0000	C(2A)-C(3A)	1.44(3)
C(2A)-H(2A)	1.0000	C(3A)-C(4A)	1.61(3)
C(3A)-H(3A1)	0.9900	C(3A)-H(3A2)	0.9900
C(4A)-C(5A)	1.44(4)	C(4A)-H(4A1)	0.9900
C(4A)-H(4A2)	0.9900	C(5A)-C(6A)	1.51(4)
C(5A)-H(5A1)	0.9900	C(5A)-H(5A2)	0.9900
C(6A)-H(6A1)	0.9900	C(6A)-H(6A2)	0.9900
C(1B)-C(6B)	1.57(3)	C(1B)-C(2B)	1.63(2)
C(1B)-H(1B)	1.0000	C(2B)-C(3B)	1.56(3)
C(2B)-H(2B)	1.0000	C(3B)-C(4B)	1.48(4)
C(3B)-H(3B1)	0.9900	C(3B)-H(3B2)	0.9900
C(4B)-C(5B)	1.60(4)	C(4B)-H(4B1)	0.9900
C(4B)-H(4B2)	0.9900	C(5B)-C(6B)	1.52(4)
C(5B)-H(5B1)	0.9900	C(5B)-H(5B2)	0.9900
C(6B)-H(6B1)	0.9900	C(6B)-H(6B2)	0.9900
C(7)-C(8)	1.38(1)	C(7)-C(12)	1.46(1)
C(8)-C(9)	1.40(1)	C(9)-C(10)	1.43(1)
C(9)-C(13)	1.55(1)	C(10)-C(11)	1.40(1)
C(10)-H(10)	0.9500	C(11)-C(12)	1.38(1)
C(11)-C(17)	1.53(1)	C(12)-H(12)	0.9500
C(13)-C(14)	1.50(1)	C(13)-C(15)	1.52(1)
C(13)-C(16)	1.56(1)	C(14)-H(14A)	0.9800
C(14)-H(14B)	0.9800	C(14)-H(14C)	0.9800
C(15)-H(15A)	0.9800	C(15)-H(15B)	0.9800
C(15)-H(15C)	0.9800	C(16)-H(16A)	0.9800
C(16)-H(16B)	0.9800	C(16)-H(16C)	0.9800
C(17)-C(18)	1.49(1)	C(17)-C(20)	1.52(1)
C(17)-C(19)	1.56(2)	C(18)-H(18A)	0.9800
C(18)-H(18B)	0.9800	C(18)-H(18C)	0.9800
C(19)-H(19A)	0.9800	C(19)-H(19B)	0.9800
C(19)-H(19C)	0.9800	C(20)-H(20A)	0.9800
C(20)-H(20B)	0.9800	C(20)-H(20C)	0.9800
C(21)-C(26)	1.35(1)	C(21)-C(22)	1.40(1)
C(22)-C(23)	1.33(1)	C(22)-H(22)	0.9500
C(23)-C(24)	1.48(2)	C(23)-H(23)	0.9500
C(24)-C(25)	1.34(2)	C(24)-H(24)	0.9500
C(25)-C(26)	1.42(1)	C(25)-H(25)	0.9500
C(26)-H(26)	0.9500	C(27)-C(28)	1.34(1)
C(27)-C(32)	1.39(1)	C(28)-C(29)	1.38(1)
C(28)-H(28)	0.9500	C(29)-C(30)	1.37(2)
C(29)-H(29)	0.9500	C(30)-C(31)	1.34(1)
C(30)-H(30)	0.9500	C(31)-C(32)	1.39(1)
C(31)-H(31)	0.9500	C(32)-H(32)	0.9500
C(33)-C(38)	1.33(1)	C(33)-C(34)	1.46(1)
C(34)-C(35)	1.47(1)	C(35)-C(36)	1.34(1)
C(35)-C(39)	1.53(1)	C(36)-C(37)	1.42(1)
C(36)-H(36)	0.9500	C(37)-C(38)	1.41(1)
C(37)-C(43)	1.54(1)	C(38)-H(38)	0.9500
C(39)-C(41)	1.51(1)	C(39)-C(40)	1.54(1)
C(39)-C(42)	1.58(1)	C(40)-H(40A)	0.9800
C(40)-H(40B)	0.9800	C(40)-H(40C)	0.9800
C(41)-H(41A)	0.9800	C(41)-H(41B)	0.9800
C(41)-H(41C)	0.9800	C(42)-H(42A)	0.9800
C(42)-H(42B)	0.9800	C(42)-H(42C)	0.9800

C(43)-C(44)	1.47(1)	C(43)-C(45)	1.52(1)
C(43)-C(46)	1.55(1)	C(44)-H(44A)	0.9800
C(44)-H(44B)	0.9800	C(44)-H(44C)	0.9800
C(45)-H(45A)	0.9800	C(45)-H(45B)	0.9800
C(45)-H(45C)	0.9800	C(46)-H(46A)	0.9800
C(46)-H(46B)	0.9800	C(46)-H(46C)	0.9800
C(47)-C(52)	1.39(1)	C(47)-C(48)	1.42(1)
C(48)-C(49)	1.40(1)	C(48)-H(48)	0.9500
C(49)-C(50)	1.37(2)	C(49)-H(49)	0.9500
C(50)-C(51)	1.42(2)	C(50)-H(50)	0.9500
C(51)-C(52)	1.39(1)	C(51)-H(51)	0.9500
C(52)-H(52)	0.9500	C(53)-C(54)	1.38(1)
C(53)-C(58)	1.44(1)	C(54)-C(55)	1.44(1)
C(54)-H(54)	0.9500	C(55)-C(56)	1.28(2)
C(55)-H(55)	0.9500	C(56)-C(57)	1.41(2)
C(56)-H(56)	0.9500	C(57)-C(58)	1.38(1)
C(57)-H(57)	0.9500	C(58)-H(58)	0.9500
O(3A)-C(62A)	1.443(8)	O(3A)-C(59A)	1.452(8)
C(59A)-C(60A)	1.50(1)	C(59A)-H(59A)	0.9900
C(59A)-H(59B)	0.9900	C(60A)-C(61A)	1.479(8)
C(60A)-H(60A)	0.9900	C(60A)-H(60B)	0.9900
C(61A)-C(62A)	1.50(1)	C(61A)-H(61A)	0.9900
C(61A)-H(61B)	0.9900	C(62A)-H(62A)	0.9900
C(62A)-H(62B)	0.9900	C(59B)-C(60B)	1.50(1)
C(59B)-H(59C)	0.9900	C(59B)-H(59D)	0.9900
C(60B)-C(61B)	1.488(8)	C(60B)-H(60C)	0.9900
C(60B)-H(60D)	0.9900	C(61B)-C(62B)	1.51(1)
C(61B)-H(61C)	0.9900	C(61B)-H(61D)	0.9900
C(62B)-H(62C)	0.9900	C(62B)-H(62D)	0.9900
O(4A)-C(63A)	1.33(2)	C(63A)-C(64A)	1.525(8)
C(63A)-C(65A)	1.53(1)	C(63A)-C(66A)	1.54(1)
C(64A)-H(64A)	0.9800	C(64A)-H(64B)	0.9800
C(64A)-H(64C)	0.9800	C(65A)-H(65A)	0.9800
C(65A)-H(65B)	0.9800	C(65A)-H(65C)	0.9800
C(66A)-H(66A)	0.9800	C(66A)-H(66B)	0.9800
C(66A)-H(66C)	0.9800	O(4B)-C(63B)	1.42(2)
C(63B)-C(65B)	1.52(1)	C(63B)-C(66B)	1.53(1)
C(63B)-C(64B)	1.541(7)	C(64B)-H(64D)	0.9800
C(64B)-H(64E)	0.9800	C(64B)-H(64F)	0.9800
C(65B)-H(65D)	0.9800	C(65B)-H(65E)	0.9800
C(65B)-H(65F)	0.9800	C(66B)-H(66D)	0.9800
C(66B)-H(66E)	0.9800	C(66B)-H(66F)	0.9800
O(4B)-Y(1)-O(4A)	9.6(7)	O(4B)-Y(1)-O(1)	93.5(5)
O(4A)-Y(1)-O(1)	102.3(4)	O(4B)-Y(1)-O(2)	97.2(7)
O(4A)-Y(1)-O(2)	95.9(5)	O(1)-Y(1)-O(2)	120.07(8)
O(4B)-Y(1)-N(2)	105.4(4)	O(4A)-Y(1)-N(2)	95.8(5)
O(1)-Y(1)-N(2)	149.1(2)	O(2)-Y(1)-N(2)	82.0(2)
O(4B)-Y(1)-N(1)	103.2(6)	O(4A)-Y(1)-N(1)	100.3(5)
O(1)-Y(1)-N(1)	82.4(3)	O(2)-Y(1)-N(1)	148.7(2)
N(2)-Y(1)-N(1)	69.88(8)	O(4B)-Y(1)-O(3A)	174.7(4)
O(4A)-Y(1)-O(3A)	175.3(5)	O(1)-Y(1)-O(3A)	82.4(3)
O(2)-Y(1)-O(3A)	82.0(3)	N(2)-Y(1)-O(3A)	79.7(2)
N(1)-Y(1)-O(3A)	79.8(2)	O(4B)-Y(1)-C(1A)	89.0(5)
O(4A)-Y(1)-C(1A)	82.7(5)	O(1)-Y(1)-C(1A)	107.6(3)
O(2)-Y(1)-C(1A)	131.3(3)	N(2)-Y(1)-C(1A)	50.0(3)
N(1)-Y(1)-C(1A)	28.2(3)	O(3A)-Y(1)-C(1A)	95.5(3)
N(2)-P(1)-C(47)	114.8(4)	N(2)-P(1)-C(53)	114.1(4)
C(47)-P(1)-C(53)	104.1(4)	N(2)-P(1)-C(33)	112.8(4)
C(47)-P(1)-C(33)	104.4(4)	C(53)-P(1)-C(33)	105.5(4)
N(1)-P(2)-C(7)	113.0(4)	N(1)-P(2)-C(21)	113.9(4)
C(7)-P(2)-C(21)	106.5(4)	N(1)-P(2)-C(27)	114.9(4)
C(7)-P(2)-C(27)	102.5(4)	C(21)-P(2)-C(27)	105.0(4)
C(8)-O(1)-Y(1)	127.3(5)	C(34)-O(2)-Y(1)	128.6(5)
C(1B)-N(1)-C(1A)	24.9(7)	C(1B)-N(1)-P(2)	125.2(8)
C(1A)-N(1)-P(2)	135.1(7)	C(1B)-N(1)-Y(1)	118.0(7)
C(1A)-N(1)-Y(1)	101.1(6)	P(2)-N(1)-Y(1)	116.5(4)

C(2A)-N(2)-C(2B)	20.2(6)	C(2A)-N(2)-P(1)	127.5(8)
C(2B)-N(2)-P(1)	130(1)	C(2A)-N(2)-Y(1)	115.7(7)
C(2B)-N(2)-Y(1)	106(1)	P(1)-N(2)-Y(1)	116.4(4)
C(2A)-C(1A)-N(1)	115(1)	C(2A)-C(1A)-C(6A)	109(1)
N(1)-C(1A)-C(6A)	113(1)	C(2A)-C(1A)-Y(1)	86.4(8)
N(1)-C(1A)-Y(1)	50.7(5)	C(6A)-C(1A)-Y(1)	162(1)
C(2A)-C(1A)-H(1A)	106.5	N(1)-C(1A)-H(1A)	106.5
C(6A)-C(1A)-H(1A)	106.5	Y(1)-C(1A)-H(1A)	76.2
C(3A)-C(2A)-C(1A)	114(2)	C(3A)-C(2A)-N(2)	113(2)
C(1A)-C(2A)-N(2)	108(1)	C(3A)-C(2A)-H(2A)	107.3
C(1A)-C(2A)-H(2A)	107.3	N(2)-C(2A)-H(2A)	107.3
C(2A)-C(3A)-C(4A)	110(2)	C(2A)-C(3A)-H(3A1)	109.6
C(4A)-C(3A)-H(3A1)	109.6	C(2A)-C(3A)-H(3A2)	109.6
C(4A)-C(3A)-H(3A2)	109.6	H(3A1)-C(3A)-H(3A2)	108.1
C(5A)-C(4A)-C(3A)	110(2)	C(5A)-C(4A)-H(4A1)	109.7
C(3A)-C(4A)-H(4A1)	109.7	C(5A)-C(4A)-H(4A2)	109.7
C(3A)-C(4A)-H(4A2)	109.7	H(4A1)-C(4A)-H(4A2)	108.2
C(4A)-C(5A)-C(6A)	116(2)	C(4A)-C(5A)-H(5A1)	108.2
C(6A)-C(5A)-H(5A1)	108.2	C(4A)-C(5A)-H(5A2)	108.2
C(6A)-C(5A)-H(5A2)	108.2	H(5A1)-C(5A)-H(5A2)	107.4
C(5A)-C(6A)-C(1A)	108(2)	C(5A)-C(6A)-H(6A1)	110.1
C(1A)-C(6A)-H(6A1)	110.1	C(5A)-C(6A)-H(6A2)	110.1
C(1A)-C(6A)-H(6A2)	110.1	H(6A1)-C(6A)-H(6A2)	108.4
N(1)-C(1B)-C(6B)	120(2)	N(1)-C(1B)-C(2B)	109(1)
C(6B)-C(1B)-C(2B)	102(2)	N(1)-C(1B)-H(1B)	108.2
C(6B)-C(1B)-H(1B)	108.2	C(2B)-C(1B)-H(1B)	108.2
N(2)-C(2B)-C(1B)	119(2)	N(2)-C(2B)-C(1B)	108(1)
C(3B)-C(2B)-C(1B)	112(2)	N(2)-C(2B)-H(2B)	105.6
C(3B)-C(2B)-H(2B)	105.6	C(1B)-C(2B)-H(2B)	105.6
C(4B)-C(3B)-C(2B)	110(2)	C(4B)-C(3B)-H(3B1)	109.7
C(2B)-C(3B)-H(3B1)	109.7	C(4B)-C(3B)-H(3B2)	109.7
C(2B)-C(3B)-H(3B2)	109.7	H(3B1)-C(3B)-H(3B2)	108.2
C(3B)-C(4B)-C(5B)	111(2)	C(3B)-C(4B)-H(4B1)	109.5
C(5B)-C(4B)-H(4B1)	109.5	C(3B)-C(4B)-H(4B2)	109.5
C(5B)-C(4B)-H(4B2)	109.5	H(4B1)-C(4B)-H(4B2)	108.1
C(6B)-C(5B)-C(4B)	107(2)	C(6B)-C(5B)-H(5B1)	110.3
C(4B)-C(5B)-H(5B1)	110.3	C(6B)-C(5B)-H(5B2)	110.3
C(4B)-C(5B)-H(5B2)	110.3	H(5B1)-C(5B)-H(5B2)	108.5
C(5B)-C(6B)-C(1B)	116(2)	C(5B)-C(6B)-H(6B1)	108.3
C(1B)-C(6B)-H(6B1)	108.3	C(5B)-C(6B)-H(6B2)	108.3
C(1B)-C(6B)-H(6B2)	108.3	H(6B1)-C(6B)-H(6B2)	107.4
C(8)-C(7)-C(12)	117.6(8)	C(8)-C(7)-P(2)	119.5(6)
C(12)-C(7)-P(2)	122.9(6)	O(1)-C(8)-C(7)	117.6(7)
O(1)-C(8)-C(9)	119.4(8)	C(7)-C(8)-C(9)	123.0(7)
C(8)-C(9)-C(10)	113.7(7)	C(8)-C(9)-C(13)	123.5(7)
C(10)-C(9)-C(13)	122.7(8)	C(11)-C(10)-C(9)	125.8(8)
C(11)-C(10)-H(10)	117.1	C(9)-C(10)-H(10)	117.1
C(12)-C(11)-C(10)	116.3(8)	C(12)-C(11)-C(17)	123.7(8)
C(10)-C(11)-C(17)	120.0(7)	C(11)-C(12)-C(7)	121.1(8)
C(11)-C(12)-H(12)	119.4	C(7)-C(12)-H(12)	119.4
C(14)-C(13)-C(15)	115(1)	C(14)-C(13)-C(9)	105.0(7)
C(15)-C(13)-C(9)	110.6(8)	C(14)-C(13)-C(16)	109(1)
C(15)-C(13)-C(16)	108(1)	C(9)-C(13)-C(16)	109.7(8)
C(13)-C(14)-H(14A)	109.5	C(13)-C(14)-H(14B)	109.5
H(14A)-C(14)-H(14B)	109.5	C(13)-C(14)-H(14C)	109.5
C(13)-C(15)-H(15A)	109.5	C(13)-C(15)-H(15B)	109.5
H(15A)-C(15)-H(15B)	109.5	C(13)-C(15)-H(15C)	109.5
H(15A)-C(15)-H(15C)	109.5	H(15B)-C(15)-H(15C)	109.5
C(13)-C(16)-H(16A)	109.5	C(13)-C(16)-H(16B)	109.5
H(16A)-C(16)-H(16B)	109.5	C(13)-C(16)-H(16C)	109.5
H(16A)-C(16)-H(16C)	109.5	H(16B)-C(16)-H(16C)	109.5
C(18)-C(17)-C(20)	105(1)	C(18)-C(17)-C(11)	110.7(8)
C(20)-C(17)-C(11)	111.2(8)	C(18)-C(17)-C(19)	107(1)
C(20)-C(17)-C(19)	116(1)	C(11)-C(17)-C(19)	107.2(8)
C(17)-C(18)-H(18A)	109.5	C(17)-C(18)-H(18B)	109.5
H(18A)-C(18)-H(18B)	109.5	C(17)-C(18)-H(18C)	109.5
H(18A)-C(18)-H(18C)	109.5	H(18B)-C(18)-H(18C)	109.5

Appendix 1. Crystallographic data

C(17)-C(19)-H(19A)	109.5	C(17)-C(19)-H(19B)	109.5
H(19A)-C(19)-H(19B)	109.5	C(17)-C(19)-H(19C)	109.5
H(19A)-C(19)-H(19C)	109.5	H(19B)-C(19)-H(19C)	109.5
C(17)-C(20)-H(20A)	109.5	C(17)-C(20)-H(20B)	109.5
H(20A)-C(20)-H(20B)	109.5	C(17)-C(20)-H(20C)	109.5
H(20A)-C(20)-H(20C)	109.5	H(20B)-C(20)-H(20C)	109.5
C(26)-C(21)-C(22)	119(1)	C(26)-C(21)-P(2)	119.6(7)
C(22)-C(21)-P(2)	121.3(8)	C(23)-C(22)-C(21)	122(1)
C(23)-C(22)-H(22)	118.8	C(21)-C(22)-H(22)	118.8
C(22)-C(23)-C(24)	118(1)	C(22)-C(23)-H(23)	120.8
C(24)-C(23)-H(23)	120.8	C(25)-C(24)-C(23)	119(1)
C(25)-C(24)-H(24)	120.6	C(23)-C(24)-H(24)	120.6
C(24)-C(25)-C(26)	120(1)	C(24)-C(25)-H(25)	119.9
C(26)-C(25)-H(25)	119.9	C(21)-C(26)-C(25)	121(1)
C(21)-C(26)-H(26)	119.5	C(25)-C(26)-H(26)	119.5
C(28)-C(27)-C(32)	121.5(8)	C(28)-C(27)-P(2)	119.2(7)
C(32)-C(27)-P(2)	119.2(7)	C(27)-C(28)-C(29)	120(1)
C(27)-C(28)-H(28)	120.2	C(29)-C(28)-H(28)	120.2
C(30)-C(29)-C(28)	121(1)	C(30)-C(29)-H(29)	119.5
C(28)-C(29)-H(29)	119.5	C(31)-C(30)-C(29)	118(1)
C(31)-C(30)-H(30)	121.1	C(29)-C(30)-H(30)	121.1
C(30)-C(31)-C(32)	124(1)	C(30)-C(31)-H(31)	118.2
C(32)-C(31)-H(31)	118.2	C(31)-C(32)-C(27)	116(1)
C(31)-C(32)-H(32)	121.8	C(27)-C(32)-H(32)	121.8
C(38)-C(33)-C(34)	124.8(7)	C(38)-C(33)-P(1)	123.8(6)
C(34)-C(33)-P(1)	111.0(6)	O(2)-C(34)-C(33)	121.6(7)
O(2)-C(34)-C(35)	126.9(7)	C(33)-C(34)-C(35)	111.5(7)
C(36)-C(35)-C(34)	121.7(7)	C(36)-C(35)-C(39)	122.2(7)
C(34)-C(35)-C(39)	116.1(7)	C(35)-C(36)-C(37)	122.9(7)
C(35)-C(36)-H(36)	118.5	C(37)-C(36)-H(36)	118.5
C(38)-C(37)-C(36)	116.3(8)	C(38)-C(37)-C(43)	122.9(8)
C(36)-C(37)-C(43)	120.7(8)	C(33)-C(38)-C(37)	120.9(8)
C(33)-C(38)-H(38)	119.5	C(37)-C(38)-H(38)	119.5
C(41)-C(39)-C(35)	113.4(7)	C(41)-C(39)-C(40)	106.6(8)
C(35)-C(39)-C(40)	113.5(7)	C(41)-C(39)-C(42)	106.9(8)
C(35)-C(39)-C(42)	111.8(8)	C(40)-C(39)-C(42)	104(1)
C(39)-C(40)-H(40A)	109.5	C(39)-C(40)-H(40B)	109.5
H(40A)-C(40)-H(40B)	109.5	C(39)-C(40)-H(40C)	109.5
H(40A)-C(40)-H(40C)	109.5	H(40B)-C(40)-H(40C)	109.5
C(39)-C(41)-H(41A)	109.5	C(39)-C(41)-H(41B)	109.5
H(41A)-C(41)-H(41B)	109.5	C(39)-C(41)-H(41C)	109.5
H(41A)-C(41)-H(41C)	109.5	H(41B)-C(41)-H(41C)	109.5
C(39)-C(42)-H(42A)	109.5	C(39)-C(42)-H(42B)	109.5
H(42A)-C(42)-H(42B)	109.5	C(39)-C(42)-H(42C)	109.5
H(42A)-C(42)-H(42C)	109.5	H(42B)-C(42)-H(42C)	109.5
C(44)-C(43)-C(45)	103(1)	C(44)-C(43)-C(37)	112.8(8)
C(45)-C(43)-C(37)	109.5(8)	C(44)-C(43)-C(46)	107(1)
C(45)-C(43)-C(46)	111(1)	C(37)-C(43)-C(46)	112.6(8)
C(43)-C(44)-H(44A)	109.5	C(43)-C(44)-H(44B)	109.5
H(44A)-C(44)-H(44B)	109.5	C(43)-C(44)-H(44C)	109.5
H(44A)-C(44)-H(44C)	109.5	H(44B)-C(44)-H(44C)	109.5
C(43)-C(45)-H(45A)	109.5	C(43)-C(45)-H(45B)	109.5
H(45A)-C(45)-H(45B)	109.5	C(43)-C(45)-H(45C)	109.5
H(45A)-C(45)-H(45C)	109.5	H(45B)-C(45)-H(45C)	109.5
C(43)-C(46)-H(46A)	109.5	C(43)-C(46)-H(46B)	109.5
H(46A)-C(46)-H(46B)	109.5	C(43)-C(46)-H(46C)	109.5
H(46A)-C(46)-H(46C)	109.5	H(46B)-C(46)-H(46C)	109.5
C(52)-C(47)-C(48)	116.0(8)	C(52)-C(47)-P(1)	123.4(7)
C(48)-C(47)-P(1)	120.6(7)	C(49)-C(48)-C(47)	121(1)
C(49)-C(48)-H(48)	119.5	C(47)-C(48)-H(48)	119.5
C(50)-C(49)-C(48)	120(1)	C(50)-C(49)-H(49)	119.8
C(48)-C(49)-H(49)	119.8	C(49)-C(50)-C(51)	121(1)
C(49)-C(50)-H(50)	119.6	C(51)-C(50)-H(50)	119.6
C(52)-C(51)-C(50)	117(1)	C(52)-C(51)-H(51)	121.4
C(50)-C(51)-H(51)	121.4	C(51)-C(52)-C(47)	125(1)
C(51)-C(52)-H(52)	117.7	C(47)-C(52)-H(52)	117.7
C(54)-C(53)-C(58)	119(1)	C(54)-C(53)-P(1)	122.9(7)
C(58)-C(53)-P(1)	118.4(8)	C(53)-C(54)-C(55)	119(1)

Appendix 1. Crystallographic data

C(53)-C(54)-H(54)	120.8	C(55)-C(54)-H(54)	120.8
C(56)-C(55)-C(54)	122(1)	C(56)-C(55)-H(55)	118.8
C(54)-C(55)-H(55)	118.8	C(55)-C(56)-C(57)	121(1)
C(55)-C(56)-H(56)	119.6	C(57)-C(56)-H(56)	119.6
C(58)-C(57)-C(56)	120(1)	C(58)-C(57)-H(57)	119.8
C(56)-C(57)-H(57)	119.8	C(57)-C(58)-C(53)	119(1)
C(57)-C(58)-H(58)	120.4	C(53)-C(58)-H(58)	120.4
C(62A)-O(3A)-C(59A)	107.9(8)	C(62A)-O(3A)-Y(1)	126.7(5)
C(59A)-O(3A)-Y(1)	124.3(5)	O(3A)-C(59A)-C(60A)	106.5(7)
O(3A)-C(59A)-H(59A)	110.4	C(60A)-C(59A)-H(59A)	110.4
O(3A)-C(59A)-H(59B)	110.4	C(60A)-C(59A)-H(59B)	110.4
H(59A)-C(59A)-H(59B)	108.6	C(61A)-C(60A)-C(59A)	106.2(7)
C(61A)-C(60A)-H(60A)	110.5	C(59A)-C(60A)-H(60A)	110.5
C(61A)-C(60A)-H(60B)	110.5	C(59A)-C(60A)-H(60B)	110.5
H(60A)-C(60A)-H(60B)	108.7	C(60A)-C(61A)-C(62A)	106.4(8)
C(60A)-C(61A)-H(61A)	110.5	C(62A)-C(61A)-H(61A)	110.5
C(60A)-C(61A)-H(61B)	110.5	C(62A)-C(61A)-H(61B)	110.5
H(61A)-C(61A)-H(61B)	108.7	O(3A)-C(62A)-C(61A)	104.6(8)
O(3A)-C(62A)-H(62A)	110.8	C(61A)-C(62A)-H(62A)	110.8
O(3A)-C(62A)-H(62B)	110.8	C(61A)-C(62A)-H(62B)	110.8
H(62A)-C(62A)-H(62B)	108.9	C(60B)-C(59B)-H(59C)	110.9
C(60B)-C(59B)-H(59D)	110.9	H(59C)-C(59B)-H(59D)	108.9
C(61B)-C(60B)-C(59B)	106.0(8)	C(61B)-C(60B)-H(60C)	110.5
C(59B)-C(60B)-H(60C)	110.5	C(61B)-C(60B)-H(60D)	110.5
C(59B)-C(60B)-H(60D)	110.5	H(60C)-C(60B)-H(60D)	108.7
C(60B)-C(61B)-C(62B)	104.8(6)	C(60B)-C(61B)-H(61C)	110.8
C(62B)-C(61B)-H(61C)	110.8	C(60B)-C(61B)-H(61D)	110.8
C(62B)-C(61B)-H(61D)	110.8	H(61C)-C(61B)-H(61D)	108.9
C(61B)-C(62B)-H(62C)	110.1	C(61B)-C(62B)-H(62D)	110.1
H(62C)-C(62B)-H(62D)	108.4	C(63A)-O(4A)-Y(1)	164(1)
O(4A)-C(63A)-C(64A)	108(1)	O(4A)-C(63A)-C(65A)	114(2)
C(64A)-C(63A)-C(65A)	108(1)	O(4A)-C(63A)-C(66A)	110(1)
C(64A)-C(63A)-C(66A)	110(1)	C(65A)-C(63A)-C(66A)	107(1)
C(63B)-O(4B)-Y(1)	159(1)	O(4B)-C(63B)-C(65B)	109(1)
O(4B)-C(63B)-C(66B)	111(2)	C(65B)-C(63B)-C(66B)	113(1)
O(4B)-C(63B)-C(64B)	105.9(7)	C(65B)-C(63B)-C(64B)	111(1)
C(66B)-C(63B)-C(64B)	107(1)	C(63B)-C(64B)-H(64D)	109.5
C(63B)-C(64B)-H(64E)	109.5	H(64D)-C(64B)-H(64E)	109.5
C(63B)-C(64B)-H(64F)	109.5	H(64D)-C(64B)-H(64F)	109.5
C(63B)-C(65B)-H(65E)	109.5	C(63B)-C(65B)-H(65D)	109.5
C(63B)-C(65B)-H(65F)	109.5	H(65D)-C(65B)-H(65E)	109.5
H(65E)-C(65B)-H(65F)	109.5	H(65D)-C(65B)-H(65F)	109.5
C(63B)-C(66B)-H(66E)	109.5	C(63B)-C(66B)-H(66D)	109.5
C(63B)-C(66B)-H(66F)	109.5	H(66D)-C(66B)-H(66E)	109.5
H(66E)-C(66B)-H(66F)	109.5	H(66D)-C(66B)-H(66F)	109.5

Appendix 1. Crystallographic data

Table 4. Anisotropic displacement parameters ($\text{\AA}^2 \times 10^3$) for pa652

atom	U11	U22	U33	U23	U13	U12
Y(1)	15(1)	25(1)	22(1)	-1(1)	4(1)	0(1)
P(1)	19(1)	24(1)	22(1)	2(1)	3(1)	3(1)
P(2)	16(1)	26(1)	22(1)	0(1)	5(1)	-1(1)
O(1)	19(3)	32(3)	28(3)	-8(3)	5(2)	-4(3)
O(2)	17(3)	36(4)	28(3)	8(3)	6(2)	4(3)
N(1)	22(3)	40(4)	20(3)	2(3)	6(3)	-5(3)
N(2)	27(4)	17(3)	27(4)	8(3)	12(3)	3(3)
C(1A)	22(7)	18(4)	21(5)	7(3)	10(5)	-8(4)
C(2A)	8(8)	32(5)	23(7)	9(4)	-6(5)	-7(6)
C(3A)	50(10)	29(5)	38(6)	12(4)	40(10)	11(8)
C(4A)	30(10)	28(5)	21(6)	1(4)	5(5)	0(6)
C(5A)	40(10)	36(7)	28(6)	8(5)	30(10)	0(8)
C(6A)	0(8)	28(4)	17(7)	6(5)	-8(6)	-2(7)
C(1B)	22(7)	18(4)	21(5)	7(3)	10(5)	-8(4)
C(2B)	8(8)	32(5)	23(7)	9(4)	-6(5)	-7(6)
C(3B)	50(10)	29(5)	38(6)	12(4)	40(10)	11(8)
C(4B)	30(10)	28(5)	21(6)	1(4)	5(5)	0(6)
C(5B)	40(10)	36(7)	28(6)	8(5)	30(10)	0(8)
C(6B)	0(8)	28(4)	17(7)	6(5)	-8(6)	-2(7)
C(7)	19(3)	18(3)	28(4)	-5(3)	0(3)	-5(3)
C(8)	20(3)	20(3)	25(4)	-8(3)	-8(3)	-1(3)
C(9)	15(3)	18(3)	24(3)	-1(3)	-10(2)	-5(2)
C(10)	30(4)	24(4)	21(4)	-8(3)	-5(3)	-5(3)
C(11)	28(4)	24(4)	24(4)	-4(3)	11(3)	-3(3)
C(12)	12(3)	22(4)	26(4)	0(3)	-5(3)	0(3)
C(13)	21(4)	62(6)	43(5)	-10(4)	24(3)	-3(3)
C(14)	16(3)	66(6)	63(6)	-4(5)	17(3)	8(3)
C(15)	58(7)	48(6)	72(7)	-23(5)	37(6)	-26(5)
C(16)	39(5)	81(8)	55(6)	-34(6)	32(5)	-7(5)
C(17)	29(4)	21(3)	39(5)	-4(3)	3(3)	-4(3)
C(18)	31(5)	170(10)	41(5)	-26(6)	4(4)	-41(6)
C(19)	90(10)	80(10)	170(10)	-90(10)	-40(10)	-5(7)
C(20)	42(5)	128(8)	43(4)	34(5)	-6(3)	-34(5)
C(21)	30(4)	25(4)	30(4)	-4(3)	16(3)	-7(3)
C(22)	46(6)	37(5)	32(5)	3(4)	15(4)	-8(4)
C(23)	40(4)	41(5)	49(5)	6(4)	14(3)	7(3)
C(24)	42(6)	73(8)	58(6)	-18(5)	31(5)	-40(5)
C(25)	22(4)	50(6)	39(5)	-5(4)	-2(3)	-5(4)
C(26)	36(5)	32(4)	40(5)	-11(4)	17(4)	-12(4)
C(27)	18(3)	29(4)	24(4)	8(3)	-4(3)	9(3)
C(28)	33(5)	31(4)	52(5)	7(4)	5(4)	15(4)
C(29)	25(5)	60(7)	43(6)	3(5)	-5(4)	4(5)
C(30)	29(5)	53(6)	52(6)	10(5)	24(4)	11(4)
C(31)	37(5)	30(4)	62(7)	3(4)	18(5)	15(4)
C(32)	44(5)	41(5)	38(5)	0(4)	16(4)	18(4)
C(33)	18(3)	37(4)	16(3)	0(3)	7(2)	-6(3)
C(34)	18(3)	30(4)	24(3)	-2(3)	12(3)	-4(3)
C(35)	27(4)	37(4)	36(4)	4(3)	25(3)	-8(3)
C(36)	23(4)	35(5)	31(4)	0(4)	16(3)	-6(3)
C(37)	19(4)	24(4)	28(4)	1(3)	-6(3)	-1(3)
C(38)	31(4)	31(4)	26(4)	1(3)	15(3)	0(4)
C(39)	26(4)	22(3)	28(4)	8(3)	0(3)	-2(3)
C(40)	48(6)	57(7)	63(6)	-3(5)	44(5)	3(5)
C(41)	29(5)	70(7)	43(5)	23(5)	10(4)	14(5)
C(42)	29(4)	82(8)	44(5)	3(5)	3(4)	-17(4)
C(43)	18(4)	62(5)	16(3)	6(3)	0(3)	5(4)
C(44)	37(4)	36(4)	140(10)	30(5)	-36(5)	-9(3)
C(45)	33(4)	160(10)	26(3)	-13(4)	-16(3)	28(5)
C(46)	18(3)	87(6)	57(6)	26(5)	4(3)	-5(4)
C(47)	22(4)	32(4)	35(4)	-1(3)	16(3)	7(3)
C(48)	22(4)	46(5)	25(3)	6(3)	-6(3)	9(3)
C(49)	32(5)	52(7)	38(5)	-8(5)	-3(4)	-7(5)
C(50)	25(4)	51(6)	47(6)	-28(5)	2(4)	-15(4)

Appendix 1. Crystallographic data

C(51)	60(7)	65(7)	39(6)	-4(5)	18(5)	-26(6)
C(52)	37(5)	43(6)	32(5)	4(4)	-2(4)	-4(4)
C(53)	18(4)	38(5)	24(4)	6(4)	2(3)	3(3)
C(54)	23(4)	37(5)	50(6)	3(4)	13(4)	8(4)
C(55)	51(5)	55(6)	53(5)	7(4)	28(4)	41(4)
C(56)	36(5)	45(5)	45(5)	6(4)	19(4)	11(4)
C(57)	25(4)	69(7)	57(6)	29(5)	26(4)	16(4)
C(58)	12(3)	46(5)	33(5)	1(4)	0(3)	-4(3)
O(3A)	19(1)	39(1)	22(1)	5(4)	5(1)	3(4)
C(59A)	19(1)	55(7)	30(2)	-13(7)	7(1)	2(7)
C(60A)	19(2)	42(6)	35(2)	6(6)	1(2)	-1(5)
C(61A)	27(2)	46(7)	24(2)	-2(6)	-1(2)	-11(6)
C(62A)	24(2)	48(3)	23(1)	4(6)	5(1)	7(6)
O(3B)	19(1)	39(1)	22(1)	5(4)	5(1)	3(4)
C(59B)	19(1)	55(7)	30(2)	-13(7)	7(1)	2(7)
C(60B)	19(2)	42(6)	35(2)	6(6)	1(2)	-1(5)
C(61B)	27(2)	46(7)	24(2)	-2(6)	-1(2)	-11(6)
C(62B)	24(2)	48(3)	23(1)	4(6)	5(1)	7(6)
O(4A)	23(3)	5(8)	9(6)	1(4)	1(4)	-1(3)
C(63A)	16(2)	46(2)	39(4)	20(10)	0(2)	12(6)
C(64A)	38(3)	59(4)	54(3)	-1(6)	10(2)	-2(6)
C(65A)	14(8)	90(10)	90(10)	-29(6)	0(6)	-22(7)
C(66A)	32(6)	40(5)	74(8)	19(7)	16(7)	13(4)
O(4B)	14(2)	43(6)	14(5)	-22(6)	-2(4)	5(6)
C(63B)	16(2)	46(2)	39(4)	20(10)	0(2)	12(6)
C(64B)	38(3)	59(4)	54(3)	-1(6)	10(2)	-2(6)
C(65B)	14(8)	90(10)	90(10)	-29(6)	0(6)	-22(7)
C(66B)	32(6)	40(5)	74(8)	19(7)	16(7)	13(4)

The anisotropic displacement factor exponent takes the form
 $2 \pi^2 [h^2 a^{*2} U(11) + \dots + 2 h k a^* b^* U(12)]$

Appendix 1. Crystallographic data

Table 5. Hydrogen Coordinates ($\text{\AA} \times 10^4$) and equivalent isotropic displacement parameters ($\text{\AA}^2 \times 10^3$) for pa652

atom	x	y	z	U(eq)
H(1A)	8149	2344	2410	23
H(2A)	10601	1886	3440	28
H(3A1)	8437	1526	1583	39
H(3A2)	9778	1217	2157	39
H(4A1)	11006	1835	1360	33
H(4A2)	9773	1669	237	33
H(5A1)	8662	2377	413	38
H(5A2)	10086	2549	375	38
H(6A1)	9376	3025	1839	21
H(6A2)	10728	2728	2465	21
H(1B)	10659	2421	3497	23
H(2B)	8192	1894	2334	28
H(3B1)	10773	1569	2362	39
H(3B2)	9496	1217	1847	39
H(4B1)	8550	1842	388	33
H(4B2)	9930	1659	240	33
H(5B1)	11000	2429	1307	38
H(5B2)	9794	2604	164	38
H(6B1)	8425	2680	1443	21
H(6B2)	9672	3045	1923	21
H(10)	9308	3707	9060	33
H(12)	11258	3653	6563	27
H(14A)	5036	3610	6908	70
H(14B)	5875	3461	6005	70
H(14C)	6184	3981	6779	70
H(15A)	7173	2644	8686	83
H(15B)	6478	2592	7248	83
H(15C)	5650	2782	8128	83
H(16A)	6135	3691	9126	82
H(16B)	7437	3966	9013	82
H(16C)	7537	3430	9715	82
H(18A)	12864	4068	7899	121
H(18B)	13000	3477	8305	121
H(18C)	13703	3914	9258	121
H(19A)	11537	4647	8415	197
H(19B)	12218	4592	9854	197
H(19C)	10664	4516	9300	197
H(20A)	12743	3700	10773	113
H(20B)	12258	3202	9947	113
H(20C)	11233	3532	10414	113
H(22)	9650	4214	3338	45
H(23)	11351	4618	2896	52
H(24)	13523	4217	3531	65
H(25)	13732	3409	4365	47
H(26)	11924	3017	4809	42
H(28)	7097	3153	2241	48
H(29)	5380	3682	1169	55
H(30)	4955	4450	2022	51
H(31)	6293	4686	3888	51
H(32)	8146	4209	4921	48
H(36)	9279	543	9074	33
H(38)	11190	591	6495	34
H(40A)	6214	1615	7095	75
H(40B)	7199	1662	8449	75
H(40C)	5732	1458	8244	75
H(41A)	6145	717	9194	71
H(41B)	7710	773	9666	71
H(41C)	7056	273	8918	71
H(42A)	5680	846	6019	80
H(42B)	4979	675	7016	80
H(42C)	6005	299	6674	80
H(44A)	11417	-353	8277	126

Appendix 1. Crystallographic data

H(44B)	11046	-275	9522	126
H(44C)	12553	-319	9551	126
H(45A)	12651	482	10789	117
H(45B)	11095	411	10481	117
H(45C)	11687	942	10177	117
H(46A)	13192	859	8709	83
H(46B)	12929	381	7788	83
H(46C)	13753	304	9190	83
H(48)	7156	1084	2108	40
H(49)	5312	589	1131	52
H(50)	4910	-176	1983	52
H(51)	6309	-448.0000	3923	65
H(52)	8065	75	4915	48
H(54)	9659	25	3324	43
H(55)	11540	-360.0000	2966	60
H(56)	13446	42	3398	48
H(57)	13753	831	4437	57
H(58)	11976	1254	4794	38
H(59A)	11262	2548	6251	42
H(59B)	11262	1960	5827	42
H(60A)	12584	1744	7622	40
H(60B)	12694	2341	7997	40
H(61A)	11634	2145	9301	41
H(61B)	11239	1588	8694	41
H(62A)	9235	1940	8063	38
H(62B)	9805	2514	8108	38
H(59C)	11188	2267	5718	42
H(59D)	11343	1710	6355	42
H(60C)	12894	2131	7804	40
H(60D)	12140	2672	7494	40
H(61C)	11471	2506	9108	41
H(61D)	11770	1902	9064	41
H(62C)	9682	1769	8112	38
H(62D)	9399	2375	8094	38
H(64A)	5601	2497	1230	77
H(64B)	4143	2285	634	77
H(64C)	5359	1896	966	77
H(65A)	4466	1358	2558	100
H(65B)	3274	1665	1646	100
H(65C)	3523	1706	3091	100
H(66A)	4119	2561	3683	73
H(66B)	3265	2630	2286	73
H(66C)	4651	2915	2788	73
H(64D)	4383	1834	4599	77
H(64E)	3074	2092	3739	77
H(64F)	4251	2446	4521	77
H(65D)	4597	1661	1526	100
H(65E)	3359	1576	2025	100
H(65F)	4761	1347	2763	100
H(66D)	4336	2912	2741	73
H(66E)	3152	2581	1891	73
H(66F)	4502	2630	1553	73

Complex 52

Table 1. Crystal data for pa781

Compound	pa781
Molecular formula	$\text{C}_{66}\text{H}_{87}\text{N}_2\text{O}_4\text{P}_2\text{Y}$
Molecular weight	1123.23
Crystal habit	Colorless Block
Crystal dimensions(mm)	0.24x0.22x0.08
Crystal system	monoclinic

Appendix 1. Crystallographic data

Space group	P2 ₁
a(Å)	10.652(1)
b(Å)	26.078(1)
c(Å)	11.444(1)
α(°)	90.00
β(°)	107.043(1)
γ(°)	90.00
V(Å ³)	3039.3(4)
Z	2
d(g·cm ⁻³)	1.227
F(000)	1196
μ(cm ⁻¹)	1.060
Absorption corrections	multi-scan ; 0.7851 min, 0.9200 max
Diffraction	KappaCCD
X-ray source	MoKα
λ(Å)	0.71069
Monochromator	graphite
T (K)	150.0(1)
Scan mode	phi and omega scans
Maximum θ	27.47
HKL ranges	-13 13 ; -33 26 ; -14 10
Reflections measured	13947
Unique data	10630
Rint	0.0321
Reflections used	9073
Criterion	I > 2σI
Refinement type	Fsqd
Hydrogen atoms	constr
Parameters refined	706
Reflections / parameter	12
wR2	0.1190
R1	0.0603
Flack's parameter	0.04(12)
Weights a, b	0.0000 ; 8.1500
GoF	1.111
difference peak / hole (e Å ⁻³)	1.117(0.074) / -0.531(0.074)

Appendix 1. Crystallographic data

Table 2. Atomic Coordinates (A x 10⁴) and equivalent isotropic displacement parameters (A² x 10³) for pa781

atom	x	y	z	U(eq)
Y(1)	2245(4)	2110(20)	5176(3)	20(1)
P(1)	770(20)	3230(20)	5580(20)	20(4)
P(2)	750(20)	1000(20)	5630(20)	21(4)
O(1)	2550(60)	2840(30)	4300(50)	30(10)
O(2)	2590(60)	1360(30)	4350(50)	30(10)
N(1)	930(70)	2640(30)	6020(60)	20(10)
N(2)	820(60)	1590(30)	5980(60)	20(10)
C(1)	340(60)	2400(30)	6900(50)	20(10)
C(2)	880(60)	1850(30)	7150(50)	20(10)
C(3)	230(70)	1560(30)	7980(70)	30(10)
C(4)	450(60)	1850(30)	9190(60)	30(10)
C(5)	-60(60)	2390(30)	8980(60)	30(10)
C(6)	580(70)	2670(30)	8120(70)	30(10)
C(7)	590(80)	3310(30)	3980(70)	20(20)
C(8)	1650(80)	3150(30)	3590(70)	20(20)
C(9)	1770(80)	3340(30)	2460(70)	20(10)
C(10)	660(80)	3570(30)	1690(70)	20(20)
C(11)	-520(80)	3650(30)	1970(70)	20(20)
C(12)	-490(80)	3550(30)	3190(70)	20(20)
C(13)	3100(100)	3300(40)	2120(80)	30(20)
C(14)	3400(100)	2740(40)	2000(100)	40(20)
C(15)	3000(100)	3590(50)	900(100)	50(30)
C(16)	4200(100)	3540(40)	3100(100)	40(20)
C(17)	-1700(100)	3870(40)	1020(80)	30(20)
C(18)	-1900(100)	3640(70)	-200(100)	100(50)
C(19)	-1700(100)	4450(50)	1000(200)	90(50)
C(20)	-3000(100)	3750(50)	1400(100)	60(30)
C(21)	-610(80)	3550(30)	5860(70)	30(20)
C(22)	-1820(80)	3330(40)	5550(80)	30(20)
C(23)	-2900(100)	3560(40)	5800(100)	40(20)
C(24)	-2800(100)	4040(50)	6300(100)	40(20)
C(25)	-1500(100)	4280(40)	6600(100)	40(20)
C(26)	-500(100)	4040(40)	6400(100)	30(20)
C(27)	2200(80)	3620(40)	6310(70)	20(20)
C(28)	2400(100)	4080(30)	5800(100)	30(20)
C(29)	3500(100)	4380(40)	6400(100)	40(20)
C(30)	4300(100)	4230(40)	7500(100)	40(20)
C(31)	4100(100)	3790(40)	8000(100)	40(20)
C(32)	3000(100)	3480(40)	7420(80)	30(20)
C(33)	580(80)	910(30)	4040(70)	20(10)
C(34)	1710(80)	1050(30)	3670(70)	20(20)
C(35)	1800(80)	850(30)	2540(80)	30(20)
C(36)	700(100)	620(30)	1750(80)	30(20)
C(37)	-520(80)	560(30)	2040(70)	20(20)
C(38)	-520(80)	670(30)	3220(70)	30(20)
C(39)	3100(100)	870(40)	2240(80)	30(20)
C(40)	3000(100)	590(50)	1000(100)	60(30)
C(41)	3600(100)	1400(40)	2100(100)	40(20)
C(42)	4100(100)	580(40)	3300(100)	40(20)
C(43)	-1700(100)	360(40)	1050(80)	30(20)
C(44)	-1600(100)	-200(50)	800(200)	110(70)
C(45)	-3000(100)	420(60)	1400(100)	60(30)
C(46)	-2000(100)	660(60)	-100(100)	70(40)
C(47)	-630(80)	660(30)	5930(70)	30(20)
C(48)	-500(100)	180(40)	6500(100)	40(20)
C(49)	-1600(100)	-60(40)	6800(100)	50(30)
C(50)	-2800(100)	180(40)	6400(100)	50(30)
C(51)	-2900(100)	650(50)	5900(100)	50(30)
C(52)	-1900(100)	900(40)	5600(100)	30(20)
C(53)	2160(80)	620(30)	6420(70)	20(20)
C(54)	2500(100)	170(40)	5910(80)	30(20)
C(55)	3600(100)	-130(40)	6500(100)	50(30)

Appendix 1. Crystallographic data

C(56)	4300(100)	30(40)	7600(100)	40(20)
C(57)	4100(100)	480(40)	8100(100)	40(20)
C(58)	3000(100)	780(40)	7540(80)	30(20)
O(3A)	160(70)	2120(50)	3410(80)	40(20)
C(59A)	-1200(100)	2150(60)	3510(60)	40(20)
C(60A)	-2050(70)	2000(50)	2290(70)	40(20)
C(61A)	-1310(70)	2210(50)	1440(60)	40(20)
C(62A)	90(70)	2080(70)	2100(100)	40(20)
O(3B)	200(100)	2090(70)	3400(100)	20(40)
C(59B)	-1100(200)	2070(80)	3600(100)	20(40)
C(60B)	-2100(100)	2240(70)	2500(100)	20(40)
C(61B)	-1500(100)	1990(70)	1500(100)	20(40)
C(62B)	0(100)	2100(100)	2100(200)	20(40)
O(4A)	3940(20)	2080(20)	6580(30)	30(7)
C(63A)	5310(30)	2110(40)	7010(40)	40(20)
C(64A)	5940(60)	2100(100)	5950(70)	60(30)
C(65A)	5800(100)	2600(50)	7800(100)	40(40)
C(66A)	5900(100)	1650(70)	7900(200)	60(60)
O(4B)	3940(20)	2080(20)	6580(30)	30(7)
C(63B)	5200(80)	2140(30)	7480(60)	40(20)
C(64B)	5000(100)	2160(80)	8750(40)	60(30)
C(65B)	5900(100)	2640(60)	7200(100)	40(40)
C(66B)	6100(100)	1670(70)	7400(200)	60(60)

U(eq) is defined as 1/3 the trace of the Uij tensor.

Appendix 1. Crystallographic data

Table 3. Bond lengths (Å) and angles (deg) for pa781

Y(1)-O(4A)	2.04(2)	Y(1)-O(1)	2.23(6)
Y(1)-O(2)	2.25(6)	Y(1)-N(1)	2.38(7)
Y(1)-N(2)	2.40(7)	Y(1)-O(3B)	2.5(1)
Y(1)-O(3A)	2.53(6)	P(1)-N(1)	1.59(7)
P(1)-C(21)	1.8(1)	P(1)-C(7)	1.81(8)
P(1)-C(27)	1.83(8)	P(2)-N(2)	1.59(7)
P(2)-C(33)	1.79(8)	P(2)-C(53)	1.81(8)
P(2)-C(47)	1.8(1)	O(1)-C(8)	1.3(1)
O(2)-C(34)	1.3(1)	N(1)-C(1)	1.5(1)
N(2)-C(2)	1.47(8)	C(1)-C(6)	1.5(1)
C(1)-C(2)	1.54(7)	C(2)-C(3)	1.5(1)
C(3)-C(4)	1.5(1)	C(4)-C(5)	1.52(7)
C(5)-C(6)	1.5(1)	C(7)-C(12)	1.4(1)
C(7)-C(8)	1.4(1)	C(8)-C(9)	1.4(1)
C(9)-C(10)	1.4(1)	C(9)-C(13)	1.5(1)
C(10)-C(11)	1.4(1)	C(11)-C(12)	1.4(1)
C(11)-C(17)	1.5(1)	C(13)-C(15)	1.5(1)
C(13)-C(16)	1.5(1)	C(13)-C(14)	1.5(1)
C(17)-C(19)	1.5(2)	C(17)-C(20)	1.5(1)
C(17)-C(18)	1.5(2)	C(21)-C(22)	1.4(1)
C(21)-C(26)	1.4(1)	C(22)-C(23)	1.4(1)
C(23)-C(24)	1.4(2)	C(24)-C(25)	1.4(2)
C(25)-C(26)	1.4(1)	C(27)-C(32)	1.4(1)
C(27)-C(28)	1.4(1)	C(28)-C(29)	1.4(1)
C(29)-C(30)	1.4(1)	C(30)-C(31)	1.4(1)
C(31)-C(32)	1.4(1)	C(33)-C(38)	1.4(1)
C(33)-C(34)	1.4(1)	C(34)-C(35)	1.4(1)
C(35)-C(36)	1.4(1)	C(35)-C(39)	1.5(1)
C(36)-C(37)	1.4(1)	C(37)-C(38)	1.4(1)
C(37)-C(43)	1.5(1)	C(39)-C(41)	1.5(1)
C(39)-C(40)	1.5(1)	C(39)-C(42)	1.5(1)
C(43)-C(45)	1.5(1)	C(43)-C(46)	1.5(1)
C(43)-C(44)	1.5(1)	C(47)-C(48)	1.4(1)
C(47)-C(52)	1.4(1)	C(48)-C(49)	1.4(1)
C(49)-C(50)	1.4(2)	C(50)-C(51)	1.4(2)
C(51)-C(52)	1.4(1)	C(53)-C(54)	1.4(1)
C(53)-C(58)	1.4(1)	C(54)-C(55)	1.4(1)
C(55)-C(56)	1.4(2)	C(56)-C(57)	1.4(1)
C(57)-C(58)	1.4(1)	O(3A)-C(62A)	1.43(1)
O(3A)-C(59A)	1.43(1)	C(59A)-C(60A)	1.50(1)
C(60A)-C(61A)	1.52(1)	C(61A)-C(62A)	1.50(1)
O(3B)-C(62B)	1.44(1)	O(3B)-C(59B)	1.44(1)
C(59B)-C(60B)	1.50(1)	C(60B)-C(61B)	1.52(1)
C(61B)-C(62B)	1.50(1)	O(4A)-C(63A)	1.40(1)
C(63A)-C(66A)	1.55(1)	C(63A)-C(64A)	1.55(1)
C(63A)-C(65A)	1.55(1)	C(63B)-C(64B)	1.55(1)
C(63B)-C(66B)	1.55(1)	C(63B)-C(65B)	1.55(1)

O(4A)-Y(1)-O(1)	100(2)	O(4A)-Y(1)-O(2)	95(2)
O(1)-Y(1)-O(2)	120(1)	O(4A)-Y(1)-N(1)	101(2)
O(1)-Y(1)-N(1)	82(2)	O(2)-Y(1)-N(1)	151(2)
O(4A)-Y(1)-N(2)	101(2)	O(1)-Y(1)-N(2)	148(2)
O(2)-Y(1)-N(2)	83(2)	N(1)-Y(1)-N(2)	70(1)
O(4A)-Y(1)-O(3B)	177(4)	O(1)-Y(1)-O(3B)	82(4)
O(2)-Y(1)-O(3B)	82(4)	N(1)-Y(1)-O(3B)	82(5)
N(2)-Y(1)-O(3B)	78(5)	O(4A)-Y(1)-O(3A)	179(3)
O(1)-Y(1)-O(3A)	81(3)	O(2)-Y(1)-O(3A)	84(3)
N(1)-Y(1)-O(3A)	80(3)	N(2)-Y(1)-O(3A)	79(3)
O(3B)-Y(1)-O(3A)	2(5)	N(1)-P(1)-C(21)	115(4)
N(1)-P(1)-C(7)	114(4)	C(21)-P(1)-C(7)	106(4)
N(1)-P(1)-C(27)	113(4)	C(21)-P(1)-C(27)	105(4)
C(7)-P(1)-C(27)	102(4)	N(2)-P(2)-C(33)	112(4)
N(2)-P(2)-C(53)	116(4)	C(33)-P(2)-C(53)	105(4)
N(2)-P(2)-C(47)	114(4)	C(33)-P(2)-C(47)	106(4)
C(53)-P(2)-C(47)	104(4)	C(8)-O(1)-Y(1)	128(5)

Appendix 1. Crystallographic data

C(34)-O(2)-Y(1)	127(5)	C(1)-N(1)-P(1)	127(5)
C(1)-N(1)-Y(1)	116(4)	P(1)-N(1)-Y(1)	117(3)
C(2)-N(2)-P(2)	131(5)	C(2)-N(2)-Y(1)	104(4)
P(2)-N(2)-Y(1)	116(3)	N(1)-C(1)-C(6)	115(6)
N(1)-C(1)-C(2)	109(5)	C(6)-C(1)-C(2)	108(5)
N(2)-C(2)-C(3)	116(6)	N(2)-C(2)-C(1)	110(5)
C(3)-C(2)-C(1)	111(6)	C(2)-C(3)-C(4)	111(6)
C(5)-C(4)-C(3)	111(6)	C(4)-C(5)-C(6)	110(6)
C(1)-C(6)-C(5)	112(6)	C(12)-C(7)-C(8)	122(7)
C(12)-C(7)-P(1)	123(6)	C(8)-C(7)-P(1)	116(6)
O(1)-C(8)-C(7)	120(7)	O(1)-C(8)-C(9)	122(7)
C(7)-C(8)-C(9)	118(7)	C(10)-C(9)-C(8)	116(7)
C(10)-C(9)-C(13)	122(7)	C(8)-C(9)-C(13)	122(7)
C(9)-C(10)-C(11)	126(7)	C(10)-C(11)-C(12)	115(7)
C(10)-C(11)-C(17)	122(7)	C(12)-C(11)-C(17)	123(8)
C(7)-C(12)-C(11)	121(8)	C(15)-C(13)-C(16)	108(8)
C(15)-C(13)-C(9)	113(7)	C(16)-C(13)-C(9)	110(7)
C(15)-C(13)-C(14)	108(8)	C(16)-C(13)-C(14)	108(8)
C(9)-C(13)-C(14)	110(7)	C(19)-C(17)-C(20)	106(10)
C(19)-C(17)-C(18)	110(10)	C(20)-C(17)-C(18)	109(10)
C(19)-C(17)-C(11)	110(8)	C(20)-C(17)-C(11)	111(8)
C(18)-C(17)-C(11)	109(8)	C(22)-C(21)-C(26)	117(8)
C(22)-C(21)-P(1)	120(7)	C(26)-C(21)-P(1)	122(7)
C(21)-C(22)-C(23)	122(9)	C(24)-C(23)-C(22)	119(9)
C(23)-C(24)-C(25)	120(9)	C(26)-C(25)-C(24)	121(9)
C(25)-C(26)-C(21)	121(9)	C(32)-C(27)-C(28)	119(8)
C(32)-C(27)-P(1)	120(7)	C(28)-C(27)-P(1)	121(6)
C(29)-C(28)-C(27)	119(9)	C(30)-C(29)-C(28)	122(9)
C(31)-C(30)-C(29)	120(9)	C(30)-C(31)-C(32)	119(9)
C(27)-C(32)-C(31)	121(9)	C(38)-C(33)-C(34)	122(8)
C(38)-C(33)-P(2)	123(6)	C(34)-C(33)-P(2)	115(6)
O(2)-C(34)-C(35)	123(7)	O(2)-C(34)-C(33)	120(7)
C(35)-C(34)-C(33)	117(7)	C(36)-C(35)-C(34)	118(8)
C(36)-C(35)-C(39)	122(8)	C(34)-C(35)-C(39)	120(7)
C(35)-C(36)-C(37)	124(8)	C(38)-C(37)-C(36)	118(7)
C(38)-C(37)-C(43)	124(8)	C(36)-C(37)-C(43)	119(7)
C(37)-C(38)-C(33)	120(8)	C(41)-C(39)-C(35)	114(8)
C(41)-C(39)-C(40)	108(8)	C(35)-C(39)-C(40)	111(8)
C(41)-C(39)-C(42)	110(8)	C(35)-C(39)-C(42)	106(7)
C(40)-C(39)-C(42)	108(8)	C(45)-C(43)-C(46)	106(10)
C(45)-C(43)-C(44)	108(10)	C(46)-C(43)-C(44)	108(10)
C(45)-C(43)-C(37)	112(7)	C(46)-C(43)-C(37)	112(8)
C(44)-C(43)-C(37)	111(8)	C(48)-C(47)-C(52)	119(8)
C(48)-C(47)-P(2)	123(7)	C(52)-C(47)-P(2)	118(7)
C(47)-C(48)-C(49)	122(10)	C(50)-C(49)-C(48)	119(10)
C(49)-C(50)-C(51)	120(10)	C(50)-C(51)-C(52)	122(10)
C(51)-C(52)-C(47)	118(9)	C(54)-C(53)-C(58)	118(8)
C(54)-C(53)-P(2)	122(6)	C(58)-C(53)-P(2)	120(6)
C(53)-C(54)-C(55)	122(9)	C(56)-C(55)-C(54)	118(10)
C(57)-C(56)-C(55)	120(8)	C(58)-C(57)-C(56)	122(9)
C(57)-C(58)-C(53)	120(9)	C(62A)-O(3A)-C(59A)	109(3)
C(62A)-O(3A)-Y(1)	126(5)	C(59A)-O(3A)-Y(1)	125(5)
O(3A)-C(59A)-C(60A)	107(4)	C(59A)-C(60A)-C(61A)	101(4)
C(62A)-C(61A)-C(60A)	102(4)	O(3A)-C(62A)-C(61A)	106(4)
C(62B)-O(3B)-C(59B)	109(4)	C(62B)-O(3B)-Y(1)	131(10)
C(59B)-O(3B)-Y(1)	120(10)	O(3B)-C(59B)-C(60B)	105(5)
C(59B)-C(60B)-C(61B)	101(5)	C(62B)-C(61B)-C(60B)	101(5)
O(3B)-C(62B)-C(61B)	106(5)	C(63A)-O(4A)-Y(1)	150(3)
O(4A)-C(63A)-C(66A)	112(2)	O(4A)-C(63A)-C(64A)	112(2)
C(66A)-C(63A)-C(64A)	107(8)	O(4A)-C(63A)-C(65A)	112(2)
C(66A)-C(63A)-C(65A)	106(7)	C(64A)-C(63A)-C(65A)	107(8)
C(64B)-C(63B)-C(66B)	109(9)	C(64B)-C(63B)-C(65B)	110(9)
C(66B)-C(63B)-C(65B)	110(9)		

Appendix 1. Crystallographic data

Table 4. Anisotropic displacement parameters ($\text{Å}^2 \times 10^3$) for pa781

atom	U11	U22	U33	U23	U13	U12
Y(1)	20(2)	22(2)	18(2)	0(4)	6(1)	0(4)
P(1)	20(10)	20(10)	20(10)	1(7)	5(7)	1(7)
P(2)	20(10)	20(10)	20(10)	-1(7)	6(8)	-2(7)
O(1)	20(30)	30(30)	20(30)	10(20)	10(20)	0(20)
O(2)	30(30)	30(30)	20(30)	-10(20)	10(20)	0(20)
N(1)	30(30)	20(30)	20(30)	0(20)	10(20)	0(20)
N(2)	20(30)	20(30)	20(30)	-10(20)	0(20)	0(20)
C(1)	30(30)	20(30)	20(30)	0(20)	10(20)	0(20)
C(2)	30(30)	30(30)	20(30)	0(20)	10(20)	0(30)
C(3)	30(30)	20(30)	30(30)	0(20)	10(30)	0(20)
C(4)	40(40)	30(30)	20(30)	0(20)	10(30)	0(30)
C(5)	30(30)	30(30)	20(30)	0(20)	10(30)	0(30)
C(6)	30(40)	20(30)	20(30)	0(20)	10(30)	0(30)
C(7)	30(40)	20(40)	20(30)	0(30)	10(30)	0(30)
C(8)	30(40)	10(40)	20(30)	0(20)	10(30)	0(30)
C(9)	20(30)	20(40)	20(30)	0(30)	0(30)	0(30)
C(10)	20(40)	30(50)	10(30)	0(30)	0(30)	0(30)
C(11)	30(40)	20(40)	20(40)	0(30)	10(30)	0(30)
C(12)	20(40)	20(40)	20(40)	0(30)	10(30)	0(30)
C(13)	30(40)	30(40)	30(40)	10(30)	10(30)	0(30)
C(14)	40(50)	40(50)	60(60)	0(40)	40(40)	10(30)
C(15)	30(50)	60(70)	50(60)	20(50)	20(40)	10(40)
C(16)	30(40)	60(60)	40(50)	0(40)	20(40)	-10(40)
C(17)	30(50)	40(50)	30(50)	10(30)	10(40)	10(30)
C(18)	60(80)	200(200)	20(50)	-20(60)	-10(50)	40(80)
C(19)	60(80)	50(70)	100(100)	30(70)	-20(70)	0(50)
C(20)	30(50)	90(80)	60(70)	20(60)	0(50)	0(50)
C(21)	30(40)	30(40)	20(40)	10(30)	10(30)	0(30)
C(22)	20(40)	40(50)	30(40)	10(30)	10(30)	10(30)
C(23)	30(50)	40(50)	30(40)	10(40)	10(40)	10(40)
C(24)	40(50)	60(70)	40(50)	10(40)	20(40)	30(50)
C(25)	50(60)	30(50)	40(50)	-10(40)	20(40)	10(40)
C(26)	30(50)	30(50)	40(50)	0(40)	20(40)	0(40)
C(27)	20(40)	30(40)	20(30)	0(30)	10(30)	0(30)
C(28)	50(50)	20(40)	40(40)	10(30)	10(40)	-10(30)
C(29)	50(60)	30(50)	40(50)	0(30)	10(40)	-10(40)
C(30)	40(50)	40(50)	50(50)	-10(40)	20(40)	-10(40)
C(31)	20(40)	50(50)	50(50)	0(40)	10(30)	0(30)
C(32)	30(40)	40(50)	30(40)	0(30)	10(30)	-10(30)
C(33)	20(40)	20(40)	20(40)	0(30)	10(30)	0(30)
C(34)	20(30)	30(40)	20(30)	10(30)	0(30)	10(30)
C(35)	20(40)	30(40)	30(40)	0(30)	10(30)	0(30)
C(36)	40(50)	20(40)	30(40)	0(30)	20(40)	0(30)
C(37)	20(40)	20(40)	20(40)	0(30)	0(30)	0(30)
C(38)	20(40)	20(40)	20(40)	0(30)	0(30)	0(30)
C(39)	30(40)	40(50)	30(40)	-10(30)	20(30)	0(30)
C(40)	40(60)	90(80)	40(60)	-40(50)	30(50)	-10(50)
C(41)	40(50)	40(50)	40(50)	0(30)	20(40)	0(30)
C(42)	30(40)	50(50)	50(50)	10(40)	20(40)	10(30)
C(43)	30(50)	30(50)	20(40)	0(30)	0(30)	0(30)
C(44)	100(100)	40(70)	200(100)	-60(80)	-100(100)	10(60)
C(45)	40(60)	100(100)	30(50)	-20(50)	10(40)	-30(50)
C(46)	50(60)	100(100)	40(60)	30(60)	0(50)	-40(60)
C(47)	30(40)	30(40)	20(40)	0(30)	10(30)	-10(30)
C(48)	40(50)	40(50)	30(50)	0(40)	20(40)	-10(40)
C(49)	60(70)	50(60)	40(50)	-10(40)	30(50)	-20(50)
C(50)	50(70)	50(60)	60(70)	-10(50)	30(50)	-20(50)
C(51)	20(40)	70(70)	50(60)	-20(50)	20(40)	0(40)
C(52)	20(40)	40(50)	40(50)	-10(30)	10(30)	0(30)
C(53)	30(40)	20(40)	30(40)	0(30)	10(30)	0(30)
C(54)	30(50)	40(50)	20(40)	0(30)	0(30)	10(30)
C(55)	50(60)	40(60)	60(70)	10(40)	30(50)	20(40)
C(56)	20(40)	50(50)	40(50)	20(40)	10(30)	10(30)

Appendix 1. Crystallographic data

C(57)	40(50)	40(50)	20(40)	0(30)	0(30)	10(40)
C(58)	20(40)	30(40)	30(40)	0(30)	0(30)	0(30)
O(3A)	20(30)	60(40)	20(30)	0(20)	10(20)	0(20)
C(59A)	20(30)	60(40)	20(30)	0(20)	10(20)	0(20)
C(60A)	20(30)	60(40)	20(30)	0(20)	10(20)	0(20)
C(61A)	20(30)	60(40)	20(30)	0(20)	10(20)	0(20)
C(62A)	20(30)	60(40)	20(30)	0(20)	10(20)	0(20)
O(3B)	30(60)	20(70)	20(60)	0(30)	10(40)	0(30)
C(59B)	30(60)	20(70)	20(60)	0(30)	10(40)	0(30)
C(60B)	30(60)	20(70)	20(60)	0(30)	10(40)	0(30)
C(61B)	30(60)	20(70)	20(60)	0(30)	10(40)	0(30)
C(62B)	30(60)	20(70)	20(60)	0(30)	10(40)	0(30)
O(4A)	30(20)	30(20)	30(20)	0(30)	0(10)	10(30)
C(63A)	30(30)	40(30)	40(60)	-20(80)	-10(30)	0(60)
C(64A)	50(50)	60(70)	60(50)	-10(80)	0(40)	20(80)
C(65A)	10(40)	50(60)	100(100)	20(80)	10(60)	-10(30)
C(66A)	60(80)	40(60)	100(100)	30(80)	10(80)	10(60)
O(4B)	30(20)	30(20)	30(20)	0(30)	0(10)	10(30)
C(63B)	30(30)	40(30)	40(60)	-20(80)	-10(30)	0(60)
C(64B)	50(50)	60(70)	60(50)	-10(80)	0(40)	20(80)
C(65B)	10(40)	50(60)	100(100)	20(80)	10(60)	-10(30)
C(66B)	60(80)	40(60)	100(100)	30(80)	10(80)	10(60)

The anisotropic displacement factor exponent takes the form
 $2 \pi^2 [h^2 a^{*2} U(11) + \dots + 2 h k a^* b^* U(12)]$

Appendix 1. Crystallographic data

Table 5. Hydrogen Coordinates (A x 10⁴) and equivalent isotropic displacement parameters (A² x 10³) for pa781

atom	x	y	z	U(eq)
H(1)	-633	2375	6506	28
H(2)	1828	1879	7609	29
H(3A)	593	1213	8136	30
H(3B)	-728	1534	7571	30
H(4A)	1	1662	9709	34
H(4B)	1404	1852	9630	34
H(5A)	134	2577	9767	33
H(5B)	-1029	2388	8610	33
H(6A)	220	3025	7973	31
H(6B)	1535	2699	8519	31
H(10)	700	3674	911	29
H(12)	-1217	3639	3464	27
H(14A)	4282	2718	1835	64
H(14B)	2757	2588	1250	64
H(14C)	3418	2540	2694	64
H(15A)	2787	3948	1022	71
H(15B)	2329	3431	261	71
H(15C)	3859	3563	787	71
H(16A)	4010	3902	3228	64
H(16B)	5010	3491	2966	64
H(16C)	4222	3362	3925	64
H(18A)	-1169	3782	-550	143
H(18B)	-2720.0002	3717	-804	143
H(18C)	-1749	3265	-159.0000	143
H(19A)	-1648	4590	1766	129
H(19B)	-2446	4579	344	129
H(19C)	-877	4546	762	129
H(20A)	-3154	3377	1316	94
H(20B)	-3749.0002	3923	796	94
H(20C)	-2901	3867	2198	94
H(22)	-1927	3000	5167	34
H(23)	-3737	3395	5571	42
H(24)	-3480	4200	6506	51
H(25)	-1445	4607	6998	47
H(26)	352	4204	6674	39
H(28)	1886	4184	5008	41
H(29)	3652	4695	6053	50
H(30)	5077	4436	7893	47
H(31)	4665	3685	8803	48
H(32)	2896	3163	7773	39
H(36)	707	510	970	34
H(38)	-1265	586	3477	30
H(40A)	2405	771	361	84
H(40B)	2715	238	1080	84
H(40C)	3892	583	912	84
H(41A)	2897	1594	1538	62
H(41B)	4376	1389	1877	62
H(41C)	3777	1571	2936	62
H(42A)	4967	583	3146	62
H(42B)	3814	219	3295	62
H(42C)	4153	739	4066	62
H(44A)	-1390	-397	1543	159
H(44B)	-833	-237	440	159
H(44C)	-2375	-324	198	159
H(45A)	-3074	775	1645	91
H(45B)	-2906	198	2143	91
H(45C)	-3725	312	754	91
H(46A)	-2694	502	-754	108
H(46B)	-1167	646	-391	108
H(46C)	-2174	1015	2	108
H(48)	318	11	6632	44
H(49)	-1428	-378	7160	56

Appendix 1. Crystallographic data

H(50)	-3479	13	6578	60
H(51)	-3748	807	5642	57
H(52)	-1995	1231	5236	39
H(54)	1941	63	5132	42
H(55)	3757	-435	6151	58
H(56)	5048	-178	8098	44
H(57)	4614	594	8902	44
H(58)	2830	1092	7892	38
H(59A)	-1345	2499	3728	43
H(59B)	-1245	1908	4149	43
H(60A)	-2922.9998	2163	2132	43
H(60B)	-2164	1622	2209	43
H(61A)	-1573	2031	638	43
H(61B)	-1441	2579	1314	43
H(62A)	322	1734	1941	43
H(62B)	696	2332	1932	43
H(59C)	-1110	2305	4306	28
H(59D)	-1293	1718	3850	28
H(60C)	-2082	2615	2371	28
H(60D)	-2951	2108	2378	28
H(61C)	-1661	1613	1467	28
H(61D)	-1799	2146	721	28
H(62C)	499	1819	1877	28
H(62D)	208	2425	1842	28
H(64A)	5709	1784	5481	90
H(64B)	6899	2127	6280	90
H(64C)	5617	2396	5405	90
H(65A)	5606	2901	7208	66
H(65B)	6739	2581	8153	66
H(65C)	5333	2642	8378	66
H(66A)	5617	1672	8598	92
H(66B)	6870	1675	8096	92
H(66C)	5621	1331	7436	92
H(64D)	4391	2454	8781	90
H(64E)	5813	2210	9382	90
H(64F)	4560	1845	8906	90
H(65D)	6114	2604	6481	66
H(65E)	6653	2705	7921	66
H(65F)	5255	2929	7155	66
H(66D)	5710	1365	7694	92
H(66E)	6965	1734	7991	92
H(66F)	6132	1628	6603	92

Appendix 1. Crystallographic data

Complex 54a

Table 1. Crystal data for pa666

Compound	pa666
Molecular formula	C ₆₅ H ₈₇ N ₂ O ₄ P ₂ Y
Molecular weight	1111.22
Crystal habit	Colorless Block
Crystal dimensions(mm)	0.40x0.26x0.22
Crystal system	monoclinic
Space group	P2 ₁ /c
a(Å)	11.409(1)
b(Å)	27.849(1)
c(Å)	21.019(1)
α(°)	90.00
β(°)	113.905(5)
γ(°)	90.00
V(Å ³)	6105.5(6)
Z	4
d(g·cm ⁻³)	1.209
F(000)	2368
μ(cm ⁻¹)	1.054
Absorption corrections	multi-scan ; 0.6778 min, 0.8012 max
Diffractometer	KappaCCD
X-ray source	MoKα
λ(Å)	0.71069
Monochromator	graphite
T (K)	150.0(1)
Scan mode	phi and omega scans
Maximum θ	25.02
HKL ranges	-13 13 ; -32 33 ; -25 25
Reflections measured	41671
Unique data	10712
Rint	0.0342
Reflections used	9775
Criterion	I > 2σ(I)
Refinement type	Fsqd
Hydrogen atoms	constr
Parameters refined	684
Reflections / parameter	14
wR2	0.1588
R1	0.0783
Weights a, b	0.0000 ; 34.668
GoF	1.159
difference peak / hole (e Å ⁻³)	3.735(0.088) / -2.505(0.088)

Appendix 1. Crystallographic data

Table 2. Atomic Coordinates (A x 10⁴) and equivalent isotropic displacement parameters (A² x 10³) for pa666

atom	x	y	z	U(eq)
Y(1)	2945(1)	2889(1)	953(1)	26(1)
P(1)	4260(1)	3755(1)	295(1)	20(1)
P(5)	3484(1)	1678(1)	1107(1)	20(1)
O(1)	2724(3)	3665(1)	1143(2)	25(1)
O(2)	2464(3)	2455(1)	1683(2)	24(1)
O(3)	1177(3)	2814(1)	125(2)	29(1)
O(4)	4919(3)	2956(1)	2023(2)	30(1)
N(1)	4308(3)	3187(1)	401(2)	19(1)
N(2)	3715(3)	2136(1)	715(2)	20(1)
C(1)	4056(4)	2874(2)	-211(2)	21(1)
C(2)	4834(5)	2407(2)	-57(2)	23(1)
C(3)	4926(4)	2155(2)	615(2)	21(1)
C(4)	6209(5)	2502(2)	32(3)	34(1)
C(5)	4188(5)	2080(2)	-687(3)	32(1)
C(6)	4526(5)	4057(2)	1094(2)	24(1)
C(7)	3615(4)	3995(2)	1385(2)	24(1)
C(8)	3698(5)	4317(2)	1936(3)	27(1)
C(9)	4797(5)	4592(2)	2238(3)	30(1)
C(10)	5801(5)	4598(2)	2016(3)	30(1)
C(11)	5616(5)	4347(2)	1416(2)	27(1)
C(12)	2577(5)	4352(2)	2165(3)	31(1)
C(13)	1327(5)	4442(2)	1531(3)	44(1)
C(14)	2472(6)	3893(2)	2539(3)	39(1)
C(15)	2759(6)	4775(2)	2670(3)	46(2)
C(16)	7037(5)	4876(2)	2430(3)	36(1)
C(17)	6752(6)	5416(2)	2426(3)	44(2)
C(18)	8043(6)	4803(2)	2134(3)	47(2)
C(19)	7595(6)	4699(2)	3189(3)	49(2)
C(20)	5505(4)	3986(2)	42(2)	22(1)
C(21)	6714(5)	3780(2)	335(3)	30(1)
C(22)	7730(5)	3974(2)	223(3)	36(1)
C(23)	7534(6)	4380(2)	-191(3)	41(1)
C(24)	6331(6)	4585(2)	-493(3)	38(1)
C(25)	5317(5)	4394(2)	-374(3)	30(1)
C(26)	2777(4)	3981(2)	-382(2)	24(1)
C(27)	2433(5)	3840(2)	-1073(2)	29(1)
C(28)	1294(5)	3985(2)	-1598(3)	38(1)
C(29)	477(5)	4281(2)	-1438(3)	40(1)
C(30)	801(5)	4430(2)	-763(3)	42(1)
C(31)	1931(5)	4278(2)	-236(3)	34(1)
C(32)	1956(4)	1687(2)	1161(2)	22(1)
C(33)	1665(4)	2087(2)	1488(2)	21(1)
C(34)	530(4)	2069(2)	1621(2)	22(1)
C(35)	-275(4)	1681(2)	1354(2)	26(1)
C(36)	-39(4)	1297(2)	993(2)	24(1)
C(37)	1109(4)	1303(2)	916(2)	22(1)
C(38)	223(5)	2473(2)	2020(3)	28(1)
C(39)	-68(5)	2943(2)	1604(3)	34(1)
C(40)	-967(5)	2352(2)	2162(3)	42(1)
C(41)	1357(5)	2543(2)	2728(3)	34(1)
C(42)	-1024(4)	890(2)	722(3)	27(1)
C(43)	-2337(5)	1093(2)	252(3)	44(1)
C(44)	-1123(6)	633(2)	1349(3)	42(1)
C(45)	-643(5)	519(2)	305(3)	40(1)
C(46)	4704(5)	1578(2)	1979(2)	24(1)
C(47)	5966(5)	1492(2)	2074(3)	34(1)
C(48)	6915(5)	1416(2)	2728(3)	43(1)
C(49)	6614(6)	1427(2)	3300(3)	46(2)
C(50)	5374(6)	1512(2)	3216(3)	40(1)
C(51)	4411(5)	1588(2)	2560(3)	31(1)
C(52)	3525(4)	1128(2)	645(2)	22(1)
C(53)	2882(5)	1133(2)	-71(3)	32(1)

Appendix 1. Crystallographic data

C(54)	2890(5)	728(2)	-456(3)	38(1)
C(55)	3520(5)	321(2)	-131(3)	38(1)
C(56)	4141(6)	307(2)	582(3)	40(1)
C(57)	4142(5)	708(2)	969(3)	32(1)
C(58)	80(5)	2660(2)	-448(3)	37(1)
C(59)	-157(6)	3036(2)	-1013(3)	50(2)
C(60)	-1064(6)	2638(3)	-270(3)	56(2)
C(61)	352(6)	2180(2)	-686(3)	49(2)
C(62)	4944(6)	2934(2)	2712(3)	45(2)
C(63)	6020(6)	3272(3)	3137(3)	56(2)
C(64)	6822(7)	3301(3)	2714(4)	60(2)
C(65)	6226(5)	2979(2)	2122(3)	44(2)

U(eq) is defined as 1/3 the trace of the Uij tensor.

Table 3. Bond lengths (Å) and angles (deg) for pa666

Y(1)-O(3)	2.072(3)	Y(1)-O(2)	2.191(3)
Y(1)-O(1)	2.232(3)	Y(1)-N(2)	2.402(4)
Y(1)-N(1)	2.432(4)	Y(1)-O(4)	2.462(3)
P(1)-N(1)	1.597(4)	P(1)-C(6)	1.791(5)
P(1)-C(20)	1.822(5)	P(1)-C(26)	1.825(5)
P(5)-N(2)	1.599(4)	P(5)-C(32)	1.793(5)
P(5)-C(46)	1.819(5)	P(5)-C(52)	1.823(5)
O(1)-C(7)	1.310(6)	O(2)-C(33)	1.322(5)
O(3)-C(58)	1.408(6)	O(4)-C(65)	1.421(6)
O(4)-C(62)	1.439(6)	N(1)-C(1)	1.481(5)
N(2)-C(3)	1.480(5)	C(1)-C(2)	1.534(6)
C(2)-C(4)	1.527(7)	C(2)-C(5)	1.527(7)
C(2)-C(3)	1.542(6)	C(6)-C(11)	1.404(7)
C(6)-C(7)	1.414(6)	C(7)-C(8)	1.436(7)
C(8)-C(9)	1.386(7)	C(8)-C(12)	1.542(7)
C(9)-C(10)	1.402(7)	C(10)-C(11)	1.381(7)
C(10)-C(16)	1.534(7)	C(12)-C(13)	1.528(8)
C(12)-C(14)	1.530(7)	C(12)-C(15)	1.542(7)
C(16)-C(18)	1.526(8)	C(16)-C(17)	1.536(8)
C(16)-C(19)	1.539(8)	C(20)-C(21)	1.386(7)
C(20)-C(25)	1.397(7)	C(21)-C(22)	1.383(7)
C(22)-C(23)	1.389(8)	C(23)-C(24)	1.380(8)
C(24)-C(25)	1.385(7)	C(26)-C(31)	1.395(7)
C(26)-C(27)	1.400(7)	C(27)-C(28)	1.380(7)
C(28)-C(29)	1.384(8)	C(29)-C(30)	1.378(8)
C(30)-C(31)	1.382(8)	C(32)-C(37)	1.393(6)
C(32)-C(33)	1.416(6)	C(33)-C(34)	1.432(6)
C(34)-C(35)	1.383(7)	C(34)-C(38)	1.526(6)
C(35)-C(36)	1.397(7)	C(36)-C(37)	1.385(6)
C(36)-C(42)	1.536(6)	C(38)-C(39)	1.533(7)
C(38)-C(41)	1.537(7)	C(38)-C(40)	1.541(7)
C(42)-C(45)	1.527(7)	C(42)-C(43)	1.531(7)
C(42)-C(44)	1.543(7)	C(46)-C(51)	1.389(7)
C(46)-C(47)	1.393(7)	C(47)-C(48)	1.379(7)
C(48)-C(49)	1.376(8)	C(49)-C(50)	1.37(1)
C(50)-C(51)	1.388(7)	C(52)-C(53)	1.383(7)
C(52)-C(57)	1.390(7)	C(53)-C(54)	1.391(7)
C(54)-C(55)	1.366(8)	C(55)-C(56)	1.373(8)
C(56)-C(57)	1.383(7)	C(58)-C(60)	1.499(8)
C(58)-C(61)	1.504(8)	C(58)-C(59)	1.522(8)
C(62)-C(63)	1.516(8)	C(63)-C(64)	1.51(1)
C(64)-C(65)	1.46(1)		
O(3)-Y(1)-O(2)	95.6(1)	O(3)-Y(1)-O(1)	96.1(1)
O(2)-Y(1)-O(1)	109.3(1)	O(3)-Y(1)-N(2)	92.9(1)
O(2)-Y(1)-N(2)	83.2(1)	O(1)-Y(1)-N(2)	163.7(1)
O(3)-Y(1)-N(1)	103.1(1)	O(2)-Y(1)-N(1)	155.8(1)
O(1)-Y(1)-N(1)	84.0(1)	N(2)-Y(1)-N(1)	80.8(1)
O(3)-Y(1)-O(4)	173.5(1)	O(2)-Y(1)-O(4)	78.3(1)
O(1)-Y(1)-O(4)	83.7(1)	N(2)-Y(1)-O(4)	88.9(1)
N(1)-Y(1)-O(4)	83.4(1)	N(1)-P(1)-C(6)	110.6(2)
N(1)-P(1)-C(20)	113.8(2)	C(6)-P(1)-C(20)	104.6(2)
N(1)-P(1)-C(26)	114.8(2)	C(6)-P(1)-C(26)	108.7(2)
C(20)-P(1)-C(26)	103.7(2)	N(2)-P(5)-C(32)	112.8(2)
N(2)-P(5)-C(46)	115.0(2)	C(32)-P(5)-C(46)	107.7(2)
N(2)-P(5)-C(52)	110.7(2)	C(32)-P(5)-C(52)	106.4(2)
C(46)-P(5)-C(52)	103.6(2)	C(7)-O(1)-Y(1)	128.5(3)
C(33)-O(2)-Y(1)	123.1(3)	C(58)-O(3)-Y(1)	167.1(3)
C(65)-O(4)-C(62)	105.3(4)	C(65)-O(4)-Y(1)	130.9(3)
C(62)-O(4)-Y(1)	123.6(3)	C(1)-N(1)-P(1)	118.6(3)
C(1)-N(1)-Y(1)	106.1(3)	P(1)-N(1)-Y(1)	114.3(2)
C(3)-N(2)-P(5)	117.3(3)	C(3)-N(2)-Y(1)	116.1(3)
P(5)-N(2)-Y(1)	116.1(2)	N(1)-C(1)-C(2)	115.1(4)
C(4)-C(2)-C(5)	108.7(4)	C(4)-C(2)-C(1)	110.9(4)
C(5)-C(2)-C(1)	106.8(4)	C(4)-C(2)-C(3)	106.4(4)

C(5)-C(2)-C(3)	110.7(4)	C(1)-C(2)-C(3)	113.3(4)
N(2)-C(3)-C(2)	115.2(4)	C(11)-C(6)-C(7)	121.6(4)
C(11)-C(6)-P(1)	120.1(4)	C(7)-C(6)-P(1)	118.2(3)
O(1)-C(7)-C(6)	120.6(4)	O(1)-C(7)-C(8)	122.5(4)
C(6)-C(7)-C(8)	116.9(4)	C(9)-C(8)-C(7)	117.8(4)
C(9)-C(8)-C(12)	122.2(4)	C(7)-C(8)-C(12)	120.0(4)
C(8)-C(9)-C(10)	124.3(5)	C(11)-C(10)-C(9)	117.1(5)
C(11)-C(10)-C(16)	122.7(5)	C(9)-C(10)-C(16)	120.2(4)
C(10)-C(11)-C(6)	120.5(5)	C(13)-C(12)-C(14)	110.2(5)
C(13)-C(12)-C(8)	109.7(4)	C(14)-C(12)-C(8)	110.8(4)
C(13)-C(12)-C(15)	107.0(5)	C(14)-C(12)-C(15)	107.5(4)
C(8)-C(12)-C(15)	111.5(4)	C(18)-C(16)-C(10)	111.7(4)
C(18)-C(16)-C(17)	108.7(5)	C(10)-C(16)-C(17)	110.4(5)
C(18)-C(16)-C(19)	108.4(5)	C(10)-C(16)-C(19)	109.0(4)
C(17)-C(16)-C(19)	108.6(5)	C(21)-C(20)-C(25)	119.1(4)
C(21)-C(20)-P(1)	118.6(4)	C(25)-C(20)-P(1)	122.0(4)
C(22)-C(21)-C(20)	121.0(5)	C(21)-C(22)-C(23)	119.4(5)
C(24)-C(23)-C(22)	120.1(5)	C(23)-C(24)-C(25)	120.4(5)
C(24)-C(25)-C(20)	119.9(5)	C(31)-C(26)-C(27)	117.8(4)
C(31)-C(26)-P(1)	122.6(4)	C(27)-C(26)-P(1)	119.6(4)
C(28)-C(27)-C(26)	121.6(5)	C(27)-C(28)-C(29)	119.3(5)
C(30)-C(29)-C(28)	120.2(5)	C(29)-C(30)-C(31)	120.4(5)
C(30)-C(31)-C(26)	120.7(5)	C(37)-C(32)-C(33)	121.2(4)
C(37)-C(32)-P(5)	120.8(4)	C(33)-C(32)-P(5)	117.9(3)
O(2)-C(33)-C(32)	119.5(4)	O(2)-C(33)-C(34)	122.0(4)
C(32)-C(33)-C(34)	118.5(4)	C(35)-C(34)-C(33)	116.9(4)
C(35)-C(34)-C(38)	122.5(4)	C(33)-C(34)-C(38)	120.6(4)
C(34)-C(35)-C(36)	125.2(4)	C(37)-C(36)-C(35)	117.0(4)
C(37)-C(36)-C(42)	123.4(4)	C(35)-C(36)-C(42)	119.6(4)
C(36)-C(37)-C(32)	120.9(4)	C(34)-C(38)-C(39)	111.1(4)
C(34)-C(38)-C(41)	109.6(4)	C(39)-C(38)-C(41)	110.3(4)
C(39)-C(38)-C(40)	111.2(4)	C(39)-C(38)-C(40)	107.0(4)
C(41)-C(38)-C(40)	107.6(4)	C(45)-C(42)-C(43)	108.2(4)
C(45)-C(42)-C(36)	112.1(4)	C(43)-C(42)-C(36)	110.1(4)
C(45)-C(42)-C(44)	108.4(5)	C(43)-C(42)-C(44)	109.4(4)
C(36)-C(42)-C(44)	108.7(4)	C(51)-C(46)-C(47)	118.7(5)
C(51)-C(46)-P(5)	121.7(4)	C(47)-C(46)-P(5)	119.6(4)
C(48)-C(47)-C(46)	121.1(5)	C(49)-C(48)-C(47)	119.7(5)
C(50)-C(49)-C(48)	120.0(5)	C(49)-C(50)-C(51)	120.8(5)
C(50)-C(51)-C(46)	119.7(5)	C(53)-C(52)-C(57)	118.8(4)
C(53)-C(52)-P(5)	116.9(4)	C(57)-C(52)-P(5)	124.2(4)
C(52)-C(53)-C(54)	119.8(5)	C(55)-C(54)-C(53)	120.6(5)
C(54)-C(55)-C(56)	120.3(5)	C(55)-C(56)-C(57)	119.7(5)
C(56)-C(57)-C(52)	120.8(5)	O(3)-C(58)-C(60)	111.1(5)
O(3)-C(58)-C(61)	108.9(5)	C(60)-C(58)-C(61)	111.3(5)
105.9(5)		C(60)-C(58)-C(59)	109.1(5)
110.3(5)		O(4)-C(62)-C(63)	104.3(5)
103.0(5)		C(65)-C(64)-C(63)	106.5(6)
104.5(5)			

Appendix 1. Crystallographic data

Table 4. Anisotropic displacement parameters ($\text{Å}^2 \times 10^3$) for pa666

atom	U11	U22	U33	U23	U13	U12
Y(1)	34(1)	24(1)	31(1)	6(1)	22(1)	7(1)
P(1)	18(1)	22(1)	21(1)	-2(1)	9(1)	-2(1)
P(5)	19(1)	20(1)	22(1)	-3(1)	11(1)	-2(1)
O(1)	22(2)	21(2)	34(2)	-6(1)	15(2)	-3(1)
O(2)	24(2)	25(2)	27(2)	-7(1)	16(1)	-8(1)
O(3)	12(2)	41(2)	21(2)	-8(2)	-6(1)	2(1)
O(4)	20(2)	49(2)	20(2)	1(2)	8(1)	-1(2)
N(1)	18(2)	22(2)	16(2)	-2(2)	7(2)	-1(2)
N(2)	14(2)	26(2)	20(2)	0(2)	9(2)	-1(2)
C(1)	22(2)	24(2)	17(2)	1(2)	8(2)	3(2)
C(2)	28(3)	23(2)	24(2)	2(2)	16(2)	2(2)
C(3)	15(2)	23(2)	24(2)	-2(2)	9(2)	-3(2)
C(4)	32(3)	35(3)	47(3)	10(2)	29(3)	8(2)
C(5)	43(3)	28(3)	31(3)	-1(2)	21(2)	6(2)
C(6)	25(2)	20(2)	27(2)	-5(2)	11(2)	-4(2)
C(7)	23(2)	22(2)	28(3)	1(2)	11(2)	1(2)
C(8)	29(3)	22(2)	30(3)	-3(2)	13(2)	-1(2)
C(9)	38(3)	25(3)	28(3)	-8(2)	16(2)	-3(2)
C(10)	35(3)	26(3)	27(3)	-5(2)	12(2)	-9(2)
C(11)	30(3)	28(3)	25(2)	-3(2)	14(2)	-5(2)
C(12)	37(3)	28(3)	34(3)	-7(2)	21(2)	-1(2)
C(13)	35(3)	52(4)	50(4)	-8(3)	23(3)	8(3)
C(14)	47(3)	43(3)	38(3)	-6(3)	28(3)	-4(3)
C(15)	55(4)	42(3)	57(4)	-23(3)	38(3)	-9(3)
C(16)	40(3)	39(3)	29(3)	-12(2)	14(2)	-17(3)
C(17)	57(4)	36(3)	45(3)	-12(3)	26(3)	-20(3)
C(18)	36(3)	52(4)	52(4)	-20(3)	17(3)	-18(3)
C(19)	48(4)	50(4)	36(3)	-5(3)	4(3)	-20(3)
C(20)	22(2)	26(2)	20(2)	-6(2)	9(2)	-7(2)
C(21)	28(3)	30(3)	32(3)	-2(2)	14(2)	-5(2)
C(22)	22(3)	44(3)	45(3)	-10(3)	18(2)	-8(2)
C(23)	41(3)	43(3)	52(4)	-9(3)	31(3)	-19(3)
C(24)	45(3)	34(3)	42(3)	1(2)	24(3)	-14(3)
C(25)	34(3)	28(3)	30(3)	-4(2)	15(2)	-6(2)
C(26)	17(2)	24(2)	28(3)	4(2)	5(2)	-3(2)
C(27)	30(3)	28(3)	23(2)	3(2)	7(2)	0(2)
C(28)	41(3)	36(3)	30(3)	10(2)	8(2)	-1(3)
C(29)	25(3)	46(3)	42(3)	21(3)	5(2)	3(2)
C(30)	32(3)	42(3)	53(4)	12(3)	19(3)	10(3)
C(31)	31(3)	34(3)	33(3)	0(2)	12(2)	2(2)
C(32)	20(2)	26(2)	20(2)	-1(2)	10(2)	-4(2)
C(33)	22(2)	22(2)	21(2)	-1(2)	11(2)	-2(2)
C(34)	13(2)	26(2)	27(2)	-1(2)	8(2)	-2(2)
C(35)	20(2)	33(3)	27(2)	4(2)	11(2)	-2(2)
C(36)	20(2)	24(2)	27(2)	2(2)	8(2)	-5(2)
C(37)	21(2)	22(2)	21(2)	-1(2)	5(2)	-2(2)
C(38)	21(2)	32(3)	35(3)	-9(2)	17(2)	-4(2)
C(39)	30(3)	34(3)	40(3)	-7(2)	16(2)	2(2)
C(40)	31(3)	52(4)	55(4)	-17(3)	30(3)	-8(3)
C(41)	32(3)	47(3)	27(3)	-8(2)	16(2)	-6(2)
C(42)	19(2)	27(3)	31(3)	0(2)	5(2)	-7(2)
C(43)	29(3)	36(3)	52(4)	-1(3)	3(3)	-5(2)
C(44)	44(3)	39(3)	41(3)	4(3)	14(3)	-15(3)
C(45)	35(3)	31(3)	53(4)	-14(3)	17(3)	-13(2)
C(46)	28(3)	19(2)	24(2)	-1(2)	9(2)	-5(2)
C(47)	26(3)	46(3)	30(3)	10(2)	12(2)	4(2)
C(48)	28(3)	56(4)	38(3)	13(3)	6(3)	2(3)
C(49)	48(4)	51(4)	29(3)	11(3)	5(3)	-3(3)
C(50)	48(4)	47(3)	23(3)	4(2)	12(3)	-3(3)
C(51)	34(3)	33(3)	27(3)	-1(2)	15(2)	-2(2)
C(52)	20(2)	22(2)	26(2)	-5(2)	13(2)	-4(2)
C(53)	32(3)	30(3)	33(3)	-6(2)	13(2)	-4(2)
C(54)	36(3)	43(3)	35(3)	-17(3)	13(3)	-12(3)

Appendix 1. Crystallographic data

C(55)	37(3)	28(3)	58(4)	-18(3)	27(3)	-6(2)
C(56)	46(3)	26(3)	54(4)	-1(3)	27(3)	6(2)
C(57)	37(3)	27(3)	33(3)	-2(2)	17(2)	0(2)
C(58)	33(3)	47(3)	30(3)	1(2)	11(2)	-2(3)
C(59)	45(4)	57(4)	45(4)	6(3)	16(3)	4(3)
C(60)	37(3)	93(6)	38(3)	-10(3)	16(3)	-8(3)
C(61)	45(4)	55(4)	38(3)	-4(3)	9(3)	-3(3)
C(62)	47(4)	59(4)	30(3)	-4(3)	16(3)	-6(3)
C(63)	39(3)	92(5)	33(3)	-14(3)	9(3)	-12(4)
C(64)	47(4)	71(5)	49(4)	-10(4)	5(3)	-6(4)
C(65)	21(3)	66(4)	38(3)	2(3)	4(2)	-4(3)

The anisotropic displacement factor exponent takes the form
 $2 \pi^2 [h^2 a^{*2} U(11) + \dots + 2 h k a^* b^* U(12)]$

Appendix 1. Crystallographic data

Table 5. Hydrogen Coordinates ($\text{\AA} \times 10^4$) and equivalent isotropic displacement parameters ($\text{\AA}^2 \times 10^3$) for pa666

atom	x	y	z	U(eq)
H(1A)	4239	3058	-562	25
H(1B)	3133	2791	-418	25
H(3A)	5231	1822	614	25
H(3B)	5578	2323	1018	25
H(4A)	6203	2653	-391	51
H(4B)	6679	2198	113	51
H(4C)	6630	2716	430	51
H(5A)	3307	2011	-745	48
H(5B)	4667	1778	-614	48
H(5C)	4175	2239	-1105	48
H(9)	4876	4790	2622	35
H(11)	6230	4371	1219	32
H(13A)	1167	4176	1202	66
H(13B)	1394	4742	1306	66
H(13C)	617	4465	1680	66
H(14A)	3274	3841	2949	59
H(14B)	2311	3619	2222	59
H(14C)	1762	3924	2685	59
H(15A)	2008	4800	2782	69
H(15B)	2858	5073	2451	69
H(15C)	3527	4720	3098	69
H(17A)	7532	5585	2728	66
H(17B)	6078	5467	2595	66
H(17C)	6466	5540	1949	66
H(18A)	8812	4989	2406	70
H(18B)	7699	4910	1648	70
H(18C)	8265	4461	2156	70
H(19A)	7799	4356	3201	73
H(19B)	6964	4748	3389	73
H(19C)	8376	4880	3459	73
H(21)	6847	3502	616	36
H(22)	8555	3831	427	43
H(23)	8230	4518	-266	50
H(24)	6197	4858	-785	46
H(25)	4496	4541	-575	36
H(27)	2997	3640	-1185	34
H(28)	1073	3882	-2063	45
H(29)	-309	4382	-1796	48
H(30)	243	4638	-658.0001	50
H(31)	2135	4376	229	40
H(35)	-1050	1674	1421	31
H(37)	1323	1042	693	27
H(39A)	664	3030	1497	51
H(39B)	-224.0000	3199	1879	51
H(39C)	-832	2901	1170	51
H(40A)	-1719	2327	1719	63
H(40B)	-1106	2606	2446	63
H(40C)	-831	2045	2410	63
H(41A)	1514	2244	2994	51
H(41B)	1154	2800	2986	51
H(41C)	2125	2630	2654	51
H(43A)	-2638	1307	523	65
H(43B)	-2949	829	65	65
H(43C)	-2266	1272	-132	65
H(44A)	-288	495	1644	63
H(44B)	-1764	377	1182	63
H(44C)	-1377.9999	864	1620	63
H(45A)	-602	674	-105	60
H(45B)	-1280	261	155	60
H(45C)	199	385	596	60
H(47)	6178	1486	1681	40
H(48)	7771	1357	2785	52

Appendix 1. Crystallographic data

H(49)	7264	1375	3752	55
H(50)	5173	1520	3613	48
H(51)	3556	1646	2508	37
H(53)	2436	1414	-301	38
H(54)	2454	732	-948	46
H(55)	3527	47	-398	46
H(56)	4568	22	807	48
H(57)	4570	697	1461	38
H(59A)	-312	3348	-847.0001	75
H(59B)	-907	2944	-1430.0001	75
H(59C)	596	3057	-1125	75
H(60A)	-894	2412	116	84
H(60B)	-1812	2529	-675.9999	84
H(60C)	-1234	2957	-131	84
H(61A)	1110	2205	-793	73
H(61B)	-387	2079	-1104	73
H(61C)	510	1942	-317	73
H(62A)	5121	2603	2899	54
H(62B)	4116	3042	2712	54
H(63A)	5683	3591	3183	67
H(63B)	6523	3140	3607	67
H(64A)	6835	3633	2551	72
H(64B)	7713	3199	2998	72
H(65A)	6307	3107	1703	53
H(65B)	6627	2657	2225	53

Complex 55

Table 1. Crystal data for pa717

Compound	pa717
Molecular formula	C ₆₆ H ₈₁ N ₂ O ₄ P ₂ Y, 2(C ₆ H ₁₂)
Molecular weight	1285.49
Crystal habit	Colorless Block
Crystal dimensions(mm)	0.30x0.18x0.12
Crystal system	monoclinic
Space group	C2/c
a(Å)	35.816(1)
b(Å)	19.399(1)
c(Å)	25.180(1)
α(°)	90.00
β(°)	123.852(1)
γ(°)	90.00
V(Å ³)	14529.2(10)
Z	8
d(g·cm ⁻³)	1.175
F(000)	5504
μ(cm ⁻¹)	0.895
Absorption corrections	multi-scan ; 0.7751 min, 0.9002 max
Diffractionmeter	KappaCCD
X-ray source	MoKα
λ(Å)	0.71069
Monochromator	graphite
T (K)	150.0(1)
Scan mode	phi and omega scans
Maximum θ	25.02
HKL ranges	-42 38 ; -23 23 ; -29 29
Reflections measured	38916
Unique data	12685
Rint	0.0564
Reflections used	9343
Criterion	I > 2σ(I)
Refinement type	Fsqd
Hydrogen atoms	constr
Parameters refined	691
Reflections / parameter	13
wR2	0.1679
R1	0.0702
Weights a, b	0.0664 ; 81.241
GoF	1.036
difference peak / hole (e Å ⁻³)	1.745(0.077) / -0.764(0.077)

Table 2. Atomic Coordinates (A x 10⁴) and equivalent isotropic displacement parameters (A² x 10³) for pa717

atom	x	y	z	U(eq)
Y(1)	1954(1)	4890(1)	2493(1)	32(1)
P(1)	1475(1)	3891(1)	3084(1)	29(1)
P(2)	3070(1)	4580(1)	3088(1)	37(1)
O(1)	1280(1)	5130(1)	2310(1)	31(1)
O(2)	2351(1)	5573(1)	2279(1)	32(1)
O(3)	1728(1)	4258(2)	1724(2)	37(1)
O(4)	2088(1)	5938(2)	3131(2)	57(1)
N(1)	1955(1)	4080(2)	3208(2)	32(1)
N(2)	2687(1)	4396(2)	3210(2)	33(1)
C(1)	2373(1)	3868(2)	3750(2)	31(1)
C(2)	2763(1)	4032(2)	3752(2)	33(1)
C(3)	3183(2)	3833(2)	4282(2)	40(1)
C(4)	3233(2)	3493(2)	4796(2)	41(1)
C(5)	2857(2)	3336(2)	4799(2)	39(1)
C(6)	2437(2)	3531(2)	4285(2)	34(1)
C(7)	1012(1)	4008(2)	2269(2)	30(1)
C(8)	946(1)	4678(2)	2009(2)	30(1)
C(9)	519(1)	4835(2)	1450(2)	30(1)
C(10)	210(2)	4301(2)	1156(2)	35(1)
C(11)	282(1)	3624(2)	1381(2)	32(1)
C(12)	687(1)	3493(2)	1955(2)	32(1)
C(13)	407(2)	5580(2)	1204(2)	36(1)
C(14)	732(2)	5826(2)	1025(3)	42(1)
C(15)	-75(2)	5661(2)	616(2)	42(1)
C(16)	454(2)	6041(2)	1734(3)	44(1)
C(17)	-56(2)	3049(2)	1016(2)	41(1)
C(18)	56(2)	2703(3)	567(3)	69(2)
C(19)	-542(2)	3322(3)	604(3)	54(2)
C(20)	-39(2)	2507(3)	1470(3)	78(2)
C(21)	1333(2)	4422(2)	3538(2)	34(1)
C(22)	883(2)	4516(3)	3337(3)	45(1)
C(23)	781(2)	4927(3)	3680(3)	61(2)
C(24)	1123(2)	5264(3)	4230(3)	60(2)
C(25)	1561(2)	5183(3)	4428(3)	54(1)
C(26)	1669(2)	4767(2)	4080(2)	43(1)
C(27)	1430(1)	2997(2)	3257(2)	32(1)
C(28)	1617(2)	2503(2)	3070(2)	39(1)
C(29)	1554(2)	1804(3)	3132(3)	51(1)
C(30)	1302(2)	1607(3)	3358(3)	54(1)
C(31)	1117(2)	2093(3)	3541(3)	51(1)
C(32)	1180(2)	2788(2)	3491(2)	42(1)
C(33)	2859(2)	4805(2)	2270(2)	39(1)
C(34)	2542(2)	5345(2)	1993(2)	34(1)
C(35)	2445(1)	5620(2)	1399(2)	33(1)
C(36)	2648(2)	5315(2)	1121(2)	38(1)
C(37)	2946(2)	4759(2)	1390(3)	43(1)
C(38)	3053(2)	4520(2)	1976(3)	41(1)
C(39)	2116(2)	6228(2)	1078(2)	37(1)
C(40)	1641(2)	6006(3)	863(3)	47(1)
C(41)	2268(2)	6840(2)	1536(3)	47(1)
C(42)	2090(2)	6488(3)	476(3)	53(1)
C(43)	3149(2)	4402(2)	1057(3)	50(1)
C(44)	3033(3)	4781(3)	452(4)	75(2)
C(45)	3662(2)	4371(3)	1511(4)	73(2)
C(46)	2964(2)	3667(3)	878(3)	66(2)
C(47)	3421(2)	5313(3)	3560(3)	46(1)
C(48)	3619(2)	5716(3)	3329(3)	62(2)
C(49)	3886(2)	6276(3)	3686(4)	84(2)
C(50)	3951(2)	6421(3)	4266(4)	84(2)
C(51)	3747(2)	6030(3)	4488(3)	81(2)
C(52)	3479(2)	5473(3)	4131(3)	60(2)
C(53)	3457(2)	3869(3)	3282(3)	47(1)

Appendix 1. Crystallographic data

C(54)	3917(2)	3969(3)	3607(4)	72(2)
C(55)	4191(2)	3405(4)	3720(5)	109(3)
C(56)	4010(3)	2762(4)	3517(5)	104(3)
C(57)	3560(3)	2659(3)	3212(4)	82(2)
C(58)	3279(2)	3216(3)	3091(3)	55(1)
C(59)	1608(2)	3741(2)	1269(2)	41(1)
C(60)	1881(2)	3805(3)	980(3)	72(2)
C(61)	1121(2)	3790(4)	771(3)	80(2)
C(62)	1712(3)	3045(3)	1614(3)	91(2)
C(63)	2453(2)	6429(4)	3352(4)	94(3)
C(64)	2487(3)	6833(5)	3846(5)	125(4)
C(65)	2090(3)	6656(4)	3871(5)	110(3)
C(66)	1792(2)	6242(4)	3288(4)	75(2)

 U(eq) is defined as 1/3 the trace of the Uij tensor.

Appendix 1. Crystallographic data

Table 3. Bond lengths (Å) and angles (deg) for pa717

Y(1)-O(3)	2.040(3)	Y(1)-O(2)	2.220(3)
Y(1)-O(1)	2.243(3)	Y(1)-N(1)	2.389(4)
Y(1)-N(2)	2.406(3)	Y(1)-O(4)	2.467(3)
P(1)-N(1)	1.606(4)	P(1)-C(7)	1.795(4)
P(1)-C(21)	1.811(5)	P(1)-C(27)	1.818(4)
P(2)-N(2)	1.604(4)	P(2)-C(33)	1.806(5)
P(2)-C(53)	1.818(5)	P(2)-C(47)	1.831(5)
O(1)-C(8)	1.327(5)	O(2)-C(34)	1.313(5)
O(3)-C(59)	1.398(5)	O(4)-C(66)	1.449(7)
O(4)-C(63)	1.454(7)	N(1)-C(1)	1.413(5)
N(2)-C(2)	1.422(6)	C(1)-C(6)	1.398(6)
C(1)-C(2)	1.430(6)	C(2)-C(3)	1.397(6)
C(3)-C(4)	1.372(7)	C(4)-C(5)	1.383(7)
C(5)-C(6)	1.383(6)	C(7)-C(12)	1.397(6)
C(7)-C(8)	1.415(6)	C(8)-C(9)	1.420(6)
C(9)-C(10)	1.390(6)	C(9)-C(13)	1.535(6)
C(10)-C(11)	1.395(6)	C(11)-C(12)	1.385(6)
C(11)-C(17)	1.522(6)	C(13)-C(15)	1.533(7)
C(13)-C(16)	1.537(7)	C(13)-C(14)	1.539(6)
C(17)-C(20)	1.530(7)	C(17)-C(19)	1.539(7)
C(17)-C(18)	1.550(8)	C(21)-C(26)	1.389(7)
C(21)-C(22)	1.406(6)	C(22)-C(23)	1.368(7)
C(23)-C(24)	1.397(8)	C(24)-C(25)	1.363(8)
C(25)-C(26)	1.395(7)	C(27)-C(32)	1.380(6)
C(27)-C(28)	1.390(6)	C(28)-C(29)	1.398(7)
C(29)-C(30)	1.364(8)	C(30)-C(31)	1.369(8)
C(31)-C(32)	1.385(7)	C(33)-C(38)	1.384(6)
C(33)-C(34)	1.411(6)	C(34)-C(35)	1.436(6)
C(35)-C(36)	1.393(6)	C(35)-C(39)	1.539(6)
C(36)-C(37)	1.397(7)	C(37)-C(38)	1.382(7)
C(37)-C(43)	1.546(7)	C(39)-C(41)	1.530(7)
C(39)-C(40)	1.534(7)	C(39)-C(42)	1.549(7)
C(43)-C(44)	1.527(8)	C(43)-C(46)	1.529(7)
C(43)-C(45)	1.532(8)	C(47)-C(52)	1.370(8)
C(47)-C(48)	1.383(7)	C(48)-C(49)	1.39(1)
C(49)-C(50)	1.38(1)	C(50)-C(51)	1.37(1)
C(51)-C(52)	1.391(8)	C(53)-C(58)	1.379(8)
C(53)-C(54)	1.386(8)	C(54)-C(55)	1.39(1)
C(55)-C(56)	1.37(1)	C(56)-C(57)	1.36(1)
C(57)-C(58)	1.390(8)	C(59)-C(61)	1.477(8)
C(59)-C(60)	1.515(7)	C(59)-C(62)	1.535(8)
C(63)-C(64)	1.42(1)	C(64)-C(65)	1.50(1)
C(65)-C(66)	1.48(1)		
O(3)-Y(1)-O(2)	95.5(1)	O(3)-Y(1)-O(1)	96.8(1)
O(2)-Y(1)-O(1)	126.1(1)	O(3)-Y(1)-N(1)	98.9(1)
O(2)-Y(1)-N(1)	147.6(1)	O(1)-Y(1)-N(1)	80.8(1)
O(3)-Y(1)-N(2)	99.4(1)	O(2)-Y(1)-N(2)	80.9(1)
O(1)-Y(1)-N(2)	146.9(1)	N(1)-Y(1)-N(2)	68.3(1)
O(3)-Y(1)-O(4)	160.6(1)	O(2)-Y(1)-O(4)	75.4(1)
O(1)-Y(1)-O(4)	76.0(1)	N(1)-Y(1)-O(4)	97.6(1)
N(2)-Y(1)-O(4)	96.0(1)	N(1)-P(1)-C(7)	113.7(2)
N(1)-P(1)-C(21)	113.2(2)	C(7)-P(1)-C(21)	104.1(2)
N(1)-P(1)-C(27)	113.5(2)	C(7)-P(1)-C(27)	104.2(2)
C(21)-P(1)-C(27)	107.3(2)	N(2)-P(2)-C(33)	114.4(2)
N(2)-P(2)-C(53)	112.6(2)	C(33)-P(2)-C(53)	105.3(2)
N(2)-P(2)-C(47)	113.5(2)	C(33)-P(2)-C(47)	104.7(2)
C(53)-P(2)-C(47)	105.6(2)	C(8)-O(1)-Y(1)	120.2(2)
C(34)-O(2)-Y(1)	122.1(3)	C(59)-O(3)-Y(1)	170.8(3)
C(66)-O(4)-C(63)	105.5(4)	C(66)-O(4)-Y(1)	127.4(3)
C(63)-O(4)-Y(1)	126.6(4)	C(1)-N(1)-P(1)	124.5(3)
C(1)-N(1)-Y(1)	118.2(3)	P(1)-N(1)-Y(1)	116.8(2)
C(2)-N(2)-P(2)	124.6(3)	C(2)-N(2)-Y(1)	117.6(3)
P(2)-N(2)-Y(1)	117.3(2)	C(6)-C(1)-N(1)	125.6(4)
C(6)-C(1)-C(2)	117.7(4)	N(1)-C(1)-C(2)	116.7(4)

Appendix 1. Crystallographic data

C(3)-C(2)-N(2)	125.6(4)	C(3)-C(2)-C(1)	118.1(4)
N(2)-C(2)-C(1)	116.2(4)	C(4)-C(3)-C(2)	122.6(4)
C(3)-C(4)-C(5)	119.7(4)	C(4)-C(5)-C(6)	119.3(4)
C(5)-C(6)-C(1)	122.6(4)	C(12)-C(7)-C(8)	121.6(4)
C(12)-C(7)-P(1)	120.4(3)	C(8)-C(7)-P(1)	117.0(3)
O(1)-C(8)-C(7)	118.6(4)	O(1)-C(8)-C(9)	123.7(4)
C(7)-C(8)-C(9)	117.7(4)	C(10)-C(9)-C(8)	117.8(4)
C(10)-C(9)-C(13)	122.4(4)	C(8)-C(9)-C(13)	119.8(4)
C(9)-C(10)-C(11)	124.9(4)	C(12)-C(11)-C(10)	116.5(4)
C(12)-C(11)-C(17)	120.9(4)	C(10)-C(11)-C(17)	122.6(4)
C(11)-C(12)-C(7)	121.1(4)	C(15)-C(13)-C(9)	112.7(4)
C(15)-C(13)-C(16)	107.4(4)	C(9)-C(13)-C(16)	108.6(4)
C(15)-C(13)-C(14)	108.3(4)	C(9)-C(13)-C(14)	109.9(4)
C(16)-C(13)-C(14)	109.8(4)	C(11)-C(17)-C(20)	111.5(4)
C(11)-C(17)-C(19)	112.1(4)	C(20)-C(17)-C(19)	107.4(4)
C(11)-C(17)-C(18)	108.3(4)	C(20)-C(17)-C(18)	109.3(5)
C(19)-C(17)-C(18)	108.1(5)	C(26)-C(21)-C(22)	118.9(4)
C(26)-C(21)-P(1)	120.0(3)	C(22)-C(21)-P(1)	121.0(4)
C(23)-C(22)-C(21)	120.2(5)	C(22)-C(23)-C(24)	120.2(5)
C(25)-C(24)-C(23)	120.4(5)	C(24)-C(25)-C(26)	120.0(5)
C(21)-C(26)-C(25)	120.3(5)	C(32)-C(27)-C(28)	119.4(4)
C(32)-C(27)-P(1)	123.2(4)	C(28)-C(27)-P(1)	116.9(3)
C(27)-C(28)-C(29)	119.6(5)	C(30)-C(29)-C(28)	120.2(5)
C(29)-C(30)-C(31)	120.3(5)	C(30)-C(31)-C(32)	120.3(5)
C(27)-C(32)-C(31)	120.2(5)	C(38)-C(33)-C(34)	122.5(4)
C(38)-C(33)-P(2)	119.8(4)	C(34)-C(33)-P(2)	117.1(4)
O(2)-C(34)-C(33)	119.9(4)	O(2)-C(34)-C(35)	123.2(4)
C(33)-C(34)-C(35)	116.9(4)	C(36)-C(35)-C(34)	118.3(4)
C(36)-C(35)-C(39)	121.6(4)	C(34)-C(35)-C(39)	120.1(4)
C(35)-C(36)-C(37)	123.8(5)	C(38)-C(37)-C(36)	117.3(4)
C(38)-C(37)-C(43)	119.6(4)	C(36)-C(37)-C(43)	123.1(5)
C(37)-C(38)-C(33)	121.0(4)	C(41)-C(39)-C(40)	110.0(4)
C(41)-C(39)-C(35)	110.6(4)	C(40)-C(39)-C(35)	110.1(4)
C(41)-C(39)-C(42)	106.7(4)	C(40)-C(39)-C(42)	107.3(4)
C(35)-C(39)-C(42)	112.0(4)	C(44)-C(43)-C(46)	108.8(5)
C(44)-C(43)-C(45)	108.1(5)	C(46)-C(43)-C(45)	109.0(5)
C(44)-C(43)-C(37)	112.1(4)	C(46)-C(43)-C(37)	108.8(4)
C(45)-C(43)-C(37)	110.0(5)	C(52)-C(47)-C(48)	120.0(5)
C(52)-C(47)-P(2)	120.4(4)	C(48)-C(47)-P(2)	119.6(5)
C(47)-C(48)-C(49)	119.9(7)	C(50)-C(49)-C(48)	119.5(6)
C(51)-C(50)-C(49)	120.5(6)	C(50)-C(49)-C(52)	120.1(7)
C(47)-C(52)-C(51)	120.0(6)	C(58)-C(53)-C(54)	120.0(5)
C(58)-C(53)-P(2)	117.9(4)	C(54)-C(53)-P(2)	122.0(4)
C(53)-C(54)-C(55)	118.9(7)	C(56)-C(55)-C(54)	120.5(7)
C(57)-C(56)-C(55)	120.8(6)	C(56)-C(57)-C(58)	119.6(7)
C(53)-C(58)-C(57)	120.1(6)	O(3)-C(59)-C(61)	109.2(4)
O(3)-C(59)-C(60)	110.3(4)	C(61)-C(59)-C(60)	111.0(5)
O(3)-C(59)-C(62)	107.5(4)	C(61)-C(59)-C(62)	109.7(5)
C(60)-C(59)-C(62)	109.0(5)	C(64)-C(63)-O(4)	108.4(6)
C(63)-C(64)-C(65)	107.0(7)	C(66)-C(65)-C(64)	105.1(6)
O(4)-C(66)-C(65)	105.0(6)		

Appendix 1. Crystallographic data

Table 4. Anisotropic displacement parameters ($\text{Å}^2 \times 10^3$) for pa717

atom	U11	U22	U33	U23	U13	U12
Y(1)	30(1)	31(1)	40(1)	5(1)	22(1)	2(1)
P(1)	31(1)	29(1)	33(1)	3(1)	20(1)	2(1)
P(2)	30(1)	35(1)	50(1)	10(1)	25(1)	5(1)
O(1)	26(2)	28(2)	42(2)	-2(1)	21(1)	-1(1)
O(2)	37(2)	28(2)	43(2)	2(1)	29(2)	1(1)
O(3)	39(2)	32(2)	42(2)	-7(1)	25(2)	-3(1)
O(4)	59(2)	55(2)	71(3)	-24(2)	44(2)	-14(2)
N(1)	31(2)	34(2)	34(2)	1(2)	20(2)	2(2)
N(2)	30(2)	39(2)	34(2)	7(2)	20(2)	3(2)
C(1)	29(2)	31(2)	35(2)	-3(2)	20(2)	2(2)
C(2)	30(2)	33(2)	37(3)	1(2)	19(2)	2(2)
C(3)	30(2)	44(3)	49(3)	5(2)	23(2)	1(2)
C(4)	36(3)	41(3)	32(3)	5(2)	12(2)	4(2)
C(5)	39(3)	37(3)	37(3)	5(2)	19(2)	2(2)
C(6)	34(2)	36(2)	34(3)	1(2)	21(2)	-1(2)
C(7)	27(2)	33(2)	37(3)	2(2)	20(2)	2(2)
C(8)	32(2)	30(2)	36(2)	2(2)	25(2)	4(2)
C(9)	31(2)	27(2)	40(3)	8(2)	25(2)	5(2)
C(10)	30(2)	36(2)	39(3)	5(2)	19(2)	4(2)
C(11)	32(2)	32(2)	38(3)	2(2)	23(2)	-1(2)
C(12)	32(2)	29(2)	38(3)	4(2)	22(2)	2(2)
C(13)	34(2)	33(2)	48(3)	4(2)	26(2)	2(2)
C(14)	42(3)	37(3)	57(3)	12(2)	33(3)	4(2)
C(15)	41(3)	34(3)	53(3)	8(2)	27(3)	2(2)
C(16)	44(3)	34(3)	59(3)	7(2)	33(3)	8(2)
C(17)	35(3)	32(2)	52(3)	4(2)	21(2)	-4(2)
C(18)	62(4)	55(4)	93(5)	-30(3)	46(4)	-15(3)
C(19)	34(3)	47(3)	68(4)	-1(3)	19(3)	-8(2)
C(20)	63(4)	67(4)	62(4)	20(3)	8(3)	-35(3)
C(21)	38(3)	34(2)	38(3)	3(2)	26(2)	0(2)
C(22)	40(3)	48(3)	51(3)	-5(2)	28(3)	2(2)
C(23)	50(3)	68(4)	81(4)	-8(3)	47(3)	3(3)
C(24)	65(4)	64(4)	73(4)	-12(3)	53(4)	5(3)
C(25)	55(3)	64(4)	48(3)	-13(3)	32(3)	-1(3)
C(26)	41(3)	47(3)	43(3)	-1(2)	25(2)	4(2)
C(27)	29(2)	34(2)	31(2)	8(2)	15(2)	3(2)
C(28)	39(3)	38(3)	40(3)	6(2)	22(2)	4(2)
C(29)	54(3)	34(3)	58(3)	4(2)	28(3)	6(2)
C(30)	55(3)	35(3)	65(4)	15(3)	30(3)	-2(2)
C(31)	53(3)	49(3)	54(3)	18(3)	31(3)	-1(2)
C(32)	44(3)	43(3)	45(3)	11(2)	28(2)	2(2)
C(33)	38(3)	34(2)	53(3)	5(2)	31(2)	5(2)
C(34)	34(2)	30(2)	45(3)	3(2)	27(2)	-3(2)
C(35)	35(2)	24(2)	47(3)	0(2)	29(2)	-4(2)
C(36)	44(3)	34(2)	51(3)	1(2)	35(2)	-2(2)
C(37)	52(3)	30(2)	70(4)	1(2)	48(3)	1(2)
C(38)	43(3)	33(3)	62(3)	9(2)	38(3)	6(2)
C(39)	44(3)	31(2)	48(3)	6(2)	34(2)	4(2)
C(40)	40(3)	54(3)	48(3)	17(2)	25(3)	10(2)
C(41)	51(3)	32(3)	72(4)	4(2)	43(3)	7(2)
C(42)	73(4)	45(3)	59(3)	16(3)	48(3)	15(3)
C(43)	65(4)	35(3)	77(4)	0(3)	57(3)	5(2)
C(44)	119(6)	56(4)	108(6)	20(4)	99(5)	29(4)
C(45)	72(4)	69(4)	113(6)	-10(4)	73(4)	7(3)
C(46)	92(5)	45(3)	96(5)	-7(3)	74(4)	-1(3)
C(47)	26(2)	43(3)	57(3)	17(2)	16(2)	5(2)
C(48)	50(3)	51(3)	86(5)	13(3)	39(3)	-8(3)
C(49)	60(4)	65(4)	112(7)	16(4)	39(4)	-20(3)
C(50)	65(4)	59(4)	83(5)	12(4)	14(4)	-22(3)
C(51)	83(5)	62(4)	61(4)	5(3)	17(4)	-21(3)
C(52)	58(4)	52(3)	53(4)	8(3)	22(3)	-13(3)
C(53)	46(3)	43(3)	70(4)	24(3)	43(3)	14(2)
C(54)	43(3)	62(4)	118(6)	36(4)	49(4)	21(3)

Appendix 1. Crystallographic data

C(55)	65(5)	89(6)	190(10)	67(6)	85(6)	41(4)
C(56)	104(6)	69(5)	190(10)	65(5)	111(7)	55(5)
C(57)	112(6)	45(4)	135(7)	27(4)	99(6)	24(4)
C(58)	64(4)	50(3)	72(4)	19(3)	52(3)	15(3)
C(59)	45(3)	40(3)	48(3)	-4(2)	31(3)	-3(2)
C(60)	88(5)	71(4)	84(5)	-31(4)	64(4)	-25(3)
C(61)	61(4)	113(6)	65(4)	-44(4)	34(4)	-7(4)
C(62)	141(7)	47(4)	74(5)	-4(3)	53(5)	-7(4)
C(63)	61(4)	99(6)	116(6)	-54(5)	46(4)	-30(4)
C(64)	139(8)	122(7)	150(10)	-81(7)	105(8)	-66(6)
C(65)	143(8)	91(6)	141(8)	-55(5)	107(7)	-46(5)
C(66)	92(5)	73(4)	94(5)	-25(4)	72(5)	-21(4)

The anisotropic displacement factor exponent takes the form
 $2 \pi^2 [h^2 a^{*2} U(11) + \dots + 2 h k a^* b^* U(12)]$

Appendix 1. Crystallographic data

Table 5. Hydrogen Coordinates (A x 10⁴) and equivalent isotropic displacement parameters (A² x 10³) for pa717

atom	x	y	z	U(eq)
H(3)	3444	3938	4287	48
H(4)	3524	3366	5147	49
H(5)	2888	3096	5150	46
H(6)	2182	3433	4297	40
H(10)	-72	4405	774	42
H(12)	744	3046	2138	38
H(14A)	639	6283	826	64
H(14B)	726	5500	723	64
H(14C)	1037	5852	1411	64
H(15A)	-287	5493	717	64
H(15B)	-112.0000	5391	260	64
H(15C)	-135	6148	494	64
H(16A)	378	6517	1580	66
H(16B)	763	6021	2110	66
H(16C)	249	5878	1850	66
H(18A)	49	3050	278	103
H(18B)	-166	2343	315	103
H(18C)	357	2497	823	103
H(19A)	-614	3565	876	82
H(19B)	-749	2934	392	82
H(19C)	-571	3639	279	82
H(20A)	261	2299	1719	118
H(20B)	-264	2149	1222	118
H(20C)	-105	2726	1761	118
H(22)	649	4292	2961	54
H(23)	477	4985	3545	73
H(24)	1051	5550	4466	72
H(25)	1793	5411	4803	65
H(26)	1974	4719	4215	52
H(28)	1786	2640	2902	46
H(29)	1687	1465	3015	61
H(30)	1254	1131	3389	64
H(31)	945	1951	3704	61
H(32)	1051	3122	3617	50
H(36)	2581	5493	726	45
H(38)	3263	4154	2179	49
H(40A)	1536	5640	542	70
H(40B)	1437	6402	678	70
H(40C)	1645	5833	1233	70
H(41A)	2258	6712	1905	71
H(41B)	2067	7232	1315	71
H(41C)	2576	6968	1683	71
H(42A)	2391	6618	593	79
H(42B)	1891	6889	300	79
H(42C)	1972	6120	155	79
H(44A)	2705	4803	152	113
H(44B)	3163	4534	252	113
H(44C)	3155	5249	562	113
H(45A)	3788	4165	1289	109
H(45B)	3744	4090	1885	109
H(45C)	3781	4839	1650	109
H(46A)	2637	3683	577	99
H(46B)	3041	3416	1264	99
H(46C)	3098	3431	677	99
H(48)	3573	5612	2928	74
H(49)	4023	6555	3529	101
H(50)	4139	6796	4515	100
H(51)	3789	6139	4885	97
H(52)	3336	5204	4284	71
H(54)	4043	4416	3750	87
H(55)	4507	3467	3940	130
H(56)	4201	2383	3590	125

Appendix 1. Crystallographic data

H(57)	3438	2208	3084	98
H(58)	2964	3147	2875	66
H(60A)	1823	4254	770	108
H(60B)	1796	3437	666	108
H(60C)	2202	3765	1319	108
H(61A)	952	3728	966	120
H(61B)	1036	3430	449	120
H(61C)	1054	4243	566	120
H(62A)	2024	3043	1986	137
H(62B)	1669	2674	1321	137
H(62C)	1509	2974	1755	137
H(63A)	2739	6181	3514	112
H(63B)	2392	6729	2994	112
H(64A)	2484	7329	3755	151
H(64B)	2770	6727	4261	151
H(65A)	2184	6386	4260	132
H(65B)	1935	7079	3870	132
H(66A)	1636	5880	3371	90
H(66B)	1564	6539	2935	90

Appendix 1. Crystallographic data

Complex 56'

Table 1. Crystal data for pa679bis

Compound	pa679bis
Molecular formula	C ₁₁₄ H ₁₄₄ N ₆ O ₆ P ₄ Y ₂ , 2(C ₆ H ₁₂)
Molecular weight	2164.36
Crystal habit	Colorless Block
Crystal dimensions(mm)	0.22x0.20x0.20
Crystal system	monoclinic
Space group	C2/c
a(Å)	27.529(1)
b(Å)	28.356(1)
c(Å)	18.325(1)
α(°)	90.00
β(°)	124.463(1)
γ(°)	90.00
V(Å ³)	11794.1(9)
Z	4
d(g·cm ⁻³)	1.219
F(000)	4608
μ(cm ⁻¹)	1.089
Absorption corrections	multi-scan ; 0.7956 min, 0.8116 max
Diffractometer	KappaCCD
X-ray source	MoKα
λ(Å)	0.71069
Monochromator	graphite
T (K)	150.0(1)
Scan mode	phi and omega scans
Maximum θ	26.02
HKL ranges	-33 33 ; -32 34 ; -16 22
Reflections measured	28082
Unique data	11468
Rint	0.0465
Reflections used	8593
Criterion	I > 2σ(I)
Refinement type	Fsqd
Hydrogen atoms	constr
Parameters refined	635
Reflections / parameter	13
wR2	0.1136
R1	0.0565
Weights a, b	0.0259 ; 50.837
GoF	1.050
difference peak / hole (e Å ⁻³)	0.584(0.072) / -0.391(0.072)

Appendix 1. Crystallographic data

Table 2. Atomic Coordinates (A x 10⁴) and equivalent isotropic displacement parameters (A² x 10³) for pa679bis

atom	x	y	z	U(eq)
Y(1)	5043(1)	3027(1)	3605(1)	24(1)
P(1)	5190(1)	3610(1)	5491(1)	27(1)
P(2)	4297(1)	1907(1)	3541(1)	28(1)
O(1)	5856(1)	3447(1)	4610(2)	28(1)
O(2)	5507(1)	2403(1)	4469(2)	26(1)
O(3)	5000	3521(1)	2500	30(1)
O(4)	5000	2639(1)	2500	31(1)
N(1)	4774(1)	3410(1)	4517(2)	31(1)
N(2)	4019(1)	3361(1)	2691(2)	32(1)
N(3)	4246(1)	2438(1)	3217(2)	29(1)
C(1)	4134(2)	3364(2)	4122(3)	38(1)
C(2)	3808(2)	3570(1)	3200(3)	37(1)
C(3)	3635(2)	3000(1)	2038(2)	34(1)
C(4)	3632(2)	2566(1)	2505(2)	34(1)
C(5)	5850(2)	3882(1)	5718(2)	28(1)
C(6)	6108(2)	3752(1)	5263(2)	26(1)
C(7)	6665(1)	3975(1)	5564(2)	26(1)
C(8)	6896(2)	4300(1)	6245(2)	31(1)
C(9)	6637(2)	4432(1)	6688(2)	34(1)
C(10)	6112(2)	4216(1)	6410(2)	31(1)
C(11)	6999(2)	3854(1)	5143(2)	30(1)
C(12)	6609(2)	3990(1)	4161(2)	34(1)
C(13)	7143(2)	3325(1)	5258(2)	32(1)
C(14)	7579(2)	4126(2)	5557(3)	41(1)
C(15)	6928(2)	4805(2)	7425(3)	47(1)
C(16A)	7555(3)	4664(3)	8170(5)	68(3)
C(17A)	7002(4)	5265(2)	7034(5)	63(2)
C(18A)	6533(4)	4967(3)	7720(7)	84(3)
C(16B)	7592(3)	4854(7)	7850(10)	68(3)
C(17B)	6549(6)	5250(3)	7130(10)	63(2)
C(18B)	6896(8)	4608(5)	8187(8)	84(3)
C(19)	4815(2)	4057(1)	5712(2)	29(1)
C(20)	4662(2)	4478(1)	5242(3)	35(1)
C(21)	4355(2)	4824(1)	5354(3)	41(1)
C(22)	4199(2)	4749(2)	5941(3)	59(1)
C(23)	4340(3)	4330(2)	6400(4)	73(2)
C(24)	4647(2)	3985(2)	6288(3)	50(1)
C(25)	5413(2)	3166(1)	6341(2)	32(1)
C(26)	5807(2)	3252(2)	7247(3)	43(1)
C(27)	5949(2)	2897(2)	7851(3)	50(1)
C(28)	5711(2)	2454(2)	7569(3)	52(1)
C(29)	5331(2)	2358(2)	6677(3)	47(1)
C(30)	5181(2)	2716(1)	6068(3)	36(1)
C(31)	4973(2)	1778(1)	4570(2)	29(1)
C(32)	5497(2)	2029(1)	4873(2)	27(1)
C(33)	6025(2)	1854(1)	5666(2)	29(1)
C(34)	5987(2)	1453(1)	6064(2)	36(1)
C(35)	5464(2)	1200(1)	5755(3)	39(1)
C(36)	4962(2)	1373(1)	5006(2)	35(1)
C(37)	6618(2)	2103(1)	6063(2)	33(1)
C(38)	6779(2)	2108(1)	5382(3)	38(1)
C(39)	7119(2)	1853(2)	6897(3)	54(1)
C(40)	6581(2)	2612(1)	6325(2)	35(1)
C(41)	5469(2)	760(2)	6246(3)	48(1)
C(42)	5583(3)	913(2)	7124(4)	85(2)
C(43)	5955(3)	432(2)	6414(4)	81(2)
C(44)	4880(3)	506(2)	5728(4)	98(2)
C(45)	4214(2)	1468(1)	2749(2)	32(1)
C(46)	4212(2)	984(1)	2884(3)	42(1)
C(47)	4202(2)	666(2)	2300(3)	50(1)
C(48)	4199(2)	821(2)	1585(3)	44(1)
C(49)	4196(2)	1298(2)	1441(3)	42(1)

Appendix 1. Crystallographic data

C(50)	4200(2)	1619(1)	2014(2)	36(1)
C(51)	3699(2)	1787(1)	3671(3)	34(1)
C(52)	3724(2)	2001(2)	4378(3)	46(1)
C(53)	3238(2)	2003(2)	4413(3)	60(1)
C(54)	2720(2)	1796(2)	3751(3)	58(1)
C(55)	2684(2)	1581(2)	3048(3)	45(1)
C(56)	3177(2)	1575(1)	3010(3)	37(1)
C(57)	4986(8)	4008(2)	2330(7)	32(3)
C(58)	4892(4)	4296(2)	2928(5)	44(2)

U(eq) is defined as 1/3 the trace of the U_{ij} tensor.

Table 3. Bond lengths (Å) and angles (deg) for pa679bis

Y(1)-O(2)	2.230(2)	Y(1)-O(4)	2.248(2)
Y(1)-O(1)	2.271(2)	Y(1)-O(3)	2.411(2)
Y(1)-N(1)	2.433(3)	Y(1)-N(2)	2.511(3)
Y(1)-N(3)	2.517(3)	Y(1)-Y(1)#2	3.9225(7)
P(1)-N(1)	1.583(3)	P(1)-C(5)	1.794(3)
P(1)-C(25)	1.819(4)	P(1)-C(19)	1.820(4)
P(2)-N(3)	1.596(3)	P(2)-C(31)	1.784(4)
P(2)-C(51)	1.824(4)	P(2)-C(45)	1.825(4)
O(1)-C(6)	1.311(4)	O(2)-C(32)	1.303(4)
O(3)-C(57)#2	1.411(4)	O(3)-C(57)	1.411(4)
O(3)-Y(1)#2	2.411(2)	O(4)-Y(1)#2	2.248(2)
O(4)-H(40)	0.76(6)	N(1)-C(1)	1.483(4)
N(2)-C(3)	1.469(5)	N(2)-C(2)	1.474(5)
N(2)-H(2N)	0.93(4)	N(3)-C(4)	1.482(4)
C(1)-C(2)	1.512(5)	C(1)-H(1A)	0.9900
C(1)-H(1B)	0.9900	C(2)-H(2A)	0.9900
C(2)-H(2B)	0.9900	C(3)-C(4)	1.502(5)
C(3)-H(3A)	0.9900	C(3)-H(3B)	0.9900
C(4)-H(4A)	0.9900	C(4)-H(4B)	0.9900
C(5)-C(10)	1.409(5)	C(5)-C(6)	1.417(5)
C(6)-C(7)	1.448(5)	C(7)-C(8)	1.382(5)
C(7)-C(11)	1.537(5)	C(8)-C(9)	1.400(5)
C(8)-H(8)	0.9500	C(9)-C(10)	1.375(5)
C(9)-C(15)	1.536(5)	C(10)-H(10)	0.9500
C(11)-C(14)	1.533(5)	C(11)-C(12)	1.533(5)
C(11)-C(13)	1.534(5)	C(12)-H(12A)	0.9800
C(12)-H(12B)	0.9800	C(12)-H(12C)	0.9800
C(13)-H(13A)	0.9800	C(13)-H(13B)	0.9800
C(13)-H(13C)	0.9800	C(14)-H(14A)	0.9800
C(14)-H(14B)	0.9800	C(14)-H(14C)	0.9800
C(15)-C(17B)	1.527(5)	C(15)-C(16A)	1.529(5)
C(15)-C(18A)	1.533(4)	C(15)-C(16B)	1.534(5)
C(15)-C(18B)	1.551(5)	C(15)-C(17A)	1.557(4)
C(16A)-H(16A)	0.9800	C(16A)-H(16B)	0.9800
C(16A)-H(16C)	0.9800	C(17A)-H(17A)	0.9800
C(17A)-H(17B)	0.9800	C(17A)-H(17C)	0.9800
C(18A)-H(18A)	0.9800	C(18A)-H(18B)	0.9800
C(18A)-H(18C)	0.9800	C(16B)-H(16D)	0.9800
C(16B)-H(16E)	0.9800	C(16B)-H(16F)	0.9800
C(17B)-H(17D)	0.9800	C(17B)-H(17E)	0.9800
C(17B)-H(17F)	0.9800	C(18B)-H(18D)	0.9800
C(18B)-H(18E)	0.9800	C(18B)-H(18F)	0.9800
C(19)-C(24)	1.386(5)	C(19)-C(20)	1.392(5)
C(20)-C(21)	1.385(5)	C(20)-H(20)	0.9500
C(21)-C(22)	1.381(6)	C(21)-H(21)	0.9500
C(22)-C(23)	1.378(6)	C(22)-H(22)	0.9500
C(23)-C(24)	1.382(6)	C(23)-H(23)	0.9500
C(24)-H(24)	0.9500	C(25)-C(30)	1.389(5)
C(25)-C(26)	1.398(5)	C(26)-C(27)	1.377(6)
C(26)-H(26)	0.9500	C(27)-C(28)	1.377(6)
C(27)-H(27)	0.9500	C(28)-C(29)	1.380(6)
C(28)-H(28)	0.9500	C(29)-C(30)	1.386(6)
C(29)-H(29)	0.9500	C(30)-H(30)	0.9500
C(31)-C(36)	1.409(5)	C(31)-C(32)	1.411(5)
C(32)-C(33)	1.443(5)	C(33)-C(34)	1.385(5)
C(33)-C(37)	1.534(5)	C(34)-C(35)	1.410(5)
C(34)-H(34)	0.9500	C(35)-C(36)	1.374(5)
C(35)-C(41)	1.533(5)	C(36)-H(36)	0.9500
C(37)-C(39)	1.534(5)	C(37)-C(38)	1.541(5)
C(37)-C(40)	1.543(5)	C(38)-H(38A)	0.9800
C(38)-H(38B)	0.9800	C(38)-H(38C)	0.9800
C(39)-H(39A)	0.9800	C(39)-H(39B)	0.9800
C(39)-H(39C)	0.9800	C(40)-H(40A)	0.9800
C(40)-H(40B)	0.9800	C(40)-H(40C)	0.9800
C(41)-C(43)	1.511(7)	C(41)-C(42)	1.517(7)
C(41)-C(44)	1.519(7)	C(42)-H(42A)	0.9800

C(42)-H(42B)	0.9800	C(42)-H(42C)	0.9800
C(43)-H(43A)	0.9800	C(43)-H(43B)	0.9800
C(43)-H(43C)	0.9800	C(44)-H(44A)	0.9800
C(44)-H(44B)	0.9800	C(44)-H(44C)	0.9800
C(45)-C(50)	1.393(5)	C(45)-C(46)	1.395(5)
C(46)-C(47)	1.389(6)	C(46)-H(46)	0.9500
C(47)-C(48)	1.379(6)	C(47)-H(47)	0.9500
C(48)-C(49)	1.377(6)	C(48)-H(48)	0.9500
C(49)-C(50)	1.384(5)	C(49)-H(49)	0.9500
C(50)-H(50)	0.9500	C(51)-C(56)	1.387(5)
C(51)-C(52)	1.398(5)	C(52)-C(53)	1.375(6)
C(52)-H(52)	0.9500	C(53)-C(54)	1.376(6)
C(53)-H(53)	0.9500	C(54)-C(55)	1.378(6)
C(54)-H(54)	0.9500	C(55)-C(56)	1.396(5)
C(55)-H(55)	0.9500	C(56)-H(56)	0.9500
C(57)-C(58)	1.500(2)	C(57)-H(57A)	0.9900
C(57)-H(57B)	0.9900	C(58)-H(58A)	0.9800
C(58)-H(58B)	0.9800	C(58)-H(58C)	0.9800
O(2)-Y(1)-O(4)	88.2(1)	O(2)-Y(1)-O(1)	86.26(8)
O(4)-Y(1)-O(1)	120.81(6)	O(2)-Y(1)-O(3)	142.48(7)
O(4)-Y(1)-O(3)	64.8(1)	O(1)-Y(1)-O(3)	86.17(7)
O(2)-Y(1)-N(1)	98.2(1)	O(4)-Y(1)-N(1)	162.89(7)
O(1)-Y(1)-N(1)	75.7(1)	O(3)-Y(1)-N(1)	115.3(1)
O(2)-Y(1)-N(2)	138.4(1)	O(4)-Y(1)-N(2)	96.66(8)
O(1)-Y(1)-N(2)	124.3(1)	O(3)-Y(1)-N(2)	73.59(7)
N(1)-Y(1)-N(2)	68.1(1)	O(2)-Y(1)-N(3)	74.5(1)
O(4)-Y(1)-N(3)	80.1(1)	O(1)-Y(1)-N(3)	151.5(1)
O(3)-Y(1)-N(3)	121.84(7)	N(1)-Y(1)-N(3)	86.3(1)
N(2)-Y(1)-N(3)	65.9(1)	O(2)-Y(1)-Y(1)#2	114.10(6)
O(4)-Y(1)-Y(1)#2	29.25(8)	O(1)-Y(1)-Y(1)#2	107.04(6)
O(3)-Y(1)-Y(1)#2	35.55(6)	N(1)-Y(1)-Y(1)#2	147.69(7)
N(2)-Y(1)-Y(1)#2	85.53(7)	N(3)-Y(1)-Y(1)#2	100.05(7)
N(1)-P(1)-C(5)	114.1(2)	N(1)-P(1)-C(25)	113.3(2)
C(5)-P(1)-C(25)	107.0(2)	N(1)-P(1)-C(19)	111.2(2)
C(5)-P(1)-C(19)	106.1(2)	C(25)-P(1)-C(19)	104.5(2)
N(3)-P(2)-C(31)	114.0(2)	N(3)-P(2)-C(51)	109.3(2)
C(31)-P(2)-C(51)	107.6(2)	N(3)-P(2)-C(45)	113.7(2)
C(31)-P(2)-C(45)	106.7(2)	C(51)-P(2)-C(45)	105.1(2)
C(6)-O(1)-Y(1)	148.8(2)	C(32)-O(2)-Y(1)	149.4(2)
C(57)#2-O(3)-C(57)	23.8(5)	C(57)#2-O(3)-Y(1)	113.7(2)
C(57)-O(3)-Y(1)	137.4(2)	C(57)#2-O(3)-Y(1)#2	137.4(2)
C(57)-O(3)-Y(1)#2	113.7(2)	Y(1)-O(3)-Y(1)#2	108.9(1)
Y(1)-O(4)-Y(1)#2	121.5(2)	Y(1)-O(4)-H(40)	119.25(8)
Y(1)#2-O(4)-H(40)	119.25(8)	C(1)-N(1)-P(1)	118.9(2)
C(1)-N(1)-Y(1)	111.4(2)	P(1)-N(1)-Y(1)	128.8(2)
C(3)-N(2)-C(2)	115.8(3)	C(3)-N(2)-Y(1)	107.4(2)
C(2)-N(2)-Y(1)	115.1(2)	C(3)-N(2)-H(2N)	107(2)
C(2)-N(2)-H(2N)	106(2)	Y(1)-N(2)-H(2N)	104(2)
C(4)-N(3)-P(2)	112.0(2)	C(4)-N(3)-Y(1)	117.7(2)
P(2)-N(3)-Y(1)	129.9(2)	N(1)-C(1)-C(2)	107.5(3)
N(1)-C(1)-H(1A)	110.2	C(2)-C(1)-H(1A)	110.2
N(1)-C(1)-H(1B)	110.2	C(2)-C(1)-H(1B)	110.2
H(1A)-C(1)-H(1B)	108.5	N(2)-C(2)-C(1)	110.7(3)
N(2)-C(2)-H(2A)	109.5	C(1)-C(2)-H(2A)	109.5
N(2)-C(2)-H(2B)	109.5	C(1)-C(2)-H(2B)	109.5
H(2A)-C(2)-H(2B)	108.1	N(2)-C(3)-C(4)	109.9(3)
N(2)-C(3)-H(3A)	109.7	C(4)-C(3)-H(3A)	109.7
N(2)-C(3)-H(3B)	109.7	C(4)-C(3)-H(3B)	109.7
H(3A)-C(3)-H(3B)	108.2	N(3)-C(4)-C(3)	109.3(3)
N(3)-C(4)-H(4A)	109.8	C(3)-C(4)-H(4A)	109.8
N(3)-C(4)-H(4B)	109.8	C(3)-C(4)-H(4B)	109.8
H(4A)-C(4)-H(4B)	108.3	C(10)-C(5)-C(6)	122.2(3)
C(10)-C(5)-P(1)	115.7(2)	C(6)-C(5)-P(1)	122.0(3)
O(1)-C(6)-C(5)	121.8(3)	O(1)-C(6)-C(7)	122.4(3)
C(5)-C(6)-C(7)	115.8(3)	C(8)-C(7)-C(6)	118.9(3)
C(8)-C(7)-C(11)	120.1(3)	C(6)-C(7)-C(11)	121.0(3)

C(7)-C(8)-C(9)	125.2(3)	C(7)-C(8)-H(8)	117.4
C(9)-C(8)-H(8)	117.4	C(10)-C(9)-C(8)	116.0(3)
C(10)-C(9)-C(15)	123.3(3)	C(8)-C(9)-C(15)	120.8(3)
C(9)-C(10)-C(5)	121.9(3)	C(9)-C(10)-H(10)	119.1
C(5)-C(10)-H(10)	119.1	C(14)-C(11)-C(12)	107.3(3)
C(14)-C(11)-C(13)	107.9(3)	C(12)-C(11)-C(13)	111.2(3)
C(14)-C(11)-C(7)	113.0(3)	C(12)-C(11)-C(7)	108.2(3)
C(13)-C(11)-C(7)	109.3(3)	C(11)-C(12)-H(12A)	109.5
C(11)-C(12)-H(12B)	109.5	H(12A)-C(12)-H(12B)	109.5
C(11)-C(12)-H(12C)	109.5	H(12A)-C(12)-H(12C)	109.5
H(12B)-C(12)-H(12C)	109.5	C(11)-C(13)-H(13A)	109.5
C(11)-C(13)-H(13B)	109.5	H(13A)-C(13)-H(13B)	109.5
C(11)-C(13)-H(13C)	109.5	H(13A)-C(13)-H(13C)	109.5
H(13B)-C(13)-H(13C)	109.5	C(11)-C(14)-H(14A)	109.5
C(11)-C(14)-H(14B)	109.5	H(14A)-C(14)-H(14B)	109.5
C(11)-C(14)-H(14C)	109.5	H(14A)-C(14)-H(14C)	109.5
H(14B)-C(14)-H(14C)	109.5	C(17B)-C(15)-C(16A)	137.1(7)
C(17B)-C(15)-C(18A)	53.2(7)	C(16A)-C(15)-C(18A)	115.6(6)
C(17B)-C(15)-C(16B)	119(1)	C(16A)-C(15)-C(16B)	31.8(6)
C(18A)-C(15)-C(16B)	132.1(8)	C(17B)-C(15)-C(9)	110.2(6)
C(16A)-C(15)-C(9)	111.5(4)	C(18A)-C(15)-C(9)	113.3(4)
C(16B)-C(15)-C(9)	112.9(7)	C(17B)-C(15)-C(18B)	104(1)
C(16A)-C(15)-C(18B)	73.3(8)	C(18A)-C(15)-C(18B)	51.6(7)
C(16B)-C(15)-C(18B)	103(1)	C(9)-C(15)-C(18B)	106.0(6)
C(17B)-C(15)-C(17A)	52.1(7)	C(16A)-C(15)-C(17A)	104.7(5)
C(18A)-C(15)-C(17A)	102.5(5)	C(16B)-C(15)-C(17A)	74.4(8)
C(9)-C(15)-C(17A)	108.1(4)	C(18B)-C(15)-C(17A)	143.7(7)
C(15)-C(16A)-H(16A)	109.5	C(15)-C(16A)-H(16B)	109.5
C(15)-C(16A)-H(16C)	109.5	C(15)-C(17A)-H(17A)	109.5
C(15)-C(17A)-H(17B)	109.5	C(15)-C(17A)-H(17C)	109.5
C(15)-C(18A)-H(18A)	109.5	C(15)-C(18A)-H(18B)	109.5
C(15)-C(18A)-H(18C)	109.5	C(15)-C(16B)-H(16D)	109.5
C(15)-C(16B)-H(16E)	109.5	H(16D)-C(16B)-H(16E)	109.5
C(15)-C(16B)-H(16F)	109.5	H(16D)-C(16B)-H(16F)	109.5
H(16E)-C(16B)-H(16F)	109.5	C(15)-C(17B)-H(17D)	109.5
C(15)-C(17B)-H(17E)	109.5	H(17D)-C(17B)-H(17E)	109.5
C(15)-C(17B)-H(17F)	109.5	H(17D)-C(17B)-H(17F)	109.5
H(17E)-C(17B)-H(17F)	109.5	C(15)-C(18B)-H(18D)	109.5
C(15)-C(18B)-H(18E)	109.5	H(18D)-C(18B)-H(18E)	109.5
C(15)-C(18B)-H(18F)	109.5	H(18D)-C(18B)-H(18F)	109.5
H(18E)-C(18B)-H(18F)	109.5	C(24)-C(19)-C(20)	119.0(3)
C(24)-C(19)-P(1)	122.9(3)	C(20)-C(19)-P(1)	118.0(3)
C(21)-C(20)-C(19)	120.7(4)	C(21)-C(20)-H(20)	119.7
C(19)-C(20)-H(20)	119.7	C(22)-C(21)-C(20)	119.5(4)
C(22)-C(21)-H(21)	120.3	C(20)-C(21)-H(21)	120.3
C(23)-C(22)-C(21)	120.3(4)	C(23)-C(22)-H(22)	119.8
C(21)-C(22)-H(22)	119.8	C(22)-C(23)-C(24)	120.2(4)
C(22)-C(23)-H(23)	119.9	C(24)-C(23)-H(23)	119.9
C(23)-C(24)-C(19)	120.3(4)	C(23)-C(24)-H(24)	119.9
C(19)-C(24)-H(24)	119.9	C(30)-C(25)-C(26)	118.5(4)
C(30)-C(25)-P(1)	117.7(3)	C(26)-C(25)-P(1)	123.8(3)
C(27)-C(26)-C(25)	120.3(4)	C(27)-C(26)-H(26)	119.9
C(25)-C(26)-H(26)	119.9	C(28)-C(27)-C(26)	120.5(4)
C(28)-C(27)-H(27)	119.8	C(26)-C(27)-H(27)	119.8
C(27)-C(28)-C(29)	120.2(4)	C(27)-C(28)-H(28)	119.9
C(29)-C(28)-H(28)	119.9	C(28)-C(29)-C(30)	119.5(4)
C(28)-C(29)-H(29)	120.3	C(30)-C(29)-H(29)	120.3
C(29)-C(30)-C(25)	121.0(4)	C(29)-C(30)-H(30)	119.5
C(25)-C(30)-H(30)	119.5	C(36)-C(31)-C(32)	122.2(3)
C(36)-C(31)-P(2)	115.0(3)	C(32)-C(31)-P(2)	122.3(3)
O(2)-C(32)-C(31)	122.2(3)	O(2)-C(32)-C(33)	121.3(3)
C(31)-C(32)-C(33)	116.5(3)	C(34)-C(33)-C(32)	118.6(3)
C(34)-C(33)-C(37)	120.4(3)	C(32)-C(33)-C(37)	121.0(3)
C(33)-C(34)-C(35)	124.8(3)	C(33)-C(34)-H(34)	117.6
C(35)-C(34)-H(34)	117.6	C(36)-C(35)-C(34)	116.2(3)
C(36)-C(35)-C(41)	123.1(4)	C(34)-C(35)-C(41)	120.7(3)
C(35)-C(36)-C(31)	121.7(3)	C(35)-C(36)-H(36)	119.2
C(31)-C(36)-H(36)	119.2	C(33)-C(37)-C(39)	112.0(3)

C(33)-C(37)-C(38)	109.6(3)	C(39)-C(37)-C(38)	107.7(3)
C(33)-C(37)-C(40)	109.8(3)	C(39)-C(37)-C(40)	107.6(3)
C(38)-C(37)-C(40)	110.1(3)	C(37)-C(38)-H(38A)	109.5
C(37)-C(38)-H(38B)	109.5	H(38A)-C(38)-H(38B)	109.5
C(37)-C(38)-H(38C)	109.5	H(38A)-C(38)-H(38C)	109.5
H(38B)-C(38)-H(38C)	109.5	C(37)-C(39)-H(39A)	109.5
C(37)-C(39)-H(39B)	109.5	H(39A)-C(39)-H(39B)	109.5
C(37)-C(39)-H(39C)	109.5	H(39A)-C(39)-H(39C)	109.5
H(39B)-C(39)-H(39C)	109.5	C(37)-C(40)-H(40A)	109.5
C(37)-C(40)-H(40B)	109.5	H(40A)-C(40)-H(40B)	109.5
C(37)-C(40)-H(40C)	109.5	H(40A)-C(40)-H(40C)	109.5
H(40B)-C(40)-H(40C)	109.5	C(43)-C(41)-C(42)	109.4(4)
C(43)-C(41)-C(44)	110.1(5)	C(42)-C(41)-C(44)	107.7(5)
C(43)-C(41)-C(35)	109.5(4)	C(42)-C(41)-C(35)	108.6(4)
C(44)-C(41)-C(35)	111.5(4)	C(41)-C(42)-H(42A)	109.5
C(41)-C(42)-H(42B)	109.5	H(42A)-C(42)-H(42B)	109.5
C(41)-C(42)-H(42C)	109.5	H(42A)-C(42)-H(42C)	109.5
H(42B)-C(42)-H(42C)	109.5	C(41)-C(43)-H(43A)	109.5
C(41)-C(43)-H(43B)	109.5	H(43A)-C(43)-H(43B)	109.5
C(41)-C(43)-H(43C)	109.5	H(43A)-C(43)-H(43C)	109.5
H(43B)-C(43)-H(43C)	109.5	C(41)-C(44)-H(44A)	109.5
C(41)-C(44)-H(44B)	109.5	H(44A)-C(44)-H(44B)	109.5
C(41)-C(44)-H(44C)	109.5	H(44A)-C(44)-H(44C)	109.5
H(44B)-C(44)-H(44C)	109.5	C(50)-C(45)-C(46)	118.2(4)
C(50)-C(45)-P(2)	118.8(3)	C(46)-C(45)-P(2)	122.7(3)
C(47)-C(46)-C(45)	120.2(4)	C(47)-C(46)-H(46)	119.9
C(45)-C(46)-H(46)	119.9	C(48)-C(47)-C(46)	120.8(4)
C(48)-C(47)-H(47)	119.6	C(46)-C(47)-H(47)	119.6
C(49)-C(48)-C(47)	119.5(4)	C(49)-C(48)-H(48)	120.3
C(47)-C(48)-H(48)	120.3	C(48)-C(49)-C(50)	120.3(4)
C(48)-C(49)-H(49)	119.9	C(50)-C(49)-H(49)	119.9
C(49)-C(50)-C(45)	121.0(4)	C(49)-C(50)-H(50)	119.5
C(45)-C(50)-H(50)	119.5	C(56)-C(51)-C(52)	118.7(3)
C(56)-C(51)-P(2)	122.2(3)	C(52)-C(51)-P(2)	117.7(3)
C(53)-C(52)-C(51)	120.4(4)	C(53)-C(52)-H(52)	119.8
C(51)-C(52)-H(52)	119.8	C(52)-C(53)-C(54)	120.5(4)
C(52)-C(53)-H(53)	119.8	C(54)-C(53)-H(53)	119.8
C(53)-C(54)-C(55)	120.3(4)	C(53)-C(54)-H(54)	119.9
C(55)-C(54)-H(54)	119.9	C(54)-C(55)-C(56)	119.6(4)
C(54)-C(55)-H(55)	120.2	C(56)-C(55)-H(55)	120.2
C(51)-C(56)-C(55)	120.5(4)	C(51)-C(56)-H(56)	119.8
C(55)-C(56)-H(56)	119.8	O(3)-C(57)-C(58)	111.4(4)
O(3)-C(57)-H(57A)	109.3	C(58)-C(57)-H(57A)	109.3
O(3)-C(57)-H(57B)	109.3	C(58)-C(57)-H(57B)	109.3
H(57A)-C(57)-H(57B)	108.0	C(57)-C(58)-H(58A)	109.5
C(57)-C(58)-H(58B)	109.5	H(58A)-C(58)-H(58B)	109.5
C(57)-C(58)-H(58C)	109.5	H(58A)-C(58)-H(58C)	109.5
H(58B)-C(58)-H(58C)	109.5		

Estimated standard deviations are given in the parenthesis.
Symmetry operators ::

1: x, y, z 2: -x, y, -z+1/2 3: x+1/2, y+1/2, z
4: -x+1/2, y+1/2, -z+1/2 5: -x, -y, -z 6: x, -y, z-1/2
7: -x+1/2, -y+1/2, -z 8: x+1/2, -y+1/2, z-1/2

Appendix 1. Crystallographic data

Table 4. Anisotropic displacement parameters ($\text{\AA}^2 \times 10^3$) for pa679bis

atom	U11	U22	U33	U23	U13	U12
Y(1)	22(1)	26(1)	23(1)	-1(1)	13(1)	-1(1)
P(1)	27(1)	32(1)	28(1)	-4(1)	18(1)	0(1)
P(2)	24(1)	31(1)	25(1)	3(1)	11(1)	-4(1)
O(1)	24(1)	32(1)	28(1)	-5(1)	15(1)	-3(1)
O(2)	25(1)	27(1)	27(1)	3(1)	15(1)	-1(1)
O(3)	33(2)	24(2)	37(2)	0	22(2)	0
O(4)	38(2)	30(2)	29(2)	0	22(2)	0
N(1)	23(2)	37(2)	34(2)	-7(1)	18(1)	-3(1)
N(2)	27(2)	31(2)	31(2)	2(1)	13(1)	-3(1)
N(3)	22(1)	32(2)	25(2)	8(1)	8(1)	-1(1)
C(1)	27(2)	50(2)	42(2)	-12(2)	21(2)	-3(2)
C(2)	23(2)	38(2)	45(2)	-4(2)	16(2)	5(2)
C(3)	26(2)	39(2)	27(2)	4(2)	9(2)	2(2)
C(4)	24(2)	36(2)	29(2)	1(2)	8(2)	-4(2)
C(5)	26(2)	33(2)	27(2)	-2(2)	15(2)	0(2)
C(6)	25(2)	27(2)	20(2)	-4(1)	10(2)	-1(1)
C(7)	21(2)	31(2)	24(2)	0(2)	12(2)	1(1)
C(8)	25(2)	35(2)	28(2)	-4(2)	13(2)	-5(2)
C(9)	34(2)	35(2)	31(2)	-7(2)	17(2)	-3(2)
C(10)	33(2)	36(2)	26(2)	-3(2)	19(2)	3(2)
C(11)	26(2)	35(2)	31(2)	-3(2)	17(2)	-2(2)
C(12)	39(2)	38(2)	32(2)	-1(2)	24(2)	4(2)
C(13)	29(2)	39(2)	30(2)	-3(2)	18(2)	3(2)
C(14)	31(2)	55(3)	41(2)	-10(2)	23(2)	-9(2)
C(15)	47(2)	56(3)	40(2)	-24(2)	25(2)	-11(2)
C(16A)	73(4)	62(7)	36(5)	-20(4)	10(4)	-4(4)
C(17A)	75(5)	44(4)	60(4)	-27(3)	32(4)	-8(4)
C(18A)	97(7)	92(7)	101(7)	-72(6)	79(7)	-51(5)
C(16B)	73(4)	62(7)	36(5)	-20(4)	10(4)	-4(4)
C(17B)	75(5)	44(4)	60(4)	-27(3)	32(4)	-8(4)
C(18B)	97(7)	92(7)	101(7)	-72(6)	79(7)	-51(5)
C(19)	26(2)	36(2)	27(2)	-7(2)	15(2)	-2(2)
C(20)	37(2)	35(2)	37(2)	-2(2)	23(2)	-1(2)
C(21)	42(2)	35(2)	46(2)	3(2)	24(2)	8(2)
C(22)	69(3)	64(3)	66(3)	16(3)	51(3)	34(3)
C(23)	103(4)	79(4)	83(4)	35(3)	80(4)	50(3)
C(24)	71(3)	47(3)	58(3)	18(2)	52(3)	26(2)
C(25)	34(2)	36(2)	35(2)	0(2)	24(2)	5(2)
C(26)	52(3)	34(2)	40(2)	0(2)	26(2)	6(2)
C(27)	51(3)	57(3)	35(2)	2(2)	21(2)	8(2)
C(28)	63(3)	47(3)	58(3)	19(2)	43(3)	11(2)
C(29)	49(3)	41(2)	57(3)	4(2)	35(2)	-1(2)
C(30)	35(2)	38(2)	43(2)	-1(2)	26(2)	-1(2)
C(31)	25(2)	32(2)	23(2)	4(2)	10(2)	1(2)
C(32)	27(2)	30(2)	25(2)	-1(2)	15(2)	0(2)
C(33)	28(2)	31(2)	30(2)	1(2)	17(2)	3(2)
C(34)	29(2)	42(2)	26(2)	7(2)	8(2)	4(2)
C(35)	40(2)	36(2)	36(2)	11(2)	19(2)	3(2)
C(36)	33(2)	34(2)	32(2)	4(2)	14(2)	-6(2)
C(37)	21(2)	39(2)	33(2)	5(2)	11(2)	2(2)
C(38)	33(2)	40(2)	49(2)	-3(2)	28(2)	1(2)
C(39)	28(2)	61(3)	55(3)	14(2)	13(2)	1(2)
C(40)	29(2)	43(2)	31(2)	-9(2)	16(2)	-10(2)
C(41)	44(2)	44(2)	45(3)	22(2)	19(2)	-1(2)
C(42)	123(5)	75(4)	72(4)	26(3)	64(4)	-5(4)
C(43)	90(4)	46(3)	115(5)	46(3)	62(4)	15(3)
C(44)	79(4)	79(4)	87(4)	48(4)	18(4)	-28(3)
C(45)	28(2)	33(2)	30(2)	2(2)	14(2)	-4(2)
C(46)	50(2)	35(2)	40(2)	5(2)	25(2)	2(2)
C(47)	69(3)	32(2)	54(3)	7(2)	38(3)	6(2)
C(48)	43(2)	48(3)	40(2)	-3(2)	23(2)	3(2)
C(49)	39(2)	50(3)	36(2)	2(2)	21(2)	-8(2)
C(50)	32(2)	36(2)	34(2)	0(2)	15(2)	-9(2)

Appendix 1. Crystallographic data

C(51)	28(2)	34(2)	37(2)	6(2)	17(2)	-4(2)
C(52)	39(2)	58(3)	40(2)	-7(2)	22(2)	-15(2)
C(53)	52(3)	87(4)	56(3)	-19(3)	40(3)	-20(3)
C(54)	42(3)	76(3)	66(3)	-5(3)	38(3)	-13(2)
C(55)	31(2)	50(3)	46(3)	4(2)	16(2)	-9(2)
C(56)	31(2)	41(2)	36(2)	3(2)	16(2)	-7(2)
C(57)	29(4)	28(3)	30(10)	9(3)	12(7)	0(4)
C(58)	52(5)	29(4)	52(5)	-7(4)	30(5)	0(4)

The anisotropic displacement factor exponent takes the form
 $2 \pi^2 [h^2 a^{*2} U(11) + \dots + 2hka^* b^* U(12)]$

Appendix 1. Crystallographic data

Table 5. Hydrogen Coordinates ($\text{\AA} \times 10^4$) and equivalent isotropic displacement parameters ($\text{\AA}^2 \times 10^3$) for pa679bis

atom	x	y	z	U(eq)
H(4O)	5000	2370(20)	2500	37
H(2N)	4050(20)	3610(10)	2380(30)	38
H(1A)	4030	3536	4485	46
H(1B)	4028	3028	4096	46
H(2A)	3380	3509	2891	45
H(2B)	3868	3916	3238	45
H(3A)	3779	2920	1666	40
H(3B)	3229	3125	1648	40
H(4A)	3403	2626	2761	40
H(4B)	3441	2303	2078	40
H(8)	7259	4445	6427	37
H(10)	5920	4294	6691	37
H(12A)	6236	3816	3872	51
H(12B)	6811	3910	3878	51
H(12C)	6529	4329	4107	51
H(13A)	6777	3143	4986	48
H(13B)	7400	3250	5890	48
H(13C)	7343	3245	4972	48
H(14A)	7774	4032	5270	61
H(14B)	7835	4054	6190	61
H(14C)	7497	4465	5475	61
H(16A)	7751	4930	8575	103
H(16B)	7774	4575	7917	103
H(16C)	7542	4395	8494	103
H(17A)	6614	5378	6547	94
H(17B)	7246	5200	6812	94
H(17C)	7192	5507	7496	94
H(18A)	6705	5246	8097	126
H(18B)	6500	4713	8053	126
H(18C)	6140	5044	7199	126
H(16D)	7658	4998	7431	103
H(16E)	7776	4542	8025	103
H(16F)	7766	5054	8381	103
H(17D)	6755	5495	7583	94
H(17E)	6172	5177	7045	94
H(17F)	6478	5363	6571	94
H(18D)	7048	4844	8658	126
H(18E)	7134	4320	8423	126
H(18F)	6486	4534	7960	126
H(20)	4771	4529	4839	42
H(21)	4251	5110	5030	49
H(22)	3995	4987	6030	71
H(23)	4225	4278	6794	88
H(24)	4743	3697	6608	60
H(26)	5978	3555	7447	51
H(27)	6212	2960	8466	59
H(28)	5808	2212	7991	62
H(29)	5175	2050	6481	56
H(30)	4915	2651	5454	43
H(34)	6340	1341	6582	43
H(36)	4598	1215	4776	42
H(38A)	6814	1782	5235	58
H(38B)	7155	2272	5633	58
H(38C)	6469	2271	4845	58
H(39A)	7034	1852	7349	81
H(39B)	7490	2020	7124	81
H(39C)	7152	1527	6752	81
H(40A)	6269	2784	5801	52
H(40B)	6959	2772	6570	52
H(40C)	6491	2605	6771	52
H(42A)	5960	1079	7473	127
H(42B)	5594	634	7450	127

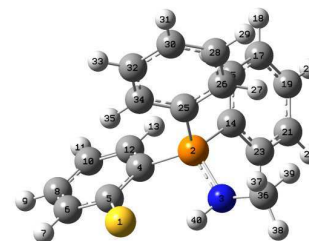
Appendix 1. Crystallographic data

H(42C)	5266	1124	7016	127
H(43A)	6337	586	6809	122
H(43B)	5902	356	5852	122
H(43C)	5940	142	6691	122
H(44A)	4900	225	6055	147
H(44B)	4789	413	5148	147
H(44C)	4571	717	5647	147
H(46)	4217	872	3378	50
H(47)	4197	337	2395	60
H(48)	4199	601	1195	53
H(49)	4191	1407	947	50
H(50)	4193	1947	1904	43
H(52)	4079	2147	4837	55
H(53)	3261	2148	4899	72
H(54)	2386	1802	3778	69
H(55)	2327	1437	2592	55
H(56)	3154	1424	2529	45
H(57A)	4665	4073	1706	39
H(57B)	5363	4102	2420	39
H(58A)	4482	4264	2740	66
H(58B)	4977	4628	2895	66
H(58C)	5156	4183	3538	66

Optimised Structures by DFT

1. Chapter 1

Monodeprotonation of 2a



Standard orientation:

Center Number	Atomic Number	Atomic Type	Coordinates (Angstroms)		
			X	Y	Z
1	16	0	-3.027033	0.242495	1.381663
2	15	0	0.111243	-0.027919	0.477180
3	7	0	0.016833	-0.084314	2.147051
4	6	0	-1.152330	-1.090448	-0.204064
5	6	0	-2.509005	-0.934018	0.219214
6	6	0	-3.440692	-1.814298	-0.391755
7	1	0	-4.480482	-1.723455	-0.090916
8	6	0	-3.062635	-2.758578	-1.328092
9	1	0	-3.819307	-3.408061	-1.763674
10	6	0	-1.721158	-2.896958	-1.718698
11	1	0	-1.427871	-3.644064	-2.450292
12	6	0	-0.773317	-2.064520	-1.149956
13	1	0	0.269782	-2.164993	-1.436947
14	6	0	1.755007	-0.695474	0.092438
15	6	0	2.451512	-0.317440	-1.063302
16	1	0	2.034948	0.432207	-1.729988
17	6	0	3.682330	-0.901103	-1.357241
18	1	0	4.218323	-0.604640	-2.254784
19	6	0	4.224447	-1.859002	-0.500836
20	1	0	5.186191	-2.310118	-0.731020
21	6	0	3.532842	-2.240503	0.649039
22	1	0	3.952645	-2.989114	1.315505
23	6	0	2.299081	-1.666552	0.945146
24	1	0	1.749339	-1.962248	1.834159
25	6	0	0.062526	1.642765	-0.238232
26	6	0	1.122254	2.535712	-0.016836
27	1	0	1.999328	2.221163	0.542974
28	6	0	1.066147	3.828924	-0.532252
29	1	0	1.889844	4.515925	-0.357300
30	6	0	-0.042892	4.234946	-1.273597
31	1	0	-0.085757	5.243691	-1.676322
32	6	0	-1.095530	3.348477	-1.500578
33	1	0	-1.961386	3.664091	-2.075861
34	6	0	-1.049879	2.056566	-0.982888
35	1	0	-1.878107	1.373612	-1.139647

Appendix 2. Optimised Structures

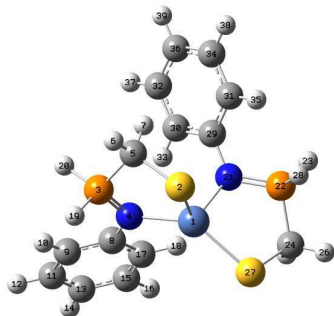
36	6	0	0.807379	0.823746	2.974862
37	1	0	0.522347	1.878488	2.857221
38	1	0	0.664383	0.540415	4.021582
39	1	0	1.872259	0.716427	2.742441
40	1	0	-0.996949	-0.043713	2.364975

 Rotational constants (GHZ): 0.2835280 0.2437411
 0.1772657

Sum of electronic and zero-point Energies= -1528.409669
 Sum of electronic and thermal Energies= -1528.389762
 Sum of electronic and thermal Enthalpies= -1528.388818
 Sum of electronic and thermal Free Energies= -1528.458991

	1	2	3
	A	A	A
Frequencies --	33.3922	43.4811	
48.4936			
Red. masses --	4.1544	5.8284	
4.5718			
Frc consts --	0.0027	0.0065	
0.0063			
IR Inten --	1.0634	1.6465	
0.0481			

Complex 18, triplet



Center Number	Atomic Number	Atomic Type	Coordinates (Angstroms)		
			X	Y	Z
1	28	0	0.201846	0.992948	-0.488104
2	16	0	0.576118	2.372836	1.328532
3	15	0	2.174141	-0.044016	1.598155
4	7	0	1.527014	-0.402627	0.164202
5	6	0	1.050426	1.046309	2.492957
6	1	0	1.575560	1.450785	3.366623

Appendix 2. Optimised Structures

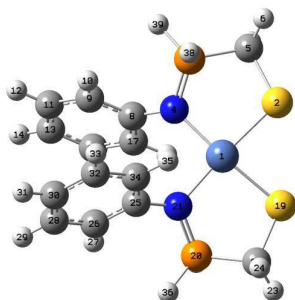
7	1	0	0.189287	0.460545	2.835260
8	6	0	2.016953	-1.425088	-0.662886
9	6	0	3.258980	-2.055555	-0.472662
10	1	0	3.918695	-1.741138	0.335026
11	6	0	3.681906	-3.072074	-1.326750
12	1	0	4.648267	-3.540568	-1.156043
13	6	0	2.886132	-3.478901	-2.394861
14	1	0	3.220373	-4.268511	-3.061866
15	6	0	1.656707	-2.850407	-2.599467
16	1	0	1.024014	-3.150028	-3.431560
17	6	0	1.223278	-1.840944	-1.747621
18	1	0	0.263188	-1.355921	-1.908387
19	1	0	3.425934	0.620611	1.590956
20	1	0	2.470248	-1.201857	2.359928
21	7	0	-1.659915	0.181039	-0.222650
22	15	0	-2.716951	1.163443	-0.944908
23	1	0	-4.014687	0.595255	-0.974207
24	6	0	-2.102733	1.512554	-2.603088
25	1	0	-2.152103	0.598077	-3.205079
26	1	0	-2.737326	2.275198	-3.068375
27	16	0	-0.389616	2.128849	-2.392422
28	1	0	-2.962531	2.442275	-0.385653
29	6	0	-1.969300	-0.476488	0.985560
30	6	0	-1.413893	-1.748080	1.209737
31	6	0	-2.789146	0.079099	1.981430
32	6	0	-1.682609	-2.439410	2.387008
33	1	0	-0.778908	-2.180486	0.442460
34	6	0	-3.061309	-0.623351	3.155222
35	1	0	-3.188495	1.083645	1.855027
36	6	0	-2.510340	-1.885509	3.366512
37	1	0	-1.250621	-3.426575	2.534935
38	1	0	-3.700028	-0.171960	3.910589
39	1	0	-2.722744	-2.432149	4.281291

 Rotational constants (GHZ): 0.2462247 0.1860907
 0.1582504

Sum of electronic and zero-point Energies= -2301.563383
 Sum of electronic and thermal Energies= -2301.540943
 Sum of electronic and thermal Enthalpies= -2301.539999
 Sum of electronic and thermal Free Energies= -2301.619293

	1	2	3
	A	A	A
Frequencies --	22.6915	25.4058	
31.6404			
Red. masses --	4.8206	5.3937	
6.2897			
Frc consts --	0.0015	0.0021	
0.0037			
IR Inten --	1.0347	0.4589	
2.3521			

Complex 18: singlet



Center Number	Atomic Number	Atomic Type	Coordinates (Angstroms)		
			X	Y	Z
1	28	0	-0.061401	-0.008349	0.064248
2	16	0	-0.059106	0.163614	2.284669
3	15	0	2.595656	0.127931	1.349255
4	7	0	1.853064	-0.319605	-0.007287
5	6	0	1.616389	-0.422996	2.748687
6	1	0	1.943876	0.055055	3.678515
7	1	0	1.684988	-1.512238	2.848417
8	6	0	2.536944	-0.983353	-1.047024
9	6	0	3.771832	-0.539227	-1.541873
10	1	0	4.199699	0.386945	-1.164519
11	6	0	4.431643	-1.247260	-2.544986
12	1	0	5.388468	-0.884187	-2.912459
13	6	0	3.862342	-2.395230	-3.090609
14	1	0	4.374775	-2.942738	-3.877161
15	6	0	2.622691	-2.831806	-2.617890
16	1	0	2.169410	-3.730772	-3.029797
17	6	0	1.967590	-2.139957	-1.604545
18	1	0	1.014196	-2.486677	-1.214647
19	16	0	-2.260299	-0.304045	0.257919
20	15	0	-1.590891	-0.064424	-2.465626
21	7	0	-0.189610	0.407231	-1.827836
22	6	0	-2.910963	0.357011	-1.325221
23	1	0	-3.846608	-0.146160	-1.593100
24	1	0	-3.063898	1.442134	-1.313961
25	6	0	0.749047	1.156146	-2.567687
26	6	0	1.136220	0.805881	-3.869353
27	1	0	0.756805	-0.111895	-4.313276
28	6	0	2.037601	1.596839	-4.579942
29	1	0	2.322503	1.305782	-5.588138
30	6	0	2.588621	2.736091	-3.998384
31	1	0	3.295946	3.348514	-4.551221
32	6	0	2.224457	3.079520	-2.694487
33	1	0	2.641127	3.970689	-2.230260
34	6	0	1.311808	2.304483	-1.986682
35	1	0	1.005003	2.578871	-0.980885

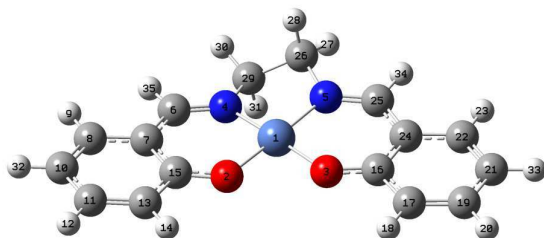
36	1	0	-1.756730	0.505437	-3.751697
37	1	0	-1.762368	-1.448178	-2.699822
38	1	0	2.761813	1.515075	1.566067
39	1	0	3.923408	-0.365036	1.365847

 Rotational constants (GHZ): 0.2688150 0.2045036
 0.1598595

Sum of electronic and zero-point Energies= -2301.551138
 Sum of electronic and thermal Energies= -2301.529209
 Sum of electronic and thermal Enthalpies= -2301.528264
 Sum of electronic and thermal Free Energies= -2301.604702

	1	2	3
	A	A	A
Frequencies --	23.9181	25.1861	
37.5125			
Red. masses --	5.9688	6.6496	
5.6170			
Frc consts --	0.0020	0.0025	
0.0047			
IR Inten --	1.1717	2.8104	
0.8091			

Chapter 3

[Ni(Salen)] singlet, square planar

Center Number	Atomic Number	Atomic Type	Coordinates (Angstroms)		
			X	Y	Z
1	28	0	0.015742	-0.046715	0.016601
2	8	0	0.016175	-0.131133	1.862897
3	8	0	1.854780	0.031940	0.166905
4	7	0	-1.830249	-0.198028	-0.119366
5	7	0	0.019572	0.118606	-1.831654
6	6	0	-2.689612	-0.189780	0.856828
7	6	0	-2.366292	-0.099710	2.235819
8	6	0	-3.411811	-0.057880	3.191663
9	1	0	-4.441013	-0.070032	2.835425
10	6	0	-3.145189	-0.004454	4.539877
11	6	0	-1.798295	0.001548	4.966531
12	1	0	-1.577088	0.040919	6.031125
13	6	0	-0.757342	-0.042443	4.066165
14	1	0	0.278215	-0.038927	4.392729
15	6	0	-0.997002	-0.090355	2.662624
16	6	0	2.729990	-0.000911	-0.782645
17	6	0	4.110790	-0.052112	-0.436183
18	1	0	4.356567	-0.064709	0.621413
19	6	0	5.088885	-0.088509	-1.404844
20	1	0	6.133153	-0.130811	-1.102207
21	6	0	4.767345	-0.071279	-2.780535
22	6	0	3.443734	-0.014028	-3.149614
23	1	0	3.168165	0.007161	-4.203107
24	6	0	2.409694	0.020396	-2.181024
25	6	0	1.060486	0.116230	-2.611335
26	6	0	-1.311926	0.340690	-2.386404
27	1	0	-1.377239	0.007962	-3.430244
28	1	0	-1.535997	1.415783	-2.351904
29	6	0	-2.282300	-0.411879	-1.490642
30	1	0	-3.316637	-0.074199	-1.634514
31	1	0	-2.235130	-1.486160	-1.716148
32	1	0	-3.952295	0.029104	5.265338
33	1	0	5.552881	-0.099013	-3.529506
34	1	0	0.886019	0.209138	-3.688324

```

35      1      0      -3.750217      -0.271966      0.597390
-----
Rotational constants (GHZ):      0.6680831      0.1727332
0.1379416

```

```

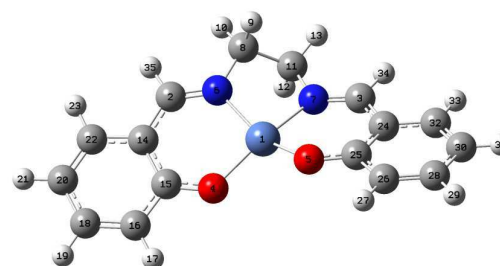
Sum of electronic and zero-point Energies=      -1046.919117
Sum of electronic and thermal Energies=      -1046.902607
Sum of electronic and thermal Enthalpies=      -1046.901663
Sum of electronic and thermal Free Energies=      -1046.963265

```

```

          1          2          3
          A          A          A
Frequencies --      30.8492      59.5601
84.2533
Red. masses --      6.2817      4.2723
5.7138
Frc consts --      0.0035      0.0089
0.0239
IR Inten  --      1.8948      0.0127
0.0919

```

[Ni(Salen)] triplet, tetrahedral

Center Number	Atomic Number	Atomic Type	Coordinates (Angstroms)		
			X	Y	Z
1	28	0	-0.439718	-0.476050	-0.156478
2	6	0	-0.213068	0.276291	2.682256
3	6	0	1.863645	-0.426269	-1.986523
4	8	0	-2.139610	0.085336	0.476245
5	8	0	-0.806197	-1.598057	-1.644983
6	7	0	0.402299	-0.087837	1.602616
7	7	0	1.379793	-0.067044	-0.839880
8	6	0	1.852221	-0.069477	1.517601
9	1	0	2.227011	-1.102133	1.537245
10	1	0	2.311583	0.482025	2.349865
11	6	0	2.213568	0.566884	0.166856
12	1	0	1.977377	1.639355	0.205246
13	1	0	3.285225	0.455293	-0.049540
14	6	0	-1.628994	0.425759	2.816973

Appendix 2. Optimised Structures

15	6	0	-2.519224	0.342150	1.690828
16	6	0	-3.898349	0.580558	1.940498
17	1	0	-4.570207	0.521685	1.089264
18	6	0	-4.365053	0.862506	3.207427
19	1	0	-5.429736	1.028342	3.357837
20	6	0	-3.488363	0.945117	4.307696
21	1	0	-3.867168	1.174158	5.299224
22	6	0	-2.142745	0.736549	4.098733
23	1	0	-1.444532	0.804750	4.932042
24	6	0	1.158085	-1.162499	-2.988668
25	6	0	-0.142178	-1.730157	-2.751988
26	6	0	-0.709993	-2.501040	-3.803274
27	1	0	-1.689988	-2.932946	-3.622826
28	6	0	-0.053388	-2.682414	-5.002328
29	1	0	-0.527699	-3.270050	-5.785505
30	6	0	1.221338	-2.125292	-5.229041
31	1	0	1.730927	-2.280263	-6.175295
32	6	0	1.809116	-1.387236	-4.225554
33	1	0	2.797880	-0.955065	-4.374368
34	1	0	2.907306	-0.171891	-2.215514
35	1	0	0.387628	0.516598	3.569886

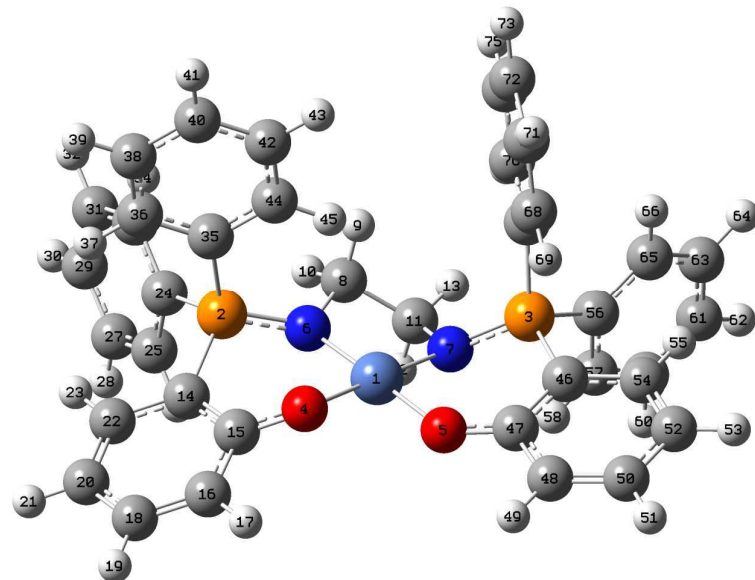
Rotational constants (GHZ): 0.7099586 0.1593090
0.1333260

Sum of electronic and zero-point Energies=-1046.906914
Sum of electronic and thermal Energies=-1046.889658
Sum of electronic and thermal Enthalpies=-1046.888714
Sum of electronic and thermal Free Energies=-1046.953803

	1	2	3
	A	A	A
Frequencies --	19.2790	47.9351	
62.5985			
Red. masses --	7.3292	4.7518	
5.9456			
Frc consts --	0.0016	0.0064	
0.0137			
IR Inten --	0.8226	0.0359	
0.0885			

Appendix 2. Optimised Structures

[Ni(phosphasalen)] square planar



Z-Matrix orientation:

Center Number	Atomic Number	Atomic Type	Coordinates (Angstroms)		
			X	Y	Z
1	28	0	0.124220	-0.131232	0.056752
2	15	0	-0.054642	-0.072813	3.120225
3	15	0	2.588596	-0.051800	-1.697128
4	8	0	-1.446577	-0.962411	0.679462
5	8	0	-0.472384	-0.676303	-1.624262
6	7	0	0.686530	0.442558	1.771597
7	7	0	1.692988	0.718873	-0.587608
8	6	0	2.079740	0.884578	1.793837
9	1	0	2.784738	0.043410	1.901627
10	1	0	2.273105	1.586790	2.617980
11	6	0	2.295023	1.560429	0.450215
12	1	0	1.767143	2.524235	0.454178
13	1	0	3.358906	1.771079	0.273815
14	6	0	-1.812762	-0.055426	2.873134
15	6	0	-2.253778	-0.561199	1.614661
16	6	0	-3.659867	-0.665248	1.432999
17	1	0	-4.009304	-1.047140	0.478028
18	6	0	-4.542414	-0.299047	2.431899
19	1	0	-5.612234	-0.391692	2.254447
20	6	0	-4.088070	0.194544	3.666243

Appendix 2. Optimised Structures

21	1	0	-4.792240	0.485643	4.440282
22	6	0	-2.723529	0.307524	3.880242
23	1	0	-2.355114	0.684675	4.831779
24	6	0	0.360262	1.040249	4.504647
25	6	0	-0.111838	2.360570	4.434343
26	1	0	-0.747921	2.660334	3.605571
27	6	0	0.228188	3.280096	5.422435
28	1	0	-0.147549	4.298237	5.364160
29	6	0	1.048866	2.895139	6.483845
30	1	0	1.313412	3.614403	7.254830
31	6	0	1.532066	1.590054	6.552469
32	1	0	2.176775	1.288589	7.373975
33	6	0	1.192160	0.664672	5.565725
34	1	0	1.574828	-0.349988	5.624180
35	6	0	0.431339	-1.759327	3.641069
36	6	0	-0.073963	-2.338525	4.813910
37	1	0	-0.752260	-1.776862	5.451917
38	6	0	0.277302	-3.640759	5.158124
39	1	0	-0.118847	-4.085324	6.067549
40	6	0	1.125853	-4.377674	4.329432
41	1	0	1.394190	-5.396613	4.597271
42	6	0	1.615459	-3.813228	3.153487
43	1	0	2.262742	-4.387957	2.496643
44	6	0	1.268302	-2.507576	2.807432
45	1	0	1.621872	-2.073656	1.876442
46	6	0	1.522734	-0.611110	-3.003789
47	6	0	0.127321	-0.803329	-2.760168
48	6	0	-0.653974	-1.196786	-3.889294
49	1	0	-1.717714	-1.335234	-3.718051
50	6	0	-0.092181	-1.406411	-5.130225
51	1	0	-0.730784	-1.711935	-5.956965
52	6	0	1.286766	-1.228902	-5.346444
53	1	0	1.722396	-1.387506	-6.328440
54	6	0	2.074326	-0.827919	-4.284158
55	1	0	3.138329	-0.661668	-4.441093
56	6	0	3.799674	1.115389	-2.405692
57	6	0	3.362674	2.428142	-2.637939
58	1	0	2.352015	2.710486	-2.354928
59	6	0	4.216355	3.356650	-3.225967
60	1	0	3.870954	4.372289	-3.400252
61	6	0	5.509837	2.983196	-3.594656
62	1	0	6.174792	3.709159	-4.055635
63	6	0	5.946800	1.678363	-3.375896
64	1	0	6.951806	1.382860	-3.665852
65	6	0	5.096150	0.745307	-2.782780
66	1	0	5.445060	-0.269489	-2.614418
67	6	0	3.577290	-1.474326	-1.083931
68	6	0	3.196318	-2.780352	-1.416192
69	1	0	2.367000	-2.938037	-2.100398
70	6	0	3.877033	-3.871469	-0.876081
71	1	0	3.574896	-4.880352	-1.145077
72	6	0	4.943035	-3.668821	-0.001118
73	1	0	5.477146	-4.519825	0.414140
74	6	0	5.327163	-2.370424	0.339703
75	1	0	6.158405	-2.208304	1.021246
76	6	0	4.647277	-1.279554	-0.195494
77	1	0	4.957315	-0.272457	0.073896

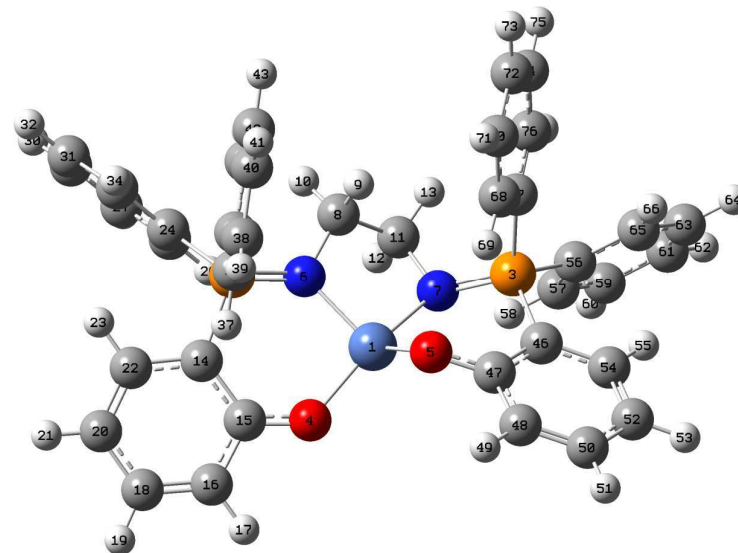
Appendix 2. Optimised Structures

Rotational constants (GHZ): 0.0989471 0.0495517
0.0473300

Sum of electronic and zero-point Energies= -2578.008478
Sum of electronic and thermal Energies= -2577.969521
Sum of electronic and thermal Enthalpies= -2577.968577
Sum of electronic and thermal Free Energies= -2578.084531

	1	2	3
	A	A	A
Frequencies --	7.0978	13.3051	
19.6091			
Red. masses --	5.3382	5.8200	
4.7240			
Frc consts --	0.0002	0.0006	
0.0011			
IR Inten --	0.0045	0.6007	
0.1290			

[Ni(Phosphasalen)] triplet



Z-Matrix orientation:

Center Number	Atomic Number	Atomic Type	Coordinates (Angstroms)		
			X	Y	Z

Appendix 2. Optimised Structures

1	28	0	0.391424	-0.586373	0.087925
2	15	0	-0.031022	-0.075297	3.117395
3	15	0	3.056662	-0.159518	-1.493694
4	8	0	-1.425223	-1.098519	0.405304
5	8	0	1.187057	-2.302429	-0.398357
6	7	0	0.665620	0.430601	1.748464
7	7	0	1.855088	0.559799	-0.680194
8	6	0	1.963349	1.096551	1.718824
9	1	0	2.781299	0.401413	1.966678
10	1	0	2.012855	1.939049	2.427011
11	6	0	2.163599	1.615434	0.290424
12	1	0	1.471195	2.452902	0.123263
13	1	0	3.182859	2.016620	0.189747
14	6	0	-1.685060	-0.674607	2.785751
15	6	0	-2.135382	-1.086238	1.486917
16	6	0	-3.491281	-1.522115	1.404467
17	1	0	-3.838870	-1.826761	0.421142
18	6	0	-4.322292	-1.568715	2.503547
19	1	0	-5.347001	-1.915116	2.383332
20	6	0	-3.863851	-1.173898	3.771279
21	1	0	-4.518355	-1.204726	4.637291
22	6	0	-2.560568	-0.729265	3.892431
23	1	0	-2.204948	-0.403861	4.867900
24	6	0	-0.164519	1.319905	4.294534
25	6	0	-0.479234	2.576250	3.757035
26	1	0	-0.600012	2.678181	2.681451
27	6	0	-0.636056	3.678167	4.593202
28	1	0	-0.878559	4.648659	4.168078
29	6	0	-0.485639	3.535683	5.973309
30	1	0	-0.610562	4.396178	6.625740
31	6	0	-0.177384	2.289131	6.514993
32	1	0	-0.061508	2.174268	7.589673
33	6	0	-0.014576	1.183823	5.679852
34	1	0	0.231095	0.216350	6.108916
35	6	0	0.912286	-1.371391	4.000565
36	6	0	0.461765	-2.697300	3.988897
37	1	0	-0.493121	-2.935863	3.528876
38	6	0	1.232654	-3.705789	4.564415
39	1	0	0.872587	-4.731137	4.552308
40	6	0	2.459440	-3.400850	5.151867
41	1	0	3.058238	-4.188718	5.602021
42	6	0	2.919603	-2.083598	5.161383
43	1	0	3.876707	-1.842366	5.616846
44	6	0	2.152444	-1.073030	4.587155
45	1	0	2.516252	-0.048521	4.605622
46	6	0	2.425491	-1.601842	-2.345404
47	6	0	1.567153	-2.498361	-1.632372
48	6	0	1.152493	-3.667309	-2.323758
49	1	0	0.503477	-4.352392	-1.785454
50	6	0	1.545040	-3.918538	-3.625500
51	1	0	1.199133	-4.824071	-4.120364
52	6	0	2.369930	-3.020836	-4.318946
53	1	0	2.663222	-3.215564	-5.346368
54	6	0	2.801055	-1.872683	-3.673828
55	1	0	3.434850	-1.169230	-4.206531
56	6	0	3.761846	0.978726	-2.740335
57	6	0	2.976765	2.068515	-3.134502
58	1	0	2.004837	2.210362	-2.669233

Appendix 2. Optimised Structures

59	6	0	3.437747	2.949513	-4.111317
60	1	0	2.823162	3.794848	-4.409891
61	6	0	4.681904	2.744203	-4.705891
62	1	0	5.040392	3.430579	-5.468912
63	6	0	5.467309	1.656065	-4.323278
64	1	0	6.436627	1.492484	-4.787173
65	6	0	5.011997	0.776758	-3.342993
66	1	0	5.631025	-0.065697	-3.045192
67	6	0	4.479293	-0.643490	-0.440937
68	6	0	4.448647	-1.885352	0.212647
69	1	0	3.611258	-2.557919	0.053903
70	6	0	5.473093	-2.241999	1.085734
71	1	0	5.440786	-3.208091	1.582561
72	6	0	6.532652	-1.365969	1.324709
73	1	0	7.332209	-1.650082	2.004496
74	6	0	6.562760	-0.124699	0.692123
75	1	0	7.383200	0.564232	0.877114
76	6	0	5.541119	0.236700	-0.185631
77	1	0	5.581722	1.203214	-0.680843

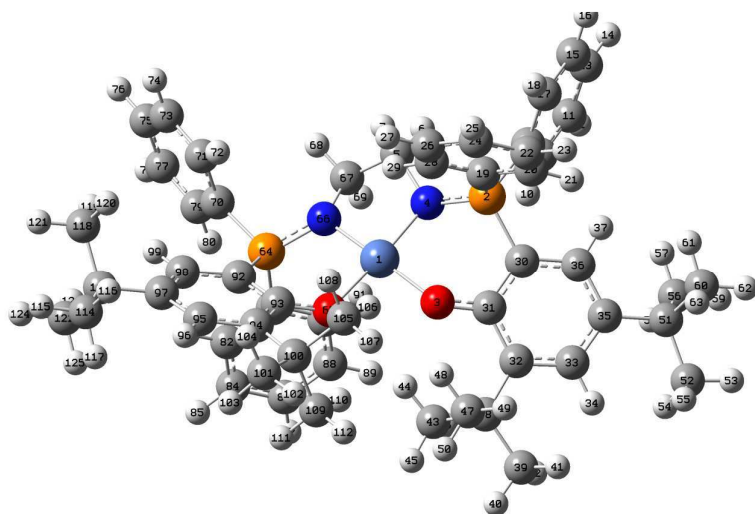
Rotational constants (GHZ): 0.1002885 0.0488261
0.0465586

Sum of electronic and zero-point Energies= -2578.011690
Sum of electronic and thermal Energies= -2577.972479
Sum of electronic and thermal Enthalpies= -2577.971534
Sum of electronic and thermal Free Energies= -2578.088748

	1	2	3
	A	A	A
Frequencies --	6.5842	12.4026	
19.7920			
Red. masses --	5.9642	6.1973	
5.3852			
Frc consts --	0.0002	0.0006	
0.0012			
IR Inten --	0.0957	0.3318	
0.6315			

Chapter 4

Complex 37a



Z-Matrix orientation:

Center Number	Atomic Number	Atomic Type	Coordinates (Angstroms)		
			X	Y	Z
1	28	0	-0.014855	0.002040	0.010012
2	15	0	-0.020430	-0.056542	3.010462
3	8	0	1.754351	-0.054966	0.712193
4	7	0	-0.833078	0.382037	1.672302
5	6	0	-2.293041	0.293298	1.604179
6	1	0	-2.771883	0.845585	2.424324
7	1	0	-2.658254	-0.746250	1.640368
8	6	0	-0.926259	0.551057	4.472485
9	6	0	-1.114793	1.937827	4.587869
10	1	0	-0.678319	2.602399	3.846986
11	6	0	-1.852648	2.459435	5.646483
12	1	0	-1.989890	3.534281	5.730968
13	6	0	-2.414113	1.603854	6.596045
14	1	0	-2.989944	2.012354	7.422647
15	6	0	-2.238646	0.226537	6.482064
16	1	0	-2.678756	-0.442766	7.216681
17	6	0	-1.499693	-0.300665	5.422742
18	1	0	-1.370928	-1.375384	5.336827
19	6	0	0.173785	-1.861967	3.229677
20	6	0	0.922046	-2.382644	4.294913
21	1	0	1.393610	-1.711930	5.009618
22	6	0	1.082120	-3.759191	4.429496

23	1	0	1.666781	-4.157259	5.254897
24	6	0	0.505684	-4.623947	3.497323
25	1	0	0.637568	-5.698110	3.600086
26	6	0	-0.223209	-4.110172	2.426605
27	1	0	-0.655068	-4.779990	1.687748
28	6	0	-0.388116	-2.732252	2.290001
29	1	0	-0.923752	-2.327030	1.435362
30	6	0	1.583852	0.699741	2.969473
31	6	0	2.271322	0.589652	1.727691
32	6	0	3.579052	1.176959	1.668329
33	6	0	4.077139	1.792026	2.814827
34	1	0	5.063912	2.233354	2.750738
35	6	0	3.403526	1.886606	4.044653
36	6	0	2.137651	1.318382	4.096832
37	1	0	1.560116	1.357383	5.017207
38	6	0	4.415337	1.101442	0.392193
39	6	0	5.759589	1.855008	0.512093
40	1	0	6.291670	1.763172	-0.442926
41	1	0	6.397747	1.426197	1.295293
42	1	0	5.607812	2.922893	0.715868
43	6	0	3.645965	1.722100	-0.802066
44	1	0	2.711856	1.184616	-0.976361
45	1	0	4.266832	1.662239	-1.705779
46	1	0	3.426739	2.779146	-0.601238
47	6	0	4.743993	-0.381624	0.084776
48	1	0	3.821531	-0.952459	-0.038192
49	1	0	5.334399	-0.813764	0.903351
50	1	0	5.329519	-0.445101	-0.841427
51	6	0	3.995907	2.573310	5.275825
52	6	0	5.402393	3.153261	5.012025
53	1	0	5.770742	3.630345	5.928875
54	1	0	5.377068	3.910895	4.219178
55	1	0	6.111303	2.366056	4.727802
56	6	0	3.080179	3.741639	5.724008
57	1	0	2.075055	3.380513	5.970668
58	1	0	2.995837	4.487242	4.924111
59	1	0	3.501463	4.226826	6.614415
60	6	0	4.113610	1.559045	6.442824
61	1	0	3.132670	1.144544	6.703499
62	1	0	4.525071	2.056053	7.331285
63	1	0	4.777419	0.731946	6.163324
64	15	0	-1.873765	0.515865	-2.291493
65	8	0	0.746479	-0.561238	-1.641255
66	7	0	-1.752958	0.243610	-0.693387
67	6	0	-2.654187	0.892812	0.260569
68	1	0	-3.708377	0.705203	0.015022
69	1	0	-2.509027	1.984582	0.308420
70	6	0	-3.639445	0.549165	-2.748933
71	6	0	-4.391911	-0.613426	-2.515705
72	1	0	-3.901083	-1.501567	-2.126606
73	6	0	-5.757234	-0.631048	-2.785433
74	1	0	-6.330978	-1.536727	-2.606984
75	6	0	-6.386518	0.511261	-3.283472
76	1	0	-7.452850	0.496118	-3.494251
77	6	0	-5.647839	1.671002	-3.507145
78	1	0	-6.135445	2.563791	-3.889880
79	6	0	-4.278951	1.693022	-3.238894
80	1	0	-3.710073	2.601615	-3.412138

Appendix 2. Optimised Structures

81	6	0	-1.163656	2.104452	-2.855758
82	6	0	-1.125739	2.430706	-4.218739
83	1	0	-1.523612	1.737415	-4.956233
84	6	0	-0.560900	3.633672	-4.633871
85	1	0	-0.530633	3.880085	-5.692141
86	6	0	-0.021706	4.513334	-3.693429
87	1	0	0.424891	5.449135	-4.019934
88	6	0	-0.040171	4.184644	-2.339394
89	1	0	0.397577	4.858110	-1.607346
90	6	0	-0.607732	2.982055	-1.919468
91	1	0	-0.590688	2.705856	-0.868488
92	6	0	-1.080917	-0.817292	-3.153831
93	6	0	0.195521	-1.191966	-2.647135
94	6	0	0.864016	-2.261781	-3.330895
95	6	0	0.232288	-2.834947	-4.432349
96	1	0	0.750178	-3.642468	-4.935167
97	6	0	-1.019494	-2.451199	-4.943513
98	6	0	-1.664864	-1.419390	-4.275020
99	1	0	-2.638665	-1.073657	-4.613506
100	6	0	2.245503	-2.736828	-2.884993
101	6	0	2.754306	-3.945963	-3.702152
102	1	0	3.736454	-4.238109	-3.310091
103	1	0	2.876443	-3.696716	-4.764036
104	1	0	2.080620	-4.807809	-3.610256
105	6	0	2.222882	-3.164803	-1.395084
106	1	0	1.927985	-2.325984	-0.761671
107	1	0	3.225058	-3.501614	-1.098501
108	1	0	1.520619	-3.996562	-1.251192
109	6	0	3.266612	-1.586477	-3.077408
110	1	0	2.965555	-0.717296	-2.489481
111	1	0	3.324886	-1.308174	-4.137837
112	1	0	4.259856	-1.915652	-2.745798
113	6	0	-1.663202	-3.110133	-6.163655
114	6	0	-0.803909	-4.256534	-6.739882
115	1	0	-1.320204	-4.691116	-7.605004
116	1	0	-0.651949	-5.050215	-5.998112
117	1	0	0.174924	-3.891856	-7.074474
118	6	0	-3.044964	-3.701906	-5.783317
119	1	0	-3.717364	-2.921870	-5.407708
120	1	0	-2.930932	-4.466747	-5.005387
121	1	0	-3.509921	-4.163773	-6.664366
122	6	0	-1.864173	-2.058731	-7.285587
123	1	0	-2.507309	-1.239572	-6.943179
124	1	0	-2.335923	-2.526570	-8.159726
125	1	0	-0.897828	-1.638723	-7.589848

Rotational constants (GHZ): 0.0557429 0.0282345
0.0262850

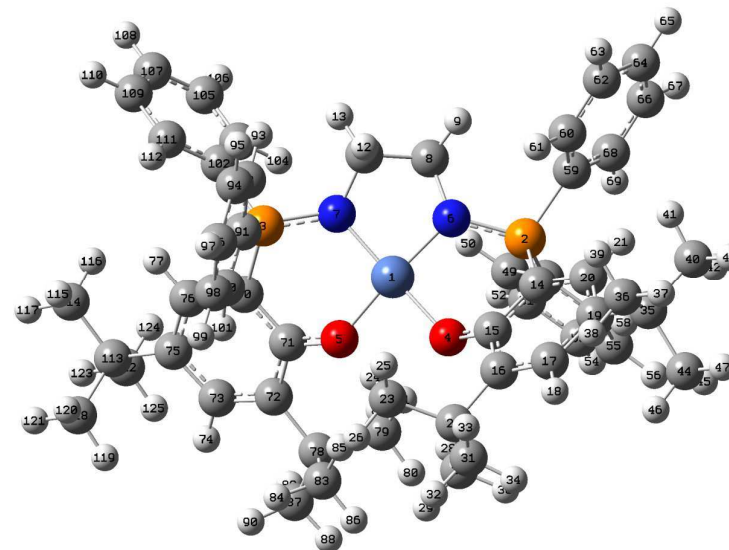
Sum of electronic and zero-point Energies= -3202.971603
Sum of electronic and thermal Energies= -3202.910930
Sum of electronic and thermal Enthalpies= -3202.909985
Sum of electronic and thermal Free Energies= -3203.069669

1 2 3

Appendix 2. Optimised Structures

Frequencies --	A 8.3015	A 12.7267	A
19.7535			
Red. masses --	4.6911	5.0398	
4.1586			
Frc consts --	0.0002	0.0005	
0.0010			
IR Inten --	0.1893	0.0662	
0.0376			

Complex [37a]⁺



Z-Matrix orientation:

Center Number	Atomic Number	Atomic Type	Coordinates (Angstroms)		
			X	Y	Z
1	28	0	-0.027215	-0.083833	0.057748
2	15	0	-0.109982	-0.204110	3.064512
3	15	0	1.914763	0.179430	-2.260311
4	8	0	-1.755362	0.131079	0.787887
5	8	0	-0.860019	-0.621487	-1.467601
6	7	0	0.791705	0.009135	1.679750
7	7	0	1.728437	-0.149652	-0.657269
8	6	0	2.249561	-0.149177	1.644983
9	1	0	2.727307	0.373813	2.480978
10	1	0	2.543375	-1.208221	1.694303
11	6	0	2.661467	0.437509	0.313752

Appendix 2. Optimised Structures

12	1	0	2.575533	1.533937	0.365832
13	1	0	3.701289	0.184626	0.069490
14	6	0	-1.452362	0.946901	2.998057
15	6	0	-2.112975	0.974969	1.747221
16	6	0	-3.208342	1.881852	1.601753
17	6	0	-3.536184	2.661108	2.707879
18	1	0	-4.367036	3.349329	2.599541
19	6	0	-2.885733	2.635063	3.956922
20	6	0	-1.824507	1.752042	4.085012
21	1	0	-1.275275	1.675384	5.017308
22	6	0	-4.025588	1.958260	0.314258
23	6	0	-3.111914	2.266783	-0.898929
24	1	0	-2.372445	1.476363	-1.038245
25	1	0	-2.597303	3.225414	-0.754047
26	1	0	-3.727983	2.338537	-1.804450
27	6	0	-4.749930	0.604356	0.097192
28	1	0	-4.026086	-0.212111	0.040098
29	1	0	-5.322443	0.639825	-0.838035
30	1	0	-5.446296	0.412591	0.923131
31	6	0	-5.107854	3.060215	0.361421
32	1	0	-5.636787	3.064820	-0.599024
33	1	0	-4.667663	4.054352	0.510284
34	1	0	-5.848932	2.871185	1.147731
35	6	0	-3.352742	3.550948	5.085233
36	6	0	-3.222963	5.032702	4.646231
37	1	0	-3.570390	5.688226	5.454299
38	1	0	-3.827455	5.237894	3.755473
39	1	0	-2.177572	5.277564	4.422516
40	6	0	-2.523594	3.360907	6.372981
41	1	0	-1.464430	3.593799	6.206055
42	1	0	-2.609145	2.336198	6.756099
43	1	0	-2.901578	4.041961	7.144259
44	6	0	-4.836453	3.256065	5.425927
45	1	0	-4.956384	2.218483	5.760036
46	1	0	-5.485017	3.420174	4.558027
47	1	0	-5.168413	3.922757	6.231399
48	6	0	-0.718802	-1.904093	3.214268
49	6	0	-0.079827	-2.952752	2.541937
50	1	0	0.760845	-2.749525	1.884729
51	6	0	-0.541123	-4.258107	2.696535
52	1	0	-0.047783	-5.070841	2.170844
53	6	0	-1.638492	-4.518493	3.517077
54	1	0	-1.998242	-5.537116	3.633439
55	6	0	-2.282733	-3.473601	4.180264
56	1	0	-3.145794	-3.675279	4.808372
57	6	0	-1.827847	-2.165935	4.030083
58	1	0	-2.342599	-1.350279	4.531456
59	6	0	0.936113	0.150533	4.499252
60	6	0	1.457879	1.446592	4.651731
61	1	0	1.208217	2.222333	3.932095
62	6	0	2.286236	1.738629	5.730853
63	1	0	2.685579	2.742032	5.848913
64	6	0	2.598292	0.745268	6.661549
65	1	0	3.242693	0.977278	7.505048
66	6	0	2.083954	-0.541124	6.512521
67	1	0	2.325602	-1.313198	7.237401
68	6	0	1.255444	-0.843158	5.432543
69	1	0	0.856364	-1.846638	5.320171

Appendix 2. Optimised Structures

70	6	0	0.837410	-0.954230	-3.119578
71	6	0	-0.427210	-1.243928	-2.552181
72	6	0	-1.259715	-2.204627	-3.210832
73	6	0	-0.767014	-2.770962	-4.383340
74	1	0	-1.392523	-3.499455	-4.885430
75	6	0	0.475264	-2.474813	-4.970318
76	6	0	1.275244	-1.550826	-4.306245
77	1	0	2.252866	-1.293101	-4.698032
78	6	0	-2.644268	-2.576228	-2.682550
79	6	0	-2.572925	-3.046969	-1.206341
80	1	0	-3.575152	-3.353273	-0.881998
81	1	0	-2.226043	-2.243465	-0.554557
82	1	0	-1.902433	-3.910810	-1.112359
83	6	0	-3.575609	-1.341586	-2.791102
84	1	0	-3.677721	-1.032533	-3.839039
85	1	0	-3.181276	-0.510348	-2.203363
86	1	0	-4.569665	-1.601838	-2.407275
87	6	0	-3.295151	-3.719702	-3.495231
88	1	0	-4.268387	-3.947622	-3.045427
89	1	0	-2.687814	-4.633167	-3.468293
90	1	0	-3.472421	-3.432064	-4.538854
91	6	0	1.555279	1.894063	-2.737910
92	6	0	2.384946	2.940198	-2.298228
93	1	0	3.294113	2.726842	-1.741755
94	6	0	2.059293	4.260529	-2.595202
95	1	0	2.706953	5.064938	-2.257800
96	6	0	0.907544	4.548386	-3.329246
97	1	0	0.657414	5.579799	-3.562003
98	6	0	0.081472	3.515136	-3.768297
99	1	0	-0.812757	3.737703	-4.343410
100	6	0	0.400317	2.190904	-3.474269
101	1	0	-0.245680	1.389050	-3.819796
102	6	0	3.627503	-0.183810	-2.731272
103	6	0	4.225868	-1.333293	-2.190880
104	1	0	3.672356	-1.947081	-1.485082
105	6	0	5.519905	-1.683667	-2.562840
106	1	0	5.981896	-2.571459	-2.140127
107	6	0	6.220278	-0.898556	-3.480737
108	1	0	7.230133	-1.175095	-3.771089
109	6	0	5.625360	0.236340	-4.028939
110	1	0	6.167689	0.844325	-4.747466
111	6	0	4.330778	0.597572	-3.657267
112	1	0	3.872899	1.482307	-4.089400
113	6	0	0.898417	-3.160972	-6.265359
114	6	0	2.284720	-2.690144	-6.753846
115	1	0	2.292442	-1.612214	-6.958560
116	1	0	3.068442	-2.923703	-6.022430
117	1	0	2.528230	-3.211788	-7.686499
118	6	0	-0.133018	-2.853980	-7.382599
119	1	0	-1.133043	-3.211731	-7.112996
120	1	0	-0.186618	-1.775555	-7.573687
121	1	0	0.171106	-3.357371	-8.308325
122	6	0	0.962130	-4.695698	-6.048476
123	1	0	1.255504	-5.184764	-6.985417
124	1	0	1.700893	-4.946245	-5.277736
125	1	0	-0.011218	-5.096572	-5.743966

Appendix 2. Optimised Structures

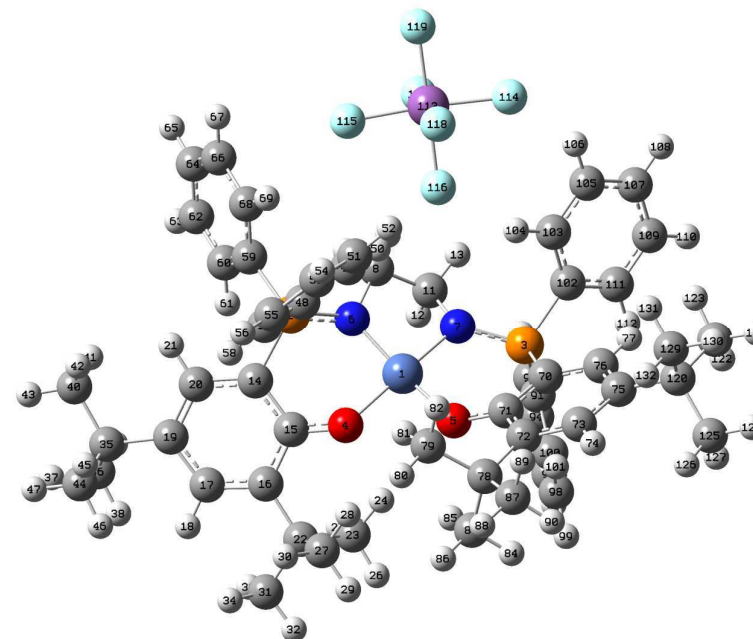
Rotational constants (GHZ): 0.0549741 0.0283287
0.0269105

Sum of electronic and zero-point Energies= -3202.773558
Sum of electronic and thermal Energies= -3202.712880
Sum of electronic and thermal Enthalpies= -3202.711936
Sum of electronic and thermal Free Energies= -3202.872181

	1	2	3
	A	A	A
Frequencies --	8.7115	12.6680	
21.1264			
Red. masses --	4.6569	5.0842	
4.0743			
Frc consts --	0.0002	0.0005	
0.0011			
IR Inten --	0.1320	0.0469	
0.0343			

Appendix 2. Optimised Structures

Complex [37a][SbF₆]



Standard orientation:

Center Number	Atomic Number	Atomic Type	Coordinates (Angstroms)		
			X	Y	Z
1	28	0	0.575883	-1.064578	0.400618
2	15	0	2.522586	1.150484	-0.084205
3	15	0	-2.230584	-1.457325	1.598869
4	8	0	2.171575	-1.711098	-0.370663
5	8	0	-0.257278	-2.454266	-0.444158
6	7	0	1.290688	0.528143	0.861413
7	7	0	-0.926930	-0.497335	1.368037
8	6	0	0.428023	1.406069	1.669942
9	1	0	1.031174	1.995890	2.369448
10	1	0	-0.154502	2.090190	1.043999
11	6	0	-0.506950	0.463965	2.393366
12	1	0	0.022543	-0.032328	3.222091
13	1	0	-1.364355	1.010249	2.805314
14	6	0	3.838880	-0.037191	-0.023484
15	6	0	3.426385	-1.389224	-0.118411
16	6	0	4.439521	-2.394660	0.005474
17	6	0	5.753314	-1.964260	0.152225

Appendix 2. Optimised Structures

18	1	0	6.519788	-2.727007	0.236632
19	6	0	6.176160	-0.621482	0.200131
20	6	0	5.183763	0.341630	0.118429
21	1	0	5.431503	1.396878	0.165080
22	6	0	4.101440	-3.882876	-0.067181
23	6	0	3.018717	-4.256176	0.978326
24	1	0	2.094301	-3.708967	0.785722
25	1	0	3.371744	-4.028036	1.992248
26	1	0	2.813263	-5.332757	0.916392
27	6	0	3.588043	-4.220105	-1.490157
28	1	0	2.708335	-3.619334	-1.729304
29	1	0	3.319079	-5.283005	-1.542031
30	1	0	4.373262	-4.022134	-2.230943
31	6	0	5.327312	-4.783809	0.206838
32	1	0	5.000978	-5.830134	0.166820
33	1	0	5.751433	-4.597228	1.201735
34	1	0	6.109557	-4.649494	-0.550619
35	6	0	7.658767	-0.288017	0.346474
36	6	0	8.209467	-0.891428	1.664463
37	1	0	9.278505	-0.662071	1.758412
38	1	0	8.088996	-1.980515	1.683366
39	1	0	7.683108	-0.468150	2.528548
40	6	0	7.915930	1.233904	0.377547
41	1	0	7.407629	1.708069	1.226265
42	1	0	7.581829	1.713743	-0.550779
43	1	0	8.992616	1.412651	0.483887
44	6	0	8.452649	-0.880408	-0.846509
45	1	0	8.098844	-0.452258	-1.792145
46	1	0	8.340537	-1.969465	-0.894859
47	1	0	9.519461	-0.648392	-0.734359
48	6	0	1.992678	1.438131	-1.789520
49	6	0	0.686493	1.861282	-2.071169
50	1	0	-0.048691	1.995609	-1.283659
51	6	0	0.320155	2.130357	-3.388947
52	1	0	-0.686355	2.481664	-3.595727
53	6	0	1.245884	1.966634	-4.418880
54	1	0	0.955963	2.179071	-5.444694
55	6	0	2.542597	1.532946	-4.139204
56	1	0	3.260168	1.397826	-4.944083
57	6	0	2.921418	1.268548	-2.826041
58	1	0	3.927771	0.921673	-2.606908
59	6	0	3.035199	2.721999	0.649421
60	6	0	3.747588	2.718434	1.861288
61	1	0	4.055197	1.778253	2.311195
62	6	0	4.058493	3.922870	2.483401
63	1	0	4.613612	3.919559	3.417636
64	6	0	3.648951	5.130943	1.913771
65	1	0	3.883595	6.069433	2.409094
66	6	0	2.929134	5.135789	0.721603
67	1	0	2.583830	6.068733	0.287180
68	6	0	2.622463	3.934747	0.083424
69	1	0	2.040377	3.953856	-0.831978
70	6	0	-2.594150	-2.227275	0.030898
71	6	0	-1.520222	-2.626111	-0.798820
72	6	0	-1.832850	-3.263305	-2.042179
73	6	0	-3.178647	-3.414985	-2.360880
74	1	0	-3.417349	-3.883822	-3.308935
75	6	0	-4.254255	-3.000657	-1.556098

Appendix 2. Optimised Structures

76	6	0	-3.931551	-2.407596	-0.342549
77	1	0	-4.713506	-2.060370	0.323795
78	6	0	-0.739043	-3.784762	-2.972511
79	6	0	0.226921	-2.645601	-3.388787
80	1	0	0.981903	-3.049394	-4.076013
81	1	0	0.733347	-2.223307	-2.519573
82	1	0	-0.323274	-1.850683	-3.907531
83	6	0	0.049321	-4.907313	-2.248475
84	1	0	-0.619024	-5.744479	-2.008321
85	1	0	0.501433	-4.526995	-1.329698
86	1	0	0.845831	-5.276369	-2.906417
87	6	0	-1.312722	-4.394200	-4.272018
88	1	0	-0.473973	-4.744558	-4.885226
89	1	0	-1.870407	-3.650780	-4.855353
90	1	0	-1.961058	-5.255372	-4.066682
91	6	0	-1.995690	-2.740709	2.872685
92	6	0	-1.851956	-2.369411	4.219565
93	1	0	-1.973011	-1.331078	4.518192
94	6	0	-1.571369	-3.332433	5.185010
95	1	0	-1.465664	-3.037954	6.225714
96	6	0	-1.429466	-4.670944	4.816501
97	1	0	-1.210985	-5.421305	5.571767
98	6	0	-1.570269	-5.045666	3.481345
99	1	0	-1.462977	-6.087640	3.192276
100	6	0	-1.851054	-4.085828	2.510444
101	1	0	-1.959913	-4.381074	1.470725
102	6	0	-3.637147	-0.437167	2.103384
103	6	0	-3.783083	0.823114	1.501694
104	1	0	-3.041041	1.194588	0.799358
105	6	0	-4.884641	1.616500	1.815955
106	1	0	-4.977654	2.593886	1.351142
107	6	0	-5.842826	1.151101	2.717400
108	1	0	-6.701204	1.772082	2.960512
109	6	0	-5.705388	-0.105111	3.308781
110	1	0	-6.454136	-0.465400	4.009344
111	6	0	-4.603307	-0.902428	3.006911
112	1	0	-4.497387	-1.878753	3.471247
113	51	0	-2.218381	4.685195	-0.445536
114	9	0	-4.048910	4.227354	-0.089900
115	9	0	-0.349103	5.009014	-0.767083
116	9	0	-1.764294	2.809997	-0.208064
117	9	0	-1.920415	4.922786	1.434310
118	9	0	-2.463074	4.318735	-2.310599
119	9	0	-2.644176	6.528559	-0.683142
120	6	0	-5.690890	-3.194098	-2.032749
121	6	0	-6.723167	-2.682582	-1.005279
122	1	0	-6.640953	-3.223231	-0.054038
123	1	0	-6.602521	-1.608529	-0.818838
124	1	0	-7.731948	-2.846272	-1.402550
125	6	0	-5.968044	-4.699382	-2.280405
126	1	0	-5.289908	-5.109910	-3.037018
127	1	0	-5.843639	-5.270851	-1.352518
128	1	0	-6.997933	-4.829820	-2.635693
129	6	0	-5.908684	-2.416076	-3.356792
130	1	0	-6.938035	-2.565275	-3.706367
131	1	0	-5.742733	-1.343282	-3.203001
132	1	0	-5.225414	-2.765151	-4.139381

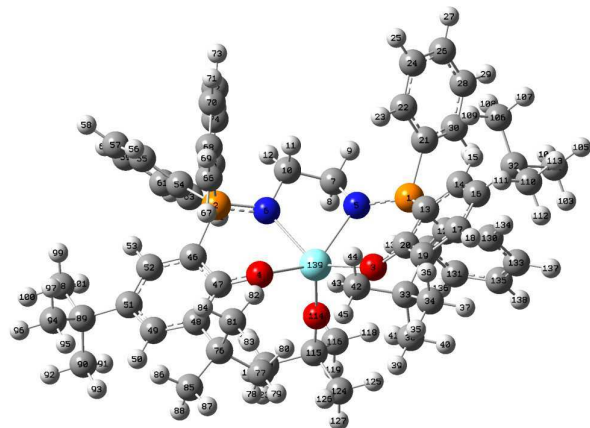
Rotational constants (GHZ): 0.0311485 0.0267516
0.0192758

Sum of electronic and zero-point Energies= -3807.522404
Sum of electronic and thermal Energies= -3807.450943
Sum of electronic and thermal Enthalpies= -3807.449999
Sum of electronic and thermal Free Energies= -3807.636885

	1	2	3
	A	A	A
Frequencies --	9.2656	11.1668	
13.5524			
Red. masses --	4.9042	6.9776	
9.2771			
Frc consts --	0.0002	0.0005	
0.0010			
IR Inten --	0.2584	1.3010	
1.0411			

Chapter 5

Complex 45



Standard orientation:

Center Number	Atomic Number	Atomic Type	Coordinates (Angstroms)		
			X	Y	Z
1	15	0	-3.041670	1.100443	0.749695
2	15	0	2.646034	1.526886	-0.673258
3	8	0	-1.682441	-1.546408	0.186293

4	8	0	1.694265	-1.331294	-0.557422
5	7	0	-1.417653	1.290192	0.733246
6	7	0	1.266582	1.541357	0.224530
7	6	0	-0.793209	2.584251	0.996913
8	1	0	-0.445665	2.655586	2.041491
9	1	0	-1.467606	3.436238	0.823905
10	6	0	0.416344	2.725643	0.078043
11	1	0	0.042199	2.836590	-0.953835
12	1	0	0.945745	3.659718	0.334312
13	6	0	-3.616466	-0.260676	-0.304621
14	6	0	-4.863085	-0.124345	-0.928537
15	1	0	-5.396951	0.818559	-0.842015
16	6	0	-5.424138	-1.168087	-1.657996
17	6	0	-4.682007	-2.357215	-1.717257
18	1	0	-5.105728	-3.187885	-2.267303
19	6	0	-3.436384	-2.549188	-1.118417
20	6	0	-2.855712	-1.460660	-0.392075
21	6	0	-3.873733	2.630273	0.137699
22	6	0	-3.581083	3.046736	-1.169287
23	1	0	-2.918296	2.448840	-1.789742
24	6	0	-4.140240	4.218292	-1.671805
25	1	0	-3.912582	4.532873	-2.687010
26	6	0	-4.992059	4.984868	-0.873884
27	1	0	-5.428612	5.899317	-1.267472
28	6	0	-5.282017	4.577284	0.426255
29	1	0	-5.943638	5.172188	1.050563
30	6	0	-4.724151	3.402678	0.933655
31	1	0	-4.954834	3.089262	1.947612
32	6	0	-6.784562	-0.987794	-2.345606
33	6	0	-2.711634	-3.899709	-1.228292
34	6	0	-3.528050	-4.943776	-2.006630
35	1	0	-2.967060	-5.885363	-2.036100
36	1	0	-3.710604	-4.640292	-3.044732
37	1	0	-4.494188	-5.153074	-1.531545
38	6	0	-2.462338	-4.475100	0.181197
39	1	0	-1.920240	-5.427021	0.109710
40	1	0	-3.414476	-4.668149	0.691157
41	1	0	-1.877884	-3.787019	0.794446
42	6	0	-1.375736	-3.717419	-1.973250
43	1	0	-0.720375	-3.016648	-1.454042
44	1	0	-1.548558	-3.340231	-2.989095
45	1	0	-0.853462	-4.679111	-2.054787
46	6	0	3.634793	0.029210	-0.414710
47	6	0	3.001774	-1.244089	-0.466360
48	6	0	3.852574	-2.400303	-0.443365
49	6	0	5.219286	-2.201993	-0.279396
50	1	0	5.855115	-3.079992	-0.238780
51	6	0	5.844938	-0.946634	-0.162602
52	6	0	5.023770	0.166731	-0.255644
53	1	0	5.449204	1.161952	-0.200988
54	6	0	3.709686	2.969550	-0.222755
55	6	0	4.582726	3.590241	-1.123520
56	1	0	4.639311	3.245825	-2.152493
57	6	0	5.383345	4.651251	-0.702041
58	1	0	6.061202	5.128156	-1.405326
59	6	0	5.313638	5.098905	0.617064
60	1	0	5.936946	5.927841	0.942826
61	6	0	4.444937	4.482849	1.518048

Appendix 2. Optimised Structures

62	1	0	4.389226	4.829604	2.546736
63	6	0	3.645513	3.420280	1.101078
64	1	0	2.965311	2.931276	1.794302
65	6	0	2.326646	1.724309	-2.484643
66	6	0	2.367073	0.610088	-3.331149
67	1	0	2.662210	-0.357082	-2.937678
68	6	0	2.028101	0.739720	-4.676774
69	1	0	2.067168	-0.130881	-5.326326
70	6	0	1.643411	1.978845	-5.188205
71	1	0	1.381530	2.077048	-6.238714
72	6	0	1.600741	3.093128	-4.350950
73	1	0	1.307528	4.062874	-4.745317
74	6	0	1.938757	2.968029	-3.004222
75	1	0	1.917320	3.846166	-2.364051
76	6	0	3.276006	-3.813090	-0.629945
77	6	0	2.296552	-4.159431	0.507499
78	1	0	2.803380	-4.127204	1.479184
79	1	0	1.899549	-5.173184	0.366846
80	1	0	1.454656	-3.466547	0.536794
81	6	0	2.553220	-3.888204	-1.989946
82	1	0	1.751172	-3.149957	-2.050846
83	1	0	2.117892	-4.885485	-2.132765
84	1	0	3.259337	-3.709112	-2.810767
85	6	0	4.366660	-4.895910	-0.631658
86	1	0	5.099216	-4.747257	-1.434363
87	1	0	3.898407	-5.873956	-0.793107
88	1	0	4.904424	-4.946193	0.323054
89	6	0	7.360975	-0.860827	0.048309
90	6	0	7.736002	-1.571848	1.363585
91	1	0	7.238825	-1.097933	2.217855
92	1	0	8.820042	-1.528896	1.530595
93	1	0	7.442538	-2.627324	1.351781
94	6	0	8.091418	-1.543009	-1.125312
95	1	0	7.814809	-2.598739	-1.220634
96	1	0	9.178340	-1.496871	-0.980140
97	1	0	7.852798	-1.048811	-2.074427
98	6	0	7.851353	0.590922	0.133858
99	1	0	7.640470	1.147654	-0.787012
100	1	0	8.936919	0.607053	0.287220
101	1	0	7.391205	1.128106	0.971509
102	6	0	-7.854804	-0.628789	-1.295737
103	1	0	-7.945294	-1.421754	-0.543981
104	1	0	-7.615851	0.304325	-0.773048
105	1	0	-8.834870	-0.498221	-1.772456
106	6	0	-6.690142	0.149785	-3.381663
107	1	0	-7.658013	0.304416	-3.876059
108	1	0	-6.397325	1.097715	-2.916618
109	1	0	-5.947392	-0.086484	-4.152633
110	6	0	-7.244542	-2.258564	-3.073343
111	1	0	-6.545032	-2.552358	-3.864637
112	1	0	-7.358691	-3.104699	-2.385512
113	1	0	-8.219020	-2.081885	-3.543870
114	8	0	0.618466	-0.930813	2.702248
115	6	0	1.046224	-1.313322	3.976299
116	6	0	0.499792	-0.319841	5.012781
117	1	0	0.852645	0.693071	4.783448
118	1	0	-0.595625	-0.318387	4.986432
119	1	0	0.821852	-0.575495	6.030273

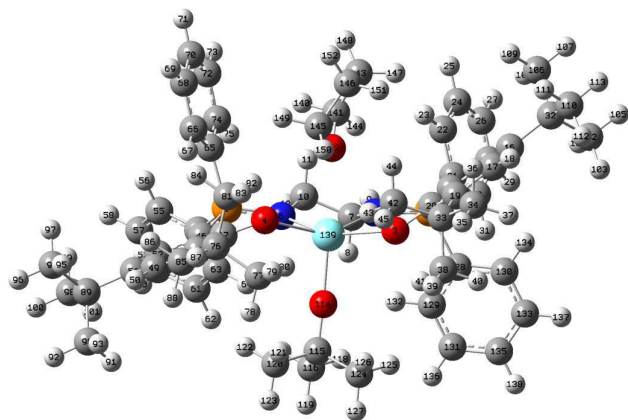
Appendix 2. Optimised Structures

120	6	0	2.581644	-1.309252	4.017394
121	1	0	2.979809	-1.991796	3.258554
122	1	0	2.961319	-0.304253	3.798451
123	1	0	2.964005	-1.617901	4.998808
124	6	0	0.517220	-2.722183	4.284070
125	1	0	-0.577753	-2.730935	4.232112
126	1	0	0.897602	-3.436243	3.544883
127	1	0	0.820921	-3.063043	5.282170
128	6	0	-3.745219	0.807062	2.434069
129	6	0	-2.973953	1.134365	3.553306
130	6	0	-5.026402	0.268433	2.607158
131	6	0	-3.487107	0.943932	4.836225
132	1	0	-1.965756	1.514934	3.420480
133	6	0	-5.535113	0.078499	3.890218
134	1	0	-5.618399	-0.016344	1.741301
135	6	0	-4.767670	0.419362	5.004971
136	1	0	-2.880861	1.196046	5.702271
137	1	0	-6.528079	-0.344380	4.019773
138	1	0	-5.164831	0.266162	6.005247
139	39	0	0.134352	-0.492134	0.768348

 Rotational constants (GHZ): 0.0461968 0.0242741
 0.0226338

Sum of electronic and zero-point Energies= -2638.893885
 Sum of electronic and thermal Energies= -2638.824020
 Sum of electronic and thermal Enthalpies= -2638.823076
 Sum of electronic and thermal Free Energies= -2639.003943

	1	2	3
	A	A	A
Frequencies --	9.6572	11.8801	
15.1770			
Red. masses --	4.9353	4.5005	
4.6516			
Frc consts --	0.0003	0.0004	
0.0006			
IR Inten --	0.0316	0.0448	
0.0863			

Complex 45-THF

Standard orientation:

Center Number	Atomic Number	Atomic Type	Coordinates (Angstroms)		
			X	Y	Z
1	15	0	-2.976916	1.314924	0.701790
2	15	0	2.873296	1.430304	-0.621434
3	8	0	-1.879829	-1.472027	0.638844
4	8	0	1.829646	-1.459837	-0.468641
5	7	0	-1.369244	1.437699	0.415928
6	7	0	1.337693	1.497557	-0.050877
7	6	0	-0.675855	2.713614	0.588325
8	1	0	-0.355045	2.865458	1.632337
9	1	0	-1.297215	3.581099	0.314352
10	6	0	0.572720	2.718905	-0.293151
11	1	0	0.254058	2.798846	-1.346174
12	1	0	1.144917	3.634457	-0.062635
13	6	0	-3.730100	-0.156999	-0.047966
14	6	0	-5.000862	-0.054829	-0.627147
15	1	0	-5.445915	0.928143	-0.755729
16	6	0	-5.703088	-1.186875	-1.032570
17	6	0	-5.097537	-2.426035	-0.768406
18	1	0	-5.647417	-3.321223	-1.031215
19	6	0	-3.844691	-2.589551	-0.176943
20	6	0	-3.087231	-1.416648	0.148841
21	6	0	-3.857890	2.800999	0.036630
22	6	0	-3.851135	3.012218	-1.349849
23	1	0	-3.406114	2.269319	-2.005847
24	6	0	-4.426728	4.158103	-1.891898
25	1	0	-4.423405	4.306602	-2.968732
26	6	0	-5.006973	5.111812	-1.053769
27	1	0	-5.455298	6.007244	-1.476671
28	6	0	-5.009222	4.913627	0.324944

29	1	0	-5.456692	5.654455	0.982529
30	6	0	-4.437171	3.763132	0.869863
31	1	0	-4.445017	3.616260	1.945615
32	6	0	-7.079973	-1.045599	-1.696310
33	6	0	-3.311787	-3.989732	0.171774
34	6	0	-4.314034	-5.102506	-0.172826
35	1	0	-3.890860	-6.069575	0.123776
36	1	0	-4.526801	-5.155013	-1.247886
37	1	0	-5.264083	-4.982515	0.361558
38	6	0	-3.040481	-4.066604	1.688840
39	1	0	-2.639577	-5.054721	1.950515
40	1	0	-3.969332	-3.918920	2.253410
41	1	0	-2.322518	-3.304650	1.999304
42	6	0	-2.013246	-4.289643	-0.599766
43	1	0	-1.238777	-3.560387	-0.356694
44	1	0	-2.191084	-4.270648	-1.682438
45	1	0	-1.638965	-5.287859	-0.337998
46	6	0	3.758993	-0.095547	-0.193012
47	6	0	3.116943	-1.367540	-0.275365
48	6	0	3.961270	-2.529403	-0.167051
49	6	0	5.310584	-2.340674	0.105830
50	1	0	5.934328	-3.222700	0.208635
51	6	0	5.934900	-1.088105	0.259492
52	6	0	5.132715	0.028143	0.081999
53	1	0	5.563959	1.019873	0.158292
54	6	0	3.847866	2.849226	0.056349
55	6	0	4.854199	3.512986	-0.654188
56	1	0	5.089422	3.216568	-1.672753
57	6	0	5.560279	4.556532	-0.055962
58	1	0	6.342611	5.066742	-0.612140
59	6	0	5.263433	4.943766	1.250283
60	1	0	5.814611	5.758094	1.713879
61	6	0	4.259005	4.286368	1.961380
62	1	0	4.024594	4.586286	2.979555
63	6	0	3.552784	3.242782	1.367435
64	1	0	2.765193	2.726277	1.910446
65	6	0	2.985544	1.633212	-2.461129
66	6	0	3.348790	0.551882	-3.271972
67	1	0	3.642606	-0.387833	-2.813180
68	6	0	3.343783	0.681428	-4.660567
69	1	0	3.634887	-0.162754	-5.280683
70	6	0	2.976514	1.890110	-5.251212
71	1	0	2.976952	1.990440	-6.333737
72	6	0	2.619024	2.974524	-4.449582
73	1	0	2.342007	3.922360	-4.904419
74	6	0	2.623294	2.848497	-3.061250
75	1	0	2.360489	3.705404	-2.446353
76	6	0	3.392521	-3.943026	-0.379661
77	6	0	2.340005	-4.277682	0.693693
78	1	0	2.796134	-4.285939	1.690004
79	1	0	1.915983	-5.273469	0.508337
80	1	0	1.526598	-3.550673	0.697706
81	6	0	2.758703	-4.033050	-1.782416
82	1	0	1.972074	-3.286436	-1.900744
83	1	0	2.324902	-5.029387	-1.939434
84	1	0	3.516462	-3.869949	-2.559505
85	6	0	4.476518	-5.030096	-0.304021
86	1	0	5.260658	-4.887540	-1.057703

Appendix 2. Optimised Structures

87	1	0	4.016023	-6.007627	-0.490332
88	1	0	4.950391	-5.077060	0.683901
89	6	0	7.429436	-1.010233	0.591275
90	6	0	7.695104	-1.712002	1.937883
91	1	0	7.137372	-1.226552	2.747045
92	1	0	8.763243	-1.675871	2.188194
93	1	0	7.394550	-2.765207	1.912647
94	6	0	8.245986	-1.707928	-0.514674
95	1	0	7.970687	-2.763038	-0.620603
96	1	0	9.318798	-1.666304	-0.286254
97	1	0	8.084728	-1.222364	-1.484413
98	6	0	7.922311	0.438903	0.703241
99	1	0	7.793165	0.986918	-0.237817
100	1	0	8.991408	0.449434	0.946640
101	1	0	7.397324	0.988209	1.493509
102	6	0	-8.054254	-0.342382	-0.730288
103	1	0	-8.165408	-0.916739	0.196829
104	1	0	-7.706549	0.661916	-0.463031
105	1	0	-9.046569	-0.238268	-1.188124
106	6	0	-6.950670	-0.205221	-2.982149
107	1	0	-7.928494	-0.085579	-3.466652
108	1	0	-6.558335	0.796343	-2.773264
109	1	0	-6.273699	-0.687935	-3.696969
110	6	0	-7.687097	-2.403427	-2.076595
111	1	0	-7.048490	-2.952992	-2.778214
112	1	0	-7.854240	-3.037308	-1.197906
113	1	0	-8.658305	-2.250947	-2.562271
114	8	0	0.660279	-0.633127	2.462654
115	6	0	1.115564	-0.823536	3.767037
116	6	0	1.407168	0.541453	4.413788
117	1	0	2.169818	1.073364	3.833285
118	1	0	0.501157	1.158364	4.433211
119	1	0	1.770518	0.434488	5.444044
120	6	0	2.409151	-1.651948	3.749950
121	1	0	2.218995	-2.630180	3.297073
122	1	0	3.176023	-1.145982	3.152994
123	1	0	2.802007	-1.810500	4.762846
124	6	0	0.042778	-1.565306	4.580051
125	1	0	-0.891844	-0.993774	4.587268
126	1	0	-0.164161	-2.539445	4.122357
127	1	0	0.360072	-1.731112	5.617976
128	6	0	-3.447189	1.263700	2.488476
129	6	0	-2.464410	1.460116	3.460837
130	6	0	-4.771621	1.023599	2.877274
131	6	0	-2.806195	1.439985	4.813740
132	1	0	-1.430698	1.595502	3.159154
133	6	0	-5.109288	1.004097	4.228088
134	1	0	-5.535578	0.839804	2.125865
135	6	0	-4.127102	1.217354	5.197351
136	1	0	-2.035551	1.586005	5.565978
137	1	0	-6.137593	0.814335	4.525217
138	1	0	-4.391483	1.198061	6.251661
139	39	0	0.087562	-0.454157	0.500638
140	1	0	0.047229	0.909192	-3.306537
141	6	0	-0.877656	0.491061	-2.883189
142	8	0	-0.546773	-0.608198	-2.034936
143	6	0	-1.773924	-0.102384	-3.980376
144	1	0	-1.353710	1.243200	-2.254220

Appendix 2. Optimised Structures

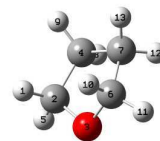
145	6	0	-0.299009	-1.701007	-2.919720
146	6	0	-1.408563	-1.606894	-3.972897
147	1	0	-2.831837	0.036229	-3.738228
148	1	0	-1.585268	0.371757	-4.948846
149	1	0	0.697378	-1.580624	-3.367836
150	1	0	-0.314542	-2.619769	-2.333651
151	1	0	-2.270623	-2.208153	-3.670181
152	1	0	-1.071016	-1.967419	-4.949641

 Rotational constants (GHZ): 0.0435340 0.0226522
 0.0213452

Sum of electronic and zero-point Energies= -2871.141187
 Sum of electronic and thermal Energies= -2871.064825
 Sum of electronic and thermal Enthalpies= -2871.063881
 Sum of electronic and thermal Free Energies= -2871.259119

	1	2	3
	A	A	A
Frequencies --	8.8309	11.9787	
16.4577			
Red. masses --	4.9587	4.3705	
5.0753			
Frc consts --	0.0002	0.0004	
0.0008			
IR Inten --	0.0318	0.0282	
0.1121			

THF



Standard orientation:

Center Number	Atomic Number	Atomic Type	Coordinates (Angstroms)		
			X	Y	Z
1	1	0	-1.334857	-0.677937	1.210686
2	6	0	-1.132251	-0.459661	0.147912
3	8	0	-0.009361	-1.198963	-0.297924
4	6	0	-0.761285	1.024588	-0.036518
5	1	0	-1.997988	-0.779510	-0.439021
6	6	0	1.117655	-0.480453	0.169223
7	6	0	0.786186	1.002566	-0.064685
8	1	0	-1.162015	1.414753	-0.977020
9	1	0	-1.159296	1.644355	0.773156
10	1	0	1.279041	-0.676639	1.243699
11	1	0	1.993907	-0.835328	-0.380747

Appendix 2. Optimised Structures

```

12      1      0      1.159698  1.331102  -1.039516
13      1      0      1.234565  1.648667  0.696559
-----

```

Rotational constants (GHZ): 7.1794263 6.9294258
4.0047528

```

Sum of electronic and zero-point Energies= -232.248141
Sum of electronic and thermal Energies= -232.243221
Sum of electronic and thermal Enthalpies= -232.242276
Sum of electronic and thermal Free Energies= -232.277148

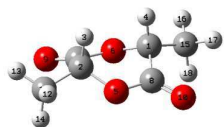
```

```

          1          2          3
          A          A          A
Frequencies -- 24.1180      282.4810
641.6987
Red. masses -- 1.5904      2.0693
2.3129
Frc consts  -- 0.0005      0.0973
0.5611
IR Inten    -- 0.0835      7.6377
3.3107

```

(R,R)-LA



Standard orientation:

Center Number	Atomic Number	Atomic Type	Coordinates (Angstroms)		
			X	Y	Z
1	6	0	1.254239	0.466248	0.434192
2	6	0	-1.254215	-0.466266	0.434179
3	1	0	-1.145206	-0.463895	1.530401
4	1	0	1.145212	0.463917	1.530407
5	8	0	-0.255738	-1.349741	-0.114353
6	8	0	0.255733	1.349744	-0.114401
7	6	0	-1.035197	0.960693	-0.059221
8	6	0	1.035184	-0.960681	-0.059227
9	8	0	-1.922040	1.708168	-0.377719
10	8	0	1.922018	-1.708166	-0.377744
11	6	0	-2.611609	-1.010992	0.049286
12	1	0	-2.725596	-2.028734	0.431650
13	1	0	-3.395455	-0.375674	0.467474
14	1	0	-2.721384	-1.022891	-1.038193
15	6	0	2.611624	1.010983	0.049297
16	1	0	2.725434	2.028856	0.431365

Appendix 2. Optimised Structures

```

17      1      0      3.395530  0.375922  0.467770
18      1      0      2.721537  1.022552  -1.038170
-----

```

Rotational constants (GHZ): 2.1988369 1.1957833
0.8179501

```

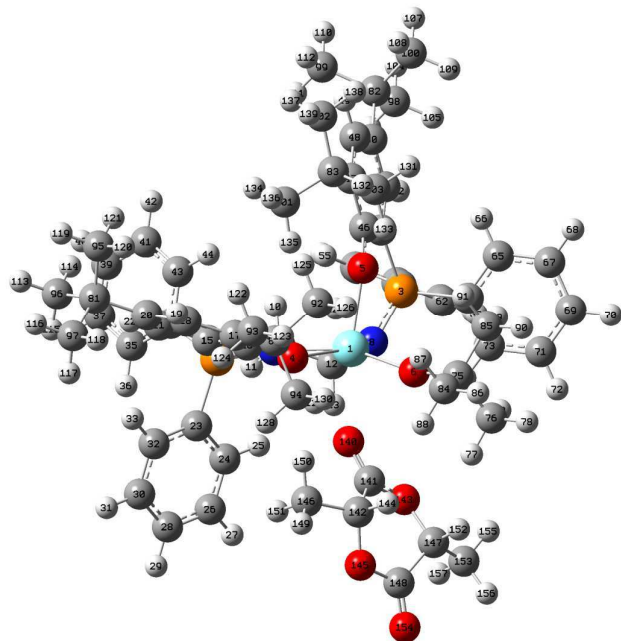
Sum of electronic and zero-point Energies= -534.017663
Sum of electronic and thermal Energies= -534.008238
Sum of electronic and thermal Enthalpies= -534.007294
Sum of electronic and thermal Free Energies= -534.052255

```

```

          1          2          3
          A          A          A
Frequencies -- 67.7468      131.3422
131.5655
Red. masses -- 5.1483      4.8822
4.7139
Frc consts  -- 0.0139      0.0496
0.0481
IR Inten    -- 6.4214      0.0079
0.2435

```

Initiation : INT1

Standard orientation:

Center Number	Atomic Number	Atomic Type	Coordinates (Angstroms)		
			X	Y	Z
1	39	0	0.017582	0.888824	-0.645241
2	15	0	-2.128598	-0.922148	1.657367
3	15	0	3.239261	0.449173	0.654520
4	8	0	-2.001922	0.173668	-1.186908
5	8	0	1.357614	-0.682214	-1.355810
6	8	0	0.271157	2.347033	-2.118365
7	7	0	-0.670585	-0.237795	1.385647
8	7	0	1.779582	1.112239	1.011518
9	6	0	0.290224	-0.228704	2.495085
10	1	0	0.899700	-1.148043	2.483660
11	1	0	-0.179270	-0.186259	3.492887
12	6	0	1.211084	0.983498	2.351118
13	1	0	0.618778	1.891128	2.534282
14	1	0	1.975929	0.944772	3.141616
15	6	0	-2.996602	-1.500170	0.172841
16	6	0	-2.859828	-0.806018	-1.059463
17	6	0	-3.706375	-1.228892	-2.143181
18	6	0	-4.564974	-2.301006	-1.927028

19	1	0	-5.194944	-2.617536	-2.751523
20	6	0	-4.676234	-3.016066	-0.719814
21	6	0	-3.876276	-2.585615	0.328152
22	1	0	-3.914514	-3.095920	1.285105
23	6	0	-3.298268	0.209527	2.553060
24	6	0	-2.792216	1.371967	3.142185
25	1	0	-1.738277	1.608602	3.034060
26	6	0	-3.641363	2.238094	3.831670
27	1	0	-3.239626	3.138486	4.290293
28	6	0	-5.003360	1.953528	3.925768
29	1	0	-5.665810	2.631000	4.458640
30	6	0	-5.516522	0.803514	3.324429
31	1	0	-6.580051	0.585954	3.382152
32	6	0	-4.668723	-0.065735	2.640102
33	1	0	-5.077110	-0.949805	2.157623
34	6	0	-1.950298	-2.395798	2.758002
35	6	0	-2.545600	-2.502207	4.017928
36	1	0	-3.194967	-1.712016	4.383753
37	6	0	-2.308656	-3.626437	4.810872
38	1	0	-2.776637	-3.703417	5.789030
39	6	0	-1.476580	-4.644587	4.350934
40	1	0	-1.294217	-5.519623	4.969743
41	6	0	-0.875474	-4.539891	3.094827
42	1	0	-0.224004	-5.331278	2.733023
43	6	0	-1.108154	-3.420244	2.301507
44	1	0	-0.637585	-3.335308	1.325019
45	6	0	3.319652	-1.196440	-0.126182
46	6	0	2.319848	-1.526544	-1.082929
47	6	0	2.436257	-2.799488	-1.739583
48	6	0	3.511512	-3.614921	-1.403248
49	1	0	3.590862	-4.574279	-1.903837
50	6	0	4.512561	-3.288291	-0.468950
51	6	0	4.393409	-2.056812	0.159045
52	1	0	5.139774	-1.742133	0.880101
53	6	0	4.312831	0.349251	2.158236
54	6	0	4.107487	-0.677715	3.091668
55	1	0	3.376657	-1.455872	2.888449
56	6	0	4.848408	-0.717002	4.270810
57	1	0	4.680375	-1.518368	4.985696
58	6	0	5.802640	0.267100	4.530579
59	1	0	6.382909	0.233757	5.449186
60	6	0	6.011351	1.290465	3.608327
61	1	0	6.756752	2.057352	3.802765
62	6	0	5.269257	1.333780	2.428217
63	1	0	5.441987	2.133968	1.714908
64	6	0	4.096166	1.616573	-0.478546
65	6	0	5.047930	1.164890	-1.398128
66	1	0	5.229754	0.099463	-1.508696
67	6	0	5.751290	2.082203	-2.177314
68	1	0	6.485252	1.728292	-2.896618
69	6	0	5.511273	3.449048	-2.036620
70	1	0	6.062547	4.162613	-2.643953
71	6	0	4.556978	3.900411	-1.124093
72	1	0	4.362628	4.965112	-1.021698
73	6	0	3.843550	2.986723	-0.349634
74	1	0	3.079348	3.317392	0.348540
75	6	0	0.589660	3.094461	-3.249782
76	6	0	0.956869	4.529510	-2.833546

Appendix 2. Optimised Structures

77	1	0	0.095067	5.010583	-2.350936
78	1	0	1.247749	5.146664	-3.693174
79	1	0	1.785616	4.509748	-2.118398
80	6	0	-3.668974	-0.517201	-3.506247
81	6	0	-5.644778	-4.199777	-0.613105
82	6	0	5.657780	-4.269368	-0.190526
83	6	0	1.413767	-3.240814	-2.797451
84	6	0	-0.616464	3.140585	-4.201547
85	6	0	1.786392	2.455303	-3.972155
86	1	0	-0.406570	3.736877	-5.099082
87	1	0	-0.889288	2.127669	-4.514093
88	1	0	-1.485057	3.578143	-3.693523
89	1	0	2.651535	2.415131	-3.301914
90	1	0	2.067713	3.014548	-4.874215
91	1	0	1.538718	1.428782	-4.264455
92	6	0	-2.280269	-0.685255	-4.150580
93	6	0	-4.702443	-1.082606	-4.493582
94	6	0	-3.981233	0.981118	-3.328932
95	6	0	-5.262433	-5.277021	-1.647384
96	6	0	-5.617966	-4.846738	0.778446
97	6	0	-7.083069	-3.718845	-0.889866
98	6	0	6.648495	-3.723507	0.846773
99	6	0	5.083282	-5.594753	0.347950
100	6	0	6.435369	-4.545919	-1.492426
101	6	0	0.014541	-3.335527	-2.160066
102	6	0	1.738231	-4.621576	-3.389714
103	6	0	1.404875	-2.233261	-3.964710
104	1	0	7.446312	-4.455759	1.018512
105	1	0	7.121295	-2.793879	0.508252
106	1	0	6.165193	-3.528343	1.811375
107	1	0	7.258357	-5.248770	-1.308511
108	1	0	5.793551	-4.981472	-2.266003
109	1	0	6.862111	-3.620186	-1.895851
110	1	0	5.889355	-6.311696	0.551060
111	1	0	4.531108	-5.429797	1.280723
112	1	0	4.396757	-6.060011	-0.367828
113	1	0	-6.319423	-5.688929	0.809875
114	1	0	-4.623721	-5.234732	1.029161
115	1	0	-5.917008	-4.140842	1.562777
116	1	0	-7.789089	-4.557034	-0.828524
117	1	0	-7.389179	-2.961110	-0.158901
118	1	0	-7.178750	-3.276133	-1.887247
119	1	0	-5.953809	-6.127823	-1.591696
120	1	0	-5.295477	-4.887696	-2.670778
121	1	0	-4.247576	-5.649290	-1.465602
122	1	0	-4.522716	-2.139453	-4.724984
123	1	0	-4.635008	-0.527486	-5.436638
124	1	0	-5.729982	-0.978418	-4.123894
125	1	0	-2.061091	-1.744483	-4.327378
126	1	0	-2.249112	-0.168000	-5.118562
127	1	0	-1.495273	-0.272423	-3.514792
128	1	0	-4.972384	1.120917	-2.879198
129	1	0	-3.233810	1.457465	-2.693154
130	1	0	-3.977777	1.483856	-4.304778
131	1	0	2.387236	-2.203837	-4.452717
132	1	0	0.663575	-2.532613	-4.716634
133	1	0	1.162630	-1.227362	-3.617784
134	1	0	0.008305	-4.089109	-1.362187

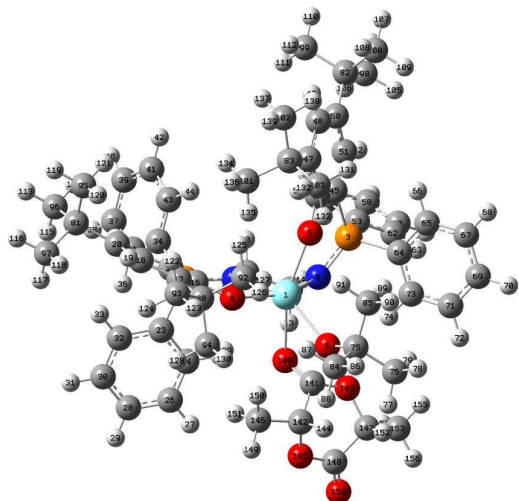
Appendix 2. Optimised Structures

135	1	0	-0.299672	-2.380312	-1.736929
136	1	0	-0.727003	-3.637717	-2.910172
137	1	0	1.727880	-5.412725	-2.629776
138	1	0	2.712008	-4.638716	-3.894223
139	1	0	0.977557	-4.876951	-4.136864
140	8	0	-0.939918	2.875589	0.585829
141	6	0	-1.220340	4.044878	0.431638
142	6	0	-2.506540	4.524246	-0.221088
143	8	0	-0.385362	4.993507	0.855103
144	1	0	-2.260793	4.776306	-1.264307
145	8	0	-2.994773	5.711997	0.437792
146	6	0	-3.611959	3.492785	-0.178234
147	6	0	-0.662431	6.364315	0.478834
148	6	0	-2.127143	6.697954	0.734867
149	1	0	-4.491038	3.881708	-0.698793
150	1	0	-3.283689	2.570981	-0.662694
151	1	0	-3.879605	3.265026	0.856857
152	1	0	-0.471351	6.452823	-0.600314
153	6	0	0.283080	7.252980	1.254091
154	8	0	-2.507571	7.754151	1.167765
155	1	0	1.318146	6.986217	1.024977
156	1	0	0.108291	8.295602	0.979489
157	1	0	0.113469	7.147774	2.329077

Rotational constants (GHZ): 0.0290047 0.0251375
0.0200209

Sum of electronic and zero-point Energies= -3172.904876
Sum of electronic and thermal Energies= -3172.823590
Sum of electronic and thermal Enthalpies= -3172.822646
Sum of electronic and thermal Free Energies= -3173.028573

	1	2	3
	A	A	A
Frequencies --	8.7438	12.8063	
13.3140			
Red. masses --	4.7748	5.6960	
5.3789			
Frc consts --	0.0002	0.0006	
0.0006			
IR Inten --	0.0481	0.1189	
0.1216			

Intitiation TS1

Standard orientation:

Center Number	Atomic Number	Atomic Type	Coordinates (Angstroms)		
			X	Y	Z
1	39	0	0.165743	0.981483	-0.441731
2	15	0	-2.355979	-0.275323	1.731502
3	15	0	3.105326	-0.595413	0.641867
4	8	0	-1.928837	0.824687	-1.070582
5	8	0	1.029264	-0.775642	-1.450449
6	8	0	0.783152	2.943333	-1.545788
7	7	0	-0.760331	0.010707	1.484442
8	7	0	1.940741	0.471657	1.066950
9	6	0	0.136432	-0.221941	2.626043
10	1	0	0.379229	-1.294042	2.708582
11	1	0	-0.301433	0.073269	3.594848
12	6	0	1.426325	0.579097	2.428641
13	1	0	1.208504	1.640378	2.602604
14	1	0	2.154968	0.271025	3.192924
15	6	0	-3.317749	-0.595905	0.227020
16	6	0	-3.024020	0.109070	-0.970321
17	6	0	-3.978158	0.005948	-2.039301
18	6	0	-5.065409	-0.844462	-1.867938
19	1	0	-5.770802	-0.930195	-2.687478
20	6	0	-5.322889	-1.601805	-0.710923
21	6	0	-4.435282	-1.439530	0.342812
22	1	0	-4.593546	-1.977455	1.271810
23	6	0	-3.187233	1.129848	2.602471
24	6	0	-2.421373	2.248784	2.941154

25	1	0	-1.368740	2.277693	2.675972
26	6	0	-3.021520	3.339287	3.572715
27	1	0	-2.421959	4.209239	3.828218
28	6	0	-4.384682	3.317239	3.861546
29	1	0	-4.851341	4.168781	4.350408
30	6	0	-5.155190	2.206952	3.510314
31	1	0	-6.221595	2.193674	3.721012
32	6	0	-4.560933	1.117274	2.878652
33	1	0	-5.169866	0.265014	2.587548
34	6	0	-2.570292	-1.751612	2.818334
35	6	0	-3.083386	-1.679913	4.116165
36	1	0	-3.436887	-0.732039	4.511179
37	6	0	-3.143137	-2.826833	4.909502
38	1	0	-3.546506	-2.763619	5.916897
39	6	0	-2.687003	-4.045816	4.413072
40	1	0	-2.735758	-4.938131	5.032109
41	6	0	-2.164549	-4.120432	3.120255
42	1	0	-1.804708	-5.068955	2.729896
43	6	0	-2.103387	-2.979103	2.325717
44	1	0	-1.694546	-3.036528	1.319939
45	6	0	2.620519	-2.088528	-0.279667
46	6	0	1.610369	-1.942205	-1.268777
47	6	0	1.290252	-3.106127	-2.047189
48	6	0	1.988515	-4.281790	-1.785611
49	1	0	1.740416	-5.155393	-2.379056
50	6	0	2.995962	-4.428032	-0.815463
51	6	0	3.299440	-3.298771	-0.067950
52	1	0	4.074685	-3.339518	0.689605
53	6	0	4.065708	-1.168903	2.110541
54	6	0	3.498868	-2.108457	2.984647
55	1	0	2.533640	-2.551382	2.753870
56	6	0	4.173505	-2.487708	4.142870
57	1	0	3.725461	-3.217206	4.812567
58	6	0	5.418490	-1.932917	4.440989
59	1	0	5.944580	-2.230851	5.344334
60	6	0	5.985844	-0.997434	3.578201
61	1	0	6.956380	-0.563605	3.804470
62	6	0	5.312683	-0.614599	2.418093
63	1	0	5.763022	0.114724	1.751438
64	6	0	4.315599	0.283627	-0.430822
65	6	0	5.123680	-0.423572	-1.328532
66	1	0	4.992053	-1.495737	-1.446822
67	6	0	6.087425	0.249958	-2.076288
68	1	0	6.710389	-0.300873	-2.776286
69	6	0	6.249630	1.627799	-1.927759
70	1	0	7.003727	2.151850	-2.509814
71	6	0	5.439728	2.333760	-1.038311
72	1	0	5.562606	3.408309	-0.929075
73	6	0	4.467037	1.667170	-0.292390
74	1	0	3.808099	2.208589	0.381175
75	6	0	1.228878	3.269197	-2.859301
76	6	0	2.387793	4.273260	-2.828280
77	1	0	2.051340	5.265190	-2.505507
78	1	0	2.818178	4.393352	-3.829556
79	1	0	3.175014	3.926699	-2.152470
80	6	0	-3.835565	0.845283	-3.320177
81	6	0	-6.541109	-2.531021	-0.653138
82	6	0	3.694370	-5.779487	-0.625205

Appendix 2. Optimised Structures

83	6	0	0.213850	-3.069715	-3.141572
84	6	0	0.068797	3.839070	-3.688500
85	6	0	1.722616	1.974043	-3.516483
86	1	0	0.380404	4.030596	-4.722932
87	1	0	-0.766870	3.132435	-3.707073
88	1	0	-0.296979	4.785167	-3.273421
89	1	0	2.546060	1.535610	-2.943006
90	1	0	2.074947	2.159782	-4.538746
91	1	0	0.914406	1.236790	-3.577146
92	6	0	-2.539190	0.487801	-4.069696
93	6	0	-4.999564	0.629833	-4.300710
94	6	0	-3.828861	2.338404	-2.939097
95	6	0	-6.443947	-3.580573	-1.777780
96	6	0	-6.638447	-3.276638	0.684766
97	6	0	-7.831620	-1.707862	-0.836573
98	6	0	4.767576	-5.725632	0.470501
99	6	0	2.655716	-6.845838	-0.224231
100	6	0	4.375375	-6.204465	-1.940987
101	6	0	-1.145824	-2.719556	-2.510782
102	6	0	0.048686	-4.420113	-3.856530
103	6	0	0.596404	-2.030657	-4.213397
104	1	0	5.239429	-6.709600	0.577104
105	1	0	5.558519	-5.004725	0.231414
106	1	0	4.342958	-5.455081	1.444492
107	1	0	4.870219	-7.176901	-1.821895
108	1	0	3.655491	-6.296184	-2.761586
109	1	0	5.132789	-5.471628	-2.243060
110	1	0	3.137387	-7.823373	-0.092580
111	1	0	2.166195	-6.577422	0.719416
112	1	0	1.874718	-6.959609	-0.984122
113	1	0	-7.512669	-3.938293	0.677227
114	1	0	-5.754309	-3.897753	0.870665
115	1	0	-6.756096	-2.587394	1.529711
116	1	0	-8.713309	-2.360663	-0.801222
117	1	0	-7.931585	-0.956491	-0.044519
118	1	0	-7.846424	-1.182005	-1.797424
119	1	0	-7.313897	-4.249621	-1.756992
120	1	0	-6.407521	-3.113162	-2.767791
121	1	0	-5.540532	-4.191030	-1.664665
122	1	0	-5.056026	-0.405683	-4.657664
123	1	0	-4.849232	1.269566	-5.178397
124	1	0	-5.967712	0.898589	-3.861435
125	1	0	-2.561639	-0.553834	-4.408550
126	1	0	-2.427823	1.127498	-4.955161
127	1	0	-1.662681	0.618339	-3.432976
128	1	0	-4.776128	2.621076	-2.463711
129	1	0	-3.017539	2.554141	-2.242062
130	1	0	-3.700045	2.960342	-3.834709
131	1	0	1.532697	-2.316793	-4.708908
132	1	0	-0.186429	-1.968280	-4.980073
133	1	0	0.731278	-1.042740	-3.771321
134	1	0	-1.425315	-3.470527	-1.761317
135	1	0	-1.124557	-1.742307	-2.027230
136	1	0	-1.931011	-2.705370	-3.276632
137	1	0	-0.271052	-5.216042	-3.172827
138	1	0	0.970110	-4.741929	-4.356939
139	1	0	-0.724925	-4.322296	-4.627149
140	8	0	0.100496	2.976513	0.744530

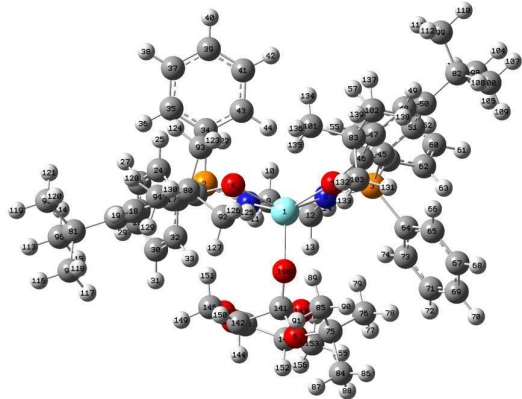
Appendix 2. Optimised Structures

141	6	0	0.613319	3.917796	0.092331
142	6	0	-0.223570	5.126930	-0.332471
143	8	0	1.895162	4.253320	0.433886
144	1	0	0.178825	5.550848	-1.257391
145	8	0	-0.084751	6.128281	0.710947
146	6	0	-1.695733	4.835239	-0.468778
147	6	0	2.265300	5.638902	0.409505
148	6	0	1.167597	6.485392	1.051557
149	1	0	-2.234149	5.756881	-0.709828
150	1	0	-1.853217	4.109395	-1.267829
151	1	0	-2.089377	4.417624	0.460590
152	1	0	2.381684	5.971163	-0.632620
153	6	0	3.585352	5.777763	1.137645
154	8	0	1.372762	7.403173	1.805722
155	1	0	4.354079	5.182961	0.636691
156	1	0	3.891900	6.826346	1.149028
157	1	0	3.487179	5.435999	2.171558

 Rotational constants (GHZ): 0.0295061 0.0259839
 0.0206903

Sum of electronic and zero-point Energies= -3172.890542
 Sum of electronic and thermal Energies= -3172.811164
 Sum of electronic and thermal Enthalpies= -3172.810220
 Sum of electronic and thermal Free Energies= -3173.007842

	1	2	3
	A	A	A
Frequencies --	-160.6767	13.0077	
13.9389			
Red. masses --	8.1828	5.1629	
4.4952			
Frc consts --	0.1245	0.0005	
0.0005			
IR Inten --	64.6273	0.0448	
0.0748			

Intitiation INT2

Standard orientation:

Center Number	Atomic Number	Atomic Type	Coordinates (Angstroms)		
			X	Y	Z
1	39	0	-0.046787	0.259134	-0.492984
2	15	0	-2.460002	-1.221958	1.515114
3	15	0	3.097951	0.320632	1.202916
4	8	0	-1.538208	-1.142025	-1.275216
5	8	0	1.789081	-0.328037	-1.488570
6	8	0	-0.811559	4.401457	-1.865901
7	7	0	-1.181206	-0.187158	1.504742
8	7	0	1.464860	0.273841	1.319330
9	6	0	-0.466666	0.011268	2.769519
10	1	0	-0.160734	-0.941930	3.233110
11	1	0	-1.080467	0.544312	3.510808
12	6	0	0.790305	0.835893	2.493709
13	1	0	0.493563	1.879828	2.310125
14	1	0	1.415455	0.829380	3.400704
15	6	0	-3.501929	-1.075927	0.042064
16	6	0	-2.855404	-1.170568	-1.217653
17	6	0	-3.687196	-1.305647	-2.375138
18	6	0	-5.066620	-1.242293	-2.190037
19	1	0	-5.695944	-1.323188	-3.069969
20	6	0	-5.712094	-1.085262	-0.949524
21	6	0	-4.896569	-1.026783	0.173168
22	1	0	-5.327246	-0.936632	1.164492
23	6	0	-3.505678	-0.914460	2.996972
24	6	0	-3.853026	-1.903634	3.922685
25	1	0	-3.531531	-2.930203	3.775317
26	6	0	-4.606271	-1.570186	5.048253
27	1	0	-4.874762	-2.343180	5.763879
28	6	0	-5.005801	-0.251183	5.258005
29	1	0	-5.588928	0.005749	6.138934

30	6	0	-4.647354	0.740504	4.344179
31	1	0	-4.934861	1.775269	4.507292
32	6	0	-3.898630	0.414482	3.216129
33	1	0	-3.607779	1.198803	2.522519
34	6	0	-1.945043	-2.997666	1.562597
35	6	0	-2.894024	-4.025274	1.489388
36	1	0	-3.952978	-3.786275	1.427454
37	6	0	-2.483440	-5.356220	1.466797
38	1	0	-3.224602	-6.149110	1.407359
39	6	0	-1.123687	-5.668878	1.502694
40	1	0	-0.804454	-6.707681	1.476855
41	6	0	-0.175460	-4.648494	1.553707
42	1	0	0.884882	-4.888191	1.559043
43	6	0	-0.584218	-3.315082	1.582433
44	1	0	0.151930	-2.515338	1.591700
45	6	0	3.701000	-0.745513	-0.134714
46	6	0	2.967415	-0.888187	-1.343568
47	6	0	3.578099	-1.653607	-2.393912
48	6	0	4.821570	-2.227135	-2.150448
49	1	0	5.272872	-2.809821	-2.946256
50	6	0	5.541584	-2.112300	-0.946961
51	6	0	4.955883	-1.350653	0.052414
52	1	0	5.464541	-1.216379	1.001112
53	6	0	3.856430	-0.286988	2.775942
54	6	0	3.263958	-1.399711	3.386963
55	1	0	2.380689	-1.846961	2.939239
56	6	0	3.798158	-1.923416	4.561178
57	1	0	3.330483	-2.785119	5.030451
58	6	0	4.929469	-1.340674	5.134107
59	1	0	5.346353	-1.749203	6.051113
60	6	0	5.523025	-0.233318	4.531042
61	1	0	6.403423	0.223887	4.975130
62	6	0	4.988374	0.295237	3.355691
63	1	0	5.454110	1.160152	2.892499
64	6	0	3.843895	1.994584	0.954805
65	6	0	4.674051	2.256830	-0.140112
66	1	0	4.892989	1.467228	-0.853099
67	6	0	5.219998	3.528240	-0.316706
68	1	0	5.863611	3.722903	-1.170663
69	6	0	4.941788	4.543184	0.596572
70	1	0	5.369155	5.533024	0.458044
71	6	0	4.112456	4.288027	1.689739
72	1	0	3.892154	5.076666	2.404508
73	6	0	3.564296	3.020792	1.868901
74	1	0	2.924012	2.832880	2.726460
75	6	0	0.385106	4.479302	-2.671764
76	6	0	1.665106	4.243289	-1.870505
77	1	0	1.725299	4.925497	-1.017919
78	1	0	2.534455	4.417192	-2.516060
79	1	0	1.718042	3.220266	-1.493615
80	6	0	-3.084685	-1.563237	-3.765450
81	6	0	-7.242142	-1.008881	-0.883614
82	6	0	6.896758	-2.812022	-0.791497
83	6	0	2.882130	-1.832868	-3.752126
84	6	0	0.355806	5.920794	-3.186615
85	6	0	0.282837	3.508057	-3.851629
86	1	0	1.196263	6.104778	-3.865494
87	1	0	-0.576246	6.113568	-3.728864

Appendix 2. Optimised Structures

88	1	0	0.419915	6.627894	-2.352461
89	1	0	0.278567	2.473583	-3.504601
90	1	0	1.128938	3.647708	-4.535696
91	1	0	-0.642144	3.690169	-4.410453
92	6	0	-2.163185	-0.404848	-4.192974
93	6	0	-2.287934	-2.882743	-3.720979
94	6	0	-4.161253	-1.710227	-4.852261
95	6	0	-7.853120	-2.302642	-1.457449
96	6	0	-7.749435	-0.838830	0.554854
97	6	0	-7.734718	0.195767	-1.709621
98	6	0	7.521307	-2.563551	0.588320
99	6	0	6.713412	-4.332595	-0.966374
100	6	0	7.877311	-2.291924	-1.861184
101	6	0	1.552692	-2.586873	-3.563063
102	6	0	3.729381	-2.647683	-4.742664
103	6	0	2.628070	-0.455604	-4.398326
104	1	0	8.483162	-3.084851	0.658418
105	1	0	7.710553	-1.497939	0.764757
106	1	0	6.883059	-2.936703	1.397900
107	1	0	8.850196	-2.790805	-1.765741
108	1	0	7.509129	-2.475331	-2.876499
109	1	0	8.036212	-1.212470	-1.753921
110	1	0	7.676066	-4.850716	-0.868963
111	1	0	6.031872	-4.732866	-0.206735
112	1	0	6.299834	-4.582188	-1.949609
113	1	0	-8.844175	-0.777966	0.557432
114	1	0	-7.465690	-1.686332	1.190246
115	1	0	-7.365661	0.078572	1.016177
116	1	0	-8.830036	0.260240	-1.681145
117	1	0	-7.327522	1.132820	-1.312625
118	1	0	-7.433550	0.119647	-2.760245
119	1	0	-8.949217	-2.257942	-1.424234
120	1	0	-7.558980	-2.465360	-2.500156
121	1	0	-7.530150	-3.176864	-0.879958
122	1	0	-1.502580	-2.842918	-2.963518
123	1	0	-1.822154	-3.078288	-4.695462
124	1	0	-2.951521	-3.724735	-3.488244
125	1	0	-1.325417	-0.285201	-3.504964
126	1	0	-1.757286	-0.598921	-5.194332
127	1	0	-2.715506	0.541266	-4.229978
128	1	0	-4.844157	-2.543747	-4.648918
129	1	0	-4.755384	-0.796185	-4.973645
130	1	0	-3.673749	-1.914110	-5.812799
131	1	0	3.577252	0.060695	-4.589846
132	1	0	2.113785	-0.579996	-5.359854
133	1	0	2.014392	0.178998	-3.757078
134	1	0	1.730631	-3.584273	-3.142033
135	1	0	0.876263	-2.050136	-2.896691
136	1	0	1.050007	-2.714259	-4.529959
137	1	0	3.916145	-3.668846	-4.388805
138	1	0	4.694394	-2.171403	-4.954762
139	1	0	3.188127	-2.726892	-5.692723
140	8	0	-0.606054	2.178162	-1.211232
141	6	0	-1.039392	3.400378	-0.898063
142	6	0	-2.585003	3.520535	-0.703339
143	8	0	-0.392891	3.774041	0.345282
144	1	0	-2.843391	4.576201	-0.843389
145	8	0	-2.972339	3.149392	0.638545

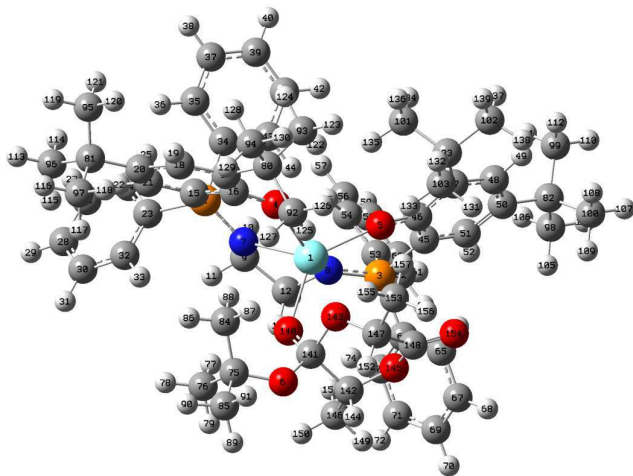
Appendix 2. Optimised Structures

146	6	0	-3.388447	2.676888	-1.661828
147	6	0	-1.157393	4.631748	1.178088
148	6	0	-2.361640	3.813849	1.637178
149	1	0	-4.458305	2.856554	-1.516226
150	1	0	-3.120309	2.944945	-2.687400
151	1	0	-3.187469	1.613863	-1.515074
152	1	0	-1.505534	5.507148	0.605311
153	6	0	-0.303676	5.103631	2.336097
154	8	0	-2.731566	3.682033	2.782177
155	1	0	0.562253	5.651593	1.953662
156	1	0	-0.884690	5.758717	2.991308
157	1	0	0.045016	4.254004	2.929507

Rotational constants (GHZ): 0.0346172 0.0216966
0.0209529

Sum of electronic and zero-point Energies= -3172.908615
Sum of electronic and thermal Energies= -3172.828667
Sum of electronic and thermal Enthalpies= -3172.827723
Sum of electronic and thermal Free Energies= -3173.030221

	1	2	3
	A	A	A
Frequencies --	8.8772	12.2809	
13.0579			
Red. masses --	4.7560	5.1340	
4.4053			
Frc consts --	0.0002	0.0005	
0.0004			
IR Inten --	0.0205	0.2605	
0.0594			

Initiation INT3

Standard orientation:

Center Number	Atomic Number	Atomic Type	Coordinates (Angstroms)		
			X	Y	Z
1	39	0	-0.129274	-0.639372	-0.132199
2	15	0	-2.608639	1.833224	-0.575665
3	15	0	3.029329	0.796290	-1.159601
4	8	0	-1.846761	-0.425480	1.219697
5	8	0	1.497323	-0.460741	1.290124
6	8	0	-1.137864	-4.155685	-2.163474
7	7	0	-1.274629	1.113466	-1.205676
8	7	0	1.400688	0.724863	-1.301641
9	6	0	-0.530319	1.894474	-2.200967
10	1	0	-0.268590	2.899866	-1.828591
11	1	0	-1.109344	2.040549	-3.126206
12	6	0	0.767336	1.162437	-2.547227
13	1	0	0.533333	0.295926	-3.184115
14	1	0	1.391788	1.847913	-3.142431
15	6	0	-3.716066	0.706179	0.305473
16	6	0	-3.143565	-0.216380	1.221753
17	6	0	-4.037270	-0.868064	2.135661
18	6	0	-5.401776	-0.639619	1.985484
19	1	0	-6.074833	-1.156203	2.661590
20	6	0	-5.979805	0.215546	1.028991
21	6	0	-5.101866	0.910768	0.209860
22	1	0	-5.480023	1.620558	-0.517697
23	6	0	-3.582090	2.639000	-1.918871
24	6	0	-3.718289	4.024633	-2.042056
25	1	0	-3.295429	4.683451	-1.289542
26	6	0	-4.395210	4.567388	-3.135042

27	1	0	-4.498786	5.645871	-3.222146
28	6	0	-4.932586	3.731229	-4.111092
29	1	0	-5.459944	4.155850	-4.961497
30	6	0	-4.787426	2.347110	-3.999956
31	1	0	-5.198635	1.691608	-4.763196
32	6	0	-4.112035	1.801621	-2.911829
33	1	0	-3.991277	0.724430	-2.830187
34	6	0	-2.185179	3.160841	0.641279
35	6	0	-3.176784	3.925897	1.269056
36	1	0	-4.224242	3.773687	1.020297
37	6	0	-2.825639	4.869416	2.231378
38	1	0	-3.599036	5.459143	2.716844
39	6	0	-1.485857	5.046266	2.582116
40	1	0	-1.215114	5.778210	3.338817
41	6	0	-0.498494	4.273098	1.974331
42	1	0	0.543434	4.392912	2.259515
43	6	0	-0.847095	3.330991	1.006113
44	1	0	-0.085893	2.705343	0.546657
45	6	0	3.565714	0.469447	0.540942
46	6	0	2.709008	-0.037266	1.555827
47	6	0	3.236569	-0.058596	2.894822
48	6	0	4.566872	0.291949	3.087433
49	1	0	4.960311	0.242135	4.096952
50	6	0	5.444872	0.714232	2.071133
51	6	0	4.902318	0.821685	0.802905
52	1	0	5.514217	1.188328	-0.015400
53	6	0	3.624231	2.502969	-1.582853
54	6	0	2.826217	3.578345	-1.173805
55	1	0	1.885964	3.380536	-0.667581
56	6	0	3.228971	4.889159	-1.416211
57	1	0	2.598866	5.715366	-1.096695
58	6	0	4.437338	5.139465	-2.067037
59	1	0	4.752679	6.162382	-2.256507
60	6	0	5.239455	4.074752	-2.473714
61	1	0	6.182176	4.263537	-2.980903
62	6	0	4.835463	2.760971	-2.234736
63	1	0	5.465332	1.938926	-2.562110
64	6	0	3.992740	-0.302355	-2.294092
65	6	0	4.654716	-1.428860	-1.795807
66	1	0	4.629881	-1.650381	-0.733477
67	6	0	5.340555	-2.277431	-2.664405
68	1	0	5.849108	-3.151060	-2.266220
69	6	0	5.364673	-2.011755	-4.031898
70	1	0	5.903607	-2.673015	-4.705964
71	6	0	4.692095	-0.898020	-4.537942
72	1	0	4.703817	-0.689463	-5.604782
73	6	0	4.008094	-0.046608	-3.674030
74	1	0	3.498436	0.825545	-4.076204
75	6	0	-2.533625	-3.852693	-2.395203
76	6	0	-2.681654	-2.960138	-3.630853
77	1	0	-2.210802	-1.990069	-3.461180
78	1	0	-3.743629	-2.811156	-3.862785
79	1	0	-2.208304	-3.433549	-4.498919
80	6	0	-3.508628	-1.755047	3.274146
81	6	0	-7.504377	0.354593	0.943245
82	6	0	6.904496	1.047299	2.398572
83	6	0	2.345120	-0.420869	4.094111
84	6	0	-3.213408	-3.235065	-1.175278

Appendix 2. Optimised Structures

85	6	0	-3.132791	-5.233151	-2.674495
86	1	0	-4.298250	-3.202940	-1.332826
87	1	0	-3.014073	-3.832293	-0.281451
88	1	0	-2.870101	-2.214783	-0.994908
89	1	0	-2.614713	-5.712628	-3.512011
90	1	0	-4.195536	-5.146472	-2.927169
91	1	0	-3.036046	-5.879611	-1.795438
92	6	0	-2.794936	-2.993980	2.705869
93	6	0	-2.532456	-0.936642	4.142115
94	6	0	-4.629694	-2.256134	4.198142
95	6	0	-8.063867	0.846131	2.292681
96	6	0	-7.934049	1.352371	-0.140931
97	6	0	-8.124468	-1.016152	0.606234
98	6	0	7.685453	1.501289	1.157552
99	6	0	6.961098	2.182227	3.440031
100	6	0	7.599181	-0.203928	2.970898
101	6	0	1.189364	0.595689	4.184809
102	6	0	3.105401	-0.366279	5.429003
103	6	0	1.782772	-1.845883	3.948854
104	1	0	8.723338	1.722521	1.433318
105	1	0	7.708104	0.723391	0.384989
106	1	0	7.260002	2.410966	0.717096
107	1	0	8.645025	0.016441	3.220930
108	1	0	7.106259	-0.560207	3.882027
109	1	0	7.586594	-1.024072	2.243833
110	1	0	8.002734	2.428656	3.683153
111	1	0	6.476320	3.088110	3.057659
112	1	0	6.460284	1.904075	4.373728
113	1	0	-9.028230	1.413427	-0.176089
114	1	0	-7.554388	2.361358	0.060462
115	1	0	-7.587624	1.049207	-1.135973
116	1	0	-9.218182	-0.942142	0.549657
117	1	0	-7.757133	-1.384375	-0.358852
118	1	0	-7.879797	-1.768589	1.363987
119	1	0	-9.156179	0.940735	2.243848
120	1	0	-7.827453	0.155154	3.108949
121	1	0	-7.647897	1.825948	2.554709
122	1	0	-1.694194	-0.565357	3.550804
123	1	0	-2.137258	-1.561001	4.953805
124	1	0	-3.044839	-0.078560	4.594673
125	1	0	-1.984891	-2.714989	2.030978
126	1	0	-2.374724	-3.593447	3.524129
127	1	0	-3.500595	-3.625896	2.153038
128	1	0	-5.178953	-1.430665	4.666855
129	1	0	-5.347981	-2.897772	3.673371
130	1	0	-4.186565	-2.854911	5.002742
131	1	0	2.593702	-2.579728	3.872529
132	1	0	1.170430	-2.100437	4.823665
133	1	0	1.162946	-1.923813	3.055742
134	1	0	1.579229	1.608487	4.346660
135	1	0	0.587676	0.598165	3.273402
136	1	0	0.532600	0.348168	5.028244
137	1	0	3.508119	0.632111	5.638644
138	1	0	3.929793	-1.088695	5.466024
139	1	0	2.414278	-0.616910	6.242276
140	8	0	-0.440558	-1.951314	-1.864430
141	6	0	-0.209138	-3.234695	-1.653739
142	6	0	1.135447	-3.787446	-2.223402

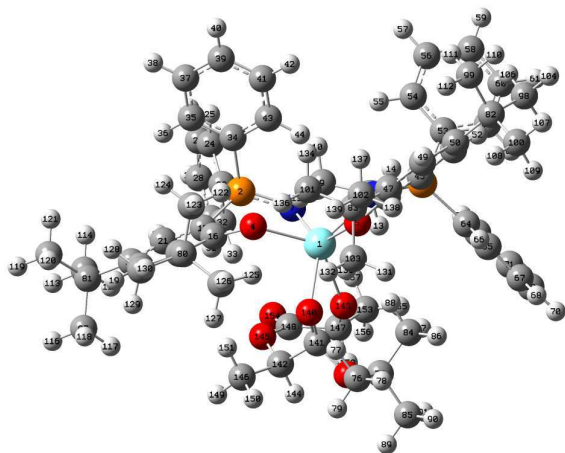
Appendix 2. Optimised Structures

143	8	0	-0.145522	-3.368915	-0.170853
144	1	0	1.017922	-4.867759	-2.362824
145	8	0	2.228612	-3.580440	-1.302787
146	6	0	1.512910	-3.144845	-3.536669
147	6	0	0.641061	-4.478565	0.266062
148	6	0	2.087524	-4.128677	-0.074831
149	1	0	2.442905	-3.577305	-3.916770
150	1	0	0.714865	-3.317327	-4.264740
151	1	0	1.643762	-2.068096	-3.411488
152	1	0	0.337395	-5.364747	-0.311952
153	6	0	0.427663	-4.755410	1.736493
154	8	0	3.035953	-4.248103	0.661901
155	1	0	-0.616868	-5.023240	1.915992
156	1	0	1.069532	-5.584097	2.049308
157	1	0	0.683324	-3.884800	2.343073

 Rotational constants (GHZ): 0.0361859 0.0217221
 0.0205308

Sum of electronic and zero-point Energies= -3172.903791
 Sum of electronic and thermal Energies= -3172.823927
 Sum of electronic and thermal Enthalpies= -3172.822983
 Sum of electronic and thermal Free Energies= -3173.023821

	1	2	3
	A	A	A
Frequencies --	9.7985	11.4469	
15.2780			
Red. masses --	4.7686	4.5840	
4.6697			
Frc consts --	0.0003	0.0004	
0.0006			
IR Inten --	0.1104	0.0352	
0.7425			

Intitiation TS2'

Standard orientation:

Center Number	Atomic Number	Atomic Type	Coordinates (Angstroms)		
			X	Y	Z
1	39	0	-0.100642	-0.504935	-0.366193
2	15	0	-2.562528	1.918362	0.111291
3	15	0	3.082089	1.174289	-0.820284
4	8	0	-1.587404	-0.549553	1.267869
5	8	0	1.675233	-1.054623	0.777783
6	8	0	-0.165965	-3.866905	-2.649192
7	7	0	-1.241830	1.521788	-0.788274
8	7	0	1.446772	1.270790	-0.865501
9	6	0	-0.500827	2.661495	-1.335821
10	1	0	-0.328997	3.447175	-0.580215
11	1	0	-1.038326	3.142756	-2.168602
12	6	0	0.860722	2.190054	-1.844831
13	1	0	0.730049	1.693193	-2.814228
14	1	0	1.479277	3.084649	-2.025850
15	6	0	-3.580953	0.499037	0.564358
16	6	0	-2.903158	-0.526835	1.274830
17	6	0	-3.712571	-1.456838	2.005663
18	6	0	-5.091364	-1.396030	1.814850
19	1	0	-5.702274	-2.124661	2.337993
20	6	0	-5.760158	-0.449978	1.014567
21	6	0	-4.975012	0.534127	0.428690
22	1	0	-5.429525	1.339053	-0.138283
23	6	0	-3.608873	3.145025	-0.781832
24	6	0	-3.815148	4.451138	-0.324630
25	1	0	-3.395312	4.772539	0.623672
26	6	0	-4.557521	5.351038	-1.089233
27	1	0	-4.714016	6.363741	-0.726241

28	6	0	-5.092954	4.953981	-2.313016
29	1	0	-5.672449	5.656640	-2.906832
30	6	0	-4.876826	3.656624	-2.778920
31	1	0	-5.282080	3.343392	-3.737448
32	6	0	-4.132944	2.752870	-2.023279
33	1	0	-3.953949	1.751049	-2.406865
34	6	0	-2.106326	2.692967	1.730370
35	6	0	-3.094268	3.120257	2.626418
36	1	0	-4.145121	3.033996	2.360619
37	6	0	-2.736050	3.634175	3.870634
38	1	0	-3.507983	3.962107	4.562202
39	6	0	-1.390540	3.712259	4.233454
40	1	0	-1.112643	4.106474	5.207731
41	6	0	-0.405542	3.268001	3.353102
42	1	0	0.641959	3.305430	3.641667
43	6	0	-0.761639	2.757454	2.104498
44	1	0	0.000502	2.383421	1.425579
45	6	0	3.667478	0.239879	0.613772
46	6	0	2.865657	-0.756824	1.233249
47	6	0	3.433374	-1.427104	2.373625
48	6	0	4.725939	-1.092846	2.759244
49	1	0	5.146308	-1.612680	3.613362
50	6	0	5.533686	-0.125982	2.130774
51	6	0	4.968680	0.539876	1.056147
52	1	0	5.529510	1.314228	0.542834
53	6	0	3.811260	2.871472	-0.694345
54	6	0	3.176031	3.778449	0.163715
55	1	0	2.279479	3.470866	0.694984
56	6	0	3.683804	5.064521	0.326795
57	1	0	3.182557	5.762835	0.992102
58	6	0	4.832203	5.455132	-0.363524
59	1	0	5.228563	6.459248	-0.235843
60	6	0	5.469225	4.557158	-1.217761
61	1	0	6.363395	4.857516	-1.757910
62	6	0	4.960076	3.268909	-1.386010
63	1	0	5.458697	2.576091	-2.057653
64	6	0	3.880702	0.459302	-2.332875
65	6	0	4.649549	-0.706304	-2.253191
66	1	0	4.811880	-1.178866	-1.288698
67	6	0	5.209742	-1.259055	-3.405257
68	1	0	5.808842	-2.163036	-3.331382
69	6	0	5.003708	-0.655348	-4.644072
70	1	0	5.441583	-1.086686	-5.540698
71	6	0	4.237860	0.508282	-4.731484
72	1	0	4.078484	0.986426	-5.694643
73	6	0	3.680047	1.064813	-3.582874
74	1	0	3.099456	1.979902	-3.661863
75	6	0	1.108734	-4.487852	-2.281091
76	6	0	0.886095	-5.439243	-1.107212
77	1	0	0.573932	-4.895694	-0.214143
78	1	0	1.816674	-5.973637	-0.884595
79	1	0	0.119570	-6.181440	-1.357730
80	6	0	-3.096862	-2.406500	3.045542
81	6	0	-7.284542	-0.511598	0.861893
82	6	0	6.948400	0.152174	2.651426
83	6	0	2.630239	-2.474127	3.160361
84	6	0	2.174391	-3.437380	-1.989369
85	6	0	1.467564	-5.269532	-3.543877

Appendix 2. Optimised Structures

86	1	0	3.151259	-3.930203	-1.917382
87	1	0	2.216098	-2.702855	-2.798283
88	1	0	1.988595	-2.915489	-1.048749
89	1	0	0.674838	-5.981554	-3.796703
90	1	0	2.397000	-5.827637	-3.388382
91	1	0	1.607351	-4.590918	-4.391988
92	6	0	-2.112408	-3.398744	2.402759
93	6	0	-2.366268	-1.545638	4.096919
94	6	0	-4.159441	-3.232511	3.787489
95	6	0	-7.957432	-0.380897	2.242376
96	6	0	-7.819613	0.611630	-0.036543
97	6	0	-7.681167	-1.859936	0.228683
98	6	0	7.665641	1.230464	1.828132
99	6	0	6.876926	0.634499	4.113769
100	6	0	7.788447	-1.138537	2.582986
101	6	0	1.371180	-1.811125	3.749622
102	6	0	3.425836	-3.066399	4.334928
103	6	0	2.231004	-3.645896	2.243070
104	1	0	8.672331	1.395704	2.229932
105	1	0	7.773927	0.935034	0.777552
106	1	0	7.135568	2.189520	1.861685
107	1	0	8.803271	-0.956908	2.959695
108	1	0	7.350466	-1.942782	3.184204
109	1	0	7.867521	-1.499058	1.550611
110	1	0	7.883738	0.829865	4.504799
111	1	0	6.295012	1.560252	4.190933
112	1	0	6.406166	-0.109986	4.765095
113	1	0	-8.907845	0.520692	-0.135678
114	1	0	-7.608962	1.603433	0.381217
115	1	0	-7.389047	0.566009	-1.043557
116	1	0	-8.771010	-1.927410	0.115035
117	1	0	-7.226275	-1.972859	-0.762148
118	1	0	-7.357201	-2.707214	0.843303
119	1	0	-9.049587	-0.429815	2.144258
120	1	0	-7.649902	-1.181444	2.923929
121	1	0	-7.700057	0.575212	2.713131
122	1	0	-1.584601	-0.940340	3.633423
123	1	0	-1.904925	-2.186894	4.859124
124	1	0	-3.072075	-0.873891	4.601062
125	1	0	-1.334852	-2.888910	1.834760
126	1	0	-1.635128	-4.006665	3.182811
127	1	0	-2.638031	-4.082069	1.725061
128	1	0	-4.879273	-2.600145	4.321152
129	1	0	-4.714210	-3.896712	3.113294
130	1	0	-3.662662	-3.865374	4.532589
131	1	0	3.123511	-4.142293	1.841040
132	1	0	1.659583	-4.390326	2.812421
133	1	0	1.616911	-3.302587	1.409935
134	1	0	1.647697	-1.008203	4.444504
135	1	0	0.737466	-1.389633	2.967981
136	1	0	0.781198	-2.549660	4.305950
137	1	0	3.715226	-2.303473	5.067811
138	1	0	4.330665	-3.591023	4.003807
139	1	0	2.796758	-3.796963	4.856832
140	8	0	-0.552556	-2.781052	-0.667780
141	6	0	-0.832322	-2.993319	-1.875808
142	6	0	-2.291159	-2.995809	-2.395020
143	8	0	-0.293242	-1.242658	-2.571968

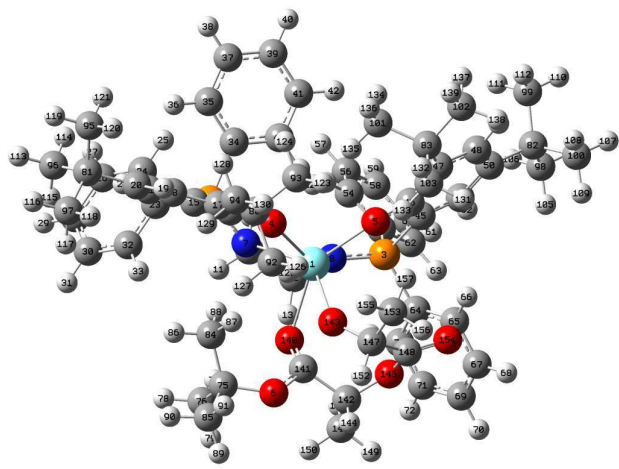
Appendix 2. Optimised Structures

144	1	0	-2.273070	-3.407585	-3.409228
145	8	0	-2.921978	-1.710758	-2.438286
146	6	0	-3.154546	-3.868223	-1.501945
147	6	0	-1.005611	-1.018721	-3.753647
148	6	0	-2.466579	-0.818076	-3.355037
149	1	0	-4.164183	-3.933832	-1.917830
150	1	0	-2.733119	-4.876036	-1.434041
151	1	0	-3.208548	-3.437168	-0.499767
152	1	0	-0.946616	-1.930943	-4.377541
153	6	0	-0.502453	0.135503	-4.606720
154	8	0	-3.183910	0.084204	-3.718166
155	1	0	0.576259	0.030688	-4.758115
156	1	0	-0.999276	0.126579	-5.583017
157	1	0	-0.717092	1.097103	-4.135704

Rotational constants (GHZ): 0.0365939 0.0220377
0.0209976

Sum of electronic and zero-point Energies= -3172.896914
Sum of electronic and thermal Energies= -3172.817498
Sum of electronic and thermal Enthalpies= -3172.816554
Sum of electronic and thermal Free Energies= -3173.015406

	1	2	3
	A	A	A
Frequencies --	-180.0881	5.8141	
11.0607			
Red. masses --	9.5350	4.5713	
5.1993			
Frc consts --	0.1822	0.0001	
0.0004			
IR Inten --	81.3810	0.0308	
0.2104			

Initiation TS2

Standard orientation:

Center Number	Atomic Number	Atomic Type	Coordinates (Angstroms)		
			X	Y	Z
1	39	0	0.119109	0.899206	0.184346
2	15	0	2.431335	-1.428767	-1.168328
3	15	0	-3.041307	-0.118891	-1.239196
4	8	0	1.879649	0.178480	1.273034
5	8	0	-1.405913	-0.000818	1.429326
6	8	0	1.399600	4.563809	-0.781018
7	7	0	1.253359	-0.341862	-1.523007
8	7	0	-1.421855	0.023271	-1.411169
9	6	0	0.492249	-0.640634	-2.746047
10	1	0	0.254670	-1.714637	-2.834660
11	1	0	1.057702	-0.371228	-3.652127
12	6	0	-0.829034	0.134572	-2.743602
13	1	0	-0.632741	1.185722	-2.992976
14	1	0	-1.464696	-0.279950	-3.542205
15	6	0	3.630942	-0.844211	0.051870
16	6	0	3.143585	-0.162421	1.198775
17	6	0	4.088349	0.111213	2.245229
18	6	0	5.411212	-0.271441	2.045433
19	1	0	6.121127	-0.056042	2.836897
20	6	0	5.903926	-0.920641	0.898278
21	6	0	4.978022	-1.212296	-0.092780
22	1	0	5.288614	-1.728643	-0.994815
23	6	0	3.370504	-1.860827	-2.699911
24	6	0	3.316447	-3.121531	-3.301063
25	1	0	2.762032	-3.927092	-2.829082
26	6	0	3.971970	-3.350613	-4.511760

27	1	0	3.925597	-4.334922	-4.970607
28	6	0	4.680229	-2.322896	-5.129984
29	1	0	5.190680	-2.503246	-6.072624
30	6	0	4.730221	-1.058961	-4.539173
31	1	0	5.278242	-0.252803	-5.020165
32	6	0	4.075899	-0.826754	-3.332715
33	1	0	4.109705	0.159174	-2.876431
34	6	0	1.765376	-3.029201	-0.519246
35	6	0	2.620063	-4.080681	-0.162917
36	1	0	3.695916	-3.973669	-0.279541
37	6	0	2.095942	-5.259745	0.361163
38	1	0	2.763822	-6.071384	0.638504
39	6	0	0.717811	-5.392734	0.541951
40	1	0	0.311113	-6.311857	0.956216
41	6	0	-0.133350	-4.341172	0.207898
42	1	0	-1.204449	-4.430803	0.368246
43	6	0	0.388310	-3.159101	-0.319879
44	1	0	-0.270426	-2.325991	-0.556372
45	6	0	-3.462974	-0.689674	0.431576
46	6	0	-2.554384	-0.626754	1.523880
47	6	0	-2.957625	-1.285479	2.739135
48	6	0	-4.234552	-1.830539	2.801933
49	1	0	-4.536765	-2.300942	3.731369
50	6	0	-5.167969	-1.824387	1.748755
51	6	0	-4.740178	-1.264617	0.557343
52	1	0	-5.395471	-1.273792	-0.307673
53	6	0	-3.706866	-1.395765	-2.410803
54	6	0	-2.932302	-2.540907	-2.634776
55	1	0	-1.962581	-2.633357	-2.154788
56	6	0	-3.397063	-3.555513	-3.467839
57	1	0	-2.784850	-4.437883	-3.636155
58	6	0	-4.644199	-3.439215	-4.082522
59	1	0	-5.007625	-4.231643	-4.731930
60	6	0	-5.422774	-2.304826	-3.861606
61	1	0	-6.395806	-2.208878	-4.336598
62	6	0	-4.956358	-1.285114	-3.031548
63	1	0	-5.568671	-0.402987	-2.869630
64	6	0	-4.040656	1.388650	-1.618087
65	6	0	-4.673381	2.095572	-0.592128
66	1	0	-4.604821	1.745884	0.433201
67	6	0	-5.379382	3.263354	-0.879931
68	1	0	-5.854272	3.811723	-0.071570
69	6	0	-5.459743	3.728497	-2.190010
70	1	0	-6.015527	4.636070	-2.412764
71	6	0	-4.820232	3.032993	-3.218501
72	1	0	-4.877938	3.394831	-4.242201
73	6	0	-4.109323	1.870050	-2.934675
74	1	0	-3.621050	1.329549	-3.742181
75	6	0	2.718595	4.197647	-1.310072
76	6	0	2.630386	4.097101	-2.832053
77	1	0	1.965986	3.282401	-3.128666
78	1	0	3.627013	3.903920	-3.245776
79	1	0	2.261615	5.035301	-3.261910
80	6	0	3.660312	0.790845	3.555506
81	6	0	7.390849	-1.281094	0.797925
82	6	0	-6.556834	-2.442198	1.943676
83	6	0	-2.002227	-1.410807	3.937751
84	6	0	3.249770	2.913542	-0.683824

Appendix 2. Optimised Structures

85	6	0	3.577614	5.389804	-0.894026
86	1	0	4.321574	2.825600	-0.897787
87	1	0	3.122873	2.932675	0.401414
88	1	0	2.751422	2.027776	-1.084676
89	1	0	3.161034	6.323329	-1.286932
90	1	0	4.595237	5.273592	-1.281682
91	1	0	3.627989	5.465219	0.197075
92	6	0	3.163294	2.219484	3.268564
93	6	0	2.544862	-0.030165	4.230420
94	6	0	4.815082	0.903869	4.564053
95	6	0	7.773201	-2.232481	1.949168
96	6	0	7.729347	-1.977355	-0.526958
97	6	0	8.242807	0.000034	0.894508
98	6	0	-7.423679	-2.325142	0.682403
99	6	0	-6.416442	-3.937616	2.290695
100	6	0	-7.285817	-1.720009	3.093954
101	6	0	-0.742018	-2.188203	3.508678
102	6	0	-2.629834	-2.177067	5.113180
103	6	0	-1.604637	-0.019510	4.459696
104	1	0	-8.409454	-2.767669	0.868463
105	1	0	-7.580123	-1.279123	0.393004
106	1	0	-6.979771	-2.854344	-0.169200
107	1	0	-8.278867	-2.158698	3.256014
108	1	0	-6.732159	-1.793676	4.036332
109	1	0	-7.415486	-0.655463	2.867059
110	1	0	-7.404073	-4.392185	2.441676
111	1	0	-5.911074	-4.479574	1.482676
112	1	0	-5.836999	-4.089063	3.207912
113	1	0	8.800448	-2.208917	-0.561208
114	1	0	7.184843	-2.922279	-0.641147
115	1	0	7.499405	-1.343440	-1.391487
116	1	0	9.311685	-0.242322	0.834093
117	1	0	8.002945	0.690460	0.077322
118	1	0	8.075504	0.530409	1.838207
119	1	0	8.839143	-2.489482	1.898810
120	1	0	7.586074	-1.781000	2.929486
121	1	0	7.195098	-3.162408	1.895632
122	1	0	1.677618	-0.132319	3.577232
123	1	0	2.227239	0.460854	5.159343
124	1	0	2.905990	-1.034183	4.485642
125	1	0	2.313074	2.223367	2.583794
126	1	0	2.853454	2.702625	4.204853
127	1	0	3.966801	2.826350	2.831993
128	1	0	5.222199	-0.076739	4.838970
129	1	0	5.636162	1.528602	4.191531
130	1	0	4.441120	1.372882	5.481837
131	1	0	-2.489747	0.552120	4.763982
132	1	0	-0.943920	-0.116972	5.330668
133	1	0	-1.078865	0.541827	3.688120
134	1	0	-1.004949	-3.201122	3.180518
135	1	0	-0.218994	-1.686430	2.692307
136	1	0	-0.048485	-2.277725	4.354467
137	1	0	-2.915125	-3.200306	4.839573
138	1	0	-3.512171	-1.666981	5.518558
139	1	0	-1.893821	-2.248542	5.922476
140	8	0	0.325280	2.640911	-1.390501
141	6	0	0.333019	3.751995	-0.804541
142	6	0	-0.910943	4.653711	-0.729946

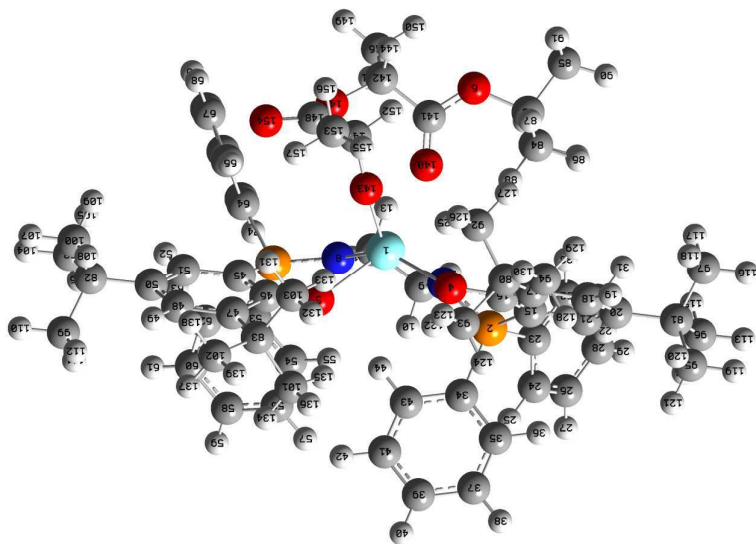
Appendix 2. Optimised Structures

143	8	0	0.214056	3.035371	1.060036
144	1	0	-0.617988	5.579557	-0.224142
145	8	0	-2.019660	4.073436	-0.047306
146	6	0	-1.386644	4.971356	-2.139241
147	6	0	-0.521649	3.912328	1.863575
148	6	0	-1.945106	3.927679	1.306355
149	1	0	-2.243226	5.649620	-2.093667
150	1	0	-0.585293	5.449391	-2.711054
151	1	0	-1.690949	4.052277	-2.646338
152	1	0	-0.106074	4.933201	1.761667
153	6	0	-0.510568	3.566010	3.342623
154	8	0	-2.960285	3.740047	1.931614
155	1	0	0.520236	3.548480	3.705108
156	1	0	-1.075599	4.312450	3.911025
157	1	0	-0.968856	2.591460	3.517894

 Rotational constants (GHZ): 0.0359933 0.0223956
 0.0210857

Sum of electronic and zero-point Energies= -3172.896536
 Sum of electronic and thermal Energies= -3172.817048
 Sum of electronic and thermal Enthalpies= -3172.816104
 Sum of electronic and thermal Free Energies= -3173.014311

	1	2	3
	A	A	A
Frequencies --	-158.3357	7.4137	
13.8111			
Red. masses --	8.0557	4.6918	
4.5893			
Frc consts --	0.1190	0.0002	
0.0005			
IR Inten --	70.8579	0.0692	
0.0282			

Intitiation INT4

Standard orientation:

Center Number	Atomic Number	Atomic Type	Coordinates (Angstroms)		
			X	Y	Z
1	39	0	-0.007816	0.549001	0.347095
2	15	0	2.602962	-1.541913	-0.849551
3	15	0	-2.998289	-0.561696	-1.327891
4	8	0	1.824352	0.059702	1.455281
5	8	0	-1.486947	-0.622519	1.424441
6	8	0	1.678567	4.398581	-1.728207
7	7	0	1.320468	-0.636935	-1.331491
8	7	0	-1.390778	-0.272688	-1.398460
9	6	0	0.610011	-1.110241	-2.524646
10	1	0	0.365814	-2.185147	-2.470683
11	1	0	1.206935	-0.976801	-3.441909
12	6	0	-0.699508	-0.332146	-2.685185
13	1	0	-0.468976	0.684995	-3.037150
14	1	0	-1.284331	-0.815592	-3.483955
15	6	0	3.729211	-0.666901	0.265213
16	6	0	3.128477	-0.031548	1.383779
17	6	0	4.001312	0.466743	2.406733
18	6	0	5.372738	0.353859	2.197843
19	1	0	6.032070	0.742790	2.966874
20	6	0	5.975129	-0.239362	1.071445
21	6	0	5.119718	-0.769385	0.114054
22	1	0	5.520105	-1.272898	-0.759336

23	6	0	3.576763	-2.115143	-2.312846
24	6	0	3.613875	-3.452376	-2.720439
25	1	0	3.121187	-4.216174	-2.126647
26	6	0	4.282418	-3.813186	-3.890914
27	1	0	4.306075	-4.856123	-4.196359
28	6	0	4.915075	-2.842890	-4.664653
29	1	0	5.436562	-3.126277	-5.575353
30	6	0	4.873547	-1.504849	-4.270039
31	1	0	5.361142	-0.742668	-4.872537
32	6	0	4.204301	-1.142101	-3.104272
33	1	0	4.167658	-0.099069	-2.803092
34	6	0	2.133680	-3.086009	0.056971
35	6	0	3.113884	-3.970076	0.526882
36	1	0	4.165773	-3.768560	0.338289
37	6	0	2.745673	-5.099619	1.253149
38	1	0	3.510479	-5.781121	1.617067
39	6	0	1.398504	-5.347503	1.525028
40	1	0	1.113142	-6.225676	2.098775
41	6	0	0.422577	-4.459729	1.077109
42	1	0	-0.625065	-4.633593	1.306563
43	6	0	0.789584	-3.329142	0.345583
44	1	0	0.032129	-2.618330	0.026105
45	6	0	-3.629712	-0.500769	0.370487
46	6	0	-2.792504	-0.636975	1.515335
47	6	0	-3.448907	-0.800672	2.785737
48	6	0	-4.836418	-0.765096	2.823617
49	1	0	-5.318767	-0.872665	3.789528
50	6	0	-5.668822	-0.592407	1.700305
51	6	0	-5.032347	-0.476864	0.477080
52	1	0	-5.620361	-0.352198	-0.426553
53	6	0	-3.437402	-2.244514	-1.985528
54	6	0	-2.461595	-3.245077	-1.961646
55	1	0	-1.459954	-3.001228	-1.623795
56	6	0	-2.769118	-4.545734	-2.358477
57	1	0	-1.998484	-5.312214	-2.336351
58	6	0	-4.060228	-4.860076	-2.778344
59	1	0	-4.302747	-5.873955	-3.086611
60	6	0	-5.042191	-3.869367	-2.799444
61	1	0	-6.051971	-4.108448	-3.123453
62	6	0	-4.734089	-2.568809	-2.406251
63	1	0	-5.507715	-1.806873	-2.433354
64	6	0	-3.992976	0.599646	-2.369945
65	6	0	-4.399809	1.826736	-1.831317
66	1	0	-4.211660	2.065576	-0.788780
67	6	0	-5.038159	2.765421	-2.639597
68	1	0	-5.349346	3.712194	-2.206708
69	6	0	-5.264791	2.495699	-3.988830
70	1	0	-5.765794	3.229640	-4.615573
71	6	0	-4.843848	1.283591	-4.535200
72	1	0	-5.013196	1.068708	-5.587475
73	6	0	-4.209725	0.338521	-3.730149
74	1	0	-3.895642	-0.607226	-4.163515
75	6	0	3.071888	3.904503	-1.792309
76	6	0	3.184296	2.784553	-2.822245
77	1	0	2.669199	1.879980	-2.491704
78	1	0	4.244739	2.552969	-2.974042
79	1	0	2.769356	3.103828	-3.785196
80	6	0	3.439495	1.065670	3.704986

Appendix 2. Optimised Structures

81	6	0	7.503396	-0.301926	0.961540
82	6	0	-7.191069	-0.536647	1.868889
83	6	0	-2.630338	-0.996989	4.072551
84	6	0	3.512601	3.471430	-0.399833
85	6	0	3.836469	5.143186	-2.248963
86	1	0	4.573839	3.201760	-0.419507
87	1	0	3.382214	4.290477	0.315207
88	1	0	2.954165	2.603160	-0.047385
89	1	0	3.492211	5.475273	-3.234114
90	1	0	4.905149	4.914648	-2.314752
91	1	0	3.702617	5.965613	-1.538882
92	6	0	2.613072	2.331438	3.405777
93	6	0	2.555229	0.017113	4.410763
94	6	0	4.548934	1.465690	4.690407
95	6	0	8.079290	-1.092216	2.153396
96	6	0	7.962522	-0.991067	-0.330823
97	6	0	8.083769	1.126130	0.972897
98	6	0	-7.915403	-0.362801	0.527176
99	6	0	-7.692606	-1.842907	2.515626
100	6	0	-7.564890	0.655203	2.772372
101	6	0	-1.713022	-2.228968	3.934618
102	6	0	-3.520867	-1.236485	5.302526
103	6	0	-1.791643	0.264473	4.356637
104	1	0	-8.998645	-0.325016	0.692611
105	1	0	-7.624845	0.567301	0.024722
106	1	0	-7.714710	-1.199111	-0.153484
107	1	0	-8.652816	0.708939	2.909455
108	1	0	-7.107671	0.570675	3.764240
109	1	0	-7.227598	1.599805	2.330449
110	1	0	-8.781748	-1.812556	2.649698
111	1	0	-7.449778	-2.708180	1.887659
112	1	0	-7.242489	-2.009237	3.500310
113	1	0	9.057943	-1.004991	-0.375685
114	1	0	7.617786	-2.030626	-0.383646
115	1	0	7.601162	-0.466486	-1.223330
116	1	0	9.179347	1.098138	0.911537
117	1	0	7.710132	1.705895	0.120345
118	1	0	7.815426	1.667361	1.886873
119	1	0	9.173603	-1.147515	2.087254
120	1	0	7.827585	-0.625309	3.111756
121	1	0	7.686206	-2.115429	2.168530
122	1	0	1.729036	-0.300481	3.772165
123	1	0	2.138126	0.438735	5.334399
124	1	0	3.146266	-0.867305	4.679838
125	1	0	1.759270	2.122093	2.758146
126	1	0	2.230929	2.755288	4.343912
127	1	0	3.238855	3.094991	2.926035
128	1	0	5.172503	0.611744	4.982154
129	1	0	5.202378	2.249552	4.287238
130	1	0	4.089736	1.862133	5.603509
131	1	0	-2.446058	1.127810	4.527449
132	1	0	-1.183076	0.116655	5.258601
133	1	0	-1.127919	0.505556	3.525710
134	1	0	-2.311483	-3.137465	3.787378
135	1	0	-1.027845	-2.122656	3.092350
136	1	0	-1.122337	-2.360714	4.850531
137	1	0	-4.150965	-2.127704	5.191669
138	1	0	-4.168187	-0.378833	5.522185

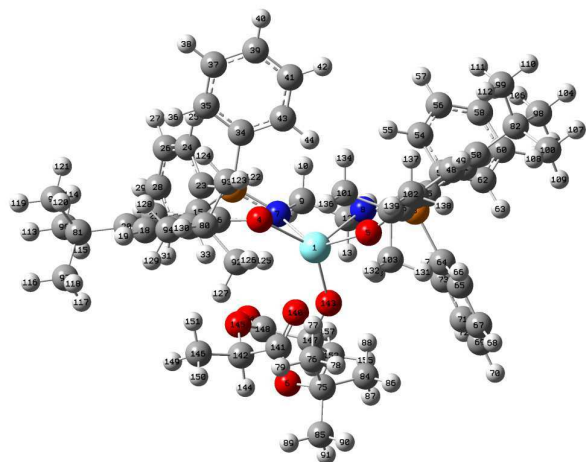
Appendix 2. Optimised Structures

139	1	0	-2.881685	-1.392934	6.179680
140	8	0	0.681029	2.425821	-1.234167
141	6	0	0.638968	3.622771	-1.455571
142	6	0	-0.637863	4.465660	-1.525850
143	8	0	-0.488761	2.373291	1.302614
144	1	0	-0.442775	5.399121	-0.984358
145	8	0	-1.774768	3.810280	-0.999753
146	6	0	-0.962798	4.791119	-2.983502
147	6	0	-0.861283	3.698682	1.323017
148	6	0	-2.046038	3.790725	0.351880
149	1	0	-1.860574	5.413852	-3.019810
150	1	0	-0.133235	5.327354	-3.451729
151	1	0	-1.161850	3.870200	-3.540218
152	1	0	-0.037249	4.350743	0.966779
153	6	0	-1.265570	4.178180	2.712307
154	8	0	-3.202886	3.677518	0.675207
155	1	0	-0.427286	4.022208	3.397803
156	1	0	-1.529585	5.243293	2.709480
157	1	0	-2.125414	3.604362	3.066047

Rotational constants (GHZ): 0.0371176 0.0212310
0.0206406

Sum of electronic and zero-point Energies= -3172.902932
Sum of electronic and thermal Energies= -3172.822041
Sum of electronic and thermal Enthalpies= -3172.821097
Sum of electronic and thermal Free Energies= -3173.025017

	1	2	3
	A	A	A
Frequencies --	8.1447	8.8934	
17.1171			
Red. masses --	4.6412	4.6930	
4.0396			
Frc consts --	0.0002	0.0002	
0.0007			
IR Inten --	0.0810	0.1797	
0.0408			

Initiation INT4'

Standard orientation:

Center Number	Atomic Number	Atomic Type	Coordinates (Angstroms)		
			X	Y	Z
1	39	0	-0.009741	0.392165	-0.471004
2	15	0	2.349633	-2.151915	0.077613
3	15	0	-3.198993	-1.066313	-0.936260
4	8	0	1.524118	0.450629	1.171541
5	8	0	-1.788697	1.128784	0.600053
6	8	0	1.341065	4.645144	-1.956675
7	7	0	1.084553	-1.661410	-0.839269
8	7	0	-1.591241	-1.374206	-0.886738
9	6	0	0.327492	-2.728050	-1.502508
10	1	0	0.132062	-3.580823	-0.829648
11	1	0	0.866306	-3.130680	-2.373908
12	6	0	-1.014202	-2.170316	-1.975660
13	1	0	-0.842307	-1.548459	-2.865506
14	1	0	-1.651363	-3.018831	-2.276560
15	6	0	3.440960	-0.810560	0.600451
16	6	0	2.823310	0.288663	1.257113
17	6	0	3.686921	1.144341	2.023346
18	6	0	5.062272	0.943111	1.919779
19	1	0	5.710494	1.613810	2.474959
20	6	0	5.678752	-0.075034	1.168871
21	6	0	4.830277	-0.980437	0.544834
22	1	0	5.232698	-1.832022	0.006810
23	6	0	3.363793	-3.380335	-0.850702
24	6	0	3.651196	-4.668250	-0.388650
25	1	0	3.297829	-4.992265	0.585683
26	6	0	4.385660	-5.548207	-1.184138
27	1	0	4.605848	-6.548022	-0.818374

28	6	0	4.829999	-5.148616	-2.443138
29	1	0	5.401486	-5.836495	-3.061551
30	6	0	4.531405	-3.869014	-2.913289
31	1	0	4.863308	-3.556643	-3.900002
32	6	0	3.796789	-2.985263	-2.126078
33	1	0	3.545686	-1.998130	-2.509018
34	6	0	1.815016	-2.960931	1.655344
35	6	0	2.750050	-3.414885	2.594394
36	1	0	3.814612	-3.321905	2.392965
37	6	0	2.321095	-3.958556	3.803193
38	1	0	3.051927	-4.307357	4.528528
39	6	0	0.957085	-4.038062	4.088324
40	1	0	0.623597	-4.455456	5.035208
41	6	0	0.024687	-3.564607	3.166765
42	1	0	-1.037375	-3.602184	3.396163
43	6	0	0.450317	-3.024849	1.952386
44	1	0	-0.272802	-2.626401	1.244257
45	6	0	-3.742571	-0.229170	0.574758
46	6	0	-2.941265	0.803902	1.135343
47	6	0	-3.472062	1.477944	2.289281
48	6	0	-4.705774	1.068961	2.784162
49	1	0	-5.092533	1.582794	3.657631
50	6	0	-5.492964	0.038464	2.240011
51	6	0	-4.983407	-0.598135	1.118774
52	1	0	-5.543548	-1.398728	0.648663
53	6	0	-4.141622	-2.652647	-1.064051
54	6	0	-3.610291	-3.769005	-0.406512
55	1	0	-2.666667	-3.671817	0.123940
56	6	0	-4.280225	-4.989681	-0.442015
57	1	0	-3.858104	-5.852651	0.066677
58	6	0	-5.487855	-5.103988	-1.131399
59	1	0	-6.010284	-6.056920	-1.159564
60	6	0	-6.023341	-3.995421	-1.785636
61	1	0	-6.964008	-4.080517	-2.323702
62	6	0	-5.352239	-2.772954	-1.755316
63	1	0	-5.772024	-1.914393	-2.271870
64	6	0	-3.793703	-0.071713	-2.378958
65	6	0	-4.288037	1.223529	-2.193420
66	1	0	-4.366371	1.631564	-1.189775
67	6	0	-4.685674	1.986931	-3.290635
68	1	0	-5.074245	2.990402	-3.135638
69	6	0	-4.593381	1.462896	-4.579043
70	1	0	-4.908815	2.056764	-5.433395
71	6	0	-4.100940	0.171273	-4.770741
72	1	0	-4.029821	-0.243244	-5.773188
73	6	0	-3.700433	-0.592679	-3.677016
74	1	0	-3.325216	-1.599979	-3.836765
75	6	0	0.241837	5.508281	-1.472183
76	6	0	0.375482	5.713787	0.031987
77	1	0	0.211219	4.786398	0.581939
78	1	0	-0.368405	6.446790	0.362782
79	1	0	1.368988	6.103119	0.279135
80	6	0	3.116806	2.178422	3.006194
81	6	0	7.207704	-0.175178	1.110654
82	6	0	-6.834038	-0.329838	2.885625
83	6	0	-2.704853	2.626112	2.961194
84	6	0	-1.098658	4.900947	-1.873714
85	6	0	0.495182	6.810958	-2.224904

Appendix 2. Optimised Structures

86	1	0	-1.899958	5.603078	-1.617969
87	1	0	-1.132016	4.725722	-2.954470
88	1	0	-1.290811	3.957298	-1.360593
89	1	0	1.479540	7.219885	-1.974885
90	1	0	-0.265405	7.550002	-1.952867
91	1	0	0.450025	6.650057	-3.306909
92	6	0	2.282525	3.243517	2.275970
93	6	0	2.237234	1.431841	4.029947
94	6	0	4.212297	2.915794	3.792641
95	6	0	7.775317	-0.369250	2.530645
96	6	0	7.674960	-1.354779	0.246920
97	6	0	7.787609	1.118565	0.506106
98	6	0	-7.540694	-1.470534	2.141201
99	6	0	-6.599976	-0.781338	4.340795
100	6	0	-7.768434	0.896186	2.878450
101	6	0	-1.353706	2.109816	3.486489
102	6	0	-3.461624	3.226498	4.156924
103	6	0	-2.479489	3.762503	1.945561
104	1	0	-8.491604	-1.702346	2.635439
105	1	0	-7.765421	-1.201362	1.102249
106	1	0	-6.939300	-2.387104	2.134317
107	1	0	-8.731417	0.649784	3.344000
108	1	0	-7.339107	1.739193	3.430976
109	1	0	-7.962002	1.233040	1.853265
110	1	0	-7.551532	-1.043038	4.821514
111	1	0	-5.946674	-1.660955	4.375844
112	1	0	-6.130090	0.006120	4.940224
113	1	0	8.770713	-1.380501	0.214631
114	1	0	7.335106	-2.315618	0.651321
115	1	0	7.313476	-1.272017	-0.784651
116	1	0	8.883950	1.072197	0.473843
117	1	0	7.422350	1.267604	-0.516683
118	1	0	7.508576	2.000981	1.092697
119	1	0	8.870414	-0.440336	2.502077
120	1	0	7.514051	0.464444	3.191484
121	1	0	7.386097	-1.288509	2.983861
122	1	0	1.430379	0.889766	3.532566
123	1	0	1.794465	2.139978	4.742171
124	1	0	2.838584	0.711470	4.597959
125	1	0	1.472200	2.787030	1.708079
126	1	0	1.852042	3.947911	2.999924
127	1	0	2.911065	3.818970	1.584471
128	1	0	4.834153	2.230759	4.381131
129	1	0	4.869237	3.503873	3.139452
130	1	0	3.739745	3.613686	4.494145
131	1	0	-3.439343	4.170746	1.603943
132	1	0	-1.912399	4.579054	2.411334
133	1	0	-1.926122	3.401502	1.076906
134	1	0	-1.505659	1.329367	4.242208
135	1	0	-0.745413	1.692784	2.682851
136	1	0	-0.791132	2.927343	3.954944
137	1	0	-3.624910	2.492743	4.955420
138	1	0	-4.433219	3.645942	3.867927
139	1	0	-2.865518	4.042787	4.581934
140	8	0	0.810020	2.774352	-0.789769
141	6	0	1.501605	3.382005	-1.589590
142	6	0	2.736516	2.810568	-2.291800
143	8	0	-0.127044	0.828963	-2.556978

Appendix 2. Optimised Structures

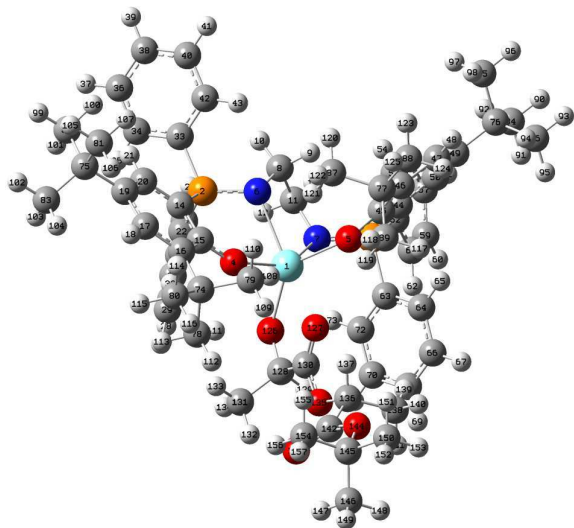
144	1	0	2.763061	3.234811	-3.302269
145	8	0	2.738685	1.392508	-2.355191
146	6	0	4.001592	3.217014	-1.540651
147	6	0	0.619293	1.255339	-3.633680
148	6	0	2.043543	0.750999	-3.363558
149	1	0	4.874406	2.854136	-2.090225
150	1	0	4.061922	4.306054	-1.453822
151	1	0	4.010360	2.768122	-0.543442
152	1	0	0.634377	2.364192	-3.696417
153	6	0	0.100031	0.734535	-4.969049
154	8	0	2.525030	-0.252059	-3.827284
155	1	0	-0.944786	1.037586	-5.084408
156	1	0	0.682803	1.134027	-5.808508
157	1	0	0.159413	-0.356782	-4.996941

 Rotational constants (GHZ): 0.0347683 0.0224534
 0.0205511

Sum of electronic and zero-point Energies= -3172.906435
 Sum of electronic and thermal Energies= -3172.825861
 Sum of electronic and thermal Enthalpies= -3172.824917
 Sum of electronic and thermal Free Energies= -3173.027356

	1	2	3
	A	A	A
Frequencies --	7.1350	10.3199	
17.6332			
Red. masses --	4.3746	5.1171	
5.4090			
Frc consts --	0.0001	0.0003	
0.0010			
IR Inten --	0.0365	0.1816	
0.0792			

Intitiation P



Standard orientation:

Center Number	Atomic Number	Atomic Type	Coordinates (Angstroms)		
			X	Y	Z
1	39	0	-0.055144	-0.046995	-0.789074
2	15	0	0.764252	-3.351957	-0.511074
3	15	0	-3.367181	0.264608	-0.903634
4	8	0	1.942830	-0.646691	-0.175997
5	8	0	-1.187643	0.779638	0.874697
6	7	0	-0.418445	-2.329791	-0.002028
7	7	0	-2.235141	-0.760145	-1.517149
8	6	0	-1.808823	-2.774197	-0.158425
9	1	0	-2.372367	-2.407199	0.713618
10	1	0	-1.909883	-3.872713	-0.152290
11	6	0	-2.449561	-2.197799	-1.424835
12	1	0	-1.965610	-2.658982	-2.294327
13	1	0	-3.517767	-2.471159	-1.471881
14	6	0	2.376128	-2.935283	0.194771
15	6	0	2.748708	-1.572952	0.278480
16	6	0	4.035179	-1.270121	0.832650
17	6	0	4.819739	-2.340614	1.252013
18	1	0	5.794169	-2.110900	1.672255
19	6	0	4.461539	-3.700798	1.169011
20	6	0	3.213672	-3.973545	0.626437
21	1	0	2.864340	-4.993879	0.513414
22	6	0	0.884721	-3.280959	-2.340340

23	6	0	-0.109255	-3.909774	-3.143274
24	1	0	-0.793676	-4.643835	-2.694532
25	6	0	-0.210228	-3.594515	-4.510606
26	1	0	-0.970301	-4.090300	-5.130185
27	6	0	0.672103	-2.656424	-5.088240
28	1	0	0.588912	-2.413952	-6.157123
29	6	0	1.676908	-2.050363	-4.308505
30	1	0	2.373389	-1.329423	-4.760154
31	6	0	1.791817	-2.358161	-2.933289
32	1	0	2.568110	-1.879229	-2.320712
33	6	0	0.445753	-5.081179	-0.020951
34	6	0	0.992419	-6.175944	-0.738268
35	1	0	1.558991	-5.997507	-1.662901
36	6	0	0.810544	-7.485422	-0.254677
37	1	0	1.234580	-8.334525	-0.806274
38	6	0	0.087957	-7.704169	0.933006
39	1	0	-0.053797	-8.728581	1.302976
40	6	0	-0.445347	-6.619834	1.654701
41	1	0	-0.998883	-6.795920	2.586367
42	6	0	-0.261760	-5.306367	1.188612
43	1	0	-0.648023	-4.445231	1.753159
44	6	0	-3.522135	0.493435	0.892005
45	6	0	-2.296021	0.716060	1.567373
46	6	0	-2.331524	0.887492	2.988641
47	6	0	-3.582385	0.870545	3.597787
48	1	0	-3.614838	1.009327	4.674161
49	6	0	-4.815187	0.684729	2.937441
50	6	0	-4.753345	0.488342	1.564502
51	1	0	-5.653387	0.305199	0.988756
52	6	0	-5.031685	-0.200310	-1.492443
53	6	0	-5.673038	-1.324072	-0.898003
54	1	0	-5.221448	-1.810481	-0.022562
55	6	0	-6.896655	-1.788783	-1.416542
56	1	0	-7.389757	-2.654262	-0.954890
57	6	0	-7.483214	-1.144307	-2.520510
58	1	0	-8.438308	-1.508508	-2.922128
59	6	0	-6.853975	-0.032782	-3.111628
60	1	0	-7.318847	0.470609	-3.969405
61	6	0	-5.629717	0.439213	-2.606273
62	1	0	-5.141699	1.308264	-3.068095
63	6	0	-2.876983	1.878109	-1.604313
64	6	0	-3.012979	3.071947	-0.850867
65	1	0	-3.386719	3.019248	0.182840
66	6	0	-2.676124	4.310879	-1.438271
67	1	0	-2.826857	5.241087	-0.873734
68	6	0	-2.204219	4.357345	-2.768360
69	1	0	-1.969486	5.327143	-3.229625
70	6	0	-2.057549	3.169199	-3.520477
71	1	0	-1.719981	3.212757	-4.565580
72	6	0	-2.383514	1.922393	-2.941517
73	1	0	-2.253244	0.982999	-3.496422
74	6	0	4.529719	0.187401	0.927550
75	6	0	5.427666	-4.788548	1.672884
76	6	0	-6.130123	0.693139	3.738970
77	6	0	-1.029203	1.069283	3.791489
78	6	0	4.579517	0.807292	-0.506670
79	6	0	3.557174	1.014125	1.827725
80	6	0	5.958360	0.284052	1.544996

Appendix 2. Optimised Structures

81	6	0	5.684229	-4.577848	3.200169
82	6	0	4.842361	-6.216624	1.458459
83	6	0	6.780462	-4.683774	0.897046
84	6	0	-7.365891	0.476915	2.814425
85	6	0	-6.094967	-0.453313	4.800918
86	6	0	-6.285818	2.069218	4.463884
87	6	0	-0.129588	-0.195043	3.596100
88	6	0	-1.301635	1.234944	5.318149
89	6	0	-0.274502	2.344643	3.292740
90	1	0	-8.284632	0.498545	3.420925
91	1	0	-7.437242	1.271204	2.057415
92	1	0	-7.315027	-0.497843	2.308062
93	1	0	-7.217934	2.083006	5.049277
94	1	0	-5.444908	2.249842	5.148823
95	1	0	-6.316015	2.886731	3.729788
96	1	0	-7.030732	-0.459231	5.380686
97	1	0	-5.977557	-1.428281	4.306727
98	1	0	-5.256597	-0.316597	5.499116
99	1	0	5.560476	-6.965515	1.827033
100	1	0	3.901118	-6.344802	2.012300
101	1	0	4.661537	-6.412273	0.391721
102	1	0	7.479460	-5.455621	1.254028
103	1	0	6.615814	-4.825300	-0.180472
104	1	0	7.246709	-3.699659	1.049183
105	1	0	6.381014	-5.342997	3.575331
106	1	0	6.121447	-3.587242	3.390515
107	1	0	4.740343	-4.652092	3.758724
108	1	0	2.540214	0.993968	1.411252
109	1	0	3.902770	2.060494	1.878191
110	1	0	3.533698	0.594418	2.845374
111	1	0	3.582822	0.758217	-0.967621
112	1	0	4.899295	1.860803	-0.445762
113	1	0	5.292046	0.252604	-1.136739
114	1	0	5.979236	-0.110964	2.571095
115	1	0	6.697025	-0.254637	0.933979
116	1	0	6.257259	1.343873	1.582143
117	1	0	-0.896963	3.238384	3.454969
118	1	0	0.666480	2.455938	3.855778
119	1	0	-0.046842	2.256380	2.221716
120	1	0	-0.648567	-1.091382	3.972308
121	1	0	0.103352	-0.347109	2.531679
122	1	0	0.815711	-0.067127	4.150772
123	1	0	-1.803569	0.349274	5.734074
124	1	0	-1.911790	2.126642	5.523458
125	1	0	-0.338413	1.355070	5.839326
126	8	0	0.488649	0.762906	-2.722748
127	8	0	0.859191	2.276883	-0.592484
128	6	0	1.005196	1.995439	-2.983546
129	1	0	0.282684	2.632458	-3.535852
130	6	0	1.181798	2.755959	-1.672619
131	6	0	2.313666	1.965812	-3.787900
132	1	0	2.697086	2.972873	-3.984194
133	1	0	3.075308	1.395135	-3.247115
134	1	0	2.120462	1.464095	-4.741521
135	8	0	1.648892	4.003173	-1.800006
136	6	0	1.668187	4.818534	-0.622789
137	1	0	1.554623	4.172292	0.253406
138	6	0	0.510333	5.806506	-0.696226

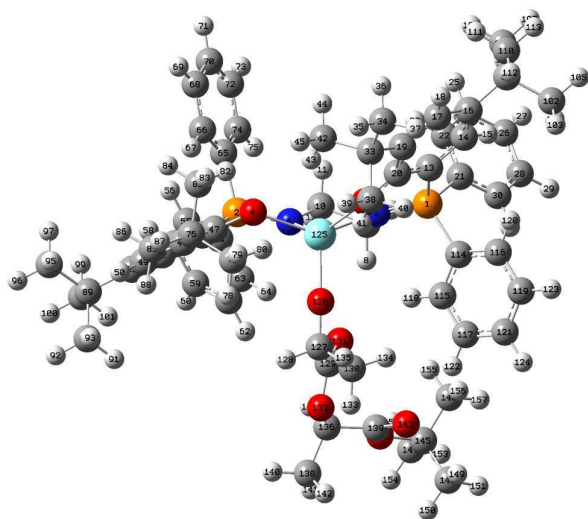
Appendix 2. Optimised Structures

139	1	0	-0.420284	5.254110	-0.854662
140	1	0	0.440457	6.380135	0.231509
141	1	0	0.647265	6.501253	-1.532421
142	6	0	3.035494	5.491618	-0.551676
143	8	0	3.938018	5.315005	-1.335147
144	8	0	3.060989	6.290942	0.526263
145	6	0	4.257655	7.064664	0.879039
146	6	0	4.584959	8.055725	-0.236335
147	1	0	4.891113	7.538138	-1.147443
148	1	0	3.713437	8.681573	-0.458553
149	1	0	5.400846	8.712709	0.085777
150	6	0	3.822574	7.797358	2.145193
151	1	0	3.541911	7.083965	2.926982
152	1	0	4.642467	8.418899	2.520459
153	1	0	2.962073	8.443560	1.942521
154	6	0	5.421014	6.119596	1.173637
155	1	0	5.133625	5.389318	1.938007
156	1	0	5.735480	5.586847	0.274245
157	1	0	6.271451	6.695096	1.556531

 Rotational constants (GHZ): 0.0258497 0.0255342
 0.0181036

Sum of electronic and zero-point Energies= -3154.452675
 Sum of electronic and thermal Energies= -3154.373325
 Sum of electronic and thermal Enthalpies= -3154.372381
 Sum of electronic and thermal Free Energies= -3154.573052

	1	2	3
	A	A	A
Frequencies --	8.9615	11.9962	
13.4847			
Red. masses --	4.8869	4.8938	
4.5457			
Frc consts --	0.0002	0.0004	
0.0005			
IR Inten --	0.2833	0.3373	
0.2848			

Intitiation P'

Standard orientation:

Center Number	Atomic Number	Atomic Type	Coordinates (Angstroms)		
			X	Y	Z
1	15	0	3.077088	0.576670	0.633863
2	15	0	-2.466922	-1.216713	1.781129
3	8	0	1.989419	-1.462569	-1.292768
4	8	0	-1.314867	-2.423945	-0.755847
5	7	0	1.489793	0.317376	0.933487
6	7	0	-1.104931	-0.383893	1.398678
7	6	0	0.753986	1.088392	1.935714
8	1	0	0.273325	1.972468	1.490238
9	1	0	1.390670	1.438345	2.762297
10	6	0	-0.335776	0.186105	2.507703
11	1	0	0.150315	-0.600836	3.108657
12	1	0	-0.960558	0.784236	3.192883
13	6	0	3.908243	-0.903740	-0.013076
14	6	0	5.228600	-1.156437	0.375817
15	1	0	5.697639	-0.505827	1.109063
16	6	0	5.944906	-2.226829	-0.152870
17	6	0	5.279790	-3.016020	-1.102705
18	1	0	5.821904	-3.846892	-1.536196
19	6	0	3.967752	-2.807972	-1.531417
20	6	0	3.232490	-1.721947	-0.961169
21	6	0	3.958755	1.044270	2.186443
22	6	0	3.920683	0.135582	3.254230
23	1	0	3.416941	-0.819742	3.130438

24	6	0	4.528223	0.453595	4.465776
25	1	0	4.498274	-0.257104	5.287676
26	6	0	5.174313	1.681473	4.622972
27	1	0	5.648951	1.928457	5.569294
28	6	0	5.209074	2.589607	3.567204
29	1	0	5.709160	3.547291	3.686708
30	6	0	4.601891	2.274240	2.350651
31	1	0	4.632929	2.985712	1.530610
32	6	0	7.384792	-2.494110	0.307749
33	6	0	3.332954	-3.717803	-2.594981
34	6	0	4.309167	-4.785956	-3.113425
35	1	0	3.804788	-5.388251	-3.878243
36	1	0	4.636181	-5.471310	-2.321920
37	1	0	5.198541	-4.343410	-3.578483
38	6	0	2.893626	-2.875051	-3.809868
39	1	0	2.415525	-3.517195	-4.561017
40	1	0	3.762240	-2.396694	-4.279395
41	1	0	2.187903	-2.095215	-3.518435
42	6	0	2.122792	-4.459715	-1.995272
43	1	0	1.359345	-3.763836	-1.643955
44	1	0	2.434909	-5.086100	-1.150128
45	1	0	1.667928	-5.114094	-2.749957
46	6	0	-3.348661	-1.825407	0.317466
47	6	0	-2.626268	-2.430844	-0.749729
48	6	0	-3.394748	-3.056571	-1.789839
49	6	0	-4.780447	-2.962457	-1.726296
50	1	0	-5.354686	-3.420064	-2.525016
51	6	0	-5.499519	-2.317432	-0.702231
52	6	0	-4.752732	-1.766791	0.327725
53	1	0	-5.249840	-1.275718	1.156256
54	6	0	-3.627183	-0.115081	2.705832
55	6	0	-4.504436	-0.570810	3.696135
56	1	0	-4.510794	-1.620124	3.978350
57	6	0	-5.373015	0.321646	4.323992
58	1	0	-6.053930	-0.037608	5.091407
59	6	0	-5.365646	1.670273	3.969297
60	1	0	-6.041647	2.364721	4.461976
61	6	0	-4.489977	2.128142	2.984204
62	1	0	-4.480141	3.179767	2.709062
63	6	0	-3.622230	1.240207	2.351772
64	1	0	-2.933179	1.588421	1.585364
65	6	0	-2.159195	-2.649096	2.907951
66	6	0	-2.202446	-3.957263	2.412315
67	1	0	-2.498654	-4.135917	1.383090
68	6	0	-1.870394	-5.030836	3.236944
69	1	0	-1.909692	-6.042987	2.842712
70	6	0	-1.492747	-4.808640	4.560571
71	1	0	-1.235638	-5.647820	5.202018
72	6	0	-1.450714	-3.507974	5.062419
73	1	0	-1.162910	-3.329512	6.095465
74	6	0	-1.781014	-2.431494	4.241098
75	1	0	-1.758177	-1.423027	4.645966
76	6	0	-2.706895	-3.833633	-2.924019
77	6	0	-1.803397	-2.903258	-3.756659
78	1	0	-2.385333	-2.081456	-4.190724
79	1	0	-1.344083	-3.465679	-4.579953
80	1	0	-1.003592	-2.473870	-3.152389
81	6	0	-1.869879	-4.979968	-2.320613

Appendix 2. Optimised Structures

82	1	0	-1.120537	-4.598088	-1.624619
83	1	0	-1.353981	-5.531490	-3.117146
84	1	0	-2.516621	-5.688075	-1.786876
85	6	0	-3.717361	-4.468441	-3.893058
86	1	0	-4.391885	-5.170623	-3.388129
87	1	0	-3.172188	-5.032298	-4.658913
88	1	0	-4.324404	-3.716495	-4.412220
89	6	0	-7.030512	-2.257523	-0.759714
90	6	0	-7.468337	-1.513731	-2.036949
91	1	0	-7.082987	-0.487395	-2.041094
92	1	0	-8.563161	-1.468205	-2.101408
93	1	0	-7.101997	-2.010140	-2.942139
94	6	0	-7.608290	-3.686681	-0.780047
95	1	0	-7.253084	-4.258455	-1.644437
96	1	0	-8.704418	-3.657515	-0.828830
97	1	0	-7.321660	-4.236949	0.123833
98	6	0	-7.626446	-1.520704	0.447393
99	1	0	-7.379695	-2.019291	1.392293
100	1	0	-8.719447	-1.495423	0.363225
101	1	0	-7.274694	-0.484032	0.505826
102	6	0	8.266262	-1.269181	-0.006649
103	1	0	8.281155	-1.065763	-1.083880
104	1	0	7.904036	-0.367554	0.499993
105	1	0	9.299489	-1.441317	0.321592
106	6	0	7.399502	-2.752785	1.827464
107	1	0	8.423341	-2.936429	2.178650
108	1	0	7.002713	-1.899555	2.388790
109	1	0	6.790578	-3.629042	2.079035
110	6	0	8.003901	-3.714353	-0.387641
111	1	0	7.440832	-4.631642	-0.179397
112	1	0	8.054938	-3.582950	-1.474873
113	1	0	9.027586	-3.865809	-0.025008
114	6	0	3.408722	1.946298	-0.558331
115	6	0	2.380459	2.843061	-0.863646
116	6	0	4.662774	2.089174	-1.166585
117	6	0	2.608249	3.887627	-1.761600
118	1	0	1.394016	2.715512	-0.427436
119	6	0	4.887553	3.134211	-2.059625
120	1	0	5.455511	1.376158	-0.954958
121	6	0	3.861494	4.033832	-2.354950
122	1	0	1.798389	4.571264	-2.001841
123	1	0	5.860521	3.239620	-2.533129
124	1	0	4.037037	4.844120	-3.058461
125	39	0	0.061007	-0.704588	-0.634321
126	8	0	-0.636856	0.639469	-2.031109
127	6	0	-1.227332	1.666798	-2.708980
128	1	0	-2.214465	1.365899	-3.109335
129	6	0	-1.527925	2.844326	-1.775827
130	6	0	-0.375252	2.143098	-3.897152
131	8	0	-1.182739	2.957941	-0.618740
132	8	0	-2.285167	3.778764	-2.402912
133	1	0	-0.858781	2.959278	-4.442894
134	1	0	0.605494	2.477663	-3.544980
135	1	0	-0.224146	1.297237	-4.575022
136	6	0	-2.657085	4.909245	-1.623955
137	1	0	-3.049180	4.576129	-0.657764
138	6	0	-3.721909	5.662224	-2.410901
139	6	0	-1.441577	5.800272	-1.353417

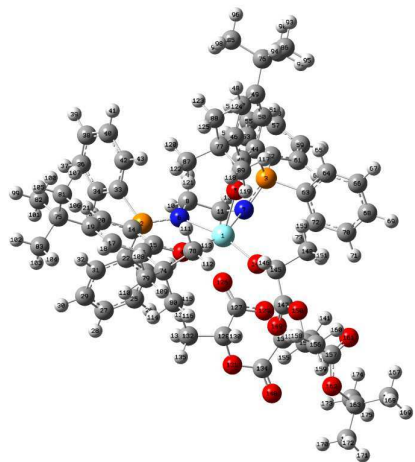
Appendix 2. Optimised Structures

140	1	0	-4.577004	5.006037	-2.597762
141	1	0	-4.060945	6.534298	-1.845023
142	1	0	-3.322348	5.994550	-3.374230
143	8	0	-0.403137	5.751443	-1.972411
144	8	0	-1.747535	6.654904	-0.370642
145	6	0	-0.803061	7.682776	0.089083
146	6	0	-0.469508	8.637067	-1.055886
147	6	0	-1.593279	8.400819	1.179652
148	6	0	0.441302	7.017030	0.671982
149	1	0	0.093328	8.131112	-1.842724
150	1	0	-1.386578	9.054289	-1.486571
151	1	0	0.132867	9.468393	-0.672851
152	1	0	-1.867058	7.705727	1.980067
153	1	0	-0.989471	9.206152	1.610780
154	1	0	-2.510987	8.836992	0.771197
155	1	0	0.159342	6.292592	1.443544
156	1	0	1.015347	6.502056	-0.100160
157	1	0	1.079483	7.778338	1.134642

Rotational constants (GHZ): 0.0271963 0.0225333
0.0172943

Sum of electronic and zero-point Energies= -3172.928365
Sum of electronic and thermal Energies= -3172.847135
Sum of electronic and thermal Enthalpies= -3172.846191
Sum of electronic and thermal Free Energies= -3173.054954

	1	2	3
	A	A	A
Frequencies --	5.6844	9.1766	
9.6599			
Red. masses --	4.4482	4.7610	
4.9915			
Frc consts --	0.0001	0.0002	
0.0003			
IR Inten --	0.0368	0.0548	
0.0026			

Propagation : INTI

Standard orientation:

Center Number	Atomic Number	Atomic Type	Coordinates (Angstroms)		
			X	Y	Z
1	39	0	-0.007996	0.010434	0.138441
2	15	0	2.612689	-2.142813	1.418463
3	15	0	1.055295	3.250232	0.934458
4	8	0	0.318276	-2.045883	-0.580577
5	8	0	1.037971	1.277947	-1.295366
6	7	0	1.897877	-0.672670	1.448566
7	7	0	0.610111	1.823400	1.611568
8	6	0	2.421859	0.309919	2.405281
9	1	0	3.261208	0.869839	1.959994
10	1	0	2.808507	-0.137830	3.337050
11	6	0	1.307253	1.288460	2.777603
12	1	0	0.560266	0.750081	3.378297
13	1	0	1.723884	2.072847	3.427144
14	6	0	2.417753	-3.060367	-0.134182
15	6	0	1.225337	-2.933697	-0.896095
16	6	0	1.064276	-3.823148	-2.013813
17	6	0	2.099132	-4.705025	-2.304670
18	1	0	1.976662	-5.363683	-3.158022
19	6	0	3.301906	-4.804673	-1.579952
20	6	0	3.432454	-3.969170	-0.480385
21	1	0	4.335131	-4.001158	0.121085
22	6	0	2.003427	-3.248466	2.778537
23	6	0	1.167919	-2.705541	3.758140
24	1	0	0.867519	-1.664925	3.682372
25	6	0	0.697013	-3.504723	4.800535
26	1	0	0.049250	-3.074846	5.560755

27	6	0	1.049532	-4.852041	4.862001
28	1	0	0.678737	-5.475729	5.671559
29	6	0	1.870133	-5.402891	3.876221
30	1	0	2.135267	-6.456514	3.912986
31	6	0	2.345462	-4.605563	2.837249
32	1	0	2.969839	-5.044405	2.063386
33	6	0	4.431781	-1.987070	1.706992
34	6	0	5.070263	-2.470124	2.852540
35	1	0	4.506539	-3.022382	3.598658
36	6	0	6.434892	-2.245455	3.041492
37	1	0	6.924678	-2.626618	3.933960
38	6	0	7.165310	-1.536301	2.090736
39	1	0	8.228397	-1.363541	2.238646
40	6	0	6.530594	-1.045984	0.947602
41	1	0	7.096453	-0.490644	0.203964
42	6	0	5.169648	-1.266826	0.756076
43	1	0	4.675457	-0.882771	-0.132732
44	6	0	2.125187	3.246422	-0.543634
45	6	0	1.931736	2.214043	-1.501545
46	6	0	2.731793	2.265119	-2.693508
47	6	0	3.632878	3.315865	-2.832696
48	1	0	4.233394	3.348267	-3.736001
49	6	0	3.820491	4.348783	-1.895153
50	6	0	3.041329	4.291396	-0.748010
51	1	0	3.130384	5.063587	0.008495
52	6	0	1.898141	4.341050	2.166254
53	6	0	3.239041	4.099794	2.500481
54	1	0	3.797735	3.327388	1.978697
55	6	0	3.865307	4.855310	3.489047
56	1	0	4.904874	4.659586	3.738936
57	6	0	3.160123	5.858933	4.153876
58	1	0	3.650089	6.450325	4.923202
59	6	0	1.827309	6.102438	3.828350
60	1	0	1.274198	6.885308	4.340857
61	6	0	1.196622	5.346116	2.840549
62	1	0	0.157996	5.543404	2.592532
63	6	0	-0.488660	4.130323	0.464502
64	6	0	-0.484471	5.101411	-0.542936
65	1	0	0.422659	5.288235	-1.111494
66	6	0	-1.646433	5.817991	-0.822064
67	1	0	-1.642453	6.567923	-1.608867
68	6	0	-2.812323	5.569630	-0.097005
69	1	0	-3.718464	6.128378	-0.317379
70	6	0	-2.819309	4.596201	0.901961
71	1	0	-3.731483	4.393897	1.457483
72	6	0	-1.661245	3.871658	1.181858
73	1	0	-1.656329	3.093232	1.939685
74	6	0	-0.217436	-3.803545	-2.863854
75	6	0	4.384149	-5.797815	-2.019921
76	6	0	4.841775	5.459732	-2.166286
77	6	0	2.589359	1.200236	-3.790996
78	6	0	-0.361525	-2.443853	-3.573056
79	6	0	-0.216764	-4.891172	-3.949933
80	6	0	-1.447860	-4.053116	-1.969308
81	6	0	4.856567	-5.447597	-3.445019
82	6	0	5.607454	-5.769356	-1.093734
83	6	0	3.812754	-7.229462	-2.012502
84	6	0	4.879200	6.497989	-1.036345

Appendix 2. Optimised Structures

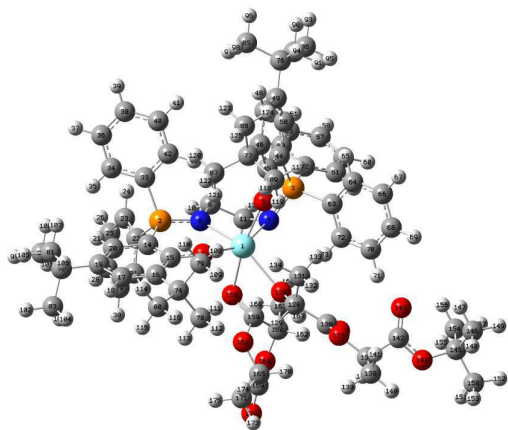
85	6	0	6.249497	4.845525	-2.299051
86	6	0	4.482918	6.191548	-3.474621
87	6	0	2.960997	-0.183097	-3.223591
88	6	0	3.514470	1.461479	-4.989998
89	6	0	1.142996	1.189865	-4.325336
90	1	0	5.620728	7.272043	-1.267266
91	1	0	3.910758	6.996410	-0.909584
92	1	0	5.159118	6.047792	-0.076614
93	1	0	5.213525	6.982924	-3.686053
94	1	0	4.472937	5.510859	-4.332771
95	1	0	3.491132	6.653370	-3.404403
96	1	0	6.993861	5.625408	-2.505808
97	1	0	6.539700	4.333223	-1.374147
98	1	0	6.298050	4.114819	-3.113908
99	1	0	6.356666	-6.488144	-1.446101
100	1	0	6.081193	-4.780929	-1.073929
101	1	0	5.346308	-6.044595	-0.064734
102	1	0	4.576390	-7.950653	-2.331200
103	1	0	3.475821	-7.511000	-1.007885
104	1	0	2.958002	-7.331102	-2.690011
105	1	0	5.624836	-6.155533	-3.782133
106	1	0	4.032292	-5.482338	-4.165743
107	1	0	5.283794	-4.438562	-3.476895
108	1	0	0.594736	-4.756810	-4.675460
109	1	0	-1.160444	-4.841242	-4.505993
110	1	0	-0.138242	-5.899617	-3.525652
111	1	0	0.481471	-2.267801	-4.251032
112	1	0	-1.284040	-2.424562	-4.168734
113	1	0	-0.399522	-1.624790	-2.852646
114	1	0	-1.369781	-5.023389	-1.462985
115	1	0	-1.543944	-3.269944	-1.215628
116	1	0	-2.360251	-4.064205	-2.580226
117	1	0	0.892991	2.159209	-4.774656
118	1	0	1.032230	0.420584	-5.100244
119	1	0	0.428199	0.985323	-3.526819
120	1	0	4.005173	-0.189346	-2.885751
121	1	0	2.324183	-0.457557	-2.381550
122	1	0	2.855627	-0.954325	-3.996902
123	1	0	4.574852	1.444006	-4.709407
124	1	0	3.301366	2.420195	-5.478437
125	1	0	3.362177	0.672932	-5.736393
126	8	0	-1.320770	-0.721053	2.090097
127	6	0	-2.523779	-0.860469	2.240501
128	6	0	-3.256000	-2.152250	1.942270
129	8	0	-3.253940	0.141052	2.706092
130	1	0	-3.700237	-2.015872	0.947104
131	8	0	-4.318797	-2.360507	2.900662
132	6	0	-2.361374	-3.371549	1.978568
133	6	0	-4.700721	0.016933	2.633974
134	6	0	-5.142482	-1.333990	3.179168
135	1	0	-2.952212	-4.259062	1.736202
136	1	0	-1.559905	-3.265451	1.244426
137	1	0	-1.913365	-3.500643	2.967494
138	1	0	-4.968116	0.063279	1.570774
139	6	0	-5.291924	1.176357	3.402462
140	8	0	-6.151475	-1.499274	3.817305
141	1	0	-4.968086	2.121134	2.958073
142	1	0	-6.381605	1.116557	3.364154

Appendix 2. Optimised Structures

143	1	0	-4.982261	1.145955	4.451080
144	8	0	-1.964307	0.226008	-0.661694
145	6	0	-2.787438	0.452210	-1.729983
146	1	0	-2.401917	-0.022862	-2.653511
147	6	0	-4.166028	-0.181527	-1.531312
148	6	0	-2.965866	1.950024	-2.036147
149	8	0	-4.595124	-0.695991	-0.515131
150	8	0	-4.898152	-0.136048	-2.665757
151	1	0	-3.608981	2.113652	-2.906703
152	1	0	-3.397399	2.463417	-1.171591
153	1	0	-1.979131	2.380035	-2.230716
154	6	0	-6.197346	-0.717407	-2.598936
155	1	0	-6.126603	-1.720174	-2.165996
156	6	0	-6.731706	-0.776573	-4.023375
157	6	0	-7.113593	0.119271	-1.701149
158	1	0	-6.058953	-1.371465	-4.648054
159	1	0	-7.723264	-1.237517	-4.032156
160	1	0	-6.801654	0.229786	-4.448074
161	8	0	-6.900833	1.266609	-1.383526
162	8	0	-8.185409	-0.616200	-1.381402
163	6	0	-9.285056	-0.072146	-0.572132
164	6	0	-9.937144	1.099502	-1.303231
165	6	0	-10.244831	-1.254120	-0.472319
166	6	0	-8.768273	0.324064	0.809417
167	1	0	-9.248335	1.941898	-1.393322
168	1	0	-10.259880	0.794689	-2.304942
169	1	0	-10.822541	1.428626	-0.747853
170	1	0	-9.758168	-2.106957	0.011709
171	1	0	-11.123665	-0.975571	0.118710
172	1	0	-10.580853	-1.565830	-1.466858
173	1	0	-8.254948	-0.518532	1.284972
174	1	0	-8.080855	1.169644	0.742609
175	1	0	-9.613403	0.607833	1.446582

Rotational constants (GHZ):			0.0238129	0.0177112	
0.0144158					
Sum of electronic and zero-point Energies=				-3706.945550	
Sum of electronic and thermal Energies=				-3706.852831	
Sum of electronic and thermal Enthalpies=				-3706.851887	
Sum of electronic and thermal Free Energies=				-3707.087665	
			1	2	3
			A	A	A
Frequencies --		5.4830		7.1954	
7.9403					
Red. masses --		5.2716		5.0952	
4.7057					
Frc consts --		0.0001		0.0002	
0.0002					
IR Inten --		0.1682		0.2483	
0.0901					

Propagation : TSI



Standard orientation:

Center Number	Atomic Number	Atomic Type	Coordinates (Angstroms)		
			X	Y	Z
1	39	0	0.146853	-0.299792	0.158811
2	15	0	3.625983	-0.666283	0.934652
3	15	0	-0.557866	2.949471	1.124399
4	8	0	1.372997	-1.577555	-1.076199
5	8	0	0.108097	1.419879	-1.227686
6	7	0	2.198447	0.102913	1.190765
7	7	0	-0.213278	1.460196	1.739019
8	6	0	2.208581	1.124585	2.246140
9	1	0	2.577157	2.088071	1.853626
10	1	0	2.862425	0.858002	3.092524
11	6	0	0.789785	1.299716	2.791931
12	1	0	0.529771	0.388170	3.344857
13	1	0	0.782959	2.123388	3.521968
14	6	0	3.562083	-2.033144	-0.261643
15	6	0	2.464823	-2.297259	-1.123987
16	6	0	2.608542	-3.390555	-2.049612
17	6	0	3.803665	-4.098391	-2.054539
18	1	0	3.903493	-4.918275	-2.757552
19	6	0	4.898980	-3.836240	-1.209971
20	6	0	4.745298	-2.791829	-0.315134
21	1	0	5.549924	-2.553831	0.373133
22	6	0	4.274840	-1.382889	2.510155
23	6	0	5.116373	-0.664809	3.368274
24	1	0	5.504252	0.304794	3.068591
25	6	0	5.466196	-1.192090	4.611857
26	1	0	6.123155	-0.629244	5.270113

27	6	0	4.972360	-2.433273	5.007908
28	1	0	5.245544	-2.843667	5.976759
29	6	0	4.122314	-3.147417	4.161744
30	1	0	3.728803	-4.112451	4.469945
31	6	0	3.770800	-2.625288	2.919865
32	1	0	3.100494	-3.178170	2.267326
33	6	0	4.913596	0.527006	0.342856
34	6	0	6.292024	0.309598	0.465364
35	1	0	6.666896	-0.569941	0.981278
36	6	0	7.196512	1.225535	-0.068430
37	1	0	8.264423	1.048567	0.031860
38	6	0	6.733517	2.363991	-0.728540
39	1	0	7.441446	3.076684	-1.144239
40	6	0	5.362895	2.584663	-0.855104
41	1	0	4.992050	3.466333	-1.370694
42	6	0	4.455425	1.670461	-0.321447
43	1	0	3.386912	1.835923	-0.430155
44	6	0	0.413726	3.568360	-0.288670
45	6	0	0.553888	2.649860	-1.365572
46	6	0	1.157009	3.138116	-2.571964
47	6	0	1.594984	4.460840	-2.587843
48	1	0	2.054826	4.825581	-3.500341
49	6	0	1.471970	5.370379	-1.521217
50	6	0	0.854158	4.896750	-0.370224
51	1	0	0.691261	5.557962	0.473689
52	6	0	-0.493035	4.242202	2.439110
53	6	0	0.742188	4.699064	2.922739
54	1	0	1.666891	4.350002	2.470836
55	6	0	0.792786	5.613363	3.973143
56	1	0	1.755508	5.961883	4.337952
57	6	0	-0.387538	6.078430	4.552473
58	1	0	-0.347308	6.792954	5.370628
59	6	0	-1.618068	5.625098	4.080338
60	1	0	-2.540876	5.984968	4.527821
61	6	0	-1.672430	4.709410	3.030371
62	1	0	-2.635129	4.360882	2.668154
63	6	0	-2.284164	2.915749	0.504965
64	6	0	-2.705252	3.886519	-0.413088
65	1	0	-2.006428	4.639257	-0.767365
66	6	0	-4.013313	3.870358	-0.890136
67	1	0	-4.334019	4.621171	-1.607896
68	6	0	-4.900572	2.880260	-0.465268
69	1	0	-5.911056	2.845473	-0.862697
70	6	0	-4.484729	1.916324	0.451511
71	1	0	-5.162404	1.127980	0.762086
72	6	0	-3.179725	1.937101	0.943641
73	1	0	-2.844154	1.176564	1.638975
74	6	0	1.465718	-3.782277	-3.002238
75	6	0	6.169986	-4.687139	-1.305767
76	6	0	1.983971	6.808031	-1.672756
77	6	0	1.299373	2.249188	-3.817050
78	6	0	0.238680	-4.223647	-2.181930
79	6	0	1.098403	-2.598832	-3.917326
80	6	0	1.841783	-4.956956	-3.920170
81	6	0	6.760060	-4.575909	-2.725556
82	6	0	7.243979	-4.234450	-0.307092
83	6	0	5.832527	-6.161747	-1.009446
84	6	0	1.748032	7.642101	-0.406142

Appendix 2. Optimised Structures

85	6	0	3.498662	6.792104	-1.958424
86	6	0	1.255980	7.500294	-2.842133
87	6	0	2.245699	1.072129	-3.517595
88	6	0	1.883890	3.008860	-5.019033
89	6	0	-0.085796	1.723640	-4.244034
90	1	0	2.136703	8.656930	-0.551702
91	1	0	0.681373	7.729237	-0.167864
92	1	0	2.258401	7.214099	0.464792
93	1	0	1.612478	8.531477	-2.961688
94	1	0	1.422017	6.979537	-3.791463
95	1	0	0.174775	7.531981	-2.664026
96	1	0	3.879057	7.813992	-2.084250
97	1	0	4.046680	6.325838	-1.130899
98	1	0	3.733976	6.236236	-2.872923
99	1	0	8.134789	-4.865334	-0.409101
100	1	0	7.552482	-3.197261	-0.485568
101	1	0	6.897469	-4.317873	0.729931
102	1	0	6.731891	-6.785912	-1.089005
103	1	0	5.427303	-6.274259	0.002901
104	1	0	5.090420	-6.557766	-1.711198
105	1	0	7.669630	-5.184109	-2.812513
106	1	0	6.054544	-4.923413	-3.488197
107	1	0	7.019237	-3.537003	-2.960276
108	1	0	0.792372	-1.726571	-3.339035
109	1	0	0.276179	-2.883310	-4.587349
110	1	0	1.955175	-2.312920	-4.539263
111	1	0	-0.083500	-3.445565	-1.489174
112	1	0	-0.595727	-4.466212	-2.854165
113	1	0	0.470265	-5.118995	-1.592846
114	1	0	2.696084	-4.721156	-4.566304
115	1	0	2.073485	-5.869077	-3.357060
116	1	0	0.991225	-5.185122	-4.573608
117	1	0	-0.745772	2.555384	-4.520778
118	1	0	0.014694	1.066643	-5.117650
119	1	0	-0.560445	1.162987	-3.437467
120	1	0	3.246166	1.437651	-3.256294
121	1	0	1.881021	0.452464	-2.696372
122	1	0	2.344326	0.434541	-4.405198
123	1	0	2.901667	3.371506	-4.829336
124	1	0	1.261193	3.862218	-5.314670
125	1	0	1.937553	2.328835	-5.877277
126	8	0	-2.037363	-1.287566	0.296106
127	8	0	-4.810569	-1.602344	0.649918
128	6	0	-2.809636	-1.747796	-0.772239
129	1	0	-2.525534	-2.784405	-1.023502
130	6	0	-4.301319	-1.820187	-0.428839
131	6	0	-2.581434	-0.880649	-2.014861
132	1	0	-3.217620	-1.203672	-2.843206
133	1	0	-2.796976	0.169054	-1.793311
134	1	0	-1.539470	-0.966369	-2.342073
135	8	0	-5.009131	-2.260890	-1.491749
136	6	0	-6.395273	-2.518099	-1.269363
137	1	0	-6.513136	-3.090210	-0.343403
138	6	0	-6.895342	-3.312440	-2.468180
139	1	0	-6.324194	-4.240384	-2.564855
140	1	0	-7.952082	-3.559455	-2.337218
141	1	0	-6.775908	-2.732970	-3.389069
142	6	0	-7.171462	-1.207979	-1.107592

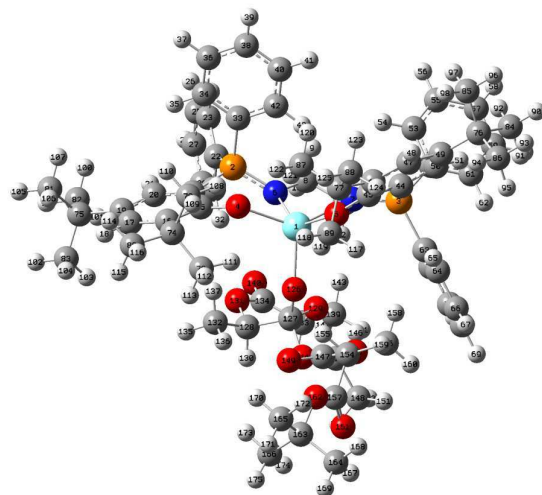
Appendix 2. Optimised Structures

143	8	0	-6.747454	-0.115754	-1.406804
144	8	0	-8.385733	-1.497203	-0.627918
145	6	0	-9.404955	-0.461137	-0.404346
146	6	0	-9.748050	0.226926	-1.723898
147	1	0	-8.899242	0.796734	-2.107150
148	1	0	-10.047838	-0.512270	-2.474981
149	1	0	-10.589212	0.911868	-1.569496
150	6	0	-10.593386	-1.266209	0.113278
151	1	0	-10.332694	-1.790832	1.038141
152	1	0	-11.436849	-0.598843	0.318764
153	1	0	-10.911533	-2.007697	-0.627015
154	6	0	-8.914602	0.523119	0.654520
155	1	0	-8.613741	-0.010784	1.562154
156	1	0	-8.066075	1.105181	0.290639
157	1	0	-9.725507	1.212030	0.916109
158	8	0	-0.229574	-1.956050	1.693880
159	6	0	-1.407266	-2.406525	1.571777
160	6	0	-2.425622	-2.191315	2.708857
161	8	0	-1.509410	-3.650338	0.996681
162	1	0	-3.416482	-2.022284	2.282043
163	6	0	-2.040938	-1.074623	3.648613
164	8	0	-2.471050	-3.397935	3.519354
165	6	0	-2.638061	-4.457443	1.364109
166	1	0	-1.910819	-0.139575	3.097939
167	1	0	-2.819828	-0.942645	4.406012
168	1	0	-1.096359	-1.313905	4.143961
169	6	0	-2.700290	-4.558712	2.885271
170	1	0	-3.566773	-3.972960	1.027093
171	6	0	-2.480596	-5.808203	0.701644
172	8	0	-2.919389	-5.577514	3.493285
173	1	0	-3.317380	-6.454531	0.977546
174	1	0	-2.451946	-5.693973	-0.385747
175	1	0	-1.554632	-6.285410	1.033166

 Rotational constants (GHZ): 0.0246569 0.0181830
 0.0141582

Sum of electronic and zero-point Energies= -3706.926246
 Sum of electronic and thermal Energies= -3706.835655
 Sum of electronic and thermal Enthalpies= -3706.834711
 Sum of electronic and thermal Free Energies= -3707.060596

	1	2	3
	A	A	A
Frequencies --	-151.9668	6.5556	
7.5380			
Red. masses --	8.6808	4.8934	
4.5524			
Frc consts --	0.1181	0.0001	
0.0002			
IR Inten --	54.4441	0.0530	
0.2015			

Propagation : INT2

Standard orientation:

Center Number	Atomic Number	Atomic Type	Coordinates (Angstroms)		
			X	Y	Z
1	39	0	-0.382446	-0.155730	-0.024264
2	15	0	-3.742024	-0.957516	-0.261233
3	15	0	1.544091	-2.975892	0.934636
4	8	0	-1.699378	0.720110	-1.533307
5	8	0	1.364516	-0.744445	-1.162397
6	7	0	-2.379603	-1.164044	0.639393
7	7	0	0.059649	-2.283533	0.901121
8	6	0	-2.295372	-2.366824	1.474538
9	1	0	-2.528495	-3.287408	0.913246
10	1	0	-2.993645	-2.326040	2.323545
11	6	0	-0.871197	-2.481796	2.017529
12	1	0	-0.724238	-1.712393	2.790307
13	1	0	-0.763246	-3.463715	2.505654
14	6	0	-3.960837	0.740599	-0.849348
15	6	0	-2.867702	1.332148	-1.532070
16	6	0	-3.103709	2.575009	-2.202122
17	6	0	-4.360923	3.157804	-2.054290
18	1	0	-4.533116	4.111092	-2.542867
19	6	0	-5.429574	2.606697	-1.323777
20	6	0	-5.210387	1.365099	-0.741142
21	1	0	-6.000232	0.866138	-0.190976
22	6	0	-5.229008	-1.418242	0.718797
23	6	0	-6.166663	-2.364843	0.293853
24	1	0	-6.057213	-2.848839	-0.672020
25	6	0	-7.244889	-2.694847	1.114817

26	1	0	-7.971686	-3.430007	0.778625
27	6	0	-7.386243	-2.088226	2.361936
28	1	0	-8.226154	-2.349671	3.000911
29	6	0	-6.445541	-1.152217	2.793495
30	1	0	-6.537243	-0.684016	3.769472
31	6	0	-5.367656	-0.815630	1.978232
32	1	0	-4.634540	-0.096409	2.333950
33	6	0	-3.752891	-2.008554	-1.783251
34	6	0	-4.755652	-1.860347	-2.749586
35	1	0	-5.546566	-1.128205	-2.605512
36	6	0	-4.728339	-2.631694	-3.909358
37	1	0	-5.507569	-2.509832	-4.657389
38	6	0	-3.694736	-3.546374	-4.116558
39	1	0	-3.671104	-4.142511	-5.025275
40	6	0	-2.684291	-3.682591	-3.165953
41	1	0	-1.866521	-4.378899	-3.333708
42	6	0	-2.711309	-2.914576	-2.001561
43	1	0	-1.909651	-2.998564	-1.271979
44	6	0	2.357196	-2.853831	-0.683411
45	6	0	2.147472	-1.731459	-1.529703
46	6	0	2.836297	-1.724170	-2.789896
47	6	0	3.683709	-2.787647	-3.081617
48	1	0	4.205986	-2.769812	-4.032133
49	6	0	3.913305	-3.890928	-2.238929
50	6	0	3.223829	-3.902311	-1.036487
51	1	0	3.344775	-4.733473	-0.350153
52	6	0	1.386407	-4.773623	1.335192
53	6	0	0.309005	-5.464350	0.765667
54	1	0	-0.395845	-4.926320	0.137428
55	6	0	0.139652	-6.824592	1.010302
56	1	0	-0.701123	-7.352841	0.568143
57	6	0	1.046351	-7.505859	1.823654
58	1	0	0.913592	-8.567601	2.015222
59	6	0	2.120828	-6.823962	2.392082
60	1	0	2.828135	-7.351456	3.026767
61	6	0	2.291119	-5.460251	2.151782
62	1	0	3.126909	-4.932862	2.602292
63	6	0	2.711154	-2.321684	2.209757
64	6	0	3.909975	-1.705731	1.835004
65	1	0	4.175892	-1.636612	0.784018
66	6	0	4.763545	-1.184544	2.807406
67	1	0	5.690949	-0.704439	2.507357
68	6	0	4.427424	-1.277703	4.156625
69	1	0	5.095192	-0.873717	4.913171
70	6	0	3.231460	-1.889141	4.536347
71	1	0	2.965486	-1.962802	5.587645
72	6	0	2.374255	-2.406090	3.568822
73	1	0	1.446717	-2.882016	3.875478
74	6	0	-2.030178	3.222102	-3.092678
75	6	0	-6.759390	3.362344	-1.214768
76	6	0	4.873685	-5.004691	-2.672756
77	6	0	2.628661	-0.584579	-3.800284
78	6	0	-0.776462	3.584354	-2.274968
79	6	0	-1.658028	2.235807	-4.217731
80	6	0	-2.524786	4.515521	-3.759225
81	6	0	-7.354978	3.574926	-2.620583
82	6	0	-7.788696	2.598332	-0.370900
83	6	0	-6.519972	4.732658	-0.550720

Appendix 2. Optimised Structures

84	6	0	4.989268	-6.113305	-1.617780
85	6	0	4.369694	-5.641981	-3.982858
86	6	0	6.279122	-4.414601	-2.901869
87	6	0	1.151082	-0.549385	-4.235927
88	6	0	3.472784	-0.765761	-5.072184
89	6	0	3.033774	0.766419	-3.178520
90	1	0	5.685346	-6.884963	-1.967029
91	1	0	5.373205	-5.729879	-0.664794
92	1	0	4.025021	-6.599433	-1.428479
93	1	0	6.977448	-5.196888	-3.225704
94	1	0	6.273189	-3.635691	-3.672140
95	1	0	6.670653	-3.969194	-1.979753
96	1	0	5.050303	-6.438292	-4.310527
97	1	0	3.373990	-6.079609	-3.845580
98	1	0	4.302770	-4.908371	-4.793715
99	1	0	-8.718716	3.175672	-0.308398
100	1	0	-8.035183	1.624541	-0.810831
101	1	0	-7.432462	2.431043	0.652220
102	1	0	-7.462157	5.289515	-0.466640
103	1	0	-6.104576	4.610264	0.456192
104	1	0	-5.820744	5.347803	-1.127644
105	1	0	-8.303674	4.123388	-2.558236
106	1	0	-6.681452	4.148993	-3.266304
107	1	0	-7.549498	2.614183	-3.111918
108	1	0	-1.290245	1.292866	-3.809231
109	1	0	-0.875899	2.667775	-4.855666
110	1	0	-2.529821	2.023420	-4.849011
111	1	0	-0.337064	2.706308	-1.799903
112	1	0	-0.017848	4.032339	-2.929786
113	1	0	-1.015019	4.312708	-1.492064
114	1	0	-3.402079	4.346169	-4.395199
115	1	0	-2.773202	5.291627	-3.024995
116	1	0	-1.728611	4.914982	-4.398555
117	1	0	4.103481	0.768650	-2.934879
118	1	0	2.850644	1.579711	-3.892377
119	1	0	2.469281	0.971063	-2.267408
120	1	0	0.869461	-1.493157	-4.719115
121	1	0	0.484889	-0.385478	-3.387352
122	1	0	0.988697	0.260635	-4.957700
123	1	0	3.216390	-1.683170	-5.615837
124	1	0	4.548587	-0.778684	-4.858424
125	1	0	3.283616	0.076521	-5.747847
126	8	0	0.109339	1.320636	1.424252
127	6	0	-0.109439	1.841607	2.628245
128	6	0	-1.366715	2.746776	2.761600
129	8	0	-0.213556	0.743706	3.562096
130	1	0	-1.196307	3.404073	3.622161
131	8	0	-2.543782	1.955271	3.036627
132	6	0	-1.639278	3.584999	1.537733
133	6	0	-1.067050	0.986761	4.671812
134	6	0	-2.475371	1.137220	4.101487
135	1	0	-2.471715	4.269990	1.727773
136	1	0	-0.741688	4.160073	1.294776
137	1	0	-1.892697	2.955809	0.681865
138	1	0	-0.775491	1.921143	5.179446
139	6	0	-0.960989	-0.164506	5.649220
140	8	0	-3.456678	0.544918	4.491304
141	1	0	0.070356	-0.252181	6.003089

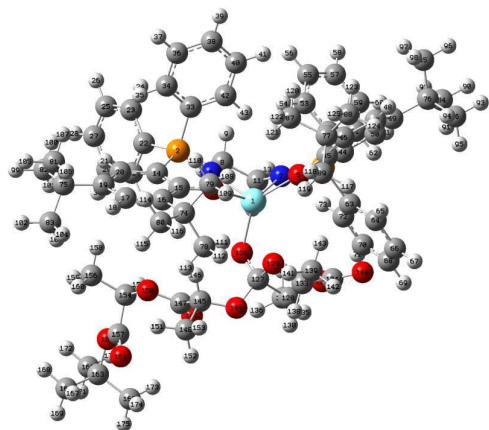
Appendix 2. Optimised Structures

142	1	0	-1.621225	0.005605	6.504141
143	1	0	-1.258436	-1.103057	5.173567
144	8	0	0.920673	2.711903	3.075075
145	6	0	2.241477	2.336787	2.765378
146	1	0	2.324195	1.251281	2.642207
147	6	0	2.686423	3.001786	1.466754
148	6	0	3.139803	2.798844	3.912519
149	8	0	2.117820	3.889516	0.879369
150	8	0	3.876589	2.486400	1.067664
151	1	0	4.188405	2.581148	3.695149
152	1	0	3.033497	3.877629	4.062806
153	1	0	2.844492	2.284516	4.831710
154	6	0	4.477693	3.135195	-0.050363
155	1	0	3.760838	3.190729	-0.874058
156	6	0	5.698968	2.315265	-0.440834
157	6	0	4.888228	4.558548	0.338120
158	1	0	5.396055	1.297111	-0.701007
159	1	0	6.191758	2.768034	-1.306090
160	1	0	6.410145	2.271494	0.390400
161	8	0	5.087136	4.917681	1.476244
162	8	0	5.043152	5.287460	-0.772249
163	6	0	5.469418	6.692349	-0.717674
164	6	0	6.867938	6.789777	-0.111395
165	6	0	5.486556	7.094214	-2.189775
166	6	0	4.442208	7.514682	0.057394
167	1	0	6.863801	6.490914	0.938618
168	1	0	7.569324	6.152074	-0.661159
169	1	0	7.224711	7.823641	-0.180450
170	1	0	4.491919	6.979435	-2.632670
171	1	0	5.792767	8.140916	-2.290030
172	1	0	6.189451	6.471821	-2.753687
173	1	0	3.441977	7.368571	-0.363670
174	1	0	4.422984	7.231952	1.111362
175	1	0	4.695033	8.578444	-0.018124

 Rotational constants (GHZ): 0.0229056 0.0194457
 0.0155023

Sum of electronic and zero-point Energies= -3706.942966
 Sum of electronic and thermal Energies= -3706.851953
 Sum of electronic and thermal Enthalpies= -3706.851009
 Sum of electronic and thermal Free Energies= -3707.080496

	1	2	3
	A	A	A
Frequencies --	5.6684	7.1784	
8.4950			
Red. masses --	5.1422	5.1340	
4.9532			
Frc consts --	0.0001	0.0002	
0.0002			
IR Inten --	0.0666	0.0599	
0.1287			

Propagation : INT3

Standard orientation:

Center Number	Atomic Number	Atomic Type	Coordinates (Angstroms)		
			X	Y	Z
1	39	0	-0.541011	-0.052198	-0.532413
2	15	0	1.086504	2.271455	1.522258
3	15	0	-3.360782	-1.302639	1.337569
4	8	0	0.509670	1.692074	-1.324359
5	8	0	-2.564404	0.375852	-1.198192
6	7	0	0.407612	0.778055	1.459373
7	7	0	-1.822656	-0.744747	1.320339
8	6	0	-0.089633	0.216196	2.721355
9	1	0	-0.736374	0.921534	3.270040
10	1	0	0.731929	-0.052934	3.403165
11	6	0	-0.903895	-1.043709	2.419093
12	1	0	-0.214103	-1.854426	2.137935
13	1	0	-1.410504	-1.354067	3.346590
14	6	0	2.129860	2.666204	0.097132
15	6	0	1.614568	2.391758	-1.196067
16	6	0	2.332293	2.926579	-2.315670
17	6	0	3.515883	3.613548	-2.059457
18	1	0	4.062304	4.006928	-2.910073
19	6	0	4.057799	3.846318	-0.781961
20	6	0	3.326088	3.371179	0.298142
21	1	0	3.671772	3.541928	1.311986
22	6	0	2.139763	2.417421	3.029973
23	6	0	1.979515	3.408720	4.001571
24	1	0	1.219216	4.174493	3.881064
25	6	0	2.794352	3.416030	5.134639
26	1	0	2.664829	4.191778	5.884894
27	6	0	3.766112	2.432649	5.305428
28	1	0	4.398739	2.440190	6.189338

29	6	0	3.920999	1.432013	4.344296
30	1	0	4.670498	0.656569	4.479312
31	6	0	3.110263	1.421312	3.212675
32	1	0	3.215598	0.635039	2.469011
33	6	0	-0.162805	3.630756	1.623624
34	6	0	0.222160	4.976788	1.572012
35	1	0	1.272070	5.240348	1.469107
36	6	0	-0.741970	5.980864	1.624883
37	1	0	-0.438348	7.023735	1.581833
38	6	0	-2.094646	5.647955	1.716275
39	1	0	-2.845674	6.433052	1.750456
40	6	0	-2.482538	4.309710	1.742861
41	1	0	-3.535840	4.045879	1.787952
42	6	0	-1.518964	3.301928	1.694268
43	1	0	-1.818237	2.256898	1.680212
44	6	0	-4.385582	-0.426581	0.121692
45	6	0	-3.847603	0.363133	-0.932239
46	6	0	-4.782165	1.152509	-1.691029
47	6	0	-6.138862	0.997458	-1.432805
48	1	0	-6.835209	1.576839	-2.029140
49	6	0	-6.682031	0.150971	-0.448205
50	6	0	-5.771341	-0.533154	0.338229
51	1	0	-6.124895	-1.162713	1.148762
52	6	0	-4.135100	-0.983607	2.993313
53	6	0	-3.869078	0.246778	3.607391
54	1	0	-3.201554	0.952411	3.121888
55	6	0	-4.453232	0.566757	4.830080
56	1	0	-4.236802	1.523845	5.297898
57	6	0	-5.314533	-0.338706	5.450943
58	1	0	-5.771722	-0.089016	6.405053
59	6	0	-5.587522	-1.563279	4.844690
60	1	0	-6.258399	-2.272256	5.323041
61	6	0	-4.999511	-1.887056	3.621514
62	1	0	-5.215747	-2.845603	3.159369
63	6	0	-3.566614	-3.120439	1.092428
64	6	0	-4.167283	-3.620955	-0.065601
65	1	0	-4.541462	-2.940713	-0.824146
66	6	0	-4.268145	-4.997929	-0.261333
67	1	0	-4.717488	-5.373562	-1.175696
68	6	0	-3.774261	-5.879177	0.696792
69	1	0	-3.855223	-6.952328	0.542649
70	6	0	-3.163820	-5.385683	1.851713
71	1	0	-2.771087	-6.070940	2.598744
72	6	0	-3.055932	-4.012105	2.048649
73	1	0	-2.583392	-3.636182	2.953002
74	6	0	1.798958	2.780868	-3.749488
75	6	0	5.377299	4.613955	-0.634300
76	6	0	-8.200803	0.049621	-0.269357
77	6	0	-4.302029	2.172264	-2.738126
78	6	0	1.748928	1.295435	-4.152362
79	6	0	0.390523	3.400978	-3.839944
80	6	0	2.682630	3.501532	-4.780119
81	6	0	5.221955	6.030031	-1.223520
82	6	0	5.804213	4.752440	0.833351
83	6	0	6.497163	3.870898	-1.388899
84	6	0	-8.586652	-0.925966	0.850926
85	6	0	-8.776110	1.435877	0.082841
86	6	0	-8.841565	-0.448697	-1.579609

Appendix 2. Optimised Structures

87	6	0	-3.413937	3.227693	-2.049277
88	6	0	-5.467005	2.922253	-3.404242
89	6	0	-3.508624	1.479243	-3.859697
90	1	0	-9.678411	-0.975788	0.939042
91	1	0	-8.224790	-1.940791	0.647006
92	1	0	-8.191487	-0.609311	1.823476
93	1	0	-9.931932	-0.516701	-1.473705
94	1	0	-8.630435	0.224663	-2.417485
95	1	0	-8.461872	-1.441530	-1.847151
96	1	0	-9.865164	1.380143	0.207809
97	1	0	-8.344336	1.811893	1.017836
98	1	0	-8.569299	2.173413	-0.700480
99	1	0	6.752501	5.299418	0.893205
100	1	0	5.066149	5.308730	1.423504
101	1	0	5.954544	3.775302	1.307251
102	1	0	7.448662	4.409714	-1.293684
103	1	0	6.634481	2.860616	-0.986805
104	1	0	6.274891	3.776036	-2.457267
105	1	0	6.161853	6.589693	-1.133739
106	1	0	4.951936	6.001325	-2.284688
107	1	0	4.440212	6.589405	-0.696290
108	1	0	-0.299657	2.921874	-3.143697
109	1	0	-0.005197	3.288879	-4.857681
110	1	0	0.426983	4.472681	-3.608207
111	1	0	1.106310	0.716386	-3.487038
112	1	0	1.361598	1.196657	-5.175204
113	1	0	2.754099	0.857257	-4.132135
114	1	0	2.755388	4.577922	-4.582746
115	1	0	3.697252	3.086913	-4.821799
116	1	0	2.240386	3.379974	-5.775927
117	1	0	-4.121055	0.715953	-4.355259
118	1	0	-3.204526	2.214190	-4.616089
119	1	0	-2.612368	1.003678	-3.461814
120	1	0	-3.981243	3.771033	-1.283788
121	1	0	-2.544010	2.770294	-1.573600
122	1	0	-3.055435	3.959216	-2.784739
123	1	0	-6.069962	3.484000	-2.680551
124	1	0	-6.130723	2.248758	-3.960277
125	1	0	-5.060976	3.644956	-4.121560
126	8	0	0.823762	-1.783916	-0.559498
127	6	0	0.736971	-2.504804	-1.659369
128	6	0	0.101293	-3.921202	-1.541970
129	8	0	-0.106318	-1.701707	-2.577823
130	1	0	0.531028	-4.538424	-2.339018
131	8	0	-1.329804	-3.888105	-1.741469
132	6	0	0.368194	-4.562257	-0.201505
133	6	0	-0.736331	-2.477141	-3.600519
134	6	0	-1.772197	-3.347958	-2.894208
135	1	0	-0.044704	-5.575488	-0.181545
136	1	0	1.447921	-4.600773	-0.034780
137	1	0	-0.088662	-3.972880	0.596944
138	1	0	0.028506	-3.121210	-4.060409
139	6	0	-1.345135	-1.586163	-4.657972
140	8	0	-2.911218	-3.513128	-3.262165
141	1	0	-0.571813	-0.951963	-5.100205
142	1	0	-1.794200	-2.202620	-5.441955
143	1	0	-2.129166	-0.957828	-4.232904
144	8	0	1.963673	-2.774139	-2.313195

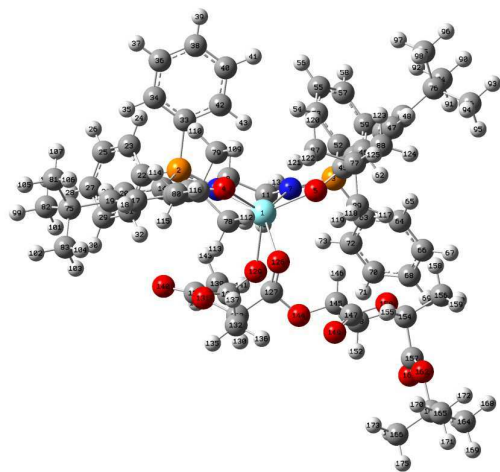
Appendix 2. Optimised Structures

145	6	0	3.037752	-1.894382	-2.075923
146	1	0	2.693709	-0.861084	-1.962568
147	6	0	3.778358	-2.295925	-0.805073
148	6	0	3.986587	-2.002202	-3.268739
149	8	0	3.683291	-3.345508	-0.215778
150	8	0	4.642950	-1.316566	-0.444610
151	1	0	4.865200	-1.369625	-3.119340
152	1	0	4.320438	-3.036992	-3.392341
153	1	0	3.463996	-1.689625	-4.177367
154	6	0	5.515255	-1.641988	0.633419
155	1	0	4.929440	-2.003048	1.484114
156	6	0	6.283719	-0.376173	0.985569
157	6	0	6.478941	-2.753462	0.205712
158	1	0	5.587765	0.423365	1.254893
159	1	0	6.953481	-0.567000	1.829343
160	1	0	6.877719	-0.042467	0.128970
161	8	0	6.761184	-2.997432	-0.944725
162	8	0	6.980194	-3.340917	1.297894
163	6	0	7.961959	-4.430475	1.201858
164	6	0	9.239050	-3.924282	0.534577
165	6	0	8.216457	-4.782356	2.664803
166	6	0	7.347454	-5.614294	0.457945
167	1	0	9.058185	-3.655053	-0.507728
168	1	0	9.628969	-3.049330	1.066739
169	1	0	10.003716	-4.708585	0.567049
170	1	0	7.289335	-5.101334	3.152094
171	1	0	8.943299	-5.598579	2.733453
172	1	0	8.613475	-3.918480	3.208565
173	1	0	6.397464	-5.901968	0.920400
174	1	0	7.166696	-5.372337	-0.590890
175	1	0	8.028860	-6.471033	0.510139

 Rotational constants (GHz): 0.0277360 0.0168430
 0.0148835

Sum of electronic and zero-point Energies= -3706.939125
 Sum of electronic and thermal Energies= -3706.848040
 Sum of electronic and thermal Enthalpies= -3706.847096
 Sum of electronic and thermal Free Energies= -3707.075061

	1	2	3
	A	A	A
Frequencies --	6.3823	8.0733	
12.8231			
Red. masses --	5.0850	4.7045	
4.9709			
Frc consts --	0.0001	0.0002	
0.0005			
IR Inten --	0.0731	0.0584	
0.0252			

Propagation : TS2'

Standard orientation:

Center Number	Atomic Number	Atomic Type	Coordinates (Angstroms)		
			X	Y	Z
1	39	0	-0.622986	-0.104832	-0.250622
2	15	0	-4.152950	0.042306	-0.389782
3	15	0	0.616101	3.194763	-1.087253
4	8	0	-1.935656	-0.947879	1.292989
5	8	0	0.854861	0.965325	0.964007
6	7	0	-2.748115	0.514481	-1.105157
7	7	0	-0.548428	2.060849	-1.261639
8	6	0	-2.856360	1.716217	-1.938517
9	1	0	-3.300131	2.563594	-1.387708
10	1	0	-3.489481	1.553467	-2.826188
11	6	0	-1.462025	2.131202	-2.402468
12	1	0	-1.137311	1.448895	-3.199909
13	1	0	-1.531456	3.136853	-2.846106
14	6	0	-4.059001	-1.557970	0.440543
15	6	0	-2.972500	-1.759747	1.332156
16	6	0	-3.091174	-2.839240	2.267841
17	6	0	-4.178326	-3.697779	2.131094
18	1	0	-4.245487	-4.537186	2.815392
19	6	0	-5.207673	-3.557883	1.182209
20	6	0	-5.147667	-2.439232	0.364555
21	1	0	-5.940303	-2.236346	-0.346588
22	6	0	-5.508481	-0.020659	-1.637666
23	6	0	-6.543024	0.919565	-1.688433
24	1	0	-6.621487	1.688943	-0.925828
25	6	0	-7.478595	0.876111	-2.722657
26	1	0	-8.280494	1.609433	-2.753581
27	6	0	-7.383486	-0.101373	-3.711118

28	1	0	-8.114988	-0.135214	-4.514742
29	6	0	-6.344900	-1.032679	-3.671186
30	1	0	-6.262147	-1.794043	-4.442403
31	6	0	-5.404610	-0.993591	-2.644197
32	1	0	-4.592714	-1.717588	-2.629803
33	6	0	-4.694321	1.224780	0.927844
34	6	0	-5.927486	1.078369	1.575558
35	1	0	-6.613761	0.292184	1.270629
36	6	0	-6.270029	1.924105	2.627752
37	1	0	-7.228037	1.804120	3.127239
38	6	0	-5.378758	2.912419	3.049173
39	1	0	-5.644292	3.566453	3.875947
40	6	0	-4.142961	3.049719	2.419537
41	1	0	-3.438166	3.805157	2.757978
42	6	0	-3.800497	2.208138	1.360805
43	1	0	-2.830270	2.295600	0.878706
44	6	0	1.246103	3.281175	0.604780
45	6	0	1.329689	2.104587	1.396756
46	6	0	1.974614	2.228684	2.676514
47	6	0	2.426876	3.484255	3.066329
48	1	0	2.904363	3.567832	4.037116
49	6	0	2.312068	4.659992	2.299564
50	6	0	1.719244	4.526755	1.053680
51	1	0	1.610127	5.391222	0.406789
52	6	0	-0.046598	4.870859	-1.503188
53	6	0	-1.235810	5.266710	-0.874959
54	1	0	-1.726903	4.592389	-0.178606
55	6	0	-1.789319	6.515341	-1.143126
56	1	0	-2.711958	6.813677	-0.651988
57	6	0	-1.161009	7.380183	-2.041064
58	1	0	-1.593747	8.355176	-2.250270
59	6	0	0.020217	6.991879	-2.669194
60	1	0	0.512207	7.661788	-3.369627
61	6	0	0.577461	5.740143	-2.403032
62	1	0	1.498061	5.444241	-2.897268
63	6	0	2.079909	3.009412	-2.211893
64	6	0	3.382454	3.246181	-1.758518
65	1	0	3.552386	3.512675	-0.719097
66	6	0	4.461024	3.141474	-2.637434
67	1	0	5.469305	3.327412	-2.276230
68	6	0	4.247549	2.800093	-3.971935
69	1	0	5.088855	2.720859	-4.655673
70	6	0	2.951903	2.552025	-4.427550
71	1	0	2.781170	2.277295	-5.465381
72	6	0	1.872713	2.652350	-3.551899
73	1	0	0.868827	2.450569	-3.913807
74	6	0	-2.102649	-3.000979	3.432071
75	6	0	-6.331515	-4.597164	1.107075
76	6	0	2.828570	5.994542	2.849623
77	6	0	2.161427	1.007731	3.589802
78	6	0	-0.676662	-3.266519	2.919200
79	6	0	-2.139206	-1.713032	4.279681
80	6	0	-2.474125	-4.166477	4.362060
81	6	0	-7.065229	-4.678666	2.460199
82	6	0	-7.364703	-4.251845	0.025577
83	6	0	-5.728649	-5.975324	0.770381
84	6	0	2.604886	7.150583	1.865230
85	6	0	2.090222	6.332637	4.159873

Appendix 2. Optimised Structures

86	6	0	4.340562	5.891496	3.130995
87	6	0	0.786145	0.468499	4.019930
88	6	0	2.944587	1.345913	4.868270
89	6	0	2.947740	-0.091659	2.848443
90	1	0	2.982070	8.084573	2.298183
91	1	0	3.134502	6.988465	0.918737
92	1	0	1.541447	7.295306	1.641418
93	1	0	4.721917	6.835884	3.540167
94	1	0	4.566986	5.100604	3.854295
95	1	0	4.895117	5.670688	2.211221
96	1	0	2.453103	7.282666	4.572881
97	1	0	1.011770	6.425398	3.986534
98	1	0	2.239569	5.559937	4.921716
99	1	0	-8.141306	-5.025332	-0.005751
100	1	0	-7.861460	-3.294768	0.226273
101	1	0	-6.908496	-4.198795	-0.969721
102	1	0	-6.515914	-6.739000	0.721692
103	1	0	-5.214074	-5.948671	-0.196812
104	1	0	-5.001156	-6.293808	1.525219
105	1	0	-7.866248	-5.427894	2.418197
106	1	0	-6.389909	-4.961713	3.274884
107	1	0	-7.514515	-3.712967	2.720498
108	1	0	-1.886294	-0.837553	3.679071
109	1	0	-1.424197	-1.783994	5.109213
110	1	0	-3.138994	-1.563602	4.706152
111	1	0	-0.333145	-2.486521	2.239621
112	1	0	0.022577	-3.324784	3.763893
113	1	0	-0.639448	-4.225442	2.388583
114	1	0	-3.469381	-4.043514	4.806092
115	1	0	-2.440375	-5.134974	3.848205
116	1	0	-1.750967	-4.209595	5.185334
117	1	0	3.935948	0.279828	2.549291
118	1	0	3.095322	-0.955963	3.508959
119	1	0	2.417325	-0.427013	1.956089
120	1	0	0.231558	1.226456	4.587216
121	1	0	0.187010	0.175832	3.156953
122	1	0	0.910002	-0.411245	4.663633
123	1	0	2.424033	2.080814	5.494276
124	1	0	3.950353	1.726441	4.650508
125	1	0	3.060065	0.434296	5.466211
126	8	0	0.940573	-1.861325	-0.063345
127	6	0	1.076366	-2.409343	-1.182323
128	6	0	0.421010	-3.743811	-1.560530
129	8	0	-0.118218	-1.218677	-2.202826
130	1	0	0.778907	-4.013783	-2.559453
131	8	0	-1.009282	-3.705477	-1.571249
132	6	0	0.838907	-4.813010	-0.566388
133	6	0	-0.752760	-1.935655	-3.222512
134	6	0	-1.625625	-2.999356	-2.551840
135	1	0	0.423155	-5.778460	-0.869822
136	1	0	1.929905	-4.877746	-0.531516
137	1	0	0.469201	-4.559221	0.429473
138	1	0	0.013842	-2.462763	-3.822061
139	6	0	-1.565025	-1.084675	-4.185280
140	8	0	-2.797012	-3.196318	-2.777059
141	1	0	-0.909868	-0.347985	-4.661091
142	1	0	-2.006260	-1.714675	-4.964899
143	1	0	-2.372574	-0.568813	-3.661300

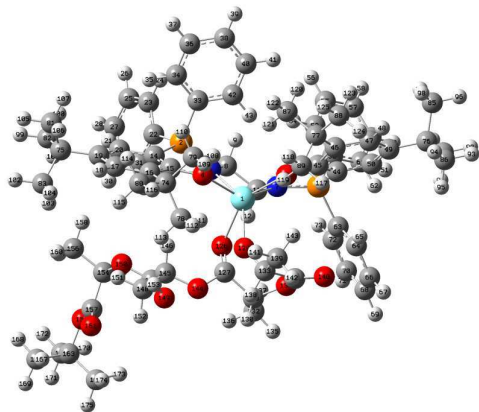
Appendix 2. Optimised Structures

144	8	0	2.230445	-2.325788	-1.881658
145	6	0	3.243857	-1.435686	-1.427755
146	1	0	2.800502	-0.625436	-0.840382
147	6	0	4.194188	-2.217862	-0.526767
148	6	0	3.963298	-0.889879	-2.653962
149	8	0	4.115630	-3.394047	-0.266359
150	8	0	5.168370	-1.405908	-0.066022
151	1	0	4.752705	-0.199656	-2.350075
152	1	0	4.413816	-1.704693	-3.228713
153	1	0	3.247380	-0.356456	-3.284044
154	6	0	6.207370	-2.051751	0.669617
155	1	0	5.766145	-2.717288	1.417293
156	6	0	7.040754	-0.962648	1.328507
157	6	0	7.049997	-2.897612	-0.291284
158	1	0	6.414129	-0.369260	2.000121
159	1	0	7.850893	-1.414163	1.907554
160	1	0	7.471098	-0.297824	0.572705
161	8	0	7.011584	-2.793115	-1.495810
162	8	0	7.833540	-3.713880	0.419521
163	6	0	8.766093	-4.646697	-0.231960
164	6	0	9.803707	-3.868161	-1.037814
165	6	0	9.417091	-5.352632	0.953648
166	6	0	7.984103	-5.636495	-1.092558
167	1	0	9.342738	-3.351642	-1.881934
168	1	0	10.308526	-3.132122	-0.402181
169	1	0	10.561458	-4.560319	-1.422007
170	1	0	8.663936	-5.869125	1.557358
171	1	0	10.143077	-6.091427	0.598154
172	1	0	9.940011	-4.634306	1.593842
173	1	0	7.213735	-6.135448	-0.495133
174	1	0	7.504746	-5.135524	-1.935622
175	1	0	8.666449	-6.401767	-1.479578

Rotational constants (GHZ): 0.0247085 0.0175735
0.0138712

Sum of electronic and zero-point Energies= -3706.929707
Sum of electronic and thermal Energies= -3706.839110
Sum of electronic and thermal Enthalpies= -3706.838166
Sum of electronic and thermal Free Energies= -3707.064660

	1	2	3
	A	A	A
Frequencies --	-166.3810	5.3813	
9.2927			
Red. masses --	9.2434	4.7056	
4.6704			
Frc consts --	0.1508	0.0001	
0.0002			
IR Inten --	102.8254	0.2094	
0.0283			

Propagation : TS2

Standard orientation:

Center Number	Atomic Number	Atomic Type	Coordinates (Angstroms)		
			X	Y	Z
1	39	0	-0.666224	0.032669	-0.664017
2	15	0	1.058174	2.128293	1.614525
3	15	0	-3.364022	-1.496336	1.194720
4	8	0	0.349223	1.890450	-1.236090
5	8	0	-2.710185	0.594549	-1.076011
6	7	0	0.366282	0.657757	1.413012
7	7	0	-1.843443	-0.896317	-1.174917
8	6	0	-0.089701	-0.034673	2.623268
9	1	0	-0.729431	0.603835	3.256078
10	1	0	0.751518	-0.358014	3.256581
11	6	0	-0.897451	-1.272597	2.226852
12	1	0	-0.209336	-2.049433	1.864954
13	1	0	-1.383111	-1.661882	3.135895
14	6	0	2.053155	2.670963	0.203953
15	6	0	1.464115	2.564590	-1.083016
16	6	0	2.125687	3.234410	-2.164876
17	6	0	3.339022	3.860981	-1.893613
18	1	0	3.846204	4.352439	-2.717439
19	6	0	3.959203	3.915158	-0.630962
20	6	0	3.275819	3.322792	0.422756
21	1	0	3.680375	3.357500	1.428893
22	6	0	2.161739	2.114582	3.096146
23	6	0	2.012513	2.981233	4.182316
24	1	0	1.244570	3.748679	4.166064
25	6	0	2.845314	2.860667	5.295813
26	1	0	2.723188	3.540785	6.134872
27	6	0	3.823947	1.870372	5.334385
28	1	0	4.469219	1.775418	6.204018
29	6	0	3.968805	0.993353	4.257789

30	1	0	4.721934	0.210278	4.291655
31	6	0	3.141741	1.111939	3.143970
32	1	0	3.242167	0.421693	2.309757
33	6	0	-0.164797	3.485570	1.909878
34	6	0	0.238406	4.824855	1.989967
35	1	0	1.287776	5.085879	1.875499
36	6	0	-0.706633	5.828035	2.192450
37	1	0	-0.388573	6.865938	2.250225
38	6	0	-2.059407	5.502137	2.305213
39	1	0	-2.796066	6.286911	2.457352
40	6	0	-2.466516	4.173428	2.201943
41	1	0	-3.521079	3.918220	2.263170
42	6	0	-1.521901	3.166600	2.000843
43	1	0	-1.837809	2.133481	1.881797
44	6	0	-4.449360	-0.582144	0.062964
45	6	0	-3.985216	0.417987	-0.835940
46	6	0	-4.986498	1.233515	-1.472400
47	6	0	-6.323172	0.910160	-1.274261
48	1	0	-7.069565	1.512791	-1.780501
49	6	0	-6.787021	-0.139919	-0.459026
50	6	0	-5.819682	-0.854622	0.225680
51	1	0	-6.115928	-1.641860	0.912644
52	6	0	-4.112983	-1.300822	2.883393
53	6	0	-3.839437	-0.117358	3.579649
54	1	0	-3.174453	0.618347	3.137234
55	6	0	-4.411022	0.116187	4.827777
56	1	0	-4.188009	1.037435	5.360126
57	6	0	-5.268244	-0.829521	5.391419
58	1	0	-5.715856	-0.647171	6.365169
59	6	0	-5.549221	-2.008078	4.702928
60	1	0	-6.216494	-2.748517	5.136730
61	6	0	-4.972892	-2.245268	3.454723
62	1	0	-5.192766	-3.170131	2.929649
63	6	0	-3.515219	-3.305333	0.851478
64	6	0	-4.066422	-3.761469	-0.348458
65	1	0	-4.444960	-3.054419	-1.079030
66	6	0	-4.107379	-5.127962	-0.623913
67	1	0	-4.523826	-5.467814	-1.567638
68	6	0	-3.600254	-6.043543	0.294319
69	1	0	-3.635601	-7.108558	0.078244
70	6	0	-3.036116	-5.593651	1.489992
71	1	0	-2.633812	-6.304920	2.207181
72	6	0	-2.990206	-4.230399	1.767599
73	1	0	-2.555685	-3.888981	2.704007
74	6	0	1.499888	3.290762	-3.566814
75	6	0	5.308329	4.625202	-0.467734
76	6	0	-8.289100	-0.419995	-0.341334
77	6	0	-4.596810	2.449493	-2.330903
78	6	0	1.403766	1.876186	-4.167511
79	6	0	0.095630	3.921734	-3.476792
80	6	0	2.323600	4.147873	-4.540964
81	6	0	5.172801	6.104034	-0.881035
82	6	0	5.812226	4.582422	0.981428
83	6	0	6.362897	3.943040	-1.361198
84	6	0	-8.584112	-1.610103	0.581790
85	6	0	-9.005858	0.818865	0.230790
86	6	0	-8.863266	-0.741468	-1.735303
87	6	0	-3.778624	3.439253	-1.477986

Appendix 2. Optimised Structures

88	6	0	-5.824609	3.211993	-2.856027
89	6	0	-3.773161	2.015128	-3.556302
90	1	0	-9.665660	-1.784920	0.626848
91	1	0	-8.114808	-2.531974	0.218023
92	1	0	-8.236409	-1.428005	1.605654
93	1	0	-9.941509	-0.937057	-1.671561
94	1	0	-8.716484	0.087234	-2.436681
95	1	0	-8.379665	-1.627647	-2.162327
96	1	0	-10.085154	0.636266	0.312355
97	1	0	-8.624606	1.063271	1.229217
98	1	0	-8.865183	1.699710	-0.405172
99	1	0	6.780011	5.092670	1.053178
100	1	0	5.122262	5.087051	1.668313
101	1	0	5.952952	3.553840	1.334095
102	1	0	7.335131	4.442906	-1.261995
103	1	0	6.489416	2.890723	-1.081071
104	1	0	6.079718	3.973543	-2.418960
105	1	0	6.133426	6.623966	-0.772643
106	1	0	4.854968	6.208963	-1.924001
107	1	0	4.434276	6.617961	-0.254683
108	1	0	-0.555187	3.347468	-2.815477
109	1	0	-0.363890	3.958069	-4.472927
110	1	0	0.158014	4.948809	-3.096036
111	1	0	0.817974	1.201982	-3.539722
112	1	0	0.931661	1.921874	-5.158166
113	1	0	2.405617	1.448156	-4.296883
114	1	0	2.428867	5.182963	-4.193877
115	1	0	3.325873	3.736860	-4.714307
116	1	0	1.812584	4.177071	-5.510499
117	1	0	-4.341174	1.311801	-4.177496
118	1	0	-3.527331	2.889265	-4.173063
119	1	0	-2.842122	1.537000	-3.252188
120	1	0	-4.371925	3.796666	-0.627274
121	1	0	-2.865822	2.978958	-1.095391
122	1	0	-3.495448	4.311966	-2.080534
123	1	0	-6.462186	3.584111	-2.044725
124	1	0	-6.439289	2.599554	-3.527059
125	1	0	-5.484179	4.081862	-3.429958
126	8	0	0.879344	-1.774276	-0.412483
127	6	0	1.022224	-2.358363	-1.503170
128	6	0	0.313721	-3.657955	-1.901323
129	8	0	-0.233146	-1.083900	-2.580883
130	1	0	0.706855	-3.952074	-2.880077
131	8	0	-1.107110	-3.572519	-1.970711
132	6	0	0.644075	-4.728717	-0.872013
133	6	0	-0.796438	-1.805910	-3.630610
134	6	0	-1.680049	-2.884058	-3.000998
135	1	0	0.220065	-5.685146	-1.190806
136	1	0	1.728066	-4.823988	-0.763800
137	1	0	0.214690	-4.454487	0.095294
138	1	0	0.006024	-2.316342	-4.199163
139	6	0	-1.586144	-0.958213	-4.615143
140	8	0	-2.836211	-3.100675	-3.273077
141	1	0	-0.936786	-0.177333	-5.021431
142	1	0	-1.960887	-1.574364	-5.439386
143	1	0	-2.440966	-0.491242	-4.122519
144	8	0	2.161389	-2.285122	-2.213269
145	6	0	3.178325	-1.386197	-1.780013

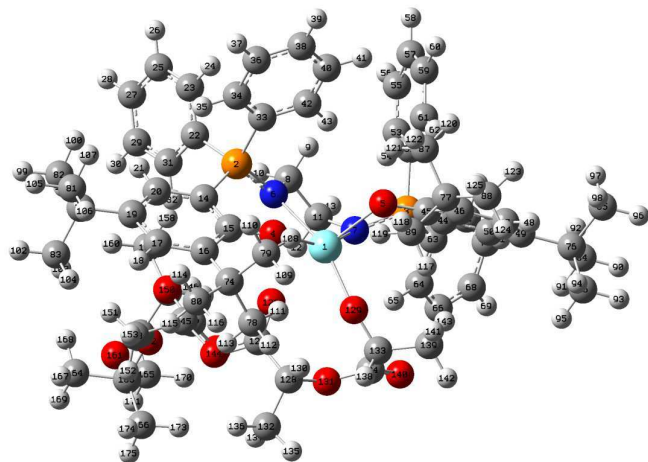
Appendix 2. Optimised Structures

146	1	0	2.732135	-0.459204	-1.407067
147	6	0	3.966954	-2.045454	-0.653562
148	6	0	4.074526	-1.109916	-2.980629
149	8	0	3.829316	-3.178304	-0.260345
150	8	0	4.886668	-1.184504	-0.169492
151	1	0	4.862195	-0.405822	-2.703902
152	1	0	4.541095	-2.034274	-3.333286
153	1	0	3.474328	-0.680447	-3.786481
154	6	0	5.819795	-1.739595	0.757678
155	1	0	5.279428	-2.266353	1.550118
156	6	0	6.637824	-0.584874	1.316816
157	6	0	6.718361	-2.749203	0.033971
158	1	0	5.981851	0.140760	1.806034
159	1	0	7.360338	-0.960464	2.046668
160	1	0	7.177760	-0.074839	0.512862
161	8	0	6.827963	-2.814424	-1.168565
162	8	0	7.366534	-3.482136	0.943103
163	6	0	8.328055	-4.525313	0.548373
164	6	0	9.491488	-3.897470	-0.215497
165	6	0	8.793675	-5.076450	1.892706
166	6	0	7.612425	-5.602380	-0.263411
167	1	0	9.162593	-3.493817	-1.174965
168	1	0	9.946958	-3.093108	0.372802
169	1	0	10.258767	-4.657735	-0.399822
170	1	0	7.948017	-5.479665	2.459240
171	1	0	9.520737	-5.880194	1.736578
172	1	0	9.268553	-4.291728	2.491083
173	1	0	6.747564	-5.984742	0.288952
174	1	0	7.271810	-5.213114	-1.224587
175	1	0	8.299050	-6.436813	-0.445133

 Rotational constants (GHZ): 0.0281900 0.0165329
 0.0145127

Sum of electronic and zero-point Energies= -3706.929471
 Sum of electronic and thermal Energies= -3706.838571
 Sum of electronic and thermal Enthalpies= -3706.837627
 Sum of electronic and thermal Free Energies= -3707.064193

	1	2	3
	A	A	A
Frequencies --	-134.4429	7.9741	
8.9059			
Red. masses --	8.1778	4.9368	
4.6802			
Frc consts --	0.0871	0.0002	
0.0002			
IR Inten --	80.8760	0.0705	
0.0467			

Propagation : INT4

Standard orientation:

Center Number	Atomic Number	Atomic Type	Coordinates (Angstroms)		
			X	Y	Z
1	39	0	0.948516	-0.502162	-0.739817
2	15	0	-1.101772	-2.169938	1.621574
3	15	0	2.860319	1.708938	1.230009
4	8	0	-0.055227	-2.424027	-1.117466
5	8	0	2.948155	-1.072344	-0.044814
6	7	0	-0.447081	-0.721326	1.237564
7	7	0	1.359189	1.318447	0.704044
8	6	0	-0.269308	0.309364	2.262165
9	1	0	0.478236	0.029192	3.022049
10	1	0	-1.203734	0.530571	2.803981
11	6	0	0.205068	1.588122	1.564349
12	1	0	-0.610113	1.959250	0.928281
13	1	0	0.385642	2.367285	2.321158
14	6	0	-1.929908	-2.969492	0.216297
15	6	0	-1.203568	-3.042343	-1.002298
16	6	0	-1.769968	-3.825671	-2.062347
17	6	0	-3.006950	-4.424329	-1.839715
18	1	0	-3.435242	-5.012450	-2.644862
19	6	0	-3.741950	-4.338828	-0.642021
20	6	0	-3.168519	-3.605443	0.389473
21	1	0	-3.672426	-3.523153	1.346330
22	6	0	-2.358748	-2.013679	2.968192
23	6	0	-2.232058	-2.672266	4.195184
24	1	0	-1.385048	-3.327122	4.375236
25	6	0	-3.193075	-2.496205	5.191585
26	1	0	-3.084695	-3.014769	6.140725
27	6	0	-4.287144	-1.663712	4.969115

28	1	0	-5.039008	-1.532248	5.743216
29	6	0	-4.415521	-0.996902	3.749655
30	1	0	-5.268400	-0.347859	3.570858
31	6	0	-3.453991	-1.163475	2.756009
32	1	0	-3.554711	-0.632162	1.813289
33	6	0	0.110839	-3.415017	2.252152
34	6	0	-0.226708	-4.772687	2.324949
35	1	0	-1.204724	-5.108044	1.988501
36	6	0	0.696168	-5.696044	2.810592
37	1	0	0.432126	-6.749430	2.860316
38	6	0	1.960715	-5.269745	3.220270
39	1	0	2.682481	-5.991904	3.593789
40	6	0	2.302661	-3.921315	3.136841
41	1	0	3.291730	-3.588651	3.438879
42	6	0	1.381690	-2.993111	2.650584
43	1	0	1.660118	-1.947916	2.556327
44	6	0	4.162446	0.962258	0.208587
45	6	0	4.062841	-0.398637	-0.205064
46	6	0	5.236009	-0.997387	-0.777883
47	6	0	6.351024	-0.191095	-0.979175
48	1	0	7.225995	-0.643220	-1.434216
49	6	0	6.431603	1.173006	-0.640484
50	6	0	5.320037	1.724626	-0.021687
51	1	0	5.329444	2.763413	0.287988
52	6	0	3.213547	1.221330	2.987550
53	6	0	2.641120	1.923703	4.058023
54	1	0	2.042381	2.811472	3.872581
55	6	0	2.852781	1.505901	5.370762
56	1	0	2.405117	2.060775	6.191483
57	6	0	3.643955	0.387016	5.629753
58	1	0	3.813978	0.065203	6.654105
59	6	0	4.226190	-0.309136	4.571288
60	1	0	4.857810	-1.171832	4.768136
61	6	0	4.012113	0.102824	3.256509
62	1	0	4.475527	-0.438444	2.436967
63	6	0	3.086300	3.541875	1.215588
64	6	0	2.375688	4.255917	0.243500
65	1	0	1.723174	3.727675	-0.445442
66	6	0	2.520686	5.639124	0.151022
67	1	0	1.973115	6.183218	-0.613592
68	6	0	3.369207	6.314475	1.027516
69	1	0	3.480245	7.393598	0.954243
70	6	0	4.080660	5.606063	1.996533
71	1	0	4.745013	6.130024	2.679173
72	6	0	3.942117	4.222397	2.091508
73	1	0	4.498906	3.675141	2.847443
74	6	0	-1.013660	-4.030348	-3.384495
75	6	0	-5.088269	-5.062620	-0.513485
76	6	0	7.706813	1.967640	-0.944577
77	6	0	5.264736	-2.493247	-1.137575
78	6	0	-0.782760	-2.678815	-4.089068
79	6	0	0.343089	-4.706634	-3.100481
80	6	0	-1.781727	-4.931236	-4.364113
81	6	0	-4.883626	-6.576658	-0.719863
82	6	0	-5.728127	-4.854771	0.866136
83	6	0	-6.069421	-4.535647	-1.579046
84	6	0	7.595641	3.431667	-0.497316
85	6	0	8.904081	1.332610	-0.209968

Appendix 2. Optimised Structures

86	6	0	7.974945	1.952160	-2.462444
87	6	0	4.946694	-3.331044	0.117341
88	6	0	6.642676	-2.942956	-1.649558
89	6	0	4.241671	-2.809876	-2.245135
90	1	0	8.523486	3.963775	-0.738779
91	1	0	6.774230	3.951125	-1.004336
92	1	0	7.439034	3.517803	0.584667
93	1	0	8.889764	2.511450	-2.697593
94	1	0	8.101857	0.932588	-2.843031
95	1	0	7.143338	2.410862	-3.009247
96	1	0	9.826074	1.887708	-0.426040
97	1	0	8.746655	1.342535	0.875052
98	1	0	9.064909	0.292342	-0.513966
99	1	0	-6.687559	-5.383236	0.912854
100	1	0	-5.096169	-5.247371	1.671571
101	1	0	-5.923244	-3.795497	1.071304
102	1	0	-7.033708	-5.054905	-1.506122
103	1	0	-6.250829	-3.462662	-1.445844
104	1	0	-5.687545	-4.686705	-2.594735
105	1	0	-5.839414	-7.109944	-0.636508
106	1	0	-4.463413	-6.800311	-1.706471
107	1	0	-4.199141	-6.983759	0.033457
108	1	0	0.946895	-4.107438	-2.416383
109	1	0	0.902295	-4.837386	-4.036129
110	1	0	0.193015	-5.697692	-2.654778
111	1	0	-0.164074	-2.014226	-3.482318
112	1	0	-0.270966	-2.838387	-5.047253
113	1	0	-1.740972	-2.185443	-4.299170
114	1	0	-1.955133	-5.933842	-3.955022
115	1	0	-2.749964	-4.502950	-4.652070
116	1	0	-1.191187	-5.049960	-5.280116
117	1	0	4.469440	-2.246889	-3.157732
118	1	0	4.274688	-3.879723	-2.490335
119	1	0	3.225823	-2.561076	-1.936178
120	1	0	5.700045	-3.158024	0.897056
121	1	0	3.961910	-3.080706	0.516144
122	1	0	4.959324	-4.400386	-0.130597
123	1	0	7.435407	-2.774531	-0.910244
124	1	0	6.924976	-2.437766	-2.581214
125	1	0	6.612197	-4.018652	-1.859474
126	8	0	-1.142901	0.745881	-1.467210
127	6	0	-1.676996	0.941466	-2.546914
128	6	0	-0.916013	1.303510	-3.819949
129	8	0	1.523306	0.118937	-2.674158
130	1	0	-0.314927	0.420508	-4.054787
131	8	0	-0.085285	2.411582	-3.481672
132	6	0	-1.789724	1.698079	-4.997926
133	6	0	1.936309	0.971985	-3.679509
134	6	0	1.280885	2.339600	-3.441535
135	1	0	-1.146481	1.943086	-5.848503
136	1	0	-2.452732	0.877219	-5.285294
137	1	0	-2.397898	2.573178	-4.754056
138	1	0	1.593167	0.608343	-4.671611
139	6	0	3.450543	1.119625	-3.761724
140	8	0	1.873345	3.356966	-3.175743
141	1	0	3.890798	0.132876	-3.932223
142	1	0	3.739434	1.786326	-4.582349
143	1	0	3.848493	1.524031	-2.827822

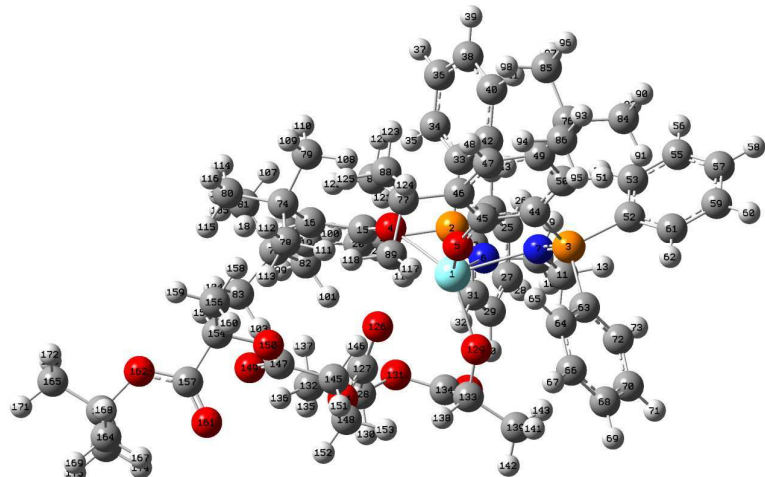
Appendix 2. Optimised Structures

144	8	0	-2.989670	0.835064	-2.730629
145	6	0	-3.797260	0.620628	-1.563932
146	1	0	-3.296593	-0.093493	-0.902989
147	6	0	-3.930292	1.962471	-0.849986
148	6	0	-5.144328	0.093078	-2.032437
149	8	0	-3.535435	3.017883	-1.278745
150	8	0	-4.570819	1.808800	0.326183
151	1	0	-5.802136	-0.046548	-1.171518
152	1	0	-5.618543	0.800193	-2.718695
153	1	0	-5.008011	-0.866879	-2.537842
154	6	0	-4.899438	3.031534	0.994600
155	1	0	-4.020484	3.682307	1.009207
156	6	0	-5.343734	2.679669	2.404954
157	6	0	-6.010955	3.739678	0.210945
158	1	0	-4.536674	2.166534	2.935678
159	1	0	-5.598185	3.593007	2.949282
160	1	0	-6.222419	2.026836	2.380107
161	8	0	-6.668145	3.206380	-0.653444
162	8	0	-6.134132	4.987962	0.664118
163	6	0	-7.128132	5.919822	0.102915
164	6	0	-8.536313	5.382807	0.347305
165	6	0	-6.883333	7.193185	0.906591
166	6	0	-6.839530	6.146547	-1.378959
167	1	0	-8.713383	4.464733	-0.216273
168	1	0	-8.691039	5.183057	1.413505
169	1	0	-9.271209	6.132520	0.033606
170	1	0	-5.857876	7.549300	0.764830
171	1	0	-7.571665	7.979553	0.579875
172	1	0	-7.043522	7.015705	1.975259
173	1	0	-5.801409	6.464635	-1.521689
174	1	0	-7.012141	5.239337	-1.960999
175	1	0	-7.495120	6.937743	-1.759602

Rotational constants (GHZ): 0.0250008 0.0179506
0.0150027

Sum of electronic and zero-point Energies= -3706.939641
Sum of electronic and thermal Energies= -3706.847652
Sum of electronic and thermal Enthalpies= -3706.846708
Sum of electronic and thermal Free Energies= -3707.078130

	1	2	3
	A	A	A
Frequencies --	5.5889	9.8541	
11.5039			
Red. masses --	5.1116	4.7133	
4.3657			
Frc consts --	0.0001	0.0003	
0.0003			
IR Inten --	0.0164	0.0693	
0.2655			

Propagation : INT4'

Standard orientation:

Center Number	Atomic Number	Atomic Type	Coordinates (Angstroms)		
			X	Y	Z
1	39	0	-0.824712	0.166482	0.524902
2	15	0	-1.845634	3.415603	-0.308544
3	15	0	-3.685556	-1.910244	0.801724
4	8	0	0.080478	1.353874	-1.149062
5	8	0	-0.878629	-1.851521	-0.346697
6	7	0	-2.120415	2.123290	0.658938
7	7	0	-3.165161	-0.358986	0.714018
8	6	0	-3.477697	2.005438	1.198811
9	1	0	-4.248246	2.220873	0.438889
10	1	0	-3.649508	2.706079	2.030401
11	6	0	-3.691554	0.581145	1.711845
12	1	0	-3.161985	0.467079	2.668449
13	1	0	-4.768979	0.447078	1.907308
14	6	0	-0.103351	3.670900	-0.711336
15	6	0	0.590878	2.557380	-1.260013
16	6	0	1.816538	2.843268	-1.952410
17	6	0	2.316690	4.141850	-1.880074
18	1	0	3.261230	4.344598	-2.374766
19	6	0	1.685500	5.219852	-1.231399
20	6	0	0.435591	4.963848	-0.682993
21	1	0	-0.140259	5.761688	-0.226544
22	6	0	-2.479987	4.948415	0.496461
23	6	0	-3.415348	5.809951	-0.085235
24	1	0	-3.792518	5.614945	-1.084623
25	6	0	-3.878422	6.919581	0.622198

26	1	0	-4.605682	7.584903	0.163534
27	6	0	-3.414648	7.170086	1.912223
28	1	0	-3.777355	8.035220	2.461970
29	6	0	-2.493747	6.302967	2.501807
30	1	0	-2.139849	6.484360	3.513286
31	6	0	-2.028327	5.191495	1.803018
32	1	0	-1.332428	4.505160	2.280975
33	6	0	-2.684316	3.269547	-1.953403
34	6	0	-2.554709	4.266474	-2.928771
35	1	0	-1.976143	5.162876	-2.718654
36	6	0	-3.140035	4.100354	-4.181994
37	1	0	-3.034743	4.877453	-4.934933
38	6	0	-3.843800	2.931104	-4.474753
39	1	0	-4.293778	2.799249	-5.455664
40	6	0	-3.951584	1.925259	-3.515883
41	1	0	-4.476927	1.002519	-3.749599
42	6	0	-3.371974	2.090880	-2.257429
43	1	0	-3.426733	1.296108	-1.516898
44	6	0	-2.998315	-2.914865	-0.540060
45	6	0	-1.628984	-2.773285	-0.898006
46	6	0	-1.111753	-3.705021	-1.862770
47	6	0	-1.983439	-4.637667	-2.414348
48	1	0	-1.583451	-5.326554	-3.151151
49	6	0	-3.346945	-4.756597	-2.089559
50	6	0	-3.830505	-3.879592	-1.130175
51	1	0	-4.869531	-3.929616	-0.824058
52	6	0	-5.529356	-1.966527	0.658648
53	6	0	-6.142271	-0.991038	-0.136638
54	1	0	-5.526737	-0.231140	-0.610669
55	6	0	-7.524912	-0.990999	-0.307093
56	1	0	-7.993602	-0.226891	-0.922025
57	6	0	-8.304826	-1.967577	0.312730
58	1	0	-9.383804	-1.967584	0.179926
59	6	0	-7.700007	-2.942207	1.105681
60	1	0	-8.304983	-3.703570	1.591416
61	6	0	-6.316524	-2.941281	1.282157
62	1	0	-5.851113	-3.698229	1.907370
63	6	0	-3.332322	-2.786184	2.393570
64	6	0	-2.398476	-3.826821	2.440234
65	1	0	-1.917911	-4.161574	1.525527
66	6	0	-2.089052	-4.437788	3.654764
67	1	0	-1.366587	-5.249811	3.679823
68	6	0	-2.707945	-4.014648	4.830129
69	1	0	-2.468377	-4.494411	5.775885
70	6	0	-3.641064	-2.978020	4.790193
71	1	0	-4.129107	-2.646422	5.703184
72	6	0	-3.951815	-2.364907	3.578500
73	1	0	-4.686482	-1.564361	3.557688
74	6	0	2.514683	1.778309	-2.812945
75	6	0	2.354809	6.598861	-1.195441
76	6	0	-4.214682	-5.815828	-2.779075
77	6	0	0.368989	-3.677627	-2.268807
78	6	0	3.026043	0.616739	-1.944925
79	6	0	1.509648	1.252076	-3.857955
80	6	0	3.720138	2.341578	-3.582153
81	6	0	2.578107	7.111016	-2.632029
82	6	0	1.502123	7.633875	-0.448819
83	6	0	3.714823	6.493528	-0.477676

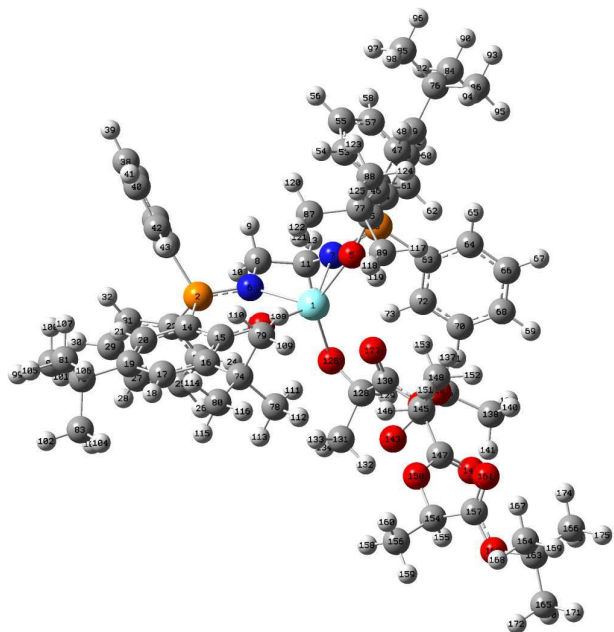
Appendix 2. Optimised Structures

84	6	0	-5.661304	-5.800114	-2.267102
85	6	0	-4.241444	-5.551969	-4.297436
86	6	0	-3.632091	-7.218721	-2.517342
87	6	0	0.694420	-2.338762	-2.954650
88	6	0	0.733015	-4.797976	-3.255800
89	6	0	1.250880	-3.868470	-1.018353
90	1	0	-6.246043	-6.570542	-2.783697
91	1	0	-5.714597	-6.010310	-1.192248
92	1	0	-6.149324	-4.835879	-2.451056
93	1	0	-4.241361	-7.986745	-3.011074
94	1	0	-2.608893	-7.313443	-2.897330
95	1	0	-3.610558	-7.438590	-1.443537
96	1	0	-4.849666	-6.308472	-4.810046
97	1	0	-4.668964	-4.566025	-4.514108
98	1	0	-3.236486	-5.581254	-4.732793
99	1	0	2.024910	8.597502	-0.424700
100	1	0	0.535169	7.796284	-0.939637
101	1	0	1.311917	7.332126	0.587736
102	1	0	4.217042	7.469447	-0.456040
103	1	0	3.583749	6.154600	0.556559
104	1	0	4.384165	5.785294	-0.978653
105	1	0	3.062793	8.095976	-2.619518
106	1	0	3.215592	6.434735	-3.211976
107	1	0	1.624196	7.207218	-3.163837
108	1	0	0.626286	0.829841	-3.374932
109	1	0	1.977505	0.473490	-4.474291
110	1	0	1.187143	2.062702	-4.523036
111	1	0	2.211922	0.152759	-1.388427
112	1	0	3.493684	-0.147723	-2.580455
113	1	0	3.781041	0.966116	-1.230774
114	1	0	3.438430	3.168629	-4.245078
115	1	0	4.516810	2.689601	-2.913073
116	1	0	4.145436	1.548594	-4.209243
117	1	0	1.075563	-4.855017	-0.570266
118	1	0	2.313223	-3.804953	-1.287390
119	1	0	1.029203	-3.104036	-0.270814
120	1	0	0.101064	-2.222627	-3.869763
121	1	0	0.483313	-1.490959	-2.301979
122	1	0	1.755249	-2.302418	-3.234059
123	1	0	0.191332	-4.707204	-4.204989
124	1	0	0.542242	-5.795685	-2.841701
125	1	0	1.803544	-4.736919	-3.485844
126	8	0	1.642231	-0.048223	1.055566
127	6	0	2.394704	0.211728	1.974786
128	6	0	2.460869	1.532186	2.732003
129	8	0	-0.651072	-0.011952	2.635453
130	1	0	2.742964	1.308402	3.767397
131	8	0	1.249671	2.268484	2.693977
132	6	0	3.532351	2.412088	2.089770
133	6	0	-0.069534	0.465238	3.789905
134	6	0	0.201296	1.955243	3.532866
135	1	0	3.644093	3.325050	2.681124
136	1	0	4.487509	1.881552	2.048416
137	1	0	3.228094	2.686985	1.075792
138	1	0	0.892964	-0.049125	3.993723
139	6	0	-0.949479	0.279722	5.021057
140	8	0	-0.527023	2.855474	3.870372
141	1	0	-1.201981	-0.780400	5.117154

Appendix 2. Optimised Structures

142	1	0	-0.437731	0.610378	5.933576
143	1	0	-1.871400	0.857404	4.913590
144	8	0	3.335434	-0.615693	2.433361
145	6	0	3.588738	-1.836676	1.724612
146	1	0	2.720439	-2.081319	1.106117
147	6	0	4.786274	-1.587373	0.813751
148	6	0	3.855256	-2.929663	2.748744
149	8	0	5.389175	-0.545598	0.723008
150	8	0	5.070224	-2.700431	0.115347
151	1	0	4.059333	-3.872022	2.235381
152	1	0	4.720083	-2.677500	3.368966
153	1	0	2.977073	-3.054889	3.388772
154	6	0	6.246614	-2.637436	-0.695677
155	1	0	6.246625	-1.699726	-1.259248
156	6	0	6.217986	-3.838913	-1.627585
157	6	0	7.478278	-2.650328	0.216831
158	1	0	5.321976	-3.804394	-2.253933
159	1	0	7.100369	-3.827720	-2.272713
160	1	0	6.207768	-4.771471	-1.054572
161	8	0	7.440148	-2.909950	1.397627
162	8	0	8.559060	-2.360487	-0.510412
163	6	0	9.902285	-2.301288	0.090904
164	6	0	10.281793	-3.671350	0.648073
165	6	0	10.784324	-1.933660	-1.098189
166	6	0	9.940277	-1.208326	1.156388
167	1	0	9.650036	-3.944294	1.495587
168	1	0	10.189302	-4.439502	-0.127733
169	1	0	11.325243	-3.652097	0.982031
170	1	0	10.477163	-0.973625	-1.525359
171	1	0	11.828606	-1.853245	-0.778949
172	1	0	10.719542	-2.697205	-1.880413
173	1	0	9.603008	-0.254482	0.737020
174	1	0	9.306976	-1.461989	2.008551
175	1	0	10.969702	-1.080886	1.509703

Rotational constants (GHZ):			0.0230639	0.0178658	
0.0133744					
Sum of electronic and zero-point Energies=				-3706.934935	
Sum of electronic and thermal Energies=				-3706.843165	
Sum of electronic and thermal Enthalpies=				-3706.842221	
Sum of electronic and thermal Free Energies=				-3707.072135	
			1	2	3
			A	A	A
Frequencies --		7.4230	9.2722		
11.3924					
Red. masses --		5.2518	4.9772		
4.4953					
Frc consts --		0.0002	0.0003		
0.0003					
IR Inten --		0.2275	0.2148		
0.0037					

Propagation : P'

Standard orientation:

Center Number	Atomic Number	Atomic Type	Coordinates (Angstroms)		
			X	Y	Z
1	39	0	1.294758	0.046618	-0.612627
2	15	0	3.783836	2.683492	-0.305088
3	15	0	2.850383	-3.106288	-0.932561
4	8	0	0.826505	1.897140	0.434719
5	8	0	0.948813	-1.577088	0.837541
6	7	0	3.385866	1.170495	-0.793640
7	7	0	3.001882	-1.499346	-1.134590
8	6	0	4.519513	0.371159	-1.277195
9	1	0	5.159592	0.045535	-0.440543
10	1	0	5.161086	0.927029	-1.983326
11	6	0	3.995219	-0.872429	-1.993573
12	1	0	3.545852	-0.560170	-2.950285
13	1	0	4.847993	-1.527214	-2.228437
14	6	0	2.406171	3.675034	0.334227
15	6	0	1.116911	3.154700	0.627378

16	6	0	0.144871	4.081628	1.149565
17	6	0	0.526848	5.402364	1.343136
18	1	0	-0.214025	6.091427	1.734595
19	6	0	1.806108	5.920903	1.062265
20	6	0	2.729901	5.027281	0.550157
21	1	0	3.728925	5.371929	0.302808
22	6	0	4.507110	3.630838	-1.725276
23	6	0	3.948782	3.374652	-2.984380
24	1	0	3.169618	2.621182	-3.079453
25	6	0	4.393626	4.078408	-4.101415
26	1	0	3.955651	3.875122	-5.075380
27	6	0	5.397190	5.039120	-3.970970
28	1	0	5.743170	5.587022	-4.843944
29	6	0	5.958179	5.294357	-2.720522
30	1	0	6.742678	6.039596	-2.615248
31	6	0	5.516284	4.591589	-1.599475
32	1	0	5.964217	4.790788	-0.629475
33	6	0	5.093087	2.678520	1.003762
34	6	0	6.427434	2.385590	0.689462
35	1	0	6.730613	2.267052	-0.347482
36	6	0	7.377033	2.258636	1.702350
37	1	0	8.410232	2.035732	1.447915
38	6	0	7.002127	2.418519	3.035862
39	1	0	7.743459	2.320622	3.824982
40	6	0	5.675429	2.706705	3.355341
41	1	0	5.379035	2.834416	4.393294
42	6	0	4.723928	2.835204	2.345367
43	1	0	3.691534	3.063436	2.595905
44	6	0	2.285193	-3.537708	0.734222
45	6	0	1.386931	-2.665585	1.409420
46	6	0	0.985781	-3.048037	2.736272
47	6	0	1.467860	-4.246151	3.250885
48	1	0	1.154171	-4.527781	4.250869
49	6	0	2.338837	-5.123085	2.576223
50	6	0	2.741953	-4.736683	1.306370
51	1	0	3.430530	-5.357707	0.742329
52	6	0	4.462433	-3.964750	-1.191504
53	6	0	5.515591	-3.645344	-0.321972
54	1	0	5.345332	-2.953434	0.498984
55	6	0	6.771883	-4.216238	-0.505517
56	1	0	7.582499	-3.966533	0.174262
57	6	0	6.988329	-5.107859	-1.558027
58	1	0	7.969571	-5.553886	-1.699479
59	6	0	5.946231	-5.425075	-2.426421
60	1	0	6.110961	-6.117910	-3.247604
61	6	0	4.685492	-4.854162	-2.246342
62	1	0	3.877080	-5.105489	-2.926689
63	6	0	1.688088	-3.882798	-2.146575
64	6	0	1.115760	-5.140493	-1.920919
65	1	0	1.327893	-5.676161	-0.999116
66	6	0	0.259757	-5.697726	-2.868946
67	1	0	-0.184729	-6.673325	-2.688312
68	6	0	-0.030273	-5.002313	-4.044189
69	1	0	-0.697313	-5.439215	-4.783335
70	6	0	0.528104	-3.743821	-4.265712
71	1	0	0.294569	-3.195582	-5.174903
72	6	0	1.382526	-3.180139	-3.317072
73	1	0	1.789390	-2.183111	-3.466665

Appendix 2. Optimised Structures

74	6	0	-1.288764	3.626106	1.466421
75	6	0	2.108667	7.402889	1.309404
76	6	0	2.809929	-6.414584	3.255002
77	6	0	0.053866	-2.149866	3.563834
78	6	0	-1.969191	3.124761	0.178320
79	6	0	-1.272079	2.508351	2.526806
80	6	0	-2.155974	4.766601	2.023742
81	6	0	1.868831	7.742892	2.793678
82	6	0	3.561786	7.760995	0.969457
83	6	0	1.183838	8.270975	0.433348
84	6	0	3.745375	-7.233334	2.354854
85	6	0	3.574534	-6.070084	4.548752
86	6	0	1.593089	-7.293796	3.604186
87	6	0	0.728646	-0.783310	3.797137
88	6	0	-0.258900	-2.743776	4.946352
89	6	0	-1.289825	-1.962444	2.830641
90	1	0	4.059307	-8.144934	2.877069
91	1	0	3.250750	-7.539617	1.425184
92	1	0	4.651082	-6.674403	2.091565
93	1	0	1.915137	-8.219585	4.098476
94	1	0	0.900299	-6.780298	4.279720
95	1	0	1.035905	-7.565876	2.700039
96	1	0	3.914876	-6.984507	5.051802
97	1	0	4.454152	-5.453609	4.329403
98	1	0	2.947654	-5.515197	5.255271
99	1	0	3.736365	8.825717	1.164483
100	1	0	4.273445	7.191901	1.579851
101	1	0	3.790421	7.577327	-0.087020
102	1	0	1.377103	9.337524	0.607212
103	1	0	1.346867	8.062580	-0.630411
104	1	0	0.126465	8.084291	0.650767
105	1	0	2.071393	8.804999	2.982475
106	1	0	0.834918	7.543963	3.096358
107	1	0	2.525385	7.150210	3.441466
108	1	0	-0.701802	1.644555	2.183657
109	1	0	-2.297923	2.183699	2.746234
110	1	0	-0.826694	2.869336	3.462445
111	1	0	-1.427982	2.283097	-0.255374
112	1	0	-2.994610	2.796899	0.388201
113	1	0	-2.020025	3.926937	-0.568331
114	1	0	-1.758745	5.170936	2.962992
115	1	0	-2.267039	5.591986	1.309981
116	1	0	-3.160370	4.379742	2.232909
117	1	0	-1.800914	-2.926965	2.716655
118	1	0	-1.944516	-1.300056	3.412541
119	1	0	-1.145276	-1.528576	1.839857
120	1	0	1.663342	-0.907191	4.358352
121	1	0	0.957398	-0.285332	2.853250
122	1	0	0.067736	-0.128775	4.379659
123	1	0	0.643076	-2.869619	5.557751
124	1	0	-0.767292	-3.713207	4.876021
125	1	0	-0.926778	-2.061764	5.486010
126	8	0	0.779603	0.317580	-2.686435
127	8	0	-1.111670	-0.558843	-1.070465
128	6	0	-0.430404	0.106008	-3.287311
129	1	0	-0.368366	-0.634432	-4.110583
130	6	0	-1.386358	-0.501421	-2.265516
131	6	0	-1.046870	1.388523	-3.872692

Appendix 2. Optimised Structures

132	1	0	-2.009106	1.195961	-4.359390
133	1	0	-1.188908	2.133260	-3.082851
134	1	0	-0.348458	1.799091	-4.608710
135	8	0	-2.515530	-0.997292	-2.769291
136	6	0	-3.427117	-1.612080	-1.849272
137	1	0	-2.865306	-2.232888	-1.145386
138	6	0	-4.399150	-2.447747	-2.669539
139	1	0	-3.853169	-3.227129	-3.209059
140	1	0	-5.134514	-2.913928	-2.009093
141	1	0	-4.929055	-1.818452	-3.390370
142	6	0	-4.165606	-0.534036	-1.066705
143	8	0	-4.241067	0.630325	-1.372422
144	8	0	-4.762776	-1.088881	0.004523
145	6	0	-5.618237	-0.223378	0.753755
146	1	0	-5.096664	0.716218	0.957945
147	6	0	-6.863754	0.082179	-0.070081
148	6	0	-5.979360	-0.945511	2.043271
149	8	0	-7.246413	-0.553475	-1.022277
150	8	0	-7.495163	1.154478	0.442317
151	1	0	-6.657445	-0.327438	2.637080
152	1	0	-6.477630	-1.893842	1.822286
153	1	0	-5.072257	-1.145613	2.620537
154	6	0	-8.755233	1.472824	-0.148986
155	1	0	-8.669696	1.408955	-1.237948
156	6	0	-9.116841	2.883534	0.290784
157	6	0	-9.795254	0.445730	0.309891
158	1	0	-8.345896	3.584723	-0.041512
159	1	0	-10.074457	3.175365	-0.148184
160	1	0	-9.192914	2.940113	1.381332
161	8	0	-9.612013	-0.350055	1.202133
162	8	0	-10.908447	0.603926	-0.411420
163	6	0	-12.098536	-0.232642	-0.188791
164	6	0	-12.628058	-0.015823	1.227051
165	6	0	-13.082242	0.301673	-1.225417
166	6	0	-11.759424	-1.695862	-0.464433
167	1	0	-11.922414	-0.384673	1.973966
168	1	0	-12.815001	1.048548	1.407988
169	1	0	-13.576646	-0.550966	1.347375
170	1	0	-12.680223	0.184601	-2.237025
171	1	0	-14.027521	-0.247359	-1.161902
172	1	0	-13.286730	1.363954	-1.055436
173	1	0	-11.323728	-1.805115	-1.463310
174	1	0	-11.054001	-2.085233	0.271977
175	1	0	-12.676091	-2.294935	-0.424312

Rotational constants (GHZ):			0.0227976	0.0136529	
0.0106176					
Sum of electronic and zero-point Energies=				-3706.959836	
Sum of electronic and thermal Energies=				-3706.867698	
Sum of electronic and thermal Enthalpies=				-3706.866754	
Sum of electronic and thermal Free Energies=				-3707.101318	
			1	2	3
			A	A	A
Frequencies --			3.7920	6.2181	
9.0497					

Appendix 2. Optimised Structures

Red. masses --	4.9559	5.0555
4.6139		
Frc consts --	0.0000	0.0001
0.0002		
IR Inten --	0.1983	0.2288
0.1065		